

General Disclaimer

One or more of the Following Statements may affect this Document

- This document has been reproduced from the best copy furnished by the organizational source. It is being released in the interest of making available as much information as possible.
- This document may contain data, which exceeds the sheet parameters. It was furnished in this condition by the organizational source and is the best copy available.
- This document may contain tone-on-tone or color graphs, charts and/or pictures, which have been reproduced in black and white.
- This document is paginated as submitted by the original source.
- Portions of this document are not fully legible due to the historical nature of some of the material. However, it is the best reproduction available from the original submission.

NASA Technical Memorandum 83335

**Bibliography of
Lewis Research Center
Technical Publications
Announced in 1982**



(NASA-TM-83335) BIBLIOGRAPHY OF LEWIS
RESEARCH CENTER TECHNICAL PUBLICATIONS
ANNOUNCED IN 1982 (NASA) 372 p
HC A16/MF A01

N83-29124

CSCC 05B

Unclass

G3/82

28125

April 1983

NASA

PREFACE

In 1982, Lewis Research Center's 934 research authors published 378 technical publications which were announced to and reached the worldwide scientific community. This number was almost the same as last year's 384 publications. The number of reports published per person per year has decreased slightly. In 1982, Lewis authors published approximately 61 percent of their research contributions in outside publications and the remainder as NASA research reports. Lewis authors primarily use society proceedings, seminar presentations, journal articles, and transactions to describe their work. Many have received awards for their contributions; among them are the following:

The 1982 Lewis Distinguished Paper Award was presented to Gary M. Johnson for his paper entitled "Surrogate-Equation Technique for Simulation of Steady Inviscid Flow."

In 1982, Marvin Goldstein, Lewis' Chief Scientist, was presented two prestigious awards. He received the Aeroacoustics Award for his important contributions to the theories of fan, jet, and jet-surface interaction noise including his comprehensive treatise *Aeroacoustics*, that has become a standard reference in the field and was published by McGraw-Hill. M. Goldstein also was presented the Pendray Aerospace Literature Award for outstanding literature contributions in aeroacoustics and unsteady aerodynamics which have significantly advanced those sciences and produced key elements in the design of high-speed fans and compressors for modern aircraft engines.

In 1982, 296 contractor-authored research reports were produced, a decrease from the previous year's output of 312. In addition, 21 patent applications were filed and 19 patents were issued.

All the publications in this collection were announced in the 1982 Issues of STAR (Scientific and Technical Aerospace Reports) and IAA (International Aerospace Abstracts).

The arrangement of the material is by NASA subject category, as noted in the Contents. The Lewis-authored items are listed first, followed by the contractor items. Within each of these groups is listed report literature, in N-number sequence, followed by the journal and conference presentations, in A-number sequence.

The various indexes will help locate specific publications by subject, author, contractor organization, contract number, and report number.

George Mandel
Chief, Publications Division

CONTENTS

	Page
AERONAUTICS (GENERAL)	1
AERODYNAMICS	3
AIR TRANSPORTATION AND SAFETY	13
AIRCRAFT DESIGN, TESTING AND PERFORMANCE	14
AIRCRAFT INSTRUMENTATION	15
AIRCRAFT PROPULSION AND POWER	16
RESEARCH AND SUPPORT FACILITIES (AIR)	31
ASTRODYNAMICS	32
GROUND SUPPORT SYSTEMS AND FACILITIES (SPACE)	33
LAUNCH VEHICLES AND SPACE VEHICLES	34
SPACE TRANSPORTATION	35
SPACECRAFT COMMUNICATIONS, COMMAND AND TRACKING	36
SPACECRAFT DESIGN, TESTING AND PERFORMANCE	37
SPACECRAFT PROPULSION AND POWER	42
CHEMISTRY AND MATERIALS (GENERAL)	48
COMPOSITE MATERIALS	49
INORGANIC AND PHYSICAL CHEMISTRY	54
METALLIC MATERIALS	58
NONMETALLIC MATERIALS	66
PROPELLANTS AND FUELS	72
ENGINEERING (GENERAL)	76
COMMUNICATIONS	78
ELECTRONICS AND ELECTRICAL ENGINEERING	81
FLUID MECHANICS AND HEAT TRANSFER	87
INSTRUMENTATION AND PHOTOGRAPHY	95
LASERS AND MASERS	98
MECHANICAL ENGINEERING	99
QUALITY ASSURANCE AND RELIABILITY	110
STRUCTURAL MECHANICS	111
EARTH RESOURCES	117
ENERGY PRODUCTION AND CONVERSION	118
ENVIRONMENT POLLUTION	139
GEOPHYSICS	140
METEOROLOGY AND CLIMATOLOGY	141
AEROSPACE MEDICINE	142
MAN/SYSTEM TECHNOLOGY AND LIFE SUPPORT	143
MATHEMATICAL AND COMPUTER SCIENCES (GENERAL)	144
COMPUTER OPERATIONS AND HARDWARE	145
COMPUTER PROGRAMMING AND SOFTWARE	146
COMPUTER SYSTEMS	147
CYBERNETICS	148
NUMERICAL ANALYSIS	149
THEORETICAL MATHEMATICS	150
ACOUSTICS	151
ATOMIC AND MOLECULAR PHYSICS	155

ORIGINAL PAGE IS
OF POOR QUALITY

OPTICS	156
PLASMA PHYSICS	157
SOLID-STATE PHYSICS	159
THERMODYNAMICS AND STATISTICAL PHYSICS	161
ADMINISTRATION AND MANAGEMENT	162
URBAN TECHNOLOGY AND TRANSPORTATION	163
ASTROPHYSICS	165
LUNAR AND PLANETARY EXPLORATION	166
SOLAR PHYSICS	167
SUBJECT INDEX (KEYWORDS)	A-1
PERSONAL AUTHOR INDEX (INCLUDES LEWIS AND CONTRACTOR AUTHORS)	B-1
CORPORATE SOURCE INDEX (CONTRACTOR ORGANIZATIONS)	C-1
CONTRACT NUMBER INDEX	D-1
REPORT/ACCESSION NUMBER INDEX (INCLUDES PATENTS)	E-1

01 AERONAUTICS (GENERAL)

N82-17083* National Aeronautics and Space Administration, Lewis Research Center, Cleveland, Ohio.

AN EXPERIMENTAL STUDY OF AIRFOIL ICING CHARACTERISTICS

Robert J. Shaw, Ray G. Sotos, and Frank R. Solano 1982 37 p refs Presented at Twentieth Aerospace Sci. Conf., Orlando, Fla., 11-14 Jan. 1982; sponsored by AIAA (NASA-TM-82790; E-1114) Avail: NTIS HC A03/MF A01 CSCL 01B

A full scale general aviation wing with a NACA 63 sub 2 A415 airfoil section was tested to determine icing characteristics for representative rime and glaze icing conditions. Measurements were made of ice accretion shapes and resultant wing section drag coefficient levels. It was found that the NACA 63 sub 2 A415 wing section was less sensitive to rime and glaze icing encounters for climb conditions. E.A.K.

N81-18004* National Aeronautics and Space Administration, Lewis Research Center, Cleveland, Ohio.

ADVANCED TECHNOLOGY FOR CONTROLLING POLLUTANT EMISSIONS FROM SUPERSONIC CRUISE AIRCRAFT

Robert A. Duerr and Larry A. Diehl /in NASA, Langley Research Center Supersonic Cruise Res. 1979, Pt. 1 Mar. 1980 p 535-549 (For primary document see N81-17981 09-01) Avail: NTIS HC A23/MF A01 CSCL 13B

Gas turbine engine combustor technology for the reduction of pollutant emissions is summarized. Variations of conventional combustion systems and advanced combustor concepts are discussed. Projected results from far term technology efforts aimed at applying the premixed prevaporized and catalytic combustion techniques to aircraft combustion systems indicate a potential for significant reductions in pollutant emission levels. M.G.

N82-19132* National Aeronautics and Space Administration, Washington, D. C.

BIBLIOGRAPHY OF NASA PUBLISHED REPORTS ON GENERAL AVIATION, 1975 TO 1981

Jun. 1981 277 p (NASA-TM-83307) Avail: NTIS HC A13/MF A01 CSCL 01B

This bibliography lists 478 documents which relate to all heavier-than-air fixed wing aircraft exclusive of military types and those used for commercial air transport. An exception is the inclusion of commuter transport aircraft types within the general aviation category. NASA publications included in this bibliography are: conference publications (CP), reference publications (RP), technical memorandums (TM, TMX), technical notes (TN), technical papers (TP), and contractor reports (CR). In addition, papers and articles on NASA general aviation programs published by technical societies (AIAA, SAE, etc.) are included, as well as those listed in NASA's Scientific and Technical Aerospace Reports (STAR) Journal. Author and subject indexes are also provided to facilitate use of the bibliography. T.M.

N82-19145* National Aeronautics and Space Administration, Lewis Research Center, Cleveland, Ohio.

ENGINE TECHNOLOGY

Anthony C. Hoffman /in NASA, Langley Research Center Elec. Flight Systems Feb. 1982 p 235-240 (For primary document see N82-19134 10-01)

Avail: NTIS HC A12/MF A01 CSCL 21E

Materials used in a presentation on development of engine technology for electric flight systems are presented. Component and system technology issues, NASA's role, and flight test requirements are outlined. J.D.H.

N82-19146* National Aeronautics and Space Administration, Lewis Research Center, Cleveland, Ohio.

POWER SYSTEMS

Robert Finke /in NASA, Langley Research Center Elec. Flight Systems Feb. 1982 p 241-246 (For primary document see N82-19134 10-01)

Avail: NTIS HC A12/MF A01 CSCL 01C

Materials illustrating a presentation of the development of power systems are presented. The technology issues and tradeoffs, the role of NASA, and testing requirements are outlined. J.D.H.

N82-19147* National Aeronautics and Space Administration, Lewis Research Center, Cleveland, Ohio.

ENVIRONMENTAL CONTROL SYSTEMS

Frank Hrach /in NASA, Langley Research Center Elec. Flight Systems Feb. 1982 p 247-252 (For primary document see N82-19134 10-01)

Avail: NTIS HC A12/MF A01 CSCL 06K

Materials illustrating a presentation on environmental control systems for electric flight systems are presented. The major technology issues, major development and application steps, the role of NASA, and required flight testing are outlined. J.D.H.

N82-21145* National Aeronautics and Space Administration, Lewis Research Center, Cleveland, Ohio.

OZONE AND AIRCRAFT OPERATIONS

Porter J. Perkins /in NASA, Marshall Space Flight Center Proc.: 5th Ann. Workshop on Meteorol. and Environ. Inputs to Aviation Systems Dec. 1981 p 40-44 refs (For primary document see N82-21139 12-01)

Avail: NTIS HC A07/MF A01 CSCL 04A

The cabin ozone problem is discussed. Cabin ozone in terms of health effects, the characteristics of ozone encounters by aircraft, a brief history of studies to define the problem, corrective actions taken, and possible future courses of action are examined. It is suggested that such actions include avoiding high ozone concentrations by applying ozone forecasting in flight planning procedures. E.A.K.

N82-21148* National Aeronautics and Space Administration, Lewis Research Center, Cleveland, Ohio.

NASA/LEWIS RESEARCH CENTER ICING RESEARCH PROGRAM

Peggy L. Evanich /in NASA, Marshall Space Flight Center Proc.: 5th Ann. Workshop on Meteorol. and Environ. Inputs to Aviation Systems Dec. 1981 p 64-75 (For primary document see N82-21139 12-01)

Avail: NTIS HC A07/MF A01 CSCL 01C

Icing requirements for commercial aircraft, light transport and general aviation aircraft, and rotorcraft were studied. The objectives was to: establish the state of the art in aircraft icing, determining the aircraft industry's icing research and technology needs, and recommending both short and long term icing programs to NASA. It is shown that all three categories of aircraft need improved and new ice protection system, icing calculational techniques, icing performance sensitivity on current and modern airfoils, and new and improved icing facilities. The need for a general aviation pilot training film concerning flight into icing conditions is also identified. E.A.K.

N82-26219* National Aeronautics and Space Administration, Lewis Research Center, Cleveland, Ohio.

SUMMARY AND RECENT RESULTS FROM THE NASA ADVANCED HIGH SPEED PROPELLER RESEARCH PROGRAM

Glenn A. Mitchell and Daniel C. Mikkelson 1982 35 p refs Presented at the 18th Joint Propulsion Conf., Cleveland, 21-23 Jun. 1982; sponsored by AIAA, SAE and ASME (NASA-TM-82891; E-1269; NAS 1.15:82891) Avail: NTIS HC A03/MF A01 CSCL 01B

Advanced high-speed propellers offer large performance improvements for aircraft that cruise in the Mach 0.7 to 0.8 speed regime. The current status of the NASA research program on high-speed propeller aerodynamics, acoustics, and aeroelastics is described. Recent wind tunnel results for five 8- to 10-blade advanced models are compared with analytical predictions. Test

ORIGINAL PAGE IS
OF POOR QUALITY

results show that blade sweep was important in achieving net efficiencies near 80 percent at Mach 0.8 and reducing near-field cruise noise by dB. Lifting line and lifting surface aerodynamic analysis codes are under development and some initial lifting line results are compared with propeller force and probe data. Some initial laser velocimeter measurements of the flow field velocities of an 8-bladed 45 deg swept propeller are shown. Experimental aeroelastic results indicate that cascade effects and blade sweep strongly affect propeller aeroelastic characteristics. Comparisons of propeller near-field noise data with linear acoustic theory indicate that the theory adequately predicts near-field noise for subsonic tip speeds but overpredicts the noise for supersonic tip speeds. Potential large gains in propeller efficiency of 7 to 11 percent at Mach 0.8 may be possible with advanced counter-rotation propellers. B.W.

ORIGINAL PAGE IS
OF POOR QUALITY

A81-32548 * # The effect of inflow velocity profiles on the performance of supersonic ejector nozzles. A. R. Bishop (NASA, Lewis Research Center, Cleveland, Ohio). *American Institute of Aeronautics and Astronautics, Aerospace Sciences Meeting, 19th, St. Louis, Mo., Jan. 12-15, 1981, Paper 81-0273*. 6 p. 5 refs.

The design of supersonic nozzles is becoming increasingly complex as conflicting requirements for low noise, higher efficiency, and wider operating range are driving the designer toward more variable geometry and multiple stream flows. Analysis techniques must be modified and expanded to take into account these additional complexities and still retain the rapid computational rate necessary for optimization and design studies. A nozzle analysis must handle more flow streams, more complex geometries, and more highly distorted initial profiles. This paper discusses some modifications to a method for calculating the performance characteristics of supersonic ejector nozzles and demonstrates the improvement in results the modifications provide. (Author)

A82-37678 * # Kevlar/PMR-15 polyimide matrix composite for a complex shaped DC-9 drag reduction fairing. R. T. Kawai, R. F. McCarthy, M. S. Willer (Douglas Aircraft Co., Long Beach, CA), and F. J. Hrach (NASA, Lewis Research Center, Cleveland, OH). *AIAA, SAE, and ASME, Joint Propulsion Conference, 18th, Cleveland, OH, June 21-23, 1982, AIAA Paper 82-1047*. 9 p. 6 refs.

The Aircraft Energy Efficiency (ACEE) Program was established by NASA to improve the fuel efficiency of commercial transport aircraft and thereby to reduce the amount of fuel consumed by the air transportation industry. One of the final items developed by the program is an improved fairing which is the aft closure for the thrust reverser actuators on the JT8D nacelles on DC-9 aircraft. The reduced-drag fairing uses, in the interest of weight savings, an advanced composite construction. The composite material contains Kevlar 49 fibers in a PMR-15 matrix. Attention is given to the aerodynamic configuration, the material system, and aspects of fabrication development. G.R.

N82-22142*# Toledo Univ., Ohio. Dept. of Chemical Engineering.

NUMERICAL SIMULATION OF ONE-DIMENSIONAL HEAT TRANSFER IN COMPOSITE BODIES WITH PHASE CHANGE

M.S. Thesis, 1980 Final Report

Kenneth J. DeWitt and Gurudutt Baliga Mar. 1982 88 p refs

(Contract NAG3-72)

(NASA-CR-165607; NAS 1.26:165607) Avail: NTIS HC A05/MF A01 CSCL 20D

A numerical simulation was developed to investigate the one dimensional heat transfer occurring in a system composed of a layered aircraft blade having an ice deposit on its surface. The finite difference representation of the heat conduction equations was done using the Crank-Nicolson implicit finite difference formulation. The simulation considers uniform or time dependent heat sources, from heaters which can be either point sources or of finite thickness. For the ice water phase change, a numerical method which approximates the latent heat effect by a large heat capacity over a small temperature interval was applied. The simulation describes the temperature profiles within the various layers of the de-icer pad, as well as the movement of the ice water interface. The simulation could also be used to predict the one dimensional temperature profiles in any composite slab having different boundary conditions. M.G.

02 AERODYNAMICS

Includes aerodynamics of bodies, combinations, wings, rotors, and control surfaces; and internal flow in ducts and turbomachinery.

For related information see also 34 *Fluid Mechanics and Heat Transfer*.

N82-11042* National Aeronautics and Space Administration, Lewis Research Center, Cleveland, Ohio.

LOW SPEED TESTING OF THE INLETS DESIGNED FOR A TANDEN-FAN V/STOL NACELLE

Robert C. Williams and Andres H. Ybarra (Vough Corp., Dallas) 1981 13 p refs Presented at the V/STOL Conf., Palo Alto, Calif., 7-9 Dec. 1981 (NASA-TM-82728, E-1031; AIAA-81-2627) Avail: NTIS HC A02/MF A01 CSCL 01A

An approximately 0.25 scale model of a tandem fan nacelle, designed for a subsonic V/STOL aircraft, was tested in a Lewis wind tunnel. Model variables included long and short aft inlet cowls and the addition of exterior strakes to the short inlet cowl. Inlet pressure recoveries and distortion were measured at pitch angles to 40 deg and at combinations of pitch and yaw to 30 deg. Airspeeds covered a range to 135 knots (69 m/sec). The short aft inlet with added strakes had the best aerodynamic performance and is considered suitable for the intended V/STOL application. T.M.

N82-11043* National Aeronautics and Space Administration, Lewis Research Center, Cleveland, Ohio.

A SUMMARY OF V/STOL INLET ANALYSIS METHODS

Danny P. Hwang 1981 12 p refs Presented at the V/STOL Conf., Palo Alto, Calif., 7-9 Dec. 1981 (NASA-TM-82725; E-1027) Avail: NTIS HC A02/MF A01 CSCL 01A

Recent extensions and applications of the methods are emphasized. They include the specification of the Kutta condition for a slotted inlet, the calculation of suction and tangential blowing for boundary layer control, and the analysis of auxiliary inlet geometries at angles of attack. A comparison is made with experiment for the slotted inlet. An optimum diffuser velocity distribution was developed. T.M.

N82-12043* National Aeronautics and Space Administration, Lewis Research Center, Cleveland, Ohio.

INTERACTION OF UPSTREAM FLOW DISTORTIONS WITH HIGH MACH NUMBER CASCADES

Gerald W. Englert 1981 21 p refs Proposed for presentation at the 27th Ann. Gas Turbine Conf., London, 18-22 Apr. 1982; sponsored by ASME (NASA-TM-82759; E-1078) Avail: NTIS HC A02/MF A01 CSCL 01A

Features of the interaction of flow distortions, such as gusts and wakes with blade rows of advance type fans and compressors having high tip Mach numbers are modeled. A typical disturbance was assumed to have harmonic time dependence and was described, at a far upstream location, in three orthogonal spatial coordinates by a double Fourier series. It was convected at supersonic relative to a linear cascade described as an unrolled annulus. Conditions were selected so that the component of this velocity parallel to the axis of the turbomachine was subsonic, permitting interaction between blades through the upstream as well as downstream flow media. A strong, nearly normal shock was considered in the blade passages which was allowed curvature and displacement. The flows before and after the shock were linearized relative to uniform mean velocities in their respective regions. Solution of the descriptive equations was by adaption of the Wiener-Hopf technique, enabling a determination of distortion patterns through and downstream of the cascade as well as pressure distributions on the blade and surfaces. Details of interaction of the disturbance with the in-passage shock were discussed. Influences of amplitude, wave length, and phase of the disturbance on lifts and moments of cascade configurations are presented. Numerical results are clarified by reference to an especially orderly pattern of upstream vertical motion in relation to the cascade parameters. R.J.F.

N82-13112* National Aeronautics and Space Administration, Lewis Research Center, Cleveland, Ohio.

THRUST MODULATION METHODS FOR A SUBSONIC V/STOL AIRCRAFT

Richard R. Woollett 1981 18 p refs Presented at V/STOL Conf., Palo Alto, Calif., 7-9 Dec. 1981; sponsored by AIAA and NASA Ames (NASA-TM-82747; E-1063) Avail: NTIS HC A02/MF A01 CSCL 01A

Low speed wind tunnel tests were conducted to assess four methods for attaining thrust modulation for V/STOL aircraft. The four methods were: (1) fan speed change, (2) fan nozzle exit area change, (3) variable pitch rotor (VPR) fan, and (4) variable inlet guide vanes (VIGV). The interrelationships between inlet and thrust modulation system were also investigated using a double slotted inlet and thick lip inlet. Results can be summarized as: (1) the VPR and VIGV systems were the most promising, (2) changes in blade angle to obtain changes in fan thrust have significant implications for the inlet, and (3) both systems attained required level of thrust with acceptable levels of fan blade stress. M.D.K.

N82-13113* National Aeronautics and Space Administration, Lewis Research Center, Cleveland, Ohio.

COMPUTATIONAL METHODS FOR INTERNAL FLOWS WITH EMPHASIS ON TURBOMACHINERY

William D. McNally and Peter M. Sockol 1981 79 p refs Presented at the Symp. on Computers in Flow Predictions and Fluid Dyn. Exp. at the ASME Winter Ann. Meeting, Washington, D.C., 16-20 Nov. 1981 (NASA-TM-82764; E-1085) Avail: NTIS HC A05/MF A01 CSCL 01A

Current computational methods for analyzing flows in turbomachinery and other related internal propulsion components are presented. The methods are divided into two classes. The inviscid methods deal specifically with turbomachinery applications. Viscous methods deal with generalized duct flows as well as flows in turbomachinery passages. Inviscid methods are categorized into the potential, stream function, and Euler approaches. Viscous methods are treated in terms of parabolic, partially parabolic, and elliptic procedures. Various grids used in association with these procedures are also discussed. Author

N82-13114* National Aeronautics and Space Administration, Lewis Research Center, Cleveland, Ohio.

THE EFFECT OF ROTOR BLADE THICKNESS AND SURFACE FINISH ON THE PERFORMANCE OF A SMALL AXIAL FLOW TURBINE

Richard J. Roelke and Jeffrey E. Haas 1982 13 p refs Proposed for presentation at the Gas Turbine Ann. Meeting, London, 18-22 Apr. 1982; sponsored by ASME Prepared in cooperation with Army Aviation Research and Development Command, Cleveland (Contract DE-A101-77CS-51040)

(NASA-TM-82726; DOE/NASA/51040-34; TR-81-C-29) Avail: NTIS HC A02/MF A01 CSCL 21E

An experimental investigation was conducted to determine the effect of blade profile inaccuracies and surface finish on the aerodynamic performance of a 11.13 cm tip diameter turbine. The as-received cast rotor blades had a significantly thicker profile than the design intent and a fairly rough surface finish. Stage test results showed an increase of one point in efficiency by smoothing the surface finish and another three points by thinning the blade profiles to near the design profile. Most of the performance gain between the as-cast thick and the thinned rotor blades both with the same surface finish, was attributed to reduced trailing edge losses of the recontoured blades. Author

N82-14051* National Aeronautics and Space Administration, Lewis Research Center, Cleveland, Ohio.

ANALYTIC INVESTIGATION OF EFFECT OF END-WALL CONTOURING ON STATOR PERFORMANCE

Robert J. Boyle, Harold E. Rholik, and Louis J. Goldman Nov. 1981 12 p refs (NASA-TP-1943; E-719) Avail: NTIS HC A02/MF A01 CSCL 01A

Calculations show improved stator performance when the tip end wall was contoured so that the inlet area was greater

then the exit area. Comparisons are made with previously published experimental data. The results of a parametric analysis of the effect contour geometry on the efficiency of a highly loaded axial stator are given. The maximum stator efficiency gain is about 0.8 percentage point, and this represents a 22 percent reduction in stator losses. The degree to which endwall contouring reduces the forces driving secondary flows was also examined. The driving forces for both cross channel and radial secondary flow were reduced. T.M.

N82-15020* National Aeronautics and Space Administration, Lewis Research Center, Cleveland, Ohio.
COMPARISON OF TWO AND THREE DIMENSIONAL FLOW COMPUTATIONS WITH LASER ANEMOMETER MEASUREMENTS IN A TRANSONIC COMPRESSOR ROTOR
Rodrick V. Chima and Anthony J. Strazisar 1982 16 p refs
Proposed for presentation at the 27th Gas Turbine Conf., London, 18-22 Apr. 1982; sponsored by ASME
(NASA-TM-82777; E-1007) Avail: NTIS HC A02/MF A01 CSCL 01A

A procedure for using an efficient axisymmetric code to generate downstream pressure input for more costly Euler codes is discussed. Two and three dimensional inviscid solutions for the flow within a transonic axial compressor rotor at design speed are compared to laser anemometer measurements at maximum flow and near stall operating points. Computational details of the 2-D axisymmetric stream function solution and the 3-D full Euler solution are described. Relative Mach number contours, shock location, and shock strength as measured and as predicted by the 3-D code are compared. Downstream of the rotor the inviscid computations agree with each other but predict higher pressure ratios than those measured. Euler codes require a downstream pressure as input. Since that pressure controls the computed mass flow and shock system, it must be consistent with an inviscid solution. E.A.K.

N82-16049* National Aeronautics and Space Administration, Lewis Research Center, Cleveland, Ohio.
APPLICATION OF IMAGE PROCESSING TECHNIQUES TO FLUID FLOW DATA ANALYSIS
Charles C. Giamati 1981 16 p Presented at the 11th Ann. Computer Output Microfilm (COMtec) Conf., Lincolnshire, Ill., 24-26 Feb. 1981
(NASA-TM-82760; E-1081) Avail: NTIS HC A02/MF A01 CSCL 01A

The application of color coding techniques used in processing remote sensing imagery to analyze and display fluid flow data is discussed. A minicomputer based color film recording and color CRT display system is described. High quality, high resolution images of two-dimensional data are produced on the film recorder. Three dimensional data, in large volume, are used to generate color motion pictures in which time is used to represent the third dimension. Several applications and examples are presented. System hardware and software is described. M.G.

N82-18175* National Aeronautics and Space Administration, Lewis Research Center, Cleveland, Ohio.
COMPARISON OF TWO PARALLEL/SERIES FLOW TURBOFAN PROPULSION CONCEPTS FOR SUPERSONIC V/STOL
R. W. Luidens, G. E. Turney, and J. Allen 1981 15 p refs
Presented at the V/STOL Conf., Palo Alto, Calif., 7-9 Dec. 1981
(NASA-TM-82743; AIAA-81-2637; E-1056) Avail: NTIS HC A02/MF A01 CSCL 01A

The thrust, specific fuel consumption, and relative merits of the tandem fan and the dual reverse flow front fan propulsion systems for a supersonic V/STOL aircraft are discussed. Consideration is given to: fan pressure ratio, fan air burning, and variable core supercharging. The special propulsion system components required are described, namely: the deflecting front inlet/nozzle, the aft subsonic inlet, the reverse pitch fan, the variable core supercharger and the low pressure forward burner. The potential benefits for these unconventional systems are indicated. Author

N82-24165* National Aeronautics and Space Administration, Lewis Research Center, Cleveland, Ohio.
EXPERIMENTAL AND ANALYTICAL RESULTS OF TANGENTIAL BLOWING APPLIED TO A SUBSONIC V/STOL INLET
Richard R. Burley and Danny P. Hwang 1982 18 p refs
Proposed for presentation at the 18th Joint Propulsion Conf., Cleveland, 21-23 Jun. 1982; sponsored by AIAA, SAE and ASME
(NASA-TM-82847; E-1217; NAS 1.15:82847) Avail: NTIS HC A02/MF A01 CSCL 01A

Engine inlets for subsonic V/STOL aircraft must operate over a wide range of conditions without internal flow separation. Experimental and analytical investigations were conducted to evaluate the effectiveness of tangential blowing to maintain attached flow to high angles of attack. The inlet had a relatively thin lip with a blowing slot located either on the lip or in the diffuser. The height and width of these slots was varied. Experimentally determined flow separation boundaries showed that lip blowing achieved higher angle of attack capability than diffuser blowing. This capability was achieved with the largest slot circumferential extent and either of the two slot heights. Predicted (analytical) separation boundaries showed good agreement except at the highest angles of attack. S.L.

N82-25213* National Aeronautics and Space Administration, Lewis Research Center, Cleveland, Ohio.
SOME ASPECTS OF CALCULATING FLOWS ABOUT THREE-DIMENSIONAL SUBSONIC INLETS
H. C. Kao 1981 19 p refs Presented at the 17th Joint Propulsion Conf., Colorado Springs, Colo., 27-29 Jul. 1981
(NASA-TM-82789; E-941; NAS 1.15:82789) Avail: NTIS HC A02/MF A01 CSCL 01A

Various three dimensional inlet models were calculated based on the potential flow model. Results are presented in the forms of surface static pressure, flow angularity, surface flow pattern, and inlet flow field. It is indicated that the extension of the lower lip can reduce the adverse pressure gradient and increase the flow separation bound. E.A.K.

N82-26234* National Aeronautics and Space Administration, Lewis Research Center, Cleveland, Ohio.
LASER ANEMOMETER MEASUREMENTS IN AN ANNULAR CASCADE OF CORE TURBINE VANES AND COMPARISON WITH THEORY
Louis J. Goldman and Richard G. Seashultz Jun. 1982 47 p refs
(NASA-TP-2018; E-876; NAS 1.60:2018) Avail: NTIS HC A03/MF A01 CSCL 01A

Laser measurements were made in an annular cascade of stator vanes operating at an exit critical velocity ratio of 0.78. Velocity and flow angles in the blade to blade plane were obtained at every 10 percent of axial chord within the passage and at 1/2 axial chord downstream of the vanes for radial positions near the hub, mean and tip. Results are presented in both plot and tabulated form and are compared with calculations from an inviscid, quasi three dimensional computer program. The experimental measurements generally agreed well with these theoretical calculations, an indication of the usefulness of this analytic approach. Author

N82-26240* National Aeronautics and Space Administration, Lewis Research Center, Cleveland, Ohio.
AERODYNAMIC PERFORMANCE OF HIGH TURNING CORE TURBINE VANES IN A TWO DIMENSIONAL CASCADE
John R. Schwab 1982 20 p refs Presented at the 18th Joint Propulsion Conf., Cleveland, 21-23 Jun. 1982; sponsored by AIAA, SAE and ASME
(NASA-TM-82894; E-1272; NAS 1.15:82894) Avail: NTIS HC A02/MF A01 CSCL 01A

Experimental and theoretical aerodynamic performance data are presented for four uncooled high turning core turbine vanes with exit angles of 74.9, 75.0, 77.5, and 79.6 degrees in a two dimensional cascade. Data for a more conservative 67.0 degree vane are included for comparison. Correction of the experimental aftermix kinetic energy losses to a common 0.100 centimeter trailing edge thickness yields a linear trend of increased loss from 0.020 to 0.025 as the vane exit angle increases from 67.0 to 79.6 degrees. The theoretical losses show

a similar trend. The experimental and theoretical vane surface velocity distributions generally agree within approximately five percent, although the suction surface theoretical velocities are generally higher than the experimental velocities as the vane exit angle increases. S.L.

N82-26241* # National Aeronautics and Space Administration, Lewis Research Center, Cleveland, Ohio

PERFORMANCE OF A 2D-CD NONAXISYMMETRIC EXHAUST NOZZLE ON A TURBOJET ENGINE AT ALTITUDE

David M. Straight 1982 28 p refs. Presented at 18th Joint Propulsion Conf., Cleveland, 21-23 Jun. 1982; sponsored by AIAA, SAE and ASME (NASA-TM-82881; E-1257; NAS 1.15:82881) Avail: NTIS HC A03/MF A01 CSCL 01A

Baseline thrust and cooling data obtained with a 2D-CD versatile research exhaust nozzle mounted on a turbojet engine in an altitude chamber are presented. The tests covered a range of nozzle pressure ratios, nozzle pressure ratios, nozzle throat areas, and internal expansion area ratios. The thrust data obtained show good agreement with theory and scale model results after correcting the data for leakage and bypass cooling flows. Additional work is needed to improve predictability of cooling performance. B.W.

N82-28247* # National Aeronautics and Space Administration, Lewis Research Center, Cleveland, Ohio.

COMPUTER PROGRAM FOR CALCULATING FULL POTENTIAL TRANSONIC, QUASI-THREE-DIMENSIONAL FLOW THROUGH A ROTATING TURBOMACHINERY BLADE ROW

Charles A. Farrell Jun. 1982 57 p refs (NASA-TP-2030; E-1013; NAS 1.60:2030) Avail: NTIS HC A04/MF A01 CSCL 01A

A fast, reliable computer code is described for calculating the flow field about a cascade of arbitrary two dimensional airfoils. The method approximates the three dimensional flow in a turbomachinery blade row by correcting for stream tube convergence and radius change in the throughflow direction. A fully conservative solution of the full potential equation is combined with the finite volume technique on a body-fitted periodic mesh, with an artificial density imposed in the transonic region to insure stability and the capture of shock waves. The instructions required to set up and use the code are included. The name of the code is QSONIC. A numerical example is also given to illustrate the output of the program. M.G.

N82-28249* # National Aeronautics and Space Administration, Lewis Research Center, Cleveland, Ohio.

A SUMMARY OF V/STOL INLET ANALYSIS METHODS

Danny P. Hwang and John M. Abbott 1982 17 p refs. To be presented at the 13th Congr. of the Intern. Council of the Aeronautical Sci. and Aircraft Systems and Technol. Conf., Seattle, 22-27 Aug. 1982; sponsored by the American Inst. of Aeronautics and Astronautics. Previously announced in IAA as A82-16902 (NASA-TM-82885; E-1263; NAS 1.15:82885) Avail: NTIS HC A02/MF A01 CSCL 01A

For abstract see A82-16902

N82-28260* # National Aeronautics and Space Administration, Lewis Research Center, Cleveland, Ohio.

COMPARISON OF LASER ANEMOMETER MEASUREMENTS AND THEORY IN AN ANNULAR TURBINE CASCADE WITH EXPERIMENTAL ACCURACY DETERMINED BY PARAMETER ESTIMATION

Louis J. Goldman and Richard G. Seasholtz 1982 15 p refs. Proposed for presentation at Symp. on Engr. Appl. of Laser Velocimetry, Phoenix, Ariz., 14-19 Nov. 1982; sponsored by ASME (NASA-TM-82860; E-1228; NAS 1.15:82860) Avail: NTIS HC A02/MF A01 CSCL 01A

Experimental measurements of the velocity components in the blade to blade (axial tangential) plane were obtained with an axial flow turbine stator passage and were compared with calculations from three turbomachinery computer programs. The theoretical results were calculated from a quasi three dimensional inviscid code, a three dimensional inviscid code, and a three

dimensional viscous code. Parameter estimation techniques and a particle dynamics calculation were used to assess the accuracy of the laser measurements, which allow a rational basis for comparison of the experimental and theoretical results. The general agreement of the experimental data with the results from the two inviscid computer codes indicates the usefulness of these calculation procedures for turbomachinery blading. The comparison with the viscous code, while generally reasonable, was not as good as for the inviscid codes. S.L.

N82-29270* # National Aeronautics and Space Administration, Lewis Research Center, Cleveland, Ohio

VELOCITY GRADIENT METHOD FOR CALCULATING VELOCITIES IN AN AXISYMMETRIC ANNULAR DUCT

Theodore Katsanis Jul. 1982 23 p refs (NASA-TP-2029; E-1104; NAS 1.60:2029) Avail: NTIS HC A02/MF A01 CSCL 01A

The velocity distribution along an arbitrary line between the inner and outer walls of an annular duct with axisymmetric swirling flow is calculated. The velocity gradient equation is used with an assumed variation of meridional streamline curvature. Upstream flow conditions can vary between the inner and outer walls, and an assumed total pressure distribution can be specified. S.L.

A82-19778 * # Three-dimensional flow calculations including

boundary layer effects for supersonic inlets at angle of attack. J. Vadyak, J. D. Hoffman (Purdue University, West Lafayette, IN), and A. R. Bishop (NASA, Lewis Research Center, Wind Tunnel and Flight Div., Cleveland, OH). *American Institute of Aeronautics and Astronautics, Aerospace Sciences Meeting, 20th, Orlando, FL, Jan. 11-14, 1982, Paper 82-0061*. 13 p. 23 refs. Grant No. NSG-3311.

An analysis is presented for calculating the steady three-dimensional flow field in supersonic mixed-compression inlets at incidence. A zonal modeling approach is employed to obtain the solution. The supersonic core flow is computed using a second-order pentahedral bicharacteristic algorithm. The bow shock wave and the reflected internal shock train are determined using a three-dimensional discrete shock fitting procedure. The boundary layer flow adjacent to both the centerbody and the cowl is computed using a second-order implicit finite difference method. The flow in a shock wave-boundary layer interaction region is computed using an integral formulation. The culmination of the present research effort is the development of a production-type computer program capable of analyzing flow in a variety of mixed-compression aircraft inlets. Numerical results and experimental correlations are presented to illustrate application of the analysis. (Author)

A82-35195 * # Experimental and analytical results of tangential blowing applied to a subsonic V/STOL inlet. R. R. Burley and D. P. Hwang (NASA, Lewis Research Center, Cleveland, OH). *AIAA, SAE, and ASME, Joint Propulsion Conference, 18th, Cleveland, OH, June 21-23, 1982, AIAA Paper 82-1084* 12 p. 9 refs.

(Previously announced in STAR as N82-24165)

A82-37684 * # Tangential blowing for control of strong normal shock - Boundary layer interactions on inlet ramps. M. F. Schwendemann (Northrop Corp., Hawthorne, CA) and B. W. Sanders (NASA, Lewis Research Center, Cleveland, OH). *AIAA, SAE, and ASME, Joint Propulsion Conference, 18th, Cleveland, OH, June 21-23, 1982, AIAA Paper 82-1082*. 10 p. 8 refs. Contract No. NAS2-9261.

The use of tangential blowing from a row of holes in an aft facing step is found to provide good control of the ramp boundary layer, normal shock interaction on a fixed geometry inlet over a wide range of inlet mass flow ratios. Ramp Mach numbers of 1.36 and 1.96 are investigated. The blowing geometry is found to have a significant effect on system performance at the highest Mach number. The use of high-temperature air in the blowing system, however, has only a slight effect on performance. The required blowing rates are significantly high for the most severe test conditions. In addition, the required blowing coefficient is found to be proportional to the normal shock pressure rise. C.R.

A82-37716 * # Aerodynamic performance of high turning core turbine vanes in a two-dimensional cascade. J. R. Schwab (NASA, Lewis Research Center, Cleveland, OH). *AIAA, SAE, and ASME, Joint Propulsion Conference, 18th, Cleveland, OH, June 21-23, 1982, AIAA Paper 82-1288*. 19 p. 6 refs.

ORIGINAL PAGE IS
OF POOR QUALITY

Experimental and theoretical aerodynamic performance data are presented for four uncooled high turning core turbine vanes with exit angles of 74.9, 75.0, 77.5, and 79.6 degrees in a two-dimensional cascade. Data for a more conservative 67.0 degree vane are included for comparison. Correction of the experimental aerodynamic kinetic energy losses to a common 0.100 centimeter trailing edge thickness yields a linear trend of increased loss from 0.020 to 0.025 as the vane exit angle increases from 67.0 to 79.6 degrees. The theoretical losses show a similar trend. The experimental and theoretical vane surface velocity distributions generally agree within approximately five percent, although the suction surface theoretical velocities are generally higher than the experimental velocities as the vane exit angle increases. (Author)

A82-37937 * # Three-dimensional shock structure in a transonic flutter cascade. D. R. Boldman, A. E. Buggele, and A. J. Decker (NASA, Lewis Research Center, Cleveland, OH). *AIAA Journal*, vol. 20, Aug. 1982, p. 1146-1148. 5 refs.

Rapid double-pulse holography was employed to obtain detailed, two-dimensional images of the shock forming during simulated flutter in a transonic flowfield. The experiment comprised a linear cascade of airfoils externally oscillated in torsion and viewed tangentially at the shock surface. Three biconvex airfoils were subjected to harmonic pitching motion about the midchord axis at a frequency of 0.53 while immersed in a Mach 0.81 flow. Failure to produce observable shocks led to use of choked flow with a Mach number near one, of which 50 holograms were taken. The images revealed a narrow shock surface with a spanwise variation in the shock properties. The method is concluded to be useful for examining transonic flowfield shocks in the presence of airfoil flutter. M.S.K.

A82-40921 * # A summary of V/STOL inlet analysis methods. D. P. Hwang and J. M. Abbott (NASA, Lewis Research Center, Cleveland, OH). In: International Council of the Aeronautical Sciences, Congress, 13th and AIAA Aircraft Systems and Technology Conference, Seattle, WA, August 22-27, 1982, Proceedings, Volume 1. (A82-40876 20-01) New York, American Institute of Aeronautics and Astronautics, 1982, p. 402-409. 24 refs.

The methods used to analyze the aerodynamic performance of V/STOL inlets at the NASA Lewis Research Center are briefly described. Recent extensions and applications of the method are emphasized. They include the specification of the Kutta condition for a slotted inlet, the calculation of suction and tangential blowing for boundary layer control, and the analysis of auxiliary inlet geometries. A comparison is made with experiment for the slotted inlet and also for tangential blowing. Finally, an optimum inlet diffuser velocity distribution is developed. (Author)

N82-11041* # Flow Research, Inc., Kent, Wash. CALCULATIONS OF TRANSONIC POTENTIAL FLOW OVER CASCADES Final Report
Wen-Huei Jou Oct. 1981 36 p refs
(Contract NAS3-22129)
(NASA-CR-165471; FRR-182) Avail: NTIS HC A03/MF A01 CSCL 01A

Transonic flow through a cascade was studied by using the full potential equation and the finite volume method of Jameson and Caughey. The C-type computational grid is generated by an electrostatic analogy and simple shearing transformation. The solution algorithm includes an option of using either an artificial density or an artificial viscosity formulation of the dissipative term. Using the developed code, flows through a cascade of NACA 0012 airfoils and flows through a cascade of shockless blades were computed. It is found that the designed flow through the shockless blade is accurately predicted, the artificial density formulation shows more tolerance to the mesh irregularity, and the C-type mesh does not extend very far upstream for a small pitch-cord ratio. T.M.

N82-16044* # Universities Space Research Association, Columbia, Md. CAS22 - FORTRAN PROGRAM FOR FAST DESIGN AND ANALYSIS OF SHOCK-FREE AIRFOIL CASCADES USING FICTITIOUS-GAS CONCEPT Final Report
Djordje S. Dulikravich and Helmut Sobieczky (DFVLR-Inst. fuer Theoretische Stromungsmechanik, Goettingen, West Germany) Washington NASA Jan. 1982 59 p refs
(Contract NAS3-22532)
(NASA-CR-3507) Avail: NTIS HC A04/MF A01 CSCL 01A

A user-oriented computer program, CAS22, was developed that is applicable to aerodynamic analysis and transonic shock-free redesign of existing two-dimensional cascades of airfoils. This FORTRAN program can be used: (1) as an analysis code for full-potential, transonic, shocked or shock-free cascade flows;

(2) as a design code for shock-free cascades that uses Sobieczky's fictitious-gas concept; and (3) as a shock-free design code followed automatically by the analysis in order to confirm that the newly obtained cascade shape provides for an entirely shock-free transonic flow field. A four-level boundary-conforming grid of an O type is generated. The shock-free design is performed by implementing Sobieczky's fictitious-gas concept of elliptic continuation from subsonic into supersonic flow domains. Recomputation inside each supersonic zone is performed by the method of characteristics in the thograph plane by using isentropic gas relations. Besides converting existing cascade shapes with multiple shocked supersonic regions into shock-free cascades, CAS22 can also unchoke previously choked cascades and make them shock free. A.R.H.

N82-17122* # McDonnell-Douglas Corp., St. Louis, Mo. TESTS OF A D VENTED THRUST DEFLECTING NOZZLE BEHIND A SIMULATED TURBOFAN ENGINE Final Report
T. L. Watson Washington NASA Jan. 1982 139 p refs
(Contract NAS3-21733)
(NASA-CR-3508; MDC-A6930) Avail: NTIS HC A07/MF A01 CSCL 01A

A D vented thrust deflecting nozzle applicable to subsonic V/STOL aircraft was tested behind a simulated turbofan engine in the vertical thrust stand. Nozzle thrust, fan operating characteristics, nozzle entrance conditions, and static pressures were measured. Nozzle performance was measured for variations in exit area and thrust deflection angle. Six core nozzle configurations, the effect of core exit axial location, mismatched core and fan stream nozzle pressure ratios, and yaw vane presence were evaluated. Core nozzle configuration affected performance at normal and engine cut operating conditions. Highest vectored nozzle performance resulted for a given exit area when core and fan stream pressure were equal. It is concluded that high nozzle performance can be maintained at both normal and engine cut conditions through control of the nozzle entrance Mach number with a variable exit area. E.A.K.

N82-18180* # United Technologies Research Center, East Hartford, Conn. AN EXPERIMENTAL INVESTIGATION OF GAPWISE PERIODICITY AND UNSTEADY AERODYNAMIC RESPONSE IN AN OSCILLATING CASCADE. VOLUME 2: DATA REPORT. PART 1: TEXT AND MODE 1 DATA Final Report
Franklin O. Carta Dec. 1981 411 p refs
(Contract NAS3-22018)
(NASA-CR-165457-Vol-2-Pt-1; R81-914618-28-Vol-2-Pt-1) Avail: NTIS HC A16/MF A01 CSCL 01A

Tests were conducted a linear cascade of airfoils oscillating in pitch to measure the unsteady pressure response on selected blade along the leading edge plane of the cascade, over the chord of the center blade, and on the sidewall in the plane of the leading edge. The tests were conducted for all 96 combinations 2 mean camberline incidence angles 2 pitching amplitudes 3 reduced frequencies and 6 interblade phase angles. The pressure data were reduced to Fourier coefficient form for direct comparison, and were also processed to yield integrated loads and particularly, the aerodynamic damping coefficient. Data obtained during the test program, reproduced from the printout of the data reduction program are compiled. A further description of the contents of this report is found in the text that follows. Author

N82-18184* # Pennsylvania State Univ., University Park. Dept. of Aerospace Engineering. NUMERICAL ANALYSIS AND FORTRAN PROGRAM FOR THE COMPUTATION OF THE TURBULENT WAKES OF TURBOMACHINERY ROTOR BLADES, ISOLATED AIRFOILS AND CASCADE OF AIRFOILS Final Report - Ph.D. Thesis Mar. 1980
C. Hah and B. Lakshminarayana Washington NASA Feb. 1982 171 p refs
(Grant NsG-3012)
(NASA-CR-3509; PSU-TURBO-81-4) Avail: NTIS HC A08/MF A01 CSCL 01A

Turbulent wakes of turbomachinery rotor blades, isolated airfoils, and a cascade of airfoils were investigated both numerically and experimentally. Low subsonic and incompressible wake flows

were examined. A finite difference procedure was employed in the numerical analysis utilizing the continuity, momentum, and turbulence closure equations in the rotating, curvilinear, and nonorthogonal coordinate system. A nonorthogonal curvilinear coordinate system was developed to improve the accuracy and efficiency of the numerical calculation. Three turbulence models were employed to obtain closure of the governing equations. The first model was comprised to transport equations for the turbulent kinetic energy and the rate of energy dissipation, and the second and third models were comprised of equations for the rate of turbulent kinetic energy dissipation and Reynolds stresses, respectively. The second model handles the convection and diffusion terms in the Reynolds stress transport equation collectively, while the third model handles them individually. The numerical results demonstrate that the second and third models provide accurate predictions, but the computer time and memory storage can be considerably saved with the second model. B.W.

N82-19139* Pennsylvania State Univ. University Park Dept of Aerospace Engineering
APPLICATION OF AN AIRFOIL STALL FLUTTER COMPUTER PREDICTION PROGRAM TO A THREE-DIMENSIONAL WING: PREDICTION VERSUS EXPERIMENT M.S. Thesis
Anthony J. Muffoletto Mar. 1982 136 p refs
(Grant Nsg-3304)
(NASA-CR-168588) Avail: NTIS HC A07/MF A01 CSCL 01A

An aerodynamic computer code, capable of predicting unsteady and C sub m values for an airfoil undergoing dynamic stall, is used to predict the amplitudes and frequencies of a wing undergoing torsional stall flutter. The code, developed at United Technologies Research Corporation (UTRC), is an empirical prediction method designed to yield unsteady values of normal force and moment, given the airfoil's static coefficient characteristics and the unsteady aerodynamic values, alpha, A and B. In this experiment, conducted in the PSU 4' x 5' subsonic wind tunnel, the wing's elastic axis, torsional spring constant and initial angle of attack are varied, and the oscillation amplitudes and frequencies of the wing, while undergoing torsional stall flutter, are recorded. These experimental values show only fair comparisons with the predicted responses. Predictions tend to be good at low velocities and rather poor at higher velocities. Author

N82-19178* Hamilton Standard, Windsor Locks, Conn.
EVALUATION OF WIND TUNNEL PERFORMANCE TESTINGS OF AN ADVANCED 45 DEG SWEEP 8-BLADED PROPELLER AT MACH NUMBERS FROM 0.45 TO 0.85 Final Report
C. Rohrbach, F. B. Metzger, D. M. Black, and R. M. Ladden
Washington NASA Mar. 1982 129 p refs
(Contract NAS3-20769)
(NASA-CR-3505) Avail: NTIS HC A07/MF A01 CSCL 01A

The increased emphasis of fuel conservation in the world and the rapid increase in the cost of jet fuel has stimulated a series of studies of both conventional and unconventional propulsion systems for commercial aircraft. The results of these studies indicate that a fuel saving of 15 to 30 percent may be realized by the use of an advanced high-speed turboprop (Prop-Fan) compared to aircraft equipped with high bypass turbofan engines of equivalent technology. The Prop-Fan propulsion system is being investigated as part of the NASA Aircraft Energy Efficient Program. This effort includes the wind tunnel testing of a series of 8 and 10-blade Prop-Fan models incorporate swept blades. Test results indicate efficiency levels near the goal of 80 percent at Mach 0.8 cruise and an altitude of 10.67 km (35,000 ft). Each successive swept model has shown improved efficiency relative to the straight blade model. The fourth model, with 45 deg swept blades reported herein, shows a net efficiency of 78.2 at the design point with a power loading of 301 kW/sq meter and a tip speed of 243.8 m/sec (800 ft/sec). Author

N82-21158* Vought Corp, Dallas, Tex.
V/STOL TANDEM FAN TRANSITION SECTION MODEL TEST
William E. Simpkin Mar. 1982 156 p refs
(Contract NAS3-22155)

(NASA-CR-165587, NAS 1.26:165587;
TR2-53200/2R-53085) Avail: NTIS HC A08/MF A01 CSCL 01A

An approximately 0.25 scale model of the transition section of a tandem fan variable cycle engine nacelle was tested in the NASA Lewis Research Center 10-by-10 foot wind tunnel. Two 12-inch, tip-turbine driven fans were used to simulate a tandem fan engine. Three testing modes simulated a V/STOL tandem fan airplane. Parallel mode has two separate propulsion streams for maximum low speed performance. A front inlet, fan, and downward vectorable nozzle forms one stream. An auxiliary top inlet provides air to the aft fan - supplying the core engine and aft vectorable nozzle. Front nozzle and top inlet closure, and removal of a blocker door separating the two streams configures the tandem fan for series mode operations as a typical aircraft propulsion system. Transition mode operation is formed by intermediate settings of the front nozzle, blocker door, and top inlet. Emphasis was on the total pressure recovery and flow distortion at the aft fan face. A range of fan flow rates were tested at tunnel airspeeds from 0 to 240 knots, and angles-of-attack from -10 to 40 deg for all three modes. In addition to the model variables for the three modes, model variants of the top inlet were tested in the parallel mode only. These lip variables were: aft lip boundary layer bleed holes, and three position turning vane. Also a bellmouth extension of the top inlet side lips was tested in parallel mode. B.W.

N82-22210* Universities Space Research Association, Columbia, Md.
DESIGN OF SUPERCRITICAL CASCADES WITH HIGH SOLIDITY
Jose M. Sanz Feb. 1982 8 p refs
(Contract NAS3-2253)
(NASA-CR-165600; NAS 1.26:165600) Avail: NTIS HC A02/MF A01 CSCL 01A

The method of complex characteristics of Garabedian and Korn was successfully used to design shockless cascades with solidities of up to one. A code was developed using this method and a new hodograph transformation of the flow onto an ellipse. This code allows the design of cascades with solidities of up to two and larger turning angles. The equations of potential flow are solved in a complex hodograph like domain by setting a characteristic initial value problem and integrating along suitable paths. The topology that the new mapping introduces permits a simpler construction of these paths of integration. M.G.

N82-22211* Boeing Commercial Airplane Co., Seattle, Wash.
AERODYNAMIC ANALYSIS OF VTOL INLETS AND DEFINITION OF A SHORT, BLOWING-LIP INLET Final Report
J. Syberg and A. L. Jones Apr. 1982 61 p refs
(Contract NAS3-22369)
(NASA-CR-165617; NAS 1.26:165617; D6-51418) Avail: NTIS HC A04/MF A01 CSCL 01A

The results indicated that, without boundary layer control, either a very long inlet or an inlet with a very high contraction ratio lip will be required to meet the stringent design requirements. It is shown that active boundary layer control is an effective means of preventing separation and that a significant reduction in inlet size can be achieved by removing only a small amount of bleed in the throat region of the inlet. A short, blowing-lip model was designed and fabricated. This model features an adjustable, blowing slot located near the hinge on the windward side of the inlet. T.M.

N82-22214* Thermo Mechanical Systems Co., Canoga Park, Calif.
DEVELOPMENT OF A LOCALLY MASS FLUX CONSERVATIVE COMPUTER CODE FOR CALCULATING 3-D VISCOUS FLOW IN TURBOMACHINES Final Report
Leonard Walitt Apr. 1982 118 p refs
(Contract NAS3-20834; DA Proj. 1L1-52209-AH-76)
(NASA-CR-3539; NAS 1.26:3539; SR-34) Avail: NTIS HC A06/MF A01 CSCL 01A

The VANS successive approximation numerical method was extended to the computation of three dimensional, viscous, transonic flows in turbomachines. A cross-sectional computer code, which conserves mass flux at each point of the cross-sectional surface of computation was developed. In the VANS numerical method, the cross-sectional computation follows a

blade-to-blade calculation. Numerical calculations were made for an axial annular turbine cascade and a transonic, centrifugal impeller with splitter vanes. The subsonic turbine cascade computation was generated in blade-to-blade surface to evaluate the accuracy of the blade-to-blade mode of marching. Calculated blade pressures at the hub, mid, and tip radii of the cascade agreed with corresponding measurements. The transonic impeller computation was conducted to test the newly developed locally mass flux conservative cross-sectional computer code. Both blade-to-blade and cross sectional modes of calculation were implemented for this problem. A triplet point shock structure was computed in the inducer region of the impeller. In addition, time-averaged shroud static pressures generally agreed with measured shroud pressures. It is concluded that the blade-to-blade computation produces a useful engineering flow field in regions of subsonic relative flow; and cross-sectional computation, with a locally mass flux conservative continuity equation, is required to compute the shock waves in regions of supersonic relative flow.

M.G.

N82-24166* Ohio State Univ., Columbus, Dept. of Aeronautical and Astronautical Engineering.

RIME ICE ACCRETION AND ITS EFFECT ON AIRFOIL PERFORMANCE Ph.D. Thesis. Final Report

Michael B. Bragg Mar. 1982 182 p refs

(Grant NAG3-28)

(NASA-CR-165599; NAS 1.26:165599) Avail: NTIS HC A09/MF A01 CSCL 01A

A methodology was developed to predict the growth of rime ice, and the resulting aerodynamic penalty on unprotected, subcritical, airfoil surfaces. The system of equations governing the trajectory of a water droplet in the airfoil flowfield is developed and a numerical solution is obtained to predict the mass flux of super cooled water droplets freezing on impact. A rime ice shape is predicted. The effect of time on the ice growth is modeled by a time-stepping procedure where the flowfield and droplet mass flux are updated periodically through the ice accretion process. Two similarity parameters, the trajectory similarity parameter and accumulation parameter, are found to govern the accretion of rime ice. In addition, an analytical solution is presented for Langmuir's classical modified inertia parameter. The aerodynamic evaluation of the effect of the ice accretion on airfoil performance is determined using an existing airfoil analysis code with empirical corrections. The change in maximum lift coefficient is found from an analysis of the new iced airfoil shape. The drag correction needed due to the severe surface roughness is formulated from existing iced airfoil and rough airfoil data. A small scale wind tunnel test was conducted to determine the change in airfoil performance due to a simulated rime ice shape.

Author

N82-26229* United Technologies Research Center, East Hartford, Conn.

AN EXPERIMENTAL INVESTIGATION OF GAPWISE PERIODICITY AND UNSTEADY AERODYNAMIC RESPONSE IN AN OSCILLATING CASCADE. 1: EXPERIMENTAL AND THEORETICAL RESULTS Final Report

Franklin O. Carta Washington NASA Jun. 1982 103 p refs (Contract NAS3-22018)

(NASA-CR-3513; NAS 1.26:3513; RB1-914618-27) Avail: NTIS HC A06/MF A01 CSCL 01A

Tests were conducted on a linear cascade of airfoils oscillating in pitch to measure the unsteady pressure response on selected blades along the leading edge plane of the cascade, over the chord of the center blade, and on the sidewall in the plane of the leading edge. The pressure data were reduced to Fourier coefficient form for direct comparison, and were also processed to yield integrated loads and, particularly, the aerodynamic damping coefficient. Results from the unsteady Verdon/Casper theory for cascaded blades with nonzero thickness and camber were compared with the experimental measurements. The three primary results are: (1) from the leading edge plane blade data, the cascade was judged to be periodic in unsteady flow over the range of parameters tested; (2) the interblade phase angle was found to be the single most important parameter affecting the stability of the oscillating cascade blades; and (3) the real blade theory and the experiment were in excellent agreement for the several cases chosen for comparison.

A.R.H.

N82-26230* Massachusetts Inst. of Tech., Cambridge Gas Turbine and Plasma Dynamics Lab.

A FORTRAN PROGRAM FOR CALCULATING THREE DIMENSIONAL, INVISCID AND ROTATIONAL FLOWS WITH SHOCK WAVES IN AXIAL COMPRESSOR BLADE ROWS: USER'S MANUAL Final Report

William T. Thompkins, Jr. Washington Jun. 1982 179 p refs

(Grant NsG-3234)

(NASA-CR-3560; NAS 1.26:3560)

Avail: NTIS

HC A09/MF A01 CSCL 01A

A FORTRAN-IV computer program was developed for the calculation of the inviscid transonic/supersonic flow field in a fully three dimensional blade passage of an axial compressor rotor or stator. Rotors may have dampers (part span shrouds). MacCormack's explicit time marching method is used to solve the unsteady Euler equations on a finite difference mesh. This technique captures shocks and smears them over several grid points. Input quantities are blade row geometry, operating conditions and thermodynamic quantities. Output quantities are three velocity components, density and internal energy at each mesh point. Other flow quantities are calculated from these variables. A short graphics package is included with the code, and may be used to display the finite difference grid, blade geometry and static pressure contour plots on blade to blade calculation surfaces or blade suction and pressure surfaces. The flow in a low aspect ratio transonic compressor was analyzed and compared with high response total pressure probe measurements and gas fluorescence static density measurements made in the MIT blowdown wind tunnel. These comparisons show that the computed flow fields accurately model the measured shock wave locations and overall aerodynamic performance.

B.W.

N82-26237* Purdue Univ., Lafayette, Ind. Thermal Sciences and Propulsion Center.

THE DESIGN AND INSTRUMENTATION OF THE PURDUE ANNULAR CASCADE FACILITY WITH INITIAL DATA ACQUISITION AND ANALYSIS

R. Charles Stauter and Sanford Fleeter May 1982 136 p refs

(Grant NsG-3285)

(NASA-CR-167861; NAS 1.26:167861; ME-TSPC-TR-82-11)

Avail: NTIS HC A07/MF A01 CSCL 01A

Three dimensional aerodynamic data, required to validate and/or indicate necessary refinements to inviscid and viscous analyses of the flow through turbomachine blade rows, are discussed. Instrumentation and capabilities for pressure measurement, probe insertion and traversing, and flow visualization are reviewed. Advanced measurement techniques including Laser Doppler Anemometers, are considered. Data processing is reviewed. Predictions were correlated with the experimental data. A flow visualization technique using helium filled soap bubbles was demonstrated.

Author

N82-26239* Universities Space Research Association, Columbia, Md.

GRID3C: COMPUTER PROGRAM FOR GENERATION OF C TYPE MULTILEVEL, THREE DIMENSIONAL AND BOUNDARY CONFORMING PERIODIC GRIDS Final Report

Djordje S. Dulikravich Mar. 1982 26 p refs

(Contract NAS3-22532)

(NASA-CR-167846; NAS 1.26:167846)

Avail: NTIS

HC A03/MF A01 CSCL 01A

A fast computer program, GRID3C, was developed for accurately generating periodic, boundary conforming, three dimensional, consecutively refined computational grids applicable to realistic axial turbomachinery geometries. The method is based on using two functions to generate two dimensional grids on a number of coaxial axisymmetric surfaces positioned between the centerbody and the outer radial boundary. These boundary fitted grids are of the C type and are characterized by quasi-orthogonality and geometric periodicity. The built in nonorthogonal coordinate stretchings and shearings cause the grid clustering in the regions of interest. The stretching parameters are part of the input to GRID3C. In its present version GRID3C can generate and store a maximum of four consecutively refined three dimensional grids. The output grid coordinates can be calculated either in the Cartesian or in the cylindrical coordinate system.

Author

ORIGINAL PAGE IS
OF POOR QUALITY

N82-28253* # Universities Space Research Association, Columbia, Md

FAST GENERATION OF THREE-DIMENSIONAL COMPUTATIONAL BOUNDARY-CONFORMING PERIODIC GRIDS OF C-TYPE Final Report

Djordje S. Dulikravich Jun. 1982 30 p refs Presented at Symp on Numerical Generation of Curvilinear Coordinating Systems and Use in Numerical Solution of Partial Differential Equations, Nashville, 13-16 Apr 1982

(Contract NAS3-22532)

(NASA-CR-165596; NAS 1.26:165596) Avail: NTIS HC A03/MF A01 CSCL 01A

A fast computer program, GRID3C, was developed to generate multilevel three dimensional, C type, periodic, boundary conforming grids for the calculation of realistic turbomachinery and propeller flow fields. The technique is based on two analytic functions that conformally map a cascade of semi-infinite slits to a cascade of doubly infinite strips on different Riemann sheets. Up to four consecutively refined three dimensional grids are automatically generated and permanently stored on four different computer tapes. Grid nonorthogonality is introduced by a separate coordinate shearing and stretching performed in each of three coordinate directions. The grids are easily clustered closer to the blade surface, the trailing and leading edges and the hub or shroud regions by changing appropriate input parameters. Hub and duct (or outer free boundary) have different axisymmetric shapes. A vortex sheet of arbitrary thickness emanating smoothly from the blade trailing edge is generated automatically by GRID3C. Blade cross sectional shape, chord length, twist angle, sweep angle, and dihedral angle can vary in an arbitrary smooth fashion in the spanwise direction S.L.

N82-29269* # Purdue Univ., Lafayette, Ind. School of Mechanical Engineering

CALCULATION OF THE FLOW FIELD INCLUDING BOUNDARY LAYER EFFECTS FOR SUPERSONIC MIXED COMPRESSION INLETS AT ANGLES OF ATTACK

Joseph Vadyak and Joe D. Hoffman Jul. 1982 406 p refs (Grant Nsg-3311)

(NASA-CR-167941; NAS 1.26:167941) Avail: NTIS HC A18/MF A01 CSCL 01A

The flow field in supersonic mixed compression aircraft inlets at angles of attack is calculated. A zonal modeling technique is employed to obtain the solution which divides the flow field into different computational regions. The computational regions consist of a supersonic core flow, boundary layer flows adjacent to both the forebody/centerbody and cowl contours, and flow in the shock wave boundary layer interaction regions. The zonal modeling analysis is described and some computational results are presented. The governing equations for the supersonic core flow form a hyperbolic system of partial differential equations. The equations for the characteristic surfaces and the compatibility equations applicable along these surfaces are derived. The characteristic surfaces are the stream surfaces, which are surfaces composed of streamlines, and the wave surfaces, which are surfaces tangent to a Mach conoid. The compatibility equations are expressed as directional derivatives along streamlines and bicharacteristics, which are the lines of tangency between a wave surface and a Mach conoid. S.L.

N82-32310* # Cincinnati Univ., Ohio. Dept. of Aerospace Engineering and Applied Mechanics.

THREE DIMENSIONAL FLOW MEASUREMENTS IN A TURBINE SCROLL

W. Tabakoff, B. V. R. Vittal, and B. Wood Jul. 1982 55 p refs (Grant NAG3-26)

(NASA-CR-167920; NAS 1.26:167920) Avail: NTIS HC A04/MF A01 CSCL 01A

A study was conducted to determine experimentally the flow behavior in combined scroll nozzle assembly of a radial inflow turbine. Hot film anemometry technique was used to measure the three dimensional flow velocity in the scroll. The through flow and secondary flow velocity components are measured at various points in three scroll sections. Author

N82-33347* # Cessna Aircraft Co., Vandalia, Ohio. Accessory Div.

IMPACT OF ADVANCED PROPELLER TECHNOLOGY ON AIRCRAFT/MISSION CHARACTERISTICS OF SEVERAL GENERAL AVIATION AIRCRAFT Final Report

Ira D. Keiter Sep. 1982 82 p refs

(Contract NAS3-21719)

(NASA-CR-167984; NAS 1.26:167984)

Avail: NTIS

HC A05/MF A01 CSCL 01A

Studies of several General Aviation aircraft indicated that the application of advanced technologies to General Aviation propellers can reduce fuel consumption in future aircraft by a significant amount. Propeller blade weight reductions achieved through the use of composites, propeller efficiency and noise improvements achieved through the use of advanced concepts and improved propeller analytical design methods result in aircraft with lower operating cost, acquisition cost and gross weight. Author

A82-15459* The three-dimensional boundary layer on a rotating helical blade, P. J. Morris (Pennsylvania State University, University Park, PA), *Journal of Fluid Mechanics*, vol. 112, Nov. 1981, p. 283-296, 8 refs. Grant No. Nsg-3265.

The laminar boundary layer on a twisted helical blade is considered. The blade geometry is the same as that proposed by Horlock and Wordsworth (1965). However, the blade is twisted about the leading edge in the manner described by Miyake and Fujita (1974). The flow may be considered to be the analog, in a rotating reference frame, of the flat-plate boundary layer in a stationary frame. It is shown that a coordinate system which is orthogonal in the blade surface may be developed. With the appropriate scaling of the dependent variables a solution for the boundary layer flow is readily obtained. The systems of ordinary differential equations for the stream function of the primary flow and the cross-flow are solved numerically. G.R.

A82-17759* # A finite element formulation of Euler equations for the solution of steady transonic flows. A. Ecer and H. U. Akay (Purdue University, Indianapolis, IN), *American Institute of Aeronautics and Astronautics, Aerospace Sciences Meeting, 20th, Orlando, FL, Jan. 11-14, 1982, Paper 82-0062*, 11 p, 14 refs. Grant No. Nsg-3294.

The main objective of the considered investigation is related to the development of a relaxation scheme for the analysis of inviscid, rotational, transonic flow problems. To formulate the equations of motion for inviscid flows in a fixed coordinate system, an Eulerian type variational principle is required. The derivation of an Eulerian variational principle which is employed in the finite element formulation is discussed. The presented numerical method describes the mathematical formulation and the application of a numerical process for the direct solution of steady Euler equations. The development of the procedure as an extension of existing potential flow formulations provides the applicability of previous procedures, e.g., proper application of the artificial viscosity for supersonic elements, and the accurate modeling of the shock. G.R.

A82-17933* # Characteristics of the flow in the annulus-wall region of an axial-flow compressor rotor blade passage. R. M. Davino (Pennsylvania State University, University Park, PA), *American Institute of Aeronautics and Astronautics Aerospace Sciences Meeting, 20th, Orlando, FL, Jan. 11-14, 1982, Paper 82-0413*, 20 p, 32 refs. Grant No. Nsg-3212.

Three-dimensional characteristics of the mean velocity and turbulence structure in the annulus-wall region of a moderately loaded compressor rotor have been investigated experimentally by employing triaxial hot-wire probes. Results are presented which indicate that the flow within and downstream of the rotor passage is highly complex due to the interaction of the annulus-wall boundary layer, blade boundary layers, tip leakage flow, and passage secondary flow. An understanding of the reported viscous flow interactions is important for establishing improved aerodynamic design criteria and efficiency, for predicting noise levels, and for determining the stall, surge, vibration, and flutter characteristics of turbomachinery.

(Author)

A82-19331 * # Interaction of compressor rotor blade wake with wall boundary layer/vortex in the end-wall region. B. Lakshminarayana and A. Ravindranath (Pennsylvania State University, University Park, PA). *American Society of Mechanical Engineers, International Symposium on Applications of Fluids Mechanics and Heat Transfer to Energy and Environmental Problems, University of Patras, Patras, Greece, June 29-July 3, 1981, Paper 81-Gr/GT-1*. 12 p. 11 refs. Members, \$2.00; nonmembers, \$4.00. Grant No. NSG-3012.

This paper reports the experimental study of the three-dimensional characteristics of the mean velocity of the rotor wake inside the annulus- and hub-wall boundary layers. The measurements were taken with a rotating three-sensor hot wire behind the rotor. This set of measurements probably represents the first set of comprehensive measurements taken inside the annulus- and hub-wall boundary layers. The wake was surveyed at several radial locations inside the boundary layer region and at several axial locations. Interaction of the wake with the annulus-wall boundary layer, secondary flow, tip-leakage flow, and the trailing vortex system results in slower decay and larger width of the wake. The presence of a strong vortex and its merger with the wake is also observed. The end-wall boundary layers and the secondary flow were found to have a substantial effect on both the decay characteristics and the profile of the wake. These and other measurements are reported and interpreted in this paper. (Author)

A82-22063 * # Effects of blade loading and rotation on compressor rotor wake in end wall regions. B. Lakshminarayana, T. R. Govindan, and B. Reynolds (Pennsylvania State University, University Park, PA). *American Institute of Aeronautics and Astronautics, Aerospace Sciences Meeting, 20th, Orlando, FL, Jan. 11-14, 1982, Paper 82-0193*. 11 p. 9 refs. Grant No. NSG-3012.

This study was carried out to understand the effects of blade loading and rotation on the rotor end wall flow structure, including the wake. The measurements were taken with a stationary three sensor hot wire located at the exit of a compressor rotor. The signal was ensemble averaged to derive all the three components of velocity and six components of stresses at the exit. Measurements were made at two different rotational speeds (1753 and 1010 rpm) and at two differing blade loadings at several radii near the hub and the annulus wall. The wake decay in the annulus wall region is found to be much more rapid than the mid span regions. Furthermore, both the loading and rotation of the blade have appreciable influence on the end wall flow and wake structure. Interaction of the annulus and hub wall boundary layers (and secondary flow resulting from these) have appreciable influence on the wake structure in the endwall regions. (Author)

A82-22081 * # Aerodynamic characteristics of airfoils with ice accretions. M. B. Bragg and G. M. Gregorek (Ohio State University, Columbus, OH). *American Institute of Aeronautics and Astronautics, Aerospace Sciences Meeting, 20th, Orlando, FL, Jan. 11-14, 1982, Paper 82-0282*. 15 p. 19 refs. Grant No. NAG3-28.

Results of a wind tunnel test to evaluate the performance of an airfoil with simulated rime ice are presented with theoretical comparisons. A NACA 65A413 airfoil was tested in the OSU 6 x 22 inch Transonic Airfoil Wind Tunnel at a Reynolds number near three million and Mach numbers from 0.20 to 0.80. The model was tested in four configurations to determine the aero-dynamic effects of the roughness and shape of a rime ice accretion. The simulated rime ice shape was obtained analytically using a time-stepping dry ice accretion computer code. Lift, drag, moment coefficients, and pressure distributions for the clean and simulated rime ice cases are reported. The measured degradation in airfoil performance is compared to an analytical method which uses existing airfoil analysis computer codes with empirical corrections for the surface roughness. A discussion of the empirical surface roughness correction and uses of other airfoil computer methods is included. (Author)

A82-26137 * Measurement and prediction of mean velocity and turbulence structure in the near wake of an airfoil. C. Hah and B. Lakshminarayana (Pennsylvania State University, University Park, PA). *Journal of Fluid Mechanics*, vol. 115, Feb. 1982, p. 251-282. 18

refs. Grant No. NSG-3012.

An experimental investigation of the near wake of a thin airfoil at various incidence angles is reported in this paper. The airfoil (NACA 0012 basic thickness form) was located in a wind tunnel, and the wake structure was measured using hot-wire sensors. The measurements of mean-velocity, turbulence intensity and Reynolds-stress components across the wake at several distances downstream show the complex nature of the near wake and its asymmetrical behavior. The asymmetry in the wake property, which is maintained up to a length of 1.5 chords downstream of the trailing edge of the blade, is dependent on the incidence angle of the inlet flow. The streamwise velocity defect in an asymmetric wake decays more slowly compared to that of a symmetric wake. The streamline curvature due to the blade loading has a substantial effect on the mean velocity profile as well as the turbulence structure. The numerical study of the same wake indicates that the existing turbulence closure models need some modification to account for the asymmetric characteristics of the wake. (Author)

A82-29003 * # Multigrid simulation of asymptotic curved-duct flows using a semi-implicit numerical technique. K. N. Ghia, U. Ghia, C. T. Shin, and D. R. Reddy (Cincinnati, University, Cincinnati, OH). In: *Computers in flow predictions and fluid dynamics experiments: Proceedings of the Winter Annual Meeting, Washington, DC, November 15-20, 1981, (A82-29001 13-02)* New York, American Society of Mechanical Engineers, 1981, p. 11-25. 19 refs. Grants No. AF-AFOSR-80-0160; No. NSG-3267.

Asymptotic flows inside curved ducts of rectangular as well as polar cross section are analyzed using the Navier-Stokes equations in terms of the axial velocity and vorticity and the cross-flow stream function. Numerical solutions of the three second-order coupled elliptic partial differential equations governing this flow are obtained efficiently using the coupled alternating-direction implicit (ADI) method as well as the multigrid strongly-implicit (SI) scheme. For the flow configuration studied, the ADI method is found to be more sensitive to the time steps used than is the SI scheme. Use of the multigrid-coupled-strongly-implicit (MG-SI) scheme makes it possible to efficiently obtain fine-grid solutions for configurations having strong secondary flow. It is shown that, for this asymptotic curved-duct flow, the similarity parameter of significance is the Dean's number K rather than the Reynolds number Re . Results are obtained for curved ducts with square cross sections for K up to 900, which here corresponds to $Re = 9,000$ for this internal flow configuration. C.R.

A82-31933 * # Finite volume calculation of three-dimensional potential flow around a propeller. W.-H. Jou (Flow Industries, Inc., Kent, WA). *American Institute of Aeronautics and Astronautics and American Society of Mechanical Engineers, Joint Thermophysics, Fluids, Plasma and Heat Transfer Conference, 3rd, St. Louis, MO, June 7-11, 1982, AIAA Paper 82-0957*. 7 p. 10 refs. Contract No. NAS3-22148.

The finite volume scheme of Jameson (1977) is used to calculate potential flow around a propeller rotating at high speed. An H-type mesh is generated and used successfully in the calculations. A test calculation with a thick blade cross section shows that the present code is capable of computing the propeller flow at the advance Mach number 0.8. The possible physical mechanisms which may play an important role in the propeller aerodynamics are discussed. V.L.

A82-31939 * # Application of a finite element algorithm for the solution of steady transonic Euler equations. H. U. Akay and A. Ecer (Purdue University, Indianapolis, IN). *American Institute of Aeronautics and Astronautics and American Society of Mechanical Engineers, Joint Thermophysics, Fluids, Plasma and Heat Transfer Conference, 3rd, St. Louis, MO, June 7-11, 1982, AIAA Paper 82-0970*. 10 p. 12 refs. Grant No. NSG-3294.

A finite element algorithm for the solution of two-dimensional, steady Euler equations is presented which, through a Clebsch-type transformation for the velocity vector, solves the conservation of mass equation with one primary variable and two additional equations for the convection of two new variables. The accuracy and efficiency of this scheme is discussed, and the second-order accuracy

attained in the analysis of the convection of the vorticity is demonstrated together with the efficient treatment of rotational and irrotational flow subregions. A sample problem is used to show the accuracy of the numerical scheme and its convergence characteristics. O.C.

A82-31947 * # Modeling parameter influences on MHD swirl combustion nozzle design. D. G. Lilley (Oklahoma State University, Stillwater, OK), A. K. Gupta (MIT, Cambridge, MA), and A. A. Busnaina, *American Institute of Aeronautics and Astronautics and American Society of Mechanical Engineers, Joint Thermophysics, Fluids, Plasma and Heat Transfer Conference, 3rd, St. Louis, MO, June 7-11, 1982, AIAA Paper 82-0984*. 10 p. 12 refs. Contract No. DE-OC01-79ET-15518; Grant No. NAG3-74.

Attention is given to a research project which has the goal to develop a two-stage slugging gasifier-combustor in the form of a high-intensity combustor, taking into account a suitable aerodynamic design of the second stage nozzle which will prevent the separation of the boundary layer as the flow turns from axial to radial direction. The specific objectives of the present investigation are to test the effect of various second-stage nozzle geometries, flow rates, swirl number, and distribution in the first and second stages upon the corresponding flowfield in the second stage. Special emphasis is given to the avoidance of boundary layer separation as the flow turns from axial to radial direction into the MHD disk generator. G.R.

A82-31964 * # Three dimensional flow field inside the passage of a low speed axial flow compressor rotor. M. Pouagare, K. N. S. Murthy, and B. Lakshminarayana (Pennsylvania State University, University Park, PA), *American Institute of Aeronautics and Astronautics and American Society of Mechanical Engineers, Joint Thermophysics, Fluids, Plasma and Heat Transfer Conference, 3rd, St. Louis, MO, June 7-11, 1982, AIAA Paper 82-1006*. 13 p. 13 refs. Grant No. NSG-3266.

Measurements of the subsonic flow in the rotor passage of a single stage axial flow compressor were made to study the nature of the flow field and to verify the existing numerical codes. The velocity and pressure fields were measured across the entire rotor passage at six axial locations and at five radial locations. A five-hole probe, rotating with the rotor, was used to measure the three components of velocity, the static and the total pressure. The experimental results are compared with the predictions from Katsanis and McNally's computer program. The agreement between the two is good for most of the cases. (Author)

A82-31965 * # Three dimensional turbulent boundary layer development on a fan rotor blade. B. Lakshminarayana, C. Hah, and T. R. Govindan (Pennsylvania State University, University Park, PA), *American Institute of Aeronautics and Astronautics and American Society of Mechanical Engineers, Joint Thermophysics, Fluids, Plasma and Heat Transfer Conference, 3rd, St. Louis, MO, June 7-11, 1982, AIAA Paper 82-1007*. 10 p. 12 refs. Grant No. NSG-3266.

This paper is concerned with an experimental study undertaken to measure the boundary layer growth on a fan rotor blade. The measurements were carried out using a miniature 'X' configuration hot wire probe at various chordwise and radial locations on both surfaces of the blade. The streamwise and radial velocity profiles as well as the corresponding intensity components are interpreted and correlated. The validity of conventional velocity profiles such as the 'law of the wall' for the streamwise profile and the hodograph plot for the cross flow profile are examined. The measured values of boundary-layer gross properties are compared with the predictions based on a momentum-integral technique. (Author)

A82-35280 * # Three-dimensional flow field in the tip region of a compressor rotor passage. I - Mean velocity profiles and annulus wall boundary layer. B. Lakshminarayana, M. Pouagare (Pennsylvania State University, University Park, PA), and R. Davino (General Electric Co., Aircraft Engine Group, Evendale, OH), *American Society of Mechanical Engineers, International Gas Turbine Conference and Exhibit, 27th, London, England, Apr. 18-22, 1982, Paper 82-GT-11*. 12 p. 15 refs. Members, \$2.00; nonmembers, \$4.00. Grant No. NSG-3212.

A rotating three-sensor, hot-wire probe has been used along with rotor blade

static pressure measurements to investigate the complex inviscid and viscous effects in the annulus wall flowfield, including the three components of mean velocity, turbulence intensity, and turbulence stress inside the rotor blade passage. It is found that the tip leakage flow originates near quarter-chord, with peak values occurring near mid-chord. The leakage flow, which is in the form of a jet within the blade row, is augmented by the blade rotation and travels further away from the suction surface than that observed in stationary blade rows and cascades. This leakage flow tends to roll up between the mid-passage and the pressure surface near the tip region; the vortex formation does not occur within the passage in this particular case. V.L.

A82-35281 * # Investigation of the tip-clearance flow inside and at the exit of a compressor rotor passage. I - Mean velocity field. A. Pandya and B. Lakshminarayana (Pennsylvania State University, University Park, PA), *American Society of Mechanical Engineers, International Gas Turbine Conference and Exhibit, 27th, London, England, Apr. 18-22, 1982, Paper 82-GT-12*. 12 p. 14 refs. Members, \$2.00; nonmembers, \$4.00. Grant No. NSG-3212.

A stationary two-sensor hot-wire probe has been used in combination with an ensemble averaging technique to measure the flow in the tip clearance region of a compressor rotor with emphasis on the leakage flow development inside the tip-clearance region and at the exit of the rotor. It is found that the presence and interaction of leakage flow, annulus boundary layer, and the scraping vortex is the dominant feature at mid-chord position. The rotation of the blade augments the leakage flow, resulting in the movement of the leakage jet toward the mid-passage. The blade-to-blade distribution of properties is shown to be highly nonuniform, except in the downstream and upstream regions. V.L.

A82-35379 * # Flow distributions and discharge coefficient effects for jet array impingement with initial crossflow. L. W. Florschütz and Y. Isoda (Arizona State University, Tempe, AZ), *American Society of Mechanical Engineers, International Gas Turbine Conference and Exhibit, 27th, London, England, Apr. 18-22, 1982, Paper 82-GT-156*. 10 p. 11 refs. Members, \$2.00; nonmembers, \$4.00. Grant No. NSG-3075.

To model the impingement cooled mid-chord region of gas turbine airfoils in cases where an initial crossflow is present, the paper presents experimentally determined flow distributions for jet arrays with ten spanwise rows of holes, which range from uniform to highly nonuniform. The jet flow after impingement is constrained to exit in a single direction along the channel formed by the jet orifice plate and the impingement surface. The streamwise distributions and crossflow velocities are presented for ratios of the initial crossflow rate to the total jet flow rate ranging from zero to unity. For crossflow to jet velocity ratios greater than a value somewhat less than unity, jet orifice discharge coefficients do not remain constant, but decrease significantly, showing a secondary dependence on z/d , where z is the channel height and d is the jet hole diameter. D.L.G.

A82-35416 * # Three-dimensional flow field in the tip region of a compressor rotor passage. II - Turbulence properties. B. Lakshminarayana, M. Pouagare (Pennsylvania State University, University Park, PA), and R. Davino (General Electric Co., Aircraft Engine Group, Evendale, OH), *American Society of Mechanical Engineers, International Gas Turbine Conference and Exhibit, 27th, London, England, Apr. 18-22, 1982, Paper 82-GT-234*. 10 p. 9 refs. Members, \$2.00; nonmembers, \$4.00. Grant No. NSG-3212.

The turbulence properties in the annulus wall region of an axial flow compressor rotor was measured using a triaxial, hot-wire probe rotating with the rotor. The flow was surveyed across the entire passage at five axial locations (leading edge, 1/4 chord, 1/2 chord, 3/4 chord, and the trailing edge location) and at six radial locations in a low-speed compressor rotor. The data derived include all three components of turbulence intensity and three components of turbulence stress. A comprehensive interpretation of the data with emphasis on features related to rotation, leakage flow, annulus wall boundary layer, and blade boundary layer interactions is included. All the components of turbulent intensities and stresses are found to be high in the leakage-flow mixing region. The radial component of intensities and stresses is found to be much higher than the corresponding streamwise components. The turbulent spectra clearly reveal the decay process of the inlet-guide-vane wake within the rotor passage. (Author)

A82-35427 * # A study of viscous flow in stator and rotor passages. Y. Sheoran and W. Tabakoff (Cincinnati, University, Cincinnati, OH), *American Society of Mechanical Engineers, International Gas Turbine Conference and Exhibit, 27th, London, England, Apr. 18-22, 1982, Paper 82-GT-248*. 17 p. 21 refs. Members, \$2.00; nonmembers, \$4.00. Army-sponsored research; Contract No. NAS3-21609.

A numerical technique to predict the viscous behavior in the three-dimensional domain of rotating and stationary blade passages is presented. The analysis is based upon the numerical integration of the incompressible Navier-Stokes equations. An approach is taken to combine the three momentum equations and the continuity equation into two sets of vorticity transport-stream function equations.

These equations are expressed along families of arbitrarily defined orthogonally intersecting surfaces placed within the blade passage. Unlike the stream surfaces, the arbitrary surfaces allow fluid to flow across. The numerical code employs a nonorthogonal body fitted coordinate system on each of the intersecting surfaces. The solution process involves the iterative combination of the solutions on the two families of intersecting surfaces for a complete solution. The results of flow in thin blade stationary and rotating polar ducts is presented.

(Author)

A82-35459 * # Aerodynamic damping measurements in a transonic compressor. E. F. Crawley (MIT, Cambridge, MA). *American Society of Mechanical Engineers, International Gas Turbine Conference and Exhibit, 27th, London, England, Apr. 18-22, 1982, Paper 82-GT-287*. 12 p. 15 refs. Members, \$2.00; nonmembers, \$4.00. Grant No. NsG-3079.

A method has been developed and demonstrated for the direct measurement of aerodynamic damping in a transonic compressor. The method is based on the inverse solution of the structural dynamic equations of motion of the blade-disk system. The equations are solved inversely to determine the forces acting on the system. If the structural dynamic equations are transformed to multiblade or modal coordinates, the damping can be measured for blade-disk modes, and related to a reduced frequency and interblade phase angle. This method of damping determination was demonstrated using a specially instrumented version of the MIT Transonic Compressor run in the MIT Blowdown Compressor Test Facility. No regions of aeroelastic instability were found. In runs at the operating point, the rotor was aerodynamically excited by a controlled two-per-revolution fixed up-stream disturbance. The disturbance was sharply terminated midway through the test. Analysis of the data in terms of multiblade modes led to a direct measurement of aerodynamic damping for three interblade phase angles.

(Author)

A82-35460 * # In-plane inertial coupling in tuned and severely mistuned bladed disks. E. F. Crawley (MIT, Cambridge, MA). *American Society of Mechanical Engineers, International Gas Turbine Conference and Exhibit, 27th, London, England, Apr. 18-22, 1982, Paper 82-GT-288*. 3 p. 8 refs. Members, \$2.00; nonmembers, \$4.00. Grant No. NsG-3079.

A model has been developed and verified for blade-disk-shaft coupling in rotors due to the in-plane rigid body modes of the disk. An analytic model has been developed which couples the in-plane rigid body modes of the disk on an elastic shaft with the blade bending modes. Bench resonance test were carried out on the MIT Compressor Rotor, typical of research rotors with flexible blades and a thick rigid disk. When the rotor was carefully tuned, the structural coupling of the blades by the disks was confined to zero and one nodal diameter modes, whose modal frequencies were greater than the blade antinodal frequency. In the case of the tuned rotor, and in two cases where severe mistuning was intentionally introduced, agreement between the predicted and observed natural frequencies is excellent. The analytic model was then extended to include the effects of constant angular rotation of the disk.

(Author)

A82-35571 * # Rapid approximate determination of nonlinear solutions - Application to aerodynamic flows and design/optimization problems. S. S. Stahara (Nielson Engineering and Research, Inc., Mountain View, CA). In: *Transonic aerodynamics, Transonic Perspective Symposium, Moffett Field, CA, February 18-20, 1981, Technical Papers. (A82-35553 17-02)* New York, American Institute of Aeronautics and Astronautics, 1982, p. 637-661. 16 refs. Contract No. NAS3-20836.

Stahara et al. (1978) have considered the use of an approximation technique which employs two or more nonlinear base solutions determined by the full computational method to predict entire families of related nonlinear solutions. The present investigation provides results for several applications of that method which demonstrate both its accuracy and its utility for engineering applications. Attention is given to the perturbation concept and methods, aspects of coordinate straining, aspects of analytical formulation, and an application to surface properties. In a discussion of the results, single and multiple parameter perturbations are considered along with a combination of the approximation method with optimization procedures. The results show that it is possible to combine in certain cases large savings in computational cost with improved optimization.

G.R.

A82-37711 * # Investigation of rotational transonic flows through ducts using a finite element scheme. H. U. Akay and A. Ecer (Purdue University, Indianapolis, IN). *AIAA, SAE, and ASME, Joint Propulsion Conference, 18th, Cleveland, OH, June 21-23, 1982, AIAA Paper 82-1267*. 8 p. 5 refs. Grant No. NsG-3294.

An application of the finite element method is presented in order to study the flow through a two-dimensional channel including the choked and nearly-choked flow conditions. The mathematical procedure provides a combined treatment of potential and Euler equations, where the steady Euler equations are solved through the integration of a pseudo-time system which is equivalent to a relaxa-

tion scheme; the isentropic, potential flow equations are embedded in this formulation. To analyze the transonic flow through a channel with near-choked flow conditions, the flow through a parallel channel with a 10 percent circular arc bump is calculated as a sample problem.

C.R.

A82-37535 * Two dimensional stagnation point flow of a dusty gas near an oscillating plate. J. Fernandez de la Mora (Yale University, New Haven, CT). *Acta Mechanica*, vol. 43, no. 3-4, 1982, p. 261-265. 11 refs. Grant No. NsG-3107.

Necessary improvements to a paper on the flow of a dusty gas by Datta and Mishra (1980) are presented. Particular attention is given to the importance of particle phase compressibility and the hyperbolic nature of the particle momentum conservation equation which prohibits downstream (wall) boundary conditions for the solid phase. Fundamental differences between particulate and ordinary flow boundary layers are discussed, and the correct conservation equations are written.

C.R.

A82-37938 * # 'Coriolis resonance' within a rotating duct. M. Kurosaka and J. E. Caruthers (Tennessee, University, Tullahoma, TN). *AIAA Journal*, vol. 20, Aug. 1982, p. 1148-1150. Grant No. NAG3-86.

An investigation of the unsteady disturbances of a fixed frequency within a radial duct rotating at a set speed is presented. The flow is assumed to be compressible, inviscid, and of a fluid which is a perfect gas. Equations are developed for the steady and the unsteady parts of the flow in cylindrical coordinates. The unsteady disturbances are expressed by Fourier decomposition in angular position, distance into the duct, and in time. It is found that a resonance is possible when the frequency of flow disturbances is twice the shaft-rotation frequency, considering only the radial and tangential disturbances and not the radial and circumferential disturbances. The particular point at which the resonance occurs indicates the occurrence is due to the Coriolis force, which is only present in the radial and tangential directions. It is noted that the Coriolis force can only be present in open-ended ducts, such as those found in centrifugal compressors.

M.S.K.

A82-41267 * Solution of the unsteady subsonic thin airfoil problem. M. H. Williams (Purdue University, West Lafayette, IN). *Quarterly Journal of Mechanics and Applied Mathematics*, vol. 35, Aug. 1982, p. 367-390. 16 refs. Grant No. NsG-3292.

The problem of a thin airfoil subject to simple harmonic disturbances in a uniform subsonic free stream is solved by extension of a technique developed earlier for a stationary strip vibrating in a uniform fluid. Explicit expressions are given for the lift and moment, acoustic directivity pattern, and total acoustic power for arbitrary upwash and, in particular, for the 'elementary disturbances': plunge, pitch and a stationary transverse gust. Numerical results for a simple skewed gust are presented and compared to the high-frequency asymptotic theory of Martinez and Widnall.

(Author)

ORIGINAL PAGE IS
OF POOR QUALITY

03 AIR TRANSPORTATION AND SAFETY

Includes passenger and cargo air transport operations; and aircraft accidents.

For related information see also 16 Space Transportation and 85 Urban Technology and Transportation.

hazard evaluation for each of the three fuels under four crash scenarios a comprehensive review and analysis and an identification of areas further development work. The conclusion was that the crash fire hazards are not significantly different when compared in general for the three fuels, although some fuels showed minor advantages in one respect or another. R.J.F.

N82-21148* National Aeronautics and Space Administration, Lewis Research Center, Cleveland, Ohio

NASA/LEWIS RESEARCH CENTER ICING RESEARCH PROGRAM

Peggy L. Evanich In NASA Marshall Space Flight Center Proc. 5th Ann Workshop on Meteorol. and Environ. Inputs to Aviation Systems Dec. 1981 p 64-75 (For primary document see N82-21139 12-01)

Avail: NTIS HC A07/MF A01 CSCL 01C

ORIGINAL PAGE IS
OF POOR QUALITY

N82-30297* National Aeronautics and Space Administration, Lewis Research Center, Cleveland, Ohio

AIRCRAFT ICING RESEARCH AT NASA

J. J. Reinmann, R. J. Shaw, and W. A. Olsen, Jr. 1982 17 p refs Presented at the 1st Intern. Workshop on Atmospheric Icing of Struct., Hanover, N.H., 1-3 Jun. 1982

(NASA-TM-82919; E-1307; NAS 1.15-82919) Avail: NTIS HC A02/MF A01 CSCL 01C

Research activity is described for ice protection systems, icing instrumentation, experimental methods, analytical modeling for the above, and in flight research. The renewed interest in aircraft icing has come about because of the new need for All-Weather Helicopters and General Aviation aircraft. Because of increased fuel costs, tomorrow's Commercial Transport aircraft will also require new types of ice protection systems and better estimates of the aeropenalties caused by ice on unprotected surfaces. The physics of aircraft icing is very similar to the icing that occurs on ground structures and structures at sea; all involve droplets that freeze on the surfaces because of the cold air. Therefore all icing research groups will benefit greatly by sharing their research information. Author

N82-10021* Kansas Univ. Center for Research, Inc., Lawrence Flight Research Lab

ICING TUNNEL TEST OF A GLYCOL-EXUDING POROUS LEADING EDGE ICE PROTECTION SYSTEM ON A GENERAL AVIATION AIRFOIL Final Report

David L. Kohlman, William G. Schwoikhard, and Alan E. Albright Sep. 1981 37 p refs

(Grant NAG3-71) (NASA-CR-185444; KU-FRL-464-1) Avail: NTIS HC A03/MF A01 CSCL 01C

Test results show that the system is very effective in preventing ice accretion (anti-ice mode) or removing ice from an airfoil. Minimum glycol flow rates required for antiicing are a function of velocity, liquid water content in the air, ambient temperature, and droplet size. Large ice caps were removed in only a few minutes using anti-ice flow rates, with the shed time being a function of the type of ice, size of the ice cap, angle of attack, and glycol flow rate. Wake surveys measurements show that no significant drag penalty is associated with the installation or operation of the system tested. T.M.

N82-19196* Little (Arthur D.), Inc., Cambridge, Mass
AN ASSESSMENT OF THE CRASH FIRE HAZARD OF LIQUID HYDROGEN FUELED AIRCRAFT Final Report

Feb. 1982 132 p refs

(Contract NAS3-22482) (NASA-CR-165526; ADL-85161) Avail: NTIS HC A07/MF A01 CSCL 01C

The crash fire hazards of liquid hydrogen fueled aircraft relative to those of mission equivalent aircraft fueled either with conventional fuel or with liquefied methane were evaluated. The aircraft evaluated were based on Lockheed Corporation design for 400 passenger, Mach 0.85, 5500 n. mile aircraft. Four crash scenarios were considered ranging from a minor incident causing some loss of fuel system integrity to a catastrophic crash. Major tasks included a review of hazardous properties of the alternate fuels and of historic crash fire data; a comparative

05 AIRCRAFT DESIGN, TESTING AND PERFORMANCE

Includes aircraft simulation technology.
For related information see also 18 *Spacecraft Design, Testing and Performance* and 39 *Structural Mechanics*.

N82-11053*# National Aeronautics and Space Administration, Lewis Research Center, Cleveland, Ohio.

SELECTED BIBLIOGRAPHY OF NACA-NASA AIRCRAFT ICING PUBLICATIONS

John J Reinmann, comp Aug. 1981 127 p
(NASA-TM-81651; E-668) Avail: NTIS HC E15/MF A01 CSCL 01C

A summary of NACA-NASA icing research from 1940 to 1982 is presented. It includes: the main results of the NACA icing program from 1940 to 1950; a selected bibliography of 132 NACA-NASA aircraft icing publications; a technical summary of each document cited in the selected bibliography; and a microfiche copy of each document cited in the selected bibliography. T.M.

A82-17894 * # The NASA MERIT program - Developing new concepts for accurate flight planning. R. Steinberg (NASA, Lewis Research Center, Cleveland, OH), *American Institute of Aeronautics and Astronautics, Aerospace Sciences Meeting, 20th, Orlando, FL, Jan. 11-14, 1982, Paper 82-0340*, 6 p.

It is noted that the rising cost of aviation fuel has necessitated the development of a new approach to upper air forecasting for flight planning. It is shown that the spatial resolution of the present weather forecast models used in fully automated computer flight planning is an important accuracy-limiting factor, and it is proposed that man be put back into the system, although not in the way he has been used in the past. A new approach is proposed which uses the application of man-computer interactive display techniques to upper air forecasting to retain the fine scale features of the atmosphere inherent in the present data base in order to provide a more accurate and cost effective flight plan. It is pointed out that, as a result of NASA research, the hardware required for this approach already exists. C.R.

A82-28322 * # Performance degradation of propeller/rotor systems due to rime ice accretion. K. D. Korkan (Texas A & M University, College Station, TX), L. Dadone (Boeing Vertol Co., Philadelphia, PA), and R. J. Shaw (NASA, Lewis Research Center, Cleveland, OH). *American Institute of Aeronautics and Astronautics, Aerospace Sciences Meeting, 20th, Orlando, FL, Jan. 11-14, 1982, Paper 82-0286*, 14 p. Grants No. NAG3-109; No. NAG3-242.

A theoretical model has been established which is applicable to both propeller and helicopter systems that determines the effect of rime ice accretion on the thrust coefficient, power coefficient, and efficiency as a function of time in a natural icing condition. Theoretical comparisons have been made with experimentally determined decrease in propeller thrust coefficient and efficiency for five natural icing conditions with good agreement. The present analytical model is also applicable to the helicopter case, where the method predicts radial and azimuthal rotor blade ice shapes in addition to torque rise as a function of time in a natural icing condition.

(Author)

N82-11052*# Kansas Univ. Center for Research, Inc., Lawrence, Flight Research Lab.

ICING TUNNEL TESTS OF A COMPOSITE POROUS LEADING EDGE FOR USE WITH A LIQUID ANTI-ICE SYSTEM

David L. Kohlman Sep. 1981 21 p refs
(Grant NAG3-71)

(NASA-CR-164966; KU-FRL-464-3) Avail: NTIS HC A02/MF A01 CSCL 01C

The efficacy of liquid ice protection systems which distribute a glycol-water solution onto leading edge surfaces through a porous skin was demonstrated in tests conducted in the NASA

Lewis icing research tunnel using a composite porous leading edge panels. The data obtained were compared with the performance of previously tested stainless steel leading edge with the same geometry. Results show: (1) anti-ice protection of a composite leading edge is possible for all the simulated conditions tested; (2) the glycol flow rates required to achieve anti-ice protection were generally much higher than those required for a stainless steel panel; (3) the low reservoir pressures of the glycol during test runs indicates that more uniform distribution of glycol, and therefore lower glycol flow rates, can probably be achieved by decreasing the porosity of the panel; and (4) significant weight savings can be achieved in fluid ice protection systems with composite porous leading edges. The resistance of composite panels to abrasion and erosion must yet be determined before they can be incorporated in production systems. A.R.H.

N82-33375*# Douglas Aircraft Co., Inc., Long Beach, Calif. **ADVANCED TURBOPROP TESTBED SYSTEMS STUDY Final Report**

I. M. Goldsmith Jul. 1982 255 p refs

(Contract NAS3-22347)

(NASA-CR-167895; NAS 1.26:167895; ACEE-22-FR-1699A) Avail: NTIS HC A12/MF A01 CSCL 01C

The proof of concept, feasibility, and verification of the advanced prop fan and of the integrated advanced prop fan aircraft are established. The use of existing hardware is compatible with having a successfully expedited testbed ready for flight. A prop fan testbed aircraft is definitely feasible and necessary for verification of prop fan/prop fan aircraft integrity. The Allison T701 is most suitable as a propulsor and modification of existing engine and propeller controls are adequate for the testbed. The airframer is considered the logical overall systems integrator of the testbed program. S.L.

A82-27098 * # Mathematical modeling of ice accretion on airfoils. C. D. MacArthur, J. L. Keller, and J. K. Luehrs (Dayton, University, Dayton, OH). *American Institute of Aeronautics and Astronautics, Aerospace Sciences Meeting, 20th, Orlando, FL, Jan. 11-14, 1982, Paper 82-0284*, 18 p, 8 refs. Grant No. NAG3-65.

The progress toward development of a computer model suitable for predicting icing behavior on airfoils over a wide range of environmental conditions and airfoil shapes is reported. The LEWICE program was formulated to solve a set of equations which describe the physical processes which occur during accretion of ice on an airfoil, including heat transfer in a time dependent mode, with the restriction that the flow must be describable by a two-dimensional flow code. Input data comprises the cloud liquid water content, mean droplet diameter, ambient air temperature, air velocity, and relative humidity. A potential flowfield around the airfoil is calculated, along with the droplet trajectories within the flowfield, followed by local values of water droplet collection efficiency at the impact points. Both glaze and rime ice conditions are reproduced, and comparisons with test results on icing of circular cylinders showed good agreement with the physical situation. M.S.K.

ORIGINAL PAGE IS
OF POOR QUALITY

06 AIRCRAFT INSTRUMENTATION

Includes cockpit and cabin display devices; and flight instruments.

For related information see also 19 *Spacecraft Instrumentation* and 35 *Instrumentation and Photography*.

N82-23241*# National Aeronautics and Space Administration, Lewis Research Center, Cleveland, Ohio.

NASA/HAA ADVANCED ROTORCRAFT TECHNOLOGY AND TILT ROTOR WORKSHOP. VOLUME 6: PROPULSION SESSION

1980 211 p Workshop held at Palo Alto, Calif., 3-5 Dec. 1980

(NASA-TM-84207; NAS 1.15:84207) Avail: NTIS HC A10/MF A01 CSCL 01C

The expressed needs and priorities of the civil helicopter users, the existing research efforts, and technology requirements as perceived by leading airframe and engine manufacturers were addressed, compared, and evaluated. Specifically, the observations and conclusions of these areas as they relate to the helicopter propulsion system are reported. Author

ORIGINAL PAGE IS
OF POOR QUALITY

A82-37691*# Optical tip clearance sensor for aircraft engine controls. G. L. Poppel (General Electric Co., Aircraft Engine Business Group, Cincinnati, OH), D. T. F. Marple (General Electric Co., Schenectady, NY), and R. J. Baumbick (NASA, Lewis Research Center, Cleveland, OH). *AIAA, SAE, and ASME, Joint Propulsion Conference, 18th, Cleveland, OH, June 21-23, 1982, AIAA Paper 82-1131*. 9 p. Contract No. NAS3-21843.

Aircraft gas turbine performance and efficiency are related to airfoil tip clearance. The possibility has been considered to obtain optimum performance and efficiency by reducing clearance to a safe minimum with the aid of a closed-loop tip clearance control system, which utilizes a tip clearance sensor. The use of optical sensing methods appears to represent a potential solution to the tip clearance measurement problem. Principles of sensor operation are discussed along with dimensional considerations and diffraction limitations. A description is presented of the study of the feasibility of a certain sensor, taking into account the test rig system, the optical components, and the mounting tube. Attention is also given to the operation of the feasibility-study sensor, performance estimations, the optical fiber bundle, light beam refraction, and aspects of aircraft engine implementation. G.R.

07 AIRCRAFT PROPULSION AND POWER

Includes prime propulsion systems and systems components, e.g., gas turbine engines and compressors; and on-board auxiliary power plants for aircraft.

For related information see also 20 *Spacecraft Propulsion and Power*, 28 *Propellants and Fuels*, and 44 *Energy Production and Conversion*.

N82-13143* National Aeronautics and Space Administration, Lewis Research Center, Cleveland, Ohio.

EFFECT OF FUEL-AIR-RATIO NONUNIFORMITY ON EMISSIONS OF NITROGEN OXIDES

Valerie J. Lyons Nov. 1981 14 p refs (NASA-TP-1798; E-648) Avail: NTIS HC A02/MF A01 CSCL 21E

The inlet fuel-air ratio nonuniformity is studied to determine how nitrogen oxide (NOx) emissions are affected. An increase in NOx emissions with increased fuel-air ratio nonuniformity for average equivalence ratios less than 0.7 and a decrease in NOx emissions for average equivalence ratios near stoichiometric is predicted. The degree of uniformity of fuel-air ratio profiles that is necessary to achieve NOx emissions goals for actual engines that use lean, premixed, prevaporized combustion systems is determined. S.L.

N82-13144* National Aeronautics and Space Administration, Lewis Research Center, Cleveland, Ohio.

A REAL TIME PEGASUS PROPULSION SYSTEM MODEL FOR VSTOL PILOTED SIMULATION EVALUATION

James R. Mihalow, Stephen P. Roth (Pratt and Whitney Aircraft Group, West Palm Beach, Fla.), and Robert Creekmore (Pratt and Whitney Aircraft Group, West Palm Beach, Fla.) 1981 18 p refs Presented at VSTOL Conf., Palo Alto, Calif., 7-9 Dec. 1981; sponsored by AIAA and NASA, Ames Research Center (NASA-TM-82770; E-1004; AIAA-81-2663) Avail: NTIS HC A02/MF A01 CSCL 21E

A real time propulsion system modeling technique suitable for use in man-in-the-loop simulator studies was developed. This technique provides the system accuracy, stability, and transient response required for integrated aircraft and propulsion control system studies. A Pegasus-Harrier propulsion system was selected as a baseline for developing mathematical modeling and simulation techniques for VSTOL. Initially, static and dynamic propulsion system characteristics were modeled in detail to form a nonlinear aerothermodynamic digital computer simulation of a Pegasus engine. From this high fidelity simulation, a real time propulsion model was formulated by applying a piece-wise linear state variable methodology. A hydromechanical and water injection control system was also simulated. The real time dynamic model includes the detail and flexibility required for the evaluation of critical control parameters and propulsion component limits over a limited flight envelope. The model was programmed for interfacing with a Harrier aircraft simulation. Typical propulsion system simulation results are presented. M.D.K.

N82-13146* National Aeronautics and Space Administration, Lewis Research Center, Cleveland, Ohio.

NASA RESEARCH IN AIRCRAFT PROPULSION

Milton A. Beheim 1982 17 p Proposed for presentation at the 27th Ann. Intern. Gas Turbine Conf., London, 18-22 Apr. 1982; sponsored by ASME (NASA-TM-82771; E-1096) Avail: NTIS HC A02/MF A01 CSCL 21E

A broad overview of the scope of research presently being supported by NASA in aircraft propulsion is presented with emphasis on Lewis Research Center activities related to civil air transports, CTOL and V/STOL systems. Aircraft systems work is performed to identify the requirements for the propulsion system that enhance the mission capabilities of the aircraft. This important source of innovation and creativity drives the direction of propulsion research. In a companion effort, component research of a generic nature is performed to provide a better basis for design and provides an evolutionary process for technological growth that increases the capabilities of all types of aircraft. Both are important. A.R.H.

N82-14090* National Aeronautics and Space Administration, Lewis Research Center, Cleveland, Ohio.

GAS TURBINE CERAMIC-COATED-VANE CONCEPT WITH CONVECTION-COOLED POROUS METAL CORE

Albert F. Kaszak (AVRADCOM Research and Technology Labs., Cleveland), Curt H. Liebert, Robert F. Handschuh, and Lawrence P. Ludwig Dec. 1981 14 p refs Sponsored in part by U.S. Army Aviation Research and Development Command, St. Louis (NASA-TP-1942; AVRADCOM-TR-81-C-7; E-732) Avail: NTIS HC A02/MF A01 CSCL 21E

Analysis and flow experiments on a ceramic-coated-porous-metal vane concept indicated the feasibility, from a heat transfer standpoint, of operating in a high-temperature (2500 F) gas turbine cascade facility. The heat transfer and pressure drop calculations provided a basis for selecting the ceramic layer thickness (to 0.08 in.), which was found to be the dominant factor in the overall heat transfer coefficient. Also an approximate analysis of the heat transfer in the vane trailing edge revealed that with trailing-edge ejection the ceramic thickness could be reduced to (0.01 in.) in this portion of the vane. B.W.

N82-14094* National Aeronautics and Space Administration, Lewis Research Center, Cleveland, Ohio.

THE USE OF OPTIMIZATION TECHNIQUES TO DESIGN CONTROLLED DIFFUSION COMPRESSOR BLADING

Nelson L. Sanger 1982 18 p refs Proposed for presentation at the 27th Ann. Intern. Gas Turbine Conf.; London, Apr. 18-22, 1982; sponsored by ASME

(NASA-TR-82763; E-1084) Avail: NTIS HC A02/MF A01 CSCL 21E

A method for automating compressor blade design using numerical optimization, and applied to the design of a controlled diffusion stator blade row is presented. A general purpose optimization procedure is employed, based on conjugate directions for locally unconstrained problems and on feasible directions for locally constrained problems. Coupled to the optimizer is an analysis package consisting of three analysis programs which calculate blade geometry, inviscid flow, and blade surface boundary layers. The optimizing concepts and selection of design objective and constraints are described. The procedure for automating the design of a two dimensional blade section is discussed, and design results are presented. E.A.K.

N82-15039* National Aeronautics and Space Administration, Lewis Research Center, Cleveland, Ohio.

COMPUTER PROGRAM FOR AERODYNAMIC AND BLADING DESIGN OF MULTISTAGE AXIAL-FLOW COMPRESSORS

James E. Crouse and William T. Gorrell Dec. 1981 105 p refs Prepared in cooperation with Army Aviation Research and Development Command, St. Louis, Mo. (NASA-TP-1946; AVRADCOM-TR-80-C-21; E-280) Avail: NTIS HC A06/MF A01 CSCL 21E

A code for computing the aerodynamic design of a multistage axial-flow compressor and, if desired, the associated blading geometry input for internal flow analysis codes is presented. Compressible flow, which is assumed to be steady and axisymmetric, is the basis for a two-dimensional solution in the meridional plane with viscous effects modeled by pressure loss coefficients and boundary layer blockage. The radial equation of motion and the continuity equation are solved with the streamline curvature method on calculation stations outside the blade rows. The annulus profile, mass flow, pressure ratio, and rotative speed are input. A number of other input parameters specify and control the blade row aerodynamics and geometry. In particular, blade element centerlines and thicknesses can be specified with fourth degree polynomials for two segments. The output includes a detailed aerodynamic solution and, if desired, blading coordinates that can be used for internal flow analysis codes. Author

N82-15040* National Aeronautics and Space Administration, Lewis Research Center, Cleveland, Ohio.

EFFECT OF FUEL INJECTOR TYPE ON PERFORMANCE AND EMISSIONS OF REVERSE-FLOW COMBUSTOR

Carl T. Norgren and Stephen M. Riddlebaugh Dec. 1981 40 p refs (NASA-TP-1945; E-556) Avail: NTIS HC A03/MF A01 CSCL 21E

The combustion process in a reverse-flow combustor suitable for a small gas turbine engine was investigated to evaluate the effect of fuel injector type on performance and emissions. Fuel injector configurations using pressure-atomizing, spill-flow, air blast, and air-assist techniques were compared and evaluated on the basis of performance obtained in a full-scale experimental combustor operated at inlet conditions corresponding to takeoff, cruise, low power, and idle and typical of a 16:1-pressure-ratio turbine engine. Major differences in combustor performance and emissions characteristics were experienced with each injector type even though the aerodynamic configuration was common to most combustor models. Performance characteristics obtained with the various fuel injector types could not have been predicted from bench-test injector spray characteristics. The effect of the number of operating fuel injectors on performance and emissions is also presented. Author

N82-15041* National Aeronautics and Space Administration, Lewis Research Center, Cleveland, Ohio.

INTERACTIVE-GRAPHIC FLOWPATH PLOTTING FOR TURBINE ENGINES

Robert R Corban Nov. 1981 51 p refs (NASA-TM-82756; E-1074) Avail: NTIS HC A04/MF A01 CSCL 21E

An engine cycle program capable of simulating the design and off-design performance of arbitrary turbine engines, and a computer code which, when used in conjunction with the cycle code, can predict the weight of the engines are described. A graphics subroutine was added to the code to enable the engineer to visualize the designed engine with more clarity by producing an overall view of the designed engine for output on a graphics device using IBM-370 graphics subroutines. In addition, with the engine drawn on a graphics screen, the program allows for the interactive user to make changes to the inputs to the code for the engine to be redrawn and reweighed. These improvements allow better use of the code in conjunction with the engine program. T.M.

N82-16084* National Aeronautics and Space Administration, Lewis Research Center, Cleveland, Ohio.

NASA RESEARCH ACTIVITIES IN AEROPROPULSION

John F. McCarthy, Jr and Richard J. Weber 1982 30 p refs Presented at the 24th Ann. Conf. on Aviation and Astronautics, Tel Aviv, Israel, 17-18 Feb. 1982 (NASA-TM-82788; E-1113) Avail: NTIS HC A03/MF A01 CSCL 21E

NASA is responsible for advancing technologies related to air transportation. A sampling of the work at NASA's Lewis Research Center aimed at improved aircraft propulsion systems is described. Particularly stressed are efforts related to reduced noise and fuel consumption of subsonic transports. Generic work in specific disciplines are reviewed including computational analysis, materials, structures, controls, diagnostics, alternative fuels, and high-speed propellers. Prospects for variable cycle engines are also discussed. Author

N82-18222* National Aeronautics and Space Administration, Lewis Research Center, Cleveland, Ohio.

EFFECTS OF FAN INLET TEMPERATURE DISTURBANCES ON THE STABILITY OF A TURBOFAN ENGINE

Mahmoud Abdelwahab Dec. 1981 36 p refs (NASA-TM-82699; E-982) Avail: NTIS HC A03/MF A01 CSCL 21E

The effects of steady-state and time-dependent fan inlet total temperature disturbances on the stability of a TF30-P-3 turbofan engine were determined. Disturbances were induced by a gaseous-hydrogen-fueled burner system installed upstream of the fan inlet. Data were obtained at a fan inlet Reynolds number index of 0.50 and at a low-pressure-rotor corrected speed of 90 percent of military speed. All tests were conducted with a 90 deg extent of the fan inlet circumference exposed to above-average temperatures. T.M.

N82-19145* National Aeronautics and Space Administration, Lewis Research Center, Cleveland, Ohio.

ENGINE TECHNOLOGY

Anthony C. Hoffman In NASA, Langley Research Center Elec. Flight Systems Feb. 1982 p 235-240 (For primary document see N82-19134 10-01)

Avail: NTIS HC A12/MF A01 CSCL 21E

N82-19220* National Aeronautics and Space Administration, Lewis Research Center, Cleveland, Ohio.

DILUTION JET BEHAVIOR IN THE TURN SECTION OF A REVERSE FLOW COMBUSTOR

Steven M. Riddlebaugh, Abraham Lipshitz (Ahuza, Haifa, Israel), and Isaac Geber (Case Western Reserve Univ., Cleveland, Ohio) Jan. 1982 15 p refs Presented at the 20th Aerospace Sci. Meeting, Orlando, Fla., 10-14 Jan. 1982; sponsored by AIAA (NASA-TM-82776; E-1107; AIAA-82-0192) Avail: NTIS HC A02/MF A01 CSCL 21E

Measurements of the temperature field produced by a single jet and a row of dilution jets issued into a reverse flow combustor are presented. The temperature measurements are presented in the form of consecutive normalized temperature profiles, and jet trajectories. Single jet trajectories were swept toward the inner wall of the turn, whether injection was from the inner or outer wall. This behavior is explained by the radially inward velocity component necessary to support irrotational flow through the turn. Comparison between experimental results and model calculations showed poor agreement due to the model's not including the radial velocity component. A widely spaced row of jets produced trajectories similar to single jets at similar test conditions, but as spacing ratio was reduced, penetration was reduced to the point where the dilution jet flow attached to the wall. Author

N82-19222* National Aeronautics and Space Administration, Lewis Research Center, Cleveland, Ohio.

PERFORMANCE OF SINGLE-STAGE AXIAL-FLOW TRANSONIC COMPRESSOR WITH ROTOR AND STATOR ASPECT RATIOS OF 1.83 AND 1.78, RESPECTIVELY, AND WITH DESIGN PRESSURE RATIO OF 1.82

Royce D. Moore and Lonnie Reid Feb. 1982 112 p refs (NASA-TP-1974; E-259) Avail: NTIS HC A06/MF A01 CSCL 21E

The overall and blade-element performance of a transonic compressor stage is presented over the stable operating flow range for speeds from 50 to 100 percent of design. The stage was designed for a pressure ratio of 1.82 at a flow 20.2 kg/sec and a tip speed of 455 m/sec. At design speed the stage achieved a peak efficiency of 0.821 at a pressure ratio of 1.817. The stage stall margin at design speed based on conditions at stall and peak efficiency was about 11 percent. Author

N82-21194* National Aeronautics and Space Administration, Lewis Research Center, Cleveland, Ohio.

PRELIMINARY RESULTS ON PERFORMANCE TESTING OF A TURBOCHARGED ROTARY COMBUSTION ENGINE

P. R. Meng, W. J. Rice, H. J. Schock, and D. P. Pringle 1982 24 p refs Presented at the 1982 Soc. of Automotive Engrs Intern. Congr. and Exposition, Detroit, 22-26 Feb. 1982 (NASA-TM-82772; E-1097; NAS 1.15:82772) Avail: NTIS HC A02/MF A01 CSCL 21E

The performance of a turbocharged rotary engine at power levels above 75 kW (100 hp) was studied. A twin rotor turbocharged Mazda engine was tested at speeds of 3000 to 6000 rpm and boost pressures to 7 psi. The NASA developed combustion diagnostic instrumentation was used to quantify indicated and pumping mean effect pressures, peak pressure, and face to face variability on a cycle by cycle basis. Results of this testing showed that a 5900 rpm a 36 percent increase in power was obtained by operating the engine in the turbocharged configuration. When operating with lean carburetor jets at 105 hp (78.3 kW) and 4000 rpm, a brake specific fuel consumption of 0.45 lbm/lb-hr was measured. B.W.

ORIGINAL PAGE IS
OF POOR QUALITY

N82-21195* National Aeronautics and Space Administration, Lewis Research Center, Cleveland, Ohio.

ANALYTICAL INVESTIGATION OF NONRECOVERABLE STALL

Leon M. Wenzel and William M. Bruton Feb. 1982 23 p refs

(NASA-TM-82792; E-1126; NAS 1.15:82792) Avail: NTIS HC A02/MF A01 CSCL 21E

A lumped parameter model of the TF34 engine is formulated to study nonrecoverable stall. Features of the model include forward and reverse flow, radial flow in the fan, and variable corrected speed. The purpose of the study is to point out those parameters to which recoverability is highly sensitive but are not well known. Experimental research may then be directed toward identification of the parameters in that category. Compressor performance in the positive flow region and radial flow in the fan are shown to be important but unknown parameters determining recoverability. Other parameters such as compressor performance during reverse flow and in-stall efficiency have relatively small impact on recoverability. Author

N82-22262* National Aeronautics and Space Administration, Lewis Research Center, Cleveland, Ohio.

THE ROLE OF MODERN CONTROL THEORY IN THE DESIGN OF CONTROLS FOR AIRCRAFT TURBINE ENGINES

J. Zeller, B. Lehtinen, and W. Merrill 1982 17 p refs Presented at 12th Aerospace Sci. Conf., Orlando, Fla., 11-14 Jan. 1982; sponsored by AIAA

(NASA-TM-82816; E-1162; NAS 1.15:82816) Avail: NTIS HC A02/MF A01 CSCL 21E

Accomplishments in applying Modern Control Theory to the design of controls for advanced aircraft turbine engines were reviewed. The results of successful research programs are discussed. Ongoing programs as well as planned or recommended future thrusts are also discussed. Author

N82-22286* National Aeronautics and Space Administration, Lewis Research Center, Cleveland, Ohio.

STRUCTURAL DYNAMICS OF SHROUDDLESS, HOLLOW FAN BLADES WITH COMPOSITE IN-LAYS

R. A. Aiello, M. S. Hirschbain, and C. C. Chamis 1982 12 p refs Presented at the 27th Ann. Intern. Gas Turbine Conf., London, 18-22 Apr. 1982; sponsored by ASME

(NASA-TM-82816; E-1163; NAS 1.15:82816) Avail: NTIS HC A02/MF A01 CSCL 21E

Structural and dynamic analyses are presented for a shrouddless, hollow titanium fan blade proposed for future use in aircraft turbine engines. The blade was modeled and analyzed using the composite blade structural analysis computer program (COBSTRAN); an integrated program consisting of mesh generators, composite mechanics codes, NASTRAN, and pre- and post-processors. Vibration and impact analyses are presented. The vibration analysis was conducted with COBSTRAN. Results show the effect of the centrifugal force field on frequencies, twist, and blade camber. Bird impact analysis was performed with the multi-mode blade impact computer program. This program uses the geometric model and modal analysis from the COBSTRAN vibration analysis to determine the gross impact response of the fan blades to bird strikes. The structural performance of this blade is also compared to a blade of similar design but with composite in-lays on the outer surface. Results show that the composite in-lays can be selected (designed) to substantially modify the mechanical performance of the shrouddless, hollow fan blade. Author

N82-22269* National Aeronautics and Space Administration, Lewis Research Center, Cleveland, Ohio.

PERFORMANCE OF SINGLE-STAGE AXIAL-FLOW TRANSONIC COMPRESSOR WITH ROTOR AND STATOR ASPECT RATIOS OF 1.63 AND 1.77, RESPECTIVELY, AND WITH DESIGN PRESSURE RATIO OF 2.05

Royce D. Moore and Lonnie Reid Apr. 1982 116 p refs (NASA-TP-2001; E-334; NAS 1.60:2001) Avail: NTIS HC A06/MF A01 CSCL 21E

The overall and blade-element performance of a transonic compressor stage is presented over the stable operating range for speeds from 50 to 100 percent of design. The stage was designed for a pressure ratio of 2.05 at a flow of 20.2 kg/sec and a tip speed of 455 m/sec. At design speed the rotor and

stage achieved peak efficiencies of 0.849 and 0.831, respectively, at the minimum flow condition. The stage stall point occurred at a flow higher than the design flow. Author

N82-24201* National Aeronautics and Space Administration, Lewis Research Center, Cleveland, Ohio.

A PIECEWISE LINEAR STATE VARIABLE TECHNIQUE FOR REAL TIME PROPULSION SYSTEM SIMULATION

James R. Mihalow and Stephen P. Roth (Pratt and Whitney Aircraft Group, West Palm Beach, Fla.) 1982 16 p refs Presented at the 13th Ann. Pittsburgh Conf. on Modelling and Simulation, Pittsburgh, 22-23 Apr. 1982; sponsored by IEEE, ISA, SCS and SMCS

(NASA-TM-82851; E-1210; NAS 1.15:82851) Avail: NTIS HC A02/MF A01 CSCL 21E

The emphasis on increased aircraft and propulsion control system integration and piloted simulation has created a need for higher fidelity real time dynamic propulsion models. A real time propulsion system modeling technique which satisfies this need and which provides the capabilities needed to evaluate propulsion system performance and aircraft system interaction on manned flight simulators was developed and demonstrated using flight simulator facilities at NASA Ames. A piecewise linear state variable technique is used. This technique provides the system accuracy, stability and transient response required for integrated aircraft and propulsion control system studies. The real time dynamic model includes the detail and flexibility required for the evaluation of critical control parameters and propulsion component limits over a limited flight envelope. The model contains approximately 7.0 K bytes of in-line computational code and 14.7 K of block data. It has an 8.9 ms cycle time on a Xerox Sigma 9 computer. A Pegasus-Harrier propulsion system was used as a baseline for developing the mathematical modeling and simulation technique. A hydromechanical and water injection control system was also simulated. The model was programmed for interfacing with a Harrier aircraft simulation at NASA Ames. Descriptions of the real time methodology and model capabilities are presented. Author

N82-24203* National Aeronautics and Space Administration, Lewis Research Center, Cleveland, Ohio.

FUTURE PROPULSION OPPORTUNITIES FOR COMMUTER AIRPLANES

William C. Strack Washington 1982 24 p refs Presented at the Commuter Airlines Meeting, Savannah, 24-26 May 1982; sponsored by the Society of Automotive Engineers

(NASA-TM-82880; E-1266; NAS 1.15:82880) Avail: NTIS HC A02/MF A01 CSCL 21E

Commuter airplane propulsion opportunities are summarized. Consideration is given to advanced technology conventional turboprop engines, advanced propellers, and several unconventional alternatives: regenerative turboprops, rotaries, and diesels. Advanced versions of conventional turboprops (including propellers) offer 15-20 percent savings in fuel and 10-15 percent in DOC compared to the new crop of 1500-2000 SHP engines currently in development. Unconventional engines could boost the fuel savings to 30-40 percent. The conclusion is that several important opportunities exist and, therefore, powerplant technology need not plateau. Author

N82-25250* National Aeronautics and Space Administration, Lewis Research Center, Cleveland, Ohio.

STGSK: A COMPUTER CODE FOR PREDICTING MULTISTAGE AXIAL FLOW COMPRESSOR PERFORMANCE BY A MEANLINE STAGE STACKING METHOD

Ronald J. Steinke May 1982 65 p refs (NASA-TP-2020; E-551; NAS 1.60:2020) Avail: NTIS HC A04/MF A01 CSCL 21E

A FORTRAN computer code is presented for off-design performance prediction of axial-flow compressors. Stage and compressor performance is obtained by a stage-stacking method that uses representative velocity diagrams at rotor inlet and outlet meanline radii. The code has options for: (1) direct user input or calculation of nondimensional stage characteristics; (2) adjustment of stage characteristics for off-design speed and blade setting angle; (3) adjustment of rotor deviation angle for off-design conditions; and (4) SI or U.S. customary units. Correlations from experimental data are used to model real flow conditions. Calculations are compared with experimental data. Author

ORIGINAL PAGE IS
OF POOR QUALITY

N82-26255*# National Aeronautics and Space Administration, Lewis Research Center, Cleveland, Ohio

EXHAUST EMISSIONS SURVEY OF A TURBOFAN ENGINE FOR FLAME HOLDER SWIRL TYPE AUGMENTORS AT SIMULATED ALTITUDE FLIGHT CONDITIONS

John E. Moss, Jr. Oct. 1981 47 p refs

(NASA-TM-82787; E-955; NAS 1.15:82787) Avail: NTIS HC A03/MF A01 CSCL 21E

Emissions of carbon dioxide, total oxides of nitrogen, unburned hydrocarbons, and carbon monoxide from an F100 afterburning two spool turbofan engine at simulated flight conditions are reported. Tests were run at Mach 0.8 at altitudes of 10.97 and 13.71 km (36,000 and 45,000 ft), and at Mach 1.2 at 13.71 km (45,000 ft). Emission measurements were made from intermediate power (nonafterburning) through maximum afterburning, using a single point gas sample probe traversed across the horizontal diameter of the exhaust nozzle. The data show that emissions vary with flight speed, altitude, power level, and radial position across the nozzle. Carbon monoxide emissions were low for intermediate and partial afterburning power. Unburned hydrocarbons were near zero for most of the simulated flight conditions. At maximum afterburning, there were regions of NOx deficiency in regions of high CO. The results suggest that the low NOx levels observed in the tests are a result of interaction with high CO in the thermal converter. CO2 emissions were proportional to local fuel air ratio for all test conditions.

T.M.

N82-26293* National Aeronautics and Space Administration, Lewis Research Center, Cleveland, Ohio

THRUST REVERSER FOR A LONG DUCT FAN ENGINE Patent

Everett A. Johnston (GE, Cincinnati) and Edward W. Ryan, inventors (to NASA) (GE, Cincinnati) Issued 14 Jul 1981 9 p Filed 30 Mar. 1979

(NASA-Case-LEW-13199-1; US-Patent-4,278,220,

US-Patent-Appl-SN-025301, US-Patent-Class-244-110B;

US-Patent-Class-60-226A) Avail: US Patent and Trademark Office CSCL 21E

A bypass duct outer cowl includes a fixed cascade disposed between axially spaced fixed cowl portions and a translatable cowl sleeve and blocker doors movably disposed on the respective radially outer and inner sides of the cascade. Actuation and linkage structure located entirely within the outer cowl provides for selectively moving the cowl sleeve rearwardly and rotating the blocker doors to a position across the bypass duct to cause the fan airflow to pass through the cascade in a thrust reversing manner. Official Gazette of the U.S. Patent and Trademark Office

N82-26294*# National Aeronautics and Space Administration, Lewis Research Center, Cleveland, Ohio

REAL TIME PRESSURE SIGNAL SYSTEM FOR A ROTARY ENGINE Patent Application

William J. Rice, inventor (to NASA) Filed 19 Feb. 1982 21 p (NASA-Case-LEW-13622-1; US-Patent-Appl-SN-350473) Avail: NTIS HC A02/MF A01 CSCL 21E

Apparatus for developing a signal which is a composite of the pressures at four different points in the chamber of a rotary type engine is disclosed. The composite signal can be read by an IMEP meter or displayed on an oscilloscope. The physical arrangement of a Wankel engine and the correlation embodying the invention is shown. The profile of the inner surface of a Wankel engine housing and the profile of a three lobed rotor together with the positions of the transducers are also shown. The timing diagrams depicting the active regions of the transducers and timing signals used in the correlator circuitry are illustrated.

S.L.

N82-26297*# National Aeronautics and Space Administration, Lewis Research Center, Cleveland, Ohio

DEVELOPMENT POTENTIAL OF INTERMITTENT COMBUSTION (I.C.) AIRCRAFT ENGINES FOR COMMUTER TRANSPORT APPLICATIONS

Edward A. Willis 1982 31 p refs Presented at the Commuter Airlines and Operations Meeting, Savannah, 23-24 May 1982 (NASA-TM-82869; E-1221; NAS 1.15:82869) Avail: NTIS HC A03/MF A01 CSCL 21E

An update on general aviation (g/a) and commuter aircraft propulsion research effort is reviewed. The following topics are

discussed: on several advanced intermittent combustion engines emphasizing lightweight diesels and rotary stratified charge engines. The current state-of-the-art is evaluated for lightweight, aircraft suitable versions of each engine. This information is used to project the engine characteristics that can be expected on near-term and long-term time horizons. The key enabling technology requirements are identified for each engine on the long-term time horizon. E.A.K.

N82-26298*# National Aeronautics and Space Administration, Lewis Research Center, Cleveland, Ohio

PROPULSION OPPORTUNITIES FOR FUTURE COMMUTER AIRCRAFT

William C. Strack 1982 27 p refs Presented at 18th Joint Propulsion Conf., Cleveland, 21-23 Jun. 1982; sponsored by AIAA, SAE and ASME

(NASA-TM-82915; E-1304; NAS 1.15:82915) Avail: NTIS HC A03/MF A01 CSCL 21E

Since 1990 propulsion improvement concepts are discussed for 1000 to 5000 SHP conventional turboprop powerplants including engines, gearboxes, and propellers. Cycle selection, power plant configurations and advanced technology elements are defined and evaluated using average stage length DOC for commuter aircraft as the primary merit criterion. B.W.

N82-26299*# National Aeronautics and Space Administration, Lewis Research Center, Cleveland, Ohio

COMPARISON OF EXPERIMENTAL AND ANALYTICAL PERFORMANCE FOR CONTOURED ENDWALL STATORS

Robert J. Boyle and Jeffrey E. Haas (Army Aviation Research and Development Command, Cleveland) 1982 15 p refs Presented at Eighteenth Joint Propulsion Conf., Cleveland, 21-23 Jun. 1982; sponsored by AIAA, SAE and ASME

(NASA-TM-82877; NAS 1.15:82877;

AVRADCOM-TR-82-C-12) Avail: NTIS HC A02/MF A01 CSCL 21E

Comparisons between predicted and experimental stator losses showed that the analysis was able to predict the change in stator loss when contoured endwalls with highly three dimensional passage geometry were used. The level of loss was predicted to within 75 percent of that measured. The predicted loss was due only to profile loss and boundary layer growth on the endwalls. The 25 percent difference was approximately 0.015 at design pressure ratio. The analysis was shown to predict the trend in stator flow angle, even for small stator geometries.

Author

N82-26300*# National Aeronautics and Space Administration, Lewis Research Center, Cleveland, Ohio

NASA RESEARCH IN SUPERSONIC PROPULSION: A DECADE OF PROGRESS

L. H. Fishbach, L. E. Stitt, J. R. Stone, and J. B. Whitlow, Jr. 1982 40 p refs Presented at 18th Joint Propulsion Conf., Cleveland, 21-23 Jun. 1982; sponsored by AIAA, SAE and ASME

(NASA-TM-82862; NAS 1.15:82862) Avail: NTIS HC A03/MF A01 CSCL 21E

A second generation, economically viable, and environmentally acceptable supersonic aircraft is reviewed. Engine selection, testbed experiments, and noise reduction research are described. Author

N82-27311*# National Aeronautics and Space Administration, Lewis Research Center, Cleveland, Ohio

QCSEE UNDER-THE-WING ENGINE ACOUSTIC DATA

Harry E. Bloomer and Nick E. Samanich May 1982 28 p refs

(NASA-TM-82691; E-972; NAS 1.15:82691) Avail: NTIS HC A03/MF A01 CSCL 21E

Both an over-the-wing (OTW) and an under-the-wing (UTW) experimental engine are discussed. The UTW engine had a variable-geometry fan exhaust nozzle and a variable-pitch fan that provided quick-response reverse thrust capability. An automatic digital control enabled optimal engine operation under all steady-state conditions as well as during forward and reverse thrust transient operation. The engine was tested at the Engine Noise Test Facility alone and with wind and flap segments to

ORIGINAL PAGE IS
OF POOR QUALITY

simulate an installation on a short-haul transport aircraft. The engine acoustic configuration was varied to give 14 test configurations. All of the acoustic test results from the UTW program at Lewis are presented as 1/3-octave-band sound pressure level (SPL) tabulations for all of the test points and some narrow-band spectra and 1/3-octave-band data plots for selected conditions. T.M.

N82-29324*# National Aeronautics and Space Administration, Lewis Research Center, Cleveland, Ohio.

QCSEE OVER-THE-WING ENGINE ACOUSTIC DATA

Harry E. Bloomer and Irvin J. Loeffler May 1982 28 p refs (NASA-TM-82708, E-890, NAS 1.15:82708) Avail: NTIS HC A03/MF A01 CSCL 21E

The over the wing (OTW) Quiet, Clean, Short Haul Experimental Engine (QCSEE) was tested at the NASA Lewis Engine Noise Test Facility. A boilerplate (nonflight weight), high throat Mach number, acoustically treated inlet and a D shaped OTW exhaust nozzle with variable position side doors were used in the tests along with wing and flap segments to simulate an installation on a short haul transport aircraft. All of the acoustic test data from 10 configurations are documented in tabular form. Some selected narrowband and 1/3 octave band plots of sound pressure level are presented. Author

N82-31329*# National Aeronautics and Space Administration, Lewis Research Center, Cleveland, Ohio.

VENTURI NOZZLE EFFECTS ON FUEL DROP SIZE AND NITROGEN OXIDE EMISSIONS

Susan M. Johnson Aug. 1982 17 p refs (NASA-TP-2028; E-1029; NAS 1.60:2028) Avail: NTIS HC A02/MF A01 CSCL 21E

The effect of a venturi nozzle on the Sauter mean diameter of a water spray produced by a simplex pressure atomizing injector in a swirling airflow was determined. A Malvern particle and droplet size distribution analyzer, Type S.T. 1800, was used to measure D sub 32 of the water sprays. The water spray was studied at ambient temperature (293 K) and atmospheric pressure. The venturi reduced D sub 32 by an average of 30 percent when installed with a simplex injector and air swirler. The venturi primarily improved atomization of the injector spray by increasing relative air velocity. The small drop size enhanced vaporization and therefore decreased oxides of nitrogen in a combustor. The decrease in drop size provided by the addition of a venturi explains the results obtained in a previous small scale research combustor wherein NOx emission indices decreased as a result of this hardware modification. S.L.

N82-32366* National Aeronautics and Space Administration, Lewis Research Center, Cleveland, Ohio.

ACTIVE CLEARANCE CONTROL SYSTEM FOR A TURBOMACHINE Patent

Richard P. Johnston, Malcolm H. Knapp, and Charles E. Coulson, inventors (to NASA) issued 11 May 1982 6 p Filed 25 Jul. 1979

(NASA-Case-LEW-12938-1; US-Patent-4,329,114; US-Patent-Appl-SN-060449; US-Patent-Class-415-145; US-Patent-Class-415-178; US-Patent-Class-60-726; US-Patent-Class-60-39.29; US-Patent-Class-60-39.07) Avail: US Patent and Trademark Office CSCL 21E

An axial compressor is provided with a cooling air manifold surrounding a portion of the shroud, and means for bleeding air from the compressor to the manifold for selectively flowing it in a modulating manner axially along the outer side of the stator/shroud to cool and shrink it during steady state operating conditions so as to obtain minimum shroud/rotor clearance conditions. Provision is also made to selectively divert the flow of cooling air from the manifold during transient periods of operation so as to alter the thermal growth or shrink rate of the stator/shroud and result in adequate clearance with the compressor rotor.

Official Gazette of the U.S. Patent and Trademark Office

N82-33389*# National Aeronautics and Space Administration, Lewis Research Center, Cleveland, Ohio.

ROTO-TIP CLEARANCE EFFECTS ON OVERALL AND BLADE-ELEMENT PERFORMANCE OF AXIAL-FLOW TRANSONIC FAN STAGE

Royce D. Moore Sep. 1982 87 p refs (NASA-TP-2049; E-559; NAS 1.60:2049) Avail: NTIS HC A05/MF A01 CSCL 21E

The effects of tip clearance on the overall and blade-element performance of an axial-flow transonic fan stage are presented. The 50-centimeter-diameter fan was tested at four tip clearances (nonrotating) from 0.061 to 0.178 centimeter. The calculated radial growth of the blades was 0.040 centimeter at design conditions. The decrease in overall stage performance with increasing clearance is attributed to the loss in rotor performance. For the rotor the effects of clearance on performance parameters extended to about 70 percent of blade span from the tip. The stage stall margin based on an assumed operating line decreased from 15.3 to 0 percent as the clearance increased from 0.061 to 0.178 centimeter. Author

A82-10952*# Thermal and flow analysis of a convection, air-cooled ceramic coated porous metal concept for turbine vanes. F. S. Stepka (NASA, Lewis Research Center, Cleveland, OH), *American Society of Mechanical Engineers and American Institute of Chemical Engineers, National Heat Transfer Conference, 20th, Milwaukee, WI, Aug. 2-5, 1981, ASME Paper 81-HT-48*, 7 p. 9 refs. Members, \$2.00; nonmembers, \$4.00.

Analysis was made of the heat transfer and pressure drop through turbine vanes made of a sintered, porous metal coated with a thin layer of ceramic and convection cooled by spanwise flow of cooling air. The analysis was made to determine the feasibility of using this concept for cooling very small turbines, primarily for short duration applications such as in missile engines. The analysis was made for gas conditions of approximately 10 and 40 atm and 1644 K and with turbine vanes made of felt-type porous metals with relative densities from 0.2 and 0.6 and ceramic coating thicknesses of 0.076 to 0.254 mm. (Author)

A82-19214*# Comparison of two parallel/series flow turbofan propulsion concepts for supersonic V/STOL. R. W. Luide, G. E. Turney, and J. Allen (NASA, Lewis Research Center, Cleveland, OH), *American Institute of Aeronautics and Astronautics and NASA Ames Research Center, V/STOL Conference, Palo Alto, CA, Dec. 7-9, 1981, AIAA Paper 81-2637*, 15 p. 5 refs.

The thrust, specific fuel consumption, and relative merits of the tandem fan and the dual reverse flow front fan propulsion systems for a supersonic V/STOL aircraft are discussed. Consideration is given to: fan pressure ratio, fan air burning, and variable core supercharging. The special propulsion system components required are described, namely: the reflecting front inlet/nozzle, the aft subsonic inlet, the reverse pitch fan, the variable core supercharger and the low pressure forward burner. The potential benefits for these unconventional systems are indicated. (Author)

A82-19221*# A real time Pegasus propulsion system model for VSTOL piloted simulation evaluation. J. R. Mihalow (NASA, Lewis Research Center, Cleveland, OH), S. P. Roth, and R. Creekmore (United Technologies Corp., Government Products Div., West Palm Beach, FL), *American Institute of Aeronautics and Astronautics and NASA Ames Research Center, V/STOL Conference, Palo Alto, CA, Dec. 7-9, 1981, AIAA Paper 81-2663*, 18 p. 6 refs.

A Pegasus-Harrier propulsion system is selected as a baseline for developing mathematical modeling and simulation techniques for VSTOL. Initially, static and dynamic propulsion system characteristics are modeled in detail to form a nonlinear aerothermodynamic digital computer simulation of a Pegasus engine. From this high fidelity simulation, a real-time propulsion model is formulated by applying a piecewise linear state variable methodology. A hydro-

mechanical and water injection control system is also simulated. It is noted that the real-time dynamic model includes the detail and flexibility required for evaluating critical control parameters and propulsion component limits over a limited flight envelope. C.R.

A82-19337 * # Aeroelastic characteristics of a cascade of mistuned blades in subsonic and supersonic flows. R. E. Kielb (NASA, Lewis Research Center, Structural Dynamics Section, Cleveland, OH) and K. R. V. Kaza (NASA, Lewis Research Center, Cleveland; Toledo, University, Toledo, OH). *American Society of Mechanical Engineers, Design Engineering Technical Conference, Hartford, CT, Sept. 20-23, 1981, Paper 81-DET-122*. 12 p. 19 refs. Members, \$2.00; nonmembers, \$4.00.

An investigation of the effects of mistuning on flutter and forced response of a cascade in subsonic and supersonic flows is presented. The aerodynamic and structural coupling between the bending and torsional motions and the aerodynamic coupling between the blades are included. It is shown that frequency mistuning always has a beneficial effect on flutter. Additionally, the results indicate that frequency mistuning may have either a beneficial or an adverse effect on forced response, depending on the engine order of the excitation and Mach number. (Author)

A82-20291 * # Dilution jet behavior in the turn section of a reverse flow combustor. S. M. Riddlebaugh (NASA, Lewis Research Center, Cleveland, OH), I. Greber (Case Western Reserve University, Cleveland, OH), and A. Lipshitz. *American Institute of Aeronautics and Astronautics, Aerospace Sciences Meeting, 20th, Orlando, FL, Jan. 11-14, 1982, Paper 82-0192*. 13 p.

Measurements of the temperature field produced by a single jet and a row of dilution jets issued into a reverse flow combustor are presented. The temperature measurements are presented in the form of consecutive normalized temperature profiles, and jet trajectories. Single jet trajectories were swept toward the inner wall of the turn, whether injection was from the inner or outer wall. This behavior is explained by the radially inward velocity component necessary to support irrotational flow through the turn. Comparison between experimental results and model calculations showed poor agreement due to the model's not including the radial velocity component. A widely spaced row of jets produced trajectories similar to single jets at similar test conditions, but as spacing ratio was reduced, penetration was reduced to the point where the dilution jet flow attached to the wall. (Author)

A82-34981 * # Turbine blade nonlinear structural and life analysis. R. L. McKnight, J. H. Laffen (General Electric Co., Cincinnati, OH), G. R. Halford, and A. Kaufman (NASA, Lewis Research Center, Cleveland, OH). *AIAA, SAE, and ASME, Joint Propulsion Conference, 18th, Cleveland, OH, June 21-23, 1982, AIAA Paper 82-1056*. 9 p. 9 refs.

The utility of advanced structural analysis and life prediction techniques was evaluated for the life assessment of a commercial air-cooled turbine blade with a history of tip cracking. Three dimensional, nonlinear finite element structural analyses were performed for the blade tip region. The computed strain-temperature history of the critical location was imposed on a uniaxial strain controlled test specimen to evaluate the validity of the structural analysis method. Experimental results indicated higher peak stresses and greater stress relaxation than the analytical predictions. Life predictions using the Strainrange Partitioning and Frequency Modified approaches predicted 1200 to 4420 cycles and 2700 cycles to crack initiation, respectively, compared to an observed life of 3000 cycles. (Author)

A82-34992 * # Experimental study of the effects of secondary air on the emissions and stability of a lean premixed combustor. G. Roffe, R. S. V. Raman (General Applied Science Laboratories, Inc., Westbury, NY), and C. J. Marek (NASA, Lewis Research Center, Cleveland, OH). *AIAA, SAE, and ASME, Joint Propulsion Conference, 18th, Cleveland, OH, June 21-23, 1982, AIAA Paper 82-1072*. 10 p. 7 refs. NASA-supported research.

A study of the effects of secondary air addition on the stability and emissions of a gas turbine combustor has been performed. Tests were conducted with two types of flameholders and varying amounts of dilution air addition. Results indicate that NO_x decreases with increasing dilution air injection, whereas CO is independent of the amount of dilution air and is related to the gas temperature

near the walls. The axial location of the dilution air addition has no effect on the performance or stability. Results also indicate that the amount of secondary air entrained by the flameholder recirculation zone is dependent on the amount of dilution air and flameholder geometry. (Author)

A82-34995 * # Advancements in real-time engine simulation technology. J. R. Szuch (NASA, Lewis Research Center, Cleveland, OH). *AIAA, SAE, and ASME, Joint Propulsion Conference, 18th, Cleveland, OH, June 21-23, 1982, AIAA Paper 82-1075*. 9 p. 21 refs. (Previously announced in STAR as N82-22915)

A82-34998 * # NASA Broad Specification Fuels Combustion Technology program - Pratt and Whitney Aircraft Phase I results and status. R. P. Lohmann (United Technologies Corp., Commercial Products Div., East Hartford, CT) and J. S. Fear (NASA, Lewis Research Center, Aerothermodynamics and Fuel Div., Cleveland, OH). *AIAA, SAE, and ASME, Joint Propulsion Conference, 18th, Cleveland, OH, June 21-23, 1982, AIAA Paper 82-1088*. 12 p. 11 refs.

In connection with increases in the cost of fuels and the reduced availability of high quality petroleum crude, a modification of fuel specifications has been considered to allow acceptance of poorer quality fuels. To obtain the information upon which a selection of appropriate fuels for aircraft can be based, the Broad Specification Fuels Combustion Technology program was formulated by NASA. A description is presented of program-related investigations conducted by an American aerospace company. The specific objective of Phase I of this program has been to evaluate the impact of the use of broadened properties fuels on combustor design through comprehensive combustor rig testing. Attention is given to combustor concepts, experimental evaluation, results obtained with single stage combustors, the stage combustor concept, and the capability of a variable geometry combustor. G.R.

A82-35000 * # NASA/General Electric broad-specification fuels combustion technology program - Phase I results and status. W. J. Dodds, E. E. Eksidt, D. W. Bahr (General Electric Co., Aircraft Engine Business Group, Cincinnati, OH), and J. S. Fear (NASA, Lewis Research Center, Cleveland, OH). *AIAA, SAE, and ASME, Joint Propulsion Conference, 18th, Cleveland, OH, June 21-23, 1982, AIAA Paper 82-1089*. 12 p. 14 refs.

A program is being conducted to develop the technology required to utilize fuels with broadened properties in aircraft gas turbine engines. The first phase of this program consisted of the experimental evaluation of three different combustor concepts to determine their potential for meeting several specific emissions and performance goals, when operated on broadened property fuels. The three concepts were a single annular combustor; a double annular combustor; and a short single annular combustor with variable geometry. All of these concepts were sized for the General Electric CF6-80 engine. A total of 24 different configurations of these concepts were evaluated in a high pressure test facility, using four test fuels having hydrogen contents between 11.8 and 14%. Fuel effects on combustor performance, durability and emissions, and combustor design features to offset these effects were demonstrated. (Author)

A82-35017 * # In-flight acoustic results from an advanced-design propeller at Mach numbers to 0.8. K. G. Mackall, P. L. Lasagna, K. Walsh (NASA, Ames Research Center, Edwards, CA), and J. H. Dittmar (NASA, Lewis Research Center, Cleveland, OH). *AIAA, SAE, and ASME, Joint Propulsion Conference, 18th, Cleveland, OH, June 21-23, 1982, AIAA Paper 82-1120*. 9 p. 6 refs.

Acoustic data for the advanced-design SR-3 propeller at Mach numbers to 0.8 and helical tip Mach numbers to 1.14 are presented. Several advanced-design propellers, previously tested in wind tunnels at the Lewis Research Center, are being tested in flight at the Dryden Flight Research Facility. The flight-test propellers are mounted on a pylon on the top of the fuselage of a JetStar airplane. Instrumentation provides near-field acoustic data for the SR-3. Acoustic data for the SR-3 propeller at Mach numbers up to 0.8, for propeller helical tip Mach numbers up to 1.14, and comparison of wind tunnel to flight data are included. Flowfield profiles measured in the area adjacent to the propeller are also included. (Author)

A82-35041 * # Evaluation of fuel injection configurations to control carbon and soot formation in small GT combustors. T. J. Rosfjord (United Technologies Research Center, East Hartford, CT) and D. Briehl (NASA, Lewis Research Center, Cleveland, OH). *AIAA, SAE, and ASME, Joint Propulsion Conference, 18th, Cleveland, OH, June 21-23, 1982, AIAA Paper 82-1175*. 12 p. 6 refs.

An experimental program to investigate hardware configurations which attempt to minimize carbon formation and soot production without sacrificing performance

In small gas turbine combustors has been conducted at the United Technologies Research Center. Four fuel injectors, embodying either airblast atomization, pressure atomization, or fuel vaporization techniques, were combined with nozzle air swirlers and injector sheaths, and evaluated at test conditions which included and extended beyond standard small gas turbine combustor operation. Extensive testing was accomplished with configurations embodying either a spill return or a T-vaporizer injector. Minimal carbon deposits were observed on the spill return nozzle for tests using either Jet A or EPBS test fuel. A more extensive film of soft carbon was observed on the vaporizer after operation at standard engine conditions, with large carbonaceous growths forming on the device during off-design operation at low combustor inlet temperature. Test results indicated that smoke emission levels depended on the combustor fluid mechanics (especially the mixing rates near the injector), the atomization quality of the injector and the fuel hydrogen content. (Author)

A82-35348 * # A computational design method for transonic turbomachinery cascades. H. Sobieczky (Deutsche Forschungs- und Versuchsanstalt für Luft- und Raumfahrt, Institut für theoretische Strömungsmechanik, Göttingen, West Germany) and D. S. Dulikravich (NASA, Lewis Research Center, Cleveland, OH). *American Society of Mechanical Engineers, International Gas Turbine Conference and Exhibit, 27th, London, England, Apr. 18-22, 1982, Paper 82-GT-117*. 10 p. 17 refs. Members, \$2.00; nonmembers, \$4.00.

This paper describes a systematical computational procedure to find configuration changes necessary to modify the resulting flow past turbomachinery cascades, channels and nozzles, to be shock-free at prescribed transonic operating conditions. The method is based on a finite area transonic analysis technique and the fictitious gas approach. This design scheme has two major areas of application. First, it can be used for design of supercritical cascades, with applications mainly in compressor blade design. Second, it provides subsonic inlet shapes including sonic surfaces with suitable initial data for the design of supersonic (accelerated) exits, like nozzles and turbine cascade shapes. This fast, accurate and economical method with a proven potential for applications to three-dimensional flows is illustrated by some design examples. (Author)

A82-35373 * # The use of optimization techniques to design controlled diffusion compressor blading. N. L. Sanger (NASA, Lewis Research Center, Cleveland, OH). *American Society of Mechanical Engineers, International Gas Turbine Conference and Exhibit, 27th, London, England, Apr. 18-22, 1982, Paper 82-GT-149*. 11 p. 17 refs. Members, \$2.00; nonmembers, \$4.00. (Previously announced in STAR as N82-14094)

A82-35389 * # NASA research in aircraft propulsion. M. A. Beheim (NASA, Lewis Research Center, Cleveland, OH). *American Society of Mechanical Engineers, International Gas Turbine Conference and Exhibit, 27th, London, England, Apr. 18-22, 1982, Paper 82-GT-177*. 10 p. Members, \$2.00; nonmembers, \$4.00. (Previously announced in STAR as N82-13146)

A82-35409 * # The effect of rotor blade thickness and surface finish on the performance of a small axial flow turbine. R. J. Roelke (NASA, Lewis Research Center, Cleveland, OH) and J. E. Haas (U.S. Army, Propulsion Laboratory, Cleveland, OH). *American Society of Mechanical Engineers, International Gas Turbine Conference and Exhibit, 27th, London, England, Apr. 18-22, 1982, Paper 82-GT-222*. 6 p. 9 refs. Members, \$2.00; nonmembers, \$4.00. (Previously announced in STAR as N82-13114)

A82-35456 * # Structural dynamics of shroudless, hollow, fan blades with composite in-lays. R. A. Aiello, M. S. Hirschbein, and C. C. Chamis (NASA, Lewis Research Center, Cleveland, OH). *American Society of Mechanical Engineers, International Gas Turbine Conference and Exhibit, 27th, London, England, Apr. 18-22, 1982, Paper 82-GT-284*. 7 p. Members, \$2.00; nonmembers, \$4.00. (Previously announced in STAR as N82-22266)

A82-40521 * # TF34 Convertible Engine System Technology Program. K. L. Abdalla (NASA, Lewis Research Center, Cleveland, OH) and A. Brooks (General Electric Co., Lynn, MA). In: *American Helicopter Society, Annual Forum, 38th, Anaheim, CA, May 4-7, 1982, Proceedings*. (A82-40505 20-01) Washington, DC, American Helicopter Society, 1982, p. 163-165. 8 refs.

The ability of the helicopter to function efficiently at zero flight speed is counter-balanced by a limitation to rather low forward flight speeds. An ability to fly efficiently at high speed would provide very significant improvements in rotorcraft productivity and economics. The implementation of such improvements would require the development of a suitable integrated power plant for both the vertical

and horizontal flight modes. The engine should be a shaft output engine in the vertical flight mode. In the horizontal mode, the propulsor can be fan or propeller. A description is presented of a program concerned with the demonstration of a convertible turbofan/turboshaft engine. The program is nominally directed toward the demonstration of a propulsion system for an X-wing aircraft. However, the principles being investigated are applicable to any convertible turbofan/turboshaft engine application. At the current early stage of the program, no barrier problems have become apparent, and interesting possibilities for high speed rotorcraft flight are envisaged. G.R.

N82-10037*# Detroit Diesel Allison, Indianapolis, Ind. **PROPULSION STUDY FOR SMALL TRANSPORT AIRCRAFT TECHNOLOGY (STAT) Contractor Final Report** J. C. Gill, R. V. Earle, D. V. Staton, P. C. Stolp, D. S. Huelster, and B. A. Zolezzi 16 Dec. 1980 186 p refs (Contract NAS3-21995) (NASA-CR-185469; DDA-EDR-10470) Avail: NTIS HC A09/MF A01 CSCL 21E

Propulsion requirements were determined for 0.5 and 0.7 Mach aircraft. Sensitivity studies were conducted on both these aircraft to determine parametrically the influence of propulsion characteristics on aircraft size and direct operating cost (DOC). Candidate technology elements and design features were identified and parametric studies conducted to select the STAT advanced engine cycle. Trade off studies were conducted to determine those advanced technologies and design features that would offer a reduction in DOC for operation of the STAT engines. These features were incorporated in the two STAT engines. A benefit assessment was conducted comparing the STAT engines to current technology engines of the same power and to 1985 derivatives of the current technology engines. Research and development programs were recommended as part of an overall technology development plan to ensure that full commercial development of the STAT engines could be initiated in 1988. T.M.

N82-10038*# Detroit Diesel Allison, Indianapolis, Ind. **PROPULSION STUDY FOR SMALL TRANSPORT AIRCRAFT TECHNOLOGY (STAT), APPENDIX B Final Report [1980]** 11 p refs (Contract NAS3-21995) (NASA-CR-185499-App-B; DDA-EDR-10470-App-B) Avail: NTIS HC A02/MF A01 CSCL 21E

Data are tabulated for two conceptual engines designed for small transport aircraft. These are the 1790 W (2400 shp) class engine and the 3579 kW (4800 shp) class engine for the 0.5 M sub N and 0.7 M sub N airplanes, respectively. All data points required to perform the STAT missions are provided including take-off, climb, cruise, loiter, and fuel allowances. The weight, dimensions, price, and maintenance costs are given as well as the installation criteria and equations used for adjusting horsepower for gearbox loss, and converting horsepower to thrust. Scaling equations are included. A.R.H.

N82-10039*# United Technologies Research Center, East Hartford, Conn. **DEVELOPMENT OF LOW MODULUS MATERIAL FOR USE IN CERAMIC GAS PATH SEAL APPLICATIONS Final Report** H. E. Eaton and R. C. Novak Oct. 1981 83 p refs (Contract NAS3-22134) (NASA-CR-165469; R81-915188-13) Avail: NTIS HC A05/MF A01 CSCL 21E

Three candidate materials were examined: Brunsond (R) Pad; plasma sprayed porous NiCrAlY; and plasma sprayed low modulus microcracked zirconia. Evaluation consisted of mechanical, thermophysical, and oxidation resistance testing along with optical microscopy and a feasibility demonstration of attaching the material to a suitable substrate. The goals of the program were the following: feasibility of fastening or depositing the low modulus system onto a broad range of substrate alloys; feasibility of depositing or forming the low modulus system to a thickness of 0.19 cm to 0.38 cm; potential to attain a modulus of elasticity in the range of 3.4 to 6.9 GPa (0.5 to 1.0 MSI), and an ultimate strength of 17.2 MPa (2.5 ksi); suitable thermal conductivity; and static oxidation life of at least 1000 hours at 1311 K. The results of the program indicate that all three systems offer attractive properties as a strain isolator material. T.M.

ORIGINAL PAGE IS
OF POOR QUALITY

N82-10040* General Electric Co., St. Petersburg, Fla.
THERMAL-BARRIER-COATED TURBINE BLADE STUDY
Final Report

P. A. Siemers and W. B. Hillig Aug. 1981 134 p refs
(Contract NAS3-21727)

(NASA-CR-165351; SRD-81-083) Avail: NTIS
HC A07/MF A01 CSCL 21E

The effects of coating TBC on a CF6-50 stage 2 high-pressure turbine blade were analyzed with respect to changes in the mean bulk temperature, cooling air requirements, and high-cycle fatigue. Localized spallation was found to have a possible deleterious effect on low-cycle fatigue life. New blade design concepts were developed to take optimum advantage of TBCs. Process and material development work and rig evaluations were undertaken which identified the most promising combination as ZrO₂ containing 8 w/o Y₂O₃ applied by air plasma spray onto a Ni22Cr-10Al-1Y bond layer. The bond layer was applied by a low-pressure, high-velocity plasma spray process onto the base alloy. During the initial startup cycles the blades experienced localized leading edge spallation caused by foreign objects. T.M.

N82-11068* Teledyne Continental Motors, Muskegon, Mich.
General Products Div
LIGHTWEIGHT DIESEL ENGINE DESIGNS FOR COMMUTER TYPE AIRCRAFT

Alex P. Brouwers Jul. 1981 70 p refs

(Contract NAS3-22149)
(NASA-CR-165470; Rept-995) Avail: NTIS HC A04/MF A01
CSCL 21E

Conceptual designs and performance of advanced technology lightweight diesel engines, suitable for commuter type aircraft power plants are defined. Two engines are discussed, a 1491 kW (2000 SHP) eight-cylinder engine and a 895 kW (1200 SHP) six-cylinder engine. High performance and related advanced technologies are proposed such as insulated cylinders, very high injection pressures and high compressor and turbine efficiencies. The description of each engine includes concept drawings, a performance analysis, and weight data. Fuel flow data are given for full and partial power up to 7620m altitude. The performance data are also extrapolated over a power range from 671 kW(900 SHP) to 1864 kW (2500 SHP). The specific fuel consumption of the 1491 kW (2000 SHP) engine is 182 g/hWh (.299 lb/HPH) at cruise altitude, its weight 620 kg (1365 lb) and specific weight .415 kg/kW (.683 lb/HP). The specific fuel consumption of the 895 kW (1200 SHP) engine is 187 g/hWh (.308 lb/HPH) at cruise altitude, its weight 465 kg (1025 lb) and specific weight .520 kg/kW (.854 lb/HP). R.J.F.

N82-12075* General Electric Co., Lynn, Mass. Aircraft Engine Group.

EFFECT OF A PART SPAN VARIABLE INLET GUIDE VANE ON TF34 FAN PERFORMANCE Final Report

Jose Alvarez and Paul W. Schneider Sep. 1981 133 p refs
(Contract NAS3-21624)

(NASA-CR-165458; RB1AEG030) Avail: NTIS
HC A07/MF A01 CSCL 21E

Experimental aerodynamic and performance data were obtained from a TF34 engine. Part span variable inlet guide vanes mounted in front of the fan on the TF34 engine were tested to demonstrate the feasibility of modulating air flow and thrust for vertical takeoff aircraft systems. The fan was mapped to stall for a range of speeds and variable inlet guide vane settings. Modulated fan tip performance and unmodulated hub performance were evaluated with a without an extended fan bypass splitter. The effect of a crosswind distortion screen on performance was also evaluated. R.J.F.

N82-13145* Pratt and Whitney Aircraft Group, East Hartford, Conn. Commercial Products Div.

SENSOR FAILURE DETECTION SYSTEM Final Report

E. C. Beattie, R. F. LaPrad, M. E. McGlone, S. M. Rock, and M. M. Akhter Aug. 1981 172 p refs Prepared in cooperation with Systems Control, Inc., Palo Alto, Calif.

(Contract NAS3-22481)
(NASA-CR-165515; PWA-5736-17) Avail: NTIS
HC A08/MF A01 CSCL 21E

Advanced concepts for detecting, isolating, and accommodating sensor failures were studied to determine their applicability to the gas turbine control problem. Five concepts were formulated

based upon such techniques as Kalman filters and a screening process led to the selection of one advanced concept for further evaluation. The selected advanced concept uses a Kalman filter to generate residuals, a weighted sum square residuals technique to detect soft failures, likelihood ratio testing of a bank of Kalman filters for isolation, and reconfiguring of the normal mode Kalman filter by eliminating the failed input to accommodate the failure. The advanced concept was compared to a baseline parameter synthesis technique. The advanced concept was shown to be a viable concept for detecting, isolating, and accommodating sensor failures for the gas turbine applications M.G.

N82-14082* General Electric Co., Cincinnati, Ohio. Aircraft Engine Business Group.

CORE COMPRESSOR EXIT STAGE STUDY. VOLUME 4: DATA AND PERFORMANCE REPORT FOR THE BEST STAGE CONFIGURATION Final Report

D. C. Wisler Apr. 1981 204 p refs

(Contract NAS3-20070)
(NASA-CR-165357; R80AEG314-Vol-4) Avail: NTIS
HC A10/MF A01 CSCL 21E

The core compressor exit stage study program develops rear stage blading designs that have lower losses in their endwall boundary layer regions. The test data and performance results for the best stage configuration consisting of Rotor-B running with Stator-B are described. The technical approach in this efficiency improvement program utilizes a low speed research compressor. Tests were conducted in two ways: (1) to use four identical stages of blading to obtain test data in a true multistage environment and (2) to use a single stage of blading to compare with the multistage test results. The effects of increased rotor tip clearances and circumferential groove casing treatment are evaluated. E.A.K.

N82-14093* General Electric Co., Cincinnati, Ohio. Aircraft Engine Business Group.

CORE COMPRESSOR EXIT STAGE STUDY. VOLUME 5: DESIGN AND PERFORMANCE REPORT FOR THE ROTOR C/STATOR B CONFIGURATION

D. C. Wisler May 1981 101 p refs

(Contract NAS3-20070)
(NASA-CR-165358; R81AEG287-Vol-5) Avail: NTIS
HC A06/MF A01 CSCL 21E

Rear stage blading designs that have lower losses in their endwall boundary layer regions were developed. The design of rotor-C and the performance results for rotor-C running with stator B are described. A low speed research compressor is utilized as the principal investigative tool. Four identical stages of blading are used to obtain data in a true multistage environment. E.A.K.

N82-14095* AiResearch Mfg. Co., Phoenix, Ariz.
POLLUTION REDUCTION TECHNOLOGY PROGRAM SMALL JET AIRCRAFT ENGINES, PHASE 3 Final Report

T. W. Bruce, F. G. Davis, T. E. Kuhn, and H. C. Mongia Dec. 1981 180 p refs

(Contract NAS3-20819)
(NASA-CR-165386; AiResearch-21-3615) Avail: NTIS
HC A09/MF A01 CSCL 21E

A series of Model TFE731-2 engine tests were conducted with the Concept 2 variable geometry airblast fuel injector combustion system installed. The engine was tested to: (1) establish the emission levels over the selected points which comprise the Environmental Protection Agency Landing-Takeoff Cycle; (2) determine engine performance with the combustion system; and (3) evaluate the engine acceleration/deceleration characteristics. The hydrocarbon (HC), carbon monoxide (CO), and smoke goals were met. Oxides of nitrogen (NOx) were above the goal for the same configuration that met the other pollutant goals. The engine and combustor performance, as well as acceleration/deceleration characteristics, were acceptable. The Concept 3 staged combustor system was refined from earlier phase development and subjected to further rig refinement testing. The concept met all of the emissions goals. E.A.K.

ORIGINAL PAGE IS
OF POOR QUALITY

N82-14088* AiResearch Mfg. Co., Phoenix, Ariz.
ERBS FUEL ADDENDUM; POLLUTION REDUCTION TECHNOLOGY PROGRAM SMALL JET AIRCRAFT ENGINES, PHASE 3 Final Report
T. W. Bruce, F. G. Davis, T. E. Kuhn, and H. C. Mongia [1982]
47 p refs
(Contract NAS3-20619)
(NASA-CR-165387; AiResearch-21-3619) Avail: NTIS
HC A03/MF A01 CSCL 21E

A Model TFE731-2 engine with a low emission, variable geometry combustion system was tested to compare the effects of operating the engine on Commercial Jet-A aviation turbine fuel and experimental referee broad specification (ERBS) fuels. Low power emission levels were essentially identical while the high power NOx emission indexes were approximately 15% lower with the ERBS fuel. The exhaust smoke number was approximately 50% higher with ERBS at the takeoff thrust setting; however, both values were still below the EPA limit of 40 for the Model TFE731 engine. Primary zone liner wall temperature ran an average of 25 K higher with ERBS fuel than with Jet-A. The possible adoption of broadened properties fuels for gas turbine applications is suggested. E.A.K.

N82-16080* United Technologies Research Center, East Hartford, Conn.
RESEARCH AND DEVELOPMENT PROGRAM FOR NON-LINEAR STRUCTURAL MODELING WITH ADVANCED TIME-TEMPERATURE DEPENDENT CONSTITUTIVE RELATIONSHIPS Final Report
Kevin P. Walker 25 Nov. 1981 187 p refs
(Contract NAS3-22055)
(NASA-CR-165533; PWA-5700-50) Avail: NTIS
HC A09/MF A01 CSCL 21E

Results of a 20-month research and development program for nonlinear structural modeling with advanced time-temperature constitutive relationships are reported. The program included: (1) the evaluation of a number of viscoplastic constitutive models in the published literature; (2) incorporation of three of the most appropriate constitutive models into the MARC nonlinear finite element program; (3) calibration of the three constitutive models against experimental data using Hastelloy-X material; and (4) application of the most appropriate constitutive model to a three dimensional finite element analysis of a cylindrical combustor liner/louver test specimen to establish the capability of the viscoplastic model to predict component structural response. M.D.K.

N82-16081* Pratt and Whitney Aircraft Group, East Hartford, Conn.
STUDY OF CONTROLLED DIFFUSION STATOR BLADING. 1. AERODYNAMIC AND MECHANICAL DESIGN REPORT
E. Canal, B. C. Chisholm, D. Lee, and D. A. Spear Jan. 1981 97 p refs
(Contract NAS3-22008)
(NASA-CR-165500; PWA-5698-28) Avail: NTIS
HC A05/MF A01 CSCL 21E

Pratt & Whitney Aircraft is conducting a test program for NASA in order to demonstrate that a controlled-diffusion stator provides low losses at high loadings and Mach numbers. The technology has shown great promise in wind tunnel tests. Details of the design of the controlled diffusion stator vanes and the multiple-circular-arc rotor blades are presented. The stage, including stator and rotor, was designed to be suitable for the first-stage of an advanced multistage, high-pressure compressor. Author

N82-17174* General Electric Co., Cincinnati, Ohio. Aircraft Engine Group.
CF6 JET ENGINE PERFORMANCE IMPROVEMENT: HIGH PRESSURE TURBINE ROUNDNESS
W. D. Howard and W. A. Fasching Jan. 1982 136 p refs
(Contract NAS3-20629)
(NASA-CR-165555; R82AEB115) Avail: NTIS
HC A07/MF A01 CSCL 21E

An improved high pressure turbine stator reducing fuel consumption in current CF6-50 turbofan engines was developed. The feasibility of the roundness and clearance response improvements was demonstrated. Application of these improvements will result in a cruise SFC reduction of 0.22 percent for new engines.

For high time engines, the improved roundness and response characteristics results in an 0.5 percent reduction in cruise SFC. A basic life capability of the improved HP turbine stator in over 800 simulated flight cycles without any sign of significant distress is shown. E.A.K.

N82-19221* Garrett Turbine Engine Co., Phoenix, Ariz.
COOLED VARIABLE-AREA RADIAL TURBINE TECHNOLOGY PROGRAM Final Report
G. D. Large and L. J. Meyer Jan. 1982 303 p refs
(Contract NAS3-22004)
(NASA-CR-165408) Avail: NTIS HC A14/MF A01 CSCL 21E

The objective of this study was a conceptual evaluation and design analyses of a cooled variable-area radial turbine capable of maintaining nearly constant high efficiency when operated at a constant speed and pressure ratio over a range of flows corresponding to 50- to 100-percent maximum engine power. The results showed that a 1589K (2400 F) turbine was feasible that would satisfy a 4000-hour duty cycle life goal. The final design feasibility is based on 1988 material technology goals. A peak aerodynamic stage total efficiency of 0.88 was predicted at 100 percent power. Two candidate stators were identified; an articulated trailing-edge and a locally movable sidewall. Both concepts must be experimentally evaluated to determine the optimum configuration. A follow-on test program is proposed for this evaluation. Author

N82-21193* National Aeronautics and Space Administration, Lewis Research Center, Cleveland, Ohio.
COLD-AIR PERFORMANCE OF A 15.41-cm-TIP-DIAMETER AXIAL-FLOW POWER TURBINE WITH VARIABLE-AREA STATOR DESIGNED FOR A 75-kW AUTOMOTIVE GAS TURBINE ENGINE Final Report
Kerry L. McLallin, Milton G. Kofskey, and Robert Y. Wong Feb. 1982 33 p refs
(Contract DE-AI01-77CS-51040)
(NASA-TM-82644; E-899; NAS 1.15:82644;
DOE/NASA/51040-20) Avail: NTIS HC A03/MF A01 CSCL 21E

An experimental evaluation of the aerodynamic performance of the axial flow, variable area stator power turbine stage for the Department of Energy upgraded automotive gas turbine engine was conducted in cold air. The interstage transition duct, the variable area stator, the rotor, and the exit diffuser were included in the evaluation of the turbine stage. The measured total blading efficiency was 0.096 less than the design value of 0.85. Large radial gradients in flow conditions were found at the exit of the interstage duct that adversely affected power turbine performance. Although power turbine efficiency was less than design, the turbine operating line corresponding to the steady state road load power curve was within 0.02 of the maximum available stage efficiency at any given speed. Author

N82-21196* Pratt and Whitney Aircraft Group, East Hartford, Conn. Commercial Products Div.
ENERGY EFFICIENT ENGINE SHROUDLESS, HOLLOW FAN BLADE TECHNOLOGY REPORT
C. J. Michael Dec. 1981 91 p refs
(Contract NAS3-20646)
(NASA-CR-165586; NAS 1.26:165586; PWA-5594-199) Avail: NTIS HC A05/MF A01 CSCL 21E

The Shroudless, Hollow Fan Blade Technology program was structured to support the design, fabrication, and subsequent evaluation of advanced hollow and shroudless blades for the Energy Efficient Engine fan component. Rockwell International was initially selected to produce hollow airfoil specimens employing the superplastic forming/diffusion bonding (SPF/DB) fabrication technique. Rockwell demonstrated that a titanium hollow structure could be fabricated utilizing SPF/DB manufacturing methods. However, some problems such as sharp internal cavity radii and unsatisfactory secondary bonding of the edge and root details prevented production of the required quantity of fatigue test specimens. Subsequently, TRW was selected to (1) produce hollow airfoil test specimens utilizing a laminate-core/hot isostatic press/diffusion bond approach, and (2) manufacture full-size hollow prototype fan blades utilizing the technology that evolved from the specimen fabrication effort. TRW established elements of blade design and defined laminate-core/hot isostatic

press/diffusion bonding fabrication techniques to produce test specimens. This fabrication technology was utilized to produce full size hollow fan blades in which the HIP'ed parts were cambered/twisted/isothermally forged, finish machined, and delivered to Pratt & Whitney Aircraft and NASA for further evaluation. Author

N82-21197* # General Electric Co., Cincinnati, Ohio. Aircraft Engine Group.

CF6 JET ENGINE DIAGNOSTICS PROGRAM: HIGH PRESSURE COMPRESSOR CLEARANCE INVESTIGATION

M. A. Radomski Jan. 1982 48 p ref

(Contract NAS3-20631)

(NASA-CR-165580; NAS 1.26:165580; R82AEB189) Avail: NTIS HC A03/MF A01 CSCL 21E

The effects of high pressure compressor clearance changes on engine performance were experimentally determined on a CF6 core engine. The results indicate that a one percent reduction in normalized average clearance, expressed as a fraction of airfoil length, improves compressor efficiency by one percent. Compressor clearances are reduced by the application of rotor bore cooling, insulation of the stator casing, and use of a low coefficient of expansion material in the aft stages. This improvement amounts to a reduction of normalized average clearance of 0.78 percent, relative to CF6-60 compressor, which is equivalent to an improvement in compressor efficiency of 0.78 percent. J.M.S.

N82-22263* # Cessna Aircraft Co., Wichita, Kans. Pawnee Div.

ADVANCED GENERAL AVIATION COMPARATIVE ENGINE/AIRFRAME INTEGRATION STUDY Final Report, Jan. 1980 - Sep. 1981

George L. Huggins and David R. Ellis Sep. 1981 133 p refs (Contract NAS3-22221)

(NASA-CR-165564; NAS 1.26:165564; Cessna-AD-217) Avail: NTIS HC A07/MF A01 CSCL 21E

The NASA Advanced Aviation Comparative Engine/Airframe Integration Study was initiated to help determine which of four promising concepts for new general aviation engines for the 1990's should be considered for further research funding. The engine concepts included rotary, diesel, spark ignition, and turboprop powerplants; a conventional state-of-the-art piston engine was used as a baseline for the comparison. Computer simulations of the performance of single and twin engine pressurized aircraft designs were used to determine how the various characteristics of each engine interacted in the design process. Comparisons were made of how each engine performed relative to the others when integrated into an airframe and required to fly a transportation mission. Author

N82-22264* # Pratt and Whitney Aircraft Group, East Hartford, Conn. Commercial Products Div.

ENERGY EFFICIENT ENGINE EXHAUST MIXER MODEL TECHNOLOGY

H. Kozlowski and M. Larkin Jun. 1981 186 p refs

(Contract NAS3-20646)

(NASA-CR-165459; NAS 1.26:165459; PWA-5594-164) Avail: NTIS HC A09/MF A01 CSCL 21E

An exhaust mixer test program was conducted to define the technology required for the Energy Efficient Engine Program. The model configurations of 1/10 scale were tested in two phases. A parametric study of mixer design options, the impact of residual low pressure turbine swirl, and integration of the mixer with the structural pylon of the nacelle were investigated. The improvement of the mixer itself was also studied. Nozzle performance characteristics were obtained along with exit profiles and oil smear photographs. The sensitivity of nozzle performance to tailpipe length, lobe number, mixer penetration, and mixer modifications like scalloping and cutbacks were established. Residual turbine swirl was found detrimental to exhaust system performance and the low pressure turbine system for Energy Efficient Engine was designed so that no swirl would enter the mixer. The impact of mixer/plug gap was also established, along with importance of scalloping, cutbacks, hoods, and plug angles on high penetration mixers. M.D.K.

N82-22265* # Pratt and Whitney Aircraft Group, East Hartford, Conn. Commercial Products Div.

ADVANCED LOW-EMISSIONS CATALYTIC-COMBUSTOR PROGRAM, PHASE 1 Final Report

G. J. Sturgess Jun. 1981 158 p refs

(Contract NAS3-20821)

(NASA-CR-159656; NAS 1.26:159656; PWA-5589-19;

ESL-TR-79-23) Avail: NTIS HC A08/MF A01 CSCL 21E

Six catalytic combustor concepts were defined, analyzed, and evaluated. Major design considerations included low emissions, performance, safety, durability, installations, operations and development. On the basis of these considerations the two most promising concepts were selected. Refined analysis and preliminary design work was conducted on these two concepts. The selected concepts were required to fit within the combustor chamber dimensions of the reference engine. This is achieved by using a dump diffuser discharging into a plenum chamber between the compressor discharge and the turbine inlet, with the combustors overlaying the pre-diffuser and the rear of the compressor. To enhance maintainability, the outer combustor case for each concept is designed to translate forward for accessibility to the catalytic reactor, liners and high pressure turbine area. The catalytic reactor is self-contained with air-cooled casing on a radiant mounting. Both selected concepts employed integrated engine-starting approaches to raise the catalytic reactor up to operating conditions. Advanced liner schemes are used to minimize required cooling air. The two selected concepts respectively employ fuel-rich initial thermal reaction followed by rapid quench and subsequent fuel-lean catalytic reaction of carbon monoxide, and, fuel-lean thermal reaction of some fuel in a continuously operating pilot combustor with fuel-lean catalytic reaction of remaining fuel in a radially-staged main combustor. Author

N82-22267* # United Technologies Research Center, East Hartford, Conn.

INVESTIGATION OF SOOT AND CARBON FORMATION IN SMALL GAS TURBINE COMBUSTORS Final Report

T. J. Rosfjord Apr. 1982 54 p refs

(Contract NAS3-22524)

(NASA-CR-167853; NAS 1.26:167853;

UTRC-R82-915387-16) Avail: NTIS HC A04/MF A01 CSCL 21E

An investigation of hardware configurations which attempt to minimize carbon and soot-production without sacrificing performance in small gas turbine combustors was conducted. Four fuel injectors, employing either airblast atomization, pressure atomization, or fuel vaporization techniques were combined with nozzle air swirlers and injector sheaths. Eight configurations were screened at sea-level takeoff and idle test conditions. Selected configurations were focused upon in an attempt to quantify the influence of combustor pressure, inlet temperature, primary zone operation, and combustor loading on soot and carbon formation. Cycle tests were also performed. It was found that smoke emission levels depended on the combustor fluid mechanics, the atomization quality of the injector and the fuel hydrogen content. R.J.F.

N82-22268* # Beech Aircraft Corp., Wichita, Kans.

ADVANCED GENERAL AVIATION ENGINE/AIRFRAME INTEGRATION STUDY

Leon A. Zmroczek Mar. 1982 131 p refs

(Contract NAS3-22220)

(NASA-CR-165565; NAS 1.26:165565) Avail: NTIS

HC A07/MF A01 CSCL 21E

A comparison of the in-airframe performance and efficiency of the advanced engine concepts is presented. The results indicate that the proposed advanced engines can significantly improve the performance and economy of general aviation airplanes. The engine found to be most promising is the highly advanced version of a rotary combustion (Wankel) engine. The low weight and fuel consumption of this engine, as well as its small size, make it suited for aircraft use. T.M.

N82-23246* # Pratt and Whitney Aircraft Group, West Palm Beach, Fla. Government Products Div.

COMPUTER MODELING OF FAN-EXIT-SPLITTER SPACING EFFECTS ON F100 RESPONSE TO DISTORTION Final Report

M. Shaw and R. W. Murdoch Mar. 1982 115 p refs

ORIGINAL PAGE IS
OF POOR QUALITY

(Contract NAS3-22739)
(NASA-CR-167879; NAS 1.26:167879; FR-15596) Avail:
NTIS HC A06/MF A01 CSCL 21E

The distortion response of the F100(3) engine was effected by the fan exit splitter configuration. The sensitivity for a proximate splitter fan is calculated to be slightly greater than a remote splitter configuration with identical airfoils. Predicted response was based upon a multiple segment parallel compressor Model modified to include a bypass ratio representation that effects the performance characteristics of the last rotor and intermediate case struts. The predicted distortion response required an accurate definition of row pre- and post-stall undistorted operation. Author

N82-23247*# Notre Dame Univ., Ind. Dept. of Electrical Engineering.

ALTERNATIVES FOR JET ENGINE CONTROL Technical Progress Report, 1 Oct. 1980 - 30 Sep. 1981

Michael K. Sain 1981 140 p refs
(Grant NSG-3048)

(NASA-CR-168894; NAS 1.26:168894; TPR-12) Avail: NTIS HC A07/MF A01 CSCL 21E

Research centered on basic topics in the modeling and feedback control of nonlinear dynamical systems is reported. Of special interest were the following topics: (1) the role of series descriptions, especially insofar as they relate to questions of scheduling, in the control of gas turbine engines; (2) the use of algebraic tensor theory as a technique for parameterizing such descriptions; (3) the relationship between tensor methodology and other parts of the nonlinear literature; (4) the improvement of interactive methods for parameter selection within a tensor viewpoint; and (5) study of feedback gain representation as a counterpart to these modeling and parameterization ideas. Author

N82-23248*# Pratt and Whitney Aircraft Group, East Hartford, Conn.

ANALYSIS OF HIGH LOAD DAMPERS Final Report
S. T. Bhat, D. F. Buono, and D. H. Hibner 21 Aug. 1981
79 p refs

(Contract NAS3-22518)

(NASA-CR-165503; NAS 1.26:165503; PWA-5779-10) Avail:
NTIS HC A05/MF A01 CSCL 21E

High load damping requirements for modern jet engines are discussed. The design of damping systems which could satisfy these requirements is also discussed. In order to evaluate high load damping requirements, engines in three major classes were studied; large transport engines, small general aviation engines, and military engines. Four damper concepts applicable to these engines were evaluated; multi-ring, cartridge, curved beam, and viscous/friction. The most promising damper concept was selected for each engine and performance was assessed relative to conventional dampers and in light of projected damping requirements for advanced jet engines. B.W.

N82-24202*# Garrett Turbine Engine Co., Phoenix, Ariz.
STUDY OF ADVANCED PROPULSION SYSTEMS FOR SMALL TRANSPORT AIRCRAFT TECHNOLOGY (STAT) PROGRAM Final Report

C. F. Baerst, R. W. Heldenbrand, and J. H. Rowse Mar. 1981
119 p refs

(Contract NAS3-21997)

(NASA-CR-165610; NAS 1.26:165610; Garrett-21-3911) Avail:
NTIS HC A06/MF A01 CSCL 21E

Definitions of takeoff gross weight, performance, and direct operating cost for both a 30 and 50 passenger airplane were established. The results indicate that a potential direct operating cost benefit, resulting from advanced technologies, of approximately 20 percent would be achieved for the 1990 engines. Of the numerous design features that were evaluated, only maintenance-related items contributed to a significant decrease in direct operating cost. Recommendations are made to continue research and technology programs for advanced component and engine development. T.M.

N82-25252*# Pennsylvania State Univ., University Park. Lab. of Turbomachinery.

THREE DIMENSIONAL MEAN VELOCITY AND TURBULENCE CHARACTERISTICS IN THE ANNULUS WALL REGION OF AN AXIAL FLOW COMPRESSOR ROTOR PASSAGE

R. Davino and B. Lakshminarayana May 1982 262 p refs
(Grant NSG-3212)

(NASA-CR-189003; NAS 1.26:189003; PSU/TURBO-82-2)
Avail: NTIS HC A12/MF A01 CSCL 21E

The experiment was performed using the rotating hot-wire technique within the rotor blade passage and the stationary hot-wire technique for the exitflow of the rotor blade passage. The measurements reveal the effect of rotation and subsequent flow interactions upon the rotor blade flowfield and wake development in the annulus-wall region. The flow near the rotor blade tips is found to be highly complex due to the interaction of the annulus-wall boundary layer, the blade boundary layers, the tip leakage flow, and the secondary flow. Within the blade passage, this interaction results in an appreciable radial inward flow as well as a defect in the mainstream velocity near the mid-passage. Turbulence levels within this region are very high. This indicates a considerable extent of flow mixing due to the viscous flow interactions. The size and strength of this loss core is found to grow with axial distance from the blade trailing edge. The nature of the rotor blade exit-flow was dominated by the wake development. T.M.

N82-25253*# Pennsylvania State Univ., University Park. Lab. of Turbomachinery.

INVESTIGATION OF THE TIP CLEARANCE FLOW INSIDE AND AT THE EXIT OF A COMPRESSOR ROTOR PASSAGE

A. Pandya and B. Lakshminarayana May 1982 147 p refs
(Grant NSG-3212)

(NASA-CR-189004; NAS 1.26:189004; PSU/TURBO-82-3)
Avail: NTIS HC A07/MF A01 CSCL 21E

The nature of the tip clearance flow in a moderately loaded compressor rotor is studied. The measurements were taken inside the clearance between the annulus-wall casing and the rotor blade tip. These measurements were obtained using a stationary two-sensor hot-wire probe in combination with an ensemble averaging technique. The flowfield was surveyed at various radial locations and at ten axial locations, four of which were inside the blade passage in the clearance region and the remaining six outside the passage. Variations of the mean flow properties in the tangential and the radial directions at various axial locations were derived from the data. Variation of the leakage velocity at different axial stations and the annulus-wall boundary layer profiles from passage-averaged mean velocities were also estimated. B.W.

N82-25254*# General Electric Co., Evendale, Ohio. Materials and Processes Technology Labs.

COST/BENEFIT STUDIES OF ADVANCED MATERIALS TECHNOLOGIES FOR FUTURE AIRCRAFT TURBINE ENGINES: MATERIALS FOR ADVANCED TURBINE ENGINES

M. Stearns and L. Wilbers May 1982 49 p

(Contract NAS3-20074)

(NASA-CR-167849; NAS 1.26:167849) Avail: NTIS HC A03/MF A01 CSCL 21E

Cost benefit studies were conducted on six advanced materials and processes technologies applicable to commercial engines planned for production in the 1985 to 1990 time frame. These technologies consisted of thermal barrier coatings for combustor and high pressure turbine airfoils, directionally solidified eutectic high pressure turbine blades, (both cast and fabricated), and mixers, tail cones, and piping made of titanium-aluminum alloys. A fabricated titanium fan blisk, an advanced turbine disk alloy with improved low cycle fatigue life, and a long-life high pressure turbine blade abrasive tip and ceramic shroud system were also analyzed. Technologies showing considerable promise as to benefits, low development costs, and high probability of success were thermal barrier coating, directionally solidified eutectic turbine blades, and abrasive-tip blades/ceramic-shroud turbine systems. R.J.F.

ORIGINAL PAGE IS
OF POOR QUALITY

N82-26257* United Technologies Corp., East Hartford, Conn. Commercial Products Div.
FRACTURE MECHANICS CRITERIA FOR TURBINE ENGINE HOT SECTION COMPONENTS Final Report
G. J. Meyers May 1982 123 p refs
(Contract NAS3-22550)
(NASA-CR-167896; NAS 1.26:167896; PWA-5772-23) Avail: NTIS HC A06/MF A01 CSCL 21E

The application of several fracture mechanics data correlation parameters to predicting the crack propagation life of turbine engine hot section components was evaluated. An engine survey was conducted to determine the locations where conventional fracture mechanics approaches may not be adequate to characterize cracking behavior. Both linear and nonlinear fracture mechanics analyses of a cracked annular combustor liner configuration were performed. Isothermal and variable temperature crack propagation tests were performed on Hastelloy X combustor liner material. The crack growth data was reduced using the stress intensity factor, the strain intensity factor, the J integral, crack opening displacement, and Tomkins' model. The parameter which showed the most effectiveness in correlation high temperature and variable temperature Hastelloy X crack growth data was crack opening displacement. S.L.

N82-26295* Pennsylvania State Univ., University Park
INVESTIGATION OF SPRAY CHARACTERISTICS FOR FLASHING INJECTION OF FUELS CONTAINING DISSOLVED AIR AND SUPERHEATED FUELS Final Report, 1 Aug. 1980 - 31 Aug. 1981
A. S. P. Solomon, L. D. Chen, and G. M. Faeth Washington
NASA Jun. 1982 90 p refs
(Grant Nsg-3306)
(NASA-CR-3563; NAS 1.26:3563) Avail: NTIS HC A05/MF A01 CSCL 21E

The flow, atomization and spreading of flashing injector flowing liquids containing dissolved gases (jet/air) as well as superheated liquids (Freon II) were considered. The use of a two stage expansion process separated by an expansion chamber, was found to be beneficial for flashing injection particularly for dissolved gas systems. Both locally homogeneous and separated flow models provided good predictions of injector flow properties. Conventional correlations for drop sizes from pressure atomized and airblast injectors were successfully modified, using the separated flow model to prescribe injector exit conditions, to correlate drop size measurements. Additional experimental results are provided for spray angle and combustion properties of sprays from flashing injectors. Author

N82-27308* Pratt and Whitney Aircraft Group, East Hartford, Conn.
PERFORMANCE DETERIORATION DUE TO ACCEPTANCE TESTING AND FLIGHT LOADS; JT9D JET ENGINE DIAGNOSTIC PROGRAM
W. J. Olsson, 22 Jan. 1982 147 p refs
(Contract NAS3-20632)
(NASA-CR-165572; NAS 1.26:165572; PWA-5512-87) Avail: NTIS HC A07/MF A01 CSCL 21E

The results of a flight loads test of the JT9D-7 engine are presented. The goals of this test program were to: measure aerodynamic and inertia loads on the engine during flight, explore the effects of airplane gross weight and typical maneuvers on these flight loads, simultaneously measure the changes in engine running clearances and performance resulting from the maneuvers, make refinements of engine performance deterioration prediction models based on analytical results of the tests, and make recommendations to improve propulsion system performance retention. The test program included a typical production airplane acceptance test plus additional flights and maneuvers to encompass the range of flight loads in revenue service. The test results indicated that aerodynamic loads, primarily at take-off, were the major cause of rub-induced that aerodynamic loads, primarily at take-off, were the major cause of rub-induced deterioration in the cold section of the engine. Differential thermal expansion between rotating and static parts plus aerodynamic loads combined to cause blade-to-seal rubs in the turbine. B.W.

N82-27310* General Electric Co., Cincinnati, Ohio. Aircraft Engine Business Group.
CORE COMPRESSOR EXIT STAGE STUDY, VOLUME 6 Final Report, Oct. 1976 - Dec. 1981
D. C. Wisler Dec. 1981 97 p refs
(Contract NAS3-20070)
(NASA-CR-165554; NAS 1.26:165554; GE-R81AEG288) Avail: NTIS HC A05/MF A01 CSCL 21E

Rear stage blading designs that have lower losses in their endwall boundary layer regions were studied. A baseline Stage A was designed as a low-speed model of stage 7 of a 10-stage compressor. Candidate rotors and stators were designed which have the potential of reducing endwall losses relative to the baseline. Rotor B uses a type of meanline in the tip region that unloads the leading edge and loads the trailing edge relative to the baseline rotor A designs. Rotor C incorporates a more skewed (hub strong) radial distribution of total pressure and smoother distribution of static pressure on the rotor tip than those of rotor B. Candidate stator B embodies twist gradients in the endwall region. Stator C embodies airfoil sections near the endwalls that have reduced trailing edge loading relative to stator A. The baseline and candidate bladings were tested using four identical stages to produce a true multistage environment. Single-stage tests were also conducted. The test data were analyzed and performances were compared. Several of the candidate configurations showed a performance improvement relative to the baseline. A.R.H.

N82-27316* Naval Air Propulsion Test Center, Trenton, N.J. Propulsion Technology and Project Engineering Dept.
ROTOR FRAGMENT PROTECTION PROGRAM: STATISTICS ON AIRCRAFT GAS TURBINE ENGINE ROTOR FAILURES THAT OCCURRED IN U.S. COMMERCIAL AVIATION DURING 1976 Final Report, 1977 - 1978
R. A. DeLucia and J. T. Salvino Sep. 1981 30 p
(NASA Order C-41581-B)
(NASA-CR-165388; NAS 1.26:165388; AD-A113767; NACP-PE-23) Avail: NTIS HC A03/MF A01 CSCL 21/5

This report presents statistical information relating to the number of gas turbine engine rotor failures which occurred in commercial aviation service use. The predominant failure involved blade fragments, 82.4 percent of which were contained. Although fewer rotor rim, disk, and seal failures occurred, 33.3%, 100% and 50% respectively were uncontained. Sixty-five percent of the 16% rotor failures occurred during the takeoff and climb stages of flight. Author (GRA)

N82-28296* Pratt and Whitney Aircraft Group, East Hartford, Conn. Commercial Products Div.
B747/JT9D FLIGHT LOADS AND THEIR EFFECT ON ENGINE RUNNING CLEARANCES AND PERFORMANCE DETERIORATION; BCAC NAIL/P AND WA JT9D ENGINE DIAGNOSTICS PROGRAMS
W. J. Olsson and R. L. Martin 19 Feb. 1982 74 p refs
Prepared in cooperation with Boeing Commercial Airplane Co., Seattle
(Contracts NAS3-20632; NAS1-15325)
(NASA-CR-165573; NAS 1.26:165573; PWA-5512-88) Avail: NTIS HC A04/MF A01 CSCL 21E

Flight loads on the 747 propulsion system and resulting JT9D blade to outer airseal running clearances during representative acceptance flight and revenue flight sequences were measured. The resulting rub induced clearance changes, and engine performance changes were then analyzed to validate and refine the JT9D-7A short term performance deterioration model. Author

N82-28297* General Electric Co., Cincinnati, Ohio. Aircraft Engine Group.
CF6 JET ENGINE PERFORMANCE IMPROVEMENT; HIGH PRESSURE TURBINE ACTIVE CLEARANCE CONTROL
S. E. Rich and W. A. Fasching Jun. 1982 136 p refs
(Contract NAS3-20629)
(NASA-CR-165556; NAS 1.26:165556; R82AEB198) Avail: NTIS HC A07/MF A01 CSCL 21E

An active clearance control system was developed which reduces fuel consumption and performance degradation. This system utilizes compressor discharge air during takeoff and fan

ORIGINAL PAGE
OF POOR QUALITY

discharge air during cruise to impinge on the shroud structure to improve the thermal response. The system was evaluated in component and engine tests. The test results demonstrated a performance improvement of 0.7 percent in cruise SFC. S.I.

N82-29323*# Teledyne CAE, Toledo, Ohio.
COOLED VARIABLE NOZZLE RADIAL TURBINE FOR ROTOR CRAFT APPLICATIONS
C. Rogo Mar 1981 205 p refs
(Contract NAS3-22005; DA Proj. 1L1-62209-AH-76)
(NASA-CR-165397; NAS 1.26:165397; Rept-1759) Avail: NTIS HC A10/MF A01 CSCL 21E

An advanced, small 2.27 kb/sec (5 lbs/sec), high temperature, variable area radial turbine was studied for a rotor craft application. Variable capacity cycles including single-shaft and free-turbine engine configurations were analyzed to define an optimum engine design configuration. Parametric optimizations were made on cooled and uncooled rotor configurations. A detailed structural and heat transfer analysis was conducted to provide a 4000-hour life HP turbine with material properties of the 1988 time frame. A pivoted vane and a moveable sidewall geometry were analyzed. Cooling and variable geometry penalties were included in the cycle analysis. A variable geometry free-turbine engine configuration with a design 1477 K (2200 F) inlet temperature and a compressor pressure ratio of 16.1 was selected. An uncooled HP radial turbine rotor with a moveable sidewall nozzle showed the highest performance potential for a time weighted duty cycle
Author

N82-31328*# Georgia Inst. of Tech., Atlanta. School of Aerospace Engineering.
DEVELOPMENT OF A SPINNING WAVE HEAT ENGINE Final Report
B. T. Zinn, E. A. Powell, and J. E. Hubbart Aug. 1982 100 p refs
(Grant NAG3-96)
(NASA-CR-165611; NAS 1.26:165611) Avail: NTIS HC A05/MF A01 CSCL 21E

A theoretical analysis and an experimental investigation were conducted to assess the feasibility of developing a spinning wave heat engine. Such an engine would utilize a large amplitude traveling acoustic wave rotating around a cylindrical chamber, and it should not suffer from the inefficiency, noise, and intermittent thrust which characterizes pulse jet engines. The objective of this investigation was to determine whether an artificially driven large amplitude spinning transverse wave could induce a steady flow of air through the combustion chamber under cold flow conditions. In the theoretical analysis the Maslari and Moore perturbation technique was extended to study flat cylinders (pancake geometry) with completely open side walls and a central opening. In the parallel experimental study, a test model was used to determine resonant frequencies and radial pressure distributions, as well as oscillatory and steady flow velocities at the inner and outer peripheries. The experimental frequency was nearly the same as the theoretical acoustic value for a model of the same outer diameter but without a central hole. Although the theoretical analysis did not predict a steady velocity component, simultaneous measurements of hotwire and microphone responses have shown that the spinning wave pumps a mean flow radially outward through the cavity.
Author

N82-32367*# Avco Lycoming Div., Stratford, Conn.
SMALL AXIAL TURBINE STATOR TECHNOLOGY PROGRAM Final Report
W. Brockett and A. Kozak Apr. 1982 89 p refs
(Contract NAS3-22109; DA Proj. 1L1-62209-AH-76)
(NASA-CR-165602; NAS 1.26:165602; LYC-82-15) Avail: NTIS HC A05/MF A01 CSCL 21E

An experimental investigation was conducted to determine the effects of surface finish, fillet radius, inlet boundary layer thickness, and free-stream inlet turbulence level on the aerodynamic performance of a small axial flow turbine stator. The principal objective of this program was to help understand why large turbine efficiency is not maintained when a large turbine is scaled to a smaller size.

The stator used in this program as a one-sixth scale of a 762 mm (30 in.) diameter stator design with 50 vanes having a vane height of 17 mm (0.666 in.) and an aspect ratio of 1.77. A comprehensive overall test matrix was used to provide a complete engineering understanding of the effects of each variable over the full range of all the other variables. The range of each variable investigated was as follows: surface finish 0.1 micro (4 micro in.) to 2.4 micro (95 micro in.); boundary layer thickness 2 to 25 percent of channel height at each wall; fillet radius 0 mm (0 in.) to 1.0 mm (.040 in.) and turbulence 2 to 12 percent.
Author

N82-32370*# Lockheed-Georgia Co., Marietta.
ADVANCED TURBOPROP TESTBED SYSTEMS STUDY. VOLUME 1: TESTBED PROGRAM OBJECTIVES AND PRIORITIES, DRIVE SYSTEM AND AIRCRAFT DESIGN STUDIES, EVALUATION AND RECOMMENDATIONS AND WIND TUNNEL TEST PLANS

E. S. Bradley, B. H. Little, W. Warnock, C. M. Jenness, J. M. Wilson, C. W. Powell, and L. Shoaf Cleveland, Ohio NASA. Lewis Research Center Jul. 1982 368 p refs 2 Vol.
(Contract NAS3-22346)
(NASA-CR-167928-Vol-1; NAS 1.26:167928-Vol-1; LG81ER0202-Vol-1) Avail: NTIS HC A16/MF A01 CSCL 21E

The establishment of propfan technology readiness was determined and candidate drive systems for propfan application were identified. Candidate testbed aircraft were investigated for testbed aircraft suitability and four aircraft selected as possible propfan testbed vehicles. An evaluation of the four candidates was performed and the Boeing KC-135A and the Gulfstream American Gulfstream II recommended as the most suitable aircraft for test application. Conceptual designs of the two recommended aircraft were performed and cost and schedule data for the entire testbed program were generated. The program total cost was estimated and a wind tunnel program cost and schedule is generated in support of the testbed program.
E.A.K.

N82-33390*# Akron Univ., Ohio. Dept. of Mechanical and Civil Engineering.
ENGINE DYNAMIC ANALYSIS WITH GENERAL NONLINEAR FINITE ELEMENT CODES. PART 2: BEARING ELEMENT IMPLEMENTATION OVERALL NUMERICAL CHARACTERISTICS AND BENCHMARKING
J. Padovan, M. Adams, J. Fertis, I. Zeld, and P. Lam Oct. 1982 229 p refs
(Grant NSG-3283)
(NASA-CR-167944; NAS 1.26:167944) Avail: NTIS HC A11/MF A01 CSCL 21E

Finite element codes are used in modelling rotor-bearing-stator structure common to the turbine industry. Engine dynamic simulation is used by developing strategies which enable the use of available finite element codes. Benchmarking the elements developed are benchmarked by incorporation into a general purpose code (ADINA); the numerical characteristics of finite element type rotor-bearing-stator simulations are evaluated through the use of various types of explicit/implicit numerical integration operators. Improving the overall numerical efficiency of the procedure is improved.
S.L.

N82-33391*# Pratt and Whitney Aircraft Group, East Hartford, Conn. Commercial Products Div.
STRUCTURAL TAILORING OF ENGINE BLADES (STAEBL) Interim Report
C. E. Platt, T. K. Pratt, and K. W. Brown Jun. 1982 359 p refs
(Contract NAS3-22525)
(NASA-CR-167949; NAS 1.26:167949; PWA-5774-21) Avail: NTIS HC A16/MF A01 CSCL 21E

A mathematical optimization procedure was developed for the structural tailoring of engine blades and was used to structurally tailor two engine fan blades constructed of composite materials without midspan shrouds. The first was a solid blade made from superhybrid composites, and the second was a hollow blade with

metal matrix composite inlays. Three major computerized functions were needed to complete the procedure: approximate analysis with the established input variables, optimization of an objective function, and refined analysis for design verification. S.L.

N82-33392* # Teledyne Continental Motors, Mobile, Ala. Aircraft Products Div.

EXHAUST EMISSIONS REDUCTION FOR INTERMITTENT COMBUSTION AIRCRAFT ENGINES Final Report

Bernard J. Rezy, Kenneth J. Stuckas, J. Ronald Tucker, and Jay E. Meyers May 1982 55 p refs

(Contract NAS3-19755)

(NASA-CR-167914; NAS 1.26:167914) Avail: NTIS HC A04/MF A01 CSCL 21E

Three concepts which, to an aircraft piston engine, provide reductions in exhaust emissions of hydrocarbons and carbon monoxide while simultaneously improving fuel economy. The three chosen concepts, (1) an improved fuel injection system, (2) an improved cooling cylinder head, and (3) exhaust air injection, when combined, show a synergistic relationship in achieving these goals. In addition, the benefits of variable ignition timing were explored and both dynamometer and flight testing of the final engine configuration were accomplished. S.L.

N82-33393* # General Electric Co., Cincinnati, Ohio. Aircraft Engine Group.

THE CF6 JET ENGINE PERFORMANCE IMPROVEMENT: LOW PRESSURE TURBINE ACTIVE CLEARANCE CONTROL

B. D. Beck and W. A. Fasching Jun. 1982 159 p refs

(Contract NAS3-20629)

(NASA-CR-165557; NAS 1.26:165557; R82AEB462) Avail: NTIS HC A08/MF A01 CSCL 21E

A low pressure turbine (LPT) active clearance control (ACC) cooling system was developed to reduce the fuel consumption of current CF6-50 turbofan engines for wide bodied commercial aircraft. The program performance improvement goal of 0.3% delta sfc was determined to be achievable with an improved impingement cooling system. The technology enables the design of an optimized manifold and piping system which is capable of a performance gain of 0.45% delta sfc. E.A.K.

N82-33394* # Pratt and Whitney Aircraft Group, East Hartford, Conn. Commercial Products Div.

ENERGY EFFICIENT ENGINE: TURBINE TRANSITION DUCT MODEL TECHNOLOGY REPORT

K. Leach and R. Thurlin Aug. 1982 113 p refs

(Contract NAS3-20646)

(NASA-CR-167996; NAS 1.26:167996; PWA-5594-215) Avail: NTIS HC A06/MF A01 CSCL 21E

The Low-Pressure Turbine Transition Duct Model Technology Program was directed toward substantiating the aerodynamic definition of a turbine transition duct for the Energy Efficient Engine. This effort was successful in demonstrating an aerodynamically viable compact duct geometry and the performance benefits associated with a low camber low-pressure turbine inlet guide vane. The transition duct design for the flight propulsion system was tested and the pressure loss goal of 0.7 percent was verified. Also, strut fairing pressure distributions, as well as wall pressure coefficients, were in close agreement with analytical predictions. Duct modifications for the integrated core/low spool were also evaluated. The total pressure loss was 1.59 percent. Although the increase in exit area in this design produced higher wall loadings, reflecting a more aggressive aerodynamic design, pressure profiles showed no evidence of flow separation. Overall, the results acquired have provided pertinent design and diagnostic information for the design of a turbine transition duct for both the flight propulsion system and the integrated core/low spool. J.M.S.

A82-10457* # Effects of vane/blade ratio and spacing on fan noise. R. A. Kantola (General Electric Co., Power Generation Group, Lynn, MA) and P. R. Gjebe (General Electric Co., Aircraft Engine Group, Cincinnati, OH). *American Institute of Aeronautics and Astronautics, Aerodynamics Conference, 7th, Palo Alto, CA, Oct. 5-7, 1981, Paper 81-2033*. 16 p. 11 refs. Contract No. NAS3-22062.

The effects of vane/blade ratio and spacing on fan noise are investigated to develop a fan noise prediction scheme which is calibrated against experimental data. A 44 blade, 0.504 diameter fan is used to demonstrate the production of fan noise data free from excess noise caused by rotor turbulence interaction. Two stator sets consisting of a cut-off set with 86 vanes, and a cut-on set of 48 vanes are used, with a total range of spacing from 0.5 to 2.3 rotor chords. The model includes viscous wake interaction noise and the potential field interactions of both the rotor and stator. A free-field acoustic environment is achieved by covering the walls, ceiling and floor with 0.7 m polyurethane foam wedges, providing less than + or - 1 dB standing wave ratio at 200 Hz. Only a 3 dB drop in tone level occurs as the spacing is increased from 0.5 to 2.3 rotor chords, and results indicate that the rotor wakes impinging on the stator vanes are the principal noise source for subsonic rotor speeds. D.L.G.

A82-11999* # Thermal expansion accommodation in a jet engine frame. M. H. Schneider (General Electric Co., Cincinnati, OH). *(American Society of Mechanical Engineers, Gas Turbine Conference and Products Show, Houston, TX, Mar. 9-12, 1981.) ASME Transactions, Journal of Engineering for Power*, vol. 103, Oct. 1981, p. 776-780. Contract No. NAS3-20643.

Design advancements to enhance stress accommodation in gas turbine engine frames are described. Consideration is given to mechanical stiffness to maintain an adequate spring rate, and to thermal stresses in both ambient and transient modes. Noting that thermal stresses occur due to differing temperatures at different parts of the frame, the matching of the thermal expansion rates of different structural materials is emphasized. Adequate stiffness is necessary to avoid dynamic reactions leading to case cracking as a result of normal imbalances of moving parts. Stress and deflection analysis of a total frame concept using a three-dimensional finite element stress analysis computer program, with modelling of all frame components, is presented, and illustrations are provided. M.S.K.

A82-12120* # On the prediction of swirling flowfields found in axisymmetric combustor geometries. D. L. Rhode, D. G. Lilley, and D. K. McLaughlin (Oklahoma State University, Stillwater, OK). In: *Fluid mechanics of combustion systems; Proceedings of the Fluids Engineering Conference, Boulder, CO, June 22, 23, 1981, (A82-12101 02-34)* New York, American Society of Mechanical Engineers, 1981, p. 257-266. 32 refs. Grant No. NAG3-74.

The paper reports research restricted to steady turbulence flow in axisymmetric geometries under low speed and nonreacting conditions. Numerical computations are performed for a basic two-dimensional axisymmetrical flow field similar to that found in a conventional gas turbine combustor. Calculations include a stairstep boundary representation of the expansion flow, a conventional k-epsilon turbulence model and realistic accommodation of swirl effects. A preliminary evaluation of the accuracy of computed flowfields is accomplished by comparisons with flow visualizations using neutrally-buoyant helium-filled soap bubbles as tracer particles. Comparisons of calculated results show good agreement, and it is found that a problem in swirling flows is the accuracy with which the sizes and shapes of the recirculation zones may be predicted, which may be attributed to the quality of the turbulence model. D.L.G.

A82-16909* # V/STOL propulsion control technology. H. Brown (General Electric Co., Cincinnati, OH). *American Institute of Aeronautics and Astronautics and NASA Ames Research Center, V/STOL Conference, Palo Alto, CA, Dec. 7-9, 1981, AIAA Paper 81-2634*. 10 p. Contract No. NAS3-22057.

Results of a NASA sponsored study of V/STOL Propulsion Control Analysis are presented. The study involved propulsion control requirements, design concepts and procedures, and control designs for supersonic V/STOL. A variable cycle engine with a

ORIGINAL PAGE IS
OF POOR QUALITY

remote augmented lift system was used as a basis for establishing typical operating requirements and control concepts, and a nonlinear engine model was developed for control development as a precursor to a real-time simulation capability. A simplified aircraft model was also used to investigate transition requirements, and a long-range technology plan was developed to define subsequent program requirements for achieving a real-time piloted simulation capability. D.L.G.

A82-17788 * # A simple finite difference procedure for the vortex controlled diffuser. A. A. Busnalna and D. G. Lilley (Oklahoma State University, Stillwater, OK). *American Institute of Aeronautics and Astronautics, Aerospace Sciences Meeting, 20th, Orlando, FL, Jan. 11-14, 1982, Paper 82-0109*. 9 p. 21 refs. USAF-supported research; Grant No. NAG3-74.

A simple prediction procedure for sudden expansion incompressible flows is developed and applied to the vortex controlled diffuser. Transient Navier-Stokes equations of an incompressible fluid are solved by means of their associated finite difference equations in terms of the primitive pressure velocity variables. A computer code is developed using a laminar flow simulation with free slip or no slip wall boundary conditions. In addition, predicted results confirm that effectiveness increases with increases in duct length and bleed flow rate. D.L.G.

A82-17796 * # An iterative finite element-integral technique for predicting sound radiation from turbofan inlets in steady flight. S. J. Horowitz, R. K. Sigman, and B. T. Zinn (Georgia Institute of Technology, Atlanta, GA). *American Institute of Aeronautics and Astronautics, Aerospace Sciences Meeting, 20th, Orlando, FL, Jan. 11-14, 1982, Paper 82-0124*. 9 p. 23 refs. Grant No. NSG-3036.

A new iterative solution technique for predicting the sound field radiated from a turbofan inlet in steady flight is presented. The sound field is divided into two regions: the sound field within and near the inlet which is computed using the finite element method and the radiation field beyond the inlet which is calculated using an integral solution technique. A continuous solution is obtained by matching the finite element and integral solutions at the interface between the two regions. The applicability of the iterative technique is demonstrated by comparison of experimental results with the theoretical results for several different inlet configurations with and without flow. These examples show that good agreement between experiment and theory is obtained within five iterations. (Author)

A82-17836 * # Water ingestion into jet engine axial compressors. T. Tsuchiya and S. N. B. Murthy (Purdue University, West Lafayette, IN). *American Institute of Aeronautics and Astronautics, Aerospace Sciences Meeting, 20th, Orlando, FL, Jan. 11-14, 1982, Paper 82-0196*. 11 p. 14 refs. Contract No. F33615-78-C-2401; Grant No. NAG3-62.

An axial flow compressor has been tested with water droplet ingestion under a variety of conditions. The results illustrate the manner in which the compressor pressure ratio, efficiency and surging characteristics are affected. A model for estimating the performance of a compressor during water ingestion has been developed and the predictions obtained compare favorably with the test results. It is then shown that with respect to five droplet-associated nonlinearly-interacting processes (namely, droplet-blade interactions, blade performance changes, centrifugal action, heat and mass transfer processes and droplet break-up), the initial water content and centrifugal action play the most dominant roles. (Author)

A82-34982 * # Blade loss transient dynamic analysis of turbomachinery. M. J. Stallone, V. Gallardo, A. F. Storage, L. J. Bach, G. Black, and E. F. Gaffney (General Electric Co., Cincinnati, OH). *AIAA, SAE, and ASME, Joint Propulsion Conference, 18th, Cleveland, OH, June 21-23, 1982, AIAA Paper 82-1057*. 8 p. Contract No. NAS3-22053.

This paper reports on work completed to develop an analytical method for predicting the transient non-linear response of a complete aircraft engine system due to the loss of a fan blade, and to validate the analysis by comparing the results against actual blade loss test data. The solution, which is based on the

component element method, accounts for rotor-to-casing rubs, high damping and rapid deceleration rates associated with the blade loss event. A comparison of test results and predicted response show good agreement except for an initial overshoot spike not observed in test. The method is effective for analysis of large systems. (Author)

A82-35081 * # A comprehensive method for preliminary design optimization of axial gas turbine stages. R. M. Jenkins (Tuskegee Institute, Tuskegee, AL). *AIAA, SAE, and ASME, Joint Propulsion Conference, 18th, Cleveland, OH, June 21-23, 1982, AIAA Paper 82-1264*. 11 p. 15 refs. Grant No. NSG-3295.

A method is presented that performs a rapid, reasonably accurate preliminary pitchline optimization of axial gas turbine annular flowpath geometry, as well as an initial estimate of blade profile shapes, given only a minimum of thermodynamic cycle requirements. No geometric parameters need be specified. The following preliminary design data are determined: (1) the optimum flowpath geometry, within mechanical stress limits; (2) initial estimates of cascade blade shapes; (3) predictions of expected turbine performance. The method uses an inverse calculation technique whereby blade profiles are generated by designing channels to yield a specified velocity distribution on the two walls. Velocity distributions are then used to calculate the cascade loss parameters. Calculated blade shapes are used primarily to determine whether the assumed velocity loadings are physically realistic. Model verification is accomplished by comparison of predicted turbine geometry and performance with four existing single stage turbines. C.D.

A82-35384 * # The influence of Coriolis forces on gyroscopic motion of spinning blades. F. Sisto, A. Chang, and M. Sutcu (Stevens Institute of Technology, Hoboken, NJ). *American Society of Mechanical Engineers, International Gas Turbine Conference and Exhibit, 27th, London, England, Apr. 18-22, 1982, Paper 82-GT-163*. 6 p. 5 refs. Members, \$2.00; nonmembers, \$4.00. Grant No. NAG3-47.

Turbomachine blades on spinning and precessing rotors experience gyroscopically induced instabilities and forcing. With vehicle-mounted turbomachines, either constant or harmonic precession occurs, depending on vehicle or mount motion. Responses of uniform cantilever beams at arbitrary stagger, subjected to the noted rotor motion, are predicted in both self-excited and forced-excitation modes taking into account Coriolis acceleration. (Author)

A82-35450 * # Progress in the development of energy efficient engine components. R. W. Bucy (General Electric Co., Cincinnati, OH). *American Society of Mechanical Engineers, International Gas Turbine Conference and Exhibit, 27th, London, England, Apr. 18-22, 1982, Paper 82-GT-275*. 7 p. 8 refs. Members, \$2.00; nonmembers, \$4.00. Contract No. NAS3-20643.

Component test results are presented for the NASA Energy Efficient Engine program, whose design goals relative to the CF6-50C reference engine include a 12% reduction in specific fuel consumption, 5% reduction in direct operating costs, and 50% reduction in specific fuel consumption deterioration rate over the course of commercial service. Emphasis is placed on the engine's high pressure compressor, which has a design pressure ratio of 23:1, and has completed a series of component tests whose resulting configuration is expected to meet all major objectives of the program. Descriptions are given of the core engine and integrated core/low spool tests, and system test benefits are discussed. Attention is given to the design features of the engine's double annular combustor, high and low pressure air turbines, and scale model exhaust mixer. O.C.

ORIGINAL PAGE IS
OF POOR QUALITY

09 RESEARCH AND SUPPORT FACILITIES (AIR)

Includes airports, hangars and runways; aircraft repair and overhaul facilities; wind tunnels; shock tube facilities; and engine test blocks.

For related information, see also 14 *Ground Support Systems and Facilities (Space)*.

N82-19221* # National Aeronautics and Space Administration, Lewis Research Center, Cleveland, Ohio.

THE AEROSPACE TECHNOLOGY LABORATORY (A PERSPECTIVE, THEN AND NOW)

James F. Connors and Robert G. Hoffman Feb. 1982 21 p refs

(NASA-TM-82754; E-1070) Avail: NTIS HC A02/MF A01 CSCL 14B

The physical changes that have taken place in aerospace facilities since the Wright brothers' accomplishment 78 years ago are highlighted. For illustrative purposes some of the technical facilities and operations of the NASA Lewis Research Center are described. These simulation facilities were designed to support research and technology studies in aerospace propulsion. Author

N82-32383* # Pratt and Whitney Aircraft Group, East Hartford, Conn. Energy Efficient Engine Component Development and Integration Program.

ENERGY EFFICIENT ENGINE: HIGH PRESSURE TURBINE UNCOOLED RIG TECHNOLOGY REPORT

W. B. Gardner Oct. 1979 242 p refs

(Contract NAS3-20646)

(NASA-CR-165149; NAS 1.26:165149; PWA-5594-92) Avail: NTIS HC A11/MF A01 CSCL 14B

Results obtained from testing five performance builds (three vane cascades and two rotating rigs of the Energy Efficient Engine uncooled rig have established the uncooled aerodynamic efficiency of the high-pressure turbine at 91.1 percent. This efficiency level was attained by increasing the rim speed and annulus area (AN(2)), and by increasing the turbine reaction level. The increase in AN(2) resulted in a performance improvement of 1.15 percent. At the design point pressure ratio, the increased reaction level rig demonstrated an efficiency of 91.1 percent. The results of this program have verified the aerodynamic design assumptions established for the Energy Efficient Engine high-pressure turbine component. Author

ORIGINAL PAGE IS
OF POOR QUALITY

13 ASTRODYNAMICS

Includes powered and free-flight trajectories; and orbit and launching dynamics.

N82-26336* # National Aeronautics and Space Administration
Lewis Research Center, Cleveland, Ohio.

MATERIAL AND PROCESSING NEEDS FOR SILICON SOLAR CELLS IN SPACE

Henry W. Brandhorst, Jr. In NASA, Marshall Space Flight Center Float Zone Workshop Sep. 1981 p 33-41 (For primary document see N82-26330 17-12)

Avail. NTIS HC A10/MF A01 CSCL 22A

The technical concerns of NASA in the area of space grade solar cells are summarized. Solar power needs are projected through 1987. The degradation of solar cell performance due to the effects of radiation on impurities and crystal defects and the improved performance of float zone silicon are illustrated. The reduction of oxygen and carbon in float zone silicon allows for much faster low temperature annealing of the defects. The effects of improved crystal purity on cell performance are summarized.

J.D.

ORIGINAL PAGE IS
OF POOR QUALITY

A82-35617 * # **A small scale lunar launcher for early lunar material utilization.** W. R. Snow, J. A. Kubby, and R. S. Dunbar (Princeton University, Princeton, NJ). In: Space manufacturing 4; Proceedings of the Fifth Conference, Princeton, NJ, May 18-21, 1981. (A82-35601 17-12) New York, American Institute of Aeronautics and Astronautics, 1981, p. 157-171, 12 refs. Grant No. NSG-3176.

A system for the launching of lunar derived oxygen or raw materials into low lunar orbit or to L2 for transfer to low earth orbit is presented. The system described is a greatly simplified version of the conventional and sophisticated approach suggested by O'Neill using mass drivers with recirculating buckets. An electromagnetic accelerator is located on the lunar surface which launches 125 kg 'smart' containers of liquid oxygen or raw materials into a transfer orbit. Upon reaching apolune a kick motor is fired to circularize the orbit at 100 km altitude or L2. These containers are collected and their payloads transferred to a tanker OTV. The empty containers then have their kick motors refurbished and then are returned to the launcher site on the lunar surface for reuse. Initial launch capability is designed for about 500T of liquid oxygen delivered to low earth orbit per year with upgrading to higher levels, delivery of lunar soil for shielding, or raw materials for processing given the demand.

(Author)

A82-35618 * # **The supply of lunar oxygen to low earth orbit.** D. G. Andrews (Boeing Co., Seattle, WA) and W. R. Snow (Princeton University, Princeton, NJ). In: Space manufacturing 4; Proceedings of the Fifth Conference, Princeton, NJ, May 18-21, 1981. (A82-35601 17-12) New York, American Institute of Aeronautics and Astronautics, 1981, p. 173-179. Grant No. NSG-3176.

Since oxygen makes up 86% of the total mass of propellants which would normally have been brought up from the earth to LEO, considerable savings are available if this oxygen can be obtained from the moon for little Delta-V penalty. This paper presents a scenario in which 400 T/yr of LOX is delivered to LEO, with the ability for upgrading to 5000 T/yr. In this scenario, cylindrical tanks of liquid oxygen with a mass of 500 kg are launched from the lunar surface by a mass driver and rendezvous with a collection station in a 100-km lunar orbit. The oxygen is removed from each tank and placed into a tanker OTV which later will transfer from low lunar orbit to LEO with an aerobraking maneuver. Launch requirements for aerobraked chemical OTVs using earth oxygen are compared to those using lunar oxygen.

B.J.

14 GROUND SUPPORT SYSTEMS AND FACILITIES (SPACE)

Includes launch complexes, research and production facilities; ground support equipment, mobile transporters; and simulators.

For related information see also 09 Research Support Facilities (Air).

A82-18310 * # Testing of a spacecraft model in a combined environment simulator. J. V. Staskus and J. C. Roche (NASA, Lewis Research Center, Cleveland, OH). (*IEEE, U.S. Defense Nuclear Agency, NASA, and DOE, Annual Conference on Nuclear and Space Radiation Effects, 18th, Seattle, WA, July 21-24, 1981.*) *IEEE Transactions on Nuclear Science*, vol. NS-28, Dec. 1981, p. 4509-4512. 7 refs.

A scale model of a satellite was tested in a large vacuum facility under electron bombardment and vacuum ultraviolet radiation to investigate the charging of dielectric materials on curved surfaces. The model was tested both stationary and rotating relative to the electron sources as well as grounded through one megohm and floating relative to the chamber. Surface potential measurements are presented and compared with the predictions of computer modelling of the stationary tests. Discharge activity observed during the stationary tests is discussed and signals from sensing devices located inside and outside of the model are presented. (Author)

A82-44659 * # Feasibility of an earth-to-space rail launcher system. E. E. Rice, L. A. Miller (Battelle Columbus Laboratories, Columbus, OH), R. A. Marshall (Australian National University, Canberra, Australia), and W. R. Kerslake (NASA, Lewis Research Center, Propulsion Systems Technology Section, Cleveland, OH). *International Astronautical Federation, International Astronautical Congress, 33rd, Paris, France, Sept. 27-Oct. 2, 1982, Paper 82-46*. 9 p. 6 refs. Contract No. NAS3-22882.

The feasibility of earth-to-space electromagnetic (railgun) launchers (ESRL) is considered, in order to determine their technical practicality and economic viability. The potential applications of the launcher include nuclear waste disposal into space, deep space probe launches, and atmospheric research. Examples of performance requirements of the ESRL system are a maximum acceleration of 10,000 g's for nuclear waste disposal in space (NWDS) missions and 2,500 g's for earth orbital missions, a 20 km/sec launch velocity for NWDS missions, and a launch azimuth of 90 degrees E. A brief configuration description is given, and test results indicate that for the 2020-2050 time period, as much as 3.0 MT per day of bulk material could be launched, and about 0.5 MT per day of high-level nuclear waste could be launched. For earth orbital missions, a significant projectile mass was approximately 6.5 MT, and an integral distributed energy store launch system demonstrated a good potential performance. ESRL prove to be economically and environmentally feasible, but an operational ESRL of the proposed size is not considered achievable before the year 2020. R.K.R.

N82-29345*# Battelle Columbus Labs, Ohio
PRELIMINARY FEASIBILITY ASSESSMENT FOR EARTH-TO-SPACE ELECTROMAGNETIC (RAILGUN) LAUNCHERS
Final Technical Report, May 1981 - Jun. 1982
Eric E. Rice, L. A. Miller, and R W Earhart 30 Jun 1982
403 p refs
(Contract NAS3-22882)
(NASA-CR-167886; NAS 1.26.167886) Avail: NTIS
HC A18/MF A01 CSCL 14B

An Earth to space electromagnetic (railgun) launcher (ESRL) for launching material into space was studied. Potential ESRL applications were identified and initially assessed to formulate preliminary system requirements. The potential applications included nuclear waste disposal in space, Earth orbital applications, deep space probe launchers, atmospheric research, and boost of chemical rockets. The ESRL system concept consisted of two separate railgun launcher tubes (one at 20 deg from the horizontal for Earth orbital missions, the other vertical for solar system escape disposal missions) powered by a common power plant. Each 2040 m launcher tube is surrounded by 10,200 homopolar generator/inductor units to transmit the power to the walls. Projectile masses are 6500 kg for Earth orbital missions and 2055 kg for nuclear waste disposal missions. For the Earth

orbital missions, the projectile requires a propulsion system, leaving an estimated payload mass of 850 kg. For the nuclear waste disposal in space mission, the high level waste mass was estimated at 250 kg. This preliminary assessment included technical, environmental, and economic analyses S.L.

A82-18319 * # NASCAP simulation of laboratory charging tests using multiple electron guns. M. J. Mandell, I. Katz, and D. E. Parks (Systems, Science and Software, La Jolla, CA). (*IEEE, U.S. Defense Nuclear Agency, NASA, and DOE, Annual Conference on Nuclear and Space Radiation Effects, 18th, Seattle, WA, July 21-24, 1981.*) *IEEE Transactions on Nuclear Science*, vol. NS-28, Dec. 1981, p. 4568-4570. 10 refs. Contracts No. NAS3-22536; No. DNA001-79-C-0079.

NASCAP calculations have been performed simulating exposure of a spacecraft-like model to multiple electron guns. The results agree well with experiment. It is found that magnetic field effects are fairly small, but substantial differential charging can result from electron gun placement. Conditions for surface flashover are readily achieved. (Author)

A82-48245 * # Real-time microcomputer simulation for space Shuttle/Centaur avionics. G. P. Szatkowski and H. C. Nelander (General Dynamics Corp., Convair Div., San Diego, CA). *Society for Computer Simulation, Conference for Modeling and Simulation on Microcomputer Systems, San Diego, CA, Jan. 28-30, 1982, Paper*. 6 p. Contract No. NAS3-22324.

The design of a simulator system for emulating the characteristics of Shuttle/Centaur avionics support equipment for launching the Solar Polar Mission and the Galileo probe are discussed. The simulators are being constructed on a modular basis for the Centaur control avionics, the Centaur Airborne Support Equipment avionics, the tanking skid ground support equipment, development mechanisms, the tanking skid ground support equipment, deployment mechanisms, the tanking onboard fluid functions, the star scanner guidance update avionics, the Orbiter command interface avionics, and the Orbiter power system. Each simulator portrays the actual working conditions, including signal delay times and harnessing. Block diagrams are provided of the interfaces and a flow diagram is presented of the software. M.S.K.

ORIGINAL PAGE IS
OF POOR QUALITY

15 LAUNCH VEHICLES AND SPACE VEHICLES

Includes boosters; manned orbital laboratories; reusable vehicles; and space stations.

A82-12623 * **Advanced 30/20 GHz communication satellites.** J. N. Sivo (NASA, Lewis Research Center, Cleveland, OH). In: *The Space Shuttle - Its current status and future impact; Proceedings of the Aerospace Congress and Exposition, Los Angeles, CA, October 13-16, 1980.* (A82-12617 02-16) Warrendale, PA, Society of Automotive Engineers, Inc., 1981, p. 75-81.

Increasing demands for satellite communications channels have filled the C-band, have begun to fill the Ku-band, and have resulted in a developmental effort to utilize 2.5 GHz of the 30/20 GHz Ka band. Problems of rain attenuation in the Ku and Ka bands are explored, and solutions are indicated in the use of antenna gain coupled with ground terminal site diversity, and higher satellite power capabilities. Tradeoffs in satellite design are focused on the number of reflectors, increased f/d, gain and sidelobe performance, and total satellite capacity. The NASA 20/3C GHz program is described, including design features of two test systems to be launched in the 1980's to examine the functioning limits of two baseline systems.

D.H.K.

ORIGINAL PAGE IS
OF POOR QUALITY

N82-27331*# **Systematics General Corp., Sterling, Va. COMMUNICATIONS SATELLITE SYSTEMS CAPACITY ANALYSIS Final Report**

Larry Browne, Taylor Hines, and Brian Tunstall Jun. 1982

114 p refs

(Contract NAS3-22888)

(NASA-CR-167911; NAS 1.26:167911) Avail: NTIS

HC A08/MF A01 CSCL 22B

Analog and digital modulation techniques are compared with regard to efficient use of the geostationary orbit by communications satellites. Included is the definition of the baseline systems (both space and ground segments), determination of interference susceptibility, calculation of orbit spacing, and evaluation of relative costs. It is assumed that voice or TV is communicated at 14/11 GHz using either FM or QPSK modulation. Both the Fixed-Satellite Service and the Broadcasting-Satellite Service are considered. For most of the cases examined the digital approach requires a satellite spacing less than or equal to that required by the analog approach.

T.M.

A82-35082 * # **Shuttle to GEO propulsion tradeoffs.** C. L. Dailey (TRW, Inc., Redondo Beach, CA) and R. M. Lovberg (California, University, La Jolla, CA). *AIAA, SAE, and ASME, Joint Propulsion Conference, 18th, Cleveland, OH, June 21-23, 1982, AIAA Paper 82-1245.* 7 p. Contract No. NAS3-22661.

An analysis has been made over a range of thruster, spacecraft and mission parameters to determine optimum electric propulsion requirements for LEO to GEO transfer missions. For this mission solar cell cover thicknesses of four to six mils each side appear to be an optimum compromise between mass and power loss due to radiation damage. The optimum range of thruster specific impulse for this mission is roughly from 1500 to 3000 seconds. Thrusters limited to much lower values of specific impulse and those requiring much higher specific impulse for good efficiency require substantially greater transfer times.

(Author)

A82-36286 * # **Centaur capabilities for communications satellite launches.** W. F. Rector, III (General Dynamics Corp., Convair Div., San Diego, CA). *American Institute of Aeronautics and Astronautics, Communications Satellite System Conference, 9th, San Diego, CA, Mar. 8, 1982, Paper 82-0558.* 6 p. Contracts No. NAS3-22914; No. NAS3-22901.

The configurations, payload capabilities, and payload envelopes for Centaur in various applications are presented. The Centaur launch record is summarized and the Atlas/Centaur launch schedule is shown. Improvements in capability are reported on, and current and proposed vehicles are depicted. Dual Delta class spacecraft will be flown using a tandem adapter or large direct broadcast satellites in a single launch model. Shuttle/Centaur will permit spacecraft weights of up to 14,000 lb to be put into orbit, including payload lengths up to 40 ft. A new capability to transfer large deployed space systems from the Shuttle to high-altitude orbits at low thrusts will be available. Spacecraft lengths requiring the full, 60-foot cargo bay and weighing 20,000 lb could be placed in geosynchronous orbit with on-orbit rendezvous and assembly of the Centaur and spacecraft in low earth orbit.

C.D.

16 SPACE TRANSPORTATION

Includes passenger and cargo space transportation e.g., shuttle operations; and rescue techniques.

For related information see also 03 Air Transportation and Safety and 85 Urban Technology and Transportation.

A82-10124 * # Design and verification of a multiple fault tolerant control system for STS applications using computer simulation. G. P. Szatkowski and J. C. Karas (General Dynamics Corp., Convair Div., San Diego, CA). In: Computers in Aerospace Conference, 3rd, San Diego, CA, October 26-28, 1981, Collection of Technical Papers. (A82-10076 01-59) New York, American Institute of Aeronautics and Astronautics, 1981, p. 349-357, Contract No. NAS3-22324. (AIAA 81-2173)

General Dynamics/Convair is under NASA's contract to integrate the Centaur upper stage into the space transportation system for future planetary missions. This requires that control of all safety critical functions be two-failure tolerant. The control system developed consists of five asynchronous computers, each contributing at their outputs to a 3-out-of-5 voting plane. Subsystem control is based on an end function redundancy management scheme. Analysis of multiple component failures and worst-case time-phase asynchrony among the computers is performed by a real-time computer simulation. The simulation emulates the hardware and subsystem interfaces, wire by wire, providing assessability to any component for the insertion of preprogrammed failures. Observability is provided via a graphics system and diagnostic software. The simulation provides an engineering tool where the integrity of control system hardware and imbedded software can be demonstrated. (Author)

ORIGINAL PAGE IS
OF POOR QUALITY

17 SPACECRAFT COMMUNICATIONS, COMMAND AND TRACKING

Includes telemetry; space communications networks; astronavigation; and radio blackout.

For related information see also *04 Aircraft Communications and Navigation* and *32 Communications*.

N82-25290*# National Aeronautics and Space Administration, Lewis Research Center, Cleveland, Ohio.

SATELLITE-AIDED LAND MOBILE COMMUNICATIONS SYSTEM IMPLEMENTATION CONSIDERATIONS

Bruce E. LeRoy 1982 10 p refs Presented at the Intern. Commun. Conf., Philadelphia, 16-19 Jun. 1982 (NASA-TM-82861; E-1229; NAS 1.15:82861) Avail: NTIS HC A02/MF A01 CSCL 09F

It was proposed that a satellite-based land mobile radio system could effectively extend the terrestrial cellular mobile system into rural and remote areas. The market, technical and economic feasibility for such a system is studied. Some of the aspects of implementing an operational mobile-satellite system are discussed. In particular, two key factors in implementation are examined: (1) bandwidth requirements; and (2) frequency sharing. Bandwidth requirements are derived based on the satellite antenna requirements, modulation characteristics and numbers of subscribers. Design trade-offs for the satellite system and potential implementation scenarios are identified. Frequency sharing is examined from a power flux density and modulation viewpoint. B.W.

ORIGINAL PAGE IS
OF POOR QUALITY

A82-27224 * Open-loop nanosecond-synchronization for wideband satellite communications. W. M. Holmes, Jr. (TRW Defense and Space Systems Group, Space Systems Div., Redondo Beach, CA). In: ITC/USA/80; Proceedings of the International Telemetry Conference, San Diego, CA, October 14-16, 1980. (A82-27174) 12-32 Research Triangle Park, NC, Instrument Society of America, 1980, p. 543-547. Contract No. NAS3-22341.

A synchronization technique for use with an onboard processing satellite communication system is discussed. The satellite oscillator is used both as the system time reference and as the frequency source for all downlink carriers and data clocks. Downlink timing is established at each system earth terminal through a combination of carrier and data-clock tracking and a downlink timing epoch signal consisting of one bit per TDMA data burst. Uplink timing is established by an open-loop range prediction process using precision ephemerides calculated and distributed by the central control station. Overall timing accuracy of the uplink signal at the satellite receiver of ± 7 nanoseconds permits unambiguous identification of each data bit position in a 128 Mbps TDMA burst. This is accomplished by means of simple, inexpensive terminal hardware using available crystal oscillators for time/frequency references and digital synthesis techniques that may be implemented in digital LSI chips. C.R.

A82-36925 * # Microwave intersatellite links for communications satellites. G. R. Welti (COMSAT Laboratories, Clarksburg, MD). *Institute of Electrical and Electronics Engineers, International Conference on Communications, Philadelphia, PA, June 14-17, 1982, Paper*. 5 p. 9 refs. Research sponsored by the International Telecommunications Satellite Organization; Contract No. NAS3-22805.

Applications and interface requirements for intersatellite links (ISLs) between commercial communications satellites are reviewed, ranging from ISLs between widely separated satellites to ISLs between clustered satellites. On-board processing architectures for ISLs employing a variety of modulation schemes are described. These schemes include FM remodulation and QPSK regeneration in combination with switching and buffering. The various architectures are compared in terms of complexity, required performance, antenna size, mass, and power. (Author)

18 SPACECRAFT DESIGN, TESTING AND PERFORMANCE

Includes spacecraft thermal and environmental control; and attitude control.

For life support systems see 54 *Man/System Technology and Life Support*. For related information see also 05 *Aircraft Design, Testing and Performance* and 39 *Structural Mechanics*.

N82-11106*# National Aeronautics and Space Administration, Lewis Research Center, Cleveland, Ohio.

TESTING OF A SPACECRAFT MODEL IN A COMBINED ENVIRONMENT SIMULATOR

J. V. Staskus and J. C. Roche 1981 11 p refs Presented at the 18th Ann. Conf. on Nucl. and Space Radiation Effects, Seattle, 20-24 Jul. 1981

(NASA-TM-82723; E-1024) Avail: NTIS HC A02/MF A01 CSCL 22B

A scale model of a satellite was tested in a large vacuum facility under electron bombardment and vacuum ultraviolet radiation to investigate the charging of dielectric materials on curved surfaces. The model was tested both stationary and rotating relative to the electron sources as well as grounded through one megohm and floating relative to the chamber. Surface potential measurements are presented and compared with the predictions of computer modelling of the stationary tests. Discharge activity observed during the stationary tests is discussed and signals from sensing devices located inside and outside of the model are presented. M.G.

N82-11107*# National Aeronautics and Space Administration, Lewis Research Center, Cleveland, Ohio.

VOLTAGE GRADIENTS IN SOLAR ARRAY CAVITIES AS POSSIBLE BREAKDOWN SITES IN SPACECRAFT-CHARGING-INDUCED DISCHARGES

N. John Stevens, Hilton E. Mills, and Lisa Orange 1981 10 p refs Presented at the Ann. Conf. on Nucl. and Space Radiation Effects, Seattle, 21-24 Jul. 1981

(NASA-TM-82710; E-1003) Avail: NTIS HC A02/MF A01 CSCL 10B

A possible explanation for environmentally-induced discharges on geosynchronous satellites exists in the electric fields formed in the cavities between solar cells - the small gaps formed by the cover slides, solar cells, metallic interconnects and insulating substrate. When exposed to a substorm environment, the cover slides become less negatively charged than the spacecraft ground. If the resultant electric field becomes large enough, then the interconnect could emit electrons (probably by field emission) which could be accelerated to space by the positive voltage on the covers. An experimental study was conducted using a small solar array segment in which the interconnect potential was controlled by a power supply while the cover slides were irradiated by monoenergetic electrons. It was found that discharges could be triggered when the interconnect potential became at least 500 volts negative with respect to the cover slides. Analytical modeling of satellites exposed to substorm environments indicates that such gradients are possible. Therefore, it appears that this trigger mechanism for discharges is possible. T.M.

N82-14213*# National Aeronautics and Space Administration, Lewis Research Center, Cleveland, Ohio.

SPACECRAFT CHARGING TECHNOLOGY, 1980

Washington Oct. 1981 1005 p refs Conf. held in Colorado Springs, 12-14 Nov. 1980; sponsored by AFGL and NASA Lewis Research Center

(NASA-CP-2182; AFGL-TR-81-0270) Avail: NTIS HC A99/MF A01 CSCL 22B

The third Spacecraft Charging Technology Conference proceedings contain 68 papers on the geosynchronous plasma environment, spacecraft modeling, charged particle environment interactions with spacecraft, spacecraft materials characterization, and satellite design and testing. The proceedings is a compilation of the state of the art of spacecraft charging and environmental interaction phenomena. For individual titles, see N82-14214 through N82-14275.

ORIGINAL PAGE IS
OF POOR QUALITY

N82-14251*# National Aeronautics and Space Administration, Lewis Research Center, Cleveland, Ohio.

SCATHA SSPM CHARGING RESPONSE: NASCAP PREDICTIONS COMPARED WITH DATA

Carolyn K. Purvis and John Staskus *In its Spacecraft Charging Technol.*, 1980 Oct. 1980 p 592-607 refs (For primary document see N82-14213 05-18)

Avail: NTIS HC A99/MF A01 CSCL 22B

Models for the satellite surface potential monitor (SSPM) units constructed in the NASCAP code and the results of comparing predictions to surface voltage and baseplate current data are reported. Several peculiarities in the test data are noted. Preliminary results from space simulations of a SCATHA model with environments representative of the day 87, 1979, eclipse injection event are presented, and their implications for predicting space response are discussed. E.A.K.

N82-14255*# National Aeronautics and Space Administration, Lewis Research Center, Cleveland, Ohio.

COMPARISON OF NASCAP MODELLING RESULTS WITH LUMPED CIRCUIT ANALYSIS

David B. Stang and Carolyn K. Purvis *In its Spacecraft Charging Technol.*, 1980 Oct. 1980 p 665-683 refs (For primary document see N82-14213 05-18)

Avail: NTIS HC A99/MF A01 CSCL 22B

Engineering design tools that can be used to predict the development of absolute and differential potentials by realistic spacecraft under geomagnetic substorm conditions are described. Two types of analyses are in use: (1) the NASCAP code, which computes quasistatic charging of geometrically complex objects with multiple surface materials in three dimensions; (2) lumped element equivalent circuit models that are used for analyses of particular spacecraft. The equivalent circuit models require very little computation time, however, they cannot account for effects, such as the formation of potential barriers, that are inherently multidimensional. Steady state potentials of structure and insulation are compared with those resulting from the equivalent circuit model. E.A.K.

N82-14258*# National Aeronautics and Space Administration, Lewis Research Center, Cleveland, Ohio.

ANALYTICAL MODELING OF SATELLITES IN GEOSYNCHRONOUS ENVIRONMENT

N. John Stevens *In its Space Charging Technol.*, 1980 Oct. 1980 p 717-729 refs (For primary document see N82-14213 05-18)

Avail: NTIS HC A99/MF A01 CSCL 22B

Experiences with surface charging of geosynchronous satellites are reviewed and mechanisms leading to discharges on satellite surfaces are considered. It was found that the large differential voltages between the surface and the substrate required to produce massive laboratory discharges do not occur on satellites in space. Analytical modeling predictions supported by dielectric charging data from P78-2, SCATHA (Spacecraft Charging at High Altitudes) flight results are discussed. Ungrounded insulator areas, buried charge layers (due to mid-energy range particles), and positive differential voltages (where structure voltages are less negative than surrounding dielectric surface voltages) are considered as possible mechanisms producing satellite charge up. J.D.H.

N82-14263*# National Aeronautics and Space Administration, Lewis Research Center, Cleveland, Ohio.

USE OF CHARGING CONTROL GUIDELINES FOR GEOSYNCHRONOUS SATELLITE DESIGN STUDIES

N. John Stevens *In its Spacecraft Charging Technol.*, 1980 Oct. 1980 p 789-801 refs (For primary document see N82-14213 05-18)

Avail: NTIS HC A99/MF A01 CSCL 22B

Several of the principle guidelines from the Spacecraft Charging Design Guidelines Handbook are presented with illustrative examples. Use of the geomagnetic substorm specification to qualify satellite designs, the evaluation of satellite designs by using analytical modelling techniques, the use of selected materials and coatings to minimize charging, the tying of all conducting elements to a common ground, and the use of electrical filtering to protect circuits from discharge induced upsets are discussed. Discharge criteria and SCATHA data are excluded. J.D.H.

N82-14271* National Aeronautics and Space Administration, Lewis Research Center, Cleveland, Ohio.

AGREEMENT FOR NASA/JAST - USAF/AFSC SPACE INTERDEPENDENCY ON SPACECRAFT ENVIRONMENT INTERACTION

C. R. Pike (AFGL) and N. John Stevens *In its Spacecraft Charging Technol.*, 1980 Oct. 1980 p 912-930 refs (For primary document see N82-14213 05-18)

Avail: NTIS HC A99/MF A01 CSCL 22B

A joint AF/NASA comprehensive program on spacecraft environment interactions consists of combined contractual and in house efforts aimed at understanding spacecraft environment interaction phenomena and relating ground test results to space conditions. Activities include: (1) a concerted effort to identify project related environmental interactions; (2) a materials investigation to measure the basic properties of materials and develop or modify materials as needed; and (3) a ground simulation investigation to evaluate basic plasma interaction phenomena and provide inputs to the analytical modeling investigation. Systems performance is evaluated by both ground tests and analysis. There is an environmental impact investigation to determine the effect of future large spacecraft on the charged particle environment. Space flight investigations are planned to verify the results. The products of this program are test standards and design guidelines which summarize the technology, specify test criteria, and provide techniques to minimize or eliminate system interactions with the charged particle environment. A.R.H.

N82-18311* National Aeronautics and Space Administration, Lewis Research Center, Cleveland, Ohio.

DESIGN PRACTICES FOR CONTROLLING SPACECRAFT CHARGING INTERACTIONS

N. John Stevens 1982 21 p refs Presented at the 20th Aerospace Sci. Meeting, Orlando, Fla., 11-14 Jan. 1982; sponsored by AIAA

(NASA-TM-82781; E-1112) Avail: NTIS HC A02/MF A01 CSCL 22B

A design guidelines handbook prepared to provide criteria for assessing and minimizing spacecraft charging interactions is described. An evaluation philosophy of analyzing specific satellite designs in a substorm environment specification with NASCAP is proposed. Criteria for possible discharges are given and a technique for computing the discharge transients is outlined. The charging of a three axis stabilized satellite is examined to illustrate the philosophy. Possible discharge locations are found and transients computed. The effect of changing selected surface coatings is evaluated and found to substantially reduce charging levels. J.M.S.

N82-23261* National Aeronautics and Space Administration, Lewis Research Center, Cleveland, Ohio.

ENVIRONMENTALLY INDUCED DISCHARGES ON SATELLITES

N. John Stevens 1982 14 p refs Presented at the 2nd EMC Seminar, Noordwijk, Netherlands, 11-13 May 1982; sponsored by ESTEC

(NASA-TM-82849; E-1219; NAS 1.15:82849) Avail: NTIS HC A02/MF A01 CSCL 22B

The problem of associated hazards to geosynchronous satellite systems from geomagnetic storm encounters is investigated. The available space flight data, coupled with analytical modeling studies, show that only relatively low differential charging is possible from environmental encounters. Using an analytical study of a discharge event on SCATHA, a discharge process is postulated where a small amount of charge is lost to space. These characteristics could then be used as inputs to a coupling model to determine the hazard to a spacecraft. The procedure is applied to a three axis stabilized satellite design. B.W.

A82-17872 * Validation of the NASCAP model using space-flight data. P. R. Stannard, I. Katz (Systems, Science and Software, La Jolla, CA), L. Gedeon, J. C. Roche (NASA, Lewis Research Center, Cleveland, OH), A. G. Rubin, and M. F. Tautz (USAF, Geophysics Laboratory, Bedford, MA). *American Institute of Aeronautics and Astronautics, Aerospace Sciences Meeting, 20th, Orlando, FL, Jan. 11-14, 1982, Paper 82-0269.* 13 p. 16 refs. Contract No. NAS3-22536.

The NASA Charging Analyzer Program (NASCAP) has been validated in a space environment. Data collected by the SCATHA (Spacecraft Charging at High Altitude) spacecraft has been used with NASCAP to simulate the charging response of the spacecraft ground conductor and dielectric surfaces with considerable success. Charging of the spacecraft ground observed in eclipse, during moderate and severe substorm environments, and in sunlight has been reproduced using the code. Close agreement between both the currents and potentials measured by the SSPM's, and the NASCAP simulated response, has been obtained for differential charging. It is concluded that NASCAP is able to predict spacecraft charging behavior in a space environment. (Author)

A82-18317 * Voltage gradients in solar array cavities as possible breakdown sites in spacecraft-charging-induced discharges. N. J. Stevens, H. E. Mills, and L. Orange (NASA, Lewis Research Center, Cleveland, OH). (*IEEE, U.S. Defense Nuclear Agency, NASA, and DOE, Annual Conference on Nuclear and Space Radiation, Effects, 18th, Seattle, WA, July 21-24, 1981.*) *IEEE Transactions on Nuclear Science*, vol. NS-28, Dec. 1981, p. 4558-4562. 35 refs.

A possible explanation for environmentally-induced discharges on geosynchronous satellites exists in the electric fields formed in the cavities between solar cells - the small gaps formed by the cover slides, solar cells, metallic interconnects and insulating substrate. When exposed to a substorm environment, the cover slides become less negatively charged than the spacecraft ground. Hence, it is possible for metallic surfaces (usually silver mesh) to be at a negative potential in a cavity that has a 'positive' surface above it. If the resultant electric field becomes large enough, then the interconnect could emit electrons (probably by field emission) which could be accelerated to space by the positive voltage on the covers. A $\frac{1}{4}$ experimental study was connected using a small solar array segment in which the interconnect potential was controlled by a power supply while the cover slides were irradiated by monoenergetic electrons. It was found that discharges could be triggered when the interconnect potential became at least 500 volts negative with respect to the cover slides. Analytical modeling of satellites exposed to substorm environments indicates that such gradients are possible. Therefore, it appears that this trigger mechanism for discharges is possible. Details of the experiment and modeling study are presented. (Author)

N82-14224* TRW Defense and Space Systems Group, Redondo Beach, Calif.

BRUSHFIRE ARC DISCHARGE MODEL

G. T. Lhouye *In NASA. Lewis Research Center Spacecraft Charging Technol.*, 1980 Oct. 1981 p 133-162 refs (For primary document see N82-14213 05-18)

(Contract NAS3-21961)

Avail: NTIS HC A99/MF A01 CSCL 22B

A one dimensional arc discharge model incorporating a brushfire-type propagation of a discharge wavefront was investigated. A set of equations, developed and their which include electrical, thermal and plasma parameters, were solutions shown to be consistent with a propagating brushfire wavefront. Voltage, current, plasma density, temperature, and resistivity profiles were obtained. Mechanical forces, magnetic and electrostatic were considered in evaluating the flashover to blowout current ratio, G' , for arc discharges with the brushfire parameters developed in the model. This ratio is an important factor in determining the electromagnetic interference (EMI) impact of arc discharges on spacecraft electrical subsystems. The conclusion of the analysis is that electrostatic forces are much more important than magnetic forces. The magnitude of the G' factor obtained, 58.5 percent, is within the range of those obtained by experimental means. Improvements in the analytical model as well in the experimental approach are recommended. M.D.K.

N82-14226* Case Western Reserve Univ., Cleveland, Ohio. **SECONDARY ELECTRON EMISSION YIELDS**

I. Krainsky, W. Lundin, W. L. Gordon, and R. W. Hoffman *In NASA. Lewis Research Center Spacecraft Charging Technol.*, 1980 Oct. 1981 p 179-197 refs (For primary document see N82-14213 05-18)

(Grant NaG-3197)

ORIGINAL PAGE IS
OF POOR QUALITY

Avail: NTIS HC A99/MF A01 CSCL 225

The secondary electron emission (SEE) characteristics for a variety of spacecraft materials were determined under UHV conditions using a commercial double pass CMA which permits sequential Auger electron spectroscopic analysis of the surface. The transparent conductive coating indium tin oxide (ITO) was examined on Kapton and borosilicate glass and indium oxide on FED Teflon. The total SEE coefficient ranges from 2.5 to 2.6 on as-received surfaces and from 1.5 to 1.6 on Ar(+)-sputtered surfaces with < 5 nm removed. A cylindrical sample carousel provides normal incidence of the primary beam as well as a multiple Faraday cup measurement of the approximately nA beam currents. Total and true secondary yields are obtained from target current measurements with biasing of the carousel. A primary beam pulsed mode to reduce electron beam dosage and minimize charging of insulating coatings was applied to Mg/F2 coated solar cell covers. Electron beam effects on ITO were found quite important at the current densities necessary to do Auger studies. M.D.K.

N82-14227*# Pennsylvania State Univ., University Park.
OBLIQUE-INCIDENCE SECONDARY EMISSION FROM CHARGED DIELECTRONICS

James W. Robinson and Paul A. Budd *In* NASA. Lewis Research Center Spacecraft Charging Technol., 1980 Oct. 1981 p 198-210 refs (For primary document see N82-14213 05-18) (Grant NsG-3166)

Avail: NTIS HC A99/MF A01 CSCL 22B

Experimental measurements and computer simulation of secondary electron emission coefficients for FEP-Teflon, for normal and oblique incidence in the presence of a normal electric field are reported. Knowledge of the electrostatic environment surrounding the specimen calculation of particle trajectories are considered. A simulation using a conformal mapping, a Green's integral, and a trajectory generator provides the necessary mathematical support for the measurements which have been made with normal fields of 1.5 and 2.7 kV/mm. When incidence is normal and energy exceeds the critical energy, the coefficient is given by V_{SB} and for oblique incidence this expression may be divided by the cosine of the angle. The parameter $V_{sub 0}$ is a function of normal field. Measurements for values of $V_{sub f}$ are presented. M.D.K.

N82-14249*# Systems Science and Software, La Jolla, Calif.
REPRESENTATION AND MATERIAL CHARGING RESPONSE OF GEOPLASMA ENVIRONMENTS

P. R. Stannard, G. W. Schueller, I. Katz, and M. J. Mandell *In* NASA. Lewis Research Center Spacecraft Charging Technol., 1980 Oct. 1980 p 560-579 refs (For primary document see N82-14213 05-18)

(Contract NAS3-21762)

Avail: NTIS HC A99/MF A01 CSCL 22B

The sensitivity of the charging response to the representation of the measured environments and material properties are discussed. Single and double Maxwellian representations are compared with direct numerical integration of the observed spectra. The effect of anisotropic incident flux distribution is modeled. In addition, the effect of the high energy radiation upon bulk conductivity and hence differential charging is examined. E.A.K.

N82-14272*# Kansas Univ., Lawrence.
NUMERICAL SIMULATION OF PLASMA INSULATOR INTERACTIONS IN SPACE. PART 1: THE SELF CONSISTENT CALCULATION

J. H. Nonnast, R. C. Chaky, T. P. Armstrong, J. Enoch, and G. G. Wiseman *In* NASA. Lewis Research Center Spacecraft Charging Technol., 1980 Oct. 1980 p 932-945 refs (For primary document see N82-14213 05-18) (Grant NsG-3290)

Avail: NTIS HC A99/MF A01 CSCL 22B

A computer program is being developed to simulate the interaction of a plasma with a conducting disk partially covered by an insulator. Initial runs consider only charge sticking to the dielectric. Results indicate that the current density drawn by the hole in the dielectric increases approximately linearly with voltage for conductor voltages between 5 volts and 250 volts. Author

N82-14273*# Kansas Univ., Lawrence.

NUMERICAL SIMULATION OF PLASMA INSULATOR INTERACTIONS IN SPACE. PART 2: DIELECTRIC EFFECTS

R. C. Chaky, J. H. Nonnast, T. P. Armstrong, J. Enoch, and G. Wiseman *In* NASA. Lewis Research Center Spacecraft Charging Technol., 1980 Oct. 1980 p 946-956 (For primary document see N82-14213 05-18)

(Grant NsG-3290)

Avail: NTIS HC A99/MF A01 CSCL 22B

Any process which may be modeled statistically for a simple plasma particle may be modeled by the particle in cell technique. The success of the calculation is then dependent on having a large enough number of particles that the statistical treatment is meaningful. Thus it is possible to include the effects of secondary emission, backscattering, charge sticking and possibly dielectric breakdown, photoemission, and spallation. The first plasma dielectric interaction included in the computer code for simulating plasma insulator interactions is secondary electron emission. A calculated current density vs. voltage curve is presented and compared to an experimental curve. A.R.H.

N82-14250*# Systems Science and Software, La Jolla, Calif.
SIMULATION OF CHARGING RESPONSE OF SCATHA (P78-2) SATELLITE

G. W. Schueller, P. R. Stannard, I. Katz, and M. J. Mandell *In* NASA. Lewis Research Center Spacecraft Charging Technol., 1980 Oct. 1980 p 580-591 refs (For primary document see N82-14213 05-18)

(Contract NAS3-21762)

Avail: NTIS HC A99/MF A01 CSCL 22B

A model of the satellite charging at high altitudes (SCATHA P78-2) satellite was used to simulate the charging response of SCATHA at geosynchronous orbit. The model includes a description of the geometry, currents to exposed surface materials, and electrical connections on the spacecraft. The charging response of the vehicle to that predicted by the NASCAP model for the Day 87, 1979 eclipse charging event, in which the spacecraft charged to several kilovolts negative during a magnetospheric substorm are compared. Double Maxwellian representations of the plasma environment reproduce the charging response observed experimentally. E.A.K.

N82-14275*# Systems Science and Software, San Diego, Calif.
CHARGING OF A LARGE OBJECT IN LOW POLAR EARTH ORBIT

D. E. Parks and I. Katz *In* NASA. Lewis Research Center Spacecraft Charging Technol., 1980 Oct. 1980 p 979-989 refs Sponsored in part by AFGL (For primary document see N82-14213 05-18)

(Contract NAS3-21762)

Avail: NTIS HC A99/MF A01 CSCL 22B

The charging of a large sphere subject to the environment encountered by the shuttle orbiter as it passes through the auroral regions in its low polar Earth orbit was investigated. The environment consists of a low temperature dense plasma and relatively intense (200 mu A/sq m) field aligned flux of energetic electrons (approximately 5 to 10 keV). The potential on a sphere in eclipse is presented as a function of the ratio kappa of the charging rate produced by precipitating electrons to the discharging rate produced by ram ions. It was found that a 5 meter conducting sphere charges to potentials of order 1 kilovolt for kappa approximately 2, even though a 0.5 meter sphere charges to less than 100 volts. It is concluded that the natural charging environment can induce large potentials (approximately 1 kilovolt) on the shuttle orbiter. A.R.H.

N82-15117*# Martin Marietta Corp., Bethesda, Md.
CRYOGENIC FLUID MANAGEMENT EXPERIMENT Final Report, Dec. 1978 - Oct. 1981

R. N. Eberhardt, W. J. Bailey, and D. A. Fester Oct. 1981 237 p refs

(Contract NAS3-21591)

(NASA-CR-165495; MCR-81-597)

Avail: NTIS HC A11/MF A01 CSCL 22B

The cryogenic fluid management experiment (CFME), designed to characterize subcritical liquid hydrogen storage and expulsion in the low-q space environment, is discussed. The experiment utilizes a fine mesh screen fluid management device to accomplish

ORIGINAL PAGE IS
OF POOR QUALITY

gas-free liquid expulsion and a thermodynamic vent system to intercept heat leak and control tank pressure. The experiment design evolved from a single flight prototype to provision for a multimission (up to 7) capability. A detailed design of the CFME, a dynamic test article, and dedicated ground support equipment were generated. All materials and parts were identified, and components were selected and specifications prepared. Long lead titanium pressurant spheres and the flight tape recorder and ground reproduce unit were procured. Experiment integration with the shuttle orbiter, Spacelab, and KSC ground operations was coordinated with the appropriate NASA centers, and experiment interfaces were defined. Phase 1 ground and flight safety reviews were conducted. Costs were estimated for fabrication and assembly of the CFME, which will become the storage and supply tank for a cryogenic fluid management facility to investigate fluid management in space. R.J.F.

N82-26377*# Systems Science and Software, San Diego, Calif. **ADDITIONAL EXTENSIONS TO THE NASCAP COMPUTER CODE, VOLUME 2** Progress Report, 9 Sep. 1980 - 22 Dec. 1981

P. R. Stannard, I. Katz, and M. J. Mandell Feb. 1982 163 p refs Sponsored in part by AFGL (Contract NAAS3-22536) (NASA-CR-167856; NAS 1.26:167856; SSS-R-82-5218) Avail: NTIS HC A08/MF A01 CSDL 22B

Particular attention is given to comparison of the actual response of the SCATHA (Spacecraft Charging AT High Altitudes) P78-2 satellite with theoretical (NASCAP) predictions. Extensive comparisons for a variety of environmental conditions confirm the validity of the NASCAP model. A summary of the capabilities and range of validity of NASCAP is presented, with extensive reference to previously published applications. It is shown that NASCAP is capable of providing quantitatively accurate results when the object and environment are adequately represented and fall within the range of conditions for which NASCAP was intended. Three dimensional electric field effects play an important role in determining the potential of dielectric surfaces and electrically isolated conducting surfaces, particularly in the presence of artificially imposed high voltages. A theory for such phenomena is presented and applied to the active control experiments carried out in SCATHA, as well as other space and laboratory experiments. Finally, some preliminary work toward modeling large spacecraft in polar Earth orbit is presented. An initial physical model is presented including charge emission. A simple code based upon the model is described along with code test results. Author

N82-26378*# Systems Science and Software, San Diego, Calif. **ADDITIONAL EXTENSIONS TO THE NASCAP COMPUTER CODE, VOLUME 3** Contractor Report, 9 Sep. 1980 - 22 Dec. 1981

M. J. Mandell and D. L. Cooke Aug. 1981 90 p refs (Contract NAS3-22536) (NASA-CR-167857; NAS 1.26:167857; SSS-R-81-5140) Avail: NTIS HC A05/MF A01 CSDL 22B

The ION computer code is designed to calculate charge exchange ion densities, electric potentials, plasma temperatures, and current densities external to a neutralized ion engine in R-Z geometry. The present version assumes the beam ion current and density to be known and specified, and the neutralizing electrons to originate from a hot-wire ring surrounding the beam orifice. The plasma is treated as being resistive, with an electron relaxation time comparable to the plasma frequency. Together with the thermal and electrical boundary conditions described below and other straightforward engine parameters, these assumptions suffice to determine the required quantities. The ION code, written in ASCII FORTRAN for UNIVAC 1100 series computers, is designed to be run interactively, although it can also be run in batch mode. The input is free-format, and the output is mainly graphical, using the machine-independent graphics developed for the NASCAP code. The executive routine calls the code's major subroutines in user-specified order, and the code allows great latitude for restart and parameter change. Author

A82-13494 * # Real-time computer simulation/emulation for verification of multi-fault-tolerant control of Centaur-in-Shuttle. G. P. Szatkowski (General Dynamics Corp., Convair Div., San Diego, CA). In: Digital Avionics Systems Conference, 4th, St. Louis, MO,

November 17-19, 1981, Collection of Technical Papers. (A82-13451 03-04) New York, American Institute of Aeronautics and Astronautics, 1981, p. 315-325. Contract No. NAS3-22324. (AIAA 81-2283)

NASA has contracted with General Dynamics to design and develop an advanced Centaur liquid upper stage for support of the Galileo and Solar Polar Interplanetary missions in 1985-86. The control of the Centaur while it resides in the Shuttle cargo bay must meet the STS safety requirements to be dual failure tolerant in all mission critical functions. The demonstration of the integrity of this control system in the event of multiple component failures and worst-case time-phase asynchronicity among the system's computers is performed by a real-time computer simulation. The simulation emulates the control hardware, subsystem interfaces, and imbedded software processes, wire-by-wire, to provide accessibility for fault insertion. Observability is provided via graphics and diagnostic software. Verification is the product of Monte Carlo simulation analysis. (Author)

A82-16904 * Numerical simulation of sheath structure and current-voltage characteristics of a conductor-dielectric disk in a plasma. R. C. Chaky, J. H. Nonnast, and J. Enoch (Kansas, University, Lawrence, KS). *Journal of Applied Physics*, vol. 52, Dec. 1981, p. 7092-7098. 16 refs. Grant No. NSG-3290.

A computer program is being developed to simulate the interaction of a plasma with a conducting disk. Two configurations are examined: (1) the conductor is a 'button' in the center of a larger dielectric disk, and (2) the conducting disk is covered by a dielectric disk to the same size with a circular hole in the center of the dielectric, exposing a region of conductor. Results of the electrostatic plasma simulation are presented both with and without secondary electron emission from the dielectric; characteristic curves and voltage profiles are included. V.L.

A82-16194 * # Modification of spacecraft potentials by thermal electron emission on ATS-5. R. C. Olsen (Alabama, University, Huntsville, AL). *Journal of Spacecraft and Rockets*, vol. 18, Nov.-Dec. 1981, p. 527-532. 7 refs. Contract No. NAS5-23481; Grant No. NSG-3150.

Electron emission experiments on Applied Technology Satellite 5 using a thermal electron emitter are reported and analyzed. Operations in eclipse charging environments showed that electron emission could partially discharge a negatively charged satellite. Typical operations resulted in kilovolt potentials being reduced to hundreds of volts for a few tens of seconds, followed by a gradual recharging over a period of minutes. Equilibrium currents were modeled with a one-dimensional current balance model. Currents on the order of 1 microampere were found, significantly below emitter capabilities. Application of a three-dimensional, time-dependent computer model showed that differential charging on the solar arrays was limiting the emitted current, preventing the complete discharge of the satellite, and allowing it to recharge in spite of the electron emitter. (Author)

A82-17793 * # Space Shuttle Orbiter charging. I. Katz and D. E. Parks (Systems, Science and Software, La Jolla, CA). *American Institute of Aeronautics and Astronautics, Aerospace Sciences Meeting, 20th, Orlando, FL, Jan. 11-14, 1982, Paper 82-0119*. 6 p. 8 refs. USAF-supported research; Contract No. NAS3-22536.

This paper considers the charging of the Space Shuttle Orbiter by energetic particles of environmental origin and from emission by accelerators. The results indicate that precipitating electrons quickly induce large voltages. High voltages may also occur when onboard accelerators inject energetic beams into the high altitude plasma. A significant conclusion from electron beam experiments is that the rockets charged to positive potentials much less than anticipated from the theory of probes in a quiescent plasma. Elementary theories predict the large negative potentials observed by firing energetic ions and predict severe differential charging of the Orbiter. (Author)

ORIGINAL PAGE IS
OF POOR QUALITY

A82-18312 * Internal breakdown of charged spacecraft dielectrics. B. L. Beers, V. W. Pine, and S. T. Ives (Beers Associates, Inc., Reston, VA). (*IEEE, U.S. Defense Nuclear Agency, NASA, and DOE, Annual Conference on Nuclear and Space Radiation Effects, 18th, Seattle, WA, July 21-24, 1981.*) *IEEE Transactions on Nuclear Science*, vol. NS-28, Dec. 1981, p. 4529-4534. 17 refs. Contract No. NAS3-22530.

It is suggested that small energy discharges of low differential voltage that are associated with internal buried charge may be an important mechanism by which sorted electrostatic energy is released from dielectrics on board orbiting spacecraft. The evidence from space given by Stevens (1980) is noted, and the laboratory experimental evidence of Frederickson is cited to demonstrate that discharges occur under circumstances with no external potential drop. Previous calculations indicating that significant internal electric fields can exist in dielectrics charged with multiple-kilovolt electron beams under conditions involving little or no external potential drop are reviewed. Attention is given to the internal discharge mechanism of Meulenbergh (1976), and new calculations suggesting that the space environment is conducive to the formation of the conditions required by this mechanism are presented. Experimental procedures for checking the suggestions made are developed. C.R.

ORIGINAL PAGE IS
OF POOR QUALITY

A82-35547 * Differential charging of high-voltage spacecraft - The equilibrium potential of insulated surfaces. I. Katz and M. J. Mandell (Systems, Science, and Software, La Jolla, CA). *Journal of Geophysical Research*, vol. 87, June 1, 1982, p. 4533-4541. 36 refs. Contract No. NAS3-22536.

A theory is presented for the steady-state potential of insulated surfaces near exposed high voltages. The term 'insulated surfaces' is used to mean either dielectric surfaces or electrically isolated metallic surfaces. The potential is bounded below by the zero of the material's I-V curve assuming total suppression of secondary electrons, and above by assuming total extraction of secondaries. Within these bounds, the material's surface potential is determined consistently with the solution to Poisson's equation external to the vehicle. The theory is compared with rocket experiments and with SCATHA satellite data. Also, an explanation is suggested for the observed 'snapover' of solar cell coverslips from near plasma ground potential to near the potential of positively biased interconnects with increasing bias voltage. (Author)

20 SPACECRAFT PROPULSION AND POWER

Includes main propulsion systems and components e.g., rocket engines; and spacecraft auxiliary power sources.

For related information see also 07 Aircraft Propulsion, 28 Propellants and Fuels, and 44 Energy Production and Conversion.

N82-20240*# National Aeronautics and Space Administration, Lewis Research Center, Cleveland, Ohio.

GEOMETRY AND STARVATION EFFECTS IN HYDRODYNAMIC LUBRICATION

David E. Brewe and Bernard J. Hamrock 1982 18 p refs Proposed for presentation at the 59th Meeting of the Propulsion and Energetics Panel Symp. on Problems in Bearings and Lubrication, Ottawa, Canada, 31 May - 3 Jun. 1982; sponsored by AGARD Prepared jointly with Army Aviation Research and Development Command, St. Louis (NASA-TM-82807; E-1147; NAS 1.15:82807; AVRADCOM-TR-82-C-17) Avail: NTIS HC A02/MF A01 CSCL 20D

Numerical methods were used to determine the effects of lubricant starvation on the minimum film thickness under conditions of a hydrodynamic point contact. Starvation was effected by varying the fluid inlet level. The Reynolds boundary conditions were applied at the cavitation boundary and zero pressure was stipulated at the meniscus or inlet boundary. A minimum-film-thickness equation as a function of both the ratio of dimensionless load to dimensionless speed and inlet supply level was determined. By comparing the film generated under the starved inlet condition with the film generated from the fully flooded inlet, an expression for the film reduction factor was obtained. Based on this factor a starvation threshold was defined as well as a critically starved inlet. The changes in the inlet pressure buildup due to changing the available lubricant supply are presented in the form of three dimensional isometric plots and also in the form of contour plots. Author

N82-24286*# National Aeronautics and Space Administration, Lewis Research Center, Cleveland, Ohio.

AN INSIGHT INTO AUXILIARY PROPULSION REQUIREMENTS OF LARGE SPACE SYSTEMS

James E. Maloy and William W. Smith (Boeing Aerospace Co., Seattle) 1982 21 p refs To be presented at the 18th Joint Propulsion Conf., Cleveland, 21-23 Jun. 1981 (NASA-TM-82827; E-1185; NAS 1.15:82827) Avail: NTIS HC A02/MF A01 CSCL 21H

Electric and chemical propulsion systems' requirements for Large Space Systems (LSS) launchable by a single Shuttle are considered. Sets of generic LSS classes (ranging in size from 30 m to 250 m) are described and the disturbance force and torque requirements for low Earth orbit (LEO), geosynchronous Earth orbit (GEO), and LEO-GEO transfer, are given. Auxiliary propulsion requirements were determined as a function of: specific impulse (250 and 500 sec. for chemical and 1000, 3000, and 10000 sec. for electric); orbit; and angle of orientation. The results were used to size the Auxiliary Propulsion System (thrustor size, fuel requirements, power processor, etc). T.M.

N82-27358*# National Aeronautics and Space Administration, Lewis Research Center, Cleveland, Ohio.

LARGE SPACE SYSTEMS/PROPULSION INTERACTIONS

Jun. 1982 253 p refs Workshop held at Cleveland, 22-23 Oct. 1981 (NASA-TM-82904; E-1288; NAS 1.15:82904) Avail: NTIS HC A12/MF A01 CSCL 22A

Material illustrating the presentations on and the conclusions of workshop panels considering the missions, systems requirements and operations, and systems design and integration is presented. For individual titles, see N82-27359 through N82-27379.

N82-27371*# National Aeronautics and Space Administration, Lewis Research Center, Cleveland, Ohio.

SYSTEMS INTEGRATION

James J. Pelouch, Jr. In: *Large Space Systems/Propulsion Interactions* Jun. 1982 p 123-126 (For primary document see N82-27358 18-20)

Avail: NTIS HC A12/MF A01 CSCL 22B

The workings of systems integration, its accomplishments, the influences of its character changes on the STS, propulsion out of the orbiter and LSS, and technological demands are discussed. The task of systems integration is to define, understand, and account for interactions between the major systems on a space mission. The safety and propulsion systems and their reliability are outlined. E.A.K.

N82-29354*# National Aeronautics and Space Administration, Lewis Research Center, Cleveland, Ohio.

A NEW STRATEGY FOR EFFICIENT SOLAR ENERGY CONVERSION: PARALLEL-PROCESSING WITH SURFACE PLASMONS

Lynn Marie Anderson 1982 13 p refs Presented at the 17th Intersoc. Energy Conversion Eng. Conf., Los Angeles, 8-13 Aug. 1982; sponsored by IEEE (NASA-TM-82867; E-1236; NAS 1.15:82867) Avail: NTIS HC A02/MF A01 CSCL 10A

An advanced concept for direct conversion of sunlight electricity, which aims at high efficiency by tailoring the conversion process to separate energy bands within the broad solar spectrum is introduced. The objective is to obtain a high level of spectrum-splitting without sequential losses or unique materials for each frequency band. In this concept, sunlight excites a spectrum of surface plasma waves which are processed in parallel on the same metal film. The surface plasmons transport energy to an array of metal-barrier-semiconductor diodes, where energy is extracted by inelastic tunneling. Diodes are tuned to different frequency bands by selecting the operating voltage and geometry, but all diodes share the same materials. Author

N82-31443*# National Aeronautics and Space Administration, Lewis Research Center, Cleveland, Ohio.

EFFECTS OF PROCESSING AND DOPANT ON RADIATION DAMAGE REMOVAL IN SILICON SOLAR CELLS

I. Weinberg, H. W. Brandhorst, Jr., C. K. Swartz, and S. Mehta (Cleveland State Univ., Ohio) 1982 15 p refs Presented at the 3rd European Symp. on Photovoltaic Generators in Space, Bath, England, 4-6 May, 1982; sponsored by RAE, the U.K. Dept. of Industry and ESA (NASA-TM-82892; E-1270; NAS 1.15:82892) Avail: NTIS HC A02/MF A01 CSCL 10A

Gallium and boron doped silicon solar cells, processed by ion-implantation followed by either laser or furnace anneal were irradiated by 1 MeV electrons and their post-irradiation recovery by thermal annealing determined. During the post-irradiation anneal, gallium-doped cells prepared by both processes recovered more rapidly and exhibited none of the severe reverse annealing observed for similarly processed 2 ohm-cm boron doped cells. Ion-implanted furnace annealed 0.1 ohm-cm boron doped cells exhibited the lowest post-irradiation annealing temperatures (200 C) after irradiation to 5×10 to the 13th e(-)/sq cm. The drastically lowered recovery temperature is attributed to the reduced oxygen and carbon content of the 0.1 ohm-cm cells. Analysis based on defect properties and annealing kinetics indicates that further reduction in annealing temperature should be attainable with further reduction in the silicon's carbon and/or divacancy content after irradiation. Author

A82-11706*# Alkaline regenerative fuel cell systems for energy storage. F. H. Schubert (Life Systems, Inc., Cleveland, OH), M. A. Reid (NASA, Lewis Research Center, Cleveland, OH), and R. E. Martin (United Technologies Corp., South Windsor, CT). In: Intersociety Energy Conversion Engineering Conference, 16th, Atlanta, GA, August 9-14, 1981, Proceedings, Volume 1. (A82-11701 02-44) New York, American Society of Mechanical Engineers, 1981, p. 61-66, 11 refs.

ORIGINAL PAGE IS
OF POOR QUALITY

A description is presented of the results of a preliminary design study of a regenerative fuel cell energy storage system for application to future low-earth orbit space missions. The high energy density storage system is based on state-of-the-art alkaline electrolyte cell technology and incorporates dedicated fuel cell and electrolysis cell modules. In addition to providing energy storage, the system can provide hydrogen and oxygen for attitude control of the satellite and for life support. During the daylight portion of the orbit the electrolysis module uses power provided by the solar array to generate H₂ and O₂ from the product water produced by the fuel cell module. The fuel cell module supplies electrical power during the dark period of the orbit. G.R.

A82-11736 * # High power solar array switching regulation. D. K. Decker, J. Cassinelli (TRW Defense and Space Systems Group, Redondo Beach, CA), and M. Valgora (NASA, Lewis Research Center, Cleveland, OH). In: Intersociety Energy Conversion Engineering Conference, 16th, Atlanta, GA, August 9-14, 1981, Proceedings, Volume 1. (A82-11701 02-44) New York, American Society of Mechanical Engineers, 1981, p. 224-231.

It is pointed out that spacecraft utilization projections for the 1980s and beyond show a trend toward extended lifetimes and larger electric power systems. The need for improved power management and energy transfer arising in connection with this trend has resulted in the conduction of a Solar Array Switching Power Management study. A description is presented of initial development work performed in the study, taking into account the characteristics for three mission classes. Attention is given to the manned LEO platform (250-kw average load), the unmanned GEO platform (50-kw average load), and an ion propulsion orbit transfer vehicle (50- to 250 kW load). G.R.

A82-11765 * # Gallium arsenide solar cells-status and prospects for use in space. H. W. Brandhorst, D. Flood, and I. Weinberg (NASA, Lewis Research Center, Cleveland, OH). In: Intersociety Energy Conversion Engineering Conference, 16th, Atlanta, GA, August 9-14, 1981, Proceedings, Volume 1. (A82-11701 02-44) New York, American Society of Mechanical Engineers, 1981, p. 409-415. 27 refs.

Gallium Arsenide solar cells now equal or surpass the ubiquitous silicon solar cells in efficiency, radiation resistance, annealability, and in the capability for producing usable power output at elevated temperatures. NASA has developed a long-range research and development program to capitalize on these manifold advantages. In this paper we review the current state and future prospects for R&D in this promising solar cell material, and indicate the progress being made toward development of GaAs cells suitable for a variety of space missions. Results are presented from studies which demonstrate conclusively that GaAs cells can provide a net mission cost and weight savings for certain important mission classes. (Author)

A82-11796 * # Multijunction high voltage concentrator solar cells. G. J. Valco, V. J. Kapoor (Case Western Reserve University, Cleveland, OH), J. C. Evans, and A.-T. Chal (NASA, Lewis Research Center, Cleveland, OH). In: Intersociety Energy Conversion Engineering Conference, 16th, Atlanta, GA, August 9-14, 1981, Proceedings, Volume 2. (A82-11701 02-44) New York, American Society of Mechanical Engineers, 1981, p. 1649-1653. NASA-supported research.

The standard integrated circuit technology has been developed to design and fabricate new innovative planar multi-junction solar cell chips for concentrated sunlight applications. This 1 cm x 1 cm cell consisted of several voltage generating regions called unit cells which were internally connected in series within a single chip resulting in high open circuit voltages. Typical open-circuit voltages of 3.6 V and short-circuit currents of 90 ma were obtained at 80 AM1 suns. A dramatic increase in both short circuit current and open circuit voltage with increased light levels was observed. (Author)

A82-15438 * # Measuring the spacecraft and environmental interactions of the 8-cm mercury ion thrusters on the P80-1 mission. J. L. Power (NASA, Lewis Research Center, Ion Auxiliary Propulsion Office, Cleveland, OH). In: Electric propulsion and its applications to space missions. (A82-15432 04-12) New York, American Institute of Aeronautics and Astronautics, 1981, p. 813-825. 14 refs.

The subject interface measurements are described for the Ion Auxiliary Propulsion System (IAPS) flight test of two 8-cm thrusters. The diagnostic devices and the effects to be measured include: 1) quartz crystal microbalances to detect nonvolatile deposition due to thruster operation; 2) warm and cold solar cell monitors for nonvolatile and volatile (mercury) deposition; 3) retarding potential ion collectors to characterize the low energy thruster ionic efflux; and 4) a probe to measure the spacecraft potential and thruster generated electron currents to biased spacecraft surfaces. The diagnostics will also assess space environmental interactions of the spacecraft and thrusters. The diagnostic data will characterize mercury thruster interfaces and provide data useful for future applications. (Author)

A82-35087 * # A simplified design procedure for life prediction of rocket thrust chambers. J. S. Porowski, W. J. O'Donnell, M. L. Badlani, B. Kasraie (O'Donnell and Associates, Inc., Pittsburgh, PA), and H. J. Kaspar (NASA, Lewis Research Center, Cleveland, OH). *AIAA, SAE, and ASME, Joint Propulsion Conference, 18th, Cleveland, OH, June 21-23, 1982, AIAA Paper 82-1251*. 9 p. 8 refs.

An analytical procedure for predicting thrust chamber life is developed. The hot-gas-wall ligaments separating the coolant and combustion gas are subjected to pressure loading and severe thermal cycling. The resulting stresses interact during plastic straining causing incremental bulging of the ligaments during each firing cycle. This mechanism of plastic ratcheting is analyzed and a method using a yield surface for combined bending and membrane loading developed for determining the incremental permanent deflection and progressive thinning near the center of the ligaments. Fatigue and tensile instability are analyzed as possible failure modes. Results of the simplified analyses compare favorably with available experimental data and finite element analysis results for OFHC (Oxygen Free High Conductivity) copper. They are also in reasonably good agreement with experimental data for NARloy Z, a copper-zirconium-silver alloy developed by the Rocketdyne Division of Rockwell International. (Author)

A82-39599 * On the cause of the flat-spot phenomenon observed in silicon solar cells at low temperatures and low intensities. V. G. Welzer and J. D. Broder (NASA, Lewis Research Center, Cleveland, OH). *Journal of Applied Physics*, vol. 53, Aug. 1982, p. 5926-5930. 15 refs.

A model is presented that explains the 'flat-spot' power-loss phenomenon observed in silicon solar cells operating under deep space (low temperature, low intensity) conditions. Evidence is presented suggesting that the effect is due to localized metallurgical interactions between the silicon substrate and the contact metallization. These reactions are shown to result in localized regions in which the PN junction is destroyed and replaced with a metal-semiconductor-like inter-depth, and metallization are presented along with a method of preventing the effect through the suppression of vacancy formation at the free surface of the contact metallization. Preliminary data indicating the effectiveness of a TiN diffusion barrier in preventing the effect are also given. (Author)

A82-44750 * # Component technology for space power systems. R. C. Finke (NASA, Lewis Research Center, Cleveland, OH). *International Astronautical Federation, International Astronautical Congress, 33rd, Paris, France, Sept. 27-Oct. 2, 1982, Paper 82-408* 10 p. 15 refs.

Progress made by NASA toward implementation of equipment for the conversion, management, and distribution of voltage power in space applications are reviewed. Work has been carried forward on components such as bipolar transistors, deep impurity semiconductors, conductors, dielectrics, magnetic devices, and rotary power transfer. Specific programs for the high voltage systems have included research on lightweight, low-cost conductors featuring graphite fibers containing electron donor materials for wires and cables with reduced mass and the conductivity of copper. Attention has also been given p-n junction technology for high-speed, high-current, high-voltage materials and diamond-like dielectric films which are hard, have high dielectric strength, and can operate up to 300 C. A transistor has been fabricated with a voltage of 1200 V at 100 A, with a gain of 10 and a 0.5 microsec rise/fall time. A 25 kW transformer has also been built which performs at 20 kHz with an efficiency of 99.2%. M.S.K.

ORIGINAL PAGE IS
OF POOR QUALITY

A82-44085 * # On the cause of the flat spot phenomenon observed in silicon solar cells at low temperatures and low intensities. V. G. Weizer and J. D. Broder (NASA, Lewis Research Center, Cleveland, OH). In: Photovoltaic Specialists Conference, 15th, Kissimmee, FL, May 12-15, 1981, Conference Record. (A82-44028 23-44) New York, Institute of Electrical and Electronics Engineers, Inc., 1981, p. 235, 236. 6 refs.

The results of an effort to determine the mechanisms involved in the flat spot (FS) effect are given. It is suggested that the FS effect is due to a resistive metal-semiconductor-like (MSL) interface in parallel with the cell PN junction. Regions responsible for the FS effect lie under the front surface metallization in these cells, where the PN junction has been destroyed and replaced with a metal silicide-semiconductor interface. Such structural changes, which appear to be due to the thermally activated dissolution of the silicon, have been induced in cells as a result of isochronal heat treatments at temperatures between 450 C and 560 C. It has been found that a 650 A layer of Ta₂O₅ evaporated over the metallization is sufficient to prevent the underlying silicon from pitting during the subsequent heat treatment, although pitting at the metal silicon ambient interface could still be observed. A.B.

N82-11111* # Boeing Aerospace Co., Seattle, Wash.
STUDY OF ELECTRICAL AND CHEMICAL PROPULSION SYSTEMS FOR AUXILIARY PROPULSION OF LARGE SPACE SYSTEMS, VOLUME 2 Final Report
W. W. Smith Nov. 1981 540 p refs 2 Vol.
(Contract NAS3-21952)
(NASA-CR-165502-Vol-2; D180-2595-4-Vol-2) Avail: NTIS HC A23/MF A01 CSCL 21H

The five major tasks of the program are reported. Task 1 is a literature search followed by selection and definition of seven generic spacecraft classes. Task 2 covers the determination and description of important disturbance effects. Task 3 applies the disturbances to the generic spacecraft and adds maneuver and stationkeeping functions to define total auxiliary propulsion systems requirements for control. The important auxiliary propulsion system characteristics are identified and sensitivities to control functions and large space system characteristics determined. In Task 4, these sensitivities are quantified and the optimum auxiliary propulsion system characteristics determined. Task 5 compares the desired characteristics with those available for both electrical and chemical auxiliary propulsion systems to identify the directions technology advances should take. T.M.

N82-12133* # Hughes Research Labs., Malibu, Calif. Ion Physics Dept.
RETROFIT AND ACCEPTANCE TEST OF 30-cm ION THRUSTERS Final Report, 12 Apr. 1978 - 1 Apr. 1981
R. L. Poeschel Jun. 1981 324 p
(Contract NAS3-21357)
(NASA-CR-165259) Avail: NTIS HC A14/MF A01 CSCL 21C

Six 30 cm mercury thrusters were modified to the J-series design and evaluated using standardized test procedures. The thruster performance meets the design objectives (lifetime objective requires verification), and documentation (drawings, etc.) for the design is completed and upgraded. The retrofit modifications are described and the test data for the modifications are presented and discussed. S.L.

N82-16172* # Rocketdyne, Canoga Park, Calif.
REUSABLE ROCKET ENGINE MAINTENANCE STUDY Final Report, Sep. 1980 - Oct. 1981
Charles A. MacGregor Jan. 1982 306 p
(Contract NAS3-22652)
(NASA-CR-165569; RI/RD81-226) Avail: NTIS HC A14/MF A01 CSCL 21H

Approximately 85,000 liquid rocket engine failure reports, obtained from 30 years of developing and delivering major pump feed engines, were reviewed and screened and reduced to 1771. These were categorized into 16 different failure modes. Failure propagation diagrams were established. The state of the art of engine condition monitoring for in-flight sensors and between flight inspection technology was determined. For the 16 failure modes, the potential measurands and diagnostic requirements were identified, assessed and ranked. Eight areas are identified requiring advanced technology development. T.M.

N82-19315* # Martin Marietta Aerospace, Denver, Colo.
PRIMARY PROPULSION/LARGE SPACE SYSTEM INTER-ACTION STUDY Final Report, Sep. 1979 - Dec. 1980
J. V. Coyner, R. H. Dergance, R. I. Robertson, and J. V. Wiggins Dec. 1981 358 p refs
(Contract NAS3-21955)
(NASA-CR-165277; MCR81-504) Avail: NTIS HC A16/MF A01 CSCL 21H

An interaction study was conducted between propulsion systems and large space structures to determine the effect of low thrust primary propulsion system characteristics on the mass, area, and orbit transfer characteristics of large space systems (LSS). The LSS which were considered would be deployed from the space shuttle orbiter bay in low Earth orbit, then transferred to geosynchronous equatorial orbit by their own propulsion systems. The types of structures studied were the expandable box truss, hoop and column, and wrap radial rib each with various surface mesh densities. The impact of the acceleration forces on system sizing was determined and the effects of single point, multipoint, and transient thrust applications were examined. Orbit transfer strategies were analyzed to determine the required velocity increment, burn time, trip time, and payload capability over a range of final acceleration levels. Variables considered were number of perigee burns, delivered specific impulse, and constant thrust and constant acceleration modes of propulsion. Propulsion stages were sized for four propellant combinations: oxygen/hydrogen, oxygen/methane, oxygen/kerosene, and nitrogen tetroxide/monomethylhydrazine, for pump fed and pressure fed engine systems. Two types of tankage configurations were evaluated, minimum length to maximize available payload volume and maximum performance to maximize available payload mass. S.L.

N82-21252* # Xerox Electro-Optical Systems, Pasadena, Calif.
INERT GAS ION THRUSTER Final Report, Mar. 1978 - Dec. 1980
William D. Ramsey Dec. 1980 90 p refs
(Contract NAS3-21345)
(NASA-CR-165521; NAS 1.26:165521; Rept-2372-5009) Avail: NTIS HC A05/MF A01 CSCL 21C

Inert gas performance with three types of 12 cm diameter magneto-electrostatic containment (MESC) ion thrusters was tested. The types tested included: (1) a hemispherical shaped discharge chamber with platinum cobalt magnets; (2) three different lengths of the hemispherical chambers with samarium cobalt magnets; and (3) three lengths of the conical shaped chambers with aluminum nickel cobalt magnets. The best argon performance was produced by a 8.0 cm long conical chamber with alnico magnets. The best xenon high mass utilization performance was obtained with the same 8.0 cm long conical thruster. The hemispherical thruster obtained 75 to 87% mass utilization at 185 to 205 eV/ion of singly charged ion equivalent beam. E.A.K.

N82-21253* # O'Donnell and Associates, Inc., Pittsburgh, Pa.
DEVELOPMENT OF A SIMPLIFIED PROCEDURE FOR THRUST CHAMBER LIFE PREDICTION Final Report
J. S. Porowski, M. Badlani, B. Kasrale, W. J. O'Donnell, and D. Peterson Oct. 1981 85 p refs
(Contract NAS3-22649)
(NASA-CR-165585; NAS 1.26:165585; ODAI-1403-12-81) Avail: NTIS HC A05/MF A01 CSCL 21H

An analytical design procedure for predicting thrust chamber life considering cyclically induced thinning and bulging of the hot gas wall is developed. The hot gas wall, composed of ligaments connecting adjacent cooling channel ribs and separating the coolant flow from the combustion gas, is subjected to pressure loading and severe thermal cycling. Thermal transients during start up and shut down cause plastic straining through the ligaments. The primary bending stress superimposed on the alternate in-plane cyclic straining causes incremental bulging of the ligaments during each firing cycle. This basic mechanism of plastic ratcheting is analyzed and a method developed for determining ligament deformation and strain. The method uses a yield surface for combined bending and membrane loading to determine the incremental permanent deflection and progressive thinning near the center of the ligaments which cause the geometry of the ligaments to change as the incremental strains accumulate. Fatigue and tensile instability are affected by these local geometry changes. Both are analyzed and a failure criterion developed. Author

ORIGINAL PAGE IS
OF POOR QUALITY

N82-22308* Aerojet Liquid Rocket Co., Sacramento, Calif.
LOW-THRUST Isp SENSITIVITY STUDY Final Report
L. Schoenman 12 Apr. 1982 265 p refs
(Contract NAS3-22665)
(NASA-CR-165621; NAS 1.26:165621) Avail: NTIS
HC A12/MF A01 CSCL 21H

A comparison of the cooling requirements and attainable specific impulse performance of engines in the 445 to 4448N thrust class utilizing LOX/RP-1, LOX/Hydrogen and LOX/Methane propellants is presented. The unique design requirements for the regenerative cooling of low-thrust engines operating at high pressures (up to 6894 kPa) were explored analytically by comparing single cooling with the fuel and the oxidizer, and dual cooling with both the fuel and the oxidizer. The effects of coolant channel geometry, chamber length, and contraction ratio on the ability to provide proper cooling were evaluated, as was the resulting specific impulse. The results show that larger contraction ratios and smaller channels are highly desirable for certain propellant combinations. T.M.

N82-24285* Colorado State Univ., Fort Collins. Dept. of Mechanical Engineering.
ELECTRIC THRUSTER RESEARCH
Harold R. Kaufman and Raymond S. Robinson Dec. 1981 151 p refs
(Grant NsG-3011)
(NASA-CR-165603; NAS 1.26:165603) Avail: NTIS
HC A08/MF A01 CSCL 21C

The multipole discharge chamber of an electrostatic ion thruster is discussed. No reductions in discharge losses were obtained, despite repeated demonstration of anode potentials more positive than the bulk of the discharge plasma. The penalty associated with biased anode operation was reduced as the magnetic integral above the biased anodes was increased. The hollow cathode is discussed. The experimental configuration of the Hall current thruster had a uniform field throughout the ion generation and acceleration regions. To obtain reliable ion generation, it was necessary to reduce the magnetic field strength, to the point where excessive electron backflow was required to establish ion acceleration. The theoretical study of ion acceleration with closed electron drift paths resulted in two classes of solutions. One class has the continuous potential variation in the acceleration region that is normally associated with a Hall current accelerator. The other class has an almost discontinuous potential step near the anode end of the acceleration region. This step includes a significant fraction of the total acceleration potential difference. Author

N82-24287* General Dynamics/Convair, San Diego, Calif.
LOW-THRUST CHEMICAL PROPULSION SYSTEM PROPELLANT EXPULSION AND THERMAL CONDITIONING STUDY. EXECUTIVE SUMMARY
F. Merino, I. Wakabayashi, R. L. Pleasant, and M. Hill Apr. 1982 42 p refs
(Contract NAS3-22650)
(NASA-CR-165622; GDC-NAS-82-001; NAS 1.26:165622)
Avail: NTIS HC A03/MF A01 CSCL 21H

Preferred techniques for providing abort pressurization and engine feed system net positive suction pressure (NPSP) for low thrust chemical propulsion systems (LTPS) were determined. A representative LTPS vehicle configuration is presented. Analysis tasks include: propellant heating analysis; pressurant requirements for abort propellant dump; and comparative analysis of pressurization techniques and thermal subcoolers. T.M.

N82-24288* General Dynamics/Convair, San Diego, Calif.
LOW-THRUST CHEMICAL PROPULSION SYSTEM PROPELLANT EXPULSION AND THERMAL CONDITIONING STUDY
F. Merino, I. Wakabayashi, R. L. Pleasant, and M. Hill Apr. 1982 210 p refs
(Contract NAS3-22650)
(NASA-CR-167841; GDC-NAS-82-002; NAS 1.26:167841)
Avail: NTIS HC A10/MF A01 CSCL 21H

Thermal conditioning systems for satisfying engine net positive suction pressure (NPSP) requirements, and propellant expulsion systems for achieving propellant dump during a return-to-launch site (RTLS) abort were studied for LH2/LO2 and LCH4/LO2 upper stage propellant combinations. A state-of-the-art thermal

conditioning system employing helium injection beneath the liquid surface shows the lowest weight penalty for LO2 and LCH4. A technology system incorporating a thermal subcooler (heat exchanger) for engine NPSP results in the lowest weight penalty for the LH2 tank. A preliminary design of two state-of-the-art and two new technology systems indicates a weight penalty difference too small to warrant development of a LH2 thermal subcooler. Analysis results showed that the LH2/LO2 propellant expulsion system is optimized for maximum dump line diameters, whereas the LCH4/LO2 system is optimized for minimum dump line diameter (LCH4) and maximum dump line diameter (LO2). The primary uncertainty is the accurate determination of two-phase flow rates through the dump system; experimentation is not recommended because this uncertainty is not considered significant. Author

N82-26381* Tuskegee Inst., Ala.
CHARACTERIZATION OF ADVANCED ELECTRIC PROPULSION SYSTEMS Final Report, 1 Jun. 1980 - 31 Jan. 1982
Pradosh K. Ray May 1982 82 p refs
(Grant NAG3-76)
(NASA-CR-167885; NAS 1.26:167885) Avail: NTIS
HC A05/MF A01 CSCL 21C

Characteristics of several advanced electric propulsion systems are evaluated and compared. The propulsion systems studied are mass driver, rail gun, MPD thruster, hydrogen free radical thruster and mercury electron bombardment ion engine. These are characterized by specific impulse, overall efficiency, input power, average thrust, power to average thrust ratio and average thrust to dry weight ratio. Several important physical characteristics such as dry system mass, accelerator length, bore size and current pulse requirement are also evaluated in appropriate cases. Only the ion engine can operate at a specific impulse beyond 2000 sec. Rail gun, MPD thruster and free radical thruster are currently characterized by low efficiencies. Mass drivers have the best performance characteristics in terms of overall efficiency, power to average thrust ratio and average thrust to dry weight ratio. But, they can only operate at low specific impulses due to large power requirements and are extremely long due to limitations of driving current. Mercury ion engines have the next best performance characteristics while operating at higher specific impulses. It is concluded that, overall, ion engines have somewhat better characteristics as compared to the other electric propulsion systems. Author

N82-28350* Colorado State Univ., Fort Collins. Dept. of Mechanical Engineering.
ELECTRIC AND MAGNETIC FIELDS
Harold R. Kaufman, Raymond S. Robinson, and Richard D. Eters Mar. 1982 42 p refs
(Grant NsG-3011)
(NASA-CR-165604; NAS 1.26:165604) Avail: NTIS
HC A03/MF A01 CSCL 21C

A number of energy momentum anomalies are described that result from the use of Abraham-Lorentz electromagnetic theory. These anomalies have in common the motion of charged bodies or current carrying conductors relative to the observer. The anomalies can be avoided by using the nonflow approach, based on internal energy of the electromagnetic field. The anomalies can also be avoided by using the flow approach, if all contributions to flow work are included. The general objective of this research is a fundamental physical understanding of electric and magnetic fields which, in turn, might promote the development of new concepts in electric space propulsion. The approach taken is to investigate quantum representations of these fields. T.M.

N82-33424* TRW Defense and Space Systems Group, Redondo Beach, Calif.
INTEGRATED PROPULSION FOR NEAR-EARTH SPACE MISSIONS. VOLUME 1: EXECUTIVE SUMMARY Final Report, 29 Sep. 1980 - 29 Sep. 1981
C. L. Dailey, H. F. Meissinger, R. H. Lovberg, and S. Zafran Oct. 1981 27 p refs
(Contract NAS3-22661)
(NASA-CR-167889-Vol-1; NAS 1.26:167889-Vol-1;
TRW-37255-6001-UT-Vol-1) Avail: NTIS HC A03/MF A01 CSCL
21C

Tradeoffs between electric propulsion system mass ratio and transfer time from LEO to GEO were conducted parametrically for various thruster efficiency, specific impulse, and other propulsion parameters. A computer model was developed for performing orbit transfer calculations which included the effects of aerodynamic drag, radiation degradation, and occultation. The tradeoff results showed that thruster technology areas for integrated propulsion should be directed towards improving primary thruster efficiency in the range from 1500 to 2500 seconds, and be continued towards reducing specific mass. Comparison of auxiliary propulsion systems showed large total propellant mass savings with integrated electric auxiliary propulsion. Stationkeeping is the most demanding on orbit propulsion requirement. At area densities above 0.5 sq m/kg, East-West stationkeeping requirements from solar pressure exceed North-South stationkeeping requirements from gravitational forces. A solar array pointing strategy was developed to minimize the effects of atmospheric drag at low altitude, enabling electric propulsion to initiate orbit transfer at Shuttle's maximum cargo carrying altitude. Gravity gradient torques are used during ascent to sustain the spacecraft roll motion required for optimum solar array illumination. A near optimum cover glass thickness of 6 mils was established for LEO to GEO transfer. Author

N82-33425*# TRW Defense and Space Systems Group, Redondo Beach, Calif.
INTEGRATED PROPULSION FOR NEAR-EARTH SPACE MISSIONS. VOLUME 2: TECHNICAL Final Report, 29 Sep. 1980 - 29 Sep. 1981

C. L. Dailey, H. F. Meissinger, R. H. Lovberg, and S. Zafran Oct. 1981 173 p refs
(Contract NAS3-22661)
(NASA-CR-167889-Vol-2; NAS 1.20-167889-Vol-2;
TRW-37255-6002-UT-Vol-2) Avail: NTIS HC A08/MF A01 CSCL 21C

The calculation approach is described for parametric analysis of candidate electric propulsion systems employed in LEO to GEO missions. Occultation relations, atmospheric density effects, and natural radiation effects are presented. A solar cell cover glass tradeoff is performed to determine optimum glass thickness. Solar array and spacecraft pointing strategies are described for low altitude flight and for optimum array illumination during ascent. Mass ratio tradeoffs versus transfer time provide direction for thruster technology improvements. Integrated electric propulsion analysis is performed for orbit boosting, inclination change, attitude control, stationkeeping, repositioning, and disposal functions as well as power sharing with payload on orbit. Comparison with chemical auxiliary propulsion is made to quantify the advantages of integrated propulsion in terms of weight savings and concomitant launch cost savings. Author

N82-11110*# Boeing Aerospace Co., Seattle, Wash.
STUDY OF ELECTRICAL AND CHEMICAL PROPULSION SYSTEMS FOR AUXILIARY PROPULSION OF LARGE SPACE SYSTEMS. VOLUME 1: EXECUTIVE SUMMARY
W. W. Smith and J. P. Clark Nov. 1981 35 p refs 2 Vol.
(Contract NAS3-21952)
(NASA-CR-165502-Vol-1; D180-25956-3-Vol-1) Avail: NTIS HC A03/MF A01 CSCL 21H

The objective was to determine the direction auxiliary propulsion research and development should take to best meet upcoming needs. The approach used was to define the important electrical and chemical propulsion characteristics in terms of the demands that will be imposed by future spacecraft. Comparison of these desired characteristics and capabilities with those presently available was then used to identify deficiencies. T.M.

A82-11762*# High- and low-resistivity silicon solar cells. A. Meulenber, Jr. and R. A. Arndt (COMSAT Laboratories, Clarksburg, MD). In: Intersociety Energy Conversion Engineering Conference, 16th, Atlanta, GA, August 9-14, 1981, Proceedings. Volume 1. (A82-11701 02-44) New York, American Society of Mechanical Engineers, 1981, p. 397-399. 13 refs. Research sponsored by the Communications Satellite Corp.; Contracts No. NAS3-21280; No. NAS3-22217.

Attention is given to recent work at COMSAT Laboratories on improving silicon solar cell efficiencies and open-circuit voltages for both high (more than 1000 ohm-cm) and low (less than 1 ohm-cm) resistivities. It is noted that open-circuit voltages above 650 mV have been obtained for 0.1 ohm-cm cells and that air mass zero efficiencies of 12.5% have been measured from 4-mil 1,250 ohm-cm. C.R.

A82-13434*# 30-cm mercury ion thruster technology. R. L. Poeschel, J. R. Beattie, P. A. Robinson, and J. W. Ward (Hughes Research Laboratories, Malibu, CA). In: Electric propulsion and its applications to space missions. (A82-15432 04-12) New York, American Institute of Aeronautics and Astronautics, 1981, p. 346-361. 21 refs. Contract No. NAS3-21040.

The LeRC/Hughes 30-cm mercury ion thruster has been developed to a state of maturity such that it has become meaningful to formulate models for describing the performance characteristics of the major subassemblies. The thruster hollow cathode and the ion optics subassemblies have been investigated with this objective and conceptual, semiquantitative models have been formulated for relating lifetime and performance capabilities to design and operating parameters. This paper summarizes the investigations, discusses the factors considered for inclusion in the models, and describes the status of the models. (Author)

A82-15435*# Characteristics of the LeRC/Hughes J-series 30-cm engineering model thruster. C. R. Collett, R. L. Poeschel, and S. Kami (Hughes Research Laboratories, Malibu, CA). In: Electric propulsion and its applications to space missions. (A82-15432 04-12) New York, American Institute of Aeronautics and Astronautics, 1981, p. 376-388. 25 refs. Contracts No. NAS3-21052; No. NAS3-21357.

As a consequence of endurance and structural tests performed on 900-series engineering model thrusters (EMT), several modifications in design were found to be necessary for achieving performance goals. The modified thruster is known as the J-series EMT. The most important of the design modifications affect the accelerator grid, gimbal mount, cathode polepiece, and wiring harness. The paper discusses the design modifications incorporated, the condition(s) they corrected, and the characteristics of the modified thruster. (Author)

A82-18191* Mass Driver Two - A status report. W. R. Snow, R. S. Dunbar, J. A. Kubby, and G. K. O'Neill (Princeton University, Princeton, NJ). (U.S. Army Armaments Research and Development Command and Defense Advanced Research Projects Agency, Conference on Electromagnetic Guns and Launchers, San Diego, CA, Nov. 4-6, 1980.) IEEE Transactions on Magnetics, vol. MAG-18, Jan. 1982, p. 127-134. 9 refs. Research supported by the Space Studies Institute; Grant No. NSG-3176.

The current status of Mass Driver Two, a linear synchronous motor for accelerating payloads or reaction mass, is discussed. Mass Driver Two combines all the essential elements of an operational mass driver with the exception of bucket recirculation and payload handling. These essential elements include: magnetic flight, vacuum environment, superconducting bucket coils, high acceleration (nominally 500 g's), optical position sensing and electronic triggering, power circuitry similar to that of a flight article, and regenerative braking. Mass Driver Two is operated on a single shot basis. V.L.

A82-18199* Mass driver reaction engine characteristics and performance in earth orbital transfer missions. W. R. Snow and R. S. Dunbar (Princeton University, Princeton, NJ). (U.S. Army Armaments Research and Development Command and Defense Advanced Research Projects Agency, Conference on Electromagnetic Guns and Launchers, San Diego, CA, Nov. 4-6, 1980.) IEEE Transactions on Magnetics, vol. MAG-18, Jan. 1982, p. 176-189. 19 refs. Research supported by the Space Studies Institute; Grant No. NSG-3176.

Configurations of a typical mass driver reaction engine (MDRE) are presented and its use for delivery of payloads to geosynchronous orbit (GEO) from low earth orbit (LEO) is discussed. Basic rocket equations are developed for LEO to GEO round-trip missions using a

single exhaust velocity. It is shown that exhaust velocities in the 5-10 km/sec range (specific impulse of 500-1000 sec) are well suited for mass drivers, minimizing the overall cost of missions. Payload delivery rate fractions show that there is little to be gained by stretching out LEO to GEO transfer times from 90 to 180 days. It therefore pays to use the shorter trip time, approximately doubling the amount of delivered payload during any fixed time of use of the MDRE.

V.L.

A82-35056 * # Propulsion system options for low-acceleration orbit transfer. L. Schoenman (Aerojet Liquid Rocket Co., Sacramento, CA). *AIAA, SAE, and ASME, Joint Propulsion Conference, 18th, Cleveland, OH, June 21-23, 1982, AIAA Paper 82-1196.* 7 p. 6 refs. Contracts No. NAS3-21940; No. NAS3-22665.

The present inventory of developed bipropellant engines suitable for the orbit transfer of large space structures is based on the use of storable propellants (nitrogen tetroxide/monomethyl hydrazine). A range of engine sizes from 22N (5 lbF) to over 26,690N (6000 lbF) is available. These engines are capable of delivering specific impulse values from 2795 to 3089 N-s/kg (285 to 315 lbF-sec/lbm). A comparison is made between the attainable specific impulse of these demonstrated engines and future low-thrust engine designs which can utilize LOX/RP-1, LOX-methane, and LOX/hydrogen propellants. The requirements for cooling these small engines for multi-hour burns as well as the merits of operating at nonoptimum performance mixture ratios to improve cooling margins and reduce tank volumes are addressed in this paper.

(Author)

ORIGINAL PAGE IS
OF POOR QUALITY

A82-37713 * # Developing a scalable inert gas ion thruster. E. James, W. Ramsey, and G. Steiner (Xerox Electro-Optical Systems, Pasadena, CA). *AIAA, SAE, and ASME, Joint Propulsion Conference, 18th, Cleveland, OH, June 21-23, 1982, AIAA Paper 82-1275.* 9 p. 9 refs. Contracts No. NAS3-22444; No. NAS3-22876.

Analytical studies to identify and then design a high performance scalable ion thruster operating with either argon or xenon for use in large space systems are presented. The magnetoelectrostatic containment concept is selected for its efficient ion generation capabilities. The iterative nature of the bounding magnetic fields allows the designer to scale both the diameter and length, so that the thruster can be adapted to spacecraft growth over time. Three different thruster assemblies (conical, hexagonal and hemispherical) are evaluated for a 12 cm diameter thruster and performance mapping of the various thruster configurations shows that conical discharge chambers produce the most efficient discharge operation, achieving argon efficiencies of 50-80% mass utilization at 240-310 eV/ion and xenon efficiencies of 60-97% at 240-280 eV/ion. Preliminary testing of the large 30 cm thruster, using argon propellant, indicates a 35% improvement over the 12 cm thruster in mass utilization efficiency. Since initial performance is found to be better than projected, a larger 50 cm thruster is already in the development stage.

N.B.

23 CHEMISTRY AND MATERIALS (GENERAL)

Includes biochemistry and organic chemistry.

NS2-15119* National Aeronautics and Space Administration, Lewis Research Center, Cleveland, Ohio.

THERMODYNAMICS AND KINETICS OF THE SULFATION OF POROUS CALCIUM SILICATE

Robert A. Miller and Fred J. Kohl 1981 18 p refs Presented at the Fall Meeting of the Electrochem. Soc., Inc., Denver, 11-17 Oct. 1981

(NASA-TM-82769; E-1023) Avail: NTIS HC A02/MF A01 CSDL 11G

The sulfation of plasma sprayed calcium silicate in flowing SO₂/air mixtures at 900 and 1000 C was investigated thermogravimetrically. Reaction products were analyzed using electron microprobe and X-ray diffraction analysis techniques, and results were compared with thermodynamic predictions. The percentage, by volume, of SO₂ in air was varied between 0.036 and 10 percent. At 10 percent SO₂ the weight gain curve displays a concave downward shoulder early in the sulfation process. An analytical model was developed which treats the initial process as one which decays exponentially with increasing time and the subsequent process as one which decays exponentially with increasing weight gain. At lower SO₂ levels the initial rate is controlled by the reactant flow rate. At 1100 C and 0.036 percent SO₂ there is no reaction, in agreement with thermodynamic predictions. S.L.

NS2-17263* National Aeronautics and Space Administration, Lewis Research Center, Cleveland, Ohio.

PERFORMANCE OF PTFE-LINED COMPOSITE JOURNAL BEARINGS

Harold E. Sliney and Frank J. Williams (North American Aviation, Inc., Los Angeles) 1982 18 p refs Presented at Ann. Meeting of the Am. Soc. of Lubrication Engr., Cincinnati, 10-13 May 1982

(NASA-TM-82779; E-1110) Avail: NTIS HC A02/MF A01 CSDL 13I

Plain cylindrical journal bearings consisting of aramid fiber reinforced epoxy outer shells and glass fiber reinforced PTFE lubricating liners were evaluated. All materials in these bearings are electrically nonconductive; thus eliminating the problem of galvanic corrosion sometimes encountered with metal bearings installed in dissimilar metal mountings. Friction and wear characteristics were determined for loads, temperatures, and oscillating conditions that are typical of current airframe bearing applications. Friction and wear characteristics were found to be compatible with most airframe bearing requirements from -23 C to 121 C. Contamination with MIL H-5606 hydraulic fluid increased wear of the PTFE liners at 121 C, but did not affect the structural integrity of the aramid/epoxy composite. Author

A82-23779* Inexpensive cross-linked polymeric separators made from water-soluble polymers. L.-C. Hsu and D. W. Sheibley (NASA, Lewis Research Center, Cleveland, OH). *Electrochemical Society, Journal*, vol. 129, Feb. 1982, p. 251-254.

Polyvinyl alcohol (PVA), cross-linked chemically with aldehyde reagents, produces membranes which demonstrate oxidation resistance, dimensional stability, low ionic resistivity (less than 0.8 Ohms sq cm), low zincate diffusivity (less than 1 x 10 to the -7th mols/sq cm per min), and low zinc dendrite penetration rate (greater than 350 min) which make them suitable for use as alkaline battery separators. They are intrinsically low in cost, and environmental health and safety problems associated with commercial production appear minimal. Preparation, property measurements, and cell test results in Ni/Zn and Ag/Zn cells are described and discussed.

(Author)

NS2-12138* Ultrasystems, Inc., Irvine, Calif. THERMAL OXIDATIVE DEGRADATION REACTIONS OF PERFLUOROALKYLETHERS Final Report, Sep. 1980 - Sep. 1981

K. L. Paciorek, T. I. Ito, and R. H. Kratzer Oct. 1981 46 p refs

(Contract NAS3-22517)

(NASA-CR-165516; SN-1020-A1-F)

Avail: NTIS

HC A03/MF A01 CSDL 07C

The mechanisms operative in thermal oxidative degradation of Fomblin Z and hexafluoropropene oxide derived fluids and the effect of alloys and additives upon these processes are investigated. The nature of arrangements responsible for the inherent thermal oxidative instability of the Fomblin Z fluids is not established. It was determined that this behavior is not associated with hydrogen end groups or peroxy linkages. The degradation rate of these fluids at elevated temperatures in oxidizing atmospheres is dependent on the surface/volume ratio. Once a limiting ratio is reached, a steady rate appears to be attained. Based on elemental analysis and oxygen consumption data, CF₂OCF₂CF₂O₂, no. CF₂CF₂O, is one of the major arrangements present. The action of the M-50 and Ti(4 Al, 4 Mn) alloys is much more drastic in the case of Fomblin Z fluids than that observed for the hexafluoropropene derived materials. The effectiveness of antioxidant anticorrosion additives, P-3 and phospho-s-triazine, in the presence of metal alloys is very limited at 316 C; at 288 C the additives arrested almost completely the fluid degradation. The phospho-s-triazine appears to be at least twice as effective as the P-3 compound; it also protected the coupon better. The Ti(4 Al, 4 Mn) alloy degraded the fluid mainly by chain scission processes this takes place to a much lesser degree with M-50. S.L.

A82-15696* Quantitative separation of tetralin hydroperoxide from its decomposition products by high performance liquid chromatography. J. H. Worstell and S. R. Daniel (Colorado School of Mines, Golden, CO). *Journal of Liquid Chromatography*, vol. 4, 1981, p. 539-547, 19 refs. Grant No. NSG-3122.

A method for the separation and analysis of tetralin hydroperoxide and its decomposition products by high pressure liquid chromatography has been developed. Elution with a single, mixed solvent from a micron-Porasil column was employed. Constant response factors (internal standard method) over large concentration ranges and reproducible retention parameters are reported.

(Author)

ORIGINAL PAGE IS
OF POOR QUALITY

24 COMPOSITE MATERIALS

Includes laminates.

N82-11117* National Aeronautics and Space Administration, Lewis Research Center, Cleveland, Ohio.**NOVEL IMPROVED PMR POLYIMIDES**

Ruth H. Pater 1981 18 p refs Presented at the 13th Natl. SAMPE Tech. Conf., Mt. Pocono, Pa., 13-15 Oct. 1981 (NASA-TM-82733; E-1045) Avail: NTIS HC A02/MF A01 CSCL 11D

A series of N-phenyladimide (PN) modified PMR polyimide composites reinforced with graphite fibers was investigated. The improved flow matrix resins consist of N-phenyladimide (PN), monomethyl ester of 5-norbornene-2, 3-dicarboxylic acid (NE), dimethyl ester of 3,3, 4,4-benzophenonetetracarboxylic acid (BTDE), and 4,4 methylenedianiline (MDA). Five modified PMR resin systems were formulated by the addition of 4 to 20 mole percent N-phenyladimide to the standard PMR-15 composition. These formulations and the control PMR resin were evaluated for rheological characteristics. The initial thermal and mechanical properties of the PN modified PMR and the control PMR/Celion 600C composites were determined. The results show that the addition of N-phenyladimide to PMR-15 significantly improved the resin flow characteristics without sacrificing the composites properties. Concentrations of 4 and 9 mole percent PN appear to improve the thermoxidative stability of PMR composites.

A.R.H.

N82-14287* National Aeronautics and Space Administration, Lewis Research Center, Cleveland, Ohio.**DURABILITY/LIFE OF FIBER COMPOSITES IN HYGRO-THERMOMECHANICAL ENVIRONMENTS**

C. C. Chamis and J. H. Sinclair 1981 28 p refs Presented at the Sixth Conf. on Composite Mater.: Testing and Design sponsored by the Am. Soc. for Testing and Mater., Phoenix, Ariz., 12-13 May 1981

(NASA-TM-82749; E-1065) Avail: NTIS HC A03/MF A01 CSCL 11D

Statistical analysis and multiple regression were used to determine and quantify the significant hygrothermomechanical variables which influence the tensile durability/life (cycle loading, fatigue) of boron-fiber/epoxy-matrix (B/E) and high-modulus-fiber/epoxy-matrix (HMS/E) composites. The use of the multiple regression analysis reduced the variables from fifteen, assumed initially, to six or less with a probability of greater than 0.999. The reduced variables were used to derive predictive models for compression and intralaminar shear durability/life of B/E and HMS/E composites assuming isoparametric fatigue behavior. The predictive models were subsequently generalized to predict the durability/life of graphite-fiber-r generalized model is of simple form, predicts conservative values compared with measured data and should be adequate for use in preliminary designs. B.W.

N82-16181* National Aeronautics and Space Administration, Lewis Research Center, Cleveland, Ohio.**PREDICTION OF COMPOSITE HYGRAL BEHAVIOR MADE SIMPLE**

Christos C. Chamis and J. H. Sinclair 1982 30 p refs Presented at the 37th Ann. Conf. of the Soc. of the Plastics Ind. (SPI), Washington, D.C., 12-15 Jan. 1982

(NASA-TM-82780; E-1022) Avail: NTIS HC A03/MF A01 CSCL 11D

A convenient procedure is described to determine the hygral behavior (moisture expansion coefficients and moisture stresses) of angleplied fiber composites using a pocket calculator. The procedure consists of equations and appropriate graphs for various (+ or - theta) ply combinations. These graphs present reduced stiffness and moisture expansion coefficients as functions of (+ or - theta) in order to simplify and expedite the use of the equations. The procedure is applicable to all types of balanced, symmetric fiber composites including interply and intraply hybrids. The versatility and generality of the procedure is illustrated using several step-by-step numerical examples. Author

N82-21258* National Aeronautics and Space Administration, Lewis Research Center, Cleveland, Ohio.**STRENGTH ADVANTAGES OF CHEMICALLY POLISHED BORON FIBERS BEFORE AND AFTER REACTION WITH ALUMINUM**

James A. DiCarlo and Robert J. Smith 1982 28 p refs Presented at the 6th Ann. Conf. on Composites and Advanced Mater., Cocoa Beach, Fla., 18-21 Jan. 1982; sponsored by the American Ceramic Society (NASA-TM-82806; E-1146; NAS 1.15:82806) Avail: NTIS HC A03/MF A01 CSCL 11D

In order to determine their strength potential, the fracture properties of different types of commercial boron fibers were measured before and after application of secondary strengthening treatments. The principal treatments employed were a slight chemical polish, which removed low strength surface flaws, and a heat treatment in oxygen, which contracted the fibers and thereby compressed intrinsic bulk flaws. Those fiber types most significantly strengthened were 200 to 400 micrometers (8 to 16 mil) diameter boron on tungsten fibers produced in a single chemical vapor deposition reactor. The slight polish increased average tensile strengths from 3.4 to 4.4 GN/m²GN/sq m (500 to 640 ksi) and reduced coefficients of variation from about 15 to 3 percent. The oxygen heat treatment plus slight polish further improved average strengths to 5.5 GN/m²GN/sq m (800 ksi) with coefficients near 3 percent. To ascertain whether these excellent properties could be retained after fabrication of B/Al composites, as produced and polished 203 micrometers (8 mil) fibers were thinly coated with aluminum, heat treated at B/Al fabrication temperatures, and then tested in tension and flexure at room temperature. The pre-polished fibers were observed to retain their superior strengths to higher temperatures than the as-produced fibers even though both were subjected to the same detrimental reaction with aluminum. Author

N82-21259* National Aeronautics and Space Administration, Lewis Research Center, Cleveland, Ohio.**TUNGSTEN FIBER REINFORCED SUPERALLOY COMPOSITE HIGH TEMPERATURE COMPONENT DESIGN CONSIDERATIONS**

Edward A. Winsa 1982 23 p refs Presented at the 111th Ann. Meeting of the Am. Inst. of Mining, Met. and Petrol. Engr., Dallas, 14-18 Feb. 1982

(NASA-TM-82811; E-1152; NAS 1.15:82811) Avail: NTIS HC A02/MF A01 CSCL 11D

Tungsten fiber reinforced superalloy composites (TFRS) are intended for use in high temperature turbine components. Current turbine component design methodology is based on applying the experience, sometimes semiempirical, gained from over 30 years of superalloy component design. Current composite component design capability is generally limited to the methodology for low temperature resin matrix composites. Often the tendency is to treat TFRS as just another superalloy or low temperature composite. However, TFRS behavior is significantly different than that of superalloys, and the high environment adds consideration not common in low temperature composite component design. The methodology used for preliminary design of TFRS components are described. Considerations unique to TFRS are emphasized. Author

N82-21260* National Aeronautics and Space Administration, Lewis Research Center, Cleveland, Ohio.**THERMAL DEGRADATION OF THE TENSILE PROPERTIES OF UNIDIRECTIONALLY REINFORCED FP-AI203/EZ 33 MAGNESIUM COMPOSITES**

R. T. Bhatt (AVRADCOM) and H. H. Grimes 1982 9 p refs Presented at the 111th Ann. Meeting of the Am. Inst. of Mining, Met. and Petro. Engr., Dallas, 14-18 Feb. 1982

(NASA-TM-82817; E-1164; NAS 1.15:82817; AVRADCOM-TR-82-C-2) Avail: NTIS HC A02/MF A01 CSCL 11D

The effects of isothermal and cyclic exposure on the room temperature axial and transverse tensile strength and dynamic flexural modulus of 35 volume percent and 55 volume percent FP-AI203/EZ 33 magnesium composites were studied. The composite specimens were continuously heated in a sand bath maintained at 350 C for up to 150 hours or thermally cycled between 50 and 250 C or 50 and 350 C for up to 3000 cycles. Each thermal cycle lasted for a total of six minutes with a hold time of two minutes at the maximum temperature. Results indicate

to significant loss in the room temperature axial tensile strength and dynamic flexural modulus of composites thermally cycled between 50 and 250 C or of composites isothermally heated at 350 C for up to 150 hours from the strength and modulus data for the untreated, as fabricated composites. In contrast, thermal cycling between 50 and 350 C caused considerable loss in both room temperature strength and modulus. Fractographic analysis and measurement of composite transverse strength and matrix hardness of thermally cycled and isothermally heated composites indicated matrix softening and fiber/matrix debonding due to void growth at the interface and matrix cracking at the likely causes of the strength and modulus loss behavior. S.L.

N82-22313*# National Aeronautics and Space Administration, Lewis Research Center, Cleveland, Ohio.
COMPRESSION BEHAVIOR OF UNIDIRECTIONAL FIBROUS COMPOSITE

J. H. Sinclair and C. C. Chamis 1982 20 p refs Presented at Symp. on Compression Testing of Homogeneous Mater. and Composites, Williamsburg, Va., 10-11 Mar. 1982; sponsored by Am. Soc. for Testing and Materials (NASA-TM-82833; E-1145; NAS 1.15:82833) Avail: NTIS HC A02/MF A01 CSCL 11D

The longitudinal compression behavior of unidirectional fiber composites is investigated using a modified Celanese test method with thick and thin test specimens. The test data obtained are interpreted using the stress/strain curves from back-to-back strain gages, examination of fracture surfaces by scanning electron microscope, and predictive equations for distinct failure modes including fiber compression failure, Euler buckling, delamination, and flexure. The results show that the longitudinal compression fracture is induced by a combination of delamination, flexure, and fiber tier breaks. No distinct fracture surface characteristics can be associated with unique failure modes. An equation is described which can be used to extract the longitudinal compression strength knowing the longitudinal tensile and flexural strengths of the same composite system. M.G.

N82-24297*# National Aeronautics and Space Administration, Lewis Research Center, Cleveland, Ohio.
FACTORS INFLUENCING THE THERMALLY-INDUCED STRENGTH DEGRADATION OF B/Al COMPOSITES

James A. DiCarlo 1982 17 p refs Presented at the Symp. on Failure Modes in Metal Matrix Composites, Dallas, 15-19 Feb. 1982; sponsored by Am. Inst. of Mining, Met. and Petrol. Engr. (NASA-TM-82823; E-1175; NAS 1.15:82823) Avail: NTIS HC A02/MF A01 CSCL 11D

Literature data related to the thermally-induced strength degradation of B/Al composites were examined in the light of fracture theories based on reaction-controlled fiber weakening. Under the assumption of a parabolic time-dependent growth for the interfacial reaction product, a Griffith-type fracture model was found to yield simple equations whose predictions were in good agreement with data for boron fiber average strength and for B/Al axial fracture strain. The only variables in these equations were the time and temperature of the thermal exposure and an empirical factor related to fiber surface smoothness prior to composite consolidation. Such variables as fiber diameter and aluminum alloy composition were found to have little influence. The basic and practical implications of the fracture model equations are discussed. Author

N82-24300*# National Aeronautics and Space Administration, Lewis Research Center, Cleveland, Ohio.
DESIGNING WITH FIBER-REINFORCED PLASTICS (PLANAR RANDOM COMPOSITES)

Christos C. Chamis Washington Mar. 1982 26 p refs (NASA-TM-82812; E-1155; NAS 1.15:82812) Avail: NTIS HC A03/MF A01 CSCL 11D

The use of composite mechanics to predict the hygrothermomechanical behavior of planar random composites (PRC) is reviewed and described. These composites are usually made from chopped fiber reinforced resins (thermoplastics or thermosets). The hygrothermomechanical behavior includes mechanical properties, physical properties, thermal properties, fracture toughness, creep and creep rupture. Properties are presented in graphical form with sample calculations to illustrate their use. Concepts such as directional reinforcement and strip hybrids are described. Typical data that can be used for preliminary design

for various PRCs are included. Several resins and molding compounds used to make PRCs are described briefly. Pertinent references are cited that cover analysis and design methods, materials, data, fabrication procedures and applications. Author

N82-26385*# National Aeronautics and Space Administration, Lewis Research Center, Cleveland, Ohio.

METHOD AND APPARATUS FOR STRENGTHENING BORON FIBERS Patent Application

James A. DiCarlo, Inventor (to NASA) Filed 23 Apr. 1982 12 p (NASA-Case-LEW-13926-1; US-Patent-AppI-SN-371354) Avail: NTIS HC A02/MF A01 CSCL 11D

The tensile strength of commercially available boron fibers produced by the chemical vapor deposition of boron onto tungsten wire substrates is increased by treating the fibers in an oxygen plus inert gas (argon) atmosphere to about 880 C. High temperature oxidation increases the residual compression of each tungsten core by forming a thin boron oxide coating on the fiber surface so that the fiber contracts axially. This increases the intrinsic strength of the fiber by raising the tensile strength level required for core initiated fracture. After cooling to room temperature the fibers are chemically polished to reduce their diameters by 0.2 mils to 0.6 mils. The reduction in diameter removes both original and oxidation induced surface flaws. The strengthened fibers are intended to be utilized as reinforcement in composite materials. Such materials may be boron/aluminum or boron/epoxy. NASA

N82-26386*# National Aeronautics and Space Administration, Lewis Research Center, Cleveland, Ohio.

ION BEAM TEXTURED GRAPHITE ELECTRODE PLATES Patent Application

James S. Sevey, Ralph Forman, Arthur N. Curren, and Edwin G. Wintucky, Inventors (to NASA) Filed 31 Mar. 1982 14 p (NASA-Case-LEW-12919-2; US-Patent-AppI-SN-364072) Avail: NTIS HC A02/MF A01 CSCL 11D

A specially textured surface of pyrolytic graphite exhibits extremely low yields of secondary electrons and reduced numbers of reflected primary electrons after impingement of high energy primary electrons. Electrode plates of this material are used in multistage depressed collectors. An ion flux having an energy between 500 eV and 1000 eV and a current density between 1.0 mA/sq cm and 6.0 mA/sq cm produces surface roughening or texturing which is in the form of needles or spires. Such textured surfaces are especially useful as anode collector plates in high efficiency electron tube devices. NASA

N82-30335*# National Aeronautics and Space Administration, Lewis Research Center, Cleveland, Ohio.

MODULUS, STRENGTH AND THERMAL EXPOSURE STUDIES OF FP-Al₂O₃/ALUMINUM AND FP-Al₂O₃/MAGNESIUM COMPOSITES

R. T. Bhatt 1981 18 p refs Presented at the Symp. on Composites and Advanced Mater., Cocoa Beach, Fla., 18-24 Jan. 1981

(NASA-TM-82868; E-1238; NAS 1.15:82868; AVADCOM-TR-81-C-1) Avail: NTIS HC A02/MF A01 CSCL 11D

The mechanical properties of FP-Al₂O₃ fiber reinforced composites prepared by liquid infiltration techniques are improved. A strengthening addition, magnesium, was incorporated with the aluminum-lithium matrix alloy usually selected for these composites because of its good wetting characteristics. This ternary composite, FP-Al₂O₃/Al-(2-3)Li-(3-5)Mg, showed improved transverse strength compared with FP-Al₂O₃/Al-(2-3)Li composites. The lower axial strengths found for the FP-Al₂O₃/Al-(2-3)Li-(3-5)Mg composites were attributed to fabrication related defects. Another technique was the use of Ti/B coated FP-Al₂O₃ fibers in the composites. This coating is readily wet by molten aluminum and permitted the use of more conventional aluminum alloys in the composites. However, the anticipated improvements in the axial and transverse strengths were not obtained due to poor bonding between the fiber coating and the matrix. A third approach studied to improve the strengths of FP-Al₂O₃ reinforced composites was the use of magnesium alloys as matrix materials. While these alloys wet fibers satisfactorily, the result indicated that the magnesium alloy composites used offered no axial strength or modulus advantage over FP-Al₂O₃/Al-(2-3)Li composites. S.L.

N82-30336* National Aeronautics and Space Administration, Lewis Research Center, Cleveland, Ohio

HIGH TEMPERATURE COMPOSITES. STATUS AND FUTURE DIRECTIONS

Robert A. Signorelli 1982 25 p refs Presented at the 4th Intern. Conf. on Composite Mater., Tokyo, 25-28 Oct 1982 (NASA-TM-82929; E-1280; NAS 1.15:82929) Avail: NTIS HC A02/MF A01 CSCL 11D

A summary of research investigations of manufacturing methods, fabrication methods, and testing of high temperature composites for use in gas turbine engines is presented. Ceramic/ceramic, ceramic/metal, and metal/metal composites are considered. Directional solidification of superalloys and eutectic alloys, fiber reinforced metal and ceramic composites, ceramic fibers and whiskers, refractory coatings, metal fiber/metal composites, matrix metal selection, and the preparation of test specimens are discussed

J.D.

N82-31449* National Aeronautics and Space Administration, Lewis Research Center, Cleveland, Ohio.

ENVIRONMENTAL AND HIGH-STRAIN RATE EFFECTS ON COMPOSITES FOR ENGINE APPLICATIONS

C. C. Chamis and G. T. Smith 1982 20 p refs Presented at the 23rd Struct. Dyn. and Mater. Conf., New Orleans, 10-12 May 1982; sponsored by AIAA, ASME, ASCE, and AHS Previously announced in IAA as A82-30119

(NASA-TM-82882; NAS 1.15:82882) Avail: NTIS HC A02/MF A01 CSCL 11D

The Lewis Research Center is conducting a series of programs intended to investigate and develop the application of composite materials to structural components for turbojet engines. A significant part of that effort is directed to establishing resistance, defect growth, and strain rate characteristics of composite materials over the wide range of environmental and load conditions found in commercial turbojet engine operations. Both analytical and experimental efforts are involved.

Author

A82-27440* Effects of nadic ester concentration and processing on physical and mechanical properties of PMR/Celion 6000 composites. F. I. Hurwitz and J. D. Whittenberger (NASA, Lewis Research Center, Cleveland, OH). In: Technology transfer; Proceedings of the Thirteenth National Technical Conference, Mount Pocono, PA, October 13-15, 1981. (A82-27401 12-24) Azusa, CA, Society for the Advancement of Material and Process Engineering, 1981, p. 477-486. 16 refs.

A82-37101* Sensitivity analysis results of the effects of various parameters on composite design. C. C. Chamis (NASA, Lewis Research Center, Structures and Mechanical Technologies Div., Cleveland, OH). In: Reinforced Plastics/Composites Institute, Annual Conference, 37th, Washington, DC, January 11-15, 1982, Preprints. (A82-37081 18-24) New York, Society of the Plastics Industry, Inc., 1982 (Session 20-B). 8 p.

Sensitivity analysis results are presented to assess the effects of a multitude of important parameters on fiber composite design and structural response. These results were obtained by using optimum design procedures in conjunction with sensitivity analyses. Sensitivity analyses were performed to assess the effects on composite optimum design and structural response of parameters such as fiber transverse and shear properties, in situ matrix elastic and strength properties, correlation coefficients used in composite micromechanics and in combined strength predictions, processing variables, and perturbations of loading conditions. The results show that matrix properties, fiber volume ratio and small perturbations of the loading conditions have significant effects on certain composite structural responses. The remaining parameters have negligible effect.

(Author)

A82-38133* On determination of fibre fraction in continuous fibre composite materials. J. D. Whittenberger, F. I. Hurwitz (NASA, Lewis Research Center, Cleveland, OH), J. J. Ricca, and R. M. Jurta (U.S. Army, Army Materials and Mechanics Research Center, Watertown, MA). *Journal of Materials Science Letters*, vol. 1, June 1982, p. 249-252.

It is pointed out that the fiber volume fraction is probably the most important parameter influencing the properties of fibrous composite materials. The present investigation is concerned with questions regarding the accurate determination of this parameter. It is found that an estimate of the fiber volume fraction based on

determinations from several coupons taken from different regions of a laminate is not accurate. At present fiber volume fractions are not directly measured but rather are calculated from the fiber weight fraction and densities of the composite and fiber. Image analysis techniques can and should be applied to determine fiber volume fraction. However, several factors have to be considered in this connection. It is necessary to make many measurements of the local fiber area fractions, and the preparation of representative planar cross sections parallel to the fiber axis may be difficult.

G.R.

A82-40796* Application of a gripping system to test a uniaxial graphite fiber reinforced composite /PMR 15/Celion 6000/ in tension at 316 C. J. D. Whittenberger and F. I. Hurwitz (NASA, Lewis Research Center, Cleveland, OH). *Polymer Composites*, vol. 3, Apr. 1982, p. 75-82. 5 refs.

A gripping system has been developed to test uniaxial, 0 deg orientation PMR 15/Celion 6000 composites at elevated temperatures. The method involves compression of grit-blasted laminate between grit-blasted metal to give a non-slipping interface for load transfer. Tensile testing at both 316 C and room temperature indicated that deformation was elastic to fracture and that the variation in tensile properties for one laminate is the same as that for several panels. In addition, the tensile properties for uniaxial PMR 15/Celion 6000 are identical at 316 C and room temperature. For nominally 51 volume percent fiber, the elastic modulus is 119.6 GPa, the fracture stress is 1370 MPa, and the strain to fracture is about 1.15 percent. In addition, data are presented which indicate that the gripping system can be used for long term, elevated temperature testing of composite materials.

(Author)

A82-42657* High-temperature resins. T. T. Serafini (NASA, Lewis Research Center, Cleveland, OH). In: Handbook of composites. (A82-42651 21-24) New York, Van Nostrand Reinhold Co., 1982, p. 89-114. 24 refs.

The basic chemistry, cure processes, properties, and applications of high temperature resins known as polyimides are surveyed. Condensation aromatic polyimides are prepared by reacting aromatic diamines with aromatic dianhydrides, aromatic tetracarboxylic acids, or with dialkyl esters of aromatic tetracarboxylic acids, depending on the intended end use. The first is for coatings or films while the latter two are more suitable for polyimide matrix resins. Prepreg solutions are made by dissolving reactants in an aprotic solvent, and advances in the addition of a diamine on the double bond and radical polymerization of the double bond are noted to have yielded a final cure product with void-free characteristics. Attention is given to properties of the Skybond, Pyralin, and NR-150B polyimide prepreg materials and characteristics of aging in the NP-150 polyimides. Finally, features of the NASA-developed PMR polyimides are reviewed.

M.S.K.

A82-45630* Forced torsional properties of PMR composites with varying nadic ester concentrations and processing histories. F. I. Hurwitz (NASA, Lewis Research Center, Cleveland, OH). *Polymer Composites*, vol. 3, July 1982, p. 152-161. 40 refs.

PMR polyimide resin was prepared from 4,4'-methylenedianiline, the dimethyl ester of 3,3',4,4'-benzophenonetetracarboxylic acid and the monomethyl ester of 5-norbornene-2,3-dicarboxylic acid (NE). The NE group serves as a chain terminator and crosslinking site. PMR/Celion 6000 composites were fabricated from resins having varying NE concentrations using two molding processes, and the laminates characterized in forced torsion. Glass transition temperatures (T_g) of 360-390 C were observed in the crosslinked resins, as compared with the literature value of 284 C reported for the uncrosslinked system. T_g did not decrease with decreasing NE concentrations over the range from 2.0 to 1.25 moles. Stoichiometry, within the range studied, showed little influence on shear properties; however, a 25% variation in matrix shear modulus with processing was observed. The $G(12)$ values determined in forced torsion were in excellent agreement with those reported from tensile tests of + or - 45 deg laminates. A branching and possible secondary crosslink mechanism is proposed based on dynamic mechanical behavior and infrared spectra of the composites.

(Author)

N82-12139* Composites Horizons, Pomona, Calif.
HYBRIDIZED POLYMER MATRIX COMPOSITE Final Report
Bruce A. Stern and Teunis Visser Sep. 1981 85 p refs
(Contract NAS3-21384)
(NASA-CR-165340) Avail: NTIS HC A05/MF A01 CSCL 11D

Under certain conditions of combined fire and impact, graphite fibers are released to the atmosphere by graphite fiber composites. The retention of graphite fibers in these situations is investigated. Hybrid combinations of graphite tape and cloth, glass cloth, and resin additives are studied with resin systems. Polyimide resins form the most resistant composites and resins based on simple

novolac epoxies the least resistant of those tested. Great improvement in the containment of the fibers is obtained in using graphite/glass hybrids, and nearly complete prevention of individual fiber release is made possible by the use of resin additives. S.L.

N82-14288* Wyoming Univ., Laramie. Composite Materials Research Group.

ANALYSIS OF CRACK PROPAGATION AS AN ENERGY ABSORPTION MECHANISM IN METAL MATRIX COMPOSITES Interim Report, Sep. 1979 - Dec. 1980

Donald F. Adams and Daniel P. Murphy Feb. 1981 159 p refs

(Grant N8G-3217)

(NASA-CR-165051; UWME-DR-101-102-1) Avail: NTIS HC A08/MF A01 CSCL 11D

The crack initiation and crack propagation capability was extended to the previously developed generalized plane strain, finite element micromechanics analysis. Also, an axisymmetric analysis was developed, which contains all of the general features of the plane analysis, including elastoplastic material behavior, temperature-dependent material properties, and crack propagation. These analyses were used to generate various example problems demonstrating the inelastic response of, and crack initiation and propagation in, a boron/aluminum composite. B.W.

N82-15123* Purdue Univ., Lafayette, Ind. Composite Materials Lab.

INDENTATION LAW FOR COMPOSITE LAMINATES

S. H. Yang 31 Jul. 1981 47 p refs

(Grant N8G-3185)

(NASA-CR-165460; CML-81-1) Avail: NTIS HC A03/MF A01 CSCL 11D

Static indentation tests are described for glass/epoxy and graphite/epoxy composite laminates with steel balls as the indenter. Beam specimens clamped at various spans were used for the tests. Loading, unloading, and reloading data were obtained and fitted into power laws. Results show that: (1) contact behavior is not appreciably affected by the span; (2) loading and reloading curves seem to follow the 1.5 power law; and (3) unloading curves are described quite well by a 2.5 power law. In addition, values were determined for the critical indentation, α sub α or which can be used to predict permanent indentations in unloading. Since α sub α or only depends on composite material properties, only the loading and an unloading curve are needed to establish the complete loading-unloading-reloading behavior. Author

N82-16176* TRW, Inc., Cleveland, Ohio.
FABRICATION OF BORON/ALUMINUM FAN BLADES FOR SCR ENGINES Final Report, Jun. 1976 - Jun. 1980

G. S. Doble Mar. 1981 49 p refs

(Contract NAS3-20360)

(NASA-CR-165294; ER-7891-F) Avail: NTIS HC A03/MF A01 CSCL 11D

The fabrication of boron/aluminum fan blades for the F-404 Supersonic Cruise Research prototype engine by rapid air bonding of fully dense monotapes is described, and the fan blades evaluated. The F-404 configuration is representative of a low aspect ratio advanced design blade with supersonic capability. Dovetail pull tests of this geometry, which substituted boron/aluminum for titanium, suggested that excessive shear stresses were present in the root. A re-designed blade, incorporating a titanium tang and root, was fabricated by hot isostatic pressing. Blades appeared well bonded but the airfoil contained sizable areas of deformation and identification from the alumina grain used as a pressure transmitting medium. The use of hot isostatic pressing with a formed steel encapsulator should eliminate this problem. J.D.H.

N82-16326* Wyoming Univ., Laramie. Composite Materials Research Group.

MICROMECHANICAL PREDICTIONS OF CRACK PROPAGATION AND FRACTURE ENERGY IN A SINGLE FIBER BORON/ALUMINUM MODEL COMPOSITE

Donald F. Adams and Jayant M. Mahishi Feb. 1982 65 p refs

(Grant N8G-3217)

(NASA-CR-168550; UWME-DR-201-101-1) Avail: NTIS HC A04/MF A01 CSCL 11D

The axisymmetric finite element model and associated computer program developed for the analysis of crack propagation in a composite consisting of a single broken fiber in an annular sheath of matrix material was extended to include a constant displacement boundary condition during an increment of crack propagation. The constant displacement condition permits the growth of a stable crack, as opposed to the catastrophic failure in an earlier version. The finite element model was refined to respond more accurately to the high stresses and steep stress gradients near the broken fiber end. The accuracy and effectiveness of the conventional constant strain axisymmetric element for crack problems was established by solving the classical problem of a penny-shaped crack in a thick cylindrical rod under axial tension. The stress intensity factors predicted by the present finite element model are compared with existing continuum results. S.L.

N82-20248* Boeing Military Airplane Development, Seattle, Wash. Advanced Airplane Branch.

ENVIRONMENTAL EFFECTS ON DEFECT GROWTH IN COMPOSITE MATERIALS Final Report

T. R. Porter Jan. 1981 418 p refs

(Contract NAS3-20405)

(NASA-CR-165213; NAS 1.26:165213) Avail: NTIS HC A18/MF A01 CSCL 11D

Data for evaluating the effects of moisture and temperature on the integrity of fiber composite components was gathered. In particular, the static and cyclic performance of three composite laminates containing flaws was investigated at room temperature and at 422 K (300 F) in wet and dry conditions. R.J.F.

N82-29363* Hughes Aircraft Co., Torrance, Calif. Electron Dynamics Div.

PYROLYTIC GRAPHITE COLLECTOR DEVELOPMENT PROGRAM Final Report

William J. Wilkins 25 Feb. 1982 23 p refs

(Contract NAS3-22505)

(NASA-CR-167909; NAS 1.26:167909; W-09170) Avail: NTIS HC A06/MF A01 CSCL 11D

Pyrolytic graphite promises to have significant advantages as a material for multistage depressed collector electrodes. Among these advantages are lighter weight, improved mechanical stiffness under shock and vibration, reduced secondary electron backstreaming for higher efficiency, and reduced outgassing at higher operating temperatures. The essential properties of pyrolytic graphite and the necessary design criteria are discussed. This includes the study of suitable electrode geometries and methods of attachment to other metal and ceramic collector components consistent with typical electrical, thermal, and mechanical requirements. Author

N82-31448* Douglas Aircraft Co., Inc., Long Beach, Calif.
KEVLAR/PMR-15 REDUCED DRAG DC-9 REVERSER STANG FAIRING

R. T. Kawai Aug. 1982 140 p refs

(Contract NAS3-21763)

(NASA-CR-165448; NAS 1.28:165448) Avail: NTIS HC A07/MF A01 CSCL 11D

A reduced drag fairing for the afterbody enclosing the thrust reverser actuators on the DC-9 has been developed with Kevlar-49/PMR-15 advanced composite material. The improved fairing reduces airplane drag 1% compared to the production baseline. Use of composites reduces weight 40% compared to an equivalent metal fairing. The Kevlar-49/PMR-15 advanced composite is an organic matrix material system that can be used at temperatures up to 500 F. Author

A82-13403 * Fatigue of Ni-Al-Mo aligned eutectics at elevated temperatures. J. M. Tartaglia (Climax Molybdenum Company of Michigan, Ann Arbor, MI) and N. S. Stoloff (Rensselaer Polytechnic Institute, Troy, NY). *Metallurgical Transactions A - Physical Metal-*

lurgy and Materials Science, vol. 12A, Nov. 1981, p. 1891-1898. 18 refs. Grants No. NAG3-22; No. AF-AFOSR-80-0015.

The elevated-temperature mechanical behavior of two aligned eutectics (Ni-8.1 wt % Al-26.4 wt % Mo and Ni-8.3 wt % Al-31.2 wt % Mo) has been investigated utilizing monotonic and cyclic testing in vacuum. Tensile yield strength and fatigue resistance increased from 25 to 725 C, but then were reduced at 825 C. The fatigue lives of specimens tested at 725 C decreased sharply with decreasing frequency. A shift from surface to internal crack initiation was observed upon increasing the test temperature from 725 to 825 C. Stage II crack propagation was observed at both temperatures, in contrast to stage I cracking at 25 C. The test results are compared to those for other nickel and cobalt-base aligned eutectics to show that the frequency effect on fatigue life is not limited to the Ni-Al-Mo system. (Author)

ORIGINAL PAGE IS
OF POOR QUALITY

A82-31339 * **Work of fracture in aluminum metal-matrix composites.** A. Skinner (Revere Research, Inc., Edison, NJ), M. J. Koczak (Drexel University, Philadelphia, PA), and A. Lawley. *Metallurgical Transactions A - Physical Metallurgy and Materials Science*, vol. 13A, Feb. 1982, p. 289-297. 13 refs. Grant No. NsG-3128.

Mechanical tests were conducted on B/Al composites and, for comparison, FP-Al₂O₃/Al composites in the as-fabricated condition and following high-temperature isothermal exposure or thermal cycling. In B/Al (1100), isothermal exposure at 773 K for 125 hr reduced toughness, measured by the work of fracture, from 76 to 10 kJ/sq m, and a similar reduction was observed after equivalent thermal cycling. In B/Al (6061), the same isothermal exposure reduced toughness from 44.6 to 8 kJ/sq m, but the effect of thermal cycling was less detrimental. In FP-Al₂O₃/Al, the work of fracture was insensitive to either type of treatment. Experimental results are interpreted in terms of matrix softening, interface properties, and fiber notch sensitivity. V.L.

A82-48220 * **Tensile properties of SiC/aluminum filamentary composite - Thermal degradation effects.** A. Skinner (Revere Research, Inc., Edison, NJ), M. J. Koczak, and A. Lawley (Drexel University, Philadelphia, PA). *Powder Metallurgy International*, vol. 14, Aug. 1982, p. 144-147. 18 refs. Grant No. NsG-3128.

Aluminum metal matrix composites with a low cost fiber, e.g. SiC, provide for an attractive combination of high elastic modulus and longitudinal strengths coupled with a low density. SiC (volume fraction 0.55)-aluminum (6061) systems have been studied in order to optimize fiber composite strength and processing parameters. A comparison of two SiC/aluminum composites produced by AVCO and DWA is provided. Fiber properties are shown to alter composite tensile properties and fracture morphology. The room temperature tensile strengths appear to be insensitive to thermal exposures at 500 C up to 150 h. The elastic modulus of the composites also appears to be stable up to 400 C, however variations in the loss modulus are apparent. The fracture morphology reflects the quality of the interfacial bond, fiber strengths and fiber processing. (Author)

25 INORGANIC AND PHYSICAL CHEMISTRY

Includes chemical analysis, e.g., chromatography; combustion theory; electrochemistry; and photochemistry.

For related information see also 77 *Thermodynamics and Statistical Physics*.

N82-19333*# National Aeronautics and Space Administration. Lewis Research Center, Cleveland, Ohio.

NASA REDOX CELL STACK SHUNT CURRENT, PUMPING POWER, AND CELL PERFORMANCE TRADEOFFS Final Report

Norman Hagedorn, Mark A. Hoberecht, and Lawrence H. Thaller Feb. 1982 33 p refs

(Contract DE-AI01-80AL-12726)

(NASA-TM-82686; DOE/NASA/12726-11; E-967) Avail: NTIS HC A03/MF A01 CSCL 10C

The NASA Redox energy storage system is under active technology development. The hardware undergoing laboratory testing is either 310 sq. cm. or 929 sq. cm. (0.33 sq. ft. or 1.0 sq. ft. per cell active area with up to 40 individual cells connected to make up a modular cell stack. This size of hardware allows rather accurate projections to be made of the shunt power/pump power tradeoffs. The modeling studies that were completed on the system concept are reviewed along with the approach of mapping the performance of Redox cells over a wide range of flow rates and depths of discharge of the Redox solutions. Methods are outlined for estimating the pumping and shunt current losses for any type of cell and stack combination. These methods are applicable to a variety of pumping options that are present with Redox systems. The results show that a fully developed Redox system has acceptable parasitic losses when using a fixed flow rate adequate to meet the worst conditions of current density and depth of discharge. These losses are reduced by about 65 percent if variable flow schedules are used. The exact value of the overall parasitics will depend on the specific system requirements of current density, voltage limits, charge, discharge time, etc. S.L.

N82-21268* National Aeronautics and Space Administration. Lewis Research Center, Cleveland, Ohio.

METHOD OF MAKING FORMULATED PLASTIC SEPARATORS FOR SOLUBLE ELECTRODE CELLS Patent

Dean W. Sheibley, inventor (to NASA) Issued 5 Jan. 1982 7 p Filed 3 Nov. 1977 Supersedes N78-25149 (16 - 16, p 2085) Continuation of US Patent Appl. SN-776146, US Patent-4,133,941, filed 10 Mar. 1977

(NASA-Case-LEW-12358-2; US-Patent-4,309,372;

US-Patent-Appl-SN-848428; US-Patent-4,133,941;

US-Patent-Appl-SN-776146; US-Patent-Class-264-453;

US-Patent-Class-264-53; US-Patent-Class-264-216;

US-Patent-Class-427-115; US-Patent-Class-427-244;

US-Patent-Class-427-246) Avail: US Patent and Trademark Office CSCL 07D

A method making a membrane comprised of a hydrochloric acid-insoluble sheet of a mixture of a rubber and a powdered ion transport material is disclosed. The sheet can be present as a coating upon a flexible and porous substrate. These membranes can be used in oxidation-reduction electrical accumulator cells wherein the reduction of one member of a couple is accompanied by the oxidation of the other member of the couple on the other side of the cell and this must be accompanied by a change in chloride ion concentration in both sides. The method comprises preparing a mixture of fine rubber particles, a solvent for the rubber and a powdered ion transport material. The mixture is formed into a sheet and dried to produce a microporous sheet. The ion transport material includes particles ranging from about 0.01 to 10 microns in size and comprises from 20 to 50 volume percent of the microporous sheet.

Official Gazette of the U.S. Patent and Trademark Office

N82-22327*# National Aeronautics and Space Administration. Lewis Research Center, Cleveland, Ohio.

CROSS-LINKED POLYVINYL ALCOHOL FILMS AS ALKALINE BATTERY SEPARATORS

Dean W. Sheibley, Michelle A. Manzo, and Olga D. Gonzalez-

Sanabria Mar. 1982 19 p refs Presented at the 158th Meeting of the Electrochim. Soc., Hollywood, Fla., 5-10 Oct. 1980

(NASA-TM-82802; E-1141; NAS 1.15:82802) Avail: NTIS HC A02/MF A01 CSCL 07D

Cross-linking methods were investigated to determine their effect on the performance of polyvinyl alcohol (PVA) films as alkaline battery separators. The following types of cross-linked PVA films are discussed: (1) PVA-dialdehyde blends post-treated with an acid or acid periodate solution (two-step method) and (2) PVA-dialdehyde blends cross-linked during film formation (drying) by using a reagent with both aldehyde and acid functionality (one-step method). Laboratory samples of each cross-linked type of film were prepared and evaluated in standard separator screening tests. The pilot-plant batches of films were prepared and compared to measure differences due to the cross-linking method. The pilot-plant materials were then tested in nickel oxide - zinc cells to compare the two methods with respect to performance characteristics and cycle life. Cell test results are compared with those from tests with Celgard. Author

N82-31450*# National Aeronautics and Space Administration. Lewis Research Center, Cleveland, Ohio.

PIEZOELECTRIC COMPOSITE MATERIALS Patent Application

L. J. Kiraly, inventor (to NASA) Filed 12 Jul. 1982 9 p

(NASA-Case-LEW-12582-1; US-Patent-Appl-SN-397281) Avail: NTIS HC A02/MF A01 CSCL 11D

A laminated structural device that has the ability to change shape, position and resonant frequency without using discrete motive components is described. The laminate may be a combination of layers of a piezoelectrically active, non-conductive matrix material. A power source selectively places various levels of charge on electrically conductive filaments imbedded in the respective layers to produce various configurations in a predetermined manner. The layers may be electrically conductive, having imbedded piezoelectrically active filaments. A combination of layers of electrically conductive material may be laminated to layers of piezoelectrically active material. NASA

N82-31459*# National Aeronautics and Space Administration. Lewis Research Center, Cleveland, Ohio.

DESIGN FLEXIBILITY OF REDOX FLOW SYSTEMS

Norman H. Hagedorn and Lawrence H. Thaller 1982 18 p refs Presented at the Intersoc. Energy Conversion Eng. Conf., Los Angeles, 8-13 Aug. 1982

(Contract DE-AI04-80AL-12726)

(NASA-TM-82854; E-1223; NAS 1.15:82854;

DOE/NASA/12726-16) Avail: NTIS HC A02/MF A01 CSCL 10C

The characteristics inherent in Redox flow systems permit considerable latitude in designing systems for specific storage applications. The first of these characteristics is the absence of plating/depilating reactions with their attendant morphology changes at the electrodes. This permits a given Redox system to operate over a wide range of depths of discharge and charge/discharge rates. The second characteristic is the separation of power generating components (stacks) from the energy storage components (tanks). This results in cost effective system design, ease of system growth via modularization, and freedom from sizing restraints so that the whole spectrum of applications, from utilities down to single residence can be considered. The final characteristic is the commonality of the reactant fluids which assures that all cells at all times are receiving reactants at the same state of charge. Since no cell can be out of balance with respect to any other cell, it is possible for some cells to be charged while others are discharging, in effect creating a DC to DC transformer. It is also possible for various groups of cells to be connected to separate loads, thus supplying a range of output voltages. Also, trim cells can be used to maintain constant bus voltage as the load is changed or as the depth of discharge increases. The commonality of reactant fluids also permits any corrective measures such as rebalancing to occur at the system level instead of at the single cell level. S.L.

ORIGINAL PAGE IS
OF POOR QUALITY

N82-33463*# National Aeronautics and Space Administration, Lewis Research Center, Cleveland, Ohio.

CHEMICAL AND ELECTROCHEMICAL BEHAVIOR OF THE Cr(3)/Cr(2) HALF CELL IN THE NASA REDOX ENERGY STORAGE SYSTEM

David A. Johnson (Spring Arbor Coll.) and Margaret A. Reid 1982 21 p refs Presented at The 162nd Meeting of the Electrochem. Soc., Detroit, 17-22 Oct. 1982

(Contract DE-AI04-80AL-12726)

(NASA-TM-82913; E-1318; DOE/NASA/12726-17; NAS 1.15:82913) Avail: NTIS HC A02/MF A01 CSCL 10C

The Cr(III) complexes in the NASA Redox Energy Storage System were isolated and identified as Cr(H₂O)₆(+3) and Cr(H₂O)₅Cl(+2) by ion exchange chromatography and visible spectrophotometry. The cell reactions during charge-discharge cycles were followed by means of visible spectrophotometry. The spectral bands were resolved into component peaks and concentrations calculated using Beer's Law. During the charge mode Cr(H₂O)₅Cl(+2) is reduced to Cr(H₂O)₅Cl(+) and during the discharge mode Cr(H₂O)₅Cl(+) is oxidized back to Cr(H₂O)₅Cl(+2). Both electrode reactions occur via a chloride-bridge inner-sphere reaction pathway. Hysteresis effects can be explained by the slow attainment of equilibrium between Cr(H₂O)₆(+3) and Cr(H₂O)₅Cl(+2). Author

A82-43194 * The premixed flame in uniform straining flow. P. A. Durbin (NASA, Lewis Research Center, Cleveland, OH), *Journal of Fluid Mechanics*, vol. 121, Aug. 1982, p. 141-161, 19 refs.

Characteristics of the premixed flame in uniform straining flow are investigated by the technique of activation-energy asymptotics. An inverse method is used, which avoids some of the restrictions of previous analyses. It is shown that this method recovers known results for adiabatic flames. New results for flames with heat loss are obtained, and it is shown that, in the presence of finite heat loss, straining can extinguish flames. A stability analysis shows that straining can suppress the cellular instability of flames with Lewis number less than unity. Strain can produce instability of flames with Lewis number greater than unity. A comparison shows quite good agreement between theoretical deductions and experimental observations of Ishizuka, Miyasaka & Law (1981). (Author)

N82-22326*# Westinghouse Electric Corp., Concordville, Pa. Combustion Turbine Systems Div.

LOW NO SUB x HEAVY FUEL COMBUSTOR CONCEPT PROGRAM. PHASE 1A: COMBUSTION TECHNOLOGY GENERATION COAL GAS FUELS Final Report

T. P. Sherlock Feb. 1982 57 p refs

(Contracts DEN3-146; DE-AI01-77ET-13111)

(NASA-CR-165614; DOE/NASA/0146-2; NAS 1.26:165614) Avail: NTIS HC A04/MF A01 CSCL 20B

Combustion tests of two scaled burners using actual coal gas from a 25 ton/day fluidized bed coal gasifier are described. The two combustor configurations studied were a ceramic lined, staged rich/lean burner and an integral, all metal multiannual swirl burner (MASB). The tests were conducted over a range of temperature and pressures representative of current industrial combustion turbine inlet conditions. Tests on the rich lean burner were conducted at three levels of product gas heating values: 104, 197 and 254 btu/scf. Corresponding levels of NO_x emissions were 5, 20 and 70 ppmv. Nitrogen was added to the fuel in the form of ammonia, and conversion efficiencies of fuel nitrogen to NO_x were on the order of 4 percent to 12 percent, which is somewhat lower than the 14 percent to 18 percent conversion efficiency when src-2 liquid fuel was used. The MASB was tested only on medium btu gas (220 to 270 btu/scf), and produced approximately 80 ppmv NO_x at rated engine conditions. Both burners operated similarly on actual coal gas and erbs fuel, and all heating values tested can be successfully burned in current machines. S.L.

N82-25337*# General Electric Co., Syracuse, N.Y. Gas Turbine Div.

LOW NO SUB x HEAVY FUEL COMBUSTOR CONCEPT PROGRAM PHASE 1A GAS TESTS

M. B. Cutrone, Kenneth W. Beebe, and Martin B. Cutrone Apr. 1982 135 p refs

(Contract DEN3-147)

(NASA-CR-167877; DOE/NASA/0147-2; NAS 1.26:167877)

Avail: NTIS HC A07/MF A01 CSCL 21B

The emissions performance of a rich lean combustor (developed for liquid fuels) for combustion of simulated coal gases ranging in heating value from 167 to 244 Btu/scf were assessed. The 244 Btu/scf gas is typical of the product gas from an oxygen blown gasifier, while the 167 Btu/scf gas is similar to that from an air blown gasifier. Although meeting NO_x goals for the 167 Btu/scf gas, NO_x performance of the rich lean combustor did not meet program goals with the 244 Btu/scf gas because of high thermal NO_x, similar to levels expected from conventional lean burning combustors. The NO_x emissions are attributed to inadequate fuel air mixing in the rich stage resulting from the design of the large central fuel nozzle delivering 71% of the total gas flow. NO_x generation from NH₃ was significant at ammonia concentrations significantly less than 0.5%. These levels occur depending on fuel gas cleanup system design. However, NO_x yield from ammonia injected into the fuel gas decreased rapidly with increasing ammonia level, and is projected to be less than 10% at NH₃ levels of 0.5% or higher. S.L.

N82-25338*# Detroit Diesel Allison, Indianapolis, Ind **LOW NO_x HEAVY FUEL COMBUSTOR CONCEPT PROGRAM ADDENDUM: LOW/MID HEATING VALUE GASEOUS FUEL EVALUATION Final Report, Apr. 1981 - Feb. 1982**

A. S. Novick and D. L. Troth Apr. 1982 77 p refs

(Contract DEN3-148)

(NASA-CR-165615; DOE/NASA/0148-2; NAS 1.26:165615; EDR-10950) Avail: NTIS HC A05/MF A01 CSCL 21B

The combustion performance of a rich/lean (RQL) combustor was evaluated when operated on low and mid heating value gaseous fuels. Two synthesized fuels were prepared having lower heating values of 10.2 MJ/cu m (274 Btu/scf) and 6.6 MJ/cu m (176 Btu/scf). These fuels were configured to be representative of actual fuels, being composed primarily of nitrogen, hydrogen, carbon monoxide, and carbon dioxide. A liquid fuel air assist fuel nozzle was modified to inject both of the gaseous fuels. The RQL combustor liner was not changed from the configuration used when the liquid fuels were tested. Both gaseous fuels were tested over a range of power levels from 50 percent load to maximum rated power of the DDN Model 570-K industrial gas turbine engine. Exhaust emissions were recorded for four power level at several rich zone equivalence ratios to determine NO_x sensitivity to the rich zone operating point. For the mid Btu heating value gas, ammonia was added to the fuel to simulate a fuel bound nitrogen type gaseous fuel. Results at the testing showed that for the low heating value fuel NO_x emissions were all below 20 ppmc and smoke was below a 10 smoke number. For the mid heating value fuel, NO_x emissions were in the 50 to 70 ppmc range with the smoke below a 10 smoke number. S.L.

A82-15732 * Moderate temperature Na cells. III - Electrochemical and structural studies of Cr_{0.5}V_{0.5}S₂ and its Na intercalates. K. M. Abraham and L. Pitts (EIC Laboratories, Inc., Newton, MA), *Electrochemical Society, Journal*, vol. 128, Dec. 1981, p. 2574-2577, 20 refs. Contract No. NAS3-21726.

Experimental results are reported on the behavior of a rechargeable Na cell incorporating a Cr_{0.5}V_{0.5}S₂ cathode. The cell operates at 130 C and uses as electrolyte a 1M solution of NaI in 1,2-bis(2-methoxy-ethoxy)ethane (triglyme). The mechanism of discharge of Cr_{0.5}V_{0.5}S₂ involves Na intercalation. It is found that the maximum rechargeable capacity of the Cr_{0.5}V_{0.5}S₂ cathode is 0.7 e(overbar)/mol. With an average cell voltage of 1.9 V, the theoretical specific energy of the cathode is 273 W-hr/kg. V.L.

A82-15743 * Moderate temperature Na cells. IV - VS2 and NbS₂Cl₂ as rechargeable cathodes in molten NaAlCl₄. K. M. Abraham, M. W. Rupich, and L. Pitts (EIC Laboratories, Inc., Newton, MA), *Electrochemical Society, Journal*, vol. 128, Dec. 1981, p. 2700-2702, 10 refs. Contract No. NAS3-21726.

ORIGINAL PAGE IS
OF POOR QUALITY

A82-17746 * # Secondary effects in combustion instabilities leading to flashback. L. Vaneveld, K. Hom, and A. K. Oppenheim (California, University, Berkeley, CA). *American Institute of Aeronautics and Astronautics, Aerospace Sciences Meeting, 20th, Orlando, FL, Jan. 11-14, 1982, Paper 82-0037*. 16 p. Grant No. NsG-3227; Contract No. W-7405-eng-48.

The secondary effects in turbulent combustion instabilities leading to flashback are investigated, including those due to buoyancy and contraction at the combustor outlet. Experiments were conducted in an oblong, rectangular cross-section combustion tunnel, where the effects of a bluff-body flame holder were generated by a rear-facing step behind a streamlined inlet nozzle. The results of experiments leading to flashback with the step mounted at the bottom of the combustion chamber were compared to those of experiments in which it was located at the top. Irrespective of the flow obstructions introduced downstream, the critical equivalence ratio for flashback was consistently lower with the step at the bottom, indicating that buoyancy was enhancing the growth of the recirculation zone that pushed the flame upstream and caused flashback. The contraction at the end of the combustion chamber had a promoting influence on the process of vortex pairing, re-enforcing the influence of the trailing vortices over that of the recirculation vortex system, and thereby curbing the tendency to flashback. Provided that the flow velocity was low, however, the characteristic features of combustion instabilities leading to flashback in the absence of contraction could still be established in its presence. J.F.

A82-20739 * # High temperature durable catalyst development. G. C. Snow and H. Tong (Acurex Corp., Mountain View, CA). *Workshop on Catalytic Combustion, 5th, San Antonio, TX, Sept. 15, 16, 1981, Paper*. 38 p. 14 refs. Research supported by the Acurex Corp.; U.S. Environmental Protection Agency Contract No. 68-02-3122; Contract No. DEN3-83.

A program has been carried out to develop a catalytic reactor capable of operation in environments representative of those anticipated for advanced automotive gas turbine engines. A reactor consisting of a graded cell honeycomb support with a combination of noble metal and metal oxide catalyst coatings was built and successfully operated for 1000 hr. At an air preheat temperature of 740 K and a propane/air ratio of 0.028 by mass, the adiabatic flame temperature was held at about 1700 K. The graded cell monolithic reaction measured 5 cm in diameter by 10.2 cm in length and was operated at a reference velocity of 14.0 m/s at 1 atm. Measured NOx levels remained below 5 ppm, while unburned hydrocarbon concentrations registered near zero and carbon monoxide levels were nominally below 20 ppm. V.L.

A82-21431 * Analysis of infrared emission from thin adsorbates. J. L. Lauer and L. E. Keller (Rensselaer Polytechnic Institute, Troy, NY). In: *International Conference on Fourier Transform Infrared Spectroscopy, Columbia, SC, June 8-12, 1981, Proceedings*. (A82-21426 08-35) Bellingham, WA, Society of Photo-Optical Instrumentation Engineers, 1981, p. 87-93. Grants No. NsG-3170; No. AF-AFOSR-78-3473; No. DAAG29-79-C-0204; Contract No. N00173-80-M-4575.

Fuel and lubricant deposits on solid surfaces, though often of similar visual appearance, differ in composition, depending on the nature of the deposit formers and the circumstances of deposition. To help establish these relations an Infrared Emission Fourier Polarization Microspectrophotometer was constructed to record infrared spectra from the deposits on their original support. By focussing on small aggregates with a reflecting microscope objective and by discriminating against the randomly polarized blackbody radiation with a rotating polarizing filter phase-locked to an amplifier, excellent Fourier emission spectra of polarized bands could be obtained. In many instances, the microscope objective was adequate without the polarizer. The analysis was calibrated against a very thin film of polyethylene terephthalate attached to a highly reflective aluminum mirror on the sample positioner. (Author)

A82-22033 * # Time resolved density measurements in premixed turbulent flames. K. V. Dandekar and F. C. Gouldin (Cornell University, Ithaca, NY). *American Institute of Aeronautics and Astronautics, Aerospace Sciences Meeting, 20th, Orlando, FL, Jan. 11-14, 1982, Paper 82-0036*. 6 p. Research supported by the General Motors Corp. and U.S. Navy; Grant No. NsG-3019.

Premixed, turbulent flames are important in connection with investigations of fundamental, turbulent-reacting-flow processes and the study of practical combustion devices, such as spark ignition engines and premixed, prevaporized gas turbine combustors which burn premixed reactants. The considered investigation is concerned with the application of laser induced Rayleigh scattering to measure the gas density in premixed, methane-air flames. A description is provided of the results of density and velocity measurements in an open, lean, premixed methane-air flame stabilized in grid turbulence of low Reynolds number. It is found that where applicable, Rayleigh scattering can be used to good advantage to measure molecular number density. Mean and rms density results show that the mean flame thickens with axial distance but that the maximum in rms does not change appreciably. G.R.

A82-28651 * Symposium /International/ on Combustion, 18th, University of Waterloo, Waterloo, Ontario, Canada, August 17-22, 1980, Proceedings. Symposium supported by Acurex Corp., U.S. Air Force, NASA, NBS, NSF, U.S. Navy, U.S. Army, U.S. Department of Energy, et al; NSF Grant No. CPE-79-23680; Contracts No. NAS3-22171; No. N00014-80-G-0079; No. DE-FG20-80PC-30197; Grants No. NBS-HA-1008; No. DAAK11-79-M-0010. Pittsburgh, PA, Combustion Institute, 1981. 1998 p. \$76.50. (For individual items see A82-28652 to A82-28738)

Problems related to combustion generated pollution are explored, taking into account the mechanism of NO formation from nitrogen compounds in hydrogen flames studied by laser fluorescence, the structure and similarity of nitric oxide production in turbulent diffusion flames, the effect of steam addition on NO formation, and the formation of NO2 by laminar flames. Other topics considered are concerned with propellant combustion, fluidized bed combustion, the combustion of droplets and sprays, premixed flame studies, fire studies, and flame stabilization. Attention is also given to coal flammability, chemical kinetics, turbulent combustion, soot, coal combustion, the modeling of combustion processes, combustion diagnostics, detonations and explosions, ignition, internal combustion engines, combustion studies, and furnaces. G.R.

A82-28694 * Flame structure in a swirl stabilized combustor inferred by radiant emission measurements. C. L. Beyler and F. C. Gouldin (Cornell University, Ithaca, NY). In: *Symposium /International/ on Combustion, 18th, Waterloo, Ontario, Canada, August 17-22, 1980, Proceedings*. (A82-28651 13-25) Pittsburgh, PA, Combustion Institute, 1981, p. 1011-1019. 25 refs. Grant No. NsG-3019.

Results of measurements of time-averaged chemiluminescent emissions from CH, OH, and CO2 and of Na tracer emissions along lateral lines-of-sight through a cylindrical premixed, swirl-stabilized combustor are reported. Assuming axial symmetry and small optical depth, raw data are inverted to obtain local emission levels from these species as a function of radius. The chemiluminescent emissions are interpreted as signatures of chemical reaction and used in determining the regions of reactions and heat release in the combustor. The data are compared with composition and velocity data obtained in the combustor for identical operating conditions. The results demonstrate that reaction occurs in a relatively narrow, turbulent flame-like combustion zone which begins upstream of the time-averaged location of the swirl-induced recirculation zone and propagates around and laterally away from the recirculation zone into the unburned gas. C.R.

A82-28708 * Numerical modeling of turbulent combustion in premixed gases. A. F. Ghoniem, A. J. Chorin, and A. K. Oppenheim (California, University, Berkeley, CA). In: *Symposium /International/ on Combustion, 18th, Waterloo, Ontario, Canada,*

ORIGINAL PAGE IS
OF POOR QUALITY

August 17-22, 1980, Proceedings. (A82-28651 13-25) Pittsburgh, PA, Combustion Institute, 1981, p. 1375-1381; Comments, p. 1381-1383. 19 refs. Contract No. W-7405-eng-48; Grant No. NsG-3227.
(Previously announced in STAR as N81-15029)

A82-28709 * Experimental and theoretical studies of the laws governing condensate deposition from combustion gases. D. E. Rosner and K. Seshadri (Yale University, New Haven, CT). In: Symposium /International/ on Combustion, 18th, Waterloo, Ontario, Canada, August 17-22, 1980, Proceedings. (A82-28651 13-25) Pittsburgh, PA, Combustion Institute, 1981, p. 1385-1393; Comments, p. 1394. 49 refs. Grants No. NsG-3107; No. NsG-3169; Contract No. F49620-76-C-0020.

A description is presented of the results of a research program directed at an improved understanding of condensate deposition rate phenomena in combustion systems. The conducted experiments make use of real-time optical laser reflectance-interference-polarization techniques in flame environments. The obtained new data and the results of previous gravimetric experiments are employed as a basis for the development of a comprehensive convective diffusion deposition theory, taking into account the assumption of a multicomponent vapor or multisize class particles 'source-free' boundary layer. The theory makes it possible to provide self-consistent salt/ash/soot deposition rate predictions over a wide variety of environmental conditions. G.R.

A82-28736 * Lean-limit extinction of propane/air mixtures in the stagnation-point flow. C. K. Law, S. Ishizuka, and M. Mizumoto (Northwestern University, Evanston, IL). In: Symposium /International/ on Combustion, 18th, Waterloo, Ontario, Canada, August 17-22, 1980, Proceedings. (A82-28651 13-25) Pittsburgh, PA, Combustion Institute, 1981, p. 1791-1797; Comments, p. 1797, 1798. 25 refs. Grant No. NAG3-53.

The extinction limits of lean propane/air mixtures in the stagnation-point flow of a flat surface were mapped as functions of the surface temperature and the mixture concentration, velocity, and temperature. The maximum flame temperatures and the flame locations were also measured. The results show that the extinction limits are extremely insensitive to the nature of the surface, which can be heated to 1000 C. On the other hand preheating the gas mixture increases the flame temperature by an almost equal amount and therefore significantly extends the extinction limits. It is also found that at extinction the maximum flame temperatures and the flame locations, which when scaled with the velocity gradient, assume almost constant values independent of the other system variables investigated. (Author)

A82-32877 * Effects of heat loss, preferential diffusion, and flame stretch on flame-front instability and extinction of propane/air mixtures. S. Ishizuka, K. Miyasaka, and C. K. Law (Northwestern University, Evanston, IL). *Combustion and Flame*, vol. 45, Mar. 1982, p. 293-308. 13 refs. Grant No. NAG3-53; Contract No. N00014-80-C-0586.

Flame configurations, flame-front cellular instability, and extinction of propane/air mixtures in the stagnation-point flow are experimentally studied for their dependence on downstream heat loss, preferential diffusion, and flame stretch. Boundaries for lean- and rich-limit extinction, stabilization of corrugated flames, and local extinction caused by sharp curvatures are mapped for varying propane concentrations and freestream velocities. Flame location and temperature at extinction are determined as functions of stagnation surface temperature, extent of preheating, propane concentration, and freestream velocity. Results substantiate the theoretical predictions of the different extinction modes for lean and rich flames in the absence of downstream heat loss, and yield useful insight on the extinction characteristics when finite downstream heat loss does exist. It is further shown that flame-front instability occurs only for rich mixtures in accordance with preferential diffusion considerations, and that flame stretch has a stabilizing effect such that flame-front instability is completely inhibited before the onset of extinction. (Author)

A82-37570 * On the opening of premixed Bunsen flame tips. C. K. Law, S. Ishizuka, and P. Cho (Northwestern University, Evanston, IL). *Combustion Science and Technology*, vol. 28, no. 3-4, 1982, p. 89-96. 13 refs. Research sponsored by the Ministry of Education of Japan; Contract No. N0014-80-C-0586; Grant No. NAG3-53.

The local extinction of Bunsen flame tip and edges of hydrocarbon/air premixtures has been experimentally investigated using a variety of burners. Results show that, while for both rich propane/air and butane/air mixtures tip opening occurs at a constant fuel equivalence ratio of 1.44 and is therefore independent of the intensity, uniformity, and configuration of the approach flow, for rich methane/air flames burning is intensified at the tip and therefore opening is not possible. These results substantiate the concept and dominance of the diffusional stratification mechanism in causing extinction, and clarify the theoretical predictions on the possible opening of two-dimensional flame wedges. (Author)

A82-37571 * Formation of oxides of nitrogen in monodisperse spray combustion of hydrocarbon fuels. A. A. Nizami, S. Singh, and N. P. Cernansky (Drexel University, Philadelphia, PA). *Combustion Science and Technology*, vol. 28, no. 3-4, 1982, p. 97-106. 21 refs. Research supported by the Philadelphia Electric Co. and General Motors Corp; NSF Grant No. ENG-76-10232; Grant No. NAG3-1.

Experimental results of exit plane NO/NO(x) emissions from atmospheric monodisperse fuel spray combustion are presented. Six different hydrocarbon fuels were studied: Isopropanol, n-propanol, n-octane, iso-octane, n-heptane and methanol. The results indicate an optimum droplet size for minimizing NO/NO(x) production for all of the test fuels. At the optimum droplet diameter, reductions in NO/NO(x) relative to the NO(x) occurred at droplet diameters of 55 and 48 microns respectively, as compared to a 50-micron droplet size for isopropanol. The occurrence of the minimum NO(x) point at different droplet diameters for the different fuels appears to be governed by the extent of prevaporization of the fuel in the spray, and is consistent with theoretical calculations based on each fuel's physical properties. Estimates are also given for the behavior of heavy fuels and of polydisperse fuel sprays in shifting the minimum NO(x) point compared to a monodisperse situation. (Author)

A82-37574 * On stability of premixed flames in stagnation - Point flow. G. I. Sivashinsky (California, University, Berkeley, CA; Tel Aviv University, Tel Aviv, Israel), C. K. Law (California, University, Berkeley, CA; Northwestern University, Evanston, IL), and G. Joulin (Poitiers, Ecole Nationale Supérieure de Mécanique et d'Aérotechnique, Poitiers, France). *Combustion Science and Technology*, vol. 28, no. 3-4, 1982, p. 155-159. 8 refs. Research supported by the Israel Commission for Basic Research and U.S.-Israel Binational Science Foundation; Grant No. NAG3-53; Contract No. N00014-80-C-0586.

A quantitative description of flame stabilization in stagnation-point flow is proposed. Asymptotic and stability analyses are made for a flame model where the density of the gas is assumed to be constant and the reaction zone is assumed to be narrow and concentrated over the flame front. It is shown that, if blowing is sufficiently strong, the corrugations disappear and a plane flame results. The phenomena cannot be fully described by means of classical linear stability analysis. C.D.

ORIGINAL PAGE IS
OF POOR QUALITY

26 METALLIC MATERIALS

Includes physical, chemical, and mechanical properties of metals, e.g., corrosion; and metallurgy.

N82-10195* National Aeronautics and Space Administration, Lewis Research Center, Cleveland, Ohio

CREEP SHEAR BEHAVIOR OF THE OXIDE DISPERSION STRENGTHENED SUPERALLOY MA 6000E

Thomas K. Glasgow 1981 19 p refs Presented at 110th Ann. Meeting of the Am. Inst. of Mining, Met. and Petroleum Engr., Chicago, 22-26 Feb. 1981
(NASA-TM-82704; E-985) Avail: NTIS HC A02/MF A01 CSCL 11F

The shear rupture life of the oxide dispersing strengthened (ODS) superalloy MA 6000E was determined at 650 and 760 C was 250 MPa. Comparisons were made at 760 C with the conventional cast superalloy B-1900+Hf, the ODS alloy MA 754, and the directionally solidified eutectic alloy gamma/gamma prime-delta was 170 MPa, and for B-1900+Hf was 360 MPa. The ODS alloy MA 6000E and gamma/gamma prime-delta failed with very little indication of ductile accommodation. Both MA 754 and B-1900+Hf showed some ductile tearing. Fracture surfaces of the ODS alloy MA 754 showed discontinuities similar size, shape, and roughness to its grain structure, but the fracture surfaces of MA 6000E were much smoother than its grain boundaries. Author

N82-11182* National Aeronautics and Space Administration, Lewis Research Center, Cleveland, Ohio.

TRENDS IN HIGH TEMPERATURE GAS TURBINE MATERIALS

S. J. Grisaffe and R. L. Dreshfield 1981 18 p refs Presented at the 1981 Aerospace Conf., Anaheim, Calif., 5-8 Oct.
(NASA-TM-82715; E-999) Avail: NTIS HC A02/MF A01 CSCL 11F

High performance - high technology materials are among the technologies that are required to allow the fruition of such improvements. Materials trends in hot section components are reviewed, and materials for future use are identified. For combustors, airfoils, and disks, a common trend of using multiple material construction to permit advances in technology is identified. S.L.

N82-11183* National Aeronautics and Space Administration, Lewis Research Center, Cleveland, Ohio.

UNIVERSAL BINDING ENERGY RELATIONS IN METALLIC ADHESION

J. Ferrante, J. R. Smith (General Motors Research Lab.), and J. H. Rose (Ames Lab.) 1981 16 p refs Presented at the Conf. on Aspects Microscopiques de l'Adhesion et de la Lubrication, Paris, 14-18 Sep. 1981
(NASA-TM-82706; E-993) Avail: NTIS HC A02/MF A01 CSCL 11F

Scaling relations which map metallic adhesive binding energy onto a single universal binding energy curve are discussed in relation to adhesion, friction, and wear in metals. The scaling involved normalizing the energy to the maximum binding energy and normalizing distances by a suitable combination of Thomas-Fermi screening lengths. The universal curve was found to be accurately represented by $E^*(A^*) = -(1 + \beta A) \exp(-\beta A^*)$ where E^* is the normalized binding energy, A^* is the normalized separation, and β is the normalized decay constant. The calculated cohesive energies of potassium, barium, copper, molybdenum, and samarium were also found to scale by similar relations, suggesting that the universal relation may be more general than for the simple free electron metals. R.J.F.

N82-11184* National Aeronautics and Space Administration, Lewis Research Center, Cleveland, Ohio.

FAILURE ANALYSIS OF A TOOL STEEL TORQUE SHAFT

John R. Reagan 1981 12 p Presented at the Conf. on Deformation, Fracture, Wear and Nondestructive Evaluation of Mater., New Orleans, 23-24 Nov. 1981; sponsored by Am. Phys. Soc. and Nat. Bureau of Standards
(NASA-TM-82758; E-1077; DOE/NASA/1011-35) Avail:

NTIS HC A02/MF A01 CSCL 11F

A low design load drive shaft used to deliver power from an experimental exhaust heat recovery system to the crankshaft of an experimental diesel truck engine failed during highway testing. An independent testing laboratory analyzed the failure by routine metallography and attributed the failure to fatigue induced by a banded microstructure. Visual examination by NASA of the failed shaft plus the knowledge of the torsional load that it carried pointed to a 100 percent ductile failure with no evidence of fatigue. Scanning electron microscopy confirmed this. Torsional test specimens were produced from pieces of the failed shaft and torsional overload testing produced identical failures to that which had occurred in the truck engine. This pointed to a failure caused by a high overload and although the microstructure was defective it was not the cause of the failure. A.R.H.

N82-12216* National Aeronautics and Space Administration, Lewis Research Center, Cleveland, Ohio.

PROGRESS IN PROTECTIVE COATINGS FOR AIRCRAFT GAS TURBINES: A REVIEW OF NASA SPONSORED RESEARCH

John P. Merutka 1981 29 p refs Presented at the 5th Ann. Conf. on Composite and Adv. Mater., Merritt Island, Fla., 19-22 Jan. 1981; sponsored by the Am. Ceramic Soc., Inc.
(NASA-TM-82740; E-711) Avail: NTIS HC A03/MF A01 CSCL 11F

Problems associated with protective coatings for advanced aircraft gas turbines are reviewed. Metallic coatings for preventing titanium fires in compressors are identified. Coatings for turbine section are also considered. Ductile aluminide coatings for protecting internal turbine-blade cooling passage surface are also identified. Composite modified external overlay MCrAlY coatings deposited by low-pressure plasma spraying are found to be better in surface protection capability than vapor deposited MCrAlY coatings. Thermal barrier coating (TBC), studies are presented. The design of a turbine airfoil is integrated with a TBC, and computer-aided manufacturing technology is applied. S.L.

N82-13281* National Aeronautics and Space Administration, Lewis Research Center, Cleveland, Ohio.

ELEVATED TEMPERATURE FATIGUE TESTING OF METALS

Marvin H. Hirschberg In AGARD Fatigue Test Methodology Oct. 1981 18 p refs (For primary document see N82-13274 04-31)
Avail: NTIS HC A12/MF A01

N82-17335* National Aeronautics and Space Administration, Lewis Research Center, Cleveland, Ohio.

REVIEW OF NASA PROGRESS IN THERMAL BARRIER COATINGS FOR STATIONARY GAS TURBINES

Philip E. Hodge, Robert A. Miller, Michael A. Gedwill, and Isidor Zaplatynsky 1981 16 p refs Presented at the Intern. Gas Turbine Conf., Houston, Tex., 9-12 Mar. 1981
(Contract EF-77-A-01-2593)
(NASA-TM-81716; DOE/NASA/2593-25; E-749) Avail: NTIS HC A02/MF A01 CSCL 11F

Ceramic thermal barrier coatings for industrial/utility gas turbines were investigated. In burner rig tests of a zirconia yttria/nickel chromium aluminum yttrium ZrO₂-12w/OY2O3/NiCrAlY coating system on air cooled superalloy specimens, ceramic coating life (spallation) was sensitive to Na and V concentration in the fuel. The locations of coating spallation correspond to areas where combustion products were predicted to condense. Three new thermal barrier coating systems were identified. These are based on calcium silicate, ZrO₂-8w/OY2O3, and a MgO-NiCrAlY cermet. The spall resistance can be increased by reducing the ceramic layer thickness from 0.038 to 0.013 cm and by the use of more oxidation/corrosion resistant bond coats. S.L.

N82-20291* National Aeronautics and Space Administration, Lewis Research Center, Cleveland, Ohio.

FRICTION AND WEAR OF IRON IN CORROSIVE METAL

George W. P. Rengstorff, Kazuhisa Miyoshi, and Donald H. Buckley

Mar. 1982 18 p refs
(NASA-TP-1985; NAS 1.60:1985; E-638) Avail: NTIS
HC A02/MF A01 CSCL 11F

Friction and wear experiments were conducted with elemental iron exposed to various corrosive media including two acids, base, and a salt. Studies involved various concentrations of nitric and sulfuric acids, sodium hydroxide, and sodium chloride. Load and reciprocating sliding speed were kept constant. With the base NaOH an increase in normality beyond 0.01 N resulted in a decrease in both friction and wear. X-ray photoelectron spectroscopy (XPS) analysis of the surface showed a decreasing concentration of ferric oxide (Fe₂O₃) on the iron surface with increasing NaOH concentration. With nitric acid (HNO₃) friction decreased in solutions to 0.05 N, beyond which no further change in friction was observed. The concentration of Fe₂O₃ on the surface continued to increase with increasing normality. XPS analysis revealed the presence of sulfates in addition of Fe₂O₃ on surfaces exposed to sulfuric acid and iron chlorides but no sodium on surfaces exposed to NaCl. Author

N82-21298* National Aeronautics and Space Administration, Lewis Research Center, Cleveland, Ohio.

EFFECT OF ALUMINUM PHOSPHATE ADDITIONS ON COMPOSITION OF THREE-COMPONENT PLASMA-SPRAYED SOLID LUBRICANT

Thomas P. Jacobson and Stanley G. Young Mar. 1982 19 p refs

(NASA-TP-1990; E-713; NAS 1.60:1990) Avail: NTIS
HC A02/MF A01 CSCL 11F

Image analysis (IA) and electron microprobe X-ray analysis (EMXA) were used to characterize a plasma-sprayed, self-lubricating coating, NASA LUBE PS106, specified by weight percent as 35NiCr-35Ag-30CaF₂. To minimize segregation of the powder mixture during the plasma-spraying procedure, monoaluminum phosphate was added to form agglomerate particles. Three concentrations of AlPO₄ were added to the mixtures: 1.25, 2.5, and 6.25 percent by weight. Analysis showed that 1.25 wt% AlPO₄ yielded a CaF₂ deficiency, 2.5 wt% kept the coating closest to specification, and 6.25 wt% yielded excess CaF₂ as well as more impurities and voids and a deficiency in silver. Photomicrographs and X-ray maps are presented. The methods of IA and EMXA complement each other, and the reasonable agreement in the results increases the confidence in determining the coating composition. Author

N82-21300* National Aeronautics and Space Administration, Lewis Research Center, Cleveland, Ohio.

FRICTION WEAR AND AUGER ANALYSIS OF IRON IMPLANTED WITH 1.5-MeV NITROGEN IONS

John Ferrante and William R. Jones, Jr. Mar. 1982 14 p refs

(NASA-TP-1989; E-678; NAS 1.60:1989) Avail: NTIS
HC A02/MF A01 CSCL 11F

The effect of implantation of 1.5-MeV nitrogen ions on the friction and wear characteristics of pure iron sliding against steel was studied in a pin-on disk apparatus. An implantation dose of 5×10^{17} to the 17th power ions/sq cm was used. Small reductions in initial and steady-state wear rates were observed for nitrogen-implanted iron riders as compared with unimplanted controls. Auger electron spectroscopy revealed a subsurface Gaussian nitrogen distribution with a maximum concentration of 15 at. % at a depth of 8×10^{-7} m. A similar analysis within the wear scar of an implanted rider after 20 microns of wear yielded only background nitrogen concentration, thus giving no evidence for diffusion of nitrogen beyond the implanted range. Author

N82-21301* National Aeronautics and Space Administration, Lewis Research Center, Cleveland, Ohio.

FRICTION AND SURFACE CHEMISTRY OF SOME FERROUS-BASE METALLIC GLASSES

Kazuhisa Miyoshi and Donald H. Buckley Mar. 1982 14 p refs

(NASA-TP-1991; E-919; NAS 1.60:1991) Avail: NTIS
HC A02/MF A01 CSCL 11F

The friction properties of some ferrous-base metallic glasses were measured both in argon and in vacuum to a temperature of 350 C. The alloy surfaces were also analyzed with X-ray photoelectron spectroscopy to identify the compounds and

elements present on the surface. The results of the investigation indicate that even when the surfaces of the amorphous alloys, or metallic glasses, are atomically clean, bulk contaminants such as boric oxide and silicon dioxide diffuse to the surfaces. Friction measurements in both argon and vacuum indicate that the alloys exhibit higher coefficients of friction in the crystalline state than they do in the amorphous state. Author

N82-22344* National Aeronautics and Space Administration, Lewis Research Center, Cleveland, Ohio.

TRIBOLOGICAL PROPERTIES AND XPS STUDIES OF ION PLATED GOLD ON NICKEL AND IRON

Kazuhisa Miyoshi, Talivaldis Spalvins, and Donald H. Buckley 1982 18 p refs Presented at Intern. Conf. on Met. Coatings, San Diego, Calif., 4-9 Apr. 1982; sponsored by American Vacuum Society

(NASA-TM-82814; E-1161; NAS 1.15:82814) Avail: NTIS
HC A02/MF A01 CSCL 11F

Tribological and X-ray photoelectron spectroscopy analysis were conducted with ion plated gold films on nickel and iron substrates in sliding contact with metals and nonmetals in a vacuum of 3×10^{-6} nPa and in an argon atmosphere. The results obtained indicated a deeper graded interface when gold was ion plated on nickel than on iron. The deep graded interface between gold and nickel may be due to the solubility of material pairs. The gold and nickel in the graded interface can form an alloy. The gold in the graded interface with iron is atomically dispersed in the iron and thus forms a physically bonded interface. This is believed to be due primarily to implantation effects. The coefficient of friction, wear and transfer of gold in contact with metal or nonmetal were greater in a vacuum of 3×10^{-6} nPa than in argon. Gold films in contact with metals had a higher coefficient of friction, wear and transfer of gold than gold films in contact with the nonmetals. These observations resulted from the greater adhesion of gold to metals than to nonmetals. Author

N82-22346* National Aeronautics and Space Administration, Lewis Research Center, Cleveland, Ohio.

PERFORMANCE OF LASER GLAZED ZrO₂ TBCs IN CYCLIC OXIDATION AND CORROSION BURNER TEST RIGS

I. Zaplatynsky 1982 21 p refs Presented at the Intern. Conf. on Met. Coatings and Process Technol., San Francisco, 4-8 Apr. 1982; sponsored by the American Vacuum Society

(NASA-TM-82830; E-1195; NAS 1.15:82830) Avail: NTIS
HC A02/MF A01 CSCL 11F

The performance of laser glazed zirconia thermal barrier coatings (TBCs) was evaluated in cyclic oxidation and cyclic corrosion tests. Plasma sprayed zirconia coatings of two thicknesses were partially melted with a CO₂ laser. The power density of the focused laser beam was varied from 35 to 75 W/sq mm, while the scanning speed was about 80 cm per minute. In cyclic oxidation tests, the specimens were heated in a burner rig for 6 minutes and cooled for 3 minutes. It is indicated that the laser treated samples have the same life as the untreated ones. However, in corrosion tests, in which the burner rig flame contained 100 PPM sodium, fuel equivalent, the laser treated samples exhibit nearly a fourfold life improvement over that of the reference samples vary. In both tests, the lives of the samples inversely with the thickness of the laser melted layer of zirconia. E.A.K.

N82-22347* National Aeronautics and Space Administration, Lewis Research Center, Cleveland, Ohio.

METHOD AND APPARATUS FOR COATING SUBSTRATES USING LASERS Patent Application

Isidor Zaplatynsky, inventor (to NASA) Filed 15 Mar. 1982 9 p

(NASA-Case-LEW-13526-1; US-Patent-Appl-SN-358398) Avail: NTIS HC A02/MF A01 CSCL 11F

A method for coating substrates using lasers is described. Metal substrates, preferably of titanium and titanium alloys, were coated by alloying or forming TiN on a substrate surface. In the process a laser beam strikes the surface of a moving substrate in the presence of purified nitrogen gas. A small area of the substrate surface is quickly heated, without melting, and reacts with the nitrogen to form a solid solution. This process of alloying or forming TiN, which occurs by diffusion of nitrogen into the titanium, is reviewed. NASA

N82-22349*# National Aeronautics and Space Administration, Lewis Research Center, Cleveland, Ohio.

SURFACE CHEMISTRY, MICROSTRUCTURE AND FRICTION PROPERTIES OF SOME FERROUS-BASE METALLIC GLASSES AT TEMPERATURES TO 750 C

Kazuhisa Miyoshi and Donald H. Buckley Apr. 1982 16 p refs

(NASA-TP-2008; E-1001; NAS 1.60:2006) Avail: NTIS HC A02/MF A01 CSCL 11B

X-ray photoelectron spectroscopy analysis, transmission electron microscopy, diffraction studies, and sliding friction experiments were conducted with ferrous-base metallic glasses in sliding contact with aluminum oxide at temperatures from room to 750 C in a vacuum of 30 nPa. The results indicate that there is a significant temperature influence on the friction properties, surface chemistry, and microstructure of metallic glasses. The relative concentrations of the various constituents at the surface of the sputtered specimens were very different from the normal bulk compositions. Contaminants can come from the bulk of the material to the surface upon heating and impart boric oxide and silicon oxide at 350 C and boron nitride above 500 C. The coefficient of friction increased with increasing temperature to 350 C. Above 500 C the coefficient of friction decreased rapidly. The segregation of contaminants may be responsible for the friction behavior. Author

N82-24322*# National Aeronautics and Space Administration, Lewis Research Center, Cleveland, Ohio.

TRIBOLOGICAL CHARACTERISTICS OF NITROGEN (N+) IMPLANTED IRON

William R. Jones and John Ferrante 1982 24 p refs Proposed for presentation at the Joint Lubrication Conf., Washington, D.C., 5-7 Oct. 1982; sponsored by the American Society of Lubrication Engineers and ASME

(NASA-TM-82839; E-1207; NAS 1.15:82839) Avail: NTIS HC A02/MF A01 CSCL 11F

The effect of implantation of nitrogen ions (1.5 MeV) on the friction and wear characteristics of pure iron sliding against M-50 steel (unimplanted) was studied in a pin-on-disk sliding friction apparatus. Test conditions included room temperature (25 C), a dry air atmosphere, a load of 1/2 kg (4.9 N), sliding velocities of 0.043 to 0.078 m/sec (15 to 25 rpm), a pure hydrocarbon lubricant (n-hexadecane), or a U.S.P. mineral oil and nitrogen ion implantation doses of 5x10 to the 15th power and 5x10 to the 17th power ions/sq cm. No differences in wear rates were observed in the low dose experiments. In the high dose experiments, small reductions in initial (40 percent) and steady state (20 percent) wear rates were observed for nitrogen implanted iron riders as compared with unimplanted controls. No differences in average friction coefficients were noted for either dose. Auger electron spectroscopy combined with argon ion bombardment revealed a subsurface Gaussian nitrogen distribution with a maximum concentration of 6 atomic percent at a depth of 0.8 microns. Similar analysis within the wear scar of an implanted rider after 20 microns of wear yielded only background nitrogen concentration. No inward migration of nitrogen ions was observed. M.G.

N82-24323*# National Aeronautics and Space Administration, Lewis Research Center, Cleveland, Ohio.

EFFECT OF OXIDE FILMS ON HYDROGEN PERMEABILITY OF CANDIDATE STIRLING ENGINE HEATER HEAD TUBE ALLOYS

Susan R. Schuon and John A. Misencik 1981 32 p refs Presented at the 110th Ann. Meeting of Am. Inst. of Mining, Met. and Petrol. Engrs., Chicago, 22-26 Feb. 1981 (Contract DE-A101-77CS-51040)

(NASA-TM-82824; E-1176; DOE/NASA/51040-38; NAS 1.15:82824) Avail: NTIS HC A03/MF A01 CSCL 11F

The effect of oxide films developed in situ from CO/CO2 doped hydrogen on high pressure hydrogen permeability at 820 C was studied on N-155, A-286, IN 800, 19-9DL, Nitronic 40, HS-188, and IN 718 tubing in a Stirling materials simulator. The hydrogen permeability decreased with increasing dopant levels of CO or CO2 and corresponding decreases in oxide porosity. Minor reactive alloying elements strongly influenced permeability. At high levels of CO or CO2, a liquid oxide formed on alloys with greater than 50 percent Fe. This caused increased permeability. The oxides formed on the inside tube walls were analyzed and their effective permeabilities were calculated. T.M.

N82-24325*# National Aeronautics and Space Administration, Lewis Research Center, Cleveland, Ohio.

CORRELATION OF TENSILE AND SHEAR STRENGTHS OF METALS WITH THEIR FRICTION PROPERTIES

Kazuhisa Miyoshi and Donald H. Buckley 1982 23 p refs Proposed for presentation at the Joint Lubrication Conf., Washington, D.C., 5-7 Oct. 1982; sponsored by ASME and the American Society of Lubrication Engineers

(NASA-TM-82828; E-1186; NAS 1.15:82828) Avail: NTIS HC A02/MF A01 CSCL 11F

The relation between the theoretical tensile and the shear strengths and the friction properties of metals in contact with diamond, boron nitride, silicon carbide, manganese-zinc ferrite, and the metals themselves in vacuum was investigated. The relationship between the actual shear strength and the friction properties of the metal was also investigated. An estimate of the theoretical uniaxial tensile strength was obtained in terms of the equilibrium surface energy, interplanar spacing of the planes perpendicular to the tensile axis, and the Young's modulus of elasticity. An estimate of the theoretical shear strength for metals was obtained from the shear modulus, the repeat distance of atoms in the direction of shear of the metal and the interplanar spacing of the shear planes. The coefficient of friction for metals was found to be related to the theoretical tensile, theoretical shear, and actual shear strengths of metals. The higher the strength of the metal, the lower the coefficient of friction. Author

N82-24326*# National Aeronautics and Space Administration, Lewis Research Center, Cleveland, Ohio.

A STATUS REVIEW OF NASA'S COSAM (CONSERVATION OF STRATEGIC AEROSPACE MATERIALS) PROGRAM Executive Status Report

Joseph R. Stephens Washington May 1982 46 p refs (NASA-TM-82852; E-1222; NAS 1.15:82852) Avail: NTIS HC A03/MF A01 CSCL 11F

The use and supply of strategic elements in nickel base superalloys for gas turbine engines are reviewed. Substitution of strategic elements, advanced processing concepts, and the identification of alternate materials are considered. Cobalt, tantalum, columbium, and chromium, the supplies of which are 91-100% imported, are the materials of major concern. J.D.

N82-26431*# National Aeronautics and Space Administration, Lewis Research Center, Cleveland, Ohio.

IMPROVED THERMAL BARRIER COATING SYSTEM Patent Application

Stephan Secura, inventor (to NASA) Filed 6 May 1982 13 p (NASA-Case-LEW-13324-1; US-Patent-Appl-SN-375784) Avail: NTIS HC A02/MF A01 CSCL 11F

A high temperature oxidation resistant thermal barrier coating system for a nickel-, cobalt-, or iron-base alloy substrate is described. An inner metal bond coating contacts the substrate, and a thermal barrier coating covers the bond coating. NiCrAlR, and CoCrAlR alloy are satisfactory as bond coating compositions where R = Y or Yb. These alloys contain, by weight, 0-35% chromium, 6-18% aluminum, and 0.05 to 1.55% yttrium or 0.05 to 3.0% ytterbium. The coatings containing ytterbium are preferred over those containing yttrium. An outer thermal barrier coating of partially stabilized zirconium oxide (zirconia) which is between 6% and 8%, by weight, of yttrium oxide (yttria) covers the bond coating. Partial stabilization provides a material with superior durability. Partially stabilized zirconia consists of mixtures of cubic, tetragonal, and monoclinic phases. NASA

N82-29415* National Aeronautics and Space Administration, Lewis Research Center, Cleveland, Ohio.

REFRACTORY COATINGS AND METHOD OF PRODUCING THE SAME Patent

William A. Brainard and Donald R. Wheeler, inventors (to NASA) Issued 22 Jun. 1982 4 p Filed 7 Dec. 1979 Supersedes N80-14232 (18 - 05, p 0583)

(NASA-Case-LEW-13169-1; US-Patent-4,336,117; US-Patent-Appl-SN-102003; US-Patent-Class-204-192C) Avail: US Patent and Trademark Office CSCL 11F

The adhesion, friction, and wear properties of sputtered refractory coatings on substrates of materials that form stable nitrides is improved by placing each substrate directly below a titanium carbide target of a commercial radiofrequency diode apparatus in a vacuum chamber. Nitrogen is bled into the system

through a nozzle resulting in a small partial pressure of about 0.5% to 2.5% during the first two minutes of deposition. The flow of nitrogen is then stopped, and the sputtering ambient is reduced to pure argon through a nozzle without interrupting the sputtering process. When nitrogen is deliberately introduced during the crucial interface formation, some of the titanium at the interface reacts to form titanium nitride while the metal of the substrate also forms the nitride. These two nitrides atomically mixed together in the interfacial region act to more strongly bond the growing titanium carbide coating as it forms on the substrate.

Official Gazette of the U.S. Patent and Trademark Office

N82-30371* National Aeronautics and Space Administration, Lewis Research Center, Cleveland, Ohio.

REFRACTORY COATINGS Patent

William A. Brainard and Donald R. Wheeler, inventors (to NASA) Issued 27 Jul. 1982 4 p Filed 29 Sep. 1980 Division of US Patent Appl. SN-102003, filed 7 Dec. 1979 (NASA-Case-LEW-13169-2; US-Patent-4,341,843; US-Patent-AppI-SN-191746; US-Patent-AppI-SN-102003; US-Patent-Class-428-457; US-Patent-Class-204-192C; US-Patent-Class-428-472) Avail: US Patent and Trademark Office CSCL 11F

A thin sputtered film is discussed which exhibits improved adherence to a substrate and has improved friction and wear characteristics. Each substrate is placed directly below a titanium carbide target of a commercial radiofrequency diode apparatus in a vacuum chamber. Nitrogen is bled into the system through a nozzle resulting in a small partial pressure of about 0.5% to 2.5% during the first two minutes of deposition. The flow of nitrogen is then stopped, and the sputtering ambient is reduced to pure argon through a nozzle without interrupting the sputtering process.

Official Gazette of the U.S. Patent and Trademark Office

N82-30372*# National Aeronautics and Space Administration, Lewis Research Center, Cleveland, Ohio

EVALUATION OF CANDIDATE STIRLING ENGINE HEATER TUBE ALLOYS AT 820 DEG AND 860 DEG C Final Report

John A. Misencik Jun. 1982 43 p refs (Contract DE-AI01-77CS-51040)

(NASA-TM-82837; E-1204; DOE/NASA/51040-39; NAS 1.15:82837) Avail: NTIS HC A03/MF A01 CSCL 11F

Seven commercial alloys were evaluated in Stirling simulator materials rigs. Five iron base alloys (N-155, A-286, Incoloy 800, 19-9DL, and 316 stainless steel), one nickel base alloy (Inconel 718), and one cobalt base alloy (HS-188) were tested in the form of thin wall tubing in a diesel fuel fired test rig. Tubes filled with hydrogen or helium at gas pressure of 21.6 MPa and temperatures of 820 and 860 C were endurance tested for 1000 and 535 hours, respectively. Results showed that under these conditions hydrogen permeated rapidly through the tube walls, thus requiring refilling during each five hour cycle. Helium was readily contained, exhibiting no measurable loss by permeation. Helium filled tubes tested at 860 C all exhibited creep-rupture failures within the 535 hour endurance test. Subsequent tensile test evaluation after removal from the rig indicated reduced room temperature ductility for some hydrogen-filled tubes compared to helium-filled tubes, suggesting possible hydrogen embrittlement in these alloys.

S.L.

N82-30373*# National Aeronautics and Space Administration, Lewis Research Center, Cleveland, Ohio.

EFFECT OF FUEL TO AIR RATIO ON MACH 0.3 BURNER RIG HOT CORROSION OF ZrO₂-Y₂O₃ THERMAL BARRIER COATINGS

Philip E. Hodge Jul. 1982 11 p refs (Contract DE-AI01-77ET-10350)

(NASA-TM-82879; E-1255; DOE/NASA/10350-32; NAS 1.15:82879) Avail: NTIS HC A02/MF A01 CSCL 11F

A Mach 0.3 burner rig test program was conducted to determine how the fuel to air mass ratio affects the durability of ZrO₂-Y₂O₃/Ni-16Cr-6Al-0.31Y thermal barrier coating systems in combustion products containing 5 ppm Na and 2 ppm V. As the fuel to air mass ratio was increased from 0.039 to 0.049, the durability of ZrO₂-6Y₂O₃, ZrO₂-8Y₂O₃ and ZrO₂-12Y₂O₃ coatings decreased. ZrO₂-8Y₂O₃ coatings were approximately 2X and 1.3X more durable than ZrO₂-12Y₂O₃ and ZrO₂-6Y₂O₃ coatings respectively at the fuel to air mass ratio of 0.039. The

number of one hour cycles endured by ZrO₂-8Y₂O₃ coatings varied from averages of 53 to 200 for the fuel to air mass ratios of 0.049 and 0.039, respectively. At the fuel to air mass ratio of 0.049, all ZrO₂-Y₂O₃ coated specimens failed in 40 to 60 one hour cycles S.L.

N82-31505* National Aeronautics and Space Administration, Lewis Research Center, Cleveland, Ohio.

NICRAL TERNARY ALLOY HAVING IMPROVED CYCLIC OXIDATION RESISTANCE Patent

Charles A. Barrett (NAS-NRC, Washington, D.C.), Carl E. Lowell (NAS-NRC, Washington, D.C.), and Abdus S. Khan (NAS-NRC, Washington, D.C.) Issued 20 Jul. 1982 3 p Filed 23 Oct. 1980 Supersedes N81-12211 (19 - 03, p 0322) Sponsored by NASA (NASA-Case-LEW-13339-1; US-Patent-4,340,425; US-Patent-AppI-SM-199769; US-Patent-Class-148-428; US-Patent-Class-410-445; US-Patent-Class-420-551; US-Patent-Class-420-528) Avail: US Patent and Trademark Office CSCL 11F

NiCrAl alloys are improved by the addition of zirconium. These alloys are in the Beta or gamma/gamma' + Beta region of the ternary system. Zirconium is added in a very low amount between 0.06 and 0.20 weight percent. There is a narrow optimum zirconium level at the low value of 0.13 weight percent. Maximum resistance to cyclic oxidation is achieved when the zirconium addition is at the optimum value.

Official Gazette of the U.S. Patent and Trademark Office

N82-32461*# National Aeronautics and Space Administration, Lewis Research Center, Cleveland, Ohio.

FAILURE MECHANISMS OF THERMAL BARRIER COATINGS EXPOSED TO ELEVATED TEMPERATURES

Robert A. Miller and Carl E. Lowell 1982 14 p refs Presented at the Intern. Conf. on Met. Coatings and Process Technol., San Diego, Calif., 4-9 Apr. 1982

(NASA-TM-82905; E-1289; NAS 1.15:82905) Avail: NTIS HC A02/MF A01 CSCL 11F

The failure of a ZrO₂-8%Y₂O₃/Ni-14% Al-0.1% Zr coating system on Rene 41 in Mach 0.3 burner rig tests was characterized. High flame and metal temperatures were employed in order to accelerate coating failure. Failure by delamination was shown to precede surface cracking or spalling. This type of failure could be duplicated by cooling down the specimen after a single long duration isothermal high temperature cycle in a burner rig or a furnace, but only if the atmosphere was oxidizing. Stresses due to thermal expansion mismatch on cooling coupled with the effects of plastic deformation of the bond coat and oxidation of the irregular bond coat are the probable life limiting factors. Heat up stresses alone could not fail the coating in the burner rig tests. Spalling eventually occurs on heat up but only after the coating has already failed through delamination.

Author

N82-33493*# National Aeronautics and Space Administration, Lewis Research Center, Cleveland, Ohio.

A STUDY OF THE NATURE OF SOLID PARTICLE IMPACT AND SHAPE ON THE EROSION MORPHOLOGY OF DUCTILE METALS

P. Veerabhadra Rao (NAS-NRC), Stanley G. Young, and Donald H. Buckley Jul. 1982 19 p refs Presented at Microscopy of the Degradation of Mater. (Wear and Erosion), MICRO 82, Intern. Symp. and Exhibition, London, 12-16 Jul. 1982; sponsored by the Royal Microscopical Society

(NASA-TM-82933; E-1298; NAS 1.15:82933) Avail: NTIS HC A02/MF A01 CSCL 11F

Impulsive versus steady jet impingement of spherical glass bead particles on metal surfaces was studied using a gas gun facility and a commercial sand blasting apparatus. Crushed glass particles were also used in the sand blasting apparatus as well as glass beads. Comparisons of the different types of erosion patterns were made. Scanning electron microscopy, surface profilometry and energy dispersive X-ray spectroscopy analysis were used to characterize erosion patterns. The nature of the

wear can be divided into cutting and deformation, each with its own characteristic features. Surface chemistry analysis indicates the possibility of complex chemical and/or mechanical interactions between erodants and target materials. S.L.

A82-10674 * Effect of gamma irradiation on the friction and wear of ultrahigh molecular weight polyethylene. W. R. Jones, W. F. Hady (NASA, Lewis Research Center, Cleveland, OH), and A. Crugnola (Lowell, University, Lowell, MA), *Wear*, vol. 70, July 15, 1981, p. 77-92. 25 refs.

The effect of sterilization gamma irradiation on the friction and wear properties of ultrahigh molecular weight polyethylene (UHMWPE) sliding against stainless steel 316L in dry air at 23 C is investigated, the results to be used in the development of artificial joints which are to surgically replace diseased human joints. A pin-on-disk sliding friction apparatus is used, a constant sliding speed in the range 0.061-0.27 m/s is maintained, a normal load of 1 kgf is applied with dead weight, and the irradiation dose levels γ/hr : 0, 2.5, and 5.0 Mrad. Wear and friction data and conditions for each of the ten tests are summarized, and include: (1) wear volume as a function of the sliding distance for the irradiation levels, (2) incremental wear rate, and (3) coefficient of friction as a function of the sliding distance. It is shown that (1) the friction and wear properties of UHMWPE are not significantly changed by the irradiation doses of 2.5 and 5.0 Mrad, (2) the irradiation increases the amount of insoluble gel as well as the amount of low molecular weight material, and (3) after run-in the wear rate is either steady or gradually decreases as a function of the sliding distance. K.S.

A82-11399 * Comparative thermal fatigue resistance of several oxide dispersion strengthened alloys. J. D. Whittenberger and P. T. Bizon (NASA, Lewis Research Center, Cleveland, OH), *International Journal of Fatigue*, vol. 3, Oct. 1981, p. 173-180. 25 refs.

The thermal fatigue resistance of several oxide dispersion strengthened (ODS) alloys has been evaluated through cyclic exposure in fluidized beds. The ODS nickel-base alloy MA 754 and ODS iron-base alloy MA 956 as well as four experimental ODS Ni-16Cr-4.5Al base alloys with and without Ta additions were examined. Both bare and coated alloys were subjected to up to 6000 cycles where each cycle consisted of a 3 minute immersion in a fluidized bed at 1130 C followed by a 3 minute immersion in a bed at 357 C. Testing revealed that the thermal fatigue resistance of the ODS nickel-base alloys was excellent and about equal to that of directionally solidified superalloys. However, the thermal fatigue resistance of MA 956 was found to be poor. Metallographic examination of tested specimens revealed that, in general, the post-test microstructures can be rationalized on the basis of previous diffusion, mechanical property, and oxidation studies. (Author)

A82-37151 * Long-term high-velocity oxidation and hot corrosion testing of several NiCrAl and FeCrAl base oxide dispersion strengthened alloys. C. E. Lowell, D. L. Deadmore, and J. D. Whittenberger (NASA, Lewis Research Center, Materials Div., Cleveland, OH), *Oxidation of Metals*, vol. 17, Apr. 1982, p. 205-221. 20 refs.

Several oxide dispersion strengthened (ODS) alloys have been tested for cyclic, long-term, high gas-velocity resistance to oxidation at 1100 C and hot corrosion at 900 C. Both nominally Ni-16Cr-4Al and Fe-20Cr-4.5Al ODS alloys were subjected up to about 2500 cycles, where each cycle consisted of 1 hr in a hot, Mach 0.3 combusted gas stream followed by a 3-min quench in an ambient temperature, Mach 0.3 air blast. For comparison to existing technology, a coated superalloy was simultaneously tested. The ODS iron alloy exhibited clearly superior behavior, surviving 3800 oxidation and 2300 hot corrosion cycles essentially unscathed. While the ODS nickel alloys exhibited adequate oxidation resistance, the long-term hot corrosion resistance could be marginal, since the best life for such alloys under these conditions was only about 1100 cycles. However, the hot corrosion resistance of the ODS Ni-base alloys is excellent in comparison to that of traditional superalloys. (Author)

A82-40041 * Crystallographic texture in oxide-dispersion-strengthened alloys. J. D. Whittenberger (NASA, Lewis Research Center, Cleveland, OH), *Materials Science and Engineering*, vol. 54, June 1982, p. 81-83. 9 refs.

Crystallographic and elastic moduli data are presented which document the degree of texture in several oxide dispersion-strengthened (ODS) nickel-base alloys. The existence of strong crystallographic textures in such multicrystalline alloys is considered important, since the small angle grain boundaries may be

partially responsible for creep threshold stresses. Gleiter (1979) has shown that ideal, low energy boundaries will act as vacancy sources only when the applied stress is greater than a threshold stress, while large angle grain boundaries will emit vacancies at all stress levels. The continued operation of a net vacancy in an ODS alloy must be avoided, since it will lead to a localized disruption of the microstructure. O.C.

A82-42774 * Structure and creep rupture properties of directionally solidified eutectic gamma/gamma-prime-alpha alloy. J. D. Whittenberger (NASA, Lewis Research Center, Cleveland, OH) and G. Wirth (Deutsche Forschungs- und Versuchsanstalt für Luft- und Raumfahrt, Cologne, West Germany), *Metal Science*, vol. 16, Aug. 1982, p. 383-388. 21 refs. Research supported by the Alexander von Humboldt-Stiftung.

A simple ternary gamma/gamma-prime-alpha alloy of nominal composition (wt-%) Ni-32Mo-6Al has been directionally solidified at 17 mm/h and tested in creep rupture at 1073, 1173, and 1273 K. A uniform microstructure consisting of square-shaped Mo fibers in a gamma + gamma-prime matrix was found despite some variation in the molybdenum and aluminum concentrations along the growth direction. Although the steady-state creep rate is well described by the normal stress temperature equation, the stress exponent (12) and the activation energy (580 kJ/mol) are high. The rupture behavior is best characterized by the Larson-Miller parameter where the constant equals 29. (Author)

A82-47393 * # The influence of gamma prime on the recrystallization of an oxide dispersion strengthened superalloy - MA 6000E. R. K. Hotzler (Queensborough Community College, Bayside, NY) and T. K. Glasgow (NASA, Lewis Research Center, Cleveland, OH), *Metallurgical Transactions A - Physical Metallurgy and Materials Science*, vol. 13A, Oct. 1982, p. 1665-1674. 15 refs.

The requirement of large, recrystallized, highly elongated grains is of primary importance to the development of suitable high temperature properties in oxide dispersion strengthened-superalloys. In the present study the recrystallization behavior of MA 6000E, a recently developed Y2O3 strengthened superalloy produced by mechanical alloying, was examined using transmission and replica microscopy. Gradient and isothermal annealing treatments were applied to extruded and hot rolled products. It was found that conversion from a very fine (0.2 micron) grain structure to a coarse (approximately 10 mm) grain structure is controlled by the dissolution of the gamma prime phase, while grain shape was controlled primarily by the thermal gradient. The fine uniform oxide dispersion appeared to have only a secondary influence in determining the grain shape as columnar grains could be grown transverse to the working direction by appropriate application of the thermal gradient. (Author)

A82-47397 * The influence of orientation on the stress rupture properties of nickel-base superalloy single crystals. R. A. MacKay (NASA, Lewis Research Center, Cleveland, OH) and P. D. Maier (Chase Brass and Copper Co., Solon, OH), *Metallurgical Transactions A - Physical Metallurgy and Materials Science*, vol. 13A, Oct. 1982, p. 1747-1754. 13 refs. Grant No. NSG-3246.

Constant load creep rupture tests were performed on MAR-M247 single crystals at 724 MPa and 774 C where the effect of anisotropy is prominent. The initial orientations of the specimens as well as the final orientations of selected crystals after stress rupture testing were determined by the Laue back-reflection X-ray technique. The stress rupture lives of the MAR-M247 single crystals were found to be largely determined by the lattice rotations required to produce intersecting slip, because second-stage creep does not begin until after the onset of intersecting slip. Crystals which required large rotations to become oriented for intersecting slip exhibited the shortest stress rupture lives, whereas crystals requiring little or no rotations exhibited the lowest minimum creep rates, and consequently, the longest stress rupture lives. V.L.

A82-47398 * Fatigue and creep-fatigue deformation of several nickel-base superalloys at 650 C. R. V. Miner, J. Gayda (NASA, Lewis Research Center, Cleveland, OH), and R. D. Maier (Chase Brass and Copper Co., Solon, OH), *Metallurgical Transactions A - Physical Metallurgy and Materials Science*, vol. 13A, Oct. 1982, p. 1755-1765. 36 refs.

Transmission electron microscopy has been used to study the bulk deformation characteristics of seven nickel-base superalloys tested in fatigue and creep-fatigue at 650 C. The alloys were Waspalloy, HIP Astroloy, H plus F Astroloy, H plus F René 95, IN 100, MERL 76, and NASA IIB-7. The amount of bulk deformation observed in all the alloys was low. In tests with inelastic strain amplitudes less than about 0.003, only some grains exhibited yielding and the majority of those had the 110 line near the tensile axis. Deformation occurred on octahedral systems for all of the alloys except MERL 76 which also showed abundant primary cube slip. Creep-fatigue cycling occasionally produced extended faults between partial dislocations, but otherwise deformation was much the same as for fatigue cycling. V.L.

ORIGINAL PAGE IS
OF POOR QUALITY

A82-47399* The influence of cobalt on the tensile and stress-rupture properties of the nickel-base superalloy MAR-M247, M. V. Nathal (NASA, Lewis Research Center, Cleveland, OH), R. D. Maler (Chase Brass and Copper Co., Solon, OH), and L. J. Ebert (Case Western Reserve University, Cleveland, OH). *Metallurgical Transactions A - Physical Metallurgy and Materials Science*, vol. 13A, Oct. 1982, p. 1767-1774. 27 refs.

A82-47400* The influence of cobalt on the microstructure of the nickel-base superalloy MAR-M247, M. V. Nathal (NASA, Lewis Research Center, Cleveland, OH), R. D. Maler (Chase Brass and Copper Co., Solon, OH), and L. J. Ebert (Case Western Reserve University, Cleveland, OH). *Metallurgical Transactions A - Physical Metallurgy and Materials Science*, vol. 13A, Oct. 1982, p. 1775-1783. 20 refs. Grant No. NSG-330.

Nickel was substituted for Co to produce 0, 5, and the standard 10% versions of MAR-M247, a cast nickel-base superalloy. The microstructures of the alloys were examined in as-cast, heat treated, aged, and stress-rupture tested conditions using a variety of metallographic techniques and differential thermal analysis. As cobalt concentration was reduced from 10 to 0 wt %, the gamma-prime weight fraction decreased from 59 to 41%; W and Ti concentrations in the gamma-prime phase increased from 5 to 8 and 2 to 3 at.%, respectively; the mean gamma-prime particle size increased from 0.6 to 0.8 micron; Cr and Al concentrations in the gamma matrix decreased from 17 to 13 and 15 to 12 at.%, respectively; and the weight fraction of carbides increased by approximately 1%. V.L.

N82-10193*# IIT Research Inst., Chicago, Ill. Materials Technology Div.

THERMAL FATIGUE AND OXIDATION DATA OF TAZ-8A AND M22 ALLOYS AND VARIATIONS Technical Report, 1 Feb. - 30 Apr. 1980

K. E. Hofer and V. E. Humphreys Sep. 1981 44 p refs (Contract NAS3-17787)

(NASA-CR-165407; IITRI-M06001-89) Avail: NTIS HC A03/MF A01 CSCL 11F

Thermal fatigue and oxidation data were obtained on 36 specimens, representing 18 distinct variations (including the base systems) of TAZ-8A and M22 alloys. Double-edge wedge specimens for these systems were cycled between fluidized beds maintained at 1088 C and 316 C with a 180 s immersion in each bed. The systems included alloys TAZ-8A, M22, and 16 variations of these alloys. Each alloy variation consisted of a unique composition with an alternation in the percentage of carbon (C1 and C2), molybdenum (M1 and M2), tungsten (W1 and W2), columbium (CB1, CB2, and CB3), tantalum (T1, T2, and T3), or boron (B1, B2, and B3) present. All of the alloys showed little weight change due to oxidation compared with other alloys previously tested in fluidized beds. Only both C1 alloy variation specimens survived 3500 cycles without cracking in the small radius, although substantial cracks were present, emanating from the end notches which were used for holding the specimen. Author

N82-13217*# Pittsburg Univ., Pa. Dept. of Metallurgical and Materials Engineering.

INVESTIGATION INTO THE ROLE OF NaCl DEPOSITED ON OXIDE AND METAL SUBSTRATES IN THE INITIATION OF HOT CORROSION Semiannual Report, 1 Apr. - 1 Oct. 1981

N. Birks 1 Oct. 1981 24 p (Grant NAG3-44)

(NASA-CR-165029; SAR-3) Avail: NTIS HC A02/MF A01 CSCL 11F

Morphological aspects of the conversion to Na₂SO₄ of NaCl deposits over the temperature range 500-700 C, in air with added SO₂ and H₂O. Progress of the reaction was observed by withdrawing samples at various times and examining them under the scanning electron microscope using EDAX to assess the extent of chloride to sulfate conversion. These initial results show that the conversion to Na₂SO₄ proceeds directly on the sodium chloride surface as well as on the surrounding substrate due to evaporation of NaCl from the solid particle. The mechanism of this reaction could involve reaction in the vapor to produce Na₂SO₄ which then deposits, alternatively Na₂SO₄ could form directly on the substrate surface due to direct reaction there between the vapors NaCl, SO₂ and O₂. A.R.H.

N82-14333*# Avco Lycoming Div., Stratford, Conn. Materials Lab.

DEVELOPMENT OF IMPROVED HIGH TEMPERATURE COATINGS FOR IN-792 + Hf Final Report

D. D. Profant and S. K. Naik Jun. 1981 95 p refs

(Contract NAS3-22371; DA Proj. 1L1-62209-AH-76) (NASA-CR-165395) Avail: NTIS HC A05/MF A01 CSCL 11F

The development for t-55 I712 engine of high temperature for integral turbine nozzles with improved thermal fatigue resistance without sacrificing oxidation/corrosion protection is discussed. The program evaluated to coating systems which comprised one baseline plasma spray coating (12% Al-NiCoCrAlY), three aluminide coatings including the baseline aluminide (701), two CoNiCrAlY (6% Al) + aluminide systems and four NiCoCrY + aluminide coating were evaluated. The two-step coating processes were investigated since it offered the advantage of tailoring the composition as well as properly coating surfaces of an integral or segmented nozzle. Cyclic burner rig thermal fatigue and oxidation/corrosion tests were used to evaluate the candidate coating systems. The plasma sprayed 12% Al-NiCoCrAlY was rated the best coating in thermal fatigue resistance and outperformed all coatings by a factor between 1.4 to 2.5 in cycles to crack initiation. However, this coatings is not applicable to integral or segmented nozzles due to the line of sight limitation of the plasma spray process. The 6% Al-CoNiCrAlY + Mod. 701 aluminide (32 w/o Al) was rated the best coating in oxidation/corrosion resistance and was rated the second best in thermal fatigue resistance. J.D.H.

N82-18368*# Westinghouse Electric Corp., Pittsburgh, Pa. **EVALUATION OF PRESENT THERMAL BARRIER COATINGS FOR POTENTIAL SERVICE IN ELECTRIC UTILITY GAS TURBINES** Final Report

R. J. Bratton, S. K. Lau, and S. Y. Lee Jul. 1982 161 p refs Sponsored in part by Electric Power Research Inst.

(Contract NAS3-21377)

(NASA-CR-165545; Rept-81-9D6-NASAC-R3) Avail: NTIS HC A08/MF A01 CSCL 11F

The resistance of present-day thermal barrier coatings to combustion gases found in electric utility turbines was assessed. The plasma sprayed coatings, both duplex and graded types, were primarily zirconia-based, although a calcium silicate was also evaluated. Both atmospheric burner rig tests and high pressure tests (135 psig) showed that several present-day thermal barrier coatings have a high potential for service in gas turbines burning the relatively clean GT No. 2 fuel. However, coating improvements are needed for use in turbines burning lower grade fuel such as residual oil. The duplex ZrO₂.8Y₂O₃/NiCrAlY coating was ranked highest and selected for near-term field testing, with Ca₂SiO₄/NiCrAlY ranked second. Graded coatings show potential for corrosive turbine operating conditions and warrant further development. The coating degradation mechanisms for each coating system subjected to the various environmental conditions are also described. B.W.

N82-18370*# TRW, Inc., Cleveland, Ohio. Materials Technology Lab.

DEVELOPMENT OF MATERIALS AND PROCESS TECHNOLOGY FOR DUAL ALLOY DISKS Final Report

James M. Marder and Charles S. Kortovich Oct. 1981 188 p refs

(Contract NAS3-21351)

(NASA-CR-165224; TRW-ER-8001-F) Avail: NTIS HC A09/MF A01 CSCL 11F

Techniques for the preparation of dual alloy disks were developed and evaluated. Four material combinations were evaluated in the form of HIP consolidated and heat treated cylindrical and plate shapes in terms of elevated temperature tensile, stress rupture and low cycle fatigue properties. The process evaluation indicated that the pe-HIP AF-115 rim/loose powder Rene 95 hub combination offered the best overall range of mechanical properties for dual disk applications. The feasibility of this dual alloy concept for the production of more complex components was demonstrated by the scale up fabrication of a prototype CFM-56 disk made from this AF-115/Rene 95 combination. The hub alloy ultimate tensile strength was approximately 92 percent of the program goal of 1520 MPa (220 ksi) at 480 C (900 F) and the rim alloy stress rupture goal of 300 hours at 675 C (1250 F)/925 MPa (134 ksi) was exceeded by 200 hours. The low cycle fatigue properties were

ORIGINAL PAGE IS
OF POOR QUALITY

equivalent to those exhibited by HIP and heat treated alloys. There was an absence of rupture notch sensitivity in both alloys. The joint tensile properties were approximately 85 percent of the weaker of the two materials (Rene 95) and the stress rupture properties were equivalent to those of the weaker of the two materials (Rene 95). Author

N82-19360*# Pratt and Whitney Aircraft, East Hartford, Conn.
TAILORED PLASMA SPRAYED MCrAlY COATINGS FOR AIRCRAFT GAS TURBINE APPLICATIONS

F. J. Pennisi and D. K. Gupta Jan. 1981 132 p refs
(NAS3-21730)

(NASA-CR-185234; PWA-5642-21) Avail: NTIS
HC A07/MF A01 CSCL 11F

Eighteen plasma sprayed coating systems, nine based on the NiCoCrAlY chemistry and nine based on the CoCrAlY composition, were evaluated to identify coating systems which provide equivalent or superior life to that shown by the electron beam physical vapor deposited NiCoCrAlY and CoCrAlY coatings respectively. NiCoCrAlY type coatings were examined on a single crystal alloy and the CoCrAlY based coatings were optimized on the B1900+ Hf alloy. Cyclic burner rig oxidation and hot corrosion and tensile ductility tests used to evaluate the various coating candidates. For the single crystal alloy, a low pressure chamber plasma sprayed NiCoCrAlY + Si coating exhibited a 2x oxidation life improvement at 1394 K (2050 F) over the vapor deposited NiCoCrAlY material while showing equivalent tensile ductility. A silicon modified low pressure chamber plasma sprayed CoCrAlY coating was found to be more durable than the baseline vapor deposited CoCrAlY coating on the B1900+ Hf alloy. S.L.

N82-26436*# Cincinnati Univ., Ohio. Dept. of Materials Science and Metallurgical Engineering.

HIGH TEMPERATURE LOW CYCLE FATIGUE MECHANISMS FOR NICKEL BASE AND A COPPER BASE ALLOY
M.S. Thesis Final Report

Chin-I Shih Washington NASA Jun. 1982 110 p refs
(Grant NsG-3263)

(NASA-CR-3543; NAS 1.26:3543) Avail: NTIS
HC A06/MF A01 CSCL 11F

Damage mechanisms were studied in Rene' 95 and NARloy Z, using optical, scanning and transmission in microscopy. In necklace Rene' 95, crack initiation was mainly associated with cracking of surface MC carbides, except for hold time tests at higher strain ranges where initiation was associated more with a grain boundary mechanism. A mixed mode of propagation with a faceted fracture morphology was typical for all cycle characters. The dependence of life on maximum tensile stress can be demonstrated by the data falling onto three lines corresponding to the three tensile hold times, in the life against maximum tensile stress plot. In NARloy Z, crack initiation was always at the grain boundaries. The mode of crack propagation depended on the cycle character. The life decreased with decreasing strain rate and with tensile holds. In terms of damage mode, different life prediction laws may be applicable to different cycle characters. A.R.H.

N82-26439*# United Technologies Corp., East Hartford, Conn. Commercial Products Div.

HOT ISOSTATICALLY PRESSED MANUFACTURE OF HIGH STRENGTH MERL 76 DISK AND SEAL SHAPES Final Report

R. D. Eng and D. J. Evans May 1982 139 p refs
(Contract NAS3-20072)

(NASA-CR-165549; NAS 1.26:165549; PWA/5574-123) Avail:
NTIS HC A07/MF A01 CSCL 11F

The feasibility of using MERL 76, an advanced high strength direct hot isostatic pressed powder metallurgy superalloy, as a full scale component in a high technology, long life, commercial turbine engine were demonstrated. The component was a JT9D first stage turbine disk. The JT9D disk rim temperature capability was increased by at least 22 C and the weight of JT9D high pressure turbine rotating components was reduced by at least 35 pounds by replacement of forged Superwaspaloy components with hot isostatic pressed (HIP) MERL 76 components. The process control plan and acceptance criteria for manufacture of MERL 76 HIP consolidated components were generated. Disk components were manufactured for spin/burst rig test, experimen-

tal engine tests, and design data generation, which established lower design properties including tensile, stress-rupture, 0.2% creep and notched ($K_t = 2.5$) low cycle fatigue properties, Sonntag, fatigue crack propagation, and low cycle fatigue crack threshold data. Direct HIP MERL 76, when compared to conventionally forged Superwaspaloy, is demonstrated to be superior in mechanical properties, increased rim temperature capability, reduced component weight, and reduced material cost by at least 30% based on 1980 costs. J.D.

N82-27462*# Michigan Technological Univ., Houghton. Dept of Metallurgical Engineering.

SOLUTE TRANSPORT DURING THE CYCLIC OXIDATION OF Ni-Cr-Al ALLOYS M.S. Thesis

James A. Nesbitt May 1982 140 p refs
(Grant NsG-3215)

(NASA-CR-165544; NAS 1.26:165544) Avail: NTIS
HC A07/MF A01 CSCL 11F

Important requirements for protective coatings of Ni-Cr-Al alloys for gas turbine superalloys are resistance to oxidation accompanied by thermal cycling, resistance to thermal fatigue cracking. The resistance to oxidation accompanied by thermal cycling is discussed. The resistance to thermal fatigue cracking is also considered. S.L.

N82-28409*# Purdue Univ., Lafayette, Ind. Dept. of Material Engineering.

EFFECTS OF COBALT ON THE MICROSTRUCTURE OF UDIMET 700 M.S. Thesis Final Report

Mayer Abraham Engel Jun. 1982 66 p refs
(Grant NAG3-57)

(NASA-CR-165605; NAS 1.26:165605) Avail: NTIS
HC A04/MF A01 CSCL 11F

Cobalt, a critical and 'strategic' alloying element in many superalloys, was systematically substituted by nickel in experimental alloys Udimet 700 containing 0.1, 4.3, 8.6, 12.8 and the standard 17.0 wt% cobalt. Electrolytic and chemical extraction techniques, X-ray diffraction, scanning electron and optical microscopy were used for the microstructural studies. The total weight fraction of gamma' was not significantly affected by the cobalt content, although a difference in the size and quantities of the primary and secondary gamma' phases was apparent. The lattice parameters of the gamma' were found to increase with increasing cobalt content while the lattice mismatch between the gamma matrix and gamma' phases decreased. Other significant effects of cobalt on the weight fraction, distribution and formation of the carbide and boride phases as well as the relative stability of the experimental alloys during long-time aging are also discussed. Author

N82-30374*# Purdue Univ., Lafayette, Ind.
MC CARBIDE STRUCTURES IN M(LC2)AR-M247
M.S. Thesis - Final Report

Stanley Walter Wawro Jun. 1982 53 p refs
(Contract NAG3-59)

(NASA-CR-167892; NAS 1.26:167892) Avail: NTIS
HC A04/MF A01 CSCL 11F

The morphologies and distribution of the MC carbides in Mar-M247 ingot stock and castings were investigated using metallographic, X-ray diffraction and energy-dispersive X-ray analysis techniques. The MC carbides were found to form script structures during solidification. The script structures were composed of three distinct parts. The central cores and elongated arms of the MC carbide script structures had compositions (Ti, Cr, Hf, Ta, W)C and lattice parameters of 4.39 A. The elongated script arms terminated in enlarged, angular 'heads'. The heads had compositions (Ti, Hf, Ta, W)C and lattice parameters of approximately 4.50 A. The heads had a higher Hf content than the cores and arms. The size of the script structures, as well as the relative amount of head-type to core and arm-type MC carbide, was found to be determined by solidification conditions. No carryover of the MC carbides from the ingot stock to the remelted and cast material was observed. Author

ORIGINAL PAGE IS
OF POOR QUALITY

N82-31509*# Colorado State Univ., Fort Collins. Dept. of Physics.

ION BEAM MICROTTEXTURING AND ENHANCED SURFACE DIFFUSION Final Report

Raymond S. Robinson Feb. 1982 54 p refs
(Grant NAG3-43)

(NASA-CR-167948; NAS 1.26:167948) Avail: NTIS HC A04/MF A01 CSCL 11F

Ion beam interactions with solid surfaces are discussed with particular emphasis on microtexturing induced by the deliberate deposition of controllable amounts of an impurity material onto a solid surface while simultaneously sputtering the surface with an ion beam. Experimental study of the optical properties of microtextured surfaces is described. Measurements of both absorptance as a function of wavelength and emissivity are presented. A computer code is described that models the sputtering and ion reflection processes involved in microtexture formation. B.W.

N82-33494*# Solar Turbines International, San Diego, Calif.
ADVANCED CERAMIC COATING DEVELOPMENT FOR INDUSTRIAL/UTILITY GAS TURBINES Final Report, 11 Mar. 1979 - 1 Sep. 1981

James W. Vogan and Alvin R. Stetson Jan. 1982 128 p refs
(Contracts DEN3-109; DE-AI01-77ET-3111)

(NASA-CR-169852; DOE/NASA/0108-1; NAS 1.26:169852; SR82-R-4792-28) Avail: NTIS HC A07/MF A01 CSCL 11F

A program was conducted with the objective of developing advanced thermal barrier coating (TBC) systems. Coating application was by plasma spray. Duplex, triplex and graded coatings were tested. Coating systems incorporated both NiCrAlY and CoCrAlY bond coats. Four ceramic overlays were tested: ZrO₂.82O₃; CaO.TiO₂; 2CaO.SiO₂; and MgO.Al₂O₃. The best overall results were obtained with a CaO.TiO₂ coating applied to a NiCrAlY bond coat. This coating was less sensitive than the ZrO₂.8Y₂O₃ coating to process variables and part geometry. Testing with fuels contaminated with compounds containing sulfur, phosphorus and alkali metals showed the zirconia coatings were destabilized. The calcium titanate coatings were not affected by these contaminants. However, when fuels were used containing 50 ppm of vanadium and 150 ppm of magnesium, heavy deposits were formed on the test specimens and combustor components that required frequent cleaning of the test rig. During the program Mars engine first-stage turbine blades were coated and installed for an engine cyclic endurance run with the zirconia, calcium titanate, and calcium silicate coatings. Heavy spalling developed with the calcium silicate system. The zirconia and calcium titanate systems survived the full test duration. It was concluded that these two TBC's showed potential for application in gas turbines. Author

A82-20742*# Improved plasma sprayed MCrAlY coatings for aircraft gas turbine applications. F. J. Pennisi and D. K. Gupta (United Technologies Corp., Pratt and Whitney Aircraft Group, East Hartford, CT). *American Vacuum Society, International Conference for Metallurgical Coatings, San Francisco, CA, Apr. 6-10, 1981, Paper*. 17 p. 11 refs. Contract No. NAS3-21730.

Eighteen plasma sprayed coating systems, nine based on the NiCoCrAlY chemistry and nine based on the CoCrAlY composition, were evaluated to identify coating systems which will provide equivalent or superior life to that shown by the electron beam physical vapor deposited NiCoCrAlY and CoCrAlY coatings respectively. NiCoCrAlY-type coatings were examined on a single crystal alloy and the CoCrAlY based coatings were optimized on the B1900 + Hf alloy. Cyclic burner rig oxidation and hot corrosion and tensile ductility tests were used to evaluate the various coating candidates. For the single crystal alloy, a low pressure chamber plasma sprayed NiCoCrAlY + Si coating exhibited a 2X oxidation life improvement at 1121 C (2050 F) over the vapor deposited NiCoCrAlY material while showing equivalent tensile ductility. A silicon modified low pressure chamber plasma sprayed CoCrAlY coating was found to be more durable than the baseline vapor deposited CoCrAlY coating on the B1900 + Hf alloy. (Author)

A82-34973* Effects of cobalt on structure, microchemistry and properties of a wrought nickel-base superalloy. R. N. Jarrett and J. K. Tien (Columbia University, New York, NY). *Metallurgical Transactions A - Physical Metallurgy and Materials Science*, vol. 13A, June 1982, p. 1021-1032, 30 refs. Grant No. NAG3-57.

The effect of cobalt on the basic mechanical properties and microstructure of wrought nickel-base superalloys has been investigated experimentally by systematically replacing cobalt by nickel in Udimet 700 (17 wt% Co) commonly used in gas turbine (jet engine) applications. It is shown that the room temperature tensile yield strength and tensile strength only slightly decrease in fine-grained (disk) alloys and are basically unaffected in coarse-grained (blading) alloys as cobalt is removed. Creep and stress rupture resistances at 760 C are found to be unaffected by cobalt level in the blading alloys and decrease sharply only when the cobalt level is reduced below 8 vol% in the disk alloys. The effect of cobalt is explained in terms of gamma prime strengthening kinetics. V.L.

A82-40335* Creep and rupture of an ODS alloy with high stress rupture ductility. M. E. McAlarney, R. M. Arsons (Delaware Research Center, Summit, NJ), T. E. Howson, J. K. Tien (Columbia University, New York, NY), and S. Baranow (Special Metals Corp., New Hartford, NY). *Metallurgical Transactions A - Physical Metallurgy and Materials Science*, vol. 13A, Aug. 1982, p. 1453-1462, 33 refs. Grant No. NSG-3050.

The creep and stress rupture properties of an oxide (Y₂O₃) dispersion strengthened nickel-base alloy, which also is strengthened by gamma-prime precipitates, was studied at 760 and 1093 C. At both temperatures, the alloy YDNiCrAl exhibits unusually high stress rupture ductility as measured by both elongation and reduction in area. Failure was transgranular, and different modes of failure were observed including crystallographic fracture at intermediate temperatures and tearing or necking almost to a chisel point at higher temperatures. While the rupture ductility was high, the creep strength of the alloy was low relative to conventional gamma prime strengthened superalloys in the intermediate temperature range and to ODS alloys in the higher temperature range. These findings are discussed with respect to the alloy composition; the strengthening oxide phases, which are inhomogeneously dispersed; the grain morphology, which is coarse and elongated and exhibits many included grains; and the second phase inclusion particles occurring at grain boundaries and in the matrix. The creep properties, in particular the high stress dependencies and high creep activation energies measured, are discussed with respect to the resisting stress model of creep in particle strengthened alloys. (Author)

A82-44529* Recrystallization and grain growth in NiAl. G. R. Haff (ODECO, New Orleans, LA) and E. M. Schulson (Dartmouth College, Hanover, NH). *Metallurgical Transactions A - Physical Metallurgy and Materials Science*, vol. 13A, Sept. 1982, p. 1563-1566, 8 refs. Grant No. NAG3-13.

Aluminide intermetallics, because of their strength, microstructural stability, and oxidation resistance at elevated temperatures, represent potential structural materials for use in advanced energy conversion systems. This inherent potential of the intermetallics can currently not be realized in connection with the general brittleness of the materials under ambient conditions. It is pointed out, however, that brittleness is not an inherent characteristic. Single crystals are ductile and polycrystals may be, too, if their grains are fine enough. The present investigation is concerned with an approach for reducing material brittleness, taking into account thermally-mechanically induced grain refinement in NiAl, a B2 aluminide which melts at 1638 C and which retains complete order to its melting point. Attention is given to the kinetics of recrystallization and grain growth of warm-worked, nickel-rich material. G.R.

A82-48244*# Applications of high-temperature powder metal aluminum alloys to small gas turbine engines. J. L. Williams, Jr. (Garrett Turbine Engine Co., Phoenix, AZ). *American Institute of Aeronautics and Astronautics, Annual Meeting, Dallas, TX, Feb. 15-18, 1982, Paper*. 13 p. Contract No. DEN3-167.

A program aimed at the development of advanced powder-metallurgy (PM) aluminum alloys for high-temperature applications up to 650 F using the concepts of rapid solidification and mechanical alloying is discussed. In particular, application of rapidly solidified PM aluminum alloys to centrifugal compressor impellers, currently used in auxiliary power units for both military and commercial aircraft and potentially for advanced automotive gas turbine engines, is examined. It is shown that substitution of high-temperature aluminum for titanium alloy impellers operating in the 360-650 F range provides significant savings in material and machining costs and results in reduced component weight, and consequently, reduced rotating group inertia requirements. V.L.

ORIGINAL PAGE IS
OF POOR QUALITY

27 NONMETALLIC MATERIALS

Includes physical, chemical, and mechanical properties of plastics, elastomers, lubricants, polymers, textiles, adhesives, and ceramic materials.

N82-11210* National Aeronautics and Space Administration, Lewis Research Center, Cleveland, Ohio.

CASTABLE HIGH TEMPERATURE FRACATORY MATERIALS Patent Application

Isidor Zaplatynsky, inventor (to NASA) Filed 13 Oct. 1981 5 p (NASA-CasJ-LEW-13080-2; US-Patent-Appl-SN-310713) Avail: NTIS HC A02/MF A01 CSCL 11B

The fabrication of chemically inert ceramic bodies that are both high refractory and porous is disclosed. A paste is formed by mixing alumina grain having a uniform particle size with colloidal silica that is stabilized with ammonia. This paste is then cast without forming a compact and dried without pressing. After drying, the cast body was sufficient green strength to be handled, and it is transferred to a furnace for curing. A green body prepared in accordance with the invention does not undergo shrinkage during either curing or prolonged subsequent heating.

NASA

N82-11211* National Aeronautics and Space Administration, Lewis Research Center, Cleveland, Ohio.

FABRICATION AND WEAR TEST OF A CONTINUOUS FIBER/PARTICULATE COMPOSITE TOTAL SURFACE HIP REPLACEMENT

Jack C. Roberts (Rensselaer Polytechnic Inst., Troy, N.Y.), Frederick F. Ling (Rensselaer Polytechnic Inst., Troy, N.Y.), and William R. Jones, Jr. 1981 29 p refs Presented at the Joint Lubrication Conf., New Orleans, 5-7 Oct. 1981; cosponsored by ASME and the Am. Soc. of Lubrication Engr. (Grant DAAG29-79-C-0204)

(NASA-TM-81746; E-709) Avail: NTIS HC A03/MF A01 CSCL 06B

Continuous fiber woven E-glass composite femoral shells having the same elastic properties as bone were fabricated. The shells were then encrusted with filled epoxy wear resistant coatings and run dry against ultrahigh molecular weight polyethylene acetabular cups in 42,000 and 250,000 cycle wear tests on a total hip simulator. The tribological characteristics of these shells articulating with the acetabular cups are comparable to a vitallium ball articulating with an ultrahigh molecular weight polyethylene cup.

S.L.

N82-14359* National Aeronautics and Space Administration, Lewis Research Center, Cleveland, Ohio.

ULTRASONIC VELOCITY FOR ESTIMATING DENSITY OF STRUCTURAL CERAMICS

S. J. Klima, G. K. Watson, T. P. Herbell, and T. J. Moore 1981 12 p refs Presented at the Automotive Technol. Develop. Contractor Coord. Meeting, Dearborn, Mich., 26-29 Oct. 1981 (Contract DE-A101-77CS-51040)

(NASA-TM-82765; DOE/NASA/51040-35; E-1026-5) Avail: NTIS HC A02/MF A01 CSCL 11B

The feasibility of using ultrasonic velocity as a measure of bulk density of sintered alpha silicon carbide was investigated. The material studied was either in the as-sintered condition or hot isostatically pressed in the temperature range from 1850 to 2050 C. Densities varied from approximately 2.8 to 3.2 g/cm³. Results show that the bulk, nominal density of structural grade silicon carbide articles can be estimated from ultrasonic velocity measurements to within 1 percent using 20 MHz longitudinal waves and a commercially available ultrasonic time intervalometer. The ultrasonic velocity measurement technique shows promise for screening out material with unacceptably low density levels.

Author

N82-15197* National Aeronautics and Space Administration, Lewis Research Center, Cleveland, Ohio.

NITRIDATION OF SILICON M.S. Thesis Case Western Reserve Univ.

Nancy J. Shaw Oct. 1981 113 p refs

(NASA-TM-82722; E-921) Avail: NTIS HC A06/MF A01 CSCL 11G

Silicon powders with three levels of impurities, principally Fe, were sintered in He or H₂. Non-densifying mechanisms of material transport were dominant in all cases. High purity Si showed coarsening in He while particle growth was suppressed in H₂. Lower purity powder coarsened in both He and H₂. The same three Si powders and Si/111/ single crystal wafers were nitrided in both N₂ and N₂/H₂ atmospheres. Hydrogen increased the degree of nitridation of all three powders and the alpha/beta ratio of the lower purity powder. Some Si₃N₄ whiskers and open channels through the surface nitride layer were observed in the presence of Fe, correlating with the nitridation-enhancing effects of Fe. Thermodynamic calculations showed that when SiO₂ is present on the Si, addition of H₂ to the nitriding atmosphere decreases the amount of SiO₂ and increases the partial pressure of Si-containing vapor species, that is, Si and SiO. Large amounts of NH₃ and SiH₄ were also predicted to form.

R.J.F.

N82-15198* National Aeronautics and Space Administration, Lewis Research Center, Cleveland, Ohio.

GEOMETRICAL ASPECTS OF THE TRIBOLOGICAL PROPERTIES OF GRAPHITE FIBER REINFORCED POLYIMIDE COMPOSITES

Robert L. Fusaro 1982 36 p refs Presented at the Ann. Meeting of the Am. Soc. of Lubrication Engrs., Cincinnati, 10-13 May 1982

(NASA-TM-82757; E-1076) Avail: NTIS HC A03/MF A01 CSCL 11D

A latin square statistical experimental test design was used to evaluate the effect of temperature, load and sliding speed on the tribological properties of graphite fiber reinforced polyimide (GFRPI) composite specimens. Hemispherically tipped composite riders were slid against 440 C HT stainless steel disks. Comparisons were made to previous studies in which hemispherically tipped 440 C HT stainless steel riders were slid against GFRPI composite disks and to studies in which GFRPI was used as a liner in plain spherical bearings. The results indicate that sliding surface geometry is especially important, in that different geometries can give completely different friction and wear results. Load, temperature, and sliding distance were found to influence the friction and wear results but sliding speed was found to have little effect. Experiments on GFRPI riders with 10 weight percent additions of graphite fluoride showed that this addition has no effect on friction and wear.

Author

N82-15199* National Aeronautics and Space Administration, Lewis Research Center, Cleveland, Ohio.

ELUCIDATION OF WEAR MECHANISMS BY FERROGRAPHIC ANALYSIS

William R. Jones, Jr. 1981 18 p refs Presented at the Tech. Symp. on Water Glycol Hydraulic Fluids at BASF Wyandotte Corp., Wyandotte, Mich., 8 Oct. 1981

(NASA-TM-82737; E-1050) Avail: NTIS HC A02/MF A01 CSCL 20K

The use of ferrographic analysis in conjunction with light and scanning electron microscopy is described for the elucidation of wear mechanisms taking place in operating equipment. Example of adhesive wear, abrasive wear, corrosive wear, rolling element fatigue, lubricant breakdown, and other wear modes are illustrated. In addition, the use of magnetic solutions to precipitate nonmagnetic debris from aqueous and nonaqueous fluids is described.

Author

N82-16239* National Aeronautics and Space Administration, Lewis Research Center, Cleveland, Ohio.

TRIBOLOGICAL CHARACTERISTICS OF A COMPOSITE TOTAL-SURFACE HIP REPLACEMENT Final Report

William R. Jones, Jr., Jack C. Roberts (Rensselaer Polytechnic Inst.), and Frederick F. Ling (Rensselaer Polytechnic Inst.) Washington NASA Jan. 1982 17 p refs Presented at the ASME-ASLE Joint Lubrication Conf., New Orleans, 5-7 Oct. 1981

(NASA-TP-1853; E-709) Avail: NTIS HC A02/MF A01 CSCL 11H

Continuous fiber, woven E-glass composite femoral shells having the same elastic properties as bone were fabricated. The

shells were then encrusted with filled epoxy wear resistant coatings and run dry against ultrahigh molecular weight polyethylene acetabular cups in 42,000 and 250,000 cycle wear tests on a total hip simulator. The tribological characteristics of these continuous fiber particulate composite femoral shells articulating with ultrahigh molecular weight polyethylene acetabular cups were comparable to those of a vitallium ball articulating with an ultrahigh molecular weight polyethylene acetabular cup. Author

N82-19373*# National Aeronautics and Space Administration, Lewis Research Center, Cleveland, Ohio.
TRIBOLOGICAL PROPERTIES AT 25 C OF SEVEN POLYIMIDE FILMS BONDED TO 440 C HIGH-TEMPERATURE STAINLESS STEEL

Robert L. Fusaro Feb. 1982 23 p refs
(NASA-TP-1944; E-758) Avail: NTIS HC A02/MF A01 CSCL 07C

The tribological properties of seven polyimide films applied to 440 C high temperature stainless steel substrates were studied at 25 C with a pin-on-disk type of friction and wear apparatus. The polyimides fell into two groups according to friction and wear properties. Group I polyimides had slightly lower friction but much higher wear than group II polyimides. The wear mechanism was predominately adhesion, but the wear particles were larger for group I polyimides. For most of the polyimides the transfer films consisted of clumps of compacted wear particles. One polyimide composition produced a very thin transfer film that sheared plastically in the contact area. Author

N82-19374*# National Aeronautics and Space Administration, Lewis Research Center, Cleveland, Ohio.
SURFACE CHEMISTRY AND WEAR BEHAVIOR OF SINGLE-CRYSTAL SILICON CARBIDE SLIDING AGAINST IRON AT TEMPERATURES TO 1500 C IN VACUUM

Kazuhiisa Miyoshi and Donald H. Buckley Feb. 1982 14 p refs
(NASA-TP-1947; E-654) Avail: NTIS HC A02/MF A01 CSCL 07C

X-ray photoelectron and Auger electron spectroscopy analyses and morphological studies of wear and metal transfer were conducted with a single-crystal silicon carbide 0001 surface in contact with iron at various temperatures to 1500 C in a vacuum of 10 to the minus 8th power pascal. The results indicate that below 800 C, carbide-carbon and silicon are primarily seen on the silicon carbide surface. Above 800 C the graphite increases rapidly with increase in temperature. The outermost surficial layer, which consists mostly of graphite and little silicon at temperatures above 1200 C is about 2 nm thick. A thicker layer, which consists of a mixture of graphite, carbide, and silicon is approximately 100 nm thick. The closer the surface sliding temperature is to 800 C, the more the metal transfer produced. Above 800 C, there was a transfer of rough, discontinuous, and thin iron debris instead of smooth, continuous and thin iron film which was observed to transfer below 800 C. Two kinds of fracture pits were observed on the silicon carbide surface: (1) a pit with a spherical asperity; and (2) multiangular shaped pits. Author

N82-20313*# National Aeronautics and Space Administration, Lewis Research Center, Cleveland, Ohio.
IMPROVED BOUNDARY LUBRICATION WITH FORMULATED C-ETHERS

William R. Loomis 1982 25 p refs Proposed for presentation at the 37th Ann. Meeting of the Am. Soc. of Lubrication Engr., Cincinnati, 10-13 May 1982
(NASA-TM-82808; E-1149; NAS 1.15:82808) Avail: NTIS HC A02/MF A01 CSCL 07C

A comparison of five recently developed C-ether-formulated fluids with an advanced formulated MIL-L-27502 candidate ester is described. Steady state wear and friction measurements were made with a sliding pin on disk friction apparatus. Conditions included disk temperatures up to 260 C, dry air test atmosphere, 1 kilogram load, 50 rpm disk speed, and test times to 130 minutes. Based on wear rates and coefficients of friction, three of the C-ether formulations as well as the C-ether base fluid gave better boundary lubrication than the ester fluid under all test conditions. The susceptibility of C-ethers to selective additive treatment (phosphinic esters or acids and other

antiwear additives) was demonstrated when two of the formulations gave somewhat improved lubrication over the base fluid. The increased operating potential for this fluid was shown in relationship to bulk oil temperature limits for MIL-L-23699 and MIL-L-27502 type esters. Author

N82-20314*# National Aeronautics and Space Administration, Lewis Research Center, Cleveland, Ohio.
SPUTTERED SILICON NITRIDE COATINGS FOR WEAR PROTECTION

Alfred Grill (Ben Gurion Univ.) and Paul R. Aron 1982 10 p refs Presented at the Intern. Conf. on Met. Coatings and Process Technol., San Diego, Calif., 4-9 Apr. 1982
(NASA-TM-82819; E-1143; NAS 1.15:82819) Avail: NTIS HC A02/MF A01 CSCL 07D

Silicon nitride films were deposited by RF sputtering on 304 stainless steel substrates in a planar RF sputtering apparatus. The sputtering was performed from a Si₃N₄ target in a sputtering atmosphere of argon and nitrogen. The rate of deposition, the composition of the coatings, the surface microhardness and the adhesion of the coatings to the substrates were investigated as a function of the process parameters, such as: substrate target distance, fraction nitrogen in the sputtering atmosphere and sputtering pressure. Silicon rich coating was obtained for fraction nitrogen below 0.2. The rate of deposition decreases continuously with increasing fraction nitrogen and decreasing sputtering pressure. It was found that the adherence of the coatings improves with decreasing sputtering pressure, almost independently of their composition. Author

N82-20316*# National Aeronautics and Space Administration, Lewis Research Center, Cleveland, Ohio.
INFLUENCE OF MINERAL OIL AND ADDITIVES ON MICROHARDNESS AND SURFACE CHEMISTRY OF MAGNESIUM OXIDE (001) SURFACE

Kazuhiisa Miyoshi, Hiroyuki Shigaki, and Donald H. Buckley Mar. 1982 11 p refs
(NASA-TP-1986; E-975; NAS 1.60:1986) Avail: NTIS HC A02/MF A01 CSCL 11H

X-ray photoelectron spectroscopy analyses and hardness experiments were conducted with cleaved magnesium oxide /001/ surfaces. The magnesium oxide bulk crystals were cleaved into specimens along the /001/ surface, and indentations were made on the cleaved surface in laboratory air, in nitrogen gas, or in degassed mineral oil with and without an additive while not exposing specimen surface to any other environment. The various additives examined contained sulfur, phosphorus, chlorine, or oleic acid. The sulfur-containing additive exhibited the highest hardness and smallest dislocation patterns evidencing plastic deformation; the chlorine-containing additive exhibited the lowest hardness and largest dislocation patterns evidencing plastic deformation. Hydrocarbon and chloride (MgCl₂) films formed on the magnesium oxide surface. A chloride film was responsible for the lowest measured hardness. Author

N82-21331*# National Aeronautics and Space Administration, Lewis Research Center, Cleveland, Ohio.
SOME PROPERTIES OF RF SPUTTERED HAFNIUM NITRIDE COATINGS

Paul R. Aron and Alfred Grill (Ben Gurion Univ. of the Negev) 1982 12 p refs Presented at the Intern. Conf. on Met. Coating and Process Technol., San Diego, Calif., 5-8 Apr. 1981
(NASA-TM-82826; E-1182; NAS 1.15:82826) Avail: NTIS HC A02/MF A01 CSCL 11F

Hafnium nitride coatings were deposited by reactive RF sputtering from a hafnium target in nitrogen and argon gas mixtures. The rate of deposition, composition, electrical resistivity and complex index of refraction were investigated as a function of target substrate distance and the fraction nitrogen, (fN₂) in the sputtering atmosphere. The relative composition of the coatings is independent on fN₂ for values above 0.1. The electric resistivity of the hafnium nitride films changes over 8 orders of magnitude when fN₂ changes from 0.10 to 0.85. The index of refraction is almost constant at 2.8(1-0.3i) up to fN₂ = 0.40 then decreases to 2.1(1 - 0.01i) for higher values of fN₂. S.L.

ORIGINAL PAGE IS
OF POOR QUALITY

N82-21332* National Aeronautics and Space Administration, Lewis Research Center, Cleveland, Ohio.

THERMAL AND OXIDATIVE DEGRADATION STUDIES OF FORMULATED C-ETHERS BY GEL-PERMEATION CHROMATOGRAPHY

William R. Jones, Jr. and Wilfredo Morales Mar. 1982 14 p refs
(NASA-TP-1994; NAS 1.60:1994; E-978) Avail: NTIS HC A02/MF A01 CSCL 07D

Gel-permeation chromatography was used to analyze C-ether lubricant formulations from high-temperature bearing tests and from micro-oxidation tests. Three mu-styragel columns (one 500 and two 100 A) and a tetrahydrofuran mobile phase were found to adequately separate the C-ether degradation products. The micro-oxidation tests yielded degradation results qualitatively similar to those observed from the bearing tests. Micro-oxidation tests conducted in air yielded more degradation than did tests in nitrogen. No great differences were observed between the thermal-oxidative stabilities of the two C-ether formulations or between the catalytic degradation activities of silver and M-50 steel. C-ether formulation I did yield more degradation than did formulation II in 111- and 25-hour bearing tests, respectively. Author

N82-22366* National Aeronautics and Space Administration, Lewis Research Center, Cleveland, Ohio.
EFFECTS OF ENVIRONMENT ON MICROHARDNESS OF MAGNESIUM OXIDE

Hiroyuki Ishigaki (Osaka Univ.) and Donald H. Buckley Apr. 1982 11 p refs
(NASA-TP-2002; E-916; NAS 1.60:2002) Avail: NTIS HC A02/MF A01 CSCL 11B

Micro-Vickers hardness measurements of magnesium oxide single crystals were conducted in various environments. These environments included air, nitrogen gas, water, mineral oil with or without various additives, and aqueous solutions with various pH values. Indentations were made on the (100) plane with the diagonals of the indentation in the (100) direction. The results indicate that a sulfur containing additive in mineral oil increased hardness, a chlorine containing additive in mineral oil decreased hardness, and aqueous solutions of hydrogen chloride decreased hardness. Other environments were found to have little effect on hardness. Mechanically polished surfaces showed larger indentation creep than did as-cleaved surfaces. Author

N82-24342* National Aeronautics and Space Administration, Lewis Research Center, Cleveland, Ohio.

PMR POLYIMIDES-REVIEW AND UPDATE

Tito T. Serafini, Peter Delvigs, and William B. Alston 1982 19 p refs Presented at the 27th Natl. S&MPE Symp. and Exhibition, San Diego, Calif., 4-6 May 1982
(NASA-TM-82821; E-1111; NAS 1.15:82821; AVRADCOM-TR-82-C-3) Avail: NTIS HC A02/MF A01 CSCL 11G

Fiber reinforced PMR polyimides are finding increased acceptance as engineering materials for high performance structural applications. Prepreg materials based on this novel class of highly processable, high temperature resistant polyimides are commercially available and the PMR concept is used by other investigators. The current status of first and second generation PMR polyimides were reviewed. Emphasis is given to the chemistry, processing and applications of the first generation material known as PMR-15. T.M.

N82-24343* National Aeronautics and Space Administration, Lewis Research Center, Cleveland, Ohio.

TRIBOLOGICAL PROPERTIES OF SINTERED POLYCRYSTALLINE AND SINGLE CRYSTAL SILICON CARBIDE

Kazuhiya Miyoshi, Donald H. Buckley, and M. Srinivasan (Carborundum) 1982 28 p refs Presented at the 84th Ann. Meeting of the Am. Ceram. Soc., Cincinnati, 2-5 May 1982
(NASA-TM-82829; E-1194; NAS 1.15:82829) Avail: NTIS HC A03/MF A01 CSCL 11G

Tribological studies and X-ray photoelectron spectroscopy analyses were conducted with sintered polycrystalline and single crystal silicon carbide surfaces in sliding contact with iron at various temperatures to 1500 C in a vacuum of 30 nPa. The results indicate that there is a significant temperature influence on both the friction properties and the surface chemistry of

silicon carbide. The main contaminants on the as received sintered polycrystalline silicon carbide surfaces are adsorbed carbon, oxygen, graphite, and silicon dioxide. The surface reveals a low coefficient of friction. This is due to the presence of the graphite on the surface. At temperatures of 400 to 600 C graphite and copious amount of silicon dioxide were observed on the polycrystalline silicon carbide surface in addition to silicon carbide. At 800 C, the amount of the silicon dioxide decreased rapidly and the silicon carbide type silicon and carbon peaks were at a maximum intensity in the XPS spectra. The coefficients of friction were high in the temperature range 400 to 800 C. Small amounts of carbon and oxygen contaminants were observed on the as received single crystal silicon carbide surface below 250 C. Silicon carbide type silicon and carbon peaks were seen on the silicon carbide in addition to very small amount of graphite and silicon dioxide at temperatures of 450 to 800 C. S.L.

N82-26468* National Aeronautics and Space Administration, Lewis Research Center, Cleveland, Ohio.

THERMAL OXIDATIVE DEGRADATION REACTIONS OF LINEAR PERFLUOROALKYL ETHERS

William R. Jones, Jr., K. J. L. Paciorek (Ultrasystems, Inc., Irvine, Calif.), T. I. Ito (Ultrasystems, Inc., Irvine, Calif.), and R. H. Kratzer (Ultrasystems, Inc., Irvine, Calif.) 1982 24 p refs Presented at the Am. Fluoropolymers Symp., Las Vegas, Nevada, 29 Mar. - 2 Apr. 1982; sponsored by the Am. Chem. Soc.
(NASA-TM-82834; E-1200; NAS 1.15:82834) Avail: NTIS HC A02/MF A01 CSCL 07C

Thermal and thermal oxidative stability studies were performed on linear perfluoro alkyl ether fluids. The effect on degradation by metal catalysts and degradation inhibitors are reported. The linear perfluoro alkylethers are inherently unstable at 316 C in an oxidizing atmosphere. The metal catalysts greatly increased the rate of degradation in oxidizing atmospheres. In the presence of these metals in an oxidizing atmosphere, the degradation inhibitors were highly effective in arresting degradation at 288 C. However, the inhibitors had only limited effectiveness at 316 C. The metals promote degradation by chain scission. Based on elemental analysis and oxygen consumption data, the linear perfluoro alkylether fluids have a structural arrangement based on difluoroformyl and tetrafluoroethylene oxide units, with the former predominating. S.L.

N82-28440* National Aeronautics and Space Administration, Lewis Research Center, Cleveland, Ohio.

TEXTURING POLYMER SURFACES BY TRANSFER CASTING Patent

Bruce A. Banks, Albert J. Weigand, and James S. Sovey, inventors (to NASA) Issued 11 May 1982 4 p Filed 19 Dec. 1980 Supersedes N81-16327 (19 - 07, p 899)
(NASA-Case-LEW-13120-1; US-Patent-4,329,385; US-Patent-AppI-SN-218587; US-Patent-Class-428-141; US-Patent-Class-204-192E; US-Patent-Class-204-192EC; US-Patent-Class-264-22; US-Patent-Class-264-220) Avail: US Patent and Trademark Office CSCL 11G

A technique for fabricating textured surfaces on polymers without altering their surface chemistries is described. A surface of a fluorocarbon polymer is exposed to a beam of ions to texture it. The polymer which is to be surface-roughened is then cast over the textured surface of the fluorocarbon polymer. After curing, the cast polymer is peeled off the textured fluorocarbon polymer, and the peeled off surface has negative replica of the textured surface. The microscopic surface texture provides large surface areas for adhesive bonding. In cardiovascular prosthesis applications the surfaces are relied on for the development of a thin adherent well nourished thrombus.

Official Gazette of the U.S. Patent and Trademark Office

N82-28441* National Aeronautics and Space Administration, Lewis Research Center, Cleveland, Ohio.

METHOD OF PROTECTING A SURFACE WITH A SILICON-SLURRY/ALUMINIDE COATING Patent

Daniel L. Deadmore and Stanley G. Young, inventors (to NASA) Issued 12 Jan. 1982 6 p Filed 20 Jun. 1980 Supersedes N80-26389 (18 - 17, p 2237)
(NASA-Case-LEW-13343-1; US-Patent-4,310,574; US-Patent-AppI-SN-161254; US-Patent-Class-427-405; US-Patent-Class-427-205; US-Patent-Class-427-253;

US-Patent-Class-428-938; US-Patent-Class-428-941) Avail: US Patent and Trademark Office CSCL 11G

A low cost coating for protecting metallic base system substrates from high temperatures, high gas velocity oxidation, thermal fatigue and hot corrosion is described. The coating is particularly useful for protecting vanes and blades in aircraft and land based gas turbine engines. A lacquer slurry comprising cellulose nitrate containing high purity silicon powder is sprayed onto the superalloy substrates. The silicon layer is then aluminized to complete the coating. The Si-Al coating is less costly to produce than advanced aluminides and protects the substrate from oxidation and thermal fatigue for a much longer period of time than the conventional aluminide coatings. While more expensive Pt-Al coatings and physical vapor deposited MCrAlY coatings may last longer and provide equal protection on certain substrates, the Si-Al coating exceeded the performance of both types of coatings on certain superalloys in high gas velocity oxidation and thermal fatigue. Also, the Si-Al coating increased the resistance of certain superalloys to hot corrosion.

Official Gazette of the U.S. Patent and Trademark Office

N82-28445* National Aeronautics and Space Administration, Lewis Research Center, Cleveland, Ohio.

ION BEAM SPUTTER DEPOSITED DIAMOND LIKE FILMS
Bruce A. Banks and Sharon K. Rutledge 1982 18 p refs
Presented at Meeting of the Greater New York Chapter of the Am. Vacuum Soc., Yorktown Heights, N.Y., 2 Jun. 1982
(NASA-TM-82873; E-1249; NAS 1.15:82873) Avail: NTIS HC A02/MF A01 CSCL 11G

A single argon ion beam source was used to sputter deposit carbon films on fused silica, copper, and tantalum substrates under conditions of sputter deposition alone and sputter deposition combined with simultaneous argon ion bombardment. Simultaneously deposited and ion bombarded carbon films were prepared under conditions of carbon atom removal to arrival ratios of 0, 0.036, and 0.71. Deposition and etch rates were measured for films on fused silica substrates. Resulting characteristics of the deposited films are: electrical resistivity of densities of 2.1 gm/cu cm for sputter deposited films and 2.2 gm/cu cm for simultaneously sputter deposited and Ar ion bombarded films. For films approximately 1700 A thick deposited by either process and at 5550 A wavelength light the reflectance was 0.2, the absorbance was 0.7, the absorption coefficient was 67,000 cm to the -1 and the transmittance was 0.1. Author

N82-29453* National Aeronautics and Space Administration, Lewis Research Center, Cleveland, Ohio.

FULLY PLASMA-SPRAYED COMPLIANT BACKED CERAMIC TURBINE SEAL Patent
Robert C. Bill and Donald W. Wisander, inventors (to NASA) Issued 22 Jun. 1982 4 p Filed 30 Mar. 1980 Supersedes N80-24619 (18 - 15, p 1985)
(NASA-Case-LEW-13268-1; US-Patent-4,336,276;
US-Patent-Appl-SN-145209; US-Patent-Class-427-34;
US-Patent-Class-415-174; US-Patent-Class-427-423) Avail: US Patent and Trademark Office CSCL 11A

A seal having a high temperature abrasion resistant lining material encircling the tips of turbine blades in turbomachinery is discussed. The minimum operating clearances between the blade tips and the lining of a high pressure turbine are maintained. A low temperature easily decomposable material, such as a polymer, in powder form is blended with a high temperature oxidation resistant metal powder. The two materials are simultaneously deposited on a substrate formed by the turbine casing. Alternately, the polymer powder may be added to the metal powder during plasma spraying. A ceramic layer is then deposited directly onto the metal polymer composite. The polymer additive mixed with the metal is then completely volatilized to provide a porous layer between the ceramic layer and the substrate.

Official Gazette of the U.S. Patent and Trademark Office

N82-29458* National Aeronautics and Space Administration, Lewis Research Center, Cleveland, Ohio.

BOUNDARY LUBRICATION: REVISITED
William R. Jones, Jr. 1982 33 p refs Presented at Meeting of the Am. Soc. of Lubrication Engr., Independence, Ohio, 9 Mar. 1982
(NASA-TM-82858; E-1181; NAS 1.15:82858) Avail: NTIS HC A03/MF A01 CSCL 11G

A review of the various lubrication regimes, with particular emphasis on boundary lubrication, is presented. The types of wear debris and extent of surface damage is illustrated for each regime. The role of boundary surface films along with their modes of formation and important physical properties are discussed. In addition, the effects of various operating parameters on friction and wear in the boundary lubrication regime are considered.

Author

N82-29459* National Aeronautics and Space Administration, Lewis Research Center, Cleveland, Ohio.

TRIBOLOGICAL EVALUATION OF COMPOSITE MATERIALS MADE FROM A PARTIALLY FLUORINATED POLYIMIDE
Robert L. Fusaro Apr. 1982 40 p refs
(NASA-TM-82832; E-1199; NAS 1.15:82832) Avail: NTIS HC A03/MF A01 CSCL 11G

Preliminary tribological studies on a new polyimide formulated from the diamine 2,2-bis [4-(4-aminophenoxy) phenyl] hexafluoropropane (4-BDAF) indicates polyimides made from this diamine have excellent potential for high temperature applications. Two different polyimides were formulated from the diamine, and five different composites were formulated using one of the polyimides. Composites were made using 10 weight percent (w/o) graphite fluoride powder, 20 w/o PTFE powder, 30 w/o silver powder, or 50 w/o carbon fibers, both graphitic and nongraphitic types. The powder additions did not improve the tribological properties as much as the carbon fibers, and the graphitic fibers produced better results than did the nongraphitic fibers. Results also indicated that improved high temperature stability and tribological properties may be obtained with a polyimide made from the dianhydride pyromellitic acid (PMDA) rather than the dianhydride benzophenonetetracarboxylic acid (BTDA). Author

N82-30401* National Aeronautics and Space Administration, Lewis Research Center, Cleveland, Ohio.

DEPOSITION OF REACTIVELY ION BEAM SPUTTERED SILICON NITRIDE COATINGS
A. Grill (Ben Gurion Univ. of the Negev) Aug. 1982 11 p refs
(NASA-TM-82942; E-1310; NAS 1.15:82942) Avail: NTIS HC A02/MF A01 CSCL 11D

An ion beam source was used to deposit silicon nitride films by reactively sputtering a silicon target with beams of Ar + N₂ mixtures. The nitrogen fraction in the sputtering gas was 0.05 to 0.80 at a total pressure of 6 to 2 millionth torr. The ion beam current was 50 mA at 500 V. The composition of the deposited films was investigated by auger electron spectroscopy and the rate of deposition was determined by interferometry. A relatively low rate of deposition of about 2 nm, one-tenth min. was found. AES spectra of films obtained with nitrogen fractions higher than 0.50 were consistent with a silicon to nitrogen ratio corresponding to Si₃N₄. However the AES spectra also indicated that the sputtered silicon nitride films were contaminated with oxygen and carbon and contained significant amounts of iron, nickel, and chromium, most probably sputtered from the holder of the substrate and target. S.L.

N82-32491* National Aeronautics and Space Administration, Lewis Research Center, Cleveland, Ohio.

OCCURRENCE OF SPHERICAL CERAMIC DEBRIS IN INDENTATION AND SLIDING CONTACT
Kazuhisa Miyoshi and Donald H. Buckley Aug. 1982 21 p refs
(NASA-TP-2048; E-1072; NAS 1.60:2048) Avail: NTIS HC A02/MF A01 CSCL 11G

Indenting experiments were conducted with the silicon carbide (0001) surface in contact with a spherical diamond indenter in air. Sliding friction experiments were also conducted with silicon carbide in contact with iron and iron-based binary alloys at room temperature and 800 C. Fracture pits with a spherical particle and spherical wear debris were observed as a result of indenting and sliding. Spherical debris may be produced by a mechanism that involves a spherical-shaped fracture along the circular or spherical stress trajectories under the inelastic deformation zone. Author

ORIGINAL PAGE IS
OF POOR QUALITY

N82-33521* National Aeronautics and Space Administration. Lewis Research Center, Cleveland, Ohio.

SURFACE TEXTURING OF FLUOROPOLYMERS Patent
Bruce A. Banks, Michael J. Mirtich, and James S. Sovey, inventors (to NASA) Issued 17 Aug. 1982 5 p Filed 19 Dec. 1980 (NASA-Case-LEW-13028-1; US-Patent-4,344,996; US-Patent-Appl-SN-218588; US-Patent-Class-428-141; US-Patent-Class-204-38B; US-Patent-Class-204-192E; US-Patent-Class-204-192EC) Avail: US Patent and Trademark Office CSCL 11G

A method is disclosed for improving surface texture for adhesive bonding, metal bonding, substrate plating, decal substrate preparation, and biomedical implant applications. The surface to be bonded is dusted in a controlled fashion to produce a disbursed layer of fine mesh particles which serve as masks. The surface texture is produced by impinging gas ions on the masked surface. The textured surface takes the form of pillars or cones. The bonding material, such as a liquid epoxy, flows between the pillars which results in a bond having increased strength. For bonding metals a thin film of metal is vapor or sputter deposited onto the textured surface. Electroplating or electroless plating is then used to increase the metal thickness in the desired amount.

Official Gazette of the U.S. Patent and Trademark Office

N82-33522*# National Aeronautics and Space Administration. Lewis Research Center, Cleveland, Ohio.

OVERLAY METALLIC-CERMET ALLOY COATING SYSTEMS Patent Application

Michael A. Gedwill, Stanley R. Levine, and Thomas K. Glasgow, inventors (to NASA) Filed 30 Jul. 1982 11 p (NASA-Case-LEW-13639-1; US-Patent-Appl-SN-403378) Avail: NTIS HC A02/MF A01 CSCL 11G

A substrate, such as a turbine blade, vane, or the like, which is subjected to high temperature use is coated with a base coating of an oxide dispersed, metallic alloy (cermet). A top coating of an oxidation, hot corrosion, erosion resistant alloy of nickel, cobalt, or iron is then deposited on the base coating. A heat treatment is used to improve the bonding. The base coating serves as an inhibitor to interdiffusion between the protective top coating and the substrate. Otherwise, the protective top coating would rapidly interact detrimentally with the substrate and degrade by spalling of the protective oxides formed on the outer surface at elevated temperatures. NASA

A82-21699* The effect of oxygen concentration on the boundary-lubricating characteristics of a C ether and a polyphenyl ether to 300 C. W. R. Jones, Jr. (NASA, Lewis Research Center, Cleveland, OH). *Wear*, vol. 73, Nov. 16, 1981, p. 123-136. 26 refs.

Ball-on-disk sliding friction experiments were carried out at 17 m/min (100 rev/min) to investigate the effect of oxygen concentration varying from 20% (air) to 0.001% (nitrogen) on the boundary-lubricating characteristics of an unformulated C ether in the temperature range 20-300 C. Results were then compared with those obtained for a five-ring polyphenylether in air and in nitrogen. The C ether yielded lower wear and lower friction coefficients than a five-ring polyphenylether in both air and nitrogen over most of the temperature range. Friction polymer was observed around the wear scars of most test specimens, with much greater quantities of friction polymer produced in a low-oxygen environment. Thus, with respect to friction polymer production, the C ether behaved very much like the polyphenylether. V.L.

A82-30021* Dynamics of solid dispersions in oil during the lubrication of point contacts. II - Molybdenum disulfide. C. Cusano (Illinois, University, Urbana, IL) and H. E. Sloney (NASA, Lewis Research Center, Cleveland, OH). (*American Society of Lubrication Engineers, Annual Meeting, 36th, Pittsburgh, PA, May 11-14, 1981.*) *ASLE Transactions*, vol. 25, Apr. 1982, p. 190-197. 18 refs. (Previously announced in STAR as N81-20275)

A82-41552* Phase stability in plasma-sprayed, partially stabilized zirconia-yttria. R. A. Miller, J. L. Smialek, and R. G. Garlick (NASA, Lewis Research Center, Cleveland, OH). In: Science and technology of zirconia. Columbus, OH, American Ceramic Society, Inc., (Advances in Ceramics, Volume 3) 1981, p. 241-253. 13 refs.

A82-42366* Effects of heating rate on density, microstructure, and strength of Si3N4-6 wt.% Y2O3 and a beta-prime sialon. S. S. Campbell and S. Dutta (NASA, Lewis Research Center, Materials Div., Cleveland, OH). (*American Ceramic Society, Annual Meeting, 83rd, Washington, DC, May 3, 1981, Paper 42-B-81.*) *American Ceramic Society Bulletin*, vol. 61, Aug. 1982, p. 854-856. 7 refs.

The effects of the heating rate during sintering/firing on the final density, microstructure, and strength of Si3N4-6 wt.% Y2O3 and beta-prime sialon, sintered for four hours at 1750 C, are examined. In Si3N4-6 wt.% Y2O3 increasing the heating rate from 7 C/min to 25 C/min to 90 C/min results in a corresponding decrease in the final density from 3.01 g/cu cm to 2.92 g/cu cm to 2.76 g/cu cm. In the beta-prime sialon composition all three heating rates produce an equivalent final density of 3.13 g/cu cm. All heating rates in both compositions produce nonhomogeneous microstructures. The room-temperature strength of Si3N4-6 wt.% Y2O3 increases from 372 to 510 MPa with increased density, while the corresponding strengths for the beta-prime sialon at equivalent densities are 345 to 445 MPa. N.B.

A82-42924* The combined effects of Fe and H2 on the nitridation of silicon. N. J. Shaw (NASA, Lewis Research Center, Cleveland, OH). *Journal of Materials Science Letters*, vol. 1, Aug. 1982, p. 337-340. 13 refs.

In view of the support offered by previous work for the suggestion that Fe may affect alpha-Si3N4 formation and microstructural development, a two-part study was conducted to differentiate the effects of H2 and Fe in, first, the nitridation of pure and of Fe-containing powder in N2 and N2-4% H2, and then the nitridation of (1 1 1) Si single crystal wafers with and without Fe powder on the surface. The degree of nitridation is most strongly affected by H2 at 1200 C, but by Fe at 1375 C, where Fe-containing samples in either atmosphere were almost completely nitrided. While neither H2 nor Fe alone changed the ratio of alpha-Si3N4 to beta-Si3N4, the combination of H2 and Fe increased it at both temperatures. O.C.

N82-17367*# TRW Defense and Space Systems Group, Redondo Beach, Calif.

IMPROVED TACK PMR

R. A. Buyny Oct. 1981 108 p refs (Contract NAS3-22026)

(NASA-CR-165432; TRW-36805-6016-UT-00) Avail: NTIS HC A06/MF A01 CSCL 07C

One reactive diluent and several high boiling solvents were investigated for providing long shelf life tack and drape to PMR polyimide prepreg materials. The most promising approach was to introduce dimethoxy ethyl ether (diglyme) to the normal methanol solvent. Compression and autoclave molding cycles were developed for the improved tack prepreg which provided up to 15% higher thermomechanical properties than conventional PMR-15 composites. Near the conclusion of this investigation, it was discovered that diglyme constituted a potential hazard because its auto ignition temperature is 464 K. Consequently, it was recommended that diglyme should not be used as a tackifier for PMR prepreps. Author

A82-18432*# Some observations in high pressure rheology of lubricants. S. Bair and W. O. Winer (Georgia Institute of Technology, Atlanta, GA). *American Society of Mechanical Engineers and American Society of Lubrication Engineers, Joint Lubrication Conference, New Orleans, LA, Oct. 5-7, 1981, ASME Paper 81-Lub-17*. 8 p. 15 refs. Members, \$2.00; nonmembers, \$4.00. Grant No. NSG-3106.

Experimental data are presented on viscosity, elastic shear modulus, and limiting shear stress of 12 liquid lubricants. It is shown that transition histories do affect the limiting shear stress of the materials in the form of isothermal compression resulting in a lower density and lower limiting stress than isobaric cooling. The measured limiting shear stress agrees with EHD traction data at slide-to-roll ratios of 0.1 or more. In pressure viscosity measurements of the polymer solutions, it is found that for some temperatures, the pressure viscosity coefficient of the blend is slightly less than that of the base, which results in the crossing of the viscosity-pressure isotherms at high pressures. D.L.G.

A82-20143 * # Strength distributions of SiC ceramics after oxidation and oxidation under load. T. E. Easler, R. C. Bradt, and R. E. Tressler (Pennsylvania State University, University Park, PA). (*American Ceramic Society, Annual Conference, 4th, Cocoa Beach, FL, Jan. 20, 1980, Paper 9-C-80C.*) *American Ceramic Society, Journal*, vol. 64, Dec. 1981, p. 731-734. 22 refs. Army-supported research; Grant No. NSG-3016.

The room-temperature strength distributions of a sintered and a hot-pressed SiC were examined as-machined, after oxidation at 1370 C, and after oxidation under load at 1370 C. The strengths were observed to be dependent on both the duration of oxidation and the magnitude of the applied load. Processes resulting in both strengthening and weakening behavior were observed to occur, at times simultaneously within the same strength distribution. This dynamic situation indicates that the strength-controlling flaw populations are highly transient in nature. (Author)

A82-20741 * # Analytical and experimental evaluation of biaxial contact stress. D. W. Richerson, D. G. Finger, and J. M. Wimmer (Garrett Turbine Engine Co., Phoenix, AZ). *International Symposium on Fracture Mechanics of Ceramics, Pennsylvania State University, University Park, PA, July 15-17, 1981, Paper 22* p. 25 refs. Research supported by the U.S. Department of Energy; Contracts No. N00014-78-C-0547; No. DEN3-167.

Contact stress analysis was conducted for ceramic-metal and ceramic-ceramic interfaces using a finite element model. Ceramics investigated included NC-132 hot-pressed silicon nitride, NC-350 reaction-bonded silicon nitride, Hexaloy SA SiC, and RBN104 reaction-bonded silicon nitride. The results are shown to be well correlated with closed-form solution both for normal and normal-tangential loading. The latter load condition is found to be especially critical for ceramic materials due to the presence of a high tensile stress at the trailing edge of the ceramic surface contact zone. It is shown that during sliding contact or biaxial loading, the magnitude of this tensile stress increases with the coefficient of friction. V.L.

A82-35064 * # Progress in ceramic component fabrication technology. R. S. Storm and R. W. Lashway (Carborundum Resistant Materials Co., Niagara Falls, NY). *AIAA, SAE, and ASME, Joint Propulsion Conference, 18th, Cleveland, OH, June 21-23, 1982, AIAA Paper 82-1211*. 6 p. Contracts No. DEN3-17; No. DEN3-168; No. DEN3-167.

Net shape techniques have been used in the production of rotating and static vehicular engine high-temperature components composed of sintered Alpha-SiC (SASC). Injection-molded rotors have been cold spin tested, as well as a slip-cast combustor assembly hot rig. SASC pistons and cylinder liners have also been constructed for an opposed piston, two-cycle diesel test rig while test results are presented. An uncooled, minimum-friction internal combustion engine with multi-fuel capability due to its elevated combustion temperatures appears to be achievable in the near term by means of SASC techniques. The flexural strength of SASC at 1500 C is 446 MPa, identical to that at room temperature, and excellent strength retention has been demonstrated after 3500 hours of cyclic exposure. O.C.

A82-35083 * # Characterization of advanced electric propulsion systems. P. K. Ray (Tuskegee Institute, Tuskegee, AL). *AIAA, SAE, and ASME, Joint Propulsion Conference, 18th, Cleveland, OH, June 21-23, 1982, AIAA Paper 82-1246*. 11 p. 7 refs. Grant No. NAG3-76.

Characteristic parameters of several advanced electric propulsion systems are evaluated and compared. The propulsion systems studied are mass driver, rail gun, argon MPD thruster, hydrogen free radical thruster and mercury electron bombardment ion engine. Overall, ion engines have somewhat better characteristics as compared to the other electric propulsion systems. (Author)

A82-35403 * # Net shape fabrication of Alpha Silicon Carbide turbine components. R. S. Storm (Carborundum Co., Niagara Falls, NY). *American Society of Mechanical Engineers, International Gas Turbine Conference and Exhibit, 27th, London, England, Apr. 18-22, 1982, Paper 82-GT-216*. 16 p. 5 refs. Members, \$2.00; nonmembers, \$4.00. Research supported by the U.S. Department of Energy; Contracts No. DEN3-17; No. DEN3-167; No. DEN3-168.

Development of Alpha Silicon Carbide components by net shape fabrication techniques has continued in conjunction with several turbine engine programs. Progress in injection molding of simple parts has been extended to much larger components. Turbine rotors fabricated by a one piece molding have been successfully spin tested above design speeds. Static components weighing up to 4.5

kg and 33 cc in diameter have also been produced using this technique. Use of sintering fixtures significantly improves dimensional control. A new Si-SiC composite material has also been developed with average strengths up to 1000 MPa (150 ksi) at 1200 C. (Author)

A82-35431 * # Fabrication of turbine components and properties of sintered silicon nitride. J. T. Neil, K. W. French, C. L. Quackenbush, and J. T. Smith (GTE Laboratories, Waltham, MA). *American Society of Mechanical Engineers, International Gas Turbine Conference and Exhibit, 27th, London, England, Apr. 18-22, 1982, Paper 82-GT-252*. 6 p. Members, \$2.00; nonmembers, \$4.00. Research supported by the U.S. Department of Energy and General Motors Corp.; Contract No. DEN3-17.

This paper presents a status report on the injection molding of sinterable silicon nitride at GTE Laboratories. The effort involves fabrication of single axial turbine blades and monolithic radial turbine rotors. The injection molding process is reviewed and the fabrication of the turbine components discussed. Oxidation resistance and strength results of current injection molded sintered silicon nitride as well as dimensional checks on sintered turbine blades demonstrate that this material is a viable candidate for high temperature structural applications. (Author)

A82-35441 * # Ceramic thermal barrier coatings for gas turbine engines. R. J. Bratton, S. K. Lau, C. A. Andersson, and S. Y. Lee (Westinghouse Research and Development Center, Pittsburgh, PA). *American Society of Mechanical Engineers, International Gas Turbine Conference and Exhibit, 27th, London, England, Apr. 18-22, 1982, Paper 82-GT-265*. 4 p. 15 refs. Members, \$2.00; nonmembers, \$4.00. Research supported by the Electric Power Research Institute and U.S. Department of Energy; Contracts No. NAS3-21377; No. DEN3-110.

The results of studies concerning the high temperature corrosion resistance of ZrO₂-Y₂O₃, ZrO₂-MgO, and Ca₂SiO₄ plasma-sprayed coatings, which may be used as gas turbine engine thermal barriers, are reported. The coatings were evaluated in atmospheric burner rig and pressurized passage tests, using GT No. 2 fuel in pure form and with sodium, sulfur and vanadium corrosive impurities doping. It is found that, while the coatings performed well in both pressurized passage and burner rig tests with pure fuel chemical reactions between the ceramic coatings and combustion gases/condensates resulted in coating degradation with impure fuels. Chemical reactions between the ceramic coatings and vanadium compounds played a critical role in coating degradation. O.C.

A82-35871 * # Effects of oxidation and oxidation under load on strength distributions of Si3N4. T. E. Easler, R. C. Bradt, and R. E. Tressler (Pennsylvania State University, University Park, PA). (*American Ceramic Society, Annual Meeting, 82nd, Chicago, IL, Apr. 29, 1980, Paper 69-B-80.*) *American Ceramic Society, Journal*, vol. 65, June 1982, p. 317-320. 18 refs. Army-supported research; Grant No. NSG-3016.

The room-temperature strength distributions of a sintered and a hot-pressed Si3N4 were examined in the as-machined condition, after oxidation at 1370 C and after oxidation under load at 1370 C. The strength-controlling flaw populations were highly transient in nature. Both the duration of oxidation and the magnitude of the applied load were observed to effect changes in strength. This dynamic situation is related to both strengthening and weakening processes, which at times may occur simultaneously in the same strength distribution. (Author)

A82-37015 * # Fabrication of sinterable silicon nitride by injection molding. C. L. Quackenbush, K. French, and J. T. Neil (GTE Laboratories, Inc., Waltham, MA). (*American Ceramic Society, Topical Meeting on Nonoxide Ceramics, Bass River, MA, Oct. 5, 6, 1981.*) *Ceramic Engineering and Science Proceedings*, vol. 3, Jan.-Feb. 1982, p. 20-34. 8 refs. Research supported by the U.S. Department of Energy; Contract No. DEN3-17.

Transformation of structural ceramics from the laboratory to production requires development of near net shape fabrication techniques which minimize finish grinding. One potential technique for producing large quantities of complex-shaped parts at a low cost, and microstructure of sintered silicon nitride fabricated by injection molding is discussed and compared to data generated from isostatically dry-pressed material. Binder selection methodology, compounding of ceramic and binder components, injection molding techniques, and problems in binder removal are discussed. Strength, oxidation resistance, and microstructure of sintered silicon nitride fabricated by injection molding is discussed and compared to data generated from isostatically dry-pressed material. (Author)

ORIGINAL PAGE IS
OF POOR QUALITY

28 PROPELLANTS AND FUELS

Includes rocket propellants, igniters, and oxidizers, storage and handling; and aircraft fuels.

For related information see also 07 *Aircraft Propulsion and Power*, 20 *Spacecraft Propulsion and Power*, and 44 *Energy Production and Conversion*.

N82-21415*# National Aeronautics and Space Administration, Lewis Research Center, Cleveland, Ohio.

RESONANCE TUBE HAZARDS IN OXYGEN SYSTEMS Ph.D. Thesis - Toledo Univ., 1975

Bert R. Phillips 1982 25 p refs Presented at Symp. on Flammability and Sensitivity of Mater. in Oxygen Enriched Atmosphere, Phoenix, Ariz., 31 Mar. - 1 Apr. 1982; sponsored by the Am. Soc. for Testing and Mater. (NASA-TM-82801; E-1140; NAS 1.15:82801) Avail: NTIS HC A02/MF A01 CSCL 21D

An experimental and analytical program was carried out to determine whether fluid dynamic oscillations could create a hazard in gaseous oxygen flow systems. The particular fluid dynamic oscillation studied was the resonance tube phenomena as it was excited in a tee-shaped configuration characteristic of configurations found in many industrial high pressure gas flow systems. The types of hazards that could be caused by the oscillations were direct heating and ignition of the piping system by the gas, the greatly augmented heating that could occur if inert contaminants were present, and the ignition of metallic contaminants. Asbestos was used as the inert contaminant; titanium, aluminum, magnesium and steel were chosen as ignitable metallic contaminants. The oscillations in the tee-shaped configuration were compared to oscillations driven by choked convergent nozzles and were found to differ markedly. Temperature generated at the end or base of the resonance tube exceeded 1089 K for both gaseous oxygen and nitrogen and reached 1645 K when asbestos was added. Aluminum in both powder and fiber form was readily ignited within the resonance tube when the supply pressures were less than 8270 kPa whereas at higher supply pressures the mixture exploded with enough violence to destroy the apparatus in less than 10 sec. In addition to aluminum, magnesium, and titanium, samples of 400 series stainless steels were also ignited within the resonance tube. The ignition occurred within a few seconds after the oxygen flow began. Author

N82-26483*# National Aeronautics and Space Administration, Lewis Research Center, Cleveland, Ohio.

EXPERIMENTS ON FUEL HEATING FOR COMMERCIAL AIRCRAFT

R. Friedman and F. J. Stockemer (Lockheed-California Co., Burbank, Calif.) 1982 15 p refs Presented at 18th Joint Propulsion Conf., Cleveland, 21-23 Jun. 1982; Sponsored by AIAA, SAE and ASME (NASA-TM-82878; E-1254; NAS 1.15:82878) Avail: NTIS HC A02/MF A01 CSCL 21D

An experimental jet fuel with a -3°C freezing point was chilled in a wing tank simulator with superimposed fuel heating to improve low temperature flowability. Heating consisted of circulating a portion of the fuel to an external heat exchanger and returning the heated fuel to the tank. Flowability was determined by the mass percent of unpumpable fuel (holdup) left in the simulator upon withdrawal of fuel at the conclusion of testing. The study demonstrated that fuel heating is feasible and improves flowability as compared to that of baseline, unheated tests. Delayed heating with initiation when the fuel reaches a prescribed low temperature limit, showed promise of being more efficient than continuous heating. Regardless of the mode or rate of heating, complete flowability (zero holdup) could not be restored by fuel heating. The severe, extreme-day environment imposed by the test caused a very small amount of subfreezing fuel to be retained near the tank surfaces even at high rates of heating. Correlations of flowability established for unheated fuel tests also could be applied to the heated test results if based on boundary-layer temperature or a solid index (subfreezing point) characteristic of the fuel. Author

N82-27519*# National Aeronautics and Space Administration, Lewis Research Center, Cleveland, Ohio.

EFFECT OF SOME NITROGEN COMPOUNDS THERMAL STABILITY OF JET A

Albert C. Antoluz Jun. 1982 20 p refs (NASA-TM-82908; NAS 1.15:82908) Avail: NTIS HC A02/MF A01 CSCL 21D

The effect of known concentrations of some nitrogen containing compounds on the thermal stability of a conventional fuel, namely, Jet A was investigated. The concentration range from 0.01 to 0.1 wt% nitrogen was examined. Solutions were made containing, individually, pyrrole, indole, quinoline, pyridine, and 4 ethylpyridine at 0.01, 0.03, 0.06, and 0.1 wt% nitrogen concentrations in Jet A. The measurements were all made by using a standard ASTM test for evaluating fuel thermal oxidation behavior, namely, ASTM D3241, 'thermal oxidation stability of turbine fuels (JFTOT procedure)'. Measurements were made at two temperature settings, and 'breakpoint temperatures' were determined. The results show that the pyrrole and indole solutions have breakpoint temperatures substantially lower than those of the Jet A used. S.L.

N82-28460*# National Aeronautics and Space Administration, Lewis Research Center, Cleveland, Ohio.

EFFECT OF HYDROCARBON FUEL TYPE ON FUEL

Edgar L. Wong and David A. Bittker Jun. 1982 13 p refs (NASA-TM-82916; E-1073; NAS 1.15:82916) Avail: NTIS HC A02/MF A01 CSCL 21D

A modified jet fuel thermal oxidation tester (JFTOT) procedure was used to evaluate deposit and sediment formation for four pure hydrocarbon fuels over the temperature range 150 to 450 C in 316-stainless-steel heater tubes. Fuel types were a normal alkane, an alkene, a naphthene, and an aromatic. Each fuel exhibited certain distinctive deposit and sediment formation characteristics. The effect of aluminum and 316-stainless-steel heater tube surfaces on deposit formation for the fuel n-decane over the same temperature range was investigated. Results showed that an aluminum surface had lower deposit formation rates at all temperatures investigated. By using a modified JFTOT procedure the thermal stability of four pure hydrocarbon fuels and two practical fuels (Jet A and home heating oil no. 2) was rated on the basis of their breakpoint temperatures. Results indicate that this method could be used to rate thermal stability for a series of fuels. Author

N82-32504*# National Aeronautics and Space Administration, Lewis Research Center, Cleveland, Ohio.

CHARACTERIZATION OF AN EXPERIMENTAL REFEREE BROADENED SPECIFICATION (ERBS) AVIATION TURBINE FUEL AND ERBS FUEL BLENDS

Gary T. Seng Aug. 1982 25 p refs (NASA-TM-82883; E-1260; NAS 1.15:82883) Avail: NTIS HC A02/MF A01 CSCL 21D

Characterization data and comparisons of these data are presented for three individual lots of a research test fuel designated as an Experimental Referee Broadened Specification (ERBS) aviation turbine fuel. This research fuel, which is a blend of kerosene and hydrotreated catalytic gas oil, is a representation of a kerojet fuel with broadened properties. To lower the hydrogen content of the ERBS fuel, a blending stock, composed of xylene bottoms and hydrotreated catalytic gas oil, was developed and employed to produce two different ERBS fuel blends. The ERBS fuel blends and the blending stock were also characterized and the results for the blends are compared to those of the original ERBS fuel. The characterization results indicate that with the exception of the freezing point for ERBS lot 2, which was slightly high, the three lots, produced over a 2 year period, met all general fuel requirements. However, although the properties of the fuels were found to be fairly consistent, there were differences in composition. Similarly, all major requirements for the ERBS fuel blends were met or closely approached, and the properties of the blended fuels were found to generally reflect those expected for the proportions of ERBS fuel and blending stock used in their production. Author

ORIGINAL PAGE IS
OF POOR QUALITY

N82-10245* Aerojet Liquid Rocket Co., Sacramento, Calif.
FUEL/OXIDIZER-RICH HIGH-PRESSURE PREBURNERS
Final Report
L. Schoenman Oct. 1981 254 p refs
(Contract NAS3-21753)
(NASA-CR-165404) Avail: NTIS HC A12/MF A01 CSCL 211

The analyses, designs, fabrication, and cold-flow acceptance testing of LOX/RP-1 preburner components required for a high-pressure staged-combustion rocket engine are discussed. Separate designs of injectors, combustion chambers, turbine simulators, and hot-gas mixing devices are provided for fuel-rich and oxidizer-rich operation. The fuel-rich design addresses the problem of non-equilibrium LOX/RP-1 combustion. The development and use of a pseudo-kinetic combustion model for predicting operating efficiency, physical properties of the combustion products, and the potential for generating solid carbon is presented. The oxygen-rich design addresses the design criteria for the prevention of metal ignition. This is accomplished by the selection of materials and the generation of well-mixed gases. The combining of unique propellant injector element designs with secondary mixing devices is predicted to be the best approach. M.G.

N82-11224* Lockheed-California Co., Burbank.
EXPERIMENTAL STUDY OF FUEL HEATING AT LOW TEMPERATURES IN A WING TANK MODEL, VOLUME 1
Final Report
Francis J. Stockemer Aug. 1981 75 p refs
(Contract NAS3-21977)
(NASA-CR-165397; LR-29935-Vol-1) Avail: NTIS HC A04/MF A01 CSCL 21D

Scale model fuel heating systems for use with aviation hydrocarbon fuel at low temperatures were investigated. The effectiveness of the heating systems in providing flowability and pumpability at extreme low temperature when some freezing of the fuel would otherwise occur is evaluated. The test tank simulated a section of an outer wing tank, and was chilled on the upper and lower surfaces. Turbine engine lubricating oil was heated, and recirculating fuel transferred the heat. Fuels included: a commercial Jet A; an intermediate freeze point distillate; a higher freeze point distillate blended according to Experimental Referee Broadened Specification guidelines; and a higher freeze point paraffinic distillate used in a preceding investigation. Each fuel was chilled to selected temperature to evaluate un-pumpable solid formation (holdup). Tests simulating extreme cold weather flight, without heating, provided baseline fuel holdup data. Heating and recirculating fuel increased bulk temperature significantly; it had a relatively small effect on temperature near the bottom of the tank. Methods which increased penetration of heated fuel into the lower boundary layer improved the capability for reducing holdup. S.L.

N82-11230* Pratt and Whitney Aircraft Group, East Hartford, Conn. Commercial Products Div.
AN ASSESSMENT OF THE USE OF ANTIMISTING FUEL IN TURBOFAN ENGINES Final Report, Sep. 1979 - Nov. 1980
A. Fiorentino, R. DeSaro, and T. Franz Jun. 1981 53 p refs
(Contract NAS3-22045)
(NASA-CR-165258; AD-A104673; PWA-5697-29; FAA-CT-81-58) Avail: NTIS HC A04/MF A01 CSCL 21/4

An evaluation was made on the effects of using antimisting kerosene (AMK) on the performance of the components from the fuel system and the combustor of a current in-service JT8D aircraft engine. The objectives were to identify problems associated with using antimisting kerosene and to determine the extent of shearing or degradation required to allow the engine components to achieve satisfactory operation. The program consisted of a literature survey and a test program which evaluated the antimisting kerosene fuel in laboratory and bench component testing, and assessed the performance of the combustor in a high pressure facility and in an altitude re-light/cold ignition facility. Performance of the fuel pump and control system was evaluated in an open loop simulation. Thus far, results of the program would not preclude the use of antimisting kerosene in a jet engine application. GRA

N82-13243* Engineering Societies Commission on Energy, Inc., Washington, D. C.
BARRIERS TO THE UTILIZATION OF SYNTHETIC FUELS FOR TRANSPORTATION Final Report
Harry W. Parker and Matthew J. Reilly Oct. 1981 25 p
(NASA Order C-57307-D; Contract DE-AI01-81CS-50006)
(NASA-CR-165517; DOE/NASA-7307/1) Avail: NTIS HC A02/MF A01 CSCL 21D

The principal types of engines for transportation uses are reviewed and the specifications for conventional fuels are compared with specifications for synthetic fuels. Synfuel processes nearing the commercialization phase are reviewed. The barriers to using synfuels can be classified into four groups: technical, such as the uncertainty that a new engine design can satisfy the desired performance criteria; environmental, such as the risk that the engine emissions cannot meet the applicable environmental standards; economic, including the cost of using a synfuel relative to conventional transportation fuels; and market, involving market penetration by offering new engines, establishing new distribution systems and/or changing user expectations. T.M.

N82-14371* United Technologies Research Center, East Hartford, Conn.
EXTERNAL FUEL VAPORIZATION STUDY Final Report
E. J. Szetela and J. A. TeVelde Nov. 1981 92 p refs
(NASA-CR-165513; UTRC-81-915326-15) HC A05/MF A01 CSCL 21D

The feasibility of external fuel vaporization in advanced aircraft gas turbine engines is addressed. Experiments were run to determine key fuel properties including boiling points, dew points, critical temperature, critical pressure, heat transfer coefficients, deposit formation rates, and deposit removal in a flowing system. Of particular concern were the heat transfer rate in the heat exchanger and the performance of the orifice used in the throttling process. Three fuels were utilized in the experiments including Jet-A. Experimental referee broad specification fuel, and a premium No. 2 diesel fuel. Engine conditions representing the NASA Energy Efficient Engine at sea level takeoff, cruise, and idle were simulated in the vaporization system and it was found that single phase flow was maintained in the heat exchanger and downstream of the throttle. Deposits encountered in the heat exchanger represented a thermal resistance as high as .0013 sq M K/watt and a deposit formation rate as high as 800 micro-gC/sq cm hr. These values are equivalent to a buildup of 0.055 cm of thickness in 36 hours resulting in a more severe fouling condition than originally anticipated. It was found that the deposit can be removed by cleaning with air at a temperature of 720 K for 10 minutes. R.J.F.

N82-16402* SRI International Corp., Menlo Park, Calif.
OXIDATION AND FORMATION OF DEPOSIT PRECURSORS IN HYDROCARBON FUELS Final Report
S. E. Buttrill, Jr., Frank R. Mayo, Bosco Lan, G. A. St. John, and David Dulin Jan. 1982 26 p refs
(Contract NAS3-22510)
(NASA-CR-165534; PYU-2115) Avail: NTIS HC A03/MF A01 CSCL 21D

A practical fuel, home heating oil no. 2 (Fuel C), and the pure hydrocarbon, n-dodecane, were subjected to mild oxidation at 130 C and the resulting oxygenated reaction products, deposit precursors, were analyzed using field ionization mass spectrometry. Results for fuel C indicated that, as oxidation was initially extended, certain oxygenated reaction products of increasing molecular weights in the form of monomers, dimers and some trimers were produced. Further oxidation time increase resulted in further increase in monomers but a marked decrease in dimers and trimers. This suggests that these larger molecular weight products have proceeded to form deposit and separated from the fuel mixture. Results for a dodecane indicated that yields for dimers and trimers were very low. Dimers were produced as a result of interaction between oxygenated products with each other rather than with another fuel molecule. This occurred even though fuel molecule concentration was 50 times, or more greater than that for these oxygenated reaction products. Author

ORIGINAL PAGE IS
OF POOR QUALITY

N82-24353*# Aerojet Liquid Rocket Co., Sacramento, Calif.
**TESTING OF FUEL/OXIDIZER-RICH, HIGH-PRESSURE
PREBURNERS** Final Report

B. R. Lawver May 1982 253 p refs

(Contract NAS3-22647)

(NASA-CR-165609; NAS 1.26:165609) Avail: NTIS
HC A12/MF A01 CSCL 211

Results of an evaluation of high pressure combustion of fuel rich and oxidizer rich LOX/RP-1 propellants using 4.0 inch diameter prototype preburner injectors and chambers are presented. Testing covered a pressure range from 8.9 to 17.5 MN/square meters (1292 to 2540 psia). Fuel rich mixture ratios ranged from 0.238 to 0.367; oxidizer rich mixture ratios ranged from 27.2 to 47.5. Performance, gas temperature uniformity, and stability data for two fuel rich and two oxidizer rich preburner injectors are presented for a conventional like-on-like (LOL) design and a platelet design injector. Kinetically limited combustion is shown by the excellent agreement of measured fuel rich gas composition and C performance data with kinetic model predictions. The oxidizer rich test results support previous equilibrium combustion predictions. Author

N82-26482*# Solar Turbines International, San Diego, Calif.
**LOW NOX HEAVY FUEL COMBUSTOR CONCEPT PRO-
GRAM**

D. J. White and Alan J. Kubasco May 1982 50 p refs

(Contract DEN3-145)

(NASA-CR-167876; NAS 1.26:167876; DOE/NASA/O145-2;
SR82-R-4994-08) Avail: NTIS HC A03/MF A01 CSCL 21D

Three simulated coal gas fuels based on hydrogen and carbon monoxide were tested during an experimental evaluation with a rich lean can combustor: these were a simulated Winkler gas, Lurgi gas and Blue Water gas. All three were simulated by mixing together the necessary pure component species, to levels typical of fuel gases produced from coal. The Lurgi gas was also evaluated with ammonia addition. Fuel burning in a rich lean mode was emphasized. Only the Blue Water gas, however, could be operated in such fashion. This showed that the expected NOx signature form could be obtained, although the absolute values of NOx were above the 75 ppm goals for most operating conditions. Lean combustion produced very low NOx well below 75 ppm with the Winkler and Lurgi gases. In addition, these low levels were not significantly impacted by changes in operating conditions. S.L.

N82-31546*# Lockheed-California Co., Burbank.
**ADDITIONAL EXPERIMENTS ON FLOWABILITY IMPROVE-
MENTS OF AVIATION FUELS AT LOW TEMPERATURES,
VOLUME 2** Final Report

Francis J. Stockemer and Ronald L. Deane Aug. 1982 56 p refs

(Contract NAS3-21977)

(NASA-CR-167912; NAS 1.26:167912) Avail: NTIS
HC A04/MF A01 CSCL 21D

An investigation was performed to study flow improver additives and scale-model fuel heating systems for use with aviation hydrocarbon fuel at low temperatures. Test were performed in a facility that simulated the heat transfer and temperature profiles anticipated in wing fuel tanks during flight of long-range commercial aircraft. The results are presented of experiments conducted in a test tank simulating a section of an outer wing integral fuel tank approximately full-scale in height, chilled through heat exchange panels bonded to the upper and lower horizontal surfaces. A separate system heated lubricating oil externally by a controllable electric heater, to transfer heat to fuel pumped from the test tank through an oil-to-fuel heat exchanger, and to recirculate the heated fuel back to the test tank. B.W.

A82-20748 * # An experiment to evaluate liquid hydrogen storage in space. R. N. Eberhardt, D. A. Fester, W. A. Johns, and J. S. Marino (Martin Marietta Aerospace, Denver, CO). *National Bureau of Standards, Cryogenic Engineering Conference, San Diego, CA, Aug. 10-14, 1981, Paper*. 9 p. Contract No. NAS3-21591.

The design and verification of a Cryogenic Fluid Management Experiment for orbital operation on the Shuttle is described. The experiment will furnish engineering data to establish design criteria

for storage and supply of cryogenic fluids, mainly hydrogen, for use in low gravity environments. The apparatus comprises an LAD (liquid acquisition device) and a TVS (thermodynamic vent system). The hydrogen will be either vented or forced out by injected helium and the flow rates will be monitored. The data will be compared with ground-based simulations to determine optimal flow rates for the pressurizing gas and the release of the cryogenic fluid. It is noted that tests on a one-g, one-third size LAD system are under way. M.S.K.

A82-22240 * Deposit formation in liquid fuels. II - The effect of selected compounds on the storage stability of Jet A turbine fuel. J. H. Worstell and S. R. Daniel (Colorado School of Mines, Golden, CO). *Fuel*, vol. 60, June 1981, p. 481-484. 30 refs. Grant No. N5G-3122.

The influence of substituted pyridines, pyrroles, indoles, and quinolines on the storage stability of conventional Jet A turbine fuel is evaluated. Significant increases in the amount of deposit formed in accelerated storage tests are found upon addition of these compounds at levels as low as one ppm nitrogen. While the effect is correlated with basicity of the nitrogen compound within a given compound class, the correlation does not hold between classes (pyridines, quinolines, etc.). Steric hindrance at the nitrogen atom greatly inhibits deposit promotion. The characteristics, but not the elemental composition, of deposits vary with the identity of the added nitrogen compound and with deposition temperature. (Author)

A82-22241 * Deposit formation in liquid fuels. I - Effect of coal-derived Lewis bases on storage stability of Jet A turbine fuel. K. E. Dahlin, S. R. Daniel, and J. H. Worstell (Colorado School of Mines, Golden, CO). *Fuel*, vol. 60, June 1981, p. 477-480. 24 refs. Grant No. N5G-3122.

The development of reasonably precise techniques for the measurement of storage stability of jet aviation fuel is described. Lewis bases, extracted by ligand-exchange from a coal-derived liquid, are shown to adversely affect storage stability (as determined by an accelerated storage test) when added to Jet A turbine fuel. JFTOT results suggesting slight decreases in thermal stability of fuel 'spiked' (i.e., contaminated with a measured quantity of reagent) with extract are reported. Addition to Jet A turbine fuel of individual heterocyclic nitrogen compounds is shown to produce comparable decreases in storage stability. (Author)

A82-23238 * Deposit formation in liquid fuels. III - The effect of selected nitrogen compounds on diesel fuel. J. H. Worstell, S. R. Daniel, and G. Frauenhoff (Colorado School of Mines, Golden, CO). *Fuel*, vol. 60, June 1981, p. 485-487. 11 refs. Grant No. N5G-3122.

The influence of substituted quinolines, pyrroles, indoles, and pyridines on deposit formation in a diesel fuel is evaluated. Significant increases in deposition rate are found which are dependent upon the basicity of the nitrogen compound within a given compound class. These effects correspond closely with those produced in a Jet A fuel. Removal of highly polar fuel components renders the nitrogen compound influence inoperative. These components are therefore participants in deposit-forming reactions. (Author)

A82-33030 * Oxidation stability of advanced reaction-bonded Si3N4 materials. L. J. Lindberg, D. W. Richerson, W. D. Carruthers (Garrett Turbine Engine Co., Phoenix, AZ), and H. M. Gersch (AIResearch Casting Co., Torrance, CA). (*American Ceramic Society, Fall Meeting, San Francisco, CA, Oct. 28, 1980, Paper 52-B-80P.*) *American Ceramic Society Bulletin*, vol. 61, May 1982, p. 574-578. 11 refs. Contracts No. N00024-76-C-5352; No. F33615-77-C-5171; No. DEN3-167.

Four slip-cast, injection-molded and isostatically-pressed specimens of reaction-bonded silicon nitride (RBSN) were subjected to static oxidation tests at 900 C for 10 hours. Specimens containing 8-10% interconnected open porosity of size greater than one micron exhibited a 20-30% decrease in average room temperature four-point

flexure strength, while those with 10% open porosity of magnitudes much smaller than one micron as well as those with 2-4% interconnected open porosity of about one micron did not decrease in strength after 900 C exposure. It was determined that preoxidation treatment at 1350 C prevents the 20-30% strength degradation due to internal oxidation, and evidence is presented which suggests that surface pit formation in some RBSN may result from cocontamination by the furnace environment rather than any intrinsic material properties. O.C.

A82-33031 * **Acoustic microscopy of silicon carbide materials.** P. K. Khandelwal, P. W. Heitman (General Motors Corp., Detroit Diesel Allison Div., Indianapolis, IN), D. Yuhas, and C. L. Vorres (Sonoscan, Inc., Bensenville, IL). *American Ceramic Society Bulletin*, vol. 61, May 1982, p. 586, 587. Research supported by the U.S. Department of Energy; Contract No. DEN3-17.

It is shown that scanning laser acoustic microscopy (SLAM) is able to detect such fracture-controlling flaws in dense silicon carbide materials as surface voids, whose diameter-by-depth size is a minimum of 75 by 17 microns in reaction-bonded SiC and 68 by 25 microns in alpha-SiC. Surface conditions such as pitting, which have been found to limit the discernibility of drilled holes, become important when pit and drilled hole sizes become comparable. O.C.

A82-35307 * # **Deposit formation in hydrocarbon fuels.** R. Roback, E. J. Szetela, and L. J. Spadaccini (United Technologies Research Center, East Hartford, CT). *American Society of Mechanical Engineers, International Gas Turbine Conference and Exhibit, 27th, London, England, Apr. 18-22, 1982, Paper 82-GT-49*, 9 p. 9 refs. Members, \$2.00; nonmembers, \$4.00. Contract No. NAS3-22277.

The hydrocarbon fuels RP-1, commercial-grade propane, JP-7 and chemically pure propane were subjected to tests in a high pressure fuel coking apparatus in order to evaluate their thermal decomposition limits and carbon deposition rates in heated copper tubes. A fuel thermal stability parametric evaluation was conducted at 136-340 atmospheres, bulk fuel velocities of 6-30 m/sec, and tube wall temperatures of 422-811 K, and the effect of inside wall material on deposit formation was evaluated in tests using nickel-plated tubes. Results show RP-1 deposit formation at wall temperatures between 600 and 800 K, with peak deposit formation near 700 K. Substitution of deoxygenated JP-7 for RP-1 showed no improvement, and the carbon deposition rates for propane fuels were found to be higher than those of either of the kerosene fuels. Nickel plating of the tube walls significantly reduced RP-1 carbon deposition rates. O.C.

A82-35312 * # **Experimental study of external fuel vaporization.** E. J. Szetela and J. A. TeVelde (United Technologies Research Center, East Hartford, CT). *American Society of Mechanical Engineers, International Gas Turbine Conference and Exhibit, 27th, London, England, Apr. 18-22, 1982, Paper 82-GT-59* 8 p. 9 refs. Members, \$2.00; nonmembers, \$4.00. Contract No. NAS3-21971.

The fuel properties used in the design of a flash vaporization system for aircraft gas turbine engines were evaluated in experiments using a flowing system to determine critical temperature and pressure, boiling points, dew points, heat transfer coefficients, deposit formation rates, and deposit removal. Three fuels were included in the experiments: Jet-A, an experimental reference broad specification fuel, and a premium No. 2 diesel fuel. Engine conditions representing a NASA Energy Efficient Engine at sea-level take-off, cruise, and idle were simulated in the vaporization system and it was found that single phase flow was maintained in the heat exchanger and downstream of the throttle. Deposits encountered in the heat exchanger represented a thermal resistance as high as 1300 sq M K/watt and a deposit formation rate over 1000 gC/sq cm hr. C.D.

31 ENGINEERING (GENERAL)

Includes vacuum technology; control engineering; display engineering; and cryogenics.

N82-13281*# National Aeronautics and Space Administration, Lewis Research Center, Cleveland, Ohio.

ELEVATED TEMPERATURE FATIGUE TESTING OF METALS

Marvin H. Hirschberg *In* AGARD Fatigue Test Methodology Oct. 1981 18 p refs (For primary document see N82-13274 04-31)

Avail: NTIS HC A12/MF A01

Material characterization and evaluation conducted for the purpose of calculating fatigue crack initiation lives of components operating at elevated temperatures are discussed. The major technology areas needed to perform a life prediction of an aircraft turbine engine hot section component and the steps required for life prediction are outlined. These include: the determination of the operating environment, the calculation of the thermal and mechanical loading of the component, the cyclic stress strain and creep behavior of the material required for structural analysis, the structural analysis to determine the local stress strain temperature time response of the material at the critical location in the component, and from a knowledge of the fatigue, creep, and failure resistance of the material, a prediction of the life of the component. E.A.K.

N82-20339*# National Aeronautics and Space Administration, Lewis Research Center, Cleveland, Ohio.

IDENTIFICATION OF MULTIVARIABLE HIGH PERFORMANCE TURBOFAN ENGINE DYNAMICS FROM CLOSED LOOP DATA

Walter Merrill 1982 16 p refs Presented at the 6th IFAC Symp. on Identification and System Parameter Estimation, Washington, D.C., 7-11 Jun. 1982 (NASA-TM-82785; E-1120; NAS 1.15:82785) Avail: NTIS HC A02/MF A01 CSCL 21E

The multivariable instrumental variable/approximate maximum likelihood (IV/AML) method or recursive time-series analysis is used to identify the multivariable (four inputs-three outputs) dynamics of the Pratt and Whitney F100 engine. A detailed nonlinear engine simulation is used to determine linear engine model structures and parameters at an operating point using open loop data. Also, the IV/AML method is used in a direct identification mode to identify models from actual closed loop engine test data. Models identified from simulated and test data are compared to determine a final model structure and parameterization that can predict engine response for a wide class of inputs. The ability of the IV/AML algorithm to identify useful dynamic models from engine test data is assessed. Author

N82-22386*# National Aeronautics and Space Administration, Lewis Research Center, Cleveland, Ohio.

ULTRASONIC SCANNING SYSTEM FOR IMAGING FLAW GROWTH IN COMPOSITES

Louis J. Kiraly and Erwin H. Meyn 1982 18 p Presented at 28th Intern. Instrumentation Symp., Las Vegas, Nev., 3-6 May 1982; sponsored by Instrument Soc. of Am. (NASA-TM-82799; E-1138; NAS 1.15:82799) Avail: NTIS HC A02/MF A01 CSCL 11D

A system for measuring and visually representing damage in composite specimens while they are being loaded was demonstrated. It uses a hobbyist grade microcomputer system to control data taking and image processing. The system scans operator selected regions of the specimen while it is under load in a tensile test machine and measures internal damage by the attenuation of a 2.5 MHz ultrasonic beam passing through the specimen. The microcomputer dynamically controls the position of ultrasonic transducers mounted on a two axis motor driven carriage. As many as 65,536 samples can be taken and filed on a floppy disk system in less than four minutes. S.L.

N82-22387*# National Aeronautics and Space Administration, Lewis Research Center, Cleveland, Ohio.

MORPHOLOGICAL AND FRICTIONAL BEHAVIOR OF SPUTTERED MoS₂ FILMS

T. Spalvins 1982 18 p refs Presented at Intern. Conf. on Met. Coatings, San Diego, Calif., 4-9 Apr. 1982; sponsored by Am. Vacuum Soc. (NASA-TM-82809; E-1150; NAS 1.15:82809) Avail: NTIS HC A02/MF A01 CSCL 11F

From the texture and growth patterns of sputtered MoS₂ films deposited on substrates, three regions are distinguished: (1) a ridge formation region; (2) an equiaxed transition zone; and (3) a columnar-fiber-like structure. The lubricating properties of sputtered MoS₂ films are visually identified with respect to optical changes before and after rubbing. The orientation of the surface microcrystallites is identified, and the change in optical properties is explained. In sliding contact the sputtered film tends to break up at the base of the columnar region. Effective lubrication occurs with the film remaining on the substrate. This film is 0.18 to 0.22 microns thick. J.M.S.

N82-22388*# National Aeronautics and Space Administration, Lewis Research Center, Cleveland, Ohio.

A HIGH SPEED IMPLEMENTATION OF THE RANDOM DECREMENT ALGORITHM

Louis J. Kiraly 1982 13 p refs Presented at 1982 Aerospace/Test Measurement Symp., Las Vegas, Nev., 2-6 May 1982; sponsored by Instrument Soc. of Am. (NASA-TM-82853; E-1192; NAS 1.15:82853) Avail: NTIS HC A02/MF A01 CSCL 09B

The algorithm is useful for measuring net system damping levels in stochastic processes and for the development of equivalent linearized system response models. The algorithm works by summing together all subrecords which occur after predefined threshold level is crossed. The random decrement signature is normally developed by scanning stored data and adding subrecords together. The high speed implementation of the random decrement algorithm exploits the digital character of sampled data and uses fixed record lengths of 2(n) samples to greatly speed up the process. The contributions to the random decrement signature of each data point was calculated only once and in the same sequence as the data were taken. A hardware implementation of the algorithm using random logic is diagrammed and the process is shown to be limited only by the record size and the threshold crossing frequency of the sampled data. With a hardware cycle time of 200 ns and 1024 point signature, a threshold crossing frequency of 5000 Hertz can be processed and a stably averaged signature presented in real time. T.M.

N82-24361*# Ohio State Univ., Columbus. THE ORTHOGONAL IN-SITU MACHINING OF SINGLE AND POLYCRYSTALLINE ALUMINUM AND COPPER, VOLUME 1 Ph.D. Thesis Final Report

Paul H. Cohen May 1982 203 p refs (Grant NsG-3164) (NASA-CR-168929; NAS 1.26:168929) Avail: NTIS HC A10/MF A01 CSCL 13H

Metal cutting is a unique deformation process characterized by large strains, exceptionally high strain rates and few constraints to the deformation. These factors, along with the difficulty of directly measuring the shear angle, make chip formation difficult to model and understand. One technique for skirting the difficulty of post mortem chip measurement is to perform a cutting experiment dynamically in a scanning electron microscope. The performance of the in-situ experiment with full instrumentation allows for component force measurement, orientation measurement (on a round single crystal disk) and a timing device, all superimposed below the deformation on the TV monitor and recorded for future viewing. This allows the shear angle to be directly measured for the screen along with the other needed information. S.L.

A82-46430 * Pressure pulsations above turbomolecular pumps. S. Danziger, B. R. F. Kendall, and J. Dormer (Pennsylvania State University, University Park, PA). *Journal of Vacuum Science and Technology*, vol. 21, Sept.-Oct. 1982, p. 893-895. 6 refs. Grant No. NsG-3301.

Lange and Singleton (1978) have observed pressure pulses above a turbomolecular pump. They reported that the mean pulse frequency increased with

the temperature of the pump cooling water and that the evolved gas was mainly hydrogen. The present investigation takes into account tests conducted with a similar pumping system. The pumping system was equipped with additional pressure-monitoring equipment in order to study these pulsations in more detail. It was found that at least two distinct types of pressure pulsations may be present in a turbomolecular-pumped ultrahigh vacuum system. The random hydrogen pulses are easily eliminated for period of days by changing the cooling water temperature. The cyclic pulses consisting mainly of water vapor are not likely to be a problem in normal experiments.

G.R.

ORIGINAL PAGE IS
OF POOR QUALITY

32 COMMUNICATIONS

Includes land and global communications; communications theory; and optical communications.

For related information see also 04 Aircraft Communications and Navigation and 17 Spacecraft Communications, Command and Tracking.

N82-31585*# Case Western Reserve Univ., Cleveland, Ohio. Inst. of Technology
COAXIAL PRIME FOCUS FEEDS FOR PARABOLOIDAL REFLECTORS
R. E. Collin, H. Schilling, and L. Hebert Jul. 1982 138 p refs (Contract NAS3-22342)
(NASA-CR-167934; NAS 1.26:167934) Avail: NTIS HC A07/MF A01 CSCL 20N

A TE₁₁ - TM₁₁ dual mode coaxial feed for use in prime focus paraboloidal antenna systems is investigated. The scattering matrix parameters of the internal bifurcation junction was determined by the residue calculus technique. The scattering parameters and radiation fields of the aperture were found from the Weinstein solution. The optimum modeing ratio for minimum cross-polarization was determined along with the corresponding optimum feed dimensions. A peak cross-polarization level of -58 dB is predicted. The frequency characteristics were also investigated and a bandwidth of 5% is predicted over which the cross-polarization remains below -30 dB, the input VSWR is below 1.15, and the phase error is less than 10 deg. Theoretical radiation patterns and efficiency curves for a paraboloidal reflector illuminated by this feed were computed. The predicted sidelobe level is below -30 dB and aperture efficiencies greater than 70% are possible. Experimental results are also presented that substantiates the theoretical results. In addition, experimental results for a 'short-cup' coaxial feed are given. The report includes extensive design data for the dual-mode feed along with performance curves showing cross-polarization as a function of feed parameters. The feed is useful for low-cost ground based receiving antennas for use in direct television satellite broadcasting service. Author

N82-13302*# Arinc Research Corp., Annapolis, Md.
THE 30/20 GHz COMMUNICATIONS SATELLITE TRUNKING NETWORK STUDY
William Kolb Oct. 1981 65 p
(Contract NAS3-22496)
(NASA-CR-165487) Avail: NTIS HC A04/MF A01 CSCL 17B

Alternative transmission media for a CONUS wide trunking network in the years 1990 and 2000 are examined. The alternative technologies comprised fiber optic cable, conventional C- and Ku-band satellites, and 30/20 GHz satellites. Three levels of implementation were considered - a 10-city network, a 20-city network, and a 40-city network. The cities selected were the major metropolitan areas with the greatest communications demand. All intercity voice, data, and video traffic carried more than 40 miles was included in the analysis. In the optimized network, traffic transmitted less than 500 miles was found to be better served by fiber optic cable in 1990. By the year 2000, the crossover point would be down to 200 miles, assuming availability of 30/20 GHz satellites. Author

N82-17420*# Future Systems, Inc., Gaithersburg, Md.
CROSS-IMPACT STUDY OF FOREIGN SATELLITE COMMUNICATIONS ON NASA'S 30/20 GHz PROGRAM
Aug. 1980 244 p refs
(Contract NAS3-21500)
(NASA-CR-165154; FSI-251) Avail: NTIS HC A11/MF A01 CSCL 17B

A comprehensive traffic demand forecast and a scenario for the transition process from current satellite systems to more advanced systems of the 1990's are presented. Systems configurations with and without the use of 30/20 GHz are described and these two alternatives are compared. It is concluded that: (1) the use of 30/20 GHz will result in increased satellite capacity, which will be needed to satisfy demand; (2) the

use of 30/20 GHz will decrease the transmission cost, especially for broadband communications; (3) in some areas, particularly Europe and Japan but also the U.S., 30/20 GHz is the only available frequency band for customer premise Earth stations because of the dense terrestrial microwave networks; and (4) the development of 30/20 GHz technology will improve U.S. markets for equipment and satellites in many world regions. A.R.H.

N82-20362*# Hughes Aircraft Co., El Segundo, Calif. Space and Communications Group.
THE 30/20 GHz FLIGHT EXPERIMENT SYSTEM, PHASE 2. VOLUME 1: EXECUTIVE SUMMARY Final Report, Apr. 1980 - Mar. 1981
L. Bronstein, Y. Kawamoto, J. J. Ribarich, J. R. Scope, B. J. Forman, S. G. Bergman, and S. Reisenfeld Jul. 1981 122 p 4 Vol.
(Contract NAS3-22340)
(NASA-CR-165409-Vol-1; NAS 1.26:165409-Vol-1; SCG-810338R) Avail: NTIS HC A06/MF A01 CSCL 17D

Summary information on the final communication system design, communication payload, space vehicle, and development plan for the 30/20 GHz flight experiment will be installed on the LEASAT spacecraft which will be placed into orbit from the space shuttle cargo bay. The communication concept has two parts: a truck service and a customer premise service (CPS). The trucking system serves four spot beams which are interconnected in a satellite switched time division multiple access mode by an IF switch matrix. The CPS covers two large areas of the eastern United States with a pair of scanning beams. M.G.

N82-20363*# Hughes Aircraft Co., El Segundo, Calif. Space and Communications Group.
THE 30/20 GHz FLIGHT EXPERIMENT SYSTEM, PHASE 2. VOLUME 2: EXPERIMENT SYSTEM DESCRIPTION Final Report, Apr. 1980 - Mar. 1981
L. Bronstein, Y. Kawamoto, J. J. Ribarich, J. R. Scope, B. J. Forman, S. G. Bergman, and S. Reisenfeld Jul. 1981 469 p 4 Vol.
(Contract NAS3-22340)
(NASA-CR-165409-Vol-2; NAS 1.26:165409-Vol-2; SCG-810339R) Avail: NTIS HC A20/MF A01 CSCL 17B

A detailed technical description of the 30/20 GHz flight experiment system is presented. The overall communication system is described with performance analyses, communication operations, and experiment plans. Hardware descriptions of the payload are given with the tradeoff studies that led to the final design. The spacecraft bus which carries the payload is discussed and its interface with the launch vehicle system is described. Finally, the hardware and the operations of the terrestrial segment are presented. R.J.F.

N82-20364*# Hughes Aircraft Co., El Segundo, Calif. Space and Communications Group.
THE 30/20 GHz FLIGHT EXPERIMENT SYSTEM, PHASE 2. VOLUME 3: EXPERIMENT SYSTEM REQUIREMENT DOCUMENT Final Report Apr. 1980 - Mar. 1981
L. Bronstein, Y. Kawamoto, J. J. Ribarich, J. R. Scope, B. J. Forman, S. G. Berman, and S. Reisenfeld Jul. 1981 25 p 4 Vol.
(Contract NAS3-22340)
(NASA-CR-165409-Vol-3; NAS 1.26:165409-Vol-3; SCG-810340R) Avail: NTIS HC A02/MF A01 CSCL 17B

An approach to the requirements document to be used to procure the system by NASA is presented. The basic approach is similar to the requirements document used in the commercial communication satellite. Enough detail requirements are given to define the system without tight constraints. R.J.F.

N82-20365*# Hughes Aircraft Co., El Segundo, Calif. Space and Communications Group.
THE 30/20 GHz FLIGHT EXPERIMENT SYSTEM, PHASE 2. VOLUME 4: EXPERIMENT SYSTEM DEVELOPMENT PLAN Final Report, Apr. 1980 - Mar. 1981
L. Bronstein, Y. Kawamoto, J. J. Ribarich, J. R. Scope, B. J. Forman, S. G. Bergman, and S. Reisenfeld Jul. 1981 40 p

4 Vol.

(Contract NAS3-22340)
(NASA-CR-165409-Vol-4; SCG-8103411R; NAS
1.26:165409-Vol-4; SCG-810341R) Avail: NTIS
HC A03/MF A01 CSCL 17B

The development plan for the 30/20 GHz flight experiment system is presented. A master program schedule with detailed development plans for each subsystem is planned with careful attention given to how technology items to ensure a minimal risk. The work breakdown structure shows the organization of the program management with detailed task definitions. The ROM costs based on the development plan are also given. R.J.F.

N82-25423*# Western Union Telegraph Co., McLean, Va. Government Systems Div.

WORLDWIDE SATELLITE MARKET DEMAND FORECAST Final Report

J. M. Bowyer, M. Frankfort, and K. M. Steinnagel 19 Jun. 1981 124 p refs

(Contract NAS3-22461)
(NASA-CR-167918; NASA-1-4-W-1-T11; NAS 1.26:167918)
Avail: NTIS HC A06/MF A01 CSCL 17B

The forecast is for the years 1981 - 2000 with benchmark years at 1985, 1990 and 2000. Two types of markets are considered for this study: Hardware (worldwide total) - satellites, earth stations and control facilities (includes replacements and spares); and non-hardware (addressable by U.S. industry) - planning, launch, turnkey systems and operations. These markets were examined for the INTELSAT System (international systems and domestic and regional systems using leased transponders) and domestic and regional systems. Forecasts were determined for six worldwide regions encompassing 185 countries using actual costs for existing equipment and engineering estimates of costs for advanced systems. Most likely (conservative growth rate estimates) and optimistic (mid range growth rate estimates) scenarios were employed for arriving at the forecasts which are presented in constant 1980 U.S. dollars. The worldwide satellite market demand forecast predicts that the market between 1981 and 2000 will range from \$35 to \$50 billion. Approximately one-half of the world market, \$16 to \$20 billion, will be generated in the United States. T.M.

N82-26526*# Ohio State Univ., Columbus.
THE TRANSMISSION OR SCATTERING OF ELASTIC WAVES BY AN INHOMOGENEITY OF SIMPLE GEOMETRY: A COMPARISON OF THEORIES

Y. C. Sheu and L. S. Fu May 1982 96 p refs
(Grant NSG-3289)
(NASA-CR-169034; NAS 1.26:169034; TR-104) Avail: NTIS
HC A05/MF A01 CSCL 20N

The extended method of equivalent inclusion developed is applied to study the specific wave problems of the transmission of elastic waves in an infinite medium containing a layer of inhomogeneity, and of the scattering of elastic waves in an infinite medium containing a perfect spherical inhomogeneity. The eigenstrains are expanded as a geometric series and the method of integration for the inhomogeneous Helmholtz operator given by Fu and Mura is adopted. The results obtained by using a limited number of terms in the eigenstrain expansion are compared with exact solutions for the layer problem and for a perfect sphere. Two parameters are singled out for this comparison: the ratio of elastic moduli, and the ratio of the mass densities. General trends for three different situations are shown. J.D.

N82-28503*# Illinois Univ., Urbana-Champaign. Electromagnetics Lab.

NASA ADAPTIVE MULTIBEAM PHASED ARRAY (AMPA): AN APPLICATION STUDY Final Report, 15 Jan. - 30 Apr. 1982

R. Mittra, S. W. Lee, and W. Gee May 1982 78 p refs
(Grant NAG3-149)
(NASA-CR-169125; NAS 1.26:169125) Avail: NTIS
HC A05/MF A01 CSCL 20N

The proposed orbital geometry for the adaptive multibeam phased array (AMPA) communication system is reviewed and some of the system's capabilities and preliminary specifications

are highlighted. Typical AMPA user link models and calculations are presented, the principal AMPA features are described, and the implementation of the system is demonstrated. System tradeoffs and requirements are discussed. Recommendations are included. A.R.H.

N82-31584*# NTL, Inc., Colmaddock, N.Y.

A NEW ANTENNA CONCEPT FOR SATELLITE COMMUNICATIONS

G. Skahill and D. Ciccolella Jun. 1982 111 p refs
(Contract NAS3-22887)
(NASA-CR-167924; NAS 1.26:167924) Avail: NTIS
HC A06/MF A01 CSCL 20N

A novel antenna configuration of two reflecting surfaces and a phased array is examined for application to satellite communications and shown to be superior in every respect to earlier designs for service to the continental United States from synchronous orbit. The vignetting that afflicts other two reflector optical systems is eliminated by use of a reflecting field element. The remaining aberrations, predominantly coma, are isolated in the time delay distribution at the surface of the array and can be compensated by ordinary array techniques. The optics exhibits infinite bandwidth and the frequency range is limited only by the design of the array. Author

A82-10679* A review of transhorizon propagation phenomena. R. K. Crane (Environmental Research and Technology, Inc., Concord, MA). (*International Union of Radio Science, Symposium on the Effects of the Lower Atmosphere on Radio Propagation at Frequencies above 1 GHz, Lennoxville, Quebec, Canada, May 26-30, 1980.*) *Radio Science*, vol. 16, Sept.-Oct. 1981, p. 649-669. 40 refs. Contract No. NASw-3336.

Interference problems underlie the current interest in transhorizon propagation. In particular, statistics of the rare, high-level fields are of interest. This paper reviews the propagation mechanisms which produce the high-level fields and summarizes recent work in the modeling of the transhorizon propagation. (Author)

A82-23486*# 30/20 GHz communications satellite multibeam antenna. W. G. Scott, H. S. Luh, A. E. Small, and E. W. Matthews (Ford Aerospace and Communications Corp., Palo Alto, CA). In: *Communications Satellite Systems Conference, 9th, San Diego, CA, March 7-11, 1982*, Collection of Technical Papers. (A82-23476 09-32) New York, American Institute of Aeronautics and Astronautics, 1982, p. 78-86. Contract No. NAS3-22498. (AIAA 82-0449)

A 20 GHz downlink satellite antenna design is described. The aperture simultaneously radiates 18 fixed, 0.3 deg width pencil beams directed at 18 cities distributed over CONUS for Trunking Service. All beams use the same trunk frequency allocation for 18 reuses of the band. The same aperture also radiates six additional 0.3 deg spot beams for Customer Premises Service (CPS) for TDMA beam hopping operation to small terminals anywhere in CONUS. Each CPS beam scans one sector of CONUS and all six beams are frequency reused in a CPS band. Offset dual reflector optics are used with a feed array and multipoint beam forming network (BFN). For so many frequency reuses, sidelobes per beam must be 30 to 40 dB down over CONUS. Novel dual reflector optics were devised with shaped surfaces providing low aberrations for all beam positions over CONUS (+ or - 12 BW by + or - 5 BW). Scan loss under 1 dB is calculated with nearly constant sidelobes. For each beam position, a 7-element cluster of feeds is activated in the feed array with coefficients adjusted by the BFN to maintain low sidelobes and thus high beam isolation for frequency reuse. (Author)

A82-23508*# Baseband-processed SS-TDMA communication system architecture and design concepts. S. Attwood and D. Sabourin (Motorola, Inc., Government Electronics Div., Scottsdale, AZ). In: *Communications Satellite Systems Conference, 9th, San Diego, CA, March 7-11, 1982*, Collection of Technical Papers. (A82-23476 09-32) New York, American Institute of Aeronautics and Astronautics, 1982, p. 234-242. Contract No. NAS3-22502.

ORIGINAL PAGE IS
OF POOR QUALITY

(AIAA 82-0482)

The architecture and system design for a commercial satellite communications system planned for the 1990's was developed by Motorola for NASA's Lewis Research Center. The system provides data communications between individual users via trunking and customer premises service terminals utilizing a central switching satellite operating in a time-division multiple-access (TDMA) mode. The major elements of the design incorporating baseband processing include: demand-assigned multiple access reservation protocol, spectral utilization, system synchronization, modulation technique and forward error control implementation. Motorola's baseband processor design, which is being proven in a proof-of-concept advanced technology development, will perform data regeneration and message routing for individual users on-board the spacecraft. (Author)

A82-23538 * # Planning satellite communication services and spectrum-orbit utilization. P. H. Sawitz (ORI, Inc., Silver Spring, MD). In: Communications Satellite Systems Conference, 9th, San Diego, CA, March 7-11, 1982, Collection of Technical Papers. (A82-23476 09-32) New York, American Institute of Aeronautics and Astronautics, 1982, p. 489-494. Contract No. NAS3-22885. (AIAA 82-0526)

The relationship between approaches to planning satellite communication services and spectrum-orbit utilization is considered, with emphasis on the fixed-satellite and the broadcasting-satellite services. It is noted that there are several possible approaches to planning space services, differing principally in the rigidity with which technical parameters are prescribed, in the time for which a plan remains in force, and in the procedures adopted for implementation and modifications. With some planning approaches, spectrum-orbit utilization is fixed at the time the plan is made. Others provide for greater flexibility by making it possible to postpone some decisions on technical parameters. In addition, the two political questions of what is equitable access and how it can be guaranteed in practice play an important role. B.J.

A82-26713 * Conversion and matched filter approximations for serial minimum-shift keyed modulation. R. E. Ziemer (Missouri-Rolla, University, Rolla, MO), C. R. Ryar, and J. H. Stillwell (Motorola, Inc., Government Electronics Div., Gilbert, AZ). *IEEE Transactions on Communications*, vol. COM-30, Mar. 1982, p. 495-509. 9 refs. Contract No. NAS3-22502.

Serial minimum-shift keyed (MSK) modulation, a technique for generating and detecting MSK using series filtering, is ideally suited for high data rate applications provided the required conversion and matched filters can be closely approximated. Low-pass implementations of these filters as parallel inphase- and quadrature-mixer structures are characterized in this paper in terms of signal-to-noise ratio (SNR) degradation from ideal and envelope deviation. Several hardware implementation techniques utilizing microwave devices or lumped elements are presented. Optimization of parameter values results in realizations whose SNR degradation is less than 0.5 dB at error probabilities of .000001. (Author)

A82-27178 * Adaptive rain fade compensation. J. C. Rautio (General Electric Co., Space Div., Philadelphia, PA). In: ITC/USA/80; Proceedings of the International Telemetry Conference, San Diego, CA, October 14-16, 1980. (A82-27176 12-32) Research Triangle Park, NC, Instrument Society of America, 1980, p. 35-46. Contract No. NAS3-21745.

A large available margin must be provided for satellite communications systems operating near 20 GHz, which occasionally experience fades due to rain attenuation. It is proposed that this margin may be achieved in high-capacity FDMA satellites by dynamically providing a large margin to those links which are experiencing deep fades, while maintaining a small fade margin on all others. Single-beam SCPC operation and multiple-beam, satellite-switched FDMA systems are described, and the optimization of the dynamic FDMA links in a severely fading environment is investigated. A solution is derived which takes into account: (1) transponder intermodulation distortion, (2) cochannel and cross-polarization antenna interference, and (3) rain fade characteristics. The sample system configuration presented shows that such systems reach availability levels approaching 0.9999 at Ka-Band. O.C.

A82-27189 * 30/20 GHz demonstration system for improving orbit utilization. W. M. Holmes, Jr. (TRW Defense and Space Systems Group, Space Systems Div., Redondo Beach, CA). In: ITC/USA/80; Proceedings of the International Telemetry Conference, San Diego, CA, October 14-16, 1980. (A82-27176 12-32) Research Triangle Park, NC, Instrument Society of America, 1980, p. 189-198. Contract No. NAS3-21933.

To guard against severe rain losses at 30 and 20 GHz, techniques are being developed which provide the high antenna gain needed to increase communications margins and frequency reuse capability through beam isolation, while providing complete coverage of the U.S. Effective bandwidths from a single satellite location may then reach tens of gigahertz, with capacity tailored to match nonuniform geographic demand patterns. Satellite onboard processing which includes forward-error-correction and the routing of channels to terminals will reduce scanning antenna requirements and increase rain margins, through the adaptive use of system margins to support those terminals experiencing rain. These antenna and onboard processing techniques are adaptable to C-band and Ku-band, in addition to Ka-band. O.C.

A82-36265 * Focal surfaces of offset dual-reflector antennas. C. J. Sletten and R. A. Shore (Solar Energy Technology, Inc., Bedford, MA). *IEE Proceedings, Part H - Microwaves, Optics and Antennas*, vol. 129, pt. H, no. 3, June 1982, p. 109-115. 9 refs. Contract No. NAS3-22343.

An analytical technique is described for finding the best focal surfaces for offset-fed dual-reflector antennas. A ray tracing procedure traces the loci of rays incident on the main reflector onto a plane or 'screen' situated perpendicular to a central ray of the antenna system. Given, then, by computer graphics, the best feed locations for azimuth and elevation plane patterns, an aperture diffraction method is used which can compute the sidelobe levels and beamwidths resulting from aperture phase errors on scanned or multibeam patterns. High-magnification Cassegrain or Gregorian antennas, with tilt angles optimised according to

ORIGINAL PAGE IS
OF POOR QUALITY

33 ELECTRONICS AND ELECTRICAL ENGINEERING

Includes test equipment and maintainability; components, e.g., tunnel diodes and transistors; microminiaturization; and integrated circuitry.

For related information see also 60 *Computer Operations and Hardware* and 76 *Solid-State Physics*.

N82-15311*# National Aeronautics and Space Administration, Lewis Research Center, Cleveland, Ohio.
PROCEEDINGS OF THE CONFERENCE ON HIGH-TEMPERATURE ELECTRONICS

1981 134 p refs Conf. held in Tucson, Ariz., 25-27 Mar. 1981 Sponsored by IEEE Industrial Electronics and Control Instrumentation Group, IEEE Solid State Circuits Council, DOE, NRC, NSF, LASL, and Arizona Univ. (NASA-T7-84039; DE81-025058; CONF-810316) Avail: NTIS HC A07/MF A01 CSCL 09C

The development of electronic devices for use in high temperature environments is addressed. The instrumental needs of planetary exploration, fossil and nuclear power reactors, turbine engine monitoring, and well logging are defined. Emphasis is placed on the fabrication and performance of materials and semiconductor devices, circuits and systems and packaging. For individual titles, see N82-15312 through N82-15337.

N82-15313*# National Aeronautics and Space Administration, Lewis Research Center, Cleveland, Ohio.

HIGH TEMPERATURE ELECTRONIC REQUIREMENTS IN AEROPULSION SYSTEMS

William C. Nieberding and J. Anthony Powell *In its Proc. of The Conf. on High-Temp. Electron.* 1981 p 13-16 refs (For primary document see N82-15311 06-33) (E-708) Avail: NTIS HC A07/MF A01 CSCL 09C

The needs for high temperature electronic and electro-optic devices as they would be used on aircraft engines in either research and development applications, or operational applications are discussed. The conclusion reached is that the temperature at which the devices must be able to function is in the neighborhood of 500 to 600 C either for R&D or for operational applications. In R&D applications the devices must function in this temperature range when in the engine but only for a moderate period of time. On an operational engine, the reliability requirements dictate that the devices be able to be burned-in at temperatures significantly higher than those at which they will function on the engine. The major point made is that semiconductor technology must be pushed well beyond the level at which silicon will be able to function. M.G.

N82-22439*# National Aeronautics and Space Administration, Lewis Research Center, Cleveland, Ohio.

THREE-DIMENSIONAL RELATIVISTIC FIELD-ELECTRON INTERACTION IN A MULTICAVITY HIGH-POWER KLYSTRON. 1: BASIC THEORY

Henry G. Kosmahl Apr. 1982 33 p refs Presented at the Intern. Electron Devices Meeting, Washington, D.C., 11 Oct. 1971; sponsored by IEEE; and the Solar Power Space System Workshop, Houston, Tex., 15-18 Jan. 1979; sponsored by NASA (NASA-TP-1992; E-1017; NAS 1.60:1992) Avail: NTIS HC A03/MF A01 CSCL 09A

A theoretical investigation of three dimensional relativistic klystron action is described. The relativistic axisymmetric equations of motion are derived from the time-dependent Lagrangian function for a charged particle in electromagnetic fields. An analytical expression of the fringing RF electric and magnetic fields within and in the vicinity of the interaction gap and the space-charge forces between axially and radially elastic deformable rings of charges are both included in the formulation. This makes an accurate computation of electron motion through the tunnel of the cavities and the drift tube spaces possible. Method of analysis is based on Lagrangian formulation. Bunching is computed using a disk model of electron stream in which the electron stream is divided into axisymmetric disks of equal charge and each disk

is assumed to consist of a number of concentric rings of equal charges. The individual representative groups of electrons are followed through the interaction gaps and drift tube spaces. Induced currents and voltages in interacting cavities are calculated by invoking the Shockley-Ramo theorem. B.W.

N82-23397*# National Aeronautics and Space Administration, Lewis Research Center, Cleveland, Ohio.

THREE-DIMENSIONAL RELATIVISTIC FIELD-ELECTRON INTERACTION IN A MULTICAVITY HIGH-POWER KLYSTRON. PART 2: WORKING EQUATIONS

Henry G. Kosmahl Apr. 1982 45 p refs Presented at the Intern. Electron Devices Meeting, Washington, D.C., 11 Oct. 1971; sponsored by IEEE Also presented at the Solar Power Space System Workshop, Houston, Tex., 15-18 Jan. 1979; sponsored by NASA. Lyndon B. Johnson Space Center (NASA-TP-2008; E-1018; NAS 1.60:2008) Avail: NTIS HC A03/MF A01 CSCL 09C

A high power multicavity klystron amplifier was designed and a computation package containing all equations and procedures needed is presented. The rigorously derived three dimensional relativistic axisymmetric equations of motion are used to compute the bunched current and the induced RF gap voltage for all interaction cavities except the input and second cavities, where the linear space charge wave theory data are employed in order to reduce the computation time. Both distance step and time step integration methods are used to compute the Fourier coefficients of both the beam current and induced current. S.L.

N82-24415* National Aeronautics and Space Administration, Lewis Research Center, Cleveland, Ohio.

MULTISTAGE DEPRESSED COLLECTOR FOR DUAL MODE OPERATION Patent

Henry C. Kosmahl, inventor (to NASA) Issued 7 Jul. 1981 6 p Filed 7 Sep. 1979 Supersedes N79-32463 (17 - 23, p 3080)

(NASA-Case-LEW-13282-1; US-Patent-4,277,721;

US-Patent-Appl-SN-073579; US-Patent-Class-315-5.38;

US-Patent-Class-315-3.6) Avail: US Patent and Trademark Office CSCL 09A

A depressed collector which captures the spent electrons of a microwave transmitting tube at high efficiency in both high and low power modes of operation is described. The collector comprises entrance and end electrodes, the end electrode having a spike extending toward entrance electrode. Intermediate electrodes and the entrance electrode each have a central aperture and, together, these electrodes capture most high power mode spent electrons. The apertures of the electrodes increase in size in a downstream direction. To capture low power mode spent electrons a low power mode electrode is positioned between the last intermediate electrode and the end electrode. This electrode has a central aperture preferably smaller but no larger than that of the last intermediate electrode. An auxiliary low power mode electrode may be added having a central aperture larger than that of the low power mode electrode. All of the electrodes are at voltages provided by a voltage divider connected between a potential.

Official Gazette of the U.S. Patent and Trademark Office

N82-24431*# National Aeronautics and Space Administration, Lewis Research Center, Cleveland, Ohio.

FIRST RESULTS OF MATERIAL CHARGING IN THE SPACE ENVIRONMENT Interim Report

N. J. Stevens, F. Berkopec, J. Staskus, P. F. Mizera, H. C. Koons, E. R. Schnauss, D. R. Croley, Jr., H. K. Kan (Aerospace Corp.), M. S. Leung (Aerospace Corp.), W. L. Lehn (AFML) et al 15 Mar. 1981 20 p refs Prepared in cooperation with SRI International, Menlo Park, Calif.

(Contract F04701-80-C-0081)

(NASA-TM-84743; NAS 1.15:84743; TOR-0081(6506-1)-1)

Avail: NTIS HC A02/MF A01 CSCL 09C

A satellite experiment, designed to measure potential charging of typical thermal control materials at near geosynchronous

ORIGINAL PAGE IS
OF POOR QUALITY

altitude, was flown as part of the SCATHA program. Direct observations of charging of typical satellite materials in a natural charging event (> 5 keV) are presented. The results show some features which differ significantly from previous laboratory simulations of the environment
S.L.

N82-24432*# National Aeronautics and Space Administration, Lewis Research Center, Cleveland, Ohio.

SIMPLIFIED dc TO dc CONVERTER Patent Application
Robert P. Gruber, inventor (to NASA) Filed 14 Apr. 1982
17 p

(NASA-Case-LEW-13495-1; US-Patent-Appl-SN-368188) Avail: NTIS HC A02/MF A01 CSCL 09A

A dc to dc converter is disclosed which has a minimum number of components, output voltage regulation, and output current limiting without any circuits converting the output to any other circuits of the converter. The converter is comprised of a transformer having a primary winding through which current is directed in alternate directions by metal oxide semiconductor transistors connected between the primary winding and a dc source or battery. A secondary winding of the transformer is connected to a rectifying and filter circuit to provide unidirectional output current. Both windings of the transformer are carried on the respective outer legs of an E-core with the center leg of the core proving a leakage reactance. This leakage reactance has the same effect as placing an inductor in series with the rectifiers in output circuit.
NASA

N82-25441*# National Aeronautics and Space Administration, Lewis Research Center, Cleveland, Ohio.

COMPUTER MODELING OF MULTIPLE-CHANNEL INPUT SIGNALS AND INTERMODULATION LOSSES CAUSED BY NONLINEAR TRAVELING WAVE TUBE AMPLIFIERS

N. Stankiewicz May 1982 26 p
(NASA-TP-1999; E-722; NAS 1.60:1999) Avail: NTIS HC A03/MF A01 CSCL 09A

The multiple channel input signal to a soft limiter amplifier as a traveling wave tube is represented as a finite, linear sum of Gaussian functions in the frequency domain. Linear regression is used to fit the channel shapes to a least squares residual error. Distortions in output signal, namely intermodulation products, are produced by the nonlinear gain characteristic of the amplifier and constitute the principal noise analyzed in this study. The signal to noise ratios are calculated for various input powers from saturation to 10 dB below saturation for two specific distributions of channels. A criterion for the truncation of the series expansion of the nonlinear transfer characteristic is given. It is found that the signal to noise ratios are very sensitive to the coefficients used in this expansion. Improper or incorrect truncation of the series leads to ambiguous results in the signal to noise ratios.
Author

N82-26568* National Aeronautics and Space Administration, Lewis Research Center, Cleveland, Ohio.

COUPLED CAVITY TRAVELING WAVE TUBE WITH VELOCITY TAPERING Patent

Denis J. Connolly, inventor (to NASA) Issued 9 Feb. 1982
7 p Filed 20 Feb. 1980

(NASA-Case-LEW-12296-1; US-Patent-4,315,194;
US-Patent-Appl-SN-122966; US-Patent-Class-315-3.6;
US-Patent-Class-315-3.5; US-Patent-Class-330-43) Avail: US Patent and Trademark Office CSCL 09A

A coupled cavity traveling wave tube with a velocity taper, which affords beam wave resynchronization and thereby enhances is described. The wave velocity reduction is achieved by reducing the resonant frequencies of the individual resonant cavities as a function of the distance from the electron gun, through changes in internal cavity dimensions. The required changes in cavity dimensions can be accomplished by gradually increasing the cavity radius decreasing the gap length from cavity to cavity. The velocity reduction is carried out without an increase in circuit resistive losses and the upper and lower cut off frequencies are reduced in approximately the same manner.
E.A.K.

N82-30474*# National Aeronautics and Space Administration, Lewis Research Center, Cleveland, Ohio.

COMPONENT TECHNOLOGY FOR SPACE POWER SYSTEMS

Robert C. Finke 1982 13 p refs Presented at the 33rd Intern. Astronautical Federation Congr., Paris, 26 Sep. - 2 Oct. 1982

(NASA-TM-82928; E-1322; NAS 1.15:82928) Avail: NTIS HC A02/MF A01 CSCL 09C

The Lewis/OAST program for the development of Component Technology for Space Power Systems is described. The program is divided into five generic areas: semiconductor devices (transistors, thyristors, and diodes); conductors (materials and transmission lines); dielectrics; magnetic devices; and thermal control devices. Examples of progress in each of the five areas is discussed. Bipolar power transistors up to 1000 V at 100 A with a gain of 10 and a 0.5 mu sec rise and fall time are presented. A new class of semiconductor devices with a possibility of switching 1000 000 V is described. Several 100 kW rotary power transformer designs and a 25 kW, 20 kHz transformer weighting 3.2 kg have been developed. Progress on the creation of diamond-like films for thermal devices and intercalated carbon fibers with the strength of steel and the conductivity of copper at one third the mass of copper is presented.
Author

N82-33636*# National Aeronautics and Space Administration, Lewis Research Center, Cleveland, Ohio.

SUMMARY OF ELECTRIC VEHICLE dc MOTOR-CONTROLLER TESTS Final Report

E. F. McBrien and H. B. Tryon Sep. 1982 30 p refs

(Contract DE-AI01-77CS-51044)
(NASA-TM-82863; E-1232; DOE/NASA/51044-28; NAS 1.15:82863) Avail: NTIS HC A03/MF A01 CSCL 13F

The differences in the performance of dc motors are evaluated when operating with chopper type controllers, and when operating on direct current. The interactions between the motor and the controller which cause these differences are investigated. Motor-controlled tests provided some of the data the quantified motor efficiency variations for both ripple free and chopper modes of operation.
S.L.

A82-16128 * # Experimental verification of a computational procedure for the design of TWT-refocuser-MDC systems. J. A. Dayton, Jr., H. G. Kosmahl, P. Ramins, and N. Stankiewicz (NASA, Lewis Research Center, Cleveland, OH). *IEEE Transactions on Electron Devices*, vol. ED-28, Dec. 1981, p. 1480-1489. 10 refs.

A comparison of analytical and experimental results is presented for a high performance dual-mode helix TWT, equipped with multistage depressed collectors (MDC), and operated over conditions ranging from saturation to the linear regime. The computations are carried out with advanced multidimensional computer programs which model the electron beam as a series of disks or rings of charge and follow their trajectories from the RF input of the TWT, through the slow-wave structure, through the refocusing system, to their points of impact in the depressed collector. TWT performance, collector efficiency, and collector current distribution are computed and compared with measurements. Very good agreement is obtained between computed and measured TWT performance and collector efficiencies. The analytical techniques were subsequently applied to the design of a smaller MDC of nearly equal efficiency. (Author)

A82-16831 * # A new approach to the minimum weight/loss design of switching power converters. F. C. Lee, S. Rahman, C. J. Wu (Virginia Polytechnic Institute and State University, Blacksburg, VA), and J. Kolacki (NASA, Lewis Research Center, Cleveland, OH). *International Power Conversion Conference, Dallas, TX, Apr. 28-30, 1981, Paper*, 11 p, 10 refs. Contract No. NAS3-21051.

A new technique using the mathematical nonlinear programming ALAG is proposed to facilitate design optimizations of switching power converters. This computer-aided approach provides a minimum weight (or loss) design down to the details of component level and concurrently satisfies all related power-circuit performance requirements. It also provides such design insights as tradeoffs between power loss and system weight as the switching frequency is increased.
(Author)

ORIGINAL PAGE IS
OF POOR QUALITY

A82-20745 * # Hard permanent magnet development trends and their application to A.C. machines. H. F. Mildrum (NASA, Lewis Research Center, Cleveland, OH). *Institute of Electrical and Electronics Engineers, Annual Meeting, Philadelphia, PA, Oct. 5-9, 1981, Paper, 8 p. 27 refs.* Research supported by the U.S. Department of Energy; Contract No. DEN3-189.

The physical and magnetic properties of Mn-Al-C, Fe-Cr-Co, and RE-TM (rare earth-transition metal intermetallics) in polymer and soft metal bonded or sintered form are considered for ac circuit machine usage. The manufacturing processes for the magnetic materials are reviewed, and the mechanical and electrical properties of the magnetic materials are compared, with consideration given to the reference Alnico magnet. The Mn-Al-C magnets have the same magnetic properties and costs as Alnico units, operate well at low temperatures, but have poor high temperature performance. Fe-Cr-Co magnets also have comparable cost to Alnico magnets, and operate at high or low temperature, but are brittle, expensive, and contain Co. RE-Co magnets possess a high energy density, operate well in a wide temperature range, and are expensive. Recommendation for exploring the rare-earth alternatives are offered. M.S.K.

A82-41845 * A remote millivolt multiplexer and amplifier module for wind tunnel data acquisition. D. B. Juanarena (Pressure Systems, Inc., Hampton, VA) and P. Z. Blumenthal (NASA, Lewis Research Center, Cleveland, OH). In: *International Instrumentation Symposium, 28th, Las Vegas, NV, May 3-6, 1982, Proceedings, Part 1.* (A82-41819 21-35) Research Triangle Park, NC, Instrument Society of America, 1982, p. 445-456. Contract No. NAS3-22950.

A 30-channel remotely located multiplexer and amplifier module is developed for the measurement of wind tunnel models, which substantially reduces the amount of wiring necessary and thus provides higher accuracy. The module provides for a wide variety of transducer voltage outputs to be multiplexed and amplified within the model, and all signals are able to exit the module on two wires. The module is self-calibrating, and when coupled with the electronically scanned pressure instrumentation widely used in wind tunnels, it allows the modular wind tunnel models to be fabricated and checked before installation into the wind tunnel. N.B.

A82-46388 * Analysis and design of a standardized control module for switching regulators. F. C. Lee, M. F. Mahmoud (Virginia Polytechnic Institute and State University, Blacksburg, VA), Y. Yu (Xerox Corp., El Segundo, CA), and J. C. Kolecki (NASA, Lewis Research Center, Cleveland, OH). *IEEE Transactions on Aerospace and Electronic Systems*, vol. AES-18, July 1982, p. 478-496. 10 refs. Contract No. NAS3-20102.

Three basic switching regulators: buck, boost, and buck/boost, employing a multiloop standardized control module (SCM) were characterized by a common small signal block diagram. Employing the unified model, regulator performances such as stability, audiosusceptibility, output impedance, and step load transient are analyzed and key performance indexes are expressed in simple analytical forms. More importantly, the performance characteristics of all three regulators are shown to enjoy common properties due to the unique SCM control scheme which nullifies the positive zero and provides adaptive compensation to the moving poles of the boost and buck/boost converters. This allows a simple unified design procedure to be devised for selecting the key SCM control parameters for an arbitrarily given power stage configuration and parameter values, such that all regulator performance specifications can be met and optimized concurrently in a single design attempt. (Author)

N82-12347*# Duke Univ., Durham, N. C. Dept of Electrical Engineering.

HIGH-FREQUENCY HIGH-VOLTAGE HIGH-POWER DC-TO-DC CONVERTERS

Thomas G. Wilson, Harry A. Owen, Jr., and Paul M. Wilson 1981 11 p refs Presented at the U.S.-Japan Sci. Seminar on Analysis and Design in Power Electron., Kobe, Japan, 25-28 Nov. 1981

(Grant NaG-3157)

Avail: NTIS HC A02/MF A01 CSCL 09C

The current and voltage waveshapes associated with the power transistor and the power diode in an example current-or-voltage step-up (buck-boost) converter were analyzed to highlight the problems and possible tradeoffs involved in the design of high voltage high power converters operating at switching frequencies in the range of 100 KHz. Although the fast switching speeds of currently available power diodes and transistors permit converter operation at high switching frequencies, the resulting time rates of changes of current coupled with parasitic inductances in series with the semiconductor switches,

produce large repetitive voltage transients across the semiconductor switches, potentially far in excess of the device voltage ratings. The need is established for semiconductor switch protection circuitry to control the peak voltages appearing across the semiconductor switches, as well as to provide the waveshaping action require for a given semiconductor device. The possible tradeoffs, as well as the factors affecting the tradeoffs that must be considered in order to maximize the efficiency of the converters are enumerated. A.R.H.

N82-13367*# Westinghouse Electric Corp., Lima, Ohio, Electrical Systems Div.

HIGH VOLTAGE DC SWITCHGEAR DEVELOPMENT FOR MULTI-KW SPACE POWER SYSTEM: AEROSPACE TECHNOLOGY DEVELOPMENT OF THREE TYPES OF SOLID STATE POWER CONTROLLERS FOR 200-1100VDC WITH CURRENT RATINGS OF 25, 50, AND 80 AMPERES WITH ONE TYPE UTILIZING AN ELECTROMECHANICAL DEVICE

Final Report

W. W. Billings Nov. 1981 187 p

(Contract NAS3-21755)

(NASA-CR-165413; WAED-81-05E)

Avail: NTIS

HC A09/MF A01 CSCL 09C

Three types of solid state power controllers (SSPCs) for high voltage, high power DC system applications were developed. The first type utilizes a SCR power switch. The second type employs an electromechanical power switch element with solid state commutation. The third type utilizes a transistor power switch. Significant accomplishments include high operating efficiencies, fault clearing, high/low temperature performance and vacuum operation. E.A.K.

N82-14447*# Virginia Polytechnic Inst. and State Univ., Blacksburg.

MODELING AND ANALYSIS OF POWER PROCESSING SYSTEMS (MAPPS). VOLUME 1: TECHNICAL REPORT

Final Technical Report, Oct. 1977 - Aug. 1980

F. C. Lee, S. Rahman, R. A. Carter, C. H. Wu, Yung Yu (TRW Defense and Space Systems Group, Redondo Beach, Calif.), and R. Chang (TRW Defense and Space Systems Group, Redondo Beach, Calif.) Dec. 1980 335 p refs

(Contract NAS3-21051)

(NASA-CR-165538; TRW-32660-6001-RU-01) Avail: NTIS

HC A15/MF A01 CSCL 09C

Computer aided design and analysis techniques were applied to power processing equipment. Topics covered include: (1) discrete time domain analysis of switching regulators for performance analysis; (2) design optimization of power converters using augmented Lagrangian penalty function technique; (3) investigation of current-injected multiloop controlled switching regulators; and (4) application of optimization for Navy VSTOL energy power system. The generation of the mathematical models and the development and application of computer aided design techniques to solve the different mathematical models are discussed. Recommendations are made for future work that would enhance the application of the computer aided design techniques for power processing systems. A.R.H.

N82-15315*# Panelvision Corp., Pittsburgh, Pa.

DEVELOPMENT OF AN 1100 DEG F CAPACITOR

Robert E. Stapleton In NASA, Lewis Research Center Proc. of the Conf. on High-Temp. Electron. 1981 p 25-28 ref Prepared in cooperation with Westinghouse Electric Corp., Pittsburgh, Pa. (For primary document see N82-15311 06-33) (Contracts NAS3-6465; NAS3-10941)

Avail: NTIS HC A07/MF A01 CSCL 09C

The feasibility of developing a high temperature capacitor for 1100 F operation which is as small and light as conventional capacitors for normal operating temperatures is discussed. Pyrolytic boron nitride (PBN) was selected for the dielectric. The PBN capacitors were made by slicing and lapping material from thick blocks and then sputtering thin film electrodes. These capacitors had breakdown strengths of 7,000 volts per mil and a dissipation factor of less than 0.001 at 1100 F. Additional processing improvements were made after testing a multi-layer or stacked PBN capacitor for 1,000 hours at 1100 F. Sputter etching the

ORIGINAL PAGE IS
OF POOR QUALITY

wafers before depositing electrodes resulted in a reduction in dissipation factor. A sputtered boron nitride film applied to the outer electrode surfaces produced a more stable capacitor. A design for a 0.1 μ F capacitor and a summary of PBN wafer fabrication costs are given. M.G.

N82-17439*# Hughes Research Labs., Malibu, Calif.
A 10KW SERIES RESONANT CONVERTER DESIGN, TRANSISTOR CHARACTERIZATION, AND BASE-DRIVE OPTIMIZATION Final Report, 6 May 1980 - 15 Sep. 1981
R. Robson and D. Hancock Nov. 1981 152 p
(Contract NAS3-22471)
(NASA-CR-165546) Avail: NTIS HC A08/MF A01 CSCL 09A

Transistors are characterized for use as switches in resonant circuit applications. A base drive circuit to provide the optimal base drive to these transistors under resonant circuit conditions is developed and then used in the design, fabrication and testing of a breadboard, spaceborne type 10 kW series resonant converter. S.L.

N82-18506*# Westinghouse Electric Corp., Pittsburgh, Pa.
HIGH VOLTAGE POWER TRANSISTOR DEVELOPMENT
Final Report, Nov. 1979 - Sep. 1981
P. L. Hower 30 Oct. 1981 54 p refs
(Contract NAS3-21949)
(NASA-CR-165547; Rpt-81-9F5-HTRAN-R5) Avail: NTIS HC A04/MF A01 CSCL 09A

Design considerations, fabrication procedures, and methods of evaluation for high-voltage power-transistor development are discussed. Technique improvements such as controlling the electric field at the surface and preserving lifetimes in the collector region which have advanced the state of the art in high-voltage transistors are discussed. These improvements can be applied directly to the development of 1200 volt, 200 ampere transistors. M.D.K.

N82-18507*# Pennsylvania State Univ., University Park. Dept. of Electrical Engineering.
SECONDARY ELECTRON EMISSION FROM A CHARGED DIELECTRIC IN THE PRESENCE OF NORMAL AND OBLIQUE ELECTRIC FIELDS M.S. Thesis
Bahram Javidi Feb. 1982 110 p refs
(Grant NsG-3166)
(NASA-CR-168558) Avail: NTIS HC A06/MF A01 CSCL 09C

The secondary electron emission coefficient was obtained for a FEP-Teflon dielectric charged with monoenergetic electrons normally incident upon the surface of the specimen. Measurements of secondary emission coefficient were done for normal and oblique incidence with different primary beam energies in the presence of normal and oblique electric fields. A collimated probing beam was directed to different points on the surface of the specimen and the released or accumulated charge was monitored using an electrometer. The measured data for different probing beam energies, different impact points and different angles of incidence were plotted vs. impact energy and impact point. Data analyzed by computer simulations to find the potential distribution on the surface of the specimen and the electric field around it, is presented and discussed. M.D.K.

N82-18508*# Pennsylvania State Univ., University Park. Dept. of Electrical Engineering.
MAPPING OF ELECTRICAL POTENTIAL DISTRIBUTIONS WITH CHARGED PARTICLE BEAMS Final Report, Nov. 1977 - Feb. 1982
James W. Robinson Feb. 1982 61 p refs
(Grant NsG-3166)
(NASA-CR-168556) Avail: NTIS HC A04/MF A01 CSCL 09C

Methods for measuring electrostatic potentials on and near dielectric surfaces charged to several kilovolts are studied. Secondary emission from those charged dielectrics is measured. Candidates for potential measurement include the induced charge, from which potential is calculated; the trajectory endpoints of either high or low energy particles traversing the region near the surface; trajectory impact on the surface; and creating ions at points of interest near the surface. Some of the methods

require computer simulations and iterative calculation if potential maps are to be generated. Several approaches are described and compared. A method using a half-cylinder as a test chamber and low-energy probing beams is adapted for the measurement of secondary emission. N.W.

N82-22438*# Duke Univ., Durham, N. C. Dept. of Electrical Engineering.
ANALYSIS OF TRANSISTOR AND SNUBBER TURN-OFF DYNAMICS IN HIGH-FREQUENCY HIGH-VOLTAGE HIGH-POWER CONVERTERS
Paul M. Wilson, Thomas G. Wilson, and Harry A. Owen, Jr.
[1982] 3 p refs
(Grant NsG-3157)
(NASA-CR-168760; NAS 1.26:168760) Avail: NTIS HC A02/MF A01 CSCL 09C

Dc to dc converters which operate reliably and efficiently at switching frequencies high enough to effect substantial reductions in the size and weight of converter energy storage elements are studied. A two winding current or voltage stepup (buck boost) dc-to-dc converter power stage submodule designed to operate in the 2.5-kW range, with an input voltage range of 110 to 180 V dc, and an output voltage of 250 V dc is emphasized. In order to assess the limitations of present day component and circuit technologies, a design goal switching frequency of 10 kHz was maintained. The converter design requirements represent a unique combination of high frequency, high voltage, and high power operation. The turn off dynamics of the primary circuit power switching transistor and its associated turn off snubber circuitry are investigated. S.L.

N82-23395*# General Electric Co., Philadelphia, Pa. Space Div.
PRELIMINARY DESIGN DEVELOPMENT OF 100 KW ROTARY POWER TRANSFER DEVICE
S. M. Weinberger Mar. 1981 165 p refs
(Contract NAS3-22266)
(NASA-CR-165431; NAS 1.26:165431; GE-81SDS4215) Avail: NTIS HC A08/MF A01 CSCL 09C

Contactless power transfer devices for transferring electrical power across a rotating spacecraft interface were studied. A power level of 100 KW was of primary interest and the study was limited to alternating current devices. Rotary transformers and rotary capacitors together with the required dc to ac power conditioning electronics were examined. Microwave devices were addressed. The rotary transformer with resonant circuit power conditioning was selected as the most feasible approach. The rotary capacitor would be larger while microwave devices would be less efficient. A design analysis was made of a 100 KW, 20 kHz power transfer device consisting of a rotary transformer, power conditioning electronics, drive mechanism and heat rejection system. The size, weight and efficiency of the device were determined. The characteristics of a baseline slip ring were presented. Aspects of testing the 100 KW power transfer device were examined. The power transfer device is a feasible concept which can be implemented using presently available technologies. Author

N82-24424*# Department of Energy, Washington, D. C.
DEVELOPMENT OF A DUAL-FIELD HETEROPOHAR POWER CONVERTER
David B. Eisenhaure, Bruce Johnson, Tim E. Blamptis, and Emery StGeorge Aug. 1981 68 p refs
(Contract NAS3-20817; DE-A101-77CS-1044)
(NASA-CR-165168; NAS 1.26:165168; R-1489) Avail: NTIS HC A04/MF A01 CSCL 10B

The design and testing of a 400 watt, dual phase, dual rotor, field modulated inductor alternator is described. The system is designed for use as a flywheel to ac utility line or flywheel to dc bus (electric vehicle) power converter. The machine is unique in that it uses dual rotors and separately controlled fields to produce output current and voltage which are in phase with each other. Having the voltage and current in phase allows the power electronics to be made of simple low cost components. Based on analytical predictions and experimental results, development of a complete 22 kilowatt (30 Hp) power conversion system is recommended. This system would include power electronics and controls and would replace the inductor alternator with an improved electromagnetic conversion system. Author

N82-24425*# Eaton Engineering and Research Center, Southfield, Mich.

STRAIGHT AND CHOPPED DC PERFORMANCE DATA FOR A GENERAL ELECTRIC 5BY436A1 DC SHUNT MOTOR WITH A GENERAL ELECTRIC EV-1 CONTROLLER Final Report

Paul C. Edie Oct. 1981 58 p

(Contract DEN3-123; DE-AI01-77CS-51044)

(NASA-CR-185507; DOE/NASA/O123-4; NAS 1.26:165507; ERC-TR-8186) Avail: NTIS HC A04/MF A01 CSCL 09C

Both straight and chopped dc motor performance data for a General Electric 5BY436A1 motor with a General Electric EV-1 controller is presented in tabular and graphical formats. Effects of motor temperature and operating voltage are also shown. The maximum motor efficiency is approximately 85% at low operating temperatures in the straight dc mode. Chopped efficiency can be assumed to be 95% under all operating conditions. For equal speeds, the motor operated in the chopped mode develops slightly more torque and draws more current than it does in the straight mode. Author

N82-25442*# Virginia Polytechnic Inst. and State Univ., Blacksburg. Dept. of Electrical Engineering.

INPUT FILTER COMPENSATION FOR SWITCHING REGULATORS Final Report

Fred C. Lee and S. S. Kelkar 1C May 1982 56 p refs (Grant NAG3-81)

(NASA-CR-169005; NAS 1.26:169005) Avail: NTIS HC A04/MF A01 CSCL 09C

The problems caused by the interaction between the input filter, output filter, and the control loop are discussed. The input filter design is made more complicated because of the need to avoid performance degradation and also stay within the weight and loss limitations. Conventional input filter design techniques are then discussed. The concept of pole zero cancellation is reviewed; this concept is the basis for an approach to control the peaking of the output impedance of the input filter and thus mitigate some of the problems caused by the input filter. The proposed approach for control of the peaking of the output impedance of the input filter is to use a feedforward loop working in conjunction with resonant loops, thus forming a total state control scheme. The design of the feedforward loop for a buck regulator is described. A possible implementation of the feedforward loop design is suggested. J.D.

A82-19310* 'Bootstrap' charging of surfaces composed of multiple materials. P. R. Stannard, I. Katz, and D. E. Parks (Systems, Science and Software, La Jolla, CA). (*IEEE, U.S. Defense Nuclear Agency, NASA, and DOE, Annual Conference on Nuclear and Space Radiation Effects, 18th, Seattle, WA, July 21-24, 1981.*) *IEEE Transactions on Nuclear Science*, vol. NS-28, Dec. 1981, p. 4563-4567. 5 refs. USAF-supported research; Contract No. NAS3-22536.

The paper examines the charging of a checkerboard array of two materials, only one of which tends to acquire a negative potential alone, using the NASA Charging Analyzer Program (NASCAP). The influence of the charging material's field causes the otherwise 'non-charging' material to acquire a negative potential due to the suppression of its secondary emission ('bootstrap' charging). The NASCAP predictions for the equilibrium potential difference between the two materials are compared to results based on an analytical model. (Author)

A82-20505* Permanent magnet properties of Mn-Al-C between -50 C and +150 C. Z. A. Abdelnour, H. F. Mildrum, and K. J. Strnat (Dayton, University, Dayton, OH). *IEEE Transactions on Magnetism*, vol. MAG-17, Nov. 1981, p. 2651-2653. 9 refs. Contract No. DEN3-189.

Anisotropic Mn-Al-C (Ni) magnets are potential substitutes for Alnico 5 and 8. The limited machinability of the alloy and the fact that it is cobalt-free made it particularly interesting. The low Curie point and the costly warm extrusion process needed for grain orientation are drawbacks. The objective of this study was a detailed magnetic characterization of the material for possible use in electric machinery. The principal subjects of the study were the largest

extruded bars presently available, of 31 mm diameter. Easy and hard axis magnetization curves and second-quadrant recoil loop fields were measured at various temperatures ranging from -50 C to +150 C. Property variations over the cross section of a bar were also studied. (Author)

A82-20743*# Power system design optimization using Lagrange multiplier techniques. Y. Yu (Xerox Corp., El Segundo, CA) and F. C. Lee (Virginia Polytechnic Institute and State University, Blacksburg, VA). *Power Conversion International Conference, Munich, West Germany, Sept. 14, 1981, Paper*. 18 p. 8 refs. Contract No. NAS3-21051.

An optimization technique using the Lagrange Multiplier Method is proposed to facilitate design of switching power converter systems. The essence of the optimization is to identify the optimal battery voltage level and switching frequency along with the detailed converter design so that the total system weight including the battery and the packaged converter is minimized, and concurrently all specified power circuit performances are satisfied. (Author)

A82-20744* A PWM transistor inverter for an ac electric vehicle drive. J. M. Slicker (Eaton Engineering and Research Center, Southfield, MI). *Institute of Electrical and Electronics Engineers, Annual Meeting, Philadelphia, PA, Oct. 5-9, 1981, Paper*. 8 p. 8 refs. Research supported by the U.S. Department of Energy; Contract No. DEN3-125.

A prototype system consisting of closely integrated motor, inverter, and transaxle has been built in order to demonstrate the feasibility of a three-phase ac transistorized inverter for electric vehicle applications. The microprocessor-controlled inverter employs monolithic power transistors to drive an oil-cooled, three-phase induction traction motor at a peak output power of 30 kW from a 144 V battery pack. Transistor safe switching requirements are discussed, and a circuit is presented for recovering trapped snubber inductor energy at transistor turn-off. V.L.

N82-23394*# Pratt and Whitney Aircraft Group, East Hartford, Conn. Commercial Products Div.

PRELIMINARY STUDY, ANALYSIS AND DESIGN FOR A POWER SWITCH FOR DIGITAL ENGINE ACTUATORS

E. C. Beattie and H. C. Zickwolf, Jr. Sep. 1979 79 p refs

(Contract NAS3-21809)

(NASA-CR-159559; NAS 1.26:159559; PWA-5643-6) Avail: NTIS HC A05/MF A01 CSCL 09A

Innovative control configurations using high temperature switches to operate actuator driving solenoids were studied. The impact on engine control system life cycle costs and reliability of electronic control and (ECU) heat dissipation due to power conditioning and interface drivers were addressed. Various power supply and actuation schemes were investigated, including optical signal transmission and electronics on the actuator, engine driven alternator, and inside the ECU. The use of a switching shunt power conditioner results in the most significant decrease in heat dissipation within the ECU. No overall control system reliability improvement is projected by the use of remote high temperature switches for solenoid drivers. J.M.S.

A82-23494*# Dynamic switch matrix for the TDMA satellite switching system. P. T. Ho, J. H. Wisniewski, J. R. Pelose, and H. M. Perasso (Ford Aerospace and Communications Corp., Western Development Laboratories Div., Palo Alto, CA). In: *Communications Satellite Systems Conference, 9th, San Diego, CA, March 7-11, 1982, Collection of Technical Papers.* (A82-23476 09-32) New York, American Institute of Aeronautics and Astronautics, 1982, p. 135-141. 11 refs. Contract No. NAS3-22501. (AIAA 82-0458)

Future high capacity satellite communication systems require signal processing on board satellites. The on-board signal processing includes switching of RF signals between multiple antennas to provide interconnection between the uplink and downlink beams. This paper describes the development of a dynamic switch matrix for a TDMA satellite switching system to be used in the next generation communications satellites. In this paper, a dynamic switch matrix,

which includes the microwave switch matrix, the distribution control unit and the timing source, will be described. Several different microwave switch matrix architectures and switching devices were evaluated and compared. A unique coupler crossbar switch matrix architecture with dual-gate field effect transistor as switching element was developed. Experimental results of both microwave switch matrix (MSM) and distribution control unit (DCU) are presented. These test results verify the MSM with coupler crossbar architecture and dual-gate FET as switching element will meet the future SS-TDMA system requirements. Finally, the reliability of the dynamic switch matrix is addressed. The analysis shows reliability of 0.9981 for 7 year space operation can be achieved for the designed dynamic switch matrix. (Author)

A82-23566 * # IMPATT power building blocks for 20 GHz spaceborne transmit amplifier. J. Asmus, Y. Cho, J. deGruyl, E. Ng, A. Giannakopoulos, and H. C. Okean (LNR Communications, Inc., Hauppauge, NY). In: Communications Satellite Systems Conference, 9th, San Diego, CA, March 7-11, 1982, Collection of Technical Papers. (A82-23476 09-32) New York, American Institute of Aeronautics and Astronautics, 1982, p. 715-720. Contracts No. NAS3-22491; No. F33615-80-C-1182. (AIAA 82-0498)

Single-stage circulator coupled IMPATT building block constituents of a 20-GHz solid state power amplifier (SSPA) currently under development for spaceborne downlink transmitter usage have been demonstrated as providing 1.5 to 2.0W RF power output at 4 to 5 dB operating gain over a 1 GHz bandwidth. Using either commercially available or recently developed in-house GaAs Schottky Read-profile IMPATT diodes, DC/RF power added efficiencies of 14 to 15% were achieved in these amplifier stages. A two stage IMPATT driver amplifier with similar RF output power capability exhibited 13 + or - 0.5 dB operating gain over a 1 GHz bandwidth. (Author)

A82-36926 * # Fast recovery, high voltage silicon diodes for AC motor controllers. V. Balodis, A. H. Berman, and C. Gaugh (Power Transistor Co., Torrance, CA). *PCI/Motorcon '82, Conference, San Francisco, CA, Mar. 29, 1982, Paper. 9 p. 5 refs.* Contract No. NAS3-22539.

The fabrication and characterization of a high voltage, high current, fast recovery silicon diode for use in AC motor controllers, originally developed for NASA for use in avionics power supplies, is presented. The diode utilizes a positive bevel PIN mesa structure with glass passivation and has the following characteristics: peak inverse voltage - 1200 volts, forward voltage at 50 amperes - 1.5 volts, reverse recovery time of 200 nanoseconds. Characterization data for the diode, included in a table, show agreement with design concepts developed for power diodes. Circuit diagrams of the diode are also given. N.B.

A82-36927 * # A 10-kW series resonant converter design, transistor characterization, and base-drive optimization. R. R. Robson and D. J. Hancock (Hughes Research Laboratories, Malibu, CA). *Institute of Electrical and Electronics Engineers, Annual Power Electronics Specialists Conference, 13th, Massachusetts Institute of Technology, Cambridge, MA, June 14-17, 1982, Paper. 12 p.* Contract No. NAS3-22471.

The development, components, and performance of a transistor-based 10 kW series resonant converter for use in resonant circuits in space applications is described. The transistors serve to switch on the converter current, which has a half-sinusoid waveform when the transistor is in saturation. The goal of the program was to handle an input-output voltage range of 230-270 Vdc, an output voltage range of 200-500 Vdc, and a current limit range of 0-20 A. Testing procedures for the D60T and D7ST transistors are outlined and base drive waveforms are presented. The total device dissipation was minimized and found to be independent of the regenerative feedback ratio at lower current levels. Dissipation was set at within 10% and rise times were found to be acceptable. The finished unit displayed a 91% efficiency at full power levels of 500 V and 20 A and 93.7% at 500 V and 10 A. M.S.I.C.

A82-40403 * Compensation mechanism in liquid encapsulated Czochralski GaAs - Importance of melt stoichiometry. D. E. Holmes, R. T. Chen, K. R. Elliott, C. G. Kirkpatrick (Rockwell International Corp., Microelectronics Research and Development Center, Thousand Oaks, CA), and P. W. Yu (Wright State University, Dayton, OH). (*Institute of Electrical and Electronics Engineers, GaAs Integrated Circuits Symposium, San Diego, CA, Oct. 27-29, 1981.*) *IEEE Transactions on Electron Devices*, vol. ED-29, July 1982, p. 1045-1051. 25 refs. Contracts No. NAS3-22224; No. F33615-81-C-1406.

It is shown that the key to reproducible growth of undoped semi-insulating GaAs by the liquid encapsulated Czochralski (LEC) technique is the control over the melt stoichiometry. Twelve crystals were grown from stoichiometric and nonstoichiometric melts. The material was characterized by secondary ion mass spectrometry, localized vibrational mode far infrared spectroscopy, Hall-effect measurements, optical absorption, and photoluminescence. A quantitative model for the compensation mechanism in the semi-insulating material was developed based on these measurements. The free carrier concentration is controlled by the balance between EL2 deep donors and carbon acceptors; furthermore, the incorporation of EL2 is controlled by the melt stoichiometry, increasing as the As atom fraction in the melt increases. As a result, semi-insulating material can be grown only from melts above a critical As composition. The practical significance of these results is discussed in terms of achieving high yield and reproducibility in the crystal growth process. (Author)

A82-43784 * Wideband, high speed switch matrix development for SS-TDMA applications. W. H. Prather, B. J. Cory, R. F. Wade, W. J. Taft, and R. E. Buzinski (General Electric Co., Fairfield, CT). In: ICC '81; International Conference on Communications, Denver, CO, June 14-18, 1981, Conference Record, Volume 1. (A82-43778 22-32) New York, Institute of Electrical and Electronics Engineers, Inc., 1981, p. 5.3.1-5.3.5. Contract No. NAS3-22500.

The paper describes the design of an SS-TDMA microwave switch matrix being developed as part of the NASA 30/20 GHz Communications Satellite Program. A critical element in the systems development is the high-speed wideband switching capability necessary for 30/20 GHz SS-TDMA trunking service interconnections. A proof-of-concept model of a 20-by-20 microwave switch matrix with a 2.5 GHz bandwidth and 10-nanosecond switching speeds is being developed to realize this capability. B.J.

A82-43867 * Near optimum delay-line detection filters for serial detection of MSK signals. R. E. Ziemer and C. R. Ryan (Motorola, Inc., Government Electronics Div., Scottsdale, AZ). In: ICC '81; International Conference on Communications, Denver, CO, June 14-18, 1981, Conference Record, Volume 3. (A82-43776 22-32) New York, Institute of Electrical and Electronics Engineers, Inc., 1981, p. 56.2.1-56.2.5. 6 refs. Contract No. NAS3-22502.

A method for designing transversal delay-line filter approximations to the matched filter for the serial detection of minimum-shift keyed (MSK) modulated signals is given. Two configurations are characterized in terms of signal-to-noise ratio degradation at a bit error rate (BER) of 10 to the -6th. One is shown to depart less than 0.3 dB from the ideal matched filter performance when its parameter values are optimized. A lumped-element equivalent is also given and shown to provide a degradation of less than 0.4 dB at a BER of 10 to the -6th. (Author)

A82-46385 * Modeling the full-bridge series-resonant power converter. R. J. King and T. A. Stuart (Toledo, University, Toledo, OH). *IEEE Transactions on Aerospace and Electronic Systems*, vol. AES-18, July 1982, p. 449-459. 8 refs. Grant No. NSG-3281.

A steady state model is derived for the full-bridge series-resonant power converter. Normalized parametric curves for various currents and voltages are then plotted versus the triggering angle of the switching devices. The calculations are compared with experimental measurements made on a 50 kHz converter and a discussion of certain operating problems is presented. (Author)

ORIGINAL PAGE IS
OF POOR QUALITY

34 FLUID MECHANICS AND HEAT TRANSFER

Includes boundary layers; hydrodynamics; fluidics; mass transfer; and ablation cooling.

For related information see also 02 Aerodynamics and 77 Thermodynamics and Statistical Physics.

N82-11397* National Aeronautics and Space Administration, Lewis Research Center, Cleveland, Ohio.

LEWIS RESEARCH CENTER'S COAL-FIRED, PRESSURIZED, FLUIDIZED-BED REACTOR TEST FACILITY

John A. Kobak and R. James Rollbuhler Oct. 1981 35 p refs
(NASA-TM-81616; E-621) Avail: NTIS HC A03/MF A01 CSCL 20D

A 200-kilowatt-thermal, pressurized, fluidized-bed (PFB) reactor, research test facility was designed, constructed, and operated as part of a NASA-funded project to assess and evaluate the effect of PFB hot-gas effluent on aircraft turbine engine materials that might have applications in stationary-power-plant turbogenerators. Some of the techniques and components developed for this PFB system are described. One of the more important items was the development of a two-in-one, gas-solids separator that removed 95+ percent of the solids in 1600 F to 1900 F gases. Another was a coal and sorbent feed and mixing system for injecting the fuel into the pressurized combustor. Also important were the controls and data-acquisition systems that enabled one person to operate the entire facility. The solid, liquid, and gas sub-systems all had problems that were solved over the 2-year operating time of the facility, which culminated in a 400-hour, hot-gas, turbine test. A.R.H.

N82-11399* National Aeronautics and Space Administration, Lewis Research Center, Cleveland, Ohio.

HIGH THERMAL POWER DENSITY HEAT TRANSFER Patent Application

James F. Morris, inventor (to NASA) Filed 30 Oct. 1980 10 p
(NASA-Case-LEW-12950-1; US-Patent-Appl-SN-202228) Avail: NTIS HC A02/MF A01 CSCL 20D

Heat from a high temperature heat pipe is transferred through a vacuum or a gap filled with electrically nonconducting gas to a cooler heat pipe. The heat pipe is used to cool the nuclear reactor while the heat pipe is connected thermally and electrically to a thermionic converter. If the receiver requires greater thermal power density, geometries are used with larger heat pipe areas for transmitting and receiving energy than the area for conducting the heat to the thermionic converter. In this way the heat pipe capability for increasing thermal power densities compensates for the comparatively low thermal power densities through the electrically non-conducting gap between the two heat pipes.

NASA

N82-17453* National Aeronautics and Space Administration, Lewis Research Center, Cleveland, Ohio.

EFFECTS OF ARC CURRENT ON THE LIFE IN BURNER RIG THERMAL CYCLING OF PLASMA SPRAYED ZrO₂-YSUB₂O₃

R. C. Hendricks and G. McDonald 1982 9 p refs Presented at the 6th Ann. Conf. on Composites, Cocoa Beach, Fla., 17-21 Jan. 1982; sponsored by the American Ceramic Society (NASA-TM-82795; E-1129) Avail: NTIS HC A02/MF A01 CSCL 20D

An analysis of thermal cycle life data for four sets of eight thermal barrier coated specimens representing arc currents (plasma gun power) of 525, 600, 800, or 950 amps is presented. The ZrO₂-BY2O₃/NiCrAlY plasma spray coated Rene 41 rods were thermal cycled to 1040 C in a Mach 0.3-Jet A/air burner flame. The experimental results indicate the existence of a minimum or threshold power level which coating life expectancy is less than 500 cycles. Above the threshold power level, coating life expectancy more than doubles and increases with arc current. T.M.

N82-19493* National Aeronautics and Space Administration, Lewis Research Center, Cleveland, Ohio.

EFFECT OF LOCATION IN AN ARRAY ON HEAT TRANSFER TO A CYLINDER IN CROSSFLOW

Robert J. Simoneau and G. James VanFossen, Jr. 1982 15 p refs Proposed for presentation at the 3rd Joint Thermophy. Fluids, Plasma and Heat Transfer Conf., St. Louis, 7-11 Jun. 1982
(NASA-TM-82797; E-1131) Avail: NTIS HC A02/MF A01 CSCL 20D

An experiment was conducted to measure the heat transfer from a heated cylinder in crossflow in an array of circular cylinders. All cylinders had a length-to-diameter ratio of 3.0. Both in-line and staggered array patterns were studied. The cylinders were spaced 2.67 diameters apart center-to-center in both the axial and transverse directions to the flow. The row containing the heated cylinder remained in a fixed position in the channel and the relative location of this row within the array was changed by adding up to five upstream rows. The working fluid was nitrogen gas at pressures from 100 to 600 kPa. The Reynolds number ranged based on cylinder diameter and average unobstructed channel velocity was from 5,000 to 125,000. Turbulence intensity; profiles were measured for each case at a point one half space upstream of the row containing the heated cylinder. The basis of comparison for all the heat transfer data was the single row with the heated cylinder. For the in-line cases the addition of a single row of cylinders upstream of the row containing the heated cylinder increased the heat transfer by an average of 50 percent above the base case. Adding up to five more rows caused no increase or decrease in heat transfer. Adding rows in the staggered array cases resulted in average increases in heat transfer of 21, 64, 58, 46, and 46 percent for one to five upstream rows, respectively. Author

N82-19494* National Aeronautics and Space Administration, Lewis Research Center, Cleveland, Ohio.

HYDRODYNAMIC AND AERODYNAMIC BREAKUP OF LIQUID SHEETS

R. Ingebo 1982 5 p refs Proposed for presentation at the 2nd Intern. Conf. on Liquid Atomization and Spray Systems, Madison, Wisc., 20-24 Jun. 1982
(NASA-TM-82800; E1139) Avail: NTIS HC A02/MF A01 CSCL 20D

The effect of hydrodynamic, aerodynamic and liquid surface forces on the mean drop diameter of water sprays that are produced by the breakup of nonswirling and swirling water sheets in quiescent air and in airflows similar to those encountered in gas turbine combustors is investigated. The mean drop diameter is used to characterize fuel sprays and it is a very important factor in determining the performance and exhaust emissions of gas turbine combustors. S.L.

N82-20467* National Aeronautics and Space Administration, Lewis Research Center, Cleveland, Ohio.

FLOW THROUGH ALIGNED SEQUENTIAL ORIFICE TYPE INLETS

Robert C. Hendricks and T. Trent Stetz Mar. 1982 53 p refs
(NASA-TP-1967; E-682; NAS 1.60:1967) Avail: NTIS HC A04/MF A01 CSCL 20D

Choked flow rate and pressure profile data were taken and studied for configurations consisting of four axially aligned, sequential orifice inlets of 0.5 length diameter ratio with separation distances of 0.66 and 32 diameters. A flow coefficient - reduced temperature plot represents the flow rate data for the two cases. At a separation distance of 32 diameters the pressure profiles dropped sharply at the entrance and partially recovered within each orifice - the exception being at low temperatures, where fluid jetting through the last orifice occurred. At a separation distance of 0.66 diameter fluid jetting was prevalent at the lower inlet temperatures. These results are in qualitative agreement with data for four axially aligned, sequential Borda inlets and for tubes with single sharp edge orifice or Borda inlets to L/D's of 105 and with a water flow visualization study. S.L.

N82-22453* National Aeronautics and Space Administration, Lewis Research Center, Cleveland, Ohio.

GENERATION OF INSTABILITY WAVES AT A LEADING EDGE

Marvin E. Goldstein 1982 12 p refs Proposed for presentation

ORIGINAL PAGE IS
OF POOR QUALITY

at the 3rd Joint Thermophys. Fluids, Plasma and Heat Transfer Conf., St. Louis, 7-11 Jun, 1982; sponsored by AIAA and ASME

(NASA-TM-82835; E-1201; NAS 1.15:82835) Avail; NTIS HC A02/MF A01 CSCL 20D

Two cases are considered. The first is concerned with mean flows of the Blasius type wherein the instabilities are represented by Tollmien-Schlichting waves. It is shown that the latter are generated fairly far downstream of the edge and are the result of a wave length reduction process that tunes the free stream disturbances to the Tollmien-Schlichting wave length. The other case is concerned with inflectional, uni-directional, transversely sheared mean flows. Such idealized flows provide a fairly good local representation to the nearly parallel flows in jets. They can support inviscid instabilities of the Kelvin-Helmholtz type. The various mathematically permissible mechanisms that can couple these instabilities to the upstream disturbances are discussed.

T.M.

N82-24449* National Aeronautics and Space Administration, Lewis Research Center, Cleveland, Ohio.

MAGNETIC HEAT PUMPING Patent Application

Gerald V. Brown, inventor (to NASA) Filed 19 Feb. 1981 20 p

(NASA-Case-LEW-12508-3; US-Patent-Appl-SN-235868) Avail; NTIS HC A02/MF A01 CSCL 20D

The method of the invention employs ferromagnetic or ferrimagnetic elements, preferably of rare-earth based material, for example gadolinium, and preferably employs a regenerator. The steps of the method comprise controlling the temperature and applied magnetic field of the element to cause the state of the element as represented on a temperature-magnetic entropy diagram repeatedly to traverse a loop. The loop may have a first portion of concurrent substantially isothermal or constant temperature and increasing applied magnetic field, a second portion of lowering temperature and constant applied magnetic field, a third portion of isothermal and decreasing applied magnetic field, and a fourth portion of increasing temperature and constant applied magnetic field. Other loops may be four-sided, with, for example, two isotherms and two adiabats (constant entropy portions). Preferably, a regenerator may be employed to enhance desired cooling or heating effects, with varied magnetic fields or varying temperatures including three-sided figures traversed by the representative point.

NASA

N82-24455* National Aeronautics and Space Administration, Lewis Research Center, Cleveland, Ohio.

FLOWS THROUGH SEQUENTIAL ORIFICES WITH HEATED SPACER RESERVOIRS

R. C. Hendricks and T. Tront Stetz (Miami Univ., Oxford, Ohio) 1982 13 p refs Presented at the 9th Intern. Cryogenics Eng. Conf./Intern. Cryogenic Mater. Conf., Kobe, Japan, 11-14 May 1982

(NASA-TM-82855; E-1224; NAS 1.15:82855) Avail; NTIS HC A02/MF A01 CSCL 20D

Flow rates and pressure thermal profiles for two phase choked flows of fluid nitrogen were studied theoretically and experimentally in a four sequential orifice configuration. Both theory and experimental evidence demonstrate that heat addition in the first spacer-reservoir adjacent to the inlet orifice is most effective in reducing the flow rate and that heat addition in the last spacer-reservoir is least effective. The flows are choked at the exit orifice for large spacings and at the inlet orifice for small spacings. The moderate addition of heat available for this experiment did not materially alter this result for large spacings; however, significant heat addition for the small spacings tended to shift the choke point to the exit orifice. Nitrogen is used as the working fluid over a range of states from liquid to gas with a reduced inlet stagnation pressure range to $P_{sub} r, o = 2$.

Author

N82-25463* National Aeronautics and Space Administration, Lewis Research Center, Cleveland, Ohio.

COVERING SOLID, FILM COOLED SURFACES WITH A DUPLEX THERMAL BARRIER COATING Patent Application

C. H. Liebert, inventor (to NASA) Filed 8 Dec. 1981 9 p (NASA-Case-LEW-13450-1; US-Patent-Appl-SN-328760) Avail; NTIS HC A02/MF A01 CSCL 20D

A thermal barrier coating is applied to solid film cooled hardware. Also, thermal barrier coating systems are used to provide corrosion resistance and thermal protection to these base metal surfaces. An inert gas, such as argon, is discharged through the apertures during the application of the thermal barrier coating system by plasma spraying. This flow of inert gas reduces both blocking of the holes and base metal oxidation during the coating operation.

NASA

N82-26611* National Aeronautics and Space Administration, Lewis Research Center, Cleveland, Ohio.

DEPOSIT FORMATION IN HYDROCARBON ROCKET FUELS WITH AN EVALUATION OF A PROPANE HEAT TRANSFER CORRELATION

Philip A. Masters and Carl A. Aukerman 1982 16 p refs Presented at 18th Joint Propulsion Conf., Cleveland, 21-23 Jun. 1982; sponsored by AIAA, SAE and ASME

(NASA-TM-82911; E-1245; NAS 1.15:82911) Avail; NTIS HC A02/MF A01 CSCL 20D

A high pressure fuel coking testing apparatus was designed and developed and was used to evaluate thermal decomposition limits and carbon decomposition rates in heated copper tubes for hydrocarbon fuels. A commercial propane (90% grade) and chemically pure (CP) propane were tested. Heat transfer to supercritical propane was evaluated at 136 atm, bulk fluid velocities of 6 to 30 m/s, and tube wall temperatures in the range of 422 to 811 K. A forced convection heat transfer correlation developed in a previous test effort verified a prediction of most of the experimental data within a $\pm 1r - 30\%$ range, with good agreement for the CP propane data. No significant differences were apparent in the predictions derived from the correlation when the carbon resistance was included with the film resistance. A post-test scanning electron microprobe analysis indicated occurrences of migration and interdiffusion of copper into the carbon deposit.

Author

N82-28574* National Aeronautics and Space Administration, Lewis Research Center, Cleveland, Ohio.

THE DRYOUT REGION IN FRICTIONALLY HEATED SLIDING CONTACTS

R. C. Hendricks, J. Braun (Akron Univ., Ohio), V. Arp, and P. J. Giarratano (NBS, Boulder, Colo.) 1982 20 p refs Proposed for presentation at the Intern. Heat Transfer Conf., Munich, 6-10 Sep. 1982; sponsored by the Am. Soc. of Mech. Engr. (NASA-TM-82796) Avail; NTIS HC A02/MF A01 CSCL 13I

Some conditions under which boiling and two-phase flow can occur in or near a wet sliding contact are determined and illustrated. The experimental apparatus consisted of a tool pressed against an instrumented slider plate and motion picture sequences at 4000 frames/sec. The temperature and photographic data demonstrated surface conditions of boiling, drying, trapped gas evolution (solutions), and volatility of fluid mixture components. The theoretical modeling and analysis are in reasonable agreement with experimental data.

Author

N82-30498* National Aeronautics and Space Administration, Lewis Research Center, Cleveland, Ohio.

FLOW VISUALIZATION STUDY OF THE HORSESHOE VORTEX IN A TURBINE STATOR CASCADE

Raymond E. Gaugler and Louis M. Russell Jun, 1982 33 p refs

(NASA-TP-1884; E-915; NAS 1.60:1884) Avail; NTIS HC A03/MF A01 CSCL 20D

Flow visualization techniques were used to show the behavior of the horseshoe vortex in a large scale turbine stator cascade. Oil drops on the end wall surface flowed in response to local shear stresses, indicating the limiting flow streamlines at the surface. Smoke injected into the flow and photographed showed time averaged flow behavior. Neutrally buoyant helium filled soap bubbles followed the flow and showed up on photographs as streaks, indicating the paths followed by individual fluid particles. Preliminary attempts to control the vortex were made by injecting air through control jets drilled in the end wall near the vane leading edge. Seventeen different hole locations were tested, one at a time, and the effect of the control jets on the path followed by smoke in the boundary layer was recorded photographically.

S.L.

ORIGINAL PAGE IS
OF POOR QUALITY

N82-32633* # National Aeronautics and Space Administration, Lewis Research Center, Cleveland, Ohio.

USE OF FIBER LIKE MATERIALS TO AUGMENT THE CYCLE LIFE OF THICK THERMOPROTECTIVE SEAL COATINGS

R. C. Hendricks and G. McDonald Aug. 1982 14 p refs Presented at Intern. Conf. on Met. Coatings and Process Technol., San Diego, Calif., 4-9 Apr. 1982; sponsored by American Vacuum Society (NASA-TM-82901; E-1284; NAS 1.15:82901) Avail: NTIS HC A02/MF A01 CSCL 20D

Some experimental and analytical studies of plasma sprayed $ZrO_2\text{-}Y_2O_3$ thick seal thermoprotective materials over NiCrAlY bond coats with testing to 1040 deg C in a Mach 0.3 burner flame are reviewed. These results indicate the need for material to have both compliance and sufficient strength to function successfully as a thick thermoprotective seal material. Fibrous materials may satisfy many of these requirements. A preliminary analysis simulating the simplified behavior of a 25 mm cylindrical SiO_2 -fiber material indicated significant radial temperature gradients, a relatively cool interface and generally acceptable stresses over the initial portion of the thermal cycle. Subsequent testing of these fiberlike materials in a Mach 0.3 Jet A/air burner flame confirmed these results. Author

N82-32634* # National Aeronautics and Space Administration, Lewis Research Center, Cleveland, Ohio.

TURBULENT SOLUTION OF THE NAVIER-STOKES EQUATIONS FOR UNIFORM SHEAR FLOW

R. G. Deissler 1981 31 p refs Presented at the Fluid Dyn. Meeting of the Am. Phys. Soc., Monterey, Calif., 23-24 Nov. 1981 (NASA-TM-82925; E-1202; NAS 1.15:82925) Avail: NTIS HC A03/MF A01 CSCL 20D

To study the nonlinear physics of uniform turbulent shear flow, the unaveraged Navier-Stokes equations are solved numerically. This extends our previous work in which mean gradients were absent. For initial conditions, modified three-dimensional-cosine velocity fluctuations are used. The boundary conditions are modified periodic conditions on a stationary three-dimensional numerical grid. A uniform mean shear is superimposed on the initial and boundary conditions. The three components of the mean-square velocity fluctuations are initially equal for the conditions chosen. As in the case of no shear the initially nonrandom flow develops into an apparently random turbulence at higher Reynolds number. Thus, randomness or turbulence can apparently arise as a consequence of the structure of the Navier-Stokes equations. Except for an initial period of adjustment, all fluctuating components grow with time. The initial equality of the three intensity components is destroyed by the shear, the transverse components becoming smaller than the longitudinal one, in agreement with experiment. Also, the shear creates a small-scale structure in the turbulence. The nonlinear solutions are compared with linearized ones. Author

A82-10964 * # Flow through axially aligned sequential apertures of the orifice and Borda types. R. C. Hendricks and T. T. Stetz (NASA, Lewis Research Center, Cleveland, OH). *American Society of Mechanical Engineers and American Institute of Chemical Engineers, National Heat Transfer Conference, 20th, Milwaukee, WI, Aug. 2-5, 1981, ASME Paper 81-HT-79*. 9 p. 17 refs. Members, \$2.00; nonmembers, \$4.00.

Choked flow rate and pressure profile data were taken and studied for two axially aligned sequential configurations consisting of: (1) Four Borda type inlets of 1.9 1/D with two separation distances of 0.8 and 30 diameters. (2) Four orifice type inlets of 0.5 1/D with two separation distances of 0.66 and 32 diameters. A flow-coefficient reduced-temperature plot can be used to represent the flow rate data for each geometry. At the larger separation distances, the pressure profiles dropped sharply at the entrance and partially recovered within each of the Borda and orifice inlet configurations; the exception being the last inlet where at low entrance temperatures, fluid jetting could occur. For the smaller

spacings fluid jetting was prevalent throughout each of the inlet configurations at lower inlet temperatures. These results are in qualitative agreement with data of tubes with single Borda or sharp-edge orifice type inlets to 105 1/D and water flow visualization studies. (Author)

A82-14848 * # Heat transfer in cooled porous region with curved boundary. R. Siegel and A. Snyder (NASA, Lewis Research Center, Cleveland, OH). *ASME, Transactions, Journal of Heat Transfer*, vol. 103, Nov. 1981, p. 765-771, 7 refs.

Heat transfer characteristics are analyzed for a cooled two-dimensional porous medium having a curved boundary. A general analytical procedure is given in combination with a numerical conformal mapping method used to transform the porous region into an upper half plane. To illustrate the method, results are evaluated for a cosine shaped boundary subjected to uniform external heating. The results show the effects of coolant starvation in the thick regions of the medium, and the extent that internal heat conduction causes the heated surface to have a more uniform temperature. (Author)

A82-16071 * Distorted turbulence in axisymmetric flow. P. A. Durbin (NASA, Lewis Research Center, Cleveland, OH). *Quarterly Journal of Mechanics and Applied Mathematics*, vol. 34, Nov. 1981, p. 489-500, 6 refs.

A solution to the rapid-distortion theory for small-scale turbulence in flow round an axisymmetric obstacle is derived. General formulae for velocity covariances and Eulerian time scales are obtained and are evaluated for the particular case of flow round a sphere. The large-scale limit for this flow is also discussed. (Author)

A82-16570 * # Toward the use of similarity theory in two-phase choked flows. R. C. Hendricks, R. J. Simoneau (NASA, Lewis Research Center, Cleveland, OH), and J. V. Sengers (Maryland, University, College Park, MD). In: *Scaling in two-phase flows; Proceedings of the Winter Annual Meeting, Chicago, IL, November 16-21, 1980*. Meeting sponsored by the American Society of Mechanical Engineers, New York, American Society of Mechanical Engineers (Heat Transfer Symposia Series. HTD Volume 14), 1980, p. 45-53, 13 refs.

Comparison of two-phase choked flows in normalized coordinates were made between pure components and available data using a reference fluid to compute the thermophysical properties. The results are favorable. Solution of the governing equations for two LNG mixtures show some possible similarities between the normalized choked flows of the two mixtures, but the departures from the pure component loci are significant. (Author)

A82-39899 * Cauchy integral method for two-dimensional solidification interface shapes. R. Siegel and D. J. Sosoka (NASA, Lewis Research Center, Cleveland, OH). *International Journal of Heat and Mass Transfer*, vol. 25, July 1982, p. 975-984, 10 refs.

A method is developed to determine the shape of steady state solidification interfaces formed when liquid above its freezing point circulates over a cold surface. The solidification interface, which is at uniform temperature, will form in a shape such that the non-uniform energy convected to it is locally balanced by conduction into the solid. The interface shape is of interest relative to the crystal structure formed during solidification; regulating the crystal structure has application in casting naturally strengthened metallic composites. The results also pertain to phase-change energy storage devices, where the solidified configuration and overall heat transfer are needed. The analysis uses a conformal mapping technique to relate the desired interface coordinates to the components of the temperature gradient at the interface. These components are unknown because the interface shape is unknown. A Cauchy integral formulation provides a second relation involving the components, and a simultaneous solution yields the interface shape. (Author)

A82-40781 * Analysis of the decay of temperature fluctuations in isotropic turbulence. P. A. Durbin (NASA, Lewis Research Center, Cleveland, OH). *Physics of Fluids*, vol. 25, Aug. 1982, p. 1328-1332, 10 refs.

The Lagrangian dispersion theory of Durbin (1980) is used to analyze experiments by Warhaft and Lumley (1978) and by Sreenivasan et al. (1980) on temperature fluctuations in grid-generated turbulence. Both theory and experiment

ORIGINAL PAGE IS
OF POOR QUALITY

show that the decay exponent m depends on the ratio of the initial length scales of velocity and temperature, although when this ratio is greater than 2.5 such dependence is negligible. The theory shows that m is not truly constant, but within the range covered by the experiments it is nearly so. The agreement between theory and experiment lends credence to the idea that the decay of fluctuations is controlled largely by turbulent relative dispersion. (Author)

N82-15360* Oklahoma State Univ., Stillwater. School of Mechanical and Aerospace Engineering.

INVESTIGATIONS OF FLOWFIELDS FOUND IN TYPICAL COMBUSTOR GEOMETRIES Semiannual Status Report, 1 Jan. - 31 Jul. 1981

D. G. Lilley and D. K. McLaughlin (Dynamics Technology, Inc., Torrance, Calif.) 31 Jul. 1981 243 p refs (Grant NAG3-74) (NASA-CR-185091; SASR-2) Avail: NTIS HC A11/MF A01 CSCL 20D

The flowfields of gas turbine combustion chambers were investigated. Six flowfield configurations with sidewall angles $\alpha = 90$ and 45 deg. and swirl vane angles $\phi = 0, 45$ and 70 deg. are characterized. Photography of neutrally-buoyant helium-filled soap bubble, tufts, and injected smoke helps to characterize the time-mean streamlines, recirculation zones and regions of highly turbulent flow. Five-hole pitot probe pressure measurements allow the determination of time-mean velocities u, v and w . An advanced computer code equipped with a standard two-equation kappa-epsilon turbulence model was used to predict corresponding flow situations and to compare results with the experimental data. J.D.H.

N82-17456* Stanford Univ., Calif. Dept. of Mechanical Engineering.

TURBULENCE BOUNDARY LAYER HEAT TRANSFER EXPERIMENTS: CONVEX CURVATURE EFFECTS INCLUDING INTRODUCTION AND RECOVERY Final Report

T. W. Simon, R. J. Moffat, J. P. Johnston, and W. M. Kays Washington NASA Feb. 1982 217 p refs (Grants NSG-3124; NAG3-3) (NASA-CR-3510; HMT-32) Avail: NTIS HC A10/MF A01 CSCL 20D

Measurements were made of the heat transfer rate through turbulent and transitional boundary layers on an isothermal, convexly curved wall and downstream flat plate. The effect of convex curvature on the fully turbulent boundary layer was a reduction of the local Stanton numbers 20% to 50% below those predicted for a flat wall under the same circumstances. The recovery of the heat transfer rates on the downstream flat wall was extremely slow. After 60 cm of recovery length, the Stanton number was still typically 15% to 20% below the flat wall predicted value. Various effects important in the modeling of curved flows were studied separately. These are: the effect of initial boundary layer thickness, the effect of freestream velocity, the effect of freestream acceleration, the effect of unheated starting length, and the effect of the maturity of the boundary layer. An existing curvature prediction model was tested against this broad heat transfer data base to determine where it could appropriately be used for heat transfer predictions. S.L.

N82-19495* Oklahoma State Univ., Stillwater. School of Mechanical and Aerospace Engineering.

INVESTIGATIONS OF FLOWFIELDS FOUND IN TYPICAL COMBUSTOR GEOMETRIES Semiannual Status Report, 1 Aug. 1981 - 31 Jan. 1982

D. G. Lilley 31 Jan. 1982 138 p refs (Grant NAG3-74) (NASA-CR-168585; SASR-3) Avail: NTIS HC A07/MF A01 CSCL 20D

Measurements and computations are being applied to an axisymmetric swirling flow, emerging from swirl vanes at angle ϕ , entering a large chamber test section via a sudden expansion of various side-wall angles α . New features are: the turbulence measurements are being performed on swirling as well as nonswirling flow; and all measurements and computations are also being performed on a confined jet flowfield with realistic downstream blockage. Recent activity falls into three categories: (1) Time-mean flowfield characterization by five-hole pitot probe

measurements and by flow visualization; (2) Turbulence measurements by a variety of single- and multi-wire hot-wire probe techniques; and (3) Flowfield computations using the computer code developed during the previous year's research program.

Author

N82-19498* United Technologies Research Center, East Hartford, Conn.

MASS AND MOMENTUM TURBULENCE TRANSPORT EXPERIMENTS WITH CONFINED COAXIAL JETS Interim Report, 18 Feb. - 18 Oct. 1981

B. V. Johnson and J. C. Bennett Nov. 1981 157 p refs (Contract NAS3-22771) (NASA-CR-165574; R81-915540-9) Avail: NTIS HC A08/MF A01 CSCL 20D

Downstream mixing of coaxial jets discharging in an expanded duct was studied to obtain data for the evaluation and improvement of turbulent transport models currently used in a variety of computational procedures throughout the propulsion community for combustor flow modeling. Flow visualization studies showed four major shear regions occurring: a wake region immediately downstream of the inner jet inlet duct; a shear region further downstream between the inner and annular jets; a recirculation zone; and a reattachment zone. A combination of turbulent momentum transport rate and two velocity component data were obtained from simultaneous measurements with a two color laser velocimeter (LV) system. Axial, radial and azimuthal velocities and turbulent momentum transport rate measurements in the $r-z$ and r - θ planes were used to determine the mean value, second central moment (or rms fluctuation from mean), skewness and kurtosis for each data set probability density function (p.d.f.). A combination of turbulent mass transport rate, concentration and velocity data were obtained system. Velocity and mass transport in all three directions as well as concentration distributions were used to obtain the mean, second central moments, skewness and kurtosis for each p.d.f. These LV/LIF measurements also exposed the existence of a large region of countergradient turbulent axial mass transport in the region where the annular jet fluid was accelerating the inner jet fluid. S.L.

N82-22455* Georgia Inst. of Tech., Atlanta. School of Aerospace Engineering.

A NEW NUMERICAL APPROACH FOR COMPRESSIBLE VISCOUS FLOWS Final Report

J. C. Wu and S. G. Lekoudis Mar. 1982 105 p refs (Grant NSG-3307) (NASA-CR-168842; NAS 1.26:168842) Avail: NTIS HC A06/MF A01 CSCL 20D

A numerical approach for computing unsteady compressible viscous flows was developed. This approach offers the capability of confining the region of computation to the viscous region of the flow. The viscous region is defined as the region where the vorticity is nonnegligible and the difference in dilatation between the potential flow and the real flow around the same geometry is also nonnegligible. The method was developed and tested. Also, an application of the procedure to the solution of the steady Navier-Stokes equations for incompressible internal flows is presented. B.W.

N82-22458* United Technologies Research Center, East Hartford, Conn.

TURBOFAN FORCED MIXER-NOZZLE INTERNAL FLOWFIELD. VOLUME 1: A BENCHMARK EXPERIMENTAL STUDY Final Report

Robert W. Paterson Washington NASA Apr. 1982 131 p refs 3 Vol. (Contract NAS3-20951) (NASA-CR-3492; NAS 1.26:3492) Avail: NTIS HC A07/MF A01 CSCL 20D

An experimental investigation of the flow field within a model turbofan forced mixer nozzle is described. Velocity and thermodynamic state variable data for use in assessing the accuracy and assisting the further development of computational procedures for predicting the flow field within mixer nozzles are provided. Velocity and temperature data suggested that the nozzle mixing

ORIGINAL PAGE IS
OF POOR QUALITY

process was dominated by circulations (secondary flows) of a length scale on the order the lobe dimensions which were associated with strong radial velocities observed near the lobe exit plane. The 'benchmark' model mixer experiment conducted for code assessment purposes is discussed. N.W.

N82-22459*# United Technologies Research Center, East Hartford, Conn.

TURBOFAN FORCED MIXER-NOZZLE INTERNAL FLOW-FIELD, VOLUME 2: COMPUTATIONAL FLUID DYNAMIC PREDICTIONS Final Report

M. J. Werle and V. N. Vasta Washington NASA Apr. 1982 90 p refs 3 Vol.

(Contract NAS3-20951)

(NASA-CR-3493; NAS 1.26.3493) Avail; NTIS HC A05/MF A01 CSCL 20D

A general program was conducted to develop and assess a computational method for predicting the flow properties in a turbofan forced mixed duct. The detail assessment of the resulting computer code is presented. It was found that the code provided excellent predictions of the kinematics of the mixing process throughout the entire length of the mixer nozzle. The thermal mixing process between the hot core and cold fan flows was found to be well represented in the low speed portion of the flowfield. N.W.

N82-22460*# United Technologies Research Center, East Hartford, Conn.

TURBOFAN FORCED MIXER-NOZZLE INTERNAL FLOW-FIELD, VOLUME 3: A COMPUTER CODE FOR 3-D MIXING IN AXISYMMETRIC NOZZLES Final Report

J. P. Kreskovsky, W. R. Briley, and H. McDonald Washington NASA Apr. 1982 129 p refs Prepared in cooperation with Scientific Research Associates, Inc., Glastonbury, Conn. 3 Vol.

(Contract NAS3-20951)

(NASA-CR-3494; NAS 1.26:3494; R81-912929) Avail; NTIS HC A07/MF A01 CSCL 20D

A finite difference method is developed for making detailed predictions of three dimensional subsonic turbulent flow in turbofan lobe mixers. The governing equations are solved by a forward-marching solution procedure which corrects an inviscid potential flow solution for viscous and thermal effects, secondary flows, total pressure distortion and losses, internal flow blockage and pressure drop. Test calculations for a turbulent coaxial jet flow verify that the turbulence model performs satisfactorily for this relatively simple flow. Lobe mixer flows are presented for two geometries typical of current mixer design. These calculations included both hot and cold flow conditions, and both matched and mismatched Mach number and total pressure in the fan and turbine streams. N.W.

N82-24452*# Southwest Research Inst., San Antonio, Tex.

STUDY OF VAPOR FLOW INTO A CAPILLARY ACQUISITION DEVICE Final Report

Franklin T. Dodge and Edgar B. Bowles Apr. 1982 64 p refs (Contract NAS3-22664)

(NASA-CR-167883; NAS 1.26:167883; SuR102-6369) Avail; NTIS HC A04/MF A01 CSCL 20D

An analytical model was developed that prescribes the conditions for vapor flow through the window screen of a start basket. Several original submodels were developed as part of this model. The submodels interrelate such phenomena as the effect of internal evaporation of the liquid, the bubble point change of a screen in the presence of wicking, the conditions for drying out of a screen through a combination of evaporation and pressure difference, the vapor inflow rate across a wet screen as a function of pressure difference, and the effect on wicking of a difference between the static pressure of the liquid reservoir and the surrounding vapor. Most of these interrelations were verified by a series of separate effects tests, which were also used to determine certain empirical constants in the models. The equations of the model were solved numerically for typical start basket designs, and a simplified start basket was constructed to verify the predictions, using both volatile and nonvolatile test liquids. The test results verified the trends predicted by the model. S.L.

N82-27686*# Pennsylvania State Univ., University Park. Turbomachinery Lab

THREE DIMENSIONAL FLOW FIELD INSIDE COMPRESSOR ROTOR, INCLUDING BLADE BOUNDARY LAYERS Semian-annual Progress Report

J. M. Galmes, M. Pouagere, and B. Lakshminarayana Jun. 1982 78 p refs

(Grant NsG-3266)

(NASA-CR-169120; NAS 1.26:169120; PSU/Turb-82-4) Avail; NTIS HC A03/MF A01 CSCL 20D

The Reynolds stress equation, pressure strain correlation, and dissipative terms and diffusion are discussed in relation to turbulence modelling using the Reynolds stress model. Algebraic modeling of Reynolds stresses and calculation of the boundary layer over an axial cylinder are examined with regards to the kinetic energy model for turbulence modelling. The numerical analysis of blade and hub wall boundary layers, and an experimental study of rotor blade boundary layer in an axial flow compressor rotor are discussed. The Patankar-Spalding numerical method for two dimensional boundary layers is included. A.R.H.

N82-31638*# Connecticut Univ., Storrs. Dept. of Mechanical Engineering.

TURBINE ENDWALL SINGLE CYLINDER PROGRAM Semian-annual Status Report, 1 Jan. - 1 Jul. 1982

Lee S. Langston 1 Jul. 1982 50 p refs

(Grant NsG-3238)

(NASA-CR-169278; NAS 1.26:169278) Avail; NTIS HC A03/MF A01 CSCL 20D

Detailed measurement of the flow field in front of a large-scale single cylinder, mounted in a wind tunnel is discussed. A better understanding of the three dimensional separation occurring in front of the cylinder on the endwall, and of the vortex system that is formed is sought. A data base with which to check analytical and numerical computer models of three dimensional flows is also anticipated. Author

N82-31639*# City Coll. Research Foundation, New York. Turbomachinery Lab.

EXPERIMENTAL STUDY OF TURBULENCE IN BLADE END WALL CORNER REGION

R. Raj Aug. 1982 110 p refs

(Grant NAG3-122)

(NASA-CR-169283; NAS 1.26:169283; RF-05438) Avail; NTIS HC A06/MF A01 CSCL 20D

Corner flows and wall pressure fluctuations, design and fabrication of the test model, preliminary results on boundary layer, flow visualization, turbulence intensity and spectra measurements are presented. The design consideration and fabrication report on the newly built wind tunnel to be used for subsequent continuation of the research effort is also presented. S.L.

N82-31641*# Cornell Univ., Ithaca, N. Y. Energy Program.

EXHAUST GAS MEASUREMENTS IN A PROPANE FUELED SWIRL STABILIZED COMBUSTOR

M. S. Aanad Aug. 1982 177 p refs

(Grant NsG-3019)

(NASA-CR-169293; NAS 1.26:169293; E-82-4) Avail; NTIS HC A09/MF A01 CSCL 20D

Exhaust gas temperature, velocity, and composition are measured and combustor efficiencies are calculated in a lean premixed swirl stabilized laboratory combustor. The radial profiles of the data between the co- and the counter swirl cases show significant differences. Co-swirl cases show evidence of poor turbulent mixing across the combustor in comparison to the counter-swirl cases. NO sub x levels are low in the combustor but substantial amounts of CO are present. Combustion efficiencies are low and surprisingly constant with varying outer swirl in contradiction to previous results under a slightly different inner swirl condition. This difference in the efficiency trends is expected

ORIGINAL PAGE IS
OF POOR QUALITY

to be a result of the high sensitivity of the combustor to changes in the inner swirl. Combustor operation is found to be the same for propane and methane fuels. A mechanism is proposed to explain the combustor operation and a few important characteristics determining combustor efficiency are identified. J.D.

NS2-31642*# Cornell Univ., Ithaca, N. Y.

FLOW PROCESS IN COMBUSTORS

F. C. Gouldin Jun. 1982 16 p refs

(Grant NsG-3019)

(NASA-CR-169294; NAS 1.26:169294)

Avail: NTIS

HC A02/MF A01 CSCL 20D

Fluid mechanical effects on combustion processes in steady flow combustors, especially gas turbine combustors were investigated. Flow features of most interest were vorticity, especially swirl, and turbulence. Theoretical analyses, numerical calculations, and experiments were performed. The theoretical and numerical work focused on noncombusting flows, while the experimental work consisted of both reacting and nonreacting flow studies. An experimental data set, e.g., velocity, temperature and composition, was developed for a swirl flow combustor for use by combustion modelers for development and validation work. J.D.

NS2-31643*# Oklahoma State Univ., Stillwater. School of Mechanical and Aerospace Engineering.

INVESTIGATIONS OF FLOWFIELDS FOUND IN TYPICAL COMBUSTOR GEOMETRIES Semiannual Status Report, 1 Feb. - 31 Jul. 1982

David G. Lilley 31 Jul. 1982 252 p refs

(Grant NAG3-74)

(NASA-CR-169295; NAS 1.26:169295; SASR-4) Avail: NTIS

HC A12/MF A01 CSCL 20D

Experimental and theoretical research undertaken on 2-D axisymmetric geometries under low speed, nonreacting, turbulent, swirling flow conditions is reported. The flow enters the test section and proceeds into a larger chamber (the expansion ratio $D/d = 2$) via a sudden or gradual expansion (sidewall angle $\alpha = 90$ and 45 degrees). Inlet swirl vanes are adjustable to a variety of vane angles with values of $\phi = 0, 38, 45, 60$ and 70 degrees being emphasized. Author

A82-10961*# A heat exchanger computational procedure for temperature-dependent fouling. L. M. Chiappetta and E. J. Szetela (United Technologies Research Center, East Hartford, CT). *American Society of Mechanical Engineers and American Institute of Chemical Engineers, National Heat Transfer Conference, 20th, Milwaukee, WI, Aug. 2-5, 1981, ASME Paper 81-HT-73*, 8 p. 14 refs, Members, \$2.00; nonmembers, \$4.00. Contract No. NAS3-21971.

A novel heat exchanger computational procedure is described which provides a means of rapidly calculating the distributions of fluid and wall temperatures, deposit formation, and pressure loss at various points in a heat exchanger. The procedure is unique in that it is capable of treating wide variations in heat exchanger geometry without recourse to restrictive assumptions concerning heat exchanger type (e.g., co-flow, counterflow, cross flow devices, etc.). The analysis has been used extensively to predict the performance of cross-counterflow heat exchangers in which one fluid behaves as a perfect gas (e.g., air) while the other fluid is assumed to be a distillate fuel. The model has been extended to include the effects on heat exchanger performance of time varying inflow conditions. Heat exchanger performance degradation due to deposit formation with time can be simulated, making this procedure useful in predicting the effects of temperature-dependent fouling. (Author)

AP7-8833*# Turbulent boundary layer heat transfer experiments. A separate effects study on a convexly-curved wall. T. W. Simon (Minnesota, University, Minneapolis, MN) and R. J. Moffat (Stanford University, Stanford, CA). *American Society of Mechanical Engineers and American Institute of Chemical Engineers, National Heat Transfer Conference, 20th, Milwaukee, WI, Aug. 2-5, 1981,*

ASME Paper 81-HT-78, 10 p. 30 refs. Members, \$2.00; nonmembers, \$4.00. Grants No. NsG-3124; No. NAG3-3.

Surface heat transfer rates have been measured for several different flows on an isothermal, convexly curved surface. The freestream velocity, boundary layer thickness, acceleration parameter, and unheated starting length were varied systematically, and both turbulent and transitional boundary layers were studied. The effect of convex curvature on heat transfer rates is significant with Stanton numbers reduced 20-25% below flat wall values for the same enthalpy thickness Reynolds number. Heat transfer rates recovered slowly on a flat wall downstream of the curved wall, and after 60 cm, the Stanton numbers were still 15-20% below flat wall values. The behavior of the boundary layer suggests the existence of an asymptotic condition. Boundary layer thickness, freestream velocity, and boundary layer maturity affect the initial response to the introduction of curvature and the rate at which the asymptotic state is approached. Convex curvature appears to increase the boundary layer's sensitivity to acceleration; it also delays and retards transition. Near-laminar or early-transitional boundary layers recover from curvature rapidly, whereas late-transitional and mature boundary layers recover slowly. J.F.

NS2-11390*# SHD Associates, Inc., Evanston, Ill. **SURFACE-TENSION INDUCED INSTABILITIES: EFFECTS OF LATERAL BOUNDARIES Final Report**

S. Rosenblat, S. H. Davis, and G. M. Hornsby Jun. 1981 130 p refs

(Contract NAS3-22274)

(NASA-CR-165530) Avail: NTIS HC A07/MF A01 CSCL 20D

Convection in circular and rectangular cylinders is analyzed. The governing equations and boundary conditions are formulated. Linear and nonlinear stability theory are considered, and the physical implications of the theory are discussed. J.D.H.

A82-13395* Eigenvalues of the Rayleigh-Bénard and Marangoni problems. S. Rosenblat, G. M. Hornsby, and S. H. Davis (SHD Associates, Inc., Evanston, IL). *Physics of Fluids*, vol. 24, Nov. 1981, p. 2115-2117. Contract No. NAS3-22274.

The eigenvalues of the linear Bénard-Marangoni stability problem are discussed, Pearson and Nield boundary conditions, which correspond to a rigid, isothermal lower boundary and a stress-free conducting upper boundary are considered. It is shown that although a critical value of the Marangoni number can be determined; the number is not, strictly speaking, an eigenvalue and cannot be used as an eigenvalue parameter for the determination of an eigenvector set. D.L.G.

A82-17824*# Mean flowfields in axisymmetric combustor geometries with swirl. D. L. Rhode, D. G. Lilley (Oklahoma State University, Stillwater, OK), and D. K. McLaughlin (Dynamics Technology, Inc., Torrance, CA). *American Institute of Aeronautics and Astronautics, Aerospace Sciences Meeting, 20th, Orlando, FL, Jan. 11-14, 1982, Paper 82-0177*. 14 p. 31 refs. Grant No. NAG3-74.

Six flowfield configurations are investigated with sidewall angles of 90 and 45 deg, and swirl vane angles of 0, 45, and 70 deg. It is found that central recirculation zones occur for the swirling flow cases investigated, which extend from the inlet to $x/D = 1.7$, where x is the axial polar coordinate, and D is the test section diameter. Five-hole pitot probe pressure measurements are used to determine time-mean velocities, and corresponding flow situations are predicted and compared to results of experimental data. Excellent agreement is found for the nonswirling flow, although poor agreement is found for swirling flow cases, especially near the inlet. The discrepancy is attributed to the lack of realism in the turbulence model, and/or to inaccurate specification of time-mean velocity and turbulence energy distributions at the inlet. D.L.G.

A82-17880*# Atomization and combustion properties of flashing injectors. A. S. P. Solomon, S. D. Rupprecht (Pennsylvania State University, University Park; Westinghouse Research Laboratories, Monroeville, PA), L.-D. Chen, and G. M. Faeth (Pennsylvania

State University, University Park, PA). *American Institute of Aeronautics and Astronautics, Aerospace Sciences Meeting, 20th, Orlando, FL, Jan. 11-14, 1982, Paper 82-0300*. 11 p. 29 refs. Grant No. NsG-3306.

Flashing injection involves expanding a fluid through an injector until a supersaturated state is reached, causing a portion of the fluid to flash to a vapor. This investigation considered the flow, atomization and spreading properties of flashing injectors flowing liquids containing dissolved gases (Jut A/air) as well as superheated liquids (Freon 11). The use of a two stage expansion process, separated by an expansion chamber, was found to be beneficial for good atomization properties of flashing injection - particularly for dissolved gas systems. Both locally homogeneous and separated flow models provided good predictions of injector flow properties. Conventional correlations for drop sizes from pressure atomized and airblast injectors were successfully modified, using the separated flow model to prescribe injector exit conditions, to correlate drop size measurements. Additional experimental results are provided for spray angle and combustion properties of sprays from flashing injectors. (Author)

A82-23832 * # Solutions of the compressible Navier-Stokes equations using the integral method. M. M. ElRefaee, J. C. Wu, and S. G. Lekoudis (Georgia Institute of Technology, Atlanta, GA). (*American Institute of Aeronautics and Astronautics, Aerospace Sciences Meeting, 19th, St. Louis, MO, Jan. 12-15, 1981, Paper 81-0046*.) *AIAA Journal*, vol. 20, Mar. 1982, p. 356-362. 16 refs. Grant No. NsG-3307.

The integral representation method was used to obtain numerical solutions of the compressible, unsteady, two-dimensional Navier-Stokes equations for subsonic flows. The equations were written with the vorticity, the dilatation, the density, and the enthalpy as the dependent variables. The method was tested by solving the following problems: the flow over a flat plate, around a circular cylinder, and around a Joukowski airfoil. The last two problems involved massive flow separation. The approach offers the capability of confining the domain of computations to the region where two quantities, the vorticity and the difference in dilatation between the real flow and the potential flow around the body, are non-negligible. (Author)

A82-24748 * Numerical analysis of confined turbulent flow. A. Lin (Cincinnati, University, Cincinnati, OH) and H. Weinstein (City College, New York, NY). *Computers and Fluids*, vol. 10, no. 1, 1982, p. 27-50. 25 refs. Grant No. NsG-3174.

The considered investigation is concerned with the development of an efficient computational method for obtaining a physical understanding of an internal turbulent field. The employed approach makes use of a 'two equation' type model for the turbulence to obtain the numerical solution of a two-dimensional confined turbulent flow. The mean flow governing equations are considered along with the governing equation of the mean temperature and concentrations, and the boundary conditions. The numerical procedure for solving the turbulent flow is discussed, taking into account an approximation to the nonlinear terms, and the inner and outer coupling. Attention is given to a stability convergence analysis, the stability characteristics, and computational examples. G.R.

A82-27000 * Numerical modelling of turbulent flow in a combustion tunnel. A. F. Ghoniem, A. J. Chorin, and A. K. Oppenheim (California, University, Lawrence Berkeley Laboratory, Berkeley, CA). *Royal Society (London), Philosophical Transactions, Series A*, vol. 304, no. 1484, Mar. 9, 1982, p. 303-325. 21 refs. Contract No. W-7405-eng-48; Grant No. NsG-3227.

A numerical technique is presented for the analysis of turbulent flow associated with combustion. The technique uses Chorin's random vortex method (rvm), an algorithm capable of tracing the action of elementary turbulent eddies and their cumulative effects without imposing any restriction upon their motion. In the past, the rvm has been used with success to treat nonreacting turbulent flows, revealing in particular the mechanics of large-scale flow patterns, the so-called coherent structures. Introduced here is a flame propagation algorithm, also developed by Chorin, in conjunction with volume sources modelling the mechanical effects of the exothermic process of combustion. As an illustration of its use, the technique is applied

to flow in a combustion tunnel where the flame is stabilized by a back-facing step. Solutions for both nonreacting and reacting flow fields are obtained which satisfactorily describe the essential features of turbulent combustion in a lean propane-air mixture that were observed in the laboratory by means of high speed Schlieren photography. (Author)

A82-31445 * Natural convection with combined driving forces. S. Ostrach (Case Western Reserve University, Cleveland, OH). *PCH/Physicochemical Hydrodynamics*, vol. 1, no. 4, 1980, p. 233-247. 29 refs. Grant No. NsG-3221.

The problem of free and natural convection with combined driving forces is considered in general and all possible configurations are identified. Dimensionless parameters are discussed in order to help categorize the various problems, and existing work is critically evaluated. Four distinct cases are considered for conventional convection and for the situation when the body force and the density gradient are parallel but opposed. Considerable emphasis is given to unstable convection in horizontal layers. C.D.

A82-31908 * # Tube entrance heat transfer with deposit formation. E. J. Szetela and D. R. Sobel (United Technologies Research Center, East Hartford, CT). *American Institute of Aeronautics and Astronautics and American Society of Mechanical Engineers, Joint Thermophysics, Fluids, Plasma and Heat Transfer Conference, 3rd, St. Louis, MO, June 7-11, 1982, AIAA Paper 82-0918*, 7 p. 21 refs. Contract No. NAS3-21971.

A two-peak wall temperature profile was observed while flowing a kerosene-type gas turbine fuel through a direct-resistance heated tube at an entrance Reynolds number of about 1500. The downstream peak gradually diminished as deposits formed inside the tube, and only one peak remained after seven hours. The observation is explained qualitatively on the basis of analytical and experimental results reported in the literature. It is shown that the temperature profile can be divided into five regions: development of the thermal boundary layer, appearance of the secondary flows, fully developed thermal boundary layer, transition to turbulent flow, and turbulent flow. Deposits increase the tube roughness and reduce the length required for laminar-turbulent transition. V.L.

A82-32225 * Effects of internal heat transfer on the structure of self-similar blast waves. A. F. Ghoniem, S. A. Berger, A. K. Oppenheim (California, University, Berkeley, CA), and M. M. Kamel (Cairo University, Cairo, Egypt). *Journal of Fluid Mechanics*, vol. 117, Apr. 1982, p. 473-491. 19 refs. NSF Grant No. ENG-78-12372; Contract No. W-7405-ENG-48; Grant No. NAG3-131.

An analysis of the problem of self-similar, nonadiabatic blast waves, where both conduction and radiation are allowed to take place, show the problem can be reducible to the integration of a system of six coupled nonlinear ordinary differential equations. Consideration of these equations shows that although radiation tends to produce uniform fields through temperature gradient attenuation, all the energy carried by radiation is deposited on the front and the bounding shock becomes increasingly overdriven. When conduction is taken into account, the distribution of gasdynamic parameters in blast waves in the case of Rosseland diffusion radiation is more uniform than in the case of the Planck emission radiation. O.C.

A82-35043 * # Bluff-body flameholder wakes - A simple numerical solution. G. H. Vatistas, S. Lin, C. K. Kwok (Concordia University, Montreal, Canada), and D. G. Lilley (Oklahoma State University, Stillwater, OK). *AIAA, SAE, and ASME, Joint Propulsion Conference, 18th, Cleveland, OH, June 21-23, 1982, AIAA Paper 82-1177*, 7 p. 22 refs. National Research Council Grant No. A-7435; Grant No. NAG3-74.

Numerical finite difference predictions are made of recirculation zones behind bluff-body flame stabilizers, showing quantitatively the effects of forebody geometry, blockage ratio, lateral position of the blockage and inlet swirl on the central recirculation zone. A simple transient Navier-Stokes solution algorithm and laminar flow simulation are used with 'free slip' and 'no slip' wall boundary conditions, thus illustrating how a basic approach may be used to solve a sophisticated fluid dynamic problem. (Author)

A82-37710 * # Turbulence measurements in a confined jet using a six-orientation hot-wire probe technique. S. I. Janjua, D. K. McLaughlin (Dynamics Technology, Inc., Torrance, CA), D. G. Lilley (Oklahoma State University, Stillwater, OK), and T. Jackson. *AIAA, SAE, and ASME, Joint Propulsion Conference, 18th, Cleveland, OH, June 21-23, 1982, AIAA Paper 82-1262.* 13 p. 22 refs. Contract No. NAG3-74.

The six-orientation hot-wire technique is applied to nonreacting axisymmetric flowfields, obtaining measurements of time-mean and rms voltages at six different orientations, thus providing enough information to determine the time-mean velocities, turbulence intensities, and shear stresses. At each location in the flow, there are six different values of each of the above quantities that can be obtained using six sets of measurements of three adjacent orientations. Flowfield surveys of both swirling and nonswirling confined jets are used to calculate estimates of the mean velocity components and the normal and shear turbulent stresses, and comparisons with independent data are made. A sensitivity analysis of the data reduction technique demonstrates that the largest uncertainties are to be expected in the turbulent shear force estimates. C.D.

A82-39501 * Nonlinear Marangoni convection in bounded layers. I - Circular cylindrical containers. II - Rectangular cylindrical containers. S. Rosenblatt, S. H. Davis, and G. M. Homsy (SHD Associates Inc., Evanston, IL). *Journal of Fluid Mechanics*, vol. 120, July 1982, p. 91-138, 25 refs. Contract No. NAS3-22274.

Liquid undergoing nonlinear Marangoni instability in a circular cylinder is examined, with attention given to roll-cell development and interaction. Surface deflections are neglected and the side walls are considered as adiabatic and impenetrable, allowing the liquid to freely slip. The nonlinear convective states are calculated and their stability is defined, the behavior and amplitude of cells forming in the liquid, heated from below, is modeled in order to derive all the transport properties. A new small parameter is formulated which is related to the critical Marangoni number of the infinite matrix expressing the eigenvalue expansion of the problem. The observed roll cell amplitudes and transport properties are shown to be available from simple eigenvalues, with double eigenvalues, indicating the existence of two roll-states as predicted by linear theory, nonlinear theory indicates transitions from one steady convective state to another. M.S.K.

A82-41203 * # Buoyancy effects on the temperature field in downward spreading flames. R. A. Altenkirch, D. C. Winchester, and R. Eichhorn (Kentucky University, Lexington, KY). *ASME, Transactions, Journal of Heat Transfer*, vol. 104, Aug. 1982, p. 560-563, 8 refs. Grant No. NSG-3114.

It is shown that flames which spread vertically down thermally thin fuels at the same Damköhler number, and therefore have the same dimensionless spread rate, also have the same dimensionless temperature fields irrespective of differences in physical size. The Frey and Tien (1976) effects of pressure on flame size are due to the effects of pressure on the character of the induced buoyant flow. O.C.

A82-44782 * # Flow aerodynamics modeling of an MHD swirl combustor - Calculations and experimental verification. A. K. Gupta, J. M. Beer, J. F. Louis (MIT, Cambridge, MA), A. A. Busnaina, and D. G. Lilley (Oklahoma State University, Stillwater, OK). *ASME, Transactions, Journal of Fluids Engineering*, vol. 104, Sept. 1982, p. 385-391; Discussion, p. 391, 392, 18 refs. Contract No. DE-AC01-79ET-15518; Grant No. NAG3-74.

This paper describes a computer code for calculating the flow dynamics of constant density flow in the second stage trumpet shaped nozzle section of a two stage MHD swirl combustor for application to a disk generator. The primitive pressure-velocity variable, finite difference computer code has been developed to allow the computation of inert nonreacting turbulent swirling flows in an axisymmetric MHD model swirl combustor. The method and program involve a staggered grid system for axial and radial velocities, and a line relaxation technique for efficient solution of the equations. Turbulence simulation is by way of a two-equation Kappa-epsilon model. The code produces as output the flowfield map of the nondimensional stream function, axial, and swirl velocity. Good agreement was obtained between the theoretical predictions and the qualitative experimental results. The best seed injector location for uniform seed distribution at combustor exit is with injector located centrally on the combustor axis at entrance to the second stage combustor. (Author)

A82-45157 * Self-adaptive closed constrained solution algorithms for nonlinear conduction. J. Padovan and S. Tovchakchaikul (Akron, University, Akron, OH). *Numerical Heat Transfer*, vol. 5, July-Sept. 1982, p. 253-274. 10 refs. Grant No. NAG3-54.

Self-adaptive solution algorithms are developed for nonlinear heat conduction problems encountered in analyzing materials for use in high temperature or cryogenic conditions. The nonlinear effects are noted to occur due to convection and radiation effects, as well as temperature-dependent properties of the materi-

als. Incremental successive substitution (ISS) and Newton-Raphson (NR) procedures are treated as extrapolation schemes which have solution projections bounded by a hyperline with an externally applied thermal load vector arising from internal heat generation and boundary conditions. Closed constraints are formulated which improve the efficiency and stability of the procedures by employing closed ellipsoidal surfaces to control the size of successive iterations. Governing equations are defined for nonlinear finite element models, and comparisons are made of results using the the new method and the ISS and NR schemes for epoxy, PVC, and CuGe. M.S.K.

ORIGINAL PAGE IS
OF POOR QUALITY

C-2

35 INSTRUMENTATION AND PHOTOGRAPHY

Includes remote sensors; measuring instruments and gages; detectors; cameras and photographic supplies; and holography.

For aerial photography see 43 *Earth Resources*. For related information see also 06 *Aircraft Instrumentation*, and 19 *Spacecraft Instrumentation*.

N82-14494*# National Aeronautics and Space Administration. Lewis Research Center, Cleveland, Ohio.

AN EXPERIMENTAL INVESTIGATION INTO THE FEASIBILITY OF A THERMOELECTRIC HEAT FLUX GAGE

Jan C. Jones (Tri State Univ.) and G. James VanFossen, Jr. Dec. 1981 17 p refs

(NASA-TM-82755; E-1071) Avail: NTIS HC A02/MF A01 CSCL 14B

An experiment was conducted to determine the feasibility of using a commercially available thermoelectric device as a heat flux gage. In certain research applications, the thermoelectric heat flux gage can provide a relatively simple means to model a warm fluid-cold wall. The experiment showed that heat flux through the gage could be correlated within two percent to the applied thermoelectric current through the device and the hot and cold side temperature with a simple algebraic equation.

Author

N82-19521*# National Aeronautics and Space Administration. Lewis Research Center, Cleveland, Ohio.

HIGH-SPEED LASER ANEMOMETER SYSTEM FOR INTRAROTOR FLOW MAPPING IN TURBOMACHINERY

J. Anthony Powell, Anthony J. Strazisar, and Richard G. Seasholtz Feb. 1982 22 p refs

(NASA-TP-1663; E-276) Avail: NTIS HC A02/MF A01 CSCL 14B

A fringe-type laser anemometer with innovative features is described. The innovative features include: (1) rapid, efficient data acquisition processes, (2) detailed graphic display of data being accumulated, and (3) input laser-beam positioning that allows greater optical access to the intrarotor region. Results are presented that demonstrate the anemometer's capability in flow mapping within a transonic axial-flow compressor rotor.

M.D.K.

N82-22481*# National Aeronautics and Space Administration. Lewis Research Center, Cleveland, Ohio.

FRINGE LOCALIZATION REQUIREMENTS FOR THREE-DIMENSIONAL FLOW VISUALIZATION OF SHOCK WAVES IN DIFFUSE-ILLUMINATION DOUBLE-PULSE HOLOGRAPHIC INTERFEROMETRY

Arthur J. Decker Apr. 1982 45 p refs

(NASA-TP-1868; NAS 1.60:1868; E-757) Avail: NTIS HC A03/MF A01 CSCL 14E

A theory of fringe localization in rapid-double-exposure, diffuse-illumination holographic interferometry was developed. The theory was then applied to compare holographic measurements with laser anemometer measurements of shock locations in a transonic axial-flow compressor rotor. The computed fringe localization error was found to agree well with the measured localization error. It is shown how the view orientation and the curvature and positional variation of the strength of a shock wave are used to determine the localization error and to minimize it. In particular, it is suggested that the view direction not deviate from tangency at the shock surface by more than 30 degrees.

Author

N82-23515*# National Aeronautics and Space Administration. Lewis Research Center, Cleveland, Ohio.

POCKELS-EFFECT CELL FOR GAS-FLOW SIMULATION

David Weimer May 1982 13 p refs

(NASA-TP-2007; E-1028; NAS 1.60:2007) Avail: NTIS HC A02/MF A01 CSCL 14B

A Pockels effect cell using a 75 cu cm DK*P crystal was developed and used as a gas flow simulator. Index of refraction gradients were produced in the cell by the fringing fields of parallel plate electrodes. Calibration curves for the device were obtained for index of refraction gradients in excess of .00025 m S.L.

N82-28605*# National Aeronautics and Space Administration. Lewis Research Center, Cleveland, Ohio.

LASER ANEMOMETER USING A FABRY-PEROT INTERFEROMETER FOR MEASURING MEAN VELOCITY AND TURBULENCE INTENSITY ALONG THE OPTICAL AXIS IN TURBOMACHINERY

Richard G. Seasholtz and Louis J. Goldman 1982 11 p refs Proposed for presentation at the Winter Ann. Meeting of the Am. Soc. of Mech. Engr., Phoenix, Ariz., 14-19 Nov. 1982

(NASA-TM-82841; E-1211; NAS 1.15:82841) Avail: NTIS HC A02/MF A01 CSCL 14B

A technique for measuring a small optical axis velocity component in a flow with a large transverse velocity component is presented. Experimental results are given for a subsonic jet operating in a laboratory environment, and for a 0.508 meter diameter turbine stator cascade. Satisfactory operation of the instrument was demonstrated in the stator cascade facility with an ambient acoustic noise level during operation of about 105 dB. In addition, the turbulence intensity measured with the interferometer was consistent with previous measurements taken with a fringe type laser anemometer.

T.M.

N82-31663*# National Aeronautics and Space Administration. Lewis Research Center, Cleveland, Ohio.

DEVELOPMENT AND UTILIZATION OF A LASER VELOCIMETER SYSTEM FOR A LARGE TRANSONIC WIND TUNNEL

Robert J. Freedman and John P. Greissing Jun. 1982 17 p refs

(NASA-TM-82886; E-1264; NAS 1.15:82886) Avail: NTIS HC A02/MF A01 CSCL 14B

The need for measurements of the velocity flow field about spinner propeller nacelle configurations at Mach numbers to 0.8 was met by a specially developed laser velocimeter system. This system, which uses an argon ion laser and 4 beam 2 color optics, was required to operate in the hostile environment associated with the operation of a large transonic wind tunnel. To overcome the conditions present in locating the sensitive optics in close proximity to the wind tunnel, an isolation system was developed. The system protects the velocimeter from the high vibrations, elevated temperatures, destructive acoustic pressures and low atmospheric pressures attendant with the operation of the wind tunnel. The system was utilized to map the flow field in front of, behind and in between the rotating blades of an advanced swept blade propeller model at a Mach number of 0.8. The data collected by the system will be used to correlate and verify computer analyses of propeller nacelle flow fields and propeller performance. R.J.F.

N82-31664*# National Aeronautics and Space Administration. Lewis Research Center, Cleveland, Ohio.

A DIGITAL OPTICAL TORQUEMETER FOR HIGH ROTATIONAL SPEED APPLICATIONS

Daniel J. Lesco, Donald R. Buchele, and Lawrence G. Oberle Aug. 1982 17 p refs

(NASA-TM-82914; E-1189; NAS 1.15:82914) Avail: NTIS HC A02/MF A01 CSCL 14B

A digital optical torquemeter system designed for applications at high rotational speeds was fabricated and tested for zero stability at speeds up to 20,000 rpm. Data obtained in a spin rig and with simulated inputs demonstrate that the system is capable of measuring torque bar twist to within 0.03 degrees at speeds of 30,000 rpm. The optical system uses fiber optic bundles to transmit light to the torque bar and to silicon avalanche detectors. The system is microcomputer based and provides measurements of

ORIGINAL PAGE IS
OF POOR QUALITY

average torque and torque as a function of angular shaft position. The torque meter requires no bearings or other contact between the rotating torque bar and the nonrotating optics, and tolerates movement of the torque bar as large as 1 mm relative to the optics. R.J.F.

N82-32662*# National Aeronautics and Space Administration, Lewis Research Center, Cleveland, Ohio.

EXTENDING THE FREQUENCY OF RESPONSE OF LIGHTLY DAMPED SECOND ORDER SYSTEMS: APPLICATION TO THE DRAG FORCE ANEMOMETER

Gustave C. Fralick Aug. 1982 26 p refs (NASA-TM-82927; E-1178; NAS 1.15:82927) Avail: NTIS HC A03/MF A01 CSCL 14B

It is shown that a conventional electronic frequency compensator does not provide adequate compensation near the resonant frequency of a lightly damped second order system, such as the drag force anemometer. The reason for this is discussed, and a simple circuit modification is presented which overcomes the difficulty. The improvement is shown in theoretical frequency response curves as well as in the experimental results from some typical drag force anemometers. Author

N82-32670*# National Aeronautics and Space Administration, Lewis Research Center, Cleveland, Ohio.

NEW VERSIONS OF OLD FLOW VISUALIZATION SYSTEMS

Walton L. Howes *In* NASA, Langley Research Center Flow Visualization and Laser Velocimetry for Wind Tunnels, Sep. 1982 p 59-64 (For primary document see N82-32663 23-35) Avail: NTIS HC A16/MF A01 CSCL 14B

A small, modified Mach-Zehnder interferometer placed in series with a much larger schlieren optical system spanning the test section is examined. In one arm of the interferometer, light from the schlieren is focused through a pinhole and recollimating lens to produce a reference beam which interferes with the remaining object beam from the other arm. The object and reference beams are separated only over a small interval following the test section, and differential vibrations are greatly reduced. Color schlieren has technical, as well as aesthetic, advantages over black-and-white schlieren. Since each color is associated with a specific amount of refraction, quantitative evaluation of certain refractive-index fields becomes possible using very simple equations derived from ray trace theory. Rainbow schlieren of an acetylene flame, and the evaluated refractive index distribution are shown. Root-mean-square refractive index fluctuations in homogeneous, isotropic turbulence were determined using the rainbow schlieren, since these fluctuations determine the root-mean-square refraction, which is indicated by the overall color of the image. E.A.K.

N82-32672*# National Aeronautics and Space Administration, Lewis Research Center, Cleveland, Ohio.

PROPELLER FLOW VISUALIZATION TECHNIQUES

George L. Stefko, F. J. Paulovich, J. P. Greissing, and E. D. Walker *In* NASA, Langley Research Center Flow Visualization and Laser Velocimetry for Wind Tunnels, Sep. 1982 p 75-89 (For primary document see N82-32663 23-35) Avail: NTIS HC A16/MF A01 CSCL 14B

Propeller flow visualization techniques were tested. The actual operating blade shape as it determines the actual propeller performance and noise was established. The ability to photographically determine the advanced propeller blade tip deflections, local flow field conditions, and gain insight into aeroelastic instability is demonstrated. The analytical prediction methods which are being developed can be compared with experimental data. These comparisons contribute to the verification of these improved methods and give improved capability for designing future advanced propellers with enhanced performance and noise characteristics. E.A.K.

N82-32675*# National Aeronautics and Space Administration, Lewis Research Center, Cleveland, Ohio.

FLOW VISUALIZATION OF SHOCK-BOUNDARY LAYER INTERACTION

Warren R. Hingst and Mark Jurkovich *In* NASA, Langley Research Center Flow Visualization and Laser Velocimetry for Wind Tunnels, Sep. 1982 p 101-108 (For primary document see N82-32663 23-35) Avail: NTIS HC A16/MF A01 CSCL 14B

Two and three-dimensional shock-boundary layer interaction data were obtained from supersonic wind tunnel tests. These interactions are studied both with and without boundary layer bleed. The data verify computational fluid dynamic codes. Surface static pressure, pitot pressure, flow angularity, and bleed rates, are studied by flow visualization techniques. Surface oil flow using fluorescent dye and laser sheet using water droplets as the scattering material are used for flow visualization. E.A.K.

N82-32686*# National Aeronautics and Space Administration, Lewis Research Center, Cleveland, Ohio.

STATUS OF LASER ANEMOMETRY IN TURBOMACHINERY RESEARCH AT THE LEWIS RESEARCH CENTER

Richard G. Seasholtz *In* NASA, Langley Research Center Flow Visualization and Laser Velocimetry for Wind Tunnels, Sep. 1982 p 227-234 refs (For primary document see N82-32663 23-35) Avail: NTIS HC A16/MF A01 CSCL 14B

Laser anemometer systems were developed for a full-annular turbine stator cascade facility and for a compressor rotor facility; both are ambient temperature axial flow facilities with a 20-inch tip diameter. The optical configurations of the two anemometers are similar single-component fringe-type backscatter systems with a probe volume diameter of 125 microns and length of about 2 mm. Laser anemometer measurements are compared with numerical solutions for a transonic axial flow compressor rotor and a turbine stator cascade. M.G.

N82-32688*# National Aeronautics and Space Administration, Lewis Research Center, Cleveland, Ohio.

DEVELOPMENT OF A LASER VELOCIMETER FOR A LARGE TRANSONIC WIND TUNNEL

John P. Greissing and Daniel L. Whipple *In* NASA, Langley Research Center Flow Visualization and Laser Velocimetry for Wind Tunnels, Sep. 1982 p 243-247 (For primary document see N82-32663 23-35) Avail: NTIS HC A16/MF A01 CSCL 14B

On a 8 x 6 Foot Supersonic Wind Tunnel a laser velocimeter was utilized in the testing of advanced high speed turbopropellers. The system, using a 15-W argon-ion laser, a 3-beam 2-axis transmitting-receiving optics package, a zoom lens with 1- to 4-m focal lengths, and a 0.4-m corner mirror was initially assembled and tested in the checkout room. During the time the system was located in the checkout area, experience was acquired in the alignment and operation of the system and the data acquisition system and software were developed. By using air jet to simulate tunnel air flow, the system worked quite well. However, problems with beam alignment arose because of reduced atmospheric pressure. Mounting the laser into a vessel maintained at atmospheric pressure with deflectors mounted to the external walls improved operation for about 2 hours before misalignment reoccurred. The system was remounted to the positioning platform in an enclosure that provides both thermal and acoustic isolation. R.J.F.

N82-32689*# National Aeronautics and Space Administration, Lewis Research Center, Cleveland, Ohio.

SEEDING CONSIDERATIONS FOR AN LV SYSTEM IN A LARGE TRANSONIC WIND TUNNEL

Robert J. Freedman *In* NASA, Langley Research Center Flow Visualization and Laser Velocimetry for Wind Tunnels, Sep. 1982 p 249-252 (For primary document see N82-32663 23-35) Avail: NTIS HC A16/MF A01 CSCL 14B

When it was decided to use a laser velocimeter to measure the properties of propellers, seeding was a great concern since large particles fail to flow and small ones are too small to be seen. Many methods were tried and weeded out by using a Malvern particle sizer. The most promising ones were tested in the tunnel and the laser velocimeter (LV) measurements compared to theoretical values of velocity as the particle approached a blunt nose body along a stagnation streamline. Data obtained from the LV system were compared with the one dimensional particle lag calculation. This figure showed the theoretical velocity over the blunt nose and a velocity profile for 5 um particles. This indicated the particles were approximately 5 um. The seeding method is shown. The seed was atomized by 2 seeders run with all 12 available atomizer jets on. The atomizer seed traveled from these two seeders through four 1 inch tubes 20 feet long to the plenum chamber where this cluster of tubes injected the seed into the air stream. The tubes were located 60 feet from the model and could be moved only by shutting the tunnel down. Future seeding plans are shown. R.J.F.

N82-32690* # National Aeronautics and Space Administration, Lewis Research Center, Cleveland, Ohio.

LV MEASUREMENTS WITH AN ADVANCED TURBOPROP

Harvey E. Neumann and J. S. Serafini in NASA, Langley Research Center Flow Visualization and Laser Velocimetry for Wind Tunnels Sep. 1982 p 253-256 (For primary document see N82-32663 23-35)

Avail: NTIS HC A16/MF A01 CSCL 14B

Nonintrusive measurements of velocity about a spinner-propeller-nacelle configuration were made at a Mach number of 0.8. A laser velocimeter (LV) specifically developed for these measurements was used to determine the flow field of the advanced swept S4-3 propeller. The data will be used to study the flow and to verify computer prediction codes. The usefulness of the LV data in detecting flow anomalies and to substantiate the data quality was demonstrated. Some typical results are given. Mach number profiles at the entrance of the propeller are compared with theoretical predictions. The LV data is in excellent agreement with the axisymmetric, compressible, inviscid theory (without blades) ahead of the propeller except near the hub. The data indicate blade blockage near the spinner. Blade to blade variations in axial velocity for four radial positions at the propeller exist are also given. The large apparent wake near the hub is associated with the hub choking. The blade to blade variation of axial velocity ahead of a shock within the blade passage is given. R.J.F.

A82-40132 * Miniature drag-force anemometer. L. N. Kraus and G. C. Fralick (NASA, Lewis Research Center, Cleveland, OH). In: Flow: Its measurement and control in science and industry; Proceedings of the Second Symposium, St. Louis, MO, March 23-26, 1981. Volume 2. (A82-40126 20-35) Research Triangle Park, NC, Instrument Society of America, 1981, p. 117-130, 8 refs.

A miniature drag-force anemometer is described which is capable of measuring unsteady as well as steady-state velocity head and flow direction. It consists of a cantilevered beam with strain gages located at the base of the beam as the force measuring element. The dynamics of the beam are like those of a lightly damped second-order system with a natural frequency as high as 40 kilohertz depending on beam geometry and material. The anemometer can be used in both forward and reversed flow. Anemometer characteristics and several designs are presented along with discussions of several applications. (Author)

N82-22479* # Pratt and Whitney Aircraft Group, East Hartford, Conn. Commercial Products Div.

THIN FILM TEMPERATURE SENSORS, PHASE 3

H. P. Grant, J. S. Przybyszewski, R. G. Cising, and W. L. Anderson 11 Jan. 1982 83 p refs (Contract NAS3-22002)

(NASA-CR-165476; NAS 1.26:165476; PWA-5708-28) Avail: NTIS HC A05/MF A01 CSCL 14B

A thin film Thermocouple system installation for engine test evaluation was designed, and an engine test plan was prepared. Film adherence, durability, accuracy, and drift characteristics were improved. Film thickness was increased to 14 microns, and drift was reduced to less than 0.02 percent of Fahrenheit temperature per hour on actual turbine blades at 1255 K. S.L.

A82-30300 * Three sensor hot wire/film technique for three dimensional mean and turbulence flow field measurement. B. Lakshminarayana (Pennsylvania State University, University Park, PA). *TSI Quarterly*, vol. 8, Jan.-Mar. 1982, p. 3-13, 49 refs. Grants No. NGL-39-009-007; No. NSG-3012; No. NSG-3032.

Methods of measuring the three dimensional flow field using a three-sensor, hot-wire probe is described in this paper, with emphasis on the techniques developed by the author's group at The Pennsylvania State University. The hot wire equations, data processing procedure, calibration techniques, and a discussion of various errors in the measurement are included. Some typical data acquired by this probe is also included. (Author)

A82-34231 * Digital imaging techniques in experimental stress analysis. W. H. Peters and W. F. Ranson (South Carolina University, Columbia, SC). *Optical Engineering*, vol. 21, May-June 1982, p. 427-431, 6 refs. Grant No. NAG3-75.

Digital imaging techniques are utilized as a measure of surface displacement components in laser speckle metrology. An image scanner which is interfaced to a computer records and stores in memory the laser speckle patterns of an object in a reference and deformed configuration. Subsets of the deformed images are numerically correlated with the references as a measure of surface displacements. Discrete values are determined around a closed contour for plane problems which then become input into a boundary integral equation method in order to calculate surface traction in the contour. Stresses are then calculated within this boundary. The solution procedure is illustrated by a numerical example of a case of uniform tension. (Author)

A82-36987 * # Experimental boundary integral equation applications in speckle interferometry. J. E. Fraley, M. A. Hamed, W. H. Peters, and W. F. Ranson. (South Carolina University, Columbia, SC). In: Society for Experimental Stress Analysis, Spring Meeting, Dearborn, MI, May 31-June 4, 1981, Proceedings (A82-36977 18-39) Brookfield Center, CT, Society for Experimental Stress Analysis, 1982, p. 66-72. Grant No. NAG3-75.

A complete data analysis system utilizing laser speckle interferometry and Experimental Integral Equation Method (EBIE) is described. A host computer provides the optical data analysis and serves as an input device to a PDP11/VAX computer for numerical analysis. The basic theory of pointwise filtering and digital correlation is described as experimental data input to the BIE method. (Author)

ORIGINAL PAGE IS
OF POOR QUALITY

36 LASERS AND MASERS

Includes parametric amplifiers.

NO2-26499# KMS Fusion, Inc., Ann Arbor, Mich.
FREE ELECTRON LASERS FOR TRANSMISSION OF ENERGY IN SPACE Final Report
S. B. Segall, H. R. Hiddleston, and G. C. Catella Oct. 1981
40 p refs
(Contract NAS3-22659)
(NASA-CR-165520; NAS 1.26:165520; KMSF-U-1185) Avail:
NTIS HC A03/MF A01 CSCL 20E

A one-dimensional resonant-particle model of a free electron laser (FEL) is used to calculate laser gain and conversion efficiency of electron energy to photon energy. The optical beam profile for a resonant optical cavity is included in the model as an axial variation of laser intensity. The electron beam profile is matched to the optical beam profile and modeled as an axial variation of current density. Effective energy spread due to beam emittance is included. Accelerators appropriate for a space-based FEL oscillator are reviewed. Constraints on the concentric optical resonator and on systems required for space operation are described. An example is given of a space-based FEL that would produce 1.7 MW of average output power at 0.5 micrometer wavelength with over 50% conversion efficiency of electrical energy to laser energy. It would utilize a 10 m-long amplifier centered in a 200 m-long optical cavity. A 3-amp, 65 meV electrostatic accelerator would provide the electron beam and recover the beam after it passes through the amplifier. Three to five shuttle flights would be needed to place the laser in orbit.

A.R.H.

ORIGINAL PAGE IS
OF POOR QUALITY

37 MECHANICAL ENGINEERING

Includes auxiliary systems (non-power); machine elements and processes; and mechanical equipment.

N82-12442* National Aeronautics and Space Administration, Lewis Research Center, Cleveland, Ohio.

MODIFIED FACE SEAL FOR POSITIVE FILM STIFFNESS Patent

Izhak Etsion (Technion - Israel Inst. of Tech.) and Abraham Lipshitz, inventors (to NASA) (Technion - Israel Inst. of Tech.) Issued 29 Sep. 1981 4 p Filed 7 Nov. 1979 Supersedes N80-12414 (18 - 03, p 0334) Sponsored by NASA (NASA-Case-LEW-12989-1; US-Patent-4,291,887; US-Patent-Appl-SN-092145; US-Patent-Class-277-27; US-Patent-Class-277-40; US-Patent-Class-277-93R) Avail: US Patent and Trademark Office CSCL 11A

The film stiffness of a face seal is improved without increasing the sealing and dam area by using an apparatus which includes a primary seal ring in the form of a nose piece. A spring forces a sealing surface on the seal ring into sealing contact with a seal to form a face seal. A circumferential clearance seal is formed in series with this face seal by a lip on the piece. The width of the surface of the lip is substantially the same as the width of the sealing surface on the face seal and the clearance between the surface on the lip and the shaft is substantially the same as the spacing between the face sealing surfaces on the face seal when the shaft is rotating. The circumferential clearance seal restricts the flow of fluid from a main cavity to an intermediate cavity with a resulting pressure drop. The hydrostatic opening face is strongly dependent on the face seal clearance, and the desired axial stiffness is achieved.

Official Gazette of the U.S. Patent and Trademark Office

N82-12446* National Aeronautics and Space Administration, Lewis Research Center, Cleveland, Ohio.

MAGNETOHYDRODYNAMICS (MHD) ENGINEERING TEST FACILITY (ETF) 200 MWe POWER PLANT. DESIGN REQUIREMENTS DOCUMENT (DRD) Final Report

H. S. Rigo, R. W. Bercaw, J. A. Burkhart, T. S. Mroz, D. J. Bents, and A. M. Hatch (MIT) Sep. 1981 88 p refs Revised (Contract DE-AI01-77ET-10769) (NASA-TM-82705; DOE/NASA/10769-20-Rev-3) Avail: NTIS HC A05/MF A01 CSCL 10B

A description and the design requirements for the 200 MWe (nominal) net output MHD Engineering Test Facility (ETF) Conceptual Design, are presented. Performance requirements for the plant are identified and process conditions are indicated at interface stations between the major systems comprising the plant. Also included are the description, functions, interfaces and requirements for each of these major systems. The latest information (1980-1981) from the MHD technology program are integrated with elements of a conventional steam electric power generating plant. M.D.K.

N82-14519* National Aeronautics and Space Administration, Lewis Research Center, Cleveland, Ohio.

APPLICATION OF SURFACE ANALYSIS TO SOLVE PROBLEMS OF WEAR

Donald H. Buckley 1981 35 p refs Presented at the Ideen Traeger der SURTEC Berlin '81, West Germany, 29 Jun. - 3 Jul. 1981 (NASA-TM-82753; E-1069) Avail: NTIS HC A03/MF A01 CSCL 20K

Results are presented for the use of surface analytical tools including field ion microscopy, Auger emission spectroscopy analysis (AES), cylindrical mirror Auger analysis and X-ray photoelectron spectroscopy (XPS). Data from the field ion microscope reveal adhesive transfer (wear) at the atomic level with the formation of surface compounds not found in the bulk, and AES reveals that this transfer will occur even in the presence of surface oxides. Both AES and XPS reveal that in abrasive wear with silicon carbide and diamond contacting the transition metals, the surface and the abrasive undergo a chemical or structural change which effects wear. With silicon carbide, silicon volatilizes leaving behind a pseudo-graphitic surface and the surface of diamond is observed to graphitize. B.W.

N82-16411* National Aeronautics and Space Administration, Lewis Research Center, Cleveland, Ohio.

EFFECT OF SEALS ON ROTOR SYSTEMS

David P. Fleming 1982 18 p refs Presented at the 52nd Shock and Vibration Symp., New Orleans 27-29 Oct. 1981; sponsored by NRL and the Machinery Vibration Monitoring and Anal. Meeting, Oak Brook, Ill., 30 Mar. - 1 Apr. 1982; sponsored by the Vibration Inst. (NASA-TM-82786; E-1121) Avail: NTIS HC A02/MF A01 CSCL 11A

Seals can exert large forces on rotors. As an example, in turbopump ring seals film stiffness as high as 90 MN/m (500,000 lb/in) have been calculated. This stiffness is comparable to the stiffness of rotor support bearings; thus seals can play an important part in supporting and stabilizing rotor systems. The work done to determine forces generated in ring seals is reviewed. Working formulas are presented for seal stiffness and damping, and geometries to maximize stiffness are discussed. An example is described where a change in seal design stabilized a previously unstable rotor. Author

N82-16412* National Aeronautics and Space Administration, Lewis Research Center, Cleveland, Ohio.

EFFECTS OF ARTIFICIALLY PRODUCED DEFECTS ON FILM THICKNESS DISTRIBUTION IN SLIDING EHD POINT CONTACTS

C. Cusano (Illinois Univ. at Urbana-Champaign) and L. D. Wedeven 1981 31 p refs Presented at the Joint Lubrication Conf., New Orleans, 5-7 Oct. 1981; sponsored by the Am. Soc. of Lubrication Engr. and ASME (NASA-TM-82732; E-1042) Avail: NTIS HC A03/MF A01 CSCL 20K

The effects of artificially produced dents and grooves on the elastohydrodynamic (EHD) film thickness profile in a sliding point contact were investigated by means of optical interferometry. The defects, formed on the surface of a highly polished ball, were held stationary at various locations within and in the vicinity of the contact region while the disk was rotating. It is shown that the defects, having a geometry similar to what can be expected in practice, can dramatically change the film thickness which exists when no defects are present in or near the contact. This change in film thickness is mainly a function of the position of the defects in the inlet region, the geometry of the defects, the orientation of the defects in the case of grooves, and the depth of the defect relative to the central film thickness. Author

N82-16413* National Aeronautics and Space Administration, Lewis Research Center, Cleveland, Ohio.

BASIC LUBRICATION EQUATIONS

Bernard J. Hamrock and Duncan Dowson (Leeds Univ.) Dec. 1981 87 p refs Repr. from Ball Bearing Lubrication, chapter 5, Sep. 1981 (NASA-TM-81693; E-209) Avail: NTIS HC A05/MF A01 CSCL 11H

Lubricants, usually Newtonian fluids, are assumed to experience laminar flow. The basic equations used to describe the flow are the Navier-Stokes equation of motion. The study of hydrodynamic lubrication is, from a mathematical standpoint, the application of a reduced form of these Navier-Stokes equations in association with the continuity equation. The Reynolds equation can also be derived from first principles, provided of course that the same basic assumptions are adopted in each case. Both methods are used in deriving the Reynolds equation, and the assumptions inherent in reducing the Navier-Stokes equations are specified. Because the Reynolds equation contains viscosity and density terms and these properties depend on temperature and pressure, it is often necessary to couple the Reynolds with energy equation. The lubricant properties and the energy equation are presented. Film thickness, a parameter of the Reynolds equation, is a function of the elastic behavior of the bearing surface. The governing elasticity equation is therefore presented. A.R.H.

N82-19540* National Aeronautics and Space Administration, Lewis Research Center, Cleveland, Ohio.

COMPOSITE SEAL FOR TURBOMACHINERY Patent

Robert C. Bill and Lawrence P. Ludwig, inventors (to NASA) Issued 20 Oct. 1981 5 p Filed 20 Nov. 1979 Division of

ORIGINAL PAGE IS
OF POOR QUALITY

US Patent Appl. SN-931090, filed 8 Aug. 1978, US Patent-4,207,024 which is a division of US Patent Appl. SN-810290, filed 27 Mar. 1977, US Patent-4,135,851 (NASA-Case-LEW-12131-3; US-Patent-4,295,786; US-Patent-4,207,024; US-Patent-4,135,851; US-Patent-Appl-SN-086255; US-Patent-Appl-SN-931090; US-Patent-Appl-SN-801290; US-Patent-Class-415-174; US-Patent-Class-415-196) Avail: US Patent and Trademark Office CSCL 11A

A gas path seal suitable for use with a turbine engine or compressor is provided. A shroud wearable or abradable by the abrasion of the rotor blades of the turbine or compressor shrouds the rotor blades. A compliant backing surrounds the shroud. The backing is a yielding deformable porous material covered with a thin ductile layer. A mounting fixture surrounds the backing.

Official Gazette of the U.S. Patent and Trademark Office

N82-20543* National Aeronautics and Space Administration, Lewis Research Center, Cleveland, Ohio.

HIGH-SPEED MOTION PICTURE CAMERA EXPERIMENTS OF CAVITATION IN DYNAMICALLY LOADED JOURNAL BEARINGS

Bo O. Jacobson and Bernard J. Hamrock 1982 22 p refs Proposed for presentation at the Joint Lubrication Conf., Washington, D.C., 5-7 Oct. 1982; sponsored by ASME and American Society of Lubrication Engineers (NASA-TM-82798; E-1137; NAS 1.15:82798) Avail: NTIS HC A02/MF A01 CSCL 131

A high-speed camera was used to investigate cavitation in dynamically loaded journal bearings. The length-diameter ratio of the bearing, the speeds of the shaft and bearing, the surface material of the shaft, and the static and dynamic eccentricity of the bearing were varied. The results reveal not only the appearance of gas cavitation, but also the development of previously unsuspected vapor cavitation. It was found that gas cavitation increases with time until, after many hundreds of pressure cycles, there is a constant amount of gas kept in the cavitation zone of the bearing. The gas can have pressure of many times the atmospheric pressure. Vapor cavitation bubbles, on the other hand, collapse at pressures lower than the atmospheric pressure and cannot be transported through a high pressure zone, nor does the amount of vapor cavitation in a bearing increase with time. Analysis is given to support the experimental findings for both gas and vapor cavitation. J.D.H.

N82-24497* National Aeronautics and Space Administration, Lewis Research Center, Cleveland, Ohio.

DEVELOPMENT OF HIGH-SPEED ROLLING-ELEMENT BEARINGS. A HISTORICAL AND TECHNICAL PERSPECTIVE

Erwin V. Zaritsky 1982 28 p refs Presented at the SKF Seventy-Fifth Anniv. Celebration Meeting, Nieuwegein, Netherlands, 9 Jun. 1982; sponsored by SKF Research and Development Center (NASA-TM-82884; E-1198; NAS 1.15:82884) Avail: NTIS HC A03/MF A01 CSCL 131

Research on large-bore ball and roller bearings for aircraft engines is described. Tapered roller bearings and small-bore bearings are discussed. Temperature capabilities of rolling element bearings for aircraft engines have moved from 450 to 589 K (350 to 600 F) with increased reliability. High bearing speeds to 3 million DN can be achieved with a reliability exceeding that which was common in commercial aircraft. Capabilities of available bearing steels and lubricants were defined and established. Computer programs for the analysis and design of rolling element bearings were developed and experimentally verified. The reported work is a summary of NASA contributions to high performance engine and transmission bearing capabilities. R.J.F.

N82-25514* National Aeronautics and Space Administration, Lewis Research Center, Cleveland, Ohio.

FRICTIONAL HEATING DUE TO ASPERITY INTERACTION OF ELASTOHYDRODYNAMIC LINE-CONTACT SURFACES

Bankim C. Majumdar and Bernard J. Hamrock May 1982 23 p refs Presented at the ASME-ASLE Joint Lubrication Conf., New Orleans, 5-7 Oct. 1981 (NASA-TP-1882; E-897; NAS 1.60:1882) Avail: NTIS

HC A02/MF A01 CSCL 20K

A numerical solution of an elasto-hydrodynamically lubricated (EHL) line contact between two long, rough-surface cylinders that considers the frictional heating of asperities was obtained. Pressure distribution, temperature distribution, film thickness and EHL load for given speeds, lubricant properties, material properties of surfaces, and surface roughness parameters were theoretically solved by simultaneous solution of the elasticity equation and the Reynolds equation for two partially lubricated rough surfaces. The pressure due to asperity contact was calculated by assuming a Gaussian distribution of surface irregularities. The elastic deformation used for film thickness computation was found from the two kinds of pressure by plane strain analysis. The temperature rise in the contact zone was calculated by using the Blok-Jaeger flash temperature model. The effects of surface roughness on EHL load for various slide-roll ratios, surface roughness parameters, surface patterns, and temperature parameters was studied. It was found that the maximum temperature rise in most cases occurred in the inlet zone, and that the minimum film thickness decreased and the maximum temperature increased as the surface roughness was increased. Author

N82-25518* National Aeronautics and Space Administration, Lewis Research Center, Cleveland, Ohio.

LUBRICATION OF RIGID ELLIPSOIDAL SOLIDS

Bernard J. Hamrock and Duncan Dowson (Leeds Univ., Engl.) May 1982 55 p refs (NASA-TM-81694; E-209; NAS 1.15:81694) Avail: NTIS HC A04/MF A01 CSCL 131

The influence of geometry on the isothermal hydrodynamic film separating two rigid solids was investigated. The minimum film thickness is derived for fully flooded conjunctions by using the Reynolds boundary conditions. It was found that the minimum film thickness had the same speed, viscosity, and load dependence as Kapitza's classical solution. However, the incorporation of Reynolds boundary conditions resulted in an additional geometry effect. Solutions using the parabolic film approximation are compared by using the exact expression for the film in the analysis. Contour plots are known that indicate in detail the pressure developed between the solids. Author

N82-25519* National Aeronautics and Space Administration, Lewis Research Center, Cleveland, Ohio.

FILM SHAPE CALCULATIONS ON SUPERCOMPUTERS

Bernard J. Hamrock 1982 10 p refs Proposed for presentation at the Joint Lubrication Conf., Washington, 4-6 Oct. 1982 (NASA-TM-82856; E-1225; NAS 1.15:82856) Avail: NTIS HC A02/MF A01 CSCL 09B

Both scalar and vector operations are described to demonstrate usefulness of supercomputers (computers with peak computing speeds exceeding 100 million operative per second) in solving tribological problems. A simple kernel of the film shape calculations in an elasto-hydrodynamic lubricated rectangular contact is presented and the relevant equations are described. Both scalar and vector versions of the film shape code are presented. The run times of the two types of code indicate that over a 50-to-1 speedup of scalar to vector computational time for vector lengths typically used in elasto-hydrodynamic lubrication analysis is obtained. A.R.H.

N82-25520* National Aeronautics and Space Administration, Lewis Research Center, Cleveland, Ohio.

LUBRICANT EFFECTS ON EFFICIENCY OF A HELICOPTER TRANSMISSION

Andrew M. Mitchell and John J. Co, 1982 16 p refs Presented at the AGARD Symp. on Probl. in Bearings and Lubrication, Ottawa, Canada, 31 May - 4 Jun. 1982 (NASA-TM-82857; E-1226; NAS 1.15:82857; AVRADCOM-TR-82-C-9) Avail: NTIS HC A02/MF A01 CSCL 01C

Eleven different lubricants were used in efficiency tests conducted on the OH-58A helicopter main transmission using the NASA Lewis Research Center's 500 hp torque regenerative helicopter transmission test stand. Tests were run at oil-in temperatures of 355 K and 372 K. The efficiency was calculated from a heat balance on the water running through an oil to water heat exchanger which the transmission was heavily insulated. Results show an efficiency range from 98.3% to 98.8% which is a 50% variation relative to the losses associated with

the maximum efficiency measured. For a given lubricant, the efficiency increased as temperature increased and viscosity decreased. There were two exceptions which could not be explained. Between lubricants, efficiency was not correlated with viscosity. There were relatively large variations in efficiency with the different lubricants whose viscosity generally fell in the 5 to 7 centistoke range. The lubricants had no significant effect on the vibration signature of the transmission. A.R.H.

N82-26674* National Aeronautics and Space Administration, Lewis Research Center, Cleveland, Ohio.
FULLY PLASMA-SPRAYED COMPLIANT BACKED CERAMIC TURBINE SEAL Patent Application
Robert C. Bill and Donald W. Wisander, inventors (to NASA) Filed 30 Nov. 1981 8 p
(NASA-Case-LEW-13268-2; US-Patent-Appl-SN-325931) Avail: NTIS HC A02/MF A01 CSCL 11A

A seal with a high temperature abradable lining material which encircles the tips of turbine blades in turbomachinery was designed. The seal is directed to maintaining the minimum operating clearances between the blade tips and the lining of a high pressure turbine. A low temperature easily decomposable material in powder form is blended with a high temperature oxidation resistant metal powder. The two materials are simultaneously deposited on a substrate formed by the turbine casing. Alternately, the polymer powder may be added to the metal powder during plasma spraying. A ceramic layer is then deposited directly onto the metal-polymer composite. The polymer additive mixed with the metal is then completely volatilized to provide a porous layer between the ceramic layer and the substrate. Thermal stresses are reduced by the porous structure which gives a cushion effect. No brazing is required by using only plasma spraying for depositing both the powders of the metal and polymer material as well as the ceramic powder. NASA

N82-26676* National Aeronautics and Space Administration, Lewis Research Center, Cleveland, Ohio.
MULTIROLLER TRACTION DRIVE SPEED REDUCER: EVALUATION FOR AUTOMOTIVE GAS TURBINE ENGINE
Douglas A. Rohn, Neil E. Anderson, and Stuart H. Loewenthal Jun. 1982 24 p refs Prepared in cooperation with Army Aviation Research and Development Command, Cleveland, Ohio (NASA-TP-2027; E-1002; NAS 1.60:2027; AVRADCOM-TR-81-C-11) Avail: NTIS HC A02/MF A01 CSCL 20A

Tests were conducted on a nominal 14:1 fixed-ratio Nasvytis multiroller traction drive retrofitted as the speed reducer in an automotive gas turbine engine. Power turbine speeds of 45,000 rpm and a drive output power of 102 kW (137 hp) were reached. The drive operated under both variable roller loading (proportional to torque) and fixed roller loading (automatic loading mechanism locked). The drive operated smoothly and efficiently as the engine speed reducer. Engine specific fuel consumption with the traction speed reducer was comparable to that with the original helical gearset. Author

N82-26681* National Aeronautics and Space Administration, Lewis Research Center, Cleveland, Ohio.
TOOTH PROFILE ANALYSIS OF CIRCULAR-CUT, SPIRAL-BEVEL GEARS
Ronald L. Huston (Cincinnati Univ.), Yael Lin (Technion - Israel Inst. of Technology), and John J. Coy 1982 20 p refs Presented at the Design Engr. Tech. Conf., Washington, D.C., 12-15 Sep. 1982; sponsored by ASME Prepared in cooperation with Army Aviation Research and Development Command, Cleveland, Ohio (NASA-TM-82840; E-1209; NAS 1.15:82840; AVRADCOM-TR-82-C-05) Avail: NTIS HC A02/MF A01 CSCL 131

An analysis of tooth profile changes in the transverse plane of circular-cut, spiral-bevel crown gears is presented. The analysis assumes a straight-line profile in the mid-transverse plane. The profile variation along the centerline is determined by using expressions for the variation of the spiral angle along the tooth centerline, together with the profile description at the mid-transverse plane. It is shown that the tooth surface is a hyperboloid and that significant variations in the pressure angle are possible. Author

N82-26643* National Aeronautics and Space Administration, Lewis Research Center, Cleveland, Ohio
RELIABILITY MODEL FOR PLANETARY GEAR
Michael Savage (Akron Univ.), Charles A. Paridon (Hewlett Packard Co., Sunnyvale, California), and John J. Coy (Army Aviation Research and Development Command, Cleveland, Ohio) 1982 22 p refs Proposed for Presentation at Design Engr. Tech. Conf., Washington, D.C., 12-15 Sep 1982; sponsored by ASME Prepared in cooperation with Army Aviation Research and Development Command (NASA-TM-82859; NAS 1.15:82859; AVRADCOM-TR-82-C-6) Avail: NTIS HC A02/MF A01 CSCL 131

A reliability model is presented for planetary gear trains in which the ring gear is fixed, the Sun gear is the input, and the planet arm is the output. The input and output shafts are coaxial and the input and output torques are assumed to be coaxial with these shafts. Thrust and side loading are neglected. This type of gear train is commonly used in main rotor transmissions for helicopters and in other applications which require high reductions in speed. The reliability model is based on the Weibull distribution of the individual reliabilities of the transmission components. The transmission's basic dynamic capacity is defined as the input torque which may be applied for one million input rotations of the Sun gear. Load and life are related by a power law. The load life exponent and basic dynamic capacity are developed as functions of the component capacities. Author

N82-26644* National Aeronautics and Space Administration, Lewis Research Center, Cleveland, Ohio
ADVANCES IN HIGH-SPEED ROLLING-ELEMENT BEARINGS
Erwin V. Zaretsky 1982 29 p refs Presented at the 16th Ann. Israel Conf. on Mechan. Engr., Haifa, Israel, 12-14 Jul. 1982; sponsored by Technion - Israel Inst. of Tech. (NASA-TM-82910; E-1295; NAS 1.15:82910) Avail: NTIS HC A03/MF A01 CSCL 131

Aircraft engine and transmission rolling-element bearing state-of-the-art is summarized. Author

N82-26645* National Aeronautics and Space Administration, Lewis Research Center, Cleveland, Ohio.
THE OPTIMAL DESIGN OF INVOLUTE GEAR TEETH WITH UNEQUAL ADDENDA
Michael Savage (Akron Univ.), John J. Coy (Army Aviation Research and Development Command, Cleveland, Ohio), and Dennis P. Townsend 1982 8 p refs Presented at Tenth World Congr. on System Simulation and Sci. Computation, Montreal, 8-13 Aug. 1982; sponsored by Intern. Assoc. for Mathematics and Computers in Simulation (NASA-TM-82866; E-1235; NAS 1.15:82866; AVRADCOM-TR-82-C-7) Avail: NTIS HC A02/MF A01 CSCL 131

The design of a gear mesh is treated with the objective of minimizing the gear size for a given gear ratio, pinion torque, pressure angle, and allowable tooth lengths. Tooth strengths considered include scoring, pitting fatigue, and bending fatigue. Kinematic involute interference is avoided. The design variation on standard spur gear teeth called the long and short addendum system, is considered. In this system the mesh center distance and pressure angle are maintained as is the ability to manufacture the teeth with standard tooling. However, the pinion and gear tooth proportions are altered in order to obtain fewer teeth numbers for the same ratio as standard gears without kinematic involute interference. The effect of this nonstandard gearing geometry with on tooth strengths and gear mesh size are studied. For a 2.1 gearing ratio, the optimal nonstandard gear design is compared with the optimal standard gear design. Author

N82-26646* National Aeronautics and Space Administration, Lewis Research Center, Cleveland, Ohio
A FINITE ELEMENT STRESS ANALYSIS OF SPUR GEARS INCLUDING FILLET RADII AND RIM THICKNESS EFFECTS
S. H. Chang (Cincinnati Univ.), R. L. Huston (Cincinnati Univ.), and J. J. Coy 1982 12 p refs Proposed for presentation at Ann. Meeting of ASME, Phoenix, Ariz., 14-19 Nov. 1982 Prepared in cooperation with Army Aviation Research and Development Command, Cleveland, Ohio (NASA-TM-82865; E-1234; NAS 1.15:82865)

AVRADCOM-TR-82-C-8) Avail: NTIS HC A02/MF A01 CSCL 131

Spur gear stress analysis results are presented for a variety of loading conditions, support conditions, fillet radii, and rim thickness. These results are obtained using the SAP IV finite-element code. The maximum stresses, occurring at the root surface, substantially increase with decreasing rim thickness for partially supported rims (that is, with loose-fitting hubs). For fully supported rims (that is, with tight-fitting hubs), the root surface stresses slightly decrease with decreasing rim thickness. The fillet radius is found to have a significant effect upon the maximum stresses at the root surface. These stresses increase with increasing fillet radius. The fillet radius has little effect upon the internal root section stresses. Author

N82-30552*# National Aeronautics and Space Administration, Lewis Research Center, Cleveland, Ohio.

PRECISION OF SPIRAL-BEVEL GEARS

F. L. Litvin (Univ. of Chicago at Chicago Circle), R. N. Goldrich (Univ. of Chicago at Chicago Circle), J. J. Coy, and E. V. Zaretsky 1982 26 p refs Presented at the Winter Ann. Meeting of the Am. Soc. of Mech. Engr., Phoenix, Ariz., 15-19 Nov. 1982 Sponsored in part by AVRADCOM Research and Technology Labs.

(NASA-TM-82888; E-1196; NAS 1.15:82888, AVRADCOM-TR-82-C-11) Avail: NTIS HC A03/MF A01 CSCL 131

The kinematic errors in spiral bevel gear trains caused by the generation of nonconjugate surfaces, by axial displacements of the gears during assembly, and by eccentricity of the assembled gears were determined. One mathematical model corresponds to the motion of the contact ellipse across the tooth surface (geometry I) and the other along the tooth surface (geometry II). The following results were obtained: (1) kinematic errors induced by errors of manufacture may be minimized by applying special machine settings, the original error may be reduced by order of magnitude, the procedure is most effective for geometry 2 gears, (2) when trying to adjust the bearing contact pattern between the gear teeth for geometry 1 gears, it is more desirable to shim the gear axially; for geometry II gears, shim the pinion axially; (3) the kinematic accuracy of spiral bevel drives are most sensitive to eccentricities of the gear and less sensitive to eccentricities of the pinion. The precision of mounting accuracy and manufacture are most crucial for the gear, and less so for the pinion. E.A.K.

N82-31691*# National Aeronautics and Space Administration, Lewis Research Center, Cleveland, Ohio.

INFLUENCE OF CORROSIVE SOLUTIONS ON MICROHARDNESS AND CHEMISTRY OF MAGNESIUM OXIDE /001/ SURFACES

Hiroyuki Ishigaki (Osaka Univ.), Kazuhisa Miyoshi, and Donald H. Buckley Aug. 1982 11 p refs (NASA-TP-2040; E-1035; NAS 1.60:2040) Avail: NTIS HC A02/MF A01 CSCL 20K

X-ray photoelectron spectroscopy analyses and hardness experiments were conducted on cleaved magnesium oxide /001/ surfaces. The magnesium oxide bulk crystals were cleaved to specimen size along the /001/ surface, and indentations were made on the cleaved surface in corrosive solutions containing HCl, NaOH, or HNO₃ and in water without exposing the specimen to any other environment. The results indicated that chloride (such as MgCl₂) and sodium films are formed on the magnesium oxide surface as a result of interactions between an HCl-containing solution and a cleaved magnesium oxide surface. The chloride films soften the magnesium oxide surface. In this case microhardness is strongly influenced by the pH value of the solution. The lower the pH, the lower the microhardness. Sodium films, which are formed on the magnesium oxide surface exposed to an NaOH containing solution, do not soften the magnesium oxide surface. Author

N82-32733*# National Aeronautics and Space Administration, Lewis Research Center, Cleveland, Ohio.

KINEMATIC PRECISION OF GEAR TRAINS

F. L. Litvin (Illinois Univ. at Chicago Circle), R. N. Goldrich (Illinois

Univ. at Chicago Circle), John J. Coy (AVRADCOM Research and Technology Lab., Cleveland, Ohio), and E. V. Zaretsky 1982 40 p refs Proposed for presentation at the Winter Ann. Meeting of the ASME, Phoenix, 15-19 Nov. 1982

(NASA-TM-82887; E-1191; NAS 1.15:82887;

AVRADCOM-TR-82-C-10) Avail: NTIS HC A03/MF A01 CSCL 131

Kinematic precision is affected by errors which are the result of either intentional adjustments or accidental defects in manufacturing and assembly of gear trains. A method for the determination of kinematic precision of gear trains is described. The method is based on the exact kinematic relations for the contact point motions of the gear tooth surfaces under the influence of errors. An approximate method is also explained. Example applications of the general approximate methods are demonstrated for gear trains consisting of involute (spur and helical) gears, circular arc (Wildhaber-Novikov) gears, and spiral bevel gears. Gear noise measurements from a helicopter transmission are presented and discussed with relation to the kinematic precision theory. S.L.

N82-32734*# National Aeronautics and Space Administration, Lewis Research Center, Cleveland, Ohio.

THE INFLUENCE OF SURFACE DENTS AND GROOVES ON TRACTION IN SLIDING EHD POINT CONTACTS

C. Cusano (Illinois Univ., Urbana-Champaign) and L. D. Wedeven 1982 14 p refs Proposed for presentation at the Joint Lubrication Conf., Washington, D.C., 5-7 Oct., 1982; sponsored by AMSE and Am. Soc. of Lubrication Engr.

(NASA-TM-82943; E-1345; NAS 1.15:32943) Avail: NTIS HC A02/MF A01 CSCL 20K

Changes in traction, caused by dents and grooves on a highly polished ball, are investigated as these defects approach and go through sliding elastohydrodynamic point contacts. The contacts are formed with the ball loading against a transparent disk. The ball and thus the topographical features are held stationary at various locations in the vicinity and within the contact while the disk is rotating. These topographical features can cause substantial changes in the traction when compared to traction obtained with smooth surfaces. S.L.

N82-32735*# National Aeronautics and Space Administration, Lewis Research Center, Cleveland, Ohio.

PLASTIC DEFORMATION AND WEAR PROCESS AT A SURFACE DURING UNLUBRICATED SLIDING

Takashi Yamamoto (Tokyo Univ. of Agriculture and Technology, Japan) and Donald H. Buckley 1982 36 p refs Proposed for presentation at the Joint Lubrication Conf., Washington, D.C., 4-6 Oct. 1982; sponsored by ASME and the Am. Soc. of Lubrication Engr.

(NASA-TM-82820; E-1168; NAS 1.15:82820) Avail: NTIS HC A03/MF A01 CSCL 20K

The plastic deformation and wear of a 304 stainless steel surface sliding against an aluminum oxide rider with a spherical surface (the radius of curvature: 1.3 cm) were observed by using scanning electron and optical microscopes. Experiments were conducted in a vacuum of one million Pa and in an environment of fifty thousandth Pa of chlorine gas at 25 C. The load was 500 grams and the sliding velocity was 0.5 centimeter per second. The deformed surface layer which accumulates and develops successively is left behind the rider, and step shaped protrusions are developed even after single pass sliding under both environmental conditions. A fully developed surface layer is gradually torn off leaving a characteristic pattern. The mechanism for tearing away of the surface layer from the contact area and sliding track contour is explained assuming the simplified process of material removal based on the adhesion theory for the wear of materials. S.L.

N82-32736*# National Aeronautics and Space Administration, Lewis Research Center, Cleveland, Ohio.

EFFECT OF SHOT PEENING ON SURFACE FATIGUE LIFE OF CARBURIZED AND HARDENED AISI 9310 SPUR GEARS

ORIGINAL PAGE IS
OF POOR QUALITY

Dennis P. Townsend and Erwin V. Zaretsky Aug. 1982 14 p refs
(NASA-TP-2047; E-936; NAS 1.60:2047) Avail: NTIS
HC A02/MF A01 CSCL 131

Surface fatigue tests were conducted on two groups of AISI 9310 spur gears. Both groups were manufactured with standard ground tooth surfaces, with the second group subjected to an additional shot peening process on the gear tooth flanks. The gear pitch diameter was 8.89 cm (3.5 in.). Test conditions were a gear temperature of 350 K (170 F), a maximum Hertz stress of 1.71 billion N/sq m (246,000 psi), and a speed of 10,000 rpm. The shot peened gears exhibited pitting fatigue lives 1.6 times the life of standard gears without shot peening. Residual stress measurements and analysis indicate that the longer fatigue life is the result of the higher compressive stress produced by the shot peening. The life for the shot peened gear was calculated to be 1.5 times that for the plain gear by using the measured residual stress difference for the standard and shot peened gears. The measured residual stress for the shot peened gears was much higher than that for the standard gears. S.L.

N02-32737*# National Aeronautics and Space Administration. Lewis Research Center, Cleveland, Ohio.

WEAR MECHANISM BASED ON ADHESION

Takashi Yamamoto and Donald H. Buckley Aug. 1982 13 p refs

(NASA-TP-2037; E-1118; NAS 1.60:2037) Avail: NTIS
HC A02/MF A01 CSCL 11A

Various concepts concerning wear mechanisms and deformation behavior observed in the sliding wear track are surveyed. The mechanisms for wear fragment formation is discussed on the basis of adhesion. The wear process under unlubricated sliding conditions is explained in relation to the concept of adhesion at the interface during the sliding process. The mechanism for tearing away the surface layer from the contact area and forming the sliding track contour is explained by assuming the simplified process of material removal based on the adhesion theory. S.L.

A82-18434 * # Effect of surface roughness on elastohydrodynamic line contact. B. C. Majumdar and B. J. Hamrock (NASA, Lewis Research Center, Cleveland, OH). *American Society of Mechanical Engineers and American Society of Lubrication Engineers, Joint Lubrication Conference, New Orleans, LA, Oct. 5-7, 1981, ASME Paper 81-Lub-23*. 7 p. 17 refs. Members, \$2.00; nonmembers, \$4.00.

A numerical solution of an elastohydrodynamic lubrication (EHL) contact between two long rough surface cylinders is obtained. A simultaneous solution of an elasticity equation and the Reynolds equation for two partially lubricated rough surfaces is used to obtain a theoretical solution of pressure distribution, elastohydrodynamic load and film thicknesses for given speeds. A theoretical solution is also found for lubricants with pressure dependent viscosity, material properties of cylinders, and surface roughness parameters. Elastic deformation is found from hydrodynamic and contact pressure using plane strain analysis, and results indicate that for a constant central film thickness, increasing the surface roughness decreases the EHL load and there is little variation in minimum film thicknesses as the surface roughness is increased. D.L.G.

A82-18436 * # Effects of ultra-clean and centrifugal filtration on rolling-element bearing life. S. H. Loewenthal (NASA, Lewis Research Center, Cleveland, OH), D. W. Moyer (Tribon Bearing Co., Cleveland, OH), and W. M. Needelman (Pall Corp., Glen Cove, NY). *American Society of Mechanical Engineers and American Society of Lubrication Engineers, Joint Lubrication Conference, New Orleans, LA, Oct. 5-7, 1981, ASME Paper 81-Lub-35*. 9 p. 20 refs. Members, \$2.00; nonmembers, \$4.00.

Fatigue tests were conducted on groups of 65-mm bore diameter deep-groove ball bearings in a MIL-L-23699 lubricant under two levels of filtration to determine the upper limit in bearing life under the strictest possible lubricant cleanliness conditions. Bearing fatigue lives, surface distress and weight loss were compared to previous

bearing fatigue tests in contaminated and noncontaminated oil filters having absolute removal ratings of 3, 20, 49, and 105 microns, with lubricant and sump temperatures maintained at 347 K. Ultra clean lubrication was found to produce bearing fatigue lives that were approximately twice that obtained in previous tests with contaminated oil using 3 micron absolute filtration. It was also observed that the centrifugal oil filter has the same effectiveness as a 30 micron absolute filter in preventing surface damage. D.L.G.

A82-18680 * Adhesion and friction of single-crystal diamond in contact with transition metals. K. Miyoshi and D. H. Buckley (NASA, Lewis Research Center, Cleveland, OH). *Applications of Surface Science*, vol. 6, 1980, p. 161-172. 12 refs.

An investigation was conducted to examine the adhesion and friction of single-crystal diamond in contact with various transition metals and the nature of metal transfer to diamond. Sliding friction experiments were conducted with diamond in sliding contact with the metals yttrium, titanium, zirconium, vanadium, iron, cobalt, nickel, tungsten, platinum, rhenium and rhodium. All experiments were conducted with loads of 0.05 to 0.3 N, at a sliding velocity of 0.003 m per minute, in a vacuum of 10 to the -8th Pa, at room temperature, and on the (111) plane of diamond with sliding in the 110 line type direction. The results of the investigation indicate that the coefficient of friction for diamond in contact with various metals is related to the relative chemical activity of the metals in high vacuum. The more active the metal, the higher the coefficient of friction. All the metals examined transferred to the surface of diamond in sliding. (Author)

A82-19335 * # Optimal tooth numbers for compact standard spur gear sets. M. Savage (Akron, University, Akron, OH), J. Coy (U.S. Army, Propulsion Laboratory, Cleveland, OH), and D. P. Townsend (NASA, Lewis Research Center, Cleveland, OH). *American Society of Mechanical Engineers, Design Engineering Technical Conference, Hartford, CT, Sept. 20-23, 1981, Paper 81-DE-115*. 9 p. 23 refs. Members, \$2.00; nonmembers, \$4.00.

The design of a standard gear mesh is treated with the objective of minimizing the gear size for a given ratio, pinion torque, and allowable tooth strength. Scoring, pitting fatigue, bending fatigue, and the kinematic limits of contact ratio and interference are considered. A design space is defined in terms of the number of teeth on the pinion and the diametral pitch. This space is then combined with the objective function of minimum center distance to obtain an optimal design region. This region defines the number of pinion teeth for the most compact design. The number is a function of the gear ratio only. A design example illustrating this procedure is also given. (Author)

A82-30022 * Effect of tangential traction and roughness on crack initiation/propagation during rolling contact. N. Soda (Tokyo, University, Tokyo, Japan) and T. Yamamoto (NASA, Lewis Research Center, Cleveland, OH; Tokyo University of Agriculture and Technology, Tokyo, Japan). *(American Society of Lubrication Engineers, Annual Meeting, 36th, Pittsburgh, PA, May 11-14, 1981.) ASLE Transactions*, vol. 25, Apr. 1982, p. 198-205; Discussion, p. 205; Authors' Closure, p. 205, 206. 17 refs. (Previously announced in STAR as N81-11395)

A82-35036 * # Small gas turbine combustor primary zone development. R. E. Sullivan, A. S. Novick, G. A. Miles (General Motors Corp., Detroit Diesel Allison Div., Indianapolis, IN), and D. Briehl (NASA, Lewis Research Center, Cleveland, OH). *AIAA, SAE, and ASME, Joint Propulsion Conference, 18th, Cleveland, OH, June 21-23, 1982, AIAA Paper 82-1159*. 11 p. 6 refs. Contract No. NAS3-22762.

Designers of small gas turbine engines prefer a close-coupled compressor to turbine shafting arrangement, which in some designs necessitates the use of a small reverse-flow annular combustor. A design methodology for obtaining the maximum performance potential of these combustors is necessary. This paper describes an approach to optimize the design process and gain insight into primary zone performance through interactive theoretical analyses and experimental tests. Three candidate combustor designs are described which address the performance limiting problem areas associated with small annular combustors. Design methodology centers around understanding and controlling primary zone

aerodynamics and the interaction of the distributed fuel with internal airflow patterns. Complete three-dimensional flow field analytical performance prediction procedures are presented and results compared with performance and emission measurements described by probes located at the exit of the primary zone. The effective use of analytical performance prediction methods in the design process is demonstrated. (Author)

A82-35062 * # Combustor development for automotive gas turbines. P. T. Ross, J. R. Williams (General Motors Corp., Detroit Diesel Allison Div., Indianapolis, IN), and D. N. Anderson (NASA, Lewis Research Center, Cleveland, OH). *AIAA, SAE, and ASME, Joint Propulsion Conference, 18th, Cleveland, OH, June 21-23, 1982, AIAA Paper 82-1208*, 9 p. 9 refs. Research supported by the U.S. Department of Energy; Contract No. DEN3-168.

The development of a combustion system for the AGT 100 automotive gas turbine engine is described. A maximum turbine inlet temperature of 1288 C is reached during the regenerative cycle, and air up to 1024 C is supplied to the combustor inlet. A premix/prevaporization ceramic combustor employing variable geometry to control burning zone temperature was developed and tested. Tests on both metal and ceramic combustors showed that emissions were a function of burner inlet temperature (BIT). At 999 C BIT, NO(x) emissions were two orders of magnitude below program goals, and at the same temperature but at a different variable geometry position, the CO was 30 times below program goal. Tests to evaluate the durability of the ceramic materials showed no failures during steady-state operation; however, some cracks developed in the dome during extended transient operation. C.D.

A82-35468 * # Nonlinear analysis of rotor-bearing systems using component mode synthesis. H. D. Nelson, W. L. Meacham (Arizona State University, Tempe, AZ), D. P. Fleming (NASA, Lewis Research Center, Cleveland, OH), and A. F. Kascak (U.S. Army, Propulsion Laboratory, Cleveland, OH). *American Society of Mechanical Engineers, International Gas Turbine Conference and Exhibit, 27th, London, England, Apr. 18-22, 1982, Paper 82-17-03*, 10 p. 19 refs. Members, \$2.00; nonmembers, \$4.00. Grant No. NAG3-6.

The method of component mode synthesis is developed to determine the forced response of nonlinear, multishaft, rotor-bearing systems. The formulation allows for simulation of system response due to blade loss, distributed unbalance, base shock, maneuver loads, and specified fixed frame forces. The motion of each rotating component of the system is described by superposing constraint modes associated with boundary coordinates and constrained precessional modes associated with internal coordinates. The precessional modes are truncated for each component and the reduced component equations are assembled with the nonlinear supports and interconnections to form a set of nonlinear system equations of reduced order. These equations are then numerically integrated to obtain the system response. A computer program, which is presently restricted to single shaft systems, has been written and results are presented for transient system response associated with blade loss dynamics with squeeze film dampers, and with interference rubs. (Author)

A82-37854 * Performance of PTFE-lined composite journal bearings. H. E. Siney (NASA, Lewis Research Center, Cleveland, OH) and F. J. Williams (Rockwell International Corp., North American Aviation Div., Los Angeles, CA). *American Society of Lubrication Engineers, Annual Meeting, 37th, Cincinnati, OH, May 10-13, 1982, Preprint 82-AM-1A-1*, 7 p. 10 refs. Contract No. NAS3-22123. (Previously announced in STAR as N82-17263)

N82-10401*# Cleveland State Univ., Ohio. Dept. of Mechanical Engineering.

A MULTI-PURPOSE METHOD FOR ANALYSIS OF SPUR GEAR TOOTH LOADING Final Report

R. Kasuba, J. W. Evans, R. August, and J. L. Frater Oct. 1981 106 p refs

(Contract NAS3-18547)

(NASA-CR-165163) Avail: NTIS HC A06/MF A01 CSCL 131

A large digitized approach was developed for the static and dynamic load analysis of spur gearing. An iterative procedure was used to calculate directly the 'variable-variable' gear mesh stiffness as a function of transmitted load, gear tooth profile errors, gear tooth deflections and gear hub torsional deformation, and position of contacting profile points. The developed approach can be used to analyze the loads, Hertz stresses, and PV for the normal and high contrast ratio gearing, presently the modeling is limited to the condition that for a given gear all teeth have identical spacing and profiles (with or without surface imperfections). Certain types of simulated sinusoidal profile errors and pitting can cause interruptions of the gear mesh stiffness

function and, thus, increase the dynamic loads in spur gearing. In addition, a finite element stress and mesh subprogram was developed for future introduction into the main program for calculating the gear tooth bending stresses under dynamic loads. A.R.H.

N82-11465*# Rocketdyne, Canoga Park, Calif. ADVANCED SUPERPOSITION METHODS FOR HIGH SPEED TURBOPUMP VIBRATION ANALYSIS Interim Report C. E. Nielson and A. D. Company 19 May 1981 96 p refs (Contract NAS3-22480) (NASA-CR-165379; RI/RD81-149) Avail: NTIS HC A05/MF A01 CSCL 131

The small, high pressure Mark 48 liquid hydrogen turbopump was analyzed and dynamically tested to determine the cause of high speed vibration at an operating speed of 92,400 rpm. This approach the design point operating speed of 95,000 rpm. The initial dynamic analysis in the design stage and subsequent further analysis of the rotor only dynamics failed to predict the vibration characteristics found during testing. An advanced procedure for dynamics analysis was used in this investigation. The procedure involves developing accurate dynamic models of the rotor assembly and casing assembly by finite element analysis. The dynamically instrumented assemblies are independently run tested to verify the analytical models. The verified models are then combined by modal superposition techniques to develop a completed turbopump model where dynamic characteristics are determined. The results of the dynamic testing and analysis obtained are presented and methods of moving the high speed vibration characteristics to speeds above the operating range are recommended. Recommendations for use of these advanced dynamic analysis procedures during initial design phases are given. Author

N82-11466*# Mechanical Technology, Inc., Latham, N. Y. PRELIMINARY STUDY OF TEMPERATURE MEASUREMENT TECHNIQUES FOR STIRLING ENGINE RECIPROCATING SEALS Final Report

Donald F. Wilcock, Leo Hoogenboom, Maarten Meinders, and Ward O. Winer Aug. 1981 82 p Prepared in cooperation with Georgia Inst. of Tech.

(Contracts DEN3-227; DE-A101-77CS-51040)

(NASA-CR-165479; DOE/NASA/O227-1; MT182-TR-4) Avail: NTIS HC A05/MF A01 CSCL 11A

Methods of determining the contact surface temperature in reciprocating seals are investigated. Direct infrared measurement of surface temperatures of a rod exiting a loaded cap seal or simulated seal are compared with surface thermocouple measurements. Significant cooling of the surface requires several milliseconds so that exit temperatures may be considered representative of internal contact temperatures. S.L.

N82-11467*# Pratt and Whitney Aircraft Group, East Hartford, Conn. Commercial Products Div.

JT8D HIGH PRESSURE COMPRESSOR PERFORMANCE IMPROVEMENT Progress Report, Sep. 1978 - Apr. 1981

W. O. Gaffin 11 Nov. 1981 47 p ref

(Contract NAS3-20630)

(NASA-CR-165531; PWA-5515-162) Avail: NTIS HC A03/MF A01 CSCL 131

An improved performance high pressure compressor with potential application to all models of the JT8D engine was designed. The concept consisted of a trenched abradable rubstrip which mates with the blade tips for each of the even rotor stages. This feature allows tip clearances to be set so blade tips run at or near the optimum radius relative to the flowpath wall, without the danger of damaging the blades during transients and maneuvers. The improved compressor demonstrated thrust specific fuel consumption and exhaust gas temperature improvements of 1.0 percent and at least 10 C over the takeoff and climb power range at sea level static conditions, compared to a bill-of-material high pressure compressor. Surge margin also improved 4 percentage points over the high power operating range. A thrust specific fuel consumption improvement of 0.7 percent at typical cruise conditions was calculated based on the sea level test results. B.W.

ORIGINAL PAGE IS
OF POOR QUALITY

N82-11468*# Rocketdyne, Canoga Park, Calif.
LIQUID OXYGEN TURBOPUMP TECHNOLOGY Final Report

C. E. Nielson Nov. 1981 252 p refs
(Contract NAS3-21356)
(NASA-CR-165487; RI/RD81-199) Avail: NTIS
HC A12/MF A01 CSCL 131

A small, high-pressure, LOX turbopump was designed, fabricated and tested. The pump is a single-stage centrifugal type with power to the pump supplied by a single-stage partial-admission axial-impulse turbine. Design conditions included an operating speed of 7330 rad/s (70,000 rpm), pump discharge pressure of 2977 N/sqcm (4318 psia), and a pump flowrate of 16.4 Kg/s (36.21 lb/s). The turbopump contains a self-compensating axial thrust balance piston to eliminate axial thrust loads on the bearings during steady-state operation. Testing of the turbopump was achieved using a gaseous hydrogen high-pressure flow to drive the turbine, which generally is propelled by LOX/LH2 combustion products, at 1041K (1874 R) inlet temperature and at a design pressure ratio of 1.424. Test data obtained with the turbopump are presented which include head-flow-efficiency performance, suction performance, balance piston performance and LOX seal performance. Mechanical performance of the turbopump is also discussed. Author

N82-12444*# Chrysler Corp., Detroit, Mich.
AGT-102 AUTOMOTIVE GAS TURBINE Summary Report
Jun. 1981 434 p refs Sponsored by NASA. Lewis Research Center Prepared jointly with Williams Research Corp., Walled Lake, Mich.

(Contract DE-AC02-76CS-52749)
(NASA-CR-165353; DOE/NASA/2749-81/1) Avail: NTIS
HC A19/MF A01 CSCL 131

Development of a gas turbine powertrain with a 30% fuel economy improvement over a comparable S1 reciprocating engine, operation within 0.41 HC, 3.4 CO, and 0.40 NOx grams per mile emissions levels, and ability to use a variety of alternate fuels is summarized. The powertrain concept consists of a single-shaft engine with a ceramic inner shell for containment of hot gases and support of twin regenerators. It uses a fixed-geometry, lean, premixed, prevaporized combustor, and a ceramic radial turbine rotor supported by an air-lubricated journal bearing. The engine is coupled to the vehicle through a widerange continuously variable transmission, which utilizes gearing and a variable-ratio metal compression belt. A response assist flywheel is used to achieve acceptable levels of engine response. The package offers a 100 lb weight advantage in a Chrysler K Car front-wheel-drive installation. Initial layout studies, preliminary transient thermal analysis, ceramic inner housing structural analysis, and detailed performance analysis were carried out for the basic engine. S.L.

N82-12445*# Bales-McCoin Tractionmatic, Inc., El Paso, Tex.
DESIGN STUDY OF A CONTINUOUSLY VARIABLE ROLLER CONE TRACTION CVT FOR ELECTRIC VEHICLES Final Report

Dan K. McCoin and R. D. Walker Sep. 1980 197 p refs
(Contract DEN3-115; EC-77-A-31-1044)
(NASA-CR-159841; DOE/NASA/0115-80/1;
Bales-McCoin-80-BMT-002) Avail: NTIS HC A09/MF A01
CSCL 131

Continuously variable ratio transmissions (CVT) featuring cone and roller traction elements and computerized controls are studied. The CVT meets or exceeds all requirements set forth in the design criteria. Further, a scalability analysis indicates the basic concept is applicable to lower and higher power units, with upward scaling for increased power being more readily accomplished. S.L.

N82-13427*# Aerojet Nuclear Systems Co., Sacramento, Calif.
LOW-THRUST CHEMICAL PROPULSION SYSTEM PUMP TECHNOLOGY Final Report

R. L. Sabiers and A. Siebenhaar Mar. 1981 201 p refs
(Contract NAS3-21960)
(NASA-CR-165219) Avail: NTIS HC A10/MF A01 CSCL
13K

Candidate pump and driver systems for low thrust cargo orbit transfer vehicle engines which deliver large space structures

to geosynchronous equatorial orbit and beyond are evaluated. The pumps operate to 68 atmospheres (1000 psi) discharge pressure and flowrates suited to cryogenic engines using either LOX/methane or LOX/hydrogen propellants in thrust ranges from 445 to 8900 N (100 to 2000 lb F). Analysis of the various pumps and drivers indicate that the low specific speed requirement will make high fluid efficiencies difficult to achieve. As such, multiple stages are required. In addition, all pumps require inducer stages. The most attractive main pumps are the multistage centrifugal pumps. S.L.

N82-14520# Massachusetts Inst. of Tech., Cambridge. National Magnet Lab.
CONCEPTUAL DESIGN OF SUPERCONDUCTING MAGNET SYSTEM FOR MAGNETOHYDRODYNAMIC (MHD) ENGINEERING TEST FACILITY (ETF) 200 MW_e POWER PLANT Final Report

Nov. 1981 259 p refs
(Grant NAG3-100)
(NASA-CR-165053; FBNML-NAS-E-2) Avail: NTIS
HC A12/MF A01 CSCL 14B

A superconducting magnet system conceptual design to meet the requirements of a magnetohydrodynamic test facility power train is presented. A detailed description of the magnet is accompanied by numerous engineering drawings. Functional requirements, system interfaces, and design criteria are reviewed. System limits, safety precautions, operational procedures, and maintenance procedures are discussed. R.J.F.

N82-16408*# Transmission Research, Inc., Cleveland, Ohio.
TRACTION CONTACT PERFORMANCE EVALUATION AT HIGH SPEEDS Interim Report

Joseph L. Tavaarwerk (Applied Tribology Ltd.) Sep. 1981
193 p refs
(Contract DEN3-35; EC-77-A-31-1011)
(NASA-CR-165226; DOE/NASA/0035-1) Avail: NTIS
HC A09/MF A01 CSCL 131

The results of traction tests performed on two fluids are presented. These tests covered a pressure range of 1.0 to 2.5 GPa, an inlet temperature range of 30 °C to 70 °C, a speed range of 10 to 80 m/sec, aspect ratios of .5 to 5 and spin from 0 to 2.1 percent. The test results are presented in the form of two dimensionless parameters, the initial traction slope and the maximum traction peak. With the use of a suitable rheological fluid model the actual traction curves measured can now be reconstituted from the two fluid parameters. More importantly, the knowledge of these parameters together with the fluid rheological model, allow the prediction of traction under conditions of spin, slip and any combination thereof. Comparison between theoretically predicted traction under these conditions and those measured in actual traction tests shows that this method gives good results. Author

N82-16410*# Eaton Corp., Southfield, Mich. Engineering and Research Center.

SMALL PASSENGER CAR TRANSMISSION TEST: CHEVROLET MALIBU 200C TRANSMISSION WITH LOCKUP
M. P. Bujold Aug. 1981 245 p refs
(Contracts DEN3-124; DE-AI01-77CS-51044)
(NASA-CR-165182; DOE/NASA/0124-6; ERC-TR-8125) Avail:
NTIS CSCL 13F

The small passenger car transmission test was initiated to supply electric vehicle manufacturers with technical information regarding the performance of commercially available transmissions. This information would enable EV manufacturers to design a more energy efficient vehicle. With this information the manufacturers would be able to estimate vehicle driving range as well as speed and torque requirements for specific road load performance characteristics. This report covers the testing of a Chevrolet Malibu 200C automatic transmission with lockup. The transmission was tested in accordance with a passenger car automatic transmission test code (SAE J651b) which required drive performance, coast performance, and no load test conditions. Under these test conditions, the transmission attained maximum efficiencies in the mid 90 percent range both for drive performance test and coast performance tests. The torque, speed and efficiency curves map the complete performance characteristics for the Chevrolet Malibu 200C automatic transmission with lockup. Author

ORIGINAL PAGE IS
OF POOR QUALITY

N82-18603*# Pratt and Whitney Aircraft Group, East Hartford, Conn. Commercial Products Div.
JTDD CERAMIC OUTER AIR SEAL SYSTEM REFINEMENT PROGRAM Progress Report, Jan. 1979 - Feb. 1981
W. O. Gaffin 27 Jan. 1982 84 p refs
(Contract NAS3-20830)
(NASA-CR-165554; PWA-5515-165) Avail: NTIS HC A05/MF A01 CSCL 11A

The abrasability and durability characteristics of the plasma sprayed system were improved by refinement and optimization of the plasma spray process and the metal substrate design. The acceptability of the final seal system for engine testing was demonstrated by an extensive rig test program which included thermal shock tolerance, thermal gradient, thermal cycle, erosion, and abrasability tests. An interim seal system design was also subjected to 2500 endurance test cycles in a JT9D-7 engine.

T.M.

N82-20540*# SKF Technology Services, King of Prussia, Pa. Technology Services.

SPHERICAL ROLLER BEARING ANALYSIS. SKF COMPUTER PROGRAM SPHERBEAN. VOLUME 1: ANALYSIS Final Report, Jun. 1978 - Dec. 1980

R. J. Kleckner and J. Pirivics Dec. 1980 86 p refs 3 Vol.
(Contract NAS3-20824)

(NASA-CR-165203; NAS 1.26:165203; AT81D006-Vol-1)
Avail: NTIS HC A05/MF A01 CSCL 13I

The models and associated mathematics used within the SPHERBEAN computer program for prediction of the thermomechanical performance characteristics of high speed lubricated double row spherical roller bearings are presented. The analysis allows six degrees of freedom for each roller and three for each half of an optionally split cage. Roller skew, free lubricant, inertial loads, appropriate elastic and friction forces, and flexible outer ring are considered. Roller quasidynamic equilibrium is calculated for a bearing with up to 30 rollers per row, and distinct roller and flange geometries are specifiable. The user is referred to the material contained here for formulation assumptions and algorithm detail.

J.D.H.

N82-20541*# SKF Technology Services, King of Prussia, Pa. Technology Services.

SPHERICAL ROLLER BEARING ANALYSIS. SKF COMPUTER PROGRAM SPHERBEAN. VOLUME 2: USER'S MANUAL Final Report, Jun. 1978 - Dec. 1980

R. J. Kleckner and G. Dyba Dec. 1980 150 p refs 3 Vol.
(Contract NAS3-20824)

(NASA-CR-165204; NAS 1.26:165204; AT81D007-Vol-2)
Avail: NTIS HC A07/MF A01 CSCL 13I

The user's guide for the SPHERBEAN computer program for prediction of the thermomechanical performance characteristics of high speed lubricated double row spherical roller bearings is presented. The material presented is structured to guide the user in the practical and correct implementation of SPHERBEAN. Input and output, guidelines for program use, and sample executions are detailed.

J.D.H.

N82-20542*# SKF Technology Services, King of Prussia, Pa. Technology Services.

SPHERICAL ROLLER BEARING ANALYSIS. SKF COMPUTER PROGRAM SPHERBEAN. VOLUME 3: PROGRAM CORRELATION WITH FULL SCALE HARDWARE TESTS Final Report, Jun. 1978 - Dec. 1980

R. J. Kleckner, J. W. Rosenlieb, and G. Dyba Dec. 1980 225 p refs 3 Vol.
(Contract NAS3-20824)

(NASA-CR-165205; NAS 1.26:165205; AT81D008-Vol-3)
Avail: NTIS HC A10/MF A01 CSCL 13I

The results of a series of full scale hardware tests comparing predictions of the SPHERBEAN computer program with measured data are presented. The SPHERBEAN program predicts the thermomechanical performance characteristics of high speed lubricated double row spherical roller bearings. The degree of correlation between performance predicted by SPHERBEAN and measured data is demonstrated. Experimental and calculated performance data is compared over a range in speed up to 19,400 rpm (0.8 MDN) under pure radial, pure axial, and combined loads.

J.D.H.

N82-24496*# Eaton Engineering and Research Center, Southfield, Mich.

SMALL PASSENGER CAR TRANSMISSION TEST: MERCURY LYNX ATX TRANSMISSION Final Report

M. P. Bujold Sep. 1981 335 p
(Contract DEN3-124; DE-A101-77CS-51044)

(NASA-CR-165510; GOE/NASA/O124-7; NAS 1.26:165510; ERC-TR-B191) Avail: NTIS HC A15/MF A01 CSCL 13I

The testing of a Mercury Lynx automatic transmission is reported. The transmission was tested in accordance with a passenger car automatic transmission test code (SAE J651b) which required drive performance, coast performance, and no load test conditions. Under these conditions, the transmission averaged maximum efficiencies in the mid-ninety percent range both for drive performance test and coast performance tests. The torque, speed, and efficiency curves are presented, which provide the complete performance characteristics for the Mercury Lynx automatic transmission.

J.D.

N82-25516*# Illinois Univ., Chicago. Dept. of Materials Engineering.

MATHEMATICAL MODELS FOR THE SYNTHESIS AND OPTIMIZATION OF SPIRAL BEVEL GEAR TOOTH SURFACES Final Report

F. L. Litvin, Parnaz Rahman, and Robert N. Goldrich Jun. 1982 122 p refs

(Grant NAG3-48)
(NASA-CR-3553; NAS 1.26:3553) Avail: NTIS HC A06/MF A01 CSCL 13I

The geometry of spiral bevel gears and to their rational design are studied. The nonconjugate tooth surfaces of spiral bevel gears are, in theory, replaced (or approximated) by conjugated tooth surfaces. These surfaces can be generated by two conical surfaces, and by a conical surface and a revolution. Although these conjugated tooth surfaces are simpler than the actual ones, the determination of their principal curvatures and directions is still a complicated problem. Therefore, a new approach, to the solution of these is proposed. Direct relationships between the principal curvatures and directions of the tool surface and those of the generated gear surface are obtained. With the aid of these analytical tools, the Hertzian contact problem for conjugate tooth surfaces can be solved. These results are useful in determining compressive load capacity and surface fatigue life of spiral bevel gears. A general theory of kinematical errors exerted by manufacturing and assembly errors is developed. This theory is used to determine the analytical relationship between gear misalignments and kinematical errors. This is important to the study of noise and vibration in geared systems.

S.L.

N82-26679*# Anderson (William J.), North Olmsted, Ohio. **BEARINGS: TECHNOLOGY AND NEEDS Final Report**

William J. Anderson May 1982 21 p refs Presented at the 59th Meeting of the Propulsion and Energetics Panel Symp. on Problems in Bearings and Lubrication, Ottawa, 31 May - 3 Jun. 1982; sponsored by AGARD

(Contract NAS3-23157; DA Proj. 1L1-62209-AH-76)
(NASA-CR-167908; NAS 1.26:167908) Avail: NTIS HC A02/MF A01 CSCL 13I

A brief status report on bearing technology and present and near-term future problems that warrant research support is presented. For rolling element bearings a material with improved fracture toughness, life data in the low Lambda region, a comprehensive failure theory verified by life data and incorporated into dynamic analyses, and an improved corrosion resistant alloy are perceived as important needs. For hydrodynamic bearings better definition of cavitation boundaries and pressure distributions for squeeze film dampers, and geometry optimization for minimum power loss in turbulent film bearings are needed. For gas film bearings, foil bearing geometries that form more nearly optimum film shapes for maximum load capacity, and more effective surface protective coatings for high temperature operation are needed.

Author

N82-26680*# California State Univ., Los Angeles. Dept. of Mechanical Engineering.

ELECTROSTATIC FUEL CONDITIONING OF INTERNAL COMBUSTION ENGINES

Phillip I. Gold 15 Jun. 1982 117 p refs
(Grant NAG3-73)

(NASA-CR-165029; NAS 1.26:165029) Avail: 'NTIS HC A06/MF A01 CSC' 21A

Diesel engines were tested to determine if they are influenced by the presence of electrostatic and magnetic fields. Field forces were applied in a variety of configurations including pretreatment of the fuel and air, however, no effect on engine performance was observed. S.L.

N82-27743*# Curtiss-Wright Corp., Wood-Ridge, N.J. Rotary Engine Facility.

ADVANCED STRATIFIED CHARGE ROTARY AIRCRAFT ENGINE DESIGN STUDY

P. Badgley, M. Berkowitz, C. Jones, D. Myers, E. Norwood, W. B. Pratt, D. R. Ellis (Cessna Aircraft Corp.), G. Huggins (Cessna Aircraft Corp.), A. Mueller (Cessna Aircraft Corp.), and J. H. Hembrey (Cessna Aircraft Corp.) 29 Jan. 1982 149 p refs (Contract NAS3-21285)

(NASA-CR-165398; NAS 1.26:165398; CW-WR-81.021) Avail: NTIS HC A07/MF A01 CSCL 21A

A technology base of new developments which offered potential benefits to a general aviation engine was compiled and ranked. Using design approaches selected from the ranked list, conceptual design studies were performed of an advanced and a highly advanced engine sized to provide 186/25C shaft Kw/HP under cruise conditions at 7620/25,000 m/ft altitude. These are turbocharged, direct-injected stratified charge engines intended for commercial introduction in the early 1980's. The engine descriptive data includes tables, curves, and drawings depicting configuration, performance, weights and sizes, heat rejection, ignition and fuel injection system descriptions, maintenance requirements, and scaling data for varying power. An engine-airframe integration study of the resulting engines in advanced airframes was performed on a comparative basis with current production type engines. The results show airplane performance, costs, noise & installation factors. The rotary-engined airplanes display substantial improvements over the baseline, including 30 to 35% lower fuel usage. A.R.H.

N82-29603*# Cincinnati Univ., Ohio. Dept. of Mechanical Engineering.

ON FINITE ELEMENT STRESS ANALYSIS OF SPUR GEARS

S. H. Chang and R. L. Huston Jul. 1982 53 p refs (Grant NsG-3188)

(NASA-CR-167938; NAS 1.26:167938) Avail: NTIS HC A04/MF A01 CSCL 13I

Spur gear stress analysis results are presented for a variety of loading conditions, support conditions, root radii, and rim thicknesses. These results are obtained using the SAP-IV finite element code. The maximum stresses, occurring at the root surface, substantially increase with decreasing rim thickness for partially supported rims (that is, with loose fitting hubs). For fully supported rims (that is, with tight fitting hubs), the root surface stresses slightly decrease with decreasing rim thickness. The fillet radius has a significant effect upon the maximum stresses at the root surface. These stresses increase with decreasing fillet radius. Finally, the fillet radius has little effect upon the internal root section stresses. S.L.

A82-11783*# The AGT101 technology - An automotive alternative. R. A. Rackley and K. A. Davis (Garrett Turbine Engine Co., Phoenix, AZ). In: Intersociety Energy Conversion Engineering Conference, 16th, Atlanta, GA, August 9-14, 1981, Proceedings, Volume 2. (A82-11701 C2-44) New York, American Society of Mechanical Engineers, 1981, p. 1403-1407, Contract No. DEN3-167.

The Advanced Gas Turbine Powertrain System Development Project is oriented at providing the United States automotive industry the technology base necessary to produce gas turbine powertrains for automotive applications that will have: (1) reduced fuel consumption, (2) the ability to use a variety of fuels, (3) low emissions, and (4) competitive cost/performance. The AGT101 powertrain being developed consists of a regenerated single-shaft gas turbine engine flat rated at 74.6 kW (100 hp) coupled to a split-differential gearbox and a Ford automatic overdrive production transmission. Performance predictions for the AGT101 powertrain represent a 59-percent improvement in mileage estimates over a 1985 conventionally-powered automobile for the combined federal driving cycle. (Author)

A82-18407* Alignment of fluid molecules in an EHD contact. J. L. Lauer, L. E. Keller, F. H. Choi, and V. W. King (Rensselaer Polytechnic Institute, Troy, NY). *American Society of Lubrication Engineers and American Society of Mechanical Engineers, Lubrication Conference, New Orleans, LA, Oct. 5-7, 1981, ASLE Preprint 81-LC-5C-1*, 8 p, 7 refs. Members, \$2.00; nonmembers, \$4.00. Grants No. AF-AFOSR-78-3473; No. NsG-3170.

Dichroic infrared emission spectra have been obtained from an operating elasto-hydrodynamic contact under conditions showing unequivocally that the molecules of the fluid are aligned under shear flow in the bulk of the fluid and that the extent of the alignment is increased by the presence of an additive in a small concentration. This work applied particularly to polyphenyl ether and to 1,1,2-trichloroethane as the additive, but similar results have been obtained with polycyclohexyls and the same additive. The observation of two separate glass transitions for the polycyclohexyl solution is an indication of the occurrence of a phase separation in the Hertzian inlet zone. A model has been developed to explain the effect of these phenomena and their relation to traction. (Author)

A82-18426*# Measurement of oil film thickness for application to elastomeric Stirling engine rod seals. A. I. Krauter (Carrier Corp., Research Div., Syracuse, NY). *American Society of Mechanical Engineers and American Society of Lubrication Engineers, Joint Lubrication Conference, New Orleans, LA, Oct. 5-7, 1981, ASME Paper 81-Lub-9*, 5 p, 10 refs. Members, \$2.00; nonmembers, \$4.00. Contract No. DEN3-22.

The rod seal in the Stirling engine has the function of separating high pressure gas from low or ambient pressure oil. An experimental apparatus was designed to measure the oil film thickness distribution for an elastomeric seal in a reciprocating application. Tests were conducted on commercial elastomeric seals having a 76 mm rod and a 3.8 mm axial width. Test conditions included 70 and 90 seal durometers, a sliding velocity of 0.8 m/sec, and a zero pressure gradient across the seal. An acrylic cylinder and a typical synthetic base automotive lubricant were used. The experimental results showed that the effect of seal hardness on the oil film thickness is considerable. A comparison between analytical and experimental oil film profiles for an elastomeric seal during relatively high speed reciprocating motion showed an overall qualitative agreement. J.F.

A82-18431*# Regimes of traction in concentrated contact lubrication. S. Bair and W. O. Winer (Georgia Institute of Technology, Atlanta, GA). *American Society of Mechanical Engineers and American Society of Lubrication Engineers, Joint Lubrication Conference, New Orleans, LA, Oct. 5-7, 1981, ASME Paper 81-Lub-16*, 5 p, 11 refs. Members, \$2.00; nonmembers, \$4.00. Grant No. NsG-3106.

Experimental evidence is presented for the existence of three regimes of traction in concentrated contacts. Data are obtained in a rolling contact simulator by varying the lubricant, temperature, rolling speed, load and surface roughness at a fixed slide-to-roll ratio. At lower thicknesses the mixed regime is encountered, and traction is increased due to asperity interaction, while at higher film thicknesses, the lubricant pressure is distributed over a greater area than the Hertzian region, resulting in a lower average pressure and reduced traction. D.L.G.

A82-18449*# Single pass rub phenomena - Analysis and experiment. F. E. Kennedy (Dartmouth College, Hanover, NH). *American Society of Mechanical Engineers and American Society of Lubrication Engineers, Joint Lubrication Conference, New Orleans, LA, Oct. 5-7, 1981, ASME Paper 81-Lub-55*, 7 p, 10 refs. Members, \$2.00; nonmembers, \$4.00. Grant No. NsG-3253.

An experimental and analytical investigation is presented of contact phenomena for the case of a fully-dense copper gas path seal segment which is rubbed by a single steel blade tip at room temperature. The experiments were executed on a pendulum-type test device, with forces, rub energy, surface temperature and residual deformation being determined for each single-path rub test. The thermal and mechanical factors influencing single-pass rub surface temperatures were modeled analytically. It is found that large plastic strains occurred on or near the contact surface of the copper rub

ORIGINAL PAGE IS OF POOR QUALITY

specimens. A study of the influence of various material properties on surface temperature showed that increased thermal conductivity of the stationary component played a role in lowering contact temperatures. Increased thermal conductivity of the moving blade tip component and increased thermal diffusivity of the stationary material also had a beneficial effect. O.C.

A82-19334 * # Surface geometry of circular cut spiral bevel gears. R. L. Huston (Cincinnati, University, Cincinnati, OH) and J. J. Coy (U.S. Army, Propulsion Laboratory, Cleveland, OH). *American Society of Mechanical Engineers, Design Engineering Technical Conference, Hartford, CT, Sept. 20-23, 1981, Paper 81-DET-114*. 6 p. 7 refs. Members, \$2.00; nonmembers, \$4.00. Grant No. NsG-3128.

An analysis of the surface geometry of spiral bevel gears formed by a circular cutter is presented. The emphasis is upon determining the tooth surface principal radii of curvature of crown (flat) gears. Specific results are presented for involute, straight, and hyperbolic cutter profiles. It is shown that the geometry of circular cut spiral bevel gears is somewhat simpler than a theoretical logarithmic spiral bevel gear. (Author)

A82-21967 * Anaerobic polymers as high vacuum leak sealants. B. R. F. Kendall (Pennsylvania State University, University Park, PA). *Journal of Vacuum Science and Technology*, vol. 20, Feb. 1982, p. 248, 249. 5 refs. Research supported by the Pennsylvania Research Corp.; Grant No. NsG-3301.

Anaerobic polymers are useful as solventless leak sealants with good vacuum properties at moderate temperatures. Loctite 290 can seal leaks in a range generally encountered in carefully constructed ultrahigh vacuum and high vacuum systems. It was found that small leaks are sealed best under vacuum, whereas large leaks should be sealed at atmospheric pressure. The high-temperature behavior of Loctite 290 is limited by its fast cure, which prevents deep penetration into small leaks; cracking eventually occurs at the entrance to the leak. Repeated thermal cycling to about 300 C is possible, however, provided viscosity, curing time, and leak size are properly matched to ensure penetration into the body of the leak. This may require special formulations for high temperature vacuum applications. J.F.

A82-27079 * # Development of CdO-graphite-Ag coatings for gas bearings to 427 C. B. Bhushan (Mechanical Technology, Inc., Latham, NY). In: *Wear of materials 1981; Proceedings of the International Conference, San Francisco, CA, March 30-April 1, 1981*. (A82-27051 12-37) New York, American Society of Mechanical Engineers, 1981, p. 735-746. 21 refs. Research supported by the Mechanical Technology, Inc.; Contracts No. DEN3-43; No. EY-76 C-02-2749.

Graphite is one of the most commonly known lubricants. Its effectiveness in a range between room temperature (RT) and 540 C is reportedly improved by adding cadmium oxide. CdO-graphite powder in a gas carrier has been used in numerous applications that rely on dry lubrication. A coating of this composition was developed and successfully tested in foil air bearings for long periods up to a temperature of 427 C and at a normal contacting load (during starting and stopping) of 14 kPa based on bearing projected area. The addition of ultra-fine silver to the CdO-graphite has improved the coating endurance. At 427 C, the CdO-graphite-Ag coating performed better than CdO-graphite without silver, both for extended periods at 14 kPa loading and for limited periods at 35 kPa. At 288 C, the coating was tested for an extended period up to 28 kPa and has also successfully completed high-speed shock tests to an acceleration level of 100g. (Author)

A82-35038 * # AGT 100 automotive gas turbine system development. H. E. G. Helms (General Motors Corp., Detroit Diesel Allison Div., Indianapolis, IN). *AIAA, SAE, and ASME, Joint Propulsion Conference, 18th, Cleveland, OH, June 21-23, 1982, AIAA Paper 82-1165*. 11 p. Research sponsored by the U.S. Department of Energy; Contract No. DEN3-168.

General Motors is developing an automotive gas turbine system that can be an alternate powerplant for future automobiles. Work sponsored by DOE and administered by NASA Lewis Research Center is emphasizing small component aero-

dynamics and high-temperature structural ceramics. Reliability requirements of the AGT 100 turbine system include chemical and structural ceramic component stability in the gas turbine environment. The power train system, its configuration and schedule are presented, and its performance tested. The aerodynamic component development is reviewed with discussions on the compressor, turbine, regenerator, interturbine duct and scroll, and combustor. Ceramic component development is also reviewed, and production cost and required capital investment are taken into consideration. D.L.G.

A82-35039 * # AGT101 automotive gas turbine system development. R. A. Rackley and J. R. Kidwell (Garrett Turbine Engine Co., Phoenix, AZ). *AIAA, SAE, and ASME, Joint Propulsion Conference, 18th, Cleveland, OH, June 21-23, 1982, AIAA Paper 82-1166*. 8 p. Research sponsored by the U.S. Department of Energy; Contract No. DEN3-167.

The AGT101 automotive gas turbine system consisting of a 74.6 kw regenerated single-shaft gas turbine engine, is presented. The development and testing of the system is reviewed, and results for aerothermodynamic components indicate that compressor and turbine performance levels are within one percent of projected levels. Ceramic turbine rotor development is encouraging with successful cold spin testing of simulated rotors to speeds over 12,043 rad/sec. Spin test results demonstrate that ceramic materials having the required strength levels can be fabricated by net shape techniques to the thick hub cross section, which verifies the feasibility of the single-stage radial rotor in single-shaft engines. D.L.G.

A82-35061 * # AGT100 turbomachinery. D. L. Tipton and T. F. McKain (General Motors Corp., Detroit Diesel Allison Div., Indianapolis, IN). *AIAA, SAE, and ASME, Joint Propulsion Conference, 18th, Cleveland, OH, June 21-23, 1982, AIAA Paper 82-1207*. 11 p. Research supported by the U.S. Department of Energy; Contract No. DEN3-168.

High-performance turbomachinery components have been designed and tested for the AGT100 automotive engine. The required wide range of operation coupled with the small component size, compact packaging, and low cost of production provide significant aerodynamic challenges. Aerodynamic design and development testing of the centrifugal compressor and two radial turbines are described. The compressor achieved design flow, pressure ratio, and surge margin on the initial build. Variable inlet guide vanes have proven effective in modulating flow capacity and in improving part-speed efficiency. With optimum use of the variable inlet guide vanes, the initial efficiency goals have been demonstrated in the critical idle-to-70% gasifier speed range. The gasifier turbine exceeded initial performance goals and demonstrated good performance over a wide range. The radial power turbine achieved 'developed' efficiency goals on the first build. (Author)

A82-35321 * # The AGT 101 advanced automotive gas turbine. R. A. Rackley and J. R. Kidwell (Garrett Turbine Engine Co., Phoenix, AZ). *American Society of Mechanical Engineers, International Gas Turbine Conference and Exhibit, 27th, London, England, Apr. 18-22, 1982, Paper 82-GT-72*. 9 p. Members, \$2.00; nonmembers, \$4.00. Research supported by the U.S. Department of Energy; Contract No. DEN3-167.

A development program is described whose goal is the accumulation of the technology base needed by the U.S. automotive industry for the production of automotive gas turbine powertrains. Such gas turbine designs must exhibit reduced fuel consumption, a multi-fuel capability, and low exhaust emissions. The AGT101 powertrain described is a 74.6 kW, regenerated single-shaft gas turbine, operating at a maximum inlet temperature of 1644 K and coupled to a split differential gearbox and automatic overdrive transmission. The engine's single stage centrifugal compressor and single stage radial inflow turbine are mounted on a common shaft, and will operate at a maximum rotor speed of 100,000 rpm. All high temperature components, including the turbine rotor, are ceramic. O.C.

A82-35462 * # Engine dynamic analysis with general nonlinear finite element codes. II - Bearing element implementation, overall numerical characteristics and benchmarking. J. Padovan, M. Adams, P. Lam (Akron, University, Akron, OH), D. Fertis, and I. Zeld (Northeastern University, Boston, MA). *American Society of Mechanical Engineers, International Gas Turbine Conference and Exhibit, 27th, London, England, Apr. 18-22, 1982, Paper 82-GT-202*. 9 p. 12 refs. Members, \$2.00; nonmembers, \$4.00. Grant No. NsG-3283.

Second-year efforts within a three-year study to develop and extend finite element (FE) methodology to efficiently handle the transient/steady state response of rotor-bearing-stator structure associated with gas turbine engines are outlined. The two main areas aim at (1) implanting the squeeze film damper element into a general purpose FE code for testing and evaluation; and (2) determining the numerical characteristics of the FE-generated rotor-bearing-stator simulation scheme. The governing FE field equations are set out and the solution methodology is presented. The choice of ADINA as the general-purpose

FE code is explained, and the numerical operational characteristics of the direct integration approach of FE-generated rotor-bearing-stator simulations is determined, including benchmarking, comparison of explicit vs. implicit methodologies of direct integration, and demonstration problems. C.D.

ORIGINAL PAGE IS
OF POOR QUALITY

A82-35480 * # Design and development of a ceramic radial turbine for the AGT101. D. G. Finger and S. K. Gupta (Garrett Turbine Engine Co., Phoenix, AZ). AIAA, SAE, and ASME, Joint Propulsion Conference, 18th, Cleveland, OH, June 21-23, 1982, AIAA Paper 82-1209, 9 p. Contract No. DEN3-167.

An acceptable and feasible ceramic turbine wheel design has been achieved, and the relevant temperature, stress, and success probability analyses are discussed. The design is described, the materials selection presented, and the engine cycle conditions analysis parameters shown. Measured MOR four-point strengths are indicated for room and elevated temperatures, and engine conditions are analyzed for various cycle states, materials, power settings, turbine inlet temperatures, and speeds. An advanced gas turbine ceramic turbine rotor thermal and stress model is developed, and cumulative probability of survival is shown for first and third-year properties of SiC and Si3N4 rotors under different operating conditions, computed for both blade and hub regions. Temperature and stress distributions for steady-state and worst-case shutdown transients are depicted. C.D.

A82-48243 * # On the automatic generation of FEM models for complex gears - A work-in-progress report. R. J. Drago (Boeing Vertol Co., Philadelphia, PA). American Gear Manufacturers Association, Meeting, San Diego, CA, Feb. 1982, Paper. 36 p. Contract No. NAS11-22143.

A description is presented of the development and use of a preprocessor to create a NASTRAN finite element model of a complex spur, helical, or spiral bevel gear quickly, inexpensively, and accurately. The preprocessor creates a ready to run NASTRAN input deck including the executive, case control, and bulk data sections. It generates nodes and solid elements to model spur, helical, or spiral bevel gear teeth with integral shafting. Either a complete gear shafting model or a symmetric model is created. The fundamental building block of the gear model is the base layer. The base layer is the mesh configuration of one layer of one tooth segment which is in turn duplicated, translated, and rotated to create the completed model of the gear. Once the base layer is created, the construction of the finite element model is straightforward. G.R.

38 QUALITY ASSURANCE AND RELIABILITY

Includes product sampling procedures and techniques; and quality control.

N82-18612*# National Aeronautics and Space Administration, Lewis Research Center, Cleveland, Ohio.

METAL HONEYCOMB TO POROUS WIREFORM SUBSTRATE DIFFUSION BOND EVALUATION

A. Vary, P. E. Moorhead, and D. R. Hull 1982 12 p refs Presented at the Spring Conf. of the Am. Soc. for Nondestructive Testing, Boston, 22-25 Mar. 1982

(NASA-TM-82793; E-959) Avail: NTIS HC A02/MF A01 CSCL 14D

Two nondestructive techniques were used to evaluate diffusion bond quality between a metal foil honeycomb and porous wireform substrate. The two techniques, cryographics and acousto-ultrasonics, are complementary in revealing variations of bond integrity and quality in shroud segments from an experimental aircraft turbine engine. S.L.

N82-19550*# National Aeronautics and Space Administration, Lewis Research Center, Cleveland, Ohio.

EXPERIENCE WITH MODIFIED AEROSPACE RELIABILITY AND QUALITY ASSURANCE METHOD FOR WIND TURBINES

William E. Klein 1982 11 p refs Proposed for Presentation at 9th Ann. Engr. Conf. on Reliability, Hershey, Penn., 16-18 Jan. 1982 Revised

(Contract DE-A101-78ET-20320)
(NASA-TM-82803; DOE/NASA/20320-38; E-1142) Avail: NTIS HC A02/MF A01 CSCL 14D

The SR&QA approach assures that the machine is not hazardous to the public or operating personnel, can operate unattended on a utility grid, demonstrates reliability operation, and helps establish the quality assurance and maintainability requirements for future wind turbine projects. The approach consisted of modified failure modes and effects analysis (FMEA) during the design phase, minimal hardware inspection during parts fabrication, and three simple documents to control activities during machine construction and operation. Five years experience shows that this low cost approach works well enough that it should be considered by others for similar projects. T.M.

N82-20551*# National Aeronautics and Space Administration, Lewis Research Center, Cleveland, Ohio.

INTERRELATION OF MATERIAL MICROSTRUCTURE, ULTRASONIC FACTORS, AND FRACTURE TOUGHNESS OF TWO PHASE TITANIUM ALLOY

Alex Vary and David R. Hull 1982 25 p refs Presented at the Spring Conf. of the Am. Soc. for Nondestructive Testing, Boston, 22-25 Mar. 1982

(NASA-TM-82810; E-1151; NAS 1.15:82810) Avail: NTIS HC A02/MF A01 CSCL 14D

The pivotal role of an alpha-beta phase microstructure in governing fracture toughness in a titanium alloy, Ti-662, is demonstrated. The interrelation of microstructure and fracture toughness is demonstrated using ultrasonic measurement techniques originally developed for nondestructive evaluation and material property characterization. It is shown that the findings determined from ultrasonic measurements agree with conclusions based on metallurgical, metallographic, and fractographic observations concerning the importance of alpha-beta morphology in controlling fracture toughness in two phase titanium alloys. Author

N82-18613*# Massachusetts Inst. of Tech., Cambridge, Dept. of Mechanical Engineering.

ULTRASONIC INPUT-OUTPUT FOR TRANSMITTING AND RECEIVING LONGITUDINAL TRANSDUCERS COUPLED TO SAME FACE OF ISOTROPIC ELASTIC PLATE Final Report

James H. Williams, Jr., Hira Karagulle, and Samson S. Lee Washington, D.C. NASA Feb. 1982 29 p refs (Grant NSG-3210)

(NASA-CR-3506) Avail: NTIS HC A03/MF A01 CSCL 14D

The quantitative understanding of ultrasonic nondestructive evaluation parameters such as the stress wave factor were studied. Ultrasonic input/output characteristics for an isotropic elastic plate with transmitting and receiving longitudinal transducers coupled to the same face were analyzed. The asymptotic normal stress is calculated for an isotropic elastic half space subjected to a uniform harmonic normal stress applied to a circular region at the surface. The radiated stress waves are traced within the plate by considering wave reflections at the top and bottom faces. The output voltage amplitude of the receiving transducer is estimated by considering only longitudinal waves. Agreement is found between the output voltage wave packet amplitudes and times of arrival due to multiple reflections of the longitudinal waves. E.A.K.

A82-14400* A pad perturbation method for the dynamic coefficients of tilting-pad journal bearings. P. E. Allaire, J. K. Parsell, and L. E. Barrett (Virginia, University, Charlottesville, VA). *Wear*, vol. 72, Oct. 1, 1981, p. 29-44. 14 refs. Contract No. EF-76-5-01-2479; Grant No. NSG-3105.

A pad assembly method for analyzing tilting-pad bearings is presented. The method results in the complete coefficient matrix for a tilting-pad bearing; the matrix is independent of the pad inertia, the pitch frequency and the number of degrees of freedom of the pad. A pad assembly method is used because it allows the collection of more bearing data with less computer time than a brute force iterative procedure. The results given show the complete dynamical matrices for a five-pad tilting-pad bearing both including and ignoring the damping effects of the unloaded (top) pads. For a symmetrical tilting-pad bearing the reduced cross-coupling coefficients are zero when the moment of inertia of the pad is ignored. (Author)

ORIGINAL PAGE IS
OF POOR QUALITY

39 STRUCTURAL MECHANICS

Includes structural element design and weight analysis; fatigue; and thermal stress.

For applications see *05 Aircraft Design, Testing and Performance* and *18 Spacecraft Design, Testing and Performance*.

N82-11491* National Aeronautics and Space Administration, Lewis Research Center, Cleveland, Ohio.

INTEGRATED ANALYSIS OF ENGINE

Christos C. Chamis 1981 24 p refs Presented at the Ann. Meeting of the ASME, Washington, D.C., 16-21 Nov. 1981 (NASA-TM-82713; E-996) Avail: NTIS HC A02/MF A01 CSCL 20K

The need for light, durable, fuel efficient, cost effective aircraft requires the development of engine structures which are flexible, made from advanced materials (including composites), resist higher temperatures, maintain tighter clearances and have lower maintenance costs. The formal quantification of any or several of these requires integrated computer programs (multi-level and/or interdisciplinary analysis programs interconnected) for engine structural analysis/design. Several integrated analysis computer programs are under development at Lewis Research Center. These programs include: (1) COBSTRAN-Composite Blade Structural Analysis, (2) CODSTRAN-Composite Durability Structural Analysis, (3) CISTRAN-Composite Impact Structural Analysis, (4) STAEBL-Strut Tailoring of Engine Blades, and (5) ESMOSS-Engine Structures Modeling Software System. Three other related programs, developed under Lewis sponsorship, are described. Author

N82-16419* National Aeronautics and Space Administration, Lewis Research Center, Cleveland, Ohio.

ELEVATED TEMPERATURE FATIGUE TESTING OF METALS

Marvin H. Hirschberg Dec. 1981 24 p refs (NASA-TM-82745; E-1058) Avail: NTIS HC A02/MF A01 CSCL 20K

The major technology areas needed to perform a life prediction of an aircraft turbine engine hot section component are discussed and the steps required for life prediction are outlined. These include the determination of the operating environment, the calculation of the thermal and mechanical loading of the component, the cyclic stress-strain and creep behavior of the material required for structural analysis, and the structural analysis to determine the local stress-strain-temperature-time response of the material at the critical location in the components. From a knowledge of the fatigue, creep, and failure resistance of the material, a prediction of the life of the component is made. Material characterization and evaluation conducted for the purpose of calculating fatigue crack initiation lives of components operating at elevated temperatures are emphasized. J.D.H.

N82-20566* National Aeronautics and Space Administration, Lewis Research Center, Cleveland, Ohio.

ELASTIC-PLASTIC FINITE-ELEMENT ANALYSES OF THERMALLY CYCLED SINGLE-EDGE WEDGE SPECIMENS

Albert Kaufman Mar. 1982 27 p refs (NASA-TP-1982; E-687; NAS 1.60:1982) Avail: NTIS HC A03/MF A01 CSCL 20K

Elastic-plastic stress-strain analyses were performed for single-edge wedge alloys subjected to thermal cycling in fluidized beds. Three cases (NASA TAZ-8A alloy under one cycling condition and 316 stainless steel alloy under two cycling conditions) were analyzed by using the MARC nonlinear, finite-element computer program. Elastic solutions from MARC showed good agreement with previously reported solutions that used the NASTRAN and ISO3DQ computer programs. The NASA TAZ-8A case exhibited no plastic strains, and the elastic and elastic-plastic analyses gave identical results. Elastic-plastic analyses of the 316 stainless steel alloy showed plastic strain reversal with a shift of the mean stresses in the compressive direction. The maximum equivalent total strain ranges for these cases were 13 to 22 percent greater than that calculated from elastic analyses. Author

N82-20566* National Aeronautics and Space Administration, Lewis Research Center, Cleveland, Ohio.

ELASTIC-PLASTIC FINITE-ELEMENT ANALYSES OF THERMALLY CYCLED DOUBLE-EDGE WEDGE SPECIMENS

Albert Kaufman and Larry E. Hunt Mar. 1982 31 p refs (NASA-TP-1973; E-626; NAS 1.60:1973) Avail: NTIS HC A03/MF A01 CSCL 20K

Elastic-plastic stress-strain analyses were performed for double-edge wedge specimens subjected to thermal cycling in fluidized beds at 316 and 1088 C. Four cases involving different nickel-base alloys (IN 100, Mar M-200, NASA TAZ-8A, and Rene 80) were analyzed by using the MARC nonlinear, finite element computer program. Elastic solutions from MARC showed good agreement with previously reported solutions obtained by using the NASTRAN and ISO3DQ computer programs. Equivalent total strain ranges at the critical locations calculated by elastic analyses agreed within 3 percent with those calculated from elastic-plastic analyses. The elastic analyses always resulted in compressive mean stresses at the critical locations. However, elastic-plastic analyses showed tensile mean stresses for two of the four alloys and an increase in the compressive mean stress for the highest plastic strain case. M.G.

N82-21604* National Aeronautics and Space Administration, Lewis Research Center, Cleveland, Ohio.

COUPLED BENDING-BENDING-TORSION FLUTTER OF A MISTUNED CASCADE WITH NONUNIFORM BLADES

Krishna Rao V. Kaza (Toledo Univ.) and Robert E. Kielb 1982 20 p refs Presented at the 23rd Struct., Structural Dyn., and Mater. Conf., New Orleans, 10-12 May 1982 (NASA-TM-82813; E-1156; NAS 1.15:82813) Avail: NTIS HC A02/MF A01 CSCL 20K

A set of aeroelastic equations describing the motion of an arbitrarily mistuned cascade with flexible, pretwisted, nonuniform blades is developed using an extended Hamilton's principle. The derivation of the equations has its basis in the geometric nonlinear theory of elasticity in which the elongations and shears are negligible compared to unity. A general expression for foreshortening of a blade is derived and is explicitly used in the formulation. The blade aerodynamic loading in the subsonic and supersonic flow regimes is obtained from two dimensional, unsteady, cascade theories. The aerodynamic, inertial and structural coupling between the bending (in two planes) and torsional motions of the blade is included. The equations are used to investigate the aeroelastic stability and to quantify the effect of frequency mistuning on flutter in turbofans. Results indicate that a moderate amount of intentional mistuning has enough potential to alleviate flutter problems in unshrouded, high aspect ratio turbofans. S.L.

N82-24501* National Aeronautics and Space Administration, Lewis Research Center, Cleveland, Ohio.

NONLINEAR STRUCTURAL AND LIFE ANALYSES OF A COMBUSTOR LINER

V. Moreno (Pratt and Whitney Aircraft Group, East Hartford, Conn.), G. J. Meyers (Pratt and Whitney Aircraft Group, East Hartford, Conn.), A. Kaufman, and G. R. Halford 1982 23 p refs Proposed for presentation at the Symp. on Advances and Trends in Struct. and Solid Mech., 4-7 Oct. 1982, Washington, D.C.; sponsored by NASA and Georgetown Univ. (NASA-TM-82846; E-1216; NAS 1.15:82846) Avail: NTIS HC A02/MF A01 CSCL 20K

Three dimensional, nonlinear finite element structural analyses were performed for a simulated combustor liner specimen to assess the capability of nonlinear analyses using classical inelastic material models to represent the thermoplastic creep response of the one half scale component. Results indicate continued cyclic hardening and ratcheting while experimental data suggested a stable stress strain response after only a few loading cycles. The computed stress strain history at the critical location was put into two life prediction methods, strainrange partitioning and a Pratt and Whitney combustor life prediction method to evaluate their ability to predict cyclic crack initiation. It is found that the life prediction analyses over predicted the observed cyclic crack initiation life. E.A.K.

N82-24502*# National Aeronautics and Space Administration, Lewis Research Center, Cleveland, Ohio.
EVALUATION OF INELASTIC CONSTITUTIVE MODELS FOR NONLINEAR STRUCTURAL ANALYSIS
Albert Kaufman 1982 22 p refs Presented at the Symp. on Nonlinear Constitutive Relations for High Temp. Appl., Akron, Ohio, 19-20 May 1982; sponsored by NASA and Akron Univ. (NASA-TM-82845; E-1215; NAS 1.15:82845) Avail: NTIS HC A02/MF A01 CSCL 20K

The influence of inelastic material models on computed stress-strain states, and therefore predicted lives, was studied for thermomechanically loaded structures. Nonlinear structural analyses were performed on a fatigue specimen which had been subjected to thermal cycling in fluidized beds and on a mechanically load cycled benchmark notch specimen. Four incremental plasticity creep models (isotropic, kinematic, combined isotropic kinematic, combined plus transient creep) were exercised using the MARC program. Of the plasticity models, kinematic hardening gave results most consistent with experimental observations. Life predictions using the computed strain histories at the critical location with a strainrange partitioning approach considerably overpredicted the crack initiation life of the thermal fatigue specimen. S.L.

N82-26701*# National Aeronautics and Space Administration, Lewis Research Center, Cleveland, Ohio.
BIRD IMPACT ANALYSIS PACKAGE FOR TURBINE ENGINE FAN BLADES
Murray S. Hirschbein 1982 20 p refs Presented at 23rd Struct. Dyn. and Mater. Conf., New Orleans, 10-12 Previously announced in IAA as A82-30162 May 1982; Sponsored by AIAA, ASME, ASCE, and AHS (NASA-TM-82831; NAS 1.15:82831) Avail: NTIS HC A02/MF A01 CSCL 20K
For abstract see A82-30162

N82-31707*# National Aeronautics and Space Administration, Lewis Research Center, Cleveland, Ohio.
LARGE DISPLACEMENTS AND STABILITY ANALYSIS OF NONLINEAR PROPELLER STRUCTURES
Robert A. Aiello 1982 18 p refs Presented at the 10th NASTRAN User's Colloq., New Orleans, 13-14 May 1982 (NASA-TM-82850; NAS 1.15:82850) Avail: NTIS HC A02/MF A01 CSCL 20K

The use of linear rigid formats in COSMIC NASTRAN without DMAP procedures for the analysis of nonlinear propeller structures is described. Approaches for updating geometry and applying follower forces for incremental loading are demonstrated. Comparisons are made with COSMIC NASTRAN rigid formats and other independent finite element programs. Specifically, the comparisons include results from the four approaches for updating the geometry using RIGID FORMAT 1, RIGID FORMATS 4 and 13, MARC and MSC/NASTRAN. It is shown that 'user friendly' updating approaches (without DMAPS) can be used to predict the large displacements and instability of these nonlinear structures. These user friendly approaches can be easily implemented by the user and predict conservative results. Author

N82-31708*# National Aeronautics and Space Administration, Lewis Research Center, Cleveland, Ohio.
TENSILE BUCKLING OF ADVANCED TURBOPROPS
C. C. Chamis and R. A. Aiello 1982 25 p refs Presented at the 23rd Struct., Struct. Dyn. and Mater. Conf., New Orleans, 10-12 May 1982; sponsored by AIAA, ASME, ASCE and AHS (NASA-TM-82896; E-1276; NAS 1.15:82896) Avail: NTIS HC A02/MF A01 CSCL 20K

Theoretical studies were conducted to determine analytically the tensile buckling of advanced propeller blades (turboprops) in centrifugal fields, as well as the effects of tensile buckling on other types of structural behavior, such as resonant frequencies and flutter. Theoretical studies were also conducted to establish the advantages of using high performance composite turboprops as compared to titanium. Results show that the vibration frequencies are not affected appreciably prior to 80 percent of the tensile

speed. Some frequencies approach zero as the tensile buckling speed is approached. Composites provide a substantial advantage over titanium on a buckling speed to weight basis. Vibration modes change as the rotor speed is increased and substantial geometric coupling is present. R.J.F.

N82-33744*# National Aeronautics and Space Administration, Lewis Research Center, Cleveland, Ohio.
NONLINEAR CONSTITUTIVE THEORY FOR TURBINE ENGINE STRUCTURAL ANALYSIS
Robert L. Thompson In NASA, Langley Research Center Res. In Struct. and Solid Mech., 1982 Oct. 1982 p 67-96 refs (For primary document see N82-33739 24-39) Avail: NTIS HC A19/MF A01 CSCL 20K

A number of viscoplastic constitutive theories and a conventional constitutive theory are evaluated and compared in their ability to predict nonlinear stress-strain behavior in gas turbine engine components at elevated temperatures. Specific application of these theories is directed towards the structural analysis of combustor liners undergoing transient, cyclic, thermomechanical load histories. The combustor liner material considered in this study is Hastelloy X. The material constants for each of the theories (as a function of temperature) are obtained from existing, published experimental data. The viscoplastic theories and a conventional theory are incorporated into a general purpose, nonlinear, finite element computer program. Several numerical examples of combustor liner structural analysis using these theories are given to demonstrate their capabilities. Based on the numerical stress-strain results, the theories are evaluated and compared. Author

A82-39852* Impact resistance of fiber composites. C. C. Chamis and J. H. Sinclair (NASA, Lewis Research Center, Cleveland, OH). In: Composite materials: Mechanics, mechanical properties and fabrication; Proceedings of the Japan-U.S. Conference, Tokyo, Japan, January 12-14, 1981. (A82-39851 19-39) Barking, Essex, England, Applied Science Publishers, 1982, p. 1-11.

Stress-strain curves are obtained for a variety of glass fiber and carbon fiber reinforced plastics in dynamic tension, over the stress-strain range of 0.00087-2070/sec. The test method is of the one-bar block-to-bar type, using a rotating disk or a pendulum as the loading apparatus and yielding accurate stress-strain curves up to the breaking strain. In the case of glass fiber reinforced plastic, the tensile strength, strain to peak impact stress, total strain and total absorbed energy all increase significantly as the strain rate increases. By contrast, carbon fiber reinforced plastics show lower rates of increase with strain rate. It is recommended that hybrid composites incorporating the high strength and rigidity of carbon fiber reinforced plastic with the high impact absorption of glass fiber reinforced plastics be developed for use in structures subjected to impact loading. O.C.

A82-40357* Extended range stress intensity factor expressions for chevron-notched short bar and short rod fracture toughness specimens. J. L. Shannon, Jr., R. T. Bubsy, W. S. Pierce (NASA, Lewis Research Center, Cleveland, OH), and D. Munz (Karlsruhe, Universität, Karlsruhe, West Germany). *International Journal of Fracture*, vol. 19, July 1982, p. R55-R58.

A82-40358* Crack displacements for J/I testing with compact specimens. T. W. Orange (NASA, Lewis Research Center, Cleveland, OH). *International Journal of Fracture*, vol. 19, July 1982, p. R59-R61. 5 refs.

The suggestion is made that the standard compact specimen (with opening displacement measured at the crack mouth) may be entirely suitable for J-integral determinations if a very simple conversion factor is used. Experimental determination of J-integral values requires the measurement of displacements at the points of load application. For the compact specimen this is a difficult task. On the basis of studies reported by Newman (1979) and Fisher and Buzzard (1980), it is suggested that for any J-based test the standard compact specimen can be used. A very good approximation to the load point displacement (within 3.4 percent) can be obtained by measuring the crack mouth displacement and multiplying by 0.773. G.R.

N82-14531*# Arizona Univ., Tucson. Dept. of Aerospace and Mechanical Engineering.
THE APPLICATION OF PROBABILISTIC DESIGN THEORY TO HIGH TEMPERATURE LOW CYCLE FATIGUE

Paul H. Wirsching Nov. 1981 224 p refs
(Grant NAG3-41)
(NASA-CR-165488) Avail: NTIS HC A10/MF A01 CSCL
20K

Metal fatigue under stress and thermal cycling is a principal mode of failure in gas turbine engine hot section components such as turbine blades and disks and combustor liners. Designing for fatigue is subject to considerable uncertainty, e.g., scatter in cycles to failure, available fatigue test data and operating environment data, uncertainties in the models used to predict stresses, etc. Methods of analyzing fatigue test data for probabilistic design purposes are summarized. The general strain life as well as homo- and hetero-scadastic models are considered. Modern probabilistic design theory is reviewed and examples are presented which illustrate application to reliability analysis of gas turbine engine components. A.R.H.

N82-17521*# Battelle Columbus Labs., Ohio.
STRESS EVALUATIONS UNDER ROLLING/SLIDING CONTACTS Final Report

J. W. Kannel and J. L. Tevaarwerk 30 Oct. 1981 54 p refs
(Contract NAS3-22808)
(NASA-CR-165561; G7782) Avail: NTIS HC A04/MF A01
CSCL 20K

The state of stress beneath traction drive type of contacts were analyzed. Computing stresses and stress reversals on various planes for points beneath the surface were examined. The effect of tangential and axial friction under gross slip conditions is evaluated with the models. Evaluations were performed on an RC (rolling contact) tester configuration and it is indicated that the classical fatigue stresses are not altered by friction forces typical of lubricated contact. Higher values of friction can result in surface shear reversal that exceeds the stresses at the depth of maximum shear reversal under rolling contact. E.A.K.

N82-19563*# Virginia Polytechnic Inst. and State Univ., Blacksburg. Dept. of Engineering Science and Mechanics.
FINITE-ELEMENT MODELING OF LAYERED, ANISOTROPIC COMPOSITE PLATES AND SHELLS: A REVIEW OF RECENT RESEARCH

J. N. Reddy In Shock and Vibration Information Center The Shock and Vibration Digest, Vol. 13, No. 12 Dec. 1981 p 3-12 refs (For primary document see N82-19562 10-39)
(Grants NAG3-208; AF-AFOSR-O142-81)
Avail: SVIC, Code 5804, Naval Research Lab., Washington, D.C. 20375; \$15.00/set CSCL 20/11

Finite element papers published in the open literature on the static bending and free vibration of layered, anisotropic, and composite plates and shells are reviewed. A literature review of large-deflection bending and large-amplitude free oscillations of layered composite plates and shells is also presented. Non-finite element literature is cited for continuity of the discussion. J.D.H.

N82-20564*# Case Western Reserve Univ., Cleveland, Ohio.
FATIGUE LIFE PREDICTION IN BENDING FROM AXIAL FATIGUE INFORMATION

S. S. Manson and U. Muralidharan Feb. 1982 38 p refs
(Grant NAG3-39)
(NASA-CR-165563; NAS 1.26:165563) Avail: NTIS
HC A03/MF A01 CSCL 20K

Bending fatigue in the low cyclic life range differs from axial fatigue due to the plastic flow which alters the linear stress-strain relation normally used to determine the nominal stresses. An approach is presented to take into account the plastic flow in calculating nominal bending stress (S sub bending) based on true surface stress. These functions are derived in closed form for rectangular and circular cross sections. The nominal bending stress and the axial fatigue stress are plotted as a function of life (N sub S) and these curves are shown for several materials of engineering interest. S.L.

N82-24503*# Georgia Inst. of Tech., Atlanta. Center for the Advancement of Computational Mechanics.

CREEP CRACK-GROWTH: A NEW PATH-INDEPENDENT T SUB O AND COMPUTATIONAL STUDIES
R. B. Stonesifer and S. N. Atluri Dec. 1981 141 p refs
(Grant NAG3-38)

ORIGINAL PAGE IS
OF POOR QUALITY

(NASA-CR-168930; NAS 1.26:168930) Avail: NTIS
HC A07/MF A01 CSCL 20K

Two path independent integral parameters which show some degree of promise as fracture criteria are the C* and delta T sub c integrals. The mathematical aspects of these parameters are reviewed. This is accomplished by deriving generalized vector forms of the parameters using conservation laws which are valid for arbitrary, three dimensional, cracked bodies with crack surface tractions (or applied displacements), body forces, inertial effects and large deformations. Two principal conclusions are that delta T sub c is a valid crack tip parameter during nonsteady as well as steady state creep and that delta T sub c has an energy rate interpretation whereas C* does not. An efficient, small displacement, infinitesimal strain, displacement based finite element model is developed for general elastic/plastic material behavior. For the numerical studies, this model is specialized to two dimensional plane stress and plane strain and to power law creep constitutive relations. S.L.

N82-26702*# Cincinnati Univ., Ohio.
MICROSTRUCTURAL EFFECTS ON THE ROOM AND ELEVATED TEMPERATURE LOW CYCLE FATIGUE BEHAVIOR OF WASPALOY M.S. Thesis Final Report

Bradley A. Lerch May 1982 194 p refs
(Grant Nsg-3263)
(NASA-CR-165497; NAS 1.26:165497) Avail: NTIS
HC A09/MF A01 CSCL 20K

Longitudinal specimens of Waspaloy containing either coarse grains with small gamma or fine grains with large gamma were tested in air at a frequency of 0.33 Hz or 0.50 Hz. The coarse grained structures exhibited planar slip on (111) planes and precipitate shearing at all temperatures. Cracks initiated by a Stage 1 mechanism and propagated by a striation forming mechanism. At 700 C and 800 C, cleavage and intergranular cracking were observed. Testing at 500 C, 700 C, and 800 C caused precipitation of grain boundary carbides. At 700 C, carbides precipitated on slip bands. The fine grained structures exhibited planar slip on (111) planes. Dislocations looped the large gamma precipitates. This structure led to stress saturation and propagation was observed. Increasing temperatures resulted in increased specimen oxidation for both heat treatments. Slip band and grain boundary oxidation were observed. At 800 C, oxidized grain boundaries were cracked by intersecting slip bands which resulted in intergranular failure. The fine specimens had crack initiation later in the fatigue life, but with more rapid propagation crack propagation. A.R.H.

N82-26706*# Cincinnati Univ., Ohio. Dept. of Materials Science and Metallurgical Engineering.
MECHANISMS OF DEFORMATION AND FRACTURE IN HIGH TEMPERATURE LOW CYCLE FATIGUE OF RENE 80 AND IN 100 Final Report

Glenn Roy Romanoski, Jr. Mar. 1982 227 p refs
(Grant Nsg-3263)
(NASA-CR-165498; NAS 1.26:165498) Avail: NTIS
HC A11/MF A01 CSCL 20K

Specimens tested for the AGARD strain range partitioning program were investigated. Rene 80 and IN 100 were tested in air and in vacuum; at 871 C, 925 C, and 1000 C; and in the coated and uncoated condition. The specimens exhibited a multiplicity of high-temperature low-cycle fatigue damage. Observations of the various forms of damage were consistent with material and testing conditions and were generally in agreement with previous studies. In every case observations support a contention that failure occurs at a particular combination of crack length and maximum stress. A failure criterion which is applicable in the regime of testing studied is presented. The predictive capabilities of this criterion are straight forward. Author

N82-26713*# Illinois Univ., Urbana-Champaign. Dept. of Theoretical and Applied Mechanics.
BOUNDARY LAYER THERMAL STRESSES IN ANGLE-PLY COMPOSITE LAMINATES, PART 1 Final Report

S. S. Wang and I. Choi Feb. 1981 56 p refs 6 Vol.
(Contract Nsg-3044)
(NASA-CR-165412; NAS 1.26:165412) Avail: NTIS
HC A04/MF A01 CSCL 20K

Thermal boundary-layer stresses (near free edges) and

displacements were determined by an eigenfunction expansion technique and the establishment of an appropriate particular solution. Current solutions in the region away from the singular domain (free edge) are found to be in excellent agreement with existing approximate numerical results. As the edge is approached, the singular term controls the near field behavior of the boundary layer. Results are presented for cases of various angle-ply graphite/epoxy laminates with $(\theta/\theta/\theta/\theta)$ configurations. These results show high interlaminar (through-the-thickness) stresses. Thermal boundary-layer thicknesses of different composite systems are determined by examining the strain energy density distribution in composites. It is shown that the boundary-layer thickness depends on the degree of anisotropy of each individual lamina, thermomechanical properties of each ply, and the relative thickness of adjacent layers. The interlaminar thermal stresses are compressive with increasing temperature. The corresponding residual stresses are tensile and may enhance interply delaminations. A.R.H.

N82-26714*# Illinois Univ., Urbana-Champaign. Dept. of Theoretical and Applied Mechanics.
ANALYSIS OF CRACKS EMANATING FROM A CIRCULAR HOLE IN UNIDIRECTIONAL FIBER REINFORCED COMPOSITES, PART 2 Final Report
S. S. Wang and J. F. Yau Feb. 1981 35 p refs 6 Vol.
(Grant NsG-3044)
(NASA-CR-165433; NAS 1.26:165433) Avail: NTIS HC A03/MF A01 CSCL 20K

An analytical method is developed for cracks emanating from a circular hole in an off-axis unidirectional fiber-reinforced composite. The method which is formulated by using conservation laws of elasticity and fundamental relationships in anisotropic fracture mechanics, provides a convenient and accurate means to examine the complicated crack behavior, when used in conjunction with a suitable numerical scheme such as the finite element method. The formulation is eventually reduced to a system of linear algebraic equations of mixed-mode stress intensity factors. Fracture parameters, describing crack-tip deformation and fracture in the composite, are obtained explicitly. Effects of material anisotropy and crack/hole geometry are examined also. Of particular interest are the energy release rates associated with crack extension; their values are evaluated for various cases. Results show that mixed-mode stress intensity factors and energy release rates associated with the cracks emanating from a hole change very appreciably with fiber orientation in the composite. $K_{sub 1}$ and G increase monotonically with increasing θ ; but $K_{sub 2}$ reaches its maximum at $\theta = 45$ deg, and then decreases gradually as θ increases further. Author

N82-26715*# Illinois Univ., Urbana-Champaign. Dept. of Theoretical and Applied Mechanics.
INTERLAMINAR CRACK GROWTH IN FIBER REINFORCED COMPOSITES DURING FATIGUE, PART 3 Final Report
S. S. Wang and H. T. Wang Feb. 1981 37 p refs 6 Vol.
(Grant NsG-3044)
(NASA-CR-165434; NAS 1.26:165434) Avail: NTIS HC A03/MF A01 CSCL 20K

Interlaminar crack growth behavior in fiber-reinforced composites subjected to fatigue loading was investigated experimentally and theoretically. In the experimental phase, inter-laminar crack propagation rates and mechanisms were determined for the cases of various geometries, laminate parameters and cyclic stress levels. A singular hybrid-stress finite element method was used in conjunction with the experimental results to examine the local crack-tip behavior and to characterize the crack propagation during fatigue. Results elucidate the basic nature of the cyclic delamination damage, and relate the interlaminar crack growth rate to the range of mixed-mode crack-tip stress intensity factors. The results show that crack growth rates are directly related to the range of the mixed-mode cyclic stress intensity factors by a power law relationship. Author

N82-26716*# Illinois Univ., Urbana-Champaign. Dept. of Theoretical and Applied Mechanics.
ANALYSIS OF INTERFACE CRACKS IN ADHESIVELY BONDED LAP SHEAR JOINTS, PART 4 Final Report
S. S. Wang and J. F. Yau Feb. 1981 39 p refs 6 Vol.
(Grant NsG-3044)
(NASA-CR-165438; NAS 1.26:165438) Avail: NTIS

HC A03/MF A01 CSCL 20K

Conservation laws of elasticity for nonhomogeneous materials were developed and were used to study the crack behavior in adhesively bonded lap shear joints. By using these laws and the fundamental relationships in fracture mechanics of interface cracks, the problem is reduced to a pair of linear algebraic equations, and stress intensity solutions can be determined directly by information extracted from the far field. The numerical results obtained show that: (1) in the lap-shear joint with a given adherend, the opening-mode stress intensity factor, ($K_{sub 1}$) is always larger than that of the shearing-mode ($K_{sub 2}$); (2) ($K_{sub 1}$) is not sensitive to adherent thickness but ($K_{sub 2}$) increases rapidly with increasing thickness; and (3) ($K_{sub 1}$) and ($K_{sub 2}$) increase simultaneously as the interfacial crack length increases. Author

N82-26717*# Illinois Univ., Urbana-Champaign. Dept. of Theoretical and Applied Mechanics.
EDGE DELAMINATION IN ANGLE-PLY COMPOSITE LAMINATES, PART 5 Final Report
S. S. Wang Feb. 1981 50 p refs 6 Vol.
(Grant NsG-3044)
(NASA-CR-165439; NAS 1.26:165439) Avail: NTIS HC A03/MF A01 CSCL 20K

A theoretical method was developed for describing the edge delamination stress intensity characteristics in angle-ply composite laminates. The method is based on the theory of anisotropic elasticity. The edge delamination problem is formulated using Lekhnitskii's complex-variable stress potentials and an especially developed eigenfunction expansion method. The method predicts exact orders of the three-dimensional stress singularity in a delamination crack tip region. With the aid of boundary collocation, the method predicts the complete stress and displacement fields in a finite-dimensional, delaminated composite. Fracture mechanics parameters such as the mixed-mode stress intensity factors and associated energy release rates for edge delamination can be calculated explicitly. Solutions are obtained for edge delaminated $(\theta/\theta/\theta/\theta)$ angle-ply composites under uniform axial extension. Effects of delamination lengths, fiber orientations, lamination and geometric variables are studied. Author

N82-26718*# Illinois Univ., Urbana-Champaign. Dept. of Theoretical and Applied Mechanics.
BOUNDARY-LAYER EFFECTS IN COMPOSITE LAMINATES: FREE-EDGE STRESS SINGULARITIES, PART 6 Final Report
S. S. Wang and I. Choi Apr. 1981 38 p refs 6 Vol.
(Grant NsG-3044)
(NASA-CR-165440; NAS 1.26:165440) Avail: NTIS HC A03/MF A01 CSCL 20K

A rigorous mathematical model was obtained for the boundary-layer free-edge stress singularity in angle-ply and crossplyed fiber composite laminates. The solution was obtained using a method consisting of complex-variable stress function potentials and eigenfunction expansions. The required order of the boundary-layer stress singularity is determined by solving the transcendental characteristic equation obtained from the homogeneous solution of the partial differential equations. Numerical results obtained show that the boundary-layer stress singularity depends only upon material elastic constants and fiber orientation of the adjacent plies. For angle-ply and crossplyed laminates the order of the singularity is weak in general. Author

N82-29619*# Georgia Inst. of Tech., Atlanta. Center for the Advancement of Computational Mechanics.
CREEP CRACK-GROWTH: A NEW PATH-INDEPENDENT INTEGRAL (T SUB C), AND COMPUTATIONAL STUDIES Ph.D. Thesis Final Report
R. B. Stonesifer and S. N. Atluri Jul. 1982 112 p refs
(Grant NAG3-38)
(NASA-CR-167897; NAS 1.26:167897) Avail: NTIS HC A06/MF A01 CSCL 20K

The development of valid creep fracture criteria is considered. Two path-independent integral parameters which show some degree of promise are the C^* and $(\Delta T)_{sub c}$ integrals. The mathematical aspects of these parameters are reviewed by deriving generalized vector forms of the parameters using conservation laws which are valid for arbitrary, three dimensional, cracked

bodies with crack surface tractions (or applied displacements), body forces, inertial effects, and large deformations. Two principal conclusions are that $(\Delta T)_{sub c}$ has an energy rate interpretation whereas C^* does not. The development and application of fracture criteria often involves the solution of boundary/initial value problems associated with deformation and stresses. The finite element method is used for this purpose. An efficient, small displacement, infinitesimal strain, displacement based finite element model is specialized to two dimensional plane stress and plane strain and to power law creep constitutive relations. A mesh shifting/remeshing procedure is used for simulating crack growth. The model is implemented with the quartz-point node technique and also with specially developed, conforming, crack-tip singularity elements which provide for the r to the $[n-(1+n)]$ power strain singularity associated with the HRR crack-tip field. Comparisons are made with a variety of analytical solutions and alternate numerical solutions for a number of problems. J.D.

N82-33736*# Dayton Univ., Ohio. Dept. of Aerospace Mechanics.

A PRELIMINARY STUDY OF CRACK INITIATION AND GROWTH AT STRESS CONCENTRATION SITES Interim Technical Report, 1 Jan. - 31 Aug. 1982

D. S. Dawicke, J. P. Gallagher, G. A. Hartman, and A. M. Rajendran Sep. 1982 30 p refs (Grant NAG3-246)

(NASA-CR-169358; NAS 1.26:169358; UDR-TR-82-119; ITR-1) Avail: NTIS HC A03/MF A01 CSCL 20K

Crack initiation and propagation models for notches are examined. The Dowling crack initiation model and the E1 Haddad et al. crack propagation model were chosen for additional study. Existing data was used to make a preliminary evaluation of the crack propagation model. The results indicate that for the crack sizes in the test, the elastic parameter K gave good correlation for the crack growth rate data. Additional testing, directed specifically toward the problem of small cracks initiating and propagating from notches is necessary to make a full evaluation of these initiation and propagation models. S.L.

A82-11298* Vibrations of cantilevered shallow cylindrical shells of rectangular planform. A. W. Leissa, J. K. Lee, and A. J. Wang (Ohio State University, Columbus, OH). *Journal of Sound and Vibration*, vol. 78, Oct. 8, 1981, p. 311-328, 25 refs, Grant No. NAG3-36.

A cantilevered, shallow shell of circular cylindrical curvature and rectangular planform exhibits free vibration behavior which differs considerably from that of a cantilevered beam or of a flat plate. Some numerical results can be found for the problem in the previously published literature, mainly obtained by using various finite element methods. The present paper is the first definitive study of the problem, presenting accurate non-dimensional frequency parameters for wide ranges of aspect ratio, shallowness ratio and thickness ratio. The analysis is based upon shallow shell theory. Numerical results are obtained by using the Ritz method, with algebraic polynomial trial functions for the displacements. Convergence is investigated, with attention being given both to the number of terms taken for each co-ordinate direction and for each of the three components of displacement. Accuracy of the results is also established by comparison with finite element results for shallow shells and with other accurate flat plate solutions. (Author)

A82-19341*# Vibrations of twisted rotating blades. A. W. Leissa, J. K. Lee (Ohio State University, Columbus, OH), and A. J. Wang. *American Society of Mechanical Engineers, Design Engineering Technical Conference, Hartford, CT, Sept. 20-23, 1981, Paper 81-DET-127*. 8 p. 22 refs. Members, \$2.00; nonmembers, \$4.00. Grant No. NAG3-36.

The literature dealing with vibrations of turbomachinery blades is voluminous, but the vast majority of it treats the blades as beams. In a previous paper a two-dimensional analytical procedure was developed and demonstrated on simple models of blades having camber. The procedure utilizes shallow shell theory along with the classical Ritz method for solving the vibration problem. Displace-

ment functions are taken as algebraic polynomials. In the present paper the method is demonstrated on blade models having camber. Comparisons are first made with results in the literature for nonrotating twisted plates and various disagreements between results are pointed out. A method for depicting mode shape information is demonstrated, permitting one to examine all three components of displacement. Finally, the analytical procedure is demonstrated on rotating twisted blade modes, both without and with camber. (Author)

A82-32303* Path-independent integrals in finite elasticity and inelasticity, with body forces, inertia, and arbitrary crack-face conditions. S. N. Atluri (Georgia Institute of Technology, Atlanta, GA). *Engineering Fracture Mechanics*, vol. 16, no. 3, 1982, p. 341-364, 17 refs. Contract No. N00014-78-C-0636; Grants No. AF-AFOSR-81-0057; (No. NAG3-38. (Previously announced in STAR as N81-32547)

A82-35408*# Comparison of beam and shell theories for the vibrations of thin turbomachinery blades. A. W. Leissa (Ohio State University, Columbus, OH) and M. S. Ewing (U.S. Air Force Academy, Colorado Springs, CO). *American Society of Mechanical Engineers, International Gas Turbine Conference and Exhibit, 27th, London, England, Apr. 18-22, 1982, Paper 82-GT-223*. 12 p. 36 refs. Members, \$2.00; nonmembers, \$4.00. Grant No. NAG3-36.

Vibration analysis of turbomachinery blades has traditionally been carried out by means of beam theory. In recent years two-dimensional methods of blade vibration analysis have been developed, most of which utilize finite elements and tend to require considerable computation time. More recently a two-dimensional method of blade analysis has evolved which does not require finite elements and is based upon shell equations. The present investigation has the primary objective to demonstrate the accuracy and limitations of blade vibration analyses which utilize one-dimensional, beam theories. It is found that beam theory is generally inadequate to determine the free vibration frequencies and mode shapes of moderate to low aspect ratio turbomachinery blades. The shallow shell theory, by contrast, is capable of representing all the vibration modes accurately. However, the one-dimensional beam theory has an important advantage over the two-dimensional shell theory for blades and vibration modes. It uses fewer degrees of freedom, thus requiring less computer time. G.R.

A82-36782* On a study of the $\Delta T/c$ and C^*/k integrals for fracture analysis under non-steady creep. R. B. Stonesifer and S. N. Atluri (Georgia Institute of Technology, Atlanta, GA). *Engineering Fracture Mechanics*, vol. 16, no. 5, 1982, p. 625-643. 14 refs. Grants No. NAG3-38; No. AF-AFOSR-81-0057.

Applications of a vector quantity, path-independent integral which has an energy interpretation to the characterization of crack-tip fields in the range from fast to slow crack propagation are examined. The crack tip characterization parameter is defined in terms of a conservation integral for an area around the crack tip in a two-dimensional cracked body. The actual physical interpretation of the parameter is shown to be the difference in crack lengths displayed by two identical bodies which have equal load histories. A steady-state value is obtained for the parameter for cases of steady-state creep and is shown to be related to the standard path-independent integral for macroscopic self-similar crack growth under mode I conditions. A finite element model is developed for viscoplastic material models, using an initial strain approach with steps in a size employed in tangent stiffness methods. M.S.K.

A82-39514* On the solution of creep induced buckling in general structure. J. Padovan and S. Tovchakchaikul (Akron, University, Akron, OH). *Computers and Structures*, vol. 15, no. 4, 1982, p. 379-392. 17 refs. Grant No. NAG3-54.

This paper considers the pre and post buckling behavior of general structures exposed to high temperature fields for long durations wherein creep effects become significant. The solution to this problem is made possible through the use of closed upper bounding constraint surfaces which enable the development of a new time stepping algorithm. This permits the stable and efficient solution of structural problems which exhibit indefinite tangent properties. Due to the manner of constraining/bounding successive iterates, the algorithm developed herein is largely self adaptive, inherently stable, sufficiently flexible to handle geometric material and boundary induced nonlinearity, and can be incorporated into either finite element or difference simulations. To illustrate the capability of the procedure, as well as, the physics of creep induced pre and post buckling behavior, the results of several numerical experiments are included. (Author)

A82-40066 * **Moving singularity creep crack growth analysis with the $\Delta T/c$ and C^* integrals.** R. B. Stonesifer and S. N. Atluri (Georgia Institute of Technology, Atlanta, GA). *Engineering Fracture Mechanics*, vol. 16, no. 6, 1982, p. 769-782. 11 refs. Grant No. NAG3-38.

The physical meaning of $\Delta T/c$ and its applicability to creep crack growth are reviewed. Numerical evaluation of $\Delta T/c$ and C^* is discussed with results being given for compact specimen and strip geometries. A moving crack-tip singularity, creep crack growth simulation procedure is described and demonstrated. The results of several crack growth simulation analyses indicate that creep crack growth in 304 stainless steel occurs under essentially steady-state conditions. Based on this result, a simple methodology for predicting creep crack growth behavior is summarized. (Author)

A82-42863 * # **On ultrasonic factors and fracture toughness.** L. S. Fu (Ohio State University, Columbus, OH). In: Symposium on Nondestructive Evaluation, 13th, San Antonio, TX, April 21-23, 1981, Proceedings. (A82-42851 21-38) San Antonio, TX, Southwest Research Institute, 1982, p. 145-160. 17 refs. Grant No. NsG-3269.

Recent experimental and theoretical studies on ultrasonics have shown that the scattering of elastic waves by material defects yields data which characterize crack properties, such as size and orientation, and also the mechanical properties of the given material. In the present study, elastodynamic fields due to the presence of a pair of inhomogeneities in a material of plate geometry are investigated by the method of equivalent inclusions. The stress amplitude change of the plates during the passage of plane time-harmonic waves is found, and the relation between fracture toughness and ultrasonic factors is determined. The approach used does not assume the existence of a sharp crack in the material. O.C.

A82-45869 * **On finite deformation elasto-plasticity.** S. Nemat-Nasser (Northwestern University, Evanston, IL). *International Journal of Solids and Structures*, vol. 18, no. 10, 1982, p. 857-872. 59 refs. Grant No. NAG3-134.

Lee (1969) has proposed a theory based on the decomposition of the total deformation gradient to an elastic and plastic part, and from it has concluded that the additive decomposition of the strain rates holds only approximately. Lubarda and Lee (1981) have declared that Lee's 'exact finite-deformation kinematics shows the almost universal assumption that the total velocity strain or rate of deformation is the sum of elastic and plastic rates to be in error'. Hence questions are raised regarding the validity of essentially all finite deformation elasto-plasticity theories. The present investigation is concerned with these questions. It is shown that the additive decomposition of the strain rates follows from all common finite elasto-plasticity concepts. Lee's theory is examined, and it is shown that this theory also leads to an additive strain rate decomposition, and therefore, his conclusion stems from misinterpretation. It is found that the elastic and the plastic strain rates considered by Lee do not correspond to the same configuration. They are, therefore, not compatible measures. G.R.

A82-46109 * **Interface cracks in adhesively bounded lap-shear joints.** S. S. Wang and J. F. Yau (Illinois, University, Urbana, IL). *International Journal of Fracture*, vol. 19, Aug. 1982, p. 295-309. 29 refs. Grant No. NsG-3044.

A study on the elastic behavior of interface cracks in adhesively bonded lap-shear joints is presented. The problem is investigated by using a recently developed method of analysis based on conservation laws in elasticity for nonhomogeneous solids and fundamental relationships in fracture mechanics of dissimilar materials. The formulation leads to a pair of linear algebraic equations in mixed-mode stress intensity factors. Singular crack-tip stress intensity solutions are determined directly by information extracted from the far field. Stress intensity factors and associated energy release rates are obtained for various cases of interest. Fundamental nature of the interfacial flaw behavior in lap-shear adhesive joints is examined in detail. (Author)

A82-46806 * # **Boundary-layer effects in composite laminates. I - Free-edge stress singularities. II - Free-edge stress solutions and basic characteristics.** S. S. Wang and I. Choi (Illinois, University, Urbana, IL). *ASME, Transactions, Journal of Applied Mechanics*, vol. 49, Sept. 1982, p. 541-560. 44 refs. Grant No. NsG-3044.

The fundamental nature of the boundary-layer effect in fiber-reinforced composite laminates is formulated in terms of the theory of anisotropic elasticity. The basic structure of the boundary-layer field solution is obtained by using Lekhnitskii's stress potentials (1963). The boundary-layer stress field is found to be singular at composite laminate edges, and the exact order or strength of the boundary layer stress singularity is determined using an eigenfunction expansion method. A complete solution to the boundary-layer problem is then derived, and the convergence and accuracy of the solution are analyzed, comparing results with existing approximate numerical solutions. The solution method is demonstrated for a symmetric graphite-epoxy composite. V.L.

ORIGINAL PAGE IS
OF POOR QUALITY

43 EARTH RESOURCES

Includes remote sensing of earth resources by aircraft and spacecraft; photogrammetry; and aerial photography.

For instrumentation see *35 Instrumentation and Photogrammetry*.

N82-14552*# National Aeronautics and Space Administration, Lewis Research Center, Cleveland, Ohio.

RELIABLE AERIAL THERMOGRAPHY FOR ENERGY CONSERVATION Final Report

John R. Jack and Robert L. Bowman Aug. 1981 35 p refs Original contains color illustrations

(Contract DE-A101-79CS-20270)
(NASA-TM-81786; DOE/NASA/20270-1; E-828) Avail: NTIS HC A03/MF A01 CSCL 08B

A method for energy conservation, the aerial thermography survey, is discussed. It locates sources of energy losses and wasteful energy management practices. An operational map is presented for clear sky conditions. The map outlines the key environmental conditions conducive to obtaining reliable aerial thermography. The map is developed from defined visual and heat loss discrimination criteria which are quantized based on flat roof heat transfer calculations. E.A.K.

N82-18664*# National Aeronautics and Space Administration, Lewis Research Center, Cleveland, Ohio.

GROUND-TRUTH OBSERVATIONS OF ICE-COVERED NORTH SLOPE LAKES IMAGED BY RADAR

W. F. Weeks Oct. 1981 24 p refs Prepared in cooperation with CRREL, Hanover, N.H.

(NASA-TM-84127; AD-A108342; CRREL-81-19) Avail: NTIS HC A02/MF A01 CSCL 08/B

Field observations support the interpretation that differences in the strength of radar returns from the ice covers of lakes on the North Slope of Alaska can be used to determine where the lake is frozen completely to the bottom. An ice/frozen soil interface is indicated by a weak return and an ice/water interface by a strong return. The immediate value of this result is that SLAR (side-looking airborne radar) imagery can now be used to prepare maps of large areas of the North Slope showing where the lakes are shallower or deeper than 1.7m (the approximate draft of the lake ice at the time of the SLAR flights). The bathymetry of these shallow lakes is largely unknown and is not obvious from their sizes or outlines. Such information could be very useful, for example in finding suitable year-round water supplies.

Author (GRA)

N82-24525*# National Aeronautics and Space Administration, Lewis Research Center, Cleveland, Ohio.

LANDSAT REMOTE SENSING: OBSERVATIONS OF AN APPALACHIAN MOUNTAIN TOP SURFACE COAL MINING AND RECLAMATION OPERATION

Oct. 1979 7 p ref Original contains color imagery. Original photography may be purchased from the EROS Data Center, Sioux Falls, S.D. 57198 Original contains color illustrations ERTS

(E82-10247; NASA-TM-84194; NAS 1.15:84194) Avail: NTIS HC A02/MF A01 CSCL 08I

The potential benefits of using LANDSAT remote sensing data by state agencies as an aide in monitoring surface coal mining operations are reviewed. A mountaintop surface mine in eastern Kentucky was surveyed over a 5 year period using satellite multispectral scanner data that were classified by computer analyses. The analyses were guided by aerial photography and by ground surveys of the surface mines procured in 1976. The application of the LANDSAT data indicates that: (1) computer classification of the various landcover categories provides information for monitoring the progress of surface mining and reclamation operations; (2) successive yearly changes in barren and revegetated areas can be qualitatively assessed for surface mines of 100 acres or more of disrupted area; (3) barren areas consisting of limestone and shale mixtures may be recognized, and revegetated areas in various stages of growth may be identified against the hilly forest background. E.A.K.

N82-13490*# Engelhard Industries, Inc., Edison, N.J.
DEVELOP AND TEST FUEL CELL POWERED ON-SITE INTEGRATED TOTAL ENERGY SYSTEM. PHASE 3: FULL-SCALE POWER PLANT DEVELOPMENT Quarterly Report, Feb. - Apr. 1981

A. Kaufman 24 Jun. 1981 50 p

(Contract DEN3-241)

(NASA-CR-185328; DOE/NASA/0241-1; QR-1) Avail: NTIS HC A03/MF A01 CSCL 10B

An integrated 5 kW power system based upon methanol fuel and a phosphoric acid fuel cell operating at about 473 K is described. Description includes test results of advanced fuel cell catalysts, a semiautomatic acid replenishment system and a completed 5 kW methanol/system reformer. The results of a preliminary system test on a reformer/stack/inverter combination are reported. An initial design for a 25 kW stack is presented. Experimental plans are outlined for data acquisition necessary for design of a 50 kW methanol/steam reformer. Activities related to complete mathematical modelling of the integrated power system, including wasteheat utilization, are described. E.A.K.

ORIGINAL PAGE IS
OF POOR QUALITY

44 ENERGY PRODUCTION AND CONVERSION

Includes specific energy conversion systems, e.g., fuel cells and batteries; global sources of energy; fossil fuels; geophysical conversion; hydroelectric power; and wind power.

For related information see also *07 Aircraft Propulsion and Power*, *20 Spacecraft Propulsion and Power*, *28 Propellants and Fuels*, and *85 Urban Technology and Transportation*.

N82-10503* National Aeronautics and Space Administration, Lewis Research Center, Cleveland, Ohio.

EFFECT OF POSITIVE PULSE CHARGE WAVEFORMS ON THE ENERGY EFFICIENCY OF LEAD-ACID TRACTION CELLS Final Report

John J. Smithrick Sep. 1981 11 p refs
(Contract DE-A101-77CS-51044)

(NASA-TM-82709; E-991; DOE/NASA/51044-22) Avail: NTIS HC A02/MF A01 CSCL 10A

The effects of four different charge methods on the energy conversion efficiency of 300 ampere hour lead acid traction cells were investigated. Three of the methods were positive pulse charge waveforms; the fourth, a constant current method, was used as a baseline of comparison. The positive pulse charge waveforms were: 120 Hz full wave rectified sinusoidal; 120 Hz silicon controlled rectified; and 1 kHz square wave. The constant current charger was set at the time average pulse current of each pulse waveform, which was 150 amps. The energy efficiency does not include charger losses. The lead acid traction cells were charged to 70 percent of rated ampere hour capacity in each case. The results of charging the cells using the three different pulse charge waveforms indicate there was no significant difference in energy conversion efficiency when compared to constant current charging at the time average pulse current value. Author

N82-13551* National Aeronautics and Space Administration, Lewis Research Center, Cleveland, Ohio.

SOLAR CELL DEVELOPMENT FOR THE POWER EXTENSION PACKAGE

Cosmo R. Baraona and James L. Cioni (NASA, Johnson Space Center) 1981 8 p refs Presented at the 16th Intersoc. Energy Conversion Conf., Atlanta, 9-14 Aug. 1981
(NASA-TM-82685; E-922) Avail: NTIS HC A02/MF A01 CSCL 10A

The PEP is a 32 kilowatt flexible substrate, retrievable, solar array system for use on the Space Shuttle. Solar cell costs will be reduced by increasing cell area and simplifying cell and coverglass fabrication processes and specifications. The cost goal is to produce cells below \$30 per watt. Two and ten ohm-cm silicon cells were investigated. In phase I of the cell development program a few thousand candidate cells will be produced and evaluated for utility and quality. In phase II a large number of cells will be fabricated to verify production readiness and cell yields and costs. This schedule is compatible with PEP initial operational capability in 1984. Approximately 140,000 large area (5.9 x 5.9 cm) cells will be required for two PEP solar arrays. The status of the cell development and testing, including a radiation damage test and side-by-side comparison of candidate cell types with pre- and post-irradiation airplane calibration of outer space short-circuit current, is reported. T.M.

N82-12553* National Aeronautics and Space Administration, Lewis Research Center, Cleveland, Ohio.

ANALYTIC INVESTIGATION OF EFFICIENCY AND PERFORMANCE LIMITS IN KLYSTRON AMPLIFIERS USING MULTIDIMENSIONAL COMPUTER PROGRAMS; MULTI-STAGE DEPRESSED COLLECTORS; AND THERMIONIC CATHODE LIFE STUDIES

H. G. Kosmahl In NASA, Johnson Space Center Workshop on Microwave Power Transmission and Reception 1980 p 139-146 refs (For primary document see N82-12538 03-44)
Avail: NTIS HC A99/MF A01 CSCL 10A

Due to complexity of the program which used a hydrodynamic, axially and radially deformable disk-ring model and the resulting

long computing time only the output gap was investigated. Results from independent studies were used to initiate the starting conditions for the electrons and the RF voltage using our program. Although this method of computation is less exact than processing the entire klystron interaction in 3-Dimensions it is shown that, for a confined flow focused throughout the penultimate cavity, radial velocities remain very small and the beam is highly laminar. It is concluded that possible errors resulting from treating only the output cavity in 3-D would remain small. T.M.

N82-12574* National Aeronautics and Space Administration, Lewis Research Center, Cleveland, Ohio.

PERFORMANCE OF ADVANCED CHROMIUM ELECTRODES FOR THE NASA REDOX ENERGY STORAGE SYSTEM Final Report

Randall F. Gahn, JoAnn Charleston, Jerri S. Ling, and Margaret A. Reid Nov. 1981 23 p refs

(Contract DE-A104-80AL-12726)

(NASA-TM-82724; E-1025; DOE/NASA/12726-15) Avail: NTIS HC A02/MF A01 CSCL 10C

Chromium electrodes were prepared for the NASA Redox Storage System with meet the performance requirements for solar-photovoltaic, wind-turbine and electric utility applications. Gold-lead catalyzed carbon felt electrodes up to 930 sq cm were fabricated and tested in single cells and multicell stacks for hydrogen evolution, coulombic efficiency, catalyst stability and electrochemical activity. Factors which affect the overall performance of a particular electrode include the carbon felt lot, the cleaning treatment and the gold catalyzed method. Effects of the chromium solution chemistry and impurities on charge/discharge performance are also presented. Author

N82-13504* National Aeronautics and Space Administration, Lewis Research Center, Cleveland, Ohio.

CATALYTIC COMBUSTION OF RESIDUAL FUELS

Daniel L. Bulzan and Robert R. Tacina 1981 20 p refs Presented at 5th Workshop on Catalytic Combustion, San Antonio, Tex., 15-16 Sep. 1981

(Contract DE-A101-77ET-10350)

(NASA-TM-82731; E-1040) Avail: NTIS HC A02/MF A01 CSCL 21B

A noble metal catalytic reactor was tested using two grades of petroleum derived residual fuels at specified inlet air temperatures, pressures, and reference velocities. Combustion efficiencies greater than 99.5 percent were obtained. Steady state operation of the catalytic reactor required inlet air temperatures of at least 800 K. At lower inlet air temperatures, upstream burning in the premixing zone occurred which was probably caused by fuel deposition and accumulation on the premixing zone walls. Increasing the inlet air temperature prevented this occurrence. Both residual fuels contained about 0.5 percent nitrogen by weight. NO sub x emissions ranged from 50 to 110 ppm by volume at 15 percent excess O₂. Conversion of fuel-bound nitrogen to NO sub x ranged from 25 to 50 percent. M.D.K.

N82-13509* National Aeronautics and Space Administration, Lewis Research Center, Cleveland, Ohio.

GAS-TURBINE CRITICAL RESEARCH AND ADVANCED TECHNOLOGY SUPPORT PROJECT Annual Report

John S. Clark, Philip E. Hodge, Carl E. Lowell, David N. Anderson, and Donald F. Schultz Mar. 1981 50 p refs

(Contract DE-A101-77ET-10350)

(NASA-TM-81708; DOE/NASA/2593-24; E-737) Avail: NTIS HC A03/MF A01 CSCL 10B

A technology data base for utility gas turbine systems capable of burning coal derived fuels was developed. The following areas are investigated: combustion; materials; and system studies. A two stage test rig is designed to study the conversion of fuel bound nitrogen to NO_x. The feasibility of using heavy fuels in catalytic combustors is evaluated. A statistically designed series of hot corrosion burner rig tests was conducted to measure the corrosion rates of typical gas turbine alloys with several fuel contaminants. Fuel additives and several advanced thermal barrier coatings are tested. Thermal barrier coatings used in conjunction with low critical alloys and those used in a combined cycle system in which the stack temperature was maintained above the acid corrosion temperature are also studied. E.A.K.

N82-14633* National Aeronautics and Space Administration, Lewis Research Center, Cleveland, Ohio
ALUMINUM BLADE DEVELOPMENT FOR THE MOD-OA 200-KILOWATT WIND TURBINE Final Report
Bradford S. Linscott, Richard K. Shaltens, and A. G. Eggers (Westinghouse Electric Corp., Pittsburgh) Dec. 1981 43 p refs (Contract DE-AB29-76ET-20370)
(NASA-TM-82594; DOE/NASA-20370/20) Avail: NTIS HC A03/MF A01 CSCL 10A

The rotor blade configuration, fabrication methods, analyses, operating experience, design modifications, and cost are described. Each 60-ft. (18.3-m.) long aluminum blade used current aircraft fixed wing and rotary wing design and fabrication technologies. Structural damage, repairs, and modifications that occurred during 6500 hours of operation are summarized. T.M.

N82-16477* National Aeronautics and Space Administration, Lewis Research Center, Cleveland, Ohio.
NEW FEATURES AND APPLICATIONS OF PRESTO, A COMPUTER CODE FOR THE PERFORMANCE OF REGENERATIVE, SUPERHEATED STEAM TURBINE CYCLES
Yung K. Choo and Patar J. Staiger Jan. 1982 39 p refs (NASA-TP-1954; E-721) Avail: NTIS HC A03/MF A01 CSCL 10B

The code was designed to analyze performance at valves-wide-open design flow. The code can model conventional steam cycles as well as cycles that include such special features as process steam extraction and induction and feedwater heating by external heat sources. Convenience features and extensions to the special features were incorporated into the PRESTO code. The features are described, and detailed examples illustrating the use of both the original and the special features are given. T.M.

N82-16478* National Aeronautics and Space Administration, Lewis Research Center, Cleveland, Ohio.
VARIABLE GAIN FOR A WIND TURBINE PITCH CONTROL Final Report
Robert C. Seidel and Arthur G. Birchenough Dec. 1981 14 p refs (Contract DE-AI01-76ET-20320)
(NASA-TM-82751; DOE/NASA/20320-34; E-1067) Avail: NTIS HC A02/MF A01 CSCL 10A

The gain variation is made in the software logic of the pitch angle controller. The gain level is changed depending upon the level of power error. The control uses low gain for low pitch activity the majority of the time. If the power exceeds ten percent offset above rated, the gain is increased to a higher gain to more effectively limit power. A variable gain control functioned well in tests on the Mod-O wind turbine. T.M.

N82-16481* National Aeronautics and Space Administration, Lewis Research Center, Cleveland, Ohio.
SUMMARY AND EVALUATION OF THE CONCEPTUAL DESIGN STUDY OF A POTENTIAL EARLY COMMERCIAL MHD POWER PLANT (CSPEC) Final Report
P. J. Staiger and P. F. Penko Jan. 1982 22 p refs (Contract DE-AI01-77ET-10769)
(NASA-TM-82734; DOE/NASA/10769-21; E-1046) Avail: NTIS HC A02/MF A01 CSCL 10B

The conceptual design study of a potential early commercial MHD power plant (CSPEC) is described and the results are summarized. Each of two contractors did a conceptual design of an approximately 1000 MWe open-cycle MHD/steam plant with oxygen enriched combustion air preheated to an intermediate temperature in a metallic heat exchanger. The contractors were close in their overall plant efficiency estimates but differed in their capital cost and cost of electricity estimates, primarily because of differences in balance-of-plant material, contingency, and operating and maintenance cost estimates. One contractor concluded that its MHD plant design compared favorably in cost of electricity with conventional coal-fired steam plants. The other contractor is making such a comparison as part of a follow-on study. Each contractor did a preliminary investigation of part-load performance and plant availability. The results of NASA studies investigating the effect of plant size and oxidizer preheat temperature on the performance of CSPEC-type MHD plants are also described. The efficiency of a 1000 MWe plant is about three points higher than of a 200 MWe plant. Preheating to

1600 F gives an efficiency about one and one-half points higher than preheating to 800 F for all plant sizes. For each plant size and preheat temperature there is an oxidizer enrichment level and MHD generator length that gives the highest plant efficiency. B.W.

N82-16495* National Aeronautics and Space Administration, Lewis Research Center, Cleveland, Ohio.
THE NASA LEWIS LARGE WIND TURBINE PROGRAM
R. L. Thomas and D. H. Baldwin 1981 24 p refs Presented at the 5th Biennial Wind Energy Conf. and Workshop, Washington, D.C., 5-7 Oct. 1981
(Contract DE-AI01-79ET-20305)
(NASA-TM-82761; DOE/NASA/20305-7; E-1082) Avail: NTIS HC A01/MF A01 CSCL 10B

The program is directed toward development of the technology for safe, reliable, environmentally acceptable large wind turbines that have the potential to generate a significant amount of electricity at costs competitive with conventional electric generation systems. In addition, these large wind turbines must be fully compatible with electric utility operations and interface requirements. Advances are made by gaining a better understanding of the system design drivers, improvements in the analytical design tools, verification of design methods with operating field data, and the incorporation of new technology and innovative designs. An overview of the program activities is presented and includes results from the first and second generation field machines (Mod-OA, -1, and -2), the design phase of the third generation wind turbine (Mod-5) and the advanced technology projects. Also included is the status of the Department of Interior WTS-4 machine. T.M.

N82-18691* National Aeronautics and Space Administration, Lewis Research Center, Cleveland, Ohio.
EXPERIMENTAL STUDY OF AN INTEGRAL CATALYTIC COMBUSTOR: HEAT EXCHANGER FOR STIRLING ENGINES
Daniel L. Bulzan 1982 20 p refs Presented at the 1982 Intern. Congr. and Exposition, Detroit, 22-26 Feb. 1982; sponsored by SAE
(Contract DE-AI01-77CS-51040)
(NASA-TM-82783; DOE/NASA/51040-36) Avail: NTIS HC A02/MF A01 CSCL 10A

The feasibility of using catalytic combustion with heat removal for the Stirling engine to reduce exhaust emissions and also improve heat transfer to the working fluid was studied using spaced parallel plates. An internally air-cooled heat exchanger was placed between two noble metal catalytic plates. A preheated fuel-air mixture passed between the plates and reacted on the surface of the catalyzed plates. Heat was removed from the catalytic surface by radiation and convection to the air-cooled heat exchangers to control temperature and minimize thermal nitrogen oxide emissions. Test conditions were inlet combustion air temperatures from 850 to 900 K, inlet velocities of about 10 m/s, equivalence ratios from 0.5 to 0.9, and pressures from 1.3x10 to the 5th power to 2.0x10 to the 5th power Pa. Propane fuel was used for all testing. Combustion efficiencies greater than 99.5 percent were measured. Nitrogen oxide emissions ranged from 1.7 to 3.3 g NO₂/kg fuel. The results demonstrate the feasibility of the concept and indicate that further investigation of the concept is warranted. A.R.H.

N82-18694* National Aeronautics and Space Administration, Lewis Research Center, Cleveland, Ohio.
ASSESSMENT OF STEAM-INJECTED GAS TURBINE SYSTEMS AND THEIR POTENTIAL APPLICATION
Robert J. Stochl Feb. 1982 21 p refs
(NASA-TM-82735; E-1047) Avail: NTIS HC A02/MF A01 CSCL 10B

Results were arrived at by utilizing and expanding on information presented in the literature. The results were analyzed and compared with those for simple gas turbine and combined cycles for both utility power generation and industrial cogeneration applications. The efficiency and specific power of simple gas turbine cycles can be increased as much as 30 and 50 percent, respectively, by the injection of steam into the combustor. Steam-injected gas turbines appear to be economically competitive

with both simple gas turbine and combined cycles for small, clean-fuel-fired utility power generation and industrial cogeneration applications. For large powerplants with integrated coal gasifiers, the economic advantages appear to be marginal. T.M.

N82-19670*# National Aeronautics and Space Administration, Lewis Research Center, Cleveland, Ohio.

PHOSPHORIC ACID FUEL CELL TECHNOLOGY STATUS
Stephen N. Simons, Robert B. King, and Paul R. Prokopius 1981
20 p refs Presented at Fuel Cells: Technol. Status and Appl.,
Chicago 16-18 Nov. 1981; sponsored by Institute of Gas
Technology

(Contract DE-AI01-80ET-17088)

(NASA-TM-82791; DOE/NASA/17088-3) Avail: NTIS
HC A02/MF A01 CSCL 10A

A review of the current phosphoric acid fuel cell system technology development efforts is presented both for multimegawatt systems for electric utility applications and for multikilowatt systems for on-site integrated energy system applications. Improving fuel cell performance, reducing cost, and increasing durability are the technology drivers at this time. Electrodes, matrices, intercell cooling, bipolar/separator plates, electrolyte management, and fuel selection are discussed. B.W.

N82-19671*# National Aeronautics and Space Administration, Lewis Research Center, Cleveland, Ohio.

MECHANISM AND MODELS FOR ZINC METAL MORPHOLOGY IN ALKALINE MEDIA

Charles E. May and Harold E. Kautz Dec. 1981 36 p refs
(NASA-TM-82768; E-1090) Avail: NTIS HC A03/MF A01
CSCL 10A

Based on experimental observations, a mechanism is presented to explain existence of the different morphologies of electrodeposited zinc in alkaline solution. The high current density dendrites appear to be due to more rapid growth on the nonbasal crystallographic planes than on the basal plane. The low current density moss apparently results from dissolution from the nonbasal planes at low cathodic voltages. Electrochemical models were sought which would produce such a phenomenon. The fundamental plating mechanism alone accounts only for different rates on different planes, not for zinc dissolution from a plane in the cathodic region. Fourteen models were explored; two models were in accord with the proposed mechanism. One involves rapid disproportionation of the zinc +1 species on the nonbasal planes. The other involves a redox reaction (corrosion) between the zinc-zincate and hydrogen-water systems. S.L.

N82-19672*# National Aeronautics and Space Administration, Lewis Research Center, Cleveland, Ohio.

PERFORMANCE AND OPERATIONAL ECONOMICS ESTIMATES FOR A COAL GASIFICATION COMBINED-CYCLE COGENERATION POWERPLANT

Joseph J. Nainiger, Raymond K. Burns, and Annie J. Easley
Mar. 1982 32 p refs

(NASA-TM-82729; E-1032) Avail: NTIS HC A03/MF A01
CSCL 10B

A performance and operational economics analysis is presented for an integrated-gasifier, combined-cycle (IGCC) system to meet the steam and baseload electrical requirements. The effect of time variations in steam and electrical requirements is included. The amount and timing of electricity purchases from sales to the electric utility are determined. The resulting expenses for purchased electricity and revenues from electricity sales are estimated by using an assumed utility rate structure model. Cogeneration results for a range of potential IGCC cogeneration system sizes are compared with the fuel consumption and costs of natural gas and electricity to meet requirements without cogeneration. The results indicate that an IGCC cogeneration system could save about 10 percent of the total fuel energy presently required to supply steam and electrical requirements without cogeneration. Also for the assumed future fuel and electricity prices, an annual operating cost savings of 21 percent to 26 percent could be achieved with such a cogeneration system. An analysis of the effects of electricity price, fuel price, and system availability indicates that the IGCC cogeneration system has a good potential for economical operation over a wide range in these assumptions. R.J.F.

N82-19673*# National Aeronautics and Space Administration, Lewis Research Center, Cleveland, Ohio

OPERATIONAL PERFORMANCE OF THE PHOTOVOLTAIC-POWERED GRAIN MILL AND WATER PUMP AT TANGAYE, UPPER VOLTA Summary Report, Mar. 1979 - Apr. 1981

James E. Mertz, Anthony F. Katojczak, and Richard DeLombard
Feb. 1982 59 p refs Sponsored in part by Bureau for
Development Support

(NASA-TM-82767; E-1089) Avail: NTIS HC A04/MF A01
CSCL 10B

The first two years of operation of a stand alone photovoltaic (PV) power system for the village of Tangaye, Upper Volta in West Africa are described. The purpose of the experiment was to demonstrate that PV systems could provide reliable electrical power for multiple use applications in remote areas where local technical expertise is limited. The 1.8 kW (peak) power system supplies 120-V (d.c.) electrical power to operate a grain mill, a water pump, and mill building lights for the village. The system was initially sized to pump a part of the village water requirements from an existing improved well, and to meet a portion of the village grain grinding requirements. The data, observations, experiences, and conclusions developed during the first two years of operation are discussed. Reports of tests of the mills used in the project are included. B.W.

N82-20668*# National Aeronautics and Space Administration, Lewis Research Center, Cleveland, Ohio.

PERFORMANCE MAPPING STUDIES IN REDOX FLOW CELLS

Mark A. Hoberecht and Lawrence H. Thaller Sep. 1981 12 p
refs

(Contract DE-AI04-80AL-12726)

(NASA-TM-82707; DOE/NASA/12726-13; NAS 1.15:82707;
DE82-003288) Avail: NTIS HC A02/MF A01 CSCL 10A

Pumping power requirements in any flow battery system constitute a direct parasitic energy loss. It is therefore useful to determine the practical lower limit for reactant flow rates. Through the use of a theoretical framework based on electrochemical first principles, two different experimental flow mapping techniques were developed to evaluate and compare electrodes as a function of flow rate. For the carbon felt electrodes presently used in NASA-Lewis Redox cells, a flow rate 1.5 times greater than the stoichiometric rate seems to be the required minimum.

Author

N82-21710*# National Aeronautics and Space Administration, Lewis Research Center, Cleveland, Ohio.

MICROPROCESSOR CONTROL SYSTEM FOR 200-KILOWATT MOD-OA WIND TURBINES Final Report

Ted W. Nyland and Arthur G. Birchenough Jan. 1982 26 p
refs

(Contract DE-AI01-76ET-20370)

(NASA-TM-82711; E-10006; NAS 1.15:82711;
DOE/NASA/20370-22) Avail: NTIS HC A03/MF A01 CSCL
10A

The microprocessor system and program used to control the operation of the 200-kW Mod-OA wind turbines is described. The system is programmed to begin startup and shutdown sequences automatically and to control yaw motion. Rotor speed and power output are controlled with integral and proportional control of the blade pitch angle. Included in the report are a description of the hardware and a discussion of the software programming technique. A listing of the PL/M software program is given. Author

N82-21712*# National Aeronautics and Space Administration, Lewis Research Center, Cleveland, Ohio.

EXPERIMENTAL PERFORMANCE OF THE REGENERATOR FOR THE CHRYSLER UPGRADED AUTOMOTIVE GAS TURBINE ENGINE Final Report

Jerry M. Winter and Ralph C. Nussle Feb. 1982 62 p refs
(Contract DE-AI01-77CS-51040)

(NASA-TM-82671; E-953; DOE/NASA/51040-32; NAS
1.15:82671) Avail: NTIS HC A04/MF A01 CSCL 10B

Automobile gas turbine engine regenerator performance was studied in a regenerator test facility that provided a satisfactory simulation of the actual engine operating environment but with independent control of airflow and gas flow. Velocity and temperature distributions were measured immediately downstream

of both the core high-pressure-side outlet and the core low-pressure-side outlet. For the original engine housing, the regenerator temperature effectiveness was 1 to 2 percent higher than the design value, and the heat transfer effectiveness was 2 to 4 percent lower than the design value over the range of test conditions simulating 50 to 100 percent of gas generator speed. Recalculating the design values to account for seal leakage decreased the design heat transfer effectiveness to values consistent with those measured herein. A baffle installed in the engine housing high-pressure-side inlet provided more uniform velocities out of the regenerator but did not improve the effectiveness. A housing designed to provide more uniform axial flow to the regenerator was also tested. Although temperature uniformity was improved, the effectiveness values were not improved. Neither did 50-percent flow, blockage (90 degree segment) applied to the high-pressure-side inlet change the effectiveness significantly. Author

N82-21714* National Aeronautics and Space Administration, Lewis Research Center, Cleveland, Ohio.

METHOD FOR PREDICTING IMPULSIVE NOISE GENERATED BY WIND TURBINE ROTORS

Larry A. Viterna 1982 7 p refs Presented at the Intern. Conf. on Noise Control Eng., San Francisco, 17-19 May 1982 (Contract D2-A101-78ET-20320)

(NASA-TM-82794; E-1128; DOE/NASA/20320-36; NAS 1.15 82794) Avail: NTIS HC A02/MF A01 CSCL 10B

Large wind turbines can generate both broad band and impulsive noises. These noises can be controlled by proper choice of rotor design parameters such as rotor location with respect to the supporting tower, tower geometry and tip speed. A method was developed to calculate the impulsive noise generated when the wind turbine blade experiences air forces that are periodic functions of the rotational frequency. This phenomenon can occur when the blades operate in the wake of the support tower and the nonuniform velocity field near the ground due to wind shear. Results from this method were compared with measured sound spectra taken at locations of one to two rotor diameters from the DOE/NASA Mod-1 wind turbine. The calculated spectra generally agreed with the measured data in both the amplitude of the predominant harmonics and the roll of rate with frequency. Measured sound pressure levels far from the Mod-1 (15 rotor diameters), however, were higher than predicted. Simultaneous measurements in the near and far field indicated that the propagation effects could enhance the sound levels by more than 10 dB above that expected by spherical dispersion. These propagation effects are believed to be due to terrain and atmospheric characteristics of the Mod-1 site. Author

N82-22648* National Aeronautics and Space Administration, Lewis Research Center, Cleveland, Ohio.

EFFECT OF ROTOR CONFIGURATION ON GUYED TOWER AND FOUNDATION DESIGNS AND ESTIMATED COSTS FOR INTERMEDIATE SITE HORIZONTAL AXIS WIND TURBINES

G. R. Frederick (Toledo Univ.), J. R. Winemiller, and J. M. Savino Mar. 1982 39 p refs (NASA-TM-82804; DOE/NASA/20320-39; NAS 1.15:82804) Avail: NTIS HC A03/MF A01 CSCL 10B

Three designs of a guyed cylindrical tower and its foundation for an intermediate size horizontal axis wind turbine generator are discussed. The primary difference in the three designs is the configuration of the rotor. Two configurations are two-blade rotors with teetering hubs - one with full span pitchable blades, the other with fixed pitch blades. The third configuration is a three-bladed rotor with a rigid hub and fixed pitch blades. In all configurations the diameter of the rotor is 38 meters and the axis of rotation is 30.4 meters above grade, and the power output is 200 kW and 400 kW. For each configuration the design is based upon for the most severe loading condition either operating wind or hurricane conditions. The diameter of the tower is selected to be 1.5 meters (since it was determined that this would provide sufficient space for access ladders within the tower) with guy rods attached at 10.7 meters above grade. Completing a design requires selecting the required thicknesses of the various cylindrical segments, the number and diameter of the guy rods, the number and size of soil anchors, and the size of the central foundation. The lower natural frequencies of vibration are determined for each design to ensure that operation near

resonance does not occur. Finally, a cost estimate is prepared for each design. A preliminary design and cost estimate of a cantilever tower (cylindrical and not guyed) and its foundation is also presented for each of the three configurations. Author

N82-22672* National Aeronautics and Space Administration, Lewis Research Center, Cleveland, Ohio.

IMPROVED CHROMIUM ELECTRODES FOR REDOX CELLS Patent Application

Vinod Jalan (Giner, Inc.), Margaret A. Reid, and Jo Ann Charleston, inventors (to NASA) Filed 26 Feb. 1982 13 p (NASA-Case-LEW-13653-1; US-Patent-Appl-SN-352821) Avail: NTIS HC A02/MF A01 CSCL 10C

An improved electrode having a gold coating for use in the anode compartment of a REDOX cell is described. The anode fluid utilizes a chromic/chromous couple. A carbon felt is soaked in methanol, rinsed in water, dried and then heated in KOH after which it is again washed in deionized water and dried. The felt is then moistened with a methanol water solution containing chloroauric acid and is stored in a dark place while still in contact with the gold-containing solution. After all the gold-containing solution is absorbed in the felt, the latter is dried by heat and then heat treated at a substantially greater temperature. The felt is then suitable for use as an electrode and is wetted with water or up to two molar HCl prior to installation in a REDOX cell. The novelty of the invention lies in the use of KOH for cleaning the felt and the use of alcohol as a carrier for the gold together with the heat treating procedure. NASA

N82-22673* National Aeronautics and Space Administration, Lewis Research Center, Cleveland, Ohio.

LIGHT WEIGHT NICKEL BATTERY PLAQUE Patent Application

M. A. Reid, R. E. Post, and D. G. Soltis, inventors (to NASA) Filed 19 Feb. 1982 9 p (NASA-Case-LEW-13349-1; US-Patent-Appl-SN-350476) Avail: NTIS HC A02/MF A01 CSCL 10C

Fabrication of a nickel plaque which may be coated with another suitable metal or compound to form an electrode for use in a fuel cell or battery is described. A flexible, porous, platable, plastic substrate is positioned against a diffuser together with an apertured support plate in a conduit. Flanges are clamped together on gaskets which prevent leakage of fluid from the conduit for bypassing of the substrate by the fluid. Treatment solutions are directed under pressure from a container by a pump through the substrate, diffuser and apertured support to a treatment solution collector. The treatment solutions are first a sensitizer, then distilled water, a catalyst solution, distilled water and, lastly, a nickel plating bath solution. T.M.

N82-23678* National Aeronautics and Space Administration, Lewis Research Center, Cleveland, Ohio.

PARAMETRIC PERFORMANCE ANALYSIS OF STEAM-INJECTED GAS TURBINE WITH A THERMIONIC-ENERGY-CONVERTER-LINED COMBUSTOR

Yung K. Choo and Raymond K. Burns Feb. 1982 21 p refs (NASA-TM-82736; E-1048; NAS 1.15:82736) Avail: NTIS HC A02/MF A01 CSCL 10B

The performance of steam-injected gas turbines having combustors lined with thermionic energy converters (STIG/TEC systems) was analyzed and compared with that of two baseline systems: a steam-injected gas turbine (without a TEC-lined combustor) and a conventional combined gas turbine/steam turbine cycle. Common gas turbine parameters were assumed for all of the systems. Two configurations of the STIG/TEC system were investigated. In both cases, steam produced in an exhaust-heat-recovery boiler cools the TEC collectors. It is then injected into the gas combustion stream and expanded through the gas turbine. The STIG/TEC system combines the advantage of gas turbine steam injection with the conversion of high-temperature combustion heat by TEC's. The addition of TEC's to the baseline steam-injected gas turbine improves both its efficiency and specific power. Depending on system configuration and design parameters, the STIG/TEC system can also achieve higher efficiency and specific power than the baseline combined cycle. Author

N82-23678*# National Aeronautics and Space Administration, Lewis Research Center, Cleveland, Ohio.
EVALUATION OF LIGHTNING ACCOMMODATION SYSTEMS FOR WIND-DRIVEN TURBINE ROTORS Final Report

H. Bankaitis Mar. 1982 49 p refs
(Contract DE-A101-76ET-20320)
(NASA-TM-82784; E-1116; DOE/NASA/20320-37; NAS 1.15:82784) Avail: NTIS HC A03/MF A01 CSCL 10B

Wind-driven turbine generators are being evaluated as an alternative source of electric energy. Areas of favorable location for the wind-driven turbines (high wind density) coincide with areas of high incidence of thunderstorm activity. These locations, coupled with the 30-m or larger diameter rotor blades, make the wind-driven turbine blades probable terminations for lightning strikes. Several candidate systems of lightning accommodation for composite-structural-material blades were designed and their effectiveness evaluated by submitting the systems to simulated lightning strikes. The test data were analyzed and system design were reviewed on the basis of the analysis. T.M.

N82-23684*# National Aeronautics and Space Administration, Lewis Research Center, Cleveland, Ohio.

WIND TURBINE DYNAMICS

Robert W. Thresher, ed. (Oregon State Univ., Corvallis) May 1981 422 p refs Workshop held in Cleveland 24-26 Feb. 1981 Sponsored in part by DOE
(NASA-CP-2185; NAS 1.55:2185; CONF-81-226; SERI/CP-635-1238) Avail: NTIS HC A18/MF A01 CSCL 10B

Recent progress in the analysis and prediction of the dynamic behavior of wind turbine generators is discussed. The following areas were addressed: (1) the adequacy of state of the art analysis tools for designing the next generation of wind power systems; (2) the use of state of the art analysis tools designers; and (3) verifications of theory which might be lacking or inadequate. Summaries of these informative discussions as well as the questions and answers which followed each paper are documented in the proceedings. For individual titles, see N82-23685 through N82-23733.

N82-23696*# National Aeronautics and Space Administration, Lewis Research Center, Cleveland, Ohio.

APPLICATIONS OF THE DOE/NASA WIND TURBINE ENGINEERING INFORMATION SYSTEM

Harold E. Neustadter and David A. Spera *In its* Wind Turbine Dyn. May 1981 p 113-120 refs (For primary document see N82-23684 14-44)
Avail: NTIS HC A18/MF A01 CSCL 10B

A statistical analysis of data obtained from the Technology and Engineering Information Systems was made. The systems analyzed consist of the following elements: (1) sensors which measure critical parameters (e.g., wind speed and direction, output power, blade loads and component vibrations); (2) remote multiplexing units (RMUs) on each wind turbine which frequency-modulate, multiplex and transmit sensor outputs; (3) on-site instrumentation to record, process and display the sensor output; and (4) statistical analysis of data. Two examples of the capabilities of these systems are presented. The first illustrates the standardized format for application of statistical analysis to each directly measured parameter. The second shows the use of a model to estimate the variability of the rotor thrust loading, which is a derived parameter. Author

N82-23699*# National Aeronautics and Space Administration, Lewis Research Center, Cleveland, Ohio.

CALCULATION OF GUARANTEED MEAN POWER FROM WIND TURBINE GENERATORS

David A. Spera *In its* Wind Turbine Dyn. May 1981 p 139-150 refs (For primary document see N82-23684 14-44)
Avail: NTIS HC A18/MF A01 CSCL 10B

A method for calculating the 'guaranteed mean' power output of a wind turbine generator is proposed. The term 'mean power' refers to the average power generated at specified wind speeds during short-term tests. Correlation of anemometers, the method of bins for analyzing non-steady data, the PROP Code for predicting turbine power, and statistical analysis of deviations in test data

from theory are discussed. Guaranteed mean power density for the Clayton Mod-OA system was found to be 8 watts per square meter less than theoretical power density at all power levels, with a confidence level of 0.999. This amounts to 4 percent of rated power. Author

N82-23707*# National Aeronautics and Space Administration, Lewis Research Center, Cleveland, Ohio.

WHIRL FLUTTER ANALYSIS OF A HORIZONTAL-AXIS WIND TURBINE WITH A TWO-BLADED TEETERING ROTOR

David C. Janetzke and Krishna R. V. Kaza (Toledo Univ.) *In* NASA, Lewis Research Center Wind Turbine Dyn. May 1981 p 201-210 refs (For primary document see N82-23684 14-44)
Avail: NTIS HC A18/MF A01 CSCL 10B

Whirl flutter and the effect of pitch-flap coupling on teetering motion of a wind turbine were investigated. The equations of motion are derived for an idealized five-degree-of-freedom mathematical model of a horizontal-axis wind turbine with a two-bladed teetering rotor. The model accounts for the out-of-plane bending motion of each blade, the teetering motion of the rotor, and both the pitching and yawing motions of the rotor support. Results show that the design is free from whirl flutter. Selected results are presented indicating the effect of variations in rotor support damping, rotor support stiffness, and pitch-flap coupling on pitching, yawing, teetering, and blade bending motions. Author

N82-23710*# National Aeronautics and Space Administration, Lewis Research Center, Cleveland, Ohio.

COMPARISON OF UPWIND AND DOWNWIND ROTOR OPERATION OF THE DOE/NASA 100-KW MOD-0 WIND TURBINE

John C. Glasgow, Dean R. Miller, and Robert D. Corrigan *In its* Wind Turbine Dyn. May 1981 p 225-234 refs (For primary document see N82-23684 14-44)
Avail: NTIS HC A18/MF A01 CSCL 10B

Tests were conducted on a 38m diameter horizontal axis wind turbine, which had first a rotor downwind of the supporting tower and then upwind of the tower. Aside from the placement of the rotor and the direction of rotation of the drive train, the wind turbine was identical for both tests. Three aspects of the test results are compared: rotor blade bending loads, rotor teeter response, and nacelle yaw moments. As a result of the tests, it is shown that while mean flatwise bending moments were unaffected by the placement of the rotor, cyclic flatwise bending tended to increase with wind speed for the downwind rotor while remaining somewhat uniform with wind speed for the upwind rotor, reflecting the effects of increased flow disturbance for downwind rotor. Rotor teeter response was not significantly affected by the rotor location relative to the tower, but appears to reflect reduced teeter stability near rated wind speed for both configurations. Teeter stability appears to return above rated wind speed, however. Nacelle yaw moments are higher for the upwind rotor but do not indicate significant design problems for either configuration. T.M.

N82-23711*# National Aeronautics and Space Administration, Lewis Research Center, Cleveland, Ohio.

A REVIEW OF RESONANCE RESPONSE IN LARGE HORIZONTAL-AXIS WIND TURBINES

Timothy L. Sullivan *In its* Wind Turbine Dyn. May 1981 p 237-244 refs (For primary document see N82-23684 14-44)
Avail: NTIS HC A18/MF A01 CSCL 10B

Field operation of the Mod-0 and Mod-1 wind turbines is described. Operational experience shows that 1 per rev excitation exists in the drive train, high aerodynamic damping prevents resonance response of the blade flatwise modes, and teetering the hub substantially reduces the chordwise blade response to odd harmonic excitation. These results can be used by designer as a guide to system frequency placement. In addition it is found that present analytical techniques can accurately predict wind turbine natural frequencies. T.M.

ORIGINAL PAGE IS
OF POOR QUALITY

N82-23730* National Aeronautics and Space Administration, Lewis Research Center, Cleveland, Ohio.

THE NASA-LERC WIND TURBINE SOUND PREDICTION CODE

Larry A. Viterna *In its* Wind Turbine Dyn. May 1981 p 411-418 refs (For primary document see: N82-23884 14-44)

Avail: NTIS HC A18/MF A01 CSCL 10B

Since regular operation of the DOE/NASA MOD-1 wind turbine began in October 1979 about 10 nearby households have complained of noise from the machine. Development of the NASA-LERC with turbine sound prediction code began in May 1980 as part of an effort to understand and reduce the noise generated by MOD-1. Tone sound levels predicted with this code are in generally good agreement with measured data taken in the vicinity MOD-1 wind turbine (less than 2 rotor diameters). Comparison in the far field indicates that propagation effects due to terrain and atmospheric conditions may be amplifying the actual sound levels by about 6 dB. Parametric analysis using the code has shown that the predominant contributions to MOD-1 rotor noise are: (1) the velocity deficit in the wake of the support tower; (2) the high rotor speed; and (3) off column operation. Author

N82-24647* National Aeronautics and Space Administration, Lewis Research Center, Cleveland, Ohio.

DESIGN OF A 35-KILOWATT BIPOLAR NICKEL-HYDROGEN BATTERY FOR LOW EARTH ORBIT APPLICATION

Robert L. Cataldo and John J. Smithrick 1982 10 p refs To be presented at the 17th Intersoc. Energy Conversion Eng. Conf., Los Angeles, 8-13 Aug. 1982; sponsored by IEEE, AIAA, ACS, AIChE, ANS, ASME and SAE

(NASA-TM-82844; E-1214; NAS 1.15:82844) Avail: NTIS HC A02/MF A01 CSCL 10C

The needs of multikilowatt storage for low Earth orbit applications are featured. The modular concept, with projected energy densities of 20-24 W-hr/lb and 700-900 W-hr/ft³, has significant improvements over state of the art capabilities. Other design features are: active cooling, a new scheme for H₂-O₂ recombination, and pore size engineering of all cell components. T.M.

N82-24717* National Aeronautics and Space Administration, Lewis Research Center, Cleveland, Ohio.

HIGH VOLTAGE V-GROOVE SOLAR CELL Patent Application

J. C. Evans, Jr., A. T. Chai, and C. P. Goradia, inventors (to NASA) Filed 18 Mar. 1982 11 p

(NASA-Case-LEW-13401-2; US-Patent-Appi-SN-359388) Avail: NTIS HC A02/MF A01 CSCL 10A

A high voltage multijunction solar cell is disclosed. The cell is composed of a plurality of discrete voltage generating regions, or unit cells, which are formed in a single semiconductor wafer and are connected together so that the voltages of the individual cells are additive. The unit cells comprise doped regions of opposite conductivity types separated by a gap. V-shaped grooves are formed in the wafer and thereafter the wafer is oriented so that ions of one conductivity type can be implanted in one face of the groove while the other face is shielded. A metallization layer is applied and selectively etched away to provide connections between the unit cells. NASA

N82-25636* National Aeronautics and Space Administration, Lewis Research Center, Cleveland, Ohio.

IMPACT OF UNIFORM ELECTRODE CURRENT DISTRIBUTION ON ETF

David J. Bents 1982 10 p refs Presented at the 20th Aerospace Sci. Meeting, Orlando, Fla., 11-14 Jan 1982

(Contract DE-AI01-77ET-10769) (NASA-TM-82875; E-1044; NAS 1.15:82875; DOE/NASA/10769-24) Avail: NTIS HC A02/MF A01 CSCL 10A

The design impacts on the ETF electrode consolidation network associated with uniform channel electrode current distribution are examined and the alternate consolidation design which occur are presented compared to the baseline (non-uniform current) design with respect to performance, and hardware requirements. A rational basis is given for comparing the requirements for the different designs and the savings that result from uniform current distribution. Performance and cost impacts upon the combined cycle plant are discussed. Author

N82-25637* National Aeronautics and Space Administration, Lewis Research Center, Cleveland, Ohio.

NASA REDOX SYSTEM DEVELOPMENT PROJECT STATUS

A. W. Nice 1981 18 p refs Presented at the 4th Battery and Electrochem Contractors Conf., Washington, 2-4 Jun. 1981 (Contract DE-AI01-80AL-12726)

(NASA-TM-82665; E-939; DOE/NASA/12726-9; NAS 1.15:82665) Avail: NTIS HC A02/MF A01 CSCL 10A

NASA-Redox energy storage systems developed for solar power applications and utility load leveling applications are discussed. The major objective of the project is to establish the technology readiness of Redox energy storage for transfer to industry for product development and commercialization by industry. The approach is to competitively contract to design, build, and test Redox systems progressively from preprototype to prototype multi-kW and megawatt systems and conduct supporting technology advancement tasks. The Redox electrode and membrane are fully adequate for multi-kW solar related applications and the viability of the Redox system technology as demonstrated for multi-kW solar related applications. The status of the NASA Redox Storage System Project is described along with the goals and objectives of the project elements. Author

N82-26790* National Aeronautics and Space Administration, Lewis Research Center, Cleveland, Ohio.

OPTIMIZATION OF THE OXIDANT SUPPLY SYSTEM FOR COMBINED CYCLE MHD POWER PLANTS

Albert J. Juhasz 1982 14 p refs Presented at the 20th Symp. on the Eng. Aspects of Magnetohydrodyn., Irvine, Calif., 14-16 Jun. 1981

(Contract DE-AI01-77ET-10769) (NASA-TM-82909; E-1294; DOE/NASA/10769-27; NAS 1.15:82909) Avail: NTIS HC A02/MF A01

An in-depth study was conducted to determine what, if any, improvements could be made on the oxidant supply system for combined cycle MHD power plants which could be reflected in higher thermal efficiency and a reduction in the cost of electricity, COE. A systematic analysis of air separation process variations which showed that the specific energy consumption could be minimized when the product stream oxygen concentration is about 70 mole percent was conducted. The use of advanced air compressors, having variable speed and guide vane position control, results in additional power savings. The study also led to the conceptual design of a new air separation process, sized for a 500 MW sub e MHD plant, referred to as an internal compression is discussed. In addition to its lower overall energy consumption, potential capital cost savings were identified for air separation plants using this process when constructed in a single large air separation train rather than multiple parallel trains, typical of conventional practice. B.W.

N82-26807* National Aeronautics and Space Administration, Lewis Research Center, Cleveland, Ohio.

MOD-2 WIND TURBINE SYSTEM CLUSTER RESEARCH TEST PROGRAM, VOLUME 1: INITIAL PLAN E-1290 Final Report

Larry H. Gordon Mar. 1982 92 p refs 2 Vol. (NASA-TM-82906; NAS 1.15:82906; DOE/NASA/20305-8)

Avail: NTIS HC A05/MF A01 CSCL 10A

Upon completion of the design and development of three Mod-2 wind turbines, a series of research experiments are planned to gather data on and evaluate the performance, environmental effects, and operation of a cluster as well as a single, large multimegawatt wind turbine. Information on the program objectives, a Mod-2 system description, a planned schedule, organizational roles, and responsibilities, is included. T.M.

N82-27838* National Aeronautics and Space Administration, Lewis Research Center, Cleveland, Ohio.

COMPARATIVE ANALYSIS OF THE CONCEPTUAL DESIGN STUDIES OF POTENTIAL EARLY COMMERCIAL MHD POWER PLANTS (CSPEC)

R. J. Sovie, J. M. Winter, A. J. Juhasz, and R. D. Berg (Gilbert Associates, Inc.) 1982 27 p refs Presented at the 20th Symp. on the Eng. Aspects of Magnetohydrodyn., Irvine, Calif., 14-16 Jun. 1982

(Contract DE-AI01-77ET-10769) (NASA-TM-82897; DOE/NASA/10769-26; NAS 1.15:82897)

Avail: NTIS HC A03/MF A01 CSCL 10B

A conceptual design study of the MHD/steam plant that incorporates the use of oxygen enriched air preheated in a metallic heat exchanger as the combustor oxidant showed that this plant is the most attractive for early commercial applications. The variation of performance and cost was investigated as a function of plant size. The contractors' results for the overall efficiencies are in reasonable agreement considering the slight differences in their plant designs. NASA LeRC is reviewing cost and performance results for consistency with those of previous studies, including studies of conventional steam plants. LeRC in house efforts show that there are still many tradeoffs to be considered for these oxygen enriched plants and considerable variations can be made in channel length and level of oxygen enrichment with little change in overall plant efficiency. A.R.H.

N82-28786*# National Aeronautics and Space Administration. Lewis Research Center, Cleveland, Ohio.
ROLLING RESISTANCE OF ELECTRIC VEHICLE TIRES FROM TRACK TESTS

Miles O. Dustin and Ralph J. Slavik Jun. 1982 26 p refs Sponsored in part by NASA (Contract DE-AI01-77CS-51044) (NASA-TM-82836; DOE/NASA/51044-24; NAS 1.15:82836) Avail: NTIS HC A03/MF A01 CSCL 13F

Special low-rolling-resistance tires were made for DOE's ETV-1 electric vehicle. Tests were conducted on these tires and on a set of standard commercial automotive tires to determine the rolling resistance as a function of time during both constant-speed tires and SAE J227a driving cycle tests. The tests were conducted on a test track at ambient temperatures that ranged from 15 to 32 C (59 to 89 F) and with tire pressures of 207 to 276 kPa (30 to 40 psi). At a contained-air temperature of 38 C (100 F) and a pressure of 207 kPa (30 psi) the rolling resistances of the electric vehicle tires and the standard commercial tires, respectively, were 0.0102 and 0.0088 kilogram per kilogram of vehicle weight. At a contained-air temperature of 38 C (100 F) and a pressure of 276 kPa (40 psi) the rolling resistances were 0.009 and 0.0074 kilogram per kilogram of vehicle weight, respectively. Author

N82-29708* National Aeronautics and Space Administration. Lewis Research Center, Cleveland, Ohio.
ADVANCED INORGANIC SEPARATORS FOR ALKALINE BATTERIES Patent

Dean W. Sheibley, inventor (to NASA) Issued 25 May 1982 5 p Filed 27 Feb. 1981 Supersedes N81-22466 (19 - 13, p 1777)

(NASA-Case-LEW-13171-1; US-Patent-4,331,746; US-Patent-Appl-SN-238790; US-Patent-Class-429-144; US-Patent-Class-429-251; US-Patent-Class-429-254) Avail: US Patent and Trademark Office CSCL 10C

A flexible, porous battery separator comprising a coating applied to a porous, flexible substrate is described. The coating comprises: (1) a thermoplastic rubber-based resin which is insoluble and unreactive in the alkaline electrolyte; (2) a polar organic plasticizer which is reactive with the alkaline electrolyte to produce a reaction product which contains a hydroxyl group and/or a carboxylic acid group; and (3) a mixture of polar particulate filler materials which are unreactive with the electrolyte, the mixture comprising at least one first filler material having a surface area of greater than 25 meters sq/gram, at least one second filler material having a surface area of 10 to 25 sq meters/gram, wherein the volume of the mixture of filler materials is less than 45% of the total volume of the fillers and the binder, the filler surface area per gram of binder is about 20 to 60 sq meters/gram, and the amount of plasticizer is sufficient to coat each filler particle. A method of forming the battery separator is also described.

Official Gazette of the U.S. Patent and Trademark Office

N82-29709* National Aeronautics and Space Administration. Lewis Research Center, Cleveland, Ohio.
METHOD OF MAKING A HIGH VOLTAGE V-GROOVE SOLAR CELL Patent

John C. Evans, Jr., An-Ti Chai, and Chandr P. Goradia, inventors (to NASA) Issued 22 Jun. 1982 6 p Filed 24 Dec. 1980 Supersedes N81-16529 (19 - 07, p 092)

(NASA-Case-LEW-13401-1; US-Patent-4,335,503; US-Patent-Appl-SN-219678; US-Patent-Class-29-572; US-Patent-Class-136-249; US-Patent-Class-148-15;

US-Patent-Class-357-30) Avail: US Patent and Trademark Office CSCL 10A

A method is provided for making a high voltage multijunction solar cell. The cell comprises a plurality of discrete voltage generating regions, or unit cells, which are formed in a single semiconductor wafer and are connected together so that the voltages of the individual cells are additive. The unit cells comprise doped regions of opposite conductivity types separated by a gap. The method includes forming V-shaped grooves in the wafer and thereafter orienting the wafer so that ions of one conductivity type can be implanted in one face of the groove while the other face is shielded. A metallization layer is applied and selectively etched away to provide connections between the unit cells. Official Gazette of the U.S. Patent and Trademark Office

N82-29717*# National Aeronautics and Space Administration. Lewis Research Center, Cleveland, Ohio.

TECHNIQUES FOR ENHANCING DURABILITY AND EQUIVALENCE RATIO CONTROL IN A RICH-LEAN, THREE-STAGE GROUND POWER GAS TURBINE COMBUSTOR

Donald F. Schultz 1982 14 p refs Presented at 1982 Joint Power Generation Conf., Denver, 17-21 Oct. 1982; sponsored by ASME

(Contract DE-AI01-77ET-10350) (NASA-TM-82922; DOE/NASA/10350-33-E-1313, NAS 1.15:82922) Avail: NTIS HC A02/MF A01 CSCL 10A

Rig tests of a can-type combustor were performed to demonstrate two advanced ground power engine combustor concepts: steam cooled rich-burn combustor primary zones for enhanced durability; and variable combustor geometry for three stage combustion equivalence ratio control. Both concepts proved to be highly successful in achieving their desired objectives. The steam cooling reduced peak liner temperatures to less than 800 K. This offers the potential of both long life and reduced use of strategic materials for liner fabrication. Three degrees of variable geometry were successfully implemented to control airflow distribution within the combustor. One was a variable blade angle axial flow air swirler to control primary airflow while the other two consisted of rotating bands to control secondary and tertiary or dilution air flow. B.W.

N82-30700*# National Aeronautics and Space Administration. Lewis Research Center, Cleveland, Ohio.

RESULTS OF CHOPPER-CONTROLLED DISCHARGE LIFE CYCLING STUDIES ON LEAD ACID BATTERIES

John G. Ewashinka and Steven M. Sidik 1982 17 p refs Presented at the 17th Intersoc. Energy Conversion Eng. Conf., Los Angeles, 8-13 Aug. 1982 Sponsored in part by DOE (NASA-TM-82912; DOE/NASA/51044-26; E-1293; NAS 1.15:82912) Avail: NTIS HC A02/MF A01 CSCL 10C

A group of 108 state of the art nominally 6 volt lead acid batteries were tested in a program of one charge/discharge cycle per day for over two years or to ultimate battery failure. The primary objective was to determine battery cycle life as a function of depth of discharge (25 to 75 percent), chopper frequency (100 to 1000 Hz), duty cycle (25 to 87.5 percent), and average discharge current (20 to 260 A). The secondary objective was to determine the types of battery failure modes, if any, were due to the above parameters. The four parameters above were incorporated in a statistically designed test program. R.J.F.

N82-30704*# National Aeronautics and Space Administration. Lewis Research Center, Cleveland, Ohio.

LEWIS PRESSURIZED, FLUIDIZED-BED COMBUSTION PROGRAM. DATA AND CALCULATED RESULTS

R. James Rollbuhler Mar. 1982 63 p refs (NASA-TM-81767; E-830; NAS 1.15:81767) Avail: NTIS HC A04/MF A01 CSCL 10B

A 200 kilowatt (thermal), pressurized, fluidized bed (PFB) reactor and research test facility were designed, constructed, and operated. The facility was established to assess and evaluate the effect of PFB hot gas effluent on aircraft turbine engine materials that may have applications in stationary powerplant turbogenerators. The facility was intended for research and development work and was designed to operate over a wide range of conditions. These conditions included the type and rate of consumption of fuel (e.g., coal) and sulfur reacting sorbent

material; the ratio of feed fuel to sorbent material; the ratio of feed fuel to combustion airflow; the depth of the fluidized reaction bed; the temperature and pressure in the reaction bed; and the type of test unit that was exposed to the combustion exhaust gases. S.L.

N82-30710*# National Aeronautics and Space Administration, Lewis Research Center, Cleveland, Ohio.
EXPERIENCE AND ASSESSMENT OF THE DOE-NASA MOD-1 2000-KILOWATT WIND TURBINE GENERATOR AT BOONE, NORTH CAROLINA Final Report
John L. Collins, Richard K. Shaltenc, Richard H. Poor (General Electric, Philadelphia), and Robert S. Barton (General Electric, Philadelphia) Apr. 1982 55 p refs
(Contract DE-A101-76ET-20366)
(NASA-TM-82721; E-1020; DOE/NASA/20366-2; NAS 1.15:82721) Avail: NTIS HC A04/MF A01 CSCL 10A

The Mod 1 program objectives are defined. The Mod 1 wind turbine is described. In addition to the steel blade operated on the wind turbine, a composite blade was designed and manufactured. During the early phase of the manufacturing cycle of Mod 1A configuration was designed that identified concepts such as partial span control, a soft tower, and upwind teetered rotors that were incorporated in second and third generation industry designs. The Mod 1 electrical system performed as designed, with voltage flicker characteristics within acceptable utility limits. Power output versus wind speed equaled or exceeded design predictions. The wind turbine control system was operated successfully at the site and remotely from the utility dispatcher's office. During wind turbine operations, television interference was experienced by the local residents. As a consequence, operations were restricted. Although not implemented, two potential solutions were identified. In addition to television interference, a few local residents complained about objectionable sound, particularly the 'thump' as the blade passed behind the tower. To eliminate objections, the sound generation level was reduced by 10 dB by reducing the rotor speed from 35 rpm to 23 rpm. Bolts in the drive train fractured. A solution was identified but not implemented. The public reaction toward the Mod 1 wind turbine program was overwhelmingly favorable. S.L.

N82-30713*# National Aeronautics and Space Administration, Lewis Research Center, Cleveland, Ohio.
INTEGRATED GASIFIER COMBINED CYCLE POLYGENERATION SYSTEM TO PRODUCE LIQUID HYDROGEN
Raymond K. Burns, Peter J. Staiger, and Richard M. Donovan Jul. 1982 37 p refs
(NASA-TM-82921; E-1308; NAS 1.15:82921) Avail: NTIS HC A03/MF A01 CSCL 10A

An integrated gasifier combined cycle (IGCC) system which simultaneously produces electricity, process steam, and liquid hydrogen was evaluated and compared to IGCC systems which cogenerate electricity and process steam. A number of IGCC plants, all employing a 15 MWe gas turbine and producing from 0 to 20 tons per day of liquid hydrogen and from 0 to 20 MWt of process steam were considered. The annual revenue required to own and operate such plants was estimated to be significantly lower than the potential market value of the products. The results indicate a significant potential economic benefit to configuring IGCC systems to produce a clean fuel in addition to electricity and process steam in relatively small industrial applications. Author

N82-30714*# National Aeronautics and Space Administration, Lewis Research Center, Cleveland, Ohio.
ASSESSMENT OF A 40-KILOWATT STIRLING ENGINE FOR UNDERGROUND MINING APPLICATIONS
James E. Cairelli, Gary G. Kelm, and Jack G. Slaby Jun. 1982 75 p refs
(Contract DI-BM-JO-100026)
(NASA-TM-82822; E-1171; NAS 1.15:82822) Avail: NTIS HC A04/MF A01 CSCL 081

An assessment of alternative power sources for underground mining applications was performed. A 40-kW Stirling research engine was tested to evaluate its performance and emission characteristics when operated with helium working gas and diesel fuel. The engine, the test facility, and the test procedures are described. Performance and emission data for the engine operating with helium working gas and diesel fuel are reported and compared with data obtained with hydrogen working gas and

unleaded gasoline fuel. Helium diesel test results are compared with the characteristics of current diesel engines and other Stirling engines. External surface temperature data are also presented. Emission and temperature results are compared with the Federal requirements for diesel underground mine engines. The durability potential of Stirling engines is discussed on the basis of the experience gained during the engine tests. Author

N82-30715*# National Aeronautics and Space Administration, Lewis Research Center, Cleveland, Ohio.
SYNTHETIC BATTERY CYCLING TECHNIQUES
Harold F. Leibbecki and Lawrence H. Thaller 1982 8 p refs
Proposed for presentation at the 4th ESTEC Spacecraft Power Conditioning Seminar, Noordwijk, Netherlands, 9-11 Nov. 1982; sponsored by ESA
(NASA-TM-82945; E-1351; NAS 1.15:82945) Avail: NTIS HC A02/MF A01 CSCL 10C

Synthetic battery cycling makes use of the fast growing capability of computer graphics to illustrate some of the basic characteristics of operation of individual electrodes within an operating electrochemical cell. It can also simulate the operation of an entire string of cells that are used as the energy storage subsystem of a power system. The group of techniques that as a class have been referred to as Synthetic Battery Cycling is developed in part to try to bridge the gap of understanding that exists between single cell characteristics and battery system behavior. Author

N82-30716*# National Aeronautics and Space Administration, Lewis Research Center, Cleveland, Ohio.
NICKEL-HYDROGEN BIPOLAR BATTERY SYSTEMS
Lawrence H. Thaller 1982 9 p refs
Proposed for presentation at the 4th ESTEC Spacecraft Power Conditioning Seminar, Noordwijk, Netherlands, 9-11 Nov. 1982; sponsored by ESA
(NASA-TM-82946; E-1352; NAS 1.15:82946) Avail: NTIS HC A02/MF A01 CSCL 10A

Nickel-hydrogen cells are currently being manufactured on a semi-experimental basis. Rechargeable nickel-hydrogen systems are described that more closely resemble a fuel cell system than a traditional nickel-cadmium battery pack. This has been stimulated by the currently emerging requirements related to large manned and unmanned low earth orbit applications. The resultant nickel-hydrogen battery system should have a number of features that would lead to improved reliability, reduced costs as well as superior energy density and cycle lives as compared to battery systems constructed from the current state-of-the-art nickel-hydrogen individual pressure vessel cells. B.W.

N82-30717*# National Aeronautics and Space Administration, Lewis Research Center, Cleveland, Ohio.
CATALYTIC COMBUSTION OF ACTUAL LOW AND MEDIUM HEATING VALUE GASES
Daniel L. Bulzan 1982 19 p refs
Presented at the Joint Power Generation Conf., Denver, 17-21 Oct. 1982
(Contract DE-A101-77ET-10350)
(NASA-TM-82930; E-1326; DOE/NASA/10350-34; NAS 1.15:82930) Avail: NTIS HC A02/MF A01 CSCL 10A

Catalytic combustion of both low and medium heating value gases using actual coal derived gases obtained from operating gasifiers was demonstrated. A fixed bed gasifier with a complete product gas cleanup system was operated in an air blown mode to produce low heating value gas. A fluidized bed gasifier with a water quench product gas cleanup system was operated in both an air enriched and an oxygen blown mode to produce low and medium heating value gas. Noble metal catalytic reactors were evaluated in 12 cm flow diameter test rigs on both low and medium heating value gases. Combustion efficiencies greater than 99.5% were obtained with all coal derived gaseous fuels. The NOx emissions ranged from 0.2 to 4 g NO2 kg fuel. E.A.K.

N82-31764* National Aeronautics and Space Administration, Lewis Research Center, Cleveland, Ohio.
HIGH VOLTAGE PLANAR MULTI-JUNCTION SOLAR CELL Patent
John C. Evans, Jr., An-Ti Chai, and Chandra P. Goradia, inventors
(to NASA) Issued 24 Dec. 1980 6 p Filed 24 Dec. 1980

Supersedes N81-16528 (19 - 07, p 0927)
(NASA-Case-LEW-13400-1; US-Patent-4,341,918;
US-Patent-Appl-SN-219677; US-Patent-Class-136-249;
US-Patent-Class-357-30) Avail: US Patent and Trademark Office
CSCL 10A

A high voltage multijunction solar cell is provided wherein a plurality of discrete voltage generating regions or unit cells are formed in a single generally planar semiconductor body. The unit cells are comprised of doped regions of opposite conductivity type separated by a gap or undiffused region. Metal contacts connect adjacent cells together in series so that the output voltages of the individual cells are additive. In some embodiments, doped field regions separated by a overlie the unit cells but the cells may be formed in both faces of the wafer.

Official Gazette of the U.S. Patent and Trademark Office

N82-31769*# National Aeronautics and Space Administration.
Lewis Research Center, Cleveland, Ohio.

MICRONIZED COAL BURNER FACILITY Patent Application
F. D. Calfo and M. W. Lupton, inventors (to NASA) Filed 30 Jun.
1982 13 p

(NASA-Case-LEW-13426-1; US-Patent-Appl-SN-393588) Avail:
NTIS HC A02/MF A01 CSCL 10B

A combustor or burner system in which the ash resulting from burning a coal in oil mixture is of submicron particle size is described. The burner system comprises a burner section, a flame exit nozzle, a fuel nozzle section, and an air tube by which preheated air is directed into the burner section. Regulated air pressure is delivered to a fuel nozzle. Means are provided for directing a mixture of coal particles and oil from a drum to a nozzle at a desired rate and pressure while means returns excess fuel to the fuel drum.

Author

N82-31776*# National Aeronautics and Space Administration.
Lewis Research Center, Cleveland, Ohio.

GAS TURBINE CRITICAL RESEARCH AND ADVANCED TECHNOLOGY (CRT) SUPPORT PROJECT Annual Report, Fiscal Year 1980

Edward R. Furman, David N. Anderson, Michael A. Gedwill, Jr.,
Carl E. Lowell, and Donald F. Schultz Jul. 1982 47 p refs
(Contract DE-AI01-77ET-10350)

(NASA-TM-82872; E-1247; NAS 1.15:82872) Avail: NTIS
HC A03/MF A01 CSCL 10A

The technical progress to provide a critical technology base for utility gas turbine systems capable of burning coal-derived fuels is summarized. Project tasks include the following: (1) combustion - to investigate the combustion of coal-derived fuels and the conversion of fuel-bound nitrogen to NO_x; (2) materials - to understand and prevent the hot corrosion of turbine hot section materials; and (3) system studies - to integrate and guide the technological efforts. Technical accomplishments include: an extension of flame tube combustion testing of propane - Toluene Fuel Mixtures to vary H₂ content from 9 to 18 percent by weight and the comparison of results with that predicted from a NASA Lewis General Chemical Kinetics Computer Code; the design and fabrication of combustor sector test section to test current and advanced combustor concepts; Testing of Catalytic combustors with residual and coal-derived liquid fuels; testing of high strength super alloys to evaluate their resistance to potential fuel impurities using doped clean fuels and coal-derived liquids; and the testing and evaluation of thermal barrier coatings and bond coatings on conventional turbine materials.

Author

N82-31777*# National Aeronautics and Space Administration.
Lewis Research Center, Cleveland, Ohio.

ON THE CAUSE OF THE 'FLAT-SPOT' PHENOMENON OBSERVED IN SILICON SOLAR CELLS AT LOW TEMPERATURES AND LOW INTENSITIES

V. G. Weizer, J. D. Broder, H. W. Brandhorst, and A. F. Forestieri
1982 14 p refs Presented at the 3rd European Symp. on
Photovoltaic Generators in Space, Bath, England, 4-6 May 1982;

sponsored by RAE, U.K. Dept. of Industry and ESA.
(NASA-TM-82903; E-1286; NAS 1.15:82903) Avail: NTIS
HC A02/MF A01 CSCL 10A

A model is presented that explains the 'flat-spot' (FS) power loss phenomenon observed in silicon solar cells operating deep space (low temperature, low intensity) conditions. Evidence is presented suggesting that the effect is due to localized metallurgical interactions between the silicon substrate and the contact metallization. These reactions are shown to result in localized regions in which the PN junction is destroyed and replaced with a metal-semiconductor-like interface. The effects of thermal treatment, crystallographic orientation, junction depth, and metallization are presented along with a method of preventing the effect through the suppression of vacancy formation at the free surface of the contact metallization. Preliminary data indicating the effectiveness of a TiN diffusion barrier in preventing the effect are also given.

Author

N82-32653*# National Aeronautics and Space Administration.
Lewis Research Center, Cleveland, Ohio.

DETERMINATION OF OPTIMUM SUNLIGHT CONCENTRATION LEVEL IN SPACE FOR 3-4 CASCADE SOLAR CELLS

Henry B. Curtis 1982 14 p refs Presented at the 3rd European Symp. on Photovoltaic Generators in Space, Bath, Engl., 4-6 May 1982; sponsored by RAE and ESA

(NASA-TM-82899; E-1282; NAS 1.15:82899) Avail: NTIS
HC A02/MF A01 CSCL 10A

The optimum range of concentration in space for III-V cascade cells has been calculated using a realistic solar cell diode equation. Temperature was varied with concentration using several models and ranged from 55 deg at one sun to between 80 deg and 200 deg C at 100 suns. A variety of series resistance and internal resistances were used. Coefficients of the diffusion and recombination terms are strongly temperature dependent. The study indicates that the maximum efficiency of 30 percent occurs in the 50 to 100 X sun concentration range provided series resistance is below 0.015 ohm sq cm and cell temperature is about 80 C at 100 suns.

Author

N82-32854*# National Aeronautics and Space Administration.
Lewis Research Center, Cleveland, Ohio.

LARGE AREA LOW-COST SPACE SOLAR CELL DEVELOPMENT

C. R. Baraona and J. L. Cioni (NASA, Johnson Space Center, Houston, Tex.) 1982 9 p refs Presented at the 3rd European Symp. on Photovoltaic Generators in Space, Bath, Engl., 4-6 May, 1982; sponsored by RAE and ESA

(NASA-TM-82902; E-1285; NAS 1.15:82902) Avail: NTIS
HC A02/MF A01 CSCL 10A

A development program to produce large-area (5.9 x 5.9 cm) space quality silicon solar cells with a cost goal of 30 \$/watt is described. Five cell types under investigation include wraparound dielectric, mechanical wraparound and conventional contact configurations with combinations of 2 or 10 ohm-cm resistivity, back surface reflectors and/or fields, and diffused or ion implanted junctions. A single step process to cut cell and cover-glass simultaneously is being developed. A description of cell developments by Applied Solar Energy Corp., Spectrolab and Spire is included. Results are given for cell and array tests, performed by Lockheed, TRW and NASA. Future large solar arrays that might use cells of this type are discussed.

Author

N82-33828# National Aeronautics and Space Administration.
Lewis Research Center, Cleveland, Ohio.

DESIGN DESCRIPTION OF THE TANGAYE VILLAGE PHOTOVOLTAIC POWER SYSTEM

James E. Martz and Anthony F. Ratajczak Jun. 1982 113 p refs

(NASA-TM-82917; E-1305; NAS 1.15:82917) Avail: NTIS
HC A06/MF A01 CSCL 10A

ORIGINAL PAGE IS
OF POOR QUALITY

The engineering design of a stand alone photovoltaic (PV) powered grain mill and water pump for the village of Tangaye, Upper Volta is described. The socioeconomic effects of reducing the time required by women in rural areas for drawing water and grinding grain were studied. The suitability of photovoltaic technology for use in rural areas by people of limited technical training was demonstrated. The PV system consists of a 1.8-kW (peak) solar cell array, 540 ampere hours of battery storage, instrumentation, automatic controls, and a data collection and storage system. The PV system is situated near an improved village well and supplies d.c. power to a grain mill and a water pump. The array is located in a fenced area and the mill, battery, instruments, controls, and data system are in a mill building. A water storage tank is located near the well. The system employs automatic controls which provide battery charge regulation and system over and under voltage protection. This report includes descriptions of the engineering design of the system and of the load that it serves; a discussion of PV array and battery sizing methodology; descriptions of the mechanical and electrical designs including the array, battery, controls, and instrumentation; and a discussion of the safety features. The system became operational on March 1, 1979.

Author

N82-33829*# National Aeronautics and Space Administration, Lewis Research Center, Cleveland, Ohio.
ON THE ROAD PERFORMANCE TESTS OF ELECTRIC TEST VEHICLE FOR CORRELATION WITH ROAD LOAD SIMULATOR Final Report

Miles O. Dustin and Ralph J. Slavik Aug. 1982 27 p refs (Contract DE-A101-77CS-51044)

(NASA-TM-82900; E-1283; DOE/NASA/51044-25; NAS 1.15:82900) Avail: NTIS HC A03/MF A01 CSCL 13F

A dynamometer (road load simulator) is used to test and evaluate electric vehicle propulsion systems. To improve correlation between system tests on the road load simulator and on the road, similar performance tests are conducted using the same vehicle. The results of track tests on the electric propulsion system test vehicle are described. The tests include range at constant speeds and over SAE J227a driving cycles, maximum accelerations, maximum gradability, and tire rolling resistance determination. Road power requirements and energy consumption were also determined from coast down tests.

S.L.

N82-33830*# National Aeronautics and Space Administration, Lewis Research Center, Cleveland, Ohio.
THEORETICAL AND EXPERIMENTAL POWER FROM LARGE HORIZONTAL-AXIS WIND TURBINES

Larry A. Viterna and David C. Janetzke Sep. 1982 21 p refs Presented at the 5th Biennial Conf. and Workshop on Wind Energy, Washington D.C., 5-7 Oct. 1981 (Contract DE-A101-76ET-20320)

(NASA-TM-82944; E-1346; DOE/NASA/20320-41; NAS 1.15:82944) Avail: NTIS HC A02/MF A01 CSCL 10A

A method for calculating the output power from large horizontal-axis wind turbines is presented. Modifications to the airfoil characteristics and the momentum portion of classical blade element-momentum theory are given that improve correlation with measured data. Improvement is particularly evident at low tip-speed ratios where aerodynamic stall can occur as the blade experiences high angles of attack. Output power calculated using the modified theory is compared with measured data for several large wind turbines. These wind turbines range in size from the DOE/NASA 100 kW Mod-0 (38 m rotor diameter) to the 2000 kW Mod-1 (61 m rotor diameter). The calculated results are in good agreement with measured data from these machines.

Author

A82-11774*# NASA preprototype redox storage system for a photovoltaic stand-alone application. N. H. Hagedorn (NASA, Lewis Research Center, Cleveland, OH). In: Intersociety Energy Conversion Engineering Conference, 16th, Atlanta, GA, August 9-14, 1981, Proceedings, Volume 1. (A82-11701 02-44) New York, American Society of Mechanical Engineers, 1981, p. 805-811.

A 1-kW preprototype redox storage system that has undergone characterization tests and been operated as the storage device for a 5-kW (peak) photovoltaic array is described and performance data are presented. Loss mechanisms are discussed, and simple design changes leading to appreciable increases in efficiency are suggested. The effects on system performance of nonequilibrium between the predominant species of complexed chromic ion in the negative electrode reactant solution are summarized. It is noted that with the aid of the prototype system, control concepts have been shown to be valid and trouble free and some insight has been gained into interactions at the mutual interfaces of the redox system, the photovoltaic array, the load, and the control devices.

C.R.

A82-44942* Advances in high output voltage silicon solar cells. R. A. Arndt, A. Meulenbergh, J. F. Allison (COMSAT Laboratories, Clarksburg, MD), and V. G. Welzer (NASA, Lewis Research Center, Cleveland, OH). In: Photovoltaic Specialists Conference, 15th, Kissimmee, FL, May 12-15, 1981, Conference Record. (A82-44928 23-44) New York, Institute of Electrical and Electronics Engineers, Inc., 1981, p. 92-96, 14 refs. Research sponsored by the Communication Satellite Corp.; Contract No. NAS3-21227.

Solar cells have been fabricated from 0.1 ohm-cm, p-type silicon by means of a two-step diffusion process of emitter formation in order to delineate the factors limiting V_{oc} in conventionally structured cells with the goal of achieving 700 mV. The cells are 200 microns thick and 2 x 2 cm in area with a planar front surface that has an anti-reflection coating of tantalum oxide, as well as Cr-Au-Ag contact metallization on both sides of the cell. The Cr-Au-Ag is applied over an aluminum diffused layer on the back, while it is applied through small holes in the anti-reflection coating on the front. Results show that the best of these cells exhibits an open-circuit voltage of 654 mV under AMO illumination.

N.B.

A82-44944* Thin foil silicon solar cells with coplanar back contacts. F. Ho, P. A. Iles (Applied Solar Energy Corp., City of Industry, CA), and C. R. Baraona (NASA, Lewis Research Center, Cleveland, OH). In: Photovoltaic Specialists Conference, 15th, Kissimmee, FL, May 12-15, 1981, Conference Record. (A82-44928 23-44) New York, Institute of Electrical and Electronics Engineers, Inc., 1981, p. 102-106, 8 refs. Contract No. NAS3-22228.

To fabricate 50 microns thick, coplanar back contact (CBC) silicon solar cells, wraparound junction design was selected and proved to be effective. The process sequence used, the cell design, and the cell performance are described. CBC cells with low solar absorptance have shown AMO efficiencies to 13%, high cells up to 14%; further improvements are projected with predictable optimization.

(Author)

A82-44957* Fabrication of multijunction high voltage concentrator solar cells by integrated circuit technology. G. J. Valco, V. J. Kapoor (Case Western Reserve University, Cleveland, OH), J. C. Evans, Jr., and A.-T. Chai (NASA, Lewis Research Center; Case Western Reserve University, Cleveland, OH). In: Photovoltaic Specialists Conference, 15th, Kissimmee, FL, May 12-15, 1981, Conference Record. (A82-44928 23-44) New York, Institute of Electrical and Electronics Engineers, Inc., 1981, p. 187-192. NASA-supported research.

Standard integrated circuit technology has been developed for the design and fabrication of planar multijunction (PMJ) solar cell chips. Each 1 cm x 1 cm solar chip consisted of six n(+)/p, back contacted, internally series interconnected unit cells. These high open circuit voltage solar cells were fabricated on 2 ohm-cm, p-type 75 microns thick, silicon substrates. A five photomask level process employing contact photolithography was used to pattern for boron diffusions, phosphorus diffusions, and contact metallization. Fabricated devices demonstrated an open circuit voltage of 3.6 volts and a short circuit current of 90 mA at 80 AMI suns. An equivalent circuit model of the planar multi-junction solar cell was developed.

(Author)

A82-45027* The effects of controls and controllable and storage loads on the performance of stand-alone photovoltaic systems. R. C. Cull (NASA, Lewis Research Center, Cleveland, OH) and A. H. Eltimsahy (Toledo, University, Toledo, OH). In: Photovoltaic Specialists Conference, 15th, Kissimmee, FL, May 12-15, 1981, Conference Record. (A82-44928 23-44) New York, Institute of Electrical and Electronics Engineers, Inc., 1981, p. 621-626. NASA-supported research.

Stand-alone photovoltaic systems have been modeled and analyzed from sunlight in to consumer product out. By including the consumer product in the analysis, concepts such as 'product storage' (a storage tank for water or cold-plates for refrigeration) and loads controllable by the system controller have been added to the system analysis. From a controls analysis viewpoint, this adds state variables to the system. The result is that the system controller can make operating control decisions on the energy flow between these various system elements

ORIGINAL PAGE IS
OF POOR QUALITY

to optimize system performance and reduce system cost. The effects on system performance of various control schemes employing these concepts are presented. Analysis of water pumping and/or refrigeration systems show possible performance improvements of greater than 15% with the addition of controllable loads with product storage. (Author)

A92-45055 * **A theory of the n-p silicon solar cell.** C. Goradia (Cleveland State University, Cleveland, OH), I. Weinberg, and C. Baraona (NASA, Lewis Research Center, Cleveland, OH). In: Photovoltaic Specialists Conference, 15th, Kissimmee, FL, May 12-15, 1981, Conference Record, (A82-44928 23-44) New York, Institute of Electrical and Electronics Engineers, Inc., 1981, p. 855-860. 11 refs. Grant No. NAG3-144.

A computer model has been developed, based on an analytical theory of the high base resistivity BSF n(+)(pi)p(+) or p(+)(nu)n(+) silicon solar cell. The model makes very few assumptions and accounts for nonuniform optical generation, generation and recombination in the junction space charge region, and bandgap narrowing in the heavily doped regions. The paper presents calculated results based on this model and compares them to available experimental data. Also discussed is radiation damage in high base resistivity n(+)(pi)p(+) space solar cells. (Author)

A82-45325 * **40-kW phosphoric acid fuel cell field test - Project plan.** R. R. Woods (Gas Research Institute, Chicago, IL) and R. A. Duscha (NASA, Lewis Research Center, Cleveland, OH). In: Fuel cells: Technology status and applications; Proceedings of the Symposium, Chicago, IL, November 16-18, 1981. (A82-45317 23-44) Chicago, IL, Institute of Gas Technology, 1982, p. 215-231.

N82-10495*# Gilbert/Commonwealth, Reading, Pa.
MAGNETOHYDRODYNAMICS MHD ENGINEERING TEST FACILITY ETF 200 MWE POWER PLANT. CONCEPTUAL DESIGN ENGINEERING REPORT CDR. VOLUME 3: COSTS AND SCHEDULES Final Report
Sep. 1981 61 p 5 Vol.
(Contracts DEN3-224; DE-AI01-77ET-10769)
(NASA-CR-165452-Vol-3; DOE/NASA/0224-1-Vol-3) Avail: NTIS HC A04/MF A01 CSCL 10B

The estimated plant capital cost for a coal fired 200 MWE electric generating plant with open cycle magnetohydrodynamics is divided into principal accounts based on Federal Energy Regulatory Commission account structure. Each principal account is defined and its estimated cost subdivided into identifiable and major equipment systems. The cost data sources for compiling the estimates, cost parameters, allotments, assumptions, and contingencies, are discussed. Uncertainties associated with developing the costs are quantified to show the confidence level acquired. Guidelines established in preparing the estimated costs are included. Based on an overall milestone schedule related to conventional power plant scheduling experience and starting procurement of MHD components during the preliminary design phase there is a 6 1/2-year construction period. The duration of the project from start to commercial operation is 79 months. The engineering phase of the project is 4 1/2 years; the construction duration following the start of the main power block is 37 months. A.R.H.

N82-10505*# Stirling Thermal Motors, Inc., Ann Arbor, Mich.
EVALUATION OF THE POTENTIAL OF THE STIRLING ENGINE FOR HEAVY DUTY APPLICATION Final Report
R. J. Meijer and B. Ziph Oct. 1981 62 p refs
(Contract NAS3-22226)
(NASA-CR-165473) Avail: NTIS HC A04/MF A01 CSCL 10B

A 150 hp four cylinder heavy duty Stirling engine was evaluated. The engine uses a variable stroke power control system, swashplate drive and ceramic insulation. The sensitivity of the design to engine size and heater temperature is investigated. Optimization shows that, with porous ceramics, indicated efficiencies as high as 52% can be achieved. It is shown that the gain in engine efficiency becomes insignificant when the heater temperature is raised above 200 degrees F. E.A.K.

N82-10506*# DHR, Inc., Washington, D.C.
MARKET ASSESSMENT OF PHOTOVOLTAIC POWER SYSTEMS FOR AGRICULTURAL APPLICATIONS IN MEXICO
William Steigelmann and Itil Asmon (ARD, Inc.) Jul. 1981

135 p refs
(Contracts DEN3-180; DE-AI01-79ET-20485)
(NASA-CR-165441; DOE/NASA/0180-3) Avail: NTIS
HC A07/MF A01 CSCL 10A

The first year of cost-competitiveness, the market potential, and the environment in which PV systems would be marketed and employed were examined. Market elements specific to Mexico addressed include: (1) useful applications and estimates of the potential market for PV systems; (2) power requirements and load profiles for applications compatible with PV usage; (3) operating and cost characteristics of power systems that compete against PV; (4) national development goals in rural electrification and rural services, technology programs and government policies that influence the demand for PV in Mexico; (5) financing mechanisms and capital available for PV acquisition; (6) channels for distribution, installation and maintenance of PV systems; and (7) appropriate methods for conducting business in Mexico. A.R.H.

N82-11545*# Stonehart Associates, Inc., Madison, Conn.
SURVEY ON AGING ON ELECTRODES AND ELECTROCATALYSTS IN PHOSPHORIC ACID FUEL CELLS Progress Report

Paul Stonehart and John Hochmuth Oct. 1981 73 p refs
(Contract DEN3-176)
(NASA-CR-165505; DOE/NASA/0176-81/3) Avail: NTIS
HC A04/MF A01 CSCL 10A

The processes which contribute to the decay in performance of electrodes used in phosphoric acid fuel cell systems are discussed. Loss of catalytic surface area, corrosion of the carbon support, electrode structure degradation, electrolyte degradation, and impurities in the reactant streams are identified as the major areas for concern. J.M.S.

N82-11546*# Spire Corp., Bedford, Mass.
PROCESSING OF SILICON SOLAR CELLS BY ION IMPLANTATION AND LASER ANNEALING Final Report
J. A. Minnucci, K. W. Matthei, and A. C. Greenwald Feb. 1981
78 p refs
(Contract NAS3-21276)
(NASA-CR-165283; FR-10066) Avail: NTIS
HC A05/MF A01 CSCL 10A

Methods to improve the radiation tolerance of silicon cells for spacecraft use are described. The major emphasis of the program was to reduce the process-induced carbon and oxygen impurities in the junction and base regions of the solar cell, and to measure the effect of reduced impurity levels on the radiation tolerance of cells. Substrates of 0.1, 1.0 and 10.0 ohm-cm float-zone material were used as starting material in the process sequence. High-dose, low-energy ion implantation was used to form the junction in n-p structures. Implant annealing was performed by conventional furnace techniques and by pulsed laser and pulsed electron beam annealing. Cells were tested for radiation tolerance at Spire and NASA-LeRC. After irradiation by 1 MeV electrons to a fluence of 10 to the 16th power per sq cm, the cells tested at Spire showed no significant process induced variations in radiation tolerance. However, for cells tested at Lewis to a fluence of 10 to the 15th power per sq cm, ion-implanted cells annealed in vacuum by pulsed electron beam consistently showed the best radiation tolerance for all cell resistivities. Author

N82-11547*# Munising Paper Div., Neenah, Wis.
DEVELOPMENT OF BATTERY SEPARATOR COMPOSITES Final Report, Oct. 1976 - Nov. 1981
George F. Schmidt and Robert E. Weber Nov. 1981 56 p refs
(Contract NAS3-20583)
(NASA-CR-165508) Avail: NTIS HC A04/MF A01 CSCL 10C

Improved inorganic-organic separators developed by NASA were commercially prepared. A single-ply asbestos substrate was developed, as well as alternative substrates based on cellulose and on polypropylene fibers. The single-ply asbestos was bound with butyl rubber and was functionally superior to the formerly used polyphenylene oxide saturated sheet. Commercially prepared separators exhibited better measured separator properties than the NASA standard. Cycle life in Ni/Zn and Ag/Zn cells was

related to substrate, decreasing in the order: asbestos > cellulose paper > nonwoven polypropylene. The cycle life of solvent-coated separators was better than aqueous in Ni/Zn cells, while aqueous coatings were better in Ag/Zn cells. T.M.

N82-12570*# Gilbert/Commonwealth, Reading, Pa.
MAGNETOHYDRODYNAMICS (MHD) ENGINEERING TEST FACILITY (ETF) 200 MW_e POWER PLANT. CONCEPTUAL DESIGN ENGINEERING REPORT (CDER). VOLUME 1: EXECUTIVE SUMMARY Final Report

Sep. 1981 48 p
(Contracts DEN3-224; DE-AI01-77ET-10769)
(NASA-CR-165452-Vol-1; DOE/NASA-0224/1-Vol-1) Avail:
NTIS HC A03/MF A01 CSCL 10B

Main elements of the design are identified and explained, and the rationale behind them was reviewed. Major systems and plant facilities are listed and discussed. Construction cost and schedule estimates are presented, and the engineering issues that should be reexamined are identified. The latest (1980-1981) information from the MHD technology program is integrated with the elements of a conventional steam power electric generating plant. T.M.

N82-12571*# Boeing Co., Seattle, Wash.
TESTING OF SOLAR CELL COVERS AND ENCAPSULANTS CONDUCTED IN A SIMULATED SPACE ENVIRONMENT Final Report

D. A. Russell Nov. 1981 267 p
(Contract NAS3-22222)
(NASA-CR-165475; D180-26590-1) Avail: NTIS
HC A12/MF A01 CSCL 10A

The materials included in the evaluation were O211 micro-sheet, FEP-A used as a cover and as an adhesive, DC 93-500 adhesive, PFA 'hard coat' used as a cover, GE 615/UV-24 used as a cover, GR 650 used as a cover, and electrostatically bonded 7070 glass. The test environments were 1 MeV electron irradiation interspersed with thermal cycling, 0.5 MeV proton irradiation interspersed with thermal cycling and UV exposure interspersed with thermal cycling. Summary data is given describing the response of the test materials both visually and electrically to the three different environments. T.M.

N82-12572*# United Technologies Corp., South Windsor, Conn.
Power Systems Div.
LOW NO SUB X HEAVY FUEL COMBUSTOR CONCEPT PROGRAM Final Report, 23 Oct. 1979 - Jul. 1981
Paul Russell, George Beal, and Bruce Hinton 15 Oct. 1981
99 p refs Prepared in cooperation with Pratt and Whitney Aircraft, East Hartford, Conn.
(Contracts DEN3-149; DE-AI01-77ET-13111)
(NASA-CR-165512; DOE/NASA/O149-1; QTR-3236) Avail:
NTIS HC A05/MF A01 CSCL 10B

A gas turbine technology program to improve and optimize the staged rich lean low NO_x combustor concept is described. Subscale combustor tests to develop the design information for optimization of the fuel preparation, rich burn, quick quench, and lean burn steps of the combustion process were run. The program provides information for the design of high pressure full scale gas turbine combustors capable of providing environmentally clean combustion of minimally of minimally processed and synthetic fuels. It is concluded that liquid fuel atomization and mixing, rich zone stoichiometry, rich zone liner cooling, rich zone residence time, and quench zone stoichiometry are important considerations in the design and scale up of the rich lean combustor. E.A.K.

N82-12573*# Stonehart Associates, Inc., Madison, Conn.
PREPARATION AND EVALUATION OF ADVANCED ELECTROCATALYSTS FOR PHOSPHORIC ACID FUEL CELLS Quarterly Report
Paul Stonehart, John Baris, John Hochmuth, and Peter Pagliaro
30 Sep. 1981 31 p
(Contracts DEN3-176; DE-AI03-80ET-17088)
(NASA-CR-165519; DOE/NASA/O176-81/4; QR-7) Avail:
NTIS HC A03/MF A01 CSCL 10A

A number of electrocatalyst combinations were prepared and characterized. These electrocatalysts were formulated to contain platinum combined with transition metal carbide forming elements

(W, Mo, V) for cathodes and platinum combined with palladium for anodes. High resolution electron microscopy was used to determine the crystallite size and dispersion of platinum-palladium alloy electrocatalysts in order to provide analytical support for the electrochemical determinations of the particle dispersions. An equation was derived which correlates palladium crystallite size with electrochemical hydrogen adsorption. Based on comparisons of electrocatalyst performances in the presence of pure hydrogen and hydrogen containing carbon monoxide, it was shown that the apparent poisoning of the electrocatalyst by carbon monoxide is influenced by the electrode structure. DOE

N82-13505*# Paragon Pacific, Inc., El Segundo, Calif.
DEVELOPMENT REPORT: AUTOMATIC SYSTEM TEST AND CALIBRATION (ASTAC) EQUIPMENT Final Report

Robert J. Thoren Jul. 1981 25 p ref
(Contracts DEN3-203; DE-AI01-76ET-20320)
(NASA-CR-165403; DOE/NASA/O203-1; PPI-3009-4) Avail:
NTIS HC A02/MF A01 CSCL 10A

A microcomputer based automatic test system was developed for the daily performance monitoring of wind energy system time domain (WEST) analyzer. The test system consists of a microprocessor based controller and hybrid interface unit which are used for inputting prescribed test signals into all WEST subsystems and for monitoring WEST responses to these signals. Performance is compared to theoretically correct performance levels calculated off line on a large general purpose digital computer. Results are displayed on a cathode ray tube or are available from a line printer. Excessive drift and/or lack of repeatability of the high speed analog sections within WEST is easily detected and the malfunctioning hardware identified using this system. E.A.K.

N82-13506*# Eaton Engineering and Research Center, Southfield, Mich.
THE AC PROPULSION SYSTEM FOR AN ELECTRIC VEHICLE. PHASE 1 Final Report

Steven Geppert Aug. 1981 307 p refs
(Contracts DEN3-125; DE-AI01-77CS-51044)
(NASA-CR-165480; DOE/NASA/O125-1; ERC-TR-8101) Avail:
NTIS HC A14/MF A01 CSCL 10B

A functional prototype of an electric vehicle ac propulsion system was built consisting of a 18.65 kW rated ac induction traction motor, pulse width modulated (PWM) transistorized inverter, two speed mechanically shifted automatic transmission, and an overall drive/vehicle controller. Design developmental steps, and test results of individual components and the complex system on an instrumented test frame are described. Computer models were developed for the inverter, motor and a representative vehicle. A preliminary reliability model and failure modes effects analysis are given. E.A.K.

N82-13507*# Case Western Reserve Univ., Cleveland, Ohio.
TRANSIENT CATALYTIC COMBUSTOR MODEL Final Report

James S. Tien May 1981 87 p refs
(Grant NSG-3230; Contract DE-AI01-77CS-51040)
(NASA-CR-165324; DOE/NASA/3230-1) Avail: NTIS
HC A05/MF A01 CSCL 10B

A quasi-steady gas phase and thermally thin substrate model is used to analyze the transient behavior of catalytic monolith combustors in fuel lean operation. The combustor response delay is due to the substrate thermal inertia. Fast response is favored by thin substrate, short catalytic bed length, high combustor inlet and final temperatures, and small gas channel diameters. The calculated gas and substrate temperature time history at different axial positions provides an understanding of how the catalytic combustor responds to an upstream condition change. The computed results also suggest that the gas residence times in the catalytic bed in the after bed space are correlatable with the nondimensional combustor response time. The model also performs steady state combustion calculations; and the computed steady state emission characteristics show agreement with available experimental data in the range of parameters covered. A catalytic combustor design for automotive gas turbine engine which has reasonably fast response (< 1 second) and can satisfy the emission goals in an acceptable total combustor length is possible. S.L.

ORIGINAL PAGE IS
OF POOR QUALITY

N82-13508* Life Systems, Inc., Cleveland, Ohio.
ENDURANCE TEST AND EVALUATION OF ALKALINE WATER ELECTROLYSIS CELLS Annual Report
K. A. Burke and F. H. Schubert Nov. 1981 46 p refs
(Contract NAS3-21287)
(NASA-CR-185424; TR-376-16) Avail: NTIS
HC A03/MF A01 CSCL 10C

Utilization in the development of multi-kW low orbit power systems is discussed. The following technological developments of alkaline water electrolysis cells for space power application were demonstrated: (1) four 92.9 cm² single water electrolysis cells, two using LST's advanced anodes and two using LST's super anodes; (2) four single cell endurance test stands for life testing of alkaline water electrolyte cells; (3) the solid performance of the advanced electrode and 365 K; (4) the breakthrough performance of the super electrode; (5) the four single cells for over 5,000 hours each significant cell deterioration or cell failure. It is concluded that the static feed water electrolysis concept is reliable and due to the inherent simplicity of the passive water feed mechanism coupled with the use of alkaline electrolyte has greater potential for regenerative fuel cell system applications than alternative electrolyzers. A rise in cell voltage occur after 2,000-3,000 hours which was attributed to deflection of the polysulfone end plates due to creepage of the thermoplastic. More end plate support was added, and the performance of the cells was restored to the initial performance level. E.A.K.

N82-13510* Acurex Corp., Mountain View, Calif. Energy and Environmental Div.
DEVELOPMENT OF A HIGH-TEMPERATURE DURABLE CATALYST FOR USE IN CATALYTIC COMBUSTORS FOR ADVANCED AUTOMOTIVE GAS TURBINE ENGINES Final Report

H. Tong, G. C. Snow, E. K. Chu, R. L. S. Chang, M. J. Angwin, and S. L. Pessagno Sep. 1981 169 p refs
(Contracts DEN3-83; DE-A101-77CS-51040)
(NASA-CR-185398; DOE/NASA/0083-1) Avail: NTIS
HC A08/MF A01 CSCL 10B

Durable catalytic reactors for advanced gas turbine engines were developed. Objectives were: to evaluate furnace aging as a cost effective catalytic reactor screening test, measure reactor degradation as a function of furnace aging, demonstrate 1,000 hours of combustion durability, and define a catalytic reactor system with a high probability of successful integration into an automotive gas turbine engine. Fourteen different catalytic reactor concepts were evaluated, leading to the selection of one for a durability combustion test with diesel fuel for combustion conditions. Eight additional catalytic reactors were evaluated and one of these was successfully combustion tested on propane fuel. This durability reactor used graded cell honeycombs and a combination of noble metal and metal oxide catalysts. The reactor was catalytically active and structurally sound at the end of the durability test. E.A.K.

N82-13511* Westinghouse Research and Development Center, Pittsburgh, Pa.
CELL MODULE AND FUEL CONDITIONER DEVELOPMENT Quarterly Report, Jul. - Sep. 1981
D. Q. Hoover, Jr. Oct. 1981 59 p
(Contracts DEN3-161; DE-A101-80ET-17088)
(NASA-CR-165462; DOE/NASA/0161-9; Rept-81-9D1-MARED-R1) Avail: NTIS HC A04/MF A01 CSCL 10A

The results of pretesting and performance testing of Stack 564 are reported. The design features, progress in fabrication and plans for assembly of Stack 800 are given. The status of endurance testing of Stack 560 is reported. The design, fabrication, test procedures and preliminary tests of the 10 kW double counterflow reformer and the reformer test stand are described. Results of vendor contacts to define the performance and cost of fuel conditioning system components are reported. The results of burner tests and continuing development of the BOLTA R program are reported. T.M.

N82-14627* DHR, Inc., Washington, D.C.
MARKET ASSESSMENT OF PHOTOVOLTAIC POWER SYSTEMS FOR AGRICULTURAL APPLICATIONS IN MOROCCO Final Report
Henry Steingass and Itil Asmon (ARD, Inc.) Sep. 1981 157 p

refs
(Contract DEN3-180; DE-A101-79ET-20485)
(NASA-CR-165477; DOE/NASA/0180-2; C4100-50) Avail:
NTIS HC A08/MF A01 CSCL 10A

Results of a month-long study in Morocco aimed at assessing the market potential for stand-alone photovoltaic systems in agriculture and rural service applications are presented. The following applications, requiring less than 15 kW of power, are described: irrigation, cattle watering, refrigeration, crop processing, potable water and educational TV. Telecommunications and transportation signalling applications, descriptions of power and energy use profiles, assessments of business environment, government and private sector attitudes towards photovoltaics, and financing were also considered. The Moroccan market presents both advantages and disadvantages for American PV manufacturers. The principle advantages of the Moroccan market are: a limited grid, interest in and present use of PV in communications applications, attractive investment incentives, and a stated policy favoring American investment. Disadvantages include: lack of government incentives for PV use, general unfamiliarity with PV technology, high first cost of PV, a well-established market network for diesel generators, and difficulty with financing. The market for PV in Morocco (1981-1986), will be relatively small, about 340 kwp. The market for PV is likely to be more favorable in telecommunications, transport signalling and some rural services. The primary market appears to be in the public (i.e., government) rather than private sector, due to financial constraints and the high price of PV relative to conventional power sector. M.D.K.

N82-14628* Institute of Gas Technology, Chicago, Ill.
STABILIZING PLATINUM IN PHOSPHORIC ACID FUEL CELLS Quarterly Report
Robert J. Remick Oct. 1981 19 p refs
(Contracts DEN3-208; DE-1101-80ET-17088)
(NASA-CR-165483; DOE/NASA-0208/3; IGT-61051; QR-3) CSCL 10A

A carbon substrate for use in fabricating phosphoric acid fuel cell cathodes was modified by catalytic oxidation to stabilize the platinum catalyst by retarding the sintering of small platinum crystallites. Results of 100-hour operational tests confirmed that the rate of platinum surface area loss observed on catalytically oxidized supports was less than that observed with unmodified supports of the same starting material. Fuel cell electrodes fabricated from Vulcan XC-72R, which was modified by catalytic in a nitric oxide atmosphere, produced low platinum sintering rates and high activity for the reduction of oxygen in the phosphoric acid environment. N.W.

N82-14636* General Dynamics/Convair, San Diego, Calif.
STUDY OF MULTI-MEGAWATT TECHNOLOGY NEEDS FOR PHOTOVOLTAIC SPACE POWER SYSTEMS. VOLUME 1: EXECUTIVE SUMMARY

D. M. Peterson and R. L. Pleasant 1 Aug. 1981 28 p refs
2 Vol.
(Contract NAS3-21951)
(NASA-CR-165323-Vol-1; Rept-111-2401-204) Avail: NTIS
HC A03/MF A01 CSCL 10A

Possible missions requiring multimewatt photovoltaic space power systems in the 1990's time frame and associated power system technology needs are examined. The following concepts for photovoltaic power approaches are considered: planar arrays, concentrating arrays, hybrid systems using Rankine engines, thermophotovoltaic and AC/DC power management approaches, battery, fuel cell, flywheel energy storage, and interactions with the electrical ion engine injection and stationkeeping system. The levels of modularity for efficient, safe, constructable, serviceable, and cost effective system design are analyzed, and the benefits of alternate approaches developed. Both manned low Earth orbit and unmanned geosynchronous Earth orbit applications were examined for technological development. Technology developments applicable to power systems which appear to have benefits independent of the absolute power level are suggested. M.D.K.

N82-14637* General Dynamics/Convair, San Diego, Calif.
STUDY OF MULTI-MEGAWATT TECHNOLOGY NEEDS FOR PHOTOVOLTAIC SPACE POWER SYSTEMS, VOLUME 2 Final Report
D. M. Peterson and R. L. Pleasant 19 Mar. 1981 285 p

refs 2 Vol.

(Contract NAS3-21951)
(NASA-CR-165323-Vol-2; GDC-AST-81-019-Vol-2) Avail:
NTIS HC A13/MF A01 CSCL 10A

Possible missions requiring multimegawatt photovoltaic space power systems in the 1990's time frame and power system technology needs associated with these missions are examined. Four specific task areas were considered: (1) missions requiring power in the 7-10 megawatt average power region; (2) alternative power systems and component technologies; (3) technology goals and sensitivity trades and analyses; and (4) technology recommendations. Specific concepts for photovoltaic power approaches considered were: planar arrays, concentrating arrays, hybrid systems using Rankine engines, thermophotovoltaic approaches; all with various photovoltaic cell component technologies. Various AC/DC power management approaches, and battery, fuel cell, and flywheel energy storage concepts are evaluated. Interactions with the electrical ion engine injection and stationkeeping system are also considered. M.D.K.

N82-15527*# Bump and Roe, Inc., Woodbury, N. Y.
MHD OXIDANT INTERMEDIATE TEMPERATURE CERAMIC HEATER STUDY Final Report

A. W. Carlson, I. L. Chait, D. P. Saari, and C. L. Marksberry
Sep. 1981 199 p refs Prepared in cooperation with Fluidyne Engineering Corp.

(Contract DEN3-107; DE-AI01-77ET-10769)
(NASA-CR-165453; DOE/NASA-0107/3) Avail: NTIS
HC A09/MF A01 CSCL 10A

The use of three types of directly fired ceramic heaters for preheating oxygen enriched air to an intermediate temperature of 1144K was investigated. The three types of ceramic heaters are: (1) a fixed bed, periodic flow ceramic brick regenerative heater; (2) a ceramic pebble regenerative heater. The heater design, performance and operating characteristics under conditions in which the particulate matter is not solidified are evaluated. A comparison and overall evaluation of the three types of ceramic heaters and temperature range determination at which the particulate matter in the MHD exhaust gas is estimated to be a dry powder are presented. E.A.K.

N82-16479*# New Mexico Univ., Albuquerque. Dept. of Electrical and Computer Engineering.

STUDY OF THE PHOTOVOLTAIC EFFECT IN THIN FILM BARIUM TITANATE Annual Report

W. W. Grannemann and Vineet S. Dharmadhikari Jan. 1982
24 p

(Grant NAG1-95)
(NASA-CR-165091; EE-273(82)NASA-931-1) Avail: NTIS
HC A02/MF A01 CSCL 10A

Ferroelectric films of barium titanate were synthesized on silicon and quartz substrates, and the photoelectric effect in the structure consisting of metal deposited ferroelectric barium titanate film silicon was studied. A photovoltage with polarity that depends on the direction of the remanent polarization was observed. The deposition of BaTiO₃ on silicon and fused quartz substrates was accomplished by an RF sputtering technique. A series of experiments to study the growth of ferroelectric BaTiO₃ films on single crystal silicon and fused quartz substrates were conducted. The ferroelectric character in these films was found on the basis of evidence from the polarization electric field hysteresis loops, capacitance voltage and capacitance temperature techniques and from X-ray diffraction studies. S.L.

N82-16480*# Engelhard Industries, Inc., Edison, N.J.
DEVELOP AND TEST FUEL CELL POWERED ON-SITE INTEGRATED TOTAL ENERGY SYSTEMS. PHASE 3: FULL-SCALE POWER PLANT DEVELOPMENT Quarterly Progress Report, Feb. - Apr. 1981

24 Jun. 1981 51 p
(Contracts DEN3-241; DE-AI01-80ET-17088)
(NASA-CR-165328; DOE/NASA/0241-1; QR-1) Avail: NTIS
HC A04/MF A01 CSCL 10A

Progress toward an integrated 5kW power system based upon methanol fuel and a phosphoric acid fuel cell operating at about 473 K is described in detail. Description includes test results of advanced fuel cell catalysts, a semi-automatic acid replenishment system and a completed 5kW methanol/steam reformer. Design features of a 5kW fuel cell stack are included.

The results of a preliminary system test on a reformer/stack/inverter combination are reported. An initial design for a 25 kW stack is presented. Experimental plans are outlined for data acquisition necessary for design of a 50 kW methanol/steam reformer. Activities related to complete mathematical modelling of the integrated power system, including wasteheat utilization are described. T.M.

N82-16482*# Energy Research Corp., Danbury, Conn.
TECHNOLOGY DEVELOPMENT FOR PHOSPHORIC ACID FUEL CELL POWERPLANT, PHASE 2 Final Technical Report

Larry Christner Dec. 1981 159 p refs
(Contracts DEN3-67; DE-AI03-79ET-11272)
(NASA-CR-165426; DOE/NASA/0067-79/7) Avail: NTIS
HC A08/MF A01 CSCL 10A

The development of materials, cell components, and reformers for on site integrated energy systems is described. Progress includes: (1) heat-treatment of 25 sq cm, 350 sq cm and 1200 sq cm cell test hardware was accomplished. Performance of fuel cells is improved by using this material; (2) electrochemical and chemical corrosion rates of heat-treated and as-molded graphite/phenolic resin composites in phosphoric acid were determined; (3) three cell, 5 in. x 16 in. stacks operated for up to 10,000 hours and 12 in. x 17 in. five cell stacks were tested for 5,000 hours; (4) a three cell 5 in. x 15 in. stack with 0.12 mg Pt/sq cm anodes and 0.25 mg Pt/sq cm cathodes was operated for 4,500 hours; and (5) an ERC proprietary high bubble pressure matrix, MAT-1, was tested for up to 10,000 hours. A.R.H.

N82-16483*# Engelhard Industries, Inc., Edison, N.J. Industries Div.

DEVELOP AND TEST FUEL CELL POWERED ON-SITE INTEGRATED TOTAL ENERGY SYSTEMS. PHASE 3: FULL-SCALE POWER PLANT DEVELOPMENT Quarterly Report, May - Jul. 1981

25 Aug. 1981 35 p refs
(Contracts DEN3-241; DE-AI01-80ET-17088)
(NASA-CR-165455; DOE/NASA/0241-2; QR-2) Avail: NTIS
HC A03/MF A01 CSCL 10B

A schematic and physical layout is given for the 5kW integrated system and the development status of individual components is described. The results of using a one dimensional mathematical model of the 5kW reformer are presented. Plans for a single-tube reformer test unit for the acquisition of temperature profile data are described. Tentative specifications for a 50kW dc to-ac inverter are listed. Performance data are given on two 3-cell stacks incorporating semiautomatic acid replenishment systems and improved electrocatalysts. A qualification test on methanol/steam reforming catalyst T2107RS is reported, including a portion in which the catalyst was deliberately poisoned with 800 ppm ethanol in the feed. Author

N82-16484*# General Electric Co., Cincinnati, Ohio. Aircraft Engine Business Group.

DEMONSTRATION OF CATALYTIC COMBUSTION WITH RESIDUAL FUEL Final Report

W. J. Dodds and E. E. Ekstedt Aug. 1981 106 p refs
(Contracts DEN3-155; DE-A101-77ET-10350)
(NASA-CR-165369; DOE/NASA/0155-1; RB1AEG590) Avail:
NTIS HC A06/MF A01 CSCL 10B

An experimental program was conducted to demonstrate catalytic combustion of a residual fuel oil. Three catalytic reactors, including a baseline configuration and two backup configurations based on baseline test results, were operated on No. 6 fuel oil. All reactors were multielement configurations consisting of ceramic honeycomb catalyzed with palladium on stabilized alumina. Stable operation on residual oil was demonstrated with the baseline configuration at a reactor inlet temperature of about 825 K (1025 F). At low inlet temperature, operation was precluded by apparent plugging of the catalytic reactor with residual oil. Reduced plugging tendency was demonstrated in the backup reactors by increasing the size of the catalyst channels at the reactor inlet, but plugging still occurred at inlet temperature below 725 K (1845 F). Operation at the original design inlet temperature of

ORIGINAL PAGE IS
OF POOR QUALITY

ORIGINAL PAGE IS
OF POOR QUALITY

889 K (600 F) could not be demonstrated. Combustion efficiency above 99.5% was obtained with less than 5% reactor pressure drop. Thermally formed NO sub x levels were very low (less than 0.5 g NO₂/kg fuel) but nearly 100% conversion of fuel-bound nitrogen to NO sub x was observed. M.D.K.

N82-16485* Ford Motor Co., Dearborn, Mich.
ADVANCED GAS TURBINE (AGT) POWERTRAIN SYSTEM INITIAL DEVELOPMENT REPORT Progress Report, 20 May - 24 Sep. 1979

Aug. 1980 150 p Prepared in cooperation with AirResearch Mfg. Co., Phoenix, Ariz.
(Contract DEN3-37)

(NASA-CR-165130; DOE/NASA/0037-80/2;
DDA-ADR-10086) Avail: NTIS HC A07/MF A01 CSCL 10B

The powertrain consists of a single shaft regenerated gas turbine engine utilizing ceramic hot section components, coupled to a slit differential gearbox with an available variable stator torque converter and an available Ford intergral overdrive four-speed automatic transmission. Predicted fuel economy using gasoline fuel over the combined federal driving cycle (CFDC) is 15.3 km/l, which represents a 59% improvement over the spark-ignition-powered baseline vehicle. Using DF2 fuel, CFDC mileage estimates are 17.43 km/l. Zero to 96.6 km/hr acceleration time is 11.9 seconds with a four-second acceleration distance of 21.0 m. The ceramic radial turbine rotor is discussed along with the control system for the powertrain. T.M.

N82-16494* IIT Research Inst., Chicago, Ill.
INTERNATIONAL MARKET ASSESSMENT OF STAND-ALONE PHOTOVOLTAIC POWER SYSTEMS FOR COTTAGE INDUSTRY APPLICATIONS Final Report

Theresa M. Philippi Nov. 1981 290 p refs
(Contracts DEN3-197; DE-AI01-79ET-20485)
(NASA-CR-165287; DOE/NASA/O197-1; IITRI-J06519) Avail: NTIS HC A13/MF A01 CSCL 10B

The final result of an international assessment of the market for stand-alone photovoltaic systems in cottage industry applications is reported. Nonindustrialized countries without centrally planned economies were considered. Cottage industries were defined as small rural manufacturers, employing less than 50 people, producing consumer and simple products. The data to support this analysis were obtained from secondary and expert sources in the U.S. and in-country field investigations of the Philippines and Mexico. The near-term market for photovoltaics for rural cottage industry applications appears to be limited to demonstration projects and pilot programs, based on an in-depth study of the nature of cottage industry, its role in the rural economy, the electric energy requirements of cottage industry, and a financial analysis of stand-alone photovoltaic systems as compared to their most viable competitor, diesel driven generators. Photovoltaics are shown to be a better long-term option only for very low power requirements. Some of these uses would include clay mixers, grinders, centrifuges, lathes, power saws and lighting of a workshop. Author

N82-17603* Gilbert/Commonwealth, Reading, Pa.
MAGNETOHYDRODYNAMICS (MHD) ENGINEERING TEST FACILITY (ETF) 200 MWe POWER PLANT CONCEPTUAL DESIGN ENGINEERING REPORT (CDER) Final Report

Sep. 1981 593 p refs
(Contracts DEN3-224; DE-AI01-77ET-10769)
(NASA-CR-165452-Vol-5; DOE/NASA/O224-1-Vol-5) Avail: NTIS HC A25/MF A01 CSCL 10B

The reference conceptual design of the magnetohydrodynamic (MHD) Engineering Test Facility (ETF), a prototype 200 MWe coal-fired electric generating plant designed to demonstrate the commercial feasibility of open cycle MHD, is summarized. Main elements of the design, systems, and plant facilities are illustrated. System design descriptions are included for closed cycle cooling water, industrial gas systems, fuel oil, boiler flue gas, coal management, seed management, slag management, plant industrial waste, fire service water, oxidant supply, MHD power train, magnet, heat recovery/seed recovery, inverter, heating, ventilating, and air conditioning, and electrical. N.W.

N82-17606* Mathematical Sciences Northwest, Inc., Bellevue, Wash.

OVERVIEW STUDY OF SPACE POWER TECHNOLOGIES FOR THE ADVANCED ENERGETICS PROGRAM

R. Taussig, S. Gross, A. Millner, M. Neugebauer, W. Phillips, J. Powell, E. Schmidt, M. Wolf, and G. Woodcock Oct. 1981 341 p refs

(Contract NAS3-22477)
(NASA-CR-165289; MSNW-1169) Avail: NTIS HC A15/MF A01 CSCL 10B

Space power technologies are reviewed to determine the state-of-the-art and to identify advanced or novel concepts which promise large increases in performance. The potential for increased performance is judged relative to benchmarks based on technologies which have been flight tested. Space power technology concepts selected for their potentially high performance are prioritized in a list of R & D topical recommendations for the NASA program on Advanced Energetics. The technology categories studied are solar collection, nuclear power sources, energy conversion, energy storage, power transmission, and power processing. The emphasis is on electric power generation in space for satellite on board electric power, for electric propulsion, or for beamed power to spacecraft. Generic mission categories such as low Earth orbit missions and geosynchronous orbit missions are used to distinguish general requirements placed on the performance of power conversion technology. Each space power technology is judged on its own merits without reference to specific missions or power systems. Recommendations include 31 space power concepts which span the entire collection of technology categories studied and represent the critical technologies needed for higher power, lighter weight, more efficient power conversion in space. Author

N82-17607* United Technologies Corp., South Windsor, Conn. Power Systems Div.

ELECTROCHEMICAL ENERGY STORAGE FOR AN ORBITING SPACE STATION

R. E. Martin Dec. 1981 61 p refs
(Contract NAS3-21293)

(NASA-CR-165436; FCR-3142) Avail: NTIS HC A04/MF A01 CSCL 10C

The system weight of a multi hundred kilowatt fuel cell electrolysis cell energy storage system based upon alkaline electrochemical cell technology for use in a future orbiting space station in low Earth orbit (LEO) was studied. Preliminary system conceptual design, fuel cell module performance characteristics, subsystem and system weights, and overall system efficiency are identified. The impact of fuel cell module operating temperature and efficiency upon energy storage system weight is investigated. The weight of an advanced technology system featuring high strength filament wound reactant tanks and a fuel cell module employing lightweight graphite electrolyte reservoir plates is defined. E.A.K.

N82-17608* Eaton Engineering and Research Center, Southfield, Mich. Engineering and Research Center.
STRAIGHT AND CHOPPED DC PERFORMANCE DATA FOR A RELIANCE EV-250AT MOTOR WITH A GENERAL ELECTRIC EV-1 CONTROLLER Final Report

Paul C. Edie Sep. 1981 58 p
(Contracts DEN3-123; DE-AI01-77CS-51044)
(NASA-CR-165447; DOE/NASA/O123-3; ERC-TR-8175) Avail: NTIS HC A04/MF A01 CSCL 10B

Straight and chopped DC motor performances for a Reliance EV-250AT motor with an EV-1 controller were examined. Effects of motor temperature and operating voltage are shown. It is found that the maximum motor efficiency is approximately 85% at low operating temperatures in the straight DC mode. Chopper efficiency is 95% under all operating conditions. For equal speeds, the motor operated in the chopped mode develops slightly more torque and draws more current than it does in the straight DC mode. E.A.K.

N82-17615* Stonehart Associates, Inc., Madison, Conn.
PREPARATION AND EVALUATION OF ADVANCED ELECTROCATALYSTS FOR PHOSPHORIC ACID FUEL CELLS Quarterly Report, Oct. - Dec. 1981

Paul Stonehart, John Baris, John Hochruth, and Peter Pagliaro Dec. 1981 44 p

(Contract DEN3-176; Contract DE-AI03-80ET-17088)
(NASA-CR-165594; DOE/NASA/0178-81/5, QR-8) Avail:
NTIS HC A03/MF A01 CSCL 10A

Two cooperative phenomena are required the development of highly efficient porous electrocatalysts: (1) is an increase in the electrocatalytic activity of the catalyst particle; and (2) is the availability of that electrocatalyst particle for the electromechanical reaction. The two processes interact with each other so that improvements in the electrochemical activity must be coupled with improvements in the availability of the electrocatalyst for reaction. Cost effective and highly reactive electrocatalysts were developed. The utilization of the electrocatalyst particles in the porous electrode structures was analyzed. It is shown that a large percentage of the electrocatalyst in anode structures is not utilized. This low utilization translates directly into a noble metal cost penalty for the fuel cell. E.A.K.

N82-18668*# Gilbert/Commonwealth, Reading, Pa.
MAGNETOHYDRODYNAMICS (MHD) ENGINEERING TEST FACILITY (ETF) 200 MWe POWER PLANT. CONCEPTUAL DESIGN ENGINEERING REPORT (CDER). VOLUME 4: SUPPLEMENTARY ENGINEERING DATA

Sep. 1981 548 p refs
(Contract DEN3-224; DE-AI01-77ET-10769)
(NASA-CR-165452-Vol-4; DOE/NASA/0224-1-Vol-4) Avail:
NTIS HC A23/MF A01 CSCL 10B

The reference conceptual design of the Magnetohydrodynamic Engineering Test Facility (ETF), a prototype 200 MWe coal-fired electric generating plant designed to demonstrate the commercial feasibility of open cycle MHD is summarized. Main elements of the design are identified and explained, and the rationale behind them is reviewed. Major systems and plant facilities are listed and discussed. Construction cost and schedule estimates, and identification of engineering issues that should be reexamined are also given. The latest (1980-1981) information from the MHD technology program are integrated with the elements of a conventional steam power electric generating plant. Supplementary Engineering Data (Issues, Background, Performance Assurance Plan, Design Details, System Design Descriptions and Related Drawings) is presented. M.D.K.

N82-18689*# Applied Solar Energy Corp., City of Industry, Calif.
DEVELOPMENT OF THIN WRAPAROUND JUNCTION SILICON SOLAR CELLS Final Report, Sep. 1980 - Nov. 1981

F. Ho and P. A. Iles Nov. 1981 43 p refs
(Contract NAS3-22228)
(NASA-CR-165570) Avail: NTIS HC A03/MF A01 CSCL 10A

The state of the art technologies was applied to fabricate 50 micro thick 2x4 cm. coplanar back contact (CBC) solar cells with AMO efficiency above 12%. A requirement was that the cells have low solar absorptance. A wraparound junction (WAJ) with wraparound metallization was chosen. This WAJ approach avoided the need for very complex fixturing, especially during rotation of the cells for providing adequate contacts over dielectric edge layers. The contact adhesion to silicon was considered better than to an insulator. It is indicated that shunt resistance caused by poor WAJ diode quality, and series resistance from the WAJ contact, give good cell performance. The cells developed reached 14 percent AMO efficiency (at 25 C), with solar absorptance values of 0.73. Space/cell environmental tests were performed on these cells and the thin CSC cells performed well. The optimized design configuration and process sequence were used to make 50 deliverable CBC cells. These cells were all above 12 percent efficiency and had an average efficiency of -13 percent. Results of environmental tests (humidity-temperature, thermal shock, and contact adherence) are also given. E.A.K.

N82-18690*# United Technologies Corp., South Windsor, Conn. Power Systems Div.

LOW NO SUBX HEAVY FUEL COMBUSTOR CONCEPT PROGRAM. PHASE 1A: COAL GAS ADDENDUM Final Report, 29 Jun. - Oct. 1981

Thomas Rosfjord and Richard Sederquist Jan. 1982 43 p refs
(Contract DEN3-149; DE-AI01-77ET-13111)
(NASA-CR-165577; DOE/NASA/0149-2; GTR-3932) Avail:

NTIS HC A03/MF A01 CSCL 10B

The performance and emissions from a rich-lean combustor fired on simulated coal gas fuels were investigated using a 12.7-cm diameter axially-staged burner originally designed for operation with high heating value liquid fuels. A simple, tubular fuel injector was substituted for the liquid fuel nozzle; no other combustor modifications were made. Four test fuels were studied including three chemically bound nitrogen-free gas mixtures with higher heating values of 88, 227, and 308 kJ/mol (103, 258 and 349 Btu/scf), and a 227 kJ/mol (258 Btu/scf) heating value doped with ammonia to produce a fuel nitrogen content of 0.5% (wt). Stable, ultra-low nitrogen oxide, smoke-free combustion was attained for the nitrogen-free fuels. Results with the doped fuel indicated that less than 5% conversion of NH3 to nitrogen oxide levels below Environmental Protection Agency limits could be achieved. In some instances, excessive CO levels were encountered. It is shown that use of a burner design employing a less fuel-rich primary zone than that found optimum for liquid fuels would yield more acceptable CO emissions. A.R.H.

N82-18693*# Structural Composites Industries, Inc., Azusa, Calif.

DESIGN, EVALUATION, AND FABRICATION OF LOW-COST COMPOSITE BLADES FOR INTERMEDIATE-SIZE WIND TURBINES Final Report

Oscar Weingart Sep. 1981 210 p refs
(Contracts DEN3-100; DE-AI01-79ET-20320)
(NASA-CR-165342; DOE/NASA/0100-1; SCI-81520) Avail:
NTIS HC A10/MF A01 CSCL 10A

Low cost approaches for production of 60 ft long glass fiber/resin composite rotor blades for the MOD-OA wind turbine were identified and evaluated. The most cost-effective configuration was selected for detailed design. Subelement and subscale specimens were fabricated for testing to confirm physical and mechanical properties of the composite blade materials, to develop and evaluate blade fabrication techniques and processes, and to confirm the structural adequacy of the root end joint. Full-scale blade tooling was constructed and a partial blade for tool and process tryout was built. Then two full scale blades were fabricated and delivered to NASA-LaRC for installation on a MOD-OA wind turbine at Clayton, New Mexico for operational testing. Each blade was 60 ft. long with 4.5 ft. chord at root end and 2575 lbs weight including metal hub adapter. The selected blade configuration was a three cell design constructed using a resin impregnated glass fiber tape winding process that allows rapid wrapping of primarily axially oriented fibers onto a tapered mandrel, with tapered wall thickness. The ring winder/transverse filament tape process combination was used for the first time on this program to produce entire rotor blade structures. This approach permitted the complete blade to be wound on stationary mandrels, an improvement which alleviated some of the tooling and process problems encountered on previous composite blade programs. Author

N82-18698*# DHR, Inc., Washington, D.C.
MARKET ASSESSMENT OF PHOTOVOLTAIC POWER SYSTEMS FOR AGRICULTURAL APPLICATIONS IN NIGERIA Final Report

David Staples, Henry Steingrass, and James Nolfi (ARD, Inc., Burlington, Vt.) Oct. 1981 115 p refs
(Contracts DEN3-180; DE-AI01-79ET-20485)
(NASA-CR-165511; DOE/NASA/0180-4; C4100-50) Avail:
NTIS HC A06/MF A01 CSCL 10A

The market potential for stand-alone photovoltaic systems in agriculture was studied. Information is presented on technical and economically feasible applications, and assessments of the business, government and financial climate for photovoltaic sales. It is concluded that the market for stand-alone systems will be large because of the availability of capital and the high premium placed on high reliability, low maintenance power systems. Various specific applications are described, mostly related to agriculture. R.J.F.

N82-19669*# Arizona State Univ., Tempe.
SOCIOECONOMIC IMPACT OF PHOTOVOLTAIC POWER AT SCHUCHULI, ARIZONA Final Report

Donald Bahr, Billy G. Garrett, and Carolyn Chrisman Oct. 1980 161 p refs
(Contracts DEN3-50; DE-AI01-79ET-20485)

(NASA-CR-165551; DOE/NASA/0050-1) Avail: NTIS
HC A08/MF A01 CSCL 10A

The social and economic impact of photovoltaic power on a small, remote native American village is studied. Village history, group life, energy use in general, and the use of photovoltaic-powered appliances are discussed. No significant impacts due to the photovoltaic power system were observed. R.J.F.

N82-20661* TRW, Inc., Redondo Beach, Calif.
**CHOPPER-CONTROLLED DISCHARGE LIFE CYCLING
STUDIES ON LEAD-ACID BATTERIES Final Report**

Joseph J. Kraml and Ernest P. Ames Mar. 1982 79 p refs
Sponsored in part by DOE

(Contract DEN3-88)
(NASA-CR-165615; NAS 1.26:165615) Avail: NTIS
HC A05/MF A01 CSCL 10C

State-of-the-art 6 volt lead-acid golf car batteries were tested. A daily charge/discharge cycling to failure points under various chopper controlled pulsed dc and continuous current load conditions was undertaken. The cycle life and failure modes were investigated for depth of discharge, average current chopper frequency, and chopper duty cycle. It is shown that battery life is primarily and inversely related to depth of discharge and discharge current. Failure mode is characterized by a gradual capacity loss with consistent evidence of cell element aging. E.A.K.

N82-21709* ECO, Inc., Cambridge, Mass.
**CATHODE CATALYSTS FOR PRIMARY PHOSPHORIC ACID
FUEL CELLS Final Report**

Dec. 1981 60 p refs
(Contracts DEN3-150; DE-A101-80ET-17088)

(NASA-CR-165578; NAS 1.26:165578;
DOE/NASA/150-81/7) Avail: NTIS HC A04/MF A01 CSCL
10A

Alkylation of carbon Vulcan XC-72, the support carbon, was shown to provide the most stable bond type for linking cobalt dehydrobenzo tetraazannulene (CoTAA) to the surface of the carbon; this result is based on data obtained by cyclic voltammetry, pulse voltammetry and by release of ¹⁴C from bonded CoTAA. Half-cell tests at 100 C in 85% phosphoric acid showed that CoTAA bonded to the surface of carbon (Vulcan XC-72) via an alkylation procedure is a more active catalyst than is platinum based on a factor of two improvement in Tafel slope; dimeric CoTAA had catalytic activity equal to platinum. Half-cell tests also showed that bonded CoTAA catalysts do not suffer a loss in potential when air is used as a fuel rather than oxygen. Commercially available polytetrafluoroethylene (PTFE) was shown to be unstable in the fuel cell environment with degradation occurring in 2000 hours or less. The PTFE was stressed at 200 C in concentrated phosphoric acid as well as electrochemically stressed in 150 C concentrated phosphoric acid; the surface chemistry of PTFE was observed to change significantly. Radiolabeled PTFE was prepared and used to verify that such chemical changes also occur in the primary fuel cell environment. R.J.F.

N82-21711* ECO, Inc., Cambridge, Mass.
**CATHODE CATALYST FOR PRIMARY PHOSPHORIC ACID
FUEL CELLS Final Report**

Fraser Walsh Dec. 1981 60 p
(Contract DEN3-150; Contract DE-A101-80ET-17088)

(NASA-CR-165578; DOE/NASA/150-81/7; NAS
1.26:165578) Avail: NTIS HC A04/MF A01 CSCL 10A

Three carbon surface functionalization procedures were carried out on Vulcan XC-72, the support carbon in the phosphoric acid fuel cell. The resulting functionalized carbons were reacted with carbon 14-labeled trimethylamine and with carbon 14-labeled dimethylamino tetraazannulene. The release of the carbon 14 from these bonded carbons was measured. Based on the results obtained, the alkylation procedure of carbon functionalization was identified as providing the most stable bond between the carbon surface and the organic electrocatalyst. R.J.F.

N82-21713* Westinghouse Electric Corp., Pittsburgh, Pa.
Advanced Energy Systems Div.

**CELL MODULE AND FUEL CONDITIONER DEVELOPMENT
Quarterly Report, Oct. - Dec. 1981**

J. M. Feret Jan. 1982 51 p
(Contract DEN3-161; Contract DE-A101-80ET-17088)

(NASA-CR-165620; DOE/NASA/0161-9A; NAS 1.26:16562;
QR-9) Avail: NTIS HC A04/MF A01 CSCL 10A

The efforts performed to develop a phosphoric acid fuel cell (PAFC) stack design having a 10 kW power rating for operation at higher than atmospheric pressure based on the existing Mark II design configuration are described. The work involves: (1) Performance of pertinent functional analysis, trade studies and thermodynamic cycle analysis for requirements definition and system operating parameter selection purposes, (2) characterization of fuel cell materials and components, and performance testing and evaluation of the repeating electrode components, (3) establishment of the state-of-the-art manufacturing technology for all fuel cell components at Westinghouse and the fabrication of short stacks of various sizes, and (4) development of a 10 kW PAFC stack design for higher pressure operation utilizing the top down systems engineering approach. Author

N82-22666* Acurex Corp., Mountain View, Calif. Energy
and Environment Div.

**COMPUTER MODEL OF CATALYTIC COMBUSTION/
STIRLING ENGINE HEATER HEAD Final Report**

E. K. Chu May 1981 188 p refs
(Contract DEN3-186; DE-A101-77CS-61040)

(NASA-CR-165378; DOE/NASA/0186-1; NAS 1.26:165378;
FR-81-75/EE) Avail: NTIS HC A09/MF A01 CSCL 10B

The basic Acurex HET code was modified to analyze specific problems for Stirling engine heater head applications. Specifically, the code can model: an adiabatic catalytic monolith reactor, an externally cooled catalytic cylindrical reactor/flat plate reactor, a conannular tube radiatively cooled reactor, and a monolithic reactor radiating to upstream and downstream heat exchangers. T.M.

N82-22675* ECO, Inc., Cambridge, Mass.
**CATHODE CATALYST FOR PRIMARY PHOSPHORIC FUEL
CELLS Quarterly Report, Jul. - Sep. 1980**

Fraser Walsh Sep. 1980 17 p refs
(Contract DEN3-150)

(NASA-CR-165198; DOE/NASA/0150-80/5; NAS
1.26:165198) Avail: NTIS HC A02/MF A01 CSCL 10A

Alkylation of Vulcan XC-72 provided the most stable bond type for linking CoTAA to the surface of the carbon; this result is based on data obtained by cyclic voltammetry, pulse voltammetry and by release of ¹⁴C from bonded CoTAA. Half-cell tests at 100 C in 85% phosphoric acid showed that CoTAA bonded to the surface of carbon (Vulcan XC-72) via an alkylation procedure is a more active catalyst than is platinum based on a factor of two improvement in Tafel slope; dimeric CoTAA has catalytic activity equal to platinum. Half-cell tests also showed that bonded CoTAA catalysts do not suffer a loss in potential when air is used as a fuel rather than oxygen. Commercially available PTFE was shown to be stable for four months in 200 C 85% phosphoric acid based on lack of change in surface wetting properties, IR and physical characteristics. When stressed electrochemically in 150 C 85% phosphoric acid, PTFE also showed no changes after one month. Author

N82-22770* DHR, Inc., Washington, D.C.
**MARKET ASSESSMENT OF PHOTOVOLTAIC POWER
SYSTEMS FOR AGRICULTURAL APPLICATIONS IN
COLOMBIA Final Report**

William Steigelmann and Sergio Neyeloff Nov. 1981 124 p
refs Presented in cooperation with Associates in Rural
Development, Inc., Burlington, Vt.

(Contracts DEN3-180; DE-A101-79ET-20485)
(NASA-CR-165524; DOE/NASA-0180/5) Avail: NTIS
HC A06/MF A01 CSCL 10B

The market potential for photovoltaic systems in the agricultural sector of Colombia is assessed. Consideration was given to over twenty specific livestock production, crop production, and rural services applications requiring less than 15 kW of power without backup power. Analysis revealed that near-term potential exists for photovoltaic technology in applications in coffee depulping, cattle watering, rural domestic users, rural water supply

ORIGINAL PAGE IS OF POOR QUALITY

and small irrigation, rural telephones, rural health posts, and vaccine refrigeration. Market size would be in the 1200 to 2500 kWp range in the 1981 to 86 timeframe. Positive factors influencing the market size include a lack of electrical services, potential for developing the Llanos Orientales Territory, high fuel costs in remote areas, balance of system availability, the presence of wealthy land owners, and a large government-sponsored contract for photovoltaic (PV)-powered rural telephone systems. The anticipated eligibility of photovoltaic equipment for loans would be a further positive factor in market potential. Important negative factors include relatively inexpensive energy in developed locations, reliance on hydropower, lack of familiarity with PV equipment, a lack of financing, and established foreign competition in PV technology. Recommendations to American PV manufacturers attempting to develop the Colombian market are given. R.J.F.

N82-23702* Massachusetts Inst of Tech. Cambridge Dept. of Aeronautics and Astronautics
REVIEW OF ANALYSIS METHODS FOR ROTATING SYSTEMS WITH PERIODIC COEFFICIENTS
John Dugundji and John H. Wandell. In NASA Lewis Research Center Wind Turbine Dyn. May 1981 p 165-172 refs (For primary document see N82-23884 14-44)
(Grant NaG-3303)
Avail: NTIS HC A18/MF A01 CSCL 10B

Two of the more common procedures for analyzing the stability and forced response of equations with periodic coefficients are reviewed: the use of Floquet methods, and the use of multiblade coordinate and harmonic balance methods. The analysis procedures of these periodic coefficient systems are compared with those of the more familiar constant coefficient systems. Author

N82-24646* Jet Propulsion Lab., California Inst. of Tech., Pasadena.
[SUBSYSTEMS DESIGN AND COMPONENT DEVELOPMENT FOR THE PARABOLIC DISH MODULE FOR SOLAR THERMAL POWER SYSTEMS] Annual Technical Report
C. K. Stein 15 Mar. 1982 30 p Prepared in cooperation with NASA, Lewis Research Center
(Contracts NAS7-10; DE-AT04-81AL-16228)
(NASA-CR-168941; DOE/JPL-1060-51; JPL-Pub-82-22; NAS 1.26:168941) Avail: NTIS HC A03/MF A01 CSCL 10A

Solar thermal power systems parabolic dish activities are summarized. Subsystem designs of concentrators, receivers, engines, power converters, and thermal transport are discussed. Analyses, test results, field tests, small community system development and the parabolic dish test site are also included. Author

N82-24648* Engelhard Industries, Inc., Edison, N.J.
DEVELOP AND TEST FUEL CELL POWERED ON-SITE INTEGRATED TOTAL ENERGY SYSTEMS: PHASE 3: FULL-SCALE POWER PLANT DEVELOPMENT Quarterly Report, Aug. - Oct. 1981
28 Apr. 1982 59 p refs
(Contracts DEN3-241; DE-AI-90ET-17088)
(NASA-CR-165568; DOE/NASA/C241-3; NAS 1.26:165568; QR-3) Avail: NTIS HC A04/MF A01 CSCL 10B

The development of a commercially viable and cost-effective phosphoric acid fuel cell powered on-site integrated energy system (OS/IES) is described. The fuel cell offers energy efficiencies in the range of 35-40% of the higher heating value of available fuels in the form of electrical energy. In addition, by utilizing the thermal energy generated for heating, ventilating and air-conditioning (HVAC), a fuel cell OS/IES could provide total energy efficiencies in the neighborhood of 80%. Also, the Engelhard fuel cell OS/IES offers the important incentive of replacing imported oil with domestically produced methanol, including coal-derived methanol. T.M.

N82-24649* Parsons (Ralph M.) Co., Pasadena, Calif.
FUEL QUALITY PROCESSING STUDY, VOLUME 1 Final Report
J. B. OHara, A. Bela, N. E. Jentz, H. T. Syverson, H. W. Klumpe, R. E. Kessler, H. T. Kotzot, and B. L. Loran Apr. 1981 203 p refs 2 Vol.

(Contracts DEN3-183; DE-AI01-77ET-13111)
(NASA-CR-165327-Vol-1; DOE/NASA/O183-1; NAS 1.26:165327-Vol-1) Avail: NTIS HC A10/MF A01 CSCL 21D

A fuel quality processing study to provide a data base for an intelligent tradeoff between advanced turbine technology and liquid fuel quality, and also, to guide the development of specifications of future synthetic fuels anticipated for use in the time period 1985 to 2000 is given. Four technical performance tests are discussed: on-site pretreating, existing refineries to upgrade fuels, new refineries to upgrade fuels, and data evaluation. The base case refinery is a modern Midwest refinery processing 200,000 BPD of a 60/40 domestic/import petroleum crude mix. The synthetic crudes used for upgrading to marketable products and turbine fuel are shale oil and coal liquids. Of these syncrudes, 50,000 BPD are processed in the existing petroleum refinery, requiring additional process units and reducing petroleum feed, and in a new refinery designed for processing each syncrude to produce gasoline, distillate fuels, resid fuels, and turbine fuel, JPGs and coke. An extensive collection of synfuel properties and upgrading data was prepared for the application of a linear program model to investigate the most economical production slate meeting petroleum product specifications and turbine fuels of various quality grades. Technical and economic projections were developed for 36 scenarios, based on 4 different crude feeds to either modified existing or new refineries operated in 2 different modes to produce 7 differing grades of turbine fuels. A required product selling price of turbine fuel for each processing route was calculated. Procedures and projected economics were developed for on-site treatment of turbine fuel to meet limitations of impurities and emission of pollutants. R.J.F.

N82-24650* Parsons (Ralph M.) Co., Pasadena, Calif.
FUEL QUALITY/PROCESSING STUDY, VOLUME 2: APPENDIX. TASK 1 LITERATURE SURVEY Final Report
J. B. OHara, A. Bela, N. E. Jentz, H. W. Klumpe, H. E. Kessler, H. T. Kotzot, and B. L. Loran Apr. 1981 274 p refs 2 Vol.
(Contract DEN3-183; DE-AI01-77ET-13111)
(NASA-CR-165327-Vol-2; DOE/NASA/O183-1; NAS 1.26:165327-Vol-2) Avail: NTIS HC A12/MF A01 CSCL 21D

The results of a literature survey of fuel processing and fuel quality are given. Liquid synfuels produced from coal and oil shale are discussed. Gas turbine fuel property specifications are discussed. On-site fuel pretreatment and emissions from stationary gas turbines are discussed. Numerous data tables and abstracts are given. R.J.F.

N82-24651* General Electric Co., Schenectady, N. Y. Gas Turbine Div.
LOW NOx HEAVY FUEL COMBUSTOR CONCEPT PROGRAM, PHASE 1 Final Report
Martin B. Cutrone Oct. 1981 251 p
(Contracts DEN3-147; DE-AI01-77ET-13111)
(NASA-CR-165449; DOE/NASA/O147-1; NAS 1.26:165449)
Avail: NTIS HC A12/MF A01 CSCL 10B

Combustion tests were completed with seven concepts, including three rich/lean concepts, three lean/lean concepts, and one catalytic combustor concept. Testing was conducted with ERBS petroleum, distillate, petroleum residual, and SRC-II coal-derived liquid fuels over a range of operating conditions for the 12:1 pressure ratio General Electric MS7001E heavy-duty turbine. Blends of ERBS and SRC-II fuels were used to vary fuel properties over a wide range. In addition, pyridine was added to the ERBS and residual fuels to vary nitrogen level while holding other fuel properties constant. Test results indicate that low levels of NOx and fuel-bound nitrogen conversion can be achieved with the rich/lean combustor concepts for fuels with nitrogen contents up to 1.0% by weight. Multinozzle rich/lean Concept 2 demonstrated dry low NOx emissions within 10-15% of the EPA New Source Performance Standards goals for SRC-II fuel, with yields of approximately 15%, while meeting program goals for combustion efficiency, pressure drop, and exhaust gas temperature profile. Similar, if not superior, potential was demonstrated by Concept 3, which is a promising rich/lean combustor design. T.M.

N82-24686*# Edde (Howard), Inc., Bellevue, Wash.
COLLECTION AND DISSEMINATION OF THERMAL ENERGY STORAGE SYSTEM INFORMATION FOR THE PULP AND PAPER INDUSTRY

Howard Edde *In* Courtesy Associates, Inc. Proc. of the DOE Thermal and Chem. Storage Ann. Contractor's Rev. Meeting Mar. 1981 p 133-136 refs (For primary document see N82-24652 15-44)

(Contract DEN3-190)
Avail: NTIS HC A16/MF A01 CSCL 10A

The collection and dissemination of thermal energy storage (TES) system technology for the pulp and paper industry with the intent of reducing fossil fuel usage is discussed. The study plan is described and a description presented of example TES systems. Author

N82-24725*# Westinghouse Electric Corp., Concordville, Pa.
LOW NO_x HEAVY FUEL COMBUSTOR CONCEPT PROGRAM, PHASE 1: COMBUSTION TECHNOLOGY GENERATION Final Report

H. G. Lew, D. R. Carl, G. Vermes, E. A. DeZubay, J. A. Schwab, and D. Prothro Oct. 1981 143 p refs
(Contract DEN3-146; DE-A101-77ET-13111)
(NASA-CR-165482; DOE/NASA/O146-1; NAS 1.26:165482)
Avail: NTIS HC A07/MF A01 CSCL 10B

The viability of low emission nitrogen oxide (NO_x) gas turbine combustors for industrial and utility application. Thirteen different concepts were evolved and most were tested. Acceptable performance was demonstrated for four of the combustors using ERBS fuel and ultralow NO_x emissions were obtained for lean catalytic combustion. Residual oil and coal derived liquids containing fuel bound nitrogen (FBN) were also used at test fuels, and it was shown that staged rich/lean combustion was effective in minimizing the conversion of FBN to NO_x. The rich/lean concept was tested with both modular and integral combustors. While the ceramic lined modular configuration produced the best results, the advantages of the all metal integral burners make them candidates for future development. An example of scaling the laboratory sized combustor to a 100 MW size engine is included in the report as are recommendations for future work. Author

N82-25635*# Detroit Diesel Allison, Indianapolis, Ind.
LOW NO_x HEAVY FUEL COMBUSTOR CONCEPT PROGRAM Final Report

A. S. Novick and D. L. Troth Oct. 1981 206 p refs
(Contracts DEN3-148; DE-A101-77ET-13111)
(NASA-CR-165367; NAS 1.26:165367; DDA-EDR-10594; DOE/NASA/O148-1) Avail: NTIS HC A10/MF A01 CSCL 10B

The development of the technology required to operate an industrial gas turbine combustion system on minimally processed, heavy petroleum or residual fuels having high levels of fuel-bound nitrogen (FBN) while producing acceptable levels of exhaust emissions is discussed. Three combustor concepts were designed and fabricated. Three fuels were supplied for the combustor test demonstrations: a typical middle distillate fuel, a heavy residual fuel, and a synthetic coal-derived fuel. The primary concept was an air staged, variable-geometry combustor designed to produce low emissions from fuels having high levels of FBN. This combustor used a long residence time, fuel-rich primary combustion zone followed by a quick-quench air mixer to rapidly dilute the fuel rich products for the fuel-lean final burnout of the fuel. This combustor, called the rich quench lean (RQL) combustor, was extensively tested using each fuel over the entire power range of the model 570 K engine. Also, a series of parametric tests was conducted to determine the combustor's sensitivity to rich-zone equivalence ratio, lean-zone equivalence ratio, rich-zone residence time, and overall system pressure drop. Minimum nitrogen oxide emissions were measured at 50 to 55 ppmv at maximum continuous power for all three fuels. Smoke was less than a 10 SAE smoke number. M.G.

N82-25640*# Giner, Inc., Waltham, Mass.
REQUIREMENTS FOR OPTIMIZATION OF ELECTRODES AND ELECTROLYTE FOR THE IRON/CHROMIUM REDOX FLOW CELL Final Report

Vinod Jalan, Herbert Stark, and Jose Giner Sep. 1981 82 p refs

(Contracts DEN3-97; DE-A104-80AL-12726)
(NASA-CR-165218; DOE/NASA/O097-80/1; NAS 1.26:165218) Avail: NTIS HC A05/MF A01 CSCL 10C

Improved catalyzation techniques that included a pretreatment of carbon substrate and provided normalized carbon surface for uniform gold deposition were developed. This permits efficient use of different batches of carbon felt materials which initially vary significantly in their physical and surface chemical properties, as well as their electrochemical behavior. Further modification of gold impregnation technique gave the best performing electrodes. In addition to the linear sweep voltammetry, cyclic voltammetry was used to determine the effects of different activation procedures on the Cr(3)/Cr(2) Redox and H₂ evolution reactions. The roles of carbon, gold and lead in the overall Redox cycle are identified. The behavior of the electrodes at both normal battery operating potentials and more extreme potentials is discussed preparing efficient and stable electrodes for the energy storage battery is implicated. E.A.K.

N82-27837*# Gilbert/Commonwealth, Reading, Pa.
MAGNETOHYDRODYNAMICS (MHD) ENGINEERING TEST FACILITY (ETF) 200 MWe POWER PLANT, CONCEPTUAL DESIGN ENGINEERING REPORT (CDER), VOLUME 2: ENGINEERING, VOLUME 3: COSTS AND SCHEDULES Final Report

Sep. 1981 163 p Volume 3 is included as MF 5 Vol.
(Contracts DEN3-224; DE-A101-77ET-10769)
(NASA-CR-165452-Vol-2; NASA-CR-165452-Vol-3; NAS 1.26:165452-Vol-3; NAS 1.26:165452-Vol-2; DOE/NASA/O224-1) Avail: NTIS HC E08/MF A01 CSCL 10B

Engineering design details for the principal systems, system operating modes, site facilities, and structures of an engineering test facility (ETF) of a 200 MWE power plant are presented. The ETF resembles a coal-fired steam power plant in many ways. It is analogous to a conventional plant which has had the coal combustor replaced with the MHD power train. Most of the ETF components are conventional. They can, however, be sized or configured differently or perform additional functions from those in a conventional coal power plant. The boiler not only generates steam, but also performs the functions of heating the MHD oxidant, recovering seed, and controlling emissions. S.L.

N82-29718*# Institute of Gas Technology, Chicago, Ill.
Engineering Research Div.

STABILIZING PLATINUM IN PHOSPHORIC ACID FUEL CELLS Final Report, Dec. 1980 - Mar. 1982

Robert J. Remick Jul. 1982 47 p refs
(Contracts DEN3-208; DE-A101-80ET-17088)
(NASA-CR-165606; DOE/NASA/O208-4; NAS 1.26:165606; Rept-61051) Avail: NTIS HC A03/MF A01 CSCL 10A

Platinum sintering on phosphoric acid fuel cell cathodes is discussed. The cathode of the phosphoric acid fuel cell uses a high surface area platinum catalyst dispersed on a conductive carbon support to minimize both cathode polarization and fabrication costs. During operation, however, the active surface area of these electrodes decreases, which in turn leads to decreased cell performance. This loss of active surface area is a major factor in the degradation of fuel cell performance over time. S.L.

N82-29719*# California Univ., Berkeley Legal Inst.
CURRENT LEGAL AND INSTITUTIONAL ISSUES IN THE COMMERCIALIZATION OF PHOSPHORIC ACID FUEL CELLS Final Report

John T. Nimmons, Kevin D. Sheehy, Joel R. Singer, and Tom C. Gardner Jan. 1982 238 p refs
(Grant NAG3-111; Contract DE-A101-80ET-17088)
(NASA-CR-167867; DOE/NASA/O111-1; NAS 1.26:167867)
Avail: NTIS HC A11/MF A01 CSCL 10A

Legal and institutional factors affecting the development and commercial diffusion of phosphoric acid fuel cells are assessed. Issues for future research and action are suggested. Perceived barriers and potential opportunities for fuel cells in central and dispersed utility operations and on-site applications are reviewed, as well as the general concept of commercialization as applied to emerging energy technologies. Author

ORIGINAL PAGE IS
OF POOR QUALITY

N82-29720*# DHR, Inc., Washington, D.C.
APPLICATION OF PHOTOVOLTAIC ELECTRIC POWER TO THE RURAL EDUCATION/COMMUNICATION NEEDS OF DEVELOPING COUNTRIES Final Report
Anil Cabraal, David Delansanta, and George Burrill Jul, 1982
61 p ref Prepared in cooperation with Associates in Rural Development, Inc., Burlington, Vt. Sponsored in part by Agency for International Development
(Contract DEN3-248)
(NASA-CR-167894; NAS 1.26:167894) Avail: NTIS HC A04/MF A01 CSCL 10B

The suitability (i.e., cost competitiveness and reliability) of photovoltaic (PV) power systems for rural applications in developing countries is considered. Potential application sectors include health delivery, education and communication where small amounts of electricity are needed to meet critical needs. Author

N82-29721*# Aerospace Corp., El Segundo, Calif.
ENVIRONMENTAL ASSESSMENT OF THE 40 KILOWATT FUEL CELL SYSTEM FIELD TEST OPERATION Final Report

Gary Bollenbacher May 1982 160 p refs
(Contract DE-A101-80ET-17088; NASA Order C-42701D)
(DOE/NASA/2701-1; NASA-CR-167923) Avail: NTIS HC A08/MF A01 CSCL 10A

This environmental assessment examines the potential environmental consequences, both adverse and beneficial, of the 40 kW fuel cell system field test operation. The assessment is of necessity generic in nature since actual test sites were not selected. This assessment provides the basis for determining the need for an environmental impact statement. In addition, this assessment provides siting criteria to avoid or minimize negative environmental impacts and standards for determining candidate test sites, if any, for which site specific assessments may be required S.L.

N82-30705*# Engelhard Industries, Inc., Edison, N.J.
DEVELOPMENT AND TEST FUEL CELL POWERED ON-SITE INTEGRATED TOTAL ENERGY SYSTEM. PHASE 3: FULL-SCALE POWER PLANT DEVELOPMENT Quarterly Report, Nov. 1981 - Jan. 1982

A. Kaufman 21 Jun. 1982 61 p refs
(Contracts DEN3-241; DE-A101-80ET-17088)
(NASA-CR-167898; DOE/NASA/0241-4; NAS 1.26:167898; QR-4) Avail: NTIS HC A04/MF A01 CSCL 10B

The on-site system application analysis is summarized. Preparations were completed for the first test of a full-sized single cell. Emphasis of the methanol fuel processor development program shifted toward the use of commercial shell-and-tube heat exchangers. An improved method for predicting the carbon-monoxide tolerance of anode catalysts is described. Other stack support areas reported include improved ABA bipolar plate bonding technology, improved electrical measurement techniques for specification-testing of stack components, and anodic corrosion behavior of carbon materials. Author

N82-30706*# Spire Corp., Bedford, Mass.
DEVELOPMENT OF A LARGE AREA SPACE SOLAR CELL ASSEMBLY Final Report, Jul. 1981 - Mar. 1982
M. B. Spitzer May 1982 65 p refs
(Contract NAS3-22236)
(NASA-CR-167929; NAS 1.26:167929; FR-10081) Avail: NTIS HC A04/MF A01 CSCL 10A

The development of a large area high efficiency solar cell assembly is described. The assembly consists of an ion implanted silicon solar cell and glass cover. The important attributes of fabrication are the use of a back surface field which is compatible with a back surface reflector, and integration of coverglass application and cell fabrications. Cell development experiments concerned optimization of ion implantation processing of 2 ohm-cm boron-doped silicon. Process parameters were selected based on these experiments and cells with area of 34.3 sq cm were fabricated. The average AMO efficiency of the twenty-five best cells was 13.9% and the best cell had an efficiency of 14.4%. An important innovation in cell encapsulation was also developed. In this technique, the coverglass is applied before the cell is sawed to final size. The coverglass and cell are then

sawed as a unit. In this way, the cost of the coverglass is reduced, since the tolerance on glass size is relaxed, and costly coverglass/cell alignment procedures are eliminated. Adhesive investigations were EVA, FEP-Teflon sheet and DC 93-500. Details of processing and results are reported. B.W.

N82-30709*# Tanksley (W. L.) and Associates, Inc., Brook Park, Ohio.

VIBRATION ANALYSIS OF THREE GUYED TOWER DESIGNS FOR INTERMEDIATE SIZE WIND TURBINES

Robert J. Christie Mar. 1982 113 p refs
(Contract NAS3-21900)
(NASA-CR-165589; DOE/NASA/1900-1; NAS 1.26:165589) Avail: NTIS HC A06/MF A01 CSCL 10A

Three guyed tower designs were analyzed for intermediate size wind turbines. The four lowest natural frequencies of vibration of the three towers concepts were estimated. A parametric study was performed on each tower to determine the effect of varying such tower properties as the inertia and stiffness of the tower and guys, the inertia values of the nacelle and rotor, and the rotational speed of the rotor. Only the two lowest frequencies were in a range where they could be excited by the rotor blade passing frequencies. These two frequencies could be tuned by varying the guy stiffness, the guy attachment point on the tower, the tower and mass stiffness, and the nacelle/rotor/power train masses. Author

N82-30711*# Ionics, Inc., Watertown, Mass.

ANION PERMSELECTIVE MEMBRANE Summary Report
Russell B. Hodgdon and Warren A. Waitz Apr. 1982 75 p
(Contracts DEN3-204; DE-A104-80AL-12726)
(NASA-CR-167872; DOE/NASA/0204-1; NAS 1.26:167872) Avail: NTIS HC A04/MF A01 CSCL 10A

The synthesis and fabrication of polymeric anion permselective membranes for redox systems are discussed. Variations of the prime candidate anion membrane formulation to achieve better resistance and/or lower permeability were explored. Processing parameters were evaluated to lower cost and fabricate larger sizes. The processing techniques to produce more membranes per batch were successfully integrated with the fabrication of larger membranes. Membranes of about 107 cm x 51 cm were made in excellent yield. Several measurements were made on the larger sample membranes. Among the data developed were water transport and transference numbers for these prime candidate membranes at 20 C. Other work done on this system included characterization of a number of specimens of candidate membranes which had been returned after service lives of up to sixteen months. Work with new polymer constituents, with new N.P.'s, catalysts and backing fabrics is discussed. Some work was also done to evaluate other proportions of the ingredients of the prime candidate system. The adoption of a flow selectivity test at elevated temperature was explored. Author

N82-30712*# Westinghouse Research and Development Center, Pittsburgh, Pa.

CELL MODULE AND FUEL CONDITIONER DEVELOPMENT

Final Report, Oct. 1979 - Jan. 1982
D. O. Hoover, Jr. Feb. 1982 393 p
(Contracts DEN3-161; DE-A101-80ET-17088)
(NASA-CR-165193; DOE/NASA/0161-10; NAS 1.26:185193; WEC-82-901-MARED-R1) Avail: NTIS HC A17/MF A01 CSCL 10A

The phosphoric acid fuel cell module (stack) development which culminated in an 80 cell air-cooled stack with separated gas cooling and feed cooling plates is described. The performance of the 80 cell stack was approx. 100 mV per cell higher than that attained during phase 1. The components and materials performed stably for over 8000 hours in a 5 cell stack. The conceptual design of a fuel conditioning system is described. Author

N82-30722*# National Bureau of Standards, Washington, D.C. Metallurgy Div.

NON-NOBLE CATALYSTS AND CATALYST SUPPORTS FOR PHOSPHORIC ACID FUEL CELLS Final Report, Oct. 1979 - Sep. 1981

A. J. McAlister Sep. 1981 38 p refs
(NASA Order C-46229-D; Contract DE-A101-80ET-17088)

(NASA-CR-165289; DOE/NASA/6229-2; NAS 1.26:165289)
Avail NTIS HC A03/MF A01 CSCL 10A

Tungsten carbide, which is active for hydrogen oxidation, is CO tolerant and has a hexagonal structure is discussed. Titanium carbide is inactive and has a cubic structure. Four different samples of the cubic alloys W sub x-Ti sub XC sub 1-y were found to be active and CO tolerant. When the activities of these cubic alloys are weighted by the reciprocal of the square to those of highly forms of WC. They offer important insight into the nature of the active sites on W-C anode catalysts for use in phosphoric acid fuel cells. E.A.K.

N82-32855*# PRC Systems Sciences Co., Tucson, Ariz.
GALLIUM ARSENIDE SOLAR ARRAY SUBSYSTEM STUDY
Final Report, Jan. 1981 - Feb. 1982

F. Q. Miller Feb. 1982 221 p refs

(Contract NAS3-22667)

(NASA-CR-167869; NAS 1.26:167869) Avail: NTIS
HC A10/MF A01 CSCL 10A

The effects on life cycle costs of a number of technology areas are examined for a gallium arsenide space solar array. Four specific configurations were addressed: (1) a 250 KWe LEO mission - planer array; (2) a 250 KWe LEO mission - with concentration; (3) a 50 KWe GEO mission planer array; (4) a 50 KWe GEO mission - with concentration. For each configuration, a baseline system conceptual design was developed and the life cycle costs estimated in detail. The baseline system requirements and design technologies were then varied and their relationships to life cycle costs quantified. For example, the thermal characteristics of the baseline design are determined by the array materials and masses. The thermal characteristics in turn determine configuration, performance, and hence life cycle costs. Author

N82-32856*# Westinghouse Electric Corp., Madison, Pa. Synthetic Fuels Div.

LOW AND MEDIUM HEATING VALUE COAL GAS CATALYTIC COMBUSTOR CHARACTERIZATION

John A. Schwab Nov. 1982 137 p refs

(Contracts DEN3-277; DE-AI01-77ET-10350)

(NASA-CR-165560; DOE/NASA/0277-1; NAS 1.26:165560) Avail:
NTIS HC A07/MF A01 CSCL 10B

Catalytic combustion with both low and medium heating value coal gases obtained from an operating gasifier was demonstrated. A practical operating range for efficient operation was determined, and also to identify potential problem areas were identified for consideration during stationary gas turbine engine design. The test rig consists of fuel injectors, a fuel-air premixing section, a catalytic reactor with thermocouple instrumentation and a single point, water cooled sample probe. The test rig included inlet and outlet transition pieces and was designed for installation into an existing test loop. S.L.

N82-33827*# Solar Turbines International, San Diego, Calif.
LOW NOx HEAVY FUEL COMBUSTOR CONCEPT PROGRAM
Final Report

David J. White, Richard T. LeCren, and Anthony P. Batakis Nov. 1981 93 p refs

(Contracts DEN3-145; DE-AI01-77ET-13111)

(NASA-CR-165481; DOE/NASA/0145-1; NAS 1.26:165481;
SR81-R-4761-21) Avail: NTIS HC A05/MF A01 CSCL 10B

A total of twelve low NOx combustor configurations, embodying three different combustion concepts, were designed and fabricated as modular units. These configurations were evaluated experimentally for exhaust emission levels and for mechanical integrity. Emissions data were obtained in depth on two of the configurations. R.J.F.

A82-11712*# Direct conversion of light to radio frequency energy. J. W. Freeman and S. Simons (Rice University, Houston, TX). In: Intersociety Energy Conversion Engineering Conference, 16th, Atlanta, GA, August 9-14, 1981, Proceedings, Volume 1. (A82-11701 02-44) New York, American Society of Mechanical

Engineers, 1981, p. 95, 96. Research supported by the Brown Foundation of Houston; Grant No. NAG3-29.

A description is presented of the test results obtained with the latest models of the phototron. The phototron was conceived as a replacement for the high voltage solar cell-high power klystron combination for the solar power satellite concept. Physically, the phototron is a cylindrical evacuated glass tube with a photocathode, two grids, and a reflector electrode in a planar configuration. The phototron can be operated either in a biased mode where a low voltage is used to accelerate the electron beam produced by the photocathode or in an unbiased mode referred to as self-oscillation. The device is easily modulated by light input or voltage to broadcast in AM or FM. The range of operation of the present test model phototrons is from 2 to 200 MHz. G.R.

A82-11816*# Characteristic dynamical energy equations for Stirling cycle analysis. V. H. Larson (Cleveland State University, Cleveland, OH). In: Intersociety Energy Conversion Engineering Conference, 16th, Atlanta, GA, August 9-14, 1981, Proceedings, Volume 2. (A82-11701 02-44) New York, American Society of Mechanical Engineers, 1981, p. 1942-1947. 12 refs. Grant No. NSG-3257.

A82-24695* An assessment of alternative fuel cell designs for residential and commercial cogeneration. R. A. Wakefield (Mattech, Inc., Washington, DC). In: The 1980's - A forest of energy decision trees; Proceedings of the Region Six Conference, San Diego, CA, February 20-22, 1980. (A82-24683 10-44) New York, Institute of Electrical and Electronics Engineers, Inc., 1980, p. 160-165. Research sponsored by the U.S. Department of Energy; Contract No. DEN3-89.

A comparative assessment of three fuel cell systems for application in different buildings and geographic locations is presented. The study was performed at the NASA Lewis Center and comprised the fuel cell design, performance in different conditions, and the economic parameters. Applications in multifamily housing, stores and hospitals were considered, with a load of 10kW-1 MW. Designs were traced through system sizing, simulation/evaluation, and reliability analysis, and a computer simulation based on a fourth-order representation of a generalized system was performed. The cells were all phosphoric acid type cells, and were found to be incompatible with gas/electric systems and more favorable economically than the gas/electric systems in hospital uses. The methodology used provided an optimized energy-use pattern and minimized back-up system turn-on. M.S.K.

A82-37078*# Winding for the wind. O. Weingart (Structural Composites Industries, Inc., Azusa, CA). In: Reinforced Plastics/Composites Institute, Annual Conference, 37th, Washington, DC, January 11-15, 1982, Preprints. (A82-37081 18-24) New York, Society of the Plastics Industry, Inc., 1982 (Session 22-C). 8 p. 5 refs. Research supported by the U.S. Department of Energy; Contract No. DEN3-100.

The mechanical properties and construction of epoxy-impregnated fiber-glass blades for wind turbines are discussed, along with descriptions of blades for the Mod 0A and Mod 5A WECS and design goals for a 4 kW WECS. Multicell structure combined with transverse filament tape winding reduces labor and material costs, while placing a high percentage of 0 deg fibers spanwise in the blades yields improved strength and elastic properties. The longitudinal, transverse, and shear modulus are shown to resist stresses exceeding the 50 lb/sq ft requirements, with constant stress resistance expected until fatigue failure is approached. Regression analysis indicates a fatigue life of 400 million operating cycles. The small WECS under prototype development features composite blades, nacelle, and tower. Rated at 5.7 kW in a 15 mph wind, the machine operates over a speed range of 9-53.9 mph and is expected to produce 16,200 kWh annually in a 10 mph average wind measured at 30 ft. M.S.K.

45 ENVIRONMENT POLLUTION

Includes air, noise, thermal and water pollution; environment monitoring; and contamination control.

ORIGINAL PAGE IS
OF POOR QUALITY

N82-13554*# United Air Lines, Inc., San Francisco, Calif. Maintenance Operations Center.

AN AUTOMATED SYSTEM FOR GLOBAL ATMOSPHERIC SAMPLING USING B-747 AIRLINERS Final Report

Ken O. Lew, Ulf R. C. Gustafsson, and Robert E. Johnson Oct. 1981 31 p refs

(Contract NAS3-17867)

(NASA-CR-165264; UAL-C-80-31-33) Avail: NTIS HC A03/MF A01 CSCL 13B

The global air sampling program utilizes commercial aircrafts in scheduled service to measure atmospheric constituents. A fully automated system designed for the 747 aircraft is described. Airline operational constraints and data and control subsystems are treated. The overall program management, system monitoring, and data retrieval from four aircraft in global service is described. E.A.K.

N82-29777*# Garrett Turbine Engine Co., Phoenix, Ariz. **COMPUTATIONS OF SOOT AND AND NO SUB X EMISSIONS FROM GARRETT TURBINE COMBUSTORS Final Report**

S. K. Srivatsa May 1982 300 p refs

(Contract NAS3-22542)

(NASA-CR-167930; NAS 1.26:167930; Rept-21-4309) Avail: NTIS HC A13/MF A01 CSCL 13B

An analytical program was conducted to compute the soot and NOx emissions from a combustor and the radiation heat transfer to the combustor walls. The program involved the formulation of an emission and radiation model and the incorporation of this model into the Garrett 3-D Combustor Performance Computer Program. Computations were performed for the idle, cruise, and take-off conditions of a JT8D can combustor. The predicted soot and NOx emissions and the radiation heat transfer to the combustor walls agree reasonably well with the limited experimental data available. Author

46 GEOPHYSICS

Includes aeronomy; upper and lower atmosphere studies; ionospheric and magnetospheric physics; and geomagnetism.

For space radiation see 93 Space Radiation.

NS2-21145*# National Aeronautics and Space Administration, Lewis Research Center, Cleveland, Ohio.

OZONE AND AIRCRAFT OPERATIONS

Porter J. Perkins in NASA, Marshall Space Flight Center Proc.: 5th Ann. Workshop on Meteorol. and Environ. Inputs to Aviation Systems Dec. 1981 p 40-44 refs (For primary document see NS2-21139 12-01)

Avail: NTIS HC A07/MF A01 CSDL 04A

A82-37450 * # Aircraft sampling of the sulfate layer near the tropopause following the eruption of Mount St. Helens. E. A. Ezberg, D. A. Otterson, W. K. Roberts, and L. C. Papathakos (NASA, Lewis Research Center, Cleveland, OH). *Journal of Geophysical Research*, vol. 87, Apr. 20, 1982, p. 3123-3127. 9 refs.

Twenty-three filter sampling flights of the NASA Lewis F-106 aircraft, were conducted in the Great Lakes region between June 4 and Dec. 23, 1980, following the major eruption of Mount St. Helens on May 18. The IPC-1478 filters were exposed over an altitude range spanning the local tropopause. A filter sample exposed above the tropopause on June 5 indicated a sulfate level 50 times the baseline measurements, which is consistent with the trajectory predictions of the leading edge of the cloud on its second transit around the earth. Subsequent measurements over a period of 7 months revealed the existence of a layer of sulfate above the tropopause that decayed to a level of about 4 times previously measured background levels by the beginning of August. Concentration of nitrate above the tropopause exhibited considerable variability and showed some enhancement compared with previously measured concentration levels. On the basis of the null results of X ray fluorescence measurements, there is no evidence of ash particle concentrations of greater than 3.4 microns/cu m persisting in the layer above the tropopause following the second transit of the cloud. (Author)

A82-31009 * Field-aligned ion streams in the earth's midnight region. R. C. Olsen (Alabama, University, Huntsville, AL). *Journal of Geophysical Research*, vol. 87, Apr. 1, 1982, p. 2301-2310. 20 refs. Grant No. NSG-3150; Contract No. NAS8-30563.

Plasma measurements from the University of California at San Diego auroral particles experiment on the geosynchronous Applied Technology Satellite 6 in the midnight region show that the low-energy ion fluxes (1-100 eV) are field aligned and are well characterized as thermal populations (1-10 eV) with a streaming velocity of 30-100 km/s along the magnetic field line. The lowest energies are found prior to injections, on quiet days, with an increase of the streaming velocity evident when an injection occurs near the satellite. Multiple peaks in the ion distribution functions are attributed to the presence of different ions species (H⁺, He⁺, O⁺, O²⁺) streaming at similar velocities, both during quiet times and as the plasma velocity increases in response to an injection.

(Author)

A82-32630 * The hidden ion population of the magnetosphere. R. C. Olsen (Alabama, University, Huntsville, AL). *Journal of Geophysical Research*, vol. 87, May 1, 1982, p. 3481-3488. 12 refs. Contracts No. NAS5-23481; No. NAS8-33982; No. F04701-77-C-0062; Grant No. NSG-3150.

The presence of a cold ion population in the magnetosphere which is normally hidden from particle detector observation by the positive charging of the spacecraft is reported. Ion and electron data were obtained from particle detectors on the ATS 6 and SCATHA satellites designed to measure the 1-eV to 80-keV plasma population. The cold, isotropic ion population, with temperature 1 eV and density 10-100/cu cm, was detected only when the spacecraft were in eclipse, when spacecraft potential had dropped from +10 V in sunlight to +4 to +5 V. The hidden ion population was found at geosynchronous altitude only during geomagnetically quiet times and when there has been an absence of geomagnetic activity for several

hours, and appears to coexist with the plasma sheet. More consistent measurements of the cold-ion population at midnight or at other local times would require the biasing of the ion detector with respect to the spacecraft, or the controlling of spacecraft potential. A.L.W.

ORIGINAL PAGE IS
OF POOR QUALITY

47 METEOROLOGY AND CLIMATOLOGY

Includes weather forecasting and modification.

NS2-16659* FWG Associates, Inc., Tullahoma, Tenn.
**DESIGN OF PROTOTYPE CHARGED PARTICLE FOG
DISPERSAL UNIT Final Report**
Frank G. Collins, Walter Frost, and Philip Kessel Washington,
D.C. NASA Dec. 1981 41 p refs
(Contract NAS3-33541)
(NASA-CR-3481; M364) Avail: NTIS HC A03/MF A01 CSCL
04B

The unit was designed to be easily modified so that certain features that influence the output current and particle size distribution could be examined. An experimental program was designed to measure the performance of the unit. The program described includes measurements in a fog chamber and in the field. Features of the nozzle and estimated nozzle characteristics are presented.

T.M.

ORIGINAL PAGE IS
OF POOR QUALITY

52 AEROSPACE MEDICINE

Includes physiological factors, biological effects of radiation; and weightlessness.

ORIGINAL PAGE IS
OF POOR QUALITY

**82-23976*# Thermo Electron Corp., Waltham, Mass.
EVALUATION OF LEFT VENTRICULAR ASSIST DEVICE
PUMP BLADDERS CAST FROM ION-SPUTTERED POLYTETRAFLUORETHYLENE MANDRELS**

Mar. 1982 103 p refs

(Contract NAS3-22476)

(NASA-CR-167904; NAS 1.26:167904; TE200-230-82) Avail:
NTIS HC A06/MF A01 CSCL 08B

A highly thromboresistant blood contacting interface for use in implantable blood pump is investigated. Biomaterials mechanics, dynamics, durability, surface morphology, and chemistry are among the critical considerations pertinent to the choice of an appropriate blood pump bladder material. The use of transfer cast biopolymers from ion beam textured surfaces is investigated to detect subtle variations in blood pump surface morphology using Biomer as the biomaterial of choice. The efficacy of ion beam sputtering as an acceptable method of fabricating textured blood interfaces is evaluated. Aortic grafts and left ventricular assist devices were implanted in calves; the blood interfaces were fabricated by transfer casting methods from ion beam textured polytetrafluorethylene mandrels. The mandrels were textured by superimposing a 15 micron screen mesh; ion sputtering conditions were 300 volts beam energy, 40 to 50 mA beam, and a mandrel to source distance of 25 microns. S.L.

54 MAN/SYSTEM TECHNOLOGY AND LIFE SUPPORT

includes human engineering; bio'chnology; and space suits and protective clothing.

ORIGINAL PAGE IS
OF POOR QUALITY

N82-16743* # National Aeronautics and Space Administration. Lewis Research Center, Cleveland, Ohio.

A HYDRODYNAMIC MODEL OF AN OUTER HAIR CELL
Bo O. Jacobson 1982 14 p refs To be presented at the 19th Ann. Northeast Bioengr. Conf., Hanover, New Hampshire, 15-16 Mar. 1982; sponsored by the Thayer School of Engineering Dartmouth Med. School, IEEE, ASME, and the American Society for Engineering Education
(NASA-TM-82773; E-1098) Avail: NTIS HC A02/MF A01 CSCL 06P

Or: the model it is possible to measure the force and the force direction for each individual hair as a function of the flow direction and velocity. Measurements were made at the man flow velocity .01 m/s, which is equivalent to a flow velocity in the real ear of about 1 micrometer/s. The kinematic viscosity of the liquid used in the model was 10,000 times higher than the viscosity of perilymph to attain hydrodynamic equality. Two different geometries for the stereocilia pattern were tested. First the force distribution for a W-shaped stereocilia pattern was recorded. This is the stereocilia pattern found in all real ears. It is found that the forces acting on the hairs are very regular and perpendicular to the legs of the W when the flow is directed from the outside of the W. When the flow is reversed, the forces are not reversed, but are much more irregular. This can eventually explain the half wave rectification of the nerve signals. As a second experiment, the force distribution for a V-shaped stereocilia pattern was recorded. Here the forces were irregular both when the flow was directed into the V and when it was directed against the edge of the V. T.M.

N82-19147* # National Aeronautics and Space Administration. Lewis Research Center, Cleveland, Ohio.

ENVIRONMENTAL CONTROL SYSTEMS

Frank Hrach In NASA, Langley Research Center Elec. Flight Systems Feb. 1982 p 247-252 (For primary document see N82-19134 10-01)

Avail: NTIS HC A12/MF A01 CSCL 06K

A82-13289 * # **Veiling glare reduction methods compared for ophthalmic applications.** D. R. Buchele (NASA, Lewis Research Center, Cleveland, OH). *Applied Optics*, vol. 20, Nov. 1, 1981, p. 3787-3791. 11 refs.

Veiling glare in ocular viewing was simulated by viewing the retina of an eye model through a sheet of light-scattering material lit from the front. Four methods of glare reduction were compared, namely, optical scanning, polarized light, viewing and illumination paths either coaxial or intersecting at the object, and closed circuit TV. Photographs show the effect of these methods on visibility. Polarized light was required to eliminate light specularly reflected from the instrument optics. The greatest glare reduction was obtained when the first three methods were utilized together. Glare reduction using TV was limited by nonuniform distribution of scattered light over the image. (Author)

59 MATHEMATICAL AND COMPUTER SCIENCES (GENERAL)

NS2-30949* National Aeronautics and Space Administration, Lewis Research Center, Cleveland, Ohio.

CONSTRUCTION OF SOLUTIONS FOR SOME NONLINEAR TWO-POINT BOUNDARY VALUE PROBLEMS

James A. Pennline 1982 24 p refs Presented at the 30th Ann. Meeting of the Soc. for Ind. and Appl. Math., Stanford, Calif., 19-23 Jul, 1982

(NASA-TM-82937; E-1335; NAS 1.15:82937) Avail: NTIS HC A02/MF A01 CSCL 12A

Constructive existence and uniqueness results for boundary value problems associated with some simple special cases of the second order equation $y'' = f(x, y, y')$ $0 < \alpha < x < \alpha + 1$, are sought. The approach considered is to convert the differential equation and boundary conditions to an integral equation via Green's functions, and then to apply fixed point and contraction map principles to a sequence of successive approximations. The approach is tested on several applied problems. Difficulties in trying to prove general theorems are discussed. M.G.

ORIGINAL PAGE IS
OF POOR QUALITY

60 COMPUTER OPERATIONS AND HARDWARE

Includes computer graphics and data processing.
For components see 33 *Electronics and Electrical Engineering*.

ORIGINAL PAGE IS
OF POOR QUALITY

N82-16748*# Virginia Polytechnic Inst. and State Univ., Blacksburg.

MODELING AND ANALYSIS OF POWER PROCESSING SYSTEMS (MAPPS). VOLUME 2: APPENDICES Final Technical Report, Oct. 1977 - Aug. 1980

F. C. Lee, S. Radman, R. A. Carter, C. H. Wu, Yuan Yu (TRW Defense and Space Systems Group, Redondo Beach, Calif.), and R. Chang (TRW Defense and Space Systems Group, Redondo Beach, Calif.) Dec. 1980 210 p refs

(Contract NAS3-21051)

(NASA-CR-165539; TRW-32660-8001-RU-01) Avail: NTIS HC A10/MF A01 CSCL 09B

The computer programs and derivations generated in support of the modeling and design optimization program are presented. Programs for the buck regulator, boost regulator, and buck-boost regulator are described. The computer program for the design optimization calculations is presented. Constraints for the boost and buck-boost converter were derived. Derivations of state-space equations and transfer functions are presented. Computer lists for the converters are presented, and the input parameters justified. J.D.H.

N82-17879*# Case Western Reserve Univ., Cleveland, Ohio.

INVESTIGATION AND EVALUATION OF A COMPUTER PROGRAM TO MINIMIZE THREE-DIMENSIONAL FLIGHT TIME TRACKS Final Report, 15 Sep. 1980 - 12 Aug. 1981

Frederic I. Parke 12 Aug. 1981 150 p

(Grant NAG3-101)

(NASA-CR-168419) Avail: NTIS HC A07/MF A01 CSCL 09B

The program for the DC 8-D3 flight planning was slightly modified for the three dimensional flight planning for DC 10 aircrafts. Several test runs of the modified program over the North Atlantic and North America were made for verifying the program. While geopotential height and temperature were used in a previous program as meteorological data, the modified program uses wind direction and speed and temperature received from the National Weather Service. A scanning program was written to collect required weather information from the raw data received in a packed decimal format. Two sets of weather data, the 12-hour forecast and 24-hour forecast based on 0000 GMT, are used for dynamic processes in testruns. In order to save computing time only the weather data of the North Atlantic and North America is previously stored in a PCF file and then scanned one by one. R.J.F.

N82-17880*# Case Western Reserve Univ., Cleveland, Ohio. Dept. of Computer Engineering and Science.

SHADED COMPUTER GRAPHIC TECHNIQUES FOR VISUALIZING AND INTERPRETING ANALYTIC FLUID FLOW MODELS Final Report, Jul. 1978 - Jun. 1981

Frederic I. Parke Jun. 1981 17 p refs

(Grant N8G-3207)

(NASA-CR-168418) Avail: NTIS HC A02/MF A01 CSCL 09B

Mathematical models which predict the behavior of fluid flow in different experiments are simulated using digital computers. The simulations predict values of parameters of the fluid flow (pressure, temperature and velocity vector) at many points in the fluid. Visualization of the spatial variation in the value of these parameters is important to comprehend and check the data generated, to identify the regions of interest in the flow, and for effectively communicating information about the flow to others. The state of the art imaging techniques developed in the field of three dimensional shaded computer graphics is applied to visualization of fluid flow. Use of an imaging technique known as 'SCAN' for visualizing fluid flow, is studied and the results are presented. S.L.

61 COMPUTER PROGRAMMING AND SOFTWARE

Includes computer programs, routines, and algorithms.

N82-31971*# National Aeronautics and Space Administration, Lewis Research Center, Cleveland, Ohio.

A GENERALIZED MEMORY TEST ALGORITHM

Edward J. Milner Jul. 1982 11 p refs
(NASA-TM-82874; E-1250; NAS 1.15:82874) Avail: NTIS HC A02/MF A01 CSCL 09B

A general algorithm for testing digital computer memory is presented. The test checks that (1) every bit can be cleared and set in each memory word, and (2) bits are not erroneously cleared and/or set elsewhere in memory at the same time. The algorithm can be applied to any size memory block and any size memory word. It is concise and efficient, requiring the very few cycles through memory. For example, a test of 16-bit-word-size memory requires only 384 cycles through memory. Approximately 15 seconds were required to test a 32K block of such memory, using a microcomputer having a cycle time of 133 nanoseconds.

Author

N82-33020*# National Aeronautics and Space Administration, Lewis Research Center, Cleveland, Ohio.

AUTOMATED PROCEDURE FOR DEVELOPING HYBRID COMPUTER SIMULATIONS OF TURBOFAN ENGINES. PART 1: GENERAL DESCRIPTION

John R. Szuch, Susan M. Krosel, and William M. Bruton Aug. 1982 120 p refs
(NASA-TP-1851; E-779; NAS 1.60:1851) Avail: NTIS HC A06/MF A01 CSCL 09B

A systematic, computer-aided, self-documenting methodology for developing hybrid computer simulations of turbofan engines is presented. The methodology that is presented makes use of a host program that can run on a large digital computer and a machine-dependent target (hybrid) program. The host program performs all the calculations and data manipulations that are needed to transform user-supplied engine design information to a form suitable for the hybrid computer. The host program also trims the self-contained engine model to match specified design-point information. Part I contains a general discussion of the methodology, describes a test case, and presents comparisons between hybrid simulation and specified engine performance data. Part II, a companion document, contains documentation, in the form of computer printouts, for the test case.

Author

N82-25810*# Systems Science and Software, San Diego, Calif. **ADDITIONAL EXTENSIONS TO THE NASCAP COMPUTER CODE, VOLUME 1 Contractor Report, 9 Sep. 1980 - 22 Dec. 1981**

M. J. Mandell, I. Katz, and P. R. Stannard Oct. 1981 246 p refs Revised
(Contract NAS3-22536)
(NASA-CR-167855; NAS 1.26:167855; SSS-R-82-5249-Rev) Avail: NTIS HC A11/MF A01 CSCL 09B

Extensions and revisions to a computer code that comprehensively analyzes problems of spacecraft charging (NASCAP) are documented. Using a fully three dimensional approach, it can accurately predict spacecraft potentials under a variety of conditions. Among the extensions are a multiple electron/ion gun test tank capability, and the ability to model anisotropic and time dependent space environments. Also documented are a greatly extended MATCHG program and the preliminary version of NASCAP/LEO. The interactive MATCHG code was developed into an extremely powerful tool for the study of material-environment interactions. The NASCAP/LEO, a three dimensional code to study current collection under conditions of high voltages and short Debye lengths, was distributed for preliminary testing.

M.G.

N82-31968*# SKF Technology Services, King of Prussia, Pa. Technology Services Div.

HIGH SPEED CYLINDRICAL ROLLER BEARING ANALYSIS. SKF COMPUTER PROGRAM CYBEAN. VOLUME 2: USER'S MANUAL Final Report

G. J. Dyba and R. J. Kleckner Jun. 1981 147 p refs
(Contract NAS3-22690)
(NASA-CR-165364; NAS 1.26:165364; SKF-AT81D049-Vol-2) Avail: NTIS HC A07/MF A01 CSCL 09B

CYBEAN (CYlindrical BEaring ANalysis) was created to detail radially loaded, aligned and misaligned cylindrical roller bearing performance under a variety of operating conditions. Emphasis was placed on detailing the effects of high speed, preload and system thermal coupling. Roller tilt, skew, radial, circumferential and axial displacement as well as flange contact were considered. Variable housing and flexible out-of-round outer ring geometries, and both steady state and time transient temperature calculations were enabled. The complete range of elastohydrodynamic contact considerations, employing full and partial film conditions were treated in the computation of raceway and flange contacts. The practical and correct implementation of CYBEAN is discussed. The capability to execute the program at four different levels of complexity was included. In addition, the program was updated to properly direct roller-to-raceway contact load vectors automatically in those cases where roller or ring profiles have small radii of curvature. Input and output architectures containing guidelines for use and two sample executions are detailed. R.J.F.

N82-31969*# SKF Technology Services, King of Prussia, Pa. **RESEARCH REPORT: USER'S MANUAL FOR COMPUTER PROGRAM AT81Y003 SHABERTH. STEADY STATE AND TRANSIENT THERMAL ANALYSIS OF A SHAFT BEARING SYSTEM INCLUDING BALL, CYLINDRICAL AND TAPERED ROLLER BEARINGS Final Report**

G. B. Hadden, R. J. Kleckner, M. A. Ragen, and L. Sheynin May 1981 254 p refs
(Contract NAS3-22690)
(NASA-CR-165365; NAS 1.26:165365; SKF-AT81D040) Avail: NTIS HC A12/MF A01 CSCL 09B

The SHABERTH program is capable of simulating the thermo-mechanical performance of a load support system consisting of a flexible shaft supported by up to five rolling element bearings. Any combination of ball, cylindrical, and tapered roller bearings can be used to support the shaft. The user can select models in calculating lubricant film thickness and traction forces. The formulation of the cage pocket/rolling element interaction model was revised to improve solution numerical convergence characteristics.

S.L.

N82-31970*# SKF Technology Services, King of Prussia, Pa. **RESEARCH REPORT: USER'S MANUAL FOR COMPUTER PROGRAM AT81Y005. PLANETSYS, A COMPUTER PROGRAM FOR THE STEADY STATE AND TRANSIENT THERMAL ANALYSIS OF A PLANETARY POWER TRANSMISSION SYSTEM Final Report**

G. B. Hadden, R. J. Kleckner, M. A. Ragen, G. J. Dyba, and L. Sheynin May 1981 142 p refs
(Contract NAS3-22690)
(NASA-CR-165366; NAS 1.26:165366; SKF-AT81D044) Avail: NTIS HC A07/MF A01 CSCL 09B

The material presented is structured to guide the user in the practical and correct implementation of PLANETSYS which is capable of simulating the thermomechanical performance of a multistage planetary power transmission. In this version of PLANETSYS, the user can select either SKF or NASA models in calculating lubricant film thickness and traction forces.

Author

62 COMPUTER SYSTEMS

Includes computer networks.

N82-22915* National Aeronautics and Space Administration,
Lewis Research Center, Cleveland, Ohio.

ADVANCEMENTS IN REAL-TIME ENGINE SIMULATION TECHNOLOGY

John R. Szuch 1982 12 p refs To be presented at the
18th Joint Propulsion Conf., Cleveland, 21-23 Jun. 1982
Sponsored in part by AIAA, SAE and ASME
(NASA-TM-82825; E-1177; NAS 1.15:82825) Avail: NTIS
HC A02/MF A01 CSCL 21E

The approaches used to develop real-time engine simulations
are reviewed. Both digital and hybrid (analog and digital)
techniques are discussed and specific examples of each are cited.
These approaches are assessed from the standpoint of their
usefulness for digital engine control development. A number of
NASA-sponsored simulation research activities, aimed at exploring
real-time simulation techniques, are described. These include the
development of a microcomputer-based, parallel processor system
for real-time engine simulation.

M.G.

ORIGINAL PAGE IS
OF POOR QUALITY

63 CYBERNETICS

Includes feedback and control theory.
For related information see also 54 *Man/System Technology and Life Support*.

ORIGINAL PAGE IS
OF POOR QUALITY

N82-30992*# National Aeronautics and Space Administration, Lewis Research Center, Cleveland, Ohio.

AESOP: A COMPUTER-AIDED DESIGN PROGRAM FOR LINEAR MULTIVARIABLE CONTROL SYSTEMS

Bruce Lehtinen and Lucille C. Geysler 1982 7 p ref Presented at the Am. Control Conf., Arlington, Va., 14-16 Jun. 1982 (NASA-TM-82871; E-1246; NAS 1.15:82871) Avail: NTIS HC A02/MF A01 CSCL 09#

An interactive computer program (AESOP) which solves quadratic optimal control and is discussed. The program can also be used to perform system analysis calculations such as transient and frequency responses, controllability, observability, etc., in support of the control and filter design computations.

M.G.

A82-13143 * Model degradation effects on sensor failure detection. G. G. Leininger (Purdue University, West Lafayette, IN). In: Joint Automatic Control Conference, Charlottesville, VA, June 17-19, 1981, Proceedings. Volume 2. (A82-13076 03-63) New York, American Institute of Chemical Engineers, 1981. 8 p. (FP-3A), 11 refs. Grants No. NsG-3171; No. NsG-317; No. NsG-3084.

This paper discusses the effects of imperfect modeling on the detection and isolation of sensor failures. For systems with non-zero set points, deterministic inputs or non-zero noise biases, the model mismatch appears as a bias on the stochastic innovation process. This bias, if left unaccounted for, would be sufficient to declare a false alarm failure in one or more sensors. A practical design procedure based upon the Generalized Likelihood Ratio (GLR) form uses a finite data window sequential t-test to detect and isolate model mismatch effects and soft sensor failures. Application to an eighth order model of the QCSEE turbofan engine is discussed. (Author)

A82-19064 * # A tensor approach to modeling of nonhomogeneous nonlinear systems. S. Yurkovich and M. Sain (Notre Dame, University, Notre Dame, IN). In: Annual Allerton Conference on Communication, Control, and Computing, 18th, Monticello, IL, October 8-10, 1980, Proceedings. (A82-19051 07-63) Urbana, IL, University of Illinois, 1980, p. 604-613. 13 refs. Grant No. NsG-3048.

Model following control methodology plays a key role in numerous application areas. Cases in point include flight control systems and gas turbine engine control systems. Typical uses of such a design strategy involve the determination of nonlinear models which generate requested control and response trajectories for various commands. Linear multivariable techniques provide trim about these motions; and protection logic is added to secure the hardware from excursions beyond the specification range. This paper reports upon experience in developing a general class of such nonlinear models based upon the idea of the algebraic tensor product. (Author)

64 NUMERICAL ANALYSIS

Includes iteration, difference equations, and numerical approximation.

N82-14649*# National Aeronautics and Space Administration, Lewis Research Center, Cleveland, Ohio.

APPLICATION OF INTEGRATION ALGORITHMS IN A PARALLEL PROCESSING ENVIRONMENT FOR THE SIMULATION OF JET ENGINES

Susan M. Krosei and Edward J. Milner 1982 26 p refs To be presented at the 15th Ann. Simulation Symp., Tampa, Fla., 17-19 Mar. 1982 (NASA-TM-82740; E-1059) Avail: NTIS HC A02/MF A01 CSCL 12A

The application of Predictor corrector integration algorithms developed for the digital parallel processing environment are investigated. The algorithms are implemented and evaluated through the use of a software simulator which provides an approximate representation of the parallel processing hardware. Test cases which focus on the use of the algorithms are presented and a specific application using a linear model of a turbofan engine is considered. Results are presented showing the effects of integration step size and the number of processors on simulation accuracy. Real time performance, interprocessor communication, and algorithm startup are also discussed. B.W.

N82-22822*# National Aeronautics and Space Administration, Lewis Research Center, Cleveland, Ohio.

MULTIPLE-GRID ACCELERATION OF LAX-WENDROFF ALGORITHMS

Gary M. Johnson Mar. 1982 22 p refs (NASA-TM-82843; E-1213; NAS 1.15:82843) Avail: NTIS HC A02/MF A01 CSCL 12A

A technique for accelerating the convergence of a one-step Lax-Wendroff method to a steady-state solution is discussed and its applicability extended to the more general class of two-step Lax-Wendroff methods. Several two-step methods which lead to quite efficient multiple grid algorithms are discussed. Computational results are presented using the full two dimensional Euler equations for both subcritical and shocked supercritical flows. Extensions and generalizations are mentioned. M.G.

N82-24859*# National Aeronautics and Space Administration, Lewis Research Center, Cleveland, Ohio.

RELAXATION SOLUTION OF THE FULL EULER EQUATIONS

Gary M. Johnson 1982 9 p refs Presented at the 8th Intern. Conf on Numerical Methods in Fluid Dyn., Aachen, West Germany, 28 Jun. - 2 Jul. 1982; sponsored by Deutsche Forschungsgemeinschaft, Dornier G.m.b.H., Messerschmitt-Boelkow-Blohm G.m.b.H., ONR and ERO (NASA-TM-82889; E-1265; NAS 1.15:82889) Avail: NTIS HC A02/MF A01 CSCL 12A

A numerical procedure for the relaxation solution of the full steady Euler equations is described. By embedding the Euler system in a second order surrogate system, central differencing may be used in subsonic regions while retaining matrix forms well suited to iterative solution procedures and convergence acceleration techniques. Hence, this method allows the development of stable, fully conservative differencing schemes for the solution of quite general inviscid flow problems. Results are presented for both subcritical and shocked supercritical internal flows. Comparisons are made with a standard time dependent solution algorithm. Author

N82-29075*# National Aeronautics and Space Administration, Lewis Research Center, Cleveland, Ohio.

ACCELERATION OF CONVERGENCE OF VECTOR SEQUENCES

Avram Sidi (Technion-Israel Inst. of Technology, Haifa), William F. Ford, and David A. Smith (Duke Univ.) 1982 10 p refs Presented at the 30th Anniv. Meeting of the Soc. for Ind. and Appl. Math., Stanford, Calif. 19-23 Jul 1982 (NASA-TM-82931, E-1324; NAS 1.15:82931) Avail: NTIS HC A02/MF A01 CSCL 12A

A general approach to the construction of accelerated

convergence methods for vector sequences is proposed. A simplified version of minimal polynomial extrapolation is emphasized. The convergence of this method is analyzed and it is shown that it is especially suitable for accelerating the convergence of vector sequences that are obtained when one solves linear systems of equations iteratively. M.G.

A82-31438* Numerical comparisons of nonlinear convergence accelerators. D. A. Smith (Duke University, Durham, NC) and W. F. Ford (NASA, Lewis Research Center, Computer Services Div., Cleveland, OH), *Mathematics of Computation*, vol. 38, Apr. 1982, p. 481-499, 23 refs. Grant No. Nsg-3160.

As part of a continuing program of numerical tests of convergence accelerators, the iterated Aitken's Delta-squared method, Wynn's epsilon algorithm, Brazinski's theta algorithm, and Levin's u transform are compared on a broad range of test problems: linearly convergence alternating, monotone, and irregular-sign series, logarithmically convergent series, power method and Bernoulli method sequences, alternating and monotone asymptotic series, and some perturbation series arising in applications. In each category either the epsilon algorithm or the u transform gives the best results of the four methods tested. In some cases differences among methods are slight, and in others they are quite striking. (Author)

ORIGINAL PAGE IS
OF POOR QUALITY

67 THEORETICAL MATHEMATICS

Includes topology and number theory.

A82-33605 * Diffraction by a finite strip. M. H. Williams (Purdue University, West Lafayette, IN). *Quarterly Journal of Mechanics and Applied Mathematics*, vol. 35, Feb. 1982, p. 103-124. 7 refs. Grant No. NsG-3292.

A new approach is presented to diffraction problems involving plane strip barriers or slit apertures. These are problems that display the effects of multiple interacting edges. The approach taken here provides exact, compact solutions. The theory is introduced through a series of examples that are, in fact, the 'standard' problems of the subject, diffraction of a plane oblique wave by a slit, for example. In each case, the solutions are found to depend explicitly on a single 'special' function and its Fourier transform. These fundamental functions are described, with the emphasis placed on practical computational methods. The example problems are all couched in the language of acoustics. C.R.

ORIGINAL PAGE IS
OF POOR QUALITY

71 ACOUSTICS

Includes sound generation, transmission and attenuation.
For noise pollution see 45 *Environment Pollution*.

N82-12890* National Aeronautics and Space Administration, Lewis Research Center, Cleveland, Ohio.

NUMERICAL TECHNIQUES IN LINEAR DUCT ACOUSTICS, 1980-81 UPDATE

Kenneth J. Baumeister 1981 51 p refs Presented at the 102 Winter Ann. Meeting, Washington, D.C., 15-20 Nov. 1981; sponsored by ASME

(NASA-TM-82730, E-1034) Avail: NTIS HC A04/MF A01 CSCL 20A

A review is presented covering finite element and finite difference analysis of small amplitude (linear) sound propagation in straight and variable area ducts. This review stresses the new work performed during the 1980-1981 time frame, although a brief discussion of earlier work is also included. Emphasis is placed on the latest state of the art in numerical techniques.

Author

N82-12891* National Aeronautics and Space Administration, Lewis Research Center, Cleveland, Ohio.

VERIFICATION OF AN ACOUSTIC TRANSMISSION MATRIX ANALYSIS OF SOUND PROPAGATION IN A VARIABLE AREA DUCT WITHOUT FLOW

J. H. Miles 1981 15 p refs Presented at the 102 Meeting of the Acoustical Soc. of Am., Miami Beach, Fla., 1-4 Dec. 1981

(NASA-TM-82741; E-1053) Avail: NTIS HC A02/MF A01 CSCL 20A

A predicted standing wave pressure and phase angle profile for a hard wall rectangular duct with a region of converging-diverging area variation is compared to published experimental measurements in a study of sound propagation without flow. The factor of 1/2 area variation used is sufficient magnitude to produce large reflections. The prediction is based on a transmission matrix approach developed for the analysis of sound propagation in a variable area duct with and without flow. The agreement between the measured and predicted results is shown to be excellent.

Author

N82-14881* National Aeronautics and Space Administration, Lewis Research Center, Cleveland, Ohio.

MODE PROPAGATION IN NONUNIFORM CIRCULAR DUCTS WITH POTENTIAL FLOW

Y. C. Cho and K. U. Ingard (MIT) 1982 15 p refs Presented at the 20th Aerospace Sci. Conf., Orlando, Fla., 11-14 Jan. 1982

(NASA-TM-82776; E-1086, AIAA-Paper-82-0122) Avail: NTIS HC A02/MF A01 CSCL 20A

A previously reported closed form solution is expanded to determine effects of isentropic mean flow on mode propagation in a slowly converging-diverging duct, a circular cosh duct. On the assumption of uniform steady fluid density, the mean flow increases the power transmission coefficient. The increase is directly related to the increase of the cutoff ratio at the duct throat. With the negligible transverse gradients of the steady fluid variables, the conversion from one mode to another is negligible, and the power transmission coefficient remains unchanged with the mean flow direction reversed. With a proper choice of frequency parameter, many different modes can be made subject to a single value of the power transmission loss. A systematic method to include the effects of the gradients of the steady fluid variables is also described.

B.W.

N82-15847* National Aeronautics and Space Administration, Lewis Research Center, Cleveland, Ohio.

APPLICATION OF STEADY STATE FINITE ELEMENT AND TRANSIENT FINITE DIFFERENCE THEORY TO SOUND PROPAGATION IN A VARIABLE AREA DUCT: A COMPARISON WITH EXPERIMENT

Kenneth J. Baumeister, W. Eversman (Missouri Univ., Rolla), R. J. Aetley (Missouri, Univ., Rolla), and J. W. White (Tennessee Univ., Knoxville) 1981 14 p refs Presented at the 7th Aeroacoustics Conf., Palo Alto, Calif., 5-7 Oct. 1981; sponsored

by AIAA

(NASA-TM-82678; E-960) Avail: NTIS HC A02/MF A01 CSCL 20A

Sound propagation without flow in a rectangular duct with a converging-diverging area variation was studied experimentally and theoretically. The area variation was of sufficient magnitude to produce large reflections and induce modal scattering. The rms (root-mean-squared) pressure and phase angle on both the flat and curved surface were measured and tabulated. The steady state finite element theory and the transient finite difference theory are in good agreement with the data. It is concluded that numerical finite difference and finite element theories appear ideally suited for handling duct propagation problems which encounter large area variations.

M.G.

N82-16808* National Aeronautics and Space Administration, Lewis Research Center, Cleveland, Ohio.

NOISE OF THE SR-3 PROPELLER MODEL AT 2 DEG AND 4 DEG ANGLE OF ATTACK

James H. Dittmar and Robert J. Jeracki Dec 1981 30 p refs

(NASA-TM-82738; E-1051) Avail: NTIS HC A03/MF A01 CSCL 20A

The noise effect of operating supersonic tip speed propellers at angle of attack with respect to the incoming flow was determined. Increases in the maximum blade passage noise were observed for the propeller operating at angle of attack. The noise increase was not symmetrical with one wall of the wind tunnel having significantly more noise increase than the other wall. This was apparently the result of the rotational direction of the propeller. The lack of symmetry of the noise at angle of attack to the use of oppositely rotating propellers on opposite sides of an airplane fuselage as a way of minimizing the noise due to operation at angle of attack.

J.D.H.

N82-16809* National Aeronautics and Space Administration, Lewis Research Center, Cleveland, Ohio.

A SHOCK WAVE APPROACH TO THE NOISE OF SUPERSONIC PROPELLERS

James H. Dittmar and Edward J. Rice Dec. 1981 19 p refs (NASA-TM-82752; E-1068) Avail: NTIS HC A02/MF A01 CSCL 20A

To model propeller noise expected for a turboprop aircraft, the pressure ratio across the shock at the propeller tip was calculated and compared with noise data from three propellers. At helical tip Mach numbers over 1.0, using only the tip shock wave, the model gave a fairly good prediction of the noise for a bladed propeller and for a propeller swept for aerodynamic purposes. However for another propeller, which was highly swept and designed to have noise cancellations from the inboard propeller sections, the shock strength from the tip over predicted the noise. In general the good agreement indicates that shock theory is a viable method for predicting the noise from these supersonic propellers but that the shock strengths from all of the blade sections need to be properly included.

M.G.

N82-19944* National Aeronautics and Space Administration, Lewis Research Center, Cleveland, Ohio.

EFFECT OF FACILITY VARIATION ON THE ACOUSTIC CHARACTERISTICS OF THREE SINGLE STREAM NOZZLES

Orlando A. Gutierrez 1980 38 p refs Presented at the 100th Meeting of the Acoust. Soc. of Am., Los Angeles, 17-21 Nov. 1980

(NASA-TM-81635; E-646) Avail: NTIS HC A03/MF A01 CSCL 20A

The characteristics of the jet noise produced by three single stream nozzles were investigated statistically at the NASA-Lewis Research Center outdoor jet acoustic facility. The nozzles consisted of a 7.6 cm diameter convergent conical, a 10.2 cm diameter convergent conical and an 8-lobe daisy nozzle with 7.6 cm equivalent diameter flow area. The same nozzles were tested previously at cold flow conditions in other facilities such as the Royal Aircraft Establishment (RAE) 7.3 m acoustic wind tunnel. The acoustic experiments at NASA covered pressure ratios from 1.4 to 2.5 at total temperatures of 811 K and ambient. The data obtained with four different microphone arrays are compared. The results are also compared with data taken at the RAE facility and with a NASA prediction procedure.

Author

N82-21036* # National Aeronautics and Space Administration, Lewis Research Center, Cleveland, Ohio.
FORWARD ACOUSTIC PERFORMANCE OF A MODEL TURBOFAN DESIGNED FOR A HIGH SPECIFIC FLOW (QF-14)

James G. Lucas, Richard P. Woodward, and Charles J. Michels
Mar. 1982 20 p refs
(NASA-TP-1968; E-777; NAS 1.60:1968) Avail: NTIS HC A02/MF A01 CSCL 20A

Forward noise and overall aerodynamic performance are presented for a high-tip-speed fan having an exceptionally high average axial Mach number at the rotor inlet. This high Mach number is intended to attenuate forward noise at both the design-speed takeoff point, and at the unconventional low-pressure-ratio, design-speed approach point. As speed was increased near design, all forward noise components were reduced, and rear noise in the discharge duct was increased, indicating that the high Mach number flow at the rotor face is attenuating forward noise at takeoff. The fan at takeoff is some 5.5 to 11 dB quieter than several reference fans. Data at the point closest to approach indicated tentatively that the design-speed approach mode was 3 dB quieter than the conventional mode.

M.G.

N82-21998* # National Aeronautics and Space Administration, Lewis Research Center, Cleveland, Ohio.

A PRELIMINARY COMPARISON BETWEEN THE SR-3 PROPELLER NOISE IN FLIGHT AND IN A WIND TUNNEL

James H. Dittmar and Paul L. Lasagna 1982 14 p refs
Presented at the 103rd Meeting of the Acoust. Soc. of Am., Chicago, 27-30 Apr. 1982

(NASA-TM-82805; E-1144; NAS 1.15:82805) Avail: NTIS HC A02/MF A01 CSCL 20A

The noise generated by supersonic-tip-speed propellers is addressed. Models of such propellers were tested for acoustics in the Lewis 8-by-6-foot wind tunnel. One of these propeller models, SR-3, was tested in flight on the Jetstar airplane and noise data were obtained. Preliminary comparisons of the maximum blade passing tone variation with helical tip Mach number taken in flight with those taken in the tunnel showed good agreement when corrected to the same test conditions. This indicated that the wind tunnel is a viable location for measuring the noise of these propeller models. Comparisons of the directivities at 0.6 and 0.7 axial Mach number showed reasonable agreement. At 0.75 and 0.8 axial Mach number the tunnel directivity data fell off more towards the front than did the airplane data. A possible explanation for this is boundary layer refraction which could be different in the wind tunnel from that in flight. This may imply that some corrections should be applied to both the airplane and wind tunnel data at the forward angles. At and aft of the peak noise angle the boundary layer refraction does not appear to be significant and no correction appears necessary.

M.G.

N82-22951* # National Aeronautics and Space Administration, Lewis Research Center, Cleveland, Ohio.

PRESSURE TRANSFER FUNCTION OF A JT15D NOZZLE DUE TO ACOUSTIC AND CONVECTED ENTROPY FLUCTUATIONS

J. H. Miles 1982 39 p refs Presented at the 103rd Meeting of the Acoust. Soc. of Am., Chicago, 26-30 Apr. 1982
(NASA-TM-82842; E-1212; NAS 1.15:82842) Avail: NTIS HC A03/MF A01 CSCL 20A

An acoustic transmission matrix analysis of sound propagation in a variable area duct with and without flow is extended to include convected entropy fluctuations. The boundary conditions used in the analysis are a transfer function relating entropy and pressure at the nozzle inlet and the nozzle exit impedance. The nozzle pressure transfer function calculated is compared with JT15D turbofan engine nozzle data. The one dimensional theory for sound propagation in a variable area nozzle with flow but without convected entropy is good at the low engine speeds where the nozzle exit Mach number is low ($M=0.2$) and the duct exit impedance model is good. The effect of convected entropy appears to be so negligible that it is obscured by the inaccuracy of the nozzle exit impedance model, the lack of information on the magnitude of the convected entropy and its phase relationship with the pressure, and the scatter in the data. An improved duct exit impedance model is required at the higher engine speeds where the nozzle exit Mach number is high ($M=0.56$) and at low frequencies (below 120 Hz).

B.W.

N82-24942* # National Aeronautics and Space Administration, Lewis Research Center, Cleveland, Ohio.

AEROACOUSTIC PERFORMANCE OF AN EXTERNALLY BLOWN FLAP CONFIGURATION WITH SEVERAL FLAP NOISE SUPPRESSION DEVICES

Daniel J. McKinzie, Jr. May 1982 30 p refs
(NASA-TP-1995; E-573; NAS 1.60:1995) Avail: NTIS HC A03/MF A01 CSCL 20A

Small scale model acoustic experiments were conducted to measure the noise produced in the flyover and sideline planes by an engine under the wing externally blown flap configuration in its approach attitude. Broadband low frequency noise reductions as large as 9 dB were produced by reducing the separation distance between the nozzle exhaust plane and the flaps. Experiments were also conducted to determine the noise suppression effectiveness in comparison with a reference configuration of three passive types of devices that were located on the jet impingement surfaces of the reference configuration. These devices produced noise reductions that varied up to 10 dB at reduced separation distances. In addition, a qualitative estimate of the noise suppression characteristics of the separate devices was made. Finally static aerodynamic performance data were obtained to evaluate the penalties incurred by these suppression devices. The test results suggest that further parametric studies are required in order to understand more fully the noise mechanisms that are affected by the suppression devices used.

M.G.

N82-31068* # National Aeronautics and Space Administration, Lewis Research Center, Cleveland, Ohio.

FINITE ELEMENT-INTEGRAL SIMULATION OF STATIC AND FLIGHT FAN NOISE RADIATION FROM THE JT15D TURBOFAN ENGINE

Kenneth J. Baumeister and Scott J. Horowitz (Lockheed-Georgia, Marietta) 1982 16 p refs Presented at the Winter Ann. Meeting of the Am. Soc. of Mech. Engr., Phoenix, Ariz., 14-19 Nov. 1982

(NASA-TM-82936; E-1332; NAS 1.15:82936) Avail: NTIS HC A02/MF A01 CSCL 20A

An iterative finite element integral technique is used to predict the sound field radiated from the JT15D turbofan inlet. The sound field is divided into two regions; the sound field within and near the inlet which is computed using the finite element method and the radiation field beyond the inlet which is calculated using an integral solution technique. The velocity potential formulation of the acoustic wave equation was employed in the program. For some single mode JT15D data, the theory and experiment are in good agreement for the far field radiation pattern as well as suppressor attenuation. Also, the computer program is used to simulate flight effects that cannot be performed on a ground static test stand.

Author

N82-32082* # National Aeronautics and Space Administration, Lewis Research Center, Cleveland, Ohio.

ROUGH ANALYSIS OF INSTALLATION EFFECTS ON TURBOPROP NOISE

Paul A. Durbin and John F. Groeneweg 1982 17 p refs Proposed for Presentation at the Acoust. Soc. of Am., Orlando, Fla., 8-12 Nov. 1982

(NASA-TM-82924; E-1316; NAS 1.15:82924) Avail: NTIS HC A02/MF A01 CSCL 20A

A rough analysis of noise from a propeller operated at angle of attack, and in the nonuniform flow due to a line vortex approximating a wing flow field suggests installation can significantly affect turboprop noise levels. On one side of the propeller, where the blades approach the horizontal plane from above, decreases of noise occur; while on the other side noise increases. The noise reduction is due to negative interference of steady and unsteady sources. An angle of attack, or distance between propeller and vortex, exists for which noise is a minimum.

Author

A82-17603 * # Propeller tip vortex - A possible contributor to aircraft cabin noise. B. A. Miller, J. H. Dittmar, and R. J. Jeracki (NASA, Lewis Research Center, Cleveland, OH). *Journal of Aircraft*, vol. 19, Jan. 1982, p. 84-86. 8 refs.

Wind tunnel model tests support the hypothesis that a propeller tip vortex may subject a downstream wing surface to greater

excitation than would be experienced by the aircraft fuselage side wall exposed to propeller-generated noise, ultimately transmitting this structural response to incident dynamic pressure to the cabin interior. Even if structure-borne excitations are less efficient than airborne excitations in the creation of cabin noise, the higher level of the former could still govern cabin noise levels. O.C.

N82-16810*# Georgia Inst. of Tech., Atlanta. School of Aerospace Engineering.
PREDICTION OF SOUND RADIATION FROM DIFFERENT PRACTICAL JET ENGINE INLETS Semiannual Status Report, 1 Jun. 1981 - 1 Dec. 1981
Ben T. Zinn and William L. Meyer 1982 127 p refs
(Grant NAG3-67)
(NASA-CR-165120) Avail: NTIS HC A07/MF A01 CSCL 20A

The computer codes necessary for this study were developed and checked against exact solutions generated by the point source method using the NASA Lewis QCSEE inlet geometry. These computer codes were used to predict the acoustic properties of the following five inlet configurations: the NASA Langley Bellmouth, the NASA Lewis JT15D-1 Ground Test Nacelle, and three finite hyperbolic inlets of 50, 70 and 90 degrees. Thirty-five computer runs were done for the NASA Langley Bellmouth. For each of these computer runs, the reflection coefficient at the duct exit plane was calculated as was the far field radiation pattern. These results are presented in both graphical and tabular form with many of the results cross plotted so that trends in the results versus cut-off ratio (wave number) and tangential mode number may be easily identified. Author

N82-18994*# California Univ., Los Angeles. School of Engineering and Applied Science.
THE VELOCITY FIELD NEAR THE ORIFICE OF A HELMHOLTZ RESONATOR IN GRAZING FLOW
Andrew F. Charvat and Bruce E. Walker Mar. 1981 53 p refs
(Grant NsG-3236)
(NASA-CR-168548; UCLA-ENG-81-101) Avail: NTIS HC A04/MF A01 CSCL 20A

Measurement of the time-dependent velocities induced inside and outside the opening of acoustically excited, two-dimensional Helmholtz resonator imbedded in a grazing flow are presented. The remarkably clear structure of the perturbation field which evokes a pulsating source and a coherently pulsating vortex-image pair is described. The simple phenomenological 'lid-model' which correlates the variation in the components of the acoustic impedance with the velocity of the grazing flow is discussed and extended. Author

N82-21031*# Avco Lycoming Div., Stratford, Conn.
YF 102 IN-DUCT COMBUSTOR NOISE MEASUREMENTS WITH A TURBINE NOZZLE, VOLUME 1 Final Report, Sep. 1979 - Mar. 1981
Craig A. Wilson and James M. OConnell Sep. 1981 63 p refs
Contract NAS3-21974

(NASA-CR-165562-Vol-1; NAS 1.26:165562-Vol-1; LYC-81-32-Vol-1) Avail: NTIS HC A04/MF A01 CSCL 20A
The internal noise generated by an Avco Lycoming YF-102 engine combustor installed in a test rig was recorded. Two configurations were tested one with and one without the first stage turbine nozzle installed. Acoustic probes and accessories were used. Internal dynamic pressure level measurements were made at ten locations within the combustor. The combustor rig, the test procedures, and data acquisition and reduction systems are described. Tables and plots of narrow band and one third octave band pressure level spectra are included. S.L.

N82-21032*# Avco Lycoming Div., Stratford, Conn.
YF 102 IN-DUCT COMBUSTOR NOISE MEASUREMENTS WITH A TURBINE NOZZLE, VOLUME 2 Final Report
Craig A. Wilson and James M. OConnell Sep. 1981 232 p refs
(Contract NAS3-21974)
(NASA-CR-165562-Vol-2; NAS 1.26:165562-Vol-2;

LYC-81-32-Vol-2) Avail: NTIS HC A11/MF A01 CSCL 20A
The internal noise generated by an Avco Lycoming YF-102 engine combustor installed in a test rig was recorded. The one third octave band pressure level spectra is presented. S.L.

N82-27090*# Georgia Inst. of Tech., Atlanta. School of Aerospace Engineering.
ACOUSTIC PROPERTIES OF TURBOFAN INLETS Final Technical Report, 1 Sep. 1974 - 31 Oct. 1981
Ben T. Zinn, Robert K. Sigman, and Scott J. Horowitz 31 Oct. 1981 6 p refs
(Grant NsG-3038)
(NASA-CR-169016; NAS 1.26:169016) Avail: NTIS HC A02/MF A01 CSCL 20A
The acoustic field within a duct containing a nonuniform steady flow was predicted. This analysis used the finite element method to calculate the velocity potential within the duct. S.L.

A82-10454*# Analytical and experimental investigation of the propagation and attenuation of sound in extended reaction lined ducts. A. S. Hersh (Hersh Acoustical Engineering, Chatsworth, CA), S. B. Dong (California University, Los Angeles, CA), and B. Walker. *American Institute of Aeronautics and Astronautics, Aeroacoustics Conference, 7th, Palo Alto, CA, Oct. 5-7, 1981, Paper 81-2014*. 31 p. 10 refs. Contract No. NAS3-21975.

Results are presented of an analytical and experimental study of the attenuation and propagation of harmonically excited sound waves in an extended reaction lined cylindrical duct. The duct geometry considered consisted of an annular outer region of bulk material surrounding an inner cylinder of air. The coupled wave equations governing the motion of the sound in both the inner and annular regions were solved numerically. The numerically predicted attenuation and propagation constants were in excellent agreement with measured values using Kevlar as the liner material for plane-wave mode (0,0) excitation over the frequency from 100 to 7,000 Hz. Although the numerical model was verified using Kevlar, it can be used with any fibrous constructed bulk liner. The results of this study demonstrate that a good start has been made on the numerical modelling of the acoustic performance of extended reaction liners. (Author)

A82-10460*# Sound generated in a cascade by three-dimensional disturbances convected in a subsonic flow. H. Atassi and G. Hamad (Notre Dame University, Notre Dame, IN). *American Institute of Aeronautics and Astronautics, Aeroacoustics Conference, 7th, Palo Alto, CA, Oct. 5-7, 1981, Paper 81-2046*. 14 p. 20 refs. Grant No. NsG-3195.

Discrete tone sound generation in a subsonic fan subject to three-dimensional disturbances is investigated. The analytical model used treats the fan rotor and stator as linear cascades of thin airfoils in a rectangular duct subject to a three-dimensional gust for which a complete aerodynamic theory already exists. The sound pressure can then be cast as the sum of a finite number of discrete sound waves (modes) the magnitude of which depends on an unknown function satisfying a singular integral equation. Similarity rules are derived to reduce the problem to that of a two-dimensional gust. Three-dimensional effects on the cut-off condition, the sound pressure, and the acoustic power are first investigated for each mode. The theory is then applied to noise generated by typical rotor-wake-defect and rotor-tip-vortex disturbances interacting with a stator. (Author)

A82-14044*# Methods for the calculation of axial wave numbers in lined ducts with mean flow. W. Eversman (Missouri-Rolla, University, Rolla, MO). *Acoustical Society of America, Meeting, 101st, Ottawa, Canada, May 18-22, 1981, Paper*. 45 p. 50 refs. Grant No. NsG-3231.

A survey is made of the methods available for the calculation of axial wave numbers in lined ducts. Rectangular and circular ducts with both uniform and non-uniform flow are considered as are ducts with peripherally varying liners. A historical perspective is provided by a discussion of the classical methods for computing attenuation when no mean flow is present. When flow is present these techniques

become either impractical or impossible. A number of direct eigenvalue determination schemes which have been used when flow is present are discussed. Methods described are extensions of the classical no-flow technique, perturbation methods based on the no-flow technique, direct integration methods for solution of the eigenvalue equation, an integration-iteration method based on the governing differential equation for acoustic transmission, Galerkin methods, finite difference methods, and finite element methods.

(Author)

A82-17663 * # Acoustic transmission in lined flow ducts - A finite element eigenvalue problem. R. J. Astley (Canterbury, University, Christchurch, New Zealand) and W. Eversman (Missouri-Rolla, University, Rolla, MO). In: International Conference on Finite Elements in Flow Problems, 3rd, Banff, Alberta, Canada, June 10-13, 1980, Proceedings, Volume 2. (A82-17651 06-34) Calgary, Alberta, Canada, University of Calgary, 1981, p. 123-132. 6 refs. Research supported by the Boeing Wichita Co.; Grant No. NsG-3231.

The problem of acoustical transmission in lined ducts with subsonic mean flow is of considerable practical interest in the context of fan noise attenuation in the ducted inlet regions of turbofan aircraft engines. If nonaxisymmetric liners are present, a loss of axial symmetry results, and the study of acoustic transmission involves the solution of a full two-dimensional eigenvalue problem. The reported investigation is concerned with such an eigenvalue problem. The employed method of solution is effectively a two-dimensional analog of an approach considered by Astley and Eversman (1979). The approach makes use of a Galerkin Finite Element Method whereby the weighting and basis functions are generated automatically by the discretization.

G.R.

A82-36195 * Conversion of acoustic energy by lossless liners. W. Möhring (Max-Planck-Institut für Strömungsforschung, Göttingen, West Germany) and W. Eversman (Missouri-Rolla, University, Rolla, MO). *Journal of Sound and Vibration*, vol. 82, June 8, 1982, p. 371-381. 16 refs. Grant No. NsG-3231.

The Blokhintzev acoustic energy equation is applied to a two-dimensional duct containing a uniform flow with a finite length lining. It is shown that the difference of the incident and outgoing acoustic energy differs in general from the energy dissipated in the liner, the difference being related to the displacements at the liner's edges. It is shown that in the case of a locally reacting lossless liner for frequencies below the first cut-off frequency and for low Mach number acoustic energy is generated if the flow and the incident sound wave are in the same direction and is absorbed if these two directions are opposite unless special edge conditions are met. Furthermore it is shown under the same conditions that the ratio of the reflection coefficient at finite flow velocity to the reflection coefficient at vanishing velocity is to first order in Mach number independent of the liner characteristics. A numerical calculation confirms these predictions at least for mass-like linear admittance.

(Author)

A82-45165 The acoustical structure of highly porous open-cell foams. R. F. Lambert (Minnesota, University, Minneapolis, MN). *Acoustical Society of America, Journal*, vol. 72, Sept. 1982, p. 879-887. 12 refs. NSF Grant No. MEA-80-11362; Grant No. NAG3-161.

This work concerns both the theoretical prediction and measurement of structural parameters in open-cell highly porous polyurethane foams. Of particular interest are the dynamic flow resistance, thermal time constant, and mass structure factor and their dependence on frequency and geometry of the cellular structure. The predictions of cell size parameters, static flow resistance, and heat transfer as accounted for by a Nusselt number are compared with measurement. Since the static flow resistance and inverse thermal time constant are interrelated via the 'mean' pore size parameter of Biot, only two independent measurements such as volume porosity and mean filament diameter are required to make the predictions for a given fluid condition. The agreements between this theory and nonacoustical experiments are excellent.

(Author)

72 ATOMIC AND MOLECULAR PHYSICS

Includes atomic structure and molecular spectra.

ORIGINAL PAGE IS
OF POOR QUALITY

NS2-21033*# Avco Lycoming Div., Stratford, Conn.
**YF 102 IN-DUCT COMBUSTOR NOISE MEASUREMENTS
WITH A TURBINE NOZZLE. VOLUME 3 Final Report**
Craig A. Wilson and James M. O'Connell Sep. 1981 244 p
refs

(Contract NAS3-21974)
(NASA-CR-165562-Vol-3; NAS 1.26:165562-Vol-3;
LYC-81-32-Vol-3) Avail: NTIS HC A11/MF A01 CSCL 20A
The internal noise generated by an Avco Lycoming YF-102
engine combustor installed in a test rig was recorded. The narrow
band pressure level spectra is presented. S.L.

74 OPTICS

Includes light phenomena.

ORIGINAL PAGE IS
OF POOR QUALITY

N82-15897 National Aeronautics and Space Administration,
Lewis Research Center, Cleveland, Ohio.

ROLE OF OPTICAL COMPUTERS IN AERONAUTICAL CONTROL APPLICATIONS

Robert J. Baumbick /in NASA. Langley Research Center Opt.
Inform. Process. for Aerospace Appl. Dec. 1981 p 33-43 (For
primary document see N82-15894 08-74)

Avail: NTIS HC A15/MF A01 CSCL 30F

The role that optical computers play in aircraft control is determined. The optical computer has the potential high speed capability required, especially for matrix/matrix operations. The optical computer also has the potential for handling nonlinear simulations in real time. They are also more compatible with fiber optic signal transmission. Optics also permit the use of passive sensors to measure process variables. No electrical energy need be supplied to the sensor. Complex interfacing between optical sensors and the optical computer is avoided if the optical sensor outputs can be directly processed by the optical computer. S.L.

75 PLASMA PHYSICS

Includes magnetohydrodynamics and plasma fusion.
For ionospheric plasmas see 46 *Geophysics*. For space
plasmas see 90 *Astrophysics*.

N82-12943*# National Aeronautics and Space Administration,
Lewis Research Center, Cleveland, Ohio.

END REGION AND CURRENT CONSOLIDATION EFFECTS UPON THE PERFORMANCE OF AN MHD CHANNEL FOR THE ETF CONCEPTUAL DESIGN

S. Y. Wang and J. Marlin Smith [1981] 9 p refs To be
presented at the 20th Aerospace Sci. Conf., Orlando, Fla.,
11-14 Jan. 1982; sponsored by AIAA
(Contract DE-A101-77ET-10769)
(NASA-TM-82744; DOE/NASA/10769-22; E-1057) Avail:
NTIS HC A02/MF A01 CSCL 201

The effects of MHD channel end regions on the overall
power generation were considered. The peak plant thermodynamic
efficiency was found to be slightly lower than for the active
region (41%). The channel operating point for the peak efficiency
was shifted to the supersonic mode (Mach No., M sub c approx.
1.1) rather than the previous subsonic operation (M sub c approx.
0.9). The sensitivity of the channel performance to the B-field,
diffuser recovery coefficient, channel load parameter, Mach
number, and combustor pressure is also discussed. In addition,
methods for operating the channel in a constant-current mode
are investigated. This mode is highly desirable from the standpoint
of simplifying the current and voltage consolidation for the inverter
system. This simplification could result in significant savings in
the cost of the equipment. The initial results indicate that this
simplification is possible, even under a strict Hall field constraint,
with reasonable plant thermodynamic efficiency (40.5%). N.W.

N82-13908*# National Aeronautics and Space Administration,
Lewis Research Center, Cleveland, Ohio.

EFFECT OF VACUUM EXHAUST PRESSURE ON THE PERFORMANCE OF MHD DUCTS AT HIGH D-FIELD

J. Marlin Smith, J. L. Morgan, and Shih-Ying Wang 1982
13 p refs Presented at the 20th Aerospace Sci. Meeting,
Orlando, Fla., 11-14 Jan. 1982; sponsored by AIAA
(Contract DE-A101-77ET-10769)
(NASA-TM-82750; DOE/NASA/10769-23; F-1066) Avail:
NTIS HC A02/MF A01 CSCL 201

The effect of area ratio variation on the performance of a
supersonic Hall MHD duct is investigated. Results indicate that
for a given combustion pressure there exists an area ratio below
which the power generating region of the duct is shock free
and the power output increases linearly with the square of the
magnetic field. For area ratios greater than this, a shock forms
in the power generating region which moves upstream with
increasing magnetic field strength resulting in a less rapid raise
in the power output. The shock can be moved downstream by
either increasing the combustion pressure or decreasing the
exhaust pressure. The influence of these effects upon duct
performance is presented. B.W.

N82-25961*# National Aeronautics and Space Administration,
Lewis Research Center, Cleveland, Ohio.

RESULTS AND COMPARISON OF HALL AND DW DUCT EXPERIMENTS

J. Marlin Smith and J. L. Morgan 1982 10 p refs Proposed
for presentation at the 20th Symp. on Eng. Aspects of Magneto-
hydrodyn., Los Angeles, 14-16 Jun. 1982
(Contract DE-A101-77ET-10769)
(NASA-TM-82864; DOE/NASA/10769-25; E1233; NAS
1.15:82864) Avail: NTIS HC A02/MF A01 CSCL 201

Experimental data from recent tests of a 45 deg diagonal
wall duct are presented and compared with the results of a
similar Hall duct. It is shown that while the peak power density
of the two devices is approximately equal that the diagonal
wall duct produces greater total power output due to its ability
to better utilize the available magnetic field. Author

A82-17889*# End region and current consolidation effects
upon the performance of an MHD channel for the ETF conceptual
design. S. Y. Wang and J. M. Smith (NASA, Lewis Research Center,
Cleveland, OH). *American Institute of Aeronautics and Astronautics,
Aerospace Sciences Meeting, 20th, Orlando, FL, Jan. 11-14, 1982,
Paper 82-0325*, 5 p. 6 refs.

It is noted that operating conditions which yielded a peak
thermodynamic efficiency (41%) for an EFT-size MHD/steam power
plant were previously (Wang et al., 1981; Staiger, 1981) identified by
considering only the active region (the primary portion for power
production) of an MHD channel. These previous efforts are extended
here to include an investigation of the effects of the channel end
regions on overall power generation. Considering these effects, the
peak plant thermodynamic efficiency is found to be slightly lowered
(40.7%); the channel operating point for peak efficiency is shifted to
the supersonic mode (Mach number of approximately 1.1) rather
than the previous subsonic operation (Mach number of approxi-
mately 0.9). Also discussed is the sensitivity of the channel
performance to the B-field, diffuser recovery coefficient, channel
load parameter, Mach number, and combustor pressure. C.R.

A82-17941*# Impact of uniform electrode current distribu-
tion on ETF. D. J. Bents (NASA, Lewis Research Center, Cleveland,
OH). *American Institute of Aeronautics and Astronautics, Aerospace
Sciences Meeting, 20th, Orlando, FL, Jan. 11-14, 1982, Paper
82-0423*, 8 p. 5 refs.

A basic reason for the complexity and sheer volume of electrode
consolidation hardware in the MHD ETF Powertrain system is the
channel electrode current distribution, which is non-uniform. If the
channel design is altered to provide uniform electrode current
distribution, the amount of hardware required decreases consider-
ably, but at the possible expense of degraded channel performance.
This paper explains the design impacts on the ETF electrode
consolidation network associated with uniform channel electrode
current distribution, and presents the alternate consolidation designs
which occur. They are compared to the baseline (non-uniform
current) design with respect to performance, and hardware require-
ments. A rational basis is presented for comparing the requirements
for the different designs and the savings that result from uniform
current distribution. Performance and cost impacts upon the
combined cycle plant are discussed. (Author)

A82-20292*# Effect of vacuum exhaust pressure on the
performance of MHD ducts at high B-field. J. M. Smith, J. L.
Morgan, and S.-Y. Wang (NASA, Lewis Research Center, Cleveland,
OH). *American Institute of Aeronautics and Astronautics, Aerospace
Sciences Meeting, 20th, Orlando, FL, Jan. 11-14, 1982, Paper
82-0396*, 10 p.

The effect of area ratio variation on the performance of a
supersonic Hall MHD duct showed that for a given combustion
pressure there exists an area ratio below which the power generating
region of the duct is shock free and the power output increases
linearly with the square of the magnetic field. For area ratios greater
than this, a shock forms in the power generating region which moves
upstream with increasing magnetic field strength resulting in a less
rapid raise in the power output. The shock can be moved
downstream by either increasing the combustion pressure or de-
creasing the exhaust pressure. The influence of these effects upon
duct performance is presented in this paper. (Author)

N82-10880*# Colorado State Univ., Fort Collins. Dept. of
Physics.
**EXPERIMENTAL SIMULATION OF BIASED SOLAR ARRAYS
WITH THE SPACE PLASMA Annual Report**
Harold R. Kaufman and Raymond S. Robinson May 1981
71 p refs
(Grant NSG-3196)
(NASA-CR-165485) Avail: NTIS HC A04/MF A01 CSCL
201

The phenomenon of unexpectedly large leakage currents
collected by small exposed areas of high voltage solar arrays
operating in a plasma environment was investigated. Polyimide
(Kapton) was the insulating material used in all tests. Both positive
bias (electron collection) and negative bias (ion collection) tests

ORIGINAL PAGE IS
OF POOR QUALITY

ORIGINAL PAGE IS OF POOR QUALITY

were performed. A mode change in the electron collection mechanism was associated with a glow discharge process and was found to be related to the neutral background density. Results indicate that the glow discharge collection mode does not occur in a space environment where the background density is considerably lower than that of the vacuum facility used. B.W.

N82-24078* # Wichita State Univ., Kans. Dept. of Mechanical Engineering.

NUMERICAL MODELING OF THREE-DIMENSIONAL CONFINED FLOWS Final Report

Mahesh S. Greywall Aug. 1981 78 p refs
(Grant NSG-3186; Contract DE-AI01-77ET-10769)
(NASA-CR-165583; NAS 1.26:165583) Avail; NTIS
HC A05/M: A01 CSDL 201

A three dimensional confined flow model is presented. The flow field is computed by calculating velocity and enthalpy along a set of streamlines. The finite difference equations are obtained by applying conservation principles to streamtubes constructed around the chosen streamlines. With appropriate substitutions for the body force terms, the approach computes three dimensional magnetohydrodynamic channel flows. A listing of a computer code, based on this approach is presented in FORTRAN IV language. The code computes three dimensional compressible viscous flow through a rectangular duct, with the duct cross section specified along the axis. S.L.

A82-11117 * Turbulence in argon shock waves. J. A. Johnson, III, J. P. Santiago, and L. I. (Rutgers University, New Brunswick, NJ). *Physics Letters*, vol. 83A, June 29, 1981, p. 443-445, 12 refs. Grant No. NSG-3280.

Irregular density fluctuations with turbulent-like behaviors are found in ionizing shock fronts produced by an arc-driven shock tube. Electric probes are used as the primary diagnostic. Spectral analyses show statistical patterns which seem frozen-in and characterizable by a dominant mode and its harmonics. (Author)

A82-17585 * Stoichiometry-controlled compensation in liquid encapsulated Czochralski GaAs. D. E. Holmes, R. T. Chen, K. R. Elliott, and C. G. Kirkpatrick (Rockwell International Microelectronics Research and Development Center, Thousand Oaks, CA). *Applied Physics Letters*, vol. 40, Jan. 1, 1982, p. 46-48, 15 refs. Contract No. NAS3-22224.

It is shown that the electrical compensation of undoped GaAs grown by the liquid encapsulated Czochralski technique is controlled by the melt stoichiometry. The concentration of the deep donor EL2 in the crystal depends on the As concentration in the melt, increasing from about 5×10 to the 15th per cu cm to 1.7×10 to the 16th per cu cm as the As atom fraction increases from 0.48 to 0.51. Furthermore, it is shown that the free-carrier concentration of semi-insulating GaAs is determined by the relative concentrations of EL2 and carbon acceptors. As a result, semi-insulating material can be obtained only above a critical As concentration (0.475-atom fraction in the material here) where the concentration of EL2 is sufficient to compensate residual acceptors. Below the critical As concentration the material is p type due to excess acceptors. (Author)

A82-20747 * # Comparative analysis of CCMHD power plants. F. N. Alyea, C. H. Marston, V. B. Mantri (General Electric Co., Energy Systems Programs Dept., Philadelphia, PA), B. G. Geisendorfer (Babcock and Wilcox Co., Fossil Power Generation Div., Barberton, OH), and H. Doss (Bechtel National, Inc., San Francisco, CA). *Symposium on the Engineering Aspects of MHD, 19th, Tullahoma, TN, June 15-17, 1981, Paper*. 8 p. Contract No. DEN3-135; No. DE-AC01-78ET-10818.

A study of Closed Cycle MHD (CCMHD) power generation systems has been conducted which emphasizes both advances in component conceptual design and overall system performance. New design data are presented for the high temperature, regenerative argon heaters (HTRH) and the heat recovery/seed recovery (HRSR) subsystem. Contamination of the argon by flue gas adsorbed in the HTRH is examined and a model for estimation of contamination

effects in operating systems is developed. System performance and cost data have been developed for the standard CCMHD/steam cycle as powered by both direct fired cyclone combustors and selected coal gasifiers. In addition, a new CCMHD thermodynamic cycle has been identified. (Author)

A82-20750 * # MHD channel performance for potential early commercial MHD power plants. D. W. Swallow (Avco-Everett Research Laboratory, Inc., Everett, MA). *Intersociety Energy Conversion Engineering Conference, 16th, Atlanta, GA, Aug. 9-14, 1981, Paper*, 7 p, 15 refs, Contract No. DEN3-51.

The commercial viability of full and part load early commercial MHD power plants is examined. The load conditions comprise a mass flow of 472 kg/sec in the channel, Rosebud coal, 34% by volume oxygen in the oxidizer preheated to 922 K, and a one percent by mass seeding with K. The full load condition is discussed in terms of a combined cycle plant with optimized electrical output by the MHD channel. Various electrical load parameters, pressure ratios, and magnetic field profiles are considered for a baseload MHD generator, with a finding that a decelerating flow rate yields slightly higher electrical output than a constant flow rate. Nominal and part load conditions are explored, with a reduced gas mass flow rate and an enriched oxygen content. An enthalpy extraction of 24.6% and an isentropic efficiency of 74.2% is predicted for nominal operation of a 526 MWe MHD generator, with higher efficiencies for part load operation. M.S.K.

A82-26952 * Standing waves along a microwave generated surface wave plasma. J. Rogers and J. Asmussen (Michigan State University, East Lansing, MI). *IEEE Transactions on Plasma Science*, vol. PS-10, Mar. 1982, p. 11-16, 24 refs. Grant No. NSG-3299.

Two surface wave plasma columns, generated by microwave power in argon at gas pressures of 0.05 torr to 330 torr, interact in the same discharge tube to form standing surface waves. Radial electric field and azimuthal magnetic field outside the discharge tube are measured to be 90 deg out of phase with respect to axial position and to decay exponentially with radial distance from the tube axis. Maximum light emission occurs at the position of maximum azimuthal magnetic field and minimum radial electric field. Electron temperature and density are measured at low pressures with double probes inserted into the plasma at a null of radial electric field. Measured electron densities compare well with those predicted by Gould-Trivelpiece surface wave theory. (Author)

76 SOLID-STATE PHYSICS

Includes superconductivity.

For related information, see also 33 *Electronics and Electrical Engineering* and 36 *Lasers and Masers*.

N82-11959* Rensselaer Polytechnic Inst., Troy, N. Y. Dept. of Electrical Computer and Systems Engineering.
LOW TEMPERATURE GROWTH AND ELECTRICAL CHARACTERIZATION OF INSULATORS FOR GaAs MISFETS Semiannual Status Report, 1 May - 31 Oct. 1981
J. M. Borrego and S. K. Gandhi 31 Oct. 1981 11 p
(Contract NAG3-175)
(NASA-CR-164972) Avail: NTIS HC A02/MF A01 CSCL 20B

Progress in the low temperature growth of oxides and layers on GaAs and the detailed electrical characterization of these oxides is reported. A plasma anodization system was designed, assembled, and put into operation. A measurement system was assembled for determining capacitance and conductance as a function of gate voltage for frequencies in the range from 1 Hz to 1 MHz. Initial measurements were carried out in Si-SiO₂ capacitors in order to test the system and in GaAs MIS capacitors fabricated using liquid anodization. J.M.S.

N82-23030* Rockwell International Corp., Thousand Oaks, Calif. Microelectronics Research and Development Center.
HIGH PURITY LOW DISLOCATION GaAs SINGLE CRYSTALS Final Report, 25 Feb. 1980 - 24 Feb. 1981
R. T. Chen, D. E. Holmes, and C. G. Kirkpatrick Jan. 1982 46 p
(Contract NAS3-22224)
(NASA-CR-165533; NAS 1.26;165593; ERC41054.36FR) Avail: NTIS HC A03/MF A01 CSCL 20B

Recent advances in GaAs bulk crystal growth using the LEC (liquid encapsulated Czochralski) technique are described. The dependence of the background impurity concentration and the dislocation density distribution on the materials synthesis and growth conditions were investigated. Background impurity concentrations as low as 4 x 10 to the 15th power were observed in undoped LEC GaAs. The dislocation density in selected regions of individual ingots was very low, below the 3000 cm².3000/sq cm threshold. The average dislocation density over a large annular ring on the wafers fell below the 10000/sq cm level for 3 inch diameter ingots. The diameter control during the program advanced to a diameter variation along a 3 inch ingot less than 2 mm. Author

A82-13754* Undoped semi-insulating LEC GaAs - A model and a mechanism. J. R. Oliver, R. D. Fairman, R. T. Chen (Rockwell International Microelectronics Research and Development Center, Thousand Oaks, CA), and P. W. Yu (Wright State University, Dayton, OH). *Electronics Letters*, vol. 17, Oct. 29, 1981, p. 839-841. 8 refs. Contract No. NAS3-22224.

Undoped semi-insulating GaAs grown by the high-pressure liquid encapsulated Czochralski (LEC) method has been produced for use in direct ion implantation in several laboratories. A clear understanding of the factors controlling impurity transport and compensation in these materials has been lacking to date. In this work, detailed characterization has been performed on undoped semi-insulating crystals grown from both SiO₂ and PBN crucibles followed by a proposed impurity model and compensation mechanism. (Author)

A82-21965* Surface diffusion activation energy determination using ion beam microtexturing. S. M. Rossmagel and R. S. Robinson (Colorado State University, Fort Collins, CO). *Journal of Vacuum Science and Technology*, vol. 20, Feb. 1982, p. 195-198. 18 refs. Grant No. NAG3-43.

The activation energy for impurity atom (adatom) surface diffusion can be determined from the temperature dependence of the spacing of sputter cones. These cones are formed on the surface during sputtering while simultaneously adding impurities. The impurities form clusters by means of surface diffusion, and these clusters in turn initiate cone formation. Values are given for the

surface diffusion activation energies for various materials on polycrystalline Cu, Al, Pb, Au, and Ni. The values for different impurity species on each of these substrates are approximately independent of impurity species within the experimental uncertainty, suggesting the absence of strong chemical bonding effects on the diffusion. (Author)

A82-30335* Quasi-liquid states observed on ion beam microtextured surfaces. S. M. Rossmagel and R. S. Robinson (Colorado State University, Fort Collins, CO). (*American Vacuum Society, National Symposium, 28th, Anaheim, CA, Nov. 2-6, 1981.*) *Journal of Vacuum Science and Technology*, vol. 20, Mar. 1982, p. 506-509. 13 refs. Grant No. NAG3-43.

Liquid-like properties have been observed on surface structures developed by means of ion beam microtexturing. The structures include cones, pyramids, or wavelike formations. The observed liquidlike effects are drips and ripples on the sides of cones, droplet formation, the apparent flow and coalescence of closely packed structures, wetting angle and other surface tension effects, and the bending of cones by additional heating. The bulk temperatures are in the range of 50-600 C. These effects are seen to some extent on Cu, Al, Au, Pb, and Ni substrates. (Author)

A82-31276* Impedance conversion using quantum limit nonreciprocity for superconductor-insulator-superconductor mixer compensation. S. R. Whiteley (California, University, Berkeley, CA). *Applied Physics Letters*, vol. 40, May 1, 1982, p. 842, 843. 8 refs. NSF Grant No. ECS-79-23877; Contract No. NAG3-88.

It is shown how a superconductor-insulator-superconductor (SIS) mixer when inductively terminated at the IF port has inductive reactance at the signal port. This reactance may be used to compensate for the geometric capacitance of a conventionally operated SIS mixer over twice the bandwidth available through signal port resonance techniques. (Author)

A82-38411* OM-VPE growth of Mg-doped GaAs. C. R. Lewis, W. T. Dietze, and M. J. Ludowise (Varian Corporate Solid State Laboratory, Palo Alto, CA). *Electronics Letters*, vol. 18, June 24, 1982, p. 569, 570. 5 refs. Contract No. NAS3-22232.

The epitaxial growth of Mg-doped GaAs by the organometallic vapor phase epitaxial process (OM-VPE) has been achieved for the first time. The doping is controllable over a wide range of input fluxes of bis (cyclopentadienyl) magnesium, (C₅H₅)₂Mg, the organometallic precursor to Mg. (Author)

A82-41546* Electron beam induced damage in ITO coated Kapton. I. Krainsky, W. L. Gordon, and R. W. Hoffman (Case Western Reserve University, Cleveland, OH). *Applications of Surface Science*, vol. 9, 1981, p. 39-46. 17 refs. Grant No. NSG-3197.

Data for the stability of thin conductive indium tin oxide films on 0.003 inch thick Kapton substrates during exposure of the surface to electron beams are reported. The electron beam energy was 3 keV and the diameter was about 0.8 mm. Thermal effects and surface modifications are considered. For primary current greater than 0.6 microamperes, an obvious dark discoloration with diameter approximately that of the beam was produced. The structure of the discolored region was studied with the scanning electron microscope, and the findings are stated. Surface modifications were explored by AES, obtaining spectra and secondary emission coefficient as a function of time for different beam intensities. In all cases beam exposure results in a decrease of the secondary yield but because of thermal effects this change, as well as composition changes, cannot be directly interpreted in terms of electron beam dosage. C.D.

A82-42912* Stationary state model for normal metal tunnel junction phenomena. S. R. Whiteley and T. K. Gustafson (California, University, Berkeley, CA). *IEEE Journal of Quantum Electronics*, vol. QE-18, Sept. 1982, p. 1387-1398. 21 refs. NSF Grant No. ECS-79-23877; Grant No. NAG3-88.

A model applicable to normal metal tunnel junctions is presented. This model, referred to herein as the stationary state model, is an extension of the extended basis function theory of Kleinman and Duke (1972). Under the assumption that elastic tunneling is the dominant transport mechanism under static bias, the theory has been extended to include the case where there is an ac component of bias potential, and the fluctuation spectrum has been derived. In this approach structure eigenstates are used as the basis, allowing observables to be evaluated without recourse to the perturbation theory inherent in the transfer Hamiltonian model. Comparison is made to the appropriate results of the first order transfer

Hamiltonian model, and it is found that there is close but not always exact agreement to lowest order in the tunneling exponential. The stationary state model should be accurate with large barrier transmission, as it includes all orders of the tunneling exponential. The model as presented here should be applicable to normal metal tunnel junctions, where elastic tunneling is the dominant transport mechanism (under static bias), up to infrared excitation frequencies. (Author)

ORIGINAL PAGE IS
OF POOR QUALITY

A82-46426 * **Ion-beam-induced topography and surface diffusion.** R. S. Robinson and S. M. Rossnagel (Colorado State University, Fort Collins, CO). (*American Vacuum Society, Annual Symposium on Plasma and Ion-Beam Processing, 13th, Yorktown Heights, NY, June 2, 1982.*) *Journal of Vacuum Science and Technology*, vol. 21, Sept.-Oct. 1982, p. 790-797. 32 refs. Grant No. NAG3-43.

It is pointed out that the development of surface topography along with enhanced surface and bulk diffusion processes accompanying ion bombardment have generated growing interest among users of ion beams and plasmas for thin film or material processing. Interest in these processes stems both from attempts to generate topographic changes for specific studies or applications and from the need to suppress or control undesirable changes. The present investigation provides a summary of the current status of impurity-induced texturing, with emphasis on recent developments. Particular attention is given to the texturing accompanying deposition of an impurity material onto a solid surface while simultaneously etching the surface with an ion beam. A description of experimental considerations is provided, and a thermal-diffusion model is discussed along with the development of sputter cones, and aspects of impact-enhanced surface diffusion. G.R.

A82-46517 * **Effect of melt stoichiometry on twin formation in LEC GaAs.** R. T. Chen and D. E. Holmes (Rockwell International Microelectronics Research and Development Center, Thousand Oaks, CA). *Electrochemical Society, Journal*, vol. 129, Oct. 1982, p. 2382, 2383. 5 refs. Contract No. NAS3-22224.

It is shown that the incidence of twin formation in large diameter, undoped, (100) LEC GaAs is reduced when the melt composition is slightly As-rich. Twenty GaAs crystals were grown from stoichiometric and nonstoichiometric melts. The results suggest that the barrier to twin formation is related to the stoichiometry of the solid at the solidification front. C.D.

77 THERMODYNAMICS AND STATISTICAL PHYSICS

Includes quantum mechanics; and Bose and Fermi statistics.

For related information see also 25 *Inorganic and Physical Chemistry* and 34 *Fluid Mechanics and Heat Transfer*.

N82-32186*# National Aeronautics and Space Administration, Lewis Research Center, Cleveland, Ohio.
THERMODYNAMIC AND TRANSPORT COMBUSTION PROPERTIES OF HYDROCARBONS WITH AIR. PART 1: PROPERTIES IN SI UNITS

Sanford Gordon Jul. 1982 397 p refs
(NASA-TP-1906; E-946; NAS 1.60:1906) Avail: NTIS HC A17/MF A01 CSCL 20M

Thermodynamic and transport combustion properties were calculated for a wide range of conditions for the reaction of hydrocarbons with air. Three hydrogen-carbon atom ratios ($H/C = 1.7, 2.0, 2.1$) were selected to represent the range of aircraft fuels. For each of these H/C ratios, combustion properties were calculated for the following conditions: Equivalence ratio: 0, 0.25, 0.5, 0.75, 1.0, 1.25 Water - dry air mass ratio: 0, 0.03 Pressure, kPa: 1.01325, 10.1325, 101.325, 1013.25, 5066.25 (or in atm: 0.01, 0.1, 1, 10, 50) Temperature, K: every 10 degrees from 200 to 900 K; every 50 degrees from 900 to 3000 K Temperature, R: every 20 degrees from 360 to 1600 R; every 100 degrees from 1600 to 5400 R. The properties presented are composition, density, molecular weight, enthalpy, entropy, specific heat at constant pressure, volume derivatives, isentropic exponent, velocity of sound, viscosity, thermal conductivity, and Prandtl number. Property tables are based on composites that were calculated by assuming both: (1) chemical equilibrium (for both homogeneous and heterogeneous phases) and (2) constant compositions for all temperatures. Properties in SI units are presented in this report for the Kelvin temperature schedules. Author

N82-32187*# National Aeronautics and Space Administration, Lewis Research Center, Cleveland, Ohio.

THERMODYNAMIC AND TRANSPORT COMBUSTION PROPERTIES OF HYDROCARBONS WITH AIR. PART 2: COMPOSITIONS CORRESPONDING TO KELVIN TEMPERATURE SCHEDULES IN PART 1

Sanford Gordon Jul. 1982 281 p refs
(NASA-TP-1907; E-947; NAS 1.60:1907) Avail: NTIS HC A13/MF A01 CSCL 20M

The equilibrium compositions that correspond to the thermodynamic and transport combustion properties for a wide range of conditions for the reaction of hydrocarbons with air are presented. Initially 55 gaseous species and 3 coin condensed species were considered in the calculations. Only 17 of these 55 gaseous species had equilibrium mole fractions greater than 0.000005 for any of the conditions studied and therefore these were the only ones retained in the final tables. J.M.S.

N82-32188*# National Aeronautics and Space Administration, Lewis Research Center, Cleveland, Ohio.

THERMODYNAMIC AND TRANSPORT COMBUSTION PROPERTIES OF HYDROCARBONS WITH AIR. PART 3: PROPERTIES IN US CUSTOMARY UNITS

Sanford Gordon Jul. 1982 362 p refs
(NASA-TP-1908; E-948; NAS 1.60:1908) Avail: NTIS HC A16/MF A01 CSCL 20M

Thermodynamic and transport properties are presented for a wide range of conditions for the reaction of hydrocarbons with air. The values given are in U.S. customary units. J.M.S.

N82-32189*# National Aeronautics and Space Administration, Lewis Research Center, Cleveland, Ohio.

THERMODYNAMIC AND TRANSPORT COMBUSTION PROPERTIES OF HYDROCARBONS WITH AIR. PART 4: COMPOSITIONS CORRESPONDING TO RANKINE TEMPERATURE SCHEDULES IN PART 3

Sanford Gordon Jul. 1982 281 p refs
(NASA-TP-1909; E-949; NAS 1.60:1909) Avail: NTIS HC A18/MF A01 CSCL 20M

The equilibrium compositions corresponding to the thermodynamic and transport combustion properties for a wide range of conditions for the reaction of hydrocarbons with air are presented. The compositions presented correspond to Rankine temperature schedules. J.M.S.

ORIGINAL PAGE IS
OF POOR QUALITY

81 ADMINISTRATION AND MANAGEMENT

Includes management planning and research.

ORIGINAL PAGE IS
OF POOR QUALITY

N82-20006* National Aeronautics and Space Administration.
Lewis Research Center, Cleveland, Ohio.

LOCAL AND NATIONAL IMPACT OF AEROSPACE RESEARCH AND TECHNOLOGY

John F. McCarthy, Jr. Dec. 1981 10 p refs Presented at
Cleveland City Club, Ohio, 4 Dec. 1981
(NASA-TM-82775; E-1106) Avail: NTIS HC A02/MF A01
CSC 05A

An overview of work at the NASA Lewis Research Center
in the areas of aeronautics, space, and energy is presented. Local
and national impact of the work is discussed. Some aspects of
the U.S. research and technology base, the aerospace industry,
and foreign competition are discussed. In conclusion, U.S. research
and technology programs are cited as vital to U.S. economic
health. Author

85 URBAN TECHNOLOGY AND TRANSPORTATION

Includes applications of space technology to urban problems, technology transfer; technology assessment; and surface and mass transportation.

For related information see 03 Air Transportation and Safety, 16 Space Transportation, and 44 Energy Production and Conversion.

N82-13013* National Aeronautics and Space Administration, Lewis Research Center, Cleveland, Ohio.

TEST RESULTS AND FACILITY DESCRIPTION FOR A 40-KILOWATT STIRLING ENGINE Final Report

Gary G. Kelm, James E. Cairrell, and Robert J. Walter Jun. 1981 47 p refs

(Contract DE-AI01-77CS-51040)

(NASA-TM-82620; DOE/NASA/51040-27; E-871) Avail: NTIS HC A03/MF A01 CSCL 10B

A 40 kilowatt Stirling engine, its test support facilities, and the experimental procedures used for these tests are described. Operating experience with the engine is discussed, and some initial test results are presented S.L.

N82-26051* National Aeronautics and Space Administration, Lewis Research Center, Cleveland, Ohio.

PRELIMINARY ANALYSIS OF A DOWNIZED ADVANCED GAS-TURBINE ENGINE IN A SUBCOMPACT CAR

John L. Klann and Roy L. Johnson 1982 25 p refs Presented at the 18th Joint Propulsion Conf., Cleveland, 21-23 Jun. 1982

(Contract DE-AI01-77CS-51040)

(NASA-TM-82848; E-1218; NAS 1.15:82848;

DOE/NASA/51040-40) Avail: NTIS HC A02/MF A01 CSCL 13F

Relative fuel economy advantages exist for a ceramic turbine engine when it is downized for a small car, as was investigated. A 75 kW (100 hp) single shaft engine under development was analytically downized to 37 kW (50 hp) and analyzed with a metal belt continuously variable transmission in a synthesized car. With gasoline, a 25% advantage was calculated over that of a current spark ignition engine, scaled to the same power, using the same transmission and car. With diesel fuel, a 21% advantage was calculated over that of a similar diesel engine vehicle. Author

N82-27191* National Aeronautics and Space Administration, Lewis Research Center, Cleveland, Ohio.

BIBLIOGRAPHY OF LEWIS RESEARCH CENTER TECHNICAL PUBLICATIONS ANNOUNCED IN 1981

May 1982 295 p

(NASA-TM-82838; E-1205, NAS 1.15:82838) Avail: NTIS HC A13/MF A01 CSCL 05B

Technical reporting that resulted from the scientific and engineering work performed and managed by the Lewis Research Center in 1981 are indexed and abstracted. All the publications were announced in the 1981 issues of STAR (Scientific and Technical Aerospace Reports) and/or IAA (International Aerospace Abstracts). Included are research reports, journal articles, conference presentations, patent applications, and theses. A total of 384 technical publications is listed. Author

N82-31160* National Aeronautics and Space Administration, Lewis Research Center, Cleveland, Ohio.

PROGRESS ON ADVANCED dc AND ac INDUCTION DRIVES FOR ELECTRIC VEHICLES

Harvey J. Schwartz 1922 16 p refs Presented at the Drive Elec. Amsterdam '82, Amsterdam, 25-29 Oct. 1982

(Contract DE-AI01-77CS-51044)

(NASA-TM-82895; E1273; NAS 1.15:82895;

DOE/NASA/51044-27) Avail: NTIS HC A02/MF A01 CSCL 13F

Progress is reported in the development of complete electric vehicle propulsion systems, and the results of tests on the Road Load Simulator of two such systems representative of advanced dc and ac drive technology are presented. One is the system used in the DOE's ETV-1 integrated test vehicle which consists

of a shunt wound dc traction motor under microprocessor control using a transistorized controller. The motor drives the vehicle through a fixed ratio transmission. The second system uses an ac induction motor controlled by transistorized pulse width modulated inverter which drives through a two speed automatically shifted transmission. The inverter and transmission both operate under the control of a microprocessor. The characteristics of these systems are also compared with the propulsion system technology available in vehicles being manufactured at the inception of the DOE program and with an advanced, highly integrated propulsion system upon which technology development was recently initiated. Author

N82-11993*# Razor Associates, Inc., Sunnyvale, Calif. JET IMPINGEMENT HEAT TRANSFER ENHANCEMENT FOR THE GPU-3 STIRLING ENGINE

Douglas C. Johnson, Craig W. Congdon, Lester L. Begg, Edward J. Britt, and Lanny G. Thieme Oct. 1981 28 p refs

(NASA-TM-82727; DOE/NASA/51040/33) Avail: NTIS HC A03/MF A01 CSCL 13F

A computer model of the combustion-gas-side heat transfer was developed to predict the effects of a jet impingement system and the possible range of improvements available. Using low temperature (315 C (600 F)) pretest data in an updated model, a high temperature silicon carbide jet impingement heat transfer system was designed and fabricated. The system model predicted that at the theoretical maximum limit, jet impingement enhanced heat transfer can: (1) reduce the flame temperature by 275 C (500 F); (2) reduce the exhaust temperature by 110 C (200 F); and (3) increase the overall heat into the working fluid by 10%, all for an increase in required pumping power of less than 0.5% of the engine power output. Initial tests on the GPU-3 Stirling engine at NASA-Lewis demonstrated that the jet impingement system increased the engine output power and efficiency by 5% - 8% with no measurable increase in pumping power. The overall heat transfer coefficient was increased by 65% for the maximum power point of the tests. A.R.H.

N82-16937*# AiResearch Mfg. Co., Phoenix, Ariz. ADVANCED GAS TURBINE (AGT) POWERTRAIN SYSTEM DEVELOPMENT FOR AUTOMOTIVE APPLICATIONS Progress Report, Oct. 1979 - Jun. 1980

Nov. 1980 431 p refs

(Contract DEN3-167)

(NASA-CR-165175; DOE/NASA/O167-80/1;

AiResearch-31-3725; PR-1) Avail: NTIS HC A19/MF A01 CSCL 13F

Progress in the development of a gas turbine engine to improve fuel economy, reduce gaseous emissions and particulate levels, and compatible with a variety of alternate fuels is reported. The powertrain is designated AGT101 and consists of a regenerated single shaft gas turbine engine, a split differential gearbox and a Ford Automatic Overdrive production transmission. The powertrain is controlled by an electronic digital microprocessor and associated actuators, instrumentation, and sensors. Standard automotive accessories are driven by engine power provided by an accessory pad on the gearbox. Component/subsystem development progress is reported in the following areas: compressor, turbine, combustion system, regenerator, gearbox/transmission, structures, ceramic components, foil gas bearing, bearings and seals, rotor dynamics, and controls and accessories. J.M.S.

N82-16938*# Boeing Computer Services Co., Tukwila, Wash. HYBRID AND ELECTRIC ADVANCED VEHICLE SYSTEMS (HEAVY) SIMULATION Final Report

Ronald A. Hammond and Richard K. McGehee Nov. 1981 89 p refs

(Contract D11N3-151; DE-AI01-77CS-51044)

(NASA-CR-165536; DOE/NASA/O151-1; BCS-40357) Avail: NTIS HC A05/MF A01 CSCL 13F

A computer program to simulate hybrid and electric advanced vehicle systems (HEAVY) is described. It is intended for use early in the design process: concept evaluation, alternative comparison, preliminary design, control and management strategy development, component sizing, and sensitivity studies. It allows the designer to quickly, conveniently, and economically predict

the performance of a proposed drive train. The user defines the system to be simulated using a library of predefined component models that may be connected to represent a wide variety of propulsion systems. The development of three models are discussed as examples. M.G.

N82-18068*# Department of Transportation, Cambridge, Mass.
FUELECONOMY AND EXHAUST EMISSIONS CHARACTERISTICS OF DIESEL VEHICLES: TEST RESULTS OF A PROTOTYPE FIAT 131TC 2.4 LITER AUTOMOBILE
S. S. Quayle Jan. 1982 58 p refs
(NASA Order C-32817-D; Contract DE-AI01-80CS-50194)
(NASA-CR-165535; DOE/NASA/2817-2;
DGT-TSC-NASA-81-2) Avail: NTIS HC A04/MF A01 CSCL 13F

The results obtained from fuel economy and emission tests conducted on a prototype Fiat 131 turbocharged diesel vehicle are presented. The vehicle was tested on a chassis dynamometer over selected drive cycles and steady-state conditions. Two fuels were used, a United States number 2 diesel and a European diesel fuel. Particulate emission rates were calculated from dilution tunnel measurements and large volume particulate samples were collected for biological and chemical analysis. It was determined that turbocharging accompanied by complementary modifications results in small but substantial improvements in regulated emissions, fuel economy, and performance. Notably, particulate levels were reduced by 30 percent. Author

N82-29235*# Mechanical Technology, Inc., Latham, N. Y.
Stirling Engine Systems Div.
AUTOMOTIVE STIRLING ENGINE DEVELOPMENT PROGRAM Quarterly Technical Progress Report, 1 Apr. - 30 Jun. 1981
Steven Piller, Al Richey, Mark Dowdy, and Kelly Mather May 1982 111 p refs
(Contracts DEN3-32; EC-77-A-31-10040)
(NASA-CR-167907; DOE/NASA/0032-15; NAS 1.26:167907;
MTI-91ASE229QT13) Avail: NTIS HC A06/MF A01 CSCL 13F

The background and history of the Stirling engine, the technology, materials, components, controls, and systems, and a technical assessment of automotive stirling engines are presented. Author

N82-31158*# Detroit Diesel Allison, Indianapolis, Ind.
CERAMIC APPLICATIONS IN TURBINE ENGINES Semianual Report, 1 Jan. - 30 Jun. 1980
S. Michael Hudson, Michael A. Janovicz, and Franklin A. Rockwood Nov. 1980 177 p
(Contracts DEN3-17; EC-77-A-31-1040)
(NASA-CR-165197; NAS 1.26:165197; EDR-10383) Avail:
NTIS HC A09/MF A01 CSCL 13F

The design and testing of gas turbine engines employing ceramic components is discussed. Thermal shock and vibration test results as well as spin tests of various engine components are discussed. R.J.F.

N82-34311*# Mechanical Technology, Inc., Latham, N. Y.
AUTOMOTIVE STIRLING ENGINE MOD 1 DESIGN REVIEW, VOLUME 1 Final Report
Aug. 1982 654 p refs Presented at Automotive Stirling Engine (ASE) Mod 1 Engine Design Review, Cleveland, 22-23 May 1980 3 Vol.
(Contracts DEN3-32; DE-AI01-77CS-51040)
(NASA-CR-167935; DOE/NASA/0032-16-Vol-1; NAS 1.26:167935; MTI-80ASE142DR1-Vol-1) Avail: NTIS HC A99/MF A01 CSCL 13F

Risk assessment, safety analysis of the automotive stirling engine (ASE) mod 1, design criteria and materials properties for the ASE mod 1 and reference engines, combustion are flower development, and the mod 1 engine starter motor are discussed. The stirling engine system, external heat system, hot engine system, cold engine system, and engine drive system are also discussed. N.W.

N82-34312*# Mechanical Technology, Inc., Latham, N. Y.
AUTOMOTIVE STIRLING ENGINE MOD 1 DESIGN REVIEW, VOLUME 3 Final Report
Aug. 1982 362 p refs Review held in Cleveland, 22-23 May 1980 3 Vol.
(Contracts DEN3-32; DE-AI01-77CS-51040)
(NASA-CR-167937; DOE/NASA/0032-18-Vol-3; NAS 1.26:167937; Rept-80ASE142DR1-Vol-3) Avail: NTIS HC A16/MF A01 CSCL 13F
Engineering drawings for the stirling engine, external heat, hot and cold engine, engine drive, and control systems and auxiliaries are provided. Vehicle integration is also illustrated. N.W.

ORIGINAL PAGE IS
OF POOR QUALITY

90 ASTROPHYSICS

Includes cosmology; and interstellar and interplanetary gases and dust.

A82-23750 * Potentials of surfaces in space. E. C. Whipple (California, University, La Jolla, CA). *Reports on Progress in Physics*, vol. 44, Nov. 1981, p. 1197-1250. 334 refs. Grants No. NGL-05-005-007; No. NAG3-152; Contract No. F04701-77-C-0062.

The subject of surface potentials on natural and artificial bodies in space is reviewed with particular emphasis on recent developments. Following a brief survey of work done up to the early 1970s on the charging of astrophysical objects in interstellar and interplanetary space and spacecraft charging, the various charging mechanisms in space are examined, including the collection of plasma particles, photoemission, and secondary electron emission by electron impact and ion impact, and the effects on charging of nonisotropic plasmas, wakes, and environmental magnetic and electric fields are considered. The concept of equilibrium potential is discussed, along with differential charging, potential barriers and discharge processes. The measurement of spacecraft potentials is then considered, and recent work on spacecraft potential modification and control by active and passive means is presented. Finally, astrophysical applications where charging effects may be important are discussed, and areas for further work are indicated.

A.L.W.

ORIGINAL PAGE IS
OF POOR QUALITY

91 LUNAR AND PLANETARY EXPLORATION

Includes planetology; and manned and unmanned flights.
For spacecraft design see *18 Spacecraft Design Testing,
and Performance*. For space stations see *15 Launch
Vehicles and Space Vehicles*.

A82-29316 4 Evidence for Pu-244 fission tracks in hibonites from Murchison carbonaceous chondrite. R. S. Rajan (California Institute of Technology, Jet Propulsion Laboratory, Earth and Space Sciences Div., Pasadena, CA; Carnegie Institution of Washington, Washington, DC) and A. S. Tamhane (Carnegie Institution of Washington, Washington, DC; Tata Institute of Fundamental Research, Bombay, India). *Earth and Planetary Science Letters*, vol. 58, no. 1, Mar. 1982, p. 129-135. 15 refs. Grant No. NA6GW-38.

ORIGINAL PAGE IS
OF POOR QUALITY

92 SOLAR PHYSICS

Includes solar activity, solar flares, solar radiation and sunspots.

A82-10156 * VLA observations of solar active regions at 6 cm wavelength. M. R. Kundu, E. J. Schmahl, and A. P. Rao (Maryland, University, College Park, MD). *Astronomy and Astrophysics*, vol. 94, no. 1, Jan. 1981, p. 72-79. 24 refs. NSF Grant No. ATM-78-21762; Grants No. NGR-21-002-199; No. NsG-5320; No. NsG-398.

Synthesized maps of two solar active regions obtained from observations with the Very Large Array (VLA) with 9-arcsec resolution are presented. The most intense sources in these regions are found to be associated with filamentary structures and magnetic neutral lines as shown in H-alpha and photospheric magnetograms. These sources are not located directly over sunspots in disagreement with earlier observations. EUV and X-ray observations have suggested that similar structures should be visible at cm wavelengths around but, outside of, sunspots if the magnetic field is sufficiently strong. These results are consistent with the locations of hot (greater than 1,000,000 K) plasmas in active regions expected from generalization based on optical photographs. Given the sizes of the radio sources, the volume emission measures of soft X-rays observed from OSO-8 rule out the possibility of thermal bremsstrahlung being of any significance, as far as the 6 cm emission is concerned. Therefore, gyroresonance absorption process is the most likely cause of 6 cm emission from these sources, and its likelihood is enhanced by the magnetic field geometry that is known to exist over filaments and neutral lines.

(Author)

A82-26003 * Time variability and structure of quiet sun sources at 6 cm wavelength. F. T. Erskine and M. R. Kundu (Maryland, University, College Park, MD). *Solar Physics*, vol. 76, Mar. 1982, p. 221-237. 14 refs. NSF Grant No. ATM-76-22415; Grants No. NGR-21-022-199; No. NsG-398.

Results are presented of a detailed study of quiet sun emitting regions at 6 cm and their correspondence with regions observed at optical wavelengths. The Westerbork Synthesis Radio Telescope was used to obtain a 12-hr synthesis map of a quiet sun region with a resolution of 6 arcsec. Comparison of this map with a Ca(+) K filtergram indicates the features on the 6-cm map to correspond to Ca(+) K chromospheric networks and cells. In addition, about 72% of the magnetic field enhancements observed on photospheric magnetograms coincides with 6-cm emissive regions. Intercomparison of the 12-hr synthesis map, a 4-hr synthesis map and 6-cm fan beam scans along with the Ca(+) K and magnetogram results reveals all of the time-varying 6-cm elements to be located on Ca(+) K networks, and about 40% of them to be coincident with magnetogram enhancements. Lifetimes of the time-varying sources vary from a few minutes to several tens of minutes, and intensity varies by factors of 2 to 7.

A.L.W.

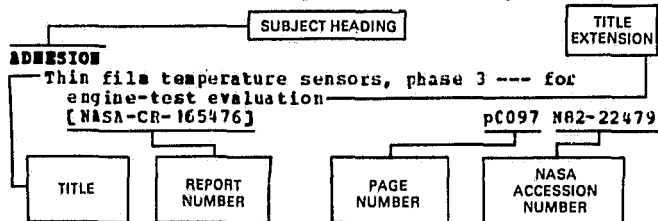
A82-27323 * Magnetic structure of a flaring region producing impulsive microwave and hard X-ray bursts. M. R. Kundu, E. J. Schmahl (Maryland, University, College Park, MD), and T. Velusamy. *Astrophysical Journal, Part 1*, vol. 253, Feb. 15, 1982, p. 963-974. 18 refs. NSF Grant No. ATM-78-2176; Grants No. NGR-21-002-199; No. NsG-5320; No. NsG-398.

Using VLA observations of the 1B/M1 flare of June 25, 1980, 6-cm 'snapshot' maps are synthesized. The spatial and temporal resolutions during the 9 minutes of the impulsive phase were, respectively, 1 arcsec x 2 arcsec and 10 s. Some displacement is noted between the locations of the burst source and the preflare loop structures seen in the preflare map. The burst peak occurred on the neutral line of the preflare polarization map, between the two oppositely polarized microwave 'loop' structures approximately 40 arcsec long. Concurrent hard X-ray observations were made of the burst, although these had no spatial resolution. The 6-cm maps show the locations of a number of the X-ray burst spikes. The 6-cm burst was fully resolved into at least eight components, many of which were bipolar.

C.R.

ORIGINAL PAGE IS
OF POOR QUALITY

Typical Subject Index Listing



The title is used to provide a description of the subject matter. When the title is insufficiently descriptive of the document content, a title extension is added, separated from the title by three hyphens. The *STAR* or *IAA* accession number is included in each entry to assist the user in locating the abstract in the abstract section. If applicable a report number is also included as an aid in identifying the document. The page and accession numbers are located beneath and to the right of the title. Under any one subject heading the accession numbers are arranged in sequence with the *IAA* accession numbers appearing first.

A

ABRASION

Elucidation of wear mechanisms by ferrographic analysis
[NASA-TM-82737] p0066 N82-15199
Composite seal for turbomachinery
[NASA-CASE-LEW-12131-3] p0099 N82-19540

ABUNDANCE

Evidence for Pu-244 fission tracks in hibonites from Murchison carbonaceous chondrite
p0166 A82-29316

AC (CURRENT)

U TERMINATING CURRENT

AC GENERATORS

Development of a dual-field heteropolar power converter
[NASA-CR-165168] p0084 N82-24424

ACCELERATED LIFE TESTS

Elevated temperature fatigue testing of metals
p0058 N82-13281

ACCELERATION (PHYSICS)

NI HIGH ACCELERATION NT PLASMA ACCELERATION

ACCESSORIES

Component technology for space power systems
[NASA-TM-82928] p0082 N82-30474

ACCRETION

U POSITION

ACCUMULATORS

NT SOLAR COLLECTORS
NI SOLAR REFLECTORS
Multistage depressed collector for dual mode operation --- for microwave transmitting tubes
[NASA-CASE-LEW-13282-1] p0081 N82-24415

ACIDS

NT PHOSPHORIC ACID

ACOUSTIC ATTENUATION

NT SHOCK WAVE ATTENUATION
On ultrasonic factors and fracture toughness
p0116 A82-42863

ACOUSTIC COMBUSTION

U COMBUSTION STABILITY

ACOUSTIC DUCTS

Analytical and experimental investigation of the propagation and attenuation of sound in extended reaction lined ducts
[AIAA PAPER 81-2014] p0153 A82-10454
Methods for the calculation of axial wave numbers in lined ducts with mean flow
p0153 A82-14044
Effect of vacuum exhaust pressure on the performance of MHD ducts at high B-field

[AIAA PAPER 82-0396] p0157 A82-20292
Conversion of acoustic energy by lossless liners
p0154 A82-36195
Numerical techniques in linear duct acoustics, 1980-81 update
[NASA-TM-82730] p0151 N82-12890
Application of steady state finite element and transient finite difference theory to sound propagation in a variable area duct: 1 comparison with experiment
[NASA-TM-82678] p0151 N82-15847

ACOUSTIC MEASUREMENT

NT NOISE MEASUREMENT

Effects of vane/blade ratio and spacing on fan noise
[AIAA PAPER 81-2033] p0029 A82-10457
Prediction of sound radiation from different practical jet engine inlets
[NASA-CR-165120] p0153 N82-16810

ACOUSTIC MICROSCOPES

Acoustic microscopy of silicon carbide materials
p0075 A82-33031

ACOUSTIC PROPAGATION

Acoustic transmission in lined flow ducts - A finite element eigenvalue problem
p0154 A82-17663
Numerical techniques in linear duct acoustics, 1980-81 update
[NASA-TM-82730] p0151 N82-12890

Verification of an acoustic transmission matrix analysis of sound propagation in a variable area duct without flow
[NASA-TM-82741] p0151 N82-12891
Application of steady state finite element and transient finite difference theory to sound propagation in a variable area duct: A comparison with experiment
[NASA-TM-82678] p0151 N82-15847

Pressure transfer function of a JT15D nozzle due to acoustic and convected entropy fluctuations
[NASA-TM-82842] p0152 N82-22951

ACOUSTIC PROPERTIES

NT ACOUSTIC VELOCITY

In-flight acoustic results from an advanced-design propeller at Mach numbers to 0.8
[AIAA PAPER 82-1120] p0021 A82-35017
The acoustical structure of highly porous open-cell foams
p0154 A82-45165

Prediction of sound radiation from different practical jet engine inlets
[NASA-CR-165120] p0153 N82-16810

Effect of facility variation on the acoustic characteristics of three single stream nozzles
[NASA-TM-81635] p0151 N82-19944

Acoustic properties of turbofan inlets
[NASA-CR-169016] p0153 N82-27090

ACOUSTIC RADIATION

U UND WAVES

ACOUSTIC SIMULATION

QCSEF over-the-wing engine acoustic data
[NASA-TM-82708] p0020 N82-29324

ACOUSTIC VELOCITY

On ultrasonic factors and fracture toughness
p0116 A82-42863

ACOUSTIC VIBRATIONS

U UND WAVES

ACOUSTICS

NT AEROACOUSTICS

Verification of an acoustic transmission matrix analysis of sound propagation in a variable area duct without flow
[NASA-TM-82741] p0151 N82-12891
Bibliography of Lewis Research Center technical publications announced in 1981
[NASA-TM-82838] p0163 N82-27191

ACQUISITION

ORIGINAL PAGE IS
OF POOR QUALITY

SUBJECT INDEX

ACQUISITION

NT DATA ACQUISITION

ACTINIDE SERIES

NT PLUTONIUM 244

ACTINOMETERS

NT INFRARED DETECTORS

ACTIVATION ENERGY

Surface diffusion activation energy determination
using ion beam microtexturing

p0159 A82-21965

ACTIVE CONTROL

CR6 jet engine performance improvement: High
pressure turbine active clearance control

[NASA-CR-165556]

p0027 A82-28297

ACTIVE VOLCANOES

U LCAOES

ACTUATORS

Electromechanical actuators

N82-19148

Preliminary study, analysis and design for a power
switch for digital engine actuators

[NASA-CR-159559]

p0085 A82-23394

Kevlar/PMR-15 reduced drag EC-9 reverser stang

fairing

[NASA-CR-165448]

p0052 A82-31448

ADAPTIVE CONTROL

NT ACTIVE CONTROL

Role of optical computers in aeronautical control
applications

p0156 A82-15897

NASA Adaptive Multibeam Phased Array (AMEA): An

application study

[NASA-CR-169125]

p0079 A82-28503

ADAPTIVE CONTROL SYSTEMS

U ADPTIVE CONTROL

ADDITIVES

NT ANTIICING ADDITIVES

NT ELASTICIZERS

Effect of aluminum phosphate additions on
composition of three-component plasma-sprayed
solid lubricant

[NASA-TP-1990]

p0059 A82-21298

Additional experiments on flowability improvements
of aviation fuels at low temperatures, volume 2

[NASA-CR-167912]

p0074 A82-31546

ADHEROMETERS

U HESION TESTS

ADHESION

Universal binding energy relations in metallic

adhesion

[NASA-TM-82706]

p0058 A82-11183

Application of surface analysis to solve problems

of wear

[NASA-TM-82753]

p0099 A82-14519

Thin film temperature sensors, phase 3 --- for
engine-test evaluation

[NASA-CR-165476]

p0097 A82-22479

Refractory coatings

[NASA-CASE-LEW-13169-2]

p0061 A82-30371

Wear mechanism based on adhesion

[NASA-TP-2037]

p0103 A82-32737

ADHESION TESTS

Adhesion and friction of single-crystal diamond in
contact with transition metals

p0103 A82-18680

ADHESIVE BONDING

Interface cracks in adhesively bounded lap-shear
joints

p0116 A82-46109

Analysis of interface cracks in adhesively bonded
lap shear joints, part 4

[NASA-CR-165438]

p0114 A82-26716

ADMITTANCE

U ECTRICAL IMPEDANCE

ADSORBENTS

Analysis of infrared emission from thin adsorbates

p0056 A82-21431

AEROACOUSTICS

Analytical and experimental investigation of the
propagation and attenuation of sound in extended
reaction lined ducts

[AIAA PAPER 81-2014]

p0153 A82-10454

Aeroacoustic performance of an externally blown
flap configuration with several flap noise

suppressor devices

[NASA-TP-1995]

p0152 A82-24942

AERODYNAMIC BUZZ

U UTTER

AERODYNAMIC CHARACTERISTICS

NT AERODYNAMIC STABILITY

Aerodynamic characteristics of airfoils with ice

accretions

[AIAA PAPER 82-0282]

p0010 A82-22081

Finite volume calculation of three-dimensional
potential flow around a propeller

[AIAA PAPER 82-0957]

p0010 A82-31933

The effect of rotor blade thickness and surface
finish on the performance of a small axial flow
turbine

[ASME PAPER 82-GT-222]

p0022 A82-35409

Rapid approximate determination of nonlinear
solutions - Application to aerodynamic flows and
design/optimization problems

p0012 A82-35571

Flow aerodynamics modeling of an MHD swirl
combustor - Calculations and experimental
verification

p0094 A82-44782

The effect of rotor blade thickness and surface
finish on the performance of a small axial flow
turbine

[NASA-TM-82726]

p0003 A82-13114

Computer program for aerodynamic and blading
design of multistage axial-flow compressors

[NASA-TP-1946]

p0016 A82-15039

Rime ice accretion and its effect on airfoil
performance

[NASA-CR-165599]

p0008 A82-24166

Laser anemometer measurements in an annular
cascade of core turbine vanes and comparison
with theory

[NASA-TP-2018]

p0004 A82-26234

Aerodynamic performance of high turning core
turbine vanes in a two dimensional cascade

[NASA-TM-82894]

p0004 A82-26240

A summary of V/STOL inlet analysis methods

[NASA-TM-82885]

p0005 A82-28249

Comparison of laser anemometer measurements and
theory in an annular turbine cascade with
experimental accuracy determined by parameter
estimation

[NASA-TM-82860]

p0005 A82-28250

Energy efficient engine: High pressure turbine
uncooled rig technology report

[NASA-CR-165149]

p0031 A82-32383

Propeller flow visualization techniques

p0096 A82-32672

AERODYNAMIC CHORDS

U RFOIL PROFILES

AERODYNAMIC CONFIGURATIONS

Effect of heavy rain on aircraft

N82-21149

Rime ice accretion and its effect on airfoil
performance

[NASA-CR-165599]

p0008 A82-24166

AERODYNAMIC FORCES

NT AERODYNAMIC INTERFERENCE

NT AERODYNAMIC LOADS

Aerodynamic damping measurements in a transonic
compressor

[ASME PAPER 82-GT-287]

p0012 A82-35459

An experimental investigation of gapwise
periodicity and unsteady aerodynamic response in
an oscillating cascade. Volume 2: Data report.

Part 1: Text and mode 1 data

[NASA-CR-165457-VOL-2-PT-1]

p0006 A82-18180

Hydrodynamic and aerodynamic breakup of liquid
sheets

[NASA-TM-82800]

p0087 A82-19494

AERODYNAMIC INTERFERENCE

Effects of vane/blade ratio and spacing on fan noise

[AIAA PAPER 81-2033]

p0029 A82-10457

An experimental study of airfoil icing
characteristics

[NASA-TM-82790]

p0001 A82-17083

AERODYNAMIC LOADS

Effects of blade loading and rotation on
compressor rotor wake in end wall regions

[AIAA PAPER 82-0193]

p0010 A82-22063

Analytic investigation of effect of end-wall
contouring on stator performance

[NASA-TP-1943]

p0003 A82-14051

Performance deterioration due to acceptance
testing and flight loads; JT90 jet engine
diagnostic program

[NASA-CR-165572]

p0027 A82-27309

ORIGINAL PAGE IS
OF POOR QUALITY

SUBJECT INDEX

AIR INLETS

- D747/JT9D flight loads and their effect on engine running clearances and performance deterioration; BCAC NAIL/P and WA JT9D engine diagnostics programs [NASA-CF-165573] p0027 N82-28296
- On the road performance tests of electric test vehicle for correlation with road load simulator [NASA-TM-82900] p0127 N82-33829
- AERODYNAMIC NOISE**
The NASA-IERC wind turbine sound prediction code p0123 N82-23730
- Aeroacoustic performance of an externally blown flap configuration with several flap noise suppression devices [NASA-TP-1995] p0152 N82-24942
- AERODYNAMIC STABILITY**
Coupled bending-bending-torsion flutter of a mistuned cascade with nonuniform blades [NASA-TM-82813] p0111 N82-21604
- An experimental investigation of gapwise periodicity and unsteady aerodynamic response in an oscillating cascade. I: Experimental and theoretical results --- turbine blades [NASA-CF-3513] p0008 N82-26229
- Large displacements and stability analysis of nonlinear propeller structures [NASA-TM-82850] p0112 N82-31707
- AERODYNAMIC STALLING**
Application of an airfoil stall flutter computer prediction program to a three-dimensional wing: Prediction versus experiment [NASA-CF-168586] p0007 N82-19169
- Performance of single-stage axial-flow transonic compressor with rotor and stator aspect ratios of 1.63 and 1.77, respectively, and with design pressure ratio of 2.05 [NASA-TP-2901] p0018 N82-22269
- AERODYNAMICS**
NT AEROTHERMODYNAMICS
NT ROTOF AERODYNAMICS
The three-dimensional boundary layer on a rotating helical blade p0009 N82-15459
- Effect of a part span variable inlet guide vane on TP34 fan performance [NASA-CR-165458] p0023 N82-12075
- Cold-air performance of a 15.41-cm-tip-diameter axial-flow power turbine with variable-area stator designed for a 75-kW automotive gas turbine engine [NASA-TM-82644] p0024 N82-21193
- Aerodynamic analysis of VTOL inlets and definition of a short, blowing-lip inlet [NASA-CR-165617] p0007 N82-22211
- AEROELASTICITY**
Aeroelastic characteristics of a cascade of mistuned blades in subsonic and supersonic flows [ASME PAPER 81-DET-122] p0021 N82-19337
- Aerodynamic damping measurements in a transonic compressor [ASME PAPER 82-GT-287] p0012 N82-35459
- Application of an airfoil stall flutter computer prediction program to a three-dimensional wing: Prediction versus experiment [NASA-CR-168586] p0007 N82-19169
- Coupled bending-bending-torsion flutter of a mistuned cascade with nonuniform blades [NASA-TM-82813] p0111 N82-21604
- Summary and recent results from the NASA advanced High Speed Propeller Research Program [NASA-TM-82891] p0001 N82-26219
- Propeller flow visualization techniques p0096 N82-32672
- AEROMAGNETISM**
U MAGNETISM
- AEROMAGNETO FLUTTER**
U UTTER
- AERONAUTICAL ENGINEERING**
NASA research in aircraft propulsion [ASME PAPER 82-GT-177] p0022 N82-35389
- NASA research in aircraft propulsion [NASA-TM-82771] p0016 N82-13146
- NASA research activities in aeropropulsion [NASA-TM-82788] p0017 N82-16084
- AERONAUTICS**
Rotor fragment protection program: Statistics on aircraft gas turbine engine rotor failures that occurred in U.S. commercial aviation during 1978 [NASA-CF-165388] p0027 N82-27316
- AEROSOLS**
Aircraft sampling of the sulfate layer near the tropopause following the eruption of Mount St. Helens p0140 N82-37450
- AEROSPACE ENGINEERING**
NT AERONAUTICAL ENGINEERING
Local and national impact of aerospace research and technology [NASA-TM-82775] p0162 N82-20006
- Bibliography of Lewis Research Center technical publications announced in 1981 [NASA-TM-82838] p0163 N82-27191
- AEROSPACE ENVIRONMENTS**
NT DEEP SPACE
NT INTERPLANETARY SPACE
First results of material charging in the space environment [NASA-TM-84743] p0081 N82-24431
- Free electron lasers for transmission of energy in space [NASA-CR-165520] p0098 N82-25499
- Additional extensions to the NASCAP computer code, volume 1 [NASA-CR-167855] p0146 N82-25810
- AEROSPACE MEDICINE**
Ozone and aircraft operations p0001 N82-21145
- AEROTHERMODYNAMICS**
A real time Pegasus propulsion system model for VSTOL piloted simulation evaluation [NASA-TM-82770] p0016 N82-13144
- Demonstration of catalytic combustion with residual fuel [NASA-CR-165369] p0131 N82-16484
- AEROZINE**
NT LIQUID FUELS
- AGE HARDENING**
U ECIPITATION HARDENING
- AGING (MATERIALS)**
Survey on aging on electrodes and electrocatalysts in phosphoric acid fuel cells [NASA-CR-165505] p0128 N82-11545
- AGRICULTURE**
Market assessment of photovoltaic power systems for agricultural applications in Mexico [NASA-CR-165441] p0128 N82-10506
- Market assessment of photovoltaic power systems for agricultural applications in Morocco [NASA-CR-165477] p0130 N82-14627
- Market assessment of photovoltaic power systems for agricultural applications in Nigeria [NASA-CR-165511] p0133 N82-18698
- Market assessment of photovoltaic power systems for agricultural applications in Colombia [NASA-CR-165524] p0134 N82-22770
- AIR BEARINGS**
U S BEARINGS
- AIR BREATHING ENGINES**
NT BRISTOL-SIDDELEY BS 53 ENGINE
NT GAS TURBINE ENGINES
NT JET ENGINES
NT TURBOFAN ENGINES
NT TURBOJET ENGINES
NT TURBOPROP ENGINES
- AIR COOLING**
Thermal and flow analysis of a convection, air-cooled ceramic coated porous metal concept for turbine vanes [ASME PAPER 81-HT-48] p0020 N82-10952
- AIR DUCTS**
Turbofan forced mixer-nozzle internal flowfield. Volume 2: Computational fluid dynamic predictions [NASA-CR-3493] p0091 N82-22459
- AIR FLOW**
Methods for the calculation of axial wave numbers in lined ducts with mean flow p0153 N82-14044
- Experimental performance of the regenerator for the Chrysler upgraded automotive gas turbine engine [NASA-TM-82671] p0120 N82-21712
- Development of a spinning wave heat engine [NASA-CR-165611] p0028 N82-31328
- Active clearance control system for a turbomachine [NASA-CASE-LEW-12938-1] p0020 N82-32366
- AIR INLETS**
U R INTAKES

AIR INTAKES

N1 ENGINE INLETS
NT SUPERSONIC INTAKES
 Low speed testing of the inlets designed for a tandem-fan V/STOL nacelle --- conducted in the Lewis 10 by 10 foot wind tunnel
 [NASA-TM-82728] p0003 N82-11042
 Aerodynamic analysis of V/STOL inlets and definition of a short, blowing-lip inlet
 [NASA-CR-165617] p0007 N82-22211

AIR JETS
 Flow distributions and discharge coefficient effects for jet array impingement with initial crossflow
 [ASME PAPER 82-GT-1561] p0011 A82-35379

AIR LOCKS
 JT90 ceramic outer air seal system refinement program
 [NASA-CR-165554] p0106 N82-18603

AIR TRANSPORTATION
 NASA research activities in aeropropulsion
 [NASA-TM-82708] p0017 N82-16084

AIRCRAFT ACCIDENTS
 An assessment of the crash fire hazard of liquid hydrogen fueled aircraft
 [NASA-CR-165261] p0013 N82-19196

AIRCRAFT CONFIGURATIONS
 NASA research in aircraft propulsion
 [ASME PAPER 82-GT-177] p0022 A82-35389
 NASA research in aircraft propulsion
 [NASA-TM-82771] p0016 N82-13146

AIRCRAFT CONSTRUCTION MATERIALS
 Cost/benefit studies of advanced materials technologies for future aircraft turbine engines: Materials for advanced turbine engines
 [NASA-CR-167849] p0026 N82-25254

AIRCRAFT CONTROL
 Role of optical computers in aeronautical control applications
 p0156 N82-15897

AIRCRAFT DESIGN
NT HELICOPTER DESIGN
 Engine technology
 p0001 N82-19145
 Power systems
 p0001 N82-19146
 Power systems
 p0001 N82-19146
 Environmental control systems
 p0001 N82-19147
 Electromechanical actuators
 N82-19148

AIRCRAFT ENGINES
NT HELICOPTER ENGINES
NT IF-34 ENGINE
NT VARIABLE CYCLE ENGINES
 V/STOL propulsion control technology
 [AIAA PAPER 81-2634] p0029 A82-16909
 Blade loss transient dynamic analysis of turbomachinery
 [AIAA PAPER P2-1057] p0030 A82-34982
 The influence of Coriolis forces on gyroscopic motion of spinning blades
 [ASME PAPER 82-GT-163] p0030 A82-35384
 Optical tip clearance sensor for aircraft engine controls
 [AIAA PAPER 82-1131] p0018 A82-37691
 Propulsion study for Small Transport Aircraft Technology (STAT), Appendix B
 [NASA-CR-165499-APP-B] p0022 N82-10038
 Lightweight diesel engine designs for commuter type aircraft
 [NASA-CR-165470] p0023 N82-11068
 JT9D high pressure compressor performance improvement
 [NASA-CR-165531] p0104 N82-11467
 Integrated analysis of engine structures
 [NASA-TM-82713] p0111 N82-11491
 Thrust modulation methods for a subsonic V/STOL aircraft
 [NASA-TM-82747] p0003 N82-13112
 A real time Pegasus propulsion system model for V/STOL piloted simulation evaluation
 [NASA-TM-82770] p0016 N82-13144
 Sensor failure detection system --- for the F100 turbofan engine
 [NASA-CR-165515] p0023 N82-13145
 High temperature electronic requirements in aeropropulsion systems

[E-708] p0081 N82-15313
 Engine technology
 p0001 N82-19145
 Power systems
 p0001 N82-19146
 Power systems
 p0001 N82-19146
 Environmental control systems
 p0001 N82-19147
 Electromechanical actuators
 N82-19148
 YF 102 in-duct combustor noise measurements with a turbine nozzle, volume 1
 [NASA-CR-165562-VOL-1] p0153 N82-21031
 YF 102 in-duct combustor noise measurements with a turbine nozzle, volume 2
 [NASA-CR-165562-VOL-2] p0153 N82-21032
 YF 102 in-duct combustor noise measurements with a turbine nozzle, volume 3
 [NASA-CR-165562-VOL-3] p0155 N82-21033
 Preliminary results on performance testing of a turbocharged rotary combustion engine
 [NASA-TM-82772] p0017 N82-21194
 Analytical investigation of nonrecoverable stall
 [NASA-TM-82792] p0018 N82-21195
 The role of modern control theory in the design of controls for aircraft turbine engines
 [NASA-TM-82815] p0018 N82-22262
 Advanced general aviation comparative engine/airframe integration study
 [NASA-CR-165564] p0025 N82-22263
 Advanced Low-Emissions Catalytic-Combustor Program, phase 1 --- aircraft gas turbine engines
 [NASA-CR-159656] p0025 N82-22265
 Advanced general aviation engine/airframe integration study
 [NASA-CR-165565] p0025 N82-22268
 Evaluation of inelastic constitutive models for nonlinear structural analysis --- for aircraft turbine engines
 [NASA-TM-82845] p0112 N82-24502
 Cost/benefit studies of advanced materials technologies for future aircraft turbine engines: Materials for advanced turbine engines
 [NASA-CR-167849] p0026 N82-25254
 Development potential of Intermittent Combustion (I.C.) aircraft engines for commuter transport applications
 [NASA-TM-82869] p0019 N82-26297
 NASA research in supersonic propulsion: A decade of progress
 [NASA-TM-82862] p0019 N82-26300
 Performance deterioration due to acceptance testing and flight loads; JT90 jet engine diagnostic program
 [NASA-CR-165572] p0027 N82-27309
 Advanced stratified charge rotary aircraft engine design study
 [NASA-CR-165398] p0107 N82-27743
 Advances in high-speed rolling-element bearings
 [NASA-TM-82910] p0101 N82-28644
 QCSSE over-the-wing engine acoustic data
 [NASA-TM-82708] p0020 N82-29324
 Advanced turboprop testbed systems study
 [NASA-CR-167895] p0014 N82-33375
 Structural tailoring of engine blades (STAEBL)
 [NASA-CR-167949] p0028 N82-33391
 Exhaust emissions reduction for intermittent combustion aircraft engines
 [NASA-CR-167914] p0029 N82-33392
 Energy efficient engine: Turbine transition duct model technology report
 [NASA-CR-167996] p0029 N82-33394

AIRCRAFT FUEL SYSTEMS
 Experimental study of external fuel vaporization
 [ASME PAPER 82-GT-59] p0075 A82-35312
 Experimental study of fuel heating at low temperatures in a wing tank model, volume 1
 [NASA-CR-165391] p0073 N82-11224
 External fuel vaporization study
 [NASA-CR-165513] p0073 N82-14371

AIRCRAFT FUELS
NT LIQUID FUELS
 The NASA MERIT program - Developing new concepts for accurate flight planning
 [AIAA PAPER 82-0340] p0614 A82-17894
 NASA Broad Specification Fuels Combustion Technology program - Pratt and Whitney Aircraft Phase I results and status

- [AIAA PAPER 82-1088] p0021 A82-34999
Experimental study of fuel heating at low
temperatures in a wing tank model, volume 1
[NASA-CR-165391] p0073 N82-11224
- External fuel vaporization study
[NASA-CR-165513] p0073 N82-14371
- An assessment of the crash fire hazard of liquid
hydrogen fueled aircraft
[NASA-CP-165526] p0013 N82-19196
- Low NOx heavy fuel combustor concept
program
[NASA-CR-165367] p0136 N82-25635
- Additional experiments on flowability improvements
of aviation fuels at low temperatures, volume 2
[NASA-CR-167912] p0074 N82-31546
- Characterization of an Experimental Referee
Broadened Specification (ERBS) aviation turbine
fuel and EPBS fuel blends
[NASA-TM-82883] p0572 N82-32504
- Impact of advanced propeller technology on
aircraft/mission characteristics of several
general aviation aircraft
[NASA-CR-167984] p0009 N82-33347
- AIRCRAFT HAZARDS**
Selected bibliography of NACA-NASA aircraft icing
publications
[NASA-TM-81651] p0014 N82-11053
- An assessment of the crash fire hazard of liquid
hydrogen fueled aircraft
[NASA-CR-165526] p0013 N82-19196
- Rime ice accretion and its effect on airfoil
performance
[NASA-CR-165599] p0008 N82-24166
- AIRCRAFT INSTRUMENTS**
NT DRAG FORCE ANEMOMETERS
NT HOT-WIRE ANEMOMETERS
Aircraft icing research at NASA
[NASA-TM-82919] p0013 N82-30297
- AIRCRAFT MANEUVERS**
Performance deterioration due to acceptance
testing and flight loads; JT90 jet engine
diagnostic program
[NASA-CR-165572] p0027 N82-27309
- AIRCRAFT MODELS**
Alternatives for jet engine control
[NASA-CP-168894] p0026 N82-23247
- AIRCRAFT NOISE**
NT JET AIRCRAFT NOISE
Sound generated in a cascade by three-dimensional
disturbances convected in a subsonic flow
[AIAA PAPER 81-2046] p0153 A82-10460
- Propeller tip vortex - A possible contributor to
aircraft cabin noise
p0152 A82-17603
- Acoustic transmission in lined flow ducts - A
finite element eigenvalue problem
p0154 A82-17663
- A shock wave approach to the noise of supersonic
propellers
[NASA-TM-82752] p0151 N82-16809
- A preliminary comparison between the SR-3
propeller noise in flight and in a wind tunnel
[NASA-TM-82805] p0152 N82-21998
- AIRCRAFT NOISE PREDICTION**
USE PREDICTION (AIRCRAFT)
- AIRCRAFT PARTS**
Geometrical aspects of the tribological properties
of graphite fiber reinforced polyimide composites
[NASA-TM-82757] p0066 N82-15198
- AIRCRAFT PERFORMANCE**
NT HELICOPTER PERFORMANCE
Kevlar/PMR-15 reduced drag DC-9 reverser stang
fairing
[NASA-CP-165448] p0052 N82-31448
- AIRCRAFT POWER SOURCES**
U RCPAFT ENGINES
- AIRCRAFT WAKES**
NT PROPELLER SLIPSTREAMS
- AIRFOIL CHARACTERISTICS**
U RFOILS
- AIRFOIL PROFILES**
The effect of rotor blade thickness and surface
finish on the performance of a small axial flow
turbine
[ASME PAPER 82-GT-2221] p0022 A82-35409
- Three-dimensional shock structure in a transonic
flutter cascade
p0006 A82-37937
- The effect of rotor blade thickness and surface
finish on the performance of a small axial flow
turbine
[NASA-TM-82726] p0003 N82-13114
- Computer program for aerodynamic and blading
design of multistage axial-flow compressors
[NASA-TP-1946] p0016 N82-15039
- An experimental study of airfoil icing
characteristics
[NASA-TM-82790] p0001 N82-17083
- Core compressor exit stage study, volume 6
[NASA-CR-165553] p0027 N82-27310
- AIRFOIL SECTIONS**
U RFOIL PROFILES
- AIRFOIL THICKNESS**
U RFOIL PROFILES
- AIRFOILS**
NT EXTERNALLY BLOWN FLAPS
NT PROPELLER BLADES
NT THIN AIRFOILS
NT TILTING ROTORS
NT WINGS
Aerodynamic characteristics of airfoils with ice
accretions
[AIAA PAPER 82-0282] p0010 A82-22081
- Mathematical modeling of ice accretion on airfoils
[AIAA PAPER 82-0284] p0014 A82-27098
- CAS22 - FORTRAN program for fast design and
analysis of shock-free airfoil cascades using
fictitious-gas concept
[NASA-CR-3507] p0006 N82-16044
- An experimental investigation of gapwise
periodicity and unsteady aerodynamic response in
an oscillating cascade, Volume 2: Data report.
Part 1: Text and model data
[NASA-CR-165457-VOL-2-PT-1] p0006 N82-18180
- Numerical analysis and FORTRAN program for the
computation of the turbulent wakes of
turbomachinery rotor blades, isolated airfoils
and cascade of airfoils
[NASA-CR-3509] p0006 N82-18184
- Application of an airfoil stall flutter computer
prediction program to a three-dimensional wing:
Prediction versus experiment
[NASA-CR-168586] p0007 N82-19169
- NASA/Lewis Research Center Icing Research Program
p0001 N82-21148
- Rime ice accretion and its effect on airfoil
performance
[NASA-CR-165599] p0008 N82-24166
- ALCOHOLS**
NT POLYVINYL ALCOHOL
- ALGEBRA**
NT EIGENVALUES
NT EIGENVECTORS
NT MATRICES (MATHEMATICS)
NT NONLINEAR EQUATIONS
NT VECTORS (MATHEMATICS)
- ALGORITHMS**
Application of integration algorithms in a
parallel processing environment for the
simulation of jet engines
[NASA-TM-82746] p0149 N82-14849
- Multiple-grid acceleration of Lax-Wendroff
algorithms
[NASA-TM-82843] p0149 N82-22922
- A generalized memory test algorithm
[NASA-TM-82874] p0146 N82-31971
- ALIPHATIC COMPOUNDS**
NT ALKYL COMPOUNDS
NT METHANE
NT PROPANE
- ALKALI HALIDES**
NT SODIUM CHLORIDES
- ALKALI METALS**
NT CESIUM
- ALKALINE BATTERIES**
Alkaline regenerative fuel cell systems for energy
storage
p0042 A82-11706
- Mechanism and models for zinc metal morphology in
alkaline media
[NASA-TM-82768] p0120 N82-19671
- Cross-linked polyvinyl alcohol films as alkaline
battery separators
[NASA-TM-82802] p0054 N82-22327
- Advanced inorganic separators for alkaline batteries
[NASA-CASE-LEW-13171-1] p0124 N82-29708
- ALKALINE EARTH OXIDES**
NT MAGNESIUM OXIDES

ALKALINITY

Endurance test and evaluation of alkaline water
electrolysis cells
[NASA-CR-165424] p0130 N82-13508

ALKALOIDS

NT QUINOLINE

ALKANES

NT METHANE

NT PROPANE

ALKYL COMPOUNDS

Thermal oxidative degradation reactions of linear
perfluoroalkyl ethers
[NASA-TM-82814] p0068 N82-26468

ALKYLATION

Cathode catalysts for primary phosphoric acid fuel
cells
[NASA-CR-165578] p0134 N82-21709

ALLOYS

NT ALUMINUM ALLOYS

NT CHROMIUM ALLOYS

NT COBALT ALLOYS

NT COPPER ALLOYS

NT EUTECTIC ALLOYS

NT HEAT RESISTANT ALLOYS

NT IRON ALLOYS

NT MAGNESIUM ALLOYS

NT MANGANESE ALLOYS

NT MOLYBDENUM ALLOYS

NT NICKEL ALLOYS

NT PLATINUM ALLOYS

NT STAINLESS STEELS

NT STEELS

NT TERNARY ALLOYS

NT TITANIUM ALLOYS

NT TUNGSTEN ALLOYS

NT WELDMENTS

NT WROUGHT ALLOYS

Elastic-plastic finite-element analyses of
thermally cycled double-edge wedge specimens
[NASA-TP-1973] p0111 N82-20566

ALTERNATING CURRENT

The ac propulsion system for an electric vehicle,
phase 1
[NASA-CR-165480] p0129 N82-13506

Progress on advanced dc and ac induction drives
for electric vehicles
[NASA-TM-82895] p0163 N82-31160

ALTERNATING CURRENT GENERATORS

U GENERATORS

ALTERNATORS (GENERATORS)

U GENERATORS

ALUMINA

U OXIDE

ALUMINIZING

U ALUMINUM COATINGS

ALUMINUM

Detection of a change in the oxidation state on
aluminum surface using angular correlation of
positron annihilation radiation A82-30374

Tensile properties of SiC/aluminum filamentary
composites - Thermal degradation effects p0053 A82-46220

Factors influencing the thermally-induced strength
degradation of B/Al composites
[NASA-TM-82823] p0050 N82-24297

The orthogonal in-situ etching of single and
polycrystalline aluminum and copper, volume 1
[NASA-CR-168929] p0076 N82-24361

ALUMINUM ALLOYS

Fatigue of Ni-Al-Mo aligned eutectics at elevated
temperatures p0052 A82-13403

Permanent magnet properties of Mn-Al-C between -50
C and +150 C p0085 A82-20505

Long-term high-velocity oxidation and hot
corrosion testing of several NiCrAl and FeCrAl
base oxide dispersion strengthened alloys p0062 A82-37151

Applications of high-temperature powder metal
aluminum alloys to small gas turbines p0065 A82-48244

Solute transport during the cyclic oxidation of
Ni-Cr-Al alloys
[NASA-CR-165544] p0064 N82-27462

NiCrAl ternary alloy having improved cyclic
oxidation resistance
[NASA-CASE-LEW-13339-1] p0061 N82-31505

ALUMINUM BORON COMPOSITES

Work of fracture in aluminum metal-matrix composites
p0053 A82-31339

Analysis of crack propagation as an energy
absorption mechanism in metal matrix composites
[NASA-CR-165051] p0052 N82-14288

Micromechanical predictions of crack propagation
and fracture energy in a single fiber
boron/aluminum model composite

[NASA-CR-168550] p0052 N82-18326
Strength advantages of chemically polished boron
fibers before and after reaction with aluminum
[NASA-TM-82806] p0049 N82-21258

ALUMINUM COATINGS

Method of protecting a surface with a
silicon-slurry/aluminide coating --- coatings
for gas turbine engine blades and vanes
[NASA-CASE-LEW-13343-1] p0068 N82-28441

ALUMINUM COMPOUNDS

NT ALUMINUM OXIDES

Recrystallization and grain growth in Al
p0065 A82-44529

ALUMINUM OXIDES

Castable high temperature refractory materials
[NASA-CASE-LEW-13080-2] p0066 N82-11210
Thermal degradation of the tensile properties of
unidirectionally reinforced FP-Al2O3/EZ 33
magnesium composites

[NASA-TM-82817] p0049 N82-21260
Modulus, strength and thermal exposure studies of
FP-Al2O3/aluminum and FP-Al2O3/magnesium
composites

[NASA-TM-82868] p0050 N82-30335
Plastic deformation and wear process at a surface
during unlubricated sliding

[NASA-TM-82820] p0102 N82-32735

ANBIT

U ELD THEORY (PHYSICS)

ANIDES

NT POLYIMIDES

AMORPHOUS MATERIALS

Friction and surface chemistry of some
ferrous-base metallic glasses
[NASA-TP-1991] p0059 N82-21301

AMPERAGE

U ELECTRIC CURRENT

AMPLIFICATION

NT POWER GAIN

AMPLIFIER DESIGN

Investigation of a comb-type slow-wave structure
for millimeter-wave masers A82-18368

IMPATT power building blocks for 20 GHz spaceborne
transmit amplifier
[AIAA 82-0498] p0086 A82-23566

AMPLIFIERS

NT MAGNETIC AMPLIFIERS

NT MICROWAVE AMPLIFIERS

NT POWER AMPLIFIERS

Analytic investigation of efficiency and
performance limits in klystron amplifiers using
multidimensional computer programs; multi-stage
depressed collectors; and thermionic cathode
life studies p0118 N82-12553

ANALOG SIMULATION

Advancements in real-time engine simulation
technology --- of digital electronic aircraft
engine controls
[AIAA PAPER 82-1075] p0021 A82-3489

Advancements in real-time engine simulation
technology
[NASA-TM-82825] p0147 N82-22915

ANALYSIS (MATHEMATICS)

NT APPROXIMATION

NT CAUCHY INTEGRAL FORMULA

NT COMPUTATIONAL FLUID DYNAMICS

NT CONFORMAL MAPPING

NT DIFFERENCE EQUATIONS

NT DIFFERENTIAL EQUATIONS

NT ERROR ANALYSIS

NT FINITE DIFFERENCE THEORY

NT FINITE ELEMENT METHOD

NT FOURIER ANALYSIS

NT FOURIER SERIES

NT HALF PLANES

NT HELMHOLTZ VORTICITY EQUATION

NT INTEGRAL EQUATIONS

NT J INTEGRAL

NT MATHIEU FUNCTION [NASA-TP-2018] p0004 N82-26234
 NT NEWTON-RAPHSON METHOD The design and instrumentation of the Purdue
 NT NONLINEAR EQUATIONS annular cascade facility with initial data
 NT NUMERICAL ANALYSIS acquisition and analysis
 NT NUMERICAL INTEGRATION [NASA-CR-167861] p0008 N82-26237
 NT PERIODIC FUNCTIONS
 NT RAYLEIGH-RITZ METHOD
 NT RELAXATION METHOD (MATHEMATICS)
 NT SINGULARITY (MATHEMATICS)
 NT TANGENTS
 NT VECTOR ANALYSIS
ANALYTIC GEOMETRY
 NT TANGENTS
ANATOMY
 NT AORTA
 NT EAR
 NT EYE (ANATOMY)
ANEMOMETERS
 NT DRAG FORCE ANEMOMETERS
 NT HOT-FILM ANEMOMETERS
 NT HOT-WIRE ANEMOMETERS
 NT LASER ANEMOMETERS
ANEMOMETRY
 U LOCALITY MEASUREMENT
ANGLE OF ATTACK
 Three-dimensional flow calculations including
 boundary layer effects for supersonic inlets at
 angle of attack
 [AIAA PAPER 82-0061] p0005 A82-19778
 Experimental and analytical results of tangential
 blowing applied to a subsonic V-STOL inlet
 [AIAA PAPER 82-1084] p0005 A82-35195
 Experimental and analytical results of tangential
 blowing applied to a subsonic V-STOL inlet
 [NASA-TM-82847] p0004 N82-24165
 Calculation of the flow field including boundary
 layer effects for supersonic mixed compression
 inlets at angles of attack
 [NASA-CR-167941] p0009 N82-29269
 Rough analysis of installation effects on
 turboprop noise
 [NASA-TM-82924] p0152 N82-32082
ANGLES (GEOMETRY)
 NT ANGLE OF ATTACK
ANGULAR CORRELATION
 Detection of a change in the oxidation state on
 aluminum surface using angular correlation of
 positron annihilation radiation
 A82-30374
ANIONS
 Anion permselective membrane
 [NASA-CR-167872] p0137 N82-30711
ANISOTROPIC MEDIA
 Permanent magnet properties of Mn-Al-C between -50
 C and +150 C
 p0065 A82-20505
ANISOTROPY
 Representation and material charging response of
 geoplasma environments
 p0039 N82-14249
ANNEALING
 Processing of silicon solar cells by ion
 implantation and laser annealing
 [NASA-CR-165283] p0128 N82-11546
ANNIHILATION REACTIONS
 NT POSITRON ANNIHILATION
ANNUAL VARIATIONS
 Illustration of a new test for detecting a shift
 in mean in precipitation series
 A82-13217
ANNULAR DUCTS
 Velocity gradient method for calculating velocities
 in an axisymmetric annular duct
 [NASA-TP-2029] p0005 N82-29270
ANNULAR FLOW
 A comprehensive method for preliminary design
 optimization of axial gas turbine stages
 [AIAA PAPER 82-1268] p0030 A82-35091
 Three-dimensional flow field in the tip region of
 a compressor rotor passage. I - Mean velocity
 profiles and annulus wall boundary layer
 [ASME PAPER 82-GT-11] p0011 A82-35280
 Three-dimensional flow field in the tip region of
 a compressor rotor passage. II - Turbulence
 properties
 [ASME PAPER 82-GT-234] p0011 A82-35416
 Laser anemometer measurements in an annular
 cascade of core turbine vanes and comparison
 with theory

ANNULAR NOZZLES
 Three dimensional mean velocity and turbulence
 characteristics in the annulus wall region of an
 axial flow compressor rotor passage
 [NASA-CR-169003] p0026 N82-25252

ANODES
 Endurance test and evaluation of alkaline water
 electrolysis cells
 [NASA-CR-165424] p0130 N82-13508

ANTARCTIC ENVIRONMENT
 U E ENVIRONMENTS
ANTARCTIC REGIONS
 An attempt at magnetic-variation sounding in the
 Antarctic
 A82-25290

ANTARCTICA
 U TARTIC REGIONS

ANTENNA ARRAYS
 NASA Adaptive Multibeam Phased Array (AMPA): An
 application study
 [NASA-CR-169125] p0079 N82-28503

ANTENNA COMPONENTS
 NT ANTENNA FEEDS
ANTENNA DESIGN
 30/20 GHz communications satellite multibeam antenna
 [AIAA 82-0449] p0079 A82-23486
 Focal surfaces of offset dual-reflector antennas
 p0080 A82-36265
 Coaxial prime focus feeds for paraboloidal
 reflectors
 [NASA-CR-167934] p0078 N82-31585

ANTENNA FEEDS
 Coaxial prime focus feeds for paraboloidal
 reflectors
 [NASA-CR-167934] p0078 N82-31585

ANTENNA FIELDS
 U TENNA RADIATION PATTERNS
ANTENNA RADIATION PATTERNS
 Focal surfaces of offset dual-reflector antennas
 p0080 A82-36265
 NASA Adaptive Multibeam Phased Array (AMPA): An
 application study
 [NASA-CR-169125] p0079 N82-28503
 Coaxial prime focus feeds for paraboloidal
 reflectors
 [NASA-CR-167934] p0078 N82-31585

ANTENNAS
 NT SATELLITE ANTENNAS
 NT SPACECRAFT ANTENNAS
 NT TWO REFLECTOR ANTENNAS
 Coupled cavity traveling wave tube with velocity
 tapering
 [NASA-CASE-LEW-12296-1] p0082 N82-26568

ANTI-FRICTION BEARINGS
 NT BALL BEARINGS
 NT ROLLER BEARINGS
ANTIICING ADDITIVES
 Icing tunnel tests of a composite porous leading
 edge for use with a liquid anti-ice system ---
 Lewis icing research tunnel
 [NASA-CR-164966] p0014 N82-11052

ANTIREFLECTION COATINGS
 Advances in high output voltage silicon solar cells
 p0127 A82-44942

AORTA
 Evaluation of left ventricular assist device pump
 bladders cast from ion-sputtered
 polytetrafluorethylene mandrels
 [NASA-CR-167904] p0142 N82-23976

APATITES
 U NERALS

APERTURES
 Diffraction by a finite strip
 p0150 A82-33605

APPALACHIAN MOUNTAINS (NORTH AMERICA)
 LANDSAT Remote Sensing: Observations of an
 Appalachian mountaintop surface coal mining and
 reclamation operation --- Kentucky
 [82-10247] p0117 N82-24525

APPROXIMATION
 NT FINITE DIFFERENCE THEORY
 NT FINITE ELEMENT METHOD
 NT NEWTON-RAPHSON METHOD
 NT RAYLEIGH-RITZ METHOD

NT RELAXATION METHOD (MATHEMATICS)
 Rapid approximate determination of nonlinear solutions - Application to aerodynamic flows and design/optimization problems p0012 A82-35571

APPROXIMATION METHODS
 U APPROXIMATION

AQUEOUS SOLUTIONS
 Inexpensive cross-linked polymeric separators made from water-soluble polymers --- for secondary alkaline nickel-zinc and silver-zinc cells p0048 A82-23778

ARC DISCHARGES
 Brushfire arc discharge model p0038 A82-14224

ARCHITECTURE (COMPUTERS)
 Film shape calculations on supercomputers [NASA-TM-82856] p0100 A82-25519

ARCTIC ENVIRONMENTS
 U E ENVIRONMENTS

ARGON PLASMA
 Turbulence in argon shock waves p0158 A82-11117

ARIP (IMPACT PREDICTION)
 U NEUTRALIZED SIMULATION

ARMATURES
 Straight and chopped DC performance data for a General Electric 5BY436A1 DC shunt motor with a General Electric KV-1 controller [NASA-CR-165507] p00P5 A82-24425

AROMATIC COMPOUNDS
 High-temperature resins p0051 A82-42657

ARRAYS
 NT ANTERNA ARRAYS
 NT PHASED ARRAYS
 NT SOLAR ARRAYS

ARSENIC COMPOUNDS
 NT GALLIUM ARSENIDES

ARSENIDES
 NT GALLIUM ARSENIDES

ARTERIES
 NT AORTA

ARTIFICIAL SATELLITES
 NT ATS 5
 NT COMMUNICATION SATELLITES
 NT SCATHA SATELLITE
 NT SOLAR POWER SATELLITES
 NT SYNCHRONOUS SATELLITES
 Potentials of surfaces in space p0165 A82-23750

ARYL COMPOUNDS
 U ONATIC COMPOUNDS

ASPECT RATIO
 Performance of single-stage axial-flow transonic compressor with rotor and stator aspect ratios of 1.63 and 1.78, respectively, and with design pressure ratio of 1.82 [NASA-TP-1974] p0017 A82-19222

ASSEMBLING
 NT ORBITAL ASSEMBLY
 A pad perturbation method for the dynamic coefficients of tilting-pad journal bearings p0110 A82-14400

ASSESSMENTS
 NT TECHNOLOGY ASSESSMENT

ASSURANCE
 Experience with modified aerospace reliability and quality assurance method for wind turbines [NASA-TM-82803] p0110 A82-19550

ASTRONOMICAL MAPS
 Time variability and structure of quiet sun sources at 6 cm wavelength p0167 A82-26003

ASTRONOMY
 NT GALILEO ASTRONOMY

ATLAS CENTAUR LAUNCH VEHICLE
 Centaur capabilities for communications satellite launches [AIAA PAPER 82-0558] p0034 A82-36286

ATLAS LAUNCH VEHICLES
 NT ATLAS CENTAUR LAUNCH VEHICLE

ATMOSPHERIC ABSORPTION
 U MOSPHERIC ATTENUATION

ATMOSPHERIC ATTENUATION
 Advanced 30/20 GHz communication satellites p0034 A82-12623
 Adaptive rain fade compensation p0080 A82-27178

ATMOSPHERIC BOUNDARY LAYER
 Natural convection with combined driving forces p0093 A82-31445

ATMOSPHERIC CIRCULATION
 Stratospheric-mesospheric midwinter disturbances - A summary of observed characteristics A82-12135
 Natural convection with combined driving forces p0093 A82-31445

ATMOSPHERIC EFFECTS
 Environmental effects on solar concentrator mirrors A82-23394
 Effect of heavy rain on aircraft A82-21149

ATMOSPHERIC ELECTRICITY
 NASA research programs responding to workshop recommendations A82-21146

ATMOSPHERIC HEATING
 Stratospheric-mesospheric midwinter disturbances - A summary of observed characteristics A82-12135

ATMOSPHERIC IONIZATION
 NT AURORAL IONIZATION

ATMOSPHERIC PHYSICS
 NT CLOUD PHYSICS

ATMOSPHERIC SCATTERING
 NT TROPOSPHERIC SCATTERING

ATMOSPHERIC SOUNDING
 Aircraft sampling of the sulfate layer near the tropopause following the eruption of Mount St. Helens p0140 A82-37450

ATMOSPHERIC TEMPERATURE
 Stratospheric-mesospheric midwinter disturbances - A summary of observed characteristics A82-12135
 Natural convection with combined driving forces p0093 A82-31445

ATOMIZATION
 U OMIZING

ATOMIZING
 Atomization and combustion properties of flashing injectors [AIAA PAPER 82-0300] p0092 A82-17880

ATS
 NT ATS 5

ATS 5
 Modification of spacecraft potentials by thermal electron emission on ATS-5 p0040 A82-16194

ATTACHMENTS
 U CESSORIES

ATTENUATION
 NT ACOUSTIC ATTENUATION
 NT ATMOSPHERIC ATTENUATION
 NT SHOCK WAVE ATTENUATION

ATTITUDE (INCLINATION)
 NT PITCH (INCLINATION)
 NT YAW

ATTITUDE CONTROL
 NT THRUST VECTOR CONTROL
 Variable gain for a wind turbine pitch control [NASA-TM-82751] p0119 A82-16478

ATTITUDE STABILITY
 NT GYROSCOPIC STABILITY

AUGER SPECTROSCOPY
 Application of surface analysis to solve problems of wear [NASA-TM-82753] p0099 A82-14519

AURORAL IONIZATION
 Charging of a large object in low polar Earth orbit --- space shuttle orbiter p0039 A82-14275

AUTOCOLLIMATORS
 U LLIMATORS

AUTOMATIC CONTROL
 NT ACTIVE CONTROL
 NT ADAPTIVE CONTROL
 NT DYNAMIC CONTROL
 NT FEEDBACK CONTROL
 NT NUMERICAL CONTROL
 NT OPTIMAL CONTROL
 Sensor failure detection system --- for the F100 turbofan engine [NASA-CR-165515] p0023 A82-13145

AUTOMATIC DATA PROCESSING
 U TA PROCESSING

AUTOMATIC ROCKET IMPACT PREDICTORS
U MPUTEFIZED SIMULATION
AUTOMOBILE ENGINES

The AGT101 technology - An automotive alternative
p0107 A82-11783

AGT 100 automotive gas turbine system development
[AIAA PAPER 82-1165] p0108 A82-35038

AGT101 automotive gas turbine system development
[AIAA PAPER 82-1166] p0108 A82-35039

AGT100 turbomachinery --- for automobiles
[AIAA PAPER 82-1277] p0108 A82-35061

Combustor development for automotive gas turbines
[AIAA PAPER 82-1208] p0104 A82-35062

The AGT 101 advanced automotive gas turbine
[ASME PAPER 82-GT-72] p0108 A82-35321

Jet impingement heat transfer enhancement for the
GPU-3 Stirling engine
[NASA-TM-82727] p0163 A82-11993

AGT-102 automotive gas turbine
[NASA-CR-165353] p0105 A82-12444

Test results and facility description for a
40-kilowatt stirling engine
[NASA-TM-82620] p0163 A82-13013

Advanced Gas Turbine (AGT) powertrain system
initial development report
[NASA-CR-165130] p0132 A82-16485

Advanced Gas Turbine (AGT) powertrain system
development for automotive applications
[NASA-CR-165175] p0163 A82-16937

Cold-air performance of a 15.41-cm-tip-diameter
axial-flow power turbine with variable-area
stator designed for a 75-kW automotive gas
turbine engine
[NASA-TM-82644] p0024 A82-21193

Preliminary results on performance testing of a
turbocharged rotary combustion engine
[NASA-TM-82772] p0017 A82-21194

Experimental performance of the regenerator for
the Chrysler upgraded automotive gas turbine
engine
[NASA-TM-82671] p0120 A82-21712

Preliminary analysis of a downsized advanced
gas-turbine engine in a subcompact car
[NASA-TM-82848] p0163 A82-26051

Multiroller traction drive speed reducer:
Evaluation for automotive gas turbine engine
[NASA-TP-2027] p0101 A82-26678

Automotive Stirling engine development program
[NASA-CR-167907] p0164 A82-29235

Evaluation of candidate stirling engine heater
tube alloys at 820 deg and 860 deg C
[NASA-TM-82837] p0061 A82-30372

Automotive Stirling Engine Mod 1 Design Review,
volume 1
[NASA-CR-167935] p0164 A82-34311

Automotive Stirling Engine Mod 1 Design Review,
volume 3 --- engineering drawings
[NASA-CR-167397] p0164 A82-34312

AUTOMOBILE FUELS
NT LIQUID FUELS
AUTOMOBILES
NT ELECTRIC AUTOMOBILES

High temperature durable catalyst development
p0056 A82-20739

Fuel economy and exhaust emissions characteristics
of diesel vehicles: Test results of a prototype
fiat 131TC 2.4 liter automobile
[NASA-CR-165535] p0164 A82-18068

AUXILIARY POWER SOURCES
NT SPACE POWER UNIT REACTORS
AUXILIARY PROPULSION

Measuring the spacecraft and environmental
interactions of the 8-cm mercury ion thrusters
on the P80-1 mission
p0043 A82-15438

Study of electrical and chemical propulsion
systems for auxiliary propulsion of large space
systems, Volume 1: Executive summary
[NASA-CR-165502-VOL-1] p0046 A82-11110

Study of electrical and chemical propulsion
systems for auxiliary propulsion of large space
systems, volume 2
[NASA-CR-165502-VOL-2] p0044 A82-11111

An insight into auxiliary propulsion requirements
of large space systems
[NASA-TM-92827] p0042 A82-24286

Large Space Systems/Propulsion Interactions
[NASA-TM-82904] p0042 A82-27358

AV-8A AIRCRAFT
U REIER AIRCRAFT
AVLANCHE DIODES

IMPATT power building blocks for 20 GHz spaceborne
transmit amplifier
[AIAA 82-0498] p0086 A82-23566

AVERAGE
NT MEAN
AVIATION
U RONAUTICS
AVONICS

Real-time microcomputer simulation for space
Shuttle/Centaur avionics
p0033 A82-48245

Bibliography of Lewis Research Center technical
publications announced in 1981
[NASA-TM-82838] p0163 A82-27191

AXES (REFERENCE LINES)
NT AXES OF ROTATION
AXES OF ROTATION

Whirl flutter analysis of a horizontal-axis wind
turbine with a two-bladed teetering rotor
p0122 A82-23707

AXIAL COMPRESSION LOADS

Compression behavior of unidirectional fibrous
composite
[NASA-TM-82833] p0050 A82-22313

AXIAL COMPRESSORS
U RECOMPRESSORS
AXIAL FLOW

Flow through axially aligned sequential apertures
of the orifice and Borda types
[ASME PAPER 81-HT-79] p0089 A82-10964

Three dimensional flow field inside the passage of
a low speed axial flow compressor rotor
[AIAA PAPER 82-1006] p0011 A82-31964

Performance of single-stage axial-flow transonic
compressor with rotor and stator aspect ratios
of 1.63 and 1.77, respectively, and with design
pressure ratio of 2.05
[NASA-TP-2001] p0018 A82-22269

STGSK: A computer code for predicting multistage
axial flow compressor performance by a meanline
stage stacking method
[NASA-TP-2020] p0018 A82-25250

Investigation of the tip clearance flow inside and
at the exit of a compressor rotor passage
[NASA-CR-169004] p0026 A82-25253

AXIAL FLOW COMPRESSORS
U RECOMPRESSORS
AXIAL FLOW PUMPS
NT TURBINE PUMPS
AXIAL FLOW TURBINES

A comprehensive method for preliminary design
optimization of axial gas turbine stages
[AIAA PAPER 82-1264] p0030 A82-35091

The use of optimization techniques to design
controlled diffusion compressor blading
[ASME PAPER 82-GT-149] p0022 A82-35373

The use of optimization techniques to design
controlled diffusion compressor blading
[NASA-TM-82763] p0016 A82-14094

Small axial turbine stator technology program
[NASA-CR-165602] p0028 A82-32367

Rotor tip clearance effects on overall and
blade-element performance of axial-flow
transonic fan stage
[NASA-TP-2049] p0020 A82-33389

AXIAL LOADS
NT AXIAL COMPRESSION LOADS

Modulus, strength and thermal exposure studies of
PP-A1203/aluminum and PP-A1203/magnesium
composites
[NASA-TM-82868] p0050 A82-30335

AXIAL STRESS

Analytical and experimental evaluation of biaxial
contact stress
p0071 A82-20741

Fatigue life prediction in bending from axial
fatigue information
[NASA-CR-165563] p0113 A82-20564

AXISYMMETRIC BODIES

GRID3C: Computer program for generation of C type
multilevel, three dimensional and boundary
conforming periodic grids
[NASA-CR-167846] p0008 A82-26239

Investigations of flowfields found in typical
combustor geometries
[NASA-CR-169295] p0092 A82-31643

ORIGINAL PAGE IS
OF POOR QUALITY

AXISYMMETRIC FLOW

NT ANNULAR FLOW
On the prediction of swirling flowfields found in axisymmetric combustor geometries p0029 A82-12120
Distorted turbulence in axisymmetric flow p0089 A82-16071
Near flowfields in axisymmetric combustor geometries with swirl [AIAA PAPER 82-0177] p0092 A82-17824
Turbulence measurements in a confined jet using a six-orientation hot-wire probe technique [AIAA PAPER 82-1262] p0094 A82-37710

AXLES

U AFTS (MACHINE ELEMENTS)

AZOLES

NT INDOLES
NT PYRROLES

B

BACKWARD FACING STEPS

Tangential blowing for control of strong normal shock - Boundary layer interactions on inlet ramps [AIAA PAPER 82-1082] p0005 A82-37684

BALL BEARINGS

Effects of ultra-clean and centrifugal filtration on rolling-element bearing life [ASME PAPER 81-LUB-35] p0103 A82-18436
Development of high-speed rolling-element bearings. A historical and technical perspective [NASA-TM-82884] p0100 A82-24497
Research report: User's manual for computer program ATBly003 SHABERTH. Steady state and transient thermal analysis of a shaft bearing system including ball, cylindrical and tapered roller bearings [NASA-CR-165365] p0146 A82-31969

BARBERM APPROXIMATION

U SPACE PROPERTIES

BARIUM COMPOUNDS

NT BARIUM TITANATES

BARIUM TITANATES

Study of the photovoltaic effect in thin film barium titanate [NASA-CR-165081] p0131 A82-16479

BAROTROPISM

NT PLANETARY WAVES

BARS

Extended range stress intensity factor expressions for chevron-notched short bar and short rod fracture toughness specimens p0112 A82-40357

BASES (FOUNDATIONS)

U FOUNDATIONS

BATTERIES

NT ELECTRIC BATTERIES

BATTERY CHARGERS

Effect of positive pulse charge waveforms on the energy efficiency of lead-acid traction cells [NASA-TM-82709] p0118 A82-10503

BATTERY SEPARATORS

U PARATORS

BEADS

A study of the nature of solid particle impact and shape on the erosion morphology of ductile metals [NASA-TM-82933] p0061 A82-33493

BEAMS (RADIATION)

NT ELECTRON BEAMS

NT ION BEAMS

NT PARTICLE BEAMS

NT RELATIVISTIC ELECTRON BEAMS

30/20 GHz communications satellite multibeam antenna [AIAA 82-0449] p0079 A82-23486

BEAMS (SUPPORTS)

NT CANTILEVER BEAMS

NT RECTANGULAR BEAMS

Comparison of beam and shell theories for the vibrations of thin turbomachinery blades [ASME PAPER 82-GT-223] p0115 A82-35408

BEARINGS

NT BALL BEARINGS

NT GAS BEARINGS

NT JOURNAL BEARINGS

NT LIQUID BEARINGS

NT ROLLER BEARINGS

Engine dynamic analysis with general nonlinear finite element codes. II - Bearing element implementation, overall numerical

characteristics and benchmarking [ASME PAPER 82-GT-292] p0108 A82-35462
Nonlinear analysis of rotor-bearing systems using component mode synthesis [ASME PAPER 82-GT-303] p0104 A82-35468
Engine dynamic analysis with general nonlinear finite element codes. Part 2: Bearing element implementation overall numerical characteristics and benchmarking [NASA-CR-167944] p0028 A82-33390
BENARD CELLS
Eigenvalues of the Rayleigh-Benard and Marangoni problems p0092 A82-13396

BENDING

Finite-element modeling of layered, anisotropic composite plates and shells: A review of recent research p0113 A82-19563

BENDING FATIGUE

Fatigue life prediction in bending from axial fatigue information [NASA-CR-165563] p0113 A82-20564

BENDING MOMENTS

Comparison of upwind and downwind rotor operation of the DOE/NASA 100-kw MOD-0 wind turbine p0122 A82-23710

BENDING VIBRATION

Coupled bending-bending-torsion flutter of a mistuned cascade with nonuniform blades [NASA-TM-82813] p0111 A82-21604

BETA FACTOR

Effect of vacuum exhaust pressure on the performance of MHD ducts at high B-field [AIAA PAPER 82-0396] p0157 A82-20292

BIBLIOGRAPHIES

Selected bibliography of NACA-NASA aircraft icing publications [NASA-TM-81651] p0014 A82-11053
Bibliography of NASA published reports on general aviation, 1975 to 1981 [NASA-TM-83307] p0001 A82-19132
Bibliography of Lewis Research Center technical publications announced in 1981 [NASA-TM-82838] p0163 A82-27191

BINARY MIXTURES

NT EUTECTIC ALLOYS

BINARY STARS

NT ECLIPSING BINARY STARS

BINARY SYSTEMS (DIGITAL)

U GITAL SYSTEMS

BINARY SYSTEMS (MATERIALS)

NT EUTECTIC ALLOYS

BINDING

Universal binding energy relations in metallic adhesion [NASA-TM-82706] p0058 A82-11183

BIOLOGICAL CELLS

U LLS (BIOLOGY)

BIOTECHNOLOGY

Evaluation of left ventricular assist device pump bladders cast from ion-sputtered polytetrafluorethylene mandrels [NASA-CR-167904] p0142 A82-23976

BIPOLAR TRANSISTORS

A 10kW series resonant converter design, transistor characterization, and base-drive optimization [NASA-CR-165546] p0084 A82-17439

BIREFRINGENCE

Pockels-effect cell for gas-flow simulation [NASA-TM-2007] p0095 A82-23515

BIT SYNCHRONIZATION

Open-loop nanosecond-synchronization for wideband satellite communications p0036 A82-27224

BIVARIATE ANALYSIS

Illustration of a new test for detecting a shift in mean in precipitation series A82-13217

BLADE TIPS

Propeller tip vortex - A possible contributor to aircraft cabin noise p0152 A82-17603
Single pass rub phenomena - Analysis and experiment [ASME PAPER 81-LUB-55] p0107 A82-18449
Turbine blade nonlinear structural and life analysis [AIAA PAPER 82-1056] p0021 A82-34981

ORIGINAL PAGE IS
OF POOR QUALITY

SUBJECT INDEX

BOUNDARY LAYER FLOW

Three-dimensional flow field in the tip region of a compressor rotor passage. I - Mean velocity profiles and annulus wall boundary layer
[ASME PAPER 82-GT-11] p0011 A82-35280

Investigation of the tip-clearance flow inside and at the exit of a compressor rotor passage. I - Mean velocity field
[ASME PAPER 82-GT-12] p0011 A82-35281

Three-dimensional flow field in the tip region of a compressor rotor passage. II - Turbulence properties
[ASME PAPER 82-GT-234] p0011 A82-35416

Optical tip clearance sensor for aircraft engine controls
[AIAA PAPER 82-1131] p0015 A82-37691

Analytic investigation of effect of end-wall contouring on stator performance
[NASA-TP-1943] p0003 A82-14051

CF6 Jet Engine Diagnostics Program: High pressure compressor clearance investigation
[NASA-CR-165580] p0025 A82-21197

Core compressor exit stage study, volume 6
[NASA-CR-165553] p0027 A82-27310

Rotor tip clearance effects on overall and blade-element performance of axial-flow transonic fan stage
[NASA-TP-20491] p0020 A82-33389

BLASIUS FLOW
Generation of instability waves at a leading edge
[NASA-TM-82845] p0087 A82-22453

BLEED-OFF
U ESSURE REDUCTION

BLENDS
U XTYPES

BLOOD PUMPS
Evaluation of left ventricular assist device pump bladders cast from ion-sputtered polytetrafluorethylene mandrels
[NASA-CR-167904] p0142 A82-23976

BLOOD VESSELS
NT AORTA

BLOWING
Experimental and analytical results of tangential blowing applied to a subsonic V/STOL inlet
[AIAA PAPER 82-1084] p0005 A82-35195

Tangential blowing for control of strong normal shock - Boundary layer interactions on inlet ramps
[AIAA PAPER 82-1082] p0005 A82-37684

Aerodynamic analysis of VTOL inlets and definition of a short, blowing-lip inlet
[NASA-CR-165617] p0007 A82-22211

Experimental and analytical results of tangential blowing applied to a subsonic V/STOL inlet
[NASA-TM-82847] p0004 A82-24165

BLOWN FLAPS
U TERNALLY BLOWN FLAPS

BLUFF BODIES
Secondary effects in combustion instabilities leading to flashback
[AIAA PAPER 82-0037] p0056 A82-17746

Bluff-body flameholder wakes - A simple numerical solution
[AIAA PAPER 82-1177] p0093 A82-35043

BODIES OF REVOLUTION
NT CYLINDRICAL BODIES
NT ROTATING CYLINDERS
NT SPHERES

BOEING AIRCRAFT
NT BOEING 747 AIRCRAFT
BOEING 747 AIRCRAFT
B747/JT9D flight loads and their effect on engine running clearances and performance deterioration; ECAC NAIL/P and WA JT9D engine diagnostics programs
[NASA-CR-165573] p0027 A82-28296

BOILING
Study of vapor flow into a capillary acquisition device --- for cryogenic rocket propellants
[NASA-CR-167883] p0091 A82-24452

The dryout region in frictionally heated sliding contacts
[NASA-TM-82796] p0088 A82-28574

BONDING
NT ADHESIVE BONDING
NT CERAMIC BONDING
NT REACTION BONDING
Surface texturing of fluoropolymers
[NASA-CASE-LEW-13028-1] p0070 A82-33521

BOOSTER ROCKET ENGINES

Fuel/oxidizer-rich high-pressure preburners --- staged-combustion rocket engine
[NASA-CR-165404] p0073 A82-10245

BORATES

Raman study of the improper ferroelectric phase transition in iron iodine boracite
A82-30297

BORON

NT BORON FIBERS

BORON COMPOUNDS

NT BORATES

NT BORON NITRIDES

BORON FIBERS

Durability/life of fiber composites in hygrothermomechanical environments
[NASA-TM-82749] p0049 A82-14287

Micromechanical predictions of crack propagation and fracture energy in a single fiber boron/aluminum metal composite
[NASA-CR-168550] p0052 A82-18326

Strength advantages of chemically polished boron fibers before and after reaction with aluminum
[NASA-TM-82806] p0049 A82-21258

Factors influencing the thermally-induced strength degradation of B/Al composites
[NASA-TM-82823] p0050 A82-24297

Method and apparatus for strengthening boron fibers --- high temperature oxidation
[NASA-CASE-LEW-13826-1] p0050 A82-26385

BORON NITRIDES

Development of an 1100 deg F capacitor
p0083 A82-15315

BORON REINFORCED MATERIALS

Durability/life of fiber composites in hygrothermomechanical environments
[NASA-TM-82749] p0049 A82-14287

Strength advantages of chemically polished boron fibers before and after reaction with aluminum
[NASA-TM-82806] p0049 A82-21258

BOROSILICATE GLASS

Secondary electron emission yields
p0038 A82-14226

BOUNDARIES

NT LIQUID-SOLID INTERFACES

BOUNDARY INTEGRAL METHOD

Experimental boundary integral equation applications in speckle interferometry
p0097 A82-36987

BOUNDARY LAYER CONTROL

Experimental and analytical results of tangential blowing applied to a subsonic V/STOL inlet
[AIAA PAPER 82-1084] p0005 A82-35195

Tangential blowing for control of strong normal shock - Boundary layer interactions on inlet ramps
[AIAA PAPER 82-1082] p0005 A82-37684

Aerodynamic analysis of VTOL inlets and definition of a short, blowing-lip inlet
[NASA-CR-165617] p0007 A82-22211

Experimental and analytical results of tangential blowing applied to a subsonic V/STOL inlet
[NASA-TM-82847] p0004 A82-24165

A summary of V/STOL inlet analysis methods
[NASA-TM-82885] p0005 A82-28249

Flow visualization of shock-boundary layer interaction
p0096 A82-32675

BOUNDARY LAYER EQUATIONS

The three-dimensional boundary layer on a rotating helical blade
p0009 A82-15459

BOUNDARY LAYER FLOW

NT BOUNDARY LAYER SEPARATION

NT SECONDARY FLOW

NT SEPARATED FLOW

Interaction of compressor rotor blade wake with wall boundary layer/vortex in the end-wall region
[ASME PAPER 81-GR/GT-1] p0010 A82-19301

Three-dimensional flow field in the tip region of a compressor rotor passage. I - Mean velocity profiles and annulus wall boundary layer
[ASME PAPER 82-GT-11] p0011 A82-35280

Nonlinear Marangoni convection in bounded layers. I - Circular cylindrical containers. II - Rectangular cylindrical containers
p0094 A82-39501

Core compressor exit stage study. Volume 4: Data and performance report for the best stage configuration

ORIGINAL PAGE IS
OF POOR QUALITY

BOUNDARY LAYER NOISE

SUBJECT INDEX

[NASA-CP-165257] p0023 N82-14092
Core compressor exit stage study, Volume 5:
Design and performance report for the Rotor
C/Stator B configuration
[NASA-CP-165358] p0023 N82-14093
Numerical modeling of three-dimensional confined
flows
[NASA-CP-165583] p0158 N82-24078
Comparison of experimental and analytical
performance for contoured endwall stators
[NASA-TN-82877] p0019 N82-26299
Three dimensional flow field inside compressor
rotor, including blade boundary layers
[NASA-CR-169120] p0091 N82-27686
Calculation of the flow field including boundary
layer effects for supersonic mixed compression
inlets at angles of attack
[NASA-CP-167941] p0009 N82-29269
Turbulent solution of the Navier-Stokes equations
for uniform shear flow
[NASA-TN-82925] p0089 N82-32634
Flow visualization of shock-boundary layer
interaction p0096 N82-32675

BOUNDARY LAYER NOISE

U DYNAMIC NOISE
U NDARY LAYERS

BOUNDARY LAYER SEPARATION

A summary of V/STOL inlet analysis methods
[NASA-TN-82725] p0003 N82-11043
Some aspects of calculating flows about
three-dimensional subsonic inlets
[NASA-TN-82789] p0004 N82-25213

BOUNDARY LAYER STABILITY

Eigenvalues of the Rayleigh-Benard and Marangoni
problems p0092 A82-13396
Three-dimensional flow calculations including
boundary layer effects for supersonic inlets at
angle of attack
[AIAA PAPER 82-0061] p0005 A82-19778

BOUNDARY LAYER TRANSITION

Turbulent boundary layer heat transfer experiments
- A separate effects study on a convexly-curved
wall
[ASME PAPER 81-HT-78] p0092 A82-10963
Turbulent boundary layer heat transfer
experiments: Convex curvature effects including
introduction and recovery
[NASA-CP-3510] p0090 N82-17456

BOUNDARY LAYERS

NT ATMOSPHERIC BOUNDARY LAYER
NT LAMINAR BOUNDARY LAYER
NT PLANETARY BOUNDARY LAYER
NT THREE DIMENSIONAL BOUNDARY LAYER
NT TURBULENT BOUNDARY LAYER

Boundary layer thermal stresses in angle-ply
composite laminates, part 1 --- graphite-epoxy
composites
[NASA-CP-165412] p0113 N82-26713
Boundary-layer effects in composite laminates:
Free-edge stress singularities, part 6
[NASA-CP-165440] p0114 N82-26718
Small axial turbine stator technology program
[NASA-CR-165602] p0028 N82-32367

BOUNDARY LUBRICATION

Regimes of traction in concentrated contact
lubrication
[ASME PAPER 81-LUB-16] p0107 A82-18431
The effect of oxygen concentration on the
boundary-lubricating characteristics of a C
ether and a polyphenyl ether to 300 C
p0070 A82-21699
Improved boundary lubrication with formulated C-
ethers
[NASA-TN-82908] p0067 N82-20313
Boundary lubrication: Revisited
[NASA-TN-82859] p0069 N82-29458

BOUNDARY VALUE PROBLEMS

NT DIRICHLET PROBLEM
Construction of solutions for some nonlinear
two-point boundary value problems
[NASA-TN-82937] p0144 N82-30949

BOW SHOCK WAVES

U OCK WAVES

BREAKAWAY

U NDARY LAYER SEPARATION

BREAKERS (ELECTRIC)

U RCUIT BREAKERS

BRISTOL-SIDDELEY BS 53 ENGINE

A real time Pegasus propulsion system model for
VSTOL piloted simulation evaluation
[AIAA PAPER 81-2663] p0020 A82-19221

BRITTLE MATERIALS

Application of a gripping system to test a
uniaxial graphite fiber reinforced composite
/PHR 15/Celion 6000/ in tension at 316 C
p0051 A82-40796

BRITTLENESS

Recrystallization and grain growth in NiAl
p0065 A82-44529

BUCKLING

NT CREEP BUCKLING
Tensile buckling of advanced turboprops
[NASA-TN-82896] p0112 N82-31708

BUNCHING

NT ELECTRON BUNCHING

BUOYANCY

Buoyancy effects on the temperature field in
downward spreading flames
p0094 A82-41203

BURNERS

On the opening of premixed Bunsen flame tips
p0057 A82-37570
Low NO sub x heavy fuel combustor concept program.
Phase 1A: Combustion technology generation coal
gas fuels
[NASA-CR-165614] p0055 N82-22326
Micronized coal burner facility
[NASA-CASE-LEW-13426-1] p0126 N82-31769

BURNING

U BUSTION

BURNING PROCESS

U BUSTION

BURNING RATE

Turbofan forced mixer-nozzle internal flowfield.
Volume 1: A benchmark experimental study
[NASA-CR-3492] p0090 N82-22458

BURSTS

NT SOLAR RADIO BURSTS

BYPASS RATIO

NASA Redox cell stack shunt current, pumping
power, and cell performance tradeoffs
[NASA-TN-82686] p0054 N82-19333

BYPASSES

Thrust reverser for a long duct fan engine --- for
turbofan engines
[NASA-CASE-LEW-13199-1] p0019 N82-26293

C

CABIN ATMOSPHERES

Environmental control systems p0001 N82-19147
Ozone and aircraft operations p0001 N82-21145

CAD (DESIGN)

U MPUTER AIDED DESIGN

CADMIUM COMPOUNDS

Development of CdO-graphite-Ag coatings for gas
bearings to 427 C
p0108 A82-27079

CADMIUM NICKEL BATTERIES

U CKEL CADMIUM BATTERIES

CALCIUM COMPOUNDS

NT CALCIUM SILICATES

CALCIUM SILICATES

Thermodynamics and kinetics of the sulfation of
porous calcium silicate
[NASA-TN-82769] p0048 N82-15119

CALCULATION

U MPUTATION

CALCULUS

NT FOURIER SERIES

NT VECTOR ANALYSIS

CAMBER

Vibrations of twisted rotating blades
[ASME PAPER 81-DET-127] p0115 A82-19341

CANTILEVER BEAMS

Miniature drag-force anemometer
p0097 A82-40132

CANTILEVER MEMBERS

NT CANTILEVER BEAMS

Vibrations of cantilevered shallow cylindrical
shells of rectangular planform
p0115 A82-11298

CANTILEVER WINGS

U NGS

CAPACITORS

Development of an 1100 deg F capacitor
p0083 N82-15315
Preliminary design development of 100 KW rotary
power transfer device
[NASA-CR-165431] p0084 N82-23395

CAPILLARY CIRCULATION

U PILLARY FLOW
CAPILLARY FLOW
Study of vapor flow into a capillary acquisition
device --- for cryogenic rocket propellants
[NASA-CR-167883] p0091 N82-24452

CARBIDES

NT SILICON CARBIDES
MC carbide structures in M(lc2)ar-M247
[NASA-CR-167892] p0064 N82-30374

CARBON

Evaluation of fuel injection configurations to
control carbon and soot formation in small GT
combustors
[AIAA PAPER 82-1175] p0021 N82-35041
Investigation of soot and carbon formation in
small gas turbine combustors
[NASA-CR-167853] p0025 N82-22267
Improved chromium electrodes for REDOX cells
[NASA-CASE-LFW-13653-1] p0121 N82-22672
Ion beam sputter deposited diamond like films
[NASA-TM-82873] p0069 N82-28445
Stabilizing platinum in phosphoric acid fuel cells
[NASA-CR-165606] p0136 N82-29718

CARBON COMPOUNDS

NT CARBIDES
NT FLUOROPOLYMERS
NT SILICON CARBIDES

CARBON DIOXIDE LASERS

Optically pumped high-pressure DF-CO2 transfer laser
A82-10193

CARBON FIBER REINFORCED PLASTICS

Impact resistance of fiber composites
p0112 A82-39852

CARBON MONOXIDE

Preparation and evaluation of advanced
electrocatalysts for phosphoric acid fuel cells
[NASA-CR-165519] p0129 N82-12573
Exhaust emissions reduction for intermittent
combustion aircraft engines
[NASA-CR-167914] p0029 N82-33392

CARBONACEOUS CHONDRITES

Evidence for Pu-244 fission tracks in hibonites
from Murchison carbonaceous chondrite
p0166 A82-29316

CARBONACEOUS ROCKS

NT COAL

CARDIOVASCULAR SYSTEM

NT AORTA

CARRIER TRANSPORT (SOLID STATE)

Stationary state model for normal metal tunnel
junction phenomena
p0159 A82-42912

CARTOGRAPHY

U PFLING

CARTRIDGE ACTUATED DEVICES

U TEACTORS

CASCADE FLOW

Sound generated in a cascade by three-dimensional
disturbances convected in a subsonic flow
[AIAA PAPER 81-2046] p0153 A82-10460
Aeroelastic characteristics of a cascade of
mistuned blades in subsonic and supersonic flows
[ASME PAPER 81-DET-122] p0021 A82-19337
A comprehensive method for preliminary design
optimization of axial gas turbine stages
[AIAA PAPER 82-1264] p0030 A82-35091
Investigation of the tip-clearance flow inside and
at the exit of a compressor rotor passage. I -
Mean velocity field
[ASME PAPER 82-GT-12] p0011 A82-35281
A computational design method for transonic
turbomachinery cascades
[ASME PAPER 82-GT-117] p0022 A82-35348
Three-dimensional flow field in the tip region of
a compressor rotor passage. II - Turbulence
properties
[ASME PAPER 82-GT-234] p0011 A82-35416
Aerodynamic performance of high turning core
turbine vanes in a two-dimensional cascade
[AIAA PAPER 82-1288] p0005 A82-37716
Three-dimensional shock structure in a transonic
flutter cascade

p0006 A82-37937
Interaction of upstream flow distortions with high
Mach number cascades
[NASA-TM-82759] p0003 N82-12043
CAS22 - FORTRAN program for fast design and
analysis of shock-free airfoil cascades using
fictitious-gas concept
[NASA-CR-3507] p0006 N82-16044
An experimental investigation of gapwise
periodicity and unsteady aerodynamic response in
an oscillating cascade. Volume 2: Data report.
Part I: Text and mode 1 data
[NASA-CR-165457-VOL-2-PT-1] p0006 N82-18180
Numerical analysis and FORTRAN program for the
computation of the turbulent wakes of
turbomachinery rotor blades, isolated airfoils
and cascade of airfoils
[NASA-CR-3509] p0006 N82-18184
Design of supercritical cascades with high solidity
[NASA-CR-165600] p0007 N82-22210
An experimental investigation of gapwise
periodicity and unsteady aerodynamic response in
an oscillating cascade. I: Experimental and
theoretical results --- turbine blades
[NASA-CR-3513] p0008 N82-26229
Aerodynamic performance of high turning core
turbine vanes in a two dimensional cascade
[NASA-TM-82894] p0004 N82-26240
Thrust reverser for a long duct fan engine --- for
turbofan engines
[NASA-CASE-LEW-13199-1] p0019 N82-26293
Computer program for calculating full potential
transonic, quasi-three-dimensional flow through
a rotating turbomachinery blade row
[NASA-TP-2030] p0005 N82-28247
Comparison of laser anemometer measurements and
theory in an annular turbine cascade with
experimental accuracy determined by parameter
estimation
[NASA-TM-82860] p0005 N82-28250
Fast generation of three-dimensional computational
boundary-conforming periodic grids of C-type ---
for turbine blades and propellers
[NASA-CR-165596] p0009 N82-28253
Flow visualization study of the horseshoe vortex
in a turbine stator cascade
[NASA-TP-1884] p0088 N82-30498

CASCADE WIND TUNNELS
Aerodynamic performance of high turning core
turbine vanes in a two-dimensional cascade
[AIAA PAPER 82-1288] p0005 A82-37716

CASCADES (FLUID DYNAMICS)
U UID DYNAMICS

CASCADE MOSFET
U ELD EFFECT TRANSISTORS

CASTING
Texturing polymer surfaces by transfer casting ---
cardiovascular prosthesis
[NASA-CASE-LEW-13120-1] p0068 N82-28440

CASTING SOLVENTS
U ASTICIZERS

CASTINGS
NT INGOTS
Castable high temperature refractory materials
[NASA-CASE-LEW-13080-2] p0066 N82-11210

CATALYSIS
Demonstration of catalytic combustion with
residual fuel
[NASA-CR-165369] p0131 N82-16484
Requirements for optimization of electrodes and
electrolyte for the iron/chromium Redox flow cell
[NASA-CR-165218] p0136 N82-25640

CATALYSTS
NT ELECTROCATALYSTS
High temperature durable catalyst development
p0056 A82-20739
Endurance test and evaluation of alkaline water
electrolysis cells
[NASA-CR-165424] p0130 N82-13508
Experimental study of an integral catalytic
combustor: Heat exchanger for Stirling engines
[NASA-TM-82783] p0119 N82-18691

CATALYTIC ACTIVITY
High temperature durable catalyst development
p0056 A82-20739
Catalytic combustion of residual fuels
[NASA-TM-82731] p0118 N82-13504
Transient catalytic combustor model
[NASA-CR-165324] p0129 N82-13507

Advanced Low-Emissions Catalytic-Combustor
Program, phase I --- aircraft gas turbine engines
[NASA-CR-159656] p0025 N82-22265
Computer model of catalytic combustion/Stirling
engine heater head
[NASA-CR-165378] p0134 N82-22666
Catalytic combustion of actual low and medium
heating value gases
[NASA-TM-82930] p0125 N82-30717
Low and medium heating value coal gas catalytic
combustor characterization
[NASA-CR-165560] p0138 N82-32856

CATHODES

NT CELL CATHODES
Stabilizing platinum in phosphoric acid fuel cells
[NASA-CR-165606] p0136 N82-29718

CATHODIC COATINGS

Mechanism and models for zinc metal morphology in
alkaline media
[NASA-TM-82768] p0120 N82-19671
CAUCHEY INTEGRAL FORMULA
Cauchy integral method for two-dimensional
solidification interface shapes
p0089 N82-39899

CAVITATION

U CAVITATION FLOW
CAVITATION FLOW
High-speed motion picture camera experiments of
cavitation in dynamically loaded journal bearings
[NASA-TM-82798] p0100 N82-20543

CAVITY RESONATORS

Analytic investigation of efficiency and
performance limits in klystron amplifiers using
multidimensional computer programs; multi-stage
depressed collectors; and thermionic cathode
life studies
p0118 N82-12553
Three-dimensional relativistic field-electron
interaction in a multicavity high-power
klystron. I: Basic theory
[NASA-TP-1992] p0081 N82-22439

CELESTIAL BODIES

NT CARBONACEOUS CHONDRITES
NT ECLIPSE BINARY STARS
NT NATURAL SATELLITES

CELL CATHODES

Moderate temperature Na cells. III -
Electrochemical and structural studies of
CrO₂Sr_{0.5}VO₂ and its Na intercalates
p0055 N82-15732
Moderate temperature Na cells. IV - VS2 and
NbS₂Cl₂ as rechargeable cathodes in molten NaAlCl₄
p0055 N82-15743
Stabilizing platinum in phosphoric acid fuel cells
[NASA-CR-165483] p0130 N82-14628
Cathode catalysts for primary phosphoric acid fuel
cells
[NASA-CR-165578] p0134 N82-21709

CELLS (BIOLOGY)

A hydrodynamic model of an outer hair cell
[NASA-TM-82773] p0143 N82-16743

CENTAUR LAUNCH VEHICLE

NT ATLAS CENTAUR LAUNCH VEHICLE
Real-time computer simulation/emulation for
verification of multi-fault-tolerant control of
Centaur-in-Shuttle
[AIAA 81-2263] p0040 N82-13494
Real-time microcomputer simulation for space
Shuttle/Centaur avionics
p0033 N82-48245

CENTAUR VEHICLE

U NTAUR LAUNCH VEHICLE

CENTIMETER WAVES

VLA observations of solar active regions at 6 cm
wavelength
p0167 N82-10156
Time variability and structure of quiet sun
sources at 6 cm wavelength
p0167 N82-26003

CENTRIFUGAL COMPRESSORS

'Coriolis resonance' within a rotating duct ---
flow induced vibrations in centrifugal compressors
p0012 N82-37938

CENTRIFUGAL PUMPS

Liquid oxygen turbopump technology
[NASA-CR-165487] p0105 N82-11468

CERAMAL PROTECTIVE COATINGS

U CTECTIVE COATINGS

CERAMIC BONDING

Review of NASA progress in thermal barrier
coatings for stationary gas turbines
[NASA-TM-81716] p0058 N82-17335

CERAMIC COATINGS

Ceramic thermal barrier coatings for gas turbine
engines
[ASME PAPER 82-GT-265] p0071 N82-35441
Evaluation of the potential of the Stirling engine
for heavy duty application
[NASA-CR-165473] p0128 N82-10505
Gas turbine ceramic-coated-vane concept with
convection-cooled porous metal core
[NASA-TP-1942] p0016 N82-14090
MHD oxidant intermediate temperature ceramic
heater study
[NASA-CR-165453] p0131 N82-15527
Review of NASA progress in thermal barrier
coatings for stationary gas turbines
[NASA-TM-81716] p0058 N82-17335
Evaluation of present thermal barrier coatings for
potential service in electric utility gas turbines
[NASA-CR-165545] p0063 N82-18368
JT9D ceramic outer air seal system refinement
program
[NASA-CR-165554] p0106 N82-18603
High temperature composites. Status and future
directions
[NASA-TM-82929] p0051 N82-30336
Use of fiber like materials to augment the cycle
life of thick thermoprotective seal coatings
[NASA-TM-82901] p0089 N82-32633

CERAMICS

Strength distributions of SiC ceramics after
oxidation and oxidation under load
[ACS PAPER 9-C-80C] p0071 N82-20143
Analytical and experimental evaluation of biaxial
contact stress
p0071 N82-20741
Progress in ceramic component fabrication technology
[AIAA PAPER 82-1211] p0071 N82-35064
Design and development of a ceramic radial turbine
for the AGT101
[AIAA PAPER 82-1209] p0109 N82-35480
Effects of oxidation and oxidation under load on
strength distributions of Si₃N₄
[ACS PAPER 69-B-80] p0071 N82-35871
Fabrication of sinterable silicon nitride by
injection molding
p0071 N82-37015
Development of low modulus material for use in
ceramic gas path seal applications
[NASA-CR-165469] p0022 N82-10039
Castable high temperature refractory materials
[NASA-CASE-LEW-13080-2] p0066 N82-11210
Ultrasonic velocity for estimating density of
structural ceramics
[NASA-TM-82765] p0066 N82-14359
Fully plasma-sprayed compliant backed ceramic
turbine seal
[NASA-CASE-LEW-13268-2] p0101 N82-26674
Fully plasma-sprayed compliant backed ceramic
turbine seal
[NASA-CASE-LEW-13268-1] p0069 N82-29453
High temperature composites. Status and future
directions
[NASA-TM-82929] p0051 N82-30336
Ceramic applications in turbine engines
[NASA-CR-165197] p0164 N82-31145
Occurrence of spherical ceramic debris in
indentation and sliding contact
[NASA-TP-2048] p0069 N82-32491
Advanced ceramic coating development for
industrial/utility gas turbines
[NASA-CR-169852] p0065 N82-33494

CESIUM

Cesiation of W/001/ - Work function lowering by
multiple dipole formation
N82-30002

CFRP

U RBON FIBER REINFORCED PLASTICS

CHALCOGENIDES

NT ALUMINUM OXIDES
NT CARBON MONOXIDE
NT HYDROGEN PEROXIDE
NT INORGANIC SULFIDES
NT MAGNESIUM OXIDES
NT METAL OXIDES
NT MOLYBDENUM SULFIDES

NT NITRIC OXIDE
 NT NITROGEN OXIDES
 NT NITROUS OXIDES
 NT OXIDES
 NT QUARTZ
 NT SILICON DIOXIDE
 NT TIN OXIDES
 NT YTTRIUM OXIDES
 NT ZIRCONIUM OXIDES
CHANNEL FLOW
 Numerical modeling of three-dimensional confined flows
 [NASA-CR-165583] p0158 N82-24078
 Study of vapor flow into a capillary acquisition device --- for cryogenic rocket propellants
 [NASA-CR-167883] p0091 N82-24452
CHAPMAN-JOUGET FLAME
 FLAME PROPAGATION
CHARACTERISTIC EQUATIONS
 U GENVALUES
 U GENVECTORS
CHARACTERISTIC FUNCTIONS
 U GENVALUES
 U GENVECTORS
CHARACTERISTIC METHOD
 U THEO OF CHARACTERISTICS
CHARACTERIZATION
 Characterization of an Experimental Referee Broadened Specification (ERBS) aviation turbine fuel and ERBS fuel blends
 [NASA-TM-82893] p0072 N82-32504
CHARGE DISTRIBUTION
 Secondary electron emission from a charged dielectric in the presence of normal and oblique electric fields
 [NASA-CP-168558] p0084 N82-18507
CHARGE EXCHANGE
 Additional extensions to the NASCAP computer code, volume 3
 [NASA-CP-167857] p0040 N82-26378
CHARGED PARTICLES
 NT ANIONS
 NT ARCS PLASMA
 NT CYLINDRICAL PLASMAS
 NT ENERGETIC PARTICLES
 NT PLASMA SHEATHS
 NT PLASMAS (PHYSICS)
 NT RELATIVISTIC ELECTRON BEAMS
 Agreement for NASA/OAST - USAF/AFSC space interdependency on spacecraft environment interaction
 p0038 N82-14271
 Mapping of electrical potential distributions with charged particle beams
 [NASA-CR-168556] p0084 N82-18508
CHARTS
 NT FLOW CHARTS
CHECKOUT EQUIPMENT
 U ST EQUIPMENT
CHEMICAL ANALYSIS
 NT CROMOMETRY
 NT SPECTROSCOPIC ANALYSIS
 Fuel economy and exhaust emissions characteristics of diesel vehicles: Test results of a prototype fiat 131TC 2.4 liter automobile
 [NASA-CR-165535] p0164 N82-18068
CHEMICAL COMPOSITION
 Effects of nadic ester concentration and processing on physical and mechanical properties of EMR/Celion 6000 composites
 p0051 N82-27440
 NASA Broad Specification Fuels Combustion Technology program - Pratt and Whitney Aircraft Phase I results and status
 [AIAA PAPER 82-1088] p0021 N82-34999
 Some properties of RF sputtered hafnium nitride coatings
 [NASA-TM-82826] p0067 N82-21331
 Thermodynamic and transport combustion properties of hydrocarbons with air. Part 2: Compositions corresponding to Kelvin temperature schedules in part 1
 [NASA-TP-1907] p0161 N82-32187
 Thermodynamic and transport combustion properties of hydrocarbons with air. Part 4: Compositions corresponding to Rankine temperature schedules in part 3
 [NASA-TP-1909] p0161 N82-32189

CHEMICAL ELEMENTS

NT ALUMINUM
 NT CARBON
 NT CESIUM
 NT CHROMIUM
 NT COBALT
 NT COPPER
 NT GOLD
 NT HYDROGEN
 NT INDIUM
 NT IRON
 NT LIQUID HYDROGEN
 NT NIOBIUM
 NT NITROGEN
 NT NITROGEN IONS
 NT OXYGEN
 NT PLATINUM
 NT PLATINUM ISOTOPES
 NT PLUTONIUM 244
 NT RARE GASES
 NT SILICON
 NT TANTALUM
 NT TITANIUM
 NT TUNGSTEN
 NT ZINC
 NT ZIRCONIUM

CHEMICAL FRACTIONATION

Quantitative separation of tetralin hydroperoxide from its decomposition products by high performance liquid chromatography
 p0048 N82-15696

CHEMICAL FUELS

NT AIRCRAFT FUELS
 NT DIESEL FUELS
 NT HYDROCARBON FUELS
 NT JET ENGINE FUELS
 NT LIQUID FUELS
 NT RP-1 ROCKET PROPELLANTS
 NT SYNTHETIC FUELS

CHEMICAL KINETICS

U ACTION KINETICS
CHEMICAL PROPERTIES
 NT HEAT OF COMBUSTION

CHEMICAL PROPULSION

Study of electrical and chemical propulsion systems for auxiliary propulsion of large space systems. Volume 1: Executive summary
 [NASA-CR-165502-VOL-1] p0046 N82-11110
 Study of electrical and chemical propulsion systems for auxiliary propulsion of large space systems, volume 2
 [NASA-CR-165502-VOL-2] p0044 N82-11111
 Low-thrust chemical propulsion system pump technology
 [NASA-CR-165219] p0105 N82-13427
 An insight into auxiliary propulsion requirements of large space systems
 [NASA-TM-82827] p0042 N82-24286
 Low-thrust chemical propulsion system propellant expulsion and thermal conditioning study. Executive summary
 [NASA-CR-165622] p0045 N82-24287
 Low-thrust chemical propulsion system propellant expulsion and thermal conditioning study
 [NASA-CR-167841] p0045 N82-24288
 Large Space Systems/Propulsion Interactions
 [NASA-TM-82904] p0042 N82-27358

CHEMICAL REACTIONS

NT ALKYLATION
 NT DEOXIDIZING
 NT ELECTROCHEMICAL OXIDATION
 NT FLUORINATION
 NT NITRIDING
 NT OXIDATION
 NT OXIDATION-REDUCTION REACTIONS
 NT SULFATION
 NT THERMAL DECOMPOSITION

Surface chemistry and wear behavior of single-crystal silicon carbide sliding against iron at temperatures to 1500 C in vacuum
 [NASA-TP-1947] p0067 N82-19374

CHEMICAL REACTORS

Catalytic combustion of residual fuels
 [NASA-TM-82731] p0118 N82-13504

CHEMICAL TESTS

NT CHEMICAL ANALYSIS
 NT CROMOMETRY
 NT SPECTROSCOPIC ANALYSIS

CHEMILUMINESCENCE

SUBJECT INDEX

CHEMILUMINESCENCE

Flame structure in a swirl stabilized combustor
Inferred by radiant emission measurements
p0056 A82-28694

CHEMNUCLEAR PROPULSION

U EMICAL PROPULSION

CHILLING

U CLING

CHIPS (ELECTRONICS)

Multi-junction high voltage concentrator solar cells
p0043 A82-11796

CHLORIDES

NT HYDROGEN CHLORIDES

NT IRON CHLORIDES

NT SODIUM CHLORIDES

CHLORINE COMPOUNDS

NT IRON CHLORIDES

NT SODIUM CHLORIDES

CHOKES (FUEL SYSTEMS)

Flow through aligned sequential orifice type inlets
[NASA-TF-1967] p0087 N82-20467

CHOKES (RESTRICTIONS)

Toward the use of similarity theory in two-phase
choked flows
p0089 A82-16570

CHONDRITES

NT CARBONACEOUS CHONDRITES

CHOPPERS (ELECTRIC)

U ELECTRIC CHOPPERS

CHROMATOGRAPHY

NT LIQUID CHROMATOGRAPHY

CHROME

U CHROMIUM

CHROMIUM

Performance of advanced chromium electrodes for
the NASA Redox Energy Storage System
[NASA-TM-82724] p0118 N82-12574

A status review of NASA's COSAM (Conservation Of
Strategic Aerospace Materials) program
[NASA-TM-82852] p0060 N82-24326

Requirements for optimization of electrodes and
electrolyte for the iron/chromium Redox flow cell
[NASA-CR-165218] p0136 N82-25640

CHROMIUM ALLOYS

Long-term high-velocity oxidation and hot
corrosion testing of several NiCrAl and FeCrAl
base oxide dispersion strengthened alloys
p0062 A82-37151

Solute transport during the cyclic oxidation of
Ni-Cr-Al alloys
[NASA-CF-165544] p0064 N82-27462

Nickel ternary alloy having improved cyclic
oxidation resistance
[NASA-CASE-LEW-13339-1] p0061 N82-31505

CHROMIUM COMPOUNDS

Moderate temperature Na cells. III -
Electrochemical and structural studies of
CrO₂·5VO₂·5S2 and its Na intercalates
p0055 A82-15732

Improved chromium electrodes for REDOX cells
[NASA-CASE-LEW-13653-1] p0121 N82-22672

Chemical and electrochemical behavior of the
Cr(3)/Cr(2) half cell in the NASA Redox Energy
Storage System
[NASA-TM-82913] p0055 N82-33463

CHROSPHERE

Time variability and structure of quiet sun
sources at 6 cm wavelength
p0167 A82-26003

CHUGGING

U COMBUSTION STABILITY

CIRCUIT BREAKERS

High voltage DC switchgear development for
multi-kV space power system: Aerospace
technology development of three types of solid
state power controllers for 200-1100VDC with
current ratings of 25, 50, and 80 amperes with
one type utilizing an electromechanical device
[NASA-CF-165413] p0083 N82-13357

CIRCUITS

NT ELECTRIC BRIDGES

NT ENCAPSULATED MICROCIRCUITS

NT EQUIVALENT CIRCUITS

NT INTEGRATED CIRCUITS

NT MATRICES (CIRCUITS)

NT MICROWAVE CIRCUITS

NT POWER SUPPLY CIRCUITS

NT SWITCHING CIRCUITS

NT TRANSISTOR CIRCUITS

Proceedings of the Conference on High-temperature

Electronics
[NASA-TM-84069] p0081 N82-15311

High voltage power transistor development
[NASA-CR-165547] p0084 N82-18506

CIRCULAR CYLINDERS

Nonlinear Marangoni convection in bounded layers.
I - Circular cylindrical containers. II -
Rectangular cylindrical containers
p0094 A82-39501

Surface-tension induced instabilities: Effects of
lateral boundaries
[NASA-CR-165530] p0092 N82-11396

Effect of location in an array on heat transfer to
a cylinder in crossflow
[NASA-TM-82797] p0087 N82-19493

CIRCULATION

NT ATMOSPHERIC CIRCULATION

CIRCULATORY SYSTEM

NT AORTA

CIVIL AVIATION

Bibliography of NASA published reports on general
aviation, 1975 to 1981
[NASA-TM-83307] p0001 N82-19132

CLARK Y AIRFOIL

U RFOIL PROFILES

CLEAN ENERGY

Interfacing wind energy conversion equipment with
utility systems
A82-21148

Mod-2 wind turbine system cluster research test
program. Volume 1: Initial plan E-1290
[NASA-TM-82906] p0123 N82-26807

CLEAN FUELS

NT FUEL OILS

CLEARANCES

Optical tip clearance sensor for aircraft engine
controls
[AIAA PAPER 82-1131] p0015 A82-37691

CF6 Jet Engine Diagnostics Program: High pressure
compressor clearance investigation
[NASA-CR-165580] p0025 N82-21197

Investigation of the tip clearance flow inside and
at the exit of a compressor rotor passage
[NASA-CR-169004] p0026 N82-25253

CF6 jet engine performance improvement: High
pressure turbine active clearance control
[NASA-CR-165556] p0027 N82-28297

Active clearance control system for a turbomachine
[NASA-CASE-LEW-12938-1] p0020 N82-32366

Rotor tip clearance effects on overall and
blade-element performance of axial-flow
transonic fan stage
[NASA-TP-2049] p0020 N82-33389

CLOSE PACKED LATTICES

Net shape fabrication of Alpha Silicon Carbide
turbine components
[ASME PAPER 82-GT-216] p0071 A82-35403

CLOSED CYCLES

Comparative analysis of CCMHD power plants ---
Closed Cycle MHD
p0158 A82-20747

CLOSED LOOP SYSTEMS

U EDBACK CONTROL

CLOUD PHYSICS

Design of prototype charged particle fog dispersal
unit
[NASA-CR-3481] p0141 N82-16659

COAL

Magnetohydrodynamics (MHD) Engineering Test
Facility (ETF) 200 MWe power plant Conceptual
Design Engineering Report (CDER)
[NASA-CR-165452-VOL-5] p0132 N82-17603

Techniques for enhancing durability and
equivalence ratio control in a rich-lean,
three-stage ground power gas turbine combustor
[NASA-TM-82922] p0124 N82-29717

COAL DERIVED GASES

Low NO sub x heavy fuel combustor concept program.
Phase IA: Coal gas addendum
[NASA-CR-165577] p0133 N82-18690

Low NO sub x heavy fuel combustor concept program.
Phase IA: Combustion technology generation coal
gas fuels
[NASA-CR-165614] p0055 N82-22326

Low NO sub x heavy fuel combustor concept program
phase IA gas tests
[NASA-CR-167877] p0055 N82-25337

- Catalytic combustion of actual low and medium heating value gases
[NASA-TM-82930] p0125 N82-30717
- Low and medium heating value coal gas catalytic combustor characterization
[NASA-CR-165560] p0138 N82-32856
- COAL DERIVED LIQUIDS**
Deposit formation in liquid fuels. I - Effect of coal-derived Lewis bases on storage stability of Jet A turbine fuel
p0074 A82-22241
- Low NOx heavy fuel combustor concept program
[NASA-CR-165367] p0136 N82-25635
- COAL GASIFICATION**
Performance and operational economics estimates for a coal gasification combined-cycle cogeneration powerplant
[NASA-TM-82729] p0120 N82-19672
- Integrated gasifier combined cycle polygeneration system to produce liquid hydrogen
[NASA-TM-82921] p0125 N82-30713
- Micronized coal burner facility
[NASA-CASE-LEW-13426-1] p0126 N82-31769
- Gas turbine critical research and advanced technology (CRT) support project
[NASA-TM-82872] p0126 N82-31776
- COAL UTILIZATION**
Lewis Research Center's coal-fired, pressurized, fluidized-bed reactor test facility
[NASA-TM-81616] p0087 N82-11397
- COATING**
NT ENCAPSULATING
NT METALLIZING
- COATINGS**
NT ALUMINUM COATINGS
NT ANTIREFLECTION COATINGS
NT CATHODIC COATINGS
NT CERAMIC COATINGS
NT ENCAPSULATING
NT GLAZES
NT GOLD COATINGS
NT METAL COATINGS
NT METALLIZING
NT PLASTIC COATINGS
NT PROTECTIVE COATINGS
NT REFRACTORY COATINGS
NT SPRAYED COATINGS
NT THERMAL CONTROL COATINGS
Deposition of reactively ion beam sputtered silicon nitride coatings
[NASA-TM-82942] p0069 N82-30401
- COAXIAL FLOW**
Mass and momentum turbulent transport experiments with confined coaxial jets
[NASA-CR-165574] p0090 N82-19496
- COAXIAL TRANSMISSION**
U ANSMISSION
- COBALT**
A status review of NASA's CCSAM (Conservation Of Strategic Aerospace Materials) program
[NASA-TM-82852] p0060 N82-24326
- COBALT ALLOYS**
Effects of cobalt on structure, microchemistry and properties of a wrought nickel-base superalloy
p0065 A82-34973
- The influence of cobalt on the tensile and stress-rupture properties of the nickel-base superalloy MAR-M247
p0063 A82-47399
- The influence of cobalt on the microstructure of the nickel-base superalloy MAR-M247
p0063 A82-47400
- Effects of cobalt on the microstructure of Udimet 700
[NASA-CR-165605] p0064 N82-28409
- Evaluation of candidate stirling engine heater tube alloys at 820 deg and 860 deg C
[NASA-TM-82877] p0061 N82-30372
- Overlay metallic-cermet alloy coating systems --- for gas turbine engines
[NASA-CASE-LEW-13639-1] p0070 N82-33522
- COEFFICIENT OF FRICTION**
Stress evaluations under rolling/sliding contacts
[NASA-CR-165561] p0113 N82-17521
- Friction and wear of iron in corrosive metal
[NASA-TP-1985] p0058 N82-20291
- COEFFICIENTS**
NT COEFFICIENT OF FRICTION
NT DISCHARGE COEFFICIENT
- NT NOZZLE THRUST COEFFICIENTS
- COGENERATION**
An assessment of alternative fuel cell designs for residential and commercial cogeneration
p0138 A82-24695
- Performance and operational economics estimates for a coal gasification combined-cycle cogeneration powerplant
[NASA-TM-82729] p0120 N82-19572
- CONJUNCTION**
Universal binding energy relations in metallic adhesion
[NASA-TM-82706] p0058 N82-11183
- COLD WEATHER TESTS**
Experiments on fuel heating for commercial aircraft
[NASA-TM-82878] p0072 N82-26483
- COLLECTORS**
U CUMULATORS
- COLLIMATORS**
Secondary electron emission from a charged dielectric in the presence of normal and oblique electric fields
[NASA-CR-168558] p0084 N82-18507
- COLLOIDS**
NT AEROSOLS
- COLOR CODING**
Application of image processing techniques to fluid flow data analysis
[NASA-TM-82760] p0004 N82-16049
- COLUMBIUM**
U OBIUM
- COMBINED CYCLE POWER GENERATION**
Assessment of steam-injected gas turbine systems and their potential application
[NASA-TM-82735] p0119 N82-18694
- Performance and operational economics estimates for a coal gasification combined-cycle cogeneration powerplant
[NASA-TM-82729] p0120 N82-19672
- Parametric performance analysis of steam-injected gas turbine with a thermionic-energy-converter-lined combustor
[NASA-TM-82736] p0121 N82-23678
- Integrated gasifier combined cycle polygeneration system to produce liquid hydrogen
[NASA-TM-82921] p0125 N82-30713
- COMBUSTIBILITY**
U AMMABILITY
- COMBUSTIBLE FLOW**
Time resolved density measurements in premixed turbulent flames
[AIAA PAPER 82-0036] p0056 A82-22033
- Numerical modeling of turbulent combustion in premixed gases
p0056 A82-28708
- The premixed flame in uniform straining flow
p0055 A82-43194
- COMBUSTION**
NT FUEL COMBUSTION
NT HYDROCARBON COMBUSTION
NT SOLID PROPELLANT COMBUSTION
NT SUPERSONIC COMBUSTION
Catalytic combustion of actual low and medium heating value gases
[NASA-TM-82930] p0125 N82-30717
- COMBUSTION CHAMBERS**
On the prediction of swirling flowfields found in axisymmetric combustor geometries
p0029 A82-12120
- Mean flowfields in axisymmetric combustor geometries with swirl
[AIAA PAPER 82-0177] p0092 A82-17824
- Dilution jet behavior in the turn section of a reverse flow combustor
[AIAA PAPER 82-0192] p0027 A82-20291
- High temperature durable catalyst development
p0056 A82-20739
- Flame structure in a swirl stabilized combustor inferred by radiant emission measurements
p0056 A82-28694
- Modeling parameter influences on MHD swirl combustion nozzle design
[AIAA PAPER 82-0984] p0011 A82-31947
- Experimental study of the effects of secondary air on the emissions and stability of a lean premixed combustor
[AIAA PAPER 82-1072] p0021 A82-34992
- NASA Broad Specification Fuels Combustion Technology program - Pratt and Whitney Aircraft

ORIGINAL PAGE IS
OF POOR QUALITY

COMBUSTION CONTROL

SUBJECT INDEX

Phase I results and status
[AIAA PAPER 82-1088] p0021 A82-34999
Small gas turbine combustor primary zone development
[AIAA PAPER 82-1159] p0103 A82-35036
Evaluation of fuel injection configurations to
control carbon and soot formation in small GT
combustors
[AIAA PAPER 82-1175] p0021 A82-35041
Combustor development for automotive gas turbines
[AIAA PAPER 82-1208] p0104 A82-35062
Turbulence measurements in a confined jet using a
six-orientation hot-wire probe technique
[AIAA PAPER 82-1262] p0094 A82-37710
Flow aerodynamics modeling of an MHD swirl
combustor - Calculations and experimental
verification p0094 A82-44782
Trends in high temperature gas turbine materials
[NASA-TM-82715] p0058 A82-11182
Low NO sub x heavy fuel combustor concept program
[NASA-CR-165512] p0129 A82-12572
Catalytic combustion of residual fuels
[NASA-TM-82731] p0118 A82-13504
Transient catalytic combustor model
[NASA-CR-165324] p0129 A82-13507
Gas-turbine critical research and advanced
technology support project
[NASA-TM-81708] p0118 A82-13509
Effect of fuel injector type on performance and
emissions of reverse-flow combustor
[NASA-TP-1945] p0016 A82-15040
Investigations of flowfields found in typical
combustor geometries
[NASA-CR-165061] p0090 A82-15360
Low NO subx heavy fuel combustor concept program.
Phase IA: Coal gas addendum
[NASA-CR-165577] p0133 A82-18690
Dilution jet behavior in the turn section of a
reverse flow combustor
[NASA-TM-82776] p0017 A82-19220
Investigations of flowfields found in typical
combustor geometries
[NASA-CR-168585] p0090 A82-19495
YF 102 in-duct combustor noise measurements with a
turbine nozzle, volume 1
[NASA-CR-165562-VOL-1] p0153 A82-21031
YF 102 in-duct combustor noise measurements with a
turbine nozzle, volume 2
[NASA-CR-165562-VOL-2] p0153 A82-21032
YF 102 in-duct combustor noise measurements with a
turbine nozzle, volume 3
[NASA-CR-165562-VOL-3] p0155 A82-21033
Advanced Low-Emissions Catalytic-Combustor
Program, phase I --- aircraft gas turbine engines
[NASA-CR-159656] p0025 A82-22265
Investigation of soot and carbon formation in
small gas turbine combustors
[NASA-CR-167853] p0025 A82-22267
Low NO sub x heavy fuel combustor concept program.
Phase IA: Combustion technology generation coal
gas fuels
[NASA-CR-165614] p0055 A82-22326
Nonlinear structural and life analyses of a
combustor liner
[NASA-TM-82846] p0111 A82-24501
Low NOx heavy fuel combustor concept program,
phase I
[NASA-CR-165449] p0135 A82-24651
Low NOx heavy fuel combustor concept program.
Phase I: Combustion technology generation
[NASA-CR-165482] p0136 A82-24725
Fracture mechanics criteria for turbine engine hot
section components
[NASA-CR-167896] p0027 A82-25257
Low NO sub x heavy fuel combustor concept program
phase IA gas tests
[NASA-CR-167877] p0055 A82-25337
Low NOx heavy fuel combustor concept program
addendum: Low/mid heating value gaseous fuel
evaluation
[NASA-CR-165615] p0055 A82-25338
Low NOx heavy fuel combustor concept
program
[NASA-CR-165367] p0136 A82-25635
Low NOx heavy fuel combustor concept
program
[NASA-CR-167876] p0074 A82-26482
Optimization of the oxidant supply system for
combined cycle MHD power plants
[NASA-TM-82909] p0123 A82-26790
Techniques for enhancing durability and
equivalence ratio control in a rich-lean,
three-stage ground power gas turbine combustor
[NASA-TM-82922] p0124 A82-29717
Computations of soot and NO sub x emissions
from gas turbine combustors
[NASA-CR-167930] p0139 A82-29777
Lewis pressurized, fluidized-bed combustion
program. Data and calculated results
[NASA-TM-81767] p0124 A82-30704
Exhaust gas measurements in a propane fueled swirl
stabilized combustor
[NASA-CR-169293] p0091 A82-31641
Flow process in combustors
[NASA-CR-169294] p0092 A82-31642
Investigations of flowfields found in typical
combustor geometries
[NASA-CR-169295] p0092 A82-31643
Micronized coal burner facility
[NASA-CASE-LEW-13426-1] p0126 A82-31769
Gas turbine critical research and advanced
technology (CRT) support project
[NASA-TM-82872] p0126 A82-31776
Nonlinear constitutive theory for turbine engine
structural analysis p0112 A82-33744
Low NOx heavy fuel combustor concept
program
[NASA-CR-165481] p0138 A82-33827
COMBUSTION CONTROL
Computer model of catalytic combustion/Stirling
engine heater head
[NASA-CR-165378] p0134 A82-22666
COMBUSTION EFFICIENCY
Atomization and combustion properties of flashing
injectors
[AIAA PAPER 82-0300] p0092 A82-17880
High temperature durable catalyst development
p0056 A82-20739
NASA Broad Specification Fuels Combustion
Technology program - Pratt and Whitney Aircraft
Phase I results and status
[AIAA PAPER 82-1088] p0021 A82-34999
Catalytic combustion of residual fuels
[NASA-TM-82731] p0118 A82-13504
Demonstration of catalytic combustion with
residual fuel
[NASA-CR-165369] p0131 A82-16484
Experimental study of an integral catalytic
combustor: Heat exchanger for Stirling engines
[NASA-TM-82783] p0119 A82-18691
Preliminary results on performance testing of a
turbocharged rotary combustion engine
[NASA-TM-82772] p0017 A82-21194
Testing of fuel/oxidizer-rich, high-pressure
preburners
[NASA-CR-165609] p0074 A82-24353
Low NOx heavy fuel combustor concept program,
phase I
[NASA-CR-165449] p0135 A82-24651
Exhaust gas measurements in a propane fueled swirl
stabilized combustor
[NASA-CR-169293] p0091 A82-31641
Low and medium heating value coal gas catalytic
combustor characterization
[NASA-CR-165560] p0138 A82-32856
COMBUSTION HEAT
U AT OF COMBUSTION
COMBUSTION INSTABILITY
U MBUSTION STABILITY
COMBUSTION PHYSICS
Symposium /International/ on Combustion, 18th,
University of Waterloo, Waterloo, Ontario,
Canada, August 17-22, 1980, Proceedings
p0056 A82-28651
Experimental and theoretical studies of the laws
governing condensate deposition from combustion
gases p0057 A82-28709
Thermodynamic and transport combustion properties
of hydrocarbons with air. Part 1: Properties
in SI units
[NASA-TP-1906] p0161 A82-32186
Thermodynamic and transport combustion properties
of hydrocarbons with air. Part 2: Compositions
corresponding to Kelvin temperature schedules in
part 1
[NASA-TP-1907] p0161 A82-32187
Thermodynamic and transport combustion properties
of hydrocarbons with air. Part 3: Properties

ORIGINAL PAGE IS
OF POOR QUALITY

SUBJECT INDEX

COMPONENT RELIABILITY

- in US customary units
[NASA-TP-1908] p0161 N82-32188
- Thermodynamic and transport combustion properties
of hydrocarbons with air. Part 4: Compositions
corresponding to Rankine temperature schedules
in part 3
[NASA-TP-1909] p0161 N82-32189
- COMBUSTION PRODUCTS**
Formation of oxides of nitrogen in monodisperse
spray combustion of hydrocarbon fuels
p0057 A82-37571
- Catalytic combustion of residual fuels
[NASA-TM-82731] p0118 N82-13504
- Low NOx sub heavy fuel combustor concept program.
Phase 1A: Coal gas addendum
[NASA-CR-165577] p0133 N82-18690
- Investigation of soot and carbon formation in
small gas turbine combustors
[NASA-CR-167853] p0025 N82-22267
- Exhaust emissions survey of a turbofan engine for
flame holder swirl type augmentors at simulated
altitude flight conditions
[NASA-TM-82787] p0019 N82-25255
- Low NOx heavy fuel combustor concept program
addendum: Low/mid heating value gaseous fuel
evaluation
[NASA-CR-165615] p0055 N82-25338
- Low NOx heavy fuel combustor concept program
[NASA-CR-165367] p0136 N82-25635
- Effect of fuel to air ratio on Mach 0.3 burner rig
hot corrosion of ZrO₂-Y₂O₃ thermal barrier
coatings
[NASA-TM-82879] p0061 N82-30373
- Exhaust gas measurements in a propane fueled swirl
stabilized combustor
[NASA-CR-169293] p0091 N82-31641
- COMBUSTION STABILITY**
NT FLAME STABILITY
Secondary effects in combustion instabilities
leading to flashback
[AIAA PAPER 82-0037] p0056 A82-17746
- Testing of fuel/oxidizer-rich, high-pressure
preburners
[NASA-CR-165609] p0074 N82-24353
- COMBUSTION WAVES**
U AMF PROPAGATION
- COMBUSTION WIND TUNNELS**
Numerical modelling of turbulent flow in a
combustion tunnel
p0093 A82-27000
- COMBUSTORS**
U COMBUSTION CHAMBERS
- COMMERCIAL AIRCRAFT**
NT BOEING 747 AIRCRAFT
NT DC 9 AIRCRAFT
NT EC 119 AIRCRAFT
Lightweight diesel engine designs for commuter
type aircraft
[NASA-CR-165470] p0023 N82-11068
- Bibliography of NASA published reports on general
aviation, 1975 to 1981
[NASA-TM-83307] p0001 N82-19132
- NASA/Lewis Research Center Icing Research Program
p0001 N82-21148
- Future propulsion opportunities for commuter
airplanes
[NASA-TM-82880] p0018 N82-24203
- COMMERCIAL AVIATION**
U VIL AVIATION
U COMMERCIAL AIRCRAFT
- COMMERCIAL ENERGY**
An assessment of alternative fuel cell designs for
residential and commercial cogeneration
p0138 A82-24695
- Magnetohydrodynamics (MHD) Engineering Test
Facility (ETF) 200 MWe power plant Conceptual
Design Engineering Report (CDER)
[NASA-CR-165452-VOL-5] p0132 N82-17603
- Development and test fuel cell powered on-site
integrated total energy systems. Phase 3:
Full-scale power plant development
[NASA-CR-167898] p0137 N82-30705
- COMMUNICATION CABLES**
NT FIBER OPTICS
- COMMUNICATION EQUIPMENT**
Baseband-processed SS-TDMA communication system
architecture and design concepts
[AIAA 82-0482] p0079 A82-23508
- COMMUNICATION NETWORKS**
The 30/20 GHz communications satellite trunking
network study
[NASA-CR-165467] p0078 N82-13302
- COMMUNICATION SATELLITES**
Advanced 30/20 GHz communication satellites
p0034 A82-12623
- 30/20 GHz communications satellite multibeam antenna
[AIAA 82-0449] p0079 A82-23486
- Dynamic switch matrix for the TDMA satellite
switching system
[AIAA 82-0458] p0085 A82-23494
- Planning satellite communication services and
spectrum-orbit utilization
[AIAA 82-0526] p0080 A82-23538
- Adaptive rain fade compensation
p0080 A82-27178
- 30/20 GHz demonstration system for improving orbit
utilization
p0080 A82-27189
- Open-loop nanosecond-synchronization for wideband
satellite communications
p0036 A82-27224
- Centaur capabilities for communications satellite
launches
[AIAA PAPER 82-0558] p0034 A82-36286
- Microwave intersatellite links for communications
satellites
p0036 A82-36925
- Wideband, high speed switch matrix development for
SS-TDMA applications
p0086 A82-43784
- The 30/20 GHz communications satellite trunking
network study
[NASA-CR-165467] p0078 N82-13302
- Cross-impact study of foreign satellite
communications on NASA's 30/20 GHz program
[NASA-CR-165154] p0078 N82-17420
- The 30/20 GHz flight experiment system, phase 2.
Volume 1: Executive summary
[NASA-CR-165409-VOL-1] p0078 N82-20362
- The 30/20 GHz flight experiment system, phase 2.
Volume 2: Experiment system description
[NASA-CR-165409-VOL-2] p0078 N82-20363
- The 30/20 GHz flight experiment system, phase 2.
Volume 3: Experiment system requirement document
[NASA-CR-165409-VOL-3] p0078 N82-20364
- The 30/20 GHz flight experiment system, phase 2.
Volume 4: Experiment system development plan
[NASA-CR-165409-VOL-4] p0078 N82-20365
- Communications satellite systems capacity analysis
[NASA-CR-167911] p0034 N82-27331
- NASA Adaptive Multibeam Phased Array (AMPA): An
application study
[NASA-CR-169125] p0079 N82-28503
- COMMUNICATION SYSTEMS**
U LECOMMUNICATION
- COMPARISON**
Application of an airfoil stall flutter computer
prediction program to a three-dimensional wing:
Prediction versus experiment
[NASA-CR-168586] p0007 N82-19169
- COMPARTMENTS**
NT AIR LOCKS
NT PRESSURE CHAMBERS
- COMPENSATION**
Compensation mechanism in liquid encapsulated
Czochralski GaAs Importance of melt stoichiometry
p0086 A82-40403
- COMPLEX VARIABLES**
NT CAUCHY INTEGRAL FORMULA
NT CONFORMAL MAPPING
NT HATHIEU FUNCTION
NT SINGULARITY (MATHEMATICS)
- COMPLIANCE (ELASTICITY)**
U DULUS OF ELASTICITY
- COMPONENT RELIABILITY**
Internal breakdown of charged spacecraft dielectrics
p0041 A82-18312
- The application of probabilistic design theory to
high temperature low cycle fatigue
[NASA-CR-165483] p0112 N82-14531
- Research and development program for non-linear
structural modeling with advanced
time-temperature dependent constitutive
relationships
[NASA-CR-165533] p0024 N82-16080
- Reliability model for planetary gear
[NASA-TM-82859] p0101 N82-28643

ORIGINAL PAGE IS
OF POOR QUALITY

COMPOSITE MATERIALS

SUBJECT INDEX

COMPOSITE MATERIALS

NT ALUMINUM BORON COMPOSITES
NT BORON REINFORCED MATERIALS
NT CARBON FIBER REINFORCED PLASTICS
NT EPOXY MATRIX COMPOSITES
NT EUTECTIC COMPOSITES
NT FIBER COMPOSITES
NT FIBER REINFORCED COMPOSITES
NT GLASS FIBER REINFORCED PLASTICS
NT GRAPHITE-EPOXY COMPOSITES
NT GRAPHITE-POLYIMIDE COMPOSITES
NT LAMINATES
NT METAL MATRIX COMPOSITES
NT POLYMER MATRIX COMPOSITES
NT RESIN MATRIX COMPOSITES
NT WHISKER COMPOSITES

Effects of nadic ester concentration and processing on physical and mechanical properties of PMR/Celion 6000 composites

p0051 A82-27440
Kevlar/PMR-15 polyimide matrix composite for a complex shaped DC-9 drag reduction fairing [AIAA PAPER 82-1047] p0002 A82-37678
Novel improved PMR polyimides [NASA-TM-82733] p0009 A82-11117
Development of battery separator composites [NASA-CR-165508] p0128 A82-11547
Indentation lay for composite laminates [NASA-CR-165460] p0052 A82-15123
Tribological characteristics of a composite total-surface hip replacement [NASA-TP-1853] p0066 A82-16239
Bibliography of Lewis Research Center technical publications announced in 1981 [NASA-TM-82838] p0163 A82-27191
Tribological evaluation of composite materials made from a partially fluorinated polyimide [NASA-TM-82832] p0069 A82-29459
Kevlar/PMR-15 reduced drag DC-9 reverser stang fairing [NASA-CR-165448] p0052 A82-31448
Environmental and High-Strain Rate effects on composites for engine applications [NASA-TM-82882] p0051 A82-31449
Structural tailoring of engine blades (STAEBL) [NASA-CR-167949] p0028 A82-33391

COMPOSITE STRUCTURES

NT LAMINATES

Structural dynamics of shroudless, hollow, fan blades with composite in-lays [ASME PAPER 82-GT-284] p0022 A82-35456
Performance of PTFE-lined composite journal bearings [ASLE PREPRINT 82-A7-1A-1] p0104 A82-37854
Icing tunnel tests of a composite porous leading edge for use with a liquid anti-ice system --- Lewis icing research tunnel [NASA-CR-164966] p0014 A82-11052
Performance of PTFE-lined composite journal bearings [NASA-TM-82779] p0048 A82-17263
Numerical simulation of one-dimensional heat transfer in composite holes with phase change --- wing deicing pads [NASA-CR-165607] p0002 A82-22142
Structural dynamics of shroudless, hollow fan blades with composite in-lays [NASA-TM-82816] p0018 A82-22266
Compression behavior of unidirectional fibrous composite [NASA-TM-82833] p0050 A82-22313
Experience and assessment of the DOE-NASA Mod-1 2000-Kilowatt wind turbine generator at Boone, North Carolina [NASA-TM-82721] p0125 A82-30710

COMPOSITES

COMPOSITE MATERIALS

COMPOSITION (PROPERTY)

NT CHEMICAL COMPOSITION

NT MOISTURE CONTENT

COMPRESSIBLE FLOW

NT TRANSONIC FLOW

Solutions of the compressible Navier-Stokes equations using the integral method [AIAA PAPER 81-0046] p0093 A82-23832
Computer program for aerodynamic and blading design of multistage axial-flow compressors [NASA-TP-1946] p0016 A82-15039
A new numerical approach for compressible viscous flows [NASA-CR-168842] p0090 A82-22455

COMPRESSION LOADS

NT AXIAL COMPRESSION LOADS

Analytical and experimental evaluation of biaxial contact stress

p0071 A82-20741

COMPRESSIVE STRENGTH

Compression behavior of unidirectional fibrous composite

[NASA-TM-82833] p0050 A82-22313

COMPRESSOR BLADES

Characteristics of the flow in the annulus-wall region of an axial-flow compressor rotor blade passage

[AIAA PAPER 82-0413] p0009 A82-17933

Three-dimensional flow field in the tip region of a compressor rotor passage. I - Mean velocity profiles and annulus wall boundary layer [ASME PAPER 82-GT-11] p0011 A82-35280

The use of optimization techniques to design controlled diffusion compressor blading [ASME PAPER 82-GT-149] p0022 A82-35373

The effect of rotor blade thickness and surface finish on the performance of a small axial flow turbine

[ASME PAPER 82-GT-222] p0022 A82-35409

Aerodynamic damping measurements in a transonic compressor

[ASME PAPER 82-GT-287] p0012 A82-35459

The effect of rotor blade thickness and surface finish on the performance of a small axial flow turbine

[NASA-TM-82726] p0003 A82-13114

Core compressor exit stage study. Volume 4: Data and performance report for the best stage configuration

[NASA-CR-165357] p0023 A82-14092

Core compressor exit stage study. Volume 5: Design and performance report for the Rotor C/Stator B configuration

[NASA-CR-165358] p0023 A82-14093

The use of optimization techniques to design controlled diffusion compressor blading

[NASA-TM-82763] p0016 A82-14094

Computer program for aerodynamic and blading design of multistage axial-flow compressors

[NASA-TP-1946] p0016 A82-15039

Performance of single-stage axial-flow transonic compressor with rotor and stator aspect ratios of 1.63 and 1.78, respectively, and with design pressure ratio of 1.82

[NASA-TP-1974] p0017 A82-19222

A FORTRAN program for calculating three dimensional, inviscid and rotational flows with shock waves in axial compressor blade rows: User's manual

[NASA-CR-3560] p0008 A82-26230

Core compressor exit stage study, volume 6

[NASA-CR-165553] p0027 A82-27310

B747/JT9D flight loads and their effect on engine running clearances and performance deterioration; BCAC NAIL/P and WA JT9D engine diagnostics programs

[NASA-CR-165573] p0027 A82-28296

COMPRESSOR EFFICIENCY

Progress in the development of energy efficient engine components

[ASME PAPER 82-GT-275] p0030 A82-35450

JT8D high pressure compressor performance improvement

[NASA-CR-165531] p0104 A82-11467

CP6 Jet Engine Diagnostics Program: High pressure compressor clearance investigation

[NASA-CR-165580] p0025 A82-21197

STGSK: A computer code for predicting multistage axial flow compressor performance by a meanline stage stacking method

[NASA-TP-2020] p0018 A82-25250

COMPRESSOR MOTORS

Interaction of compressor rotor blade wake with wall boundary layer/vortex in the end-wall region

[ASME PAPER 81-GR/GT-1] p0010 A82-19301

Effects of blade loading and rotation on compressor rotor wake in end wall regions

[AIAA PAPER 82-0193] p0010 A82-22063

Three dimensional flow field inside the passage of a low speed axial flow compressor rotor

[AIAA PAPER 82-1036] p0011 A82-31964

Investigation of the tip-clearance flow inside and at the exit of a compressor rotor passage. I -

- Mean velocity field
[ASME PAPER 82-GT-12] p0011 A82-35281
- Three-dimensional flow field in the tip region of
a compressor rotor passage. II - Turbulence
properties p0093 A82-32225
[ASKE PAPER 82-GT-234] p0011 A82-35416
- In-plane inertial coupling in tuned and severely
mistuned bladed disks p0093 A82-35043
[ASME PAPER 82-GT-288] p0012 A82-35460
- Performance of single-stage axial-flow transonic
compressor with rotor and stator aspect ratios
of 1.63 and 1.78, respectively, and with design
pressure ratio of 1.82 p0022 A82-35348
[NASA-TP-1974] p0017 A82-19222
- High-speed laser anemometer system for intrarotor
flow mapping in turbomachinery p0011 A82-35379
[NASA-TP-1663] p0095 A82-19521
- Performance of single-stage axial-flow transonic
compressor with rotor and stator aspect ratios
of 1.63 and 1.77, respectively, and with design
pressure ratio of 2.05 p0012 A82-35571
[NASA-TP-2001] p0018 A82-22269
- Investigation of the tip clearance flow inside and
at the exit of a compressor rotor passage p0012 A82-37711
[NASA-CR-169004] p0026 A82-25253
- A FORTRAN program for calculating three
dimensional, inviscid and rotational flows with
shock waves in axial compressor blade rows:
User's manual p0006 A82-40921
[NASA-CR-3560] p0008 A82-26230
- Three dimensional flow field inside compressor
rotor, including blade boundary layers p0094 A82-44782
[NASA-CR-169120] p0091 A82-27686
- Active clearance control system for a turbomachine p0004 A82-15020
[NASA-CASE-LEW-12938-1] p0020 A82-32366
- Status of laser anemometry in turbomachinery
research at the Lewis Research Center p0096 A82-32686
- COMPRESSORS**
- NT CENTRIFUGAL COMPRESSORS
- NT SUPERCHARGERS
- NT TRANSONIC COMPRESSORS
- NT TURBOCOMPRESSORS
- JTD high pressure compressor performance
improvement p0104 A82-11467
[NASA-CR-165531]
- Investigation of the tip clearance flow inside and
at the exit of a compressor rotor passage p0026 A82-25253
[NASA-CR-169004]
- COMPUTATION**
- NT GRID CALCULATION
- File shape calculations on supercomputers p0100 A82-25519
[NASA-TM-82856]
- COMPUTATIONAL FLUID DYNAMICS**
- The three-dimensional boundary layer on a rotating
helical blade p0009 A82-15459
- Toward the use of similarity theory in two-phase
choked flows p0089 A82-16570
- A simple finite difference procedure for the
vertex controlled diffuser p0030 A82-17788
[AIAA PAPER 82-0109]
- Forms of three-dimensional supersonic free jets in
linear approximation p0093 A82-23832
A82-19196
- Three-dimensional flow calculations including
boundary layer effects for supersonic inlets at
angle of attack p0005 A82-19778
[AIAA PAPER 82-0061]
- Solutions of the compressible Navier-Stokes
equations using the integral method p0093 A82-23832
[AIAA PAPER 91-0046]
- Numerical analysis of confined turbulent flow p0093 A82-24748
- Numerical modelling of turbulent flow in a
combustion tunnel p0093 A82-27000
- Multi-grid simulation of asymptotic curved-duct
flows using a semi-implicit numerical technique p0010 A82-29003
- Natural convection with combined driving forces p0093 A82-31445
- Finite volume calculation of three-dimensional
potential flow around a propeller p0010 A82-31933
[AIAA PAPER 82-0957]
- Application of a finite element algorithm for the
solution of steady transonic Euler equations p0010 A82-31939
[AIAA PAPER 82-0970]
- Effects of internal heat transfer on the structure
of self-similar blast waves p0093 A82-32225
- Small gas turbine combustor primary zone development
[AIAA PAPER 82-1159] p0103 A82-35036
- Bluff-body flameholder wakes - A simple numerical
solution p0093 A82-35043
[AIAA PAPER 82-1177]
- A computational design method for transonic
turbomachinery cascades p0022 A82-35348
[ASME PAPER 82-GT-117]
- Flow distributions and discharge coefficient
effects for jet array impingement with initial
crossflow p0011 A82-35379
[ASME PAPER 82-GT-156]
- A study of viscous flow in stator and rotor passages
[ASME PAPER 82-GT-248] p0011 A82-35427
- Rapid approximate determination of nonlinear
solutions - Application to aerodynamic flows and
design/optimization problems p0012 A82-35571
- Investigation of rotational transonic flows
through ducts using a finite element scheme p0012 A82-37711
[AIAA PAPER 82-1267]
- A summary of V/STOL inlet analysis methods p0006 A82-40921
- Flow aerodynamics modeling of an MHD swirl
combustor - Calculations and experimental
verification p0094 A82-44782
- Comparison of two and three dimensional flow
computations with laser anemometer measurements
in a transonic compressor rotor p0004 A82-15020
[NASA-TM-82777]
- Numerical analysis and FORTRAN program for the
computation of the turbulent wakes of
turbomachinery rotor blades, isolated airfoils
and cascade of airfoils p0006 A82-18184
[NASA-CR-3509]
- Development of a locally mass flux conservative
computer code for calculating 3-D viscous flow
in turbomachines p0007 A82-22214
[NASA-CR-3539]
- A new numerical approach for compressible viscous
flows p0090 A82-22455
[NASA-CR-168842]
- Turbofan forced mixer-nozzle internal flowfield.
Volume 2: Computational fluid dynamic predictions p0091 A82-22459
[NASA-CR-3493]
- Multiple-grid acceleration of Lax-Wendroff
algorithms p0149 A82-22922
[NASA-TM-82843]
- Rime ice accretion and its effect on airfoil
performance p0008 A82-24166
[NASA-CR-165599]
- Computer program for calculating full potential
transonic, quasi-three-dimensional flow through
a rotating turbomachinery blade row p0005 A82-28247
[NASA-TP-2030]
- Past generation of three-dimensional computational
boundary-conforming periodic grids of C-type ---
for turbine blades and propellers p0009 A82-28253
[NASA-CR-165596]
- Flow process in combustors p0092 A82-31642
[NASA-CR-169294]
- COMPUTER AIDED DESIGN**
- Experimental verification of a computational
procedure for the design of TWT-refocuser-MDC
systems --- Multistage Depressed Collectors p0082 A82-16128
- A new approach to the minimum weight/loss design
of switching power converters p0082 A82-16831
- Modeling and Analysis of Power Processing Systems
(MAPPS). Volume 1: Technical report p0083 A82-14447
[NASA-CR-165538]
- Computer program for aerodynamic and blading
design of multistage axial-flow compressors p0016 A82-15039
[NASA-TP-1946]
- Interactive-graphic flowpath plotting for turbine
engines p0017 A82-15041
[NASA-TM-82756]
- CAS22 - FORTRAN program for fast design and
analysis of shock-free airfoil cascades using
fictitious-gas concept p0006 A82-16044
[NASA-CR-3507]
- Design of supercritical cascades with high solidity
[NASA-CR-165600] p0007 A82-22210

- The optimal design of involute gear teeth with unequal addenda
[NASA-TM-82866] p0101 N82-28645
- AESOP: A computer-aided design program for linear multivariable control systems
[NASA-TM-82871] p0148 N82-30992
- Automated procedure for developing hybrid computer simulations of turbofan engines. Part 1: General description
[NASA-TP-1851] p0146 N82-33020
- Structural tailoring of engine blades (STAEBL)
[NASA-CR-167949] p0028 N82-3339;
- COMPUTER GRAPHICS**
- Interactive-graphic flowpath plotting for turbine engines
[NASA-TM-82756] p0017 N82-15041
- Shaded computer graphic techniques for visualizing and interpreting analytic fluid flow models
[NASA-CR-168418] p0145 N82-17880
- Synthetic battery cycling techniques
[NASA-TM-82945] p0125 N82-30715
- COMPUTER METHODS**
- U MPUTER PROGRAMS**
- COMPUTER PROGRAMS**
- NT NASTRAM**
- NT OPERATING SYSTEMS (COMPUTERS)**
- On the automatic generation of FEM models for complex gears - A work-in-progress report
p0109 N82-48243
- Integrated analysis of engine structures
[NASA-TM-82713] p0111 N82-11491
- Numerical simulation of plasma insulator interactions in space. Part 1: The self consistent calculation
p0039 N82-14277
- Numerical simulation of plasma insulator interactions in space. Part 2: Dielectric effects
p0039 N82-14273
- CAS22 - FORTRAN program for fast design and analysis of shock-free airfoil cascades using fictitious-gas concept
[NASA-CR-3507] p0006 N82-16044
- Research and development program for non-linear structural modeling with advanced time-temperature dependent constitutive relationships
[NASA-CR-165533] p0024 N82-16080
- Modeling and Analysis of Power Processing Systems (MAPPS). Volume 2: Appendices
[NASA-CR-165539] p0145 N82-16748
- Prediction of sound radiation from different practical jet engine inlets
[NASA-CR-165120] p0153 N82-16810
- Hybrid and electric advanced vehicle systems (heavy) simulation
[NASA-CR-165536] p0163 N82-16938
- Investigation and evaluation of a computer program to minimize three-dimensional flight time tracks
[NASA-CR-168419] p0145 N82-17879
- Numerical analysis and FORTRAN program for the computation of the turbulent wakes of turbomachinery rotor blades, isolated airfoils and cascade of airfoils
[NASA-CR-3509] p0006 N82-18184
- Application of an airfoil stall flutter computer prediction program to a three-dimensional wing: Prediction versus experiment
[NASA-CR-168586] p0007 N82-19169
- Investigations of flowfields found in typical combustor geometries
[NASA-CR-168585] p0090 N82-19495
- Development of a locally mass flux conservative computer code for calculating 3-D viscous flow in turbomachines
[NASA-CR-3539] p0007 N82-22214
- SIGSTR: A computer code for predicting multistage axial flow compressor performance by a meanline stage stacking method
[NASA-TP-2029] p0018 N82-25250
- Additional extensions to the NASCAP computer code, volume 1
[NASA-CR-167855] p0146 N82-25810
- A FORTRAN program for calculating three dimensional, inviscid and rotational flows with shock waves in axial compressor blade rows: User's manual
[NASA-CR-3560] p0008 N82-26230
- Bird impact analysis package for turbine engine fan blades
[NASA-TM-82831] p0112 N82-26701
- Computer program for calculating full potential transonic, quasi-three-dimensional flow through a rotating turbomachinery blade row
[NASA-TP-2030] p0005 N82-28247
- AESOP: A computer-aided design program for linear multivariable control systems
[NASA-TM-82871] p0148 N82-30992
- Finite element-integral simulation of static and flight fan noise radiation from the JT15D turbofan engine
[NASA-TM-82936] p0152 N82-31068
- Large displacements and stability analysis of nonlinear propeller structures
[NASA-TM-82850] p0112 N82-31707
- High speed cylindrical roller bearing analysis. S/P computer program CYBEAM. Volume 2: User's manual
[NASA-CR-165364] p0146 N82-31968
- Automated procedure for developing hybrid computer simulations of turbofan engines. Part 1: General description
[NASA-TP-1851] p0146 N82-33020
- COMPUTER SIMULATION**
- U MPUTERIZED SIMULATION**
- COMPUTER STORAGE DEVICES**
- A generalized memory test algorithm
[NASA-TM-82874] p0146 N82-31971
- COMPUTER SYSTEMS PROGRAMS**
- NT OPERATING SYSTEMS (COMPUTERS)**
- COMPUTER TECHNIQUES**
- The NASA MBRIT program - Developing new concepts for accurate flight planning
[AIAA PAPER 82-0340] p0014 N82-17894
- COMPUTERIZED CONTROL**
- U MERICAN CONTROL**
- COMPUTERIZED DESIGN**
- U MPUTER AIDED DESIGN**
- COMPUTERIZED SIMULATION**
- NT ANALOG SIMULATION**
- NT DIGITAL SIMULATION**
- Design and verification of a multiple fault tolerant control system for STS applications using computer simulation
[AIAA 81-2173] p0035 N82-10124
- Maximum entropy image reconstruction from projections
A82-11053
- Real-time computer simulation/emulation for verification of multi-fault-tolerant control of Centaur-in-Shuttle
[AIAA 81-2283] p0040 N82-13494
- A simple finite difference procedure for the vortex controlled diffuser
[AIAA PAPER 82-0109] p0030 N82-17788
- Validation of the NASCAP model using spaceflight data
[AIAA PAPER 82-0269] p0038 N82-17872
- A real time Pegasus propulsion system model for VSTOL piloted simulation evaluation
[AIAA PAPER 81-2663] p0020 N82-19221
- Mathematical modeling of ice accretion on airfoils
[AIAA PAPER 82-0284] p0014 N82-27098
- On the automatic generation of FEM models for complex gears - A work-in-progress report
p0109 N82-48243
- Oblique-incidence secondary emission from charged dielectronics
p0039 N82-14227
- New features and applications of PRESTO, a computer code for the performance of regenerative, superheated steam turbine cycles
[NASA-TP-1954] p0119 N82-16477
- Hybrid and electric advanced vehicle systems (heavy) simulation
[NASA-CR-165536] p0163 N82-16938
- Mapping of electrical potential distributions with charged particle beams
[NASA-CR-168556] p0084 N82-18508
- Numerical simulation of one-dimensional heat transfer in composite bodies with phase change --- wing deicing pads
[NASA-CR-165607] p0002 N82-22142
- Additional extensions to the NASCAP computer code, volume 2
[NASA-CR-167856] p0040 N82-26377

ORIGINAL PAGE IS
OF POOR QUALITY

SUBJECT INDEX

CONVECTIVE HEAT TRANSFER

- Finite element-integral simulation of static and flight fan noise radiation from the JT15D turbofan engine [NASA-TP-82936] p0152 N82-31068
- Automated procedure for developing hybrid computer simulations of turbofan engines. Part I: General description [NASA-TP-1851] p0146 N82-33020
- COMPUTERS**
 NT DIGITAL COMPUTERS
 NT HYBRID COMPUTERS
 NT MICROCOMPUTERS
- CONCENTRATION (COMPOSITION)**
 NT MOISTURE CONTENT
- CONCENTRATORS**
 Subsystems design and component development for the parabolic dish module for solar thermal power systems [NASA-CR-168941] p0135 N82-24646
 Determination of optimum sunlight concentration level in space for 3-4 cascade solar cells [NASA-TN-82899] p0126 N82-32853
- CONDENSATES**
 Experimental and theoretical studies of the laws governing condensate deposition from combustion gases p0057 A82-28709
- CONDENSATION**
 Effects of condensation and surface action on the structure of steady-state fronts A82-19360
- CONDITIONS**
 NT KUTTA-JOUKOWSKI CONDITION
- CONDUCTING MEDIA**
 U INDUCTORS
- CONVECTIVE HEAT TRANSFER**
 Heat transfer in cooled porous region with curved boundary p0089 A82-14848
 Self-adaptive closed constrained solution algorithms for nonlinear conduction p0094 A82-45157
 Numerical simulation of one-dimensional heat transfer in composite bodies with phase change --- wing leading pads [NASA-CR-165607] p0002 N82-22142
- CONDUCTORS**
 NT ELECTRIC CONDUCTORS
 NT ELECTROLYTES
 NT ION EXCHANGE MEMBRANE ELECTROLYTES
 NT MOLTEN SALT ELECTROLYTES
 NT METAL CONDUCTORS
 NT SUPERCONDUCTORS
 Component technology for space power systems [NASA-TN-82928] p0082 N82-24474
- CONFERENCES**
 Symposium /International/ on Combustion, 18th, University of Waterloo, Waterloo, Ontario, Canada, August 17-22, 1980, Proceedings p0056 A82-28651
 Spacecraft Charging Technology, 1980 [NASA-CP-2182] p0037 N82-14213
 Proceedings of the Conference on High-temperature Electronics [NASA-TN-84969] p0081 N82-15311
 Future propulsion opportunities for commuter airplanes [NASA-TN-82880] p0018 N82-24203
- CONFLUENCE**
 U MERGENCE
- CONFORMAL MAPPING**
 Oblique-incidence secondary emission from charged dielectrics p0039 N82-14227
- CONFORMAL TRANSFORMATIONS**
 U NORMAL MAPPING
- CONSERVATION**
 NT ENERGY CONSERVATION
- CONSERVATION LAWS**
 Multiple-grid acceleration of Lax-Wendroff algorithms [NASA-TN-82843] p0149 N82-22922
- CONSTITUTIONAL DIAGRAMS**
 U ASE DIAGRAMS
- CONSTITUTIVE EQUATIONS**
 Nonlinear structural and life analyses of a combustor liner [NASA-TN-82846] p0111 N82-24501
- Nonlinear constitutive theory for turbine engine structural analysis p0112 N82-33744
- CONSTRUCTION**
 Study of multi-megawatt technology needs for photovoltaic space power systems, Volume I: Executive summary [NASA-CR-165323-VOL-1] p0130 N82-14636
- CONSTRUCTION IN SPACE**
 U BITAL ASSEMBLY
- CONSUMABLES (SPACECRAFT)**
 NT PROPELLANT STORAGE
 NT STORABLE PROPELLANTS
- CONSUMPTION**
 NT ENERGY CONSUMPTION
 NT FUEL CONSUMPTION
- CONTACT RESISTANCE**
 Rolling resistance of electric vehicle tires from track tests [NASA-TN-82836] p0124 N82-28786
- CONTAMINANTS**
 NT TRACE CONTAMINANTS
- CONTAMINATION**
 NT FUEL CONTAMINATION
- CONTOURS**
 Analytic investigation of effect of end-wall contouring on stator performance [NASA-TP-1943] p0003 N82-14051
 Comparison of experimental and analytical performance for contoured endwall stators [NASA-TN-82877] p0019 N82-26299
- CONTROL DEVICES**
 U NTROL EQUIPMENT
- CONTROL EQUIPMENT**
 The effects of controls and controllable and storage loads on the performance of stand-alone photovoltaic systems p0127 A82-45027
 Sensor failure detection system --- for the F100 turbofan engine [NASA-CR-165515] p0023 N82-13145
- CONTROL SIMULATION**
 A tensor approach to modeling of nonhomogeneous nonlinear systems p0148 A82-19064
- CONTROL SURFACES**
 NT EXTERNALLY BLOWN FLAPS
 NT GUIDE VANES
 NT JET VANES
- CONTROL THEORY**
 The role of modern control theory in the design of controls for aircraft turbine engines [NASA-TN-82815] p0018 N82-22262
- CONTROLLED ATMOSPHERES**
~~CONTROLLED ATMOSPHERES~~
- CONTROL SYSTEMS**
 Fast recovery, high voltage silicon diodes for AC motor controllers p0086 A82-36926
 Straight and chopped DC performance data for a General Electric 5BY436A1 DC shunt motor with a General Electric EV-1 controller [NASA-CR-165507] p0085 N82-24425
 Summary of electric vehicle dc motor-controller tests [NASA-TN-82863] p0082 N82-33636
- CONVECTION**
 NT FREE CONVECTION
 Gas turbine ceramic-coated-vane concept with convection-cooled porous metal core [NASA-TP-1942] p0016 N82-14090
- CONVECTIVE FLOW**
 Sound generated in a cascade by three-dimensional disturbances convected in a subsonic flow [AIAA PAPER 81-2046] p0153 A82-10460
 Heat transfer in cooled porous region with curved boundary p0089 A82-14848
 Nonlinear Marangoni convection in bounded layers. I - Circular cylindrical containers. II - Rectangular cylindrical containers p0094 A82-39501
- CONVECTIVE HEAT TRANSFER**
 Effects of condensation and surface motion on the structure of steady-state fronts A82-19360
 An experimental investigation into the feasibility of a thermoelectric heat flux gage [NASA-TN-82755] p0095 N82-14494

CONVERGENCE

SUBJECT INDEX

CONVERGENCE

Numerical comparisons of nonlinear convergence accelerators

p0149 A82-31438

Acceleration of convergence of vector sequences
[NASA-TM-82931] p0149 N82-29075

CONVERTIBLES

B 5701 AIRCRAFT

CONVERTERS

A 10-KV series resonant converter design, transistor characterization, and base-drive optimization p0086 A82-36927

CONVEKITY

Turbulent boundary layer heat transfer experiments; Convex curvature effects including introduction and recovery [NASA-CR-3510] p0090 N82-17456

COOLING

NT AIR COOLING

NT FILM COOLING

NT SWFAN COOLING

Low-thrust Isp sensitivity study [NASA-CR-165621] p0045 N82-22309

COPPER

The orthogonal in-situ machining of single and polycrystalline aluminum and copper, volume I [NASA-CR-168929] p0076 N82-24361

COPPER ALLOYS

High temperature low cycle fatigue mechanisms for nickel base and a copper base alloy [NASA-CR-3542] p0064 N82-26436

COBES

Core compressor exit stage study, Volume 4: Data and performance report for the best stage configuration [NASA-CR-165357] p0023 N82-14092

Core compressor exit stage study, Volume 5: Design and performance report for the Rotor C/Stator B configuration [NASA-CR-165358] p0023 N82-14093

CORIOLIS EFFECT

The influence of Coriolis forces on gyroscopic motion of spinning blades [ASME PAPER 82-GT-163] p0030 A82-35384
'Coriolis resonance' within a rotating duct --- flow induced vibrations in centrifugal compressors p0012 A82-37938

CORNER FLOW

Dilution jet behavior in the turn section of a reverse flow combustor [AIAA PAPER 82-C192] p0021 A82-20291
Experimental study of turbulence in blade end wall corner region [NASA-CR-169283] p0091 N82-31639

CORPUSCULAR RADIATION

NT ELECTRON BEAMS

NT FERRORETIC PARTICLES

NT RELATIVISTIC ELECTRON BEAMS

CORRELATION

NT ANGULAR CORRELATION

CORROSION

NT HCT CORROSION

Influence of corrosive solutions on microhardness and chemistry of magnesium oxide /001/ surfaces [NASA-TP-2042] p0102 N82-31691

CORROSION PREVENTION

Method of protecting a surface with a silicon-slurry/aluminate coating --- coatings for gas turbine engine blades and vanes [NASA-CR-165498] p0068 N82-28441

CORROSION RESISTANCE

NT OXIDATION RESISTANCE

Development of improved high temperature coatings for IN-792 + HF [NASA-CR-165395] p0063 N82-14333

Review of NASA progress in thermal barrier coatings for stationary gas turbines [NASA-TM-81716] p0058 N82-17335

Covering solid, film cooled surfaces with a duplex thermal barrier coating [NASA-CR-165498] p0088 N82-25463

CORROSION TESTS

Long-term high-velocity oxidation and hot corrosion testing of several NiCrAl and FeCrAl base oxide dispersion strengthened alloys p0062 A82-37151

Friction and wear of iron in corrosive metal [NASA-TP-1985] p0058 N82-20291

CONUNDUM

U URANIUM OXIDES

COST ANALYSIS

Cost/benefit studies of advanced materials technologies for future aircraft turbine engines; Materials for advanced turbine engines [NASA-CR-167849] p0026 N82-25254

COST EFFECTIVENESS

Comparative analysis of CCHHD power plants --- Closed Cycle MHD p0158 A82-20747

COST ESTIMATES

Magnetohydrodynamics MHD Engineering Test Facility 2TF 200 MWe power plant. Conceptual Design Engineering Report CDR. Volume 3: Costs and schedules [NASA-CR-165452-VOL-3] p0128 N82-10495
Summary and evaluation of the conceptual design study of a potential early commercial MHD power plant (CSPEC) [NASA-TM-82734] p0113 N82-16481

COSTS

NT LIFE CYCLE COSTS

COUNTER-ROTATING WHEELS

Precision of spiral-bevel gears [NASA-TM-82888] p0102 N82-30552

COUPLING

In-plane inertial coupling in tuned and severely mistuned bladed disks [ASME PAPER 82-GT-288] p0012 A82-35460
Coupled cavity traveling wave tube with velocity tapering [NASA-CASE-LEW-12296-1] p0082 N82-26568

COVERINGS

Testing of solar cell covers and encapsulants conducted in a simulated space environment [NASA-CR-165475] p0129 N82-12571

CONNELL METHOD

U MECHANICAL INTEGRATION

COOLINGS

Low speed testing of the inlets designed for a tandem-fan V/STOL nacelle --- conducted in the Lewis 10 by 10 foot wind tunnel [NASA-TM-82728] p0003 N82-11042
Thrust reverser for a long duct fan engine --- for turbofan engines [NASA-CASE-LEW-13199-1] p0019 N82-26293

CRACK FORMATION

U ACK INITIATION

CRACK GEOMETRY

Creep crack-growth: A new path-independent T sub o and computational studies [NASA-CR-168930] p0113 N82-24503

CRACK INITIATION

Effect of tangential traction and roughness on crack initiation/propagation during rolling contact p0103 A82-30022

Turbine blade nonlinear structural and life analysis [AIAA PAPER 82-1056] p0021 A82-34981

Analysis of crack propagation as an energy absorption mechanism in metal matrix composites [NASA-CR-165051] p0052 N82-14288

Elevated temperature fatigue testing of metals [NASA-TM-82745] p0111 N82-16119

Mechanisms of deformation and fracture in high temperature low cycle fatigue of Rene 80 and IN 100 [NASA-CR-165498] p0113 N82-26706

A preliminary study of crack initiation and growth at stress concentration sites [NASA-CR-169358] p0115 N82-33738

CRACK PROPAGATION

Effect of tangential traction and roughness on crack initiation/propagation during rolling contact p0103 A82-30022

Effects of oxidation and oxidation under load on strength distributions of Si3N4 [ACS PAPER 69-B-80] p0071 A82-35871

On a study of the /Delta T/c and C/asterisk/ integrals for fracture analysis under non-steady creep p0115 A82-36782

Moving singularity creep crack growth analysis with the /Delta T/c and C/asterisk/ integrals --- path-independent vector and energy rate line integrals p0116 A82-40066

C-3

- Crack displacements for J/I/ testing with compact specimens p0063 A82-47399
- Creep shear behavior of the oxide dispersion strengthened superalloy MA 6000E [NASA-TM-82704] p0056 A82-10195
- CREEP TESTS**
Fatigue and creep-fatigue deformation of several nickel-base superalloys at 650 C p0062 A82-47398
- CRISTATIONS**
U AVELING WAVE TUBES
- CRIVICES**
U ACKS
- CRITERIA**
WT STRUCTURAL DESIGN CRITERIA
- CRITICAL HATCH NUMBER**
U CH NUMBER
- CRITICAL REYNOLDS NUMBER**
U INOLDS NUMBER
- CROSS FLOW**
Flow distributions and discharge coefficient effects for jet array impingement with initial crossflow [ASME PAPER 82-GT-156] p0011 A82-35379
- CROSS POLARIZATION**
Coaxial prime focus feeds for paraboloidal reflectors [NASA-CR-167934] p0078 A82-31585
- CROSSLINKING**
Cross-linked polyvinyl alcohol films as alkaline battery separators [NASA-TM-82802] p0054 A82-22327
- CRYOGENIC FLUID STORAGE**
An experiment to evaluate liquid hydrogen storage in space A82-20748
- Cryogenic fluid management experiment [NASA-CR-165495] p0039 A82-15117
- CRYOGENIC FLUIDS**
NT LIQUID HYDROGEN
NT LIQUID OXYGEN
- CRYOGENIC ROCKET PROPELLANTS**
NT LIQUID FUELS
Study of vapor flow into a capillary acquisition device --- for cryogenic rocket propellants [NASA-CR-167883] p0091 A82-24452
- CRYOGENICS**
Flows through sequential orifices with heated spacer reservoirs [NASA-TM-82855] p0088 A82-24455
- CRYSTAL DEFECTS**
NT CRYSTAL DISLOCATIONS
NT VACANCIES (CRYSTAL DEFECTS)
Material and processing needs for silicon solar cells in space p0032 A82-26336
- CRYSTAL DISLOCATIONS**
On finite deformation elasto-plasticity p0116 A82-45869
The influence of orientation on the stress rupture properties of nickel-base superalloy single crystals p0062 A82-47397
High purity low dislocation GaAs single crystals [NASA-CR-165593] p0159 A82-23030
- CRYSTAL GROWTH**
NT CZOCHRALSKI METHOD
NT DIRECTIONAL SOLIDIFICATION (CRYSTALS)
NT VAPOR PHASE EPITAXY
Undoped semi-insulating LEC GaAs - A model and a mechanism --- Liquid Encapsulated Czochralski p0159 A82-13754
- CRYSTAL LATTICES**
NT CLOSE PACKED LATTICES
NT FACE CENTERED CUBIC LATTICES
- CRYSTAL OPTICS**
Investigation of a comb-type slow-wave structure for millimeter-wave masers A82-18368
Pockels-effect cell for gas-flow simulation [NASA-TP-2007] p0095 A82-23515
- CRYSTAL RECTIFIERS**
Fast recovery, high voltage silicon diodes for AC motor controllers p0086 A82-36926
- CRYSTAL STRUCTURE**
Cauchy integral method for two-dimensional solidification interface shapes p0089 A82-39899
- Analysis of crack propagation as an energy absorption mechanism in metal matrix composites [NASA-CR-165051] p0052 N82-14288
- Micromechanical predictions of crack propagation and fracture energy in a single fiber boron/aluminum model composite [NASA-CR-168550] p0052 N82-18326
- Environmental effects on defect growth in composite materials [NASA-CR-165213] p0052 N82-20248
- Ultrasonic scanning system for imaging flaw growth in composites [NASA-TM-82799] p0076 N82-22386
- Creep crack-growth: A new path-independent T sub o and computational studies [NASA-CR-168930] p0113 N82-24503
- Fracture mechanics criteria for turbine engine hot section components [NASA-CR-167896] p0027 N82-25257
- Interlaminar crack growth in fiber reinforced composites during fatigue, part 3 [NASA-CR-165434] p0114 N82-26715
- Creep crack-growth: A new path-independent integral (T sub c), and computational studies [NASA-CR-167897] p0114 N82-29619
- A preliminary study of crack initiation and growth at stress concentration sites [NASA-CR-169358] p0115 N82-33738
- (CRACKING (FRACTURING))**
NT STRESS CORROSION CRACKING
Interface cracks in adhesively bonded lap-shear joints p0116 A82-46109
- CRACKS**
Analysis of cracks emanating from a circular hole in unidirectional fiber reinforced composites, part 2 [NASA-CR-165433] p0114 N82-26714
Analysis of interface cracks in adhesively bonded lap shear joints, part 4 [NASA-CR-165438] p0114 N82-26716
- CRASHES**
An assessment of the crash fire hazard of liquid hydrogen fueled aircraft [NASA-CR-165526] p0013 N82-19196
- CRATERS**
NT LUNAR CRATERS
NT METEORITE CRATERS
- CREEP ANALYSIS**
Moving singularity creep crack growth analysis with the $\Delta T/c$ and $C^*/\text{asterisk}/$ integrals --- path-independent vector and energy rate line integrals p0116 A82-40066
Creep crack-growth: A new path-independent integral (T sub c), and computational studies [NASA-CR-167897] p0114 N82-29619
- CREEP BUCKLING**
On the solution of creep induced buckling in general structure p0115 A82-39514
- CREEP PROPERTIES**
NT SHEAR CREEP
On a study of the $\Delta T/c$ and $C^*/\text{asterisk}/$ integrals for fracture analysis under non-steady creep p0115 A82-36782
Creep crack-growth: A new path-independent T sub o and computational studies [NASA-CR-168930] p0113 N82-24503
- CREEP RUPTURE STRENGTH**
Creep and rupture of an ODS alloy with high stress rupture ductility --- Oxide Dispersion Strengthened p0065 A82-40335
Structure and creep rupture properties of directionally solidified eutectic gamma/gamma-prime-alpha alloy p0062 A82-42774
The influence of orientation on the stress rupture properties of nickel-base superalloy single crystals p0062 A82-47397
The influence of cobalt on the tensile and stress-rupture properties of the nickel-base superalloy MAR-M247

Mechanism and models for zinc metal morphology in alkaline media
[NASA-TM-82768] p0120 N82-19671
Morphological and frictional behavior of sputtered MoS₂ films
[NASA-TM-82809] p0076 N82-22387
CRYSTAL SURFACES
Influence of mineral oil and additives on microhardness and surface chemistry of magnesium oxide (CO) surface
[NASA-TP-1986] p0067 N82-20316
CRYSTALLIZATION
NT DIRECTIONAL SOLIDIFICATION (CRYSTALS)
NT BICRYSTALLIZATION
CRYSTALLOGRAPHY
Crystallographic texture in oxide-dispersion-strengthened alloys
p0062 N82-40041

CRYSTALS
NT DOPED CRYSTALS
NT LIQUID CRYSTALS
NT POLYCRYSTALS
NT SINGLE CRYSTALS
CUBIC LATTICES
NT FACE CENTERED CUBIC LATTICES
CURING
High-temperature resins
p0051 N82-42657

CURRENT CONVERTERS (AC TO DC)
Simplified dc to dc converter
[NASA-CASE-LBN-13495-1] p0082 N82-24432
CURRENT DENSITY
On the cause of the flat spot phenomenon observed in silicon solar cells at low temperatures and low intensities
p0044 N82-44965
Additional extensions to the NASCAP computer code, volume 3
[NASA-CR-167857] p0040 N82-26378

CURRENT DISTRIBUTION
Impact of uniform electrode current distribution on ETF --- Engineering Test Facility MHD generator
[AIAA PAPER 82-0423] p0157 N82-17941
Impact of uniform electrode current distribution on ETF
[NASA-TM-82875] p0123 N82-25636

CURRENT REGULATORS
Input filter compensation for switching regulators
[NASA-CR-169005] p0085 N82-25442

CURRENT STABILIZERS
CURRENT REGULATORS
CURVATURE
Turbulent boundary layer heat transfer experiments: Convex curvature effects including introduction and recovery
[NASA-CR-3510] p0090 N82-17456

CURVED SURFACES
U MTOURS
U APES
CURVES (GEOMETRY)
Precision of spiral-bevel gears
[NASA-TM-82888] p0102 N82-30552

CUTTERS
Surface geometry of circular cut spiral bevel gears
[ASME PAPER 81-DET-114] p0108 N82-19334

CUTTING
NT METAL CUTTING
Surface geometry of circular cut spiral bevel gears
[ASME PAPER 81-DET-114] p0108 N82-19334

CYCLES
NT STIRLING CYCLE
NT STRESS CYCLES
NT THERMODYNAMIC CYCLES

CYLINDRICAL AFTERBODIES
U LINDRICAL BODIES
CYLINDRICAL BODIES
NT ROTATING CYLINDERS
Surface-tension induced instabilities: Effects of lateral boundaries
[NASA-CR-165530] p0092 N82-11390
Turbine endwall single cylinder program
[NASA-CR-169278] p0091 N82-31638

CYLINDRICAL FLASHES
Standing waves along a microwave generated surface wave plasma
p0158 N82-26952

CYLINDRICAL SHELLS
Vibrations of cantilevered shallow cylindrical shells of rectangular planform

CYLINDROIDS
U LINDRICAL BODIES
CZOCHEWSKI METHOD
Stoichiometry-controlled compensation in liquid encapsulated Czochralski GaAs
p0158 N82-17585
Compensation mechanism in liquid encapsulated Czochralski GaAs Importance of melt stoichiometry
p0086 N82-40403
Effect of melt stoichiometry on twin formation in LEC GaAs --- Liquid Encapsulated Czochralski technique
p0160 N82-46517

D

DARHO (DATA ANALYSIS)
U TA PROCESSING
DAMAGE
NT IMPACT DAMAGE
NT RADIATION DAMAGE
DAMPING
NT VIBRATION DAMPING
An experimental investigation of gapwise periodicity and unsteady aerodynamic response in an oscillating cascade. Volume 2: Data report. Part 1: Text and mode 1 data
[NASA-CR-165457-VOL-2-P1-1] p0006 N82-18180
Extending the frequency of response of lightly damped second order systems: Application to the drag force anemometer
[NASA-TM-82927] p0096 N82-32662

DAMPING FACTOR
U MPING
DAMPING IN PITCH
U MPING
U TCH (INCLINATION)
DAMPING IN ROLL
U MPING
DAMPING IN YAW
U MPING
U W
DAMPNESS
U ISTURE CONTENT
DANGER
U ZARDS
DART TURBOPROP ENGINES
U RBOPROP ENGINES
DATA ACQUISITION
A remote millivolt multiplexer and amplifier module for wind tunnel data acquisition
p0083 N82-41845

DATA ADAPTIVE EVALUATOR/MONITOR
U TA PROCESSING
DATA ANALYSIS
U TA PROCESSING
DATA PROCESSING
NT OPTICAL DATA PROCESSING
NT PARALLEL PROCESSING (COMPUTERS)
NT SIGNAL PROCESSING
Applications of the DOE/NASA wind turbine engineering information system
p0122 N82-23696

DATA PROCESSING EQUIPMENT
NT DIGITAL COMPUTERS
NT HYBRID COMPUTERS
NT MICROCOMPUTERS
NT MICROPROCESSORS

DATA TRANSMISSION
NT FREQUENCY DIVISION MULTIPLE ACCESS
DC (CURRENT)
U RECT CURRENT
DC 9 AIRCRAFT
Kevlar/PMR-15 reduced drag DC-9 reverser stang fairing
[NASA-CR-165448] p0052 N82-31448

DC 10 AIRCRAFT
Investigation and evaluation of a computer program to minimize three-dimensional flight time tracks
[NASA-CR-168419] p0145 N82-17879
Advanced turboprop testbed systems study
[NASA-CR-167895] p0014 N82-33375

DEADWEIGHT
U ATIC LOADS
DEBRIS
Occurrence of spherical ceramic debris in indentation and sliding contact
[NASA-TP-2048] p0069 N82-32491

ORIGINAL PAGE IS
OF POOR QUALITY

- DECAY**
 NT CHEMILUMINESCENCE
 NT ELECTRON EMISSION
 NT EXHAUST EMISSION
 NT MICROWAVE EMISSION
 NT SECONDARY EMISSION
 NT SOLAR RADIO BURSTS
 NT SOLAR RADIO EMISSION
- DECOMPOSITION**
 NT PROPELLANT DECOMPOSITION
 NT THERMAL DECOMPOSITION
 Quantitative separation of tetralin hydroperoxide from its decomposition products by high performance liquid chromatography p0048 A82-15696
- DECOMPRESSION**
 U PRESSURE REDUCTION
- DEEP SPACE**
 NT INTERPLANETARY SPACE
 On the cause of the flat-spot phenomenon observed in silicon solar cells at low temperatures and low intensities --- in deep space environments p0043 A82-39599
- DEFECTS**
 NT CRYSTAL DEFECTS
 NT CRYSTAL DISLOCATIONS
 NT SURFACE DEFECTS
 NT VACANCIES (CRYSTAL DEFECTS)
 Environmental and High-Strain Rate effects on composites for engine applications [NASA-TM-82082] p0051 A82-31449
- DEFLATING**
 U PRESSURE REDUCTION
- DEFORMATION**
 NT PLASTIC DEFORMATION
 On finite deformation elastic-plasticity p0116 A82-45869
- DEGRADATION**
 NT THERMAL DEGRADATION
 Model degradation effects on sensor failure detection p0148 A82-13143
- DEICERS**
 Numerical simulation of one-dimensional heat transfer in composite bodies with phase change --- wing deicing pads [NASA-CR-165607] p0002 A82-22142
- DEICING**
 Aircraft icing research at NASA [NASA-TM-82919] p0013 A82-30297
- DEICING SYSTEMS**
 U ICEFS
- DELAMINATING**
 Interlaminar crack growth in fiber reinforced composites during fatigue, part 3 [NASA-CR-165434] p0114 A82-26715
 Edge delamination in angle-ply composite laminates, part 5 [NASA-CR-165439] p0114 A82-26717
- DELAY LINES**
 Near optimum delay-line detection filters for serial detection of MSK signals p0086 A82-43867
- DENSIMETERS**
 NT ULTRASONIC DENSIMETERS
- DENSITY (MASS/VOLUME)**
 NT GAS DENSITY
 Ultrasonic velocity for estimating density of structural ceramics [NASA-TM-82765] p0066 A82-14359
 The transmission or scattering of elastic waves by an inhomogeneity of simple geometry: A comparison of theories [NASA-CR-169034] p0079 A82-26526
- DENSITY (NUMBER/VOLUME)**
 NT ELECTRON DISTRIBUTION
 NT ION DENSITY (CONCENTRATION)
 NT MAGNETOSPHERIC ION DENSITY
- DENSITY MEASUREMENT**
 Time resolved density measurements in premixed turbulent flames [AIAA PAPER 82-0036] p0056 A82-22033
- DEOXIDIZING**
 Stabilizing platinum in phosphoric acid fuel cells [NASA-CR-165483] p0130 A82-14628
- DEPENDENCE**
 NT TEMPERATURE DEPENDENCE
- DEPOSITION**
 NT ELECTRODEPOSITION
- NT VACUUM DEPOSITION
 NT VAPOR DEPOSITION
 Deposit formation in liquid fuels. II - The effect of selected compounds on the storage stability of Jet A turbine fuel p0074 A82-22240
 Ion beam sputter deposited diamond like films [NASA-TM-82673] p0069 A82-28445
 Deposition of reactively ion beam sputtered silicon nitride coatings [NASA-TM-82942] p0069 A82-30401
 Ion beam microtexturing and enhanced surface diffusion [NASA-CR-167948] p0065 A82-31509
- DEPOSITS**
 Analysis of infrared emission from thin adsorbates p0056 A82-21431
 Deposit formation in liquid fuels. III - The effect of selected nitrogen compounds on diesel fuel p0074 A82-23238
 Deposit formation in hydrocarbon fuels [ASME PAPER 82-GT-49] p0075 A82-35307
 Deposit formation in hydrocarbon rocket fuels with an evaluation of a propane heat transfer correlation [NASA-TM-82911] p0088 A82-26611
- DEPRESSURIZATION**
 U PRESSURE REDUCTION
- DEPTH MEASUREMENT**
 Ground-truth observations of ice-covered North Slope Lakes imaged by radar [NASA-TM-84127] p0117 A82-18664
- DESIGN**
 Summary and evaluation of the conceptual design study of a potential early commercial MHD power plant (CSPEC) [NASA-TM-82734] p0119 A82-16481
- DESIGN ANALYSIS**
 End region and current consolidation effects upon the performance of an MHD channel for the ETP conceptual design --- Engineering Test Facility [AIAA PAPER 82-0325] p0157 A82-17889
 An experiment to evaluate liquid hydrogen storage in space A82-20748
 MHD channel performance for potential early commercial MHD power plants p0158 A82-20750
 Baseband-processed SS-TDMA communication system architecture and design concepts [AIAA 82-0482] p0079 A82-23508
 A comprehensive method for preliminary design optimization of axial gas turbine stages [AIAA PAPER 82-1264] p0030 A82-35091
 A computational design method for transonic turbomachinery cascades [ASME PAPER 82-GT-117] p0022 A82-35348
 Analysis and design of a standardized control module for switching regulators p0083 A82-46388
 Conceptual design of superconducting magnet system for Magnetohydrodynamic (MHD) Engineering Test Facility (ETF) 200 MWe power plant [NASA-CR-165053] p0105 A82-14520
 Study of controlled diffusion stator blading. I. Aerodynamic and mechanical design report [NASA-CR-165500] p0024 A82-16081
 Summary and evaluation of the conceptual design study of a potential early commercial MHD power plant (CSPEC) [NASA-TM-82734] p0119 A82-16481
 Modeling and Analysis of Power Processing Systems (MAPPS). Volume 2: Appendices [NASA-CR-165539] p0145 A82-16748
 Design, evaluation, and fabrication of low-cost composite blades for intermediate-size wind turbines [NASA-CR-165342] p0133 A82-18693
 Cooled variable-area radial turbine technology program [NASA-CR-165408] p0024 A82-19221
 Advanced Low-Emissions Catalytic-Combustor Program, phase 1 --- aircraft gas turbine engines [NASA-CR-159656] p0025 A82-22265
 Preliminary design development of 100 KW rotary power transfer device [NASA-CR-165431] p0084 A82-23395

- Comparative analysis of the conceptual design studies of potential early commercial MHD power plants (CSPEC)
[NASA-TM-82897] p0123 N82-27838
- Pyrolytic graphite collector development program
[NASA-CR-167909] p0052 N82-29363
- Vibration analysis of three guyed tower designs for intermediate size wind turbines
[NASA-CR-165589] p0137 N82-30709
- Design flexibility of Redox flow systems --- for energy storage applications
[NASA-TM-82854] p0054 N82-31459
- DETECTION**
NT SIGNAL DETECTION
NT ULTRASONIC FLAW DETECTION
Sensor failure detection system --- for the F100 turbofan engine
[NASA-CR-165515] p0023 N82-13145
NASA research programs responding to workshop recommendations
N82-21146
- DETONATION WAVES**
Effects of internal heat transfer on the structure of self-similar blast waves
p0093 N82-32225
- DEUTERIUM FLUORIDE LASERS**
U LASERS
- DEVELOPING NATIONS**
International market assessment of stand-alone photovoltaic power systems for cottage industry applications
[NASA-CR-165287] p0132 N82-16494
Application of photovoltaic electric power to the rural education/communication needs of developing countries
[NASA-CR-167894] p0137 N82-29720
Design description of the Tangaye Village photovoltaic power system
[NASA-TM-82917] p0126 N82-33828
- DF LASERS**
Optically pumped high-pressure DF-CO2 transfer laser
A82-10193
- DIAGRAMS**
NT PHASE DIAGRAMS
NT S-N DIAGRAMS
NT STRESS-STRAIN DIAGRAMS
- DIAMONDS**
Adhesion and friction of single-crystal diamond in contact with transition metals
p0103 N82-18680
- DIELECTRIC MATERIALS**
U DIELECTRICS
- DIELECTRIC PROPERTIES**
Spacecraft Charging Technology, 1980
[NASA-CR-2182] p0037 N82-14213
Oblique-incidence secondary emission from charged dielectrics
p0039 N82-14227
- DIELECTRICS**
NT LOSSLESS MATERIALS
Numerical simulation of sheath structure and current-voltage characteristics of a conductor-dielectric disk in a plasma
p0040 N82-15904
Testing of a spacecraft model in a combined environment simulator
p0033 N82-18310
Internal breakdown of charged spacecraft dielectrics
p0041 N82-18312
Testing of a spacecraft model in a combined environment simulator
[NASA-TM-82723] p0037 N82-11106
Numerical simulation of plasma insulator interactions in space. Part 1: The self consistent calculation
p0039 N82-14272
Numerical simulation of plasma insulator interactions in space. Part 2: Dielectric effects
p0039 N82-14273
Development of an 1100 deg F capacitor
p0083 N82-15315
Secondary electron emission from a charged dielectric in the presence of normal and oblique electric fields
[NASA-CR-168558] p0084 N82-18507
Mapping of electrical potential distributions with charged particle beams
[NASA-CR-168556] p0084 N82-18508
- Component technology for space power systems
[NASA-TM-82928] p0082 N82-30474
- DIESEL ENGINES**
Lightweight diesel engine designs for commuter type aircraft
[NASA-CR-165470] p0023 N82-11068
Fuel economy and exhaust emissions characteristics of diesel vehicles: Test results of a prototype fiat 131TC 2.4 liter automobile
[NASA-CR-165535] p0164 N82-18068
Advanced general aviation comparative engine/airframe integration study
[NASA-CR-165564] p0025 N82-22263
Electrostatic fuel conditioning of internal combustion engines
[NASA-CR-169029] p0106 N82-26680
- DIESEL FUELS**
NT LIQUID FUELS
Deposit formation in liquid fuels. III - The effect of selected nitrogen compounds on diesel fuel
p0074 N82-23238
Fuel economy and exhaust emissions characteristics of diesel vehicles: Test results of a prototype fiat 131TC 2.4 liter automobile
[NASA-CR-165535] p0164 N82-18068
- DIFFERENCE EQUATIONS**
Multiple-grid acceleration of Lax-Wendroff algorithms
[NASA-TM-82843] p0149 N82-22922
- DIFFERENTIAL ALGEBRA**
U TRICES (MATHEMATICS)
- DIFFERENTIAL EQUATIONS**
NT HELMHOLTZ VORTICITY EQUATION
Construction of solutions for some nonlinear two-point boundary value problems
[NASA-TM-82937] p0144 N82-30949
- DIFFERENTIAL GEOMETRY**
NT TENSOR ANALYSIS
Surface geometry of circular cut spiral bevel gears
[ASME PAPER 81-DET-114] p0108 N82-19334
- DIFFERENTIAL OPERATORS**
U DIFFERENTIAL EQUATIONS
- DIFFACTION**
NT WAVE DIFFACTION
DIFFACTION PATTERNS
Diffraction by a finite strip
p0150 N82-33605
- DIFFUSE RADIATION**
Effects of internal heat transfer on the structure of self-similar blast waves
p0093 N82-32225
- DIFFUSION**
NT PARTICLE DIFFUSION
NT SURFACE DIFFUSION
Study of controlled diffusion stator blading. I. Aerodynamic and mechanical design report
[NASA-CR-165500] p0024 N82-16081
Determination of optimum sunlight concentration level in space for 3-4 cascade solar cells
[NASA-TM-82899] p0126 N82-32853
- DIFFUSION BONDING**
U DIFFUSION WELDING
- DIFFUSION EFFECT**
U DIFFUSION
- DIFFUSION FLAMES**
On the opening of premixed Bunsen flame tips
p0057 N82-37570
- DIFFUSION WELDING**
Metal honeycomb to porous wireform substrate diffusion bond evaluation
[NASA-TM-82793] p0110 N82-18612
- DIFLUORO COMPOUNDS**
NT POLYTETRAFLUOROETHYLENE
- DIGITAL COMPUTERS**
NT MICROCOMPUTERS
Development report: Automatic System Test and Calibration (ASTAC) equipment
[NASA-CR-165403] p0129 N82-13505
Role of optical computers in aeronautical control applications
p0156 N82-15897
- DIGITAL SIMULATION**
Numerical simulation of sheath structure and current-voltage characteristics of a conductor-dielectric disk in a plasma
p0040 N82-15904
Multigrid simulation of asymptotic curved-duct flows using a semi-implicit numerical technique

ORIGINAL PAGE IS OF POOR QUALITY

SUBJECT INDEX

DOMESTIC SATELLITE COMMUNICATIONS SYSTEMS

- Advancements in real-time engine simulation technology --- of digital electronic aircraft engine controls [AIAA PAPER 82-1075] p0010 A82-29003
- A real time Pegasus propulsion system model for VSTOL piloted simulation evaluation [NASA-TN-82770] p0021 A82-34995
- Application of integration algorithms in a parallel processing environment for the simulation of jet engines [NASA-TN-82746] p0016 A82-13144
- Advancements in real-time engine simulation technology [NASA-TN-82825] p0149 A82-14849
- DIGITAL SYSTEMS**
- A digital optical torque meter for high rotational speed applications [NASA-TN-82914] p0147 A82-22915
- DIGITAL TECHNIQUES**
- Digital imaging techniques in experimental stress analysis p0097 A82-34231
- A multi-purpose method for analysis of spur gear tooth loading [NASA-CR-165183] p0104 A82-10401
- Preliminary study, analysis and design for a power switch for digital engine actuators [NASA-CR-159559] p0085 A82-23394
- DILUTION**
- Dilution jet behavior in the turn section of a reverse flow combustor [AIAA PAPER 82-0192] p0021 A82-20291
- Dilution jet behavior in the turn section of a reverse flow combustor [NASA-TN-82778] p0017 A82-19220
- DIMENSIONLESS NUMBERS**
- NT MACH NUMBER
- NT REYNOLDS NUMBER
- DIMENSIONS**
- NT FILM THICKNESS
- DIODES**
- NT AVALANCHE DIODES
- NT CRYSTAL RECTIFIERS
- NT SEMICONDUCTOR DIODES
- DIOXIDES**
- NT HYDROGEN PEROXIDE
- NT QUARTZ
- NT SILICON DIOXIDE
- DIRECT CURRENT**
- Straight and chopped DC performance data for a reluctance HV-250AT motor with a General Electric EV-1 controller [NASA-CR-165447] p0132 A82-17608
- Analysis of transistor and snubber turn-off dynamics in high-frequency high-voltage high-power converters [NASA-CR-168769] p0084 A82-22438
- Straight and chopped DC performance data for a General Electric 5BY436A1 DC shunt motor with a General Electric EV-1 controller [NASA-CR-165507] p0085 A82-24425
- Simplified dc to dc converter [NASA-CASE-LFW-13495-1] p0082 A82-24432
- Progress on advanced dc and ac induction drives for electric vehicles [NASA-TN-82095] p0163 A82-31160
- Summary of electric vehicle dc motor-controller tests [NASA-TN-82863] p0082 A82-33636
- DIRECT POWER GENERATORS**
- NT ALKALINE BATTERIES
- NT FUEL CELLS
- NT HYDROGEN OXYGEN FUEL CELLS
- NT MAGNETOHYDRODYNAMIC GENERATORS
- NT NICKEL ZINC BATTERIES
- NT PHOSPHORIC ACID FUEL CELLS
- NT REGENERATIVE FUEL CELLS
- NT SOLAR CELLS
- NT THERMIONIC CONVERTERS
- Develop and test fuel cell powered on-site integrated total energy system, Phase 3: Full-scale power plant development [NASA-CR-165328] p0117 A82-13490
- DIRECTIONAL ANTENNAS**
- NT TWO REFLECTOR ANTENNAS
- DIRECTIONAL CONTROL**
- NT THRUST VECTOR CONTROL
- DIRECTIONAL SOLIDIFICATION (CRYSTALS)**
- Structure and creep rupture properties of directionally solidified eutectic gamma/gamma-prime-alpha alloy p0062 A82-42774
- DIRECTIONAL STABILITY**
- NT GYROSCOPIC STABILITY
- DIRECTIONAL PROBLEMS**
- The use of a structural method to calculate the electrostatic field of a magnetron A82-18370
- DISCHARGE COEFFICIENT**
- Flow distributions and discharge coefficient effects for jet array impingement with initial crossflow [ASME PAPER 82-GT-156] p0011 A82-35379
- Electric thruster research [NASA-CR-165603] p0045 A82-24285
- DISHES**
- U RABOLIC REFLECTORS
- DISKS (SHAPES)**
- NT ROTATING DISKS
- Development of materials and process technology for dual alloy disks [NASA-CR-165224] p0063 A82-10370
- Hot isostatically pressed manufacture of high strength HEBL 76 disk and seal shapes [NASA-CR-165549] p0064 A82-26439
- DISLOCATIONS (MATERIALS)**
- NT CRYSTAL DISLOCATIONS
- DISPERSION PRECIPITATION HARDENING**
- U RCIPITATION HARDENING
- DISPERSIONS**
- NT AEROSOLS
- DISPLACEMENT**
- Large displacements and stability analysis of nonlinear propeller structures [NASA-TN-82850] p0112 A82-31707
- DISPLACEMENT MEASUREMENT**
- Experimental boundary integral equation applications in speckle interferometry p0097 A82-36987
- Crack displacements for J/I/ testing with compact specimens p0112 A82-40358
- DISPLAY DEVICES**
- NT DIAG FORCE ANEMOMETERS
- NT FLOW DIRECTION INDICATORS
- NT HOT-FILM ANEMOMETERS
- NT HOT-WIRE ANEMOMETERS
- DISPOSAL**
- NT WASTE DISPOSAL
- DISSIPATION**
- NT ENERGY DISSIPATION
- DISSOLVED GASES**
- Investigation of spray characteristics for flashing injection of fuels containing dissolved air and superheated fuels [NASA-CR-3563] p0027 A82-26295
- DISTORTION**
- NT FLOW DISTORTION
- NT SIGNAL DISTORTION
- Computer modeling of fan-exit-splitter spacing effects on F100 response to distortion [NASA-CR-167879] p0025 A82-23246
- DISTRIBUTION (PROPERTY)**
- NT ANTENNA RADIATION PATTERNS
- NT CHARGE DISTRIBUTION
- NT CURRENT DISTRIBUTION
- NT DIFFRACTION PATTERNS
- NT ELECTRON DISTRIBUTION
- NT FLOW DISTRIBUTION
- NT ION DISTRIBUTION
- NT LOAD DISTRIBUTION (FORCES)
- NT SPATIAL DISTRIBUTION
- NT STRESS CONCENTRATION
- NT TEMPERATURE DISTRIBUTION
- NT VELOCITY DISTRIBUTION
- DISTRIBUTION MOMENTS**
- NT MEAN
- DISTURBANCE THEORY**
- U TURBATION THEORY
- DIVERGENCE**
- NT MAGNETIC CHARGE DENSITY
- DOCUMENTS**
- NT BIBLIOGRAPHIES
- NT USER MANUALS (COMPUTER PROGRAMS)
- DOMESTIC SATELLITE COMMUNICATIONS SYSTEMS**
- Baseband-processed S₁-TDMA communication system

DOPED CRYSTALS

SUBJECT INDEX

architecture and design concepts
[AIAA 82-0482] p0079 A82-23508

DOPED CRYSTALS
CN-VPE growth of Mg-doped GaAs ---
Organometallic Vapor Phase Epitaxy p0159 A82-38411

DOPING (ADDITIVES)
U DITIVES

DOUGLAS AIRCRAFT
MT DC 9 AIRCRAFT
MT EC 10 AIRCRAFT
DOUGLAS DC-9 AIRCRAFT
U 9 AIRCRAFT

DRAG
Stress evaluations under rolling/sliding contacts
[NASA-CR-165561] p0113 N82-17521
Kevlar/PMR-15 reduced drag DC-9 reverser stang
fairing p0052 N82-31448
[NASA-CR-165448]

DRAG EFFECT
U AG

DRAG FORCE ANEMOMETERS
Miniature drag-force anemometer p0097 A82-40132
Extending the frequency of response of lightly
damped second order systems: Application to the
drag force anemometer
[NASA-TM-82927] p0096 N82-32662

DRAG REDUCTION
Kevlar/PMR-15 polyimide matrix composite for a
complex shaped DC-9 drag reduction fairing
[AIAA PAPER 82-1047] p0002 A82-37678

DRIFT (INSTRUMENTATION)
Thin film temperature sensors, phase 3 --- for
engine-test evaluation
[NASA-CR-165476] p0097 N82-22479

DRONE HELICOPTERS
U HELICOPTERS

DROP SIZE
Water ingestion into jet engine axial compressors
[AIAA PAPER 82-0196] p0030 A82-17836
Formation of oxides of nitrogen in monodisperse
spray combustion of hydrocarbon fuels
p0057 A82-37571
Hydrodynamic and aerodynamic breakup of liquid
sheets
[NASA-TM-82800] p0087 N82-19494
Venturi nozzle effects on fuel drop size and
nitrogen oxide emissions
[NASA-TP-2028] p0020 N82-31329

DRY CELLS
NT NICKEL ZINC BATTERIES

DRY FRICTION
Single pass rub phenomena - Analysis and experiment
[ASME PAPER 81-LUB-55] p0107 A82-18449
Morphological and frictional behavior of sputtered
MoS2 films
[NASA-TM-82809] p0076 N82-22387
The dryout region in frictionally heated sliding
contacts
[NASA-TM-82796] p0088 N82-28574

DUCT GEOMETRY
Effect of vacuum exhaust pressure on the
performance of MHD ducts at high B-field
[NASA-TM-82750] p0157 N82-13908
Mode propagation in nonuniform circular ducts with
potential flow
[NASA-TM-82766] p0151 N82-14881
Application of steady state finite element and
transient finite difference theory to sound
propagation in a variable area duct: A
comparison with experiment
[NASA-TM-82678] p0151 N82-15847
Energy efficient engine: Turbine transition duct
model technology report
[NASA-CR-167996] p0029 N82-33394

DUCTED BODIES
Acoustic properties of turbofan inlets
[NASA-CR-169016] p0153 N82-27090

DUCTED FLOW
Acoustic transmission in lined flow ducts - A
finite element eigenvalue problem
p0154 A82-17663
Multigrid simulation of asymptotic curved-duct
flows using a semi-implicit numerical technique
p0010 A82-29003
Investigation of rotational transonic flows
through ducts using a finite element scheme
[AIAA PAPER 82-1267] p0012 A82-37711

'Coriolis resonance' within a rotating duct ---
flow induced vibrations in centrifugal compressors
p0012 A82-37938

Computational methods for internal flows with
emphasis on turbomachinery p0003 N82-13113
[NASA-TM-82764]
Mode propagation in nonuniform circular ducts with
potential flow p0151 N82-14881
[NASA-TM-82766]
Velocity gradient method for calculating velocities
in an axisymmetric annular duct p0005 N82-29270
[NASA-TP-2029]

DUCTILITY
Creep and rupture of an ODS alloy with high stress
rupture ductility --- Oxide Dispersion
Strengthened p0065 A82-40335
[NASA-TM-82758]
Failure analysis of a tool steel torque shaft
p0058 N82-11184
Composite seal for turbomachinery
[NASA-CASE-LEW-12131-3] p0099 N82-19540
A study of the nature of solid particle impact and
shape on the erosion morphology of ductile metals
[NASA-TM-82933] p0061 N82-33493

DUCTS
NT ACOUSTIC DUCTS
NT AIR DUCTS
NT ANNULAR DUCTS

Verification of an acoustic transmission matrix
analysis of sound propagation in a variable area
duct without flow p0151 N82-12891
[NASA-TM-82741]
End region and current consolidation effects upon
the performance of an MHD channel for the ETF
conceptual design
[NASA-TM-82744] p0157 N82-12943
Mode propagation in nonuniform circular ducts with
potential flow p0151 N82-14881
[NASA-TM-82766]
Results and comparison of Hall and DW duct
experiments
[NASA-TM-82864] p0157 N82-25961

SUBJECT WIND SHEAR MECHANISM
WIND SHEAR

DURABILITY
Durability/life of fiber composites in
hygrothermomechanical environments
[NASA-TM-82749] p0049 N82-14287
JT9D ceramic outer air seal system refinement
program
[NASA-CR-165554] p0105 N82-18603
Techniques for enhancing durability and
equivalence ratio control in a rich-lean,
three-stage ground power gas turbine combustor
[NASA-TM-82922] p0124 N82-29717
Effect of fuel to air ratio on Mach 0.3 burner rig
hot corrosion of ZrO2-Y2O3 thermal barrier
coatings
[NASA-TM-82879] p0061 N82-30373

DYNAMIC CHARACTERISTICS
NT AERODYNAMIC STABILITY
NT BOUNDARY LAYER STABILITY
NT COMBUSTION STABILITY
NT DRAG
NT FLAME STABILITY
NT FLOW CHARACTERISTICS
NT FLOW DISTRIBUTION
NT FLOW STABILITY
NT FLOW VELOCITY
NT GYROSCOPIC STABILITY
NT ROTARY STABILITY
NT TRANSIENT RESPONSES

Spherical roller bearing analysis. SKF computer
program SPHERBEAN. Volume 3: Program
correlation with full scale hardware tests
[NASA-CR-165205] p0106 N82-20542
Analysis of transistor and snubber turn-off
dynamics in high-frequency high-voltage
high-power converters
[NASA-CR-168760] p0084 N82-22438

DYNAMIC CONTROL
The effects of controls and controllable and
storage loads on the performance of stand-alone
photovoltaic systems p0127 A82-45027

DYNAMIC LOADS
NT AERODYNAMIC LOADS
NT ROLLING CONTACT LOADS
NT SHOCK LOADS

- NT THRUST LOADS
A multi-purpose method for analysis of spur gear
tooth loading
[NASA-CR-165163] p0104 N82-10401
- DYNAMIC PROPERTIES
U NAMIC CHARACTERISTICS
- DYNAMIC RESPONSE
NT TRANSIENT RESPONSE
CFG jet engine performance improvement: High
pressure turbine roundness
[NASA-CR-165555] p0024 N82-17174
- DYNAMIC STABILITY
NT AEROELASTIC STABILITY
NT BOUNDARY LAYER STABILITY
NT COMBUSTION STABILITY
NT FLAME STABILITY
NT FLOW STABILITY
NT GYROSCOPIC STABILITY
NT ROTARY STABILITY
- DYNAMIC STRUCTURAL ANALYSIS
A pad perturbation method for the dynamic
coefficients of tilting-pad journal bearings
p0110 N82-14400
- Blade loss transient dynamic analysis of
turbomachinery
[AIAA PAPER 82-1057] p0030 N82-34982
- Structural dynamics of shroudless, hollow, fan
blades with composite in-lays
[ASME PAPER 82-GT-284] p0022 N82-35456
- Aerodynamic damping measurements in a transonic
compressor
[ASME PAPER 82-GT-287] p0012 N82-35459
- Engine dynamic analysis with general nonlinear
finite element codes II - Bearing element
implementation, overall numerical
characteristics and benchmarking
[ASME PAPER 82-GT-292] p0108 N82-35462
- Sensitivity analysis results of the effects of
various parameters on composite design
p0051 N82-37101
- Forced torsional properties of FRP composites with
varying matrix concentrations and
processing histories
p0051 N82-45630
- Structural dynamics of shroudless, hollow fan
blades with composite in-lays
[NASA-TM-82816] p0018 N82-22266
- Wind turbine dynamics
[NASA-CF-2185] p0122 N82-23684
- DYNAMIC TESTS
Advanced superposition methods for high speed
turbopump vibration analysis
[NASA-CF-165379] p0104 N82-11465
- E**
- E GLASS
Tribological characteristics of a composite
total-surface hip replacement
[NASA-TP-1053] p0066 N82-16239
- EAR
A hydrodynamic model of an outer hair cell
[NASA-TM-82773] p0143 N82-16743
- EARTH ATMOSPHERE
NT MESOSPHERE
NT STRATOSPHERE
NT TROPOPAUSE
- EARTH ORBITS
Charging of a large object in low polar Earth orbit
--- space shuttle orbiter
p0039 N82-14275
- Nickel-hydrogen bipolar battery systems
[NASA-TM-82946] p0125 N82-30716
- EARTH RESOURCES
NT COAL
NT FOSSIL FUELS
- EARTH SATELLITES
NT ATS 5
NT COMMUNICATION SATELLITES
NT SCATHA SATELLITE
NT SOLAR POWER SATELLITES
NT SYNCHRONOUS SATELLITES
- ECP
U TERNALLY BLOWN FLAPS
- EBULLITION
U ILLING
- ECLIPSING BINARY STARS
Ultraviolet observations of the 1980 eclipse of
the symbiotic star CI Cygni
- ECONOMIC ANALYSIS
Socioeconomic impact of photovoltaic power at
Schuchull, Arizona
[NASA-CR-165551] p0133 N82-19669
- Performance and operational economics estimates
for a coal gasification combined-cycle
cogeneration powerplant
[NASA-TM-82729] p0120 N82-19672
- Satellite-aided land mobile communications system
implementation considerations
[NASA-TM-82861] p0036 N82-25290
- ECONOMIC DEVELOPMENT
Barriers to the utilization of synthetic fuels for
transportation
[NASA-CR-165517] p0073 N82-13243
- Design description of the Tangaya Village
photovoltaic power system
[NASA-TM-82917] p0126 N82-33828
- ECONOMIC FACTORS
Local and national impact of aerospace research
and technology
[NASA-TM-82775] p0162 N82-20006
- ECONOMIC IMPACT
Socioeconomic impact of photovoltaic power at
Schuchull, Arizona
[NASA-CR-165551] p0133 N82-19669
- Kevlar/PMR-15 reduced drag DC-9 reverser stang
fairing
[NASA-CR-165448] p0052 N82-31448
- EDDIES
U RTICES
- EDGE LOADING
Boundary-layer effects in composite laminates. I -
Free-edge stress singularities. II - Free-edge
stress solutions and basic characteristics
p0116 N82-46806
- EDGES
NT LEADING EDGES
Edge delamination in angle-ply composite
laminates, part 5
[NASA-CR-165439] p0114 N82-26717
- Boundary-layer effects in composite laminates:
Free-edge stress singularities, part 6
[NASA-CR-165440] p0114 N82-26718
- EFFECTIVENESS
NT COST EFFECTIVENESS
- EFFECTORS
U NTROL EQUIPMENT
- EFFICIENCY
NT COMBUSTION EFFICIENCY
NT COMPRESSOR EFFICIENCY
NT ENERGY CONVERSION EFFICIENCY
NT POWER EFFICIENCY
NT PROPELLER EFFICIENCY
NT PROPULSIVE EFFICIENCY
NT THERMODYNAMIC EFFICIENCY
NT TRANSMISSION EFFICIENCY
- EIGENFUNCTIONS
U GENVECTORS
- EIGENSTATES
U GENVECTORS
- EIGENVALUES
Eigenvalues of the Rayleigh-Benard and Marangoni
problems
p0092 N82-13396
- Acoustic transmission in lined flow ducts - A
finite element eigenvalue problem
p0154 N82-17663
- EIGENVECTORS
Boundary layer thermal stresses in angle-ply
composite laminates, part 1 --- graphite-epoxy
composites
[NASA-CR-165412] p0113 N82-26713
- EJECTION
NT STELLAR MASS EJECTION
- ELASTIC CONSTANTS
U ASTIC PROPERTIES
- ELASTIC MEDIA
On a study of the $\Delta T/c$ and $C^*/\text{asterisk}$ /
integrals for fracture analysis under non-steady
creep
p0115 N82-36782
- ELASTIC MODULUS
U DULUS OF ELASTICITY
- ELASTIC PLATES
Ultrasonic input-output for transmitting and
receiving longitudinal transducers coupled to
same face of isotropic elastic plate

[NASA-CF-3506] p0110 N82-18613

ELASTIC PROPERTIES

NT AFFOELASTICITY

NT ELASTOPLASTICITY

NT MODULUS OF ELASTICITY

NT THERMOVISCOELASTICITY

NT VISCOELASTICITY

Path-independent integrals in finite elasticity and inelasticity, with body forces, inertia, and arbitrary crack-face conditions p0115 A82-32303

Elastic-plastic finite-element analyses of thermally cycled double-edge wedge specimens [NASA-TP-1973] p0111 N82-20566

ELASTIC STABILITY

U BENDING

ELASTIC WAVES

NT AEROBONAVIC NOISE

NT AIRCRAFT NOISE

NT DETONATION WAVES

NT ENGINE NOISE

NT JET AIRCRAFT NOISE

NT NOISE (SCAND)

NT NORMAL SHOCK WAVES

NT PLASMA WAVES

NT SHOCK WAVES

NT SOUND WAVES

NT TOLLMIEN-SCHLICHTING WAVES

NT ULTRASONIC RADIATION

NT UNLOADING WAVES

Ultrasonic input-output for transmitting and receiving longitudinal transducers coupled to same face of isotropic elastic plate [NASA-CR-3506] p0110 N82-18613

ELASTICITY

U ELASTIC PROPERTIES

ELASTICIZERS

U ELASTICIZERS

ELASTODYNAMICS

NT ELASTOHYDRODYNAMICS

Motion of a rigid punch at the boundary of an orthotropic viscoelastic half-plane A82-26436

ELASTOHYDRODYNAMICS

Alignment of fluid molecules in an EHD contact [ASLE PREPRINT 81-LC-FC-1] p0107 A82-18407

Regimes of traction in concentrated contact lubrication [ASME PAPER 81-LUB-16] p0107 A82-18431

Effects of artificially produced defects on film thickness distribution in sliding EHD point contacts [NASA-TM-82732] p0099 N82-16412

Basic lubrication equations [NASA-TM-81693] p0099 N82-16413

Frictional heating due to asperity interaction of elastohydrodynamic line-contact surfaces [NASA-TR-1882] p0100 N82-25514

Film shape calculations on supercomputers [NASA-TM-82856] p0100 N82-25519

The influence of surface dents and grooves on traction in sliding EHD point contacts [NASA-TM-82943] p0102 N82-32734

ELASTOMERS

Measurement of oil film thickness for application to elastomeric Stirling engine rod seals [ASME PAPER 81-LUB-9] p0107 A82-18426

ELASTOPLASTICITY

On finite deformation elasto-plasticity p0116 A82-45869

Elastic-plastic finite-element analyses of thermally cycled single-edge wedge specimens [NASA-TP-1982] p0111 N82-20565

ELECTRIC ARCS

Effects of arc current on the life in burner rig thermal cycling of plasma sprayed ZrO₂sub2-y sub20 sub3 [NASA-TM-82795] p0087 N82-17453

ELECTRIC AUTOMOBILES

Progress on advanced dc and ac induction drives for electric vehicles [NASA-TM-82895] p0163 N82-21160

ELECTRIC BATTERIES

NT ALKALINE BATTERIES

NT LEAD ACID BATTERIES

NT NICKEL CADMIUM BATTERIES

NT NICKEL HYDROGEN BATTERIES

NT NICKEL ZINC BATTERIES

NT REDOX CELLS

NT SILVER ZINC BATTERIES

NT STORAGE BATTERIES

Performance of advanced chromium electrodes for the NASA Redox Energy Storage System [NASA-TM-82724] p0118 N82-12574

ELECTRIC BRIDGES

Modeling the full-bridge series-resonant power converter p0086 A82-46385

ELECTRIC CHARGE

NT ELECTRIC DIPOLES

NT ELECTROSTATIC CHARGE

ELECTRIC CHOPPERS

Straight and chopped DC performance data for a reliance EV-250AT motor with a General Electric EV-1 controller [NASA-CR-165447] p0132 N82-17608

Chopper-controlled discharge life cycling studies on lead-acid batteries [NASA-CR-165616] p0134 N82-20661

Straight and chopped DC performance data for a General Electric 5B1436A1 DC shunt motor with a General Electric EV-1 controller [NASA-CR-165507] p0085 N82-24425

Results of chopper-controlled discharge life cycling studies on lead acid batteries [NASA-TM-82912] p0124 N82-30700

ELECTRIC CIRCUITS

U CIRCUITS

ELECTRIC CONDUCTORS

Numerical simulation of sheath structure and current-voltage characteristics of a conductor-dielectric disk in a plasma p0040 A82-15904

SCATHA SSPM charging response: NASCAP predictions compared with data p0037 N82-14251

ELECTRIC CURRENT

NT ALTERNATING CURRENT

NT ARC DISCHARGES

NT DIRECT CURRENT

NT ELECTRIC ARCS

NT ELECTRIC DISCHARGES

NT LIGHTNING

NT PLASMA CURRENTS

NT RADIO FREQUENCY DISCHARGE

Multijunction high voltage concentrator solar cells p0043 A82-11796

Effect of positive pulse charge waveforms on the energy efficiency of lead-acid traction cells [NASA-TM-82709] p0118 N82-10503

ELECTRIC DIPOLES

Cessation of W/001/ - Work function lowering by multiple dipole formation A82-30002

ELECTRIC DISCHARGES

NT ARC DISCHARGES

NT ELECTRIC ARCS

NT LIGHTNING

NT RADIO FREQUENCY DISCHARGE

Modification of spacecraft potentials by thermal electron emission on ATS-5 p0040 A82-16194

Internal breakdown of charged spacecraft dielectrics p0041 A82-18312

Voltage gradients in solar array cavities as possible breakdown sites in spacecraft-charging-induced discharges p0038 A82-18317

Voltage gradients in solar array cavities as possible breakdown sites in spacecraft-charging-induced discharges [NASA-TM-82710] p0037 N82-11107

Analytical modeling of satellites in geosynchronous environment p0037 N82-14258

ELECTRIC ENERGY STORAGE

NASA Redox system development project status [NASA-TM-82665] p0123 N82-25637

Chemical and electrochemical behavior of the Cr(3)/Cr(2) half cell in the NASA Redox Energy Storage System [NASA-TM-82913] p0055 N82-33463

ELECTRIC FIELDS

The use of a structural method to calculate the electrostatic field of a magnetron A82-18370

Experimental simulation of biased solar arrays with the space plasma

- [NASA-CF-165485] p0157 N82-10880
Pockels-effect cell for gas-flow simulation
- [NASA-TP-2007] p0095 N82-23515
Electrostatic fuel conditioning of internal combustion engines
- [NASA-CR-169029] p0106 N82-26680
Electric and magnetic fields
- [NASA-CF-165604] p0045 N82-28350
- ELECTRIC FILTERS**
Input filter compensation for switching regulators
[NASA-CR-169005] p0085 N82-25444
- ELECTRIC GENERATORS**
NT AC GENERATORS
NT ALKALINE BATTERIES
NT DIRECT POWER GENERATORS
NT FUEL CELLS
NT HYDROGEN OXYGEN FUEL CELLS
NT MAGNETOHYDRODYNAMIC GENERATORS
NT NICKEL ZINC BATTERIES
NT FUSIONIC ACID FUEL CELLS
NT REGENERATIVE FUEL CELLS
NT SOLAR CELLS
NT SOLAR GENERATORS
NT THERMIONIC CONVERTERS
NT TURBOGENERATORS
Interfacing wind energy conversion equipment with utility systems A82-21148
- The NASA Lewis large wind turbine program
[NASA-TM-82761] p0119 N82-16495
Application of photovoltaic electric power to the rural education/communication needs of developing countries
[NASA-CR-167894] p0137 N82-29720
Environmental assessment of the 40 kilowatt fuel cell system field test operation
[DOE/NASA/2701-1] p0137 N82-29721
Experience and assessment of the DOE-NASA Mod-1 2000-Kilowatt wind turbine generator at Boone, North Carolina
[NASA-TM-82721] p0125 N82-30710
On the cause of the flat-spot phenomenon observed in silicon solar cells at low temperatures and low intensities
[NASA-TM-82903] p0126 N82-31777
- ELECTRIC HYBRID VEHICLES**
Hybrid and electric advanced vehicle systems (heavy) simulation
[NASA-CR-165536] p0163 N82-16938
- ELECTRIC MOTOR VEHICLES**
A PWM transistor inverter for an ac electric vehicle drive p0085 A82-20744
Design study of a continuously variable roller cone traction CVT for electric vehicles
[NASA-CR-159841] p0105 N82-12445
The ac propulsion system for an electric vehicle, phase 1
[NASA-CF-165480] p0129 N82-13506
Hybrid and electric advanced vehicle systems (heavy) simulation
[NASA-CF-165536] p0163 N82-16938
Straight and chopped DC performance data for a General Electric 5BY436A1 DC shunt motor with a General Electric EV-1 controller
[NASA-CR-165507] p0085 N82-24425
Rolling resistance of electric vehicle tires from track tests
[NASA-TM-82836] p0124 N82-28786
Summary of electric vehicle dc motor-controller tests
[NASA-TM-82863] p0082 N82-33636
On the road performance tests of electric test vehicle for correlation with road load simulator
[NASA-TM-82900] p0127 N82-33829
- ELECTRIC MOTORS**
NT INDUCTION MOTORS
NT SYNCHRONOUS MOTORS
Hard permanent magnet development trends and their application to A.C. machines p0083 A82-20745
Fast recovery, high voltage silicon diodes for AC motor controllers p0086 A82-36926
Straight and chopped DC performance data for a reliance EV-250AT motor with a General Electric EV-1 controller
[NASA-CR-165447] p0132 N82-17608
- Engine technology p0001 N82-19145
Power systems p0001 N82-19146
Power systems p0001 N82-19146
Environmental control systems p0001 N82-19147
Electromechanical actuators N82-19148
Straight and chopped DC performance data for a General Electric 5BY436A1 DC shunt motor with a General Electric EV-1 controller
[NASA-CR-165507] p0085 N82-24425
- ELECTRIC POTENTIAL**
NT OPEN CIRCUIT VOLTAGE
High- and low-resistivity silicon solar cells p0046 A82-11762
Modification of spacecraft potentials by thermal electron emission on ATS-5 p0040 A82-16194
Voltage gradients in solar array cavities as possible breakdown sites in spacecraft-charging-induced discharges p0038 A82-18317
'Bootstrap' charging of surfaces composed of multiple materials p0085 A82-18318
Potentials of surfaces in space p0165 A82-23750
Differential charging of high-voltage spacecraft - The equilibrium potential of insulated surfaces p0041 A82-35547
Numerical simulation of plasma insulator interactions in space. Part 1: The self consistent calculation p0039 N82-14272
Mapping of electrical potential distributions with charged particle beams
[NASA-CR-168556] p0084 N82-18508
Impact of uniform electrode current distribution on ETF
[NASA-TM-82875] p0123 N82-25636
Additional extensions to the NASCAP computer code, volume 3
[NASA-CR-167857] p0040 N82-26378
Determination of optimum sunlight concentration level in space for 3-4 cascade solar cells
[NASA-TM-82899] p0126 N82-32853
- ELECTRIC POWER**
High power solar array switching regulation p0043 A82-11736
- ELECTRIC POWER CONVERSION**
U ELECTRIC GENERATORS
ELECTRIC POWER PLANTS
NT FUEL CELL POWER PLANTS
Comparative analysis of CCMHD power plants --- Closed Cycle MHD p0158 A82-20747
MHD channel performance for potential early commercial MHD power plants p0158 A82-0750
An assessment of alternative fuel cell designs for residential and commercial cogeneration p0138 A82-24695
Magnetohydrodynamics MHD Engineering Test Facility ETF 200 MWe power plant. Conceptual Design Engineering Report CDEK. Volume 3: Costs and schedules
[NASA-CR-165452-VOL-3] p0128 N82-10495
Magnetohydrodynamics (MHD) Engineering Test Facility (ETF) 200 MWe power plant. Design Requirements Document (DRD)
[NASA-TM-82705] p0099 N82-12446
Magnetohydrodynamics (MHD) Engineering Test Facility (ETF) 200 MWe power plant. Conceptual Design Engineering Report (CDEK). Volume 1: Executive summary
[NASA-CR-165452-VOL-1] p0129 N82-12570
Summary and evaluation of the conceptual design study of a potential early commercial MHD power plant (CSPEC)
[NASA-TM-82734] p0119 N82-16481
Develop and test fuel cell powered on-site integrated total energy systems. Phase 3: Full-scale power plant development
[NASA-CR-165455] p0131 N82-16483
Magnetohydrodynamics (MHD) Engineering Test Facility (ETF) 200 MWe power plant Conceptual

- Design Engineering Report (CDER)
[NASA-CR-165452-VOL-5] p0132 N82-17603
- Maqnetohydrodynamics (MHD) Engineering Test
Facility (ETF) 200 MWe power plant. Conceptual
Design Engineering Report (CDER). Volume 4:
Supplementary engineering data
[NASA-CR-165452-VOL-4] p0133 N82-18688
- Performance and operational economics estimates
for a coal gasification combined-cycle
cogeneration powerplant
[NASA-TM-82729] p0120 N82-19672
- Maqnetohydrodynamics (MHD) Engineering Test
Facility (ETF) 200 MWe power plant. Conceptual
Design Engineering Report (CDER). Volume 2:
Engineering. Volume 3: Costs and schedules
[NASA-CR-165452-VOL-2] p0136 N82-27837
- Development and test fuel cell powered on-site
integrated total energy systems. Phase 3:
Full-scale power plant development
[NASA-CR-167898] p0137 N82-30705
- ELECTRIC POWER SUPPLIES**
- NT SPACECRAFT POWER SUPPLIES
- NASA preprototype redox storage system for a
photovoltaic stand-alone application
p0127 N82-11774
- Power system design optimization using Lagrange
multiplier techniques
p0085 N82-20743
- Modeling the full-bridge series-resonant power
converter
p0086 N82-46385
- International market assessment of stand-alone
photovoltaic power systems for cottage industry
applications
[NASA-CR-165287] p0132 N82-16494
- Calculation of guaranteed mean power from wind
turbine generators
p0122 N82-23699
- ELECTRIC POWER TRANSMISSION**
- Preliminary design development of 100 KW rotary
power transfer device
[NASA-CR-165431] p0084 N82-23395
- ELECTRIC PROPULSION**
- NT ELECTROMAGNETIC PROPULSION
- NT SOLAR ELECTRIC PROPULSION
- Characterization of advanced electric propulsion
systems
[AIAA PAPER 82-1246] p0071 N82-35083
- Study of electrical and chemical propulsion
systems for auxiliary propulsion of large space
systems. Volume 1: Executive summary
[NASA-CR-165502-VOL-1] p0046 N82-11110
- Study of electrical and chemical propulsion
systems for auxiliary propulsion of large space
systems, volume 2
[NASA-CR-165502-VOL-2] p0044 N82-11111
- Inert gas ion thruster
[NASA-CR-165521] p0044 N82-21252
- An insight into auxiliary propulsion requirements
of large space systems
[NASA-TM-82827] p0042 N82-24286
- Characterization of advanced electric propulsion
systems
[NASA-CR-167885] p0045 N82-26381
- Large Space Systems/Propulsion Interactions
[NASA-TM-82904] p0042 N82-27358
- Electric and magnetic fields
[NASA-CR-165604] p0045 N82-28350
- Integrated propulsion for near-Earth space
missions. Volume 1: Executive summary
[NASA-CR-167889-VOL-1] p0045 N82-33424
- Integrated propulsion for near-Earth space
missions. Volume 2: Technical
[NASA-CR-167889-VOL-2] p0046 N82-33425
- ELECTRIC ROCKET ENGINES**
- NT ELECTROSTATIC ENGINES
- NT ION ENGINES
- NT MERCURY ION ENGINES
- ELECTRICAL CONDUCTIVITY**
- U ELECTRIC RESISTIVITY
- ELECTRICAL ENERGY**
- U ELECTRIC POWER
- ELECTRICAL ENGINEERING**
- Bibliography of Lewis Research Center technical
publications announced in 1981
[NASA-TM-82838] p0163 N82-27191
- ELECTRICAL IMPEDANCE**
- NT CONTACT RESISTANCE
- NT ELECTRICAL RESISTANCE
- Impedance conversion using quantum limit
nonreciprocity for
superconductor-insulator-superconductor mixer
compensation
p0159 N82-31276
- ELECTRICAL INSULATION**
- Low temperature growth and electrical
characterization of insulators for GaAs MISFETS
[NASA-CR-164972] p0159 N82-11959
- ELECTRICAL LEADS**
- U ELECTRIC CONDUCTORS
- ELECTRICAL PROPERTIES**
- NT CHARGE DISTRIBUTION
- NT CONTACT RESISTANCE
- NT DIELECTRIC PROPERTIES
- NT ELECTRICAL IMPEDANCE
- NT ELECTRICAL RESISTANCE
- NT ELECTRICAL RESISTIVITY
- NT FERROELECTRICITY
- NT PHOTOVOLTAIC EFFECT
- NT PIEZOELECTRICITY
- ELECTRICAL RESISTANCE**
- NT CONTACT RESISTANCE
- Large area low-cost space solar cell development
[NASA-TM-82902] p0126 N82-32854
- ELECTRICAL RESISTIVITY**
- A theory of the n-i-p silicon solar cell
p0128 N82-45055
- Some properties of RF sputtered hafnium nitride
coatings
[NASA-TM-82826] p0067 N82-21331
- Method of making a high voltage V-groove solar cell
[NASA-CASE-LEW-13401-1] p0124 N82-29700
- ELECTRICITY**
- NT ALTERNATING CURRENT
- NT ATMOSPHERIC ELECTRICITY
- Integrated gasifier combined cycle polygeneration
system to produce liquid hydrogen
[NASA-TM-82921] p0125 N82-30713
- ELECTRIFICATION**
- Market assessment of photovoltaic power systems
for agricultural applications in Mexico
[NASA-CR-165441] p0128 N82-10506
- Socioeconomic impact of photovoltaic power at
Schuchuli, Arizona
[NASA-CR-165551] p0133 N82-19669
- ELECTRO-OPTICS**
- High temperature electronic requirements in
aeropropulsion systems
[E-708] p0081 N82-15313
- Pockels-effect cell for gas-flow simulation
[NASA-TP-2007] p0095 N82-23515
- ELECTROCATALYSTS**
- Survey on aging on electrodes and electrocatalysts
in phosphoric acid fuel cells
[NASA-CR-165505] p0124 N82-11545
- Preparation and evaluation of advanced
electrocatalysts for phosphoric acid fuel cells
[NASA-CR-165519] p0129 N82-12573
- Development of a high-temperature durable catalyst
for use in catalytic combustors for advanced
automotive gas turbine engines
[NASA-CR-165396] p0130 N82-13510
- Stabilizing platinum in phosphoric acid fuel cells
[NASA-CR-165483] p0130 N82-14628
- Preparation and evaluation of advanced
electrocatalysts for phosphoric acid fuel cells
[NASA-CR-165594] p0132 N82-17615
- Cathode catalysts for primary phosphoric acid fuel
cells
[NASA-CR-165578] p0134 N82-21709
- Cathode catalyst for primary phosphoric fuel cells
[NASA-CR-165198] p0134 N82-22675
- Non-noble catalysts and catalyst supports for
phosphoric acid fuel cells
[NASA-CR-165289] p0137 N82-30722
- ELECTROCHEMICAL CELLS**
- NT ALKALINE BATTERIES
- NT ELECTRIC BATTERIES
- NT FUEL CELLS
- NT HYDROGEN OXYGEN FUEL CELLS
- NT LEAD ACID BATTERIES
- NT NICKEL CADMIUM BATTERIES
- NT NICKEL HYDROGEN BATTERIES
- NT NICKEL ZINC BATTERIES
- NT PHOSPHORIC ACID FUEL CELLS
- NT REDOX CELLS
- NT REGENERATIVE FUEL CELLS
- NT SILVER ZINC BATTERIES

- NT STORAGE BATTERIES**
Moderate temperature Na cells III - Electrochemical and structural studies of Cr_{0.5}V_{0.5}S₂ and its Na intercalates p0055 A82-15732
- Endurance test and evaluation of alkaline water electrolysis cells [NASA-CF-165423] p0130 N82-13508
- Preparation and evaluation of advanced electrocatalysts for phosphoric acid fuel cells [NASA-CF-165534] p0132 N82-17615
- ELECTROCHEMICAL OXIDATION**
Chemical and electrochemical behavior of the Cr(3)/Cr(2) half cell in the NASA Redox Energy Storage System [NASA-TM-82913] p0055 N82-33463
- ELECTROCHEMISTRY**
Moderate temperature Na cells IV - VS2 and NbS₂Cl₂ as rechargeable cathodes in molten NaAlCl₄ p0055 A82-15743
- Synthetic battery cycling techniques [NASA-TM-82945] p0125 N82-30715
- ELECTRODE FILM BARRIERS**
Cross-linked polyvinyl alcohol films as alkaline battery separators [NASA-TM-82802] p0054 N82-22327
- ELECTRODEPOSITION**
Mechanism and models for zinc metal morphology in alkaline media [NASA-TM-82768] p0120 N82-19671
- ELECTRODES**
NT ANODES
NT CATHODES
NT CELL CATHODES
NT PLASMA ELECTRODES
NT SOLID ELECTRODES
- Survey on aging on electrodes and electrocatalysts in phosphoric acid fuel cells [NASA-CF-165505] p0128 N82-11545
- Performance of advanced chromium electrodes for the NASA Redox Energy Storage System [NASA-TM-82724] p0118 N82-12574
- Technology development for phosphoric acid fuel cell powerplant, phase 2 [NASA-CF-165426] p0131 N82-16482
- Performance mapping studies in Redox flow cells [NASA-TM-82707] p0120 N82-20668
- Method of making formulated plastic separators for soluble electrode cells [NASA-CASE-LPW-12358-2] p0054 N82-21268
- Improved chromium electrodes for REDOX cells [NASA-CASE-LPW-13653-1] p0121 N82-22672
- Light weight nickel battery plaque [NASA-CASE-LEW-13349-1] p0121 N82-22673
- Multistage depressed collector for dual mode operation --- for microwave transmitting tubes [NASA-CASE-LPW-13282-1] p0081 N82-24415
- Impact of uniform electrode current distribution on ETF [NASA-TM-82875] p0123 N82-25636
- NASA Redox system development project status [NASA-TM-82665] p0123 N82-25637
- Ion beam textured graphite electrode plates --- high efficiency electron tube devices [NASA-CASE-LEW-12919-2] p0050 N82-26386
- Pyrolytic graphite collector development program [NASA-CF-167909] p0052 N82-29363
- Synthetic battery cycling techniques [NASA-TM-82945] p0125 N82-30715
- Nickel-hydrogen bipolar battery systems [NASA-TM-82946] p0125 N82-30716
- ELECTRODYNAMICS**
Representation and material charging response of quoplasma environments p0039 N82-14249
- ELECTROGENERATORS**
ELECTRIC GENERATORS
- ELECTROLYTES**
NT ION EXCHANGE MEMBRANE ELECTROLYTES
NT MOLTEN SALT ELECTROLYTES
- Improved chromium electrodes for REDOX cells [NASA-CASE-LEW-13653-1] p0121 N82-22672
- Requirements for optimization of electrodes and electrolyte for the iron/chromium Redox flow cell [NASA-CR-165218] p0136 N82-25640
- ELECTROLYTIC CELLS**
Endurance test and evaluation of alkaline water electrolysis cells [NASA-CF-165424] p0130 N82-13508
- ELECTROMAGNETIC ACCELERATION**
A small scale lunar launcher for early lunar material utilization p0032 A82-35617
- ELECTROMAGNETIC CONTROL**
ELECTROMAGNETS
- ELECTROMAGNETIC FIELDS**
On a free-electron-laser in a uniform magnetic field - A solution for arbitrarily strong electromagnetic radiation fields A82-28409
- Three-dimensional relativistic field-electron interaction in a multicavity high-power klystron. I: Basic theory [NASA-TP-1992] p0081 N82-22439
- ELECTROMAGNETIC INTERACTIONS**
NT PLASMA-ELECTROMAGNETIC INTERACTION
- ELECTROMAGNETIC INTERFERENCE**
NT RADIO FREQUENCY INTERFERENCE
Brushfire arc discharge model p0038 N82-14224
- ELECTROMAGNETIC PROPERTIES**
NT DIREFRINGENCE
NT DIELECTRIC PROPERTIES
NT FERROELECTRICITY
NT OPTICAL PROPERTIES
NT PHOTOVOLTAIC EFFECT
NT REFLECTANCE
NT REFRACTIVITY
NT TRANSMITTANCE
- ELECTROMAGNETIC PROPULSION**
NT MASS DRIVERS (PAYLOAD DELIVERY)
Preliminary feasibility assessment for earth-to-space electromagnetic (Railgun) launchers [NASA-CR-167886] p0033 N82-29345
- ELECTROMAGNETIC RADIATION**
NT CENTIMETER WAVES
NT FAR ULTRAVIOLET RADIATION
NT GAMMA RAYS
NT INFRARED RADIATION
NT MICROWAVE EMISSION
NT MILLIMETER WAVES
NT POLARIZED LIGHT
NT SOLAR RADIO BURSTS
NT SOLAR RADIO EMISSION
NT SOLAR X-RAYS
NT SUNLIGHT
- ELECTROMAGNETIC SCATTERING**
NT LIGHT SCATTERING
NT RAMAN SPECTRA
NT RAYLEIGH SCATTERING
- ELECTROMAGNETIC SPECTRA**
NT INFRARED SPECTRA
NT RAMAN SPECTRA
NT STELLAR SPECTRA
NT ULTRAVIOLET SPECTRA
- ELECTROMAGNETIC WAVE FILTERS**
NT ELECTRIC FILTERS
NT MATCHED FILTERS
- ELECTROMAGNETIC WAVE TRANSMISSION**
NT LIGHT SCATTERING
NT MICROWAVE TRANSMISSION
NT TRANSHORIZON RADIO PROPAGATION
- ELECTROMAGNETICS**
ELECTROMAGNETISM
- ELECTROMAGNETISM**
Conceptual design of superconducting magnet system for Magnetohydrodynamic (MHD) Engineering Test Facility (ETF) 200 Mwe power plant [NASA-CR-165053] p0105 N82-14520
- Development of a dual-field heteropolar power converter [NASA-CR-165168] p0084 N82-24424
- ELECTROMAGNETS**
NT SUPERCONDUCTING MAGNETS
Permanent magnet properties of Mn-Ni-C between -50 C and +150 C p0085 A82-20505
- ELECTROMECHANICAL DEVICES**
Electromechanical actuators N82-19148
- ELECTRON BEAMS**
NT RELATIVISTIC ELECTRON BEAMS
Electron beam induced damage in ITO coated Kapton --- Indium Tin Oxide p0159 A82-41546
- Secondary electron emission yields p0038 N82-14226

ORIGINAL PAGE IS
OF POOR QUALITY

ELECTRON BOMBARDMENT

SUBJECT INDEX

- Secondary electron emission from a charged dielectric in the presence of normal and oblique electric fields
[NASA-CR-168558] p0084 N82-18507
- ELECTRON BOMBARDMENT**
Testing of a spacecraft model in a combined environment simulator
[NASA-TN-82723] p0037 N82-11106
Ion beam textured graphite electrode plates --- high efficiency electron tube devices
[NASA-CASE-LEW-12919-2] p0050 N82-26386
- ELECTRON BUNCHING**
Three-dimensional relativistic field-electron interaction in a multicavity high-power klystron. Part 2: Working Equations
[NASA-TP-2008] p0081 N82-23397
- ELECTRON CAPTURE**
Multistage depressed collector for dual mode operation --- for microwave transmitting tubes
[NASA-CASE-LEW-13282-1] p0081 N82-24415
- ELECTRON COLLISIONS**
U ELECTRON SCATTERING
- ELECTRON COMPOUNDS**
U THERMALICS
- ELECTRON DISTRIBUTION**
The use of a structural method to calculate the electrostatic field of a magnetron
A82-18370
- ELECTRON EMISSION**
NT SECONDARY EMISSION
Modification of spacecraft potentials by thermal electron emission on ATS-5
p0040 A82-16194
Spacecraft Charging Technology, 1980
[NASA-CP-2182] p0037 N82-14213
Secondary electron emission yields
p0038 N82-14226
Oblique-incidence secondary emission from charged dielectrics
p0039 N82-14227
Secondary electron emission from a charged dielectric in the presence of normal and oblique electric fields
[NASA-CR-168558] p0084 N82-18507
- ELECTRON GUNS**
NASCAP simulation of laboratory charging tests using multiple electron guns
p0033 A82-18319
- ELECTRON INTERACTIONS**
U ELECTRON SCATTERING
- ELECTRON IRRADIATION**
Internal breakdown of charged spacecraft dielectrics
p0041 A82-18312
NASCAP simulation of laboratory charging tests using multiple electron guns
p0033 A82-18319
Spacecraft Charging Technology, 1980
[NASA-CP-2182] p0037 N82-14213
- ELECTRON MICROSCOPY**
Preparation and evaluation of advanced electrocatalysts for phosphoric acid fuel cells
[NASA-CR-165519] p0129 N82-12573
Elucidation of wear mechanisms by ferrographic analysis
[NASA-TN-82737] p0066 N82-15199
- ELECTRON PATHS**
U ELECTRON TRAJECTORIES
- ELECTRON RADIATION**
NT ELECTRON BEAMS
NT RELATIVISTIC ELECTRON BEAMS
- ELECTRON SCATTERING**
Three-dimensional relativistic field-electron interaction in a multicavity high-power klystron. Part 2: Working Equations
[NASA-TP-2008] p0081 N82-23397
- ELECTRON TRAJECTORIES**
Three-dimensional relativistic field-electron interaction in a multicavity high-power klystron. 1: Basic theory
[NASA-TP-1992] p0081 N82-22439
- ELECTRON TUBES**
NT KLYSTRONS
NT MAGNETRONS
NT TRAVELING WAVE TUBES
- ELECTRON TUNNELING**
Impedance conversion using quantum limit nonreciprocity for superconductor-insulator-superconductor mixer compensation
- Stationary state model for normal metal tunnel junction phenomena
p0159 A82-31276
p0159 A82-42912
- ELECTRONIC AMPLIFIERS**
U PLIFIERS
- ELECTRONIC CONTROL**
A PWM transistor inverter for an electric vehicle drive
p0085 A82-20744
Preliminary study, analysis and design for a power switch for digital engine actuators
[NASA-CR-159559] p0085 N82-23394
- ELECTRONIC EQUIPMENT**
NT AVALANCHE DIODES
NT BIPOLAR TRANSISTORS
NT CRYSTAL RECTIFIERS
NT ELECTRONIC MODULES
NT ELECTRONIC PACKAGING
NT FIELD EFFECT TRANSISTORS
NT METAL OXIDE SEMICONDUCTORS
NT MIS (SEMICONDUCTORS)
NT PHOTOVOLTAIC CELLS
NT SEMICONDUCTOR DEVICES
NT SEMICONDUCTOR DIODES
NT SOLID STATE DEVICES
NT TRANSISTORS
- ELECTRONIC MODULES**
A remote millivolt multiplexer and amplifier module for wind tunnel data acquisition
p0083 A82-41845
Analysis and design of a standardized control module for switching regulators
p0083 A82-46388
- ELECTRONIC PACKAGING**
Proceedings of the Conference on High-temperature Electronics
[NASA-TN-84069] p0081 N82-15311
- ELECTRONIC SWITCHES**
U ITCHING CIRCUITS
- ELECTRONS**
NT RELATIVISTIC ELECTRON BEAMS
- ELECTROPHYSICS**
NT ELECTRO-OPTICS
- ELECTROSEISMIC EFFECT**
U ELECTRIC CURRENT
- ELECTROSTATIC CHARGE**
Potentials of surfaces in space
p0165 A82-23750
Simulation of charging response of SCATHA (P78-2) satellite
p0039 N82-14250
SCATHA SSPM charging response: NASCAP predictions compared with data
p0037 N82-14251
Comparison of NASCAP modelling results with lumped circuit analysis
p0037 N82-14255
Mapping of electrical potential distributions with charged particle beams
[NASA-CR-168556] p0084 N82-18508
- ELECTROSTATIC ENGINES**
Electric thruster research
[NASA-CR-165603] p0045 N82-24285
- ELECTROSTATIC FIELDS**
U ELECTRIC FIELDS
- ELECTROSTATIC PLASMA**
U ASMAS (PHYSICS)
- ELECTROSTATICS**
Numerical simulation of plasma insulator interactions in space. Part 1: The self consistent calculation
p0039 N82-14272
Numerical simulation of plasma insulator interactions in space. Part 2: Dielectric effects
p0039 N82-14273
- ELEMENT ABUNDANCE**
U UNANCE
- ELEMENTARY EXCITATIONS**
NT PLASMONS
- ELEMENTARY PARTICLE INTERACTIONS**
NT ELECTRON CAPTURE
- ELLIPTICAL ORBITS**
NT TRASPOR ORBITS
- EMISSION**
NT CHEMILUMINESCENCE
NT ELECTRON EMISSION
NT EXHAUST EMISSION

NT MICROWAVE EMISSION
 NT SECONDARY EMISSION
 NT SOLAR RADIO BURSTS
 NT SOLAR RADIO EMISSION
EMISSION SPECTRA
 Alignment of fluid molecules in an MHD contact
 [ASLE PREPRINT 81-LC-5C71] p0107 A82-18407
 Analysis of infrared emission from thin adsorbates
 p0056 A82-21431

EMISSIVITY
 Ion beam microtexturing and enhanced surface
 diffusion
 [NASA-CR-167948] p0065 A82-31509

EMITTERS
 NT THERMIONIC EMITTERS
 High voltage power transistor development
 [NASA-CR-165547] p0084 A82-18506

ENCAPSULATED MICROCIRCUITS
 Stoichiometry-controlled compensation in liquid
 encapsulated Czochralski GaAs p0158 A82-17585

ENCAPSULATING
 Undoped semi-insulating LEC GaAs - A model and a
 mechanism --- Liquid Encapsulated Czochralski
 p0159 A82-13754
 Testing of solar cell covers and encapsulants
 conducted in a simulated space environment
 [NASA-CR-165475] p0129 A82-12571
 Development of a large area space solar cell
 assembly
 [NASA-CR-167929] p0137 A82-30706

END PLATES
 Turbine endwall single cylinder program
 [NASA-CR-169278] p0091 A82-31638

ENERGETIC PARTICLES
 NT ARGON PLASMA
 NT CYLINDRICAL PLASMAS
 NT PLASMAS (PHYSICS)
 Space Shuttle Orbiter charging
 [AIAA PAPER 82-0119] p0040 A82-17793

ENERGY ABSORPTION
 Analysis of crack propagation as an energy
 absorption mechanism in metal matrix composites
 [NASA-CR-165051] p0052 A82-14288

ENERGY ABSORPTION FILMS
 Thin foil silicon solar cells with coplanar back
 contacts
 p0127 A82-44944

ENERGY BANDS
 A new strategy for efficient solar energy
 conversion: Parallel-processing with surface
 plasmons
 [NASA-TM-82867] p0042 A82-29354

ENERGY CONSERVATION
 Reliable aerial thermography for energy conservation
 [NASA-TM-81766] p0117 A82-14552
 Advanced Gas Turbine (AGT) powertrain system
 initial development report
 [NASA-CR-165130] p0132 A82-16485
 Develop and test fuel cell powered on-site
 integrated total energy systems: Phase 3:
 Full-scale power plant development
 [NASA-CR-165568] p0135 A82-24648
 The CF6 jet engine performance improvement: Low
 pressure turbine active clearance control
 [NASA-CR-165557] p0029 A82-33393

ENERGY CONSUMPTION
 Collection and dissemination of thermal energy
 storage system information for the pulp and
 paper industry
 p0136 A82-24686

ENERGY CONVERSION
 NT PHOTOTHERMAL CONVERSION
 NT SATELLITE SOLAR ENERGY CONVERSION
 NT SOLAR ENERGY CONVERSION
 Conversion of acoustic energy by lossless liners
 p0154 A82-36195
 Modeling the full-bridge series-resonant power
 converter
 p0086 A82-46385
 Phosphoric acid fuel cell technology status
 [NASA-TM-82791] p0120 A82-19670
 Cell module and fuel conditioner development
 [NASA-CR-165626] p0134 A82-21713
 Collection and dissemination of thermal energy
 storage system information for the pulp and
 paper industry
 p0136 A82-24686

Free electron lasers for transmission of energy in
 space
 [NASA-CR-165520] p0098 A82-25499
ENERGY CONVERSION EFFICIENCY
 Optically pumped high-pressure DF-CO2 transfer laser
 A82-10193
 Direct conversion of light to radio frequency energy
 --- using photoklystrons for solar power
 satellites
 p0138 A82-11712
 High- and low-resistivity silicon solar cells
 p0046 A82-11762
 Comparative analysis of CCMHD power plants ---
 Closed Cycle MHD
 p0158 A82-20747
 MHD channel performance for potential early
 commercial MHD power plants
 p0158 A82-20750
 Effect of positive pulse charge waveforms on the
 energy efficiency of lead-acid traction cells
 [NASA-TM-82709] p0118 A82-10503
 Evaluation of the potential of the Stirling engine
 for heavy duty application
 [NASA-CR-165473] p0128 A82-10505
 Develop and test fuel cell powered on-site
 integrated total energy system. Phase 3:
 Full-scale power plant development
 [NASA-CR-165328] p0117 A82-13490
 Cell module and fuel conditioner development
 [NASA-CR-165462] p0130 A82-13511
 Study of multi-megawatt technology needs for
 photovoltaic space power systems, volume 2
 [NASA-CR-165323-VOL-2] p0130 A82-14637
 Performance mapping studies in Redox flow cells
 [NASA-TM-82707] p0120 A82-20668
 Energy efficient engine exhaust mixer model
 technology
 [NASA-CR-165459] p0025 A82-22264
 Low NO sub x heavy fuel combustor concept program.
 Phase 1A: Combustion technology generation coal
 gas fuels
 [NASA-CR-165614] p0055 A82-22326
 Parametric performance analysis of steam-injected
 gas turbine with a
 thermionic-energy-converter-lined combustor
 [NASA-TM-82736] p0121 A82-23678

ENERGY CONVERTERS
 U RECT POWER GENERATORS

ENERGY DISSIPATION
 Aerodynamic performance of high turning core
 turbine vanes in a two-dimensional cascade
 [AIAA PAPER 82-1288] p0005 A82-37716
 On the cause of the flat spot phenomenon observed
 in silicon solar cells at low temperatures and
 low intensities
 p0044 A82-44965
 Micromechanical predictions of crack propagation
 and fracture energy in a single fiber
 boron/aluminum model composite
 [NASA-CR-168550] p0052 A82-16726
 Frictional heating due to asperity interaction
 elastohydrodynamic line-contact surfaces
 [NASA-TP-1882] p0100 A82-20510

ENERGY EXCHANGE
 U ERGY TRANSFER

ENERGY LOSSES
 U ERGY DISSIPATION

ENERGY METHODS
 NT STRAIN ENERGY METHODS

ENERGY POLICY
 Effect of positive pulse charge waveforms on the
 energy efficiency of lead-acid traction cells
 [NASA-TM-82709] p0118 A82-10503
 Performance of advanced chromium electrodes for
 the NASA Redox Energy Storage System
 [NASA-TM-82724] p0118 A82-12574
 Barriers to the utilization of synthetic fuels for
 transportation
 [NASA-CR-165517] p0073 A82-13243
 Component technology for space power systems
 [NASA-TM-82928] p0082 A82-30474

ENERGY STORAGE
 NT ELECTRIC ENERGY STORAGE
 NT HEAT STORAGE
 Alkaline regenerative fuel cell systems for energy
 storage
 p0042 A82-11706
 Deposit formation in liquid fuels. III - The
 effect of selected nitrogen compounds on diesel

- fuel
p0074 A82-23238
- The effects of controls and controllable and storage loads on the performance of stand-alone photovoltaic systems
p0127 A82-45027
- Performance of advanced chromium electrodes for the NASA Redox Energy Storage System
[NASA-TM-82724] p0118 N82-12574
- Electrochemical energy storage for an orbiting space station
[NASA-CR-165436] p0132 N82-17697
- Performance mapping studies in Redox flow cells
[NASA-TM-82707] p0120 N82-20668
- Develop and test fuel cell powered on-site integrated total energy systems: Phase 3: Full-scale power plant development
[NASA-CR-165568] p0135 N82-24648
- Requirements for optimization of electrodes and electrolyte for the iron/chromium Redox flow cell
[NASA-CR-165210] p0136 N82-25640
- Synthetic battery cycling techniques
[NASA-TM-82945] p0125 N82-30715
- Nickel-hydrogen bipolar battery systems
[NASA-TM-82946] p0125 N82-30716
- Design flexibility of Redox flow systems --- for energy storage applications
[NASA-TM-82854] p0054 N82-31459
- ENERGY STORAGE DEVICES**
- U ERGY STORAGE**
- ENERGY TECHNOLOGY**
- Low NO subx heavy fuel combustor concept program. Phase 1A: Coal gas addendum
[NASA-CR-165577] p0133 N82-18690
- Results and comparison of Hall and DW duct experiments
[NASA-TM-82864] p0157 N82-25961
- ENERGY TRANSFER**
- Characteristic dynamic energy equations for Stirling cycle analysis
p0138 A82-11816
- ENGINE AIRFRAME INTEGRATION**
- Advanced general aviation engine/airframe integration study
[NASA-CR-165565] p0025 N82-22268
- ENGINE CONTROL**
- NT ROCKET ENGINE CONTROL**
- NT TURBOJET ENGINE CONTROL**
- M/STOL propulsion control technology
[AIAA PAPER 61-2634] p0029 A82-16909
- A tensor approach to modeling of nonhomogeneous nonlinear systems
p0148 A82-19064
- Optical tip clearance sensor for aircraft engine controls
[AIAA PAPER 82-1131] p0015 A82-37691
- Sensor failure detection system --- for the F100 turbofan engine
[NASA-CR-165515] p0023 N82-13145
- Role of optical computers in aeronautical control applications
p0156 N82-15897
- Preliminary study, analysis and design for a power switch for digital engine actuators
[NASA-CR-159559] p0085 N82-23394
- ENGINE DESIGN**
- NT ROCKET ENGINE DESIGN**
- The AGT101 technology - An automotive alternative
p0107 A82-11783
- Thermal expansion accommodation in a jet engine frame
p0029 A82-11999
- NASA Eroad Specification Fuels Combustion Technology program - Pratt and Whitney Aircraft Phase I results and status
[AIAA PAPER 82-1088] p0021 A82-34999
- Small gas turbine combustor primary zone development
[AIAA PAPER 82-1159] p0103 A82-35036
- AGT100 turbomachinery --- for automobiles
[AIAA PAPER 82-1207] p0108 A82-35061
- Combustor development for automotive gas turbines
[AIAA PAPER 82-1208] p0104 A82-35062
- The AGT 101 advanced automotive gas turbine
[ASME PAPER 82-GT-72] p0108 A82-35321
- Developing a scalable inert gas ion thruster
[AIAA PAPER 82-1275] p0047 A82-37713
- TF34 Convertible Engine System Technology Program
p0022 A82-40521
- Propulsion study for Small Transport Aircraft Technology (STAT)
[NASA-CR-165499] p0022 N82-10037
- Propulsion study for Small Transport Aircraft Technology (STAT), Appendix B
[NASA-CR-165499-APP-B] p0022 N82-10038
- Lightweight diesel engine designs for commuter type aircraft
[NASA-CR-165470] p0023 N82-11068
- Integrated analysis of engine structures
[NASA-TM-82713] p0111 N82-11491
- Test results and facility description for a 40-kilowatt stirling engine
[NASA-TM-82620] p0163 N82-13013
- Interactive-graphic flowpath plotting for turbine engines
[NASA-TM-82756] p0017 N82-15041
- Advanced Gas Turbine (AGT) powertrain system initial development report
[NASA-CR-165130] p0132 N82-16485
- Advanced Gas Turbine (AGT) powertrain system development for automotive applications
[NASA-CR-165175] p0163 N82-16937
- Cooled variable-area radial turbine technology program
[NASA-CR-165408] p0024 N82-19221
- Forward acoustic performance of a model turbofan designed for a high specific flow (QF-14)
[NASA-TP-1968] p0152 N82-21036
- Cold-air performance of a 15.41-cm-tip-diameter axial-flow power turbine with variable-area stator designed for a 75-kW automotive gas turbine engine
[NASA-TM-82644] p0024 N82-21193
- Energy efficient engine shroudless, hollow fan blade technology report
[NASA-CR-165586] p0024 N82-21196
- The role of modern control theory in the design of controls for aircraft turbine engines
[NASA-TM-82815] p0018 N82-22262
- Energy efficient engine exhaust mixer model technology
[NASA-CR-165459] p0025 N82-22264
- Computer model of catalytic combustion/Stirling engine heater head
[NASA-CR-165378] p0134 N82-22666
- Alternatives for jet engine control
[NASA-CR-168894] p0026 N82-23247
- Study of advanced propulsion systems for Small Transport Aircraft Technology (STAT) program
[NASA-CR-165610] p0026 N82-24202
- Low NOx heavy fuel combustor concept program
[NASA-CR-165367] p0136 N82-25635
- Propulsion opportunities for future commuter aircraft
[NASA-TM-82915] p0019 N82-26298
- Advanced stratified charge rotary aircraft engine design study
[NASA-CR-165398] p0107 N82-27743
- Automotive Stirling engine development program
[NASA-CR-167907] p0164 N82-29235
- QCSEE over-the-wing engine acoustic data
[NASA-TM-82708] p0020 N82-29324
- Assessment of a 40-kilowatt stirling engine for underground mining applications
[NASA-TM-82822] p0125 N82-30714
- Development of a spinning wave heat engine
[NASA-CR-165611] p0028 N82-31328
- Advanced turboprop testbed systems study. Volume 1: Testbed program objectives and priorities, drive system and aircraft design studies, evaluation and recommendations and wind tunnel test plans
[NASA-CR-167928-VOL-1] p0028 N82-32370
- Low and medium heating value coal gas catalytic combustor characterization
[NASA-CR-165560] p0138 N82-32856
- Automated procedure for developing hybrid computer simulations of turbofan engines. Part 1: General description
[NASA-TP-1851] p0146 N82-33020
- Engine dynamic analysis with general nonlinear finite element codes. Part 2: Bearing element implementation overall numerical characteristics and benchmarking
[NASA-CR-167944] p0028 N82-33390
- Structural tailoring of engine blades (STARBL)
[NASA-CR-167949] p0028 N82-33391

ENGINE FAILURE

- Reusable rocket engine maintenance study
[NASA-CR-165569] p0044 N82-16172
- Analytical investigation of nonrecoverable stall
[NASA-TM-82792] p0018 N82-21195
- Computer modeling of fan-exit-splitter spacing effects on F100 response to distortion
[NASA-CR-167979] p0025 N82-23246
- Rotor fragment protection program: Statistics on aircraft gas turbine engine rotor failures that occurred in U.S. commercial aviation during 1978
[NASA-CR-165388] p0027 N82-27316

ENGINE INLETS

- An iterative finite element-integral technique for predicting sound radiation from turbofan inlets in steady flight
[AIAA PAPER 82-0124] p0030 A82-17796
- A summary of V/STOL inlet analysis methods
[NASA-TM-82725] p0003 N82-11043
- Effect of a part span variable inlet guide vane on TF34 fan performance
[NASA-CR-165458] p0023 N82-12075
- Prediction of sound radiation from different practical jet engine inlets
[NASA-CR-165120] p0153 N82-16810
- Effects of fan inlet temperature disturbances on the stability of a turbofan engine
[NASA-TM-82699] p0017 N82-18222
- V/STOL Tandem Fan transition section model test --- in the Lewis Research Center 10-by-10 foot wind tunnel
[NASA-CR-165587] p0007 N82-21150
- Energy efficient engine: Turbine transition duct model technology report
[NASA-CR-167996] p0029 N82-33394

ENGINE MONITORING INSTRUMENTS

- High temperature electronic requirements in aeropropulsion systems
[E-708] p0081 N82-15313

ENGINE NOISE

- An iterative finite element-integral technique for predicting sound radiation from turbofan inlets in steady flight
[AIAA PAPER 82-0124] p0030 A82-17796
- YF 102 in-duct combustor noise measurements with a turbine nozzle, volume 1
[NASA-CR-165562-VOL-1] p0153 N82-21031
- YF 102 in-duct combustor noise measurements with a turbine nozzle, volume 2
[NASA-CR-165562-VOL-2] p0153 N82-21032
- YF 102 in-duct combustor noise measurements with a turbine nozzle, volume 3
[NASA-CR-165562-VOL-3] p0155 N82-21033
- Forward acoustic performance of a model turbofan designed for a high specific flow (QP-14)
[NASA-TM-1968] p0152 N82-21036
- Pressure transfer function of a JT15D nozzle due to acoustic and convected entropy fluctuations
[NASA-TM-82042] p0152 N82-22951
- OCSEE under-the-wing engine acoustic data
[NASA-TM-82691] p0019 N82-27311
- OCSEE over-the-wing engine acoustic data
[NASA-TM-82708] p0020 N82-29324
- Finite element-integral simulation of static and flight fan noise radiation from the JT15D turbofan engine
[NASA-TM-82936] p0152 N82-31068
- Rough analysis of installation effects on turboprop noise
[NASA-TM-82924] p0152 N82-32082

ENGINE PARTS

- Progress in ceramic component fabrication technology
[AIAA PAPER 82-1211] p0071 A82-35064
- The AGT 101 advanced automotive gas turbine
[ASME PAPER 82-GT-72] p0108 A82-35321
- Fabrication of turbine components and properties of sintered silicon nitride
[ASME PAPER 82-GT-252] p0071 A82-35431
- Progress in the development of energy efficient engine components
[ASME PAPER 82-GT-275] p0030 A82-35450
- Engine dynamic analysis with general nonlinear finite element codes. II - Bearing element implementation, overall numerical characteristics and benchmarking
[ASME PAPER 82-GT-292] p0108 A82-35462
- Elevated temperature fatigue testing of metals
[NASA-TM-82745] p0111 N82-16419

- Elastic-plastic finite-element analysis of thermally cycled double-edge wedge specimens
[NASA-TT-1973] p0111 N82-20566
- Effect of oxide films on hydrogen permeability of candidate Stirling engine heater head tube alloys
[NASA-TM-82824] p0060 N82-24323
- Cost/benefit studies of advanced materials technologies for future aircraft turbine engines: Materials for advanced turbine engines
[NASA-CR-167849] p0026 N82-25254
- Propulsion opportunities for future commuter aircraft
[NASA-TM-82915] p0019 N82-26298
- Method of protecting a surface with a silicon-slurry/alumina coating --- coatings for gas turbine engine blades and vanes
[NASA-CASE-LEW-13343-1] p0068 N82-28441
- Evaluation of candidate Stirling engine heater tube alloys at 820 deg and 860 deg C
[NASA-TM-82837] p0061 N82-30372
- Automotive Stirling Engine Mod 1 Design Review, volume 1
[NASA-CR-167935] p0164 N82-34311
- Automotive Stirling Engine Mod 1 Design Review, volume 3 --- engineering drawings
[NASA-CR-167397] p0164 N82-34312

ENGINE TESTS

- Characteristics of the LeRC/Hughes J-series 30-cm engineering model thruster
p0046 A82-15435
- AGT100 turbomachinery --- for automobiles
[AIAA PAPER 82-1207] p0108 A82-35061
- Compressor development for automotive gas turbines
[AIAA PAPER 82-1208] p0104 A82-35062
- Progress in the development of energy efficient engine components
[ASME PAPER 82-GT-275] p0030 A82-35450
- Propulsion study for Small Transport Aircraft Technology (STAT), Appendix B
[NASA-CR-165499-APP-B] p0022 N82-10038
- Pollution reduction technology program small jet aircraft engines, phase 3
[NASA-CR-165386] p0023 N82-14095
- ERDS fuel addendum: Pollution reduction technology program small jet aircraft engines, phase 3
[NASA-CR-165387] p0024 N82-14096
- Comparison of two parallel/series flow turbofan propulsion concepts for supersonic V/STOL
[NASA-TM-82743] p0004 N82-18178
- Preliminary results on performance testing of a turbocharged rotary combustion engine
[NASA-TM-82772] p0017 N82-21194
- CF6 Jet Engine Diagnostics Program: High pressure compressor clearance investigation
[NASA-CR-165580] p0025 N82-21197
- Performance deterioration due to acceptance testing and flight loads; JT90 jet engine diagnostic program
[NASA-CR-165572] p0027 N82-27309
- Energy efficient engine: High pressure turbine uncooled rig technology report
[NASA-CR-165149] p0031 N82-32383

ENGINEERING DEVELOPMENT

U DUCT DEVELOPMENT

ENGINES

- NT BOOSTER ROCKET ENGINES
- NT BRISTOL-SIDDELEY BS 53 ENGINE
- NT DIESEL ENGINES
- NT ELECTROSTATIC ENGINES
- NT GAS TURBINE ENGINES
- NT HELICOPTER ENGINES
- NT HYDROGEN OXYGEN ENGINES
- NT INTERNAL COMBUSTION ENGINES
- NT ION ENGINES
- NT JET ENGINES
- NT LIQUID PROPELLANT ROCKET ENGINES
- NT MERCURY ION ENGINES
- NT PISTON ENGINES
- NT ROCKET ENGINES
- NT TF-34 ENGINE
- NT TURBINE ENGINES
- NT TURBOFAN ENGINES
- NT TURBOJET ENGINES
- NT TURBOPROP ENGINES
- NT VARIABLE CYCLE ENGINES
- NT WANKEL ENGINES

ENTHALPY

- Numerical modeling of three-dimensional confined

- flows
[NASA-CF-165583] p0158 N82-24078
- ENTROPY**
Pressure transfer function of a JT15D nozzle due to acoustic and convected entropy fluctuations
[NASA-TM-82842] p0152 N82-22951
- ENTROPY (STATISTICS)**
NT MAXIMUM ENTROPY METHOD
- ENVIRONMENT EFFECTS**
Environmental assessment of the 40 kilowatt fuel cell system field test operation
[COE/NASA/2701-1] p0137 N82-29721
- ENVIRONMENT MODELS**
Environmentally induced discharges on satellites
[NASA-TM-82849] p0038 N82-23261
- ENVIRONMENT PROTECTION**
Advanced technology for controlling pollutant emissions from supersonic cruise aircraft
p0001 N81-18004
- ENVIRONMENT SIMULATION**
NT ACOUSTIC SIMULATION
NT SPACE ENVIRONMENT SIMULATION
Agreement for NASA/OAST - USAF/AISC space interdependency on spacecraft environment interaction
p0038 N82-14271
- ENVIRONMENT SIMULATORS**
NT SOLAR SIMULATORS
- ENVIRONMENTAL CONTROL**
Environmental control systems
p0001 N82-19147
- ENVIRONMENTAL MONITORING**
LANDSAT Remote Sensing: Observations of an Appalachian mountaintop surface coal mining and reclamation operation --- Kentucky
[82-10247] p0117 N82-24525
- ENVIRONMENTAL QUALITY**
An automated system for global atmospheric sampling using D-747 airliners
[NASA-CF-165264] p0139 N82-13554
- ENVIRONMENTAL TESTS**
NT COLD WEATHER TESTS
NT CORROSION TESTS
NT HIGH TEMPERATURE TESTS
NT LOW TEMPERATURE TESTS
Environmental effects on defect growth in composite materials
[NASA-CR-165213] p0052 N82-20248
Effects of environment on microhardness of magnesium oxide
[NASA-TP-2002] p0068 N82-22366
- ENVIRONMENTS**
NT AEROSPACE ENVIRONMENTS
NT CUFOMOSPHERE
NT DEEP SPACE
NT HIGH TEMPERATURE ENVIRONMENTS
NT ICE ENVIRONMENTS
NT INTERPLANETARY SPACE
NT LOW TEMPERATURE ENVIRONMENTS
NT MESOSPHERE
- EPITAXY**
NT VAPOR PHASE EPITAXY
- EPOXY MATRIX COMPOSITES**
Durability/life of fiber composites in hydrothermomechanical environments
[NASA-TM-82749] p0049 N82-14287
Prediction of composite hygral behavior made simple
[NASA-TM-82780] p0049 N82-16181
- EPOXY RESINS**
Tribological characteristics of a composite total-surface hip replacement
[NASA-TP-1853] p0066 N82-16239
- EQUATIONS OF MOTION**
NT EULER EQUATIONS OF MOTION
NT HELMHOLTZ VORTICITY EQUATION
NT NAVIER-STOKES EQUATION
NT BENOULES EQUATION
Basic lubrication equations
[NASA-TM-81693] p0099 N82-16413
- EQUILIBRIUM DIAGRAMS**
U ASE DIAGRAMS
- EQUIVALENT CIRCUITS**
Comparison of NASCAP modelling results with lumped circuit analysis
p0037 N82-14255
- ERRECTION**
U NSTRUCTION
- EROSION**
A study of the nature of solid particle impact and shape on the erosion morphology of ductile metals
[NASA-TM-82933] p0061 N82-33493
- EROR ANALYSIS**
Conversion and matched filter approximations for serial minimum-shift keyed modulation
p0080 N82-26713
- ESTERS**
Effects of nadic ester concentration and processing on physical and mechanical properties of PBR/Celion 6000 composites
p0051 N82-27440
Forced torsional properties of PBR composites with varying nadic ester concentrations and processing histories
p0051 N82-45630
Improved boundary lubrication with formulated C-ethers
[NASA-TM-82808] p0067 N82-20313
- ESTIMATES**
NT COST ESTIMATES
- ESTIMATING**
NT PARAMETER IDENTIFICATION
- ETHERS**
NT POLYPHENYL ETHER
Thermal and oxidative degradation studies of formulated C-ethers by gel-permeation chromatography
[NASA-TP-1994] p0068 N82-21332
Thermal oxidative degradation reactions of linear perfluoroalkyl ethers
[NASA-TM-82834] p0068 N82-26468
- EUCLIDEAN GEOMETRY**
NT ANGLE OF ATTACK
NT RECTANGLES
NT TANGENTS
- EULER EQUATIONS OF MOTION**
A finite element formulation of Euler equations for the solution of steady transonic flows
[AIAA PAPER 82-0062] p0009 N82-17759
Application of a finite element algorithm for the solution of steady transonic Euler equations
[AIAA PAPER 82-0970] p0010 N82-31929
Comparison of two and three dimensional flow computations with laser anemometer measurements in a transonic compressor motor
[NASA-TM-82777] p0004 N82-15020
Multiple-grid acceleration of Lax-Wendroff algorithms
[NASA-TM-82843] p0149 N82-22922
Relaxation solution of the full Euler equations
[NASA-TM-82889] p0149 N82-24859
- EUTECTIC ALLOYS**
Fatigue of Ni-Al-Mo aligned eutectics at elevated temperatures
p0052 N82-13403
Structure and creep rupture properties of directionally solidified eutectic gamma/gamma-prime alloy
p0062 N82-42774
- EUTECTIC COMPOSITES**
High temperature composites. Status and future directions
[NASA-TM-82929] p0051 N82-30336
- EUTECTIC DIAGRAMS**
U ASE DIAGRAMS
- EUTECTICS**
NT EUTECTIC ALLOYS
- EVALUATION**
Investigation and evaluation of a computer program to minimize three-dimensional flight track
[NASA-CR-168419] p0144 N82-17879
Tribological evaluation of composite materials made from a partially fluorinated polyimide
[NASA-TM-82832] p0069 N82-29459
- EVAPORATION**
NT PROPELLANT EVAPORATION
- EVAPORATIVE COOLING**
NT FILM COOLING
NT SWEAT COOLING
- EXCHANGING**
NT CHARGE EXCHANGE
- EXECUTIVE AIRCRAFT**
U HERAL AVIATION AIRCRAFT
U SSENGER AIRCRAFT
- EXHAUST EMISSION**
Experimental study of the effects of secondary air on the emissions and stability of a lean premixed combustor
[AIAA PAPER 82-1072] p0021 N82-34992

- Combustor development for automotive gas turbines
 [AIAA PAPER 82-1206] p0104 A82-35062
 AOT-102 automotive gas turbine
 [NASA-CR-165353] p0105 A82-12444
 Effect of fuel-air-ratio nonuniformity on
 emissions of nitrogen oxides
 [NASA-TD-1790] p0016 A82-13143
 Exhaust emissions survey of a turbofan engine for
 flame holder swirl type augmentors at simulated
 altitude flight conditions
 [NASA-TM-82707] p0019 A82-25255
 Low NOx heavy fuel combustor concept program
 phase IA gas tests
 [NASA-CR-167477] p0055 A82-25337
 Low NOx heavy fuel combustor concept program
 addendum: Low/mid heating value gaseous fuel
 evaluation
 [NASA-CR-165615] p0055 A82-25338
 Low NOx heavy fuel combustor concept program
 [NASA-CR-167476] p0074 A82-26482
 Exhaust emissions reduction for intermittent
 combustion aircraft engines
 [NASA-CR-167914] p0029 A82-33392
- EXHAUST FLOW SIMULATION**
NT FLIGHT SIMULATION
- EXHAUST CASES**
 Effect of vacuum exhaust pressure on the
 performance of HMD ducts at high B-field
 [AIAA PAPER 82-0396] p0157 A82-20292
 Advanced technology for controlling pollutant
 emissions from supersonic cruise aircraft
 p0001 A81-18004
 ERBS fuel addendum: Pollution reduction
 technology program small jet aircraft engines,
 phase J
 [NASA-CR-165387] p0024 A82-14096
 Fuel economy and exhaust emissions characteristics
 of diesel vehicles: Test results of a prototype
 Fiat 131TC 2.4 liter automobile
 [NASA-CR-165535] p0164 A82-18068
 Exhaust emissions survey of a turbofan engine for
 flame holder swirl type augmentors at simulated
 altitude flight conditions
 [NASA-TM-82707] p0019 A82-25255
 Low NOx heavy fuel combustor concept program
 [NASA-CR-165367] p0136 A82-25635
 Low pressure fluidized-bed combustion
 program. Data and calculated results
 [NASA-TM-81767] p0124 A82-30704
 Venturi nozzle effects on fuel drop size and
 nitrogen oxide emissions
 [NASA-TP-2020] p0020 A82-31329
 Exhaust gas measurements in a propane fueled swirl
 stabilized combustor
 [NASA-CR-169293] p0091 A82-31641
- EXHAUST JETS**
U HAUST GASKS
- EXHAUST NOZZLES**
 Energy efficient engine exhaust mixer model
 technology
 [NASA-CR-165459] p0025 A82-22264
 Pressure transfer function of a JT15D nozzle due
 to acoustic and convected entropy fluctuations
 [NASA-TM-82842] p0152 A82-22951
 Performance of a 2D-CD nonaxisymmetric exhaust
 nozzle on a turbojet engine at altitude
 [NASA-TM-82801] p0005 A82-26241
- EXHAUST SYSTEMS**
 Energy efficient engine exhaust mixer model
 technology
 [NASA-CR-165459] p0025 A82-22264
 Computer modeling of fan-exit-splitter spacing
 effects on F100 response to distortion
 [NASA-CR-167879] p0025 A82-23246
- EXPANSION**
NT THERMAL EXPANSION
- EXPANSION WAVES**
U ASTIC WAVES
- EXPERIMENTATION**
 Effect of location in an array on heat transfer to
 a cylinder in crossflow
 [NASA-TM-82797] p0087 A82-19493
- EXPLODING CONDUCTOR CIRCUITS**
U RCUITS
- EXPORTS**
U TERNATIONAL TRADE
- EXPULSION**
 Low-thrust chemical propulsion system propellant
 expulsion and thermal conditioning study.
- Executive summary
 [NASA-CR-165622] p0045 A82-24287
 Low-thrust chemical propulsion system propellant
 expulsion and thermal conditioning study
 [NASA-CR-167841] p0045 A82-24288
- EXTERNALLY BLOWN FLAPS**
 Aeroacoustic performance of an externally blown
 flap configuration with several flap noise
 suppression devices
 [NASA-TP-1995] p0152 A82-24942
- EXTINCTION**
 Lean-limit extinction of propane/air mixtures in
 the stagnation-point flow
 p0057 A82-28736
- EXTRAPOLATION**
 Acceleration of convergence of vector sequences
 [NASA-TM-82931] p0149 A82-29075
- EXTRATERRESTRIAL ENVIRONMENTS**
NT CHROMOSPHERE
NT DEEP SPACE
NT INTERPLANETARY SPACE
EXTRATERRESTRIAL RADIATION
NT SOLAR RADIO BURSTS
NT SOLAR RADIO EMISSION
NT SOLAR X-RAYS
NT SUNLIGHT
EXTRATERRESTRIAL RADIO WAVES
NT SOLAR RADIO BURSTS
NT SOLAR RADIO EMISSION
EXTRATERRESTRIAL RESOURCES
 A small scale lunar launcher for early lunar
 material utilization
 p0032 A82-35617
- EXTREMELY HIGH FREQUENCIES**
 Advanced 30/20 GHz communication satellites
 p0034 A82-12623
- EYE (ANATOMY)**
 Vailing glare reduction methods compared for
 ophthalmic applications
 p0143 A82-13289
- F**
- FAB (PROGRAMMING LANGUAGE)**
U RTRAN
- FABRICATION**
NT SPACE MANUFACTURING
 Programs in ceramic component fabrication technology
 [AIAA PAPER 82-1211] p0071 A82-35064
 Net shape fabrication of Alpha Silicon Carbide
 turbine components
 [AEM PAPER 82-GT-216] p0071 A82-35403
 Solar cell development for the power extension
 package
 [NASA-TM-82685] p0118 A82-11551
 Cell module and fuel conditioner development
 [NASA-CR-165462] p0130 A82-13511
 Technology development for phosphoric acid fuel
 cell powerplant, phase 2
 [NASA-CR-165426] p0131 A82-16482
 High voltage power transistor development
 [NASA-CR-165547] p0084 A82-18506
 Energy efficient engine shroudless, hollow fan
 blade technology report
 [NASA-CR-165586] p0024 A82-21196
 Cell module and fuel conditioner development
 [NASA-CR-165620] p0134 A82-21713
 Advanced inorganic separators for alkaline batteries
 [NASA-CASE-LNW-13171-1] p0124 A82-29708
 Method of making a high voltage V-groove solar cell
 [NASA-CASE-LNW-13401-1] p0124 A82-29709
- FACE CENTERED CUBIC LATTICES**
 The influence of gamma prime on the
 recrystallization of an oxide dispersion
 strengthened superalloy - AA 6008
 p0062 A82-47393
 The influence of cobalt on the microstructure of
 the nickel-base superalloy MAR-M247
 p0063 A82-47400
- FADING**
NT SIGNAL FADING
- FAILURE**
NT ENGINE FAILURE
NT STRUCTURAL FAILURE
NT SYSTEM FAILURES
- FAILURE ANALYSIS**
 Model degradation effects on sensor failure
 detection
 p0148 A82-13143

Failure analysis of a tool steel torque shaft
[NASA-TM-82758] p0058 N82-11184

FAILURE MODES

Reusable rocket engine maintenance study
[NASA-CR-165569] p0044 N82-16172

Failure mechanisms of thermal barrier coatings
exposed to elevated temperatures
[NASA-TM-82905] p0061 N82-32461

FAIRINGS

Kevlar/PHR-15 polyimide matrix composite for a
complex shaped DC-9 drag reduction fairing
[AIAA PAPER 82-1047] p0002 A82-37679

FAN BLADES

Effects of vane/blade ratio and spacing on fan noise
[AIAA PAPER 81-2033] p0029 A82-10457

Three dimensional turbulent boundary layer
development on a fan rotor blade
[AIAA PAPER 82-1007] p0011 A82-31965

Blade loss transient dynamic analysis of
turbomachinery
[AIAA PAPER 82-1057] p0030 A82-34982

Structural dynamics of shroudless, hollow, fan
blades with composite in-lays
[ASME PAPER 82-GT-284] p0022 A82-35456

Thrust modulation methods for a subsonic V/STOL
aircraft
[NASA-TM-82747] p0003 N82-13112

Structural dynamics of shroudless, hollow fan
blades with composite in-lays
[NASA-TM-82816] p0018 N82-22266

Bird impact analysis package for turbine engine
fan blades
[NASA-TM-82831] p0112 N82-26701

Structural tailoring of engine blades (STAEBL)
[NASA-CR-167949] p0028 N82-33391

FAR ULTRAVIOLET RADIATION

Testing of a spacecraft model in a combined
environment simulator
[NASA-TM-82723] p0037 N82-11106

FARM CROPS

NT GRAINS (FOOD)

FATIGUE (MATERIALS)

NT BENDING FATIGUE
NT METAL FATIGUE
NT THERMAL FATIGUE

Endurance test and evaluation of alkaline water
electrolysis cells
[NASA-CR-165424] p0130 N82-13508

Interlaminar crack growth in fiber reinforced
composites during fatigue, part 3
[NASA-CR-165434] p0114 N82-26715

FATIGUE DIAGRAMS

U N DIAGRAMS

FATIGUE LIFE

Comparative thermal fatigue resistance of several
oxide dispersion strengthened alloys
p0062 A82-11399

Turbine blade nonlinear structural and life analysis
[AIAA PAPER 82-1056] p0021 A82-34981

A simplified design procedure for life prediction
of rocket thrust chambers
[AIAA PAPER 82-1251] p0043 A82-35067

Elevated temperature fatigue testing of metals
p0058 N82-13281

The application of probabilistic design theory to
high temperature low cycle fatigue
[NASA-CR-165486] p0112 N82-14531

Elevated temperature fatigue testing of metals
[NASA-TM-82745] p0111 N82-16419

Stress evaluations under rolling/sliding contacts
[NASA-CR-165561] p0113 N82-17521

Fatigue life prediction in bending from axial
fatigue information
[NASA-CR-165563] p0113 N82-20564

Development of a simplified procedure for thrust
chamber life prediction
[NASA-CR-165585] p0044 N82-21253

High temperature low cycle fatigue mechanisms for
nickel base and a copper base alloy
[NASA-CR-3543] p0064 N82-26436

Effect of shot peening on surface fatigue life of
carburized and hardened AISI 9310 spur gears
[NASA-IP-2047] p0102 N82-32736

FATIGUE TESTS

Effects of ultra-clean and centrifugal filtration
on rolling-element bearing life
[ASME PAPER 81-LUB-35] p0103 A82-18436

Elevated temperature fatigue testing of metals
p0058 N82-13281

Fatigue tests with a corrosive environment
N82-13282

Mechanisms of deformation and fracture in high
temperature low cycle fatigue of Rene 80 and IN
100
[NASA-CR-165498] p0113 N82-26706

FAULT MECHANICS

U ACTURE MECHANICS

FAULT TOLERANCE

Design and verification of a multiple fault
tolerant control system for STS applications
using computer simulation
[AIAA 81-2173] p0035 A82-10124

FCC LATTICES

U CE CENTERED CUBIC LATTICES

FDNA

U EQUENCY DIVISION MULTIPLE ACCESS

FEASIBILITY ANALYSIS

Feasibility of an earth-to-space rail launcher
system --- emphasizing nuclear waste disposal
application
[IAF PAPER 82-46] p0033 A82-44659

An experimental investigation into the feasibility
of a thermoelectric heat flux gage
[NASA-TM-82755] p0095 N82-14494

FEEDBACK CONTROL

Open-loop nanosecond-synchronization for wideband
satellite communications
p0036 A82-27224

Analysis and design of a standardized control
module for switching regulators
p0083 A82-46388

Identification of multivariable high performance
turbofan engine dynamics from closed loop data
[NASA-TM-82785] p0076 N82-20339

AESOP: A computer-aided design program for linear
multivariable control systems
[NASA-TM-82871] p0148 N82-30992

FEEDING (SUPPLYING)

Input filter compensation for switching regulators
[NASA-CR-169005] p0085 N82-25442

FERROALLOYS

U OM ALLOYS

FERROELECTRICITY

Raman study of the improper ferroelectric phase
transition in iron iodine boracite
A82-30297

Study of the photovoltaic effect in thin film
barium titanate
[NASA-CR-165081] p0131 N82-16479

FERROGRAPHY

Elucidation of wear mechanisms by ferrographic
analysis
[NASA-TM-82737] p0066 N82-15199

FERROUS METALS

Friction and surface chemistry of some
ferrous-base metallic glasses
[NASA-TP-1991] p0059 N82-21301

FET (TRANSISTORS)

U ELD EFFECT TRANSISTORS

FIBER COMPOSITES

NT CARBON FIBER REINFORCED PLASTICS
NT GLASS FIBER REINFORCED PLASTICS

Sensitivity analysis results of the effects of
various parameters on composite design
p0051 A82-37101

Durability/life of fiber composites in
hygrothermomechanical environments
[NASA-TM-82749] p0049 N82-14287

Prediction of composite hygral behavior made simple
[NASA-TM-82780] p0049 N82-16181

Environmental effects on defect growth in
composite materials
[NASA-CR-165213] p0052 N82-20248

Compression behavior of unidirectional fibrous
composite
[NASA-TM-82833] p0050 N82-23313

FIBER OPTICS

The 30/20 GHz communications satellite trunking
network study
[NASA-CR-165467] p0078 N82-13302

Role of optical computers in aeronautical control
applications
p0156 N82-15897

Preliminary study, analysis and design for a power
switch for digital engine actuators
[NASA-CR-159559] p0085 N82-23394

FIBER ORIENTATION

Compression behavior of unidirectional fibrous

composites [NASA-TM-82833] p0050 N82-22313

FIBER REINFORCED COMPOSITES

On determination of fibre fraction in continuous fibre composite materials p0051 A82-38133

Forced torsional properties of FRP composites with varying nadic ester concentrations and processing histories p0051 A82-45630

Tensile properties of SiC/aluminum filamentary composites - Thermal degradation effects p0053 A82-46220

Boundary-layer effects in composite laminates. I - Free-edge stress singularities. II - Free-edge stress solutions and basic characteristics p0116 A82-46806

Geometrical aspects of the tribological properties of graphite fiber reinforced polyimide composites [NASA-TM-82757] p0066 N82-15198

Tungsten fiber reinforced superalloy composite high temperature component design considerations [NASA-TM-82811] p0049 N82-21259

Thermal degradation of the tensile properties of unidirectionally reinforced FP-AI203/EZ 33 magnesium composites [NASA-TM-82817] p0049 N82-21260

Designing with fiber-reinforced plastics (planar random composites) [NASA-TM-82812] p0050 N82-24300

Analysis of cracks emanating from a circular hole in unidirectional fiber reinforced composites, part 2 [NASA-CR-165433] p0114 N82-26714

Interlaminar crack growth in fiber reinforced composites during fatigue, part 3 [NASA-CR-165434] p0114 N82-26715

Edge delamination in angle-ply composite laminates, part 5 [NASA-CR-165439] p0114 N82-26717

Boundary-layer effects in composite laminates: Free-edge stress singularities, part 6 [NASA-CR-165440] p0114 N82-26718

Modulus, strength and thermal exposure studies of FP-AI203/aluminum and FP-AI203/magnesium composites [NASA-TM-82868] p0050 N82-30335

High temperature composites. Status and future directions [NASA-TM-82929] p0051 N82-30336

FIBER RELEASE

Hybridized polymer matrix composite [NASA-CR-165340] p0051 N82-12139

FIBRE STRENGTH

Tensile properties of SiC/aluminum filamentary composites - Thermal degradation effects p0053 A82-46220

Indentation law for composite laminates [NASA-CR-165460] p0052 N82-15123

Strength advantages of chemically polished boron fibers before and after reaction with aluminum [NASA-TM-82806] p0049 N82-21258

Method and apparatus for strengthening boron fibers --- high temperature oxidation [NASA-CASE-LEW-13826-1] p0050 N82-26385

FIBERGLASS

U AES FIBERS

FIBERS

NT BORON FIBERS

NT GLASS FIBERS

NT HAIR

NT REINFORCING FIBERS

FIELD EFFECT TRANSISTORS

Low temperature growth and electrical characterization of insulators for GaAs MISFETS [NASA-CR-164972] p0159 N82-11959

FIELD THEORY (PHYSICS)

Electric and magnetic fields [NASA-CR-165604] p0045 N82-28350

FIGHTER AIRCRAFT

NT BARRIER AIRCRAFT

FILAMENTS (SOLAR PHYSICS)

U LAR PROMINENCES

FILLETS

A finite element stress analysis of spur gears including fillet radii and rim thickness effects [NASA-TM-82865] p0101 N82-28646

On finite element stress analysis of spur gears [NASA-CR-167938] p0107 N82-29607

FILM COOLING

Covering solid, film cooled surfaces with a duplex thermal barrier coating [NASA-CASE-LEW-13450-1] p0088 N82-25463

FILM THICKNESS

Alignment of fluid molecules in an EHD contact [ASLE PREPRINT 81-LC-5C-1] p0107 A82-18407

Measurement of oil film thickness for application to elastomeric Stirling engine rod seals [ASME PAPER 81-LUB-9] p0107 A82-18426

Effects of artificially produced defects on film thickness distribution in sliding EHD point contacts [NASA-TM-82732] p0099 N82-16412

Geometry and starvation effects in hydrodynamic lubrication [NASA-TM-82807] p0042 N82-20240

Lubrication of rigid ellipsoidal solids [NASA-TM-81694] p0100 N82-25518

FILTRING

U LTRATION

FILTRATION

Effects of ultra-clean and centrifugal filtration on rolling-element bearing life [ASME PAPER 81-LUB-35] p0103 A82-18436

FINISHES

NT GLAZES

FINITE DIFFERENCE THEORY

A simple finite difference procedure for the vortex controlled diffuser [AIAA PAPER 82-0109] p0030 A82-17788

Bluff-body flameholder wakes - A simple numerical solution [AIAA PAPER 82-1177] p0093 A82-35043

Numerical techniques in linear duct acoustics, 1980-81 update [NASA-TM-82730] p0151 N82-12890

Application of steady state finite element and transient finite difference theory to sound propagation in a variable area duct: A comparison with experiment [NASA-TM-82678] p0151 N82-15847

Turbofan forced mixer-nozzle internal flowfield. Volume 3: A computer code for 3-D mixing in axisymmetric nozzles [NASA-CR-3494] p0091 N82-22460

FINITE ELEMENT METHOD

Acoustic transmission in lined flow ducts - A finite element eigenvalue problem p0154 A82-17663

A finite element formulation of Euler equations for the solution of steady transonic flows [AIAA PAPER 82-0062] p0009 A82-17759

An iterative finite element-integral technique for predicting sound radiation from turbofan inlets in steady flight [AIAA PAPER 82-0124] p0030 A82-17796

Application of a finite element algorithm for the solution of steady transonic Euler equations [AIAA PAPER 82-0970] p0010 A82-31939

Engine dynamic analysis with general nonlinear finite element codes. II - Bearing element implementation, overall numerical characteristics and benchmarking [ASME PAPER 82-GT-292] p0108 A82-35462

Investigation of rotational transonic flows through ducts using a finite element scheme [AIAA PAPER 82-1267] p0012 A82-37711

On the automatic generation of FEM models for complex gears - A work-in-progress report p0109 A82-48243

A multi-purpose method for analysis of spur gear tooth loading [NASA-CR-165163] p0104 N82-10401

Numerical techniques in linear duct acoustics, 1980-81 update [NASA-TM-82730] p0151 N82-12890

Application of steady state finite element and transient finite difference theory to sound propagation in a variable area duct: A comparison with experiment [NASA-TM-82678] p0151 N82-15847

Research and development program for non-linear structural modeling with advanced time-temperature dependent constitutive relationships [NASA-CR-165533] p0024 N82-16080

Elastic-plastic finite-element analyses of thermally cycled double-edge wedge specimens

ORIGINAL PAGE IS OF POOR QUALITY

FINITE VOLUME METHOD

SUBJECT INDEX

- [NASA-TP-1973] p0111 N82-20566
 Nonlinear structural and life analyses of a combustor liner [NASA-TM-82846] p0111 N82-24501
 A finite element stress analysis of spur gears including fillet radii and rim thickness effects [NASA-TM-82865] p0101 N82-28646
 Finite element-integral simulation of static and flight fan noise radiation from the JT15D turbofan engine [NASA-TM-82936] p0152 N82-31068
 Large displacements and stability analysis of nonlinear propeller structures [NASA-TM-82850] p0112 N82-31707
- FINITE VOLUME METHOD**
 Finite volume calculation of three-dimensional potential flow around a propeller [AIAA PAPER 82-0957] p0010 A82-31933
- FIRE PREVENTION**
 An assessment of the crash fire hazard of liquid hydrogen fueled aircraft [NASA-CF-165526] p0013 N82-19196
- FIRES**
 Hybridized polymer matrix composite [NASA-CF-165340] p0051 N82-12139
- FISHTAILING**
 U W
- FISSION**
 Evidence for Pu-244 fission tracks in hibonites from Murchison carbonaceous chondrite p0166 A82-29316
- FIXED-WING AIRCRAFT**
 U AIRCRAFT CONFIGURATIONS
- FLAME FRONTS**
 U FLAME PROPAGATION
- FLAME HOLDERS**
 Experimental study of the effects of secondary air on the emissions and stability of a lean premixed combustor [AIAA PAPER 82-1072] p0021 A82-34992
 Bluff-body flameholder wakes - A simple numerical solution [AIAA PAPER 82-1177] p0093 A82-35043
- FLAME INTERACTION**
 U CHEMICAL REACTIONS
 U FLAME PROPAGATION
- FLAME PROPAGATION**
 Secondary effects in combustion instabilities leading to flashback [AIAA PAPER 82-0037] p0056 A82-17746
 Numerical modelling of turbulent flow in a combustion tunnel p0093 A82-27000
 Flame structure in a swirl stabilized combustor inferred by radiant emission measurements p0056 A82-28694
 Numerical modeling of turbulent combustion in premixed gases p0056 A82-28708
 Effects of heat loss, preferential diffusion, and flame stretch on flame-front instability and extinction of propane/air mixtures p0057 A82-32877
 On the opening of premixed Bunsen flame tips p0057 A82-37570
 On stability of premixed flames in stagnation - Point flow p0057 A82-37574
 Buoyancy effects on the temperature field in downward spreading flames p0094 A82-41203
- FLAME STABILITY**
 Flame structure in a swirl stabilized combustor inferred by radiant emission measurements p0056 A82-28694
 Lean-limit extinction of propane/air mixtures in the stagnation-point flow p0057 A82-28736
 Effects of heat loss, preferential diffusion, and flame stretch on flame-front instability and extinction of propane/air mixtures p0057 A82-32877
 On stability of premixed flames in stagnation - Point flow p0057 A82-37574
 The premixed flame in uniform straining flow p0055 A82-43194
- FLAME TEMPERATURE**
 Effects of heat loss, preferential diffusion, and flame stretch on flame-front instability and extinction of propane/air mixtures p0057 A82-32877
 Buoyancy effects on the temperature field in downward spreading flames p0094 A82-41203
- FLAMES**
 NT DIFFUSION FLAMES
 NT PREMIXED FLAMES
- FLAMMABILITY**
 Resonance tube hazards in oxygen systems [NASA-TM-82801] p0072 N82-21415
- FLAMMABLE GASES**
 NT GASEOUS FUELS
 NT LIQUEFIED NATURAL GAS
- FLAP CONTROL**
 U AIRCRAFT CONTROL
- FLAPS (CONTROL SURFACES)**
 NT EXTERNALLY BLOWN FLAPS
- FLASHBACK**
 Secondary effects in combustion instabilities leading to flashback [AIAA PAPER 82-0037] p0056 A82-17746
- FLASHING (VAPORIZING)**
 Atomization and combustion properties of flashing injectors [AIAA PAPER 82-0300] p0092 A82-17880
 Experimental study of external fuel vaporization [ASME PAPER 82-GT-59] p0075 A82-35312
 External fuel vaporization study [NASA-CR-165513] p0073 N82-14371
 Investigation of spray characteristics for flashing injection of fuels containing dissolved air and superheated fuels [NASA-CR-3563] p0027 N82-26295
- FLAT PLATES**
 Two dimensional stagnation point flow of a dusty gas near an oscillating plate p0012 A82-37535
- FLAWS**
 U DEFECTS
- FLEXING**
 Thermal degradation of the tensile properties of unidirectionally reinforced PP-AI203/EZ 33 magnesium composites [NASA-TM-82817] p0049 N82-21260
- FLEXURE**
 U BENDING
- FLIGHT CONTROL**
 NT THRUST VECTOR CONTROL
 A tensor approach to modeling of nonhomogeneous nonlinear systems p0148 A82-19064
- FLIGHT PLANS**
 The NASA MERIT program - Developing new concepts for accurate flight planning [AIAA PAPER 82-0340] p0014 A82-17894
 Investigation and evaluation of a computer program to minimize three-dimensional flight time tracks [NASA-CR-168419] p0145 N82-17879
 Ozone and aircraft operations p0001 N82-21145
- FLIGHT SIMULATION**
 A real time Pegasus propulsion system model for VSTOL piloted simulation evaluation [AIAA PAPER 81-2663] p0020 A82-19221
- FLIGHT SIMULATORS**
 A real time Pegasus propulsion system model for VSTOL piloted simulation evaluation [NASA-TM-82770] p0016 N82-13144
- FLIGHT TESTS**
 Measuring the spacecraft and environmental interactions of the 8-cm mercury ion thrusters on the P80-1 mission p0043 A82-15438
 In-flight acoustic results from an advanced-design propeller at Mach numbers to 0.8 [AIAA PAPER 82-1120] p0021 A82-35017
 A preliminary comparison between the SR-3 propeller noise in flight and in a wind tunnel [NASA-TM-82805] p0152 N82-21998
- FLIGHT TIME**
 Investigation and evaluation of a computer program to minimize three-dimensional flight time tracks [NASA-CR-168419] p0145 N82-17879
- FLOOD PREDICTIONS**
 Dynamics of snow cover in mountain regions of the Aral Sea basin, studied using satellite photographs

- AR2- 27462
- FLOQUET THEOREM**
Review of analysis methods for rotating systems with periodic coefficients p0135 N82-23702
- FLOW CHARACTERISTICS**
- NT BOUNDARY LAYER STABILITY**
NT FLAME STABILITY
NT FLOW DISTRIBUTION
NT FLOW STABILITY
NT FLOW VELOCITY
- Characteristics of the flow in the annulus-wall region of an axial-flow compressor rotor blade passage [AIAA PAPER 82-0413] p0009 A82-17933
- Novel improved PMR polyimides [NASA-TM-82733] p0049 N82-11117
- Mode propagation in nonuniform circular ducts with potential flow [NASA-TM-82766] p0151 N82-14881
- Calculation of the flow field including boundary layer effects for supersonic mixed compression inlets at angles of attack [NASA-CR-167941] p0009 N82-29269
- FLOW CHARTS**
Interactive-graphic flowpath plotting for turbine engines [NASA-TM-82756] p0017 N82-15041
- FLOW COEFFICIENTS**
NT DISCHARGE COEFFICIENT
- FLOW DIRECTION INDICATORS**
Miniature drag-force anemometer p0097 A82-40132
- FLOW DISTORTION**
Distorted turbulence in axisymmetric flow p0089 A82-16071
- FLOW DISTRIBUTION**
The effect of inflow velocity profiles on the performance of supersonic ejector nozzles [AIAA PAPER 81-0273] p0002 A81-32548
- On the prediction of swirling flowfields found in axisymmetric combustor geometries p0029 A82-12120
- Mean flowfields in axisymmetric combustor geometries with swirl [AIAA PAPER 82-0177] p0092 A82-17824
- Three-dimensional flow calculations including boundary layer effects for supersonic inlets at angle of attack [AIAA PAPER 82-0061] p0005 A82-19778
- Numerical analysis of confined turbulent flow p0093 A82-24748
- In-flight acoustic results from an advanced-design propeller at Mach numbers to 0.8 [AIAA PAPER 82-1120] p0021 A82-35017
- Small gas turbine combustor primary zone development [AIAA PAPER 82-1159] p0103 A82-35036
- Three-dimensional flow field in the tip region of a compressor rotor passage. I - Mean velocity profiles and annulus wall boundary layer [ASME PAPER 82-GT-11] p0011 A82-35280
- Flow distributions and discharge coefficient effects for jet array impingement with initial crossflow [ASME PAPER 82-GT-156] p0011 A82-35379
- Turbulence measurements in a confined jet using a six-orientation hot-wire probe technique [AIAA PAPER 82-1262] p0094 A82-37710
- Interaction of upstream flow distortions with high Mach number cascades [NASA-TM-E2759] p0003 N82-12043
- Core compressor exit stage study. Volume 4: Data and performance report for the best stage configuration [NASA-CR-165357] p0023 N82-14092
- Core compressor exit stage study. Volume 5: Design and performance report for the Rotor C/Stator B configuration [NASA-CR-165358] p0023 N82-14093
- Investigations of flowfields found in typical combustor geometries [NASA-CR-165061] p0090 N82-15360
- Investigations of flowfields found in typical combustor geometries [NASA-CR-168585] p0090 N82-19495
- Turbofan forced mixer-nozzle internal flowfield. Volume 1: A benchmark experimental study [NASA-CR-3492] p0090 N82-22458
- Turbofan forced mixer-nozzle internal flowfield. Volume 2: computational fluid dynamic predictions [NASA-CR-3493] p0091 N82-22459
- Investigation of the tip clearance flow inside and at the exit of a compressor rotor passage [NASA-CR-169004] p0026 N82-25253
- A FORTRAN program for calculating three dimensional, inviscid and rotational flows with shock waves in axial compressor blade rows: User's manual [NASA-CR-3560] p0008 N82-26230
- Three dimensional flow field inside compressor rotor, including blade boundary layers [NASA-CR-169120] p0091 N82-27686
- Turbine endwall single cylinder program [NASA-CR-169278] p0091 N82-31638
- Investigations of flowfields found in typical combustor geometries [NASA-CR-169295] p0092 N82-31643
- Development and utilization of a laser velocimeter system for a large transonic wind tunnel [NASA-TM-82886] p0095 N82-31663
- Propeller flow visualization techniques p0096 N82-32672
- LV measurements with an advanced turboprop p0097 N82-32690
- FLOW EQUATIONS**
NT HELMHOLTZ VORTICITY EQUATION
- A finite element formulation of Euler equations for the solution of steady transonic flows [AIAA PAPER 82-0062] p0009 A82-17759
- An example of a solution to transonic equations for shock-free flow about a symmetric profile A82-26439
- Development of a locally mass flux conservative computer code for calculating 3-D viscous flow in turbomachines [NASA-CR-3539] p0007 N82-22214
- Computer program for calculating full potential transonic, quasi-three-dimensional flow through a rotating turbomachinery blade row [NASA-TP-2030] p0005 N82-28247
- FLOW FIELDS**
FLOW DISTRIBUTION
- FLOW GEOMETRY**
Thermal and flow analysis of a convection, air-cooled ceramic coated porous metal concept for turbine vanes [ASME PAPER 81-HT-48] p0020 A82-10952
- Turbulent boundary layer heat transfer experiments - A separate effects study on a convexly-curved wall [ASME PAPER 81-HT-78] p0092 A82-10963
- Flow through axially aligned sequential apertures of the orifice and Borda types [ASME PAPER 81-HT-79] p0089 A82-10964
- Mean flowfields in axisymmetric combustor geometries with swirl [AIAA PAPER 82-0177] p0092 A82-17824
- Multi-grid simulation of asymptotic curved-duct flows using a semi-implicit numerical technique p0010 A82-29003
- Bluff-body flameholder wakes - A simple numerical solution [AIAA PAPER 82-1177] p0093 A82-35043
- A comprehensive method for preliminary design optimization of axial gas turbine stages [AIAA PAPER 82-1264] p0030 A82-35091
- The use of optimization techniques to design controlled diffusion compressor blading [ASME PAPER 82-GT-149] p0022 A82-35373
- The use of optimization techniques to design controlled diffusion compressor blading [NASA-TM-82763] p0016 N82-14094
- Investigations of flowfields found in typical combustor geometries [NASA-CR-165061] p0090 N82-15360
- FLOW MEASUREMENT**
Interaction of compressor rotor blade wake with wall boundary layer/vortex in the end-wall region [ASME PAPER 81-GT-11] p0010 A82-19301
- Three sensor hot wire/film technique for three dimensional mean and turbulence flow field measurement p0097 A82-30300
- Three dimensional flow field inside the passage of a low speed axial flow compressor rotor [AIAA PAPER 82-1006] p0011 A82-31964

Three dimensional turbulent boundary layer development on a fan rotor blade [AIAA PAPER 82-1007] p0011 A82-31965
Flow distributions and discharge coefficient effects for jet array impingement with initial crossflow [ASME PAPER 82-GT-156] p0011 A82-35379
Turbulence measurements in a confined jet using a six-orientation hot-wire probe technique [AIAA PAPER 82-1262] p0094 A82-37710
Miniature drag-force anemometer p0097 A82-40132
Extending the frequency of response of lightly damped second order systems: Application to the drag force anemometer [NASA-TM-82927] p0096 N82-32662
Status of laser anemometry in turbomachinery research at the Lewis Research Center p0096 N82-32686

FLOW PATTERNS

U ON DISTRIBUTION

FLOW RATE

U ON VELOCITY

FLOW SEPARATION

U ONDARY LAYER SEPARATION

U PARATED FLOW

FLOW STABILITY

NT BOUNDARY LAYER STABILITY

NT FLAME STABILITY

Nonlinear Marangoni convection in bounded layers.

I - Circular cylindrical containers, II -
Pectangular cylindrical containers p0094 A82-39501

FLOW THEORY

NT MIXING LENGTH FLOW THEORY

Distorted turbulence in axisymmetric flow p0089 A82-16071

FLOW VELOCITY

The effect of inflow velocity profiles on the performance of supersonic ejector nozzles [AIAA PAPER 81-0273] p0002 A81-32548

Flow through axially aligned sequential apertures of the orifice and Borda types [ASME PAPER 81-HT-79] p0089 A82-10964

Distorted turbulence in axisymmetric flow p0089 A82-16071

Secondary effects in combustion instabilities leading to flashback [AIAA PAPER 82-0037] p0056 A82-17746

Measurement and prediction of mean velocity and turbulence structure in the near wake of an airfoil p0010 A82-26137

Investigation of the tip-clearance flow inside and at the exit of a compressor rotor passage. I - Mean velocity field [ASME PAPER 82-GT-12] p0011 A82-35281

The velocity field near the orifice of a Helmholtz resonator in grazing flow [NASA-CR-168548] p0153 N82-18994

NASA Redox cell stack shunt current, pumping power, and cell performance tradeoffs [NASA-TM-82686] p0054 N82-19333

High-speed laser anemometer system for intrarotor flow mapping in turbomachinery [NASA-TF-1663] p0095 N82-19521

Flow through aligned sequential orifice type inlets [NASA-TP-1967] p0087 N82-20467

Performance mapping studies in Redox flow cells [NASA-TM-82707] p0120 N82-20668

Numerical modeling of three-dimensional confined flows [NASA-CR-165583] p0158 N82-24078

Three dimensional mean velocity and turbulence characteristics in the annulus wall region of an axial flow compressor rotor passage [NASA-CR-169003] p0026 N82-25252

Acoustic properties of turbfan inlets [NASA-CR-169016] p0153 N82-27090

Laser anemometer using a Fabry-Perot interferometer for measuring mean velocity and turbulence intensity along the optical axis in turbomachinery [NASA-TM-82841] p0095 N82-28605

Velocity gradient method for calculating velocities in an axisymmetric annular duct [NASA-TP-2029] p0005 N82-29270

FLOW VISUALIZATION

NT NUMERICAL FLOW VISUALIZATION

Flow through axially aligned sequential apertures of the orifice and Borda types [ASME PAPER 81-HT-79] p0089 A82-10964
Secondary effects in combustion instabilities leading to flashback [AIAA PAPER 82-0037] p0056 A82-17746
Application of image processing techniques to fluid flow data analysis [NASA-TM-82760] p0004 N82-16049
Shaded computer graphic techniques for visualizing and interpreting analytic fluid flow models [NASA-CR-168418] p0145 N82-17880
Fringe localization requirements for three-dimensional flow visualization of shock waves in diffuse-illumination double-pulse holographic interferometry [NASA-TP-1868] p0095 N82-22481
New versions of old flow visualization systems p0096 N82-32670
Propeller flow visualization techniques p0096 N82-32672
Flow visualization of shock-boundary layer interaction p0096 N82-32675

FLOWMETERS

NT HOT-WIRE FLOWMETERS

FLUID BOUNDARIES

NT LIQUID-SOLID INTERFACES

FLUID DYNAMICS

NT AERODYNAMICS

NT AEROTHERMODYNAMICS

NT COMPUTATIONAL FLUID DYNAMICS

NT CYLINDRICAL PLASMAS

NT ELASTOHYDRODYNAMICS

NT GAS DYNAMICS

NT HYDRODYNAMICS

NT MAGNETOHYDRODYNAMICS

NT ROTOR AERODYNAMICS

Eigenvalues of the Rayleigh-Benard and Marangoni

problems p0092 A82-13396

Effect of location in an array on heat transfer to

a cylinder in crossflow [NASA-TM-82797] p0087 N82-19493

FLUID FILMS

NT SQUEEZE FILMS

Measurement of oil film thickness for application

to elastomeric Stirling engine rod seals [ASME PAPER 81-LUB-9] p0107 A82-18426

FLUID FLOW

NT AIR FLOW

NT AIR JETS

NT ANNULAR FLOW

NT AXIAL FLOW

NT AXISYMMETRIC FLOW

NT BLASIUS FLOW

NT BOUNDARY LAYER FLOW

NT BOUNDARY LAYER SEPARATION

NT CAPILLARY FLOW

NT CASCADE FLOW

NT CAVITATION FLOW

NT CHANNEL FLOW

NT COAXIAL FLOW

NT COMBUSTIBLE FLOW

NT COMPRESSIBLE FLOW

NT CONVECTIVE FLOW

NT CORNER FLOW

NT CROSS FLOW

NT DUCTED FLOW

NT FUEL FLOW

NT GAS FLOW

NT INCOMPRESSIBLE FLOW

NT INLET FLOW

NT INVISCID FLOW

NT JET FLOW

NT LAMINAR FLOW

NT LIQUID FLOW

NT NONUNIFORM FLOW

NT NOZZLE FLOW

NT ORIFICE FLOW

NT OSCILLATING FLOW

NT PARALLEL FLOW

NT PIPE FLOW

NT POTENTIAL FLOW

NT PROPELLANT TRANSFER

NT RADIAL FLOW

NT RECIRCULATIVE FLUID FLOW

NT REVERSED FLOW

NT SECONDARY FLOW

- NT SEPARATED FLOW
 NT SHEAR FLOW
 NT STAGNATION FLOW
 NT STEADY FLOW
 NT SUBSONIC FLOW
 NT SUPERCRITICAL FLOW
 NT SUPERSONIC FLOW
 NT SUPERSONIC JET FLOW
 NT THREE DIMENSIONAL FLOW
 NT TRANSONIC FLOW
 NT TURBULENT FLOW
 NT TWO DIMENSIONAL FLOW
 NT TWO PHASE FLOW
 NT UNIFORM FLOW
 NT UNSTEADY FLOW
 NT VISCOUS FLOW
 NT WALL FLOW
 NT WATER FLOW
- Application of image processing techniques to
 Fluid flow data analysis
 [NASA-TM-82760] p0004 N82-16049
 A hydrodynamic model of an outer hair cell
 [NASA-TM-82773] p0143 N82-16743
 Shaded computer graphic techniques for visualizing
 and interpreting analytic fluid flow models
 [NASA-CR-168418] p0145 N82-1788A
 Investigations of flowfields found in typical
 combustor geometries
 [NASA-CR-168585] p0090 N82-19495
 Analytical investigation of nonrecoverable stall
 [NASA-TM-82792] p0018 N82-21195
 Experiments on fuel heating for commercial aircraft
 [NASA-TM-82878] p0072 N82-26483
- FLUID INJECTION**
 NT GAS INJECTION
- FLUID JETS**
 NT AIR JETS
 NT FREE JETS
- FLUID MECHANICS**
 NT AERODYNAMICS
 NT AEROTHERMODYNAMICS
 NT COMPUTATIONAL FLUID DYNAMICS
 NT CYLINDRICAL PLASMAS
 NT ELASTOHYDRODYNAMICS
 NT FLUID DYNAMICS
 NT GAS DYNAMICS
 NT HYDRODYNAMICS
 NT MAGNETOHYDRODYNAMICS
 NT ROTOF AERODYNAMICS
- Modified face seal for positive film stiffness
 [NASA-CASE-LEW-12989-1] p0099 N82-12442
 Flows through sequential orifices with heated
 spacer reservoirs
 [NASA-TM-82855] p0089 N82-24455
- FLUIDIZED BED PROCESSORS**
 Lewis Research Center's coal-fired, pressurized,
 fluidized-bed reactor test facility
 [NASA-TM-81616] p0087 N82-11397
 Elastic-plastic finite-element analyses of
 thermally cycled single-edge wedge specimens
 [NASA-TF-1982] p0111 N82-20565
 Lewis pressurized, fluidized-bed combustion
 program. Data and calculated results
 [NASA-TM-81767] p0124 N82-30704
 Catalytic combustion of actual low and medium
 heating value gases
 [NASA-TM-82930] p0125 N82-30717
- FLUORINATION**
 Technological evaluation of composite materials
 made from a partially fluorinated polyimide
 [NASA-TM-82832] p0069 N82-29459
- FLUORINE COMPOUNDS**
 NT FLUOROPOLYMERS
 NT POLYTETRAFLUOROETHYLENE
- FLUORINE ORGANIC COMPOUNDS**
 NT FLUOROPOLYMERS
- FLUORO COMPOUNDS**
 NT FLUOROPOLYMERS
 NT POLYTETRAFLUOROETHYLENE
- FLUOROPOLYMERS**
 NT POLYTETRAFLUOROETHYLENE
 NT TEFLON (TRADEMARK)
- Texturing polymer surfaces by transfer casting ---
 cardiovascular prosthesis
 [NASA-CASE-LEW-13120-1] p0068 N82-28440
 Surface texturing of fluoropolymers
 [NASA-CASE-LEW-13028-1] p0070 N82-33521
- FLUTTER**
 NT TRANSONIC FLUTTER
- Aeroelastic characteristics of a cascade of
 mistuned blades in subsonic and supersonic flows
 [ASME PAPER 81-DET-122] p0021 N82-19337
 Coupled bending-torsion flutter of a
 mistuned cascade with nonuniform blades
 [NASA-TM-82813] p0111 N82-21604
- FLUTTER ANALYSIS**
 Three-dimensional shock structure in a transonic
 flutter cascade
 p0006 N82-37937
 Solution of the unsteady subsonic thin airfoil
 problem
 p0012 N82-41267
- FLUX (RATE)**
 NT HEAT FLUX
FLUX DENSITY
 NT CURRENT DENSITY
 NT LUMINOUS INTENSITY
 NT RADIANT FLUX DENSITY
- FLUX MAPPING**
 U PPING
- FLOWMETERS**
 U ASURING INSTRUMENTS
FLYING PLATFORM STABILITY
 U DYNAMIC STABILITY
- FLYWHEELS**
 Development of a dual-field heteropolar power
 converter
 [NASA-CR-165168] p0084 N82-24424
- FOCUSING**
 Experimental verification of a computational
 procedure for the design of TWT-refocuser-MDC
 systems --- Multistage Depressed Collectors
 p0082 N82-16128
 Focal surfaces of offset dual-reflector antennas
 p0080 N82-36265
- FOG DISPERSAL**
 Design of prototype charged particle fog dispersal
 unit
 [NASA-CR-3481] p0141 N82-16659
- FOILS (MATERIALS)**
 NT METAL FOILS
 Thin foil silicon solar cells with coplanar back
 contacts
 p0127 N82-44944
- FOKKER BOND TESTERS**
 U HESION TESTS
- FORCE FIELDS**
 U ELD THEORY (PHYSICS)
- FORCED OSCILLATION**
 U RCED VIBRATION
- FORCED VIBRATION**
 The influence of Coriolis forces on gyroscopic
 motion of spinning blades
 [ASME PAPER 82-GT-163] p0030 N82-35384
 Review of analysis methods for rotating systems
 with periodic coefficients
 p0135 N82-23702
- FORCED VIBRATORY MOTION EQUATIONS**
 U RCED VIBRATION
- FORECASTING**
 NT PERFORMANCE PREDICTION
 NT PREDICTION ANALYSIS TECHNIQUES
 NT TECHNOLOGICAL FORECASTING
 NT WEATHER FORECASTING
- Ozone and aircraft operations
 p0001 N82-21145
 Worldwide satellite market demand forecast
 [NASA-CR-167918] p0079 N82-25423
- FORECASTS**
 U RECASTING
- FORM**
 U APES
- FORMING TECHNIQUES**
 NT CASTING
 NT INJECTION MOLDING
- FORTRAN**
 STGSK: A computer code for predicting multistage
 axial flow compressor performance by a meanline
 stage stacking method
 [NASA-TF-2020] p0018 N82-25250
- FOSSIL FUELS**
 NT COAL
 Collection and dissemination of thermal energy
 storage system information for the pulp and
 paper industry
 p0136 N82-24686
- FOSSIL METEORITE CRATERS**
 U TEORITE CRATERS

FOUNDATIONS

Effect of rotor configuration on guyed tower and foundation designs and estimated costs for intermediate site horizontal axis wind turbines [NASA-TN-82804] p0121 N82-22649

FOURIER ANALYSIS
NT FOURIER SERIES
An experimental investigation of gapwise periodicity and unsteady aerodynamic response in an oscillating cascade. Volume 2: Data report. Part 1: Text and mode 1 data [NASA-CR-165457-VOL-2-PT-1] p0006 N82-18180

FOURIER SERIES
Numerical comparisons of nonlinear convergence accelerators p0149 N82-31438

FRACTIONATION

NT CHEMICAL FRACTIONATION

FRACTOGRAPHY

Microstructural effects on the room and elevated temperature low cycle fatigue behavior of Waspaloy [NASA-CR-165497] p0113 N82-26702

FRACTURE MECHANICS
On a study of the $\Delta T/c$ and $C^*/\text{asterisk}$ integrals for fracture analysis under non-steady creep p0115 N82-36782

Micromechanical predictions of crack propagation and fracture energy in a single fiber boron/aluminum model composite [NASA-CR-168550] p0052 N82-18326

Creep crack-growth: A new path-independent T_{sub} and computational studies [NASA-CR-168930] p0113 N82-24503

Fracture mechanics criteria for turbine engine hot section components [NASA-CR-167836] p0027 N82-25257

High temperature low cycle fatigue mechanisms for nickel base and a copper base alloy [NASA-CR-3543] p0064 N82-26436

Analysis of cracks emanating from a circular hole in unidirectional fiber reinforced composites, part 2 [NASA-CR-165433] p0114 N82-26714

Analysis of interface cracks in adhesively bonded lap shear joints, part 4 [NASA-CR-165438] p0114 N82-26716

FRACTURE RESISTANCE

U ACTURE STRENGTH

FRACTURE STRENGTH

Strength distributions of SiC ceramics after oxidation and oxidation under load [ACS PAPER 9-C-80C] p0071 N82-20143

Work of fracture in aluminum metal-matrix composites p0053 N82-31339

Effects of oxidation and oxidation under load on strength distributions of Si3N4 [ACS PAPER 69-B-80] p0071 N82-35871

Extended range stress intensity factor expressions for chevron-notched short bar and short rod fracture toughness specimens p0112 N82-40357

On ultrasonic factors and fracture toughness p0116 N82-42863

Interrelation of material microstructure, ultrasonic factors, and fracture toughness of two phase titanium alloy [NASA-TN-82810] p0110 N82-20551

Factors influencing the thermally-induced strength degradation of B/A1 composites [NASA-TN-82823] p0050 N82-24297

FRACTURE TOUGHNESS

U ACTURE STRENGTH

FRACTURES (MATERIALS)

Creep crack-growth: A new path-independent integral ($T_{sub} c$), and computational studies [NASA-CR-167897] p0114 N82-29619

FRACTURING

Environmental effects on defect growth in composite materials [NASA-CR-165213] p0052 N82-20248

FRAGMENTS

Rotor fragment protection program: Statistics on aircraft gas turbine engine rotor failures that occurred in U.S. commercial aviation during 1978 [NASA-CR-165388] p0027 N82-27316

FRAMES

Thermal expansion accommodation in a jet engine frame

FREE CONVECTION

Eigenvalues of the Rayleigh-Denard and Marangoni problems p0029 N82-11999

Natural convection with combined driving forces p0092 N82-13396
p0093 N82-31445

FREE ELECTRON LASERS

On a free-electron-laser in a uniform magnetic field - A solution for arbitrarily strong electromagnetic radiation fields p0092 N82-13396
p0093 N82-31445

Free electron lasers for transmission of energy in space [NASA-CR-165520] p0098 N82-25499

FREE JETS

Forms of three-dimensional supersonic free jets in linear approximation p0098 N82-25499
N82-19196

FREE OSCILLATIONS

U EE VIBRATION

FREE VIBRATION

Vibrations of cantilevered shallow cylindrical shells of rectangular planform p0115 N82-11298

Comparison of beam and shell theories for the vibrations of thin turbomachinery blades [ASME PAPER 82-GT-223] p0115 N82-35408

Finite-element modeling of layered, anisotropic composite plates and shells: A review of recent research p0113 N82-19563

FREQUENCIES

NT EXTREMELY HIGH FREQUENCIES

NT HIGH FREQUENCIES

NT RESONANT FREQUENCIES

Extending the frequency of response of lightly damped second order systems: Application to the drag force anemometer [NASA-TN-82927] p0096 N82-32662

FREQUENCY BANDS

U EQUENCIES

FREQUENCY CONVERSION

U EQUENCY CONVERTERS

FREQUENCY CONVERTERS

A 10kW series resonant converter design, transistor characterization, and base-drive optimization [NASA-CR-165546] p0084 N82-17439

FREQUENCY DIVISION MULTIPLE ACCESS

Baseband-processed SS-TDMA communication system architecture and design concepts [AIAA 82-0482] p0079 N82-23508

FREQUENCY MODULATION

NT FREQUENCY SHIFT KEYING

Communications satellite systems capacity analysis [NASA-CR-167911] p0034 N82-27331

FREQUENCY SHIFT KEYING

Conversion and matched filter approximations for serial minimum-shift keyed modulation p0080 N82-26713

Near optimum delay-line detection filters for serial detection of MSK signals p0086 N82-43867

FREQUENCY TRANSLATION

U EQUENCY CONVERTERS

FRICTION

NT DRY FRICTION

NT SLIDING FRICTION

Application of surface analysis to solve problems of wear [NASA-TN-82753] p0099 N82-14519

Stress evaluations under rolling/sliding contacts [NASA-CR-165561] p0113 N82-17521

Tribological properties at 25 C of seven polyimide films bonded to 440 C high-temperature stainless steel [NASA-TP-1944] p0067 N82-19373

Friction and wear of iron in corrosive metal [NASA-TP-1985] p0058 N82-20291

Friction and surface chemistry of some ferrous-base metallic glasses [NASA-TP-1991] p0059 N82-21301

Correlation of tensile and shear strengths of metals with their friction properties [NASA-TN-82828] p0060 N82-24325

Frictional heating due to asperity interaction of elastohydrodynamic line-contact surfaces [NASA-TP-1882] p0100 N82-25514

Lubricant effects on efficiency of a helicopter:
transmission
[NASA-TM-82857] p0100 N82-25520
Boundary lubrication: Revisited
[NASA-TM-82858] p0069 N82-29458
Refractory coatings
[NASA-CASE-LRW-13169-2] p0061 N82-30371

FRICTION COEFFICIENT
U EFFICIENT OF FRICTION
FRICTION FACTOR
The effect of oxygen concentration on the
boundary-lubricating characteristics of a C
ether and a polyphenyl ether to 300 C
p0070 N82-21699
Surface chemistry, microstructure and friction
properties of some ferrous-base metallic glasses
at temperatures to 750 C
[NASA-TP-2006] p0060 N82-22349

FRICTION LOSS COEFFICIENT
U FRICTION FACTOR
FRICTION REDUCTION
Stress evaluations under rolling/sliding contacts
[NASA-CR-165561] p0113 N82-17521

FRINGE PATTERNS
U REFRACTION PATTERNS
FRONTAL AREAS (METEOROLOGY)
U ONTS (METEOROLOGY)
FRONTS (METEOROLOGY)
Effects of condensation and surface motion on the
structure of steady-state fronts
N82-19360

FROST
Effect of heavy rain on aircraft
N82-21149

FUEL CELL CATALYSTS
U ELECTROCATALYSTS
FUEL CELL POWER PLANTS
40-kW phosphoric acid fuel cell field test -
Project plan
p0128 N82-45325
Phosphoric acid fuel cell technology status
[NASA-TM-82791] p0120 N82-19670

FUEL CELLS
NT HYDROGEN OXYGEN FUEL CELLS
NT PHOSPHORIC ACID FUEL CELLS
NT REGENERATIVE FUEL CELLS
An assessment of alternative fuel cell designs for
residential and commercial cogeneration
p0138 N82-24695
Develop and test fuel cell powered on-site
integrated total energy systems. Phase 3:
Full-scale power plant development
[NASA-CP-165328] p0117 N82-13490
Develop and test fuel cell powered on-site
integrated total energy systems. Phase 3:
Full-scale power plant development
[NASA-CR-165455] p0131 N82-16483
Preparation and evaluation of advanced
electrocatalysts for phosphoric acid fuel cells
[NASA-CR-165554] p0132 N82-17615
Cell module and fuel conditioner development
[NASA-CP-165620] p0134 N82-21713
Cathode catalyst for primary phosphoric fuel cells
[NASA-CP-165198] p0134 N82-22675
Requirements for optimization of electrodes and
electrolyte for the iron/chromium Redox flow cell
[NASA-CP-165218] p0136 N82-25640
Stabilizing platinum in phosphoric acid fuel cells
[NASA-CR-165606] p0136 N82-29710
Development and test fuel cell powered on-site
integrated total energy systems. Phase 3:
Full-scale power plant development
[NASA-CP-167899] p0137 N82-30705
Non-noble catalysts and catalyst supports for
phosphoric acid fuel cells
[NASA-CR-165289] p0137 N82-30722

FUEL COMBUSTION
Symposium /International/ on Combustion, 18th,
University of Waterloo, Waterloo, Ontario,
Canada, August 17-22, 1980, Proceedings
p0056 N82-28651
Experimental and theoretical studies of the laws
governing condensate deposition from combustion
gases
p0057 N82-28709
NASA Broad Specification Fuels Combustion
Technology program - Pratt and Whitney Aircraft
Phase I results and status
[AIAA PAPER 82-1088] p0021 N82-34999

NASA/General Electric broad-specification fuels
combustion technology program - Phase I results
and status
[AIAA PAPER 82-1089] p0021 N82-35000
Buoyancy effects on the temperature field in
downward spreading flames
p0094 N82-41203
Effect of fuel-air-ratio nonuniformity on
emissions of nitrogen oxides
[NASA-TP-1798] p0016 N82-13143
Catalytic combustion of residual fuels
[NASA-TM-82731] p0118 N82-13504
Demonstration of catalytic combustion with
residual fuel
[NASA-CR-165369] p0131 N82-16484
Advanced Low-Emissions Catalytic-Combustor
Program, phase 1 --- aircraft gas turbine engines
[NASA-CR-159656] p0025 N82-22265
Low NOx heavy fuel combustor concept program,
phase 1
[NASA-CR-165449] p0135 N82-24651
Low NOx heavy fuel combustor concept program
[NASA-CR-167876] p0074 N82-26482
Electrostatic fuel conditioning of internal
combustion engines
[NASA-CR-169020] p0106 N82-26680
Effect of hydrocarbon fuel type on fuel
[NASA-TM-82916] p0072 N82-28460
Low and medium heating value coal gas catalytic
combustor characterization
[NASA-CR-165560] p0138 N82-32856
Low NOx heavy fuel combustor concept program
[NASA-CR-165481] p0138 N82-33827

FUEL CONSUMPTION
Comparison of two parallel/series flow turbofan
propulsion concepts for supersonic V/STOL
[AIAA PAPER 81-2637] p0020 N82-19214
The AGT 101 advanced automotive gas turbine
[ASME PAPER 82-GT-72] p0108 N82-35321
Progress in the development of energy efficient
engine components
[ASME PAPER 82-GT-275] p0030 N82-35450
AGT-102 automotive gas turbine
[NASA-CR-165353] p0105 N82-12444
NASA research activities in aeropropulsion
[NASA-TM-82788] p0017 N82-16084
Advanced Gas Turbine (AGT) powertrain system
initial development report
[NASA-CR-165130] p0132 N82-16485
CF6 jet engine performance improvement: High
pressure turbine roundness
[NASA-CR-165555] p0024 N82-17174
Advanced general aviation comparative
engine/airframe integration study
[NASA-CR-165564] p0025 N82-22263
Energy efficient engine exhaust mixer model
technology
[NASA-CR-165459] p0025 N82-22264
Straight and chopped DC performance data for a
General Electric 5BY436A1 DC shunt motor with a
General Electric EV-1 controller
[NASA-CR-165507] p0085 N82-24425
Preliminary analysis of a downsized advanced
gas-turbine engine in a subcompact car
[NASA-TM-82848] p0163 N82-26051
CF6 jet engine performance improvement: High
pressure turbine active clearance control
[NASA-CR-165556] p0027 N82-28297
Impact of advanced propeller technology on
aircraft/mission characteristics of several
general aviation aircraft
[NASA-CR-167984] p0009 N82-33347
Exhaust emissions reduction for intermittent
combustion aircraft engines
[NASA-CR-167914] p0029 N82-33392
Advanced ceramic coating development for
industrial/utility gas turbines
[NASA-CR-169852] p0065 N82-33494

FUEL CONTAMINATION
Deposit formation in liquid fuels. III - The
effect of selected nitrogen compounds on diesel
fuel
p0074 N82-23238
Advanced ceramic coating development for
industrial/utility gas turbines
[NASA-CR-169852] p0065 N82-33494

FUEL FLOW
NT PROPELLANT TRANSFER

- Tube entrance heat transfer with deposit formation
[AIAA PAPER 82-0918] p0093 A82-31908
- FUEL INJECTION**
- Atomization and combustion properties of flashing injectors
[AIAA PAPER 82-0300] p0092 A82-17880
- Evaluation of fuel injection configurations to control carbon and soot formation in small GT combustors
[AIAA PAPER 82-1175] p0021 A82-35041
- Pollution reduction technology program small jet aircraft engines, phase 3
[NASA-CR-165786] p0023 A82-14095
- External fuel vaporization study
[NASA-CR-165513] p0073 A82-14371
- Effect of fuel injector type on performance and emissions of reverse-flow combustor
[NASA-TP-1945] p0016 A82-15040
- Investigation of spray characteristics for flashing injection of fuels containing dissolved air and superheated fuels
[NASA-CR-35563] p0027 A82-26295
- FUEL OILS**
- NT LIQUID FUELS**
- Demonstration of catalytic combustion with residual fuel
[NASA-CR-165369] p0131 A82-16484
- Oxidation and formation of deposit precursors in hydrocarbon fuels
[NASA-CR-165534] p0073 A82-18402
- FUEL PRODUCTION**
- NT LIQUID FUELS**
- Fuel quality processing study, volume 1
[NASA-CR-165327-VOL-1] p0135 A82-24649
- Fuel quality/processing study, Volume 2: Appendix, Task 1 literature survey
[NASA-CR-165327-VOL-2] p0135 A82-24650
- FUEL SPRAYS**
- Formation of oxides of nitrogen in monodisperse spray combustion of hydrocarbon fuels
p0057 A82-37571
- FUEL SYSTEMS**
- NT AIRCRAFT FUEL SYSTEMS**
- Demonstration of catalytic combustion with residual fuel
[NASA-CR-165369] p0131 A82-16484
- FUEL TANK PRESSURIZATION**
- Low-thrust chemical propulsion system propellant expulsion and thermal conditioning study. Executive summary
[NASA-CR-165622] p0045 A82-24287
- Low-thrust chemical propulsion system propellant expulsion and thermal conditioning study
[NASA-CR-167841] p0045 A82-24288
- FUEL TANKS**
- NT WING TANKS**
- Additional experiments on flowability improvements of aviation fuels at low temperatures, volume 2
[NASA-CR-167912] p0074 A82-31546
- FUEL TESTS**
- Deposit formation in liquid fuels. II - The effect of selected compounds on the storage stability of Jet A turbine fuel
p0074 A82-22240
- Evaluation of fuel injection configurations to control carbon and soot formation in small GT combustors
[AIAA PAPER 82-1175] p0021 A82-35041
- Deposit formation in hydrocarbon fuels
[ASME PAPER 82-GT-49] p0075 A82-35307
- Experimental study of external fuel vaporization
[ASME PAPER 82-GT-59] p0075 A82-35312
- Catalytic combustion of residual fuels
[NASA-TM-82731] p0118 A82-13504
- Fuel economy and exhaust emissions characteristics of diesel vehicles: Test results of a prototype fiat 131TC 2.4 liter automobile
[NASA-CR-165535] p0164 A82-18068
- Testing of fuel/oxidizer-rich, high-pressure preburners
[NASA-CR-165609] p0074 A82-24353
- Characterization of an Experimental Reference Broadened Specification (ERBS) aviation turbine fuel and ERBS fuel blends
[NASA-TM-82883] p0072 A82-32504
- FUEL-AIR RATIO**
- Effects of heat loss, preferential diffusion, and flame stretch on flame-front instability and extinction of propane/air mixtures p0057 A82-32877
- On the opening of premixed (unseen) flame tips p0057 A82-37570
- Effect of fuel-air-ratio nonuniformity on emissions of nitrogen oxides
[NASA-TP-1798] p0016 A82-13143
- Catalytic combustion of residual fuels
[NASA-TM-82731] p0118 A82-13504
- Low NOx heavy fuel combustor concept program. Phase I: Combustion technology generation
[NASA-CR-165482] p0136 A82-24725
- Effect of fuel to air ratio on Mach 0.3 burner rig hot corrosion of ZrO₂-Y₂O₃ thermal barrier coatings
[NASA-TM-82879] p0061 A82-30373
- FUELS**
- NT AIRCRAFT FUELS**
- NT COAL**
- NT CRYOGENIC ROCKET PROPELLANTS**
- NT DIESEL FUELS**
- NT FOSSIL FUELS**
- NT FUEL OILS**
- NT GASEOUS FUELS**
- NT HYDROCARBON FUELS**
- NT JET ENGINE FUELS**
- NT LIQUEFIED NATURAL GAS**
- NT LIQUID FUELS**
- NT RP-1 ROCKET PROPELLANTS**
- NT SYNTHETIC FUELS**
- FUNCTIONAL ANALYSIS**
- NT INTEGRAL EQUATIONS**
- NT J INTEGRAL**
- FUNCTIONS (MATHEMATICS)**
- NT CONFORMAL MAPPING**
- NT HATHIEU FUNCTION**
- NT PERIODIC FUNCTIONS**
- NT TANGENTS**
- NT TRANSFER FUNCTIONS**
- PURAN RESINS**
- NT KEVLAR (TRADEMARK)**
- G**
- GAGES**
- U ASURING INSTRUMENTS**
- GALLIUM ARSENIDES**
- Gallium arsenide solar cells-status and prospects for use in space
p0043 A82-11765
- Undoped semi-insulating LEC GaAs - A model and a mechanism --- Liquid Encapsulated Czochralski
p0159 A82-13754
- Stoichiometry-controlled compensation in liquid encapsulated Czochralski GaAs
p0158 A82-17585
- OM-VPE growth of Mg-doped GaAs --- OrganoMetallic-Vapor Phase Epitaxy
p0159 A82-38411
- Compensation mechanism in liquid encapsulated Czochralski GaAs importance of melt stoichiometry
p0086 A82-40403
- Effect of melt stoichiometry on twin formation in LEC GaAs --- Liquid Encapsulated Czochralski technique
p0160 A82-46517
- Low temperature growth and electrical characterization of insulators for GaAs MISFETS
[NASA-CR-164972] p0159 A82-11959
- High purity low dislocation GaAs single crystals
[NASA-CR-165593] p0159 A82-23030
- Gallium arsenide solar array subsystem study
[NASA-CR-167869] p0138 A82-32855
- GALLIUM COMPOUNDS**
- NT GALLIUM ARSENIDES**
- GALVANIC CELLS**
- U ELECTROLYTIC CELLS**
- GAMMA RADIATION**
- U XMA RAYS**
- GAMMA RAYS**
- Effect of gamma irradiation on the friction and wear of ultrahigh molecular weight polyethylene
p0062 A82-10674
- GAPS**
- Method of making a high voltage v-groove solar cell
[NASA-CASE-LEW-13404-1] p0124 A82-29709
- GAS ANALYSIS**
- NT OZONOMETRY**
- GAS BEARINGS**
- Development of CdO-graphite-Ag coatings for gas

bearings to 427 C p0108 A82-27079

Bearings: Technology and needs [NASA-CR-167008] p0106 A82-26679

GAS DENSITY

CAS22 - FORTRAN program for fast design and analysis of shock-free airfoil cascades using fictitious-gas concept [NASA-CR-3507] p0006 A82-16044

GAS DYNAMICS

NT AERODYNAMICS

NT APROTHERMODYNAMICS

NT ROTOR AERODYNAMICS

Characteristic dynamic energy equations for Stirling cycle analysis p0138 A82-11816

Effects of internal heat transfer on the structure of self-similar blast waves p0093 A82-32225

GAS FLOW

NT AIP FLOW

NT TIPE FLOW

Two dimensional stagnation point flow of a dusty gas near an oscillating plate p0012 A82-37535

High-speed motion picture camera experiments of cavitation in dynamically loaded journal bearings [NASA-TN-82798] p0100 A82-20543

Pockels-effect cell for gas-flow simulation [NASA-TP-2007] p0095 A82-23515

Study of vapor flow into a capillary acquisition device --- for cryogenic rocket propellants [NASA-CR-167883] p0091 A82-24452

Covering solid, film cooled surfaces with a duplex thermal barrier coating [NASA-CASE-LEW-13450-1] p0088 A82-25463

GAS INJECTION

Assessment of steam-injected gas turbine systems and their potential application [NASA-TN-82735] p0119 A82-18694

GAS IONIZATION

NT ANGROBAL IONIZATION

GAS LASERS

NT CARBON DIOXIDE LASERS

NT DF LASERS

GAS LUBRICATED BEARINGS

U S BEARINGS

GAS MIXTURES

Numerical modeling of turbulent combustion in premixed gases p0056 A82-28708

GAS PHASES

U EOP PHASES

GAS STREAMS

Dilution jet behavior in the turn section of a reverse flow combustor [NASA-TN-82776] p0017 A82-19220

GAS TURBINE ENGINES

NT DP1STOL-SIDDELEY BS 53 ENGINE

NT JET ENGINES

NT TURBOFAN ENGINES

NT TURBOJET ENGINES

NT TURBOPROP ENGINES

The AGT101 technology - An automotive alternative p0107 A82-11783

Thermal expansion accommodation in a jet engine frame p0029 A82-11999

High temperature durable catalyst development p0056 A82-20739

Blade loss transient dynamic analysis of turbomachinery [AIAA PAPER 82-1057] p0030 A82-34982

Experimental study of the effects of secondary air on the emissions and stability of a lean premixed combustor [AIAA PAPER 82-1072] p0021 A82-34992

Advancements in real-time engine simulation technology --- of digital electronic aircraft engine controls [AIAA PAPER 82-1075] p0021 A82-34995

NASA/General Electric broad-specification fuels combustion technology program - Phase I results and status [AIAA PAPER 82-1089] p0021 A82-35000

Small gas turbine combustor primary zone development [AIAA PAPER 82-1159] p0103 A82-35036

AGT 100 automotive gas turbine system development [AIAA PAPER 82-1165] p0108 A82-35038

AGT101 automotive gas turbine system development [AIAA PAPER 82-1166] p0108 A82-35039

Evaluation of fuel injection configurations to control carbon and soot formation in small GT combustors [AIAA PAPER 82-1175] p0021 A82-35041

AGT100 turbomachinery --- for automobiles [AIAA PAPER 82-1207] p0108 A82-35061

Combustor development for automotive gas turbines [AIAA PAPER 82-1208] p0104 A82-35062

The AGT 101 advanced automotive gas turbine [ASME PAPER 82-GT-72] p0108 A82-35321

The use of optimization techniques to design controlled diffusion compressor blading [ASME PAPER 82-GT-149] p0022 A82-35373

Ceramic thermal barrier coatings for gas turbine engines [ASME PAPER 82-GT-265] p0071 A82-35441

Progress in the development of energy efficient engine components [ASME PAPER 82-GT-275] p0030 A82-35450

Engine dynamic analysis with general nonlinear finite element codes. II - Bearing element implementation, overall numerical characteristics and benchmarking [ASME PAPER 82-GT-292] p0108 A82-35462

Design and development of a ceramic radial turbine for the AGT101 [AIAA PAPER 82-1209] p0109 A82-35480

Optical tip clearance sensor for aircraft engine controls [AIAA PAPER 82-1131] p0015 A82-37691

Applications of high-temperature powder metal aluminum alloys to small gas turbines p0065 A82-48244

Development of low modulus material for use in ceramic gas path seal applications [NASA-CR-165469] p0022 A82-10039

Evaluation of the potential of the Stirling engine for heavy duty application [NASA-CR-165473] p0128 A82-10505

Progress in protective coatings for aircraft gas turbines: A Review of NASA sponsored research [NASA-TN-82740] p0058 A82-12216

AGT-102 automotive gas turbine p0105 A82-12444

Low NO sub x heavy fuel combustor concept program [NASA-CR-165512] p0129 A82-12572

Gas-turbine critical research and advanced technology support project [NASA-TN-81708] p0118 A82-13509

Development of a high-temperature durable catalyst for use in catalytic combustors for advanced automotive gas turbine engines [NASA-CR-165396] p0130 A82-13510

The use of optimization techniques to design controlled diffusion compressor blading [NASA-TN-82763] p0016 A82-14094

ERBS fuel addendum: Pollution reduction technology program small jet aircraft engines, phase 3 [NASA-CR-165387] p0024 A82-14096

External fuel vaporization study [NASA-CR-165513] p0073 A82-14371

Effect of fuel injector type on performance and emissions of reverse-flow combustor [NASA-TP-1945] p0016 A82-15040

Research and development program for non-linear structural modeling with advanced time-temperature dependent constitutive relationships [NASA-CR-165333] p0024 A82-16080

Demonstration of catalytic combustion with residual fuel [NASA-CR-165369] p0131 A82-16484

Advanced Gas Turbine (AGT) powertrain system initial development report [NASA-CR-165130] p0132 A82-16485

Dilution jet behavior in the turn section of a reverse flow combustor [NASA-TN-82776] p0017 A82-19220

Cooled variable-area radial turbine technology program [NASA-CR-165408] p0024 A82-19221

Cold-air performance of a 15.41-cm-tip-diameter axial-flow power turbine with variable-area stator designed for a 75-kW automotive gas turbine engine [NASA-TN-82644] p0024 A82-21193

- Experimental performance of the regenerator for the Chrysler upgraded automotive gas turbine engine
[NASA-TM-82671] p0120 N82-21712
- Investigation of soot and carbon formation in small gas turbine combustors
[NASA-CR-167853] p0025 N82-22267
- Advancements in real-time engine simulation technology
[NASA-TM-82825] p0147 N82-22915
- Analysis of high load dampers
[NASA-CR-165503] p0026 N82-23248
- Evaluation of inelastic constitutive models for nonlinear structural analysis --- for aircraft turbine engines
[NASA-TM-82845] p0112 N82-24502
- Cost/benefit studies of advanced materials technologies for future aircraft turbine engines: Materials for advanced turbine engines
[NASA-CR-167849] p0026 N82-25254
- Low NOx heavy fuel combustor concept program addendum: Low/mid heating value gaseous fuel evaluation
[NASA-CR-165615] p0055 N82-25338
- Low NOx heavy fuel combustor concept program
[NASA-CR-165367] p0136 N82-25635
- Preliminary analysis of a downsized advanced gas-turbine engine in a subcompact car
[NASA-TM-82848] p0163 N82-26051
- Multitroller traction drive speed reducer: Evaluation for automotive gas turbine engine
[NASA-TP-2027] p0101 N82-26678
- Rotor fragment protection program: Statistics on aircraft gas turbine engine rotor failures that occurred in U.S. commercial aviation during 1978
[NASA-CR-165388] p0027 N82-27316
- Techniques for enhancing durability and equivalence ratio control in a rich-lean, three-stage ground power gas turbine combustor
[NASA-TM-82922] p0124 N82-29717
- Ceramic applications in turbine engines
[NASA-CR-165197] p0164 N82-31158
- Active clearance control system for a turbomachine
[NASA-CASE-LEW-12939-1] p0020 N82-32366
- Low and medium heating value coal gas catalytic combustor characterization
[NASA-CR-165560] p0138 N82-32856
- Engine dynamic analysis with general nonlinear finite element codes. Part 2: Bearing element implementation overall numerical characteristics and benchmarking
[NASA-CR-167944] p0028 N82-33390
- Energy efficient engine: Turbine transition duct model technology report
[NASA-CR-167996] p0029 N82-33394
- Overlay metallic-cermet alloy coating systems --- for gas turbine engines
[NASA-CASE-LEW-13639-1] p0070 N82-33522
- GAS TURBINES**
- A comprehensive method for preliminary design optimization of axial gas turbine stages
[AIAA PAPER 82-1264] p0030 N82-35091
- Trends in high temperature gas turbine materials
[NASA-TM-82715] p0058 N82-11182
- Gas turbine ceramic-coated-vane concept with convection-cooled porous metal core
[NASA-TP-1942] p0016 N82-14090
- Investigations of flowfields found in typical combustor geometries
[NASA-CR-165061] p0090 N82-15360
- Advanced Gas Turbine (AGT) powertrain system development for automotive applications
[NASA-CR-165175] p0163 N82-16937
- Review of NASA progress in thermal barrier coatings for stationary gas turbines
[NASA-TM-81716] p0058 N82-17335
- Evaluation of present thermal barrier coatings for potential service in electric utility gas turbines
[NASA-CR-165543] p0063 N82-18368
- Low NO subx heavy fuel combustor concept program. Phase 1A: Coal gas addendum
[NASA-CR-165577] p0133 N82-18690
- Assessment of steam-injected gas turbine systems and their potential application
[NASA-TM-82735] p0119 N82-18694
- Tailored plasma sprayed MCrAlY coatings for aircraft gas turbine applications
[NASA-CR-165234] p0064 N82-19360
- Hydrodynamic and aerodynamic breakup of liquid sheets
[NASA-TM-82800] p0087 N82-19494
- Parametric performance analysis of steam-injected gas turbine with a thermionic-energy-converter-lined combustor
[NASA-TM-82736] p0121 N82-23678
- Low NOx heavy fuel combustor concept program. Phase 1: Combustion technology generation
[NASA-CR-165482] p0136 N82-24725
- Aerodynamic performance of high turning core turbine vanes in a two dimensional cascade
[NASA-TM-82894] p0004 N82-26240
- Low NOx heavy fuel combustor concept program
[NASA-CR-167876] p0074 N82-26482
- Solute transport during the cyclic oxidation of Ni-Cr-Al alloys
[NASA-CR-165544] p0064 N82-27462
- Lewis pressurized, fluidized-bed combustion program. Data and calculated results
[NASA-TM-81767] p0124 N82-30704
- Gas turbine critical research and advanced technology (CRT) support project
[NASA-TM-82872] p0126 N82-31776
- Three dimensional flow measurements in a turbine scroll
[NASA-CR-167920] p0009 N82-32310
- Use of fiber like materials to augment the cycle life of thick thermoprotective seal coatings
[NASA-TM-82901] p0089 N82-32633
- Advanced ceramic coating development for industrial/utility gas turbines
[NASA-CR-169852] p0065 N82-33494
- GAS-ION INTERACTIONS**
- Inert gas ion thruster
[NASA-CR-165521] p0044 N82-21252
- GAS-METAL INTERACTIONS**
- Investigation into the role of NaCl deposited on oxide and metal substrates in the initiation of hot corrosion
[NASA-CR-165029] p0063 N82-13217
- Method and apparatus for coating substrates using lasers
[NASA-CASE-LEW-13526-1] p0059 N82-22347
- Refractory coatings and method of producing the same
[NASA-CASE-LEW-13169-1] p0060 N82-29415
- GAS-SOLID INTERACTIONS**
- NT GAS-METAL INTERACTIONS**
- GASOUS CAVITATION**
- U VITATION FLOW**
- U S FLOW**
- GASOUS FUELS**
- NT LIQUID FUELS**
- Low NOx heavy fuel combustor concept program addendum: Low/mid heating value gaseous fuel evaluation
[NASA-CR-165615] p0055 N82-25338
- Catalytic combustion of actual low and medium heating value gases
[NASA-TM-82930] p0125 N82-30717
- GASES**
- NT ARGON PLASMA**
- NT CARBON MONOXIDE**
- NT CHARGED PARTICLES**
- NT DISSOLVED GASES**
- NT EXHAUST GASES**
- NT GAS MIXTURES**
- NT GAS STREAMS**
- NT HIGH TEMPERATURE GASES**
- NT HYDROGEN**
- NT LIQUEFIED NATURAL GAS**
- NT LIQUID HYDROGEN**
- NT LIQUID OXYGEN**
- NT NITROGEN**
- NT NITROGEN IONS**
- NT OXYGEN**
- NT OZONE**
- NT RARE GASES**
- Catalytic combustion of actual low and medium heating value gases
[NASA-TM-82930] p0125 N82-30717
- GASIFICATION**
- NT COAL GASIFICATION**
- GASOLINE**
- NT LIQUID FUELS**
- GASP**
- U OBAL AIR SAMPLING PROGRAM**
- GAUSSIAN NOISE**
- U NDOM NOISE**

ORIGINAL PAGE IS
OF POOR QUALITY

SUBJECT INDEX

GRANULAR MATERIALS

GEAR TEETH

Surface geometry of circular cut spiral bevel gears
[ASME PAPER 81-DET-114] p0108 A82-19334
Optimal tooth numbers for compact standard spur
gear sets
[ASME PAPER 81-DET-115] p0103 A82-19335
A multi-purpose method for analysis of spur gear
tooth loading
[NASA-CR-165163] p0104 A82-10401
Mathematical models for the synthesis and
optimization of spiral bevel gear tooth surfaces
--- for helicopter transmissions
[NASA-CR-3553] p0106 A82-25516
Tooth profile analysis of circular-cut,
spiral-bevel gears
[NASA-TM-82840] p0101 A82-26681
The optimal design of involute gear teeth with
unequal addenda
[NASA-TM-82866] p0101 A82-28645
Precision of spiral-bevel gears
[NASA-TM-82888] p0102 A82-30552
Effect of shot peening on surface fatigue life of
carburized and hardened AISI 9310 spur gears
[NASA-TP-2047] p0102 A82-32736

GEARS

NT RACKS (GEARS)

On the automatic generation of FEM models for
complex gears - A work-in-progress report
p0109 A82-48243
Lubricant effects on efficiency of a helicopter
transmission
[NASA-TM-82857] p0100 A82-25520
Tooth profile analysis of circular-cut,
spiral-bevel gears
[NASA-TM-82840] p0101 A82-26681
Reliability model for planetary gear
[NASA-TM-82859] p0101 A82-28643
A finite element stress analysis of spur gears
including fillet radii and rim thickness effects
[NASA-TM-82865] p0101 A82-28646
On finite element stress analysis of spur gears
[NASA-CR-167938] p0107 A82-29607
Precision of spiral-bevel gears
[NASA-TM-82888] p0102 A82-30552
Kinematic precision of gear trains
[NASA-TM-82887] p0102 A82-32733

GEL PERMEATION CHROMATOGRAPHY

U QUIC CHROMATOGRAPHY

GELLED ROCKET PROPELLANTS

NT LIQUID FUELS

GENERAL AVIATION AIRCRAFT

NASA research in aircraft propulsion
[ASME PAPER 82-GT-177] p0022 A82-35389
NASA research in aircraft propulsion
[NASA-TM-82771] p0016 A82-13146
Bibliography of NASA published reports on general
aviation, 1975 to 1981
[NASA-TM-83307] p0001 A82-19132
NASA/Lewis Research Center Icing Research Program
p0001 A82-21148
Propulsion opportunities for future commuter
aircraft
[NASA-TM-82915] p0019 A82-26298

GEOLOGY

NT VOLCANOES

GEOMAGNETIC FIELD

U MAGNETISM

GEOMAGNETIC STORMS

U NETIC STORMS

GEOMAGNETISM

An attempt at magnetic-variation sounding in the
Antarctic
A82-25290
Design practices for controlling spacecraft
charging interactions
[NASA-TM-82781] p0038 A82-18311

GEOMETRIC RECTIFICATION (IMAGERY)

GRID3C: Computer program for generation of C type
multilevel, three dimensional and boundary
conforming periodic grids
[NASA-CF-167846] p0008 A82-26239

GEOMETRICAL HYDROMAGNETICS

U GNETOHYDRODYNAMICS

GEOMETRY

NT ANGLE OF ATTACK
NT CRACK GEOMETRY
NT CURVATURE
NT CURVES (GEOMETRY)
NT DIFFERENTIAL GEOMETRY

NT DUCT GEOMETRY
NT FLOW GEOMETRY
NT NOZZLE GEOMETRY
NT RECTANGLES
NT TANGENTS
NT TENSOR ANALYSIS
NT VECTOR ANALYSIS

GEOPOTENTIAL

Representation and material charging response of
geoplasma environments
p0039 A82-14249
SCATHA SSPM charging response: NASCAP predictions
compared with data
p0037 A82-14251

GEOSTATIONARY SATELLITES

U NCHRONOUS SATELLITE(S)

GEOSYNCHRONOUS ORBITS

Mass driver react/on engine characteristics and
performance in earth orbital transfer missions
p0046 A82-18199
Shuttle to GEO propulsion tradeoffs
[AIAA PAPER 82-1245] p0034 A82-35082
Centaur capabilities for communications satellite
launches
[AIAA PAPER 82-0558] p0034 A82-36286
Design practices for controlling spacecraft
charging interactions
[NASA-TM-82781] p0038 A82-18311

GEOTHERMAL RESOURCES

NT VOLCANOES

GEOTHERMAL HEATERS

U ATING EQUIPMENT

GLARE

Veiling glare reduction methods compared for
ophthalmic applications
p0143 A82-13289

GLASS

NT BOROSILICATE GLASS

NT E GLASS

NT GLASS FIBERS

NT METALLIC GLASSES

GLASS FIBER REINFORCED PLASTICS

Winding for the wind
p0138 A82-37078
Impact resistance of fiber composites
p0112 A82-39852
Fabrication and wear test of a continuous
fiber/particulate composite total surface hip
replacement
[NASA-TM-81746] p0066 A82-11211

GLASS FIBERS

Design, evaluation, and fabrication of low-cost
composite blades for intermediate-size wind
turbines
[NASA-CR-165342] p0133 A82-10693

GLAUBERT COEFFICIENT

U RODYNAMIC FORCES

U CH NUMBER

GLAZES

An experimental study of airfoil icing
characteristics
[NASA-TM-82790] p0001 A82-17083
Performance of laser glazed ZrO2 TBCs in cyclic
oxidation and corrosion burner test rigs
[NASA-TM-82830] p0059 A82-22346

GLOBAL AIR SAMPLING PROGRAM

An automated system for global atmospheric
sampling using B-747 airliners
[NASA-CR-165264] p0139 A82-13554

GOLD

Tribological properties and XPS studies of ion
plated gold on nickel and iron
[NASA-TM-82814] p0059 A82-22344

GOLD COATINGS

Improved chromium electrodes for REDOX cells
[NASA-CASE-LEW-13653-1] p0121 A82-22672

GOLD PLATE

U LD COATINGS

GRADIENTS

NT PRESSURE GRADIENTS

NT TEMPERATURE GRADIENTS

(GRAINS (FOOD))

Operational performance of the
photovoltaic-powered grain mill and water pump
at Tangaya, Upper Volta
[NASA-TM-82767] p0120 A82-19673

GRANULAR MATERIALS

Recrystallization and grain growth in NiAl
p0065 A82-44529

GRAPHITE

**ORIGINAL PAGE IS
OF POOR QUALITY**

SUBJECT INDEX

GRAPHITE

NT EYECLYTIC GRAPHITE
Development of CdO-graphite-Ag coatings for gas bearings to 427 C
p0108 N82-27079

Novel improved PBR polyimides
[NASA-TM-82733] p0049 N82-11117

GRAPHITE-EPOXY COMPOSITES
Hybridized polymer matrix composite
[NASA-CR-165340] p0051 N82-12139
Boundary layer thermal stresses in angle-ply composite laminates, part I --- graphite-epoxy composites
[NASA-CR-165412] p0113 N82-26713

GRAPHITE-POLYIMIDE COMPOSITES
Application of a gripping system to test a uniaxial graphite fiber reinforced composite /EMR 15/Celion 6000/ in tension at 316 C
p0051 N82-40796
Geometrical aspects of the tribological properties of graphite fiber reinforced polyimide composites
[NASA-TM-82757] p0066 N82-15198
Tribological evaluation of composite materials made from a partially fluorinated polyimide
[NASA-TM-82832] p0069 N82-29459

GRAVITY GRADIENT SATELLITES
NT ATS 5

GROOVES
NI V GROOVES
The influence of surface dents and grooves on traction in sliding EHD point contacts
[NASA-TM-82943] p0102 N82-32734

GROUND TRUTH
Ground-truth observations of ice-covered North Slope Lakes imaged by radar
[NASA-TM-84127] p0117 N82-18664

GROWTH
NT CRYSTAL GROWTH
NT CZCCHRAISKI METHOD
NT DIRECTIONAL SOLIDIFICATION (CRYSTALS)
NT VAPOR PHASE EPITAXY

GUIDE VANES
NI JET VANES
Effect of a part span variable inlet guide vane on TF34 fan performance
[NASA-CR-165458] p0023 N82-12075
YF 102 in-duct combustor noise measurements with a turbine nozzle, volume 1
[NASA-CR-165562-VOL-1] p0153 N82-21031
YF 102 in-duct combustor noise measurements with a turbine nozzle, volume 2
[NASA-CR-165562-VOL-2] p0153 N82-21032
YF 102 in-duct combustor noise measurements with a turbine nozzle, volume 3
[NASA-CR-165562-VOL-3] p0155 N82-21033
Energy efficient engine: Turbine transition duct model technology report
[NASA-CR-167996] p0029 N82-33394

GUN LAUNCHERS
Mass Driver Two - A status report
p0046 N82-18191
Feasibility of an earth-to-space rail launcher system --- emphasizing nuclear waste disposal application
[IAF PAPER 82-46] p0033 N82-44659

GUY WIRES
Vibration analysis of three guyed tower designs for intermediate size wind turbines
[NASA-CR-165589] p0137 N82-30709

GYROPLANES
U LICOPTERS

GYROSCOPIC DRIFT
U ROSCOPIIC STABILITY

GYROSCOPIC STABILITY
The influence of Coriolis forces on gyroscopic motion of spinning blades
[ASME PAPER 82-GT-163] p0030 N82-35384

H

HAFNIUM COMPOUNDS
Some properties of RF sputtered hafnium nitride coatings
[NASA-TM-82826] p0067 N82-21331

HAIR
A hydrodynamic model of an outer hair cell
[NASA-TM-82773] p0143 N82-16743

HAIR PLANES
Motion of a rigid punch at the boundary of an

orthotropic viscoelastic half-plane

A82-26436

HALIDES
NT HYDROGEN CHLORIDES
NT IRON CHLORIDES
NT SODIUM CHLORIDES

HALL ACCELERATORS
Results and comparison of Hall and DV duct experiments
[NASA-TM-82864] p0157 N82-25961

HALL COEFFICIENT
U LL EFFECT

HALL CURRENTS
U LL EFFECT

HALL EFFECT
Effect of vacuum exhaust pressure on the performance of MHD ducts at high D-field
[NASA-TM-82750] p0157 N82-13908

HALOGEN COMPOUNDS
NT FLUOROPOLYMERS
NT HYDROGEN CHLORIDES
NT IRON CHLORIDES
NT POLYTETRAFLUOROETHYLENE
NT SODIUM CHLORIDES

HALOGENATION
NT FLUORINATION

HANDBOOKS
NT USER MANUALS (COMPUTER PROGRAMS)

HARDENING (MATERIALS)
NT HOT PRESSING
NT NITRIDING
NT PRECIPITATION HARDENING
NT SHOT PEENING

HARDNESS
NT MICROHARDNESS

HARDNESS TESTS
Effects of environment on microhardness of magnesium oxide
[NASA-TF-2002] p0068 N82-22366

HARRIER AIRCRAFT
A real time Pegasus propulsion system model for VSTOL piloted simulation evaluation
[NASA-TM-82770] p0016 N82-13144

HAUSER SIDDELEY AIRCRAFT
NT HARRIER AIRCRAFT

HAZARDS
NT AIRCRAFT HAZARDS
Resonance tube hazards in oxygen systems
[NASA-TM-82801] p0072 N82-21415

HEAT
NT PROCESS HEAT

HEAT CONDUCTION
U NDUCTIVE HEAT TRANSFER

HEAT CONTENT
U THALPY

HEAT DISSIPATION
U OLING

HEAT DISSIPATION CHILLING
U OLING

HEAT EFFECTS
U MPERATURE EFFECTS

HEAT EQUATIONS
U ERMOYNAMICS

HEAT EXCHANGERS
A heat exchanger computational procedure for temperature-dependent fouling
[ASME PAPER 81-HT-75] p0092 N82-10961
External fuel vaporization study
[NASA-CR-165513] p0073 N82-14371
MHD oxidant intermediate temperature ceramic heater study
[NASA-CR-165453] p0131 N82-15527
Experimental study of an integral catalytic combustor: Heat exchanger for Stirling engines
[NASA-TM-82783] p0119 N82-18691
Computer model of catalytic combustion/Stirling engine heater head
[NASA-CR-165378] p0134 N82-22666
Development and test fuel cell powered on-site integrated total energy systems. Phase 3: Full-scale power plant development
[NASA-CR-167898] p0137 N82-30705

HEAT FLUX
An experimental investigation into the feasibility of a thermoelectric heat flux gage
[NASA-TM-82755] p0095 N82-14494

HEAT GAIN
U ATING

HEAT OF COMBUSTION

Low NO sub x heavy fuel combustor concept program.
Phase 1A: Combustion technology generation coal
gas fuels
[NASA-CF-165614] p0055 N82-22326

HEAT PIPES

High thermal power density heat transfer ---
thermionic converters
[NASA-CASE-LFK-12950-1] p0087 N82-11399

HEAT PUMPS

An experimental investigation into the feasibility
of a thermoelectric heat flux pump
[NASA-TM-82755] p0095 N82-14494
Magnetic heat pumping
[NASA-CASE-LEW-12508-3] p0088 N82-24449

HEAT REGULATION

U MPFFATURE CONTROL

HEAT RESISTANCE

U ERMAL PPSISTANCE

HEAT RESISTANT ALLOYS

NT MOLYBDENUM ALLOYS

NT UDIRET ALLOYS

NT WASPALOY

Effects of cobalt on structure, microchemistry and
properties of a wrought nickel-base superalloy
p0065 A82-34973

The influence of gamma prime on the
recrystallization of an oxide dispersion
strengthened superalloy - MA 6000E
p0062 A82-47393

The influence of orientation on the stress rupture
properties of nickel-base superalloy single
crystals
p0062 A82-47397

Fatigue and creep-fatigue deformation of several
nickel-base superalloys at 650 C
p0062 A82-47398

The influence of cobalt on the tensile and
stress-rupture properties of the nickel-base
superalloy MAR-M247
p0063 A82-47399

The influence of cobalt on the microstructure of
the nickel-base superalloy MAR-M247
p0063 A82-47400

Applications of high-temperature powder metal
aluminum alloys to small gas turbines
p0065 A82-48244

Thermal fatigue and oxidation data of TAZ-8A and
M22 alloys and variations
[NASA-CR-165407] p0063 N82-10193

Creep shear behavior of the oxide dispersion
strengthened superalloy MA 6000E
[NASA-TM-82704] p0058 N82-10195

Trends in high temperature gas turbine materials
[NASA-TM-82715] p0058 N82-11182

A status review of NASA's CCSAM (Conservation Of
Strategic Aerospace Materials) program
[NASA-TM-82852] p0060 N82-24326

Hot isostatically pressed manufacture of high
strength HERRL 76 disk and seal shapes
[NASA-CR-165549] p0064 N82-26439

Mechanisms of deformation and fracture in high
temperature low cycle fatigue of Rene 80 and IN
100
[NASA-CF-165498] p0113 N82-26706

Solute transport during the cyclic oxidation of
Ni-Cr-Al alloys
[NASA-CR-165544] p0064 N82-27462

High temperature composites. Status and future
directions
[NASA-TM-82929] p0051 N82-30336

Overlay metallic-cermet alloy coating systems ---
for gas turbine engines
[NASA-CASE-LEW-13639-1] p0070 N82-33522

HEAT SHIELDING

Pyrolytic graphite collector development program
[NASA-CR-167909] p0052 N82-29363

HEAT STORAGE

Collection and dissemination of thermal energy
storage system information for the pulp and
paper industry
p0136 N82-24686

HEAT TESTS

U GH TEMPERATURE TESTS

HEAT TRANSFER

NT CONDUCTIVE HEAT TRANSFER

NT CONVECTIVE HEAT TRANSFER

NT RADIATIVE HEAT TRANSFER

Thermal and flow analysis of a convection,
air-cooled ceramic coated porous metal concept
for turbine vanes
[ASME PAPER 81-HT-48] p0020 A82-16952

Turbulent boundary layer heat transfer experiments
- A separate effects study on a convexly-curved
wall
[ASME PAPER 81-HT-70] p0092 A82-10961

Tube entrance heat transfer with deposit formation
[AIAA PAPER 82-0918] p0093 A82-31908

Effects of internal heat transfer on the structure
of self-similar blast waves
p0093 A82-32225

Cauchy integral method for two-dimensional
solidification interface shapes
p0089 A82-39899

Jet impingement heat transfer enhancement for the
GPU-3 Stirling engine
[NASA-TM-82727] p0163 N82-11993

Gas turbine ceramic-coated-vane concept with
convection-cooled porous metal core
[NASA-TP-1942] p0016 N82-14090

External fuel vaporization study
[NASA-CR-165513] p0073 N82-14371

Turbulent boundary layer heat transfer
experiments: Convex curvature effects including
introduction and recovery
[NASA-CR-3510] p0090 N82-17456

Effect of location in an array on heat transfer to
a cylinder in crossflow
[NASA-TM-82797] p0007 N82-19493

Low-thrust chemical propulsion system propellant
expulsion and thermal conditioning study.
Executive summary
[NASA-CR-165622] p0045 N82-24287

Low-thrust chemical propulsion system propellant
expulsion and thermal conditioning study
[NASA-CR-167841] p0045 N82-24288

Flows through sequential orifices with heated
spacer reservoirs
[NASA-TM-82855] p0088 N82-24455

Comparison of laser anemometer measurements and
theory in an annular turbine cascade with
experimental accuracy determined by parameter
estimation
[NASA-TM-82860] p0005 N82-28250

The dryout region in frictionally heated sliding
contacts
[NASA-TM-82796] p0088 N82-28574

Cooled variable nozzle radial turbine for rotor
craft applications
[NASA-CR-165397] p0028 N82-29323

HEAT TRANSMISSION

NT CONDUCTIVE HEAT TRANSFER

NT CONVECTIVE HEAT TRANSFER

NT HEAT TRANSFER

NT RADIATIVE HEAT TRANSFER

HEAT TREATMENT

NT ANNEALING

NT NITRIDING

HEATERS

MHD oxidant intermediate temperature ceramic
heater study
[NASA-CR-165453] p0131 N82-15527

HEATING

NT ATMOSPHERIC HEATING

NT RADIANT HEATING

NT SUPERHEATING

Experiments on fuel heating for commercial aircraft
[NASA-TM-82878] p0072 N82-26483

HEATING EQUIPMENT

NT VAPORIZERS

Experimental study of fuel heating at low
temperatures in a wing tank model, volume 1
[NASA-CR-165391] p0073 N82-11224

Additional experiments on flowability improvements
of aviation fuels at low temperatures, volume 2
[NASA-CR-167912] p0074 N82-31546

HEAVY ELEMENTS

NT PLUTONIUM 244

HELICOPTER ATTITUDE INDICATORS

U LICOPTERS

HELICOPTER DESIGN

NASA/HAA Advanced Rotorcraft Technology and Tilt
Rotor Workshop. Volume 5: Propulsion Session
[NASA-TM-84207] p0015 N82-23241

HELICOPTER ENGINES

TF34 Convertible Engine System Technology Program
p0022 A82-40521

ORIGINAL PAGE IS
OF POOR QUALITY

HELICOPTER PERFORMANCE

SUBJECT INDEX

NASA/HAA Advanced Rotorcraft Technology and Tilt Rotor Workshop. Volume 5: Propulsion Session
[NASA-TM-84207] p0015 N82-23241

Mathematical models for the synthesis and optimization of spiral bevel gear tooth surfaces --- for helicopter transmissions
[NASA-CR-3553] p0106 N82-25516

HELICOPTER PERFORMANCE
Performance degradation of propeller/rotor systems due to rime ice accretion
[AIAA PAPER 82-0286] p0014 A82-28322

HELICOPTERS
Lubricant effects on efficiency of a helicopter transmission
[NASA-TM-82857] p0100 N82-25520
Reliability model for planetary gear
[NASA-TM-82859] p0101 N82-28643

HELIOMAGNETISM
U LAR MAGNETIC FIELD

HELIX TUBES
U AVELING WAVE TUBES

HELIXES
U RVES (GEOMETRY)

HELVOLTZ VORTICITY EQUATION
The velocity field near the orifice of a Helmholtz resonator in grazing flow
[NASA-CR-168548] p0153 N82-18994

HERMETIC SEALS
Anaerobic polymers as high vacuum leak sealants
p0108 A82-21967

HETEROCYCLIC COMPOUNDS
NT INDOLES
NI PYBROLES
Deposit formation in liquid fuels. II - The effect of selected compounds on the storage stability of Jet A turbine fuel
p0074 A82-22240

HEXAGONAL CELLS
Net shape fabrication of Alpha Silicon Carbide turbine components
[ASME PAPER 82-GT-216] p0071 A82-35403

HIGH ACCELERATION
Mass Driver Two - A status report
p0046 A82-18191

HIGH ENERGY ELECTRONS
NT RELATIVISTIC ELECTRON BEAMS

HIGH FREQUENCIES
High-frequency high-voltage high-power DC-to-DC converters
p0083 N82-12347

HIGH MELTING COMPOUNDS
U FRACTORY MATERIALS

HIGH PRESSURE
Optically pumped high-pressure DF-CO2 transfer laser
A82-10193

Some observations in high pressure rheology of lubricants
[ASME PAPER 81-LUB-17] p0070 A82-18432

Some observations in high pressure rheology of lubricants
[ASME PAPER 81-LUB-17] p0070 A82-18432

JTBD high pressure compressor performance improvement
[NASA-CR-165531] p0104 N82-11467

CF6 jet engine performance improvement: High pressure turbine roundness
[NASA-CR-165555] p0024 N82-17174

Energy efficient engine: High pressure turbine uncooled rig technology report
[NASA-CR-165149] p0031 N82-32383

HIGH SPEED
Summary and recent results from the NASA advanced High Speed Propeller Research Program
[NASA-TM-82891] p0001 N82-26219

HIGH SPEED FLIGHT
U GH SPEED

HIGH TEMPERATURE
High thermal power density heat transfer --- thermionic converters
[NASA-CASE-LEW-12950-1] p0087 N82-11399
Tribological properties at 25 C of seven polyimide films bonded to 440 C high-temperature stainless steel
[NASA-TP-1944] p0067 N82-19373
Performance of laser glazed ZrO2 TBCs in cyclic oxidation and corrosion burner test rigs
[NASA-TM-82930] p0059 N82-22346

HIGH TEMPERATURE ALLOYS
U AT RESISTANT ALLOYS

HIGH TEMPERATURE ENVIRONMENTS
Proceedings of the Conference on High-temperature Electronics
[NASA-TM-84069] p0081 N82-15311
High temperature electronic requirements in aeropropulsion systems
[E-708] p0081 N82-15313
Development of an 1100 deg F capacitor
p0083 N82-15315
Fully plasma-sprayed compliant backed ceramic turbine seal
[NASA-CASE-LEW-13268-1] p0069 N82-29453

HIGH TEMPERATURE FLUIDS
NT HIGH TEMPERATURE GASES

HIGH TEMPERATURE GASES
Method and apparatus for strengthening boron fibers --- high temperature oxidation
[NASA-CASE-LEW-13826-1] p0050 N82-24385

HIGH TEMPERATURE LUBRICANTS
Thermal oxidative degradation reactions of perfluoroalkylethers
[NASA-CR-165516] p0048 N82-12135

HIGH TEMPERATURE MATERIALS
U FRACTORY MATERIALS

HIGH TEMPERATURE TESTS
Development of CdO-graphite-Ag coatings for gas bearings to 427 C
p0108 A82-27079
Work of fracture in aluminum metal-matrix composites
p0053 A82-31339
Ceramic thermal barrier coatings for gas turbine engines
[ASME PAPER 82-GT-265] p0071 A82-35441
Application of a gripping system to test a uniaxial graphite fiber reinforced composite /PHR 15/Celion 6000/ in tension at 316 C
p0051 A82-40796
Fatigue and creep-fatigue deformation of several nickel-base superalloys at 650 C
p0062 A82-47398
Elevated temperature fatigue testing of metals
[NASA-TM-82745] p0111 N82-16419
High temperature low cycle fatigue mechanisms for nickel base and a copper base alloy
[NASA-CR-3543] p0064 N82-26436
Mechanisms of deformation and fracture in high temperature low cycle fatigue of Rene 80 and IN 100
[NASA-CR-165498] p0113 N82-26706
Failure mechanisms of thermal barrier coatings exposed to elevated temperatures
[NASA-TM-82905] p0061 N82-32461

HIGH VACUUM
Anaerobic polymers as high vacuum leak sealants
p0108 A82-21967

HIGH VOLTAGES
Space Shuttle Orbiter charging
[AIAA PAPER 82-0119] p0040 A82-17793
Differential charging of high-voltage spacecraft - The equilibrium potential of insulated surfaces
p0041 A82-35547
Fast recovery, high voltage silicon diodes for AC motor controllers
p0086 A82-26926
Fabrication of multi-junction high voltage concentrator solar cells by integrated circuit technology
p0127 A82-44957
High-frequency high-voltage high-power DC-to-DC converters
p0083 N82-12347
High voltage power transistor development
[NASA-CR-165547] p0084 N82-18506
High voltage V-groove solar cell
[NASA-CASE-LEW-13401-2] p0123 N82-24717
High voltage planar multi-junction solar cell
[NASA-CASE-LEW-13400-1] p0125 N82-31764

HINGE MOMENTS
U ROUE

HOHNANN TRAJECTORIES
U ANSPER ORBITS

HOHNANN TRANSFER ORBITS
U ANSPER ORBITS

HOLDERS
NT FLAME HOLDERS

HOLE GEOMETRY (MECHANICS)
Analysis of cracks emanating from a circular hole in unidirectional fiber reinforced composites, part 2

ORIGINAL PAGE IS
OF POOR QUALITY

SUBJECT INDEX

HYDRODYNAMICS

- [NASA-CF-165433] p0114 N82-26714
- HOLOGRAPHIC INTERFEROMETRY**
Fringe localization requirements for three-dimensional flow visualization of shock waves in diffuse-illumination double-pulse holographic interferometry [NASA-TP-1868] p0095 N82-22481
- HOMOSPHERE**
NT STRATOSPHERE
- HONEYCOMB STRUCTURES**
Development of a high-temperature durable catalyst for use in catalytic combustors for advanced automotive gas turbine engines [NASA-CR-165396] p0130 N82-13510
Metal honeycomb to porous wireform substrate diffusion bond evaluation [NASA-TM-82793] p0110 N82-18612
- HORIZONTAL ORIENTATION**
Effect of rotor configuration on guyed tower and foundation designs and estimated costs for intermediate site horizontal axis wind turbines [NASA-TM-82804] p0121 N82-22649
Whirl flutter analysis of a horizontal-axis wind turbine with a two-bladed teetering rotor p0122 N82-23707
Comparison of upwind and downwind rotor operation of the DOE/NASA 100-kW MOD-0 wind turbine p0122 N82-23710
A review of resonance response in large horizontal-axis wind turbines p0122 N82-23711
- HOT CORROSION**
NT TEMPERATURE DEPENDENCE
Improved plasma sprayed MCrAlY coatings for aircraft gas turbine applications p0065 N82-20742
Long-term high-velocity oxidation and hot corrosion testing of several NiCrAl and FeCrAl base oxide dispersion strengthened alloys p0062 N82-37151
Investigation into the role of NaCl deposited on oxide and metal substrates in the initiation of hot corrosion [NASA-CR-165029] p0063 N82-13217
Gas-turbine critical research and advanced technology support project [NASA-TM-81708] p0118 N82-13509
- HOT GAS SYSTEMS**
U GH TEMPERATURE GASES
- HOT GASES**
U GH TEMPERATURE GASES
- HOT JET EXHAUST**
U GH TEMPERATURE GASES
U T EXHAUST
- HOT JETS**
U T FLOW
- HOT PRESSING**
Hot isostatically pressed manufacture of high strength MRL 76 disk and seal shapes [NASA-CR-165549] p0064 N82-26439
- HOT-FILM ANEMOMETERS**
Three sensor hot wire/film technique for three dimensional mean and turbulence flow field measurement p0097 N82-30300
- HOT-WIRE ANEMOMETERS**
Three sensor hot wire/film technique for three dimensional mean and turbulence flow field measurement p0097 N82-30300
- HOT-WIRE FLOWMETERS**
Turbulence measurements in a confined jet using a hot-wire probe technique [AIAA PAPER 82-1262] p0094 N82-37710
Investigations of flowfields found in typical combustor geometries [NASA-CR-163585] p0090 N82-19495
- HOT-WIRE TURBULENCE METERS**
U T-WIRE FLOWMETERS
- HOUSINGS**
NT COWLINGS
- HYBRID COMPUTERS**
Development report: Automatic System Test and Calibration (ASTAC) equipment [NASA-CF-165403] p0129 N82-13505
Role of optical computers in aeronautical control applications p0156 N82-15897
- HYDRAULIC ACTUATORS**
U TUATORS
- HYDRAULIC FLUIDS**
Elucidation of wear mechanisms by ferrographic analysis [NASA-TM-82737] p0066 N82-15199
- HYDRAULIC PUMPS**
U PPS
- HYDROAEROMECHANICS**
U RODYNAMICS
- HYDROCARBON COMBUSTION**
Lean-limit extinction of propane/air mixtures in the stagnation-point flow p0057 N82-28736
On the opening of premixed Bunsen flame tips p0057 N82-37570
Formation of oxides of nitrogen in monodisperse spray combustion of hydrocarbon fuels p0057 N82-37571
Thermodynamic and transport combustion properties of hydrocarbons with air. Part 1: Properties in SI units [NASA-TP-1906] p0161 N82-32186
Thermodynamic and transport combustion properties of hydrocarbons with air. Part 2: Compositions corresponding to Kelvin temperature schedules in part 1 [NASA-TP-1907] p0161 N82-32187
Thermodynamic and transport combustion properties of hydrocarbons with air. Part 3: Properties in US customary units [NASA-TP-1908] p0161 N82-32188
Thermodynamic and transport combustion properties of hydrocarbons with air. Part 4: Compositions corresponding to Rankine temperature schedules in part 3 [NASA-TP-1909] p0161 N82-32189
- HYDROCARBON FUELS**
NT DIESEL FUELS
NT FOSSIL FUELS
NT JET ENGINE FUELS
NT LIQUID FUELS
NT RP-1 ROCKET PROPELLANTS
Deposit formation in hydrocarbon fuels [ASME PAPER 82-GT-49] p0075 N82-35307
Gas-turbine critical research and advanced technology support project [NASA-TM-81708] p0118 N82-13509
Oxidation and formation of deposit precursors in hydrocarbon fuels [NASA-CR-165534] p0073 N82-18402
Deposit formation in hydrocarbon rocket fuels with an evaluation of a propane heat transfer correlation [NASA-TM-82911] p0088 N82-26611
Effect of hydrocarbon fuel type on fuel [NASA-TM-82916] p0072 N82-28460
Additional experiments on flowability improvements of aviation fuels at low temperatures, volume 2 [NASA-CR-167912] p0074 N82-31546
- HYDROCARBONS**
NT LIQUEFIED NATURAL GAS
NT METHANE
NT PROPANE
Quantitative separation of tetralin hydroperoxide from its decomposition products by high performance liquid chromatography p0048 N82-15696
Exhaust emissions reduction for intermittent combustion aircraft engines [NASA-CR-167914] p0029 N82-33392
- HYDRODYNAMIC EQUATIONS**
NT HELMHOLTZ VORTICITY EQUATION
- HYDRODYNAMIC STABILITY**
U OW STABILITY
- HYDRODYNAMICS**
NT CYLINDRICAL PLASMAS
NT ELASTOHYDRODYNAMICS
NT MAGNETOHYDRODYNAMICS
A hydrodynamic model of an outer hair cell [NASA-TM-82773] p0143 N82-16743
Hydrodynamic and aerodynamic breakup of liquid sheets [NASA-TM-82800] p0087 N82-19494
Geometry and starvation effects in hydrodynamic lubrication [NASA-TM-82807] p0042 N82-20240
Lubrication of rigid ellipsoidal solids [NASA-TM-81694] p0100 N82-25518

HYDROGEN

HYDROGEN

NT LIQUID HYDROGEN
The combined effects of Fe and H2 on the nitridation of silicon
p0070 A82-42924
Effect of oxide films on hydrogen permeability of candidate Stirling engine heater head tube alloys
[NASA-TM-82024] p0060 A82-24323

HYDROGEN AIR FUEL CELLS
U DROGEN OXYGEN FUEL CELLS

HYDROGEN CHLORIDES
Effects of environment on microhardness of magnesium oxide
[NASA-TP-2002] p0068 A82-22366

HYDROGEN COMPOUNDS
NT HYDROGEN PEROXIDE

HYDROGEN FUELS
NT LIQUID FUELS

HYDROGEN OXYGEN ENGINES
Low-thrust Isp sensitivity study
[NASA-CR-165621] p0045 A82-22309

HYDROGEN OXYGEN FUEL CELLS
Electrochemical energy storage for an orbiting space station
[NASA-CR-165436] p0132 A82-17607

HYDROGEN PEROXIDE
Quantitative separation of tetralin hydroperoxide from its decomposition products by high performance liquid chromatography
p0048 A82-15696

HYDROLOGY
Dynamics of snow cover in mountain regions of the Aral Sea basin, studied using satellite photographs
A82-27462

HYDROMAGNETICS
U GNETOHYDRODYNAMICS

HYDROMAGNETISM
U GNETOHYDRODYNAMICS

HYDROMECHANICS
NT ELASTOHYDRODYNAMICS
NT HYDRODYNAMICS
NT MAGNETOHYDRODYNAMICS

HYDROX ENGINES
U DROGEN OXYGEN ENGINES

HYDROXYL COMPOUNDS
NT POLYVINYL ALCOHOL

HYGIAL PROPERTIES
Prediction of composite hygral behavior made simple
[NASA-TM-82780] p0049 A82-16181

HYPERGOLIC ROCKET PROPELLANTS
NT LIQUID FUELS

HYPERSONIC WIND TUNNELS
NT CASCADE WIND TUNNELS
NT SHOCK TUNNELS

HYPERVELOCITY CRATERING
U PERVELOCITY PROJECTILES

HYPERVELOCITY IMPACT
The development of central peaks in lunar craters
A82-14333

HYPERVELOCITY PROJECTILES
Mass Driver Two - A status report
p0046 A82-18191

HYPERVELOCITY WIND TUNNELS
NT CASCADE WIND TUNNELS
NT SHOCK TUNNELS

ICE
NT LAKE ICE

ICE ENVIRONMENTS
NASA/Lewis Research Center Icing Research Program
p0001 A82-21148

ICE FORMATION
Aerodynamic characteristics of airfoils with ice accretions
[AIAA PAPER 82-0282] p0010 A82-22081
Mathematical modeling of ice accretion on airfoils
[AIAA PAPER 82-0284] p0014 A82-27098
Performance degradation of propeller/rotor systems due to rime ice accretion
[AIAA PAPER 82-0286] p0014 A82-28322
Selected bibliography of NACA-NASA aircraft icing publications
[NASA-TM-81651] p0014 A82-11053
An experimental study of airfoil icing characteristics
[NASA-TM-82790] p0001 A82-17083

NASA/Lewis Research Center Icing Research Program
p0001 A82-21148
Rime ice accretion and its effect on airfoil performance
[NASA-CR-165599] p0008 A82-24166
Aircraft icing research at NASA
[NASA-TM-82919] p0013 A82-30297

ICE OBSERVATION
U E REPORTING

ICE PREVENTION
Icing tunnel tests of a composite porous leading edge for use with a liquid anti-ice system --- Lewis icing research tunnel
[NASA-CR-164966] p0014 A82-11052
Selected bibliography of NACA-NASA aircraft icing publications
[NASA-TM-81651] p0014 A82-11053
Numerical simulation of one-dimensional heat transfer in composite bodies with phase change --- wing deicing pads
[NASA-CR-165607] p0002 A82-22142
Aircraft icing research at NASA
[NASA-TM-82919] p0013 A82-30297

ICE REPORTING
Ground-truth observations of ice-covered North Slope Lakes imaged by radar
[NASA-TM-84127] p0117 A82-18664

ICING
U E FORMATION

IDENTIFYING
NT PARAMETER IDENTIFICATION

IGFET
U ELD EFFECT TRANSISTORS

IGNITION
Resonance tube hazards in oxygen systems
[NASA-TM-82801] p0072 A82-21415

IMAGE PROCESSING
NT GEOMETRIC RECTIFICATION (IMAGERY)
Reliable aerial thermography for energy conservation
[NASA-TM-81766] p0117 A82-14552
Application of image processing techniques to fluid flow data analysis
[NASA-TM-82760] p0004 A82-16049

IMAGE RECONSTRUCTION
Maximum entropy image reconstruction from projections
A82-11053

IMAGERY
NT SATELLITE-BORNE PHOTOGRAPHY
NT SCHLIEREN PHOTOGRAPHY

IMAGING TECHNIQUES
Digital imaging techniques in experimental stress analysis
p0097 A82-34231
Application of image processing techniques to fluid flow data analysis
[NASA-TM-82760] p0004 A82-16049
Shaded computer graphic techniques for visualizing and interpreting analytic fluid flow models
[NASA-CR-168418] p0145 A82-17880

IMMITTANCE
U ELECTRICAL IMPEDANCE

IMPACT
NT ECONOMIC IMPACT
NT HYPERVELOCITY IMPACT
NT ION IMPACT

IMPACT DAMAGE
Hybridized polymer matrix composite
[NASA-CR-165340] p0051 A82-12139
Bird impact analysis package for turbine engine fan blades
[NASA-TM-82831] p0112 A82-26701
A study of the nature of solid particle impact and shape on the erosion morphology of ductile metals
[NASA-TM-82933] p0061 A82-33493

IMPACT RESISTANCE
Impact resistance of fiber composites
p0112 A82-39852
Environmental and High-Strain Rate effects on composites for engine applications
[NASA-TM-82882] p0051 A82-31449

IMPACT SENSITIVITY
U PACT RESISTANCE

IMPACT TESTS
Indentation law for composite laminates
[NASA-CR-165460] p0052 A82-15123

IMPACT DIODES
U ALANCHE DIODES

- IMPEDANCE**
 NT CONTACT RESISTANCE
 NT ELECTRICAL IMPEDANCE
 NT ELECTRICAL RESISTANCE
- IMPELLER BLADES**
 U TOR BLADES (TUPBCNACHINFRY)
- IMPELLERS**
 Applications of high-temperature powder metal aluminum alloys to small gas turbines p0065 A82-48244
- IMPERFECTIONS**
 U FACTS
- IMPINGEMENT**
 NT JET IMPINGEMENT
 A study of the nature of solid particle impact and shape on the erosion morphology of ductile metals [NASA-TM-82933] p0061 N82-33493
- IMPLANTATION**
 NT ION IMPLANTATION
- IMPURITIES**
 Surface diffusion activation energy determination using ion beam microtexturing p0159 A82-21965
 Quasi-liquid states observed on ion beam microtextured surfaces p0159 A82-30335
 Material and processing needs for silicon solar cells in space p0032 N82-26336
- INCOMPRESSIBLE FLOW**
 A simple finite difference procedure for the vortex controlled diffuser [AIAA PAPER 82-0109] p0030 A82-17788
 Numerical analysis of confined turbulent flow p0093 A82-24748
- INDENTATION**
 Indentation law for composite laminates [NASA-CR-165460] p0052 N82-15123
 Occurrence of spherical ceramic debris in indentation and sliding contact [NASA-TP-2048] p0069 N82-32491
- INDEPENDENT VARIABLES**
 NT LATTICE PARAMETERS
- INDICATING INSTRUMENTS**
 NT DRAG FORCE ANEMOMETERS
 NT FLOW DIRECTION INDICATORS
 NT HOT-FILM ANEMOMETERS
 NT HOT-WIRE ANEMOMETERS
 NT LASER ANEMOMETERS
- INDIUM**
 Secondary electron emission yields p0038 N82-14226
- INDIUM COMPOUNDS**
 Electron beam induced damage in ITO coated Kapton --- Indium Tin Oxide p0159 A82-41546
- INDOLES**
 Deposit formation in liquid fuels. III - The effect of selected nitrogen compounds on diesel fuel p0074 A82-23238
- INDUCED FLUID FLOW**
 U UID FLOW
- INDUCTION MOTORS**
 A PWM transistor inverter for an ac electric vehicle drive p0085 A82-20744
 Progress on advanced dc and ac induction drives for electric vehicles [NASA-TM-82895] p0163 N82-31160
- INDUCTION SYSTEMS**
 U TAKE SYSTEMS
- INDUCTORS**
 Development of a dual-field heteropolar power converter [NASA-CR-165168] p0084 N82-24424
- INDUSTRIAL WASTES**
 Collection and dissemination of thermal energy storage system information for the pulp and paper industry p0136 N82-24686
- INELASTIC STRESS**
 Research and development program for non-linear structural modeling with advanced time-temperature dependent constitutive relationships [NASA-CR-165533] p0024 N82-16080
 Evaluation of inelastic constitutive models for nonlinear structural analysis --- for aircraft turbine engines [NASA-TM-82845] p0112 N82-24502
- INERT GASES**
 U RE GASES
- INERTIA**
 NT INERTIA PRINCIPLE
 INERTIA PRINCIPLE
 In-plane inertial coupling in tuned and severely mistuned bladed disks [ASME PAPER 82-GT-288] p0012 A82-35460
- INERTIA WHEELS**
 U UNTER-ROTATING WHEELS
- INFORMATION MANAGEMENT**
 Applications of the DOE/NASA wind turbine engineering information system p0122 N82-23696
- INFRARED DETECTORS**
 Raman study of the improper ferroelectric phase transition in iron iodine boracite A82-30297
- INFRARED INSTRUMENTS**
 NT INFRARED DETECTORS
- INFRARED RADIATION**
 Analysis of infrared emission from thin adsorbates p0056 A82-21431
- INFRARED SPECTRA**
 Alignment of fluid molecules in an EHD contact [ASLE PREPRINT 81-LC-5C-1] p0107 A82-18407
- INGESTION (ENGINES)**
 Water ingestion into jet engine axial compressors [AIAA PAPER 82-0196] p0030 A82-17836
- INGOTS**
 MC carbide structures in M(1c2)ar-M247 [NASA-CR-167892] p0064 N82-30374
- INHIBITORS**
 NT WEAR INHIBITORS
- INITIAL VALUE PROBLEMS**
 U UNDAARY VALUE PROBLEMS
- INJECTION**
 NT FUEL INJECTION
 NT GAS INJECTION
- INJECTION CARBURATORS**
 U EL INJECTION
- INJECTION MOLDING**
 Fabrication of turbine components and properties of sintered silicon nitride [ASME PAPER 82-GT-252] p0071 A82-35431
 Fabrication of sinterable silicon nitride by injection molding p0071 A82-37015
- INJECTORS**
 Atomization and combustion properties of flashing injectors [AIAA PAPER 82-0300] p0092 A82-17880
 Testing of fuel/oxidizer-rich, high-pressure preburners [NASA-CR-165609] p0074 N82-24353
- INLET FLOW**
 The effect of inflow velocity profiles on the performance of supersonic ejector nozzles [AIAA PAPER 81-0273] p0002 A81-32548
 Flow through axially aligned sequential apertures of the orifice and Borda types [ASME PAPER 81-HT-79] p0089 A82-10964
 Experimental and analytical results of tangential blowing applied to a subsonic V/STOL inlet [AIAA PAPER 82-1084] p0005 A82-35195
 Tangential blowing for control of strong normal shock - Boundary layer interactions on inlet ramps [AIAA PAPER 82-1082] p0005 A82-37684
 A summary of V/STOL inlet analysis methods p0006 A82-40921
 A summary of V/STOL inlet analysis methods [NASA-TM-82725] p0003 N82-11043
 Effect of a part span variable inlet guide vane on TP34 fan performance [NASA-CR-165458] p0023 N82-12075
 Thrust modulation methods for a subsonic V/STOL aircraft [NASA-TM-82747] p0003 N82-13112
 Geometry and starvation effects in hydrodynamic lubrication [NASA-TM-82807] p0042 N82-20240
 Experimental and analytical results of tangential blowing applied to a subsonic V/STOL inlet [NASA-TM-82847] p0004 N82-24165
 Some aspects of calculating flows about three-dimensional subsonic inlets [NASA-TM-82789] p0004 N82-25213

- Investigation of the tip clearance flow inside and at the exit of a compressor rotor passage
[NASA-CF-169004] p0026 N82-25253
- Acoustic properties of turbfan inlets
[NASA-CF-169016] p0153 N82-27090
- A summary of V/STOL inlet analysis methods
[NASA-TM-828P5] p0005 N82-28249
- Calculation of the flow field including boundary layer effects for supersonic mixed compression inlets at angles of attack
[NASA-CF-167941] p0009 N82-29269
- INLET NOZZLES**
- YF 102 in-duct combustor noise measurements with a turbine nozzle, volume 1
[NASA-CR-165562-VOL-1] p0153 N82-21031
- YF 102 in-duct combustor noise measurements with a turbine nozzle, volume 2
[NASA-CR-165562-VOL-2] p0153 N82-21032
- YF 102 in-duct combustor noise measurements with a turbine nozzle, volume 3
[NASA-CF-165562-VOL-3] p0155 N82-21033
- Aerodynamic analysis of V/STOL inlets and definition of a short, blowing-lip inlet
[NASA-CF-1656171] p0007 N82-22211
- INLET PRESSURE**
- Computer modeling of fan-exit-splitter spacing effects on F100 response to distortion
[NASA-CR-167879] p0025 N82-23246
- INLET TEMPERATURE**
- Computer modeling of fan-exit-splitter spacing effects on F100 response to distortion
[NASA-CF-167879] p0025 N82-23246
- INLETS (DEVICES)**
- INTAKE SYSTEMS**
- INOCULATION**
- Seeding considerations for an LV system in a large transonic wind tunnel
p0096 N82-32689
- INORGANIC COATINGS**
- NT CERMIC COATINGS**
- INORGANIC PEROXIDES**
- NT HYDROGEN PEROXIDE**
- INORGANIC SULFIDES**
- NT MOLYBDENUM SULFIDES**
- Moderate temperature Na cells III - Electrochemical and structural studies of Cr_{0.5}V_{0.5}S₂ and its Na intercalates
p0055 N82-15732
- INSENSITIVITY**
- U NSITIVITY**
- INSULATION**
- Development of a large area space solar cell assembly
[NASA-CR-167929] p0137 N82-30706
- INSTABILITY**
- U ABILITY**
- INSTALLATION**
- U STALLING**
- INSTALLING**
- Rough analysis of installation effects on turboprop noise
[NASA-TM-82924] p0152 N82-32082
- INSTRUMENT COMPENSATION**
- Extending the frequency of response of lightly damped second order systems: Application to the drag force anemometer
[NASA-TM-82927] p0096 N82-32662
- INSTRUMENT DRIFT**
- U IFT (INSTRUMENTATION)**
- INSULATING MATERIALS**
- U SULATION**
- INSULATION**
- NT ELECTRICAL INSULATION**
- Experimental simulation of biased solar arrays with the space plasma
[NASA-CR-165485] p0157 N82-10880
- INSULATORS**
- SCATHA SSPM charging response: NASCAP predictions compared with data
p0037 N82-14251
- Numerical simulation of plasma insulator interactions in space. Part 1: The self consistent calculation
p0039 N82-14272
- Numerical simulation of plasma insulator interactions in space. Part 2: Dielectric effects
p0039 N82-14273
- INTAKE SYSTEMS**
- NT AIR INTAKES**
- NT ENGINE INLETS**
- NT INTERNAL COMPRESSION INLETS**
- NT NOSE INLETS**
- NT SUPERSONIC INLETS**
- Performance of single-stage axial-flow transonic compressor with rotor and stator aspect ratios of 1.63 and 1.78, respectively, and with design pressure ratio of 1.82
[NASA-TP-1974] p0017 N82-19222
- INTEGRAL EQUATIONS**
- NT J INTEGRAL**
- Solutions of the compressible Navier-Stokes equations using the integral method
[AIAA PAPER 81-0046] p0093 N82-23832
- Path-independent integrals in finite elasticity and inelasticity, with body forces, inertia, and arbitrary crack-face conditions
p0115 N82-32303
- On a study of the $\Delta T/c$ and $C/asterisk/$ integrals for fracture analysis under non-steady creep
p0115 N82-36782
- Construction of solutions for some nonlinear two-point boundary value problems
[NASA-TM-82937] p0144 N82-30949
- INTEGRATED CIRCUITS**
- NT ENCAPSULATED MICROCIRCUITS**
- Multijunction high voltage concentrator solar cells
p0043 N82-11796
- Compensation mechanism in liquid encapsulated Czochralski GaAs importance of melt stoichiometry
p0086 N82-40403
- Fabrication of multijunction high voltage concentrator solar cells by integrated circuit technology
p0127 N82-44957
- INTEGRATED ENERGY SYSTEMS**
- Develop and test fuel cell powered on-site integrated total energy systems. Phase 3: Full-scale power plant development
[NASA-CR-165455] p0131 N82-16483
- Develop and test fuel cell powered on-site integrated total energy systems: Phase 3: Full-scale power plant development
[NASA-CR-165568] p0135 N82-24648
- INTEGRODIFFERENTIAL EQUATIONS**
- U PFERENTIAL EQUATIONS**
- U TEGRAL EQUATIONS**
- INTERACTIVE GRAPHICS**
- U MPUTER GRAPHICS**
- INTERCALATION**
- Moderate temperature Na cells. III - Electrochemical and structural studies of Cr_{0.5}V_{0.5}S₂ and its Na intercalates
p0055 N82-15732
- INTERFACES**
- NT LIQUID-SOLID INTERFACES**
- NT SOLID-SOLID INTERFACES**
- Systems integration
p0042 N82-27371
- INTERFACIAL ENERGY**
- Universal binding energy relations in metallic adhesion
[NASA-TM-82706] p0058 N82-11183
- INTERFACIAL STRAIN**
- U TERFACIAL TENSION**
- INTERFACIAL TENSION**
- Interface cracks in adhesively bounded lap-shear joints
p0116 N82-46109
- Fatigue life prediction in bending from axial fatigue information
[NASA-CR-165563] p0113 N82-20564
- Factors influencing the thermally-induced strength degradation of B/Al composites
[NASA-TM-82823] p0050 N82-24297
- INTERFEROMETERS**
- NT MACH-ZEHNDER INTERFEROMETERS**
- INTERFEROMETRY**
- NT HOLOGRAPHIC INTERFEROMETRY**
- NT LASER INTERFEROMETRY**
- INTERMETALLICS**
- Hard permanent magnet development trends and their application to A.C. machines
p0083 N82-20745
- Recrystallization and grain growth in NiAl
p0065 N82-44529

INTERMITTENCY
Development potential of Intermittent Combustion (I.C.) aircraft engines for commuter transport applications [NASA-TM-82869] p0019 N82-26297

INTERMODULATION
Computer modeling of multiple-channel input signals and intermodulation losses caused by nonlinear traveling wave tube amplifiers [NASA-TP-1999] p0082 N82-25441

INTERNAL COMBUSTION ENGINES
NT BRISTOL-SIDDELEY BS 53 ENGINE
NT DIESEL ENGINES
NT GAS TURBINE ENGINES
NT HELICOPTER ENGINES
NT JET ENGINES
NT TURBOFAN ENGINES
NT TURBOJET ENGINES
NT TURBOPROP ENGINES
NT WANKEL ENGINES
Barriers to the utilization of synthetic fuels for transportation [NASA-CR-165517] p0073 N82-13243
Development of a high-temperature durable catalyst for use in catalytic combustors for advanced automotive gas turbine engines [NASA-CR-165396] p0130 N82-13510
ERPs fuel addendum: Pollution reduction technology program small jet aircraft engines, phase 3 [NASA-CF-165387] p0024 N82-14096
Development potential of Intermittent Combustion (I.C.) aircraft engines for commuter transport applications [NASA-TM-82869] p0019 N82-26297
Electrostatic fuel conditioning of internal combustion engines [NASA-CR-169029] p0106 N82-26680

INTERNAL COMPRESSION INLETS
Three-dimensional flow calculations including boundary layer effects for supersonic inlets at angle of attack [AIAA PAPER 82-0061] p0005 A82-19778

INTERNAL STRESS
U SIGNAL STRESS

INTERNAL WAVES
NT PLANETARY WAVES

INTERNATIONAL TRADE
International market assessment of stand-alone photovoltaic power systems for cottage industry applications [NASA-CR-165287] p0132 N82-16494

INTERPLANETARY PROPULSION
U TERPLANETARY SPACECRAFT
UCKET ENGINES

INTERPLANETARY SPACE
Potentials of surfaces in space p0165 A82-23750

INTERPLANETARY SPACECRAFT
Research report: User's manual for computer program AT81Y005. PLANETSYS, a computer program for the steady state and transient thermal analysis of a planetary power transmission system [NASA-CF-165366] p0146 N82-31970

INVERTERS
NT STATIC INVERTERS
The ac propulsion system for an electric vehicle, phase 1 [NASA-CF-165480] p0129 N82-13506

INVESTIGATION
Analytical investigation of nonrecoverable stall [NASA-TM-82792] p0018 N82-21195

INVISCID FLOW
N^o STAGNATION FLOW
A FORTRAN program for calculating three dimensional, inviscid and rotational flows with shock waves in axial compressor blade rows: User's manual [NASA-CF-3560] p0008 N82-26230
The design and instrumentation of the Purdue annular cascade facility with initial data acquisition and analysis [NASA-CF-167861] p0008 N82-26237

ION BEAMS
Surface diffusion activation energy determination using ion beam microtexturing p0159 A82-21965
Quasi-liquid states observed on ion beam microtextured surfaces p0159 A82-30335

Ion-beam-induced topography and surface diffusion p0160 A82-46426
Ion beam textured graphite electrode plates --- high efficiency electron tube devices [NASA-CASE-LEW-12919-2] p0050 N82-26386
Ion beam sputter deposited diamond like films [NASA-TM-82873] p0069 N82-28445
Deposition of reactively ion beam sputtered silicon nitride coatings [NASA-TM-82942] p0069 N82-30401
Ion beam microtexturing and enhanced surface diffusion [NASA-CR-167948] p0065 N82-31509

ION CURRENTS
NT ION BEAMS

ION DENSITY (CONCENTRATION)
NT MAGNETOSPHERIC ION DENSITY
Additional extensions to the NASCAP computer code, volume 3 [NASA-CR-167857] p0040 N82-26378

ION DISTRIBUTION
The hidden ion population of the magnetosphere p0140 A82-32630

ION ENGINES
NT MERCURY ION ENGINES
Characterization of advanced electric propulsion systems [AIAA PAPER 82-1246] p0071 A82-35083
Developing a scalable inert gas ion thruster [AIAA PAPER 82-1275] p0047 A82-37713
Electric thruster research [NASA-CR-165603] p0045 N82-24285
Additional extensions to the NASCAP computer code, volume 3 [NASA-CR-167857] p0040 N82-26378
Characterization of advanced electric propulsion systems [NASA-CR-167885] p0045 N82-26381

ION EXCHANGE MEMBRANE ELECTROLYTES
Method of making formulated plastic separators for soluble electrode cells [NASA-CASE-LEW-12358-2] p0054 N82-21268

ION IMPACT
Ion-beam-induced topography and surface diffusion p0160 A82-46426

ION IMPLANTATION
Undoped semi-insulating LEC GaAs - A model and a mechanism --- Liquid Encapsulated Czochralski p0159 A82-13754
Stoichiometry-controlled compensation in liquid encapsulated Czochralski GaAs p0158 A82-17585
Processing of silicon solar cells by ion implantation and laser annealing [NASA-CR-165283] p0128 N82-11546
Friction wear and auger analysis of iron implanted with 1.5-MeV nitrogen ions [NASA-TP-1989] p0059 N82-21300
Tribological characteristics of nitrogen (N+) implanted iron [NASA-TM-82839] p0060 N82-24322

ION MICROSCOPES
Application of surface analysis to solve problems of wear [NASA-TM-82753] p0099 N82-14519

ION MOTION
Field-aligned ion streams in the earth's midnight region p0140 A82-31009

ION PLATING
Tribological properties and XPS studies of ion plated gold on nickel and iron [NASA-TM-82814] p0059 N82-22344

ION-GAS INTERACTIONS
U S-ION INTERACTIONS

IONIC PROPELLANTS
U N ENGINES

IONIZATION
NT AURORAL IONIZATION

IONIZED GASES
NT ARGON PLASMA
NT CHARGED PARTICLES
NT PLASMA SHEATHS
NT PLASMAS (PHYSICS)

IONIZED PLASMAS
U ASMAS (PHYSICS)

IONIZING RADIATION
NT FAR ULTRAVIOLET RADIATION

J

NT GLAMA FAYS
NT SOLAR X-RAYS
IONOSPHERIC SOUNDING

An attempt at magnetic-variation sounding in the
Antarctic

A82-25290

IONS

NT ANIONS
NT NITROGEN IONS
IP (IMPACT PREDICTION)
U NEUTRALIZED SIMULATION

IRON

The combined effects of Fe and H2 on the
nitridation of silicon

p0070 A82-42924

Surface chemistry and wear behavior of
single-crystal silicon carbide sliding against
iron at temperatures to 1500 C in vacuum
[NASA-TP-1947] p0067 A82-19374

Friction and wear of iron in corrosive metal
[NASA-TP-1985] p0058 A82-20291

Friction wear and auger analysis of iron implanted
with 1.5-MeV nitrogen ions
[NASA-TP-1989] p0059 A82-21300

Tribological characteristics of nitrogen (N+)
implanted iron
[NASA-TM-82B39] p0060 A82-24322

IRON ALLOYS

NT STAINLESS STEELS
NT STEELS

Long-term high-velocity oxidation and hot
corrosion testing of several NiCrAl and FeCrAl
base oxide dispersion strengthened alloys
p0062 A82-37151

Evaluation of candidate stirling engine heater
tube alloys at 820 deg and 860 deg C
[NASA-TM-82A37] p0061 A82-30372

Overlay metallic-cermet alloy coating systems ---
for gas turbine engines
[NASA-CASE-LFW-13639-1] p0070 A82-33522

IRON CHLORIDES

Improved chromium electrodes for REDOX cells
[NASA-CASE-LFW-13653-1] p0121 A82-22672

IRON COMPOUNDS

NT IRON CHLORIDES

Raman study of the improper ferroelectric phase
transition in iron iodine boracite
A82-30297

IRON-CHROMIUM REDOX BATTERIES

NASA preprototype redox storage system for a
photovoltaic stand-alone application
p0127 A82-11774

IRRADIATION

NT ELECTRON IRRADIATION

IRROTATIONAL FLOW

U TENTIAL FLOW

ISING MODEL

U THERMICAL MODELS

ISOLATORS

NT VIBRATION ISOLATORS

ISOSTATIC PRESSURE

Hot isostatically pressed manufacture of high
strength MERL 76 disk and seal shapes
[NASA-CR-165549] p0064 A82-26439

ISOTOPIES

NT PLATINUM ISOTOPIES

NT PLUTONIUM 244

ISOTROPIC TURBULENCE

Analysis of the decay of temperature fluctuations
in isotropic turbulence
p0089 A82-40781

Ultrasonic input-output for transmitting and
receiving longitudinal transducers coupled to
same face of isotropic elastic plate
[NASA-CR-3506] p0110 A82-18613

ITERATION

NT ITERATIVE SOLUTION

ITERATIVE SOLUTION

Maximum entropy image reconstruction from
projections
A82-11053

An iterative finite element-integral technique for
predicting sound radiation from turbofan inlets
in steady flight
[AIAA PAPER 82-0124] p0030 A82-17796

Self-adaptive closed constrained solution
algorithms for nonlinear conduction
p0094 A82-45157

J INTEGRAL

Crack displacements for J/I testing with compact
specimens

p0112 A82-43358

JEEPS

U TOMOBILES

JET AIRCRAFT

NT BOEING 747 AIRCRAFT

NT DC 9 AIRCRAFT

NT DC 10 AIRCRAFT

NT TURBOPROP AIRCRAFT

JET AIRCRAFT NOISE

Effect of facility variation on the acoustic
characteristics of three single stream nozzles
[NASA-TM-81635] p0151 A82-19944

Forward acoustic performance of a model turbofan
designed for a high specific flow (QP-14)
[NASA-TP-1968] p0152 A82-21036

Aeroacoustic performance of an externally blown
flap configuration with several flap noise
suppression devices
[NASA-TP-1995] p0152 A82-24942

QCSEE under-the-wing engine acoustic data
[NASA-TM-82691] p0019 A82-27311

JET DAMPING

U MPING

JET DRIVE

U T PROPULSION

JET ENGINE FUELS

NT LIQUID FUELS

Deposit formation in liquid fuels, II - The effect
of selected compounds on the storage stability
of Jet A turbine fuel
p0074 A82-22240

Deposit formation in liquid fuels, I - Effect of
coal-derived Lewis bases on storage stability of
Jet A turbine fuel
p0074 A82-22241

NASA/General Electric broad-specification fuels
combustion technology program - Phase I results
and status
[AIAA PAPER 82-1089] p0021 A82-35000

Experimental study of fuel heating at low
temperatures in a wing tank model, volume 1
[NASA-CR-165391] p0073 A82-11224

Pollution reduction technology program small jet
aircraft engines, phase 3
[NASA-CR-165386] p0023 A82-14095

An assessment of the crash fire hazard of liquid
hydrogen fueled aircraft
[NASA-CR-165526] p0013 A82-19196

Experiments on fuel heating for commercial aircraft
[NASA-TM-82878] p0072 A82-26483

Effect of some nitrogen compounds thermal
stability of jet A
[NASA-TM-82908] p0072 A82-27519

Characterization of an Experimental Referee
Broadened Specification (ERBS) aviation turbine
fuel and ERBS fuel blends
[NASA-TM-82883] p0072 A82-32504

JET ENGINES

NT BRISTOL-SIDDELEY BS 53 ENGINE

NT TURBOFAN ENGINES

NT TURBOJET ENGINES

NT TURBOPROP ENGINES

Thermal expansion accommodation in a jet engine
frame
p0029 A82-11999

Water ingestion into jet engine axial compressors
[AIAA PAPER 82-0196] p0030 A82-17836

Pollution reduction technology program small jet
aircraft engines, phase 3
[NASA-CR-165386] p0023 A82-14095

ERBS fuel addendum: Pollution reduction
technology program small jet aircraft engines,
phase 3
[NASA-CR-165387] p0024 A82-14096

Application of integration algorithms in a
parallel processing environment for the
simulation of jet engines
[NASA-TM-82746] p0149 A82-14849

Prediction of sound radiation from different
practical jet engine inlets
[NASA-CR-165120] p0153 A82-16810

CP6 jet engine performance improvement: High
pressure turbine roundness

[NASA-CF-165555] p0024 N82-17174
CF6 Jet Engine Diagnostics Program: High pressure
compressor clearance investigation
[NASA-CF-165580] p0025 N82-21197
Alternatives for jet engine control
[NASA-CF-168894] p0026 N82-23247
B747/JT9D flight loads and their effect on engine
running clearances and performance
deterioration; BCAC NAIL/E and WA JT9D engine
diagnostics programs
[NASA-CF-165573] p0027 N82-28296
CF6 jet engine performance improvement: High
pressure turbine active clearance control
[NASA-CF-165556] p0027 N82-28297
The CF6 jet engine performance improvement: Low
pressure turbine active clearance control
[NASA-CR-165557] p0029 N82-33393

JET EXHAUST
Methods for the calculation of axial wave numbers
in lined ducts with mean flow
p0153 N82-14044
Advanced technology for controlling pollutant
emissions from supersonic cruise aircraft
p0001 N81-18004

JET FLAMES
U T FLOW

JET FLOW
NT AIR JETS
NT SUPERSONIC JET FLOW
Dilution jet behavior in the turn section of a
reverse flow combustor
[AIAA PAPER 82-0192] p0021 A82-20291
Dilution jet behavior in the turn section of a
reverse flow combustor
[NASA-TM-82776] p0017 N82-19220
Mass and momentum turbulent transport experiments
with confined coaxial jets
[NASA-CR-165574] p0090 N82-19496

JET FUELS
U T ENGINE FUELS

JET IMPINGEMENT
Flow distributions and discharge coefficient
effects for jet array impingement with initial
crossflow
[ASME PAPER 82-GT-156] p0011 A82-35379
Jet impingement heat transfer enhancement for the
GPU-3 Stirling engine
[NASA-TM-82727] p0163 N82-11993

JET NOISE
U 1 AIRCRAFT NOISE

JET PROPULSION
Development potential of Intermittent Combustion
(I.C.) aircraft engines for commuter transport
applications
[NASA-TM-82869] p0019 N82-26297

JET VANES
Effects of vane/blade ratio and spacing on fan noise
[AIAA PAPER 81-2033] p0029 A82-10457
Aerodynamic performance of high turning core
turbine vanes in a two dimensional cascade
[NASA-TM-82894] p0004 N82-26240

JETAVATORS
U IDF VANES

JOINTS (JUNCTIONS)
NT LAF JOINTS

JOURNAL BEARINGS
A pad perturbation method for the dynamic
coefficients of tilting-pad journal bearings
p0110 A82-14400
Performance of PTFE-lined composite journal bearings
[ASLE PREPRINT 82-AM-1A-1] p0104 A82-37854
Performance of PTFE-lined composite journal bearings
[NASA-TM-82779] p0048 N82-17263
High-speed motion picture camera experiments of
cavitation in dynamically loaded journal bearings
[NASA-TM-82798] p0100 N82-20543
Bearings: Technology and needs
[NASA-CR-167908] p0106 N82-26679

JOURNALS (SHAFTS)
U AETS (MACHINE ELEMENTS)

JUNCTIONS
Impedance conversion using quantum limit
nonreciprocity for
superconductor-insulator-superconductor mixer
compensation
p0159 A82-31276

K

K BAND
U TREMELY HIGH FREQUENCIES

KAPTON (TRADEMARK)
Electron beam induced damage in ITO coated Kapton
--- Indium Tin Oxide
p0148 A82-13143
p0148 N82-30992
p0159 A82-41546
p0038 N82-14226

Secondary electron emission yields
p0081 N82-24431
First results of material charging in the space
environment
[NASA-TM-84743] p0081 N82-24431

KELVIN-HELMHOLTZ INSTABILITY
Generation of instability waves at a leading edge
[NASA-TM-82835] p0087 N82-22453

KENTUCKY
LANDSAT Remote Sensing: Observations of an
Appalachian mountain top surface coal mining and
reclamation operation --- Kentucky
[E82-10247] p0117 N82-24525

KEROGEN
NT LIQUID FUELS

KEROSENE
NT LIQUID FUELS

KEVLAR (TRADEMARK)
Kevlar/PMR-15 polyimide matrix composite for a
complex shaped DC-9 drag reduction fairing
[AIAA PAPER 82-1047] p0002 A82-37678
Kevlar/PMR-15 reduced drag DC-9 reverser stang
fairing
[NASA-CR-165448] p0052 N82-31448

KEYING
NT FREQUENCY SHIFT KEYING

KINEMATICS
Tooth profile analysis of circular-cut,
spiral-bevel gears
[NASA-TM-82840] p0101 N82-26681
Kinematic precision of gear trains
[NASA-TM-82887] p0102 N82-32733

KINETIC EQUATIONS
NT HELMHOLTZ VORTICITY EQUATION

KINETIC FRICTION
NT SLIDING FRICTION

KINETIC THEORY
NT MIXING LENGTH FLOW THEORY

KINETICS
NT REACTION KINETICS

KIRCHHOFF-HELMHOLTZ FLOW
U PE FLOW

KIRCHHOFF-HUYGENS PRINCIPLE
U VE PROPAGATION

KLYSTRONS
Direct conversion of light to radio frequency energy
--- using photoklystrons for solar power
satellites
p0138 A82-11712
Analytic investigation of efficiency and
performance limits in klystron amplifiers using
multidimensional computer programs; multi-stage
depressed collectors; and thermionic cathode
life studies
p0118 N82-12553
Three-dimensional relativistic field-electron
interaction in a multicavity high-power
klystron. 1: Basic theory
[NASA-TP-1992] p0081 N82-22439
Three-dimensional relativistic field-electron
interaction in a multicavity high-power
klystron. Part 2: Working Equations
[NASA-TP-2008] p0081 N82-23397

KUTTA-ZOUKOWSKI CONDITION
A summary of V/STOL inlet analysis methods
[NASA-TM-82885] p0005 N82-28249

L

LABORATORIES
The aerospace technology laboratory (a

- perspective, then and now)
[NASA-TM-82754] p0031 N82-19229
- LAGRANGE MULTIPLIERS**
Power system design optimization using Lagrange multiplier techniques p0085 A82-20743
- LAKE ICE**
Ground-truth observations of ice-covered North Slope Lakes imaged by radar [NASA-TM-84127] p0117 N82-18664
- LAKES**
Ground-truth observations of ice-covered North Slope Lakes imaged by radar [NASA-TM-84127] p0117 N82-18664
- LAMINAR BOUNDARY LAYER**
The three-dimensional boundary layer on a rotating helical blade p0009 A82-15459
- LAMINAR BOUNDARY LAYER SEPARATION**
U MINAR BOUNDARY LAYER
- LAMINAR FLAMES**
U MINAR FLOW
- LAMINAR FLOW**
NT BLASIUS FLOW
A simple finite difference procedure for the vortex controlled diffuser [AIAA PAPER 82-0109] p0030 A82-17788
Numerical modeling of three-dimensional confined flows [NASA-CR-165583] p0158 N82-24078
- LAMINAR FLOW CONTROL**
U UNDARY LAYER CONTROL
U MINAR BOUNDARY LAYER
- LAMINAR JETS**
U T FLOW
U MINAR FLOW
- LAMINAR WAKES**
Bluff-body flameholder wakes - A simple numerical solution [AIAA PAPER 82-1177] p0093 A82-35043
- LAMINATED MATERIALS**
U TIMATES
- LAMINATES**
On determination of fibre fraction in continuous fibre composite materials p0051 A82-38133
Application of a gripping system to test a uniaxial graphite fiber reinforced composite /PMR 15/Celion 6000/ in tension at 316 C p0051 A82-40796
Boundary-layer effects in composite laminates, I - Free-edge stress singularities, II - Free-edge stress solutions and basic characteristics p0116 A82-46806
Indentation law for composite laminates [NASA-CR-165460] p0052 N82-15123
Ultrasonic scanning system for imaging flaw growth in composites [NASA-TM-82799] p0076 N82-22386
Piezoelectric composite materials [NASA-CASE-LEW-12582-1] p0054 N82-31450
- LAMINATIONS**
U MINATES
- LAND MOBILE SATELLITE SERVICE**
Satellite-aided land mobile communications system implementation considerations [NASA-TM-82861] p0036 N82-25290
- LANDFORMS**
NT APPALACHIAN MOUNTAINS (NORTH AMERICA)
NT MOUNTAINS
NT PEAKS (LANDFORMS)
NT VOLCANOES
- LANDSCAPE**
U PCGRAPHY
- LANGUAGES**
NT FORTRAN
- LAP JOINTS**
Interface cracks in adhesively bonded lap-shear joints p0116 A82-46109
Analysis of interface cracks in adhesively bonded lap shear joints, part 4 [NASA-CR-165438] p0114 N82-26716
- LAPLACE EQUATION**
The use of a structural method to calculate the electrostatic field of a magnetron A82-18370
- LARGE SPACE STRUCTURES**
Propulsion system options for low-acceleration
- orbit transfer [AIAA PAPER 82-1196] p0047 A82-35056
Developing a scalable inert gas ion thruster [AIAA PAPER 82-1275] p0047 A82-37713
Study of electrical and chemical propulsion systems for auxiliary propulsion of large space systems. Volume 1: Executive summary [NASA-CR-165502-VOL-1] p0046 N82-11110
Study of electrical and chemical propulsion systems for auxiliary propulsion of large space systems, volume 2 [NASA-CR-165502-VOL-2] p0044 N82-11111
An insight into auxiliary propulsion requirements of large space systems [NASA-TM-82827] p0042 N82-24286
Large Space Systems/Propulsion Interactions [NASA-TM-82904] p0042 N82-27358
Systems integration p0042 N82-27371
- LASER ANEMOMETERS**
Comparison of two and three dimensional flow computations with laser anemometer measurements in a transonic compressor rotor [NASA-TM-82777] p0004 N82-15020
High-speed laser anemometer system for intrarotor flow mapping in turbomachinery [NASA-TP-1663] p0095 N82-19521
Laser anemometer measurements in an annular cascade of core turbine vanes and comparison with theory [NASA-TP-2018] p0004 N82-26234
Laser anemometer using a Fabry-Perot interferometer for measuring mean velocity and turbulence intensity along the optical axis in turbomachinery [NASA-TM-82841] p0095 N82-28605
Status of laser anemometry in turbomachinery research at the Lewis Research Center p0096 N82-32686
- LASER APPLICATIONS**
Digital imaging techniques in experimental stress analysis p0097 A82-34231
Performance of laser glazed ZrO2 TBCs in cyclic oxidation and corrosion burner test rigs [NASA-TM-82830] p0059 N82-22346
Method and apparatus for coating substrates using lasers [NASA-CASE-LEW-13526-1] p0059 N82-22347
Development and utilization of a laser velocimeter system for a large transonic wind tunnel [NASA-TM-82886] p0095 N82-31663
- LASER CAVITIES**
Free electron lasers for transmission of energy in space [NASA-CR-165520] p0098 N82-25499
- LASER DOPPLER VELOCIMETERS**
Development of a laser velocimeter for a large transonic wind tunnel p0096 N82-32688
Seeding considerations for an LV system in a large transonic wind tunnel p0096 N82-32689
LV measurements with an advanced turboprop p0097 N82-32690
- LASER INTERFEROMETRY**
Experimental and theoretical studies of the laws governing condensate deposition from combustion gases p0057 A82-28709
Experimental boundary integral equation applications in speckle interferometry p0097 A82-36987
- LASER MICROSCOPY**
Acoustic microscopy of silicon carbide materials p0075 A82-33031
- LASERS**
NT CARBON DIOXIDE LASERS
NT DF LASERS
NT FREE ELECTRON LASERS
NT PULSED LASERS
- LATIN SQUARE METHOD**
Geometrical aspects of the tribological properties of graphite fiber reinforced polyimide composites [NASA-TM-82757] p0066 N82-15198
- LATTICE IMPERFECTIONS**
U YSTAL DEFECTS
- LATTICE PARAMETERS**
The influence of orientation on the stress rupture

- properties of nickel-base superalloy single crystals
 Effects of cobalt on the microstructure of Udimet 700
 [NASA-CR-165605] p0062 A82-47397
 p0064 A82-28409
- LAUNCH VEHICLES**
 NT ATLAS CENTAUR LAUNCH VEHICLE
 NT CENTAUR LAUNCH VEHICLE
- LAUNCHERS**
 NT GUN LAUNCHERS
 NT ROCKET LAUNCHERS
- LAUNCHING**
 NT ORBITAL LAUNCHING
 NT SPACECRAFT LAUNCHING
- LAWS**
 NT CONSERVATION LAWS
- LEAD ACID BATTERIES**
 Effect of positive pulse charge waveforms on the energy efficiency of lead-acid traction cells
 [NASA-TN-82769] p0118 A82-10503
 Chopper-controlled discharge life cycling studies on lead-acid batteries
 [NASA-CR-165616] p0134 A82-20661
 Results of chopper-controlled discharge life cycling studies on lead acid batteries
 [NASA-TN-82912] p0124 A82-30700
- LEADING EDGES**
 Icing tunnel tests of a composite porous leading edge for use with a liquid anti-ice system --- Lewis icing research tunnel
 [NASA-CR-164966] p0014 A82-11052
 Generation of instability waves at a leading edge
 [NASA-TN-82835] p0087 A82-22453
- LEWIS BASE**
 Deposit formation in liquid fuels. I - Effect of coal-derived Lewis bases on storage stability of Jet A turbine fuel
 p0074 A82-22241
- LIFE (DURABILITY)**
 NT FATIGUE LIFE
 NT SERVICE LIFE
 NT STORAGE STABILITY
 Durability/life of fiber composites in hydrothermo-mechanical environments
 [NASA-TN-82749] p0099 A82-14287
 Chopper-controlled discharge life cycling studies on lead-acid batteries
 [NASA-CR-165616] p0134 A82-20661
- LIFE CYCLE COSTS**
 Gallium arsenide solar array subsystem study
 [NASA-CR-167869] p0138 A82-32855
- LIFETIME (DURABILITY)**
 U FE (DURABILITY)
- LIGHT (VISIBLE RADIATION)**
 NT POLARIZED LIGHT
 NT SUNLIGHT
- LIGHT ALLOYS**
 NT ALUMINUM ALLOYS
 NT MAGNESIUM ALLOYS
- LIGHT EMISSION**
 NT CHEMILUMINESCENCE
- LIGHT INTENSITY**
 NT MINCOS INTENS.
- LIGHT SCATTERING**
 Veiling glare reduction methods compared for ophthalmic applications
 p0143 A82-13289
- LIGHT TRANSMISSION**
 NT LIGHT SCATTERING
- LIGHTNING**
 NASA research programs responding to workshop recommendations
 A82-21146
- LIGHTNING SUPPRESSION**
 Evaluation of lightning accommodation systems for wind-driven turbine rotors
 [NASA-TN-82784] p0122 A82-23679
- LINEAR FILTERS**
 NT KALMAN FILTERS
- LINEARITY**
 Effect of vacuum exhaust pressure on the performance of MHD ducts at high D-field
 [NASA-TN-82750] p0157 A82-13908
- LINERS**
 U RINGS
- LININGS**
 Analytical and experimental investigation of the propagation and attenuation of sound in extended reaction lined ducts
 [AIAA PAPER 81-2014] p0153 A82-10454
 Conversion of acoustic energy by lossless liners
 p0154 A82-36195
- Nonlinear structural and life analyses of a combustor liner
 [NASA-TN-82846] p0111 A82-24501
 Fully plasma-sprayed compliant backed ceramic turbine seal
 [NASA-CASE-LEW-13268-1] p0069 A82-29453
 Nonlinear constitutive theory for turbine engine structural analysis
 p0112 A82-33744
- LIQUEFIED GASES**
 NT LIQUEFIED NATURAL GAS
 NT LIQUID HYDROGEN
 NT LIQUID OXYGEN
- LIQUEFIED NATURAL GAS**
 Toward the use of similarity theory in two-phase choked flows
 p0089 A82-16570
- LIQUID AMMONIA**
 NT LIQUID FUELS
- LIQUID BEARINGS**
 Bearings; Technology and needs
 [NASA-CR-167908] p0106 A82-26679
- LIQUID CHROMATOGRAPHY**
 Quantitative separation of tetralin hydroperoxide from its decomposition products by high performance liquid chromatography
 p0048 A82-15696
 Thermal and oxidative degradation studies of formulated C-ethers by gel-permeation chromatography
 [NASA-TP-1994] p0068 A82-21332
- LIQUID COOLING**
 NT FILM COOLING
- LIQUID CRYSTALS**
 Stoichiometry-controlled compensation in liquid encapsulated Czochralski GaAs
 p0158 A82-17585
- LIQUID FLOW**
 NT WATER FLOW
 Nonlinear Marangoni convection in bounded layers.
 I - Circular cylindrical containers. II - Rectangular cylindrical containers
 p0094 A82-39501
- LIQUID FUELS**
 Deposit formation in liquid fuels. I - Effect of coal-derived Lewis bases on storage stability of Jet A turbine fuel
 p0074 A82-22241
- LIQUID HYDROGEN**
 NT LIQUID FUELS
 An experiment to evaluate liquid hydrogen storage in space
 A82-20748
 An assessment of the crash fire hazard of liquid hydrogen fueled aircraft
 [NASA-CR-165526] p0013 A82-19196
 Integrated gasifier combined cycle polygeneration system to produce liquid hydrogen
 [NASA-TN-82921] p0125 A82-30713
- LIQUID OXIDIZERS**
 Testing of fuel/oxidizer-rich, high-pressure preburners
 [NASA-CR-165609] p0074 A82-24353
- LIQUID OXYGEN**
 The supply of lunar oxygen to low earth orbit
 p0032 A82-35618
 Liquid oxygen turbopump technology
 [NASA-CR-165487] p0105 A82-11460
 Low-thrust Isp sensitivity study
 [NASA-CR-165621] p0045 A82-22309
 Testing of fuel/oxidizer-rich, high-pressure preburners
 [NASA-CR-165609] p0074 A82-24353
- LIQUID PHASES**
 Quasi-liquid states observed on ion beam microtextured surfaces
 p0159 A82-30335
- LIQUID PROPELLANT ROCKET ENGINES**
 NT HYDROGEN OXYGEN ENGINES
 Propulsion system options for low-acceleration orbit transfer
 [AIAA PAPER 82-1196] p0047 A82-35056
 Reusable rocket engine maintenance study
 [NASA-CR-165569] p0044 A82-16172

LIQUID ROCKET PROPELLANTS

SUBJECT INDEX

Low-thrust Isp sensitivity study
[NASA-CR-165621] p0045 N82-22304

LIQUID ROCKET PROPELLANTS
NT CRYOGENIC ROCKET PROPELLANTS
NT LIQUID FUELS
NT RP-1 ROCKET PROPELLANTS

LIQUID SURFACES
Hydrodynamic and aerodynamic breakup of liquid sheets
[NASA-TM-82900] p0087 N82-19494

LIQUID-GAS MIXTURES
NT AEROSOLS

LIQUID-SOLID INTERFACES
Heat transfer in cooled porous region with curved boundary p0089 A82-14848
Cauchy integral method for two-dimensional solidification interface shapes p0089 A82-39899

LIQUIDS
NT CRYOGENIC ROCKET PROPELLANTS
NT HYDRAULIC FLUIDS
NT LIQUID FUELS
NT LIQUID HYDROGEN
NT LIQUID OXIDIZERS
NT LIQUID OXYGEN
NT RP-1 ROCKET PROPELLANTS

LNG
U DEIFIED NATURAL GAS

LOAD DISTRIBUTION (FORCES)
Strength distributions of SiC ceramics after oxidation and oxidation under load
[ACS PAPER 9-C-80C] p0071 A82-20143

LOAD FACTORS
U ADS (FORCES)

LOAD TESTING MACHINES
Application of a gripping system to test a uniaxial graphite fiber reinforced composite /FHR 15/Celion 6000/ in tension at 316 C p0051 A82-40796

LOAD TESTS
Indentation law for composite laminates
[NASA-CR-165460] p0052 N82-15123

LOADING FORCES
U ADS (FORCES)

LOADING WAVES
U ASTIC WAVES
U ADS (FORCES)

LOADS (FORCES)
NT AERODYNAMIC LOADS
NT AXIAL COMPRESSION LOADS
NT AXIAL LOADS
NT COMPRESSION LOADS
NT DYNAMIC LOADS
NT EDGE LOADING
NT ROLLING CONTACT LOADS
NT SHOCK LOADS
NT STATIC LOADS
NT THRUST LOADS
Effect of seals on rotor systems
[NASA-TM-82786] p0099 N82-16411

LONG TERM EFFECTS
Survey on aging on electrodes and electrocatalysts in phosphoric acid fuel cells
[NASA-CP-165505] p0128 N82-11545

LONG WAVES (METEOROLOGY)
U ANETARY WAVES

LOSSLESS MATERIALS
Conversion of acoustic energy by lossless liners p154 A82-36195

LOW PASS FILTERS
Conversion and matched filter approximations for serial minimum-shift keyed modulation p0080 A82-26713

LOW PRESSURE
The CP6 jet engine performance improvement: Low pressure turbine active clearance control
[NASA-CR-165557] p0029 N82-33393
Energy efficient engine: Turbine transition duct model technology report
[NASA-CR-167996] p0029 N82-33394

LOW TEMPERATURE
On the cause of the flat spot phenomenon observed in silicon solar cells at low temperatures and low intensities p0044 A82-44965
Additional experiments on flowability improvements of aviation fuels at low temperatures, volume 2
[NASA-CR-167912] p0074 N82-31546

LOW TEMPERATURE ENVIRONMENTS
Experimental study of fuel heating at low temperatures in a wing tank model, volume 1
[NASA-CR-165391] p0073 N82-11224
On the cause of the flat-spot phenomenon observed in silicon solar cells at low temperatures and low intensities
[NASA-TM-82903] p0126 N82-31777

LOW TEMPERATURE TESTS
On the cause of the flat-spot phenomenon observed in silicon solar cells at low temperatures and low intensities --- in deep space environments p0043 A82-39599

LOW THRUST PROPULSION
NT ELECTROMAGNETIC PROPULSION
NT SOLAR ELECTRIC PROPULSION
Propulsion system options for low-acceleration orbit transfer
[AIAA PAPER 82-1196] p0047 A82-35056
Low-thrust chemical propulsion system pump technology
[NASA-CR-165219] p0105 N82-13427
Low-thrust chemical propulsion system propellant expulsion and thermal conditioning study. Executive summary
[NASA-CR-165622] p0045 N82-24287
Low-thrust chemical propulsion system propellant expulsion and thermal conditioning study
[NASA-CR-167841] p0045 N82-24268

LOW WEIGHT
A new approach to the minimum weight/loss design of switching power converters p0082 A82-16831

LOX (OXYGEN)
U QUID OXYGEN

LOX-HYDROGEN ENGINES
U DROGEN OXYGEN ENGINES

LUBRICANTS
NT HIGH TEMPERATURE LUBRICANTS
NT LUBRICATING OILS
NT SOLID LUBRICANTS
Alignment of fluid molecules in an EHD contact
[ASLE PREPRINT 81-LC-5C-1] p0107 A82-18467
Traction contact performance evaluation at high speeds
[NASA-CR-165226] p0105 N82-16409
Thermal and oxidative degradation studies of formulated C-ethers by gel-permeation chromatography
[NASA-TP-1994] p0068 N82-21332
Morphological and frictional behavior of sputtered MoS2 films
[NASA-TM-82809] p0076 N82-22387
Lubricant effects on efficiency of a helicopter transmission
[NASA-TM-82857] p0100 N82-25520

LUBRICATING OILS
Regimes of traction in concentrated contact lubrication
[ASME PAPER 81-LUB-16] p0107 A82-18431
Some observations in high pressure rheology of lubricants
[ASME PAPER 81-LUB-17] p0070 A82-18432
Some observations in high pressure rheology of lubricants
[ASME PAPER 81-LUB-17] p0070 A82-18432
Effects of ultra-clean and centrifugal filtration on rolling-element bearing life
[ASME PAPER 81-LUB-35] p0103 A82-18436

LUBRICATION
NT BOUNDARY LUBRICATION
NT SELF LUBRICATION
Application of surface analysis to solve problems of wear
[NASA-TM-82753] p0099 N82-14519
Elucidation of wear mechanisms by ferrographic analysis
[NASA-TM-82737] p0066 N82-15199
Basic lubrication equations
[NASA-TM-81693] p0099 N82-16413
Geometry and starvation effects in hydrodynamic lubrication
[NASA-TM-82807] p0042 N82-20240
Frictional heating due to asperity interaction of elastohydrodynamic line-contact surfaces
[NASA-TP-1882] p0100 N82-25514
Lubrication of rigid ellipsoidal solids
[NASA-TM-81694] p0100 N82-25518

ORIGINAL PAGE IS
OF POOR QUALITY

- File shape calculations on supercomputers
[NASA-TM-82356] p0100 N82-25519
- LUNAR BANDS**
U ASTIC DEFORMATION
- LUMINESCENCE**
NT CHEMILUMINESCENCE
- LUMINESCENT INTENSITY**
U MINOUS INTENSITY
- LUMINOUS FLUX DENSITY**
U MINOUS INTENSITY
- LUMINOUS INTENSITY**
On the cause of the flat spot phenomenon observed
in silicon solar cells at low temperatures and
low intensities p0044 A82-44965
- LUMPED PARAMETER SYSTEMS**
Comparison of NASCAP modelling results with lumped
circuit analysis p0037 N82-14255
- LUNAR CRATERS**
The development of central peaks in lunar craters
A82-14333
- LUNAR SCATTERING**
U FFUSE RADIATION
- LUNAR SOIL**
A small scale lunar launcher for early lunar
material utilization p0032 A82-35617
- The supply of lunar oxygen to low earth orbit
p0032 A82-35618
- LUNAR TRAJECTORIES**
NT MOON-EARTH TRAJECTORIES
- M**
- MACH NUMBER**
In-flight acoustic results from an advanced-design
propeller at Mach numbers to 6.8
[AIAA PAPER 82-1120] p0021 A82-35017
- MACH-ZEHNDER INTERFEROMETERS**
New versions of old flow visualization systems
p0096 N82-32670
- MACHINE LIFE**
U RVICE LIFE
- MACHINE STORAGE**
U MEMORY STORAGE DEVICES
- MACHINE TOOLS**
NT MILLING MACHINES
- MACHINERY**
Precision of spiral-bevel gears
[NASA-TM-82888] p0102 N82-30552
- MAGNESIUM ALLOYS**
Thermal degradation of the tensile properties of
unidirectionally reinforced FP-AL203/BZ 33
magnesium composites p0049 N82-21260
- Modulus, strength and thermal exposure studies of
FP-AL203/aluminum and FP-AL203/magnesium
composites [NASA-TM-82868] p0050 N82-30335
- MAGNESIUM COMPOUNDS**
NT MAGNESIUM OXIDES
- MAGNESIUM OXIDES**
Influence of mineral oil and additives on
microhardness and surface chemistry of magnesium
oxide (001) surface [NASA-TP-1986] p0067 N82-20316
- Effects of environment on microhardness of
magnesium oxide [NASA-TP-2002] p0068 N82-22366
- Influence of corrosive solutions on microhardness
and chemistry of magnesium oxide (001) surfaces
[NASA-TP-2040] p0102 N82-31691
- MAGNETIC AMPLIFIERS**
Three-dimensional relativistic field-electron
interaction in a multicavity high-power
klystron. Part 2: Working Equations
[NASA-TP-2008] p0081 N82-23397
- MAGNETIC CHARGE DENSITY**
Representation and material charging response of
geoplasma environments p0039 N82-14249
- MAGNETIC DISTURBANCES**
NT MAGNETIC STORMS
- MAGNETIC FIELD CONFIGURATIONS**
On a free-electron-laser in a uniform magnetic
field - A solution for arbitrarily strong
electromagnetic radiation fields A82-28409
- Electrostatic fuel conditioning of internal
combustion engines
[NASA-CR-169029] p0106 N82-26680
- MAGNETIC FIELDS**
NT GEOMAGNETISM
- NT SOLAR MAGNETIC FIELD**
Three-dimensional relativistic field-electron
interaction in a multicavity high-power
klystron. 1: Basic theory [NASA-TP-1992] p0081 N82-22439
- Electric and magnetic fields
[NASA-CR-165604] p0045 N82-28350
- MAGNETIC METALS**
U TALS
- MAGNETIC PROPERTIES**
NT GEOMAGNETISM
- Permanent magnet properties of Mn-Al-C between -50
C and +150 C p0085 A82-20505
- MAGNETIC PUMPING**
Magnetic heat pumping
[NASA-CASE-LEW-12508-3] p0088 N82-24449
- MAGNETIC SIGNATURES**
Magnetic structure of a flaring region producing
impulsive microwave and hard X-ray bursts
p0167 A82-27323
- MAGNETIC STORMS**
Environmentally induced discharges on satellites
[NASA-TM-82849] p0038 N82-23261
- MAGNETIC SUBSTORMS**
U GNETIC STORMS
- MAGNETIC VARIATIONS**
An attempt at magnetic-variation sounding in the
Antarctic A82-25290
- MAGNETOGASDYNAMICS**
U GNETOHYDRODYNAMICS
- MAGNETOGRAMS**
U GNETIC SIGNATURES
- MAGNETOHYDRODYNAMIC ACCELERATION**
U ASMA ACCELERATION
- MAGNETOHYDRODYNAMIC GENERATORS**
End region and current consolidation effects upon
the performance of an MHD channel for the ETF
conceptual design --- Engineering Test Facility
[AIAA PAPER 82-0325] p0157 A82-17889
- Impact of uniform electrode current distribution
on ETF --- Engineering Test Facility MHD generator
[AIAA PAPER 82-0423] p0157 A82-17941
- Effect of vacuum exhaust pressure on the
performance of MHD ducts at high B-field
[AIAA PAPER 82-0396] p0157 A82-20292
- Comparative analysis of CCMHD power plants ---
Closed Cycle MHD p0158 A82-20747
- MHD channel performance for potential early
commercial MHD power plants p0158 A82-20750
- Modeling parameter influences on MHD swirl
combustion nozzle design [AIAA PAPER 82-0984] p0011 A82-31947
- Flow aerodynamics modeling of an MHD swirl
combustor - Calculations and experimental
verification p0094 A82-44782
- Magnetohydrodynamics MHD Engineering Test Facility
ETF 200 MWe power plant. Conceptual Design
Engineering Report CDER. Volume 3: Costs and
schedules [NASA-CR-165452-VOL-3] p0128 N82-10495
- Magnetohydrodynamics (MHD) Engineering Test
Facility (ETF) 200 MWe power plant. Design
Requirements Document (DRD) [NASA-TM-82705] p0099 N82-12446
- Magnetohydrodynamics (MHD) Engineering Test
Facility (ETF) 200 MWe power plant. Conceptual
Design Engineering Report (CDER). Volume 1:
Executive summary [NASA-CR-165452-VOL-1] p0129 N82-12570
- End region and current consolidation effects upon
the performance of an MHD channel for the ETF
conceptual design [NASA-TM-82744] p0157 N82-12943
- Conceptual design of superconducting magnet system
for Magnetohydrodynamic (MHD) Engineering Test
Facility (ETF) 200 MWe power plant
[NASA-CR-165053] p0105 N82-14520
- MHD oxidant intermediate temperature ceramic
heater study

- [NASA-CR-165453] p0131 N82-15527
Summary and evaluation of the conceptual design study of a potential early commercial MHD power plant (CSPEC)
- [NASA-TM-82734] p0119 N82-16481
Magnetohydrodynamics (MHD) Engineering Test Facility (ETF) 200 MWe power plant Conceptual Design Engineering Report (CDER)
- [NASA-CR-165452-VOL-5] p0132 N82-17603
Impact of uniform electrode current distribution on ETF
- [NASA-TM-82875] p0123 N82-25636
Optimization of the oxidant supply system for combined cycle MHD power plants
- [NASA-TM-82909] p0123 N82-26790
Magnetohydrodynamics (MHD) Engineering Test Facility (ETF) 200 MWe power plant. Conceptual Design Engineering Report (CDER). Volume 2: Engineering. Volume 3: Costs and schedules
- [NASA-CR-165452-VOL-2] p0136 N82-27037
Comparative analysis of the conceptual design studies of potential early commercial MHD power plants (CSPEC)
- [NASA-TM-82897] p0123 N82-27838
MAGNETOHYDRODYNAMIC TURBULENCE
NT PLASMA TURBULENCE
MAGNETOHYDRODYNAMIC WAVES
NT PLASMA WAVES
MAGNETOHYDRODYNAMICS
NT CYLINDRICAL PLASMAS
Characterization of advanced electric propulsion systems
- [AIAA PAPER 82-1246] p0071 A82-35083
Effect of vacuum exhaust pressure on the performance of MHD ducts at high B-field
- [NASA-TM-82750] p0157 N82-13908
Magnetohydrodynamics (MHD) Engineering Test Facility (ETF) 200 MWe power plant. Conceptual Design Engineering Report (CDER). Volume 4: Supplementary engineering data
- [NASA-CR-165452-VOL-4] p0133 N82-18688
Results and comparison of Hall and DW duct experiments
- [NASA-TM-82864] p0157 N82-25961
MAGNETOIONIC PLASMA
U AEMAS (PHYSICS)
MAGNETOPLASMAS
U ASMAS (PHYSICS)
MAGNETOSPHERIC ION DENSITY
The hidden ion population of the magnetosphere
- p0140 A82-32630
MAGNETRONS
The use of a structural method to calculate the electrostatic field of a magnetron
- A82-18370
MAGNETS
NT ELECTROMAGNETS
NT SUPERCONDUCTING MAGNETS
Hard permanent magnet development trends and their application to A.C. machines
- p0083 A82-20745
MAN MACHINE SYSTEMS
The NASA MMRIT program - Developing new concepts for accurate flight planning
- [AIAA PAPER 82-0340] p0014 A82-17894
MANAGEMENT
NT INFORMATION MANAGEMENT
MANEUVERS
NT AIRCRAFT MANEUVERS
MANGANESE ALLOYS
Permanent magnet properties of Mn-Al-C between -50 C and +150 C
- p0085 A82-20505
MANIFOLDS
Active clearance control system for a turbomachine
- [NASA-CASE-LEW-12938-1] p0020 N82-32366
MANNED SPACECRAFT
NT SPACE STATIONS
MANUALS
NT USER MANUALS (COMPUTER PROGRAMS)
MANUFACTURING
NT SPACE MANUFACTURING
MAPPING
NT THEMATIC MAPPING
NT THERMAL MAPPING
Mapping of electrical potential distributions with charged particle beams
- [NASA-CR-168556] p0084 N82-18508
MAPS
NT ASTRONOMICAL MAPS
MARANGONI CONVECTION
Nonlinear Marangoni convection in bounded layers.
I - Circular cylindrical containers. II - Rectangular cylindrical containers
- p0094 A82-39501
MARKET RESEARCH
Market assessment of photovoltaic power systems for agricultural applications in Mexico
- [NASA-CR-165441] p0128 N82-10506
Market assessment of photovoltaic power systems for agricultural applications in Morocco
- [NASA-CR-165477] p0130 N82-14627
International market assessment of stand-alone photovoltaic power systems for cottage industry applications
- [NASA-CR-165287] p0132 N82-16494
Cross-impact study of foreign satellite communications on NASA's 30/20 GHz program
- [NASA-CR-165154] p0078 N82-17420
Market assessment of photovoltaic power systems for agricultural applications in Nigeria
- [NASA-CR-165511] p0133 N82-18698
Market assessment of photovoltaic power systems for agricultural applications in Colombia
- [NASA-CR-165524] p0134 N82-22770
Worldwide satellite market demand forecast
- [NASA-CR-167918] p0079 N82-25423
MASER RESONATORS
U SERS
MASERS
Investigation of a comb-type slow-wave structure for millimeter-wave masers
- A82-18368
MASS DRIVERS (PAYLOAD DELIVERY)
Mass Driver Two - A status report
- p0046 A82-18191
Mass driver reaction engine characteristics and performance in earth orbital transfer missions
- p0046 A82-18199
Characterization of advanced electric propulsion systems
- [AIAA PAPER 82-1246] p0071 A82-35083
A small scale lunar launcher for early lunar material utilization
- p0032 A82-35617
Characterization of advanced electric propulsion systems
- [NASA-CR-167885] p0045 N82-26381
MASS FLOW RATE
Three dimensional flow measurements in a turbine scroll
- [NASA-CR-167920] p0009 N82-32310
MASS TRANSFER
Mass and momentum turbulent transport experiments with confined coaxial jets
- [NASA-CR-165574] p0090 N82-19496
MATCHED FILTERS
Conversion and matched filter approximations for serial minimum-shift keyed modulation
- p0080 A82-26713
Near optimum delay-line detection filters for serial detection of MSK signals
- p0086 A82-43867
MATERIALS HANDLING
NT PROPELLANT TRANSFER
NT REMOTE HANDLING
MATERIALS SCIENCE
Materials science issues encountered during the development of thermochemical concepts --- in screening of reactions for solar energy applications
- A82-10021
MATHEMATICAL LOGIC
NT ALGORITHMS
MATHEMATICAL MODELS
NT ANALOG SIMULATION
NT DIGITAL SIMULATION
Model degradation effects on sensor failure detection
- p0148 A82-13143
'Bootstrap' charging of surfaces composed of multiple materials
- p0085 A82-18318
Numerical modelling of turbulent flow in a combustion tunnel
- p0093 A82-27000

- Performance degradation of propeller/rotor systems
due to rim ice accretion
[AIAA PAPER 82-0286] p0014 A82-20322
- Numerical modeling of turbulent combustion in
premixed gases p0056 A82-28408
- Modeling parameter influences on MHD swirl
combustion nozzle design
[AIAA PAPER 82-0904] p0011 A82-31947
- Stationary state model for normal metal tunnel
junction phenomena p0159 A82-42912
- Surface-tension induced instabilities: Effects of
lateral boundaries
[NASA-CF-165530] p0092 N82-11390
- Integrated analysis of engine structures
[NASA-TM-82713] p0111 N82-11491
- Numerical techniques in linear duct acoustics,
1980-81 update p0151 N82-12890
- A real time Pegasus propulsion system model for
VSTOL piloted simulation evaluation
[NASA-TM-82770] p0016 N82-13144
- Modeling and Analysis of Power Processing Systems
(MAPPS). Volume 1: Technical report
[NASA-CR-165530] p0083 N82-14447
- Finite-element modeling of layered, anisotropic
composite plates and shells: A review of recent
research p0113 N82-19563
- Identification of multivariable high performance
turbofan engine dynamics from closed loop data
[NASA-TM-82785] p0076 N82-20339
- Spherical roller bearing analysis. SKF computer
program SPHERBEAN. Volume 1: Analysis
[NASA-CR-165203] p0106 N82-20540
- Analytical investigation of nonrecoverable stall
[NASA-TM-82792] p0018 N82-21195
- The NASA-LoRC wind turbine sound prediction code
p0123 N82-23730
- Computer modeling of multiple-channel input
signals and intermodulation losses caused by
nonlinear traveling wave tube amplifiers
[NASA-TR-1999] p0082 N82-25441
- Reliability model for planetary gear
[NASA-TM-82859] p0101 N82-28643
- MATHIEU EQUATION**
- MATHIEU FUNCTION**
- MATHIEU FUNCTION**
- The influence of Coriolis forces on gyroscopic
motion of spinning blades
[ASME PAPER 82-GT-163] p0030 A82-35384
- MATRICES (CIRCUITS)**
- Dynamic switch matrix for the TDMA satellite
switching system
[AIAA 82-0458] p0085 A82-23494
- MATRICES (MATHEMATICS)**
- NT EIGENVALUES**
- NT EIGENVECTORS**
- Verification of an acoustic transmission matrix
analysis of sound propagation in a variable area
duct without flow
[NASA-TM-82741] p0151 N82-12891
- MATRIX ANALYSIS**
- MATRICES (MATHEMATICS)**
- MATRIX MATERIALS**
- High-temperature resins p0051 A82-42657
- Modulus, strength and thermal exposure studies of
FP-Al2O3/aluminum and FP-Al2O3/magnesium
composites p0050 N82-30335
- MAXIMUM ENTROPY METHOD**
- Maximum entropy image reconstruction from
projections A82-11053
- MAXWELL EQUATION**
- Simulation of charging response of SCATHA (P78-2)
satellite p0039 N82-14250
- MCDONNELL AIRCRAFT**
- NT EC 10 AIRCRAFT**
- MCDONNELL DOUGLAS AIRCRAFT**
- NT EC 9 AIRCRAFT**
- NT EC 10 AIRCRAFT**
- MEAN**
- Illustration of a new test for detecting a shift
in mean in precipitation series A82-13217
- Laser anemometer using a Fabry-Perot
interferometer for measuring mean velocity and
turbulence intensity along the optical axis in
turbomachinery [NASA-TM-82841] p0095 N82-28605
- MEASURE AND INTEGRATION**
- NT J INTEGRAL**
- NT NUMERICAL INTEGRATION**
- MEASURING INSTRUMENTS**
- NT DRAG FORCE ANEMOMETERS**
- NT ENGINE MONITORING INSTRUMENTS**
- NT FLOW DIRECTION INDICATORS**
- NT HOT-FILM ANEMOMETERS**
- NT HOT-WIRE ANEMOMETERS**
- NT HOT-WIRE FLOWMETERS**
- NT INFRARED DETECTORS**
- NT LASER ANEMOMETERS**
- NT LASER DOPPLER VELOCIMETERS**
- NT MACH-ZEHNDER INTERFEROMETERS**
- NT OPTICAL MEASURING INSTRUMENTS**
- NT OPTICAL SCANNERS**
- NT STRAIN GAGES**
- NT TORQUEMETERS**
- NT ULTRASONIC DENSIMETERS**
- An experimental investigation into the feasibility
of a thermoelectric heat flux gage
[NASA-TM-82755] p0095 N82-14494
- MECHANICAL DEVICES**
- Elucidation of wear mechanisms by ferrographic
analysis [NASA-TM-82737] p0066 N82-15199
- International market assessment of stand-alone
photovoltaic power systems for cottage industry
applications [NASA-CR-165287] p0132 N82-16494
- Precision of spiral-bevel gears
[NASA-TM-82888] p0102 N82-30552
- MECHANICAL DRIVES**
- NT TRANSMISSIONS (MACHINE ELEMENTS)**
- Low-thrust chemical propulsion system pump
technology [NASA-CR-165219] p0105 N82-13427
- The ac propulsion system for an electric vehicle,
phase 1 [NASA-CR-165480] p0129 N82-13506
- Traction contact performance evaluation at high
speeds [NASA-CR-165226] p0105 N82-16409
- Advanced general aviation comparative
engine/airframe integration study
[NASA-CR-165564] p0025 N82-22263
- Kinematic precision of gear trains
[NASA-TM-82887] p0102 N82-32733
- Automotive Stirling Engine Mod 1 Design Review,
volume 3 --- engineering drawings [NASA-CR-167397] p0164 N82-34312
- MECHANICAL ENGINEERING**
- Bibliography of Lewis Research Center technical
publications announced in 1981
[NASA-TM-82838] p0163 N82-27191
- MECHANICAL MEASUREMENT**
- NT DISPLACEMENT MEASUREMENT**
- NT FLOW MEASUREMENT**
- NT PRESSURE MEASUREMENT**
- NT STRESS MEASUREMENT**
- NT VELOCITY MEASUREMENT**
- MECHANICAL PROPERTIES**
- NT AEROELASTICITY**
- NT BRITTLENESS**
- NT COMPRESSIVE STRENGTH**
- NT CREEP PROPERTIES**
- NT CREEP RUPTURE STRENGTH**
- NT DUCTILITY**
- NT ELASTIC PROPERTIES**
- NT ELASTOPLASTICITY**
- NT FATIGUE LIFE**
- NT FIBER STRENGTH**
- NT FRACTURE STRENGTH**
- NT MICROHARDNESS**
- NT MODULUS OF ELASTICITY**
- NT NOTCH STRENGTH**
- NT PIEZOELECTRICITY**
- NT PLASTIC PROPERTIES**
- NT POISSON RATIO**
- NT SHEAR CREEP**
- NT SHEAR PROPERTIES**
- NT SHEAR STRENGTH**
- NT STIFFNESS**
- NT STRESS CYCLES**

- NT TENSILE PROPERTIES p0108 A82-27079
 NT TENSILE STRENGTH
 NT THERMAL RESISTANCE
 NT THERMOPLASTICITY A82-30002
 NT THERMOVISCOELASTICITY
 NT VISCOELASTICITY
 NT VISCOPLASTICITY
 Fatigue of Ni-Al-Mo aligned eutectics at elevated temperatures p0052 A82-13403
 Effects of nadic ester concentration and processing on physical and mechanical properties of FMB/Celion 6000 composites p0051 A82-27440
 Effects of cobalt on structure, microchemistry and properties of a wrought nickel-base superalloy p0065 A82-34973
 Winding for the wind p0138 A82-37078
 Effects of heating rate on density, microstructure, and strength of Si₃N₄-6 wt.% Y₂O₃ and a beta-prime sialon [ACS PAPER 42-B-81] p0070 A82-42366
 Technology development for phosphoric acid fuel cell powerplant, phase 2 [NASA-CR-165426] p0131 A82-16482
- MECHANICAL RESONANCE**
 U SONANT VIBRATION
METAL TWISSING
 Effect of melt stoichiometry on twin formation in LEC GaAs --- Liquid Encapsulated Czochralski technique p0160 A82-46517
- MEDIA**
 NT ANISOTROPIC MEDIA
 NT ELASTIC MEDIA
MEDICAL EQUIPMENT
 NT ELCOE PUMPS
 NT PROSTHETIC DEVICES
MEDICAL SCIENCE
 NT OPHTHALMOLOGY
 Ozone and aircraft operations p0001 A82-21145
- MEETINGS**
 U REFERENCES
- MELTING**
 Numerical simulation of one-dimensional heat transfer in composite bodies with phase change --- wing deicing pads [NASA-CR-165607] p0002 A82-22142
- MELTS (CRYSTAL GROWTH)**
 Compensation mechanism in liquid encapsulated Czochralski GaAs Importance of melt stoichiometry p0086 A82-40403
 Effect of melt stoichiometry on twin formation in LEC GaAs --- Liquid Encapsulated Czochralski technique p0160 A82-46517
- MEMBRANE ANALOGY**
 U STRUCTURAL ANALYSIS
MEMBRANE THEORY
 U STRUCTURAL ANALYSIS
MEMBRANES
 NT ION EXCHANGE MEMBRANE ELECTROLYTES
 Anion permselective membrane [NASA-CR-167872] p0137 A82-30711
- MERCURY ION ENGINES**
 30-cm mercury ion thruster technology p0046 A82-15434
 Measuring the spacecraft and environmental interactions of the 8-cm mercury ion thrusters on the P80-1 mission p0043 A82-15438
 Retrofit and acceptance test of 30-cm ion thrusters [NASA-CR-165259] p0044 A82-12133
- MESFET**
 U FLD EFFECT TRANSISTORS
- MESOSPHERE**
 Stratospheric-mesospheric midwinter disturbances - A summary of observed characteristics A82-12135
- METAL COATINGS**
 NT ALUMINUM COATINGS
 NT GOLD COATINGS
 Improved plasma sprayed MCrAlY coatings for aircraft gas turbine applications p0065 A82-20742
 Development of CdO-graphite-Ag coatings for gas hearings to 427 C
- Cessation of W/001/ - Work function lowering by multiple dipole formation p0108 A82-27079
 Progress in protective coatings for aircraft gas turbines: A Review of NASA sponsored research [NASA-TM-82740] p0058 A82-12216
 Method and apparatus for coating substrates using lasers p0059 A82-22347
 Light weight nickel battery plaque [NASA-CASE-LEW-13349-1] p0121 A82-22673
 Improved thermal barrier coating system [NASA-CASE-LEW-13324-1] p0060 A82-26431
- METAL CORROSION**
 U EROSION
METAL CUTTING
 The orthogonal in-situ machining of single and polycrystalline aluminum and copper, volume 1 [NASA-CR-168929] p0076 A82-24361
- METAL FATIGUE**
 Comparative thermal fatigue resistance of several oxide dispersion strengthened alloys p0062 A82-11399
 Fatigue and creep-fatigue deformation of several nickel-base superalloys at 650 C p0062 A82-47398
 Elevated temperature fatigue testing of metals p0058 A82-13284
 Fatigue tests with a corrosive environment A82-13282
 Evaluation of inelastic constitutive models for nonlinear structural analysis --- for aircraft turbine engines p0112 A82-24502
 High temperature low cycle fatigue mechanisms for nickel base and a copper base alloy [NASA-CR-3543] p0064 A82-26436
 Microstructural effects on the room and elevated temperature low cycle fatigue behavior of Waspaloy [NASA-CR-165497] p0113 A82-26702
 Mechanisms of deformation and fracture in high temperature low cycle fatigue of Rene 80 and IN 100 [NASA-CR-165498] p0113 A82-26706
- METAL FILMS**
 Tribological properties and XPS studies of ion plated gold on nickel and iron [NASA-TM-82814] p0059 A82-22344
 Boundary lubrication: Revisited [NASA-TM-82858] p0069 A82-29458
- METAL FINISHING**
 NT SHOT PEENING
- METAL FOILS**
 Metal honeycomb to porous wireform substrate diffusion bond evaluation [NASA-TM-82793] p0110 A82-18612
- METAL HALIDES**
 NT IRON CHLORIDES
 NT SODIUM CHLORIDES
- METAL INSULATOR SEMICONDUCTORS**
 U S (SEMICONDUCTORS)
- METAL MATRIX COMPOSITES**
 NT EUTECTIC COMPOSITES
 Work of fracture in aluminum metal-matrix composites p0053 A82-31339
 Tensile properties of SiC/aluminum filamentary composites - Thermal degradation effects p0053 A82-46220
 Analysis of crack propagation as an energy absorption mechanism in metal matrix composites [NASA-CR-165051] p0052 A82-14288
 Tungsten fiber reinforced superalloy composite high temperature component design considerations [NASA-TM-82811] p0049 A82-21259
 Factors influencing the thermally-induced strength degradation of B/Al composites [NASA-TM-82823] p0050 A82-24297
 Method and apparatus for strengthening boron fibers --- high temperature oxidation [NASA-CASE-LEW-13826-1] p0050 A82-26385
 High temperature composites. Status and future directions [NASA-TM-82929] p0051 A82-30336
- METAL OXIDE SEMICONDUCTORS**
 High voltage V-groove solar cell [NASA-CASE-LEW-13401-2] p0123 A82-24717
- METAL OXIDES**
 NT ALUMINUM OXIDES

- NT MAGNESIUM OXIDES
 NT TIN OXIDES
 NT YTTRIUM OXIDES
 NT ZIRCONIUM OXIDES
 Comparative thermal fatigue resistance of several oxide dispersion strengthened alloys p0062 A82-11399
 Development of CdO-graphite-Aq coatings for gas bearings to 427 C p0108 A82-2079
 Crystallographic texture in oxide-dispersion-strengthened alloys p0062 A82-40041
- METAL PARTICLES**
 NT METAL POWDER
- METAL POLISHING**
 Strength advantages of chemically polished boron fibers before and after reaction with aluminum [NASA-TM-82806] p0049 N82-21258
- METAL POWDER**
 Development of materials and process technology for dual alloy disks [NASA-CP-165224] p0063 N82-18370
- METAL SURFACES**
 Single pass rub phenomena - Analysis and experiment [ASME PAPER P1-LUB-55] p0107 A82-18449
 Cessation of $\omega/001$ - Work function lowering by multiple dipole formation A82-30002
 Detection of a change in the oxidation state on aluminum surface using angular correlation of positron annihilation radiation A82-30374
 Stationary state model for normal metal tunnel junction phenomena p0159 A82-42912
 Universal binding energy relations in metallic adhesion [NASA-TM-82706] p0058 N82-11183
 Investigation into the role of NaCl deposited on oxide and metal substrates in the initiation of hot corrosion [NASA-CR-165029] p0063 N82-13217
 Gas turbine ceramic-coated-vane concept with convection-cooled porous metal core [NASA-TP-1942] p0016 N82-14090
 Friction and wear of iron in corrosive metal [NASA-TP-1985] p0058 N82-20291
 A study of the nature of solid particle impact and shape on the erosion morphology of ductile metals [NASA-TM-82933] p0061 N82-33493
 Overlay metallic-cermet alloy coating systems --- for gas turbine engines [NASA-CASE-LEW-13639-1] p0070 N82-33522
- METAL WHISKER REINFORCEMENT**
 U ISKER COMPOSITES
- METALLIC GLASSES**
 Friction and surface chemistry of some ferrous-base metallic glasses [NASA-TP-1991] p0059 N82-21301
 Surface chemistry, microstructure and friction properties of some ferrous-base metallic glasses at temperatures to 750 C [NASA-TP-2006] p0060 N82-22349
- METALLIZING**
 Advances in high output voltage silicon solar cells p0127 A82-44942
- METALLOGRAPHY**
 The influence of gamma prime on the recrystallization of an oxide dispersion strengthened superalloy - MA 6000E p0062 A82-47393
 Microstructural effects on the room and elevated temperature low cycle fatigue behavior of Waspaloy [NASA-CR-165497] p0113 N82-26702
- METALLOIDS**
 NT SILICON
- METALLOORGANIC COMPOUNDS**
 U GANOMETALLIC COMPOUNDS
- METALS**
 NT ALUMINUM
 NT ALUMINUM COATINGS
 NT CESIUM
 NT CHROMIUM
 NT COBALT
 NT FERROUS METALS
 NT GOLD
 NT GOLD COATINGS
 NT INDIUM
- NT IRON
 NT METAL COATINGS
 NT METAL FILMS
 NT METAL FOLDS
 NT METAL MATRIX COMPOSITES
 NT METAL POWDER
 NT NIOBIUM
 NT PLATINUM
 NT PLATINUM ISOTOPES
 NT PLUTONIUM 244
 NT TANTALUM
 NT TITANIUM
 NT TRANSITION METALS
 NT TUNGSTEN
 NT ZINC
 NT ZIRCONIUM
 Correlation of tensile and shear strengths of metals with their friction properties [NASA-TM-82828] p0060 N82-24325
- METEORITE COMPRESSION TESTS**
 U CHANICAL PROPERTIES
METEORITE CRATERS
 The development of central peaks in lunar craters A82-14333
- METEORITES**
 NT CARBONACEOUS CHONDRITES
METEOROID CRATERS
 U TEORITE CRATERS
METEOROLOGY
 NT WEATHER FORECASTING
METERS
 U ASURING INSTRUMENTS
METHANE
 Low-thrust Isp sensitivity study [NASA-CR-165621] p0045 N82-22309
- METHOD OF CHARACTERISTICS**
 Design of supercritical cascades with high solidity [NASA-CR-165600] p0007 N82-22210
- MEXICO**
 Market assessment of photovoltaic power systems for agricultural applications in Mexico [NASA-CR-165441] p0128 N82-10506
- MICROCIRCUITS**
 U CROELECTRONICS
MICROCOMPUTERS
 Real-time microcomputer simulation for space Shuttle/Centaur avionics p0033 A82-48245
 Development report: Automatic System Test and Calibration (ASTAC) equipment [NASA-CR-165403] p0129 N82-13505
- MICROELECTRONICS**
 Proceedings of the Conference on High-temperature Electronics [NASA-TM-84069] p0081 N82-15311
 Method of making a high voltage V-groove solar cell [NASA-CASE-LEW-13401-1] p0124 N82-29709
- MICROHARDNESS**
 Influence of mineral oil and additives on microhardness and surface chemistry of magnesium oxide (001) surface [NASA-TP-1986] p0067 N82-20316
 Effects of environment on microhardness of magnesium oxide [NASA-TP-2002] p0068 N82-22366
 Influence of corrosive solutions on microhardness and chemistry of magnesium oxide /001/ surfaces [NASA-TP-2040] p0102 N82-31691
- MICROINDENTATION**
 U CROHARDNESS
MICROPROCESSORS
 Microprocessor control system for 200-kilowatt Mod-0A wind turbines [NASA-TM-82711] p0120 N82-21710
- MICROSCOPES**
 NT ACOUSTIC MICROSCOPES
 NT ION MICROSCOPES
MICROSCOPY
 NT ELECTRON MICROSCOPY
 NT LASER MICROSCOPY
- MICROSTRUCTURE**
 Quasi-liquid states observed on ion beam microtextured surfaces p0159 A82-30335
 Effects of cobalt on structure, microchemistry and properties of a wrought nickel-base superalloy p0065 A82-34973
 Effects of heating rate on density, microstructure, and strength of Si3N4-6 wt.%

- Y203 and a beta-prime sialon
[ACS PAPER 42-B-81] p0070 882-42366
Structure and creep rupture properties of
directionally solidified eutectic
gamma/gamma-prime-alpha alloy p0062 882-42774
The influence of cobalt on the microstructure of
the nickel-base superalloy MAR-M247 p0063 882-47400
Ultrasonic velocity for estimating density of
structural ceramics p0066 882-14359
[NASA-TM-82765]
Interrelation of material microstructure,
ultrasonic factors, and fracture toughness of
two phase titanium alloy p0110 882-20551
[NASA-TM-82810]
Surface chemistry, microstructure and friction
properties of some ferrous-base metallic glasses
at temperatures to 750 C p0060 882-22349
[NASA-TP-2006]
Microstructural effects on the room and elevated
temperature low cycle fatigue behavior of Waspaloy
[NASA-CR-165497] p0113 882-26702
Effects of cobalt on the microstructure of Udimet
700 p0064 882-28409
[NASA-CR-165605]
Ion beam microtexturing and enhanced surface
diffusion p0065 882-31509
[NASA-CR-167948]
- MICROWAVE AMPLIFIERS**
IMPATT power building blocks for 20 GHz spaceborne
transmit amplifier p0086 882-23566
[AIAA 82-0498]
- MICROWAVE CIRCUITS**
Dynamic switch matrix for the TDMA satellite
switching system p0085 882-23494
[AIAA 82-0458]
- MICROWAVE EMISSION**
Magnetic structure of a flaring region producing
impulsive microwave and hard X-ray bursts p0167 882-27323
- MICROWAVE EQUIPMENT**
NT KLYSTRONS
NT MAGNETRONS
NT MICROWAVE AMPLIFIERS
NT TRAVELING WAVE TUBES
A new antenna concept for satellite communications
[NASA-CR-167924] p0079 882-31584
- MICROWAVE FREQUENCIES**
NT EXTREMELY HIGH FREQUENCIES
- MICROWAVE SWITCHING**
Wideband, high speed switch matrix development for
SS-TDMA applications p0086 882-43784
- MICROWAVE TRANSMISSION**
A review of transhorizon propagation phenomena p0079 882-10679
30/20 GHz demonstration system for improving orbit
utilization p0080 882-27189
Microwave intersatellite links for communications
satellites p0036 882-36925
Analytic investigation of efficiency and
performance limits in klystron amplifiers using
multidimensional computer programs; multi-stage
depressed collectors; and thermionic cathode
life studies p0118 882-12553
The 30/20 GHz flight experiment system, phase 2.
Volume 1: Executive summary p0078 882-20362
[NASA-CR-165409-VOL-1]
The 30/20 GHz flight experiment system, phase 2.
Volume 2: Experiment system description p0078 882-20363
[NASA-CR-165409-VOL-2]
The 30/20 GHz flight experiment system, phase 2.
Volume 3: Experiment system requirement document p0078 882-20364
[NASA-CR-165409-VOL-3]
The 30/20 GHz flight experiment system, phase 2.
Volume 4: Experiment system development plan p0078 882-20365
[NASA-CR-165409-VOL-4]
- MICROWAVE TUBES**
NT KLYSTRONS
NT MAGNETRONS
NT TRAVELING WAVE TUBES
- MICROWAVES**
NT CENTIMETER WAVES
NT MICROWAVE EMISSION
NT MILLIMETER WAVES
- MIDDLE ATMOSPHERE**
NT MESOSPHERE
NT STRATOSPHERE
- MIE SCATTERING**
NT RAYLEIGH SCATTERING
- MILLIMETER WAVES**
Investigation of a comb-type slow-wave structure
for millimeter-wave masers 882-18342
- MILLING MACHINES**
Operational performance of the
photovoltaic-powered grain mill and water pump
at Tangaye, Upper Volta p0120 882-19673
[NASA-TM-82767]
Design description of the Tangaye Village
photovoltaic power system p0126 882-33828
[NASA-TM-82917]
- MINERAL OILS**
Influence of mineral oil and additives on
microhardness and surface chemistry of magnesium
oxide (001) surface p0067 882-20316
[NASA-TP-1986]
- MINERALS**
NT GRAPHITE
NT QUARTZ
Evidence for Pu-244 fission tracks in hibonites
from Murchison carbonaceous chondrite p0166 882-29316
- MINES (EXCAVATIONS)**
LANDSAT Remote Sensing: Observations of an
Appalachian mountaintop surface coal mining and
reclamation operation --- Kentucky p0117 882-24525
[E82-10247]
- MINIMIZATION**
U TIMIZATION
- MINING**
NT STRIP MINING
Assessment of a 40-kilowatt stirling engine for
underground mining applications p0125 882-30714
[NASA-TM-82822]
- MIRRORS**
Environmental effects on solar concentrator mirrors
882-23394
- MIS (SEMICONDUCTORS)**
Low temperature growth and electrical
characterization of insulators for GaAs MISFETS
[NASA-CR-164972] p0159 882-11959
- MISSILE STABILIZATION**
U ABILIZATION
- MIXING**
NT PREMIXING
NT SIGNAL MIXING
NT TURBULENT MIXING
- MIXING LENGTH FLOW THEORY**
Turbofan forced mixer-nozzle internal flowfield.
Volume 1: A benchmark experimental study p0090 882-22458
[NASA-CR-3492]
Turbofan forced mixer-nozzle internal flowfield.
Volume 2: Computational fluid dynamic predictions p0091 882-22459
[NASA-CR-3493]
Turbofan forced mixer-nozzle internal flowfield.
Volume 3: A computer code for 3-D mixing in
axisymmetric nozzles p0091 882-22460
[NASA-CR-3494]
- MIXTURES**
NT AEROSOLS
NT AQUEOUS SOLUTIONS
NT EUTECTIC ALLOYS
NT GAS MIXTURES
NT METAL MATRIX COMPOSITES
NT SIALON
Characterization of an Experimental Referee
Broadened Specification (ERBS) aviation turbine
fuel and ERBS fuel blends p0072 882-32504
[NASA-TM-82883]
- MOBILE COMMUNICATION SYSTEMS**
NT LAND MOBILE SATELLITE SERVICE
- MOBILITY**
Satellite-aided land mobile communications system
implementation considerations p0036 882-25290
[NASA-TM-82861]
- MODAL RESPONSE**
Advanced superposition methods for high speed
turbopump vibration analysis p0104 882-11465
[NASA-CR-165379]
- MODE OF VIBRATION**
U BRATION MODE
MODE SHAPES
U DAL RESPONSE

ORIGINAL PAGE IS
OF POOR QUALITY

SUBJECT INDEX

NACELLES

MODELS

NT AIRCRAFT MODELS
NT ANALOG SIMULATION
NT DIGITAL SIMULATION
NT ENVIRONMENT MODELS
NT MATHEMATICAL MODELS
NT SCALE MODELS
NT SPACECRAFT MODELS
NT WIND TUNNEL MODELS

MODES

NT FAILURE MODES
NT PROPAGATION MODES
NT VIBRATION MODES

MODULATION

NT FREQUENCY MODULATION
NT FREQUENCY SHIFT KEYING
NT INTERMODULATION
NT PULSE DURATION MODULATION

MODULES

NT ELECTRONIC MODULES

MODULUS OF ELASTICITY

Some observations in high pressure rheology of lubricants
[ASME PAPER 81-LUB-171] p0070 A82-18432
Some observations in high pressure rheology of lubricants
[ASME PAPER 81-LUB-171] p0070 A82-18432
Crystallographic texture in oxido-dispersion-strengthened alloys
p0062 A82-40041
The transmission or scattering of elastic waves by an inhomogeneity of simple geometry: A comparison of theories
[NASA-CR-169034] p0079 A82-26026

MOND CIRCLES

U ACQUIRE MECHANICS

MOISTURE

Environmental effects on defect growth in composite materials
[NASA-CR-165213] p0052 A82-20248

MOISTURE CORRECTION

Water ingestion into jet engine axial compressors
[AIAA PAPER 82-0196] p0030 A82-17836

MOLECULAR PUMPS

Pressure pulsations above turbomolecular pumps
p0076 A82-46430

MOLECULAR SPECTRA

NT RAMAN SPECTRA

MOLECULAR WEIGHT

Effect of gamma irradiation on the friction and wear of ultrahigh molecular weight polyethylene
p0062 A82-10674

MOLIERE FORMULA

U ATOM DISTRIBUTION

MOLTEN SALT ELECTROLYTES

Moderate temperature Na cells, IV - V52 and NbS₂Cl₂ as rechargeable cathodes in molten NaAlCl₄
p0055 A82-15743

MOLYBDENUM ALLOYS

Structure and creep rupture properties of directionally solidified eutectic gamma/gamma-prime-alpha alloy
p0062 A82-42774

MOLYBDENUM SULFIDES

Morphological and frictional behavior of sputtered MoS₂ films
[NASA-TN-82809] p0076 A82-22387

MOMENTS

NT BENDING MOMENTS
NT MEAN
NT TORQUE

MOMENTUM TRANSFER

Effects of condensation and surface motion on the structure of steady-state fronts
A82-19360
Mass and momentum turbulent transport experiments with confined coaxial jets
[NASA-CR-165574] p0090 A82-19496

MONOCRYSTALS

U NGLE CRYSTALS

MONOLITHIC CIRCUITS

U INTEGRATED CIRCUITS

MONOMERS

Oxidation and formation of deposit precursors in hydrocarbon fuels
[NASA-CR-165534] p0073 A82-18402

NONPROPELLANTS

NT LIQUID FUELS

MOON-EARTH TRAJECTORIES

The supply of lunar oxygen to low earth orbit
p0032 A82-35618

MOROCCO

Market assessment of photovoltaic power systems for agricultural applications in Morocco
[NASA-CR-165477] p0130 A82-14627

MORPHOLOGY

Mechanism and models for zinc metal morphology in alkaline media
[NASA-TN-82768] p0120 A82-19671
Morphological and frictional behavior of sputtered MoS₂ films
[NASA-TN-82809] p0076 A82-22387
Evaluation of left ventricular assist device pump bladders cast from ion-sputtered polytetrafluoroethylene mandrels
[NASA-CR-167904] p0142 A82-23976

MOS (SEMICONDUCTORS)

U TAL OXIDE SEMICONDUCTORS

MOSFET

U ELD EFFECT TRANSISTORS

MOTION EQUATIONS

U EQUATIONS OF MOTION

MOTION STABILITY

NT AERODYNAMIC STABILITY
NT BOUNDARY LAYER STABILITY
NT FLAME STABILITY
NT FLOW STABILITY
NT GYROSCOPIC STABILITY
NT ROTARY STABILITY

MOTOR VEHICLES

NT AUTOMOBILES
NT ELECTRIC AUTOMOBILES
NT ELECTRIC MOTOR VEHICLES

MOTORS

NT ELECTRIC MOTORS
NT INDUCTION MOTORS
NT SYNCHRONOUS MOTORS

MOUNTAINS

NT APPALACHIAN MOUNTAINS (NORTH AMERICA)
Dynamics of snow cover in mountain regions of the Aral Sea basin, studied using satellite photographs
A82-27462

MULTICHANNEL COMMUNICATION

A remote millivolt multiplexer and amplifier module for wind tunnel data acquisition
p0003 A82-41845

MULTILAYER STRUCTURES

U MINUTES

MULTIPHASE FLOW

NT TWO PHASE FLOW

MULTIPLE ACCESS

NT FREQUENCY DIVISION MULTIPLE ACCESS
NT TIME DIVISION MULTIPLE ACCESS

MULTIPLY TRANSMISSION

U MULTIPLEXING

MULTIPLERS

U MULTIPLEXING

MULTIPLYING

A remote millivolt multiplexer and amplifier module for wind tunnel data acquisition
p0083 A82-41845

MULTIPELLANTS

UCKET PROPELLANTS

MULTISTAGE COMPRESSORS

U RBOCOMPRESSORS

MULTISTAGE ROCKET VEHICLES

NT ATLAS CENTAUR LAUNCH VEHICLE
Fuel/oxidizer-rich high-pressure preburners --- staged-combustion rocket engine
[NASA-CR-165404] p0073 A82-10245
Research report: User's manual for computer program AT81Y005. PLANETSYS, a computer program for the steady state and transient thermal analysis of a planetary power transmission system
[NASA-CR-165366] p0146 A82-31970

MULTIVARIATE STATISTICAL ANALYSIS

NT BIVARIATE ANALYSIS
Identification of multivariable high performance turbofan engine dynamics from closed loop data
[NASA-TN-82785] p0076 A82-20339

N

NACELLES

Low speed testing of the inlets designed for a tandem-fan V/STOL nacelle --- conducted in the

- Lewis 10 by 10 foot wind tunnel
[NASA-TM-82728] p0003 N82-11042
- Thrust modulation methods for a subsonic V/STOL aircraft
[NASA-TM-82747] p0003 N82-13112
- Performance deterioration due to acceptance testing and flight loads; JT90 jet engine diagnostic program
[NASA-CR-165572] p0027 N82-27309
- Advanced turboprop testbed systems study
[NASA-CR-167895] p0014 N82-33375
- NASA PROGRAMS**
- NT SUPERSONIC CRUISE AIRCRAFT RESEARCH**
- 30/20 GHz demonstration system for improving orbit utilization
p0080 A82-27189
- Lewis Research Center's coal-fired, pressurized, fluidized-bed reactor test facility
[NASA-TM-81616] p0087 N82-11397
- Summary and recent results from the NASA advanced High Speed Propeller Research Program
[NASA-TM-82891] p0001 N82-26219
- NASA STRUCTURAL ANALYSIS PROGRAM**
- U STRAN**
- NASTRAN**
- On the automatic generation of FEM models for complex gears - A work-in-progress report
p0109 A82-48243
- Large displacements and stability analysis of nonlinear propeller structures
[NASA-TM-82850] p0112 N82-31707
- NATIONS**
- NT DEVELOPING NATIONS**
- NATURAL FREQUENCIES**
- U SONANT FREQUENCIES**
- NATURAL GAS**
- NT LIQUEFIED NATURAL GAS**
- NATURAL SATELLITES**
- Potentials of surfaces in space
p0165 A82-23750
- NAVIER-STOKES EQUATION**
- A simple finite difference procedure for the vortex controlled diffuser
[AIAA PAPER 82-0109] p0030 A82-17788
- Solutions of the compressible Navier-Stokes equations using the integral method
[AIAA PAPER 81-0046] p0093 A82-23832
- Multigrad simulation of asymptotic curved-duct flows using a semi-implicit numerical technique
p0010 A82-29003
- Basic lubrication equations
[NASA-TM-81693] p0099 N82-16413
- Turbulent solution of the Navier-Stokes equations for uniform shear flow
[NASA-TM-82925] p0089 N82-32634
- NEAR WAKES**
- Measurement and prediction of mean velocity and turbulence structure in the near wake of an airfoil
p0010 A82-26137
- NETWORK ANALYSIS**
- Analysis and design of a standardized control module for switching regulators
p0083 A82-46388
- NETWORK SYNTHESIS**
- A new approach to the minimum weight/loss design of switching power converters
p0082 A82-16831
- Power system design optimization using Lagrange multiplier techniques
p0085 A82-20743
- A 10-kw series resonant converter design, transistor characterization, and base-drive optimization
p0086 A82-36927
- Impact of uniform electrode current distribution on ETF
[NASA-TM-82875] p0123 N82-25636
- NEWTON-RAPHSON METHOD**
- Self-adaptive closed constrained solution algorithms for nonlinear conduction
p0094 A82-45157
- NEWTONIAN FLUIDS**
- Basic lubrication equations
[NASA-TM-81693] p0099 N82-16413
- NICKEL ALLOYS**
- NT UDINET ALLOYS**
- NT NASPALOY**
- Comparative thermal fatigue resistance of several oxide dispersion strengthened alloys
p0062 A82-11399
- Fatigue of Ni-Al-Mo aligned eutectics at elevated temperatures
p0052 A82-13403
- Effects of cobalt on structure, microchemistry and properties of a wrought nickel-base superalloy
p0065 A82-34973
- Long-term high-velocity oxidation and hot corrosion testing of several NiCrAl and FeCrAl base oxide dispersion strengthened alloys
p0062 A82-37151
- Crystallographic texture in oxide-dispersion-strengthened alloys
p0062 A82-40041
- Creep and rupture of an ODS alloy with high stress rupture ductility --- Oxide Dispersion Strengthened
p0065 A82-40335
- Structure and creep rupture properties of directionally solidified eutectic gamma/gamma-prime-alpha alloy
p0062 A82-42774
- The influence of gamma prime on the recrystallization of an oxide dispersion strengthened superalloy - MA 6000E
p0062 A82-47393
- The influence of orientation on the stress rupture properties of nickel-base superalloy single crystals
p0062 A82-47397
- Fatigue and creep-fatigue deformation of several nickel-base superalloys at 650 C
p0062 A82-47398
- The influence of cobalt on the tensile and stress-rupture properties of the nickel-base superalloy MA8-M247
p0063 A82-47399
- The influence of cobalt on the microstructure of the nickel-base superalloy MA8-M247
p0063 A82-47400
- Thermal fatigue and oxidation data of TAZ-8A and M22 alloys and variations
[NASA-CR-165407] p0063 N82-10193
- Development of materials and process technology for dual alloy disks
[NASA-CR-165224] p0063 N82-18370
- A status review of NASA's COSAM (Conservation Of Strategic Aerospace Materials) program
[NASA-TM-82852] p0060 N82-24326
- High temperature low cycle fatigue mechanisms for nickel base and a copper base alloy
[NASA-CR-3543] p0064 N82-26436
- Mechanisms of deformation and fracture in high temperature low cycle fatigue of Rene 80 and IN 100
[NASA-CR-165498] p0113 N82-26706
- Solute transport during the cyclic oxidation of Ni-Cr-Al alloys
[NASA-CR-165544] p0064 N82-27462
- Effects of cobalt on the microstructure of Udinet 700
[NASA-CR-165605] p0064 N82-28409
- Evaluation of candidate stirling engine heater tube alloys at 820 deg and 860 deg C
[NASA-TM-82837] p0061 N82-30372
- MC carbide structures in M(lc2)ar-M247
[NASA-CR-167892] p0064 N82-30374
- Nickel ternary alloy having improved cyclic oxidation resistance
[NASA-CASE-LEW-13339-1] p0061 N82-31505
- Overlay metallic-cermet alloy coating systems --- for gas turbine engines
[NASA-CASE-LEW-13639-1] p0070 N82-33522
- NICKEL CADMIUM BATTERIES**
- Synthetic battery cycling techniques
[NASA-TM-82945] p0125 N82-30715
- NICKEL COMPOUNDS**
- Recrystallization and grain growth in NiAl
p0065 A82-44529
- NICKEL HYDROGEN BATTERIES**
- Design of a 35-kilowatt bipolar nickel-hydrogen battery for low Earth orbit application
[NASA-TM-82844] p0123 N82-24647
- Nickel-hydrogen bipolar battery systems
[NASA-TM-82946] p0125 N82-30716
- NICKEL PLATE**
- Light weight nickel battery plaque

ORIGINAL PAGE IS
OF POOR QUALITY

SUBJECT INDEX

NOISE REDUCTION

[NASA-CASE-LEW-13349-1] p0121 N82-22673
NICKEL ZINC BATTERIES
 Development of battery separator composites
 [NASA-CR-165508] p0128 N82-11547
 Cross-linked polyvinyl alcohol films as alkaline
 battery separators
 [NASA-TM-82802] p0054 N82-22327
NIGHT X LAYER
 U GHT SKY
NIGHT F LAYER
 U GHT SKY
NIGHT SKY
 Field-aligned ion streams in the earth's midnight
 region
 p0140 N82-31009
NIOBIUM
 A status review of NASA's COSAM (Conservation Of
 Strategic Aerospace Materials) program
 [NASA-TM-82852] p0060 N82-24326
NITRIC OXIDE
 Stabilizing platinum in phosphoric acid fuel cells
 [NASA-CR-165483] p0130 N82-14628
 Low NO sub x heavy fuel combustor concept program.
 Phase 1A: Combustion technology generation coal
 gas fuels
 [NASA-CR-165614] p0055 N82-22326
NITRIDES
 NT BORON NITRIDES
 NT SILICON NITRIDES
 Some properties of PF sputtered hafnium nitride
 coatings
 [NASA-TM-82826] p0067 N82-21331
 Refractory coatings and method of producing the same
 [NASA-CASE-LEW-13169-1] p0060 N82-29415
NITRIDING
 The combined effects of Fe and H2 on the
 nitridation of silicon
 p0070 N82-42924
 Nitridation of silicon
 [NASA-TM-82722] p0066 N82-15197
NITROGEN
 NI NITROGEN IONS
 Techniques for enhancing durability and
 equivalence ratio control in a rich-lean,
 three-stage ground power gas turbine combustor
 [NASA-TM-82922] p0124 N82-29717
NITROGEN COMPOUNDS
 NT BORON NITRIDES
 NT NITRIC OXIDE
 NT NITRIDES
 NT NITROGEN OXIDES
 NT NITRUS OXIDES
 NT POLYIMIDES
 NT QUINCLINE
 NT SILICON NITRIDES
 Deposit formation in liquid fuels. II - The effect
 of selected compounds on the storage stability
 of Jet A turbine fuel
 p0074 N82-22240
 Effect of some nitrogen compounds thermal
 stability of Jet A
 [NASA-TM-82908] p0072 N82-27519
NITROGEN IONS
 Friction wear and auger analysis of iron implanted
 with 1.5-MeV nitrogen ions
 [NASA-TP-1989] p0059 N82-21300
NITROGEN OXIDES
 NI NITRIC OXIDE
 NT NITROUS OXIDES
 Formation of oxides of nitrogen in monodisperse
 spray combustion of hydrocarbon fuels
 p0057 N82-37571
 Low NO sub x heavy fuel combustor concept program
 [NASA-CR-165512] p0129 N82-12572
 Effect of fuel-air-ratio nonuniformity on
 emissions of nitrogen oxides
 [NASA-TP-1798] p0016 N82-13143
 Low NO subx heavy fuel combustor concept program.
 Phase 1A: Coal gas addendum
 [NASA-CR-165577] p0133 N82-18690
 Low NOx heavy fuel combustor concept program,
 phase 1
 [NASA-CR-165449] p0135 N82-24651
 Low NOx heavy fuel combustor concept program.
 Phase 1: Combustion technology generation
 [NASA-CR-165482] p0136 N82-24725
 Low NOx heavy fuel combustor concept
 program
 [NASA-CR-167876] p0074 N82-26482
 Computations of soot and and NO sub x emissions
 from gas turbine combustors
 [NASA-CR-167930] p0139 N82-29777
 Venturi nozzle effects on fuel drop size and
 nitrogen oxide emissions
 [NASA-TP-2028] p0020 N82-31329
NITROUS OXIDES
 Catalytic combustion of residual fuels
 [NASA-TM-82731] p0118 N82-13504
 Low NO sub x heavy fuel combustor concept program
 phase 1A gas tests
 [NASA-CR-167877] p0055 N82-25337
 Low NOx heavy fuel combustor concept
 program
 [NASA-CR-165481] p0138 N82-33827
NOBLE GASES
 U RE GASES
NOBLE METALS
 NT GOLD
NOISE (SOUND)
 NT AERODYNAMIC NOISE
 NT AIRCRAFT NOISE
 NT ENGINE NOISE
 NT JET AIRCRAFT NOISE
 Tooth profile analysis of circular-cut,
 spiral-bevel gears
 [NASA-TM-82840] p0101 N82-26681
NOISE ATTENUATION
 U ISE REDUCTION
NOISE ELIMINATION
 U ISE REDUCTION
NOISE GENERATORS
 Sound generated in a cascade by three-dimensional
 disturbances convected in a subsonic flow
 [AIAA PAPER 81-2046] p0153 N82-10460
NOISE HAZARDS
 U ZARDS
 U ISE (SOUND)
NOISE MEASUREMENT
 Noise of the SR-3 propeller model at 2 deg and 4
 deg angle of attack
 [NASA-TM-82738] p0151 N82-16808
 Effect of facility variation on the acoustic
 characteristics of three single stream nozzles
 [NASA-TM-81635] p0151 N82-19944
 YF 102 in-duct combustor noise measurements with a
 turbine nozzle, volume 1
 [NASA-CR-165562-VOL-1] p0153 N82-21031
 YF 102 in-duct combustor noise measurements with a
 turbine nozzle, volume 2
 [NASA-CR-165562-VOL-2] p0153 N82-21032
 YF 102 in-duct combustor noise measurements with a
 turbine nozzle, volume 3
 [NASA-CR-165562-VOL-3] p0155 N82-21033
 Method for predicting impulsive noise generated by
 wind turbine rotors
 [NASA-TM-82794] p0121 N82-21714
 A preliminary comparison between the SR-3
 propeller noise in flight and in a wind tunnel
 [NASA-TM-82805] p0152 N82-21998
NOISE PREDICTION
 An iterative finite element-integral technique for
 predicting sound radiation from turbofan inlets
 in steady flight
 [AIAA PAPER 82-0124] p0030 N82-17796
NOISE PREDICTION (AIRCRAFT)
 Effects of vane/blade ratio and spacing on fan noise
 [AIAA PAPER 81-2033] p0029 N82-10457
 A shock wave approach to the noise of supersonic
 propellers
 [NASA-TM-82752] p0151 N82-16809
NOISE PROPAGATION
 Method for predicting impulsive noise generated by
 wind turbine rotors
 [NASA-TM-82794] p0121 N82-21714
 Propeller flow visualization techniques
 p0096 N82-32672
NOISE REDUCTION
 Maximum entropy image reconstruction from
 projections
 A82-11053
 Acoustic transmission in lined flow ducts - A
 finite element eigenvalue problem
 p0154 N82-17663
 NASA research activities in aeropropulsion
 [NASA-TM-82788] p0017 N82-16084
 Forward acoustic performance of a model turbofan
 designed for a high specific flow (QF-14)
 [NASA-TP-1968] p0152 N82-21036

A high speed implementation of the random decrement algorithm [NASA-TM-82853] p0076 N82-22388
The NASA-LeRC wind turbine sound prediction code p0123 N82-23730
Aeroacoustic performance of an externally blown flap configuration with several flap noise suppression devices [NASA-TP-1995] p0152 N82-24942
NASA research in supersonic propulsion: A decade of progress [NASA-TM-82862] p0019 N82-26300
QCSSE under-the-wing engine acoustic data [NASA-TM-82691] p0019 N82-27311
Rough analysis of installation effects on turbo-prop noise [NASA-TM-82924] p0152 N82-32082

NOISE SPECTRA
Stationary state model for normal metal tunnel junction phenomena p0159 A82-42912

NOISE SUPPRESSORS
U ISE REDUCTION
NOMINAL VALUES
U PROXIMATION
NONADIABATIC PROCESSES
U AT TRANSFER
NONCONDUCTORS
U ELECTRICAL INSULATION
NONEUCLIDIAN GEOMETRY
U SPHERICAL GEOMETRY
NONISOTROPY
U ISOTROPY
NONLINEAR EQUATIONS
Numerical comparisons of nonlinear convergence accelerators p0149 A82-31438
Rapid approximate determination of nonlinear solutions - Application to aerodynamic flows and design/optimization problems p0012 A82-35571
Construction of solutions for some nonlinear two-point boundary value problems [NASA-TM-82927] p0144 N82-30949

NONLINEAR SYSTEMS
A tensor approach to modeling of nonhomogeneous nonlinear systems p0148 A82-19064
Nonlinear analysis of rotor-bearing systems using component mode synthesis [ASME PAPER 82-GT-303] p0104 A82-35468
Self-adaptive closed constrained solution algorithms for nonlinear conduction p0094 A82-45157
Nonlinear structural and life analyses of a combustor liner [NASA-TM-82846] p0111 N82-24501

NONREFLECTION
U ENERGY ABSORPTION
NONUNIFORM FLOW
Effect of fuel-air-ratio nonuniformity on emissions of nitrogen oxides [NASA-TP-1798] p0016 N82-13143
Rough analysis of installation effects on turbo-prop noise [NASA-TM-82924] p0152 N82-32082

NONVISCOUS FLOW
U VISCID FLOW
NORMAL SHOCK WAVES
Tangential blowing for control of strong normal shock - Boundary layer interactions on inlet ramps [AIAA PAPER 82-1082] p0005 A82-37684

NOSE INLETS
Thrust modulation methods for a subsonic V/STOL aircraft [NASA-TM-82747] p0003 N82-13112

NOTCH STRENGTH
A preliminary study of crack initiation and growth at stress concentration sites [NASA-CR-169358] p0115 N82-33738

NOTCH TESTS
Extended range stress intensity factor expressions for chevron-notched short bar and short rod fracture toughness specimens p0112 A82-40357

NOTCHED METALS
U ICH TESTS
NOZZLE COEFFICIENT
U ZYLE FLOW

NOZZLE DESIGN
Modeling parameter influences on MHD swirl combustion nozzle design [AIAA PAPER 82-0984] p0011 A82-31947
Three dimensional flow measurements in a turbine scroll [NASA-CR-167920] p0009 N82-32310

NOZZLE FLOW
The effect of inflow velocity profiles on the performance of supersonic ejector nozzles [AIAA PAPER 81-0273] p0002 A81-32548
An example of a solution to transonic equations for shock-free flow about a symmetric profile A82-26439
Flow aerodynamics modeling of an MHD swirl combustor - Calculations and experimental verification p0094 A82-44782
Turbofan forced mixer-nozzle internal flowfield. Volume 1: A benchmark experimental study [NASA-CR-3492] p0090 N82-22458
Turbofan forced mixer-nozzle internal flowfield. Volume 2: Computational fluid dynamic predictions [NASA-CR-3493] p0091 N82-22459
Turbofan forced mixer-nozzle internal flowfield. Volume 3: A computer code for 3-D mixing in axisymmetric nozzles [NASA-CR-3494] p0091 N82-22460
Venturi nozzle effects on fuel drop size and nitrogen oxide emissions [NASA-TP-2028] p0020 N82-31329
Three dimensional flow measurements in a turbine scroll [NASA-CR-167920] p0009 N82-32310

NOZZLE GEOMETRY
Tests of a D vented thrust deflecting nozzle behind a simulated turbofan engine [NASA-CR-3508] p0006 N82-17122
Effect of facility variation on the acoustic characteristics of three single stream nozzles [NASA-TM-81635] p0151 N82-19944
Aerodynamic analysis of VTOL inlets and definition of a short, blowing-lip inlet [NASA-CR-165617] p0007 N82-22211
A summary of V/STOL inlet analysis methods [NASA-TM-82885] p0005 N82-28249

NOZZLE THRUST COEFFICIENTS
Thrust modulation methods for a subsonic V/STOL aircraft [NASA-TM-82747] p0003 N82-13112
Tests of a D vented thrust deflecting nozzle behind a simulated turbofan engine [NASA-CR-3508] p0006 N82-17122

NOZZLE WALLS
Core compressor exit stage study. Volume 4: Data and performance report for the best stage configuration [NASA-CR-165357] p0023 N82-14092
Core compressor exit stage study. Volume 5: Design and performance report for the Rotor C/Stator B configuration [NASA-CR-165358] p0023 N82-14093

NOZZLES
Development of improved high temperature coatings for IN-792 + HF [NASA-CR-165395] p0063 N82-14333

NUCLEAR AUXILIARY POWER UNITS
NT SPACE POWER UNIT REACTORS
NUCLEAR CAPTURE
NT ELECTRON CAPTURE
NUCLEAR ELECTRIC POWER GENERATION
NT SPACE POWER UNIT REACTORS
NUCLEAR INTERACTIONS
NT ELECTRON CAPTURE
NUCLEAR POWER REACTORS
NT SPACE POWER UNIT REACTORS
NUCLEAR RADIATION
NT GAMMA RAYS
NUCLEAR REACTIONS
NT ELECTRON CAPTURE
NT ELECTRON SCATTERING
NT POSITRON ANNIHILATION
NUCLEAR REACTORS
NT SPACE POWER UNIT REACTORS
NUCLEAR WASTES
U DIOACTIVE WASTES
NUCLIDES
NT PLATINUM ISOTOPES
NT PLUTONIUM 244

NUMERICAL ANALYSIS

NT APPROXIMATION
 NT BOUNDARY INTEGRAL METHOD
 NT COMPUTATIONAL FLUID DYNAMICS
 NT DIFFERENCE EQUATIONS
 NT ERROR ANALYSIS
 NT FINITE DIFFERENCE THEORY
 NT FINITE ELEMENT METHOD
 NT FINITE VOLUME METHOD
 NT ITERATIVE SOLUTION
 NT NEWTON-RAPHSON METHOD
 NT NUMERICAL INTEGRATION
 NT RAYLEIGH-RITZ METHOD
 NT RELAXATION METHOD (MATHEMATICS)
 Numerical analysis and FORTRAN program for the computation of the turbulent wakes of turbomachinery rotor blades, isolated airfoils and cascade of airfoils
 [NASA-CR-3509] p0006 N82-18184
 Geometry and starvation effects in hydrodynamic lubrication
 [NASA-TM-82807] p0042 N82-20240
 A new numerical approach for compressible viscous flows
 [NASA-CR-168842] p0090 N82-22455
 Boundary-layer effects in composite laminates: Free-edge stress singularities, part 6
 [NASA-CR-165440] p0114 N82-26718
 Three dimensional flow field inside compressor rotor, including blade boundary layers
 [NASA-CR-169120] p0091 N82-27686
 Turbulent solution of the Navier-Stokes equations for uniform shear flow
 [NASA-TM-82925] p0089 N82-32634

NUMERICAL CONTROL

Design study of a continuously variable roller cone traction CVT for electric vehicles
 [NASA-CR-159841] p0105 N82-12445

NUMERICAL FLOW VISUALIZATION

Numerical analysis of confined turbulent flow
 p0093 A82-24748
 Numerical modelling of turbulent flow in a combustion tunnel
 p0093 A82-27000
 Numerical modeling of turbulent combustion in premixed gases
 p0056 A82-28708

NUMERICAL INTEGRATION

Application of integration algorithms in a parallel processing environment for the simulation of jet engines
 [NASA-TM-82746] p0149 N82-14849

NUMERICAL STABILITY

Self-adaptive closed constrained solution algorithms for nonlinear conduction
 p0094 A82-45157

O RING SEALS

Effect of seals on rotor systems
 [NASA-TM-82786] p0099 N82-16411

OILS

NT FUEL OILS
 NT LUBRICATING OILS
 NT MINERAL OILS
 Measurement of oil film thickness for application to elastomeric Stirling engine rod seals
 [ASME PAPER 81-1118-9] p0107 A82-18426

ONBOARD DATA PROCESSING

Dynamic switch matrix for the TDMA satellite switching system
 [AIAA 82-2458] p0085 A82-23494
 Baseband-processed SS-TDMA communication system architecture and design concepts
 [AIAA 82-0482] p0079 A82-23508
 34/20 GHz demonstration system for improving orbit utilization
 p0080 A82-27189
 Open-loop nanosecond-synchronization for wideband satellite communications
 p0036 A82-27224

OMNISOTROPY

U ISOTROPY

OPEN CIRCUIT VOLTAGE

Multi junction high voltage concentrator solar cells
 p0043 A82-11796
 Moderate temperature Na cells, IV - VS2 and H₂SO₄ as rechargeable cathodes in molten NaAlCl₄

p0055 A82-15743
 Advances in high output voltage silicon solar cells
 p0127 A82-44942
 Fabrication of multijunction high voltage concentrator solar cells by integrated circuit technology
 p0127 A82-44957

OPENINGS

NT APERTURES

OPERATING SYSTEMS (COMPUTERS)

Microprocessor control system for 200-kilowatt Mod-OA wind turbines
 [NASA-TM-82711] p0120 N82-21710

OPERATING TEMPERATURE

Research report: User's manual for computer program AT81y003 SHABERTH. Steady state and transient thermal analysis of a shaft bearing system including ball, cylindrical and tapered roller bearings
 [NASA-CR-165365] p0146 N82-31969

OPHTHALMOLOGY

Veiling glare reduction methods compared for ophthalmic applications
 p0143 A82-13289

OPTICAL DATA PROCESSING

Experimental boundary integral equation applications in speckle interferometry
 p0097 A82-36987
 Role of optical computers in aeronautical control applications
 p0156 N82-15897

OPTICAL EQUIPMENT

NT COLLIMATORS

NT LASER DOPPLER VELOCIMETERS

NT OPTICAL MEASURING INSTRUMENTS

NT OPTICAL SCANNERS

A digital optical torque meter for high rotational speed applications
 [NASA-TM-82914] p0095 N82-31664

OPTICAL GENERATORS

U SER CAVITIES

OPTICAL MEASURING INSTRUMENTS

NT OPTICAL SCANNERS

Optical tip clearance sensor for aircraft engine controls
 [AIAA PAPER 82-1131] p0015 A82-37691

OPTICAL PROPERTIES

NT BIREFRINGENCE

NT PHOTOVOLTAIC EFFECT

NT REFLECTANCE

NT REFRACTIVITY

NT TRANSMITTANCE

Ion beam microtexturing and enhanced surface diffusion
 [NASA-CR-167948] p0065 N82-31509

OPTICAL PUMPING

Optically pumped high-pressure DF-CO₂ transfer laser
 A82-10193

OPTICAL SCANNERS

Reliable aerial thermography for energy conservation
 [NASA-TM-81766] p0117 N82-14552

OPTICAL SENSORS

U TICAL MEASURING INSTRUMENTS

OPTICAL CONTROL

AESOP: A computer-aided design program for linear multivariable control systems
 [NASA-TM-82871] p0148 N82-30992

OPTIMIZATION

NT OPTIMAL CONTROL

Optimal tooth numbers for compact standard spur gear sets
 [ASME PAPER 81-DET-115] p0103 A82-19335
 Power system design optimization using Lagrange multiplier techniques
 p0085 A82-20743

The use of optimization techniques to design controlled diffusion compressor blading
 [ASME PAPER 82-GT-149] p0022 A82-35373

The use of optimization techniques to design controlled diffusion compressor blading
 [NASA-TM-82763] p0016 N82-14094

Mathematical models for the synthesis and optimization of spiral bevel gear tooth surfaces --- for helicopter transmissions
 [NASA-CR-3553] p0106 N82-25516

Optimization of the oxidant supply system for combined cycle MHD power plants
 [NASA-TM-82909] p0123 N82-26790

- The optimal design of involute gear teeth with unequal addenda
[NASA-TM-82866] p0101 N82-28645
- OPTIMUM CONTROL**
U TIMAL CONTROL
- ORBIT CALCULATION**
Integrated propulsion for near-Earth space missions. Volume 2: Technical
[NASA-CR-167889-VOL-2] p0086 N82-33425
- ORBIT SPECTRUM UTILIZATION**
Planning satellite communication services and spectrum-orbit utilization
[AIAA 82-0526] p0080 N82-23538
30/20 GHz demonstration system for improving orbit utilization p0080 N82-27189
- ORBIT TRANSFER VEHICLES**
Low-thrust chemical propulsion system pump technology
[NASA-CR-165219] p0105 N82-13427
Large Space Systems/Propulsion Interactions
[NASA-TM-82904] p0042 N82-27358
- ORBITAL ASSEMBLY**
Centaur capabilities for communications satellite launches
[AIAA PAPER 82-0558] p0034 N82-36286
- ORBITAL LAUNCHING**
Real-time computer simulation/emulation for verification of multi-fault-tolerant control of Centaur-in-Shuttle
[AIAA 81-2283] p0040 N82-13494
- ORBITAL TRANSFER**
U TRANSFER ORBITS
- ORBITING SATELLITES**
U TYPICAL SATELLITES
- ORBITS**
NT EARTH ORBITS
NT GEOSYNCHRONOUS ORBITS
NT POLAR ORBITS
NT SATELLITE ORBITS
NT SPACECRAFT ORBITS
NT TRANSFER ORBITS
- ORES**
U NERALS
- ORGANIC COMPOUNDS**
NT ORGANIC SULFUR COMPOUNDS
NT QUINOLINE
ORGANIC SULFUR COMPOUNDS
Improved boundary lubrication with formulated C-ethers
[NASA-TM-82808] p0067 N82-20313
- ORGANOMETALLIC COMPOUNDS**
OM-VPE growth of Mg-doped GaAs --- Organometallic-Vapor Phase Epitaxy p0159 N82-38411
- ORIFICE FLOW**
Flow through axially aligned sequential apertures of the orifice and Borda types
[ASME PAPER 81-HT-79] p0089 N82-10964
Flow through aligned sequential orifice type inlets
[NASA-TP-1967] p0087 N82-20467
Flows through sequential orifices with heated spacer reservoirs
[NASA-TM-82855] p0088 N82-24455
- ORIFICES**
The velocity field near the orifice of a Helmholtz resonator in grazing flow
[NASA-CR-168548] p0153 N82-18994
- ORTHOTROPIC PLATES**
Motion of a rigid punch at the boundary of an orthotropic viscoelastic half-plane
A82-26436
- OSCILLATING FLOW**
Two dimensional stagnation point flow of a dusty gas near an oscillating plate
p0012 N82-37535
An experimental investigation of gapwise periodicity and unsteady aerodynamic response in an oscillating cascade. Volume 2: Data report. Part 1: Text and mode 1 data
[NASA-CR-165457-VOL-2-PT-1] p0006 N82-18180
- OSCILLATIONS**
NT WING OSCILLATIONS
- OSCILLATORS**
NT MAGNETRONS
- OTV**
U BIT TRANSFER VEHICLES
- OXIDATION**
NT ELECTROCHEMICAL OXIDATION
- Strength distributions of SiC ceramics after oxidation and oxidation under load
[ACS PAPER 9-C-80C] p0071 N82-20143
Detection of a change in the oxidation state on aluminum surface using angular correlation of positron annihilation radiation
A82-30374
- Effects of oxidation and oxidation under load on strength distributions of Si3N4
[ACS PAPER 69-B-80] p0071 N82-35871
Thermal fatigue and oxidation data of TAZ-8A and M22 alloys and variations
[NASA-CR-705407] p0063 N82-10193
Thermal oxidative degradation reactions of perfluoroalkylethers
[NASA-CR-165516] p0048 N82-12135
Oxidation and formation of deposit precursors in hydrocarbon fuels
[NASA-CR-165534] p0073 N82-18402
Thermal and oxidative degradation studies of formulated C-ethers by gel-permeation chromatography
[NASA-TP-1994] p0068 N82-21332
Method and apparatus for strengthening boron fibers --- high temperature oxidation
[NASA-CASE-LEW-13826-1] p0050 N82-26385
Thermal oxidative degradation reactions of linear perfluoroalkylethers
[NASA-TM-82834] p0068 N82-26468
Solute transport during the cyclic oxidation of Ni-Cr-Al alloys
[NASA-CR-165544] p0064 N82-27462
Effect of some nitrogen compounds thermal stability of jet A
[NASA-TM-82908] p0072 N82-27519
- OXIDATION RESISTANCE**
Improved plasma sprayed MCrAlY coatings for aircraft gas turbine applications
p0065 N82-20742
Inexpensive cross-linked polymeric separators made from water-soluble polymers --- for secondary alkaline nickel-zinc and silver-zinc cells
p0048 N82-23778
Oxidation stability of advanced reaction-bonded Si3N4 materials
[ACS PAPER 52-B-80P] p0074 N82-33030
Ceramic thermal barrier coatings for gas turbine engines
[ASME PAPER 82-GT-265] p0071 N82-35441
Long-term high-velocity oxidation and hot corrosion testing of several NiCrAl and FeCrAl base oxide dispersion strengthened alloys
p0062 N82-37151
Development of improved high temperature coatings for IN-792 + HF
[NASA-CR-165395] p0063 N82-14333
Review of NASA progress in thermal barrier coatings for stationary gas turbines
[NASA-TM-81716] p0058 N82-17335
Tailored plasma sprayed MCrAlY coatings for aircraft gas turbine applications
[NASA-CR-165234] p0064 N82-19360
Improved thermal barrier coating system
[NASA-CASE-LEW-13324-1] p0060 N82-26431
NiCrAl ternary alloy having improved cyclic oxidation resistance
[NASA-CASE-LEW-13339-1] p0061 N82-31505
- OXIDATION-REDUCTION REACTIONS**
Method of making formulated plastic separators for soluble electrode cells
[NASA-CASE-LEW-12358-2] p0054 N82-21268
Chemical and electrochemical behavior of the Cr(3)/Cr(2) half cell in the NASA Redox Energy Storage System
[NASA-TM-82913] p0055 N82-33463
- OXIDE FILMS**
Oxidation stability of advanced reaction-bonded Si3N4 materials
[ACS PAPER 52-B-80P] p0074 N82-33030
Electron beam induced damage in ITO coated Kapton --- Indium Tin Oxide
p0159 N82-41546
Effect of oxide films on hydrogen permeability of candidate Stirling engine heater head tube alloys
[NASA-TM-82824] p0060 N82-24323
- OXIDES**
NT ALUMINUM OXIDES
NT CARBON MONOXIDE
NT HYDROGEN PEROXIDE

- NT MAGNESIUM OXIDES
NT METAL OXIDES
NT NITRIC OXIDE
NT NITROGEN OXIDES
NT NITROUS OXIDES
NT QUARTZ
NT SILICON DIOXIDE
NT TIN OXIDES
NT YTTRIUM OXIDES
NT ZIRCONIUM OXIDES
Investigation into the role of NaCl deposited on
oxide and metal substrates in the initiation of
hot corrosion
[NASA-CF-165029] p0063 N82-13217
- OXIDIZERS**
NT LIQUID OXIDIZERS
NT LIQUID OXYGEN
Optimization of the oxidant supply system for
combined cycle MHD power plants
[NASA-TM-82909] p0123 N82-26790
- OXYALKYLATION**
U KYLATION
- OXYGEN**
NT LIQUID OXYGEN
NT OZONE
The effect of oxygen concentration on the
boundary-lubricating characteristics of a C
ether and a polyphenyl ether to 300 C
MHD oxidant intermediate temperature ceramic
heater study
[NASA-CF-165453] p0131 N82-15527
- OXYGEN PRODUCTION**
Optimization of the oxidant supply system for
combined cycle MHD power plants
[NASA-TM-82909] p0123 N82-26790
- OXYGEN SUPPLY EQUIPMENT**
Resonance tube hazards in oxygen systems
[NASA-TM-82801] p0072 N82-21415
- OXYGEN SYSTEMS**
U YGEN SUPPLY EQUIPMENT
- OZONE**
An automated system for global atmospheric
sampling using B-747 airliners
[NASA-CR-165264] p0139 N82-13554
Ozone and aircraft operations
p0001 N82-21145
- OZONOMETRY**
Ozone and aircraft operations
p0001 N82-21145
- P**
- P-I-N DIODES**
U I-N JUNCTIONS
- P-I-N JUNCTIONS**
A theory of the n-i-p silicon solar cell
p0128 N82-45055
High voltage V-groove solar cell
[NASA-CAS2-LEW-1340-1-2] p0123 N82-24717
- PACKAGING**
NT ELECTRONIC PACKAGING
Development of thin wraparound junction silicon
solar cells
[NASA-CR-165570] p0133 N82-18689
- PACKET SWITCHING**
Wideband, high speed switch matrix development for
SS-TDMA applications
p0086 N82-43784
- PACKET TRANSMISSION**
NT PACKET SWITCHING
- PAD**
A pad perturbation method for the dynamic
coefficients of tilting-pad journal bearings
p0110 N82-14400
- PAPER (MATERIAL)**
Collection and dissemination of thermal energy
storage system information for the pulp and
paper industry
p0136 N82-24686
- PARABOLIC REFLECTORS**
Subsystems design and component development for
the parabolic dish module for solar thermal
power systems
[NASA-CR-168941] p0135 N82-24646
Coaxial prime focus feeds for paraboloidal
reflectors
[NASA-CF-167934] p0078 N82-31585
- PARALLEL FLOW**
NT PIPE FLOW
NT THREE DIMENSIONAL FLOW
Comparison of two parallel/series flow turbofan
propulsion concepts for supersonic V/STOL
[AIAA PAPER 81-2637] p0020 N82-19214
- PARALLEL PROCESSING (COMPUTERS)**
Application of integration algorithms in a
parallel processing environment for the
simulation of jet engines
[NASA-TM-82746] p0149 N82-14849
- PARAMAGNETIC AMPLIFIERS**
U SERS
- PARAMETER IDENTIFICATION**
Modeling parameter influences on MHD swirl
combustion nozzle design
[AIAA PAPER 82-0984] p0011 N82-31947
A 10KW series resonant converter design,
transistor characterization, and base-drive
optimization
[NASA-CR-165546] p0084 N82-17439
Shaded computer graphic techniques for visualizing
and interpreting analytic fluid flow models
[NASA-CR-168418] p0145 N82-17880
Identification of multivariable high performance
turbofan engine dynamics from closed loop data
[NASA-TM-82785] p0076 N82-20339
- PARAMETERIZATION**
NT PARAMETER IDENTIFICATION
- PARTIAL DIFFERENTIAL EQUATIONS**
NT HELMHOLTZ VORTICITY EQUATION
- PARTICLE BEAMS**
NT ELECTRON BEAMS
NT ION BEAMS
NT RELATIVISTIC ELECTRON BEAMS
Mapping of electrical potential distributions with
charged particle beams
[NASA-CR-168556] p0084 N82-18508
- PARTICLE DENSITY (CONCENTRATION)**
NT ELECTRON DISTRIBUTION
NT ION DENSITY (CONCENTRATION)
NT MAGNETOSPHERIC ION DENSITY
- PARTICLE DIFFUSION**
Experimental and theoretical studies of the laws
governing condensate deposition from combustion
gases
p0057 N82-28709
- PARTICLE EMISSION**
NT ELECTRON EMISSION
NT SECONDARY EMISSION
- PARTICLE INTERACTIONS**
NT ELECTRON CAPTURE
- PARTICLE MOTION**
Three-dimensional relativistic field-electron
interaction in a multicavity high-power
klystron. I: Basic theory
[NASA-TP-1992] p0081 N82-22439
- PARTICLE TRACKS**
Evidence for Pu-244 fission tracks in hibonites
from Murchison carbonaceous chondrite
p0166 N82-29316
- PARTICLE TRAJECTORIES**
NT ELECTRON TRAJECTORIES
Mapping of electrical potential distributions with
charged particle beams
[NASA-CR-168556] p0084 N82-18508
- PARTICLES**
NT AEROSOLS
NT ANIONS
NT ARGON PLASMA
NT CHARGED PARTICLES
NT CYLINDRICAL PLASMAS
NT ELECTRON BEAMS
NT EMERGETIC PARTICLES
NT PLASMA SHEATHS
NT PLASMAS (PHYSICS)
NT RELATIVISTIC ELECTRON BEAMS
NT RELATIVISTIC PARTICLES
NT SOOT
- PASSENGER AIRCRAFT**
NT BOEING 747 AIRCRAFT
NT DC 10 AIRCRAFT
Lightweight diesel engine designs for commuter
type aircraft
[NASA-CR-165470] p0023 N82-11068
- PAYLOAD INTEGRATION PLAN**
Cryogenic fluid management experiment
[NASA-CR-165495] p0039 N82-15117

ORIGINAL PAGE IS
OF POOR QUALITY

PAYLOADS

PAYLOADS

NT SPACE SHUTTLE PAYLOADS
NT SPACEBORNE EXPERIMENTS
NT SPACILAP PAYLOADS
PDM (MODULATION)
U LSE DURATION MODULATION
PEAKS (LANDFORMS)
The development of central peaks in lunar craters
A82-14333

PREHEATING

NT SHOT PREHEATING
PEGASUS ENGINE
U ISTOL-SIDDELEY DS 57 ENGINE

PERCENTAGE

U TIOS

PERFLUORO COMPOUNDS

Thermal oxidative degradation reactions of
perfluoroalkylethers
[NASA-CR-165516] p0048 A82-12135
Thermal oxidative degradation reactions of linear
perfluoroalkylethers
[NASA-TM-82834] p0068 A82-26468

PERFORMANCE PREDICTION

NT PREDICTION ANALYSIS TECHNIQUES
A heat exchanger computational procedure for
temperature-dependent fouling
[ASME PAPER 81-NT-75] p0092 A82-10961
On the prediction of swirling flowfields found in
axisymmetric combustor geometries
p0029 A82-12120
Measurement and prediction of mean velocity and
turbulence structure in the near wake of an
airfoil
p0010 A82-26137

Performance degradation of propeller/rotor systems
due to rime ice accretion
[AIAA PAPER 82-0286] p0014 A82-28322

Small gas turbine combustor primary zone development
[AIAA PAPER 82-1159] p0103 A82-35036

Jet impingement heat transfer enhancement for the
GFJ-3 Stirling engine
[NASA-TM-82727] p0163 A82-11993

Spherical roller bearing analysis. SKF computer
program SPHERBEAN. Volume 1: Analysis
[NASA-CR-165203] p0106 A82-20540

Spherical roller bearing analysis. SKF computer
program SPHERBEAN. Volume 2: User's manual
[NASA-CR-165204] p0106 A82-20541

Nonlinear constitutive theory for turbine engine
structural analysis
p0112 A82-33744

Theoretical and experimental power from large
horizontal-axis wind turbines
[NASA-TM-82944] p0127 A82-33830

PERFORMANCE TESTS

Experimental verification of a computational
procedure for the design of TWT-refocuser-MDC
systems --- Multistage Depressed Collectors
p0082 A82-16128

An experiment to evaluate liquid hydrogen storage
in space
A82-20748

Environmental effects on solar concentrator mirrors
A82-23394

Ceramic thermal barrier coatings for gas turbine
engines
[ASME PAPER 82-GT-265] p0071 A82-35441

Pressure pulsations above turbomolecular pumps
p0076 A82-46430

Effect of fuel injector type on performance and
emissions of reverse-flow combustor
[NASA-TP-1945] p0016 A82-15040

Evaluation of wind tunnel performance testings of
an advanced 45 deg swept 8-bladed propeller at
Mach numbers from 0.45 to 0.85
[NASA-CR-3505] p0007 A82-19178

Preliminary results on performance testing of a
turbocharged rotary combustion engine
[NASA-TM-82772] p0017 A82-21194

Experimental performance of the regenerator for
the Chrysler upgraded automotive gas turbine
engine
[NASA-TM-82671] p0120 A82-21712

Small passenger car transmission test: Mercury
Lynx ATX transmission
[NASA-CR-165510] p0106 A82-24496

Results of chopper-controlled discharge life
cycling studies on lead acid batteries
[NASA-TM-82912] p0124 A82-30700

SUBJECT INDEX

Ceramic applications in turbine engines
[NASA-CR-165197] p0164 A82-31158

PERFUSION

U PERFUSION

PERIOD EQUATIONS

U PERIODIC FUNCTIONS

PERIODIC FUNCTIONS

U PERIODIC FUNCTIONS

NT TANGENTS

Review of analysis methods for rotating systems
with periodic coefficients
p0135 A82-23702

PERIODIC VARIATIONS

NT ANNUAL VARIATIONS

PERIPHERAL EQUIPMENT (COMPUTERS)

NT COMPUTER STORAGE DEVICES

PERMEABILITY

Effect of oxide films on hydrogen permeability of
candidate Stirling engine heater head tube alloys
[NASA-TM-82824] p0060 A82-24323

PEROXIDES

NT HYDROGEN PEROXIDE

PERTURBATION THEORY

A pad perturbation method for the dynamic
coefficients of tilting-pad journal bearings
p0110 A82-14400

Stationary state model for normal metal tunnel
junction phenomena
p0159 A82-42912

PETROLEUM PRODUCTS

NT DIESEL FUELS

NT LUBRICATING OILS

PHASE DIAGRAMS

Phase stability in plasma-sprayed, partially
stabilized zirconia-yttria
p0070 A82-41552

PHASE TRANSFORMATIONS

NT BOILING

NT FLASHING (VAPORIZING)

NT MELTING

NT PROPELLANT EVAPORATION

NT VAPORIZING

Raman study of the improper ferroelectric phase
transition in iron iodine boracite
A82-30297

Effects of cobalt on the microstructure of Udimet
700
[NASA-CR-165605] p0064 A82-28409

PHASED ARRAYS

NASA Adaptive Multibeam Phased Array (ANPA): An
application study
[NASA-CR-169125] p0079 A82-28503

PHOSPHORIC ACID

Develop and test fuel cell powered on-site
integrated total energy systems. Phase 3:
Full-scale power plant development
[NASA-CR-165455] p0131 A82-16483

Preparation and evaluation of advanced
electrocatalysts for phosphoric acid fuel cells
[NASA-CR-165594] p0132 A82-17615

Cell module and fuel conditioner development
[NASA-CR-165620] p0134 A82-21713

Cathode catalyst for primary phosphoric acid fuel cells
[NASA-CR-165198] p0134 A82-22675

Stabilizing platinum in phosphoric acid fuel cells
[NASA-CR-165606] p0136 A82-29718

Non-noble catalysts and catalyst supports for
phosphoric acid fuel cells
[NASA-CR-165289] p0137 A82-30722

40-kW phosphoric acid fuel cell field test -
Project plan
p0128 A82-45325

Survey on aging on electrodes and electrocatalysts
in phosphoric acid fuel cells
[NASA-CR-165505] p0128 A82-11545

Preparation and evaluation of advanced
electrocatalysts for phosphoric acid fuel cells
[NASA-CR-165519] p0129 A82-12573

Cell module and fuel conditioner development
[NASA-CR-165462] p0130 A82-13511

Stabilizing platinum in phosphoric acid fuel cells
[NASA-CR-165483] p0130 A82-14628

Technology development for phosphoric acid fuel
cell powerplant, phase 2
[NASA-CR-165426] p0131 A82-14492

Phosphoric acid fuel cell technology status
[NASA-TM-82791] p0120 A82-19670

Cathode catalysts for primary phosphoric acid fuel
cells

- [NASA-CR-165578] p0134 N82-21709
Develop and test fuel cell powered on-site
integrated total energy systems: Phase 3:
Full-scale power plant development
- [NASA-CR-165668] p0135 N82-24648
Current legal and institutional issues in the
commercialization of phosphoric acid fuel cells
- [NASA-CR-167867] p0136 N82-29719
Environmental assessment of the 40 kilowatt fuel
cell system field test operation
- [DOE/NASA/2701-1] p0137 N82-29721
Cell module and fuel conditioner development
- [NASA-CR-165193] p0137 N82-30712
- PHOSPHORUS COMPOUNDS**
NT PHOSPHORIC ACID
- PHOTOCONDUCTORS**
High voltage V-groove solar cell
[NASA-CASE-LEW-13401-2] p0123 N82-24717
- PHOTOCURRENTS**
U RECTIFIC CURRENT
- PHOTOELECTRIC CELLS**
NT PHOTOVOLTAIC CELLS
- PHOTOELECTRICITY**
Operational performance of the
photovoltaic-powered grain mill and water pump
at Tangaye, Upper Volta
[NASA-TM-82767] p0120 N82-19573
- PHOTOELECTRON SPECTROSCOPY**
Application of surface analysis to solve problems
of wear
[NASA-TM-82753] p0099 N82-14519
- PHOTOELECTRONICS**
U PHOTOELECTRICITY
- PHOTOEMISSIVITY**
U ISSIVITY
- PHOTOGRAPHY**
NT FRACTOGRAPHY
NT SATELLITE-BORNE PHOTOGRAPHY
NT SCHLIERN PHOTOGRAPHY
- PHOTORESISTORS**
U PHOTOCONDUCTORS
- PHOTOSENSORS**
U PHOTOELECTRICITY
- PHOTOSPHERE**
Time variability and structure of quiet sun
sources at 6 cm wavelength
p0167 N82-26003
- PHOTOTHERMAL CONVERSION**
Materials science issues encountered during the
development of thermochemical concepts --- in
screening of reactions for solar energy
applications
A82-10021
- PHOTOTHERMOTROPISM**
U ISOTROPY
U DEFLECTION EFFECTS
- PHOTOVOLTAIC CELLS**
NASA preprototype redox storage system for a
photovoltaic stand-alone application
p0127 N82-11774
The effects of controls and controllable and
storage loads on the performance of stand-alone
photovoltaic systems
p0127 N82-45027
International market assessment of stand-alone
photovoltaic power systems for cottage industry
applications
[NASA-CR-165287] p0132 N82-16494
Development of thin wraparound junction silicon
solar cells
[NASA-CR-165570] p0133 N82-18489
Market assessment of photovoltaic power systems
for agricultural applications in Nigeria
[NASA-CR-165511] p0133 N82-18698
Operational performance of the
photovoltaic-powered grain mill and water pump
at Tangaye, Upper Volta
[NASA-TM-82767] p0120 N82-19673
Method of making a high voltage V-groove solar cell
[NASA-CASE-LEW-13401-1] p0124 N82-29709
Development of a large area space solar cell
assembly
[NASA-CP-167929] p0137 N82-30706
High voltage planar multijunction solar cell
[NASA-CASE-LEW-13400-1] p0125 N82-31764
Large area low-cost space solar cell development
[NASA-TM-82902] p0126 N82-32854
Design description of the Tangaye Village
photovoltaic power system
- [NASA-TM-82917] p0126 N82-33828
PHOTOVOLTAIC CONVERSION
Market assessment of photovoltaic power systems
for agricultural applications in Mexico
[NASA-CR-165441] p0128 N82-10506
Market assessment of photovoltaic power systems
for agricultural applications in Morocco
[NASA-CR-165477] p0130 N82-14627
Study of multi-megawatt technology needs for
photovoltaic space power systems. Volume 1:
Executive Summary
[NASA-CR-165323-VOL-1] p0130 N82-14636
Study of multi-megawatt technology needs for
photovoltaic space power systems, volume 2
[NASA-CR-165323-VOL-2] p0130 N82-14637
Market assessment of photovoltaic power systems
for agricultural applications in Nigeria
[NASA-CR-165511] p0133 N82-18698
Socioeconomic impact of photovoltaic power at
Schuchuli, Arizona
[NASA-CR-165551] p0133 N82-19669
Operational performance of the
photovoltaic-powered grain mill and water pump
at Tangaye, Upper Volta
[NASA-TM-82767] p0120 N82-19673
Application of photovoltaic electric power to the
rural education/communication needs of
developing countries
[NASA-CR-167894] p0137 N82-29720
- PHOTOVOLTAIC EFFECT**
Study of the photovoltaic effect in thin film
barium titanate
[NASA-CR-165081] p0131 N82-16479
Market assessment of photovoltaic power systems
for agricultural applications in Colombia
[NASA-CR-165524] p0134 N82-22770
Determination of optimum sunlight concentration
level in space for 3-4 cascade solar cells
[NASA-TM-82899] p0126 N82-32853
- PHUGOID OSCILLATIONS**
U TCH (INCLINATION)
- PIEZOELECTRICITY**
Piezoelectric composite materials
[NASA-CASE-LEW-12582-1] p0054 N82-31450
- PINNACLES**
U AKS (LANDFORMS)
- PIPE FLOW**
Tube entrance heat transfer with deposit formation
[AIAA PAPER 82-0918] p0093 N82-31908
- PIPES (TUBES)**
Resonance tube hazards in oxygen systems
[NASA-TM-82801] p0072 N82-21415
- PISTON ENGINES**
NT DIESEL ENGINES
Preliminary study of temperature measurement
techniques for Stirling engine reciprocating seals
[NASA-CR-165479] p0104 N82-11466
Advanced general aviation comparative
engine/airframe integration study
[NASA-CR-165564] p0025 N82-22263
Exhaust emissions reduction for intermittent
combustion aircraft engines
[NASA-CR-167914] p0029 N82-33392
- PITCH (INCLINATION)**
Variable gain for a wind turbine pitch control
[NASA-TM-82751] p0119 N82-16478
- PITCH ANGLES**
U TCH (INCLINATION)
- PLANAR STRUCTURES**
High voltage planar multijunction solar cell
[NASA-CASE-LEW-13400-1] p0125 N82-31764
- PLANE STRAIN**
Moving singularity creep crack growth analysis
with the $\Delta T/c$ and $C^*/\text{asterisk}/$ integrals
--- path-independent vector and energy rate line
integrals
p0116 N82-40066
- PLANETARY BOUNDARY LAYER**
Effects of condensation and surface motion on the
structure of steady-state fronts
A82-19360
- PLANETARY SATELLITES**
U TURAL SATELLITES
- PLANETARY SPACECRAFT**
U TERPLANETARY SPACECRAFT
- PLANETARY WAVES**
Stratospheric-mesospheric midwinter disturbances -
A summary of observed characteristics
A82-12135

PLANFORMS

NT RECTANGULAR PLANFORMS

PLASMA DESIGN

Magnetohydrodynamics (MHD) Engineering Test Facility (ETF) 200 MWe power plant. Design Requirements Document (DRD) [NASA-TM-82705] p0099 N82-12446

Magnetohydrodynamics (MHD) Engineering Test Facility (ETF) 200 MWe power plant. Conceptual Design Engineering Report (CDER). Volume 1: Executive summary [NASA-CR-165452-VOL-1] p0129 N82-12570

Magnetohydrodynamics (MHD) Engineering Test Facility (ETF) 200 MWe power plant Conceptual Design Engineering Report (CDER) [NASA-CR-165452-VOL-5] p0132 N82-17603

Magnetohydrodynamics (MHD) Engineering Test Facility (ETF) 200 MWe power plant. Conceptual Design Engineering Report (CDER). Volume 2: Engineering, Volume 3: Costs and schedules [NASA-CR-165452-VOL-2] p0136 N82-27837

Comparative analysis of the conceptual design studies of potential early commercial MHD power plants (CSPEC) [NASA-TM-82897] p0123 N82-27838

PLASMA ACCELERATION
Electric thruster research [NASA-CR-165603] p0045 N82-24285

PLASMA CURRENTS
End region and current consolidation effects upon the performance of an MHD channel for the ETF conceptual design --- Engineering Test Facility [AIAA PAPER 82-0325] p0157 A82-17889
Brushfire arc discharge model p0038 N82-14224

PLASMA CYLINDERS
NT CYLINDRICAL PLASMAS

PLASMA DIAGNOSTICS
Field-aligned ion streams in the earth's midnight region p0140 A82-31009

PLASMA ELECTRODES
Impact of uniform electrode current distribution on ETF --- Engineering Test Facility MHD generator [AIAA PAPER 82-0423] p0157 A82-17941

PLASMA INTERACTIONS
NT PLASMA-ELECTROMAGNETIC INTERACTION
Spacecraft Charging Technology, 1980 [NASA-CP-2192] p0037 N82-14213
Agreement for NASA/OAST - USAF/AFSC space interdependency on spacecraft environment interaction p0038 N82-14271
Numerical simulation of plasma insulator interactions in space. Part 1: The self consistent calculation p0039 N82-14272
Numerical simulation of plasma insulator interactions in space. Part 2: Dielectric effects p0039 N82-14273

PLASMA LAYERS
NT PLASMA SHEATHS

PLASMA PHYSICS
Experimental simulation of biased solar arrays with the space plasma [NASA-CR-165485] p0157 N82-10880

PLASMA SHEATHS
Numerical simulation of sheath structure and current-voltage characteristics of a conductor-dielectric disk in a plasma p0040 A82-15904

PLASMA SOUND WAVES
U ASMA WAVES

PLASMA SPRAYING
Improved plasma sprayed MCrAlY coatings for aircraft gas turbine applications p0065 A82-20742
Phase stability in plasma-sprayed, partially stabilized zirconia-yttria p0070 A82-41552
Thermal-barrier-coated turbine blade study [NASA-CP-165351] p0023 N82-10040
Progress in protective coatings for aircraft gas turbines: A Review of NASA sponsored research [NASA-TM-82740] p0058 N82-12216
Thermodynamics and kinetics of the sulfation of porous calcium silicate [NASA-TM-82769] p0048 N82-15119

Effects of arc current on the life in burner rig thermal cycling of plasma sprayed ZrOsub2-Ysub2Osub3 [NASA-TM-82795] p0087 N82-17453
Tailored plasma sprayed MCrAlY coatings for aircraft gas turbine applications [NASA-CR-165234] p0064 N82-19360
Effect of aluminum phosphate additions on composition of three-component plasma-sprayed solid lubricant [NASA-TP-1990] p0059 N82-21298
Fully plasma-sprayed compliant backed ceramic turbine seal [NASA-CASE-LEW-13268-2] p0101 N82-26674
Fully plasma-sprayed compliant backed ceramic turbine seal [NASA-CASE-LEW-13268-1] p0069 N82-29453
Use of fiber like materials to augment the cycle life of thick thermoprotective seal coatings [NASA-TM-82901] p0089 N82-32633
Advanced ceramic coating development for industrial/utility gas turbines [NASA-CR-169852] p0065 N82-33494

PLASMA TEMPERATURE
Additional extensions to the NASCAP computer code, volume 3 [NASA-CR-167857] p0040 N82-26378

PLASMA THEORY
U ASMA PHYSICS

PLASMA TURBULENCE
Turbulence in argon shock waves p0158 A82-11117

PLASMA WAVES
Turbulence in argon shock waves p0158 A82-11117
Standing waves along a microwave generated surface wave plasma p0158 A82-26952

PLASMA-ELECTROMAGNETIC INTERACTION
Standing waves along a microwave generated surface wave plasma p0158 A82-26952

PLASMAS (PHYSICS)
NT ARGON PLASMA
NT CYLINDRICAL PLASMAS
Representation and material charging response of geoplasma environments p0039 N82-14249

PLASMASPHERE
Representation and material charging response of geoplasma environments p0039 N82-14249
Simulation of charging response of SCATHA (P78-2) satellite p0039 N82-14250
SCATHA SSPM charging response: NASCAP predictions compared with data p0037 N82-14251

PLASHOIDS
U ASMAS (PHYSICS)

PLASHONS
A new strategy for efficient solar energy conversion: Parallel-processing with surface plasmons [NASA-TM-82867] p0042 N82-29354

PLASTIC COATINGS
Advanced inorganic separators for alkaline batteries [NASA-CASE-LEW-13171-1] p0124 N82-29708

PLASTIC DEFORMATION
A simplified design procedure for life prediction of rocket thrust chambers [AIAA PAPER 82-1251] p0043 A82-35087
The orthogonal in-situ machining of single and polycrystalline aluminum and copper, volume 1 [NASA-CR-168929] p0076 N82-24361
Plastic deformation and wear process at a surface during unlubricated sliding [NASA-TM-82820] p0102 N82-32735

PLASTIC FILMS
U LYMERIC FILMS

PLASTIC PROPERTIES
NT ELASTOPLASTICITY
NT THERMOPLASTICITY
NT VISCOPLASTICITY
Elastic-plastic finite-element analyses of thermally cycled double-edge wedge specimens [NASA-TP-1973] p0111 N82-20566

PLASTIC YIELDING
U ASTIC DEFORMATION

- ELASTICITY**
U ASTIC PROPERTIES
- ELASTICIZERS**
Advanced inorganic separators for alkaline batteries
[NASA-CASE-LEW-13171-1] p0124 N82-29708
- ELASTICS**
NT CARBON FIBER REINFORCED PLASTICS
NT EPXY RESINS
NT KEVLAR (TRADEMARK)
NT POLYETHYLENES
NT POLYTETRAFLUOROETHYLENE
NT POLYVINYL ALCOHOL
NT TEFLON (TRADEMARK)
NT THERMOPLASTIC FILMS
NT THERMOPLASTIC RESINS
NT THERMOSETTING RESINS
- PLATES (STRUCTURAL MEMBERS)**
NT ELASTIC PLATES
NT END PLATES
NT ORTHOTROPIC PLATES
Finite-element modeling of layered, anisotropic composite plates and shells: A review of recent research
p0113 N82-19563
Cell module and fuel conditioner development
[NASA-CR-165193] p0137 N82-30712
- PLATING**
NT ION PLATING
NT NICKEL PLATE
- PLATINUM**
NT PLATINUM ISOTOPES
Stabilizing platinum in phosphoric acid fuel cells
[NASA-CR-165483] p0130 N82-14620
Stabilizing platinum in phosphoric acid fuel cells
[NASA-CR-165606] p0136 N82-29718
- PLATINUM ALLOYS**
Preparation and evaluation of advanced electrocatalysts for phosphoric acid fuel cells
[NASA-CR-165519] p0129 N82-12573
- PLATINUM ISOTOPES**
Preparation and evaluation of advanced electrocatalysts for phosphoric acid fuel cells
[NASA-CR-165594] p0132 N82-17615
- PLUTONIUM**
NT PLUTONIUM 244
PLUTONIUM ISOTOPES
NT PLUTONIUM 244
PLUTONIUM 244
Evidence for Pu-244 fission tracks in hibonites from Murchison carbonaceous chondrite
p0166 N82-29316
- PLY ORIENTATION**
Boundary layer thermal stresses in angle-ply composite laminates, part 1 --- graphite-epoxy composites
[NASA-CR-165412] p0113 N82-26713
Edge delamination in angle-ply composite laminates, part 5
[NASA-CR-165439] p0114 N82-26717
Boundary-layer effects in composite laminates: Free-edge stress singularities, part 6
[NASA-CR-165440] p0114 N82-26718
- POCKELS EFFECT**
U REFFINGENCE
- POINT DEFECTS**
NT VACANCIES (CRYSTAL DEFECTS)
- POINT MATCHING METHOD (MATHEMATICS)**
U NDARY VALUE PROBLEMS
- POISSON FLOW**
U MINAR FLOW
- POISSON RATIO**
Indentation law for composite laminates
[NASA-CR-165460] p0052 N82-15123
- POLAR ORBITS**
Charging of a large object in low polar Earth orbit --- space shuttle orbiter
p0039 N82-14275
- POLAR REGIONS**
NT ANTARCTIC REGIONS
- POLARIZATION (WAVES)**
NT CROSS POLARIZATION
- POLARIZED ELECTROMAGNETIC RADIATION**
NT POLARIZED LIGHT
- POLARIZED LIGHT**
Veiling glare reduction methods compared for ophthalmic applications
p0143 N82-13289
- POLARIZED RADIATION**
NT POLARIZED LIGHT
- POLICIES**
NT ENERGY POLICY
- POLISHED METALS**
U TAL POLISHING
- POLISHING**
NT METAL POLISHING
- POLLUTION CONTROL**
Advanced technology for controlling pollutant emissions from supersonic cruise aircraft
p0001 N81-18004
Pollution reduction technology program small jet aircraft engines, phase 3
[NASA-CR-165386] p0023 N82-14095
ERBS fuel addendum: Pollution reduction technology program small jet aircraft engines, phase 3
[NASA-CR-165387] p0024 N82-14096
Low NOx heavy fuel combustor concept program. Phase 1: Combustion technology generation
[NASA-CR-165482] p0136 N82-24725
- POLYAMIDE RESINS**
NT KEVLAR (TRADEMARK)
- POLYCRYSTALS**
Tribological properties of sintered polycrystalline and single crystal silicon carbide
[NASA-TM-82829] p0068 N82-24343
The orthogonal in-situ machining of single and polycrystalline aluminum and copper, volume 1
[NASA-CR-168929] p0076 N82-24361
- POLYETHYLENES**
Effect of gamma irradiation on the friction and wear of ultrahigh molecular weight polyethylene
p0062 A82-10674
- POLYGONS**
NT RECTANGLES
- POLYIMIDE RESINS**
Effects of nadic ester concentration and processing on physical and mechanical properties of PMR/Celion 6000 composites
p0051 A82-27440
Kevlar/PMR-15 polyimide matrix composite for a complex shaped DC-9 drag reduction fairing
[AIAA PAPER 82-1047] p0002 A82-37678
High-temperature resins
p0051 A82-42657
Forced torsional properties of PMR composites with varying nadic ester concentrations and processing histories
p0051 A82-45630
Novel improved PMR polyimides
[NASA-TM-82733] p0049 N82-11117
- POLYIMIDES**
NT KAPTON (TRADEMARK)
Novel improved PMR polyimides
[NASA-TM-82733] p0049 N82-11117
Tribological properties at 25 C of seven polyimide films bonded to 440 C high-temperature stainless steel
[NASA-TP-1944] p0067 N82-19373
PMR polyimides-review and update
[NASA-TM-82821] p0068 N82-24342
Tribological evaluation of composite materials made from a partially fluorinated polyimide
[NASA-TM-82832] p0069 N82-29459
- POLYMER CHEMISTRY**
High-temperature resins
p0051 A82-42657
Evaluation of left ventricular assist device pump bladders cast from ion-sputtered polytetrafluoroethylene mandrels
[NASA-CR-167904] p0142 N82-23976
- POLYMER MATRIX COMPOSITES**
Hybridized polymer matrix composite
[NASA-CR-165340] p0051 N82-12139
PMR polyimides-review and update
[NASA-TM-82821] p0068 N82-24342
- POLYMER PHYSICS**
Effects of nadic ester concentration and processing on physical and mechanical properties of PMR/Celion 6000 composites
p0051 A82-27440
- POLYMERIC FILMS**
NT KAPTON (TRADEMARK)
Inexpensive cross-linked polymeric separators made from water-soluble polymers --- for secondary alkaline nickel-zinc and silver-zinc cells
p0048 A82-23778
Tribological properties at 25 C of seven polyimide films bonded to 440 C high-temperature stainless

steel
[NASA-TP-1944] p0067 N82-19373
Texturing polymer surfaces by transfer casting ---
cardiovascular prosthesis
[NASA-CASE-LEW-13120-1] p0068 N82-28440

POLYMERIZATION
PHP polyimides-review and update
[NASA-TM-82821] p0068 N82-24342
Anion permselective membrane
[NASA-CR-167872] p0137 N82-30711

POLYMERS
Anaerobic polymers as high vacuum leak sealants
p0108 N82-21967

POLYPHENYL ETHER
The effect of oxygen concentration on the
boundary-lubricating characteristics of a c
ether and a polyphenyl ether to 300 c
p0070 N82-21699
Improved boundary lubrication with formulated C-
ethers
[NASA-TM-82898] p0067 N82-20313

POLYTETRAFLUOROETHYLENE
Performance of PTFE-lined composite journal bearings
[ASLE PREPRINT 92-AM-1A-1] p0104 N82-37854
Performance of PTFE-lined composite journal bearings
[NASA-TM-82779] p0048 N82-17263
Evaluation of left ventricular assist device pump
bladders cast from ion-sputtered
polytetrafluoroethylene mandrels
[NASA-CR-167904] p0142 N82-23976

POLYURETHANE FOAM
The acoustical structure of highly porous
open-cell foams
p0154 N82-45165

POLYVINYL ALCOHOL
Inexpensive cross-linked polymeric separators made
from water-soluble polymers --- for secondary
alkaline nickel-zinc and silver-zinc cells
p0048 N82-23778
Cross-linked polyvinyl alcohol films as alkaline
battery separators
[NASA-TM-82802] p0054 N82-22327

POROUS MATERIALS
The acoustical structure of highly porous
open-cell foams
p0154 N82-45165
Development of low modulus material for use in
ceramic gas path seal applications
[NASA-CR-165469] p0022 N82-10039
Icing tunnel tests of a composite porous leading
edge for use with a liquid anti-ice system ---
Lewis icing research tunnel
[NASA-CR-164966] p0014 N82-11052
Castable high temperature fracture materials
[NASA-CASE-LEW-13080-2] p0066 N82-11210
Gas turbine ceramic-coated-vane concept with
convection-cooled porous metal core
[NASA-TP-1942] p0016 N82-14090
Composite seal for turbomachinery
[NASA-CASE-LEW-12131-3] p0099 N82-19540

POROUS WALLS
Thermal and flow analysis of a convection,
air-cooled ceramic coated porous metal concept
for turbine vanes
[ASME PAPER 91-HT-48] p0020 N82-10952
Heat transfer in cooled porous region with curved
boundary
p0089 N82-14848

POSITRON ANNIHILATION
Detection of a change in the oxidation state on
aluminum surface using angular correlation of
positron annihilation radiation
A82-30374

POTENTIAL ENERGY
NET ELECTRIC POTENTIAL
NET OPEN CIRCUIT VOLTAGE

POTENTIAL FLOW
Finite volume calculation of three-dimensional
potential flow around a propeller
[AIAA PAPER 82-C957] p0010 N82-31933
Mode propagation in nonuniform circular ducts with
potential flow
[NASA-TM-82766] p0151 N82-14881
Computer program for calculating full potential
transonic, quasi-three-dimensional flow through
a rotating turbomachinery blade row
[NASA-TP-2030] p0005 N82-28247

POWDER (PARTICLES)
NET METAL POWDER

POWDER METALLURGY

The combined effects of Fe and H₂ on the
nitridation of silicon
p0070 N82-42924
Applications of high-temperature powder metal
aluminum alloys to small gas turbines
p0065 N82-48244
Trends in high temperature gas turbine materials
[NASA-TM-82715] p0058 N82-11182
Effect of aluminum phosphate additions on
composition of three-component plasma-sprayed
solid lubricant
[NASA-TP-1990] p0059 N82-21298
Hot isostatically pressed manufacture of high
strength MERL 76 disk and seal shapes
[NASA-CR-165549] p0064 N82-26439

POWDERED METALS
U TAL POWDER

POWER AMPLIFIERS
IMPATT power building blocks for 20 GHz spaceborne
transmit amplifier
[AIAA 82-0498] p0086 N82-23566

POWER CONDITIONING
High power solar array switching regulation
p0043 N82-11736
Component technology for space power systems
[TAP PAPER 82-408] p0043 N82-44750
High-frequency high-voltage high-power DC-to-DC
converters
p0083 N82-12347
Modeling and Analysis of Power Processing Systems
(NAPPS). Volume 1: Technical report
[NASA-CR-165538] p0083 N82-14447
Modeling and Analysis of Power Processing Systems
(NAPPS). Volume 2: Appendices
[NASA-CR-165539] p0145 N82-16748
Power systems
p0001 N82-19146
Power systems
p0001 N82-19146

POWER CONVERTERS
Analysis of transistor and snubber turn-off
dynamics in high-frequency high-voltage
high-power converters
[NASA-CR-168760] p0084 N82-22438
Development of a dual-field heteropolar power
converter
[NASA-CR-165168] p0084 N82-24424

POWER DENSITY (ELECTROMAGNETIC)
U DIANT FLUX DENSITY

POWER EFFICIENCY
Shuttle to GEO propulsion tradeoffs
[AIAA PAPER 82-1245] p0034 N82-35082
On the cause of the flat-spot phenomenon observed
in silicon solar cells at low temperatures and
low intensities --- in deep space environments
p0043 N82-39599
Summary and evaluation of the conceptual design
study of a potential early commercial MHD power
plant (CSPEC)
[NASA-TM-82734] p0119 N82-16481
Straight and chopped DC performance data for a
General Electric 5BY436A1 DC shunt motor with a
General Electric EV-1 controller
[NASA-CR-165507] p0085 N82-24425

POWER GAIN
On a free-electron-laser in a uniform magnetic
field - A solution for arbitrarily strong
electromagnetic radiation fields
A82-28409
Variable gain for a wind turbine pitch control
[NASA-TM-82751] p0119 N82-16478

POWER GENERATORS
U ELECTRIC GENERATORS

POWER PROCESSING SYSTEMS
U WER CONDITIONING

POWER SUPPLY CIRCUITS
A new approach to the minimum weight/loss design
of switching power converters
p0082 N82-16831
Power system design optimization using Lagrange
multiplier techniques
p0085 N82-20743
High voltage DC switchgear development for
multi-kW space power system: Aerospace
technology development of three types of solid
state power controllers for 200-1100VDC with
current ratings of 25, 50, and 80 amperes with
one type utilizing an electromechanical device

- [NASA-CR-165413] p0083 N82-13357
Preliminary study, analysis and design for a power switch for digital engine actuators
[NASA-CR-159559] p0085 N82-23394
- POWERED LIFT AIRCRAFT**
QCSZE over-the-wing engine acoustic data
[NASA-TM-82708] p0020 N82-29324
- PREBURNERS**
Fuel/oxidizer-rich high-pressure preburners --- staged-combustion rocket engine
[NASA-CR-165404] p0073 N82-10245
Testing of fuel/oxidizer-rich, high-pressure preburners
[NASA-CR-165609] p0074 N82-24353
- PRECIPITATION (METEOROLOGY)**
NT FAIN
NT SNOW COVER
Illustration of a new test for detecting a shift in mean in precipitation series
A82-13217
- PRECIPITATION HARDENING**
Comparative thermal fatigue resistance of several oxide dispersion strengthened alloys
p0062 A82-11399
Long-term high-velocity oxidation and hot corrosion testing of several NiCrAl and FeCrAl base oxide dispersion strengthened alloys
p0062 A82-37151
Crystallographic texture in oxide-dispersion-strengthened alloys
p0062 A82-40041
Creep and rupture of an ODS alloy with high stress rupture ductility --- Oxide Dispersion Strengthened
p0065 A82-40335
Creep shear behavior of the oxide dispersion strengthened superalloy MA 6000E
[NASA-TM-82704] p0058 N82-10195
- PREDICTION ANALYSIS TECHNIQUES**
Turbine blade nonlinear structural and life analysis
[AIAA PAPER 82-1056] p0021 A82-34981
Blade loss transient dynamic analysis of turbomachinery
[AIAA PAPER 82-1057] p0030 A82-34982
Prediction of composite hygral behavior made simple
[NASA-TM-82780] p0049 N82-16181
Prediction of sound radiation from different practical jet engine inlets
[NASA-CR-165120] p0153 N82-16810
Application of an airfoil stall flutter computer prediction program to a three-dimensional wing: Prediction versus experiment
[NASA-CR-168586] p0007 N82-19169
The NASA-LeRC wind turbine sound prediction code
p0123 N82-23730
Large displacements and stability analysis of nonlinear propeller structures
[NASA-TM-82850] p0112 N82-31707
- PREDICTIONS**
NT FLCCD PREDICTIONS
NT NOISE PREDICTION
NT NOISE PREDICTION (AIRCRAFT)
NT PERFORMANCE PREDICTION
- PREHEATERS**
U ATING EQUIPMENT
- PREHEATING**
U ATING
- PREMIXED FLAMES**
Time resolved density measurements in premixed turbulent flames
[AIAA PAPER 82-0036] p0056 A82-22033
Flame structure in a swirl stabilized combustor inferred by radiant emission measurements
p0056 A82-28694
Lean-limit extinction of propane/air mixtures in the stagnation-point flow
p0057 A82-28736
Experimental study of the effects of secondary air on the emissions and stability of a lean premixed combustor
[AIAA PAPER 82-1072] p0021 A82-34992
On the opening of premixed Bunsen flame tips
p0057 A82-37570
On stability of premixed flames in stagnation - Point flow
p0057 A82-37574
The premixed flame in uniform straining flow
p0055 A82-43194
- PREMIXING**
Effect of fuel-air-ratio nonuniformity on emissions of nitrogen oxides
[NASA-TP-1798] p0016 N82-13143
- PREPREGS**
On determination of fibre fraction in continuous fibre composite materials
p0051 A82-38133
- PRESSINTERING**
U NTERING
- PRESSURE**
NT HIGH PRESSURE
NT HIGH VACUUM
NT INLET PRESSURE
NT ISOSTATIC PRESSURE
NT LOW PRESSURE
NT LUMINOUS INTENSITY
NT SOUND PRESSURE
NT ULTRAHIGH VACUUM
NT WALL PRESSURE
- PRESSURE CHAMBERS**
Levis, pressurized, fluidized-bed combustion program. Data and calculated results
[NASA-TM-81767] p0124 N82-30704
- PRESSURE EFFECTS**
Effect of vacuum exhaust pressure on the performance of MHD ducts at high B-field
[AIAA PAPER 82-0396] p0157 A82-20292
Effect of vacuum exhaust pressure on the performance of MHD ducts at high D-field
[NASA-TM-82750] p0157 N82-13908
- PRESSURE GRADIENTS**
Real time pressure signal system for a rotary engine
[NASA-CASE-LEW-13622-1] p0019 N82-26294
Comparison of experimental and analytical performance for contoured endwall stators
[NASA-TM-82877] p0019 N82-26299
Experimental study of turbulence in blade end wall corner region
[NASA-CR-169283] p0091 N82-31639
- PRESSURE MEASUREMENT**
Flow through aligned sequential orifice type inlets
[NASA-TP-1967] p0087 N82-20467
- PRESSURE PROBES**
U ESSURE SENSORS
- PRESSURE PULSES**
Pressure pulsations above turbomolecular pumps
p0076 A82-46430
- PRESSURE RATIO**
Performance of single-stage axial-flow transonic compressor with rotor and stator aspect ratios of 1.63 and 1.78, respectively, and with design pressure ratio of 1.82
[NASA-TP-1974] p0017 N82-19222
Performance of single-stage axial-flow transonic compressor with rotor and stator aspect ratios of 1.63 and 1.77, respectively, and with design pressure ratio of 2.05
[NASA-TP-2001] p0018 N82-22269
- PRESSURE REDUCTION**
Thermal and flow analysis of a convection, air-cooled ceramic coated porous metal concept for turbine vanes
[ASME PAPER 81-HT-48] p0020 A82-10952
- PRESSURE SENSORS**
Real time pressure signal system for a rotary engine
[NASA-CASE-LEW-13622-1] p0019 N82-26294
- PRESSURE TRANSDUCERS**
U ESSURE SENSORS
- PRESSURE VESSELS**
NT PREBURNERS
- PRESSURE WAVES**
U ASTIC WAVES
- PRESSURE WELDING**
NT DIFFUSION WELDING
- PRESSURIZING**
NT FUEL TANK PRESSURIZATION
- PRETWISTING**
U ISTING
- PREVENTION**
NT CORROSION PREVENTION
NT FIRE PREVENTION
NT ICE PREVENTION
- PRIMARY BATTERIES**
NT ALKALINE BATTERIES
NT NICKEL ZINC BATTERIES
- PRIVATE AIRCRAFT**
U NERAL AVIATION AIRCRAFT

PROBABILITY

U OPERABILITY THEORY

PROBABILITY THEORY

The application of probabilistic design theory to high temperature low cycle fatigue
[NASA-CR-165408] p0112 N82-14531

PROBLEM SOLVING

NI ITERATIVE SOLUTION

Multiple-grid acceleration of Lax-Wendroff algorithms
[NASA-TM-82843] p0149 N82-22922
Construction of solutions for some nonlinear two-point boundary value problems
[NASA-TM-82937] p0144 N82-30949

PROCEDURES

NT BOUNDARY INTEGRAL METHOD

NT FINITE ELEMENT METHOD

NT FINITE VOLUME METHOD

PROCESS CONTROL (INDUSTRY)

Fuel quality processing study, volume 1
[NASA-CR-165327-VOL-1] p0135 N82-24649
Fuel quality/processing study volume 2:
Appendix. Task 1 literature survey
[NASA-CR-165327-VOL-2] p0135 N82-24650

PROCESS HEAT

Collection and dissemination of thermal energy storage system information for the pulp and paper industry
p0136 N82-24686

PRODUCT DEVELOPMENT

AGT 100 automotive gas turbine system development
[AIAA PAPER 82-1165] p0108 N82-35038
AGT 101 automotive gas turbine system development
[AIAA PAPER 82-1166] p0108 N82-35039
Integrated analysis of engine structures
[NASA-TM-82713] p0111 N82-11491
Solar cell development for the power extension package
[NASA-TM-82685] p0118 N82-11551
Cooled variable-area radial turbine technology program
[NASA-CR-165408] p0024 N82-19221
Local and national impact of aerospace research and technology
[NASA-TM-82775] p0162 N82-20006
Energy efficient engine shroudless, hollow fan blade technology report
[NASA-CR-165586] p0024 N82-21196
Pyrolytic graphite collector development program
[NASA-CR-167909] p0052 N82-29363
Current legal and institutional issues in the commercialization of phosphoric acid fuel cells
[NASA-CR-167867] p0136 N82-29719
Component technology for space power systems
[NASA-TM-82928] p0082 N82-30474

PRODUCTION COSTS

Comparative analysis of the conceptual design studies of potential early commercial MHD power plants (CSPEC)
[NASA-TM-82897] p0123 N82-27838

PRODUCTION ENGINEERING

Technology development for phosphoric acid fuel cell powerplant, phase 2
[NASA-CR-165426] p0131 N82-16482

PRODUCTION METHODS

U PRODUCTION ENGINEERING

PRODUCTS

NT REACTION PRODUCTS

PROGRAM VERIFICATION (COMPUTERS)

Experimental verification of a computational procedure for the design of TWT-refocuser-MDC systems --- Multistage Depressed Collectors
p0082 N82-16128
Spherical roller bearing analysis. SKP computer program SPHERBEAN, Volume 3: Program correlation with full scale hardware tests
[NASA-CR-165205] p0106 N82-20542
Additional extensions to the NASCAP computer code, volume 2
[NASA-CR-167856] p0040 N82-26377
A generalized memory test algorithm
[NASA-TM-82874] p0146 N82-31971

PROGRAMMING LANGUAGES

NT FORTRAN

PROGRAMS

NT NASA PROGRAMS

NT SUPERSONIC CRUISE AIRCRAFT RESEARCH

PROJECTILES

NT HYPERVELOCITY PROJECTILES

PROMINENCES

NT SOLAR PROMINENCES

PROP-FAN TECHNOLOGY

Advanced turboprop testbed systems study, Volume 1: Testbed program objectives and priorities, drive system and aircraft design studies, evaluation and recommendations and wind tunnel test plans
[NASA-CR-167928-VOL-1] p0028 N82-32370
Advanced turboprop testbed systems study
[NASA-CR-167895] p0014 N82-33375

PROPAGATION (EXTENSION)

NT CRACK PROPAGATION

NT FLAME PROPAGATION

PROPAGATION MODES

Analytical and experimental investigation of the propagation and attenuation of sound in extended reaction lined ducts
[AIAA PAPER 81-2014] p0153 N82-10454
Mode propagation in nonuniform circular ducts with potential flow
[NASA-TM-82766] p0151 N82-14881

PROPAGATION VELOCITY

Buoyancy effects on the temperature field in downward spreading flames
p0094 N82-41203

PROPANE

Lean-limit extinction of propane/air mixtures in the stagnation-point flow
p0057 N82-28736
Effects of heat loss, preferential diffusion, and flame stretch on flame-front instability and extinction of propane/air mixtures
p0057 N82-32877
Deposit formation in hydrocarbon fuels
[ASME PAPER 82-GT-49] p0075 N82-35307
Deposit formation in hydrocarbon rocket fuels with an evaluation of a propane heat transfer correlation
[NASA-TM-82911] p0088 N82-26611

PROPELLANT COMBUSTION

NT SOLID PROPELLANT COMBUSTION

PROPELLANT DECOMPOSITION

Deposit formation in hydrocarbon fuels
[ASME PAPER 82-GT-49] p0075 N82-35307

PROPELLANT EVAPORATION

Study of vapor flow into a capillary acquisition device --- for cryogenic rocket propellants
[NASA-CR-167883] p0091 N82-24452

PROPELLANT PROPERTIES

NASA/General Electric broad-specification fuels combustion technology program - Phase I results and status
[AIAA PAPER 82-1089] p0021 N82-35000
Characterization of an Experimental Referee Broadened Specification (EBBS) aviation turbine fuel and ERBS fuel blends
[NASA-TM-82883] p0072 N82-32504

PROPELLANT STORAGE

Cryogenic fluid management experiment
[NASA-CR-165495] p0039 N82-15117

PROPELLANT TANKS

Cryogenic fluid management experiment
[NASA-CR-165495] p0039 N82-15117

PROPELLANT TRANSFER

Cryogenic fluid management experiment
[NASA-CR-165495] p0039 N82-15117

PROPELLANTS

NT CRYOGENIC ROCKET PROPELLANTS

NT ROCKET PROPELLANTS

NT RP-1 ROCKET PROPELLANTS

NT STORABLE PROPELLANTS

PROPELLER BLADES

Tensile buckling of advanced turboprops
[NASA-TM-82896] p0112 N82-31708
Impact of advanced propeller technology on aircraft/mission characteristics of several general aviation aircraft
[NASA-CR-167984] p0009 N82-33347

PROPELLER EFFICIENCY

Performance degradation of propeller/rotor systems due to rime ice accretion
[AIAA PAPER 82-0286] p0014 N82-28322
Evaluation of wind tunnel performance testings of an advanced 45 deg swept 8-bladed propeller at Mach numbers from 0.45 to 0.85
[NASA-CR-3505] p0007 N82-19178

PROPELLER FANS

In-flight acoustic results from an advanced-design

ORIGINAL PAGE IS
OF POOR QUALITY

SUBJECT INDEX

PROTECTIVE COATINGS

propeller at Mach numbers to 0.8
[AIAA PAPER 82-1120] p0021 A82-35017

PROPELLER SLIPSTREAMS

Propeller tip vortex - A possible contributor to
aircraft cabin noise p0152 A82-17603

Fast generation of three-dimensional computational
boundary-conforming periodic grids of C-type ---
for turbine blades and propellers
[NASA-CR-165596] p0009 A82-28253

PROPELLERS

NT PROPELLER FANS

Finite volume calculation of three-dimensional
potential flow around a propeller
[AIAA PAPER 82-0957] p0010 A82-31933

Noise of the SP-3 propeller model at 2 deg and 4
deg angle of attack
[NASA-TM-82738] p0151 A82-16808

A shock wave approach to the noise of supersonic
propellers
[NASA-TM-82752] p0151 A82-16809

Evaluation of wind tunnel performance testings of
an advanced 45 deg swept 8-bladed propeller at
Mach numbers from 0.45 to 0.85
[NASA-CR-3505] p0007 A82-19178

A preliminary comparison between the SR-3
propeller noise in flight and in a wind tunnel
[NASA-TM-82805] p0152 A82-21998

Future propulsion opportunities for commuter
airplanes
[NASA-TM-82880] p0018 A82-24203

Summary and recent results from the NASA advanced
High Speed Propeller Research Program
[NASA-TM-82891] p0001 A82-26219

Propulsion opportunities for future commuter
aircraft
[NASA-TM-82915] p0019 A82-26298

Large displacements and stability analysis of
nonlinear propeller structures
[NASA-TM-82850] p0112 A82-31707

Rough analysis of installation effects on
turbo-prop noise
[NASA-TM-82924] p0152 A82-32082

Propeller flow visualization techniques
p0096 A82-32672

Development of a laser velocimeter for a large
transonic wind tunnel.
p0096 A82-32688

LV measurements with an advanced turbo-prop
p0097 A82-32690

PROPULSION

NT AUXILIARY PROPULSION

NT CHEMICAL PROPULSION

NT ELECTRIC PROPULSION

NT ELECTROMAGNETIC PROPULSION

NT JET PROPULSION

NT LOW THRUST PROPULSION

NT MASS DRIVERS (PAYLOAD DELIVERY)

NT SOLAR ELECTRIC PROPULSION

NT SPACECRAFT PROPULSION

NASA research activities in aeropropulsion
[NASA-TM-82788] p0017 A82-16084

A piecewise linear state variable technique for
real time propulsion system simulation
[NASA-TM-82851] p0018 A82-24201

PROPULSION SYSTEM CONFIGURATIONS

NASA research in aircraft propulsion
[ASME PAPER 82-GT-177] p0022 A82-35389

Computational methods for internal flows with
emphasis on turbomachinery
[NASA-TM-82764] p0003 A82-13113

NASA research in aircraft propulsion
[NASA-TM-82771] p0016 A82-13146

The role of modern control theory in the design of
controls for aircraft turbine engines
[NASA-TM-82815] p0018 A82-22262

Future propulsion opportunities for commuter
airplanes
[NASA-TM-82880] p0018 A82-24203

Integrated propulsion for near-Earth space
missions. Volume 1: Executive summary
[NASA-CR-167889-VOL-1] p0045 A82-33424

Integrated propulsion for near-Earth space
missions. Volume 2: Technical
[NASA-CR-167889-VOL-2] p0046 A82-33425

PROPULSION SYSTEM PERFORMANCE

30-cm mercury ion thruster technology
p0046 A82-15434

Characteristics of the Lorc/Hughes J-series 30-cm
engineering model thruster
p0046 A82-15435

Measuring the spacecraft and environmental
interactions of the 8-cm mercury ion thrusters
on the P80-1 mission
p0043 A82-15438

V/STOL propulsion control technology
[AIAA PAPER 81-2634] p0029 A82-16909

A real time Pegasus propulsion system model for
VSTOL piloted simulation evaluation
[AIAA PAPER 81-2663] p0020 A82-19221

Characterization of advanced electric propulsion
systems
[AIAA PAPER 82-1246] p0071 A82-35083

JT8D high pressure compressor performance
improvement
[NASA-CR-165531] p0104 A82-11467

The ac propulsion system for an electric vehicle,
phase I
[NASA-CR-165480] p0129 A82-13506

Advanced Gas Turbine (AGT) powertrain system
development for automotive applications
[NASA-CR-165175] p0163 A82-16937

Comparison of two parallel/series flow turbofan
propulsion concepts for supersonic V/STOL
[NASA-TM-82743] p0004 A82-18178

NASA/HAA Advanced Rotorcraft Technology and Tilt
Rotor Workshop. Volume 5: Propulsion Session
[NASA-TM-84207] p0015 A82-23241

A piecewise linear state variable technique for
real time propulsion system simulation
[NASA-TM-82851] p0018 A82-24201

Summary and recent results from the NASA advanced
High Speed Propeller Research Program
[NASA-TM-82891] p0001 A82-26219

Propulsion opportunities for future commuter
aircraft
[NASA-TM-82915] p0019 A82-26298

Systems integration
p0042 A82-27371

On the road performance tests of electric test
vehicle for correlation with road load simulator
[NASA-TM-82900] p0127 A82-33829

PROPULSIVE EFFICIENCY

NT PROPELLER EFFICIENCY

Propulsion study for Small Transport Aircraft
Technology (STAT), Appendix B
[NASA-CR-165499-APP-B] p0022 A82-10038

Small passenger car transmission test: Chevrolet
Malibu 200C transmission with lockup
[NASA-CR-165182] p0105 A82-16410

PROSTHETIC DEVICES

Fabrication and wear test of a continuous
fiber/particulate composite total surface hip
replacement
[NASA-TM-81746] p0066 A82-11211

Texturing polymer surfaces by transfer casting ---
cardiovascular prosthesis
[NASA-CASE-LEW-13120-1] p0068 A82-28440

PROTECTION

NT CORROSION PREVENTION

NT ENVIRONMENT PROTECTION

NT THERMAL PROTECTION

PROTECTIVE COATINGS

NT CERAMIC COATINGS

NT REFRACTORY COATINGS

Thermal-barrier-coated turbine blade study
[NASA-CR-165351] p0023 A82-10040

Fabrication and wear test of a continuous
fiber/particulate composite total surface hip
replacement
[NASA-TM-81746] p0066 A82-11211

Progress in protective coatings for aircraft gas
turbines: A Review of NASA sponsored research
[NASA-TM-82740] p0058 A82-12216

Tailored plasma sprayed MCrAlY coatings for
aircraft gas turbine applications
[NASA-CR-165234] p0064 A82-19360

Sputtered silicon nitride coatings for wear
protection
[NASA-TM-82819] p0067 A82-20314

Effect of aluminum phosphate additions on
composition of three-component plasma-sprayed
solid lubricant
[NASA-TP-1990] p0059 A82-21298

Some properties of RF sputtered hafnium nitride
coatings
[NASA-TM-82826] p0067 A82-21331

Covering solid, film cooled surfaces with a duplex thermal barrier coating
[NASA-CASE-LEW-13450-1] p0088 N82-25463

Method of protecting a surface with a silicon-slurry/alumina coatings --- coatings for gas turbine engine blades and vanes
[NASA-CASE-LEW-13343-1] p0068 N82-28441

Advanced ceramic coating development for industrial/utility gas turbines
[NASA-CF-169852] p0065 N82-33494

Overlay metallic-cermet alloy coating systems --- for gas turbine engines
[NASA-CASE-LEW-13639-1] p0070 N82-33522

PULSATING FLOW

U STEADY FLOW

PULSE CHARGING

Effect of positive pulse charge waveforms on the energy efficiency of lead-acid traction cells
[NASA-TM-82709] p0118 N82-10503

PULSE DURATION MODULATION

A PWM transistor inverter for an ac electric vehicle drive

p0085 A82-20744

PULSE MODULATION

NT PULSE DURATION MODULATION

PULSE TIME MODULATION

NT PULSE DURATION MODULATION

PULSE WIDTH MODULATION

U LSE DURATION MODULATION

PULSED LASERS

Optically pumped high-pressure DF-CO2 transfer laser
A82-10193

PULSES

NT PRESSURE PULSES

PUMPS

NT RECIPROCATING PUMPS

NT CENTRIFUGAL PUMPS

NT MOLECULAR PUMPS

NT TURBINE PUMPS

Low-thrust chemical propulsion system pump technology

[NASA-CF-165219] p0105 N82-13427

NASA Redox cell stack shunt current, pumping power, and cell performance tradeoffs

[NASA-TM-82688] p0054 N82-19333

Operational performance of the photovoltaic-powered grain mill and water pump at Tangaye, Upper Volta

[NASA-TM-82767] p0120 N82-19673

Design description of the Tangaye Village photovoltaic power system

[NASA-TM-82917] p0126 N82-33828

PUNCHES

Motion of a rigid punch at the boundary of an orthotropic viscoelastic half-plane

A82-26436

PWM (MODULATION)

U LSE DURATION MODULATION

PYREX (TRADEMARK)

U ROSILLICATE GLASS

PYROGRAPHALLOY

U POSITIVE MATERIALS

U POLYLYTIC GRAPHITE

U FRACTORY MATERIALS

PYROLYTIC GRAPHITE

Ion beam textured graphite electrode plates --- high efficiency electron tube devices

[NASA-CASE-LEW-12919-2] p0050 N82-26386

Pyrolytic graphite collector development program

[NASA-CF-167009] p0052 N82-29363

PYROLYTIC MATERIALS

NT PYROLYTIC GRAPHITE

PYROMETRY

U TEMPERATURE MEASUREMENT

PYROLES

NT INDOLES

Deposit formation in liquid fuels. III - The effect of selected nitrogen compounds on diesel fuel

p0074 A82-23238

P78-2 SATELLITE

U ATHA SATELLITE

QUALITY

NT ENVIRONMENTAL QUALITY

QUALITY CONTROL

Experience with modified aerospace reliability and

quality assurance method for wind turbines
[NASA-TM-82803] p0110 N82-19550

Fuel quality processing study, volume 1
[NASA-CR-165327-VOL-1] p0135 N82-24649

Fuel quality/processing study, volume 2:
Appendix. Task 1 literature survey
[NASA-CR-165327-VOL-2] p0135 N82-24650

QUARRIES

U NES (EXCAVATIONS)

QUARTZ

First results of material charging in the space environment

[NASA-TM-84743] p0081 N82-24431

QUINOLINE

Deposit formation in liquid fuels. III - The effect of selected nitrogen compounds on diesel fuel

p0074 A82-23238

R

RACKS (GEARS)

Optimal tooth numbers for compact standard spur gear sets

[ASME PAPER 81-DET-115] p0103 A82-19335

RADIAL FLOW

Design and development of a ceramic radial turbine for the AGT101

[AIAA PAPER 82-1209] p0109 A82-35480

'Coriolis resonance' within a rotating duct --- flow induced vibrations in centrifugal compressors

p0012 A82-37938

Cooled variable nozzle radial turbine for rotor craft applications

[NASA-CR-165397] p0028 N82-29323

Three dimensional flow measurements in a turbine scroll

[NASA-CR-167920] p0009 N82-32310

RADIANT FLUX DENSITY

NT LUMINOUS INTENSITY

Calculation of guaranteed mean power from wind turbine generators

p0122 N82-23699

RADIANT HEATING

High thermal power density heat transfer --- thermionic converters

[NASA-CASE-LEW-12950-1] p0087 N82-11399

RADIANT INTENSITY

U DIANT FLUX DENSITY

RADIATION ABSORPTION

NT ATMOSPHERIC ATTENUATION

RADIATION DAMAGE

Electron beam induced damage in ITO coated Kapton --- Indium Tin Oxide

p0159 A82-41546

Solar cell development for the power extension package

[NASA-TM-82685] p0118 N82-11551

Effects of processing and dopant on radiation damage removal in silicon solar cells

[NASA-TM-82892] p0042 N82-31443

RADIATION DISTRIBUTION

NT ANTENNA RADIATION PATTERNS

NT DIFFRACTION PATTERNS

RADIATION EFFECTS

NT RADIATION DAMAGE

Effect of gamma irradiation on the friction and wear of ultrahigh molecular weight polyethylene

p0062 A82-10674

NASCAP simulation of laboratory charging tests using multiple electron guns

p0033 A82-18319

Testing of solar cell covers and encapsulants conducted in a simulated space environment

[NASA-CR-165475] p0129 N82-12571

RADIATION HEATING

U DIANT HEATING

RADIATION INTENSITY

U DIANT FLUX DENSITY

RADIATION MEASURING INSTRUMENTS

NT INFRARED DETECTORS

RADIATION PRESSURE

NT LUMINOUS INTENSITY

NT SOUND PRESSURE

RADIATION RESISTANCE

U DIANT TOLERANCE

RADIATION SPECTRA

NT EMISSION SPECTRA

NT INFRARED SPECTRA

Q

- NT RAMAN SPECTRA
 NT STELLAR SPECTRA
 NT ULTRAVIOLET SPECTRA
RADIATION TOLERANCE
 Processing of silicon solar cells by ion
 implantation and laser annealing
 [NASA-CR-165283] p0128 N82-11546
- RADIATIVE HEAT TRANSFER**
 Computer model of catalytic combustion/Stirling
 engine heater head
 [NASA-CR-165378] p0134 N82-22666
 Computations of soot and NO sub x emissions
 from gas turbine combustors
 [NASA-CR-167930] p0139 N82-29777
- RADIATIVE TRANSFER**
 NT RADIATIVE HEAT TRANSFER
 Numerical comparisons of nonlinear convergence
 accelerators p0149 A82-31438
- RADIO ASTRONOMY**
 VLA observations of solar active regions at 6 cm
 wavelength p0167 A82-10156
- RADIO BURSTS**
 NT SOLAR RADIO BURSTS
- RADIO COMMUNICATION**
 NT TIME DIVISION MULTIPLE ACCESS
 Satellite-aided land mobile communications system
 implementation considerations
 [NASA-TM-82861] p0036 N82-25290
- RADIO EMISSION**
 NT SOLAR RADIO BURSTS
 NT SOLAR RADIO EMISSIONS
- RADIO EQUIPMENT**
 NT SPACECRAFT ANTENNAS
 NT TRANSDUCERS
- RADIO FREQUENCIES**
 NT EXTREMELY HIGH FREQUENCIES
 NT HIGH FREQUENCIES
- RADIO FREQUENCY DISCHARGE**
 Standing waves along a microwave generated surface
 wave plasma p0158 A82-26952
 Three-dimensional relativistic field-electron
 interaction in a multicavity high-power
 klystron. Part 2: Working Equations
 [NASA-TP-2008] p0081 N82-23397
- RADIO FREQUENCY INTERFERENCE**
 A review of transhorizon propagation phenomena
 p0079 A82-10679
- RADIO INTERFERENCE**
 U DIO FREQUENCY INTERFERENCE
- RADIO RELAY SYSTEMS**
 NT TIME DIVISION MULTIPLE ACCESS
- RADIO TRANSMISSION**
 NT MICROWAVE TRANSMISSION
 NT TRANSORIZON RADIO PROPAGATION
- RADIO WAVES**
 NT CENTIMETER WAVES
 NT MICROWAVE EMISSION
 NT MILLIMETER WAVES
 NT SOLAR RADIO BURSTS
 NT SOLAR RADIO EMISSIONS
- RADIOACTIVE ISOTOPIES**
 NT RADIUM 224
- RADIOACTIVE WASTES**
 Feasibility of an earth-to-space rail launcher
 system --- emphasizing nuclear waste disposal
 application
 [IAF PAPER 82-46] p0033 A82-44659
- RADIOMETERS**
 NT INFRARED DETECTORS
- RADIOSENSITIVITY**
 U EMISSION TOLERANCE
- RAILGUN ACCELERATORS**
 Characterization of advanced electric propulsion
 systems
 [AIAA PAPER 82-1246] p0071 A82-35083
 Feasibility of an earth-to-space rail launcher
 system --- emphasizing nuclear waste disposal
 application
 [IAF PAPER 82-46] p0033 A82-44659
 Characterization of advanced electric propulsion
 systems
 [NASA-CR-167885] p0045 N82-26381
 Preliminary feasibility assessment for
 Earth-to-space electromagnetic (Railgun) launchers
 [NASA-CR-167886] p0073 A82-29345
- RAIN**
 Adaptive rain fade compensation p0080 A82-27178
- RAINSTORMS**
 NT THUNDERSTORMS
 Effect of heavy rain on aircraft N82-21149
- RAMAN EFFECT**
 U RAN SPECTRA
RAMAN SCATTERING
 U RAN SPECTRA
RAMAN SPECTRA
 Raman study of the improper ferroelectric phase
 transition in iron iodine boracite A82-30297
- RANDOM NOISE**
 A high speed implementation of the random
 decrement algorithm
 [NASA-TM-82853] p0076 N82-22388
- RAPID QUENCHING (METALLURGY)**
 Applications of high-temperature powder metal
 aluminum alloys to small gas turbines
 p0065 A82-48244
- RARE GASES**
 Developing a scalable inert gas ion thruster
 [AIAA PAPER 82-1275] p0047 A82-37713
 Inert gas ion thruster
 [NASA-CR-165521] p0044 N82-21252
- REFRACTION WAVES**
 U ASTIC WAVES
- RASERS**
 U SERS
- RATE METERS**
 U ASURING INSTRUMENTS
- RATES (PER TIME)**
 NT ACOUSTIC VELOCITY
 NT BURNING RATE
 NT CURRENT DENSITY
 NT FLOW VELOCITY
 NT HEAT FLUX
 NT HIGH ACCELERATION
 NT HIGH SPEED
 NT LUMINOUS INTENSITY
 NT MASS FLOW RATE
 NT PLASMA ACCELERATION
 NT PROPAGATION VELOCITY
 NT RADIANT FLUX DENSITY
 NT ROTOR SPEED
 NT STRAIN RATE
 NT SUBSONIC SPEED
 NT SUPERSONIC SPEEDS
 NT TIP SPEED
 NT WIND VELOCITY
- RATIOS**
 NT ASPECT RATIO
 NT FUEL-AIR RATIO
 NT MACH NUMBER
 NT POISSON RATIO
 NT PRESSURE RATIO
 NT REYNOLDS NUMBER
 NT SCALE (RATIO)
 NT SIGNAL TO NOISE RATIOS
 The transmission or scattering of elastic waves by
 an inhomogeneity of simple geometry: A
 comparison of theories
 [NASA-CR-169034] p0079 N82-26526
- RAY TRACING**
 Focal surfaces of offset dual-reflector antenna//
 p0080 A82-36265
- RAYLEIGH SCATTERING**
 Time resolved density measurements in premixed
 turbulent flames
 [AIAA PAPER 82-0036] p0056 A82-22033
- RAYLEIGH-BENARD CONVECTION**
 NT BENARD CELLS
- RAYLEIGH-RITZ METHOD**
 Vibrations of cantilevered shallow cylindrical
 shells of rectangular planform p0115 A82-11298
- REACTION BONDING**
 Oxidation stability of advanced reaction-bonded
 Si3N4 materials
 [ACS PAPER 52-B-80P] p0074 A82-33030
- REACTION CONTROL**
 Mass driver reaction engine characteristics and
 performance in earth orbital transfer missions
 p0046 A82-18199
- REACTION JETS**
 U T FLOW

REACTION KINETICS

Symposium /International/ on Combustion, 18th,
University of Waterloo, Waterloo, Ontario,
Canada, August 17-22, 1980, Proceedings

Investigation into the role of NaCl deposited on
oxide and metal substrates in the initiation of
hot corrosion

[NASA-CR-165029] p0063 N82-13217
Thermodynamics and kinetics of the sulfation of
porous calcium silicate
[NASA-TN-82769] p0048 N82-15119

REACTION PRODUCTS

Quantitative separation of tetralin hydroperoxide
from its decomposition products by high
performance liquid chromatography

p0048 N82-15696
Oxidation and formation of deposit precursors in
hydrocarbon fuels
[NASA-CR-165534] p0073 N82-18402

REACTION RATE

U ACTION KINETICS

REACTION MATERIALS

Materials science issues encountered during the
development of thermochemical concepts --- in
screening of reactions for solar energy
applications

A82-10021

REAL TIME OPERATION

A real time Pegasus propulsion system model for
VSTOL piloted simulation evaluation

[AIAA PAPER 81-2663] p0020 N82-19221
Advancements in real-time engine simulation
technology --- of digital electronic aircraft
engine controls

[AIAA PAPER 82-1075] p0021 N82-34995
Real-time microcomputer simulation for space
Shuttle/Centaur avionics

A real time Pegasus propulsion system model for
VSTOL piloted simulation evaluation

[NASA-TN-82770] p0016 N82-13144
Advancements in real-time engine simulation
technology

[NASA-TN-82825] p0147 N82-22915
A piecewise linear state variable technique for
real time propulsion system simulation

[NASA-TN-82851] p0018 N82-24201
Real time pressure signal system for a rotary engine
[NASA-CASE-LEW-13622-1] p0019 N82-26294

REAL VARIABLES

NT DIFFERENTIAL EQUATIONS

NT FOURIER SERIES

NT HELMHOLTZ VORTICITY EQUATION

NT J INTEGRAL

NT NONLINEAR EQUATIONS

NT NUMERICAL INTEGRATION

NT PERIODIC FUNCTIONS

NT TANGENTS

NT VECTOR ANALYSIS

REARWARD FACING STEPS

U CKWARD FACING STEPS

REB

U LATIVISTIC ELECTRON BEAMS

RECEIVERS

Subsystems design and component development for
the parabolic dish module for solar thermal
power systems

[NASA-CR-168941] p0135 N82-24646

RECEIVING SYSTEMS

U CEIVERS

RECIPROCATING ENGINES

U STION ENGINES

RECIRCULATIVE FLUID FLOW

On the prediction of swirling flowfields found in
axisymmetric combustor geometries

p0029 N82-12120
Flame structure in a swirl stabilized combustor
inferred by radiant emission measurements

p0056 N82-28694
Bluff-body flameholder wakes - A simple numerical
solution

[AIAA PAPER 82-1177] p0093 N82-35043

RECLAMATION

LANDSAT Remote Sensing: Observations of an
Appalachian mountaintop surface coal mining and
reclamation operation --- Kentucky

[E82-17247] p0117 N82-24525

RECRYSTALLIZATION

Recrystallization and grain growth in NiAl

The influence of gamma prime on the
recrystallization of an oxide dispersion
strengthened superalloy - MA-6000E

p0062 N82-47393

RECTANGLES

Surface-tension induced instabilities: Effects of
lateral boundaries

[NASA-CR-165530] p0092 N82-11390

RECTANGULAR BEAMS

Fatigue life prediction in bending from axial

fatigue information

[NASA-CR-165563] p0113 N82-20564

RECTANGULAR PLANFORMS

Vibrations of cantilevered shallow cylindrical

shells of rectangular planform

p0115 N82-11298

RECTIFICATION

NT GEOMETRIC RECTIFICATION (IMAGERY)

RECTIFIERS

NT AVALANCHE DIODES

NT CRYSTAL RECTIFIERS

RECOVERATORS

U GENERATORS

REDOX CELLS

Performance of advanced chromium electrodes for
the NASA Redox Energy Storage System

[NASA-TN-82724] p0118 N82-12574
NASA Redox cell stack shunt current, pumping
power, and cell performance tradeoffs

[NASA-TN-82686] p0054 N82-19333
Performance mapping studies in Redox
flow cells

[NASA-TN-82707] p0120 N82-20668
Improved chromium electrodes for REDOX cells

[NASA-CASE-LEW-13653-1] p0121 N82-22672
NASA Redox system development project status

[NASA-TN-82665] p0123 N82-25637
Requirements for optimization of electrodes and
electrolyte for the iron/chromium Redox flow cell

[NASA-CR-165218] p0136 N82-25640
Anion permselective membrane

[NASA-CR-167872] p0137 N82-30711
Design flexibility of Redox flow systems --- for
energy storage applications

[NASA-TN-82854] p0054 N82-31459
Chemical and electrochemical behavior of the
Cr(3)/Cr(2) half cell in the NASA Redox Energy
Storage System

[NASA-TN-82913] p0055 N82-33463

REDUCTION (CHEMISTRY)

NT DEOXIDIZING

REDUCTION (MATHEMATICS)

U TIMIZATION

REFINING

Fuel quality processing study, volume 1

[NASA-CR-165327-VOL-1] p0135 N82-24649

Fuel quality/processing study, Volume 2:

Appendix. Task 1 literature survey

[NASA-CR-165327-VOL-2] p0135 N82-24650

REFLECTANCE

Environmental effects on solar concentrator mirrors

A82-23394

REFLECTION COEFFICIENT

U FLECTANCE

REFLECTIVITY

U FLECTANCE

REFLECTORS

NT PARABOLIC REFLECTORS

NT SOLAR COLLECTORS

NT SOLAR REFLECTORS

REFRACTION

NT BIREFRINGENCE

REFRACTIVE INDEX

U FRACTIVITY

REFRACTIVITY

Some properties of RF sputtered hafnium nitride

coatings

[NASA-TN-82826] p0067 N82-21331

Pockels-effect cell for gas-flow simulation

[NASA-TP-2007] p0095 N82-23515

REFRACTORY COATINGS

Refractory coatings and method of producing the same

[NASA-CASE-LEW-13169-1] p0060 N82-29415

Refractory coatings

[NASA-CASE-LEW-13169-2] p0061 N82-30371

REFRACTORY MATERIALS

NT CHROMIUM

- NT MOLYBDENUM ALLOYS**
NT NiCBIUM
NT TANTALUM
NT TUNGSTEN
 Trends in high temperature gas turbine materials
 [NASA-TM-82715] p0058 N82-11182
 Castable high temperature refractory materials
 [NASA-CASE-LEW-13780-2] p0066 N82-11210
 MC carbide structures in M(1c3)ar-M247
 [NASA-CP-167892] p0064 N82-30374
- REFRACTORY METAL ALLOYS**
NT MOLYBDENUM ALLOYS
REFRACTORY METALS
NT NiCBIUM
NT NiCBIUM
NT TANTALUM
NT TUNGSTEN
REFRASIL (TRADEMARK)
U LIGCN DIOXIDE
REFRIGERATING
 Magnetic heat pumping
 [NASA-CASE-LEW-12508-3] p0088 N82-24449
REGENERATION (ENGINEERING)
 New features and applications of PRESTO, a
 computer code for the performance of
 regenerative, superheated steam turbine cycles
 [NASA-TP-1954] p0119 N82-16477
REGENERATIVE CYCLES
U GENERATION (ENGINEERING)
REGENERATIVE FUEL CELLS
 Alkaline regenerative fuel cell systems for energy
 storage
 p0042 A82-11706
 Electrochemical energy storage for an orbiting
 space station
 [NASA-CP-165436] p0132 N82-17607
REGENERATORS
 Experimental performance of the regenerator for
 the Chrysler upgraded automotive gas turbine
 engine
 [NASA-TP-82671] p0120 N82-21712
 Magnetic heat pumping
 [NASA-CASE-LEW-12508-3] p0088 N82-24449
- REGIONS**
NT ANTARCTIC REGIONS
REGULATORS
NT CURRENT REGULATORS
NT VOLTAGE REGULATORS
 Analysis and design of a standardized control
 module for switching regulators
 p0083 A82-46388
- REHEATING**
U ATING
REIGNITION
U NITION
REINFORCED MATERIALS
U MPOSITE MATERIALS
REINFORCED PLASTICS
NT GLASS FIBER REINFORCED PLASTICS
REINFORCED SHELLS
 Fabrication and wear test of a continuous
 fiber/particulate composite total surface hip
 replacement
 [NASA-TM-81746] p0066 N82-11211
REINFORCING FIBERS
NT BOFON FIBERS
 Hybridized polymer matrix composite
 [NASA-CP-165340] p0051 N82-12139
- RELATIVISTIC ELECTRON BEAMS**
 Three-dimensional relativistic field-electron
 interaction in a multicavity high-power
 klystron. Part 2: Working Equations
 [NASA-TP-2008] p0081 N82-23397
RELATIVISTIC PARTICLES
NT RELATIVISTIC ELECTRON BEAMS
 Three-dimensional relativistic field-electron
 interaction in a multicavity high-power
 klystron. 1: Basic theory
 [NASA-TP-1992] p0081 N82-22439
- RELAXATION METHOD (MATHEMATICS)**
 Relaxation solution of the full Euler equations
 [NASA-TM-82889] p0149 N82-24859
- RELEASING**
NT FIBER RELEASE
RELIABILITY
NT COMPONENT RELIABILITY
 Experience with modified aerospace reliability and
 quality assurance method for wind turbines
 [NASA-TM-82803] p0110 N82-19550
- RELIABILITY CONTROL**
U ALITY CONTROL
U LIABILITY ENGINEERING
RELIABILITY ENGINEERING
 Design and verification of a multiple fault
 tolerant control system for STS applications
 using computer simulation
 [AIAA 81-2173] p0035 A82-10124
 Liquid oxygen turbopump technology
 [NASA-CR-165487] p0105 N82-11469
- REHEATING**
U LTINS
REMOTE HANDLING
 A remote millivolt multiplexer and amplifier
 module for wind tunnel data acquisition
 p0083 A82-41845
- REMOTE REGIONS**
NT ANTARCTIC REGIONS
RESEARCH
NT MARKET RESEARCH
 Aircraft icing research at NASA
 [NASA-TM-82919] p0013 N82-30297
RESEARCH AND DEVELOPMENT
 Gallium arsenide solar cells-status and prospects
 for use in space
 p0043 A82-11765
 NASA/General Electric broad-specification fuels
 combustion technology program - Phase I results
 and status
 [AIAA PAPER 82-1089] p0021 A82-35000
- RESEARCH FACILITIES**
 The aerospace technology laboratory (a
 perspective, then and now)
 [NASA-TM-82754] p0031 N82-19229
- RESIDENTIAL ENERGY**
 An assessment of alternative fuel cell designs for
 residential and commercial cogeneration
 p0138 A82-24695
- RESIDUAL STRESS**
 Effect of shot peening on surface fatigue life of
 carburized and hardened AISI 9310 spur gears
 [NASA-TP-2047] p0102 N82-32736
- RESIN MATRIX COMPOSITES**
 High-temperature resins
 p0051 A82-42657
 Design, evaluation, and fabrication of low-cost
 composite blades for intermediate-size wind
 turbines
 [NASA-CR-165342] p0133 N82-18693
- RESINS**
NT EPOXY RESINS
NT KEVLAR (TRADEMARK)
NT POLYIMIDE RESINS
NT THERMOPLASTIC FILMS
NT THERMOPLASTIC RESINS
NT THERMOSETTING RESINS
RESISTIVITY
U ECTRICAL RESISTIVITY
RESONANCE
NT RESONANT VIBRATION
 Resonance tube hazards in oxygen systems
 [NASA-TM-82801] p0072 N82-21415
 A review of resonance response in large
 horizontal-axis wind turbines
 p0122 N82-23711
- RESONANCE TESTING**
 In-plane inertial coupling in tuned and severely
 mistuned bladed disks
 [ASHZ PAPER 82-CT-288] p0012 A82-35460
- RESONANT CAVITIES**
U VITY RESONATORS
RESONANT FREQUENCIES
 A 10-kW series resonant converter design,
 transistor characterization, and base-drive
 optimization
 p0086 A82-36927
 A 10kW series resonant converter design,
 transistor characterization, and base-drive
 optimization
 [NASA-CR-165546] p0084 N82-17439
 A review of resonance response in large
 horizontal-axis wind turbines
 p0122 N82-23711
- RESONANT VIBRATION**
 'Coriolis resonance' within a rotating duct ---
 flow induced vibrations in centrifugal compressors
 p0012 A82-37938
- RESONATORS**
NT CAVITY RESONATORS

ORIGINAL PAGE IS
OF POOR QUALITY

RESOURCES

SUBJECT INDEX

- The velocity field near the orifice of a Helmholtz resonator in grazing flow
[NASA-CR-168548] p0153 N82-18994
- RESOURCES**
 NT COAL
 NT EXTRATERRESTRIAL RESOURCES
 NT FOSSIL FUELS
- RESPONDERS**
 U ANSWERS
- RESPONSES**
 NT DYNAMIC RESPONSE
 NT MODAL RESPONSE
 NT TRANSIENT RESPONSE
- RETRIEVERS (DEVICES)**
 Thrust reverser for a long duct fan engine --- for turbofan engines
[NASA-CASE-LXW-13199-1] p0019 N82-26293
- RETROFITTING**
 Retrofit and acceptance test of 30-cm ion thrusters
[NASA-CR-165259] p0044 N82-12133
- REVERSE FIELD PINCH**
 NT CYLINDRICAL PLASMAS
- REVERSED FLOW**
 Comparison of two parallel/series flow turbofan propulsion concepts for supersonic V/STOL
[AIAA PAPER 81-2637] p0020 A82-19214
 Dilution jet behavior in the turn section of a reverse flow combustor
[AIAA PAPER 82-0192] p0021 A82-20291
 Small gas turbine combustor primary zone development
[AIAA PAPER 82-1159] p0103 A82-35036
 Dilution jet behavior in the turn section of a reverse flow combustor
[NASA-TM-82776] p0017 N82-19220
- REYNOLDS EQUATION**
 Basic lubrication equations
[NASA-TM-81693] p0099 N82-16413
- REYNOLDS LAW**
 U REYNOLDS EQUATION
- REYNOLDS NUMBER**
 A new numerical approach for compressible viscous flows
[NASA-CR-168842] p0090 N82-22455
 Turbulent solution of the Navier-Stokes equations for uniform shear flow
[NASA-TM-82975] p0089 N82-32634
- RHEOLOGY**
 Some observations in high pressure rheology of lubricants
[ASME PAPER 81-LUB-17] p0070 A82-18432
 Some observations in high pressure rheology of lubricants
[ASME PAPER 81-LUB-17] p0070 A82-18432
 Traction contact performance evaluation at high speeds
[NASA-CR-165226] p0105 N82-16403
- RICHARDSON-DUSHMAN EQUATION**
 U TEMPERATURE EFFECTS
- RIMS**
 A finite element stress analysis of spur gears including fillet radii and rim thickness effects
[NASA-TM-82965] p0101 N82-28646
 On finite element stress analysis of spur gears
[NASA-CR-167938] p0107 N82-29607
- RISK**
 Automotive Stirling Engine Mod 1 Design Review, volume 1
[NASA-CR-167935] p0164 N82-34311
- ROCKET BOOSTERS**
 U OTHER ROCKET ENGINES
- ROCKET CHAMBERS**
 U ROCKET CHAMBERS
- ROCKET ENGINE CONTROL**
 Mass driver reaction engine characteristics and performance in earth orbital transfer missions
p0046 A82-18199
- ROCKET ENGINE DESIGN**
 Characteristics of the LeRC/Hughes J-series 30-cm engineering model thruster
p0046 A82-15435
- ROCKET ENGINES**
 NT BOOSTER ROCKET ENGINES
 NT ELECTROSTATIC ENGINES
 NT HYDROGEN OXYGEN ENGINES
 NT ION ENGINES
 NT LIQUID PROPELLANT ROCKET ENGINES
 NT MERCURY ION ENGINES
 Development of a simplified procedure for thrust chamber life prediction
- [NASA-CR-165585] p0044 N82-21253
 Characterization of advanced electric propulsion systems
[NASA-CR-167885] p0045 N82-26381
- ROCKET LAUNCHERS**
 Preliminary feasibility assessment for Earth-to-space electromagnetic (Railgun) launchers
[NASA-CR-167886] p0033 N82-29345
- ROCKET LAUNCHING**
 NT ORBITAL LAUNCHING
- ROCKET PROPELLANT TANKS**
 U PROPELLANT TANKS
- ROCKET PROPELLANTS**
 NT CRYOGENIC ROCKET PROPELLANTS
 NT LIQUID FUELS
 NT RP-1 ROCKET PROPELLANTS
 Deposit formation in hydrocarbon rocket fuels with an evaluation of a propane heat transfer correlation
[NASA-TM-82911] p0088 N82-26611
- ROCKET THRUST**
 Primary propulsion/large space system interaction study
[NASA-CR-165277] p0044 N82-18315
- ROCKET VEHICLES**
 NT ATLAS CENTAUR LAUNCH VEHICLE
 NT CENTAUR LAUNCH VEHICLE
 NT MULTISTAGE ROCKET VEHICLES
- ROCKETS**
 NT COAL
- RODS**
 Extended range stress intensity factor expressions for chevron-notched short bar and short rod fracture toughness specimens
p0112 A82-40357
- ROLLER BEARINGS**
 Spherical roller bearing analysis. SKF computer program SPHERBEAN. Volume 1: Analysis
[NASA-CR-165203] p0106 N82-20540
 Spherical roller bearing analysis. SKF computer program SPHERBEAN. Volume 2: User's manual
[NASA-CR-165204] p0106 N82-20541
 Spherical roller bearing analysis. SKF computer program SPHERBEAN. Volume 3: Program correlation with full scale hardware tests
[NASA-CR-165205] p0106 N82-20542
 Development of high-speed rolling-element bearings. A historical and technical perspective
[NASA-TM-82884] p0100 N82-20497
 Bearings: Technology and needs
[NASA-CR-167908] p0106 N82-26679
 Advances in high-speed rolling-element bearings
[NASA-TM-82910] p0101 N82-28644
 High speed cylindrical roller bearing analysis. SKF computer program CYBEAN. Volume 2: User's manual
[NASA-CR-165364] p0146 N82-31968
 Research report: User's manual for computer program AT81Y003 SHABERTH. Steady state and transient thermal analysis of a shaft bearing system including ball, cylindrical and tapered roller bearings
[NASA-CR-165365] p0146 N82-31969
- ROLLERS**
 Design study of a continuously variable roller cone traction CVT for electric vehicles
[NASA-CR-159841] p0105 N82-12445
- ROLLING CONTACT LOADS**
 Regimes of traction in concentrated contact lubrication
[ASME PAPER 81-LUB-16] p0107 A82-18431
 Effect of tangential traction and roughness on crack initiation/propagation during rolling contact
p0103 A82-30022
 On the road performance tests of electric test vehicle for correlation with road load simulator
[NASA-TM-82900] p0127 N82-33829
- ROLLUP SOLAR ARRAYS**
 U LAR ARRAYS
- ROSSBY WAVES**
 U METEOROLOGICAL WAVES
- ROTARY DRIVES**
 U MECHANICAL DRIVES
- ROTARY STABILITY**
 NT GYROSCOPIC STABILITY
 Review of analysis methods for rotating systems with periodic coefficients
p0135 N82-23702

ROTARY WING AIRCRAFT

NT HELICOPTERS

ROTARY WINGS

NT TILTING ROTORS

ROTATING BODIES

NT COMPRESSOR ROTORS

NT FLYWHEELS

NT IMPELLERS

NT ROTATING CYLINDERS

NT ROTATING DISKS

NT ROTORS

NT TILTING ROTORS

NT TURBINE WHEELS

Vibrations of twisted rotating blades

[ASME PAPER 81-DET-127]

p0115 A82-19341

ROTATING CYLINDERS

Research report: User's manual for computer program AT81Y003 SHABFPTH. Steady state and transient thermal analysis of a shaft bearing system including ball, cylindrical and tapered roller bearings

[NASA-CR-165165]

p0146 A82-31969

ROTATING DISKS

In-plane inertial coupling in tuned and nontuned bladed disks

[ASME PAPER 82-GT-208]

p0012 A82-35460

ROTATING ELECTRICAL MACHINES

Preliminary design development of 100 KW rotary power transfer device

[NASA-CR-165431]

p0084 A82-23395

ROTATING FLUIDS

Investigation of rotational transonic flows through ducts using a finite element scheme

[AIAA PAPER 82-1267]

p0012 A82-37711

'Coriolis resonance' within a rotating duct ---

Flow induced vibrations in centrifugal compressors

p0012 A82-37938

ROTATING GENERATORS

NT AC GENERATORS

NT TURBOGENERATORS

ROTATING SHAFTS

NT SHAFTS (MACHINE ELEMENTS)

A digital optical torque meter for high rotational speed applications

[NASA-TM-82914]

p0095 A82-31664

ROTATING VEHICLES

U TAPPING PCDIES

ROTATIONAL FLOW

U WIND FLOW

U ROTICES

ROTOR AERODYNAMICS

Three dimensional turbulent boundary layer development on a fan rotor blade

[AIAA PAPER 82-1007]

p0011 A82-31965

Aerodynamic performance of high turning core turbine vanes in a two-dimensional cascade

[AIAA PAPER 82-1288]

p0005 A82-37716

Study of controlled diffusion stator blading. I. Aerodynamic and mechanical design report

[NASA-CR-165500]

p0024 A82-16081

Numerical analysis and FORTRAN program for the computation of the turbulent wakes of turbomachinery rotor blades, isolated airfoils and cascade of airfoils

[NASA-CR-3509]

p0006 A82-18184

Wind turbine dynamics

[NASA-CR-2105]

p0122 A82-23684

Applications of the DOE/NASA wind turbine engine ring information system

[NASA-CR-165388]

p0027 A82-27316

An experimental investigation of gapwise periodicity and unsteady aerodynamic response in an oscillating cascade. I: Experimental and theoretical results --- turbine blades

[NASA-CR-3513]

p0008 A82-26229

ROTOR BLADES

The three-dimensional boundary layer on a rotating helical blade

[NASA-CR-165168]

p0009 A82-15459

Characteristics of the flow in the annulus-wall region of an axial-flow compressor rotor blade passage

[AIAA PAPER 82-1411]

p0009 A82-17933

Interaction of compressor rotor blade wake with wall boundary layer/vortex in the end-wall region

[ASME PAPER 81-GR/GT-1]

p0010 A82-19301

In-plane inertial coupling in tuned and nontuned bladed disks

[ASME PAPER 82-GT-288]

p0012 A82-35460

Rotor tip clearance effects on overall and blade-element performance of axial-flow

transonic fan stage

[NASA-TP-2049]

p0020 A82-33389

ROTOR BLADES (TURBOMACHINERY)

Effects of vane/blade ratio and spacing on fan noise

[AIAA PAPER 81-2033]

p0029 A82-10457

A study of viscous flow in stator and rotor passages

[ASME PAPER 82-GT-248]

p0011 A82-35427

Thrust modulation methods for a subsonic V/STOL aircraft

[NASA-TM-82747]

p0003 A82-13112

Computational methods for internal flows with emphasis on turbomachinery

[NASA-CR-82764]

p0003 A82-13113

Aluminum blade development for the Mod-OA 200-kilowatt wind turbine

[NASA-TM-82594]

p0119 A82-14633

Study of controlled diffusion stator blading. I. Aerodynamic and mechanical design report

[NASA-CR-165500]

p0024 A82-16081

Numerical analysis and FORTRAN program for the computation of the turbulent wakes of turbomachinery rotor blades, isolated airfoils and cascade of airfoils

[NASA-CR-3509]

p0006 A82-18184

Design, evaluation, and fabrication of low-cost composite blades for intermediate-size wind turbines

[NASA-CR-165342]

p0133 A82-18693

Coupled bending-bending-torsion flutter of a mistuned cascade with nonuniform blades

[NASA-TM-82813]

p0111 A82-21604

Method for predicting impulsive noise generated by wind turbine rotors

[NASA-CR-82794]

p0121 A82-21714

Performance of single-stage axial-flow transonic compressor with rotor and stator aspect ratios of 1.63 and 1.77, respectively, and with design pressure ratio of 2.05

[NASA-TP-2001]

p0018 A82-22269

Evaluation of lightning accommodation systems for wind-driven turbine rotors

[NASA-TM-82784]

p0122 A82-23679

Comparison of upwind and downwind rotor operation of the DOE/NASA 100-kW MOD-0 wind turbine

[NASA-CR-165388]

p0122 A82-23710

Rotor fragment protection program: Statistics on aircraft gas turbine engine rotor failures that occurred in U.S. commercial aviation during 1978

[NASA-CR-165388]

p0027 A82-27316

ROTOR DISKS

U RBINE WHEELS

ROTOR HUBS

U TORS

ROTOR SPEED

Effects of blade loading and rotation on compressor rotor wake in end wall regions

[AIAA PAPER 82-0193]

p0010 A82-22063

ROTORCRAFT AIRCRAFT

NASA/Lewis Research Center Icing Research Program

[NASA-CR-165388]

p0001 A82-21148

Cooled variable nozzle radial turbine for rotorcraft applications

[NASA-CR-165397]

p0028 A82-29314

ROTORS

NT COMPRESSOR ROTORS

NT FLYWHEELS

NT IMPELLERS

NT TILTING ROTORS

NT TURBINE WHEELS

Nonlinear analysis of rotor-bearing systems using component mode synthesis

[ASME PAPER 82-GT-303]

p0104 A82-35468

Effect of seals on rotor systems

[NASA-TM-82786]

p0099 A82-16411

Effect of rotor configuration on guyed tower and foundation designs and estimated costs for intermediate site horizontal axis wind turbines

[NASA-TM-82804]

p0121 A82-22649

Development of a dual-field heteropolar power converter

[NASA-CR-165168]

p0084 A82-24424

Rotor fragment protection program: Statistics on aircraft gas turbine engine rotor failures that occurred in U.S. commercial aviation during 1978

[NASA-CR-165388]

p0027 A82-27316

Engine dynamic analysis with general nonlinear finite element codes. Part 2: Bearing element

implementation overall numerical characteristics
and benchmarking
[NASA-CR-167934] p0028 N82-33390
Theoretical and experimental power from large
horizontal-axis wind turbines
[NASA-TN-82944] p0127 N82-33830

ROUGHNESS
NT SURFACE ROUGHNESS
RF-1 ROCKET PROPELLANTS
NT LIQUID FUELS
Deposit formation in hydrocarbon fuels
[ASME PAPER 82-GT-49] p0075 AF3-35307
Low-thrust Isp sensitivity study
[NASA-CR-165621] p0045 N82-22309

ROBBER
NT ELASTOMERS
RURAL AREAS
Design description of the Tanqaye Village
photovoltaic power system
[NASA-TN-82917] p0126 N82-33820

S

S-N DIAGRAMS
The application of probabilistic design theory to
high temperature low cycle fatigue
[NASA-CR-165488] p0112 N82-14531

SAFETY
Experience with modified aerospace reliability and
quality assurance method for wind turbines
[NASA-TN-82803] p0110 N82-19550

SAFETY FACTORS
Automotive Stirling Engine Mod 1 Design Review,
volume 1
[NASA-CR-167935] p0164 N82-34311

SATELLITE ANTENNAS
30/20 GHz communications satellite multibeam antenna
[AIAA 82-0449] p0079 A82-23486

SATELLITE COMMUNICATION
U AIRCRAFT COMMUNICATION

SATELLITE DESIGN
Advanced 30/20 GHz communication satellites
p0034 A82-12623
Use of charging control guidelines for
geosynchronous satellite design studies
p0037 N82-14263
Design practices for controlling spacecraft
charging interactions
[NASA-TN-82781] p0038 N82-18311

SATELLITE LAUNCHING
U AIRCRAFT LAUNCHING

SATELLITE NETWORKS
Advanced 30/20 GHz communication satellites
p0034 A82-12623
Planning satellite communication services and
spectrum-orbit utilization
[AIAA 82-0526] p0080 A82-23538
Microwave intersatellite links for communications
satellites
p0036 A82-36925

SATELLITE ORBIT CALCULATION
U EIT CALCULATION

SATELLITE ORBITS
NT GEOSYNCHRONOUS ORBITS
NT SOLAR ORBITS
Mass driver reaction engine characteristics and
performance in earth orbital transfer missions
p0046 A82-18199

SATELLITE SOLAR ENERGY CONVERSION
Alkaline regenerative fuel cell systems for energy
storage
p0042 A82-11706
Gallium arsenide solar array subsystem study
[NASA-CR-167869] p0138 N82-32855

SATELLITE SOLAR POWER STATIONS
Component technology for space power systems
[NASA-TN-82928] p0082 N82-30474

SATELLITE SOUNDING
Field-aligned ion streams in the earth's midnight
region
p0140 A82-31009

SATELLITE TRANSMISSION
IMPATT power building blocks for 20 GHz spaceborne
transmit amplifier
[AIAA 82-0498] p0086 A82-23566
Simulation of charging response of SCATHA (P78-2)
satellite
p0039 N82-14250

Satellite-aided land mobile communications system
implementation considerations
[NASA-TN-82861] p0036 N82-25290

SATELLITE-BORNE PHOTOGRAPHY
Dynamics of snow cover in mountain regions of the
Aral Sea basin, studied using satellite
photographs
A82-27462

SATELLITES
NT ARTIFICIAL SATELLITES
NT ATS 5
NT COMMUNICATION SATELLITES
NT NATURAL SATELLITES
NT SCATHA SATELLITE
NT SOLAR POWER SATELLITES
NT SYNCHRONOUS SATELLITES
Environmentally induced discharges on satellites
[NASA-TN-82849] p0038 N82-23261

SCALAR MAGNETIC CHARGE
U NETIC CHARGE DENSITY

SCALE (RATIO)
Universal binding energy relations in metallic
adhesion
[NASA-TN-82706] p0058 N82-11183

SCALE MODELS
Testing of a spacecraft model in a combined
environment simulator
p0033 A82-18310

SCANNERS
NT OPTICAL SCANNERS
SCANNING LASER ACOUSTIC MICROSCOPE (SLAM)
U OUSTIC MICROSCOPES

SCAR PROGRAM
U PERSONIC CRUISE AIRCRAFT RESEARCH

SCARS (GEOLOGY)
U OSION

SCATHA SATELLITE
Validation of the NASCAP model using spaceflight
data
[AIAA PAPER 82-0269] p0038 A82-17872
Representation and material charging response of
geoplasma environments
p0039 N82-14249
Simulation of charging response of SCATHA (P78-2)
satellite
p0039 N82-14250
SCATHA SSPM charging response: NASCAP predictions
compared with data
p0037 N82-14251
Comparison of NASCAP modelling results with lumped
circuit analysis
p0037 N82-14255

SCATTERING
NT ELECTRON SCATTERING
NT LIGHT SCATTERING
NT RAMAN SPECTRA
NT RAYLEIGH SCATTERING
NT TROPOSPHERIC SCATTERING
NT WAVE SCATTERING

SCHEDULES
Magnetohydrodynamics MHD Engineering Test Facility
ETP 200 MWe power plant. Conceptual Design
Engineering Report CDER. Volume 3: Costs and
schedules
[NASA-CR-165452-VOL-3] p0128 N82-10495

SCHEDULING
NT PREDICTION ANALYSIS TECHNIQUES

SCHLIEREN PHOTOGRAPHY
New versions of old flow visualization systems
p0096 N82-32670

SCROTTY EFFECT
U RK FUNCTIONS

SCIENTIFIC SATELLITES
NT ATS 5

SEALS (STOPPERS)
NT HERMETIC SEALS
NT O RING SEALS
Measurement of oil film thickness for application
to elastomeric Stirling engine rod seals
[ASME PAPER 81-LUB-9] p0107 A82-18426
Anaerobic polymers as high vacuum leak sealants
p0108 A82-21967
Development of low modulus material for use in
ceramic gas path seal applications
[NASA-CR-165469] p0022 N82-10039
Preliminary study of temperature measurement
techniques for Stirling engine reciprocating seals
[NASA-CR-165479] p0104 N82-11466

- Modified face seal for positive film stiffness
[NASA-CASE-LEW-12989-1] p0099 N82-12442
- J19D ceramic outer air seal system refinement
program
[NASA-CR-165554] p0106 N82-18603
- Composite seal for turbomachinery
[NASA-CASE-LEW-12131-3] p0099 N82-19540
- Flow through aligned sequential orifice type inlets
[NASA-TP-1967] p0087 N82-20467
- Fully plasma-sprayed compliant backed ceramic
turbine seal
[NASA-CASE-LEW-13268-2] p0101 N82-26674
- Fully plasma-sprayed compliant backed ceramic
turbine seal
[NASA-CASE-LEW-13268-1] p0069 N82-29453
- SEASONAL VARIATIONS**
U ACUAL VARIATIONS
- SECONDARY BATTERIES**
U ORAGE BATTERIES
- SECONDARY EMISSION**
Numerical simulation of plasma insulator
interactions in space. Part 2: Dielectric
effects
p0039 N82-14273
- SECONDARY FLOW**
Experimental study of the effects of secondary air
on the emissions and stability of a lean
premixed combustor
[AIAA PAPER 82-1072] p0021 A82-34992
- SECULAR PERTURBATION**
U NG TERM EFFECTS
- SEDIMENTARY ROCKS**
NT COAL
- SEEDING (INOCULATION)**
U OCULATION
- SELF DEPLOYING SPACE STATIONS**
U ACE STATIONS
- SELF INDUCED VIBRATION**
NT TRANSONIC FLUTTER
- SELF LUBRICATING MATERIALS**
Performance of PTFE-lined composite journal bearings
[ASLE PREPRINT 82-AH-1A-1] p0104 A82-37854
Performance of PTFE-lined composite journal bearings
[NASA-TM-82779] p0048 N82-17263
- SELF LUBRICATION**
Effect of aluminum phosphate additions on
composition of three-component plasma-sprayed
solid lubricant
[NASA-TE-1990] p0059 N82-21298
- SELF REGULATING**
U TOMATIC CONTROL
- SEMICONDUCTOR DEVICES**
NT AVALANCHE DIODES
NT BIPOLAR TRANSISTORS
NT FIELD EFFECT TRANSISTORS
NT METAL OXIDE SEMICONDUCTORS
NT MIS (SEMICONDUCTORS)
NT PHOTOVOLTAIC CELLS
NT TRANSISTORS
Proceedings of the Conference on High-temperature
Electronics
[NASA-TM-84069] p0081 N82-15311
High temperature electronic requirements in
aeropropulsion systems
[E-708] p0081 N82-15313
Component technology for space power systems
[NASA-TM-82928] p0082 N82-30474
- SEMICONDUCTOR DIODES**
NT AVALANCHE DIODES
High-frequency high-voltage high-power DC-to-DC
converters
p0083 N82-12347
- SEMICONDUCTOR JUNCTIONS**
NT P-I-N JUNCTIONS
NT SILICON JUNCTIONS
Fabrication of multijunction high voltage
concentrator solar cells by integrated circuit
technology
p0127 A82-44957
High voltage planar multijunction solar cell
[NASA-CASE-LEW-13400-1] p0125 N82-31764
- SEMICONDUCTORS (MATERIALS)**
NT METAL OXIDE SEMICONDUCTORS
NT MIS (SEMICONDUCTORS)
NT PHOTOCONDUCTORS
Undoped semi-insulating LEC GaAs - A model and a
mechanism --- Liquid Encapsulated Czochralski
p0159 A82-13754
- SENSE ORGANS**
NT EAR
NT EYE (ANATOMY)
- SENSIBILITY**
U NSITIVITY
- SENSING**
U TECTION
- SENSITIVITY**
NT IMPACT RESISTANCE
NT RADIATION TOLERANCE
Sensitivity analysis results of the effects of
various parameters on composite design
p0051 A82-37101
- SEPARATED FLOW**
NT BOUNDARY LAYER SEPARATION
Flow through aligned sequential orifice type inlets
[NASA-TP-1967] p0087 N82-20467
- SEPARATORS**
Inexpensive cross-linked polymeric separators made
from water-soluble polymers --- for secondary
alkaline nickel-zinc and silver-zinc cells
p0048 A82-23778
Development of battery separator composites
[NASA-CR-165508] p0128 N82-11547
Method of making formulated plastic separators for
soluble electrode cells
[NASA-CASE-LEW-12358-2] p0054 N82-21268
Cross-linked polyvinyl alcohol films as alkaline
battery separators
[NASA-TM-82802] p0054 N82-22327
Advanced inorganic separators for alkaline batteries
[NASA-CASE-LEW-13171-1] p0124 N82-29708
- SERIES (MATHEMATICS)**
NT FOURIER SERIES
- SERVICE LIFE**
Effects of ultra-clean and centrifugal filtration
on rolling-element bearing life
[ASME PAPER 81-LUB-35] p0103 A82-18436
Effects of arc current on the life in burner rig
thermal cycling of plasma sprayed ZrOsub2-
Ysub2Osub3
[NASA-TM-82795] p0087 N82-17453
Fracture mechanics criteria for turbine engine hot
section components
[NASA-CR-167896] p0027 N82-25257
Results of chopper-controlled discharge life
cycling studies on lead acid batteries
[NASA-TM-82912] p0124 N82-30700
- SHADOWGRAPH PHOTOGRAPHY**
NT SCHLIEREN PHOTOGRAPHY
- SHAFTS (MACHINE ELEMENTS)**
Failure analysis of a tool steel torque shaft
[NASA-TM-82758] p0058 N82-11184
Research report: User's manual for computer
program AT81y003 SHABERTH. Steady state and
transient thermal analysis of a shaft bearing
system including ball, cylindrical and tapered
roller bearings
[NASA-CR-165365] p0146 N82-31969
- SHALLOW SHELLS**
Vibrations of cantilevered shallow cylindrical
shells of rectangular planform
p0115 A82-11298
- SHAPES**
NT CONVEXITY
Film shape calculations on supercomputers
[NASA-TM-82856] p0100 N82-25519
- SHEAR CREEP**
Motion of a rigid punch at the boundary of an
orthotropic viscoelastic half-plane
A82-26436
- SHEAR FATIGUE**
U EAR STRESS
- SHEAR FLOW**
Alignment of fluid molecules in an EHD contact
[ASLE PREPRINT 81-LC-5C-1] p0107 A82-18407
Turbulent solution of the Navier-Stokes equations
for uniform shear flow
[NASA-TM-82925] p0089 N82-32634
- SHEAR PROPERTIES**
NT SHEAR STRENGTH
Analysis of interface cracks in adhesively bonded
lap shear joints, part 4
[NASA-CR-165438] p0114 N82-26716
- SHEAR STRENGTH**
Creep shear behavior of the oxide dispersion
strengthened superalloy MA 6000E
[NASA-TM-82704] p0058 N82-10195

ORIGINAL PAGE IS
OF POOR QUALITY

SHEAR STRESS

SUBJECT INDEX

Correlation of tensile and shear strengths of metals with their friction properties
[NASA-TM-82928] p0060 N82-24325

SHEAR STRESS
NT OBSIONAL STRESS
Some observations in high pressure rheology of lubricants
[ASME PAPER 81-LUB-17] p0070 A82-18432
Some observations in high pressure rheology of lubricants
[ASME PAPER 81-LUB-17] p0070 A82-18432

SHEARING STRESS
U EAR STRESS

SHEATHS
NT PLASMA SHEATHS

SHELL THEORY
Vibrations of twisted rotating blades
[ASME PAPER 81-DET-127] p0115 A82-19341
Comparison of beam and shell theories for the vibrations of thin turbomachinery blades
[ASME PAPER 82-GT-223] p0115 A82-35408

SHELLS (STRUCTURAL FORMS)
NT CYLINDRICAL SHELLS
NT REINFORCED SHELLS
NT SHALLOW SHELLS
Finite-element modeling of layered, anisotropic composite plates and shells: A review of recent research
p0113 N82-19563

SHIELDING
NT HEAT SHIELDING
NT SPACECRAFT SHIELDING

SHOCK DIFFUSERS
U OCK WAVE ATTENUATION

SHOCK LOADS
Flow visualization of shock-boundary layer interaction
p0096 N82-32675

SHOCK RESISTANCE
NT IMPACT RESISTANCE

SHOCK TUBES
NT SHOCK TUNNELS
Turbulence in argon shock waves
p0158 A82-11117

SHOCK TUNNELS
Flow visualization of shock-boundary layer interaction
p0096 N82-32675

SHOCK WAVE ATTENUATION
CAS22 - FORTRAN program for fast design and analysis of shock-free airfoil cascades using fictitious-gas concept
[NASA-CR-3507] p0006 N82-16044

SHOCK WAVE CONTROL
An example of a solution to transonic equations for shock-free flow about a symmetric profile
A82-26439

SHOCK WAVE GENERATORS
NT SHOCK TUBES
NT SHOCK TUNNELS

SHOCK WAVE INTERACTION
Turbulence in argon shock waves
p0158 A82-11117

SHOCK WAVE PROFILES
Three-dimensional shock structure in a transonic flutter cascade
p0006 A82-37937

SHOCK WAVE PROPAGATION
The development of central peaks in lunar craters
A82-14333
Three-dimensional shock structure in a transonic flutter cascade
p0006 A82-37937

SHOCK WAVES
NT DETONATION WAVES
NT NORMAL SHOCK WAVES
A shock wave approach to the noise of supersonic propellers
[NASA-TM-82752] p0151 N82-16809
Prinque localization requirements for three-dimensional flow visualization of shock waves in diffuse-illumination double-pulse holographic interferometry
[NASA-TP-1868] p0095 N82-22481

SHORT HAUL AIRCRAFT
Propulsion study for Small Transport Aircraft Technology (STAT)
[NASA-CR-165499] p0022 N82-10037

SECRET WAVE RADIATION
NT CENTIMETER WAVES
NT MICROWAVE EMISSION
NT MILLIMETER WAVES

SHOT PEENING
Effect of shot peening on surface fatigue life of carburized and hardened AISI 9310 spur gears
[NASA-TP-2047] p0102 N82-32736

SHROUDED BODIES
U ROUDS

SHROUDS
Composite seal for turbomachinery
[NASA-CASE-LEM-12131-3] p0099 N82-19540
Active clearance control system for a turbomachine
[NASA-CASE-LEM-12938-1] p0020 N82-32366

SHUNTS
U PASSES
U RCUTS

SHUTTLE ORBITERS
U ACE SHUTTLE ORBITERS

SIALON
Effects of heating rate on density, microstructure, and strength of Si3N4-6 wt.% Y2O3 and a beta-prime sialon
[ACS PAPER 42-B-81] p0070 A82-42366

SIGNAL DETECTION
wear optimum delay-line detection filters for serial detection of MSK signals
p0086 A82-43867

SIGNAL DISTORTION
Computer modeling of multiple-channel input signals and intermodulation losses caused by nonlinear traveling wave tube amplifiers
[NASA-TP-1999] p0082 N82-25441

SIGNAL FADEOUT
U GNAL FADING

SIGNAL FADING
Adaptive rain fade compensation
p0080 A82-27178

SIGNAL GENERATORS
Real time pressure signal system for a rotary engine
[NASA-CASE-LEM-13622-1] p0019 N82-26294

SIGNAL MIXING
Impedance conversion using quantum limit nonreciprocity for superconductor-insulator-superconductor mixer compensation
p0159 A82-31276

SIGNAL PROCESSING
A high speed implementation of the random decrement algorithm
[NASA-TM-82853] p0076 N82-22388

SIGNAL RECEPTION
A review of transhorizon propagation phenomena
p0079 A82-10679

SIGNAL TO NOISE RATIOS
Conversion and matched filter approximations for serial minimum-shift keyed modulation
p0080 A82-26713
Near optimum delay-line detection filters for serial detection of MSK signals
p0086 A82-43867

SIGNAL TRANSMISSION
NT FREQUENCY DIVISION MULTIPLE ACCESS
NT MICROWAVE TRANSMISSION
NT SATELLITE TRANSMISSION
NT TRANSHORIZON RADIO PROPAGATION

SIGNALS: RES
NT MAGNETIC SIGNATURES

SILICA
U LICON DIOXIDE

SILICATES
NT CALCIUM SILICATES

SILICON
Fast recovery, high voltage silicon diodes for AC motor controllers
p0086 A82-36926
Nitridation of silicon
[NASA-TM-82722] p0066 N82-15197
Material and processing needs for silicon solar cells in space
p0032 N82-26336
Method of protecting a surface with a silicon-slurry/aluminide coating --- coatings for gas turbine engine blades and vanes
[NASA-CASE-LEM-13343-1] p0068 N82-28441
Development of a large area space solar cell assembly
[NASA-CR-167929] p0137 N82-30706

- Effects of processing and dopant on radiation damage removal in silicon solar cells
[NASA-TM-82892] p0042 N82-31443
- Large area low-cost space solar cell development
[NASA-TM-82902] p0126 N82-32854
- SILICON CARBIDES**
- Strength distributions of SiC ceramics after oxidation and oxidation under load
[ACS PAPER 9-C-80C] p0071 A82-20143
- Acoustic microscopy of silicon carbide materials
p0075 A82-33031
- Progress in ceramic component fabrication technology
[AIAA PAPER 82-1211] p0071 A82-35064
- Net shape fabrication of Alpha Silicon Carbide turbine components
[ASME PAPER 82-GT-216] p0071 A82-35403
- Design and development of a ceramic radial turbine for the AGT101
[AIAA PAPER 82-1209] p0109 A82-35480
- Tensile properties of SiC/aluminum filamentary composites - Thermal degradation effects
p0053 A82-46220
- Ultrasonic velocity for estimating density of structural ceramics
[NASA-TM-82765] p0066 N82-14359
- Surface chemistry and wear behavior of single-crystal silicon carbide sliding against iron at temperatures to 1500 C in vacuum
[NASA-TP-1947] p0067 N82-19374
- Tribological properties of sintered polycrystalline and single crystal silicon carbide
[NASA-TM-82829] p0068 N82-24343
- Occurrence of spherical ceramic debris in indentation and sliding contact
[NASA-TP-2048] p0069 N82-32491
- SILICON COMPOUNDS**
- NT CALCIUM SILICATES
- NT QUARTZ
- NT SILICON CARBIDES
- NT SILICON DIOXIDE
- NT SILICON NITRIDES
- SILICON DIOXIDE**
- NT QUARTZ
- Castable high temperature refractory materials
[NASA-CASE-LEW-13080-2] p0066 N82-11210
- SILICON FILMS**
- Study of the photovoltaic effect in thin film barium titanate
[NASA-CR-165081] p0131 N82-16479
- Development of thin wraparound junction silicon solar cells
[NASA-CR-165570] p0133 N82-18689
- Sputtered silicon nitride coatings for wear protection
[NASA-TM-82819] p0067 N82-20314
- SILICON JUNCTIONS**
- Advances in high output voltage silicon solar cells
p0127 A82-44942
- SILICON NITRIDES**
- Oxidation stability of advanced reaction-bonded Si3N4 materials
[ACS PAPER 52-B-80P] p0074 A82-33030
- Fabrication of turbine components and properties of sintered silicon nitride
[ASME PAPER 82-GT-252] p0071 A82-35431
- Design and development of a ceramic radial turbine for the AGT101
[AIAA PAPER 82-1209] p0109 A82-35480
- Effects of oxidation and oxidation under load on strength distributions of Si3N4
[ACS PAPER 69-E-80] p0071 A82-35871
- Fabrication of sinterable silicon nitride by injection molding
p0071 A82-37015
- Effects of heating rate on density, microstructure, and strength of Si3N4-6 wt.% Y2O3 and a beta-prime sialon
[ACS PAPER 42-B-81] p0070 A82-42366
- The combined effects of Fe and H2 on the nitridation of silicon
p0070 A82-42924
- Nitridation of silicon
[NASA-TM-82722] p0066 N82-15197
- Sputtered silicon nitride coatings for wear protection
[NASA-TM-82819] p0067 N82-20314
- Deposition of reactively ion beam sputtered silicon nitride coatings
[NASA-TM-82942] p0069 N82-30401
- SILICON OXIDES**
- NT QUARTZ
- NT SILICON DIOXIDE
- SILICON RECTIFIERS**
- U YSTAL RECTIFIERS
- SILICON SOLAR CELLS**
- U LAR CELLS
- SILVER OXIDE ZINC BATTERIES**
- U LVER ZINC BATTERIES
- SILVER ZINC BATTERIES**
- Development of battery separator composites
[NASA-CR-165508] p0128 N82-11547
- SIMULATION**
- NT ACOUSTIC SIMULATION
- NT ANALOG SIMULATION
- NT COMPUTERIZED SIMULATION
- NT CONTROL SIMULATION
- NT DIGITAL SIMULATION
- NT ENVIRONMENT SIMULATION
- NT FLIGHT SIMULATION
- NT SPACE ENVIRONMENT SIMULATION
- NT SYSTEMS SIMULATION
- A piecewise linear state variable technique for real time propulsion system simulation
[NASA-TM-82851] p0018 N82-24201
- SIMULATORS**
- NT CONTROL SIMULATION
- NT FLIGHT SIMULATORS
- NT SOLAR SIMULATORS
- Real-time microcomputer simulation for space Shuttle/Centaur avionics
p0033 A82-48245
- SINGLE CRYSTALS**
- Adhesion and friction of single-crystal diamond in contact with transition metals
p0103 A82-18680
- The influence of orientation on the stress rupture properties of nickel-base superalloy single crystals
p0062 A82-47397
- Surface chemistry and wear behavior of single-crystal silicon carbide sliding against iron at temperatures to 1500 C in vacuum
[NASA-TP-1947] p0067 N82-19374
- High purity low dislocation GaAs single crystals
[NASA-CR-165593] p0159 N82-23030
- Tribological properties of sintered polycrystalline and single crystal silicon carbide
[NASA-TM-82829] p0068 N82-24343
- The orthogonal in-situ machining of single and polycrystalline aluminum and copper, volume 1
[NASA-CR-168929] p0076 N82-24361
- SINGULARITY (MATHEMATICS)**
- Moving singularity creep crack growth analysis with the $\Delta T/c$ and $C/asterisk/$ integrals
--- path-independent vector and energy rate line integrals
p0116 A82-40066
- SINTERING**
- Fabrication of turbine components and properties of sintered silicon nitride
[ASME PAPER 82-GT-252] p0071 A82-35431
- Fabrication of sinterable silicon nitride by injection molding
p0071 A82-37015
- Stabilizing platinum in phosphoric acid fuel cells
[NASA-CR-165483] p0130 N82-14628
- Nitridation of silicon
[NASA-TM-82722] p0066 N82-15197
- Tribological properties of sintered polycrystalline and single crystal silicon carbide
[NASA-TM-82829] p0068 N82-24343
- Stabilizing platinum in phosphoric acid fuel cells
[NASA-CR-165606] p0136 N82-29718
- SIZE (DIMENSIONS)**
- The optimal design of involute gear teeth with unequal addenda
[NASA-TM-82866] p0101 N82-28645
- SKY**
- NT NIGHT SKY
- SLIDING**
- Friction and wear of iron in corrosive metal
[NASA-TP-1985] p0058 N82-20291
- SLIDING CONTACT**
- Single pass rub phenomena - Analysis and experiment
[ASME PAPER 81-LUB-55] p0107 A82-18449
- SLIDING FRICTION**
- Effect of gamma irradiation on the friction and wear of ultrahigh molecular weight polyethylene

- Adhesion and friction of single-crystal diamond in contact with transition metals p0062 A82-10674
- Geometrical aspects of the tribological properties of graphite fiber reinforced polyimide composites [NASA-TM-82757] p0103 A82-18680
- Effects of artificially produced defects on film thickness distribution in sliding EHD point contacts [NASA-TM-82732] p0066 N82-13198
- Surface chemistry and wear behavior of single-crystal silicon carbide sliding against iron at temperatures to 1500 C in vacuum [NASA-TP-1947] p0099 N82-16412
- Friction wear and auger analysis of iron implanted with 1.5-MeV nitrogen ions [NASA-TP-1989] p0067 N82-19374
- Surface chemistry, microstructure and friction properties of some ferrous-base metallic glasses at temperatures to 750 C [NASA-TP-2006] p0059 N82-21300
- Tribological characteristics of nitrogen (N+) implanted iron [NASA-TM-82839] p0060 N82-22349
- The dryout region in frictionally heated sliding contacts [NASA-TM-82796] p0069 N82-32491
- Occurrence of spherical ceramic debris in indentation and sliding contact [NASA-TP-2048] p0102 N82-32734
- The influence of surface dents and grooves on traction in sliding EHD point contacts [NASA-TM-82943] p0102 N82-32735
- Elastic deformation and wear process at a surface during unlubricated sliding [NASA-TM-82820] p0103 N82-32737
- Wear mechanism based on adhesion [NASA-TP-2037]
- SLIPSTREAMS**
NT PROPELLER SLIPSTREAMS
- SLOREY PROPELLANTS**
NT LIQUID FUELS
- SNOW COVER**
Dynamics of snow cover in mountain regions of the Aral Sea basin, studied using satellite photographs A82-27462
- SOCIAL FACTORS**
Socioeconomic impact of photovoltaic power at Schuchuli, Arizona [NASA-CR-165551] p0133 N82-19669
- Current legal and institutional issues in the commercialization of phosphoric acid fuel cells [NASA-CR-167867] p0136 N82-29719
- SOCIOLOGY**
NT SOCIAL FACTORS
- SODIUM CHLORIDES**
Investigation into the role of NaCl deposited on oxide and metal substrates in the initiation of hot corrosion [NASA-CR-165029] p0063 N82-13217
- SODIUM COMPOUNDS**
NT SODIUM CHLORIDES
Moderate temperature Na cells. III - Electrochemical and structural studies of CrO.5VO.5S2 and its Na intercalates p0055 A82-15732
- SOFTWARE (COMPUTERS)**
U NEUTER PROGRAMS
- SOILS**
NT LUNAR SOIL
- SOLAR ACTIVITY**
NT SOLAR FLARES
NT SOLAR PROMINENCES
VIA observations of solar active regions at 6 cm wavelength p0167 A82-10156
- SOLAR ARRAYS**
High power solar array switching regulation p0043 A82-11736
- Voltage gradients in solar array cavities as possible breakdown sites in spacecraft-charging-induced discharges p0038 A82-18317
- Component technology for space power systems [IAF PAPER 82-408] p0043 A82-44750
- Experimental simulation of biased solar arrays with the space plasma
- [NASA-CR-165485] p0157 N82-10880
- Voltage gradients in solar array cavities as possible breakdown sites in spacecraft-charging-induced discharges [NASA-TM-82710] p0037 N82-11107
- Solar cell development for the power extension package [NASA-TM-82685] p0118 N82-11551
- Study of multi-megawatt technology needs for photovoltaic space power systems. Volume 1: Executive summary [NASA-CR-165323-VOL-1] p0130 N82-14636
- Large area low-cost space solar cell development [NASA-TM-82902] p0126 N82-32854
- Gallium arsenide solar array subsystem study [NASA-CR-167869] p0138 N82-32855
- SOLAR CELLS**
High- and low-resistivity silicon solar cells p0046 A82-11762
- Gallium arsenide solar cells-status and prospects for use in space p0043 A82-11765
- Multi-junction high voltage concentrator solar cells p0043 A82-11796
- Shuttle to GEO propulsion tradeoffs [AIAA PAPER 82-1245] p0034 A82-35082
- On the cause of the flat-spot phenomenon observed in silicon solar cells at low temperatures and low intensities --- in deep space environments p0043 A82-39599
- Advances in high output voltage silicon solar cells p0127 A82-44942
- Thin foil silicon solar cells with coplanar back contacts p0127 A82-44944
- Fabrication of multi-junction high voltage concentrator solar cells by integrated circuit technology p0127 A82-44957
- On the cause of the flat spot phenomenon observed in silicon solar cells at low temperatures and low intensities p0044 A82-44965
- A theory of the n-i-p silicon solar cell p0128 A82-45055
- Processing of silicon solar cells by ion implantation and laser annealing [NASA-CR-165283] p0128 N82-11546
- Solar cell development for the power extension package [NASA-TM-82685] p0118 N82-11551
- Testing of solar cell covers and encapsulants conducted in a simulated space environment [NASA-CR-165475] p0129 N82-12571
- Study of multi-megawatt technology needs for photovoltaic space power systems. Volume 1: Executive summary [NASA-CR-165323-VOL-1] p0130 N82-14636
- Development of thin wraparound junction silicon solar cells [NASA-CR-165570] p0133 N82-18689
- High purity low dislocation GaAs single crystals [NASA-CR-165593] p0159 N82-23030
- High voltage V-groove solar cell [NASA-CASE-LEW-13401-2] p0123 N82-24717
- Material and processing needs for silicon solar cells in space p0032 N82-26336
- Method of making a high voltage V-groove solar cell [NASA-CASE-LEW-13401-1] p0124 N82-29709
- Development of a large area space solar cell assembly [NASA-CR-167929] p0137 N82-30706
- Effects of processing and dopant on radiation damage removal in silicon solar cells [NASA-TM-82892] p0042 N82-31443
- High voltage planar multi-junction solar cell [NASA-CASE-LEW-13400-1] p0125 N82-31764
- On the cause of the flat-spot phenomenon observed in silicon solar cells at low temperatures and low intensities [NASA-TM-82903] p0126 N82-31777
- Determination of optimum sunlight concentration level in space for 3-4 cascade solar cells [NASA-TM-82899] p0126 N82-32853
- Large area low-cost space solar cell development [NASA-TM-82902] p0126 N82-32854
- SOLAR COLLECTORS**
NT SOLAR REFLECTORS

- Fabrication of multi-junction high voltage concentrator solar cells by integrated circuit technology
p0127 A82-44957
- SOLAR CONVERTERS**
U LAR GENERATORS
SOLAR ELECTRIC PROPULSION
Shuttle to GEO propulsion tradeoffs [AIAA PAPER 82-1245]
p0034 A82-35082
- SOLAR ENERGY**
Study of multi-megawatt technology needs for photovoltaic space power systems. Volume 1: Executive summary [NASA-CR-165323-VOL-1]
p0130 A82-14636
Study of multi-megawatt technology needs for photovoltaic space power systems, volume 2 [NASA-CR-165323-VOL-2]
p0130 A82-14637
NASA Redox system development project status [NASA-TM-82665]
p0123 A82-25637
- SOLAR ENERGY CONVERSION**
Materials science issues encountered during the development of thermochemical concepts --- in screening of reactions for solar energy applications
A82-10021
Market assessment of photovoltaic power systems for agricultural applications in Morocco [NASA-CR-165477]
p0130 A82-14627
Market assessment of photovoltaic power systems for agricultural applications in Nigeria [NASA-CR-165511]
p0133 A82-18698
Operational performance of the photovoltaic-powered grain mill and water pump at Tanqaye, Upper Volta [NASA-TM-82767]
p0120 A82-19673
A new strategy for efficient solar energy conversion: Parallel-processing with surface plasmons [NASA-TM-82867]
p0042 A82-29354
Design description of the Tanqaye Village photovoltaic power system [NASA-TM-82917]
p0126 A82-33828
- SOLAR FLARES**
Magnetic structure of a flaring region producing impulsive microwave and hard X-ray bursts
p0167 A82-27323
- SOLAR GENERATORS**
NT SOLAR CELLS
Socioeconomic impact of photovoltaic power at Schuchuli, Arizona [NASA-CR-165551]
p0133 A82-19669
- SOLAR MAGNETIC FIELD**
VLA observations of solar active regions at 6 cm wavelength
p0167 A82-10156
Time variability and structure of quiet sun sources at 6 cm wavelength
p0167 A82-26003
- SOLAR NOISE**
U LAR RADIO EMISSION
SOLAR POWER GENERATION
U LAR GENERATORS
SOLAR POWER SATELLITES
Direct conversion of light to radio frequency energy --- using photoklystrons for solar power satellites
p0138 A82-11712
Study of multi-megawatt technology needs for photovoltaic space power systems. Volume 1: Executive summary [NASA-CR-165323-VOL-1]
p0130 A82-14636
Study of multi-megawatt technology needs for photovoltaic space power systems, volume 2 [NASA-CR-165323-VOL-2]
p0130 A82-14637
- SOLAR POWER SOURCES**
U LAR GENERATORS
SOLAR PROMINENCES
VLA observations of solar active regions at 6 cm wavelength
p0167 A82-10156
- SOLAR PROPULSION**
NT SOLAR ELECTRIC PROPULSION
SOLAR RADIATION
NT SOLAR RADIO BURSTS
NT SOLAR RADIO EMISSION
NT SOLAR X-RAYS
NT SUNLIGHT
SOLAR RADIO BURSTS
Magnetic structure of a flaring region producing impulsive microwave and hard X-ray bursts
p0167 A82-27323
- SOLAR RADIO EMISSION**
NT SOLAR RADIO BURSTS
VLA observations of solar active regions at 6 cm wavelength
p0167 A82-10156
Time variability and structure of quiet sun sources at 6 cm wavelength
p0167 A82-26003
- SOLAR RADIO WAVES**
U LAR RADIO EMISSION
SOLAR RECEIVERS
U LAR COLLECTORS
SOLAR REFLECTORS
Environmental effects on solar concentrator mirrors
A82-23394
Subsystems design and component development for the parabolic dish module for solar thermal power systems [NASA-CR-168941]
p0135 A82-24646
- SOLAR SIMULATORS**
Development of a large area space solar cell assembly [NASA-CR-167929]
p0137 A82-30706
- SOLAR X-RAYS**
Magnetic structure of a flaring region producing impulsive microwave and hard X-ray bursts
p0167 A82-27323
- SOLENOIDS**
Preliminary study, analysis and design for a power switch for digital engine actuators [NASA-CR-159559]
p0085 A82-23394
- SOLID ELECTRODES**
Moderate temperature Na cells. IV - VS2 and MoS₂/Cl₂ as rechargeable cathodes in molten NaAlCl₄
p0055 A82-15743
- SOLID LUBRICANTS**
Development of CdO-graphite-Ag coatings for gas bearings to 427 C
p0108 A82-27079
Tribological properties at 25 C of seven polyimide films bonded to 400 C high-temperature stainless steel [NASA-TP-1944]
p0067 A82-19373
- SOLID PROPELLANT COMBUSTION**
Symposium /International/ on Combustion, 18th, University of Waterloo, Waterloo, Ontario, Canada, August 17-22, 1980, Proceedings
p0056 A82-28651
- SOLID ROCKET PROPELLANTS**
NT LIQUID FUELS
SOLID ROTATION
U TATING BODIES
SOLID STATE DEVICES
NT AVALANCHE DIODES
NT BIPOLAR TRANSISTORS
NT CRYSTAL RECTIFIERS
NT FIELD EFFECT TRANSISTORS
NT METAL OXIDE SEMICONDUCTORS
NT MIS (SEMICONDUCTORS)
NT PHOTOVOLTAIC CELLS
NT SEMICONDUCTOR DEVICES
NT TRANSISTORS
High voltage DC switchgear development for multi-kW space power system: Aerospace technology development of three types of solid state power controllers for 200-1100VDC with current ratings of 25, 50, and 80 amperes with one type utilizing an electromechanical device [NASA-CR-165413]
p0083 A82-13357
- SOLID STATE PHYSICS**
Ion-beam-induced topography and surface diffusion
p0160 A82-46426
- SOLID SURFACES**
NT CRYSTAL SURFACES
Application of surface analysis to solve problems of wear [NASA-TM-82753]
p0099 A82-14519
- SOLID-SOLID INTERFACES**
Single pass rub phenomena - Analysis and experiment [ASME PAPER 81-LUB-55]
p0107 A82-18449
Adhesion and friction of single-crystal diamond in contact with transition metals
p0103 A82-18680
Analytical and experimental evaluation of biaxial contact stress
p0071 A82-20741

ORIGINAL PAGE IS
OF POOR QUALITY

SUBJECT INDEX

SOLIDIFICATION

Interface cracks in adhesively bounded lap-shear joints

p0116 A82-46109

SOLIDIFICATION

Cauchy integral method for two-dimensional solidification interface shapes

p0089 A82-39899

SOLUTIONS

NT AQUEOUS SOLUTIONS
NT GAS MIXTURES

SONIC FLOW

U ANSONIC FLOW

SONIC SPEED

U OUSTIC VELOCITY

SOOT

Evaluation of fuel injection configurations to control carbon and soot formation in small GT combustors

[AIAA PAPER 82-1175] p0021 A82-35041

Investigation of soot and carbon formation in small gas turbine combustors

[NASA-CR-167853] p0025 N82-22267

Computations of soot and and NO sub x emissions from gas turbine combustors

[NASA-CR-167930] p0139 N82-29777

SORBEENTS

NT ADSORBENTS

SOUND

U OUSTICS

SOUND ABSORPTION

U UND TRANSMISSION

SOUND BARRIER

U OUSTIC VELOCITY

SOUND FIELDS

An iterative finite element-integral technique for predicting sound radiation from turbofan inlets in steady flight

[AIAA PAPER 82-0124] p0030 A82-17796

SOUND MEASUREMENT

U OUSTIC MEASUREMENT

SOUND PRESSURE

Propeller tip vortex - A possible contributor to aircraft cabin noise

p0152 A82-17603

SOUND PROPAGATION

Analytical and experimental investigation of the propagation and attenuation of sound in extended reactive lined ducts

[AIAA PAPER 81-2014] p0153 A82-10454

Methods for the calculation of axial wave numbers in lined ducts with mean flow

p0153 A82-14044

Numerical techniques in linear duct acoustics, 1980-81 update

[NASA-TM-82730] p0151 N82-12890

Verification of an acoustic transmission matrix analysis of sound propagation in a variable area duct without flow

[NASA-TM-82741] p0151 N82-12891

Application of steady state finite element and transient finite difference theory to sound propagation in a variable area duct: A comparison with experiment

[NASA-TM-82678] p0151 N82-15847

Pressure transfer function of a JT15D nozzle due to acoustic and convected entropy fluctuations

[NASA-TM-82842] p0152 N82-22951

SOUND TRANSMISSION

Verification of an acoustic transmission matrix analysis of sound propagation in a variable area duct without flow

[NASA-TM-82741] p0151 N82-12891

SOUND VELOCITY

U OUSTIC VELOCITY

SOUND WAVES

NT AERO DYNAMIC NOISE

NT AIRCRAFT NOISE

NT ENGINE NOISE

NT JET AIRCRAFT NOISE

NT NOISE (SOUND)

Development of a spinning wave heat engine

[NASA-CR-165611] p0028 N82-31328

SOUNDING

NT ATMOSPHERIC SOUNDING

NT IONOSPHERIC SOUNDING

NT SATELLITE SOUNDING

SOUTHERN HEMISPHERE

NT ANTARCTIC REGIONS

SPACE COMMUNICATION

NT SPACECRAFT COMMUNICATION

SPACE ENVIRONMENT

U ROSPACE ENVIRONMENTS

SPACE ENVIRONMENT SIMULATION

Validation of the NASCAP model using spaceflight data

[AIAA PAPER 82-0269] p0038 A82-17872
Testing of a spacecraft model in a combined environment simulator

p0033 A82-18310

NASCAP simulation of laboratory charging tests using multiple electron guns

p0033 A82-18319

Spacecraft Charging Technology, 1980

[NASA-CR-2182] p0037 N82-14213

SPACE INDUSTRIALIZATION

The supply of lunar oxygen to low earth orbit

p0032 A82-35618

SPACE MANUFACTURING

A small scale lunar launcher for early lunar material utilization

p0032 A82-35617

Study of multi-megawatt technology needs for photovoltaic space power systems, volume 2

[NASA-CR-165323-VOL-2] p0130 N82-14637

SPACE PLASMAS

Field-aligned ion streams in the earth's midnight region

p0140 A82-31009

Experimental simulation of biased solar arrays with the space plasma

[NASA-CR-165485] p0157 N82-10880

Agreement for NASA/OAST - USAF/AFSC space interdependency on spacecraft environment interaction

p0038 N82-14271

Design practices for controlling spacecraft charging interactions

[NASA-TM-82781] p0038 N82-18311

SPACE PLATFORMS

Large Space Systems/Propulsion Interactions

[NASA-TM-82904] p0042 N82-27358

SPACE POWER REACTORS

NT SPACE POWER UNIT REACTORS

SPACE POWER UNIT REACTORS

Electrochemical energy storage for an orbiting space station

[NASA-CR-165436] p0132 N82-17607

SPACE SHUTTLE ORBITERS

Space Shuttle Orbiter charging

[AIAA PAPER 82-0119] p0040 A82-17793

Shuttle to GEO propulsion tradeoffs

[AIAA PAPER 82-1245] p0034 A82-35082

Real-time microcomputer simulation for space Shuttle/Centaur avionics

p0033 A82-48245

Charging of a large object in low polar Earth orbit --- space shuttle orbiter

p0039 N82-14275

Cryogenic fluid management experiment

[NASA-CR-165495] p0039 N82-15117

SPACE SHUTTLE PAYLOADS

NT SPACEBORNE EXPERIMENTS

Real-time computer simulation/emulation for verification of multi-fault-tolerant control of Centaur-in-Shuttle

[AIAA 81-2283] p0040 A82-13494

Cryogenic fluid management experiment

[NASA-CR-165495] p0039 N82-15117

The 30/20 GHz flight experiment system, phase 2.

Volume 1: Executive summary p0078 N82-20362

The 30/20 GHz flight experiment system, phase 2.

Volume 2: Experiment system description p0078 N82-20363

[NASA-CR-165409-VOL-2] p0078 N82-20363

The 30/20 GHz flight experiment system, phase 2.

Volume 3: Experiment system requirement document p0078 N82-20364

[NASA-CR-165409-VOL-3] p0078 N82-20364

The 30/20 GHz flight experiment system, phase 2.

Volume 4: Experiment system development plan p0078 N82-20365

[NASA-CR-165409-VOL-4] p0078 N82-20365

SPACE STATIONS

Large Space Systems/Propulsion Interactions

[NASA-TM-82904] p0042 N82-27358

SPACE STORAGE

An experiment to evaluate liquid hydrogen storage in space

A82-20748

- SPACE SYSTEMS ENGINEERING
U ROSPACE ENGINEERING
SPACE TRANSPORTATION
NT SPACE SHUTTLE ORBITERS
NT SPACE TRANSPORTATION SYSTEM
SPACE TRANSPORTATION SYSTEM
NT SPACE SHUTTLE ORBITERS
Design and verification of a multiple fault tolerant control system for STS applications using computer simulation [AIAA 81-2173] p0035 A82-10124
Large Space Systems/Propulsion Interactions [NASA-TN-82904] p0042 N82-27358
Systems integration p0042 N82-27371
- SPACE VEHICLE CONTROL
U ACRRAFT CONTROL
SPACEBORNE EXPERIMENTS
Field-aligned ion streams in the earth's midnight region p0140 A82-31009
Cryogenic fluid management experiment [NASA-CR-165495] p0039 N82-15117
SPACEBORNE PHOTOGRAPHY
NT SATELLITE-BORNE PHOTOGRAPHY
SPACECRAFT ANTENNAS
A new antenna concept for satellite communications [NASA-CR-167924] p0079 N82-31584
SPACECRAFT CHARGING
Numerical simulation of sheath structure and current-voltage characteristics of a conductor-dielectric disk in a plasma p0040 A82-15904
Modification of spacecraft potentials by thermal electron emission on ATS-5 p0040 A82-16194
Space Shuttle Orbiter charging [AIAA PAPER 82-0119] p0040 A82-17793
Validation of the NASCAP model using spaceflight data [AIAA PAPER 82-0269] p0038 A82-17872
Testing of a spacecraft model in a combined environment simulator p0033 A82-18310
Internal breakdown of charged spacecraft dielectrics p0041 A82-18312
Voltage gradients in solar array cavities as possible breakdown sites in spacecraft-charging-induced discharges p0038 A82-18317
'Bootstrap' charging of surfaces composed of multiple materials p0085 A82-18318
NASCAP simulation of laboratory charging tests using multiple electron guns p0033 A82-18319
Differential charging of high-voltage spacecraft - The equilibrium potential of insulated surfaces p0041 A82-35547
Testing of a spacecraft model in a combined environment simulator [NASA-TN-82723] p0037 N82-11106
Voltage gradients in solar array cavities as possible breakdown sites in spacecraft-charging-induced discharges [NASA-TN-82710] p0037 N82-11107
Spacecraft Charging Technology, 1980 [NASA-CP-2182] p0037 N82-14213
Brushfire arc discharge model p0038 N82-14224
Secondary electron emission yields p0038 N82-14226
Oblique-incidence secondary emission from charged dielectrics p0039 N82-14227
Comparison of NASCAP modelling results with lumped circuit analysis p0037 N82-14255
Analytical modeling of satellites in geosynchronous environment p0037 N82-14258
Use of charging control guidelines for geosynchronous satellite design studies p0037 N82-14263
Agreement for NASA/OAST - USAF/AFSC space interdependency on spacecraft environment interaction p0038 N82-14271
- Charging of a large object in low polar Earth orbit --- space shuttle orbiter p0039 N82-14275
Design practices for controlling spacecraft charging interactions [NASA-TN-82781] p0038 N82-18311
Environmentally induced discharges on satellites [NASA-TN-82849] p0038 N82-23261
First results of material charging in the space environment [NASA-TN-84743] p0081 N82-24431
Additional extensions to the NASCAP computer code, volume 1 p0146 N82-25810
Additional extensions to the NASCAP computer code, volume 2 p0040 N82-26377
Additional extensions to the NASCAP computer code, volume 3 [NASA-CR-167857] p0040 N82-26378
- SPACECRAFT COMMUNICATION
Advanced 30/20 GHz communication satellites p0034 A82-12623
Microwave intersatellite links for communications satellites p0036 A82-36925
The 30/20 GHz flight experiment system, phase 2. Volume 1: Executive summary [NASA-CR-165409-VOL-1] p0078 N82-20362
The 30/20 GHz flight experiment system, phase 2. Volume 2: Experiment system description [NASA-CR-165409-VOL-2] p0078 N82-20363
The 30/20 GHz flight experiment system, phase 2. Volume 3: Experiment system requirement document [NASA-CR-165409-VOL-3] p0078 N82-20364
The 30/20 GHz flight experiment system, phase 2. Volume 4: Experiment system development plan [NASA-CR-165409-VOL-4] p0078 N82-20365
A new antenna concept for satellite communications [NASA-CR-167924] p0079 N82-31584
- SPACECRAFT COMPONENTS
Internal breakdown of charged spacecraft dielectrics p0041 A82-18312
Component technology for space power systems [IAF PAPER 82-408] p0043 A82-44750
- SPACECRAFT CONTROL
Design and verification of a multiple fault tolerant control system for STS applications using computer simulation [AIAA 81-2173] p0035 A82-10124
- SPACECRAFT DESIGN
NT SATELLITE DESIGN
Spacecraft Charging Technology, 1980 [NASA-CP-2182] p0037 N82-14213
- SPACECRAFT LAUNCHING
Centaur capabilities for communications satellite launches [AIAA PAPER 82-0558] p0034 A82-36286
- SPACECRAFT MODELS
Testing of a spacecraft model in a combined environment simulator [NASA-TN-82723] p0037 N82-11106
Brushfire arc discharge model p0038 N82-14224
- SPACECRAFT ORBITAL ASSEMBLY
U BITAL ASSEMBLY
SPACECRAFT ORBITS
NT GEOSYNCHRONOUS ORBITS
NT POLAR ORBITS
NT SATELLITE ORBITS
NT TRANSFER ORBITS
Integrated propulsion for near-Earth space missions. Volume 1: Executive summary [NASA-CR-167889-VOL-1] p0045 N82-33424
Integrated propulsion for near-Earth space missions. Volume 2: Technical [NASA-CR-167889-VOL-2] p0046 N82-33425
- SPACECRAFT POWER SUPPLIES
High power solar array switching regulation p0043 A82-11736
High- and low-resistivity silicon solar cells p0046 A82-11762
Gallium arsenide solar cells-status and prospects for use in space p0043 A82-11765
Multijunction high voltage concentrator solar cells p0043 A82-11796
A 10-kW series resonant converter design, transistor characterization, and base-drive

optimization p0086 A82-36927

Component technology for space power systems p0043 A82-44750
[IAF PAPER 82-408]

Processing of silicon solar cells by ion implantation and laser annealing p0128 A82-11546
[NASA-CR-165283]

Overview study of Space Power Technologies for the advanced energetics program --- spacecraft p0132 A82-17606
[NASA-CP-165269]

Design of a 35-kilowatt bipolar nickel-hydrogen battery for low Earth orbit application p0123 A82-24647
[NASA-TM-82844]

SPACECRAFT PROPULSION

NT ELECTROMAGNETIC PROPULSION

NT MASS DRIVERS (PAYLOAD DELIVERFY)

NT SOLAR ELECTRIC PROPULSION

30-cm mercury ion thruster technology p0046 A82-15434

Characteristics of the LeRC/Hughes J-series 30-cm engineering model thruster p0046 A82-15435

Propulsion system options for low-acceleration orbit transfer p0047 A82-35056
[AIAA PAPER 82-1196]

Developing a scalable inert gas ion thruster p0047 A82-37713
[AIAA PAPER 82-1275]

Primary propulsion/large space system interaction study p0044 A82-18315
[NASA-CR-165277]

Large Space Systems/Propulsion Interactions p0042 A82-27358
[NASA-TM-82904]

Research report: User's manual for computer program AT81Y005. PLANETSYS, a computer program for the steady state and transient thermal analysis of a planetary power transmission system p0146 A82-31970
[NASA-CR-165366]

Integrated propulsion for near-Earth space missions. Volume 1: Executive summary p0045 A82-33424
[NASA-CR-167889-VOL-1]

Integrated propulsion for near-Earth space missions. Volume 2: Technical p0046 A82-33425
[NASA-CR-167889-VOL-2]

SPACECRAFT SHIELDING

Secondary electron emission yields p0038 A82-14226

SPACECRAFT TRAJECTORIES

NT MOON-EARTH TRAJECTORIES

SPACECRAFT PAYLOADS

Cryogenic fluid management experiment p0039 A82-15117
[NASA-CR-165495]

SPARWISE BLOWING

NT BLOWING

SPATIAL DISTRIBUTION

Representation and material charging response of geoplasmic environments p0039 A82-14249

SPATIAL ISOTROPY

U ATIAL DISTRIBUTION

SPECIFIC GRAVITY

U NSITY (MASS/VOLUME)

SPECIFIC IMPULSE

Propulsion system options for low-acceleration orbit transfer p0047 A82-35056
[AIAA PAPER 82-1196]

SPECKLE PATTERNS

Digital imaging techniques in experimental stress analysis p0097 A82-34231

Experimental boundary integral equation applications in speckle interferometry p0097 A82-36987

SPECTRA

NT EMISSION SPECTRA

NT INFRARED SPECTRA

NT NOISE SPECTRA

NT RAMAN SPECTRA

NT STELLAR SPECTRA

NT ULTRAVIOLET SPECTRA

SPECTROSCOPIC ANALYSIS

Analysis of infrared emission from thin adsorbates p0056 A82-21431

SPECTROSCOPY

NT AUGER SPECTROSCOPY

NT PHOTOELECTRON SPECTROSCOPY

NT SPECTROSCOPIC ANALYSIS

NT X RAY SPECTROSCOPY

SPECTRUM ANALYSIS

NT MAXIMUM ENTROPY METHOD

SPEED

U LOCITY

SPEED CONTROL

Multiroller traction drive speed reducer: Evaluation for automotive gas turbine engine [NASA-TP-2027] p0101 A82-26678

SPEED INDICATORS

NT DRAG FORCE ANEMOMETERS

NT HOT-FILM ANEMOMETERS

NT HOT-WIRE ANEMOMETERS

NT LASER ANEMOMETERS

SPEED REGULATION

U EED CONTROL

SPHERES

Distorted turbulence in axisymmetric flow p0089 A82-16071

SPIN

NT ELECTRON CAPTURE

SPIN-ORBIT INTERACTIONS

NT ELECTRON CAPTURE

SPIRAL WRAPPING

Mathematical models for the synthesis and optimization of spiral bevel gear tooth surfaces --- for helicopter transmissions p0106 A82-25516
[NASA-CR-3553]

SPRAY CHARACTERISTICS

Atomization and combustion properties of flashing injectors p0092 A82-17880
[AIAA PAPER 82-0300]

Venturi nozzle effects on fuel drop size and nitrogen oxide emissions p0020 A82-31329
[NASA-TP-2028]

SPRAY NOZZLES

Hydrodynamic and aerodynamic breakup of liquid sheets p0087 A82-19494
[NASA-TM-82800]

SPRAYED COATINGS

Improved plasma sprayed HCrAlY coatings for aircraft gas turbine applications p0065 A82-20742

Phase stability in plasma-sprayed, partially stabilized zirconia-yttria p0070 A82-41552

Evaluation of present thermal barrier coatings for potential service in electric utility gas turbines [NASA-CR-165545] p0063 A82-18368

JT9D ceramic outer air seal system refinement program [NASA-CR-165554] p0106 A82-18603

Sputtered silicon nitride coatings for wear protection p0067 A82-20314
[NASA-TM-82819]

SPRAYED PROTECTIVE COATINGS

U OTECTIVE COATINGS

U RAYED COATINGS

SPRAYING

NT PLASMA SPRAYING

SPUR (REACTORS)

U ACE POWER UNIT REACTORS

SPUTTERING

Surface diffusion activation energy determination using ion beam microtexturing p0159 A82-21965

Quasi-liquid states observed on ion beam microtextured surfaces p0159 A82-30335

Sputtered silicon nitride coatings for wear protection [NASA-TM-82819] p0067 A82-20314

Some properties of RF sputtered hafnium nitride coatings [NASA-TM-82826] p0067 A82-21331

Morphological and frictional behavior of sputtered MoS₂ films [NASA-TM-82809] p0076 A82-22387

Ion beam textured graphite electrode plates --- high efficiency electron tube devices [NASA-CASE-LEW-12919-2] p0050 A82-26386

Ion beam sputter deposited diamond like films [NASA-TM-82873] p0069 A82-28445

Refractory coatings and method of producing the same [NASA-CASE-LEW-13169-1] p0060 A82-29415

Deposition of reactively ion beam sputtered silicon nitride coatings [NASA-TM-82942] p0069 A82-30401

Ion beam microtexturing and enhanced surface diffusion [NASA-CR-167948] p0065 A82-31509

SQUEEZE FILMS

Engine dynamic analysis with general nonlinear finite element codes. II - Bearing element implementation, overall numerical characteristics and benchmarking [ASME PAPER 82-GT-292] p0108 N82-35462

STABILITY

NT AERODYNAMIC STABILITY
NT BOUNDARY LAYER STABILITY
NT COMBUSTION STABILITY
NT FLAME STABILITY
NT FLOW STABILITY
NT GYROSCOPIC STABILITY
NT ROTARY STABILITY
NT STORAGE STABILITY
NT THERMAL STABILITY
 Effects of fan inlet temperature disturbances on the stability of a turbofan engine [NASA-TM-82699] p0017 N82-18222

STABILIZATION

Effect of seals on rotor systems [NASA-TM-82786] p0099 N82-16411

STACKING FAULTS

U YSTAL DEFECTS

STACKS

Cell module and fuel conditioner development [NASA-CR-165462] p0130 N82-13511
 NASA Redox cell stack shunt current, pumping power, and cell performance tradeoffs [NASA-TM-82696] p0054 N82-19333
 Cell module and fuel conditioner development [NASA-CP-165193] p0137 N82-30712

STAGNATION FLOW

Lean-limit extinction of propane/air mixtures in the stagnation-point flow p0057 N82-28736
 Effects of heat loss, preferential diffusion, and flame stretch on flame-front instability and extinction of propane/air mixtures p0057 N82-32877
 Two dimensional stagnation point flow of a dusty gas near an oscillating plate p0012 N82-37535
 On stability of premixed flames in stagnation-point flow p0057 N82-37574

STAGNATION POINT

Some aspects of calculating flows about three-dimensional subsonic inlets [NASA-TM-82788] p0004 N82-25213

STAGNATION REGION

U AGNATION POINT

STAINLESS STEELS

Geometrical aspects of the tribological properties of graphite fiber reinforced polyimide composites [NASA-TM-82757] p0066 N82-15198
 Tribological properties at 25 C of seven polyimide films bonded to 440 C high-temperature stainless steel [NASA-TP-1944] p0067 N82-19373
 Sputtered silicon nitride coatings for wear protection [NASA-TM-82819] p0067 N82-20314
 Elastic-plastic finite-element analyses of thermally cycled single-edge wedge specimens [NASA-TP-1982] p0111 N82-20565
 Effect of oxide films on hydrogen permeability of candidate Stirling engine heater head tube alloys [NASA-TM-82824] p0060 N82-24323
 Creep crack-growth: A new path-independent T sub o and computational studies [NASA-CR-168930] p0113 N82-24503
 Plastic deformation and wear process at a surface during unlubricated sliding [NASA-TM-82820] p0102 N82-32735

STANDING WAVES

Standing waves along a microwave generated surface wave plasma p0158 N82-26952
 Verification of an acoustic transmission matrix analysis of sound propagation in a variable area duct without flow [NASA-TM-82741] p0151 N82-12891

STARS

NT ECLIPSING BINARY STARS

STATIC INVERTERS

A PWM transistor inverter for an ac electric vehicle drive p0085 N82-20744

STATIC LOADS

A multi-purpose method for analysis of spur gear tooth loading [NASA-CR-165163] p0104 N82-10401
 Endurance test and evaluation of alkaline water electrolysis cells [NASA-CR-165424] p0130 N82-13508

STATICS

NT ELECTROSTATICS

STATIONS

NT SPACE STATIONS

STATISTICAL ANALYSIS

NT BIVARIATE ANALYSIS

NT MULTIVARIATE STATISTICAL ANALYSIS

NT STATISTICAL TESTS

Durability/life of fiber composites in hydrothermomechanical environments [NASA-TM-82749] p0049 N82-14287
 Applications of the DOE/NASA wind turbine engineering information system p0122 N82-23696
 Rotor fragment protection program: Statistics on aircraft gas turbine engine rotor failures that occurred in U.S. commercial aviation during 1978 [NASA-CR-165388] p0027 N82-27316

STATISTICAL PROBABILITY

U OBABILITY THEORY

STATISTICAL TESTS

Illustration of a new test for detecting a shift in mean in precipitation series N82-13217

STATOR BLADES

A study of viscous flow in stator and rotor passages [ASME PAPER 82-GT-248] p0011 N82-35427
 Analytic investigation of effect of end-wall contouring on stator performance [NASA-TP-1943] p0003 N82-14051
 Performance of single-stage axial-flow transonic compressor with rotor and stator aspect ratios of 1.63 and 1.78, respectively, and with design pressure ratio of 1.82 [NASA-TP-1974] p0017 N82-19222
 Laser anemometer measurements in an annular cascade of core turbine vanes and comparison with theory [NASA-TP-2018] p0004 N82-26234
 Engine dynamic analysis with general nonlinear finite element codes. Part 2: Bearing element implementation overall numerical characteristics and benchmarking [NASA-CR-167944] p0028 N82-33390

STATORS

Analytic investigation of effect of end-wall contouring on stator performance [NASA-TP-1943] p0003 N82-14051
 Cold-air performance of a 15.41-cm-tip-diameter axial-flow power turbine with variable-area stator designed for a 75-kW automotive gas turbine engine [NASA-TM-82644] p0024 N82-21193
 Comparison of experimental and analytical performance for contoured endwall stators [NASA-TM-82877] p0019 N82-26299
 Flow visualization study of the horseshoe vortex in a turbine stator cascade [NASA-TP-1884] p0088 N82-30498
 Small axial turbine stator technology program [NASA-CR-165602] p0028 N82-32367
 Status of laser anemometry in turbomachinery research at the Lewis Research Center p0096 N82-32686

STAYS

U Y WIRES

STEADY FLOW

A finite element formulation of Euler equations for the solution of steady transonic flows [AIAA PAPER 82-0062] p0009 N82-17759
 Application of a finite element algorithm for the solution of steady transonic Euler equations [AIAA PAPER 82-0970] p0010 N82-31239

STEADY STATE

Transient catalytic combustor model [NASA-CR-165324] p0129 N82-13507
 Creep crack-growth: A new path-independent T sub o and computational studies [NASA-CR-168930] p0113 N82-24503
 Research report: User's manual for computer program AT81y003 SHABERTH. Steady state and transient thermal analysis of a shaft bearing

ORIGINAL PAGE IS
OF POOR QUALITY

STEAM

SUBJECT INDEX

- system including ball, cylindrical and tapered roller bearings
[NASA-CR-165365] p0146 N82-31969
- STEAM**
Techniques for enhancing durability and equivalence ratio control in a rich-lean, three-stage ground power gas turbine combustor
[NASA-TM-82922] p0124 N82-29717
- STEAM TURBINES**
New features and applications of PRESTO, a computer code for the performance of regenerative, superheated steam turbine cycles
[NASA-TP-1954] p0119 N82-16477
Assessment of steam-injected gas turbine systems and their potential application
[NASA-TM-82735] p0119 N82-18694
Parametric performance analysis of steam-injected gas turbine with a thermal-energy-converter-lined combustor
[NASA-TM-82736] p0121 N82-23678
- STEELS**
NT STAINLESS STEELS
Failure analysis of a tool steel torque shaft
[NASA-TM-82758] p0058 N82-11184
- STEEP GRADIENT AIRCRAFT**
U STOL AIRCRAFT
- STELLAR ATMOSPHERES**
NT CHEMOSPHERE
- STELLAR FLARES**
NT SOLAR FLARES
- STELLAR MAGNETIC FIELDS**
NT SOLAR MAGNETIC FIELD
- STELLAR MASS EJECTION**
Ultraviolet observations of the 1980 eclipse of the symbiotic star CI Cygni
A82-27331
- STELLAR SPECTRA**
Ultraviolet observations of the 1980 eclipse of the symbiotic star CI Cygni
A82-27331
- STELLAR STRUCTURE**
Time variability and structure of quiet sun sources at 6 cm wavelength
p0167 A82-16003
- STERILIZATION EFFECTS**
NT THERMAL DEGRADATION
- STIFFNESS**
Modified face seal for positive film stiffness
[NASA-CASE-LEW-12989-1] p0099 N82-12442
- STIMULATED EMISSION DEVICES**
NT CARBON DIOXIDE LASERS
NT DP LASERS
NT FREE ELECTRON LASERS
NT MASERS
NT PULSED LASERS
- STIRLING CYCLE**
Characteristic dynamic energy equations for Stirling cycle analysis
p0138 A82-11816
Measurement of oil film thickness for application to elastomeric Stirling engine rod seals
[ASME PAPER 81-LUB-9] p0107 A82-18426
Evaluation of the potential of the Stirling engine for heavy duty application
[NASA-CR-165473] p0128 N82-10505
Preliminary study of temperature measurement techniques for Stirling engine reciprocating seals
[NASA-CR-165479] p0104 N82-11466
Jet impingement heat transfer enhancement for the GEU-3 Stirling engine
[NASA-TM-82727] p0163 N82-11993
Test results and facility description for a 40-kilowatt Stirling engine
[NASA-TM-82620] p0163 N82-13013
Experimental study of an integral catalytic combustor: Heat exchanger for Stirling engines
[NASA-TM-82783] p0119 N82-18691
Computer model of catalytic combustion/Stirling engine heater head
[NASA-CR-165378] p0134 N82-22666
Effect of oxide films on hydrogen permeability of candidate Stirling engine heater head tube alloys
[NASA-TM-82824] p0060 N82-24323
Automotive Stirling engine development program
[NASA-CR-167907] p0164 N82-29235
Evaluation of candidate Stirling engine heater tube alloys at 820 deg and 860 deg C
[NASA-TM-82837] p0061 N82-30372
- Assessment of a 40-kilowatt Stirling engine for underground mining applications
[NASA-TM-82822] p0125 N82-30714
Automotive Stirling Engine Mod 1 Design Review, volume 1
[NASA-CR-167935] p0164 N82-34311
Automotive Stirling Engine Mod 1 Design Review, volume 3 --- engineering drawings
[NASA-CR-167397] p0164 N82-34312
- STOICHIOMETRY**
Stoichiometry-controlled compensation in liquid encapsulated Czochralski GaAs
p0158 A82-17585
Compensation mechanism in liquid encapsulated Czochralski GaAs: Importance of melt stoichiometry
p0086 A82-40403
Effect of melt stoichiometry on twin formation in LEC GaAs --- Liquid Encapsulated Czochralski technique
p0160 A82-45517
- STONY METEORITES**
NT CARBONACEOUS CHONDRITES
- STORABLE PROPELLANTS**
NT AIRCRAFT FUELS
NT RP-1 ROCKET PROPELLANTS
Propulsion system options for low-acceleration orbit transfer
[AIAA PAPER 82-1196] p0047 A82-35056
- STORAGE BATTERIES**
NT LEAD ACID BATTERIES
NT NICKEL CADMIUM BATTERIES
NT NICKEL HYDROGEN BATTERIES
NT NICKEL ZINC BATTERIES
NT SILVER ZINC BATTERIES
NASA preprototype redox storage system for a photovoltaic stand-alone application
p0127 A82-11774
Moderate temperature Na cells, IV - VS2 and NbS2Cl2 as rechargeable cathodes in molten NaAlCl4
p0055 A82-15743
Inexpensive cross-linked polymeric separators made from water-soluble polymers --- for secondary alkaline nickel-zinc and silver-zinc cells
p0048 A82-23778
Chopper-controlled discharge life cycling studies on lead-acid batteries
[NASA-CR-165616] p0134 N82-20661
Requirements for optimization of electrodes and electrolyte for the iron/chromium Redox flow cell
[NASA-CR-165218] p0136 N82-25640
- STORAGE STABILITY**
Deposit formation in liquid fuels, II - The effect of selected compounds on the storage stability of Jet A turbine fuel
p0074 A82-22240
Deposit formation in liquid fuels, I - Effect of coal-derived Lewis bases on storage stability of Jet A turbine fuel
p0074 A82-22241
- STORMS**
NT MAGNETIC STORMS
NT RAINSTORMS
NT THUNDERSTORMS
- STORMS (METEOROLOGY)**
NT RAINSTORMS
NT THUNDERSTORMS
- STRAIN AGING**
U PRECIPITATION HARDENING
- STRAIN DISTRIBUTION**
U RESS CONCENTRATION
- STRAIN ENERGY METHODS**
Moving singularity creep crack growth analysis with the $\Delta T/c$ and $C/asterisk/$ integrals --- path-independent vector and energy rate line integrals
p0116 A82-40066
- STRAIN FATIGUE**
U TIGUE (MATERIALS)
- STRAIN GAGES**
Miniature drag-force anemometer
p0097 A82-40132
- STRAIN RATE**
On finite deformation elasto-plasticity
p0116 A82-45869
Indentation law for composite laminates
[NASA-CR-165460] p0052 N82-15123
- STRAIN SOFTENING**
U PLASTIC DEFORMATION

- STRATA**
 NT SUBSTRATES
STRATIFICATION
 NT INTERCALATION
STRATOSPHERE
 Stratospheric-mesospheric midwinter disturbances -
 A summary of observed characteristics A82-12135
- STREAM FUNCTIONS (FLUIDS)**
 Computational methods for internal flows with
 emphasis on turbomachinery
 [NASA-TM-82764] p0003 N82-13113
- STREAMLINE FLOW**
 U MINAR FLOW
- STREAMLINED BODIES**
 NT PAIRINGS
- STREAMS**
 NT GAS STREAMS
- STRENGTH OF MATERIALS**
 U MECHANICAL PROPERTIES
- STRESS ANALYSIS**
 Turbine blade nonlinear structural and life analysis
 [AIAA PAPER 82-1056] p0021 A82-34981
 A simplified design procedure for life prediction
 of rocket thrust chambers
 [AIAA PAPER 82-1251] p0043 A82-35087
 Effects of oxidation and oxidation under load on
 strength distributions of Si3N4
 [ACS PAPER 69-B-80] p0071 A82-35871
 Experimental boundary integral equation
 applications in speckle interferometry
 p0097 A82-36987
 On the solution of creep induced buckling in
 general structure p0115 A82-39514
 Forced torsional properties of FRP composites with
 varying nadic ester concentrations and
 processing histories p0051 A82-45630
 Boundary-layer effects in composite laminates, I -
 Free-edge stress singularities, II - Free-edge
 stress solutions and basic characteristics p0116 A82-46806
 A multi-purpose method for analysis of spur gear
 tooth loading
 [NASA-CR-165163] p0104 N82-10401
 Elastic-plastic finite-element analyses of
 thermally cycled double-edge wedge specimens
 [NASA-TP-1973] p0111 N82-20566
 Development of a simplified procedure for thrust
 chamber life prediction
 [NASA-CR-165585] p0044 N82-21253
 Tooth profile analysis of circular-cut,
 spiral-bevel gears
 [NASA-TM-82840] p0101 N82-26681
 Boundary layer thermal stresses in angle-ply
 composite laminates, part 1 --- graphite-epoxy
 composites p0113 N82-26713
 Analysis of cracks emanating from a circular hole
 in unidirectional fiber reinforced composites,
 part 2 p0114 N82-26714
 Interlaminar crack growth in fiber reinforced
 composites during fatigue, part 3 p0114 N82-26715
 Analysis of interface cracks in adhesively bonded
 lap shear joints, part 4 p0114 N82-26716
 Edge delamination in angle-ply composite
 laminates, part 5 p0114 N82-26717
 Boundary-layer effects in composite laminates:
 Free-edge stress singularities, part 6 p0114 N82-26718
 [NASA-CR-165440]
 The optimal design of involute gear teeth with
 unequal addenda p0101 N82-28645
 [NASA-TM-82866]
 A finite element stress analysis of spur gears
 including fillet radii and rim thickness effects
 [NASA-TM-82965] p0101 N82-28646
 On finite element stress analysis of spur gears
 [NASA-CR-167938] p0107 N82-29607
 Environmental and High-Strain Rate effects on
 composites for engine applications
 [NASA-TM-82982] p0051 N82-31449
- STRESS CALCULATIONS**
 U BESS ANALYSIS
- STRESS CONCENTRATION**
 Elevated temperature fatigue testing of metals
 p0058 N82-13281
 A preliminary study of crack initiation and growth
 at stress concentration sites
 [NASA-CR-169358] p0115 N82-33738
- STRESS CORROSION**
 NT STRESS CORROSION CRACKING
STRESS CORROSION CRACKING
 Fatigue tests with a corrosive environment N82-13282
- STRESS CYCLES**
 Stress evaluations under rolling/sliding contacts
 [NASA-CR-165561] p0113 N82-17521
- STRESS DISTRIBUTION**
 U BESS CONCENTRATION
- STRESS INTENSITY FACTORS**
 Extended range stress intensity factor expressions
 for chevron-notched short bar and short rod
 fracture toughness specimens p0112 A82-40357
 Interface cracks in adhesively bonded lap-shear
 joints p0116 A82-46109
- STRESS MEASUREMENT**
 Digital imaging techniques in experimental stress
 analysis p0097 A82-34231
 On finite deformation elasto-plasticity p0116 A82-45869
- STRESS RUPTURE STRENGTH**
 U BESS RUPTURE STRENGTH
- STRESS-STRAIN DIAGRAMS**
 Impact resistance of fiber composites p0112 A82-39852
- STRESS-STRAIN DISTRIBUTION**
 U BESS CONCENTRATION
- STRESS-STRAIN RELATIONSHIPS**
 Elastic-plastic finite-element analyses of
 thermally cycled single-edge wedge specimens
 [NASA-TP-1982] p0111 N82-20565
 Elastic-plastic finite-element analyses of
 thermally cycled double-edge wedge specimens
 [NASA-TP-1973] p0111 N82-20566
 Nonlinear constitutive theory for turbine engine
 structural analysis p0112 N82-33744
- STRESSES**
 NT AXIAL STRESS
 NT RESIDUAL STRESS
 NT SHEAR STRESS
 NT TENSILE STRESS
 NT THERMAL STRESSES
 NT TORSIONAL STRESS
- STRIP MINING**
 LANDSAT Remote Sensing: Observations of an
 Appalachian mountaintop surface coal mining and
 reclamation operation --- Kentucky
 [E82-10247] p0117 N82-24525
- STRUCTURAL ANALYSIS**
 NT DYNAMIC STRUCTURAL ANALYSIS
 NT FLUTTER ANALYSIS
 NT STRAIN ENERGY METHODS
 On the solution of creep induced buckling in
 general structure p0115 A82-39514
 On the automatic generation of FEM models for
 complex gears - A work-in-progress report
 p0109 A82-40243
 Integrated analysis of engine structures
 [NASA-TM-82713] p0111 N82-11491
 Research and development program for non-linear
 structural modeling with advanced
 time-temperature dependent constitutive
 relationships p0024 N82-16080
 [NASA-CR-165533]
 Development of a simplified procedure for thrust
 chamber life prediction
 [NASA-CR-165585] p0044 N82-21253
 Evaluation of inelastic constitutive models for
 nonlinear structural analysis --- for aircraft
 turbine engines p0112 N82-24502
 [NASA-TM-82845]
 Bird impact analysis package for turbine engine
 fan blades p0112 N82-26701
 [NASA-TM-82831]
 Cooled variable nozzle radial turbine for rotor
 craft applications p0028 N82-29323
 [NASA-CR-165397]

- MC carbide structures in M(1c2)ar-M247
[NASA-CR-167892] p0064 N82-30374
- Environmental and High-Strain Rate effects on
composites for engine applications
[NASA-TM-82882] p0051 N82-31449
- Nonlinear constitutive theory for turbine engine
structural analysis p0112 N82-33744
- STRUCTURAL BEAMS**
U AMS (SUPPORTS)
- STRUCTURAL DESIGN**
Optimal tooth numbers for compact standard spur
gear sets
[ASME PAPER 81-DET-115] p0103 A82-19335
Winding for the vint p0138 A82-37078
- The application of probabilistic design theory to
high temperature low cycle fatigue
[NASA-CR-165488] p0112 N82-14531
- STRUCTURAL DESIGN CRITERIA**
Sensitivity analysis results of the effects of
various parameters on composite design p0051 A82-37101
- Magnetohydrodynamics MHD Engineering Test Facility
ETP 200 MWe power plant, Conceptual Design
Engineering Report CDER, Volume 3: Costs and
schedules p0128 N82-10495
[NASA-CR-165452-VOL-3]
- Magnetohydrodynamics (MHD) Engineering Test
Facility (ETP) 200 MWe power plant, Design
Requirements Document (DRD) p0099 N82-12446
[NASA-TM-82705]
- Magnetohydrodynamics (MHD) Engineering Test
Facility (ETP) 200 MWe power plant, Conceptual
Design Engineering Report (CDER), Volume 2:
Engineering, Volume 3: Costs and schedules
[NASA-CR-165452-VOL-2] p0136 N82-27837
- STRUCTURAL DYNAMICS**
U NANC STRUCTURAL ANALYSIS
- STRUCTURAL FAILURE**
Turbine blade nonlinear structural and life analysis
[AIAA PAPER 82-1056] p0021 A82-34981
- STRUCTURAL FATIGUE**
U TIGUE (MATERIALS)
- STRUCTURAL FOUNDATIONS**
U UNDATIONS
- STRUCTURAL MEMBERS**
NT BEAMS (SUPPORTS)
NT CANTILEVER BEAMS
NT ELASTIC PLATES
NT END PLATES
NT FLAT PLATES
NT ORTHOTROPIC PLATES
NT PLATES (STRUCTURAL MEMBERS)
NT RECTANGULAR BEAMS
NT STRUTS
NT TROSSES
- STRUCTURAL VIBRATION**
NT BENDING VIBRATION
NT FLUTTER
NT TRANSONIC FLUTTER
Vibrations of cantilevered shallow cylindrical
shells of rectangular planform p0115 A82-11298
- STRUCTURAL WEIGHT**
Performance deterioration due to acceptance
testing and flight loads; JT90 jet engine
diagnostic program p0027 N82-27309
[NASA-CR-165572]
- STRUTS**
Energy efficient engine: Turbine transition duct
model technology report p0029 N82-33394
[NASA-CR-167996]
- STS**
U ACE TRANSPORTATION SYSTEM
- STUDIES**
U VESTIGATION
- SUBCIRCUITS**
U RCUITS
- SUBLAYERS**
U BSTRATES
- SUBREFLECTORS**
Focal surfaces of offset dual-reflector antennas
p0080 A82-36265
- SUBSONIC FLOW**
Sound generated in a cascade by three-dimensional
disturbances convected in a subsonic flow
[AIAA PAPER 81-2046] p0153 A82-10460
- Aeroelastic characteristics of a cascade of
mistuned blades in subsonic and supersonic flows
[ASME PAPER 81-DET-122] p0021 A82-19337
- Solutions of the compressible Navier-Stokes
equations using the integral method
[AIAA PAPER 81-0046] p0093 A82-23832
- Three dimensional flow field inside the passage of
a low speed axial flow compressor rotor
[AIAA PAPER 82-1006] p0011 A82-31964
- Solution of the unsteady subsonic thin airfoil
problem p0012 A82-41267
- Some aspects of calculating flows about
three-dimensional subsonic inlets
[NASA-TM-82789] p0004 N82-25213
- SUBSONIC SPEED**
Thrust modulation methods for a subsonic V/STOL
aircraft
[NASA-TM-82747] p0003 N82-13112
- SUBSTRATES**
Transient catalytic combustor model
[NASA-CR-165324] p0129 N82-13507
- Refractory coatings
[NASA-CASE-LEW-13169-2] p0061 N82-30371
- Ion beam microtexturing and enhanced surface
diffusion
[NASA-CR-167948] p0065 N82-31509
- SULFATES**
Aircraft sampling of the sulfate layer near the
tropopause following the eruption of Mount St.
Helens p0140 A82-37450
- SULFATION**
Thermodynamics and kinetics of the sulfation of
porous calcium silicate
[NASA-TM-82769] p0048 N82-15119
- SULFIDES**
NT INORGANIC SULFIDES
NT HOLYBDENUM SULFIDES
- SULFUR COMPOUNDS**
NT INORGANIC SULFIDES
NT HOLYBDENUM SULFIDES
NT ORGANIC SULFUR COMPOUNDS
NT SULFATES
- SUNLIGHT**
Determination of optimum sunlight concentration
level in space for 3-4 cascade solar cells
[NASA-TM-82899] p0126 N82-32853
- SUPERALLOYS**
U AT RESISTANT ALLOYS
- SUPERCHARGERS**
Preliminary results on performance testing of a
turbocharged rotary combustion engine
[NASA-TM-82772] p0017 N82-21194
- Advanced stratified charge rotary aircraft engine
design study
[NASA-CR-165398] p0107 N82-27743
- SUPERCHARGING**
U PERCHARGERS
- SUPERCONDUCTING MAGNETS**
Conceptual design of superconducting magnet system
for Magnetohydrodynamic (MHD) Engineering Test
Facility (ETP) 200 MWe power plant
[NASA-CR-165053] p0105 N82-14520
- SUPERCONDUCTORS**
Impedance conversion using quantum limit
nonreciprocity for
superconductor-insulator-superconductor mixer
compensation p0159 A82-31276
- SUPERCritical FLOW**
Design of supercritical cascades with high solidity
[NASA-CR-165600] p0007 N82-22210
- SUPERHEATING**
Investigation of spray characteristics for
flashing injection of fuels containing dissolved
air and superheated fuels
[NASA-CR-3563] p0027 N82-26295
- SUPERHYBRID MATERIALS**
NT GRAPHITE-EPOXY COMPOSITES
- SUPERSONIC AIRCRAFT**
V/STOL propulsion control technology
[AIAA PAPER 81-2634] p0029 A82-16909
- Comparison of two parallel/series flow turbofan
propulsion concepts for supersonic V/STOL
[AIAA PAPER 81-2637] p0020 A82-19214
- NASA research in supersonic propulsion: A decade
of progress
[NASA-TM-82862] p0019 N82-26300

SUPERSONIC COMBUSTION

Effect of vacuum exhaust pressure on the performance of MHD ducts at high D-field
[NASA-TM-82750] p0157 N82-13908

SUPERSONIC CRUISE AIRCRAFT RESEARCH

Advanced technology for controlling pollutant emissions from supersonic cruise aircraft
p0001 N81-18004

SUPERSONIC FLOW

Aerodynamic characteristics of a cascade of mistuned blades in subsonic and supersonic flows
[ASME PAPER 81-DET-122] p0021 182-19337

A shock wave approach to the noise of supersonic propellers
[NASA-TM-82752] p0151 N82-16809

A FORTRAN program for calculating three dimensional, inviscid and rotational flows with shock waves in axial compressor blade rows: User's manual
[NASA-CR-3560] p0008 N82-26230

Calculation of the flow field including boundary layer effects for supersonic mixed compression inlets at angles of attack
[NASA-CR-167941] p0009 N82-29269

SUPERSONIC FLOW INLETS**U PERSONIC INLETS****SUPERSONIC INLETS**

Three-dimensional flow calculations including boundary layer effects for supersonic inlets at angle of attack
[AIAA PAPER 82-0061] p0005 N82-19778

Calculation of the flow field including boundary layer effects for supersonic mixed compression inlets at angles of attack
[NASA-CR-167941] p0009 N82-29269

SUPERSONIC JET FLOW

Forms of three-dimensional supersonic free jets in linear approximation
A82-19196

SUPERSONIC NOZZLES

The effect of inflow velocity profiles on the performance of supersonic ejector nozzles
[AIAA PAPER 81-0273] p0002 N81-32548

SUPERSONIC SPEEDS

Noise of the SR-3 propeller model at 2 deg and 4 deg angle of attack
[NASA-TM-82738] p0151 N82-16808

SUPERSONIC WIND TUNNELS

Flow visualization of shock-boundary layer interaction
p0096 N82-32675

LV measurements with an advanced turboprop
p0097 N82-32690

SURFACE DEFECTS

Acoustic microscopy of silicon carbide materials
p0075 N82-33031

Effects of artificially produced defects on film thickness distribution in sliding EHD point contacts
[NASA-TM-82732] p0099 N82-16412

Boundary lubrication: Revisited
[NASA-TM-82858] p0069 N82-29458

SURFACE DIFFUSION

Surface diffusion activation energy determination using ion beam microtexturing
p0159 N82-21965

Ion-beam-induced topography and surface diffusion
p0160 N82-46426

SURFACE ENERGY

Universal binding energy relations in metallic adhesion
[NASA-TM-82706] p0058 N82-11183

SURFACE FINISHING

Small axial turbine stator technology program
[NASA-CR-165602] p0028 N82-32367

Surface texturing of fluoropolymers
[NASA-CASE-LEW-13028-1] p0070 N82-33521

SURFACE GEOMETRY

Surface geometry of circular cut spiral bevel gears
[ASME PAPER 81-DET-114] p0108 N82-19334

Geometrical aspects of the tribological properties of graphite fiber reinforced polyamide composites
[NASA-TM-82757] p0066 N82-15198

SURFACE INTERACTIONS**U RFACE REACTIONS****SURFACE PROPERTIES****NT ADHESION****NT COEFFICIENT OF FRICTION****NT INTERFACIAL TENSION****NT SURFACE DEFECTS****NT SURFACE ENERGY****NT SURFACE ROUGHNESS****NT SURFACE TEMPERATURE****NT WALL TEMPERATURE**

Potentials of surfaces in space
p0165 N82-23750

Quasi-liquid states observed on ion beam microtextured surfaces
p0159 N82-30335

Differential charging of high-voltage spacecraft - The equilibrium potential of insulated surfaces
p0041 N82-35547

Simulation of charging response of SCATHA (P78-2) satellite
p0039 N82-14250

Surface chemistry and wear behavior of single-crystal silicon carbide sliding against iron at temperatures to 1500 C in vacuum
[NASA-TP-1947] p0067 N82-19374

Boundary lubrication: Revisited
[NASA-TM-82858] p0069 N82-29458

Influence of corrosive solutions on microhardness and chemistry of magnesium oxide (001) surfaces
[NASA-TP-2040] p0102 N82-31691

SURFACE REACTIONS

Universal binding energy relations in metallic adhesion
[NASA-TM-82706] p0058 N82-11183

Influence of mineral oil and additives on microhardness and surface chemistry of magnesium oxide (001) surface
[NASA-TP-1986] p0067 N82-20316

Tribological properties of sintered polycrystalline and single crystal silicon carbide
[NASA-TM-82829] p0068 N82-24343

SURFACE ROUGHNESS

Effect of tangential traction and roughness on crack initiation/propagation during rolling contact
p0103 N82-30022

The effect of rotor blade thickness and surface finish on the performance of a small axial flow turbine
[ASME PAPER 82-GT-222] p0022 N82-35409

The effect of rotor blade thickness and surface finish on the performance of a small axial flow turbine
[NASA-TM-82726] p0003 N82-13114

Evaluation of left ventricular assist device pump bladders cast from ion-sputtered polytetrafluoroethylene mandrels
[NASA-CR-167904] p0142 N82-23976

Frictional heating due to asperity interaction of elastohydrodynamic line-contact surfaces
[NASA-TP-1882] p0100 N82-25514

Ion beam textured graphite electrode plates --- high efficiency electron tube devices
[NASA-CASE-LEW-12919-2] p0050 N82-26386

Texturing polymer surfaces by transfer casting --- cardiovascular prosthesis
[NASA-CASE-LEW-13120-1] p0068 N82-28440

The influence of surface dents and grooves on traction in sliding EHD point contacts
[NASA-TM-82943] p0102 N82-32734

SURFACE TEMPERATURE**NT WALL TEMPERATURE**

Single pass rub phenomena - Analysis and experiment
[ASME PAPER 81-LUB-55] p0107 N82-18449

Preliminary study of temperature measurement techniques for Stirling engine reciprocating seals
[NASA-CR-165479] p0104 N82-11466

SURFACE TENSION**U TERFACIAL TENSION****SURFACE TREATMENT****U RFACE FINISHING****SURFACE VEHICLES****NT AUTOMOBILES****NT ELECTRIC AUTOMOBILES****NT ELECTRIC HYBRID VEHICLES****NT ELECTRIC MOTOR VEHICLES****SURFACE WAVES**

Standing waves along a microwave generated surface wave plasma
p0158 N82-26952

SURVEYING**U RVEYS****SURVEYS**

Fuel quality/processing study. Volume 2:

Appendix. Task 1 literature survey
[NASA-CR-165327-VOL-2] p0135 N82-24650

SWEAT COOLING
Heat transfer in cooled porous region with curved boundary p0089 A82-14848

SWELLING
Prediction of composite hygral behavior made simple [NASA-TM-82780] p0049 N82-16181

SWIRLING
Near flowfields in axisymmetric combustor geometries with swirl [AIAA PAPER 82-0177] p0092 A82-17824
Modeling parameter influences on MHD swirl combustion nozzle design [AIAA PAPER 82-0984] p0011 A82-31947

SWIRLING WAKES
U RECURRENT WAKES

SWITCHES
NT SWITCHING CIRCUITS

SWITCHING
NT MICROWAVE SWITCHING
NT PACKET SWITCHING
Input filter compensation for switching regulators [NASA-CR-169005] p0085 N82-25442

SWITCHING CIRCUITS
High power solar array switching regulation p0043 A82-11736
A new approach to the minimum weight/loss design of switching power converters p0082 A82-16831
Dynamic switch matrix for the TDMA satellite switching system [AIAA 82-0458] p0085 A82-23494
A 10-kW series resonant converter design, transistor characterization, and base-drive optimization p0086 A82-36927
Wideband, high speed switch matrix development for SS-TDMA applications p0086 A82-43784
Modeling the full-bridge series-resonant power converter p0086 A82-46385
Analysis and design of a standardized control module for switching regulators p0083 A82-46388
A 10kW series resonant converter design, transistor characterization, and base-drive optimization [NASA-CR-165546] p0084 N82-17839
Analysis of transistor and snubber turn-off dynamics in high-frequency high-voltage high-power converters [NASA-CR-168760] p0084 N82-22438

SWITCHING ELEMENTS
U SWITCHING CIRCUITS

SYMMETRICAL BODIES
NT AXISYMMETRIC BODIES
NT CYLINDRICAL BODIES
NT FAIRINGS
NT ROTATING CYLINDERS
NT SPHERES

SYNCHRONISM
NT BIT SYNCHRONIZATION

SYNCHRONOUS MOTORS
Mass Driver Two - A status report p0046 A82-18191

SYNCHRONOUS SATELLITES
Voltage gradients in solar array cavities as possible breakdown sites in spacecraft-charging-induced discharges p0038 A82-18317
Planning satellite communication services and spectrum-orbit utilization [AIAA 82-0526] p0080 A82-23538
Analytical modeling of satellites in geosynchronous environment p0037 N82-14258
Use of charging control guidelines for geosynchronous satellite design studies p0037 N82-14263
Communications satellite systems capacity analysis [NASA-CR-167911] p0034 N82-27331

SYNTHETIC FIBERS
NT GLASS FIBERS

SYNTHETIC FUELS
NT LIQUID FUELS

Low NO sub x heavy fuel combustor concept program [NASA-CR-165512] p0129 N82-12572
Barriers to the utilization of synthetic fuels for transportation [NASA-CR-165517] p0073 N82-13243
Fuel quality processing study, volume 1 [NASA-CR-165327-VOL-1] p0135 N82-24649
Fuel quality/processing study. Volume 2: Appendix. Task 1 literature survey [NASA-CR-165327-VOL-2] p0135 N82-24650
Low NOx heavy fuel combustor concept program [NASA-CR-165367] p0136 N82-25635
Techniques for enhancing durability and equivalence ratio control in a rich-lean, three-stage ground power gas turbine combustor [NASA-TM-82922] p0124 N82-29717

SYNTHETIC RESINS
NT EPOXY RESINS
NT KEVLAR (TRADEMARK)
NT THERMOPLASTIC FILMS
NT THERMOPLASTIC RESINS
NT THERMOSETTING RESINS

SYNTHETIC RUBBERS
NT ELASTOMERS

SYSTEM FAILURES
Model degradation effects on sensor failure detection p0148 A82-13143
Sensor failure detection system --- for the F100 turbofan engine [NASA-CR-165515] p0023 N82-13145

SYSTEMS DESIGN
U STEMS ENGINEERING

SYSTEMS ENGINEERING
Magnetohydrodynamics (MHD) Engineering Test Facility (ETF) 200 MWe power plant. Design Requirements Document (DRD) [NASA-TM-82705] p0099 N82-12446
Magnetohydrodynamics (MHD) Engineering Test Facility (ETF) 200 MWe power plant. Conceptual Design Engineering Report (CDPR). Volume 4: Supplementary engineering data [NASA-CR-165452-VOL-4] p0133 N82-18688

SYSTEMS INTEGRATION
Systems integration p0042 N82-27371

SYSTEMS SIMULATION
Design and verification of a multiple fault tolerant control system for STS applications using computer simulation [AIAA 81-2173] p0035 A82-10124
A tensor approach to modeling of nonhomogeneous nonlinear systems p0148 A82-19064
Modeling the full-bridge series-resonant power converter p0086 A82-46385

T

TAILORING
U SIGN

TANGENTS
Experimental and analytical results of tangential blowing applied to a subsonic V/STOL inlet [AIAA PAPER 82-1084] p0005 A82-35195
Experimental and analytical results of tangential blowing applied to a subsonic V/STOL inlet [NASA-TM-82847] p0004 N82-24165

TANKS (CONTAINERS)
NT FUEL TANKS
NT PROPELLANT TANKS
NT WING TANKS

TANTALUM
A status review of NASA's COSAM (Conservation of Strategic Aerospace Materials) program [NASA-TM-82852] p0060 N82-24326

TDMA
U THE DIVISION MULTIPLE ACCESS

TECHNOLOGICAL FORECASTING
Propulsion study for Small Transport Aircraft Technology (STAT) [NASA-CR-165499] p0022 N82-10037
Overview study of Space Power Technologies for the advanced energetics program --- spacecraft [NASA-CR-165269] p0132 N82-17606

TECHNOLOGIES
NT BIOTECHNOLOGY
NT ENERGY TECHNOLOGY

TECHNOLOGY ASSESSMENT

The AGT101 technology - An automotive alternative
p0107 A82-11783

30-cm mercury ion thruster technology
p0046 A82-15434

Comparative analysis of CCMHD power plants ---
Closed Cycle MHD
p0158 A82-20747

An assessment of alternative fuel cell designs for
residential and commercial cogeneration
p0138 A82-24695

Component technology for space power systems
[IAF PAPER 82-408]
p0043 A82-44750

Numerical techniques in linear duct acoustics,
1980-81 update
[NASA-TM-82730]
p0151 N82-12890

Study of multi-megawatt technology needs for
photovoltaic space power systems. Volume 1:
Executive summary
[NASA-CR-165323-VOL-1]
p0130 N82-14636

Study of multi-megawatt technology needs for
photovoltaic space power systems, volume 2
[NASA-CR-165323-VOL-2]
p0130 N82-14637

Overview study of Space Power Technologies for the
advanced energetics program --- spacecraft
[NASA-CR-165269]
p0132 N82-17606

Cell module and fuel conditioner development
[NASA-CR-165620]
p0134 N82-21713

PMR polyimides-review and update
[NASA-TM-82921]
p0068 N82-24342

Cost/benefit studies of advanced materials
technologies for future aircraft turbine
engines: Materials for advanced turbine engines
[NASA-CR-167849]
p0026 N82-25254

TECHNOLOGY TRANSFER

Local and national impact of aerospace research
and technology
[NASA-TM-82775]
p0162 N82-20006

TECHNOLOGY UTILIZATION

Market assessment of photovoltaic power systems
for agricultural applications in Mexico
[NASA-CR-165441]
p0128 N82-10506

TEETERING

Whirl flutter analysis of a horizontal-axis wind
turbine with a two-bladed teetering rotor
p0122 N82-23707

TEFLON (TRADEMARK)

Secondary electron emission yields
p0038 N82-14226

Oblique-incidence secondary emission from charged
dielectrics
p0039 N82-14227

Secondary electron emission from a charged
dielectric in the presence of normal and oblique
electric fields
[NASA-CR-168558]
p0084 N82-18507

First results of material charging in the space
environment
[NASA-TM-84743]
p0081 N82-24431

TELECHEMISTRY

U NCTE HANDLING

TELECOMMUNICATION

NT FREQUENCY DIVISION MULTIPLE ACCESS

NT MULTICHANNEL COMMUNICATION

NT RADIO COMMUNICATION

NT SPACECRAFT ANTENNAS

NT SPACECRAFT COMMUNICATION

NT TIME DIVISION MULTIPLE ACCESS

NT WIDEBAND COMMUNICATION

Worldwide satellite market demand forecast
[NASA-CR-167918]
p0079 N82-25423

TELEGEN THEORY

U TQOK ANALYSIS

U TQOK SYNTHESIS

TEMPERATURE

NT ATMOSPHERIC TEMPERATURE

NT FLAME TEMPERATURE

NT HIGH TEMPERATURE

NT INLET TEMPERATURE

NT LOW TEMPERATURE

NT OPERATING TEMPERATURE

NT PLASMA TEMPERATURE

NT SURFACE TEMPERATURE

NT WALL TEMPERATURE

TEMPERATURE CONTROL

Magnetic heat pumping
[NASA-CASE-LEW-12508-3]
p0088 N82-24449

TEMPERATURE DEPENDENCE

A heat exchanger computational procedure for

temperature-dependent fouling
[ASME PAPER 81-HT-75]
p0092 A82-10961

TEMPERATURE DIFFERENCES

TEMPERATURE GRADIENTS

TEMPERATURE DISTRIBUTION

Analysis of the decay of temperature fluctuations
in isotropic turbulence
p0089 A82-40781

Buoyancy effects on the temperature field in
downward spreading flames
p0094 A82-41203

TEMPERATURE EFFECTS

Permanent magnet properties of Mn-Al-C between -50
C and +150 C
p0085 A82-20505

On the solution of creep induced buckling in
general structure
p0115 A82-39514

Creep and rupture of an ODS alloy with high stress
rupture ductility --- Oxide Dispersion
Strengthened
p0065 A82-40335

Effects of heating rate on density,
microstructure, and strength of Si3N4-6 wt.%
Y2O3 and a beta-prime sialon
[ACS PAPER 42-B-81]
p0070 A82-42366

Effects of fan inlet temperature disturbances on
the stability of a turbofan engine
[NASA-TM-82699]
p0017 N82-18222

Environmental effects on defect growth in
composite materials
[NASA-CR-165213]
p0052 N82-20248

TEMPERATURE FIELDS

TEMPERATURE DISTRIBUTION

TEMPERATURE GRADIENTS

Frictional heating due to asperity interaction of
elastohydrodynamic line-contact surfaces
[NASA-TP-1882]
p0100 N82-25514

Use of fiber like materials to augment the cycle
life of thick thermoprotective seal coatings
[NASA-TM-82901]
p0089 N82-32633

TEMPERATURE INVERSIONS

NT INTERFACIAL TENSION

TEMPERATURE MEASUREMENT

Dilution jet behavior in the turn section of a
reverse flow combustor
[AIAA PAPER 82-0192]
p0021 A82-20291

Preliminary study of temperature measurement
techniques for Stirling engine reciprocating seals
[NASA-CR-165479]
p0104 N82-11466

TEMPERATURE SENSORS

Thin film temperature sensors, phase 3 --- for
engine-test evaluation
[NASA-CR-165476]
p0097 N82-22479

TENSILE PROPERTIES

On determination of fibre fraction in continuous
fibre composite materials
p0051 A82-38133

Tensile properties of SiC/aluminum filamentary
composites - Thermal degradation effects
p0053 A82-46220

The influence of cobalt on the tensile and
stress-rupture properties of the nickel-base
superalloy MAR-M247
p0063 A82-47399

TENSILE STRENGTH

Strength advantages of chemically polished boron
fibers before and after reaction with aluminum
[NASA-TM-82806]
p0049 N82-21258

Thermal degradation of the tensile properties of
unidirectionally reinforced FP-AI203/EZ 33
magnesium composites
[NASA-TM-82817]
p0049 N82-21260

Correlation of tensile and shear strengths of
metals with their friction properties
[NASA-TM-82828]
p0060 N82-24375

Method and apparatus for strengthening boron fibers
--- high temperature oxidation
[NASA-CASE-LEW-13826-1]
p0050 N82-26385

TENSILE STRESS

Ultrasonic scanning system for imaging flaw growth
in composites
[NASA-TM-82799]
p0076 N82-22386

Tensile buckling of advanced turboprops
[NASA-TM-82896]
p0112 N82-31708

TENSILE TESTS

Impact resistance of fiber composites
p0112 A82-39852

- Application of a gripping system to test a uniaxial graphite fiber reinforced composite /EMR 15/Celion 6000/ in tension at 316 C p0051 A82-40796
- SENSOR ANALYSIS**
A tensor approach to modeling of nonhomogeneous nonlinear systems p0148 A82-19064
- Alternatives for jet engine control [NASA-CR-168894] p0026 N82-23247
- TERNARY ALLOYS**
Hard permanent magnet development trends and their application to A.C. machines p0083 A82-20745
- TERNARY SYSTEMS**
Nical ternary alloy having improved cyclic oxidation resistance [NASA-CASE-LEW-13339-1] p0061 N82-31505
- TERNARY SYSTEMS (DIGITAL)**
DIGITAL SYSTEMS
- TERRESTRIAL MAGNETISM**
MAGNETISM
- TEST BEDS**
TEST EQUIPMENT
- TEST CHAMBERS**
HIGH PRESSURE CHAMBERS
- TEST EQUIPMENT**
Advanced turboprop testbed systems study. Volume 1: Testbed program objectives and priorities, drive system and aircraft design studies, evaluation and recommendations and wind tunnel test plans [NASA-CR-167928-VOL-1] p0028 N82-32370
- TEST FACILITIES**
NT CASCADE WIND TUNNELS
NT COMBUSTION WIND TUNNELS
NT SHOCK TUNNELS
NT SUPERSONIC WIND TUNNELS
NT TRANSONIC WIND TUNNELS
End region and current consolidation effects upon the performance of an MHD channel for the ETF conceptual design --- Engineering Test Facility [AIAA PAPER 82-0325] p0157 A82-17889
Impact of uniform electrode current distribution on ETF --- Engineering Test Facility MHD generator [AIAA PAPER 82-0423] p0157 A82-17941
Magnetohydrodynamics (MHD) Engineering Test Facility (ETF) 200 MWe power plant. Conceptual Design Engineering Report CDER. Volume 3: Costs and schedules [NASA-CR-165452-VOL-3] p0128 N82-10495
Levis Research Center's coal-fired, pressurized, fluidized-bed reactor test facility [NASA-TM-81616] p0087 N82-11397
Magnetohydrodynamics (MHD) Engineering Test Facility (ETF) 200 MWe power plant. Design Requirements Document (DRD) [NASA-TM-82705] p0099 N82-12446
Magnetohydrodynamics (MHD) Engineering Test Facility (ETF) 200 MWe power plant Conceptual Design Engineering Report (CDER) [NASA-CR-165452-VOL-5] p0132 N82-17603
Magnetohydrodynamics (MHD) Engineering Test Facility (ETF) 200 MWe power plant. Conceptual Design Engineering Report (CDER). Volume 4: Supplementary engineering data [NASA-CR-165452-VOL-4] p0133 N82-18688
The aerospace technology laboratory (a perspective, then and now) [NASA-TM-82754] p0631 N82-19229
Magnetohydrodynamics (MHD) Engineering Test Facility (ETF) 200 MWe power plant. Conceptual Design Engineering Report (CDER). Volume 2: Engineering. Volume 3: Costs and schedules [NASA-CR-165452-VOL-2] p0136 N82-27857
- TESTERS**
TEST EQUIPMENT
- TESTING MACHINES**
TEST EQUIPMENT
- TETRAGONS**
TRIANGLES
- TEXTURES**
Crystallographic texture in oxide-dispersion-strengthened alloys p0062 A82-40041
Texturing polymer surfaces by transfer casting --- cardiovascular prosthesis [NASA-CASE-LEW-13120-1] p0068 N82-28440
- Ion beam microtexturing and enhanced surface diffusion [NASA-CR-167948] p0065 N82-31509
Surface texturing of fluoropolymers [NASA-CASE-LEW-13028-1] p0070 N82-33521
- TF-34 ENGINE**
TP34 Convertible Engine System Technology Program p0022 A82-40521
Effect of a part span variable inlet guide vane on TP34 fan performance [NASA-CR-165458] p0023 N82-12075
- TRAWING**
TRILING
- THERMATIC MAPPING**
LANDSAT Remote Sensing: Observations of an Appalachian mountaintop surface coal mining and reclamation operation --- Kentucky [E82-10247] p0117 N82-24525
- THEOREMS**
ST FLOQUET THEOREM
- THERMAL CONDUCTIVITY**
Self-adaptive closed constrained solution algorithms for nonlinear conduction p0094 A82-45157
Gas-turbine critical research and advanced technology support project [NASA-TM-81708] p0118 N82-13509
- THERMAL CONTROL COATINGS**
Ceramic thermal barrier coatings for gas turbine engines [ASME PAPER 82-GT-265] p0071 A82-35441
Development of improved high temperature coatings for TN-792 + HF [NASA-CR-165395] p0063 N82-14333
Review of NASA progress in thermal barrier coatings for stationary gas turbines [NASA-TM-81716] p0058 N82-17335
Effects of arc current on the life in burner rig thermal cycling of plasma sprayed ZrO₂-Y₂O₃ [NASA-TM-82795] p0087 N82-17453
Evaluation of present thermal barrier coatings for potential service in electric utility gas turbines [NASA-CR-165545] p0063 N82-18368
Performance of laser glazed ZrO₂ TBCs in cyclic oxidation and corrosion burner test rigs [NASA-TM-82830] p0059 N82-22346
First results of material charging in the space environment [NASA-TM-84743] p0081 N82-24431
Improved thermal barrier coating system [NASA-CASE-LEW-13324-1] p0060 N82-26431
Effect of fuel to air ratio on Mach 0.3 burner rig hot corrosion of ZrO₂-Y₂O₃ thermal barrier coatings [NASA-TM-82879] p0061 N82-30373
Failure mechanisms of thermal barrier coatings exposed to elevated temperatures [NASA-TM-82905] p0061 N82-32461
- THERMAL CONVECTION**
FREE CONVECTION
- THERMAL CURRENTS**
UNVECTIVE FLOW
- THERMAL CYCLING TESTS**
High temperature durable catalyst development p0056 A82-20739
Anaerobic polymers as high vacuum leak sealants p0108 A82-21967
Work of fracture in aluminum metal-matrix composites p0053 A82-31339
A simplified design procedure for life prediction of rocket thrust chambers [AIAA PAPER 82-1251] p0043 A82-35087
Thermal fatigue and oxidation data of TAZ-8A and M22 alloys and variations [NASA-CR-165407] p0063 N82-10193
Effects of arc current on the life in burner rig thermal cycling of plasma sprayed ZrO₂-Y₂O₃ [NASA-TM-82795] p0087 N82-17453
Elastic-plastic finite-element analyses of thermally cycled single-edge wedge specimens [NASA-TP-1982] p0111 N82-20565
Elastic-plastic finite-element analyses of thermally cycled double-edge wedge specimens [NASA-TP-1973] p0111 N82-20566
High temperature low cycle fatigue mechanisms for nickel base and a copper base alloy [NASA-CR-3543] p0064 N82-26436

- Microstructural effects on the room and elevated temperature low cycle fatigue behavior of Waspaloy [NASA-CR-165497] p0113 N82-26702
- Failure mechanisms of thermal barrier coatings exposed to elevated temperatures [NASA-TM-82905] p0061 N82-32461
- Use of fiber like materials to augment the cycle life of thick thermoprotective seal coatings [NASA-TM-82901] p0089 N82-32633
- THERMAL DECOMPOSITION**
Deposit formation in hydrocarbon fuels [ASME PAPER 82-GT-49] p0075 N82-35307
- THERMAL DEGRADATION**
Tensile properties of SiC/aluminum filamentary composites - Thermal degradation effects p0053 N82-46220
- Thermal oxidative degradation reactions of perfluoroalkylethers [NASA-CR-165516] p0048 N82-12135
- Thermal degradation of the tensile properties of unidirectionally reinforced FP-Al2O3/EZ 33 magnesium composites [NASA-TM-82817] p0049 N82-21260
- Thermal and oxidative degradation studies of formulated C-ethers by gel-permeation chromatography [NASA-TP-1994] p0068 N82-21332
- Thermal oxidative degradation reactions of linear perfluoroalkylethers [NASA-TM-82834] p0068 N82-26468
- THERMAL EFFECTS**
TEMPERATURE EFFECTS
- THERMAL EFFICIENCY**
THERMODYNAMIC EFFICIENCY
- THERMAL ENERGY STORAGE**
HEAT STORAGE
- THERMAL EXPANSION**
Thermal expansion accommodation in a jet engine frame p0029 N82-11999
- THERMAL FATIGUE**
Comparative thermal fatigue resistance of several oxide dispersion strengthened alloys p0062 N82-11399
- Thermal expansion accommodation in a jet engine frame p0029 N82-11999
- Fatigue of Ni-Al-Mo aligned eutectics at elevated temperatures p0052 N82-13403
- Thermal fatigue and oxidation data of TAZ-9A and M22 alloys and variations [NASA-CR-165407] p0063 N82-10193
- Development of improved high temperature coatings for IN-792 + HF [NASA-CR-165395] p0063 N82-14333
- THERMAL MAPPING**
Reliable aerial thermography for energy conservation [NASA-TM-81766] p0117 N82-14552
- THERMAL POWER**
THERMOGENERATORS
- THERMAL PROPERTIES**
THERMODYNAMIC PROPERTIES
- THERMAL PROTECTION**
Progress in protective coatings for aircraft gas turbines: A Review of NASA sponsored research [NASA-TM-82740] p0058 N82-12216
- Covering solid, film cooled surfaces with a duplex thermal barrier coating [NASA-CASE-LEW-13450-1] p0088 N82-25463
- Use of fiber like materials to augment the cycle life of thick thermoprotective seal coatings [NASA-TM-82901] p0089 N82-32633
- THERMAL RESISTANCE**
A heat exchanger computational procedure for temperature-dependent fouling [ASME PAPER 81-HT-75] p0092 N82-10961
- Thermal-barrier-coated turbine blade study [NASA-CR-165351] p0023 N82-10040
- THERMAL SHIELDING**
HEAT SHIELDING
- THERMAL STABILITY**
HEAT TEMPERATURE DEPENDENCE
Deposit formation in liquid fuels. I - Effect of coal-derived Lewis bases on storage stability of Jet A turbine fuel p0074 N82-22241
- Oxidation stability of advanced reaction-bonded Si3N4 materials
- [ACS PAPER 52-B-80P] p0074 N82-33030
- Phase stability in plasma-sprayed, partially stabilized zirconia-yttria p0070 N82-41552
- Thermal oxidative degradation reactions of perfluoroalkylethers [NASA-CR-165516] p0048 N82-12135
- Effect of some nitrogen compounds thermal stability of jet A [NASA-TM-82908] p0072 N82-27519
- Effect of hydrocarbon fuel type on fuel [NASA-TM-82916] p0072 N82-28460
- THERMAL STRESSES**
The application of probabilistic design theory to high temperature low cycle fatigue [NASA-CR-165488] p0112 N82-14531
- Factors influencing the thermally-induced strength degradation of B/Al composites [NASA-TM-82823] p0050 N82-24297
- Fully plasma-sprayed compliant backed ceramic turbine seal [NASA-CASE-LEW-13268-2] p0101 N82-26674
- Boundary layer thermal stresses in angle-ply composite laminates, part I --- graphite-epoxy composites [NASA-CR-165412] p0113 N82-26713
- Modulus, strength and thermal exposure studies of FP-Al2O3/aluminum and FP-Al2O3/magnesium composites [NASA-TM-82868] p0050 N82-30335
- THERMIONIC CONVERTERS**
High thermal power density heat transfer --- thermionic converters [NASA-CASE-LEW-12950-1] p0087 N82-11399
- Parametric performance analysis of steam-injected gas turbine with a thermionic-energy-converter-lined combustor [NASA-TM-82736] p0121 N82-23678
- THERMIONIC EMITTERS**
Modification of spacecraft potentials by thermal electron emission on ATS-5 p0040 N82-16194
- THERMIONIC REACTORS**
THERMIONIC ENGINES
- THERMOCHEMICAL PROPERTIES**
HEAT OF COMBUSTION
- THERMOCHEMISTRY**
Materials science issues encountered during the development of thermochemical concepts --- in screening of reactions for solar energy applications N82-10021
- THERMOCOUPLES**
Thin film temperature sensors, phase 3 --- for engine-test evaluation [NASA-CR-165476] p0097 N82-22479
- THERMODYNAMIC CYCLES**
HEAT STIRLING CYCLE
Evaluation of the potential of the Stirling engine for heavy duty application [NASA-CR-165473] p0128 N82-10505
- New features and applications of PRESTO, a computer code for the performance of regenerative, superheated steam turbine cycles [NASA-TP-1954] p0119 N82-16477
- Evaluation of inelastic constitutive models for nonlinear structural analysis --- for aircraft turbine engines [NASA-TM-82845] p0112 N82-24502
- THERMODYNAMIC EFFICIENCY**
End region and current consolidation effects upon the performance of an MHD channel for the ETF conceptual design --- Engineering Test Facility [AIAA PAPER 82-0325] p0157 N82-17889
- Evaluation of the potential of the Stirling engine for heavy duty application [NASA-CR-165473] p0128 N82-10505
- End region and current consolidation effects upon the performance of an MHD channel for the ETF conceptual design [NASA-TM-82744] p0157 N82-12943
- Summary and evaluation of the conceptual design study of a potential early commercial MHD power plant (CSPEC) [NASA-TM-82734] p0119 N82-16481
- Development of thin wraparound junction silicon solar cells [NASA-CR-165570] p0133 N82-18689

THERMODYNAMIC PROPERTIES

NT EMISSIVITY
 NT ENTHALPY
 NT ENTROPY
 NT HEAT OF COMBUSTION
 NT SURFACE ENERGY
 NT THERMAL CONDUCTIVITY
 NT THERMAL EXPANSION
 NT THERMAL STABILITY
 NT THERMOPHYSICAL PROPERTIES
 Experimental study of external fuel vaporization
 [ASME PAPER 82-GT-59] p0075 A82-35312
 Thermodynamics and kinetics of the sulfation of
 porous calcium silicate
 [NASA-TM-82769] p0048 A82-15119
 Designing with fiber-reinforced plastics (planar
 random composites)
 [NASA-TM-82812] p0050 A82-24300
 Research report: User's manual for computer
 program AT81Y005. PLANETSYS, a computer program
 for the steady state and transient thermal
 analysis of a planetary power transmission system
 [NASA-CR-165366] p0146 A82-31970
 Thermodynamic and transport combustion properties
 of hydrocarbons with air. Part 1: Properties
 in SI units
 [NASA-TP-1906] p0161 A82-32186
 Thermodynamic and transport combustion properties
 of hydrocarbons with air. Part 2: Compositions
 corresponding to Kelvin temperature schedules in
 part 1
 [NASA-TP-1907] p0161 A82-32187
 Thermodynamic and transport combustion properties
 of hydrocarbons with air. Part 3: Properties
 in US customary units
 [NASA-TP-1908] p0161 A82-32188
 Thermodynamic and transport combustion properties
 of hydrocarbons with air. Part 4: Compositions
 corresponding to Rankine temperature schedules
 in part 3
 [NASA-TP-1909] p0161 A82-32189
 Large area low-cost space solar cell
 development
 [NASA-TM-82902] p0126 A82-32854

THERMODYNAMICS

NT AEROTHERMODYNAMICS
 NT COMBUSTION PHYSICS
 Materials science issues encountered during the
 development of thermochemical concepts --- in
 screening of reactions for solar energy
 applications
 A82-10021
 Computational methods for internal flows with
 emphasis on turbomachinery
 [NASA-TM-82764] p0003 A82-13113
 Effect of location in an array on heat transfer to
 a cylinder in crossflow
 [NASA-TM-82797] p0087 A82-19493
 Spherical roller bearing analysis. SKF computer
 program SPHERBEAN. Volume 1: Analysis
 [NASA-CR-165203] p0106 A82-20540
 Spherical roller bearing analysis. SKF computer
 program SPHERBEAN. Volume 2: User's manual
 [NASA-CR-165204] p0106 A82-20541
 Spherical roller bearing analysis. SKF computer
 program SPHERBEAN. Volume 3: Program
 correlation with full scale hardware tests
 [NASA-CR-165205] p0106 A82-20542
 Low-thrust chemical propulsion system propellant
 expulsion and thermal conditioning study.
 Executive summary
 [NASA-CP-165622] p0045 A82-24287
 Low-thrust chemical propulsion system propellant
 expulsion and thermal conditioning study
 [NASA-CR-167841] p0045 A82-24288

THERMOMECHANICS

U HYDRODYNAMICS

THERMOMETRY

U TEMPERATURE MEASUREMENT

THERMOPHYSICAL PROPERTIES

NT EMISSIVITY

NT TEMPERATURE DEPENDENCE

NT THERMAL CONDUCTIVITY

NT THERMAL STABILITY

Toward the use of similarity theory in two-phase
 choked flows
 p0089 A82-16570

THERMOPHYSICS

U HYDRODYNAMICS

THERMOPLASTIC FILMS

Advanced inorganic separators for alkaline batteries
 [NASA-CASE-LEW-13171-1] p0124 A82-29708

THERMOPLASTIC RESINS

NT THERMOPLASTIC FILMS

Method of making formulated plastic separators for
 soluble electrode cells
 [NASA-CASE-LEW-12358-2] p0054 A82-21268
 Designing with fiber-reinforced plastics (planar
 random composites)
 [NASA-TM-82812] p0050 A82-24300
 Advanced inorganic separators for alkaline batteries
 [NASA-CASE-LEW-13171-1] p0124 A82-29708

THERMOSTABILITY

Nonlinear structural and life analyses of a
 combustor liner
 [NASA-TM-82846] p0111 A82-24501

THERMOSETTING RESINS

NT EPOXY RESINS

NT KEVLAR (TRADEMARK)
 Designing with fiber-reinforced plastics (planar
 random composites)
 [NASA-TM-82812] p0050 A82-24300

THERMOSTABILITY

U THERMAL STABILITY

THERMOTROPISM

U ISOTROPY

U TEMPERATURE EFFECTS

THERMOVISCOELASTICITY

Research and development program for non-linear
 structural modeling with advanced
 time-temperature dependent constitutive
 relationships
 [NASA-CR-165533] p0024 A82-16080

THICKNESS

The effect of rotor blade thickness and surface
 finish on the performance of a small axial flow
 turbine
 [ASME PAPER 82-GT-222] p0022 A82-35409

The effect of rotor blade thickness and surface
 finish on the performance of a small axial flow
 turbine
 [NASA-TM-82726] p0003 A82-13114

Gas turbine ceramic-coated-vane concept with
 convection-cooled porous metal core
 [NASA-TP-1942] p0016 A82-14090

A finite element stress analysis of spur gears
 including fillet radii and rim thickness effects
 [NASA-TM-82865] p0101 A82-28646

Small axial turbine stator technology program
 [NASA-CR-165602] p0028 A82-32367

THIN AIRFOILS

Measurement and prediction of mean velocity and
 turbulence structure in the near wake of an
 airfoil
 p0010 A82-26137

Solution of the unsteady subsonic thin airfoil
 problem
 p0012 A82-41267

THIN FILMS

NT ENERGY ABSORPTION FILMS

Ion-beam-induced topography and surface diffusion
 p0160 A82-46426

Study of the photovoltaic effect in thin film
 barium titanate
 [NASA-CR-165081] p0131 A82-16479

Morphological and frictional behavior of sputtered
 MoS₂ films
 [NASA-TM-82809] p0076 A82-22387

Thin film temperature sensors, phase 3 --- for
 engine-test evaluation
 [NASA-CR-165476] p0097 A82-22479

Ion beam sputter deposited diamond like films
 [NASA-TM-82873] p0069 A82-28445

The dryout region in frictionally heated sliding
 contacts
 [NASA-TM-82796] p0088 A82-28574

THIN WALLS

On the solution of creep induced buckling in
 general structure
 p0115 A82-39514

THREE DIMENSIONAL BOUNDARY LAYER

The three-dimensional boundary layer on a rotating
 helical blade
 p0009 A82-15459

Three dimensional turbulent boundary layer
 development on a fan rotor blade
 [AIAA PAPER 82-1007] p0011 A82-31965

- THREE DIMENSIONAL FLOW**
NT SECONDARY FLOW
 Characteristics of the flow in the annulus-wall region of an axial-flow compressor rotor blade passage
 [AIAA PAPER 82-0413] p0009 A82-17933
 Forms of three-dimensional supersonic free jets in linear approximation
 A82-19196
 Three-dimensional flow calculations including boundary layer effects for supersonic inlets at angle of attack
 [AIAA PAPER 82-0061] p0005 A82-19778
 Three sensor hot wire/film technique for three dimensional mean and turbulence flow field measurement
 p0097 A82-30300
 Finite volume calculation of three-dimensional potential flow around a propeller
 [AIAA PAPER 82-0957] p0010 A82-31933
 Three dimensional flow field inside the passage of a low speed axial flow compressor rotor
 [AIAA PAPER 82-1006] p0011 A82-31964
 Three-dimensional flow field in the tip region of a compressor rotor passage. I - Mean velocity profiles and annulus wall boundary layer
 [ASME PAPER 82-GT-11] p0011 A82-35280
 Three-dimensional flow field in the tip region of a compressor rotor passage. II - Turbulence properties
 [ASME PAPER 82-GT-234] p0011 A82-35416
 Three-dimensional shock structure in a transonic flutter cascade
 p0006 A82-37937
 Development of a locally mass flux conservative computer code for calculating 3-D viscous flow in turbomachines
 [NASA-CR-3539] p0007 A82-22214
 Turbofan forced mixer-nozzle internal flowfield. Volume 3: A computer code for 3-D mixing in axisymmetric nozzles
 [NASA-CR-3494] p0091 A82-22460
 Fringe localization requirements for three-dimensional flow visualization of shock waves in diffuse-illumination double-pulse holographic interferometry
 [NASA-TP-1869] p0095 A82-22481
 Numerical modeling of three-dimensional confined flows
 [NASA-CR-165583] p0158 A82-24070
 Some aspects of calculating flows about three-dimensional subsonic inlets
 [NASA-TM-82789] p0004 A82-25213
 Three dimensional mean velocity and turbulence characteristics in the annulus wall region of an axial flow compressor rotor passage
 [NASA-CR-169003] p0026 A82-25252
 The design and instrumentation of the Purdue annular cascade facility with initial data acquisition and analysis
 [NASA-CR-167861] p0008 A82-26237
 Comparison of experimental and analytical performance for contoured endwall stators
 [NASA-TM-82877] p0019 A82-26299
 Three dimensional flow field inside compressor rotor, including blade boundary layers
 [NASA-CR-169120] p0091 A82-27696
 Computer program for calculating full potential transonic, quasi-three-dimensional flow through a rotating turbomachinery blade row
 [NASA-TP-2030] p0005 A82-28247
 Turbine endwall single cylinder program
 [NASA-CR-169278] p0097 A82-31038
 Three dimensional flow measurements in a turbine scroll
 [NASA-CR-167920] p0009 A82-32310
- THREE DIMENSIONAL MOTION**
NT SECONDARY FLOW
NT THREE DIMENSIONAL FLOW
- THROTTLING**
 External fuel vaporization study
 [NASA-CR-165513] p0073 A82-14371
- THRUST**
NT ROCKET THRUST
THRUST CHAMBERS
 A simplified design procedure for life prediction of rocket thrust chambers
 [AIAA PAPER 92-1251] p0043 A82-35087
- Development of a simplified procedure for thrust chamber life prediction
 [NASA-CR-165585] p0044 A82-21253
- THRUST CONTROL**
NT THRUST VECTOR CONTROL
 V/STOL propulsion control technology
 [AIAA PAPER 81-2634] p0029 A82-16909
 Thrust modulation methods for a subsonic V/STOL aircraft
 [NASA-TM-82747] p0003 A82-13112
- THRUST DISTRIBUTION**
 Tests of a D vented thrust deflecting nozzle behind a simulated turbofan engine
 [NASA-CR-3508] p0006 A82-17122
 Inert gas ion thruster
 [NASA-CR-165521] p0044 A82-21252
- THRUST LOADS**
 Applications of the DOE/NASA wind turbine engineering information system
 p0122 A82-23696
- THRUST REVERSAL**
 Thrust reverser for a long duct fan engine --- for turbofan engines
 [NASA-CASE-LEW-13199-1] p0019 A82-26293
- THRUST VECTOR CONTROL**
 Effect of a part span variable inlet guide vane on TP34 fan performance
 [NASA-CR-165458] p0023 A82-12075
 A real time Pegasus propulsion system model for VSTOL piloted simulation evaluation
 [NASA-TM-82770] p0016 A82-13144
 Performance of a 2D-CD nonaxisymmetric exhaust nozzle on a turbojet engine at altitude
 [NASA-TM-82881] p0005 A82-26241
- THRUSTORS**
UCKET ENGINES
THUNDERSTORMS
 NASA research programs responding to workshop recommendations
 A82-21146
- TILTING ROTORS**
 A pad perturbation method for the dynamic coefficients of tilting-pad journal bearings
 p0110 A82-14400
- TIME**
NT FLIGHT TIME
TIME DIVISION MULTIPLE ACCESS
 30/20 GHz communications satellite multibeam antenna
 [AIAA 82-0449] p0079 A82-23486
 Dynamic switch matrix for the TDMA satellite switching system
 [AIAA 82-0458] p0085 A82-23494
 Baseband-processed SS-TDMA communication system architecture and design concepts
 [AIAA 82-0482] p0079 A82-23508
 Open-loop nanosecond-synchronization for wideband satellite communications
 p0036 A82-27224
 Wideband, high speed switch matrix development for SS-TDMA applications
 p0086 A82-43784
- TIME MARCHING**
 On the solution of creep induced buckling in general structure
 p0115 A82-39514
- TIME SERIES ANALYSIS**
 Illustration of a new test for detecting a shift in mean in precipitation series
 A82-13217
 Identification of multivariable high performance turbofan engine dynamics from closed loop data
 [NASA-TM-82785] p0076 A82-20339
- TIN COMPOUNDS**
NT TIN OXIDES
TIN OXIDES
 Electron beam induced damage in ITO coated Kapton --- Indium Tin Oxide
 p0159 A82-41546
 Secondary electron emission yields
 p0038 A82-14226
- TIP SPEED**
 Forward acoustic performance of a model turbofan designed for a high specific flow (QE-14)
 [NASA-TP-1968] p0152 A82-21036
- TIPS**
NT BLADE TIPS
- TIRES**
 Rolling resistance of electric vehicle tires from track tests

TITANATES

[NASA-TM-82836] p0124 N82-28786
On the road performance tests of electric test
vehicle for correlation with road load simulator
[NASA-TM-82900] p0127 N82-33829

TITANATES
NT BARIUM TITANATES

TITANIUM

Structural dynamics of shroudless, hollow, fan
blades with composite in-lays
[ASME PAPER 82-GT-284] p0022 A82-35456
Energy efficient engine shroudless, hollow fan
blade technology report
[NASA-CR-165586] p0024 N82-21196
Structural dynamics of shroudless, hollow fan
blades with composite in-lays
[NASA-TM-82816] p0018 N82-22266

TITANIUM ALLOYS

Interrelation of material microstructure,
ultrasonic factors, and fracture toughness of
two phase titanium alloy
[NASA-TM-82810] p0110 N82-20551
Method and apparatus for coating substrates using
lasers
[NASA-CASE-LEW-13526-1] p0059 N82-22347

TITANIUM COMPOUNDS

NT BARIUM TITANATES

TOLERANCES (PHYSIOLOGY)

NT RADIATION TOLERANCE

TOLLEMI-SCHLICHTING WAVES

Generation of instability waves at a leading edge
[NASA-TM-82835] p0087 N82-22453

TRONOMETRY

U PRESSURE MEASUREMENT

TOOLS

NT MILLING MACHINES

TOPOGRAPHY

Ion-beam-induced topography and surface diffusion
p0160 A82-46426

TORQUE

Small passenger car transmission test: Chevrolet
Malibu 200C transmission with lockup
[NASA-CR-165182] p0105 N82-16410
Small passenger car transmission test: Mercury
Lynx ATX transmission
[NASA-CR-165510] p0106 N82-24496

TORQUE MEASURING APPARATUS

U EQUIMETERS

TORQUEMETERS

A digital optical torquemeter for high rotational
speed applications
[NASA-TM-82914] p0095 N82-31664

TORSIONAL STRESS

Forced torsional properties of FMR composites with
varying nadic ester concentrations and
processing histories
p0051 A82-45630
Failure analysis of a tool steel torque shaft
[NASA-TM-82758] p0058 N82-11184

TOTAL ENERGY SYSTEMS

Develop and test fuel cell powered on-site
integrated total energy system. Phase 3:
Full-scale power plant development
[NASA-CR-165328] p0117 N82-13490
Technology development for phosphoric acid fuel
cell powerplant, phase 2
[NASA-CR-165426] p0131 N82-16482
Develop and test fuel cell powered on-site
integrated total energy systems. Phase 3:
Full-scale power plant development
[NASA-CR-165455] p0131 N82-16483

TOWERS

Effect of rotor configuration on guyed tower and
foundation designs and estimated costs for
intermediate site horizontal axis wind turbines
[NASA-TM-82804] p0121 N82-22649
Vibration analysis of three guyed tower designs
for intermediate size wind turbines
[NASA-CR-165589] p0137 N82-30709

TRACE CONTAMINANTS

An automated system for global atmospheric
sampling using B-747 airliners
[NASA-CR-165264] p0139 N82-13554

TRACTION

Regimes of traction in concentrated contact
lubrication
[ASME PAPER 81-LUB-16] p0107 A82-18431
Design study of a continuously variable roller
cone traction CVT for electric vehicles
[NASA-CR-159841] p0105 N82-12445

Traction contact performance evaluation at high
speeds
[NASA-CR-165226] p0105 N82-16409
Stress evaluations under rolling/sliding contacts
[NASA-CR-165561] p0113 N82-17521
Multicollar traction drive speed reducer:
Evaluation for automotive gas turbine engine
[NASA-TR-2027] p0101 N82-26679
The influence of surface dents and grooves on
traction in sliding EHD point contacts
[NASA-TM-82943] p0102 N82-32734

TRAINING SIMULATORS

NT FLIGHT SIMULATORS

TRAJECTORIES

NT ELECTRON TRAJECTORIES
NT MOON-EARTH TRAJECTORIES
NT PARTICLE TRAJECTORIES

TRANSCENDENTAL FUNCTIONS

NT PERIODIC FUNCTIONS

NT TANGENTS

TRANSDUCERS

NT PRESSURE SENSORS

TRANSFER FUNCTIONS

Pressure transfer function of a JT15D nozzle due
to acoustic and convected entropy fluctuations
[NASA-TM-82842] p0152 N82-22951

TRANSFER ORBITS

Mass driver reaction engine characteristics and
performance in earth orbital transfer missions
p0046 A82-18199

Propulsion system options for low-acceleration
orbit transfer
[AIAA PAPER 82-1196] p0047 A82-35056

Shuttle to GEO propulsion tradeoffs
[AIAA PAPER 82-1245] p0034 A82-35082

A small scale lunar launcher for early lunar
material utilization
p0032 A82-35617

Centaur capabilities for communications satellite
launches
[AIAA PAPER 82-0558] p0034 A82-36286

TRANSFORMERS

Preliminary design development of 100 KW rotary
power transfer device
[NASA-CR-165431] p0084 N82-23395
Component technology for space power systems
[NASA-TM-82928] p0082 N82-30474

TRANSORIZON RADIO PROPAGATION

A review of transhorizon propagation phenomena
p0079 A82-10679

TRANSIENT LOADS

NT SHOCK LOADS

TRANSIENT RESPONSE

Blade loss transient dynamic analysis of
turbomachinery
[AIAA PAPER 82-1057] p0030 A82-34982
Engine dynamic analysis with general nonlinear
finite element codes. II - Bearing element
implementation, overall numerical
characteristics and benchmarking
[ASME PAPER 82-GT-292] p0108 A82-35462
Transient catalytic combustor model
[NASA-CR-165324] p0129 N82-13507

TRANSISTOR CIRCUITS

A PWM transistor inverter for an ac electric
vehicle drive
p0085 A82-20744
A 10-kW series resonant converter design,
transistor characterization, and base-drive
optimization
p0086 A82-36927

Analysis of transistor and snubber turn-off
dynamics in high-frequency high-voltage
high-power converters
[NASA-CR-168760] p0084 N82-22438

TRANSISTORS

NT BIPOLAR TRANSISTORS
NT FIELD EFFECT TRANSISTORS
High voltage power transistor development
[NASA-CR-165547] p0084 N82-18506

TRANSITION METALS

NT CHROMIUM
NT COBALT
NT GOLD
NT IRON
NT NIOBIUM
NT PLATINUM
NT PLATINUM ISOTOPES
NT TANTALUM

- NT TITANIUM
NT IUNGSTEN
N^o ZINC
N^o ZIFCCNIUM
Adhesion and friction of single-crystal diamond in contact with transition metals p0103 A82-18680
- TRANSLATIONAL MOTION**
NT SECONDARY FLOW
NT THREE DIMENSIONAL FLOW
TRANSPLANAR SPACE
O TERPLANETARY SPACE
TRANSMISSION
NT ACOUSTIC PROPAGATION
NT CONDUCTIVE HEAT TRANSFER
NT CONVECTIVE HEAT TRANSFER
NT ELECTRIC POWER TRANSMISSION
NT FREQUENCY DIVISION MULTIPLE ACCESS
NT HEAT TRANSFER
NT LIGHT SCATTERING
NT MICROWAVE TRANSMISSION
NT MULTIPLEXING
NT RADIATIVE HEAT TRANSFER
NT SATELLITE TRANSMISSION
NT SHOCK WAVE PROPAGATION
NT SOUND TRANSMISSION
NT TRANSHORIZON RADIO PROPAGATION
NT WAVE PROPAGATION
Advances in high-speed rolling-element bearings [NASA-TM-82910] p0101 A82-28644
Precision of spiral-bevel gears [NASA-TP-82888] p0102 A82-30552
- TRANSMISSION EFFICIENCY**
Conversion and matched filter approximations for serial minimum-shift keyed modulation p0080 A82-26713
Small passenger car transmission test: Mercury Lynx ATX transmission [NASA-CR-165510] p0106 A82-24496
- TRANSMISSION LINES**
NT WAVEGUIDES
The 30/20 GHz communications satellite trunking network study [NASA-CR-165467] p0078 A82-13302
- TRANSMISSION LOSS**
A review of transhorizon propagation phenomena p0079 A82-10679
On the cause of the flat-spot phenomenon observed in silicon solar cells at low temperatures and low intensities --- in deep space environments p0043 A82-39599
- TRANSMISSIONS (MACHINE ELEMENTS)**
Design study of a continuously variable roller cone traction CVT for electric vehicles [NASA-CR-159841] p0105 A82-12445
Small passenger car transmission test: Chevrolet Malibu 200C transmission with lockup [NASA-CR-165182] p0105 A82-16410
Advanced Gas Turbine (AGT) powertrain system initial development report [NASA-CR-165130] p0132 A82-16485
Small passenger car transmission test: Mercury Lynx ATX transmission [NASA-CR-165510] p0106 A82-24496
Mathematical models for the synthesis and optimization of spiral bevel gear tooth surfaces --- for helicopter transmissions [NASA-CR-35531] p0106 A82-25516
Lutical effects on efficiency of a helicopter transmission [NASA-TM-82857] p0100 A82-25520
Multicoller traction drive speed reducer: Evaluation for automotive gas turbine engine [NASA-TP-2027] p0101 A82-26678
Tooth profile analysis of circular-cut, spiral-bevel gears [NASA-TM-82846] p0101 A82-26681
Reliability model for planetary gear [NASA-TM-82859] p0101 A82-28643
Kinematic precision of gear trains [NASA-TM-82887] p0102 A82-32733
- TRANSMITTANCE**
Free electron lasers for transmission of energy in space [NASA-CR-165520] p0098 A82-25499
- TRANSONIC AIRCRAFT**
U PERSONIC AIRCRAFT
TRANSONIC COMPRESSORS
Aerodynamic damping measurements in a transonic compressor [ASME PAPER 82-GT-287] p0012 A82-35459
Performance of single-stage axial-flow transonic compressor with rotor and stator aspect ratios of 1.63 and 1.78, respectively, and with design pressure ratio of 1.82 [NASA-TP-1974] p0017 A82-19222
- TRANSONIC FLOW**
A finite element formulation of Euler equations for the solution of steady transonic flows [AIAA PAPER 82-0062] p0009 A82-17759
An example of a solution to transonic equations for shock-free flow about a symmetric profile A82-26439
Application of a finite element algorithm for the solution of steady transonic Euler equations [AIAA PAPER 82-0970] p0010 A82-31939
A computational design method for transonic turbomachinery cascades [ASME PAPER 82-GT-117] p0022 A82-35348
Investigation of rotational transonic flows through ducts using a finite element scheme [AIAA PAPER 82-1267] p0012 A82-37711
High-speed laser anemometer system for intrarotor flow mapping in turbomachinery [NASA-TP-1663] p0095 A82-19521
Development of a locally mass flux conservative computer code for calculating 2-D viscous flow in turbomachines [NASA-CR-3539] p0007 A82-22214
Computer program for calculating full potential transonic, quasi-three-dimensional flow through a rotating turbomachinery blade row [NASA-TP-2030] p0005 A82-28247
- TRANSONIC FLUTTER**
Three-dimensional shock structure in a transonic flutter cascade p0006 A82-37937
- TRANSONIC INLETS**
U PERSONIC INLETS
TRANSONIC WIND TUNNELS
Development and utilization of a laser velocimeter system for a large transonic wind tunnel [NASA-TM-82886] p0095 A82-31663
Development of a laser velocimeter for a large transonic wind tunnel p0096 A82-32688
Seeding considerations for an LV system in a large transonic wind tunnel p0096 A82-32689
- TRANSONICS**
U ANSONIC FLOW
TRANSPARATION COOLING
U EAT COOLING
TRANSPONDERS
Cross-impact study of foreign satellite communications on NASA's 30/20 GHz program [NASA-CR-165154] p0078 A82-17420
- TRANSPORT AIRCRAFT**
NT BOEING 747 AIRCRAFT
NT DC 9 AIRCRAFT
NT DC 10 AIRCRAFT
NT SHORT HAUL AIRCRAFT
Propulsion study for Small Transport Aircraft Technology (STAT) [NASA-CR-165499] p0022 A82-10037
Propulsion study for Small Transport Aircraft Technology (STAT), Appendix B [NASA-CR-165499-APP-B] p0022 A82-10038
Study of advanced propulsion systems for Small Transport Aircraft Technology (STAT) program [NASA-CR-165610] p0026 A82-24202
- TRANSPORT COEFFICIENTS**
U ANSPORT PROPERTIES
TRANSPORT PROPERTIES
NT ELECTRICAL RESISTIVITY
NT THERMAL CONDUCTIVITY
NT VISCOSITY
Natural convection with combined driving forces p0093 A82-31445
Thermodynamic and transport combustion properties of hydrocarbons with air. Part 1: Properties in SI units [NASA-TP-1906] p0161 A82-32186
Thermodynamic and transport combustion properties of hydrocarbons with air. Part 2: Compositions corresponding to Kelvin temperature schedules in part 1 [NASA-TP-1907] p0161 A82-32187

- Thermodynamic and transport combustion properties of hydrocarbons with air. Part 3: Properties in US customary units
[NASA-TP-1908] p0161 N82-32188
- Thermodynamic and transport combustion properties of hydrocarbons with air. Part 4: Compositions corresponding to Rankine temperature schedules in part 3
[NASA-TP-1909] p0161 N82-32189
- TRANSPORT THEORY**
NT MIXING LENGTH FLOW THEORY
- TRANSPORTATION**
NT AIR TRANSPORTATION
NT SPACE SHUTTLE ORBITERS
NT SPACE TRANSPORTATION SYSTEM
Barriers to the utilization of synthetic fuels for transportation
[NASA-CR-165517] p0073 N82-13243
- TRANSURANIUM ELEMENTS**
NT PLUTONIUM 244
- TRAPATT DIODES**
U AVALANCHE DIODES
- TRAVELING WAVE TUBES**
Experimental verification of a computational procedure for the design of TWT-refocuser-MDC systems --- Multistage Depressed Collectors
p0082 N82-16128
Multistage depressed collector for dual mode operation --- for microwave transmitting tubes
[NASA-CASE-LEW-13282-1] p0081 N82-24415
Computer modeling of multiple-channel input signals and intermodulation losses caused by nonlinear traveling wave tube amplifiers
[NASA-TP-1999] p0082 N82-25441
- TRIBOLOGY**
Universal binding energy relations in metallic adhesion
[NASA-TM-82706] p0058 N82-11183
Application of surface analysis to solve problems of wear
[NASA-TM-82753] p0099 N82-14519
Geometrical aspects of the tribological properties of graphite fiber reinforced polyamide composites
[NASA-TM-82757] p0066 N82-15198
Elucidation of wear mechanisms by ferrographic analysis
[NASA-TM-82737] p0066 N82-15199
Tribological characteristics of a composite total-surface hip replacement
[NASA-TP-1853] p0066 N82-16239
Effects of artificially produced defects on film thickness distribution in sliding EHD point contacts
[NASA-TM-82732] p0099 N82-16412
Tribological properties at 25 C of seven polyamide films bonded to 440 C high-temperature stainless steel
[NASA-TP-1944] p0067 N82-19373
Tribological properties and XPS studies of ion plated gold on nickel and iron
[NASA-TM-82814] p0059 N82-22344
Tribological characteristics of nitrogen (N+) implanted iron
[NASA-TM-82839] p0060 N82-24322
Correlation of tensile and shear strengths of metals with their friction properties
[NASA-TM-82828] p0060 N82-24325
Tribological properties of sintered polycrystalline and single crystal silicon carbide
[NASA-TM-82829] p0068 N82-24343
Film shape calculations on supercomputers
[NASA-TM-82856] p0100 N82-25519
- TRIGGERS**
U TRUATONS
- TRIGONOMETRIC FUNCTIONS**
NT TANGENTS
- TROPOPAUSE**
Aircraft sampling of the sulfate layer near the tropopause following the eruption of Mount St. Helens
p0140 N82-37450
- TROPOSPHERIC SCATTERING**
A review of transhorizon propagation phenomena
p0079 N82-10679
- TROPOSPHERIC WAVES**
NT PLANETARY WAVES
- TRUNCATION (MATHEMATICS)**
U PROXIMATION
- TRUNKS (LINES)**
U TRANSMISSION LINES
- TRUCTIONS**
U APTS (MACHINE ELEMENTS)
- TRUSSES**
Primary propulsion/large space system interaction study
[NASA-CR-165277] p0044 N82-18315
- TUBING**
U PES (TUBES)
- TUNGSTEN**
Cesiation of W/001/ - Work function lowering by multiple dipole formation
A82-30002
Betrofit and acceptance test of 30-cm ion thrusters
[NASA-CR-165259] p0044 N82-12133
Tungsten fiber reinforced superalloy composite high temperature component design considerations
[NASA-TM-82811] p0049 N82-21259
- TUNNEL RESISTORS**
U ELECTRON TUNNELING
- TURBINE BLADES**
Thermal and flow analysis of a convection, air-cooled ceramic coated porous metal concept for turbine vanes
[ASME PAPER 81-HT-48] p0020 N82-10952
Aeroelastic characteristics of a cascade of mistuned blades in subsonic and supersonic flows
[ASME PAPER 81-DET-122] p0021 N82-19337
Improved plasma sprayed MCrAlY coatings for aircraft gas turbine applications
p0065 N82-20742
Effects of blade loading and rotation on compressor rotor wake in end wall regions
[AIAA PAPER 82-0193] p0010 N82-22063
Turbine blade nonlinear structural and life analysis
[AIAA PAPER 82-1056] p0021 N82-34981
A comprehensive method for preliminary design optimization of axial gas turbine stages
[AIAA PAPER 82-1264] p0030 N82-35091
The effect of rotor blade thickness and surface finish on the performance of a small axial flow turbine
[ASME PAPER 82-GT-222] p0022 N82-35409
Fabrication of turbine components and properties of sintered silicon nitride
[ASME PAPER 82-GT-252] p0071 N82-35431
Structural dynamics of shroudless, hollow, fan blades with composite in-lays
[ASME PAPER 82-GT-284] p0022 N82-35456
Fabrication of sinterable silicon nitride by injection molding
p0071 N82-37015
Winding for the wind
p0138 N82-37078
Aerodynamic performance of high turning core turbine vanes in a two-dimensional cascade
[AIAA PAPER 82-1288] p0005 N82-37716
Thermal-barrier-coated turbine blade study
[NASA-CR-165351] p0023 N82-10040
Creep shear behavior of the oxide dispersion strengthened superalloy MA 6000E
[NASA-TM-82704] p0058 N82-10195
Trends in high temperature gas turbine materials
[NASA-TM-82715] p0058 N82-11182
Progress in protective coatings for aircraft gas turbines: A Review of NASA sponsored research
[NASA-TM-82740] p0058 N82-12216
The effect of rotor blade thickness and surface finish on the performance of a small axial flow turbine
[NASA-TM-82726] p0003 N82-13114
Variable gain for a wind turbine pitch control
[NASA-TM-82751] p0119 N82-16478
Energy efficient engine shroudless, hollow fan blade technology report
[NASA-CR-165586] p0024 N82-21196
Tungsten fiber reinforced superalloy composite high temperature component design considerations
[NASA-TM-82811] p0049 N82-21259
Structural dynamics of shroudless, hollow fan blades with composite in-lays
[NASA-TM-82816] p0018 N82-22266
Thin film temperature sensors, phase 3 --- for engine-test evaluation
[NASA-CR-165476] p0097 N82-22479
Review of analysis methods for rotating systems with periodic coefficients
p0135 N82-23702

- Laser anemometer measurements in an annular cascade of core turbine vanes and comparison with theory
[NASA-TP-2018] p0004 N82-26234
- The design and instrumentation of the Purdue annular cascade facility with initial data acquisition and analysis
[NASA-CR-167861] p0008 N82-26237
- Fully plasma-sprayed compliant backed ceramic turbine seal
[NASA-CASE-LEW-13268-2] p0101 N82-26674
- Comparison of laser anemometer measurements and theory in an annular turbine cascade with experimental accuracy determined by parameter estimation
[NASA-TM-82860] p0005 N82-28250
- Past generation of three-dimensional computational boundary-conforming periodic grids of C-type --- for turbine blades and propellers
[NASA-CR-165596] p0009 N82-28253
- Method of protecting a surface with a silicon-slurry/aluminide coating --- coatings for gas turbine engine blades and vanes
[NASA-CASE-LEW-13343-1] p0068 N82-28441
- Fully plasma-sprayed compliant backed ceramic turbine seal
[NASA-CASE-LEW-13268-1] p0069 N82-29453
- Experience and assessment of the DOE-NASA Mod-1 2000-Kilowatt wind turbine generator at Boone, North Carolina
[NASA-TM-82721] p0125 N82-30710
- Advanced ceramic coating development for industrial/utility gas turbines
[NASA-CR-169952] p0065 N82-33494
- TURBINE ENGINES**
- NT BRISTOL-SIDDELEY BS 53 ENGINE
- NT GAS TURBINE ENGINES
- NT JET ENGINES
- NT TURBOFAN ENGINES
- NT TURBOJET ENGINES
- NT TURBOCOMPRESSOR ENGINES
- Interactive-graphic flowpath plotting for turbine engines
[NASA-TM-82756] p0017 N82-15041
- Elevated temperature fatigue testing of metals
[NASA-TM-82745] p0111 N82-16419
- Cooled variable-area radial turbine technology program
[NASA-CF-165408] p0024 N82-19221
- The role of modern control theory in the design of controls for aircraft turbine engines
[NASA-TM-82815] p0018 N82-22262
- Advanced general aviation engine/airframe integration study
[NASA-CF-165565] p0025 N82-22268
- Fracture mechanics criteria for turbine engine hot section components
[NASA-CF-167896] p0027 N82-25257
- Bird impact analysis package for turbine engine fan blades
[NASA-TM-82831] p0112 N82-26701
- Energy efficient engine: High pressure turbine uncooled rig technology report
[NASA-CR-165149] p0031 N82-32383
- TURBINE PUMPS**
- Advanced superposition methods for high speed turbopump vibration analysis
[NASA-CF-165379] p0104 N82-11465
- Liquid oxygen turbopump technology
[NASA-CR-165487] p0105 N82-11468
- TURBINE WHEELS**
- Net shape fabrication of Alpha Silicon Carbide turbine components
[ASME PAPER 82-GT-2161] p0071 N82-35403
- Fabrication of turbine components and properties of sintered silicon nitride
[ASME PAPER 82-GT-252] p0071 N82-35431
- Design and development of a ceramic radial turbine for the AGT101
[AIAA PAPER 82-1209] p0109 N82-35480
- Fatigue and creep-fatigue deformation of several nickel-base superalloys at 650 C
p0062 N82-47398
- TURBINES**
- NT AXIAL FLOW TURBINES
- NT GAS TURBINES
- NT STEAM TURBINES
- NT WIND TURBINES
- Analytic investigation of effect of end-wall contouring on stator performance
[NASA-TP-1943] p0003 N82-14051
- The NASA Lewis large wind turbine program
[NASA-TM-82761] p0119 N82-16495
- CF6 jet engine performance improvement: High pressure turbine active clearance control
[NASA-CR-165556] p0027 N82-28297
- Cooled variable nozzle radial turbine for rotor craft applications
[NASA-CR-165397] p0028 N82-29323
- Flow visualization study of the horseshoe vortex in a turbine stator cascade
[NASA-TP-1884] p0088 N82-30498
- Turbine endwall single cylinder program
[NASA-CR-169278] p0091 N82-31638
- The CF6 jet engine performance improvement: Low pressure turbine active clearance control
[NASA-CR-165557] p0029 N82-33393
- TURBOCOMPRESSORS**
- U PERCHARGERS
- U RBOCOMPRESSORS
- TURBOCOMPRESSORS**
- Water ingestion into jet engine axial compressors
[AIAA PAPER 82-0196] p0030 N82-17836
- Characteristics of the flow in the annulus-wall region of an axial-flow compressor rotor blade passage
[AIAA PAPER 82-0413] p0009 N82-17933
- Three dimensional flow field inside the passage of a low speed axial flow compressor rotor
[AIAA PAPER 82-1006] p0011 N82-31964
- Investigation of the tip-clearance flow inside and at the exit of a compressor rotor passage. I - Mean velocity field
[ASME PAPER 82-GT-12] p0011 N82-35281
- The use of optimization techniques to design controlled diffusion compressor blading
[ASME PAPER 82-GT-149] p0022 N82-35373
- The effect of rotor blade thickness and surface finish on the performance of a small axial flow turbine
[ASME PAPER 82-GT-222] p0022 N82-35409
- Progress in the development of energy efficient engine components
[ASME PAPER 82-GT-275] p0030 N82-35450
- The effect of rotor blade thickness and surface finish on the performance of a small axial flow turbine
[NASA-TM-82726] p0003 N82-13114
- The use of optimization techniques to design controlled diffusion compressor blading
[NASA-TM-82763] p0016 N82-14094
- Computer program for aerodynamic and blading design of multistage axial-flow compressors
[NASA-TP-1946] p0016 N82-15039
- Analytical investigation of nonrecoverable stall
[NASA-TM-82792] p0018 N82-21195
- Computer modeling of fan-exit-splitter spacing effects on F100 response to distortion
[NASA-CR-167879] p0025 N82-23246
- STGSK: A computer code for predicting multistage axial flow compressor performance by a meanline stage stacking method
[NASA-TP-2020] p0018 N82-25250
- Three dimensional mean velocity and turbulence characteristics in the annulus wall region of an axial flow compressor rotor passage
[NASA-CR-169003] p0026 N82-25252
- Core compressor exit stage study, volume 6
[NASA-CR-165553] p0027 N82-27310
- Advanced stratified charge rotary aircraft engine design study
[NASA-CR-165398] p0107 N82-27743
- TURBOCONVERTERS**
- U RBOGENERATORS
- TURBOELECTRIC CONVERSION**
- U RBOGENERATORS
- TURBOFAN ENGINES**
- NT BRISTOL-SIDDELEY BS 53 ENGINE
- NT TF-34 ENGINE
- An iterative finite element-integral technique for predicting sound radiation from turbofan inlets in steady flight
[AIAA PAPER 82-0124] p0030 N82-17796
- Comparison of two parallel/series flow turbofan propulsion concepts for supersonic V/STOL
[AIAA PAPER 81-2637] p0020 N82-19214

- Sensor failure detection system --- for the P100
turbofan engine
[NASA-CR-165515] p0023 N82-13145
- Tests of a D vented thrust deflecting nozzle
behind a simulated turbofan engine
[NASA-CR-3508] p0006 N82-17122
- CF6 jet engine performance improvement: High
pressure turbine roundness
[NASA-CR-165555] p0024 N82-17174
- Comparison of two parallel/series flow turbofan
propulsion concepts for supersonic V/STOL
[NASA-TM-82743] p0004 N82-18178
- Effects of fan inlet temperature disturbances on
the stability of a turbofan engine
[NASA-TM-82699] p0017 N82-18222
- Identification of multivariable high performance
turbofan engine dynamics from closed loop data
[NASA-TM-82785] p0076 N82-20339
- Forward acoustic performance of a model turbofan
designed for a high specific flow (QF-14)
[NASA-TP-1968] p0152 N82-21036
- V/STOL Tandem Fan transition section model test
--- in the Lewis Research Center 10-by-10 foot
wind tunnel
[NASA-CR-165507] p0007 N82-21158
- Energy efficient engine shroudless, hollow fan
blade technology report
[NASA-CR-165586] p0024 N82-21196
- Energy efficient engine exhaust mixer model
technology
[NASA-CR-165459] p0025 N82-22264
- Turbofan forced mixer-nozzle internal flowfield.
Volume 1: A benchmark experimental study
[NASA-CR-3492] p0090 N82-22458
- Turbofan forced mixer-nozzle internal flowfield.
Volume 2: Computational fluid dynamic predictions
[NASA-CR-3493] p0091 N82-22459
- Turbofan forced mixer-nozzle internal flowfield.
Volume 3: A computer code for 3-D mixing in
axisymmetric nozzles
[NASA-CR-3494] p0091 N82-22460
- Computer modeling of fan-exit-splitter spacing
effects on P100 response to distortion
[NASA-CR-167879] p0025 N82-23246
- Alternatives for jet engine control
[NASA-CR-168894] p0026 N82-23247
- Exhaust emissions survey of a turbofan engine for
flame holder swirl type augmentors at simulated
altitude flight conditions
[NASA-TM-82787] p0019 N82-25255
- Thrust reverser for a long duct fan engine --- for
turbofan engines
[NASA-CASE-LEW-13199-1] p0019 N82-26293
- Acoustic properties of turbofan inlets
[NASA-CR-169016] p0153 N82-27090
- Performance deterioration due to acceptance
testing and flight loads; JT90 jet engine
diagnostic program
[NASA-CR-165572] p0027 N82-27309
- Finite element-integral simulation of static and
flight fan noise radiation from the JT15D
turbofan engine
[NASA-TM-82936] p0152 N82-31068
- Rough analysis of installation effects on
turbo-prop noise
[NASA-TM-82924] p0152 N82-32082
- Automated procedure for developing hybrid computer
simulations of turbofan engines. Part 1:
General description
[NASA-TP-1851] p0146 N82-33020
- The CF6 jet engine performance improvement: Low
pressure turbine active clearance control
[NASA-CR-165557] p0029 N82-33393
- TURBOGENERATORS**
- Lewis Research Center's coal-fired, pressurized,
fluidized-bed reactor test facility
[NASA-TM-81616] p0087 N82-11397
- Aluminum Blade development for the Mod-0A
200-kilowatt wind turbine
[NASA-TM-82594] p0119 N82-14633
- New features and applications of PRESTO, a
computer code for the performance of
regenerative, superheated steam turbine cycles
[NASA-TP-1954] p0119 N82-16477
- Assessment of steam-injected gas turbine systems
and their potential application
[NASA-TM-82735] p0119 N82-18694
- Experience with modified aerospace reliability and
quality assurance method for wind turbines
[NASA-TM-82803] p0110 N82-19550
- TURBOJET ENGINE CONTROL**
- Performance of a 2D-CD nonaxisymmetric exhaust
nozzle on a turbojet engine at altitude
[NASA-TM-82881] p0005 N82-26241
- TURBOJET ENGINES**
- NT BRISTOL-SIDDELEY BS 53 ENGINE
- NT TURBOFAN ENGINES
- NT TURBOPROP ENGINES
- Development of high-speed rolling-element
bearings. A historical and technical perspective
[NASA-TM-82884] p0100 N82-24497
- Performance of a 2D-CD nonaxisymmetric exhaust
nozzle on a turbojet engine at altitude
[NASA-TM-82881] p0005 N82-26241
- Environmental and High-Strain Rate effects on
composites for engine applications
[NASA-TM-82882] p0051 N82-31449
- TURBOMACHINE BLADES**
- NT COMPRESSOR BLADES
- NT ROTOR BLADES (TURBOMACHINERY)
- NT STATOR BLADES
- NT TURBINE BLADES
- Vibrations of twisted rotating blades
[ASME PAPER 81-DET-127] p0115 N82-19341
- The influence of Coriolis forces on gyroscopic
motion of spinning blades
[ASME PAPER 82-GT-163] p0030 N82-35384
- Comparison of beam and shell theories for the
vibrations of thin turbomachinery blades
[ASME PAPER 82-GT-223] p0115 N82-35408
- Interaction of upstream flow distortions with high
Mach number cascades
[NASA-TM-82759] p0003 N82-12043
- Design of supercritical cascades with high solidity
[NASA-CR-165600] p0007 N82-22210
- An experimental investigation of gapwise
periodicity and unsteady aerodynamic response in
an oscillating cascade. I: Experimental and
theoretical results --- turbine blades
[NASA-CR-3513] p0008 N82-26229
- Computer program for calculating full potential
transonic, quasi-three-dimensional flow through
a rotating turbomachinery blade row
[NASA-TP-2030] p0005 N82-28247
- TURBOMACHINERY**
- NT AXIAL FLOW TURBINES
- NT CENTRIFUGAL COMPRESSORS
- NT CENTRIFUGAL PUMPS
- NT GAS TURBINES
- NT STEAM TURBINES
- NT TURBINE PUMPS
- NT TURBINES
- NT TURBOCOMPRESSORS
- NT TURBOGENERATORS
- NT WIND TURBINES
- AGT100 turbomachinery --- for automobiles
[AIAA PAPER 82-1207] p0108 N82-35061
- A computational design method for transonic
turbomachinery cascades
[ASME PAPER 82-GT-117] p0022 N82-35348
- High-speed laser anemometer system for intrarotor
flow mapping in turbomachinery
[NASA-TP-1663] p0095 N82-19521
- Composite seal for turbomachinery
[NASA-CASE-LEW-12131-3] p0099 N82-19540
- Development of a locally mass flux conservative
computer code for calculating 3-D viscous flow
in turbomachines
[NASA-CR-3539] p0007 N82-22214
- GRID3C: Computer program for generation of C type
multilevel, three dimensional and boundary
conforming periodic grids
[NASA-CR-167846] p0008 N82-26239
- Fully plasma-sprayed compliant backed ceramic
turbine seal
[NASA-CASE-LEW-13268-1] p0069 N82-29453
- TURBOPROP AIRCRAFT**
- A shock wave approach to the noise of supersonic
propellers
[NASA-TM-82752] p0151 N82-16809
- A preliminary comparison between the SR-3
propeller noise in flight and in a wind tunnel
[NASA-TM-82805] p0152 N82-21998
- Advanced turboprop testbed systems study. Volume
1: Testbed program objectives and priorities,
drive system and aircraft design studies,
evaluation and recommendations and wind tunnel
test plans

- [NASA-CR-167028-VOL-1] p0028 N82-32370
- TURBOPROP ENGINES**
- Propulsion study for Small Transport Aircraft Technology (STAT) [NASA-CR-165499] p0022 N82-10037
- Evaluation of wind tunnel performance testings of an advanced 45 deg swept 8-bladed propeller at Mach numbers from 0.45 to 0.85 [NASA-CR-3505] p0007 N82-19178
- Advanced general aviation comparative engine/airframe integration study [NASA-CR-165564] p0025 N82-22263
- Study of advanced propulsion systems for Small Transport Aircraft Technology (STAT) program [NASA-CR-165610] p0026 N82-24202
- Future propulsion opportunities for commuter airplanes [NASA-TM-82880] p0018 N82-24203
- Summary and recent results from the NASA advanced High Speed Propeller Research Program [NASA-TM-82891] p0001 N82-26219
- Propulsion opportunities for future commuter aircraft [NASA-TM-82915] p0019 N82-26298
- Rough analysis of installation effects on turbo-prop noise [NASA-TM-82924] p0152 N82-32082
- Advanced turbo-prop testbed systems study. Volume 1: Testbed program objectives and priorities, drive system and aircraft design studies, evaluation and recommendations and wind tunnel test plans [NASA-CR-167928-VOL-1] p0028 N82-32370
- Advanced turbo-prop testbed systems study [NASA-CR-167895] p0014 N82-33375
- TURBOPUMPS**
- U RBINE PUMPS**
- TURBOROTORS**
- U RBINE WHEELS**
- TURBULENCE**
- NT ISOTROPIC TURBULENCE**
- NT PLASMA TURBULENCE**
- Effect of location in an array on heat transfer to a cylinder in crossflow [NASA-TM-82797] p0087 N82-19493
- Three dimensional mean velocity and turbulence characteristics in the annulus wall region of an axial flow compressor rotor passage [NASA-CR-169003] p0026 N82-25252
- Laser anemometer using a Fabry-Perot interferometer for measuring mean velocity and turbulence intensity along the optical axis in turbomachinery [NASA-TM-82841] p0095 N82-28605
- Small axial turbine stator technology program [NASA-CR-165602] p0028 N82-32367
- Turbulent solution of the Navier-Stokes equations for uniform shear flow [NASA-TM-82925] p0089 N82-32634
- TURBULENCE BOUNDARY LAYER**
- Turbulent boundary layer heat transfer experiments - A separate effects study on a convexly-curved wall [ASME PAPER 81-HT-78] p0092 A82-10963
- Three dimensional turbulent boundary layer development on a fan rotor blade [AIAA PAPER 82-1007] p0011 A82-31965
- Turbulent boundary layer heat transfer experiments: Convex curvature effects including introduction and recovery [NASA-CR-3510] p0090 N82-17456
- TURBULENCE FLOW**
- NT CAVITATION FLOW**
- On the prediction of swirling flowfields found in axisymmetric combustor geometries p0029 A82-12120
- Distorted turbulence in axisymmetric flow p0089 A82-16071
- Secondary effects in combustion instabilities leading to flashback [AIAA PAPER 82-0037] p0056 A82-17746
- Characteristics of the flow in the annulus-wall region of an axial-flow compressor rotor blade passage [AIAA PAPER 82-0413] p0009 A82-17933
- Time resolved density measurements in premixed turbulent flames [AIAA PAPER 82-0036] p0056 A82-22033
- Numerical analysis of confined turbulent flow p0093 A82-24748
- Numerical modelling of turbulent flow in a combustion tunnel p0093 A82-27000
- Numerical modeling of turbulent combustion in premixed gases p0056 A82-28708
- Three sensor hot wire/film technique for three dimensional mean and turbulence flow field measurement p0097 A82-30300
- Three-dimensional flow field in the tip region of a compressor rotor passage. II - Turbulence properties [ASME PAPER 82-GT-234] p0011 A82-35416
- Analysis of the decay of temperature fluctuations in isotropic turbulence p0089 A82-40781
- Investigations of flowfields found in typical combustor geometries [NASA-CR-168585] p0090 N82-19495
- Mass and momentum turbulent transport experiments with confined coaxial jets [NASA-CR-165574] p0090 N82-19496
- Turbofan forced mixer-nozzle internal flowfield. Volume 3: A computer code for 3-D mixing in axisymmetric nozzles [NASA-CR-3494] p0091 N82-22460
- Three dimensional flow field inside compressor rotor, including blade boundary layers [NASA-CR-169120] p0031 N82-27686
- Experimental study of turbulence in blade end wall corner region [NASA-CR-169283] p0091 N82-31639
- Flow process in combustors [NASA-CR-169294] p0092 N82-31642
- TURBULENCE JETS**
- Turbulence measurements in a confined jet using a six-orientation hot-wire probe technique [AIAA PAPER 82-1262] p0094 A82-37710
- TURBULENCE MIXING**
- Mass and momentum turbulent transport experiments with confined coaxial jets [NASA-CR-165574] p0090 N82-19496
- TURBULENCE WAKES**
- NT PROPELLER SLIPSTREAMS**
- Interaction of compressor rotor blade wake with wall boundary layer/vortex in the end-wall region [ASME PAPER 81-GT-1] p0010 A82-19301
- Effects of blade loading and rotation on compressor rotor wake in end wall regions [AIAA PAPER 82-0193] p0010 A82-22063
- Measurement and prediction of mean velocity and turbulence structure in the near wake of an airfoil p0010 A82-26137
- Numerical analysis and FORTRAN program for the computation of the turbulent wakes of turbomachinery rotor blades, isolated airfoils and cascade of airfoils [NASA-CR-3509] p0006 N82-18184
- TVC (CONTROL)**
- U RUST VECTOR CONTROL**
- TWINNING**
- NT MECHANICAL TWINNING**
- TWISTING**
- Vibrations of twisted rotating blades [ASME PAPER 81-DET-127] p0115 A82-19341
- TWO DIMENSIONAL FLOW**
- Numerical analysis of confined turbulent flow p0093 A82-24748
- An example of a solution to transonic equations for shock-free flow about a symmetric profile A82-26439
- Investigation of rotational transonic flows through ducts using a finite element scheme [AIAA PAPER 82-1267] p0012 A82-37711
- Aerodynamic performance of high turning core turbine vanes in a two-dimensional cascade [AIAA PAPER 82-1288] p0005 A82-37716
- Aerodynamic performance of high turning core turbine vanes in a two dimensional cascade [NASA-TM-82894] p0004 N82-26240
- Flow visualization study of the horseshoe vortex in a turbine stator cascade [NASA-TP-1884] p0088 N82-30498
- TWO PHASE FLOW**
- Toward the use of similarity theory in two-phase

choked flows p0089 A82-16570
Two dimensional stagnation point flow of a dusty
gas near an oscillating plate p0012 A82-37535
Flows through sequential orifices with heated
spacer reservoirs p0088 A82-24455
[NASA-TM-82855]
The dryout region in frictionally heated sliding
contacts p0088 A82-28574
[NASA-TM-82796]
TWO REFLECTOR ANTENNAS
Focal surfaces of offset dual-reflector antennas p0080 A82-36265

U

UDINET ALLOYS
Effects of cobalt on the microstructure of Udimet
700 p0064 A82-28409
[NASA-CF-165605]
ULTRAHIGH VACUUM
Anaerobic polymers as high vacuum leak sealants p0108 A82-21967
ULTRASONIC DENSIMETERS
Ultrasonic velocity for estimating density of
structural ceramics p0066 A82-14359
[NASA-TM-82765]
ULTRASONIC FLAW DETECTION
Acoustic microscopy of silicon carbide materials p0075 A82-33031
On ultrasonic factors and fracture toughness p0116 A82-42863
ULTRASONIC RADIATION
Ultrasonic input-output for transmitting and
receiving longitudinal transducers coupled to
same face of isotropic elastic plate p0110 A82-18613
[NASA-CF-3506]
ULTRASONIC TESTS
Ultrasonic velocity for estimating density of
structural ceramics p0066 A82-14359
[NASA-TM-82765]
Interrelation of material microstructure,
ultrasonic factors, and fracture toughness of
two phase titanium alloy p0110 A82-20551
[NASA-TM-82810]
Ultrasonic scanning system for imaging flaw growth
in composites p0076 A82-22386
[NASA-TM-E2799]
ULTRASONIC WAVES
ULTRASONIC RADIATION
ULTRAVIOLET RADIATION
NT FAB ULTRAVIOLET RADIATION
ULTRAVIOLET SPECTRA
Ultraviolet observations of the 1980 eclipse of
the symbiotic star CI Cygni p0082 A82-27331
UNDERGROUND STRUCTURES
Assessment of a 40-kilowatt stirling engine for
underground mining applications p0125 A82-30714
[NASA-TM-82822]
UNIFORM FLOW
NT ELASIOUS FLOW
Conversion of acoustic energy by lossless liners p0154 A82-36195
Turbulent solution of the Navier-Stokes equations
for uniform shear flow p0089 A82-32634
[NASA-TM-82925]
UNIPOLAR TRANSISTORS
U FLD EFFECT TRANSISTORS
UNITED STATES OF AMERICA
NT KENTUCKY
UNLOADING WAVES
Indentation law for composite laminates p0052 A82-15123
[NASA-CR-165460]
UNSTEADY FLOW
NT OSCILLATING FLOW
Solutions of the compressible Navier-Stokes
equations using the integral method p0093 A82-23832
[AIAA PAPER 81-0046]
An experimental investigation of gapwise
periodicity and unsteady aerodynamic response in
an oscillating cascade. 1: Experimental and
theoretical results --- turbine blades p0008 A82-26229
[NASA-CR-3513]
UPPER ATMOSPHERE
NT MESOSPHERE
UPSTREAM
Interaction of upstream flow distortions with high

Mach number cascades p0003 A82-12043
[NASA-TM-82759]
USER MANUALS (COMPUTER PROGRAMS)
Spherical roller bearing analysis. SKF computer
program SPHERBEAN. Volume 2: User's manual p0106 A82-20541
[NASA-CR-165204]
High speed cylindrical roller bearing analysis.
SKF computer program CYBEAN. Volume 2: User's
manual p0146 A82-31968
[NASA-CR-165364]
Research report: User's manual for computer
program AT81Y005. PLANETSYS, a computer program
for the steady state and transient thermal
analysis of a planetary power transmission system p0146 A82-31970
[NASA-CR-165366]

UTILITIES

Interfacing wind energy conversion equipment with
utility systems A82-21148
Evaluation of present thermal barrier coatings for
potential service in electric utility gas turbines
[NASA-CR-165545] p0063 A82-18368
Phosphoric acid fuel cell technology status p0120 A82-19670
[NASA-TM-82791]

UTILIZATION

NT COAL UTILIZATION
NT LASER APPLICATIONS
NT WASTE ENERGY UTILIZATION
NT WINDPOWER UTILIZATION

V

V BAND

U TREMELY HIGH FREQUENCIES

V GROOVES

High voltage V-groove solar cell p0123 A82-24717
[NASA-CASE-LEM-13401-2]

V/STOL AIRCRAFT

NT HELICOPTERS

NT VERTICAL TAKEOFF AIRCRAFT

V/STOL propulsion control technology p0029 A82-16909
[AIAA PAPER 81-2634]
Comparison of two parallel/series flow turbofan
propulsion concepts for supersonic V/STOL p0020 A82-19214
[AIAA PAPER 81-2637]
A real time Pegasus propulsion system model for
VSTOL piloted simulation evaluation p0020 A82-19221
[AIAA PAPER 81-2663]
Experimental and analytical results of tangential
blowing applied to a subsonic V/STOL inlet p0005 A82-35195
[AIAA PAPER 82-1084]
A summary of V/STOL inlet analysis methods p0006 A82-40921

Low speed testing of the inlets designed for a
tandem-fan V/STOL nacelle --- conducted in the
Lewis 10 by 10 foot wind tunnel p0003 A82-11042
[NASA-TM-82728]

A summary of V/STOL inlet analysis methods p0003 A82-11043
[NASA-TM-82725]

Thrust modulation methods for a subsonic V/STOL
aircraft p0003 A82-13112
[NASA-TM-82747]

A real time Pegasus propulsion system model for
VSTOL piloted simulation evaluation p0016 A82-13144
[NASA-TM-82770]

Comparison of two parallel/series flow turbofan
propulsion concepts for supersonic V/STOL p0004 A82-18178
[NASA-TM-82743]

V/STOL Tandem Fan transition section model test
--- in the Lewis Research Center 10-by-10 foot
wind tunnel p0007 A82-21158
[NASA-CR-165587]

Experimental and analytical results of tangential
blowing applied to a subsonic V/STOL inlet p0004 A82-24165
[NASA-TM-82847]

A summary of V/STOL inlet analysis methods p0005 A82-28249
[NASA-TM-82885]

VACANCIES (CRYSTAL DEFECTS)

On the cause of the flat-spot phenomenon observed
in silicon solar cells at low temperatures and
low intensities p0126 A82-31777
[NASA-TM-82903]

VACUUM

NT HIGH VACUUM

NT ULTRAHIGH VACUUM

VACUUM APPARATUS

NT MOLECULAR PUMPS

VACUUM DEPOSITION

Refractory coatings and method of producing the same

- [NASA-CASE-LEW-13169-1] p0060 N82-29415
- VACUUM SYSTEMS**
Effect of vacuum exhaust pressure on the performance of MHD ducts at high B-field
[AIAA PAPER 82-0295] p0157 A82-20292
Effect of vacuum exhaust pressure on the performance of MHD ducts at high D-field
[NASA-TM-82750] p0157 N82-13902
- VACUUM PUMPS**
NT MOLECULAR PUMPS
- VACUUM TUBE OSCILLATORS**
NT KLYSTRONS
NT MAGNETRONS
NT TRAVELING WAVE TUBES
- VACUUM TUBES**
NT KLYSTRONS
NT MAGNETRONS
NT TRAVELING WAVE TUBES
- VACUUM ULTRAVIOLET RADIATION**
U R ULTRAVIOLET RADIATION
- WADMIUM COMPOUNDS**
Moderate temperature Na colls. III -
Electrochemical and structural studies of
CrO₂·5VO₂·5S₂ and its Na intercalates
p0055 A82-15732
- VANES**
NT GUIDE VANES
NT JET VANES
Aerodynamic performance of high turning core turbine vanes in a two-dimensional cascade
[AIAA PAPER 82-1288] p0005 A82-37716
Gas turbine ceramic-coated-vane concept with convection-cooled porous metal core
[NASA-TP-1942] p0016 N82-14090
Method of protecting a surface with a silicon-nitride/aluminate coating --- coatings for gas turbine engine blades and vanes
[NASA-CASE-LEW-13343-1] p0068 N82-28441
- VAPOR DEPOSITION**
NT VACUUM DEPOSITION
Experimental and theoretical studies of the laws governing condensate deposition from combustion gases
p0057 A82-28709
An experimental study of airfoil icing characteristics
[NASA-TM-82790] p0001 N82-17083
- VAPOR GENERATORS**
U PORIZERS
- VAPOR PHASE EPITAXY**
OM-VPE growth of Mg-doped GaAs --- Organometallic-Vapor Phase Epitaxy
p0159 A82-38411
- VAPOR PHASES**
Transient catalytic combustor model
[NASA-CR-165324] p0129 N82-13507
- VAPORIZERS**
Experimental study of external fuel vaporization
[ASME PAPER 82-GT-59] p0075 A82-35312
Retrofit and acceptance test of 30-cm ion thrusters
[NASA-CF-165259] p0044 N82-12133
- VAPORIZING**
NT BOILING
NT COAL GASIFICATION
NT FLASHING (VAPORIZING)
NT PROPELLANT EVAPORATION
Electrostatic fuel conditioning of internal combustion engines
[NASA-CF-169029] p0106 N82-26680
- VAPORS**
High-speed motion picture camera experiments of cavitation in dynamically loaded journal bearings
[NASA-TM-82798] p0100 N82-20543
- VARIABLE CYCLE ENGINES**
V/SICL Tandem Fan transition section model test --- in the Lewis Research Center 10-by-10 foot wind tunnel
[NASA-CR-165587] p0007 N82-21158
- VARIABLE GEOMETRY STRUCTURES**
Pollution reduction technology program small jet aircraft engines, phase 3
[NASA-CF-165386] p0023 N82-14095
- VARIANCE (STATISTICS)**
NT BIVARIATE ANALYSIS
NT MULTIVARIATE STATISTICAL ANALYSIS
- VARIATIONS**
NT ANNUAL VARIATIONS
NT MAGNETIC VARIATIONS
- VASCULAR SYSTEM**
NT AORTA
- VCM**
U RIABLE CYCLE ENGINES
- VECTOR ANALYSIS**
Acceleration of convergence of vector sequences
[NASA-TM-82931] p0149 N82-29075
- VECTOR SPACES**
NT EIGENVALUES
NT EIGENVECTORS
NT MATRICES (MATHEMATICS)
NT VECTORS (MATHEMATICS)
- VECTORS (MATHEMATICS)**
NT EIGENVECTORS
Acceleration of convergence of vector sequences
[NASA-TM-82931] p0149 N82-29075
- VELOCITY**
NT ACOUSTIC VELOCITY
NT FLOW VELOCITY
NT HIGH SPEED
NT PROPAGATION VELOCITY
NT ROTOR SPEED
NT SUBSONIC SPEED
NT SUPERSONIC SPEEDS
NT TIP SPEED
NT WIND VELOCITY
Small passenger car transmission test: Chevrolet Malibu 200C transmission with lockup
[NASA-CR-165182] p0105 N82-16410
Small passenger car transmission test: Mercury Lynx ATX transmission
[NASA-CR-165510] p0106 N82-24496
- VELOCITY COUPLING**
Coupled cavity traveling wave tube with velocity tapering
[NASA-CASE-LEW-12296-1] p0082 N82-26568
- VELOCITY DISTRIBUTION**
The effect of inflow velocity profiles on the performance of supersonic ejector nozzles
[AIAA PAPER 81-0273] p0002 A81-32548
Multigrad simulation of asymptotic curved-duct flows using a semi-implicit numerical technique
p0010 A82-29003
Three dimensional turbulent boundary layer development on a fan rotor blade
[AIAA PAPER 82-1007] p0011 A82-31965
Investigation of the tip-clearance flow inside and at the exit of a compressor rotor passage. I - Mean velocity field
[ASME PAPER 82-GT-12] p0011 A82-35281
Velocity gradient method for calculating velocities in an axisymmetric annular duct
[NASA-TP-2029] p0005 N82-29270
Development and utilization of a laser velocimeter system for a large transonic wind tunnel
[NASA-TM-82886] p0095 N82-31663
- VELOCITY FIELDS**
U LOCITY DISTRIBUTION
- VELOCITY MEASUREMENT**
Measurement and prediction of mean velocity and turbulence structure in the near wake of an airfoil
p0011 A82-26137
The velocity field near the orifice of a Helmholtz resonator in grazing flow
[NASA-CR-168548] p0153 N82-18994
Comparison of laser anemometer measurements and theory in an annular turbine cascade with experimental accuracy determined by parameter estimation
[NASA-TM-82860] p0005 N82-28250
Laser anemometer using a Fabry-Perot interferometer for measuring mean velocity and turbulence intensity along the optical axis in turbomachinery
[NASA-TM-82841] p0095 N82-28605
Development and utilization of a laser velocimeter system for a large transonic wind tunnel
[NASA-TM-82886] p0095 N82-31663
- VELOCITY PROFILES**
U LOCITY DISTRIBUTION
- VENTURI TUBES**
Venturi nozzle effects on fuel drop size and nitrogen oxide emissions
[NASA-TP-2028] p0020 N82-31329
- VERTICAL TAKEOFF AIRCRAFT**
Aerodynamic analysis of VTOL inlets and definition of a short, blowing-lip inlet
[NASA-CR-165617] p0007 N82-22211

C-4

VIBRATION

NT PENDING VIBRATION
 NT FLUTTER
 NT FORCED VIBRATION
 NT FREE VIBRATION
 NT RESONANT VIBRATION
 NT STRUCTURAL VIBRATION
 NT TRANSONIC FLUTTER
 VIBRATION DAMPERS
 U ERATION ISOLATORS
 VIBRATION DAMPING
 Aerodynamic damping measurements in a transonic
 compressor
 [ASME PAPER 82-GT-287] p0012 A82-35459
 Analysis of high load dampers
 [NASA-CR-165503] p0026 A82-23248
 VIBRATION ISOLATORS
 Analysis of high load dampers
 [NASA-CR-165503] p0026 A82-23248
 VIBRATION MODE
 Vibrations of twisted rotating blades
 [ASME PAPER 81-DET-127] p0115 A82-19341
 Nonlinear analysis of rotor-bearing systems using
 component mode synthesis
 [ASME PAPER 82-GT-303] p0104 A82-35468
 Advanced superposition methods for high speed
 turbopump vibration analysis
 [NASA-CR-165379] p0104 A82-11465
 VIBRATION PROTECTION
 U ERATION ISOLATORS
 VIBRATION TESTS
 Vibration analysis of three quayed tower designs
 for intermediate size wind turbines
 [NASA-CR-165589] p0137 A82-30709
 VISCOELASTIC FLOW
 U SCOELASTICITY
 VISCOELASTICITY
 NT THERMOVISCOELASTICITY
 Motion of a rigid punch at the boundary of an
 orthotropic viscoelastic half-plane
 A82-26436
 VISCOPLASTIC FLOW
 U SCOPLASTICITY
 VISCOPLASTICITY
 On a study of the $\Delta T/c$ and $C/asterisk/$
 integrals for fracture analysis under non-steady
 creep
 p0115 A82-36782
 Research and development program for non-linear
 structural modeling with advanced
 time-temperature dependent constitutive
 relationships
 [NASA-CR-165533] p0024 A82-16080
 Nonlinear constitutive theory for turbine engine
 structural analysis
 p0112 A82-33744
 VISCOSITY
 Some observations in high pressure rheology of
 lubricants
 [ASME PAPER 81-LUB-17] p0070 A82-18432
 Some observations in high pressure rheology of
 lubricants
 [ASME PAPER 81-LUB-17] p0070 A82-18432
 VISCOUS FLOW
 NT BOUNDARY LAYER FLOW
 NT BOUNDARY LAYER SEPARATION
 NT SECONDARY FLOW
 NT SEPARATED FLOW
 A study of viscous flow in stator and rotor passages
 [ASME PAPER 82-GT-248] p0011 A82-35427
 Computational methods for internal flows with
 emphasis on turbomachinery
 [NASA-TM-82764] p0003 A82-13113
 Development of a locally mass flux conservative
 computer code for calculating 3-D viscous flow
 in turbomachines
 [NASA-CR-3539] p0007 A82-22214
 A new numerical approach for compressible viscous
 flows
 [NASA-CR-168842] p0090 A82-22455
 The design and instrumentation of the Purdue
 annular cascade facility with initial data
 acquisition and analysis
 [NASA-CR-167861] p0008 A82-26237
 VISUALIZATION OF FLOW
 U OW VISUALIZATION
 VOLATILIZATION
 U ERIZING

VOLCANOES

Aircraft sampling of the sulfate layer near the
 tropopause following the eruption of Mount St.
 Helens
 p0140 A82-37450
 VOLT-AMPERE CHARACTERISTICS
 Numerical simulation of sheath structure and
 current-voltage characteristics of a
 conductor-dielectric disk in a plasma
 p0040 A82-15904
 End region and current consolidation effects upon
 the performance of an HD channel for the ETF
 conceptual design --- Engineering Test Facility
 [AIAA PAPER 82-0325] p0157 A82-17889
 Impedance conversion using quantum limit
 nonreciprocity for
 superconductor-insulator-superconductor mixer
 compensation
 p0159 A82-31276
 Advances in high output voltage silicon solar cells
 p0127 A82-44942
 On the cause of the flat spot phenomenon observed
 in silicon solar cells at low temperatures and
 low intensities
 p0044 A82-44965
 Modeling the full-bridge series-resonant power
 converter
 p0086 A82-46385

VOLTAGE

U ECTRIC POTENTIAL
 VOLTAGE CONVERTERS (DC TO DC)
 A new approach to the minimum weight/loss design
 of switching power converters
 p0082 A82-16831
 High-frequency high-voltage high-power DC-to-DC
 converters
 p0083 A82-12347
 Modeling and Analysis of Power Processing Systems
 (MAPPS). Volume I: Technical report
 [NASA-CR-165538] p0083 A82-14447
 Simplified dc to dc converter
 [NASA-CASE-LEW-13495-1] p0082 A82-24432
 VOLTAGE GENERATORS
 NT PHOTOVOLTAIC CELLS
 VOLTAGE REGULATORS
 Modeling and Analysis of Power Processing Systems
 (MAPPS). Volume I: Technical report
 [NASA-CR-165538] p0083 A82-14447
 VORTEX COLUMNS
 U RTICES
 VORTEX DISTURBANCES
 U RTICES
 VORTEX FLOW
 U RTICES
 VORTEX TUBES
 U RTICES
 VORTICES
 Propeller tip vortex - A possible contributor to
 aircraft cabin noise
 p0152 A82-17603
 Application of a finite element algorithm for the
 solution of steady transonic Euler equations
 [AIAA PAPER 82-0970] p0010 A82-31939
 Flow visualization study of the horseshoe vortex
 in a turbine stator cascade
 [NASA-TP-1884] p0088 A82-30498
 Turbine endwall single cylinder program
 [NASA-CR-169278] p0091 A82-31638
 Flow process in combustors
 [NASA-CR-169294] p0092 A82-31642
 VTOL AIRCRAFT
 U RTICAL TAKEOFF AIRCRAFT

W

WAFERS

Method of making a high voltage V-groove solar cell
 [NASA-CASE-LEW-13401-1] p0124 A82-29709
 Development of a large area space solar cell
 assembly
 [NASA-CR-167929] p0137 A82-30706
 High voltage planar multijunction solar cell
 [NASA-CASE-LEW-13400-1] p0125 A82-31764
 WAKES
 NT LAMINAR WAKES
 NT NEAR WAKES
 NT PROPELLER SLIPSTREAMS
 NT TURBULENT WAKES

- The NASA-LeRC wind turbine sound prediction code
p0123 N82-23730
- WALL FLOW**
Turbulent boundary layer heat transfer experiments
- A separate effects study on a convexly-curved wall
[ASME PAPER 81-HT-78] p0092 A82-10963
Heat transfer in cooled porous region with curved boundary
p0089 A82-14848
Interaction of compressor rotor blade wake with wall boundary layer/vortex in the end-wall region
[ASME PAPER 81-GR/GT-1] p0010 A82-19301
Effects of blade loading and rotation on compressor rotor wake in end wall regions
[AIAA PAPER 82-2193] p0010 A82-22063
Numerical analysis of confined turbulent flow
p0093 A82-24748
Three-dimensional flow field in the tip region of a compressor rotor passage. I - Mean velocity profiles and annulus wall boundary layer
[ASME PAPER 82-GT-11] p0011 A82-35280
Three-dimensional flow field in the tip region of a compressor rotor passage. II - Turbulence properties
[ASME PAPER 82-GT-234] p0011 A82-35416
Analytic investigation of effect of end-wall contouring on stator performance
[NASA-TP-1943] p0003 N82-14051
Development of a simplified procedure for thrust chamber life prediction
[NASA-CF-165585] p0044 N82-21253
Three dimensional mean velocity and turbulence characteristics in the annulus wall region of an axial flow compressor rotor passage
[NASA-CR-169003] p0026 N82-25252
Comparison of experimental and analytical performance for contoured endwall stators
[NASA-TM-82877] p0019 N82-26299
Velocity gradient method for calculating velocities in an axisymmetric annular duct
[NASA-TP-2029] p0005 N82-29270
- WALL PRESSURE**
A simplified design procedure for life prediction of rocket thrust chambers
[AIAA PAPER 82-1251] p0043 A82-35087
Experimental study of turbulence in blade end wall corner region
[NASA-CF-169283] p0091 N82-31639
- WALL TEMPERATURE**
A heat exchanger computational procedure for temperature-dependent fouling
[ASME PAPER 81-HT-75] p0092 A82-10961
Tube entrance heat transfer with deposit formation
[AIAA PAPER 82-0918] p0093 A82-31908
- WALLS**
NT NOZZLE WALLS
NT FOCUS WALLS
NT THIN WALLS
- WASHEL ENGINES**
Advanced general aviation engine/airframe integration study
[NASA-CR-165565] p0025 N82-22268
Real time pressure signal system for a rotary engine
[NASA-CASE-LEW-13622-1] p0019 N82-26294
Advanced stratified charge rotary aircraft engine design study
[NASA-CR-165398] p0107 N82-27743
- WARNING**
U ATING
- WASPALLOY**
Microstructural effects on the room and elevated temperature low cycle fatigue behavior of Waspalloy
[NASA-CR-165497] p0113 N82-26702
- WASTE DISPOSAL**
Feasibility of an earth-to-space rail launcher system --- emphasizing nuclear waste disposal application
[IAF PAPER 82-46] p0033 A82-44659
- WASTE ENERGY UTILIZATION**
Collection and dissemination of thermal energy storage system information for the pulp and paper industry
p0136 N82-24686
- WASTES**
NT INDUSTRIAL WASTES
NT RADIOACTIVE WASTES
- WATER CONTENT**
U ISTURE CONTENT
- WATER FLOW**
Dynamics of snow cover in mountain regions of the Aral Sea basin, studied using satellite photographs
A82-27462
- WAVE ATTENUATION**
NT ACOUSTIC ATTENUATION
NT SHOCK WAVE ATTENUATION
- WAVE DIFFRACTION**
Diffraction by a finite strip
p0150 A82-33605
- WAVE DISPERSION**
Investigation of a comb-type slow-wave structure for millimeter-wave masers
A82-18368
- WAVE EQUATIONS**
Effects of internal heat transfer on the structure of self-similar blast waves
p0093 A82-32225
Diffraction by a finite strip
p0150 A82-33605
The transmission or scattering of elastic waves by an inhomogeneity of simple geometry: A comparison of theories
[NASA-CR-169034] p0079 N82-26526
- WAVE INTERACTION**
NT SHOCK WAVE INTERACTION
Coupled cavity traveling wave tube with velocity tapering
[NASA-CASE-LEW-12296-1] p0082 N82-26568
- WAVE PROPAGATION**
NT ACOUSTIC PROPAGATION
NT LIGHT SCATTERING
NT SHOCK WAVE PROPAGATION
Methods for the calculation of axial wave numbers in lined ducts with mean flow
p0153 A82-14044
Generation of instability waves at a leading edge
[NASA-TM-82835] p0087 N82-22453
The transmission or scattering of elastic waves by an inhomogeneity of simple geometry: A comparison of theories
[NASA-CR-169034] p0079 N82-26526
- WAVE SCATTERING**
NT LIGHT SCATTERING
NT RAMAN SPECTRA
NT RAYLEIGH SCATTERING
NT TROPOSPHERIC SCATTERING
The transmission or scattering of elastic waves by an inhomogeneity of simple geometry: A comparison of theories
[NASA-CR-169034] p0079 N82-26526
- WAVEFORMS**
Ultrasonic input-output for transmitting and receiving longitudinal transducers coupled to same face of isotropic elastic plate
[NASA-CR-3506] p0110 N82-18613
- WAVEGUIDES**
Coupled cavity traveling wave tube with velocity tapering
[NASA-CASE-LEW-12296-1] p0082 N82-26568
- WEAR**
Application of surface analysis to solve problems of wear
[NASA-TM-82753] p0099 N82-4519
Elucidation of wear mechanisms by ferrographic analysis
[NASA-TM-82737] p0066 N82-15199
Effects of artificially produced defects on film thickness distribution in sliding EHD point contacts
[NASA-TM-82732] p0099 N82-16412
Tribological properties at 25 C of seven polyimide films bonded to 440 C high-temperature stainless steel
[NASA-TP-1944] p0067 N82-19373
Surface chemistry and wear behavior of single-crystal silicon carbide sliding against iron at temperatures to 1500 C in vacuum
[NASA-TP-1947] p0067 N82-19374
Friction wear and auger analysis of iron implanted with 1.5-MeV nitrogen ions
[NASA-TP-1989] p0059 N82-21300
Tribological characteristics of nitrogen (N+) implanted iron
[NASA-TM-82839] p0060 N82-24322
Tooth profile analysis of circular-cut, spiral-bevel gears
[NASA-TM-82840] p0101 N82-26681

- The dryout region in frictionally heated sliding contacts
[NASA-TM-82796] p0088 N82-28574
- Boundary lubrication: Revisited
[NASA-TM-82858] p0069 N82-29458
- Refractory coatings
[NASA-CASE-LEN-13169-2] p0061 N82-30371
- Plastic deformation and wear process at a surface during unlubricated sliding
[NASA-TM-82820] p0102 N82-32735
- Wear mechanism based on adhesion
[NASA-TP-2037] p0103 N82-32737
- WEAR INHIBITORS**
- Composite seal for turbomachinery
[NASA-CASE-LEN-12131-3] p0099 N82-19540
- WEAR TESTS**
- Effect of gamma irradiation on the friction and wear of ultrahigh molecular weight polyethylene
p0062 N82-10674
- The effect of oxygen concentration on the boundary-lubricating characteristics of a C ether and a polyphenyl ether to 300 C
p0070 N82-21699
- Development of CdO-graphite-Ag coatings for gas bearings to 427 C
p0108 N82-27079
- Elucidation of wear mechanisms by ferrographic analysis
[NASA-TM-82737] p0066 N82-15199
- Friction and wear of iron in corrosive metal
[NASA-TP-1985] p0058 N82-20291
- Sputtered silicon nitride coatings for wear protection
[NASA-TM-82819] p0067 N82-20314
- Lubricant effects on efficiency of a helicopter transmission
[NASA-TM-82857] p0100 N82-25520
- Occurrence of spherical ceramic debris in indentation and sliding contact
[NASA-TP-2048] p0069 N82-32491
- WEATHER**
- Effect of heavy rain on aircraft
N82-21149
- WEATHER CONDITIONS**
- U ATHER**
- WEATHER FORECASTING**
- The NASA MERIT program - Developing new concepts for accurate flight planning
[AIAA PAPER 82-0340] p0014 N82-17894
- NASA research programs responding to workshop recommendations
N82-21146
- WEATHER FRONTS**
- U CNTS (METEOROLOGY)**
- WEATHER MODIFICATION**
- NT FOG DISPERSAL**
- NT LIGHTNING SUPPRESSION**
- WEATHERING**
- Environmental effects on solar concentrator mirrors
N82-23394
- WEBS (MEMBRANES)**
- U MEMANES**
- WEDGES**
- Elastic-plastic finite-element analyses of thermally cycled single-edge wedge specimens
[NASA-TP-1982] p0111 N82-20565
- Elastic-plastic finite-element analyses of thermally cycled double-edge wedge specimens
[NASA-TP-1973] p0111 N82-20566
- WEIGHT (MASS)**
- NT STRUCTURAL WEIGHT**
- WEIGHT REDUCTION**
- Power system design optimization using Lagrange multiplier techniques
p0085 N82-20743
- WELDING**
- NT DIFFUSION WELDING**
- WETNESS**
- U TSTURE CONTENT**
- WHEELS**
- NT COUNTER-ROTATING WHEELS**
- NT FLYWHEELS**
- NT TURBINE WHEELS**
- WHIRL INSTABILITY**
- U TARY STABILITY**
- WHISKER COMPOSITES**
- High temperature composites. Status and future directions
[NASA-TM-82929] p0051 N82-30336
- WIDEBAND COMMUNICATION**
- Open-loop nanosecond-synchronization for wideband satellite communications
p0036 N82-27224
- Wideband, high speed switch matrix development for SS-TDMA applications
p0086 N82-43784
- Cross-impact study of foreign satellite communications on NASA's 30/20 GHz program
[NASA-CR-165154] p0078 N82-17420
- NIGHTMAN THEORY**
- U ELD THEORY (PHYSICS)**
- WIND CIRCULATION**
- U HOSPHERIC CIRCULATION**
- WIND ENERGY**
- U NDPOWER UTILIZATION**
- WIND SHEAR**
- Effect of heavy rain on aircraft
N82-21149
- WIND TUNNEL APPARATUS**
- The design and instrumentation of the Purdue annular cascade facility with initial data acquisition and analysis
[NASA-CR-167861] p0008 N82-26237
- WIND TUNNEL BALANCES**
- U ND TUNNEL APPARATUS**
- WIND TUNNEL MODELS**
- Thrust modulation methods for a subsonic V/STOL aircraft
[NASA-TM-82747] p0003 N82-13112
- WIND TUNNEL TESTS**
- Propeller tip vortex - A possible contributor to aircraft cabin noise
p0152 N82-17603
- Aerodynamic characteristics of airfoils with ice accretions
[AIAA PAPER 82-0282] p0010 N82-22081
- In-flight acoustic results from an advanced-design propeller at Mach numbers to 0.8
[AIAA PAPER 82-1120] p0021 N82-35017
- A remote millivolt multiplexer and amplifier module for wind tunnel data acquisition
p0083 N82-41845
- Icing tunnel tests of a composite porous leading edge for use with a liquid anti-ice system --- Lewis icing research tunnel
[NASA-CR-164966] p0014 N82-11052
- Study of controlled diffusion stator blading. I. Aerodynamic and mechanical design report
[NASA-CR-165500] p0024 N82-16081
- An experimental investigation of gapwise periodicity and unsteady aerodynamic response in an oscillating cascade. Volume 2: Data report. Part 1: Text and mode 1 data
[NASA-CR-165457-VOL-2-PT-1] p0006 N82-18180
- Application of an airfoil stall flutter computer prediction program to a three-dimensional wing: Prediction versus experiment
[NASA-CR-168586] p0007 N82-19169
- Evaluation of wind tunnel performance testings of an advanced 45 deg swept 8-bladed propeller at Mach numbers from 0.45 to 0.85
[NASA-CR-3505] p0007 N82-19178
- V/STOL Tandem Fan transition section model test --- in the Lewis Research Center 10-by-10 foot wind tunnel
[NASA-CR-165587] p0007 N82-21158
- A preliminary comparison between the SR-3 propeller noise in flight and in a wind tunnel
[NASA-TM-82805] p0152 N82-21998
- An experimental investigation of gapwise periodicity and unsteady aerodynamic response in an oscillating cascade. I: Experimental and theoretical results --- turbine blades
[NASA-CR-3513] p0008 N82-26229
- Turbine endwall single cylinder program
[NASA-CR-169278] p0091 N82-31638
- WIND TUNNELS**
- NT CASCADE WIND TUNNELS**
- NT COMBUSTION WIND TUNNELS**
- NT SHOCK TUNNELS**
- NT SUPERSONIC WIND TUNNELS**
- NT TRANSONIC WIND TUNNELS**
- WIND TURBINES**
- Winding for the wind
p0138 N82-37078
- Microprocessor control system for 200-kilowatt Mod-OA wind turbines
[NASA-TM-82711] p0120 N82-21710

- Method for predicting impulsive noise generated by wind turbine rotors
[NASA-TM-82794] p0121 N82-21714
- Effect of rotor configuration on guyed tower and foundation designs and estimated costs for intermediate site horizontal axis wind turbines
[NASA-TM-82804] p0121 N82-22649
- Evaluation of lightning accommodation systems for wind-driven turbine rotors
[NASA-TM-82784] p0122 N82-23679
- Wind turbine dynamics
[NASA-CP-2185] p0122 N82-23684
- Applications of the DOE/NASA wind turbine engineering information system
p0122 N82-23696
- Calculation of guaranteed mean power from wind turbine generators
p0122 N82-23699
- Whirl flutter analysis of a horizontal-axis wind turbine with a two-bladed teetering rotor
p0122 N82-23707
- Comparison of upwind and downwind rotor operation of the DOE/NASA 100-kw MOD-0 wind turbine
p0122 N82-23710
- A review of resonance response in large horizontal-axis wind turbines
p0122 N82-23711
- The NASA-LERC wind turbine sound prediction code
p0123 N82-23730
- Mod-2 wind turbine system cluster research test program. Volume 1: Initial plan E-1290
[NASA-TM-82906] p0123 N82-26807
- Vibration analysis of three guyed tower designs for intermediate size wind turbines
[NASA-CR-165589] p0137 N82-30709
- Experience and assessment of the DOE-NASA Mod-1 2000-kilowatt wind turbine generator at Boone, North Carolina
[NASA-TM-82721] p0125 N82-30710
- Theoretical and experimental power from large horizontal-axis wind turbines
[NASA-TM-82944] p0127 N82-33830
- WIND VELOCITY**
Calculation of guaranteed mean power from wind turbine generators
p0122 N82-23699
- WINDMILLS (WINDPOWERED MACHINES)**
Microprocessor control system for 200-kilowatt Mod-0A wind turbines
[NASA-TM-82711] p0120 N82-21710
- Wind turbine dynamics
[NASA-CP-2185] p0122 N82-23684
- Theoretical and experimental power from large horizontal-axis wind turbines
[NASA-TM-82944] p0127 N82-33830
- WINDPOWER UTILIZATION**
The NASA Lewis large wind turbine program
[NASA-TM-82761] p0119 N82-16495
- Mod-2 wind turbine system cluster research test program. Volume 1: Initial plan E-1290
[NASA-TM-82906] p0123 N82-26807
- Theoretical and experimental power from large horizontal-axis wind turbines
[NASA-TM-82944] p0127 N82-33830
- WINDPOWERED GENERATORS**
Interfacing wind energy conversion equipment with utility systems
A82-21148
- Aluminum blade development for the Mod-0A 200-kilowatt wind turbine
[NASA-TM-82594] p0119 N82-14633
- The NASA Lewis large wind turbine program
[NASA-TM-82761] p0119 N82-16495
- Design, evaluation, and fabrication of low-cost composite blades for intermediate-size wind turbines
[NASA-CR-165342] p0133 N82-18693
- Experience with modified aerospace reliability and quality assurance method for wind turbines
[NASA-TM-82893] p0110 N82-19550
- Effect of rotor configuration on guyed tower and foundation designs and estimated costs for intermediate site horizontal axis wind turbines
[NASA-TM-82804] p0121 N82-22649
- Evaluation of lightning accommodation systems for wind-driven turbine rotors
[NASA-TM-82784] p0122 N82-23679
- Wind turbine dynamics
[NASA-CP-2185] p0122 N82-23684
- Mod-2 wind turbine system cluster research test program. Volume 1: Initial plan E-1290
[NASA-TM-82906] p0123 N82-26807
- WING OSCILLATIONS**
Solution of the unsteady subsonic thin airfoil problem
p0012 A82-41267
- WING TANKS**
Experimental study of fuel heating at low temperatures in a wing tank model, volume 1
[NASA-CR-165391] p0073 N82-11224
- WINGS**
NT TILTING ROTORS
Numerical simulation of one-dimensional heat transfer in composite bodies with phase change --- wing delcing pads
[NASA-CR-165607] p0002 N82-22142
- WIRE**
NT GUY WIRES
- WIRE CLOTH**
Metal honeycomb to porous wireform substrate diffusion bond evaluation
[NASA-TM-82793] p0110 N82-18612
- Study of vapor flow into a capillary acquisition device --- for cryogenic rocket propellants
[NASA-CR-167883] p0091 N82-24452
- WIRE MESH**
U RE CLOTH
- WORK FUNCTIONS**
Cesiation of W/001/ - Work function lowering by multiple dipole formation
A82-30002
- WRAPAROUND CONTACT SOLAR CELLS**
U LAB CELLS
- WROUGHT ALLOYS**
Effects of cobalt on structure, microchemistry and properties of a wrought nickel-base superalloy
p0065 A82-34973
- X**
- X RAY SPECTROGRAPHY**
U RAY SPECTROSCOPY
- X RAY SPECTROMETRY**
U RAY SPECTROSCOPY
- X RAY SPECTROSCOPY**
Application of surface analysis to solve problems of wear
[NASA-TM-82753] p0099 N82-14519
- X RAYS**
NT SOLAR X-RAYS
- Y**
- YAW**
Comparison of upwind and downwind rotor operation of the DOE/NASA 100-kw MOD-0 wind turbine
p0122 N82-23710
- YANMETERS**
U W
- YOUNG MODULUS**
U DULUS OF ELASTICITY
- YTTRIUM COMPOUNDS**
NT YTTRIUM OXIDES
- YTTRIUM OXIDES**
Creep and rupture of an ODS alloy with high stress rupture ductility --- Oxide Dispersion Strengthened
p0065 A82-40335
- Phase stability in plasma-sprayed, partially stabilized zirconia-yttria
p0070 A82-41552
- Effects of heating rate on density, microstructure, and strength of Si3N4-6 wt.% Y2O3 and a beta-prime sialon
[ACS PAPER 42-B-81] p0070 A82-42366
- The influence of gamma prime on the recrystallization of an oxide dispersion strengthened superalloy - MA 6000E
p0062 A82-47393
- Effect of fuel to air ratio on Mach 0.3 burner rig hot corrosion of ZrO2-Y2O3 thermal barrier coatings
[NASA-TM-82879] p0061 N82-30373
- Z**
- SEWER DIODES**
U ALANCHE DIODES

ORIGINAL PAGE IS
OF POOR QUALITY

ZINC

SUBJECT INDEX

ZINC

Mechanism and models for zinc metal morphology in
alkaline media
[NASA-TM-82768] p0120 N82-19671

ZINC NICKEL BATTERIES

U CREI ZINC BATTERIES

ZINC SILVER BATTERIES

U LVEE ZINC BATTERIES

ZINC SILVER OXIDE BATTERIES

U LVEE ZINC BATTERIES

ZIRCONIUM

Nicral ternary alloy having improved cyclic
oxidation resistance
[NASA-CASE-LEW-13339-1] p0061 N82-31505

ZIRCONIUM COMPOUNDS

NT ZIRCONIUM OXIDES

ZIRCONIUM OXIDES

Phase stability in plasma-sprayed, partially
stabilized zirconia-yttria p0070 A82-41552

Performance of laser glazed ZrO₂ TBCs in cyclic
oxidation and corrosion burner test rigs
[NASA-TM-82830] p0059 N82-22346

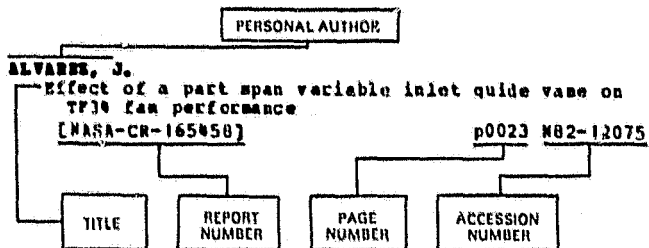
Effect of fuel to air ratio on Mach 0.3 burner rig
hot corrosion of ZrO₂-Y₂O₃ thermal barrier
coatings

[NASA-TM-82879] p0061 N82-30373

Failure mechanisms of thermal barrier coatings
exposed to elevated temperatures
[NASA-TM-82905] p0061 N82-32461

PERSONAL AUTHOR INDEX

Typical Personal Author Index Listing



Listings in this index are arranged alphabetically by personal author. The title of the document provides the user with a brief description of the subject matter. The report number helps to indicate the type of document listed (e.g., NASA report, translation, NASA contractor report). The page and accession numbers are located beneath, and to the right of the title. Under any one author's name the accession numbers are arranged in sequence with the AA accession numbers appearing first.

A

- ANAD, M. S.**
Exhaust gas measurements in a propane fueled swirl
stabilized combustor
[NASA-CR-169293] p0091 N82-31641
- ABBOTT, J. H.**
A summary of V/STOL inlet analysis methods
p0006 A82-40921
A summary of V/STOL inlet analysis methods
[NASA-TN-82805] p0005 N82-28249
- ABDALLA, K. L.**
TF34 Convertible Engine System Technology Program
p0022 A82-40521
- ABDELWOUZ, Z. A.**
Permanent magnet proportion of Mn-Al-C between -50
C and +150 C
p0085 A82-20505
- ABDELWAHAB, M.**
Effects of fan inlet temperature disturbances on
the stability of a turbofan engine
[NASA-TN-82699] p0017 N82-18222
- ABRAMAN, K. M.**
Moderate temperature Na cells. III -
Electrochemical and structural studies of
CrO₂SVG₂SS2 and its Na intercalates
p0055 A82-15732
Moderate temperature Na cells. IV - VS2 and
NbS₂Cl₂ as rechargeable cathodes in molten NaAlCl₄
p0055 A82-15743
- ADAMS, D. F.**
Analysis of crack propagation as an energy
absorption mechanism in metal matrix composites
[NASA-CR-165051] p0052 N82-14288
Micromechanical predictions of crack propagation
and fracture energy in a single fiber
boron/aluminum model composite
[NASA-CR-168550] p0052 N82-18326
- ADAMS, M.**
Engine dynamic analysis with general nonlinear
finite element codes. II - Bearing element
implementation, overall numerical
characteristics and benchmarking
[ASME PAPER 82-GT-292] p0108 A82-35462
Engine dynamic analysis with general nonlinear
finite element codes. Part 2: Bearing element
implementation overall numerical characteristics
and benchmarking
[NASA-CR-167944] p0028 N82-33390
- AIELLO, R. A.**
Structural dynamics of shroudless, hollow, fan
blades with composite in-lays
[ASME PAPER 82-GT-284] p0022 A82-35456

- Structural dynamics of shroudless, hollow fan
blades with composite in-lays
[NASA-TN-82816] p0018 N82-22266
Large displacements and stability analysis of
nonlinear propeller structures
[NASA-TN-82850] p0112 N82-31707
Tensile buckling of advanced turboprops
[NASA-TN-82896] p0112 N82-31708
- AKAY, M. U.**
A finite element formulation of Euler equations
for the solution of steady transonic flows
[AIAA PAPER 82-0062] p0009 A82-17759
Application of a finite element algorithm for the
solution of steady transonic Euler equations
[AIAA PAPER 82-0970] p0010 A82-31939
Investigation of rotational transonic flows
through ducts using a finite element scheme
[AIAA PAPER 82-1267] p0012 A82-37711
- AKHTER, M. H.**
Sensor failure detection system
[NASA-CR-165515] p0023 N82-13145
- ALLIEN, F. E.**
A pad perturbation method for the dynamic
coefficients of tilting-pad journal bearings
p0110 A82-14400
- ALLEN, J.**
Comparison of two parallel/series flow turbofan
propulsion concepts for supersonic V/STOL
[AIAA PAPER 81-2637] p0020 A82-19214
Comparison of two parallel/series flow turbofan
propulsion concepts for supersonic V/STOL
[NASA-CR-16743] p0004 A82-18170
- ALLISON, G. W.**
Advances in high output voltage silicon solar cells
p0127 A82-44942
- ALSTON, W. B.**
PMR polyimides-review and update
[NASA-TN-82821] p0068 N82-24342
- ALTENKIRCH, R. A.**
Buoyancy effects on the temperature field in
downward spreading flames
p0094 A82-41203
- ALVAREZ, J.**
Effect of a part span variable inlet guide vane on
TF34 fan performance
[NASA-CR-165458] p0023 N82-12075
- ALYEA, F. W.**
Comparative analysis of CCMHD power plants
p0158 A82-20747
- AMES, E. P.**
Chopper-controlled discharge life cycling studies
on lead-acid batteries
[NASA-CR-165616] p0134 N82-20661
- ANDERSON, D. M.**
Combustor development for automotive gas turbines
[AIAA PAPER 82-1208] p0104 A82-35062
Gas-turbine critical research and advanced
technology support project
[NASA-TN-81708] p0118 N82-13509
Gas turbine critical research and advanced
technology (CRT) support project
[NASA-TN-82872] p0126 N82-31776
- ANDERSON, L. M.**
A new strategy for efficient solar energy
conversion: Parallel-processing with surface
plasmons
[NASA-TN-82867] p0042 N82-29354
- ANDERSON, M. E.**
Multiroller traction drive speed reducer:
Evaluation for automotive gas turbine engine
[NASA-TP-2027] p0101 N82-26678
- ANDERSON, W. J.**
Bearings: Technology and needs
[NASA-CR-167908] p0106 N82-26679

ORIGINAL PAGE IS
OF POOR QUALITY

ANDERSON, W. L.

PERSONAL AUTHOR INDEX

- ANDERSON, W. L.
Thin film temperature sensors, phase 3
[NASA-CR-165476] p0097 N82-22479
- ANDERSSON, C. A.
Ceramic thermal barrier coatings for gas turbine engines
[ASME PAPER 82-GT-265] p0071 A82-35441
- ANDREWS, D. G.
The supply of lunar oxygen to low earth orbit
p0032 A82-35618
- ANGWIN, M. J.
Development of a high-temperature durable catalyst for use in catalytic combustors for advanced automotive gas turbine engines
[NASA-CR-165396] p0130 N82-13510
- ANTOINE, A. C.
Effect of some nitrogen compounds thermal stability of jet A
[NASA-TM-82908] p0072 N82-27519
- ARMSTRONG, T. P.
Numerical simulation of plasma insulator interactions in space. Part 1: The self consistent calculation
p0039 N82-14272
- Numerical simulation of plasma insulator interactions in space. Part 2: Dielectric effects
p0039 N82-14273
- ARNDT, R. A.
High- and low-resistivity silicon solar cells
p0086 A82-11762
Advances in high output voltage silicon solar cells
p0127 A82-44942
- ARON, P. E.
Sputtered silicon nitride coatings for wear protection
[NASA-TM-82819] p0067 N82-20314
Some properties of RF sputtered hafnium nitride coatings
[NASA-TM-82026] p0067 N82-21331
- ARP, V.
The dryout region in frictionally heated sliding contacts
[NASA-TM-82796] p0088 N82-28574
- ARSONS, R. M.
Creep and rupture of an ODS alloy with high stress rupture ductility
p0065 A82-40335
- ASHON, I.
Market assessment of photovoltaic power systems for agricultural applications in Mexico
[NASA-CR-165441] p0128 N82-10506
Market assessment of photovoltaic power systems for agricultural applications in Morocco
[NASA-CR-165477] p0130 N82-14627
- ASHUS, J.
IMPATT power building blocks for 20 GHz spaceborne transmit amplifier
[AIAA 82-0498] p0086 A82-23566
- ASHUSSEN, J.
Standing waves along a microwave generated surface wave plasma
p0158 A82-26952
- ASTLEY, R. J.
Acoustic transmission in lined flow ducts - A finite element eigenvalue problem
p0154 A82-17663
Application of steady state finite element and transient finite difference theory to sound propagation in a variable area duct: A comparison with experiment
[NASA-TM-82678] p0151 N82-15847
- ATASSI, E.
Sound generated in a cascade by three-dimensional disturbances convected in a subsonic flow
[AIAA PAPER 81-2046] p0153 A82-10460
- ATLURY, S. W.
Path-independent integrals in finite elasticity and inelasticity, with body forces, inertia, and arbitrary crack-face conditions
p0115 A82-32303
On a study of the $\Delta T/c$ and $C/\text{asterisk}/$ integrals for fracture analysis under non-steady creep
p0115 A82-36782
Moving singularity creep crack growth analysis with the $\Delta T/c$ and $C/\text{asterisk}/$ integrals
p0116 A82-40066
- Creep crack-growth: A new path-independent T sub o and computational studies
[NASA-CR-166930] p0113 N82-24503
Creep crack-growth: A new path-independent integral (T sub c), and computational studies
[NASA-CR-167897] p0114 N82-29619
- ATTWOOD, S.
Baseband-processed SS-TDMA communication system architecture and design concepts
[AIAA 82-0482] p0079 A82-23508
- AUGUST, R.
A multi-purpose method for analysis of spur gear tooth loading
[NASA-CR-165163] p0104 N82-10401
- AUKERMAN, C. A.
Deposit formation in hydrocarbon rocket fuels with an evaluation of a propane heat transfer correlation
[NASA-TM-82911] p0088 N82-26611

B

- BACH, L. J.
Blade loss transient dynamic analysis of turbomachinery
[AIAA PAPER 82-1057] p0030 A82-34982
- BADGLEY, P.
Advanced stratified charge rotary aircraft engine design study
[NASA-CR-165398] p0107 N82-27743
- BADLANI, M.
Development of a simplified procedure for thrust chamber life prediction
[NASA-CR-165585] p0044 N82-21353
- BADLANI, M. L.
A simplified design procedure for life prediction of rocket thrust chambers
[AIAA PAPER 82-1251] p0043 A82-35087
- BAERST, C. F.
Study of advanced propulsion systems for Small Transport Aircraft Technology (STAT) program
[NASA-CR-165610] p0026 N82-24202
- BAHR, D.
Socioeconomic impact of photovoltaic power at Schuchuli, Arizona
[NASA-CR-165551] p0133 N82-19669
- BAHR, D. W.
NASA/General Electric broad-specification fuels combustion technology program - Phase I results and status
[AIAA PAPER 82-1009] p0021 A82-35000
- BAILEY, W. J.
Cryogenic fluid management experiment
[NASA-CR-165495] p0039 N82-15117
- BAIR, S.
Regimes of traction in concentrated contact lubrication
[ASME PAPER 81-LUB-16] p0107 A82-18431
Some observations in high pressure rheology of lubricants
[ASME PAPER 81-LUB-17] p0070 A82-18432
Some observations in high pressure rheology of lubricants
[ASME PAPER 81-LUB-17] p0070 A82-18432
- BALDWIN, D. M.
The NASA Lewis large wind turbine program
[NASA-TM-82761] p0119 N82-16495
- BALIGA, G.
Numerical simulation of one-dimensional heat transfer in composite bodies with phase change
[NASA-CR-165607] p0002 N82-22142
- BALODIS, V.
Fast recovery, high voltage silicon diodes for AC motor controllers
p0086 A82-36926
- BANKAITIS, E.
Evaluation of lightning accommodation systems for wind-driven turbine rotors
[NASA-TM-82784] p0122 N82-23679
- BANKS, B. A.
Texturing polymer surfaces by transfer casting
[NASA-CASE-LEW-13120-1] p0068 N82-28440
Ion beam sputter deposited diamond like films
[NASA-TM-82873] p0069 N82-28445
Surface texturing of fluoropolymers
[NASA-CASE-LEW-13028-1] p0070 N82-33521
- BARA, M.
Maximum entropy image reconstruction from projections

- BABSON, S.**
Creep and rupture of an ODS alloy with high stress
rupture ductility
p0065 A82-40335
- BABSON, C.**
A theory of the n-i-p silicon solar cell
p0128 A82-45055
- BABSON, C. R.**
Thin foil silicon solar cells with coplanar back
contacts
p0127 A82-44944
- Solar cell development for the power extension
package
[NASA-TM-82685] p0118 A82-11524
- Large area low-cost space solar cell development
[NASA-TM-82902] p0126 A82-32854
- BABIS, J.**
Preparation and evaluation of advanced
electrocatalysts for phosphoric acid fuel cells
[NASA-CR-165519] p0129 A82-12573
- Preparation and evaluation of advanced
electrocatalysts for phosphoric acid fuel cells
[NASA-CR-165594] p0132 A82-17615
- BABBETT, C. A.**
Nical ternary alloy having improved cyclic
oxidation resistance
[NASA-CASE-LEW-13339-1] p0061 A82-31505
- BABBETT, L. E.**
A pad perturbation method for the dynamic
coefficients of tilting-pad journal bearings
p0110 A82-14400
- BABBIGER, H. T.**
Environmental effects on solar concentrator mirrors
A82-23394
- BARTON, R. S.**
Experience and assessment of the DOE-NASA Mod-1
2000-kilowatt wind turbine generator at Boone,
North Carolina
[NASA-TM-82721] p0125 A82-30710
- BATAKIS, A. P.**
Low NOx heavy fuel combustor concept program
[NASA-CR-165481] p0138 A82-33827
- BAUNDICK, R. J.**
Optical tip clearance sensor for aircraft engine
controls
[AIAA PAPER 82-1131] p0015 A82-37691
- Role of optical computers in aeronautical control
applications
p0156 A82-15897
- BAUMEISTER, K. J.**
Numerical techniques in linear duct acoustics,
1980-81 update
[NASA-TM-82730] p0151 A82-12890
- Application of steady state finite element and
transient finite difference theory to sound
propagation in a variable area duct: A
comparison with experiment
[NASA-TM-82670] p0151 A82-15847
- Finite element-integral simulation of static and
flight fan noise radiation from the JT15D
turbofan engine
[NASA-TM-82936] p0152 A82-31068
- BEAL, G.**
Low NO sub x heavy fuel combustor concept program
[NASA-CR-165512] p0129 A82-12572
- BEATTIE, E. C.**
Sensor failure detection system
[NASA-CR-165515] p0023 A82-13145
- Preliminary study, analysis and design for a power
switch for digital engine actuators
[NASA-CR-159559] p0085 A82-23394
- BEATTIE, J. R.**
30-cm mercury ion thruster technology
p0046 A82-15434
- BECK, E. D.**
The CF6 jet engine performance improvement: Low
pressure turbine active clearance control
[NASA-CR-165557] p0029 A82-33393
- BEER, K. W.**
Low NO sub x heavy fuel combustor concept program
phase 1A gas tests
[NASA-CR-167877] p0055 A82-25337
- BEER, J. H.**
Flow aerodynamics modeling of an MHD swirl
combustor - Calculations and experimental
verification
p0094 A82-44782
- BEES, B. L.**
Internal breakdown of charged spacecraft dielectrics
p0041 A82-18312
- BECK, L. L.**
Jet impingement heat transfer enhancement for the
GP3-3 Stirling engine
[NASA-TM-82727] p0163 A82-11993
- BEHN, M. A.**
NASA research in aircraft propulsion
[ASME PAPER 82-GT-177] p0022 A82-35389
- NASA research in aircraft propulsion
[NASA-TM-82771] p0016 A82-13146
- BEHL, A.**
Fuel quality processing study, volume 1
[NASA-CR-165327-VOL-1] p0135 A82-24649
- Fuel quality/processing study, Volume 2:
Appendix. Task 1 literature survey
[NASA-CR-165327-VOL-2] p0135 A82-24650
- BEHRETT, J. C.**
Mass and momentum turbulent transport experiments
with confined coaxial jets
[NASA-CR-165574] p0090 A82-19496
- BEITS, D. J.**
Impact of uniform electrode current distribution
on ETP
[AIAA PAPER 82-0423] p0157 A82-17941
- Magnetohydrodynamics (MHD) Engineering Test
Facility (ETF) 200 MWe power plant. Design
Requirements Document (DRD)
[NASA-TM-82705] p0099 A82-12446
- Impact of uniform electrode current distribution
on ETP
[NASA-TM-82875] p0123 A82-25636
- BEICAW, R. W.**
Magnetohydrodynamics (MHD) Engineering Test
Facility (ETF) 200 MWe power plant. Design
Requirements Document (DRD)
[NASA-TM-82705] p0099 A82-12446
- BEIG, R. D.**
Comparative analysis of the conceptual design
studies of potential early commercial MHD power
plants (CSPEC)
[NASA-TM-82897] p0123 A82-27638
- BERGER, S. A.**
Effects of internal heat transfer on the structure
of self-similar blast waves
p0093 A82-32225
- BERGMAN, S. C.**
The 30/20 GHz flight experiment system, phase 2.
Volume 1: Executive summary
[NASA-CR-165409-VOL-1] p0078 A82-20362
- The 30/20 GHz flight experiment system, phase 2.
Volume 2: Experiment system description
[NASA-CR-165409-VOL-2] p0078 A82-20363
- The 30/20 GHz flight experiment system, phase 2.
Volume 4: Experiment system development plan
[NASA-CR-165409-VOL-4] p0078 A82-20365
- BERKOPIC, F.**
First results of material charging in the space
environment
[NASA-TM-84743] p0081 A82-24431
- BERKOWITZ, M.**
Advanced stratified charge rotary aircraft engine
design study
[NASA-CR-165398] p0107 A82-27743
- BERMAN, A. H.**
Fast recovery, high voltage silicon diodes for AC
motor controllers
p0086 A82-36926
- BERMAN, S. G.**
The 30/20 GHz flight experiment system, phase 2.
Volume 3: Experiment system requirement document
[NASA-CR-165409-VOL-3] p0078 A82-20364
- BETHA, R. H.**
Environmental effects on solar concentrator mirrors
A82-23394
- BEYLER, C. L.**
Flame structure in a swirl stabilized combustor
inferred by radiant emission measurements
p0056 A82-28694
- BHAT, S. T.**
Analysis of high load dampers
[NASA-CR-165503] p0026 A82-23248
- BHATT, R. T.**
Thermal degradation of the tensile properties of
unidirectionally reinforced FP-K1203/EZ 33
magnesium composites
[NASA-TM-82817] p0049 A82-21260

BRUSHAN, B.

- Modulus, strength and thermal exposure studies of
FP-AL2O3/aluminum and FP-AL2O3/magnesium
composites
[NASA-TM-82868] p0050 N82-30335
- BRUSHAN, B.**
Development of CdO-graphite-Ag coatings for gas
bearings to 427 C p0108 A82-27079
- BIGHAM, J.**
Electromechanical actuators N82-22148
- BILL, B. C.**
Composite seal for turbomachinery
[NASA-CASE-LEW-12131-3] p0099 N82-19540
Fully plasma-sprayed compliant backed ceramic
turbine seal
[NASA-CASE-LEW-13268-2] p0101 N82-26674
Fully plasma-sprayed compliant backed ceramic
turbine seal
[NASA-CASE-LEW-13268-1] p0069 N82-29453
- BILLINGS, W. W.**
High voltage DC switchgear development for
multi-kw space power system: Aerospace
technology development of three types of solid
state power controllers for 200-1100VDC with
current ratings of 25, 50, and 80 amperes with
one type utilizing an electromechanical device
[NASA-CR-165413] p0083 N82-13357
- BIRCHENHOUGH, A. G.**
Variable gain for a wind turbine pitch control
[NASA-TM-82751] p0119 N82-16478
Microprocessor control system for 200-kilowatt
Mod-OA wind turbines
[NASA-TM-82711] p0120 N82-21710
- BIRKS, W.**
Investigation into the role of NaCl deposited on
oxide and metal substrates in the initiation of
hot corrosion
[NASA-CR-165029] p0063 N82-13217
- BISHOP, A. M.**
The effect of inflow velocity profiles on the
performance of supersonic ejector nozzles
[AIAA PAPER 81-0273] p0002 A81-32548
Three-dimensional flow calculations including
boundary layer effects for supersonic inlets at
angle of attack
[AIAA PAPER 82-0061] p0005 A82-19778
- BITTNER, D. A.**
Effect of hydrocarbon fuel type on fuel
[NASA-TM-82916] p0072 N82-28460
- BIXON, P. T.**
Comparative thermal fatigue resistance of several
oxide dispersion strengthened alloys p0062 A82-11399
- BLACK, D. M.**
Evaluation of wind tunnel performance testings of
an advanced 45 deg swept 8-bladed propeller at
Mach numbers from 0.45 to 0.85
[NASA-CR-3505] p0007 N82-19178
- BLACK, G.**
Blade loss transient dynamic analysis of
turbomachinery
[AIAA PAPER 82-1057] p0030 A82-34982
- BLIANPTIS, T.**
Development of a dual-field heteropolar power
converter
[NASA-CR-165168] p0084 N82-24424
- BLOCHER, H. E.**
QCSSE under-the-wing engine acoustic data
[NASA-TM-82691] p0019 N82-27311
QCSSE over-the-wing engine acoustic data
[NASA-TM-82708] p0020 N82-29324
- BLUMENTHAL, P. Z.**
A remote millivolt multiplexer and amplifier
module for wind tunnel data acquisition p0083 A82-41845
- BOIANCHUK, A. A.**
Ultraviolet observations of the 1980 eclipse of
the symbiotic star CI Cygni A82-27331
- BOLDMAN, D. B.**
Three-dimensional shock structure in a transonic
flutter cascade p0006 A82-37937
- BOLLEWEACHER, G.**
Environmental assessment of the 40 kilowatt fuel
cell system field test operation
[DOE/NASA/2701-1] p0137 N82-29721
- BOND, J. W.**
The development of central peaks in lunar craters
A82-14333
- BORRICO, J. M.**
Low temperature growth and electrical
characterization of insulators for GaAs MISFETS
[NASA-CR-164972] p0159 N82-11959
- BOYLES, E. B.**
Study of vapor flow into a capillary acquisition
device
[NASA-CR-167883] p0091 N82-24452
- BONMAN, E. M.**
Reliable aerial thermography for energy conservation
[NASA-TM-81766] p0117 N82-14552
- BOYER, J. M.**
Worldwide satellite market demand forecast
[NASA-CR-167918] p0079 N82-25423
- BOYLE, E. J.**
Analytic investigation of effect of end-wall
contouring on stator performance
[NASA-TF-1943] p0003 N82-14051
Comparison of experimental and analytical
performance for contoured endwall stators
[NASA-TM-82877] p0019 N82-26299
- BRADLEY, E. S.**
Advanced turboprop testbed systems study. Volume
1: Testbed program objectives and priorities,
drive system and aircraft design studies,
evaluation and recommendations and wind tunnel
test plans
[NASA-CR-167928-VOL-1] p0028 N82-32370
- BRADY, E. G.**
Strength distributions of SiC ceramics after
oxidation and oxidation under load
[ACS PAPER 9-C-80C] p0071 A82-20143
Effects of oxidation and oxidation under load on
strength distributions of Si3N4
[ACS PAPER 69-B-80] p0071 A82-35871
- BRAGG, H. B.**
Aerodynamic characteristics of airfoils with ice
accretions
[AIAA PAPER 82-0282] p0010 A82-22081
Rime ice accretion and its effect on airfoil
performance
[NASA-CR-165599] p0008 N82-24166
- BRATHARD, W. A.**
Refractory coatings and method of producing the same
[NASA-CASE-LEW-13169-1] p0060 N82-29415
Refractory coatings
[NASA-CASE-LEW-13169-2] p0061 N82-30371
- BRANDHORST, H. W.**
Gallium arsenide solar cells-status and prospects
for use in space p0043 A82-11765
- BRANDHORST, H. W., JR.**
Material and processing needs for silicon solar
cells in space p0032 N82-26336
Effects of processing and dopant on radiation
damage removal in silicon solar cells
[NASA-TM-82892] p0042 N82-31443
On the cause of the flat-spot phenomenon observed
in silicon solar cells at low temperatures and
low intensities
[NASA-TM-82903] p0126 N82-31777
- BRATTON, E. J.**
Ceramic thermal barrier coatings for gas turbine
engines
[ASME PAPER 82-GT-265] p0071 A82-35441
Evaluation of present thermal barrier coatings for
potential service in electric utility gas turbines
[NASA-CR-165545] p0063 N82-18368
- BRAUN, J.**
The dryout region in frictionally heated sliding
contacts
[NASA-TM-82796] p0088 N82-28574
- BREWE, D. M.**
Geometry and starvation effects in hydrodynamic
lubrication
[NASA-TM-82807] p0042 N82-20240
- BRINEL, D.**
Small gas turbine combustor primary zone development
[AIAA PAPER 82-1159] p0103 A82-35036
Evaluation of fuel injection configurations to
control carbon and soot formation in small GT
combustors
[AIAA PAPER 82-1175] p0021 A82-35041
- BRILEY, W. E.**
Turbofan forced mixer-nozzle internal flowfield.

- Volume 7: A computer code for 3-D mixing in axisymmetric nozzles
[NASA-CR-3144] p0091 N82-22460
- BRITT, E. J.**
Jet impingement heat transfer enhancement for the GPU-3 Stirling engine
[NASA-TN-82727] p0163 N82-11993
- BROCKERT, W.**
Small axial turbine stator technology program
[NASA-CR-165602] p0028 N82-32367
- BRODER, J. D.**
On the cause of the flat-spot phenomenon observed in silicon solar cells at low temperatures and low intensities
p0043 N82-39599
On the cause of the flat spot phenomenon observed in silicon solar cells at low temperatures and low intensities
p0044 N82-44965
On the cause of the flat-spot phenomenon observed in silicon solar cells at low temperatures and low intensities
[NASA-TN-82903] p0126 N82-31777
- BROWSTEIN, L.**
The 30/20 GHz flight experiment system, phase 2.
Volume 1: Executive summary
[NASA-CR-165409-VOL-1] p0070 N82-20362
The 30/20 GHz flight experiment system, phase 2.
Volume 2: Experiment system description
[NASA-CR-165409-VOL-2] p0070 N82-20363
The 30/20 GHz flight experiment system, phase 2.
Volume 3: Experiment system requirement document
[NASA-CR-165409-VOL-3] p0070 N82-20364
The 30/20 GHz flight experiment system, phase 2.
Volume 4: Experiment system development plan
[NASA-CR-165409-VOL-4] p0070 N82-20365
- BROOKS, A.**
TF34 Convertible Engine System Technology Program
p0022 N82-40521
- BROWERS, A. P.**
Lightweight diesel engine designs for commuter type aircraft
[NASA-CR-165470] p0023 N82-11068
- BROWN, G. V.**
Magnetic heat pumping
[NASA-CASE-LRW-12508-3] p0008 N82-24449
- BROWN, H.**
V/STOL propulsion control technology
[AIAA PAPER 81-2634] p0029 N82-16909
- BROWN, K. W.**
Structural tailoring of engine blades (STARBL)
[NASA-CR-167949] p0028 N82-33391
- BROWNE, L.**
Communications satellite systems capacity analysis
[NASA-CR-167911] p0034 N82-27331
- BRUCE, T. W.**
Pollution reduction technology program small jet aircraft engines, phase 1
[NASA-CR-165306] p0023 N82-14095
EFUS fuel addendum: Pollution reduction technology program small jet aircraft engines, phase 1
[NASA-CR-165307] p0024 N82-14096
- BRYTON, W. M.**
Analytical investigation of nonrecoverable stall
[NASA-TN-82792] p0018 N82-21195
Automated procedure for developing hybrid computer simulations of turbofan engines. Part 1: General description
[NASA-TN-1051] p0146 N82-33020
- BURSEY, R. T.**
Extended range stress intensity factor expressions for chevron-notched short bar and short rod fracture toughness specimens
p0112 N82-40357
- BURNELE, D. R.**
Veiling glare reduction methods compared for ophthalmic applications
p0143 N82-13289
A digital optical torquemeter for high rotational speed applications
[NASA-TN-82914] p0095 N82-31664
- BUCKLEY, D. E.**
Adhesion and friction of single-crystal diamond in contact with transition metals
p0103 N82-18680
Application of surface analysis to solve problems of wear
[NASA-TN-82753] p0099 N82-14519
- Surface chemistry and wear behavior of single-crystal silicon carbide sliding against iron at temperatures to 1500 C in vacuums
[NASA-TN-1947] p0067 N82-19374
Friction and wear of iron in corrosive metal
[NASA-TN-1985] p0058 N82-20291
Influence of mineral oil and additives on microhardness and surface chemistry of magnesium oxide (001) surface
[NASA-TN-1986] p0067 N82-20316
Friction and surface chemistry of some ferrous-base metallic glasses
[NASA-TN-1991] p0059 N82-21301
Tribological properties and XPS studies of ion plated gold on nickel and iron
[NASA-TN-82014] p0059 N82-22344
Surface chemistry, microstructure and friction properties of some ferrous-base metallic glasses at temperatures to 750 C
[NASA-TN-2006] p0060 N82-22349
Effects of environment on microhardness of magnesium oxide
[NASA-TN-2002] p0068 N82-22366
Correlation of tensile and shear strengths of metals with their friction properties
[NASA-TN-82028] p0060 N82-24325
Tribological properties of sintered polycrystalline and single crystal silicon carbide
[NASA-TN-82829] p0068 N82-24343
Influence of corrosive solutions on microhardness and chemistry of magnesium oxide (001) surfaces
[NASA-TN-2040] p0102 N82-31691
Occurrence of spherical ceramic debris in indentation and sliding contact
[NASA-TN-2048] p0069 N82-32491
Plastic deformation and wear process at a surface during unlubricated sliding
[NASA-TN-82020] p0102 N82-32735
Wear mechanisms based on adhesion
[NASA-TN-2037] p0103 N82-32737
A study of the nature of solid particle impact and shape on the erosion morphology of ductile metals
[NASA-TN-82933] p0061 N82-33493
- BUCK, E. W.**
Progress in the development of energy efficient engine components
[ASME PAPER 82-GT-275] p0030 N82-35450
- BUDD, P. A.**
Oblique-incidence secondary emission from charged dielectrics
p0039 N82-14227
- BUGGEL, A. E.**
Three-dimensional shock structure in a transonic flutter cascade
p0006 N82-37937
- BUJOLD, M. P.**
Small passenger car transmission test: Chevrolet Malibu 200C transmission with lockup
[NASA-CR-165182] p0105 N82-16410
Small passenger car transmission test: Mercury Lynx ATX transmission
[NASA-CR-165510] p0106 N82-24496
- BULMAN, D. L.**
Catalytic combustion of residual fuels
[NASA-TN-82731] p0118 N82-13504
Experimental study of an integral catalytic combustor: Heat exchanger for Stirling engines
[NASA-TN-82783] p0119 N82-18691
Catalytic combustion of actual low and medium heating value gases
[NASA-TN-82930] p0125 N82-30717
- BUOED, D. F.**
Analysis of high load dampers
[NASA-CR-165503] p0026 N82-23248
- BURKE, K. A.**
Endurance test and evaluation of alkaline water electrolysis cells
[NASA-CR-165424] p0130 N82-13508
- BURKHART, J. A.**
Magnetohydrodynamics (MHD) Engineering Test Facility (ETF) 200 MWe power plant. Design Requirements Document (DRD)
[NASA-TN-82705] p0099 N82-12446
- BURLBY, R. B.**
Experimental and analytical results of tangential blowing applied to a subsonic V/STOL inlet
[AIAA PAPER 82-1084] p0005 N82-35195
Experimental and analytical results of tangential blowing applied to a subsonic V/STOL inlet

ORIGINAL PAGE IS
OF POOR QUALITY

BURNS, R. K.

PERSONAL AUTHOR INDEX

[NASA-TM-82847] p0004 N82-24165
BURNS, R. K.
 Performance and operational economics estimates for a coal gasification combined-cycle cogeneration powerplant [NASA-TM-82729] p0120 N82-19672
 Parametric performance analysis of steam-injected gas turbine with a thermionic-energy-converter-lined combustor [NASA-TM-82736] p0121 N82-23678
 Integrated gasifier combined cycle polygeneration system to produce liquid hydrogen [NASA-TM-82921] p0125 N82-30713
MURKILL, G.
 Application of photovoltaic electric power to the rural education/communication needs of developing countries [NASA-CF-167894] p0137 N82-29720
BUSHAWA, A. A.
 A simple finite difference procedure for the vortex controlled diffuser [AIAA PAPER 82-0109] p0030 A82-17782
 Modeling parameter influences on MHD swirl combustion nozzle design [AIAA PAPER 82-0984] p0011 A82-31947
 Flow aerodynamics modeling of an MHD swirl combustor - Calculations and experimental verification p0094 A82-44782
BUTTRILL, S. E., JR.
 Oxidation and formation of deposit precursors in hydrocarbon fuels [NASA-CR-165534] p0073 N82-18402
BUZINSKI, B. E.
 Wideband, high speed switch matrix development for 3S-TDMA applications p0086 A82-43784

C

CABRAL, A.
 Application of photovoltaic electric power to the rural education/communication needs of developing countries [NASA-CR-167894] p0137 N82-29720
CABRELLI, J. E.
 Test results and facility description for a 4C-kilowatt stirling engine [NASA-TM-82620] p0163 N82-13013
 Assessment of a 40-kilowatt stirling engine for underground mining applications [NASA-TM-82822] p0125 N82-30714
CALFO, F. E.
 Micronized coal burner facility [NASA-CASE-LEW-13426-1] p0126 N82-31769
CAMPANI, A. D.
 Advanced superposition methods for high speed turbopump vibration analysis [NASA-CR-165379] p0104 N82-11465
CANBELL, S. S.
 Effects of heating rate on density, microstructure, and strength of S13N4-6 wt.% Y2O3 and a beta-prime sialon [ACS PAPER 42-B-91] p0070 A82-42366
CARAL, E.
 Study of controlled diffusion stator blading. I. Aerodynamic and mechanical design report [NASA-CF-165500] p0024 N82-16081
CARL, D. R.
 Low NOx heavy fuel combustor concept program. Phase I: Combustion technology generation [NASA-CF-165482] p0136 N82-24725
CARLSON, A. W.
 MHD oxidant intermediate temperature ceramic heater study [NASA-CF-165453] p0131 N82-15527
CARRUTHERS, W. D.
 Oxidation stability of advanced reaction-bonded S13N4 materials [ACS PAPER 52-E-80P] p0074 A82-33030
CARTA, F. O.
 An experimental investigation of gapwise periodicity and unsteady aerodynamic response in an oscillating cascade. Volume 2: Data report. Part 1: Text and model data [NASA-CF-165457-VOL-2-P1-1] p0006 N82-18180
 An experimental investigation of gapwise periodicity and unsteady aerodynamic response in an oscillating cascade. 1: Experimental and

theoretical results [NASA-CR-3513] p0008 N82-26229
CARTER, R. A.
 Modeling and Analysis of Power Processing Systems (MPPS). Volume 1: Technical report [NASA-CR-165538] p0083 N82-14447
 Modeling and Analysis of Power Processing Systems (MPPS). Volume 2: Appendices [NASA-CR-165539] p0145 N82-16740
CARUTHERS, J. E.
 'Coriolis resonance' within a rotating duct p0012 A82-37938
CASSINELLI, J.
 High power solar array switching regulation p0043 A82-11736
CATALDO, B. L.
 Design of a 35-kilowatt bipolar nickel-hydrogen battery for low Earth orbit application [NASA-TM-82844] p0123 N82-24647
CATELLA, G. C.
 Free electron lasers for transmission of energy in space [NASA-CR-165520] p0098 N82-25499
CERNANSKY, M. P.
 Formation of oxides of nitrogen in monodisperse spray combustion of hydrocarbon fuels p0057 A82-37571
CHAI, A. T.
 High voltage V-groove solar cell [NASA-CASE-LEW-13401-2] p0123 N82-24717
 Method of making a high voltage V-groove solar cell [NASA-CASE-LEW-13401-1] p0124 N82-29709
 High voltage planar multijunction solar cell [NASA-CASE-LEW-13400-1] p0125 N82-31764
CHAI, A.-T.
 Multijunction high voltage concentrator solar cells p0043 A82-11756
 Fabrication of multijunction high voltage concentrator solar cells by integrated circuit technology p0127 A82-44957
CHAIT, I. L.
 MHD oxidant intermediate temperature ceramic heater study [NASA-CR-165453] p0131 N82-15527
CHAKY, B. C.
 Numerical simulation of sheath structure and current-voltage characteristics of a conductor-dielectric disk in a plasma p0040 A82-15904
 Numerical simulation of plasma insulator interactions in space. Part 1: The self consistent calculation p0039 N82-14272
 Numerical simulation of plasma insulator interactions in space. Part 2: Dielectric effects p0039 N82-14273
CHANIS, C. C.
 Structural dynamics of shroudless, hollow, fan blades with composite in-lays [ASME PAPER 82-GT-284] p0022 A82-35456
 Sensitivity analysis results of the effects of various parameters on composite design p0051 A82-37101
 Impact resistance of fiber composites p0112 A82-39852
 Integrated analysis of engine structures [NASA-TM-82713] p0111 N82-11491
 Durability/life of fiber composites in hydrothermomechanical environments [NASA-TM-82749] p0049 N82-14287
 Prediction of composite hygral behavior made simple [NASA-TM-82780] p0049 N82-16181
 Structural dynamics of shroudless, hollow fan blades with composite in-lays [NASA-TM-82816] p0018 N82-22266
 Compression behavior of unidirectional fibrous composite [NASA-TM-82833] p0050 N82-22313
 Designing with fiber-reinforced plastics (planar random composites) [NASA-TM-82812] p0050 N82-24300
 Environmental and High-Strain Rate effects on composites for engine applications [NASA-TM-82882] p0051 N82-31449
 Tensile buckling of advanced turboprops [NASA-TM-82896] p0112 N82-31708

- CHANG, A.**
The influence of Coriolis forces on gyroscopic motion of spinning blades
[ASME PAPER 82-GT-163] p0030 A82-35384
- CHANG, R.**
Modeling and Analysis of Power Processing Systems (MAPPS). Volume 1: Technical report
[NASA-CR-165538] p0083 A82-14447
Modeling and Analysis of Power Processing Systems (MAPPS). Volume 2: Appendices
[NASA-CR-165539] p0145 A82-16748
- CHANG, M. L.**
Computer model of catalytic combustion/Stirling engine heater head
[NASA-CR-165378] p0134 A82-22666
- CHANG, M. L. S.**
Development of a high-temperature durable catalyst for use in catalytic combustors for advanced automotive gas turbine engines
[NASA-CR-165396] p0130 A82-13510
- CHANG, S. R.**
A finite element stress analysis of spur gears including fillet radii and rim thickness effects
[NASA-TN-82865] p0101 A82-28646
On finite element stress analysis of spur gears
[NASA-CR-167938] p0107 A82-29607
- CHARLESTON, J.**
Performance of advanced chromium electrodes for the NASA Redox Energy Storage System
[NASA-TN-82724] p0118 A82-12574
- CHARLESTON, J. A.**
Improved chromium electrodes for REDOX cells
[NASA-CASE-LEW-13653-1] p0121 A82-22672
- CHARBET, A. Y.**
The velocity field near the orifice of a Helmholtz resonator in grazing flow
[NASA-CR-160548] p0153 A82-18994
- CHEN, D. E.**
Detection of a change in the oxidation state on aluminum surface using angular correlation of positron annihilation radiation
A82-30374
- CHEN, L. S.**
Investigation of spray characteristics for flashing injection of fuels containing dissolved salt and superheated fuels
[NASA-CR-3563] p0027 A82-26295
- CHEN, L.-D.**
Atomization and combustion properties of flashing injectors
[AIAA PAPER 82-0300] p0092 A82-17880
- CHEN, R. T.**
Undoped semi-insulating LEC GaAs - A model and a mechanism
p0159 A82-13754
Stoichiometry-controlled compensation in liquid encapsulated Czochralski GaAs
p0153 A82-17585
Compensation mechanism in liquid encapsulated Czochralski GaAs Importance of melt stoichiometry
p0086 A82-40403
Effect of melt stoichiometry on twin formation in LEC GaAs
p0160 A82-46517
High purity low dislocation GaAs single crystals
[NASA-CR-165593] p0159 A82-23030
- CHENG, J. H.**
Detection of a change in the oxidation state on aluminum surface using angular correlation of positron annihilation radiation
A82-30374
- CHERNOV, I. A.**
An example of a solution to transonic equations for shock-free flow about a symmetric profile
A82-26439
- CHERNOV, V. IU.**
Dynamics of snow cover in mountain regions of the Aral Sea basin, studied using satellite photographs
A82-27462
- CHEPARK, M. T.**
Investigation of a comb-type slow-wave structure for millimeter-wave masers
A82-18368
- CHIAPPETTA, L. H.**
A heat exchanger computational procedure for temperature-dependent fouling
[ASME PAPER 81-HT-75] p0092 A82-10961
- CAINA, R. V.**
Comparison of two and three dimensional flow computations with laser anemometer measurements in a transonic compressor rotor
[NASA-TN-82777] p0004 A82-15020
- CHEN, S.**
Environmental effects on solar concentrator mirrors
A82-23394
- CHRISOLIN, B. C.**
Study of controlled diffusion stator mixing. I. Aerodynamic and mechanical design report
[NASA-CR-165500] p0224 A82-16081
- CHO, P.**
On the opening of premixed Bunsen flame tips
p0057 A82-37570
- CHO, Y.**
INPAT power building blocks for 20 GHz spaceborne transmit amplifier
[AIAA 82-0498] p0086 A82-23566
- CHO, Y. C.**
Mode propagation in nonuniform circular ducts with potential flow
[NASA-TN-82766] p0151 A82-14881
- CHOI, P. H.**
Alignment of fluid molecules in an EHD contact
[ASLE PREPRINT 81-LC-5C-1] p0107 A82-18407
- CHOI, I.**
Boundary-layer effects in composite laminates. I - Free-edge stress singularities. II - Free-edge stress solutions and basic characteristics
p0116 A82-46806
Boundary layer thermal stresses in angle-ply composite laminates, part 1
[NASA-CR-165412] p0113 A82-26713
Boundary-layer effects in composite laminates: Free-edge stress singularities, part 6
[NASA-CR-165440] p0114 A82-26718
- CHOO, Y. K.**
New features and applications of PRESTO, a computer code for the performance of regenerative, superheated steam turbine cycles
[NASA-TP-1954] p0119 A82-16477
Parametric performance analysis of steam-injected gas turbine with a thermionic-energy-converter-lined combustor
[NASA-TN-82736] p0121 A82-23678
- CHORIN, A. J.**
Numerical modelling of turbulent flow in a combustion tunnel
p0093 A82-27000
Numerical modeling of turbulent combustion in premixed gases
p0056 A82-28708
- CHOU, L. C.**
Effects of condensation and surface motion on the structure of steady-state fronts
A82-19360
- CHRISHAN, C.**
Socioeconomic impact of photovoltaic power at Schuchuli, Arizona
[NASA-CR-165551] p0133 A82-19669
- CHRISTIE, R. J.**
Vibration analysis of three guyed tower designs for intermediate size wind turbines
[NASA-CR-165589] p0137 A82-30709
- CHRISTNER, L.**
Technology development for phosphoric acid fuel cell powerplant, phase 2
[NASA-CR-165426] p0131 A82-16482
- CHU, B. K.**
Development of a high-temperature durable catalyst for use in catalytic combustors for advanced automotive gas turbine engines
[NASA-CR-165396] p0130 A82-13510
Computer model of catalytic combustion/Stirling engine heater head
[NASA-CR-165378] p0134 A82-22666
- CHUANG, S. Y.**
Detection of a change in the oxidation state on aluminum surface using angular correlation of positron annihilation radiation
A82-30374
- CICCOLELLA, D.**
A new antenna concept for satellite communications
[NASA-CR-167924] p0079 A82-31584
- CIOWI, J. L.**
Solar cell development for the power extension package
[NASA-TN-82685] p0118 A82-11551

- Large area low-cost space solar cell development
[NASA-TM-82902] p0126 N82-32854
- CLAYG, B. G.**
Thin film temperature sensor phase 3
[NASA-CR-165476] p0097 N82-22479
- CLARK, J. F.**
Study of electrical and chemical propulsion systems for auxiliary propulsion of large space systems. Volume 1: Executive summary
[NASA-CR-165502-VOL-1] p0046 N82-11110
- CLARK, J. S.**
Gas-turbine critical research and advanced technology support project
[NASA-TM-81708] p0118 N82-13509
- COHEN, P. B.**
The orthogonal in-situ machining of single and polycrystalline aluminum and copper, volume 1
[NASA-CR-168929] p0076 N82-24361
- COLLETT, C. B.**
Characteristics of the TeRC/Hughes J-series 30-cm engineering model thruster
p0046 A82-15435
- COLLIN, B. E.**
Coaxial prime focus feeds for paraboloidal reflectors
[NASA-CR-167934] p0078 N82-31585
- COLLINS, F. G.**
Design of prototype charged particle fog dispersal unit
[NASA-CR-34811] p0141 N82-16659
- COLLINS, J. L.**
Experience and assessment of the DOE-NASA Mod-1 2000-Kilowatt wind turbine generator at Boone, North Carolina
[NASA-TM-82721] p0125 N82-30710
- CONGDON, C. W.**
Jet impingement heat transfer enhancement for the GPU-3 Stirling engine
[NASA-TM-82727] p0163 N82-11993
- CONNELLY, D. J.**
Coupled cavity traveling wave tube with velocity tapering
[NASA-CASE-LEW-12296-1] p0082 N82-26568
- CONNORS, J. F.**
The aerospace technology laboratory (a perspective, then and now)
[NASA-TM-82754] p0031 N82-19229
- COOKE, D. L.**
Additional extensions to the NASCAP computer code, volume 3
[NASA-CR-167857] p0040 N82-26378
- CORBAN, B. B.**
Interactive-graphic flowpath plotting for turbine engines
[NASA-TM-82756] p0017 N82-15041
- CONNELIUS, C. J.**
Effects of condensation and surface motion on the structure of steady-state fronts
A82-19360
- CORRIGAN, B. D.**
Comparison of upwind and downwind rotor operation of the DOE/NASA 100-kw MOD-0 wind turbine
p0122 N82-23710
- CORY, B. J.**
Wideband, high speed switch matrix development for SS-TDMA applications
p0086 A82-43784
- COULSON, C. E.**
Active clearance control system for a turbomachine
[NASA-CASE-LEW-12938-1] p0020 N82-32366
- COY, J.**
Optimal tooth numbers for compact standard spur gear sets
[ASME PAPER 81-DET-115] p0102 A82-19335
- COY, J. J.**
Surface geometry of circular cut spiral bevel gears
[ASME PAPER 81-DET-114] p0108 A82-19334
- Lubricant effects on efficiency of a helicopter transmission
[NASA-TM-82857] p0100 N82-25520
- Tooth profile analysis of circular-cut, spiral-bevel gears
[NASA-TM-82840] p0101 N82-26681
- Reliability model for planetary gear
[NASA-TM-82859] p0101 N82-28643
- The optimal design of involute gear teeth with unequal addenda
[NASA-TM-82866] p0101 N82-28645
- A finite element stress analysis of spur gears including fillet radii and rim thickness effects
[NASA-TM-82865] p0101 N82-28646
- Precision of spiral-bevel gears
[NASA-TM-82888] p0102 N82-30552
- Kinematic precision of gear trains
[NASA-TM-82887] p0102 N82-32733
- COYNER, J. V.**
Primary propulsion/large space system interaction study
[NASA-CR-165277] p0044 N82-18315
- CRANE, R. K.**
A review of transhorizon propagation phenomena
p0079 A82-10679
- CRAWLEY, E. F.**
Aerodynamic damping measurements in a transonic compressor
[ASME PAPER 82-GT-287] p0012 A82-35459
- In-plane inertial coupling in tuned and severely mistuned bladed disks
[ASME PAPER 82-GT-288] p0012 A82-35460
- CREEKMORE, B.**
A real time Pegasus propulsion system model for VSTOL piloted simulation evaluation
[AIAA PAPER 81-2663] p0020 A82-19221
- A real time Pegasus propulsion system model for VSTOL piloted simulation evaluation
[NASA-TM-82770] p0016 N82-13144
- CROLEY, D. E., JR.**
First results of material charging in the space environment
[NASA-TM-84743] p0081 N82-24431
- CROUSE, J. E.**
Computer program for aerodynamic and blading design of multistage axial-flow compressors
[NASA-TP-1946] p0016 N82-15039
- CRUGNOLA, A.**
Effect of gamma irradiation on the friction and wear of ultrahigh molecular weight polyethylene
p0062 A82-10674
- CULL, R. C.**
The effects of controls and controllable and storage loads on the performance of stand-alone photovoltaic systems
p0127 A82-45027
- CURREN, A. M.**
Ion beam textured graphite electrode plates
[NASA-CASE-LEW-12919-2] p0050 N82-26386
- CURTIS, E. B.**
Determination of optimum sunlight concentration level in space for 3-4 cascade solar cells
[NASA-TM-82899] p0126 N82-32853
- CUSANO, C.**
Effects of artificially produced defects on film thickness distribution in sliding EHD point contacts
[NASA-TM-82732] p0099 N82-16412
- The influence of surface dents and grooves on traction in sliding EHD point contacts
[NASA-TM-82943] p0102 N82-32734
- CUTROSE, E. B.**
Low NOx heavy fuel combustor concept program, phase 1
[NASA-CR-165449] p0135 N82-24651
- Low NO sub x heavy fuel combustor concept program phase 1A gas tests
[NASA-CR-167877] p0055 N82-25337
- Low NO sub x heavy fuel combustor concept program phase 1A gas tests
[NASA-CR-167877] p0055 N82-25337
- D**
- DADONE, L.**
Performance degradation of propeller/rotor systems due to rime ice accretion
[AIAA PAPER 82-0286] p0014 A82-28322
- DANLIE, K. E.**
Deposit formation in liquid fuels. I - Effect of coal-derived Lewis bases on storage stability of Jet A turbine fuel
p0074 A82-22241
- DAILEY, C. L.**
Shuttle to GEO propulsion tradeoffs
[AIAA PAPER 82-1245] p0034 A82-35082
- Integrated propulsion for near-Earth space missions. Volume 1: Executive summary
[NASA-CR-167889-VOL-1] p0045 N82-33424

- Integrated propulsion for near-Earth space missions, Volume 2: Technical [NASA-CR-167889-VOL-2] p0046 N82-33425
- CANDEKAR, K. V.**
Time resolved density measurements in premixed turbulent flames [AIAA PAPER 82-0036] p0056 A82-22033
- CANIEL, S. R.**
Quantitative separation of tetralin hydroperoxide from its decomposition products by high performance liquid chromatography p0048 A82-15696
- Deposit formation in liquid fuels, II - The effect of selected compounds on the storage stability of Jet A turbine fuel p0074 A82-22240
- Deposit formation in liquid fuels, I - Effect of coal-derived Lewis bases on storage stability of Jet A turbine fuel p0074 A82-22241
- Deposit formation in liquid fuels, III - The effect of selected nitrogen compounds on diesel fuel p0074 A82-22238
- CANEIGER, S.**
Pressure pulsations above turbomolecular pumps p0076 A82-46430
- DAVINO, R.**
Three-dimensional flow field in the tip region of a compressor rotor passage I - Mean velocity profiles and annulus wall boundary layer [ASME PAPER 82-GT-11] p0011 A82-35280
- Three-dimensional flow field in the tip region of a compressor rotor passage, II - Turbulence properties [ASME PAPER 82-GT-2341] p0011 A82-35416
- Three dimensional mean velocity and turbulence characteristics in the annulus wall region of an axial flow compressor rotor passage [NASA-CR-169003] p0026 N82-25252
- DAVINO, R. H.**
Characteristics of the flow in the annulus-wall region of an axial-flow compressor rotor blade passage [AIAA PAPER 82-0413] p0009 A82-17933
- DAVIS, F. G.**
Pollution reduction technology program small jet aircraft engines, phase 3 [NASA-CR-165386] p0023 N82-14095
- FMS fuel addendum: Pollution reduction technology program small jet aircraft engines, phase 3 [NASA-CR-165387] p0024 N82-14096
- DAVIS, K. A.**
The AGT101 technology - An automotive alternative p0037 A82-11783
- DAVIS, S. M.**
Eigenvalues of the Rayleigh-Benard and Marangoni problems p0092 A82-13396
- Nonlinear Marangoni convection in bounded layers. I - Circular cylindrical containers, II - Rectangular cylindrical containers p0094 A82-39501
- Surface-tension induced instabilities: Effects of lateral boundaries [NASA-CR-165530] p0092 N82-11390
- DAWICKE, D. S.**
A preliminary study of crack initiation and growth at stress concentration sites [NASA-CR-169358] p0115 N82-33738
- DAYTON, J. A., JR.**
Experimental verification of a computational procedure for the design of TWT-refocuser-NDC systems p0082 A82-16128
- DEARBORN, D. L.**
Long-term high-velocity oxidation and hot corrosion testing of several NiCrAl and FeCrAl base oxide dispersion strengthened alloys p0062 A82-37151
- Method of protecting a surface with a silicon-slurry/alumina coating [NASA-CASE-LEW-13343-1] p0068 N82-28441
- DEANE, R. L.**
Additional experiments on flowability improvements of aviation fuels at low temperatures, volume 2 [NASA-CR-167912] p0074 N82-31546
- DECKER, A. J.**
Three-dimensional shock structure in a transonic flutter cascade p0006 A82-37937
- Fringe localization requirements for three-dimensional flow visualization of shock waves in diffuse-illumination double-pulse holographic interferometry [NASA-TP-1868] p0095 N82-22481
- DECKER, D. K.**
High power solar array switching regulation p0043 A82-11736
- DEGRUYL, J.**
IMPATT power building blocks for 20 GHz spaceborne transmit amplifier [AIAA 82-0498] p0086 A82-23566
- DEISSLENG, R. G.**
Turbulent solution of the Navier-Stokes equations for uniform shear flow [NASA-TN-82925] p0089 N82-32634
- DELAUSANTA, D.**
Application of photovoltaic electric power to the rural education/communication needs of developing countries [NASA-CR-167894] p0137 N82-29720
- DELOMBARD, R.**
Operational performance of the photovoltaic-powered grain mill and water pump at Tanqaya, Upper Volta [NASA-TN-82767] p0120 N82-19673
- DELUCCIA, R. A.**
Rotor fragment protection program: Statistics on aircraft gas turbine engine rotor failures that occurred in U.S. commercial aviation during 1978 [NASA-CR-165388] p0027 N82-27316
- DELVIGS, P.**
PMR polyimides-review and update [NASA-TN-82021] p0068 N82-24342
- DEMGACHE, R. M.**
Primary propulsion/large space system interaction study [NASA-CR-165277] p0044 N82-18315
- DEWITT, K. J.**
Numerical simulation of one-dimensional heat transfer in composite bodies with phase change [NASA-CR-165607] p0002 N82-22142
- DEWOBAY, R. A.**
Low NOx heavy fuel combustor concept program. Phase 1: Combustion technology generation [NASA-CR-165482] p0136 N82-24725
- DHARMADEVIKAR, V. S.**
Study of the photovoltaic effect in thin film barium titanate [NASA-CR-165081] p0131 N82-16479
- DICARLO, J. A.**
Strength advantages of chemically polished boron fibers before and after reaction with aluminum [NASA-TN-82806] p0049 N82-21258
- Factors influencing the thermally-induced strength degradation of B/Al composites [NASA-TN-82823] p0050 N82-24297
- Method and apparatus for strengthening boron fibers [NASA-CASE-LEW-13826-1] p0050 N82-26385
- DINEL, L. A.**
Advanced technology for controlling pollutant emissions from supersonic cruise aircraft p0001 N81-18004
- DIETZ, W. T.**
OH-VPE growth of Mg-doped GaAs p0159 A82-38411
- DITTMAR, J. M.,**
Propeller tip vortex - A possible contributor to aircraft cabin noise p0152 A82-17603
- In-flight acoustic results from an advanced-design propeller at Mach numbers to 0.8 [AIAA PAPER 82-1120] p0021 A82-35017
- Noise of the SR-3 propeller model at 2 deg and 4 deg angle of attack [NASA-TN-82738] p0151 N82-16808
- A shock wave approach to the noise of supersonic propellers [NASA-TN-82752] p0151 N82-16809
- A preliminary comparison between the SR-3 propeller noise in flight and in a wind tunnel [NASA-TN-82805] p0152 N82-21998
- DODDS, W. J.**
NASA/General Electric broad-specification fuels combustion technology program - Phase I results

ORIGINAL PAGE IS
OF POOR QUALITY

DODGE, F. T.

PERSONAL AUTHOR INDEX

and status
[AIAA PAPER 82-1089] p0021 A82-35000
Demonstration of catalytic combustion with
residual fuel
[NASA-CR-165369] p0131 N82-16484

DODGE, F. T.
Study of vapor flow into a capillary acquisition
device
[NASA-CR-167003] p0091 N82-24452

DONG, S. B.
Analytical and experimental investigation of the
propagation and attenuation of sound in extended
reaction lined ducts
[AIAA PAPER 81-2014] p0153 A82-10454

DOMOVAN, M. M.
Integrated gasifier combined cycle polygeneration
system to produce liquid hydrogen
[NASA-TM-82921] p0125 N82-30713

DORNER, J.
Pressure pulsations above turbomolecular pumps
p0076 A82-46430

DOSS, H.
Comparative analysis of CCMHD power plants
p0158 A82-20747

DOUDY, M.
Automotive Stirling engine development program
[NASA-CR-167937] p0164 N82-29235

DOWSON, D.
Basic lubrication equations
[NASA-TM-81693] p0099 N82-16413
Lubrication of rigid ellipsoidal solids
[NASA-TM-81694] p0100 N82-25518

DRAGO, R. J.
On the automatic generation of YEM models for
complex gears - A work-in-progress report
p0109 A82-48243

DRESHFIELD, R. L.
Trends in high temperature gas turbine materials
[NASA-TM-82715] p0058 N82-11182

DEWEE, M. A.
Advanced technology for controlling pollutant
emissions from supersonic cruise aircraft
p0001 N81-18004

DUJONDJI, J.
Review of analysis methods for rotating systems
with periodic coefficients
p0135 N82-23702

DULIKRAVICH, D. S.
A computational design method for transonic
turbomachinery cascades
[ASME PAPER 82-67-117] p0022 A82-35348
CAS22 - FORTRAN program for fast design and
analysis of shock-free airfoil cascades using
fictitious-gas concept
[NASA-CR-1597] p0006 N82-16044

GRIBCC: Computer program for generation of C type
multilevel, three dimensional and boundary
conforming periodic grids
[NASA-CR-167846] p0008 N82-26239
Fast generation of three-dimensional computational
boundary-conforming periodic grids of C-type
[NASA-CR-165596] p0009 N82-28253

DULIN, D.
Oxidation and formation of deposit precursors in
hydrocarbon fuels
[NASA-CR-165534] p0073 N82-18402

DUNBAR, R. S.
Mars Driver Two - A status report
p0046 A82-18191
Mars driver reaction engine characteristics and
performance in earth orbital transfer missions
p0046 A82-18199
A small scale lunar launcher for early lunar
material utilization
p0032 A82-35617

DUREEM, P. A.
Distorted turbulence in axisymmetric flow
p0089 A82-16071
Analysis of the decay of temperature fluctuations
in isotropic turbulence
p0089 A82-40781
The premixed flame in uniform straining flow
p0055 A82-43194
Rough analysis of installation effects on
turboprop noise
[NASA-TM-82924] p0152 N82-32082

DUSCHA, R. A.
40-KW phosphoric acid fuel cell field test -
project plan

p0128 A82-45325

DUSTIN, M. J.
Rolling resistance of electric vehicle tires from
track tests
[NASA-TM-82836] p0124 N82-28786
On the road performance tests of electric test
vehicle for correlation with road load simulator
[NASA-TM-82900] p0127 N82-33829

DUTTA, S.
Effects of heating rate on density,
microstructure, and strength of Si3N4-6 wt.%
Y2O3 and a beta-prime sialon
[ASIS PAPER 42-D-81] p0070 A82-42366

DYBA, G.
Spherical roller bearing analysis. SKF computer
program SPHERBEAM. Volume 3: Program
correlation with full scale hardware tests
[NASA-CR-165205] p0106 N82-20542

DYBA, G. J.
Spherical roller bearing analysis. SKF computer
program SPHERBEAM. Volume 2: User's manual
[NASA-CR-165204] p0106 N82-20541
High speed cylindrical roller bearing analysis.
SKF computer program CYBEAM. Volume 2: User's
manual
[NASA-CR-165364] p0146 N82-31968
Research report: User's manual for computer
program AT811005. PLANETSYS, a computer program
for the steady state and transient thermal
analysis of a planetary power transmission system
[NASA-CR-165366] p0146 N82-31970

E

EBERHART, R. W.
Preliminary feasibility assessment for
Earth-to-space electromagnetic (Railgun) launchers
[NASA-CR-167866] p0033 N82-29345

EBBLE, R. V.
Propulsion study for Small Transport Aircraft
Technology (STAT)
[NASA-CR-165499] p0022 N82-10037

EASLEE, T. E.
Strength distributions of SiC ceramics after
oxidation and oxidation under load
[ACS PAPER 9-C-80C] p0071 A82-20143
Effects of oxidation and oxidation under load on
strength distributions of Si3N4
[ACS PAPER 69-B-80] p0071 A82-35071

EASLEY, A. J.
Performance and operational economics estimates
for a coal gasification combined-cycle
cogeneration powerplant
[NASA-TM-82729] p0120 N82-19672

EATON, H. E.
Development of low modulus material for use in
ceramic gas path seal applications
[NASA-CR-165469] p0022 N82-10039

EBERHARDT, R. E.
An experiment to evaluate liquid hydrogen storage
in space
A82-20748
Cryogenic fluid management experiment
[NASA-CR-165495] p0039 N82-15117

EBERT, L. J.
The influence of cobalt on the tensile and
stress-rupture properties of the nickel-base
superalloy MAR-M247
p0063 A82-47399
The influence of cobalt on the microstructure of
the nickel-base superalloy MAR-M247
p0063 A82-47400

ECHE, A.
A finite element formulation of Euler equations
for the solution of steady transonic flows
[AIAA PAPER 82-0062] p0009 A82-17759
Application of a finite element algorithm for the
solution of steady transonic Euler equations
[AIAA PAPER 82-0970] p0010 A82-31939
Investigation of rotational transonic flows
through ducts using a finite element scheme
[AIAA PAPER 82-1267] p0012 A82-37711

EDDE, H.
Collection and dissemination of thermal energy
storage system information for the pulp and
paper industry
p0136 N82-24686

EDIE, P. C.
Straight and chopped DC performance data for a

- Reliance HV-250AT motor with a General Electric
HV-1 controller
[NASA-CR-165447] p0132 N82-17608
Straight and chopped DC performance data for a
General Electric 5HY436A) DC shunt motor with a
General Electric HV-1 controller
[NASA-CR-165507] p0005 N82-24425
- ROBERTS, A. G.
Aluminum blade development for the Mod-CA
200-kilowatt wind turbine
[NASA-TM-82594] p0119 N82-14633
- RICHMOND, R.
Buoyancy effects on the temperature field in
downward spreading flames
p0094 N82-41203
- RISHBAUM, D. B.
Development of a dual-field heteropolar power
converter
[NASA-CR-165160] p0004 N82-24424
- RUSTBY, W. K.
NASA/General Electric broad-specification fuels
combustion technology program - Phase I results
and status
[AIAA PAPER 82-1009] p0021 N82-35000
Demonstration of catalytic combustion with
residual fuel
[NASA-CR-165169] p0131 N82-16484
- WELICHT, W. B.
Stoichiometry-controlled combustion in liquid
encapsulated Crochalski GaAs
p0158 N82-17505
Combustion mechanism in liquid encapsulated
Crochalski GaAs Importance of melt stoichiometry
p0086 N82-40403
- WELLS, D. W.
Advanced general aviation comparative
engine/airframe integration study
[NASA-CR-165564] p0025 N82-22263
Advanced stratified charge rotary aircraft engine
design study
[NASA-CR-165398] p0107 N82-27743
- WELFAER, H. M.
Solutions of the compressible Navier-Stokes
equations using the integral method
[AIAA PAPER 81-0046] p0093 N82-23832
- WELLS, A. M.
The effects of control and controllable and
storage loads on the performance of stand-alone
photovoltaic systems
p0127 N82-45027
- WEG, R. D.
Hot isostatically pressed manufacture of high
strength HfZr 76 disk and seal shapes
[NASA-CR-165549] p0064 N82-26439
- WEGEL, M. A.
Effects of cobalt on the microstructure of Udimet
700
[NASA-CR-165603] p0064 N82-28409
- WEGERT, G. W.
Interaction of upstream flow distortions with high
Mach number cascades
[NASA-TM-82759] p0003 N82-12043
- WEGNER, S.
Numerical simulation of sheath structure and
current-voltage characteristics of a
conductor-dielectric disk in a plasma
p0040 N82-15904
Numerical simulation of plasma insulator
interactions in space. Part I: The self
consistent calculation
p0039 N82-14272
Numerical simulation of plasma insulator
interactions in space. Part 2: Dielectric
effects
p0039 N82-14273
- WESKINE, F. J.
Time variability and structure of quiet sun
sources at 6 cm wavelength
p0167 N82-26003
- WESION, J.
Modified face seal for positive film stiffness
[NASA-CR-LEW-12989-1] p0099 N82-12442
- WETTERS, R. D.
Electric and magnetic fields
[NASA-CR-165604] p0045 N82-28350
- WIVANICH, P. L.
NASA/Lewis Research Center Icing Research Program
p0001 N82-21140
- WVANS, D. J.
Hot isostatically pressed manufacture of high
strength HfZr 76 disk and seal shapes
[NASA-CR-165549] p0064 N82-26439
- WVANS, J. C.
Multijunction high voltage concentrator solar cells
p0043 N82-11796
- WVANS, J. C., JR.
Fabrication of multijunction high voltage
concentrator solar cells by integrated circuit
technology
p0127 N82-44957
High voltage V-groove solar cell
[NASA-CR-LEW-13401-2] p0123 N82-24717
Method of making a high voltage V-groove solar cell
[NASA-CR-LEW-13401-1] p0124 N82-29709
High voltage planar multijunction solar cell
[NASA-CR-LEW-13400-1] p0125 N82-31764
- WVANS, J. W.
A multi-purpose method for analysis of spur gear
tooth loading
[NASA-CR-165163] p0104 N82-10401
- WVANS, W.
Methods for the calculation of axial wave numbers
in lined ducts with mean flow
p0153 N82-14044
Acoustic transmission in lined flow ducts - A
finite element eigenvalue problem
p0154 N82-17663
Conversion of acoustic energy by lossless liners
p0154 N82-36195
Application of steady state finite element and
transient finite difference theory to sound
propagation in a variable area duct: A
comparison with experiment
[NASA-TM-82670] p0151 N82-15047
- WVANS, J. C.
Results of chopper-controlled discharge life
cycling studies on lead acid batteries
[NASA-TM-82912] p0124 N82-30700
- WVING, W. B.
Comparison of beam and shell theories for the
vibrations of thin turbomachinery blades
[ASME PAPER 82-07-223] p0115 N82-35400

F

- FABIN, G. S.
Atomization and combustion properties of flashing
injectors
[AIAA PAPER 82-0300] p0092 N82-17080
Investigation of spray characteristics for
flashing injection of fuels containing dissolved
air and superheated fuels
[NASA-CR-3563] p0027 N82-26295
- FABIAN, W. D.
Undoped semi-insulating LRC GaAs - A model and a
mechanism
p0159 N82-13754
- FARRILL, G. A.
Computer program for calculating full potential
transonic, quasi-three-dimensional flow through
a rotating turbomachinery blade row
[NASA-TM-2030] p0005 N82-28247
- FASCHING, W. A.
CF6 jet engine performance improvement: High
pressure turbine roundness
[NASA-CR-165555] p0024 N82-17174
CF6 jet engine performance improvement: High
pressure turbine active clearance control
[NASA-CR-165556] p0027 N82-20297
The CF6 jet engine performance improvement: Low
pressure turbine active clearance control
[NASA-CR-165557] p0029 N82-33393
- FERNANDEZ DE LA ROSA, J. S.
NASA Broad Specification Fuels Combustion
Technology Program - Pratt and Whitney Aircraft
Phase I results and status
[AIAA PAPER 82-1088] p0021 N82-34999
NASA/General Electric broad-specification fuels
combustion technology program - Phase I results
and status
[AIAA PAPER 82-1087] p0021 N82-35000
- FERNANDEZ DE LA ROSA, J. S.
Cell module and fuel conditioner development
[NASA-CR-165620] p0134 N82-21713
- FERNANDEZ DE LA ROSA, J. S.
Two dimensional stagnation point flow of a dusty
gas near an oscillating plate

- FERRANTE, J. p0012 A82-37535
Universal binding energy relations in metallic adhesion
[NASA-TM-82706] p0058 A82-11183
Friction wear and asper analysis of iron implanted with 1.5-MeV nitrogen ions
[NASA-TR-1989] p0059 A82-21300
Tribological characteristics of nitrogen (N+) implanted iron
[NASA-TM-82839] p0060 A82-24322
- FERTIS, D.
Engine dynamic analysis with general nonlinear finite element codes. II - Bearing element implementation, overall numerical characteristics and benchmarking
[ASME PAPER 82-GT-292] p0100 A82-35462
- FERTIS, J.
Engine dynamic analysis with general nonlinear finite element codes. Part 2: Bearing element implementation overall numerical characteristics and benchmarking
[NASA-CR-167944] p0028 A82-33390
- FESTER, D. A.
An experiment to evaluate liquid hydrogen storage in space A82-20748
Cryogenic fluid management experiment
[NASA-CR-165495] p0039 A82-15117
- FINGER, D. G.
Analytical and experimental evaluation of biaxial contact stress p0071 A82-20741
Design and development of a ceramic radial turbine for the AGT101
[AIAA PAPER 82-1209] p0109 A82-35480
- FISKE, R.
Power systems p0001 A82-19146
Power systems p0001 A82-19146
Component technology for space power systems
[NASA-TM-82928] p0082 A82-30474
- FISKE, R. C.
Component technology for space power systems
[IAF PAPER 82-400] p0043 A82-44750
- FISHBACH, L. H.
NASA research in supersonic propulsion: A decade of progress
[NASA-TM-82862] p0019 A82-26300
- FLEETER, S.
The design and instrumentation of the Purdue annular cascade facility with initial data acquisition and analysis
[NASA-CR-167861] p0008 A82-26237
- FLENNING, D. P.
Nonlinear analysis of rotor-bearing systems using component mode synthesis
[ASME PAPER 82-GT-303] p0104 A82-35468
Effect of seals on rotor systems
[NASA-TM-82785] p0099 A82-16411
- FLOOD, D.
Gallium arsenide solar cells-status and prospects for use in space p0043 A82-11765
- FLORSCHUETZ, L. W.
Flow distributions and discharge coefficient effects for jet array impingement with initial crossflow
[ASME PAPER 82-GT-156] p0011 A82-35379
- FORD, W. F.
Numerical comparisons of nonlinear convergence accelerators p0149 A82-31438
Acceleration of convergence of vector sequences
[NASA-TM-82931] p0149 A82-29075
- FORSTNER, A. F.
On the cause of the flat-spot phenomenon observed in silicon solar cells at low temperatures and low intensities
[NASA-TM-82903] p0126 A82-31777
- FORMAN, B. J.
The 30/20 GHz flight experiment system, phase 2. Volume 1: Executive summary
[NASA-CR-165409-VOL-1] p0078 A82-20362
The 30/20 GHz flight experiment system, phase 2. Volume 2: Experiment system description
[NASA-CR-165409-VOL-2] p0078 A82-20362
- The 30/20 GHz flight experiment system, phase 2. Volume 3: Experiment system requirement document
[NASA-CR-165409-VOL-3] p0078 A82-20364
The 30/20 GHz flight experiment system, phase 2. Volume 4: Experiment system development plan
[NASA-CR-165409-VOL-4] p0078 A82-20365
- FORMAN, M.
Ion beam textured graphite electrode plates
[NASA-CASE-LEW-12919-2] p0050 A82-26386
- FRALBY, J. E.
Experimental boundary integral equation applications in speckle interferometry p0097 A82-36987
- FRALICK, G. C.
Miniature drag-force anemometer p0097 A82-40132
Extending the frequency of response of lightly damped second order systems: Application to the drag force anemometer
[NASA-TM-82927] p0096 A82-32662
- FRANKFORT, M.
Worldwide satellite market demand forecast
[NASA-CR-167918] p0079 A82-25423
- FRATER, J. L.
A multi-purpose method for analysis of spur gear tooth loading
[NASA-CR-165163] p0104 A82-10401
- FRAUENHOFF, G.
Deposit formation in liquid fuels. III - The effect of selected nitrogen compounds on diesel fuel p0074 A82-23238
- FREDERICK, G. R.
Effect of rotor configuration on guyed tower and foundation designs and estimated costs for intermediate site horizontal axis wind turbines
[NASA-TM-82804] p0121 A82-22649
- FREEDMAN, M. J.
Development and utilization of a laser velocimeter system for a large transonic wind tunnel
[NASA-TM-82886] p0095 A82-31663
Seeding considerations for an LV system in a large transonic wind tunnel p0096 A82-32689
- FREEDMAN, A. J.
Cosiation of W/001/ - Work function lowering by multiple dipole formation A82-30002
- FREEDMAN, J. W.
Direct conversion of light to radio frequency energy p0138 A82-11712
- FRENCH, K.
Fabrication of sinterable silicon nitride by injection molding p0071 A82-37015
- FRENCH, K. W.
Fabrication of turbine components and properties of sintered silicon nitride
[ASME PAPER 82-GT-252] p0071 A82-35431
- FRIEDMAN, M.
Experiments on fuel heating for commercial aircraft
[NASA-TM-82878] p0072 A82-26483
- FROST, W.
Design of prototype charged particle fog dispersal unit
[NASA-CR-3481] p0141 A82-16659
- FU, L. S.
On ultrasonic factors and fracture toughness p0116 A82-42863
The transmission or scattering of elastic waves by an inhomogeneity of simple geometry: A comparison of theories
[NASA-CR-169034] p0079 A82-26526
- FURMAN, E. R.
Gas turbine critical research and advanced technology (CRT) support project
[NASA-TM-82872] p0126 A82-31776
- FUSARO, E. L.
Geometrical aspects of the tribological properties of graphite fiber reinforced polyimide composites
[NASA-TM-82757] p0066 A82-15198
Tribological properties at 25 C of seven polyimide films bonded to 440 C high-temperature stainless steel
[NASA-TR-1944] p0067 A82-19373
Tribological evaluation of composite materials made from a partially fluorinated polyimide
[NASA-TM-82832] p0069 A82-29459

G

- GAFFIN, L. O.**
JT8D high pressure compressor performance improvement
[NASA-CR-165531] p0104 N82-11467
JT9D ceramic outer air seal system refinement program
[NASA-CR-165554] p0106 N82-18603
- GAFFNEY, E. F.**
Blade loss transient dynamic analysis of turbomachinery
[AIAA PAPER 82-1057] p0030 A82-34982
- GANN, B. F.**
Performance of advanced chromium electrodes for the NASA Redox Energy Storage System
[NASA-TM-82724] p0118 N82-12574
- GALLAGHER, J. P.**
A preliminary study of crack initiation and growth at stress concentration sites
[NASA-CR-169358] p0115 N82-33738
- GALLARDO, V.**
Blade loss transient dynamic analysis of turbomachinery
[AIAA PAPER 82-1057] p0030 A82-34982
- GALNIS, J. H.**
Three dimensional flow field inside compressor rotor, including blade boundary layers
[NASA-CR-169120] p0091 N82-27686
- GARDNER, T. C.**
Current legal and institutional issues in the commercialization of phosphoric acid fuel cells
[NASA-CR-167867] p0136 N82-29719
- GARDNER, W. B.**
Energy efficient engine: High pressure turbine uncooled rig technology report
[NASA-CR-165149] p0031 N82-32383
- GARLICK, R. G.**
Phase stability in plasma-sprayed, partially stabilized zirconia-yttria
p0070 A82-41552
- GARRETT, B. G.**
Socioeconomic impact of photovoltaic power at Schuchuli, Arizona
[NASA-CR-165551] p0133 N82-19669
- GAUGH, C.**
Fast recovery, high voltage silicon diodes for AC motor controllers
p0086 A82-36926
- GAUGLER, R. E.**
Flow visualization study of the horseshoe vortex in a turbine stator cascade
[NASA-TP-1884] p0088 N82-30498
- GAYDA, J.**
Fatigue and creep-fatigue deformation of several nickel-base superalloys at 650 C
p0062 A82-47398
- GEDRON, L.**
Validation of the NASCAP model using spaceflight data
[AIAA PAPER 82-0269] p0038 A82-17872
- GEDWILL, M. A.**
Review of NASA progress in thermal barrier coatings for stationary gas turbines
[NASA-TM-81716] p0058 N82-17335
Gas turbine critical research and advanced technology (CRT) support project
[NASA-TM-82872] p0126 N82-31776
Overlay metallic-cermet alloy coating systems
[NASA-CASE-LEW-13639-1] p0070 N82-33522
- GEE, W.**
NASA Adaptive Multibeam Phased Array (AMPA): An application study
[NASA-CR-169125] p0079 N82-28503
- GEISENDORFER, B. G.**
Comparative analysis of CCMHD power plants
p0158 A82-20747
- GELL, Y.**
On a free-electron-laser in a uniform magnetic field - A solution for arbitrarily strong electromagnetic radiation fields
A82-28409
- GEPPERT, S.**
The ac propulsion system for an electric vehicle, phase I
[NASA-CR-165480] p0129 N82-13506
- GERSCHE, R. H.**
Oxidation stability of advanced reaction-bonded Si3N4 materials
[ACS PAPER 52-B-80P] p0074 A82-33079
- GHYSER, L. C.**
AZSOP: A computer-aided design program for linear multivariable control systems
[NASA-TM-82871] p0148 N82-30992
- GUANDINI, S. K.**
Low temperature growth and electrical characterization of insulators for GaAs MISFETS
[NASA-CR-164972] p0159 N82-11959
- GHIA, K. M.**
Multigrid simulation of asymptotic curved-duct flows using a semi-implicit numerical technique
p0010 A82-29003
- GHIA, U.**
Multigrid simulation of asymptotic curved-duct flows using a semi-implicit numerical technique
p0010 A82-29003
- GHOSH, A. F.**
Numerical modeling of turbulent flow in a combustion tunnel
p0093 A82-27000
Numerical modeling of turbulent combustion in premixed gases
p0056 A82-28708
Effects of internal heat transfer on the structure of self-similar blast waves
p0093 A82-32225
- GIANATI, C. C.**
Application of image processing techniques to fluid flow data analysis
[NASA-TM-82760] p0004 N82-16049
- GIANNAKOPOULOS, A.**
INPAT power building blocks for 20 GHz spaceborne transmit amplifier
[AIAA 82-0498] p0086 A82-23566
- GIARRATANO, P. J.**
The dryout region in frictionally heated sliding contacts
[NASA-TM-82796] p0088 N82-28574
- GILL, J. C.**
Propulsion study for Small Transport Aircraft Technology (STAT)
[NASA-CR-165499] p0022 N82-10037
- GINDER, J.**
Requirements for optimization of electrodes and electrolyte for the iron/chromium Redox flow cell
[NASA-CR-165218] p0136 N82-25640
- GLASCOB, J. C.**
Comparison of upwind and downwind rotor operation of the DOE/NASA 100-kw MOD-0 wind turbine
p0122 N82-23710
- GLASCOB, T. K.**
The influence of gamma prime on the recrystallization of an oxide dispersion strengthened superalloy - MA 6000E
p0062 A82-47393
Creep shear behavior of the oxide dispersion strengthened superalloy MA 6000E
[NASA-TM-82704] p0058 N82-10195
Overlay metallic-cermet alloy coating systems
[NASA-CASE-LEW-13639-1] p0070 N82-33522
- GLIEBE, P. R.**
Effects of vane/blade ratio and spacing on fan noise
[AIAA PAPER 81-2033] p0029 A82-10457
- GOLD, P. I.**
Electrostatic fuel conditioning of internal combustion engines
[NASA-CR-169029] p0106 N82-26680
- GOLDMAN, L. J.**
Analytic investigation of effect of end-wall contouring on stator performance
[NASA-TP-1943] p0003 N82-14051
Laser anemometer measurements in an annular cascade of core turbine vanes and comparison with theory
[NASA-TP-2018] p0004 N82-26234
Comparison of laser anemometer measurements and theory in an annular turbine cascade with experimental accuracy determined by parameter estimation
[NASA-TM-82860] p0005 N82-28250
Laser anemometer using a Fabry-Perot interferometer for measuring mean velocity and turbulence intensity along the optical axis in turbomachinery
[NASA-TM-82841] p0095 N82-28605
- GOLDBRICH, R. H.**
Mathematical models for the synthesis and

- optimization of spiral bevel gear tooth surfaces
[NASA-CR-3553] p0106 N82-25516
- Precision of spiral-bevel gears
[NASA-TN-82889] p0102 N82-30552
- Kinematic precision of gear trains
[NASA-TN-82887] p0102 N82-32733
- GOLDSMITH, I. H.**
Advanced turboprop testbed systems study
[NASA-CR-167895] p0014 N82-33375
- GOLDSTEIN, H. E.**
Generation of instability waves at a leading edge
[NASA-TN-82835] p0087 N82-22453
- GONZALEZ-SANABRIA, G. D.**
Cross-linked polyvinyl alcohol films as alkaline
battery separators
[NASA-TN-82802] p0054 N82-22327
- GONADIA, C.**
A theory of the n-i-p silicon solar cell
p0128 N82-45055
- GONADIA, C. P.**
High voltage V-groove solar cell
[NASA-CASE-LEW-13401-2] p0123 N82-24717
Method of making a high voltage V-groove solar cell
[NASA-CASE-LEW-13401-1] p0124 N82-29709
High voltage planar multi-junction solar cell
[NASA-CASE-LEW-13400-1] p0125 N82-31764
- GORDON, L. H.**
Mod-2 wind turbine system cluster research test
program. Volume 1: Initial plan E-1290
[NASA-TN-82906] p0123 N82-26807
- GORDON, S.**
Thermodynamic and transport combustion properties
of hydrocarbons with air. Part 1: Properties
in SI units
[NASA-TP-1906] p0161 N82-32186
Thermodynamic and transport combustion properties
of hydrocarbons with air. Part 2: Compositions
corresponding to Kelvin temperature schedules in
part 1
[NASA-TP-1907] p0161 N82-32187
Thermodynamic and transport combustion properties
of hydrocarbons with air. Part 3: Properties
in US customary units
[NASA-TP-1908] p0161 N82-32188
Thermodynamic and transport combustion properties
of hydrocarbons with air. Part 4: Compositions
corresponding to Rankine temperature schedules
in part 3
[NASA-TP-1909] p0161 N82-32189
- GORDON, W. L.**
Electron beam induced damage in ITO coated Kapton
p0159 N82-41546
Secondary electron emission yields
p0038 N82-14226
- GORNELL, W. T.**
Computer program for aerodynamic and blading
design of multistage axial-flow compressors
[NASA-TP-1946] p0016 N82-15039
- GOULDIN, F. C.**
Time resolved density measurements in premixed
turbulent flames
[AIAA PAPER 82-0036] p0056 N82-22033
Flame structure in a swirl stabilized combustor
inferred by radiant emission measurements
p0056 N82-28694
Flow process in combustors
[NASA-CR-169294] p0092 N82-31642
- GOVINDAN, T. R.**
Effects of blade loading and rotation on
compressor rotor wake in end wall regions
[AIAA PAPER 82-0193] p0010 N82-22063
Three dimensional turbulent boundary layer
development on a fan rotor blade
[AIAA PAPER 82-1007] p0011 N82-31965
- GRABITZ, G.**
Forms of three-dimensional supersonic free jets in
linear approximation
N82-19196
- GRANDEMANU, W. W.**
Study of the photovoltaic effect in thin film
barium titanate
[NASA-CR-165081] p0131 N82-16479
- GRANT, H. P.**
Thin film temperature sensors, phase 3
[NASA-CR-165476] p0097 N82-22479
- GREBER, I.**
Dilution jet behavior in the turn section of a
reverse flow combustor
[AIAA PAPER 82-0192] p0021 N82-20291
- Dilution jet behavior in the turn section of a
reverse flow combustor
[NASA-TN-82776] p0017 N82-19220
- GREENWALD, A. C.**
Processing of silicon solar cells by ion
implantation and laser annealing
[NASA-CR-165283] p0128 N82-11546
- GREENGARD, G. H.**
Aerodynamic characteristics of airfoils with ice
accrretions
[AIAA PAPER 82-0282] p0010 N82-22081
- GREISSING, J. P.**
Development and utilization of a laser velocimeter
system for a large transonic wind tunnel
[NASA-TN-82886] p0095 N82-31663
Propeller flow visualization techniques
p0096 N82-32672
Development of a laser velocimeter for a large
transonic wind tunnel
p0096 N82-32686
- GRYVALL, M. S.**
Numerical modeling of three-dimensional confined
flows
[NASA-CR-165583] p0158 N82-24078
- GRILL, A.**
Sputtered silicon nitride coatings for wear
protection
[NASA-TN-82819] p0067 N82-20314
Some properties of RF sputtered hafnium nitride
coatings
[NASA-TN-82826] p0067 N82-21331
Deposition of reactively ion beam sputtered
silicon nitride coatings
[NASA-TN-82942] p0069 N82-30401
- GRINES, M. M.**
Thermal degradation of the tensile properties of
unidirectionally reinforced RP-AI203/EZ 33
magnesium composites
[NASA-TN-82817] p0049 N82-21260
- GRISAPPE, S. J.**
Trends in high temperature gas turbine materials
[NASA-TN-82715] p0058 N82-11182
- GROENEWEG, J. F.**
Pough analysis of installation effects on
turboprop noise
[NASA-TN-82924] p0152 N82-32082
- GROSS, S.**
Overview study of Space Power Technologies for the
advanced energetics program
[NASA-CR-165269] p0172 N82-17606
- GRUBER, E. P.**
Simplified dc to dc converter
[NASA-CASE-LEW-13495-1] p0082 N82-24432
- GUPTA, A. K.**
Modeling parameter influences on MHD swirl
combustion nozzle design
[AIAA PAPER 82-0984] p0011 N82-31947
Flow aerodynamics modeling of an MHD swirl
combustor - Calculations and experimental
verification
p0094 N82-44782
- GUPTA, D. K.**
Improved plasma sprayed NiCrAlY coatings for
aircraft gas turbine applications
p0065 N82-20742
Tailored plasma sprayed NiCrAlY coatings for
aircraft gas turbine applications
[NASA-CR-165234] p0064 N82-19360
- GUPTA, S. K.**
Design and development of a ceramic radial turbine
for the AGT101
[AIAA PAPER 82-1209] p0109 N82-35480
- GUSTAFSON, T. K.**
Stationary state model for normal metal tunnel
junction phenomena
p0159 N82-42912
- GUSTAFSSON, U. R. C.**
An automated system for global atmospheric
sampling using B-747 airliners
[NASA-CR-165264] p0139 N82-13554
- GUTIERREZ, O. A.**
Effect of facility variation on the acoustic
characteristics of three single stream nozzles
[NASA-TN-81635] p0151 N82-19944

H

HAAS, J. E.
The effect of rotor blade thickness and surface

- finish on the performance of a small axial flow turbine
[ASME PAPER 82-GT-222] p0022 A82-35409
- The effect of rotor blade thickness and surface finish on the performance of a small axial flow turbine
[NASA-TM-82736] p0003 N82-13114
- Comparison of experimental and analytical performance for contoured endwall stators
[NASA-TM-82077] p0019 N82-26299
- WADSWORTH, G. B.**
Research report: User's manual for computer program AT81Y003 SHADERTH. Steady state and transient thermal analysis of a shaft bearing system including ball, cylindrical and tapered roller bearings
[NASA-CR-165165] p0146 N82-31969
- Research report: User's manual for computer program AT81Y005. PLANETEYS, a computer program for the steady state and transient thermal analysis of a planetary power transmission system
[NASA-CR-165366] p0146 N82-31970
- WADY, M. F.**
Effect of gamma irradiation on the friction and wear of ultrahigh molecular weight polyethylene
p0062 A82-10674
- WAPP, G. R.**
Recrystallization and grain growth in NiAl
p0065 A82-44529
- WAGNER, W.**
NASA Redox cell stack shunt current, pumping power, and cell performance tradeoffs
[NASA-TM-82686] p0054 N82-19333
- WAGNER, W. H.**
NASA preprototype redox storage system for a photovoltaic stand-alone application
p0127 A82-11774
- Design flexibility of Redox flow systems
[NASA-TM-82854] p0054 N82-31459
- WAN, C.**
Measurement and prediction of mean velocity and turbulence structure in the near wake of an airfoil
p0010 A82-26137
- Three dimensional turbulent boundary layer development on a fan rotor blade
[AIAA PAPER 82-1007] p0011 A82-31965
- Numerical analysis and FORTRAN program for the computation of the turbulent wakes of turbomachinery rotor blades, isolated airfoils and cascade of airfoils
[NASA-CR-3509] p0006 N82-18184
- WALFORD, G. R.**
Turbine blade nonlinear structural and life analysis
[AIAA PAPER 82-1056] p0021 A82-34981
- Nonlinear structural and life analyses of a combustor liner
[NASA-TM-82846] p0111 N82-24501
- WARAD, G.**
Sound generated in a cascade by three-dimensional disturbances convected in a subsonic flow
[AIAA PAPER 81-2046] p0153 A82-10460
- WARREN, M. A.**
Experimental boundary integral equation applications in speckle interferometry
p0097 A82-36987
- WARREN, R. A.**
Hybrid and electric advanced vehicle systems (heavy) simulation
[NASA-CR-165536] p0163 N82-16938
- WARREN, B. J.**
Basic lubrication equations
[NASA-TM-81691] p0099 N82-16413
- Geometry and starvation effects in hydrodynamic lubrication
[NASA-TM-82807] p0042 N82-20240
- High-speed motion picture camera experiments of cavitation in dynamically loaded journal bearings
[NASA-TM-82798] p0100 N82-20543
- Frictional heating due to asperity interaction of elastohydrodynamic line-contact surfaces
[NASA-TM-1882] p0100 N82-25514
- Lubrication of rigid ellipsoidal solids
[NASA-TM-81694] p0100 N82-25518
- Film shape calculations on supercomputers
[NASA-TM-82856] p0100 N82-25519
- WARREN, D.**
A 10kW series resonant converter design, transistor characterization, and base-drive optimization
[NASA-CR-165546] p0084 N82-17439
- WARREN, D. J.**
A 10-kW series resonant converter design, transistor characterization, and base-drive optimization
p0086 A82-36927
- WATSON, R. F.**
Gas turbine ceramic-coated-vane concept with convection-cooled porous metal core
[NASA-TP-1942] p0016 N82-14090
- WATSON, G. A.**
A preliminary study of crack initiation and growth at stress concentration sites
[NASA-CR-169358] p0115 N82-33738
- WATSON, A. M.**
Magneto-hydrodynamics (MHD) Engineering Test Facility (ETF) 200 MWe power plant. Design Requirements Document (DRD)
[NASA-TM-82705] p0099 N82-12446
- WATSON, L.**
Coaxial prime focus feeds for paraboloidal reflectors
[NASA-CR-167934] p0078 N82-31585
- WATSON, F. W.**
Acoustic microscopy of silicon carbide materials
p0075 A82-33031
- WATSON, R. W.**
Study of advanced propulsion systems for Small Transport Aircraft Technology (STAT) program
[NASA-CR-165610] p0026 N82-24202
- WATSON, M. E. G.**
AGT 100 automotive gas turbine system development
[AIAA PAPER 82-1165] p0108 A82-35038
- WATSON, J. M.**
Advanced stratified charge rotary aircraft engine design study
[NASA-CR-165398] p0107 N82-27743
- WATSON, R. C.**
Flow through axially aligned sequential apertures of the orifice and Borda types
[ASME PAPER 81-HT-79] p0089 A82-10964
- Toward the use of similarity theory in two-phase choked flows
p0089 A82-16570
- Effects of arc current on the life in burner rig thermal cycling of plasma sprayed ZrO₂-Y₂O₃
[NASA-TM-82795] p0087 N82-17453
- Flow through aligned sequential orifice type inlets
[NASA-TP-1967] p0087 N82-20467
- Flows through sequential orifices with heated spacer reservoirs
[NASA-TM-82855] p0088 N82-24455
- The dryout region in frictionally heated sliding contacts
[NASA-TM-82796] p0088 N82-28574
- Use of fiber like materials to augment the cycle life of thick thermal protective seal coatings
[NASA-TM-82901] p0089 N82-32633
- WATSON, T. P.**
Ultrasonic velocity for estimating density of structural ceramics
[NASA-TM-82765] p0066 N82-14359
- WATSON, A. S.**
Analytical and experimental investigation of the propagation and attenuation of sound in extended reaction lined ducts
[AIAA PAPER 81-2014] p0153 A82-10454
- WATSON, D. M.**
Analysis of high load dampers
[NASA-CR-165503] p0026 N82-23248
- WATSON, H. R.**
Free electron lasers for transmission of energy in space
[NASA-CR-165520] p0098 N82-25499
- WATSON, M.**
Low-thrust chemical propulsion system propellant expulsion and thermal conditioning study. Executive summary
[NASA-CR-165622] p0045 N82-24287
- Low-thrust chemical propulsion system propellant expulsion and thermal conditioning study
[NASA-CR-167841] p0045 N82-24288
- WATSON, W. B.**
Thermal-barrier-coated turbine blade study
[NASA-CR-165351] p0023 N82-10040
- WATSON, T.**
Communications satellite systems capacity analysis

- [NASA-CR-167911] p0034 N82-27331
- NINGST, W. E.**
Flow visualization of shock-boundary layer interaction p0096 N82-32675
- NINTON, B.**
Low NO sub x heavy fuel combustor concept program [NASA-CR-165512] p0129 N82-12572
- NIRSCHBERG, H. S.**
Structural dynamics of shrouded, hollow, fan blades with composite in-lays [ASME PAPER 82-GT-284] p0022 N82-35456
Structural dynamics of shrouded, hollow fan blades with composite in-lays [NASA-TM-82816] p0018 N82-22266
Bird impact analysis package for turbine engine fan blades [NASA-TM-82831] p0112 N82-26701
- NIRSCHBERG, H. S.**
Elevated temperature fatigue testing of metals p0058 N82-13281
Elevated temperature fatigue testing of metals [NASA-TM-82745] p0111 N82-16419
- NISKES, J. E.**
Coastion of W/OO1/ - Work function lowering by multiple dipole formation A82-30002
- NO, F.**
Thin foil silicon solar cells with coplanar back contacts p0127 N82-44944
Development of thin wraparound junction silicon solar cells [NASA-CR-165570] p0133 N82-18689
- NO, F. T.**
Dynamic switch matrix for the TEMSA satellite switching system [AIAA 82-0458] p0085 N82-23494
- NOBENECHT, H. A.**
NASA Redox cell stack shunt current, pumping power, and cell performance tradeoffs [NASA-TM-82686] p0054 N82-19333
Performance mapping studies in Redox flow cells [NASA-TM-82707] p0120 N82-20668
- NOCHNUTH, J.**
Survey on aging on electrodes and electrocatalysts in phosphoric acid fuel cells [NASA-CR-165505] p0128 N82-11545
Preparation and evaluation of advanced electrocatalysts for phosphoric acid fuel cells [NASA-CR-165519] p0129 N82-12573
Preparation and evaluation of advanced electrocatalysts for phosphoric acid fuel cells [NASA-CR-165594] p0132 N82-17615
- NOGDON, R. B.**
Anion permselective membrane [NASA-CR-167872] p0137 N82-30711
- HODGE, P. E.**
Gas-turbine critical research and advanced technology support project [NASA-TM-81708] p0118 N82-13509
Review of NASA progress in thermal barrier coatings for stationary gas turbines [NASA-TM-81716] p0058 N82-17335
Effect of fuel to air ratio on Mach 0.3 burner rig hot corrosion of ZrO₂-Y₂O₃ thermal barrier coatings [NASA-TM-82879] p0061 N82-30373
- HOFER, K. E.**
Thermal fatigue and oxidation data of TAZ-8A and M22 alloys and variations [NASA-CR-1654C7] p0063 N82-10193
- HOFFMAN, A. C.**
Engine technology p0001 N82-19145
- HOFFMAN, J. D.**
Three-dimensional flow calculations including boundary layer effects for supersonic inlets at angle of attack [AIAA PAPER 82-0061] p0005 N82-19778
Calculation of the flow field including boundary layer effects for supersonic mixed compression inlets at angles of attack [NASA-CR-167941] p0009 N82-29269
- HOFFMAN, R. G.**
The aerospace technology laboratory (a perspective, then and now) [NASA-TM-82754] p0031 N82-19229
- HOFFMAN, R. W.**
Electron beam induced damage in ITO coated Kapton p0159 N82-41546
Secondary electron emission yields p0038 N82-14226
- HOLMES, D. E.**
Stoichiometry-controlled compensation in liquid encapsulated Czochralski GaAs p0158 N82-17585
Compensation mechanism in liquid encapsulated Czochralski GaAs Importance of melt stoichiometry p0086 N82-40403
Effect of melt stoichiometry on twin formation in LEC GaAs p0160 N82-46517
High purity low dislocation GaAs single crystals [NASA-CR-165593] p0159 N82-23030
- HOLMES, W. M., JR.**
30/20 GHz demonstration system for improving orbit utilization p0080 N82-27189
Open-loop nanosecond-synchronization for wideband satellite communications p0036 N82-27224
- HOM, K.**
Secondary effects in combustion instabilities leading to flashback [AIAA PAPER 82-0037] p0056 N82-17746
- HORSY, G. M.**
Eigenvalues of the Rayleigh-Benard and Marangoni problems p0092 N82-13396
Nonlinear Marangoni convection in bounded layers. I - Circular cylindrical containers. II - Rectangular cylindrical containers p0094 N82-39501
- HOOGENDOORN, L.**
Preliminary study of temperature measurement techniques for Stirling engine reciprocating seals [NASA-CR-165479] p0104 N82-11466
- HOOPER, D. Q., JR.**
Cell module and fuel conditioner development [NASA-CR-165462] p0130 N82-13511
Cell module and fuel conditioner development [NASA-CR-165193] p0137 N82-30712
- HORNBY, G. M.**
Surface-tension induced instabilities: Effects of lateral boundaries [NASA-CR-165530] p0092 N82-11390
- HORNWITZ, S. J.**
An iterative finite element-integral technique for predicting sound radiation from turbofan inlets in steady flight [AIAA PAPER 82-0124] p0030 N82-17796
Acoustic properties of turbofan inlets [NASA-CR-169016] p0153 N82-27090
Finite element-integral simulation of static and flight fan noise radiation from the JT15D turbofan engine [NASA-TM-82936] p0152 N82-31068
- HOTELER, R. K.**
The influence of gamma prime on the recrystallization of an oxide dispersion strengthened superalloy - MA 6000X p0062 N82-47393
- HOWARD, V. D.**
CF6 jet engine performance improvement: High pressure turbine roundness [NASA-CR-165555] p0024 N82-17174
- HOWER, P. L.**
High voltage power transistor development [NASA-CR-165547] p0084 N82-18506
- HOWES, W. L.**
New versions of old flow visualization systems p0096 N82-32670
- HOWSON, T. E.**
Creep and rupture of an ODS alloy with high stress rupture ductility p0065 N82-40335
- HRACH, F.**
Environmental control systems p0001 N82-19147
- HRACH, F. J.**
Kevlar/PMR-15 polyimide matrix composite for a complex shaped DC-9 drag reduction fairing [AIAA PAPER 82-1047] p0002 N82-37678
- HU, L.-C.**
Inexpensive cross-linked polymeric separators made from water-soluble polymers

- MOBBARTT, J. E.
Development of a spinning wave heat engine
[NASA-CR-165611] p0048 N82-23778
- MOUSSON, S. M.
Ceramic applications in turbine engines
[NASA-CR-165197] p0020 N82-31320
- MUELSTER, D. S.
Propulsion study for Small Transport Aircraft
Technology (STAT)
[NASA-CR-165499] p0164 N82-31158
- MUGGINS, G.
Advanced stratified charge rotary aircraft engine
design study
[NASA-CR-165398] p0022 N82-10037
- MUGGINS, G. L.
Advanced general aviation comparative
engine/airframe integration study
[NASA-CR-165564] p0107 N82-27743
- MULL, D. E.
Metal honeycomb to porous wireform substrate
diffusion bond evaluation
[NASA-TM-82793] p0025 N82-22263
- MULL, D. E.
Metal honeycomb to porous wireform substrate
diffusion bond evaluation
[NASA-TM-82793] p0110 N82-18612
- MULL, D. E.
Interrelation of material microstructure,
ultrasonic factors, and fracture toughness of
two phase titanium alloy
[NASA-TM-82810] p0110 N82-20551
- MURPHY, V. E.
Thermal fatigue and oxidation data of TA2-8A and
M22 alloys and variations
[NASA-CR-165407] p0063 N82-10193
- MURT, L. E.
Elastic-plastic finite-element analyses of
thermally cycled double-edge wedge specimens
[NASA-TP-1973] p0051 A82-27440
- MURVITZ, P. I.
Effects of nadic ester concentration and
processing on physical and mechanical properties
of FBR/Celion 6000 composites
[NASA-TP-1973] p0051 A82-27440
- MURVITZ, P. I.
On determination of fibre fraction in continuous
fibre composite materials
[NASA-TP-1973] p0051 A82-30133
- MURVITZ, P. I.
Application of a gripping system to test a
uniaxial graphite fiber reinforced composite
/EMF 15/Celion 6000/ in tension at 316 C
[NASA-TP-1973] p0051 A82-40796
- MURVITZ, P. I.
Forced torsional properties of FBR composites with
varying nadic ester concentrations and
processing histories
[NASA-TP-1973] p0051 A82-45630
- MUSTON, B. L.
Surface geometry of circular cut spiral bevel gears
[ASME PAPER 81-ET-114] p0108 N82-19334
- MUSTON, B. L.
Tooth profile analysis of circular-cut,
spiral-bevel gears
[NASA-TM-82840] p0101 N82-26681
- MUSTON, B. L.
A finite element stress analysis of spur gears
including fillet radii and rim thickness effects
[NASA-TM-82865] p0101 N82-28646
- MUSTON, B. L.
On finite element stress analysis of spur gears
[NASA-CR-167938] p0107 N82-29607
- MWANG, D. P.
Experimental and analytical results of tangential
blowing applied to a subsonic V/STOL inlet
[AIAA PAPER 82-1084] p0005 A82-35195
- MWANG, D. P.
A summary of V/STOL inlet analysis methods
[NASA-TM-82725] p0006 A82-40921
- MWANG, D. P.
A summary of V/STOL inlet analysis methods
[NASA-TM-82725] p0003 N82-11043
- MWANG, D. P.
Experimental and analytical results of tangential
blowing applied to a subsonic V/STOL inlet
[NASA-TM-82847] p0004 N82-24165
- MWANG, D. P.
A summary of V/STOL inlet analysis methods
[NASA-TM-82885] p0005 N82-28249
- I, L.
Turbulence in argon shock waves
[NASA-TM-82944] p0158 N82-11117
- ILES, P. A.
Thin foil silicon solar cells with coplanar back
contacts
[NASA-CR-165570] p0127 N82-44944
- ILES, P. A.
Development of thin wraparound junction silicon
solar cells
[NASA-CR-165570] p0133 N82-48689
- INGARD, K. U.
Mode propagation in nonuniform circular ducts with
potential flow
[NASA-TM-82766] p0151 N82-14881
- INGRAM, E.
Hydrodynamic and aerodynamic breakup of liquid
sheets
[NASA-TM-82800] p0087 N82-19494
- ISHIGAKI, H.
Effects of environment on microhardness of
magnesium oxide
[NASA-TP-2002] p0068 N82-22366
- ISHIGAKI, H.
Influence of corrosive solutions on microhardness
and chemistry of magnesium oxide /001/ surfaces
[NASA-TP-2040] p0102 N82-31691
- ISHIKAWA, S.
Lean-limit extinction of propane/air mixtures in
the stagnation-point flow
[NASA-TP-2040] p0057 A82-28736
- ISHIKAWA, S.
Effects of heat loss, preferential diffusion, and
flame stretch on flame-front instability and
extinction of propane/air mixtures
[NASA-TP-2040] p0057 A82-32877
- ISHIKAWA, S.
On the opening of premixed Bunsen flame tips
[NASA-TP-2040] p0057 A82-37570
- ISODA, Y.
Flow distributions and discharge coefficient
effects for jet array impingement with initial
crossflow
[ASME PAPER 82-GT-156] p0011 A82-35379
- ITO, T. T.
Thermal oxidative degradation reactions of
perfluoroalkylethers
[NASA-CR-165516] p0048 N82-12135
- ITO, T. T.
Thermal oxidative degradation reactions of linear
perfluoroalkylethers
[NASA-TM-82834] p0068 N82-26468
- IVANOV, V. A.
An example of a solution to transonic equations
for shock-free flow about a symmetric profile
[NASA-TP-1973] p0051 A82-26439
- IVES, S. T.
Internal breakdown of charged spacecraft dielectrics
[NASA-TP-1973] p0041 A82-18312
- JACK, J. E.
Reliable aerial thermography for energy conservation
[NASA-TM-81766] p0117 N82-14552
- JACKSON, T.
Turbulence measurements in a confined jet using a
six-orientation hot-wire probe technique
[AIAA PAPER 82-1262] p0094 A82-37710
- JACOBSON, B. O.
A hydrodynamic model of an outer hair cell
[NASA-TM-82773] p0143 N82-16743
- JACOBSON, B. O.
High-speed motion picture camera experiments of
cavitation in dynamically loaded journal bearings
[NASA-TM-82798] p0100 N82-20543
- JACOBSON, T. P.
Effect of aluminum phosphate additions on
composition of three-component plasma-sprayed
solid lubricant
[NASA-TP-1990] p0059 N82-21298
- JALAN, V.
Improved chromium electrodes for REDOX cells
[NASA-CASE-LEW-13653-1] p0121 N82-22672
- JALAN, V.
Requirements for optimization of electrodes and
electrolyte for the iron/chromium Redox flow cell
[NASA-CR-165218] p0136 N82-25640
- JAMES, E.
Developing a scalable inert gas ion thruster
[AIAA PAPER 82-1275] p0047 A82-37713
- JANETTE, D. C.
Whirl flutter analysis of a horizontal-axis wind
turbine with a two-bladed teetering rotor
[NASA-TM-82944] p0122 N82-23707
- JANETTE, D. C.
Theoretical and experimental power from large
horizontal-axis wind turbines
[NASA-TM-82944] p0127 N82-33830
- JANJUA, S. J.
Turbulence measurements in a confined jet using a
six-orientation hot-wire probe technique
[AIAA PAPER 82-1262] p0094 A82-37710
- JANOVICK, M. A.
Ceramic applications in turbine engines
[NASA-CR-165197] p0164 N82-31158

JARRETT, R. M.

PERSONAL AUTHOR INDEX

- JARRETT, R. M.
Effects of cobalt on structure, microchemistry and properties of a wrought nickel-base superalloy
[NASA-CR-168558] p0065 A82-34973
- JAVIDI, B.
Secondary electron emission from a charged dielectric in the presence of normal and oblique electric fields
[NASA-CR-168558] p0084 A82-18501
- JENKINS, R. M.
A comprehensive method for preliminary design optimization of axial gas turbine stages
[AIAA PAPER 82-1264] p0030 A82-35091
- JENNESS, C. M.
Advanced turboprop testbed systems study. Volume 1: Testbed program objectives and priorities, drive system and aircraft design studies, evaluation and recommendations and wind tunnel test plans
[NASA-CR-167928-VOL-1] p0028 A82-32370
- JENTZ, M. E.
Fuel quality processing study, volume 1
[NASA-CR-165327-VOL-1] p0135 A82-24649
Fuel quality/processing study Volume 2: Appendix, Task 1 literature survey
[NASA-CR-165327-VOL-2] p0135 A82-24650
- JERACKI, R. J.
Propeller tip vortex - A possible contributor to aircraft cabin noise
p0152 A82-17603
Noise of the SR-3 propeller model at 2 deg and 4 deg angle of attack
[NASA-TM-82738] p0151 A82-16808
- JOHNS, W. A.
An experiment to evaluate liquid hydrogen storage in space
A82-20748
- JOHNSON, R. L.
Preliminary analysis of a downsized advanced gas-turbine engine in a subcompact car
[NASA-TM-82848] p0163 A82-26051
- JOHNSON, B.
Development of a dual-field heteropolar power converter
[NASA-CR-165168] p0084 A82-24424
- JOHNSON, B. V.
Mass and momentum turbulent transport experiments with confined coaxial jets
[NASA-CR-165574] p0090 A82-19496
- JOHNSON, D. A.
Chemical and electrochemical behavior of the Cr(3)/Cr(2) half cell in the NASA Redox Energy Storage System
[NASA-TM-82913] p0055 A82-33463
- JOHNSON, D. C.
Jet impingement heat transfer enhancement for the GPU-3 Stirling engine
[NASA-TM-82727] p0163 A82-11993
- JOHNSON, G. M.
Multiple-grid acceleration of Lax-Wendroff algorithms
[NASA-TM-82843] p0149 A82-22922
Relaxation solution of the full Euler equations
[NASA-TM-82889] p0149 A82-24559
- JOHNSON, J. A., III
Turbulence in argon shock waves
p0158 A82-11117
- JOHNSON, R. E.
An automated system for global atmospheric sampling using B-747 airliners
[NASA-CR-165264] p0139 A82-13554
- JOHNSON, S. M.
Venturi nozzle effects on fuel drop size and nitrogen oxide emissions
[NASA-TP-2028] p0020 A82-31329
- JOHNSTON, E. A.
Thrust reverser for a long duct fan engine
[NASA-CASE-LEW-13199-1] p0019 A82-26293
- JOHNSTON, J. P.
Turbulent boundary layer heat transfer experiments: Convex curvature effects including introduction and recovery
[NASA-CR-3510] p0090 A82-17456
- JOHNSTON, R. P.
Active clearance control system for a turbomachine
[NASA-CASE-LEW-12938-1] p0020 A82-32366
- JONES, A. L.
Aerodynamic analysis of VTCI inlets and definition of a short, blowing-lip inlet
[NASA-CR-165617] p0007 A82-22211
- JONES, C.
Advanced stratified charge rotary aircraft engine design study
[NASA-CR-165398] p0107 A82-27743
- JONES, J. C.
An experimental investigation into the feasibility of a thermoelectric heat flux gage
[NASA-TM-82755] p0095 A82-14494
- JONES, W. E.
Effect of gamma irradiation on the friction and wear of ultrahigh molecular weight polyethylene
p0062 A82-10674
Tribological characteristics of nitrogen (N₂) implanted iron
[NASA-TM-82839] p0060 A82-24322
- JONES, W. E., JR.
The effect of oxygen concentration on the boundary-lubricating characteristics of a C ether and a polyphenyl ether to 300 C
p0070 A82-21699
Fabrication and wear test of a continuous fiber/particulate composite total surface hip replacement
[NASA-TM-81746] p0066 A82-11211
Elucidation of wear mechanisms by ferrographic analysis
[NASA-TM-82737] p0066 A82-15199
Tribological characteristics of a composite total-surface hip replacement
[NASA-TP-1853] p0066 A82-16239
Friction wear and auger analysis of iron implanted with 1.5-MeV nitrogen ions
[NASA-TP-1989] p0059 A82-21300
Thermal and oxidative degradation studies of formulated C-ethers by gel-permeation chromatography
[NASA-TP-1994] p0068 A82-21332
Thermal oxidative degradation reactions of linear perfluoroalkyl leathers
[NASA-TM-82834] p0068 A82-26468
Boundary lubrication: Revisited
[NASA-TM-82858] p0069 A82-29458
- JOU, W.-H.
Finite volume calculation of three-dimensional potential flow around a propeller
[AIAA PAPER 82-0957] p0010 A82-31933
- JOULIN, G.
On stability of premixed flames in stagnation - Point flow
p0057 A82-37574
- JUANARENA, D. B.
A remote millivolt multiplexer and amplifier module for wind tunnel data acquisition
p0083 A82-41845
- JUNASZ, A. J.
Optimization of the oxidant supply system for combined cycle MHD power plants
[NASA-TM-82909] p0123 A82-26790
Comparative analysis of the conceptual design studies of potential early commercial MHD power plants (CSPEC)
[NASA-TM-82897] p0123 A82-27838
- JURKOVICH, M.
Flow visualization of shock-boundary layer interaction
p0096 A82-32675
- JURTA, R. M.
On determination of fibre fraction in continuous fibre composite materials
p0051 A82-38133

K

- KAFATORS, M.
Ultraviolet observations of the 1980 eclipse of the symbiotic star CI Cygni
A82-27331
- KANEL, H. M.
Effects of internal heat transfer on the structure of self-similar blast waves
p0093 A82-32225
- KANI, S.
Characteristics of the LeRC/Hughes J-series 30-cm engineering model thruster
p0046 A82-15435
- KAN, H. K.
First results of material charging in the space environment

- [NASA-TN-89743] p0081 N82-24431
- KAMMEL, J. W.**
Stress evaluations under rolling/sliding contacts
[NASA-CR-165561] p0113 N82-17521
- KAMTOLA, M. A.**
Effects of vane/blade ratio and spacing on fan noise
[AIAA PAPER 81-2033] p0029 N82-10457
- KAO, H. C.**
Some aspects of calculating flows about
three-dimensional subsonic inlets
[NASA-TN-82789] p0004 N82-25213
- KAPOON, V. J.**
Multijunction high voltage concentrator solar cells
p0043 N82-11796
Fabrication of multijunction high voltage
concentrator solar cells by integrated circuit
technology p0127 N82-44957
- KARACULLE, M.**
Ultrasonic input-output for transmitting and
receiving longitudinal transducers coupled to
same face of isotropic elastic plate
[NASA-CR-1506] p0110 N82-18613
- KARAS, J. C.**
Design and verification of a multiple fault
tolerant control system for SFS applications
using computer simulation
[AIAA 81-2173] p0035 N82-10124
- KARO, A. H.**
Cancellation of W/OO1/ - Work function lowering by
multiple dipole formation N82-30002
- KARSAK, A. F.**
Nonlinear analysis of rotor-bearing systems using
component mode synthesis
[ASME PAPER 82-GT-303] p0104 N82-35468
Gas turbine ceramic-coated-vane concept with
convection-cooled porous metal core
[NASA-TP-1942] p0016 N82-14090
- KASPER, E. J.**
A simplified design procedure for life prediction
of rocket thrust chambers
[AIAA PAPER 82-1251] p0043 N82-35087
- KASHAIF, B.**
A simplified design procedure for life prediction
of rocket thrust chambers
[AIAA PAPER 82-1251] p0043 N82-35087
- KASHALE, B.**
Development of a simplified procedure for thrust
chamber life prediction
[NASA-CR-165585] p0044 N82-21253
- KASUNA, E.**
A multi-purpose method for analysis of spur gear
tooth loading
[NASA-CR-165163] p0104 N82-10401
- KATSAWIS, T.**
Velocity gradient method for calculating velocities
in an axisymmetric annular duct
[NASA-TP-2029] p0005 N82-29270
- KATS, I.**
Space Shuttle Orbiter charging
[AIAA PAPER 82-0119] p0040 N82-17793
Validation of the NASCAP model using spaceflight
data
[AIAA PAPER 82-0269] p0038 N82-17872
'Bootstrap' charging of surfaces composed of
multiple materials p0085 N82-18318
NASCAP simulation of laboratory charging tests
using multiple electron guns p0033 N82-18319
Differential charging of high-voltage spacecraft -
The equilibrium potential of insulated surfaces
p0041 N82-35547
Representation and material charging response of
geoplasma environments p0039 N82-14249.
Simulation of charging response of SCATHA (P78-2)
satellite p0039 N82-14250
Charging of a large object in low polar Earth orbit
p0039 N82-14275
Additional extensions to the NASCAP computer code,
volume 1 p0146 N82-25810
[NASA-CR-167855]
Additional extensions to the NASCAP computer code,
volume 2 p0040 N82-26377
[NASA-CF-167856]
- KAUFMAN, A.**
Turbine blade nonlinear structural and life analysis
[AIAA PAPER 82-1056] p0021 N82-34981
Develop and test fuel cell powered on-site
integrated total energy system. Phase 3:
Full-scale power plant development
[NASA-CR-165328] p0117 N82-13490
Elastic-plastic finite-element analyses of
thermally cycled single-edge wedge specimens
[NASA-TP-1982] p0111 N82-20565
Elastic-plastic finite-element analyses of
thermally cycled double-edge wedge specimens
[NASA-TP-1973] p0111 N82-20566
Nonlinear structural and life analyses of a
combustor liner
[NASA-TN-82846] p0111 N82-24501
Evaluation of inelastic constitutive models for
nonlinear structural analysis
[NASA-TN-82845] p0112 N82-24502
Development and test fuel cell powered on-site
integrated total energy system. Phase 3:
Full-scale power plant development
[NASA-CR-167898] p0137 N82-30705
- KAUFMAN, M. E.**
Experimental simulation of biased solar arrays
with the space plasma
[NASA-CR-165485] p0157 N82-10880
Electric thruster research p0045 N82-24285
Electric and magnetic fields
[NASA-CR-165604] p0045 N82-28350
- KAUTH, M. E.**
Mechanism and models for zinc metal morphology in
alkaline media
[NASA-TN-82768] p0120 N82-19671
- KAWAY, E. T.**
Kevlar/PHR-15 polyimide matrix composite for a
complex shaped DC-9 drag reduction fairing
[AIAA PAPER 82-1047] p0002 N82-37678
Kevlar/PHR-15 reduced drag DC-9 reverser stang
fairing p0052 N82-31448
- KAWAMOTO, Y.**
The 30/20 GHz flight experiment system, phase 2.
Volume 1: Executive summary
[NASA-CR-165409-VOL-1] p0078 N82-20362
The 30/20 GHz flight experiment system, phase 2.
Volume 2: Experiment system description
[NASA-CR-165409-VOL-2] p0078 N82-20363
The 30/20 GHz flight experiment system, phase 2.
Volume 3: Experiment system requirement document
[NASA-CR-165409-VOL-3] p0078 N82-20364
The 30/20 GHz flight experiment system, phase 2.
Volume 4: Experiment system development plan
[NASA-CR-165409-VOL-4] p0078 N82-20365
- KAYS, W. H.**
Turbulent boundary layer heat transfer
experiments: Convex curvature effects including
introduction and recovery
[NASA-CR-3510] p0090 N82-17456
- KAZA, K. E. V.**
Aceroelastic characteristics of a cascade of
mistuned blades in subsonic and supersonic flows
[ASME PAPER 81-DET-122] p0021 N82-19337
Coupled bending-bending-torsion flutter of a
mistuned cascade with nonuniform blades
[NASA-TN-82813] p0111 N82-21604
Whirl flutter analysis of a horizontal-axis wind
turbine with a two-bladed teetering rotor
p0122 N82-23707
- KEITNER, I. D.**
Impact of advanced propeller technology on
aircraft/mission characteristics of several
general aviation aircraft
[NASA-CR-167984] p0009 N82-33347
- KELKAR, S. S.**
Input filter compensation for switching regulators
[NASA-CR-169005] p0085 N82-25442
- KELLEN, J. L.**
Mathematical modeling of ice accretion on airfoils
[AIAA PAPER 82-0284] p0014 N82-27098
- KELLEN, L. E.**
Alignment of fluid molecules in an EHD contact
[ASLE PREPRINT 81-IC-5C-1] p0107 N82-18407
Analysis of infrared emission from thin adsorbates
p0056 N82-21431
- KELLS, G. G.**
Test results and facility description for a
40-kilowatt stirling engine

- [NASA-TM-82620] p0163 N82-13013
Assessment of a 40-kilowatt stirling engine for
underground mining applications
[NASA-TM-82822] p0125 N82-30714
- KENDALL, B. E. F.
Anaerobic polymers as high vacuum leak sealants
p0108 A82-21967
Pressure pulsations above turbo-molecular pumps
p0076 A82-46430
- KENNEDY, F. E.
Single pass sub phenomena - Analysis and experiment
[ASME PAPER 81-LUB-55] p0107 A82-18449
- KENSLAKE, W. E.
Feasibility of an earth-to-space rail launcher
system
[IAF PAPER 82-46] p0033 A82-44659
- KESSEL, P.
Design of prototype charged particle fog dispersal
unit
[NASA-CR-3481] p0141 N82-16659
- KESSELER, W. E.
Fuel quality/processing study. Volume 2:
Appendix. Task 1 literature survey
[NASA-CR-165327-VOL-2] p0135 N82-24650
- KESSELER, R. E.
Fuel quality processing study, volume 1
[NASA-CR-165327-VOL-1] p0135 N82-24649
- KHAB, A. S.
Micral ternary alloy having improved cyclic
oxidation resistance
[NASA-CASE-LEW-13339-1] p0061 N82-31505
- KHANDLWAL, P. K.
Acoustic microscopy of silicon carbide materials
p0075 A82-33031
- KIDWELL, J. E.
AGT 101 automotive gas turbine system development
[AIAA PAPER 82-1166] p0108 A82-35039
The AGT 101 advanced automotive gas turbine
[ASME PAPER 82-GT-72] p0108 A82-35321
- KIEHL, R. E.
Aeroelastic characteristics of a cascade of
mistuned blades in subsonic and supersonic flows
[ASME PAPER 81-DET-122] p0021 A82-19337
Coupled bending-torsion flutter of a
mistuned cascade with nonuniform blades
[NASA-TM-82813] p0111 N82-21604
- KIN, Q.
Raman study of the improper ferroelectric phase
transition in iron iodine boracite
A82-30297
- KING, E. B.
Phosphoric acid fuel cell technology status
[NASA-TM-82791] p0120 N82-19670
- KING, B. J.
Modeling the full-bridge series-resonant power
converter
p0086 A82-46385
- KING, V. W.
Alignment of fluid molecules in an EHD contact
[ASLE PREPRINT 81-LC-5C-1] p0107 A82-18407
- KIRBY, L. J.
Ultrasonic scanning system for imaging flaw growth
in composites
[NASA-TM-82799] p0076 N82-22386
A high speed implementation of the random
decrement algorithm
[NASA-TM-82853] p0076 N82-22388
Piezoelectric composite materials
[NASA-CASE-LEW-12582-1] p0054 N82-31450
- KIRKPATRICK, C. G.
Stoichiometry-controlled compensation in liquid
encapsulated Czochralski GaAs
p0158 A82-17585
Compensation mechanism in liquid encapsulated
Czochralski GaAs importance of melt stoichiometry
p0086 A82-40403
High purity low dislocation GaAs single crystals
[NASA-CR-165593] p0159 N82-23030
- KLANN, J. L.
Preliminary analysis of a downsized advanced
gas-turbine engine in a subcompact case
[NASA-TM-82848] p0163 N82-26051
- KLECKNER, H. J.
Spherical roller bearing analysis. SKF computer
program SPHERBEAN. Volume 1: Analysis
[NASA-CR-165203] p0106 N82-20540
Spherical roller bearing analysis. SKF computer
program SPHERBEAN. Volume 2: User's manual
[NASA-CR-165204] p0106 N82-20541
- Spherical roller bearing analysis. SKF computer
program SPHERBEAN. Volume 3: Program
correlation with full scale hardware tests
[NASA-CR-165205] p0106 N82-20542
- High speed cylindrical roller bearing analysis.
SKF computer program CYBEAN. Volume 2: User's
manual
[NASA-CR-165364] p0146 N82-31968
Research report: User's manual for computer
program AT81Y003 SHABERTH. Steady state and
transient thermal analysis of a shaft bearing
system including ball, cylindrical and tapered
roller bearings
[NASA-CR-165365] p0146 N82-31969
Research report: User's manual for computer
program AT81Y003. PLANETSYS, a computer program
for the steady state and transient thermal
analysis of a planetary power transmission system
[NASA-CR-165366] p0146 N82-31970
- KLEIN, W. E.
Experience with modified aerospace reliability and
quality assurance method for wind turbines
[NASA-TM-82803] p0110 N82-19550
- KLEIN, S. J.
Ultrasonic velocity for estimating density of
structural ceramics
[NASA-TM-82765] p0066 N82-14359
- KLUMPF, M. E.
Fuel quality processing study, volume 1
[NASA-CR-165327-VOL-1] p0135 N82-24649
Fuel quality/processing study. Volume 2:
Appendix. Task 1 literature survey
[NASA-CR-165327-VOL-2] p0135 N82-24650
- KNAPP, H. H.
Active clearance control system for a turbomachine
[NASA-CASE-LEW-12938-1] p0020 N82-32366
- KOBAN, J. A.
Lewis Research Center's coal-fired, pressurized,
fluidized-bed reactor test facility
[NASA-TM-81616] p0087 N82-11397
- KOCEAN, M. J.
Work of fracture in aluminum metal-matrix composites
p0053 A82-31339
Tensile properties of SiC/aluminum filamentary
composites - Thermal degradation effects
p0053 A82-46220
- KOPFKEY, H. G.
Cold-air performance of a 15.41-cm-tip-diameter
axial-flow power turbine with variable-area
stator designed for a 75-kW automotive gas
turbine engine
[NASA-TM-82644] p0024 N82-21193
- KOHL, F. J.
Thermodynamics and kinetics of the sulfation of
porous calcium silicate
[NASA-TM-82769] p0048 N82-15119
- KOHLMAN, D. L.
Ice tunnel tests of a composite porous leading
edge for use with a liquid anti-ice system
[NASA-CR-164966] p0014 N82-11052
- KOLACKI, J.
A new approach to the minimum weight/loss design
of switching power converters
p0082 A82-16831
- KOLB, H.
The 30/20 GHz communications satellite trunking
network study
[NASA-CR-165467] p0078 N82-13302
- KOLECKI, J. C.
Analysis and design of a standardized control
module for switching regulators
p0083 A82-46388
- KOONS, H. C.
First results of material charging in the space
environment
[NASA-TM-84743] p0081 N82-24431
- KORHAN, K. D.
Performance degradation of propeller/rotor systems
due to zinc ice accretion
[AIAA PAPER 82-0286] p0014 A82-28322
- KORTOVICH, C. S.
Development of materials and process technology
for dual alloy disks
[NASA-CR-165224] p0063 N82-18370
- KOSHAKI, M. C.
Multistage depressed collector for dual mode
operation
[NASA-CASE-LEW-13282-1] p0081 N82-24415

- KOSMANL, M. G.**
Experimental verification of a computational procedure for the design of TWT-refocuser-MDC systems p0082 A82-16128
- Analytic investigation of efficiency and performance limits in klystron amplifiers using multidimensional computer programs; multi-stage depressed collectors; and thorionic cathode life studies p0118 A82-12553
- Three-dimensional relativistic field-electron interaction in a multicavity high-power klystron. I: Basic theory [NASA-TP-1992] p0081 A82-22439
- Three-dimensional relativistic field-electron interaction in a multicavity high-power klystron. Part 2: Working Equations [NASA-TP-2098] p0081 A82-23397
- KOTZOT, M. T.**
Fuel quality processing study, volume 1 [NASA-CR-165327-VOL-1] p0135 A82-24649
- Fuel quality/processing study. Volume 2: Appendix. Task 1 literature survey [NASA-CR-165327-VOL-2] p0135 A82-24650
- KOZAK, A.**
Small axial turbine stator technology program [NASA-CF-165602] p0028 A82-32367
- KOZYLOWSKI, H.**
Energy efficient engine exhaust mixer model technology [NASA-CF-165459] p0025 A82-22264
- KRAINSKY, I.**
Electron beam induced damage in ITO coated Kapton p0159 A82-41546
- Secondary electron emission yields p0038 A82-14226
- KRAKAUER, H.**
Cessation of W/001/ - Work function lowering by multiple dipole formation A82-30002
- KREHL, J. J.**
Chopper-controlled discharge life cycling studies on lead-acid batteries [NASA-CR-165616] p0134 A82-20661
- KRATZER, R. H.**
Thermal oxidative degradation reactions of perfluoroalkylethers [NASA-CR-165516] p0048 A82-12135
- Thermal oxidative degradation reactions of linear perfluoroalkylethers [NASA-TM-82834] p0068 A82-26468
- KRAUSE, L. M.**
Miniature drag-force anemometer p0097 A82-40132
- KRAUTER, A. I.**
Measurement of oil film thickness for application to elastomeric Stirling engine rod seals [ASME PAPER 81-LNB-9] p0107 A82-18426
- KRESKOVSKY, J. P.**
Turbofan forced mixer-nozzle internal flowfield. Volume 3: A computer code for 3-D mixing in axisymmetric nozzles [NASA-CR-3494] p0091 A82-22460
- KROSEL, S. M.**
Application of integration algorithms in a parallel processing environment for the simulation of jet engines [NASA-TM-82746] p0149 A82-14849
- Automated procedure for developing hybrid computer simulations of turbofan engines. Part 1: General description [NASA-TP-1851] p0146 A82-33020
- KUBASCO, A. J.**
Low NOx heavy fuel combustor concept program [NASA-CR-167876] p0074 A82-26482
- KUBBY, J. A.**
Mass Driver Two - A status report p0046 A82-18191
- A small scale lunar launcher for early lunar material utilization p0032 A82-35617
- KUHN, T. E.**
Pollution reduction technology program small jet aircraft engines, phase 3 [NASA-CR-165386] p0023 A82-14095
- EFES fuel addendum: Pollution reduction technology program small jet aircraft engines, phase 3**
- [NASA-CR-165387] p0024 A82-14096
- KUNDE, M. E.**
VIA observations of solar active regions at 6 cm wavelength p0167 A82-10156
- Time variability and structure of quiet sun sources at 6 cm wavelength p0167 A82-26003
- Magnetic structure of a flaring region producing impulsive microwave and hard X-ray bursts p0167 A82-27323
- KUMOSAKA, M.**
'Coriolis resonance' within a rotating duct p0012 A82-37938
- KUOK, C. K.**
Bluff-body flameholder wakes - A simple numerical solution [AIAA PAPER 82-1177] p0093 A82-35043
- L**
- LABITZKE, K.**
Stratospheric-mesospheric midwinter disturbances - A summary of observed characteristics A82-12135
- LADDER, E. H.**
Evaluation of wind tunnel performance testings of an advanced 45 deg swept 8-bladed propeller at Mach numbers from 0.45 to 0.85 [NASA-CR-3505] p0007 A82-19178
- LAPLEN, J. H.**
Turbine blade nonlinear structural and life analysis [AIAA PAPER 82-1056] p0021 A82-34981
- LAKSHMINARAYANA, S.**
Interaction of compressor rotor blade wake with wall boundary layer/vortex in the end-wall region [ASME PAPER 81-GT-1] p0010 A82-19301
- Effects of blade loading and rotation on compressor rotor wake in end wall regions [AIAA PAPER 82-0193] p0010 A82-22063
- Measurement and prediction of mean velocity and turbulence structure in the near wake of an airfoil p0010 A82-26137
- Three sensor hot wire/film technique for three dimensional mean and turbulence flow field measurement p0097 A82-30300
- Three dimensional flow field inside the passage of a low speed axial flow compressor rotor [AIAA PAPER 82-1006] p0011 A82-31964
- Three dimensional turbulent boundary layer development on a fan rotor blade [AIAA PAPER 82-1007] p0011 A82-31965
- Three-dimensional flow field in the tip region of a compressor rotor passage. I - Mean velocity profiles and annulus wall boundary layer [ASME PAPER 82-GT-11] p0011 A82-35280
- Investigation of the tip-clearance flow inside and at the exit of a compressor rotor passage. I - Mean velocity field [ASME PAPER 82-GT-12] p0011 A82-35281
- Three-dimensional flow field in the tip region of a compressor rotor passage. II - Turbulence properties [ASME PAPER 82-GT-234] p0011 A82-35416
- Numerical analysis and FORTRAN program for the computation of the turbulent wakes of turbomachinery rotor blades, isolated airfoils and cascade of airfoils [NASA-CR-3509] p0006 A82-18184
- Three dimensional mean velocity and turbulence characteristics in the annulus wall region of an axial flow compressor rotor passage [NASA-CR-169003] p0026 A82-25282
- Investigation of the tip clearance flow inside and at the exit of a compressor rotor passage [NASA-CR-169004] p0026 A82-25253
- Three dimensional flow field inside compressor rotor, including blade boundary layers [NASA-CR-169120] p0091 A82-27686
- LAW, P.**
Engine dynamic analysis with general nonlinear finite element codes. II - Bearing element implementation, overall structural characteristics and bearing marking [ASME PAPER 82-GT-292] p0108 A82-35462
- Engine dynamic analysis with general nonlinear finite element codes. Part 2: Bearing element

implementation overall numerical characteristics and benchmarking [NASA-CR-167944] p0026 N82-33390

LANSBERT, R. F.
The acoustical structure of highly porous open-cell foams p0154 A82-45165

LAW, B.
Oxidation and formation of deposit precursors in hydrocarbon fuels [NASA-CR-165534] p0073 N82-18402

LANGSTON, L. S.
Turbine endwall single cylinder program [NASA-CR-169278] p0091 N82-31638

LAPRAD, B. F.
Sensor failure detection system [NASA-CR-165515] p0023 N82-13145

LARGE, G. D.
Cooled variable-area radial turbine technology program [NASA-CR-165408] p0024 N82-19221

LARKIN, B.
Energy efficient engine exhaust mixer model technology [NASA-CR-165459] p0025 N82-22264

LARSON, V. W.
Characteristic dynamic energy equations for Stirling cycle analysis p0138 A82-14816

LASAGNA, P. L.
In-flight acoustic results from an advanced-design propeller at Mach numbers to C.8 [AIAA PAPER 82-1120] p0021 A82-35017
A preliminary comparison between the SR-3 propeller noise in flight and in a wind tunnel [NASA-TM-82805] p0152 N82-21998

LASHWAY, B. W.
Progress in ceramic component fabrication technology [AIAA PAPER 82-1211] p0071 A82-35064

LAU, S. K.
Ceramic thermal barrier coatings for gas turbine engines [ASME PAPER 82-GT-265] p0071 A82-35441
Evaluation of present thermal barrier coatings for potential service in electric utility gas turbines [NASA-CR-165545] p0063 N82-18368

LAUER, J. L.
Alignment of fluid molecules in an EHD contact [ASLE PREPRINT 81-LC-5C-11] p0107 A82-18407
Analysis of infrared emission from thin adsorbates p0056 A82-21431

LAVRINOVICH, A. A.
Investigation of a comb-type slow-wave structure for millimeter-wave masers A82-18368

LAW, C. K.
Lean-limit extinction of propane/air mixtures in the stagnation-point flow p0057 A82-28736
Effects of heat loss, preferential diffusion, and flame stretch on flame-front instability and extinction of propane/air mixtures p0057 A82-32877
On the opening of premixed Bunsen flame tips p0057 A82-37570
On stability of premixed flames in stagnation-point flow p0057 A82-37574

LAWLEY, A.
Work of fracture in aluminum metal-matrix composites p0053 A82-31339
Tensile properties of SiC/aluminum filamentary composites - Thermal degradation effects p0053 A82-46220

LAWVER, B. R.
Testing of fuel/oxidizer-rich, high-pressure preburners [NASA-CP-165609] p0074 N82-24353

LEACH, K.
Energy efficient engine: Turbine transition duct model technology report [NASA-CR-167996] p0029 N82-33394

LECHEN, B. T.
Low NOx heavy fuel combustor concept program [NASA-CR-165481] p0138 N82-33827

LEE, D.
Study of controlled diffusion stator blading. I. Aerodynamic and mechanical design report [NASA-CR-165500] p0024 N82-16081

LEE, F. C.
A new approach to the minimum weight/loss design of switching power converters p0082 A82-16831
Power system design optimization using Lagrange multiplier techniques p0085 A82-20743
Analysis and design of a standardized control module for switching regulators p0083 A82-46388
Modeling and Analysis of Power Processing Systems (MAPPS). Volume 1: Technical report [NASA-CR-165538] p0083 N82-14447
Modeling and Analysis of Power Processing Systems (MAPPS). Volume 2: Appendices [NASA-CR-165539] p0145 N82-16748
Input filter compensation for switching regulators [NASA-CR-169005] p0085 N82-25442

LEE, J. K.
Vibrations of cantilevered shallow cylindrical shells of rectangular planform p0115 A82-11298
Vibrations of twisted rotating blades [ASME PAPER 81-DET-127] p0115 A82-19341

LEE, S. S.
Ultrasonic input-output for transmitting and receiving longitudinal transducers coupled to same face of isotropic elastic plate [NASA-CR-3506] p0110 N82-18613

LEE, S. W.
NASA Adaptive Multibeam Phased Array (ANPA): An application study [NASA-CR-169125] p0079 N82-28503

LEE, S. Y.
Ceramic thermal barrier coatings for gas turbine engines [ASME PAPER 82-GT-265] p0071 A82-35441
Evaluation of present thermal barrier coatings for potential service in electric utility gas turbines [NASA-CR-165545] p0063 N82-18368

LEEN, W. L.
First results of material charging in the space environment [NASA-TM-84743] p0081 N82-24431

LEHTINEN, B.
The role of modern control theory in the design of controls for aircraft turbine engines [NASA-TM-82815] p0018 N82-22262
AESOP: A computer-aided design program for linear multivariable control systems [NASA-TM-82871] p0148 N82-30992

LEIBCKI, H. F.
Synthetic battery cycling techniques [NASA-TM-82945] p0125 N82-30715

LEININGER, G. C.
Model degradation effects on sensor failure detection p0148 A82-13143

LEISSA, A. W.
Vibrations of cantilevered shallow cylindrical shells of rectangular planform p0115 A82-11298
Vibrations of twisted rotating blades [ASME PAPER 81-DET-127] p0115 A82-19341
Comparison of beam and shell theories for the vibrations of thin turbomachinery blades [ASME PAPER 82-GT-223] p0115 A82-35408

LEKROUDIS, S. G.
Solutions of the compressible Navier-Stokes equations using the integral method [AIAA PAPER 81-0006] p0093 A82-23832
A new numerical approach for compressible viscous flows [NASA-CR-168842] p0090 N82-22455

LENCH, B. A.
Microstructural effects on the room and elevated temperature low cycle fatigue behavior of Waspaloy [NASA-CR-165497] p0113 N82-26702

LEROY, B. E.
Satellite-aided land mobile communications system implementation considerations [NASA-TM-82861] p0036 N82-25290

LESCO, D. J.
A digital optical torque meter for high rotational speed applications [NASA-TM-82914] p0095 N82-31664

LEUNG, M. S.
First results of material charging in the space environment

[NASA-TM-84743] p0081 N82-24431
LEVINE, S. E.
 Overlay metallic-cermet alloy coating systems
 [NASA-CASE-LEW-13639-1] p0070 N82-33522

LEVUSH, E.
 On a free-electron-laser in a uniform magnetic field - A solution for arbitrarily strong electromagnetic radiation fields
 A82-28409

LEW, H. G.
 Low NOx heavy fuel combustor concept program.
 Phase I: Combustion technology generation
 [NASA-CR-165482] p0136 N82-24725

LEW, K. G.
 An automated system for global atmospheric sampling using B-747 airliners
 [NASA-CR-165264] p0139 N82-13554

LEWIS, C. E.
 OM-VPE growth of Mg-doped GaAs
 p0159 A82-38411

LEZBERG, F. A.
 Aircraft sampling of the sulfate layer near the tropopause following the eruption of Mount St. Helens
 p0140 A82-37450

LIEBERT, C. E.
 Gas turbine ceramic-coated-vane concept with convection-cooled porous metal core
 [NASA-TP-1942] p0016 N82-14090
 Covering solid, film cooled surfaces with a duplex thermal barrier coating
 [NASA-CASE-LEW-13450-1] p0088 N82-25463

LILLY, D. G.
 On the prediction of swirling flowfields found in axisymmetric combustor geometries
 p0029 A82-12120
 A simple finite difference procedure for the vortex controlled diffuser
 [AIAA PAPER 82-0109] p0030 A82-17788
 Mean flowfields in axisymmetric combustor geometries with swirl
 [AIAA PAPER 82-0177] p0092 A82-17824
 Modeling parameter influences on MHD swirl combustor nozzle design
 [AIAA PAPER 82-0984] p0011 A82-31947
 Bluff-body flameholder wakes - A simple numerical solution
 [AIAA PAPER 82-1177] p0093 A82-35043
 Turbulence measurements in a confined jet using a six-orientation hot-wire probe technique
 [AIAA PAPER 82-1262] p0094 A82-37710
 Flow aerodynamics modeling of an MHD swirl combustor - Calculations and experimental verification
 p0094 A82-44782
 Investigations of flowfields found in typical combustor geometries
 [NASA-CR-165461] p0090 N82-15360
 Investigations of flowfields found in typical combustor geometries
 [NASA-CR-168585] p0090 N82-19495
 Investigations of flowfields found in typical combustor geometries
 [NASA-CR-169295] p0092 N82-31643

LIN, A.
 Numerical analysis of confined turbulent flow
 p0093 A82-24748

LIN, S.
 Bluff-body flameholder wakes - A simple numerical solution
 [AIAA PAPER 82-1177] p0093 A82-35043

LIN, Y.
 Tooth profile analysis of circular-cut, spiral-bevel gears
 [NASA-TM-82840] p0101 N82-26681

LINDBERG, L. J.
 Oxidation stability of advanced reaction-bonded Si3N4 materials
 [ACS PAPER 52-B-80P] p0074 A82-33030

LING, F. F.
 Fabrication and wear test of a continuous fiber/particulate composite total surface hip replacement
 [NASA-TM-81746] p0066 N82-11211
 Tribological characteristics of a composite total-surface hip replacement
 [NASA-TP-1853] p0066 N82-16239

LING, J. S.
 Performance of advanced chromium electrodes for the NASA Redox Energy Storage System
 [NASA-TM-82724] p0118 N82-12574

LINSCOTT, B. S.
 Aluminum blade development for the Mod-OA 200-kilowatt wind turbine
 [NASA-TM-82594] p0119 N82-14633

LIPSITT, A.
 Dilution jet behavior in the turn section of a reverse flow combustor
 [AIAA PAPER 82-0192] p0021 A82-20291
 Modified face seal for positive film stiffness
 [NASA-CASE-LEW-12909-1] p0099 N82-12442
 Dilution jet behavior in the turn section of a reverse flow combustor
 [NASA-TM-82776] p0017 N82-19220

LITTLE, B. S.
 Advanced turboprop testbed systems study. Volume 1: Testbed program objectives and priorities, drive system and aircraft design studies, evaluation and recommendations and wind tunnel test plans
 [NASA-CR-167928-VOL-1] p0028 N82-32370

LITVIN, P. L.
 Mathematical models for the synthesis and optimization of spiral bevel gear tooth surfaces
 [NASA-CR-3553] p0106 N82-25516
 Precision of spiral-bevel gears
 [NASA-TM-82888] p0102 N82-30552
 Kinematic precision of gear trains
 [NASA-TM-82887] p0102 N82-32733

LIU, G. T.
 Brushfire arc discharge model
 p0038 N82-14224

LOEFFLER, I. J.
 QCSEE over-the-wing engine acoustic data
 [NASA-TM-82708] p0020 N82-29324

LOEWENTHAL, S. M.
 Effects of ultra-clean and centrifugal filtration on rolling-element bearing life
 [ASME PAPER 81-LUB-35] p0103 A82-18436
 Multiroller traction drive speed reducer: Evaluation for automotive gas turbine engine
 [NASA-TP-2027] p0101 N82-26678

LOHMAN, R. P.
 NASA Broad Specification Fuels Combustion Technology program - Pratt and Whitney Aircraft Phase I results and status
 [AIAA PAPER 82-1088] p0021 A82-34999

LOONIS, W. E.
 Improved boundary lubrication with formulated C-ethers
 [NASA-TM-82808] p0067 N82-20313

LORAN, B. L.
 Fuel quality processing study, volume 1
 [NASA-CR-165327-VOL-1] p0135 N82-24649
 Fuel quality/processing study. Volume 2: Appendix. Task 1 literature survey
 [NASA-CR-165327-VOL-2] p0135 N82-24650

LOUIS, J. F.
 Flow aerodynamics modeling of an MHD swirl combustor - Calculations and experimental verification
 p0094 A82-44782

LOVBERG, R. E.
 Integrated propulsion for near-Earth space missions. Volume 1: Executive summary
 [NASA-CR-167889-VOL-1] p0045 N82-33424
 Integrated propulsion for near-Earth space missions. Volume 2: Technical
 [NASA-CR-167889-VOL-2] p0046 N82-33425

LOVBERG, R. E.
 Shuttle to GEO propulsion tradeoffs
 [AIAA PAPER 82-1245] p0034 A82-35082

LOWELL, C. E.
 Long-term high-velocity oxidation and hot corrosion testing of several NiCrAl and FeCrAl base oxide dispersion strengthened alloys
 p0062 A82-37151
 Gas-turbine critical research and advanced technology support project
 [NASA-TM-81708] p0118 N82-13509
 NiCrAl ternary alloy having improved cyclic oxidation resistance
 [NASA-CASE-LEW-13339-1] p0061 N82-31505
 Gas turbine critical research and advanced technology (CRT) support project
 [NASA-TM-82872] p0126 N82-31776
 Failure mechanisms of thermal barrier coatings exposed to elevated temperatures

[NASA-TM-82905] p0061 N82-32461
LUCAS, J. G.
 Forward acoustic performance of a model turbofan
 designed for a high specific flow (QF-14)
 [NASA-TP-1968] p0152 N82-21036
LUBOWITZ, H. J.
 CH-VPE growth of Hq-doped GaAs p0159 N82-38411
LUBWIG, L. P.
 Gas turbine ceramic-coated-vane concept with
 convection-cooled porous metal core
 [NASA-TP-1942] p0016 N82-14090
 Composite seal for turbomachinery
 [NASA-CASE-LEW-12131-3] p0099 N82-19540
LUERS, J. K.
 Mathematical modeling of ice accretion on airfoils
 [AIAA PAPER 82-0284] p0014 N82-27098
 Effect of heavy rain on aircraft N82-21149
LUH, H. S.
 30/20 GHz communications satellite multibeam antenna
 [AIAA 82-6449] p0079 N82-23486
LUIDENS, R. W.
 Comparison of two parallel/series flow turbofan
 propulsion concepts for supersonic V/STOL
 [AIAA PAPER 81-2637] p0020 N82-19214
 Comparison of two parallel/series flow turbofan
 propulsion concepts for supersonic V/STOL
 [NASA-TM-82743] p0004 N82-18178
LUNDIN, W.
 Secondary electron emission yields p0038 N82-14226
LUPION, H. W.
 Micronized coal burner facility
 [NASA-CASE-LEW-13426-1] p0126 N82-31769
LYONS, V. J.
 Effect of fuel-air-ratio nonuniformity on
 emissions of nitrogen oxides
 [NASA-TP-1798] p0016 N82-13143

M

MACARTHUR, C. D.
 Mathematical modeling of ice accretion on airfoils
 [AIAA PAPER 82-0284] p0014 N82-27098
MACCABEGOR, C. A.
 Reusable rocket engine maintenance study
 [NASA-CR-165569] p0044 N82-16172
MACKALL, K. G.
 In-flight acoustic results from an advanced-design
 propeller at Mach numbers to 0.8
 [AIAA PAPER 82-1120] p0021 N82-35017
MACKAY, R. A.
 The influence of orientation on the stress rupture
 properties of nickel-base superalloy single
 crystals p0062 N82-47397
MACKLIS, S. L.
 Interfacing wind energy conversion equipment with
 utility systems N82-21148
MAHISHI, J. M.
 Micromechanical predictions of crack propagation
 and fracture energy in a single fiber
 boron/aluminum model composite
 [NASA-CR-168550] p0052 N82-18326
MARHOUD, H. F.
 Analysis and design of a standardized control
 module for switching regulators p0083 N82-46388
MAYER, R. D.
 The influence of orientation on the stress rupture
 properties of nickel-base superalloy single
 crystals p0062 N82-47397
 Fatigue and creep-fatigue deformation of several
 nickel-base superalloys at 650 C p0062 N82-47398
 The influence of cobalt on the tensile and
 stress-rupture properties of the nickel-base
 superalloy MAR-M247 p0063 N82-47399
 The influence of cobalt on the microstructure of
 the nickel-base superalloy MAR-M247 p0063 N82-47400
MAJUMDAR, B. C.
 Frictional heating due to asperity interaction of
 elastohydrodynamic line-contact surfaces
 [NASA-TP-1882] p0100 N82-25514

MALOV, J. E.
 An insight into auxiliary propulsion requirements
 of large space systems
 [NASA-TM-82827] p0042 N82-24286
MARDELL, H. J.
 NASCAP simulation of laboratory charging tests
 using multiple electron guns p0033 N82-18319
 Differential charging of high-voltage spacecraft -
 The equilibrium potential of insulated surfaces
 p0041 N82-35547
 Representation and material charging response of
 geoplasma environments p0039 N82-14249
 Simulation of charging response of SCATHA (P78-2)
 satellite p0039 N82-14250
 Additional extensions to the NASCAP computer code,
 volume 1 p0146 N82-25810
 [NASA-CR-167855]
 Additional extensions to the NASCAP computer code,
 volume 2 p0040 N82-26377
 [NASA-CR-167856]
 Additional extensions to the NASCAP computer code,
 volume 3 p0040 N82-26378
 [NASA-CR-167857]
MANSON, S. S.
 Fatigue life prediction in bending from axial
 fatigue information p0113 N82-20564
 [NASA-CR-165563]
MANTH, V. B.
 Comparative analysis of CCHHD power plants
 p0158 N82-20747
MARCO, H. A.
 Cross-linked polyvinyl alcohol films as alkaline
 battery separators
 [NASA-TM-82802] p0054 N82-22327
MAR, E.
 Materials science issues encountered during the
 development of thermochemical concepts N82-10021
MARDEN, J. E.
 Development of materials and process technology
 for dual alloy disks
 [NASA-CR-165224] p0063 N82-18370
MARREK, C. J.
 Experimental study of the effects of secondary air
 on the emissions and stability of a lean
 premixed combustor
 [AIAA PAPER 82-1072] p0021 N82-34992
MARINO, J. S.
 An experiment to evaluate liquid hydrogen storage
 in space N82-20748
MARSHBERRY, C. L.
 MHD oxidant intermediate temperature ceramic
 heater study
 [NASA-CR-165453] p0131 N82-15527
MARPLE, D. T. F.
 Optical tip clearance sensor for aircraft engine
 controls
 [AIAA PAPER 82-1131] p0015 N82-37691
MARSHALL, R. A.
 Feasibility of an earth-to-space rail launcher
 system
 [IAF PAPER 82-46] p0033 N82-44659
MARSTON, C. E.
 Comparative analysis of CCHHD power plants
 p0158 N82-20747
MARTIN, E. E.
 Alkaline regenerative fuel cell systems for energy
 storage p0042 N82-11706
 Electrochemical energy storage for an orbiting
 space station
 [NASA-CR-165436] p0132 N82-17607
MARTIN, E. L.
 B747/JT9D flight loads and their effect on engine
 running clearances and performance
 deterioration; BCAC MAIL/P and WA JT9D engine
 diagnostics programs p0027 N82-28296
 [NASA-CR-165573]
MARTE, J. E.
 Operational performance of the
 photovoltaic-powered grain mill and water pump
 at Tanqaye, Upper Volta
 [NASA-TM-82767] p0120 N82-19673
 Design description of the Tanqaye Village
 photovoltaic power system

- [NASA-TM-82917] p0126 N82-33028
MASTERS, P. A.
 Deposit formation in hydrocarbon rocket fuels with an evaluation of a propane heat transfer correlation
 [NASA-TM-82911] p0088 N82-26611
- MATHER, K.**
 Automotive Stirling engine development program
 [NASA-CR-167907] p0164 N82-29235
- MATTHEI, K. W.**
 Processing of silicon solar cells by ion implantation and laser annealing
 [NASA-CR-165283] p0128 N82-11546
- MATTHEWS, E. W.**
 30/20 GHz communications satellite multibeam antenna
 [AIAA 82-0449] p0079 N82-23486
- MAY, C. E.**
 Mechanisms and models for zinc metal morphology in alkaline media
 [NASA-TM-82768] p0120 N82-19671
- MAYO, F. E.**
 Oxidation and formation of deposit precursors in hydrocarbon fuels
 [NASA-CR-165534] p0073 N82-18402
- MCALPNEY, M. E.**
 Creep and rupture of an ODS alloy with high stress rupture ductility
 p0065 N82-40335
- MCALISTER, A. J.**
 Non-noble catalysts and catalyst supports for phosphoric acid fuel cells
 [NASA-CR-165209] p0137 N82-30722
- MCBEHN, E. F.**
 Summary of electric vehicle dc motor-controller tests
 [NASA-TM-82863] p0082 N82-33636
- MCCARTHY, J. F., JR.**
 NASA research activities in aeropropulsion
 [NASA-TM-82788] p0017 N82-16084
 Local and national impact of aerospace research and technology
 [NASA-TM-82775] p0162 N82-20006
- MCCARTHY, E. F.**
 Kevlar/PMR-15 polyimide matrix composite for a complex shaped DC-9 drag reduction fairing
 [AIAA PAPER 82-1047] p0002 N82-37678
- MCCOIN, D. K.**
 Design study of a continuously variable roller cone traction CVT for electric vehicles
 [NASA-CR-159041] p0105 N82-12445
- MCDONALD, G.**
 Effects of arc current on the life in burner rig thermal cycling of plasma sprayed ZrO₂sub3
 [NASA-TM-82795] p0087 N82-17453
 Use of fiber like materials to augment the cycle life of thick thermoprotective seal coatings
 [NASA-TM-82901] p0089 N82-32633
- MCDONALD, N.**
 Turbofan forced mixer-nozzle internal flowfield. Volume 3: A computer code for 3-D mixing in axisymmetric nozzles
 [NASA-CR-3494] p0091 N82-22460
- MCGHEE, R. K.**
 Hybrid and electric advanced vehicle systems (heavy) simulation
 [NASA-CR-165536] p0163 N82-16938
- MCGLOTH, M. E.**
 Sensor failure detection system
 [NASA-CR-165515] p0023 N82-13145
- MCKAIN, T. F.**
 AGT100 turbomachinery
 [AIAA PAPER 82-1207] p0108 N82-35061
- MCKINLEY, D. J., JR.**
 Aeroacoustic performance of an externally blown flap configuration with several flap noise suppression devices
 [NASA-TM-1995] p0152 N82-24942
- MCKNIGHT, B. L.**
 Turbine blade nonlinear structural and life analysis
 [AIAA PAPER 82-1056] p0021 N82-34981
- MCLALLIN, K. L.**
 Cold-air performance of a 15.41-cm-tip-diameter axial-flow power turbine with variable-area stator designed for a 75-kw automotive gas turbine engine
 [NASA-TM-82644] p0024 N82-21193
- MCLAUGHLIN, D. K.**
 On the prediction of swirling flowfields found in axisymmetric combustor geometries
 p0029 N82-12120
- Mean flowfields in axisymmetric combustor geometries with swirl**
 [AIAA PAPER 82-0177] p0092 N82-17824
 Turbulence measurements in a confined jet using a six-orientation hot-wire probe technique
 [AIAA PAPER 82-1262] p0094 N82-37710
 Investigations of flowfields found in typical combustor geometries
 [NASA-CR-165061] p0090 N82-15360
- MCHALLY, W. D.**
 Computational methods for internal flows with emphasis on turbomachinery
 [NASA-TM-82764] p0003 N82-13113
- MCHAM, W. L.**
 Nonlinear analysis of rotor-bearing systems using component mode synthesis
 [ASME PAPER 82-GT-303] p0104 N82-35468
- MCHTA, S.**
 Effects of processing and dopant on radiation damage removal in silicon solar cells
 [NASA-TM-82892] p0042 N82-31443
- MCHIE, R. C.**
 Interfacing wind energy conversion equipment with utility systems
 N82-21148
- MCHJER, R. J.**
 Evaluation of the potential of the Stirling engine for heavy duty application
 [NASA-CR-165473] p0128 N82-10505
- MCHNDERS, W.**
 Preliminary study of temperature measurement techniques for Stirling engine reciprocating seals
 [NASA-CR-165479] p0104 N82-11466
- MCHSSINGER, M. F.**
 Integrated propulsion for near-Earth space missions. Volume 1: Executive summary
 [NASA-CR-167889-VOL-1] p0045 N82-33424
 Integrated propulsion for near-Earth space missions. Volume 2: Technical
 [NASA-CR-167889-VOL-2] p0046 N82-33425
- MCHO, P. S.**
 Preliminary results on performance testing of a turbocharged rotary combustion engine
 [NASA-TM-82772] p0017 N82-21194
- MCHINO, F.**
 Low-thrust chemical propulsion system propellant expulsion and thermal conditioning study. Executive summary
 [NASA-CR-165622] p0045 N82-24287
 Low-thrust chemical propulsion system propellant expulsion and thermal conditioning study
 [NASA-CR-167841] p0045 N82-24288
- MCHILL, W.**
 Identification of multivariable high performance turbofan engine dynamics from closed loop data
 [NASA-TM-82785] p0076 N82-20339
 The role of modern control theory in the design of controls for aircraft turbine engines
 [NASA-TM-82815] p0018 N82-22262
- MCHUTKA, J. P.**
 Progress in protective coatings for aircraft gas turbines: A Review of NASA sponsored research
 [NASA-TM-82740] p0058 N82-12216
- MCHTGER, F. B.**
 Evaluation of wind tunnel performance testings of an advanced 45 deg swept 8-bladed propeller at Mach numbers from 0.45 to 0.85
 [NASA-CR-3505] p0007 N82-19178
- MCHULENBERG, A.**
 Advances in high output voltage silicon solar cells
 p0127 N82-44942
- MCHULENBERG, A., JR.**
 High- and low-resistivity silicon solar cells
 p0046 N82-11762
- MCHYER, L. J.**
 Cooled variable-area radial turbine technology program
 [NASA-CR-165408] p0024 N82-19221
- MCHYER, W. L.**
 Prediction of sound radiation from different practical jet engine inlets
 [NASA-CR-165120] p0153 N82-16810
- MCHYERS, G. J.**
 Nonlinear structural and life analyses of a combustor liner
 [NASA-TM-82846] p0111 N82-24501

Fracture mechanics criteria for turbine engine hot section components
[NASA-CR-167896] p0027 N82-25257

HEYBES, J. E.
Exhaust emissions reduction for intermittent combustion aircraft engines
[NASA-CR-167914] p0029 N82-33392

HEYB, E. E.
Ultrasonic scanning system for imaging flaw growth in composites
[NASA-TM-82799] p0076 N82-22386

MICHAEL, C. J.
Energy efficient engine shroudless, hollow fan blade technology report
[NASA-CR-165586] p0024 N82-21196

MICHALTSIANSKY, A. G.
Ultraviolet observations of the 1980 eclipse of the symbiotic star CI Cygni
A82-27331

MICHAELS, C. J.
Forward acoustic performance of a model turbofan designed for a high specific flow (QF-14)
[NASA-TP-1968] p0152 N82-21036

MINALOEY, J. R.
A real time Pegasus propulsion system model for VSTOL piloted simulation evaluation
[AIAA PAPER 81-2663] p0020 A82-19221
A real time Pegasus propulsion system model for VSTOL piloted simulation evaluation
[NASA-TM-82770] p0016 N82-13144
A piecewise linear state variable technique for real time propulsion system simulation
[NASA-TM-82851] p0018 N82-24201

MIRKELSON, D. C.
Summary and recent results from the NASA advanced High Speed Propeller Research Program
[NASA-TM-82891] p0001 N82-26219

MILBURN, H. F.
Permanent magnet properties of Mn-Al-C between -50 C and +150 C
p0085 A82-20505
Hard permanent magnet development trends and their application to A.C. machines
p0083 A82-20745

MILMS, G. A.
Small gas turbine combustor primary zone development
[AIAA PAPER 82-1159] p0103 A82-35036

MILMS, J. E.
Verification of an acoustic transmission matrix analysis of sound propagation in a variable area duct without flow
[NASA-TM-82741] p0151 N82-12891
Pressure transfer function of a JT15D nozzle due to acoustic and convected entropy fluctuations
[NASA-TM-82842] p0152 N82-22951

MILLAN, P. P., JR.
Applications of high-temperature powder metal aluminum alloys to small gas turbines
p0065 A82-48244

MILLER, B. A.
Propeller tip vortex - A possible contributor to aircraft cabin noise
p0152 A82-17603

MILLER, D. R.
Comparison of upwind and downwind rotor operation of the DOE/NASA 100-kW MOD-0 wind turbine
p0122 N82-23710

MILLER, P. Q.
Gallium arsenide solar array subsystem study
[NASA-CR-167869] p0138 N82-32855

MILLER, L. A.
Feasibility of an earth-to-space rail launcher system
[IAE PAPER 82-46] p0033 A82-44659
Preliminary feasibility assessment for Earth-to-space electromagnetic (Railgun) launchers
[NASA-CR-167886] p0033 N82-29345

MILLER, H. A.
Phase stability in plasma-sprayed, partially stabilized zirconia-yttria
p0070 A82-41552
Thermodynamics and kinetics of the sulfation of porous calcium silicate
[NASA-TM-82769] p0048 N82-15119
Review of NASA progress in thermal barrier coatings for stationary gas turbines
[NASA-TM-81716] p0058 N82-17335
Failure mechanisms of thermal barrier coatings exposed to elevated temperatures

[NASA-TM-82905] p0061 N82-32461

MILLNER, A.
Overview study of Space Power Technologies for the advanced energetics program
[NASA-CR-165269] p0132 N82-17606

MILLS, M. E.
Voltage gradients in solar array cavities as possible breakdown sites in spacecraft-charging-induced discharges
p0038 A82-18317
Voltage gradients in solar array cavities as possible breakdown sites in spacecraft-charging-induced discharges
[NASA-TM-82710] p0037 N82-11107

MILNER, E. J.
Application of integration algorithms in a parallel processing environment for the simulation of jet engines
[NASA-TM-82746] p0149 N82-14849
A generalized memory test algorithm
[NASA-TM-82874] p0146 N82-31971

MINZER, M. V.
Fatigue and creep-fatigue deformation of several nickel-base superalloys at 650 C
p0062 A82-47398

MINUCCI, J. A.
Processing of silicon solar cells by ion implantation and laser annealing
[NASA-CR-165283] p0128 N82-11546

MINTICH, M. J.
Surface texturing of fluoropolymers
[NASA-CASE-LEW-13028-1] p0070 N82-33521

MISERICIK, J.
Effect of oxide films on hydrogen permeability of candidate Stirling engine heater head tube alloys
[NASA-TM-82824] p0060 N82-24323
Evaluation of candidate Stirling engine heater tube alloys at 820 deg and 860 deg C
[NASA-TM-82837] p0061 N82-30372

MITCHELL, A. E.
Lubricant effects on efficiency of a helicopter transmission
[NASA-TM-82857] p0100 N82-25520

MITCHELL, G. A.
Summary and recent results from the NASA advanced High Speed Propeller Research Program
[NASA-TM-82891] p0001 N82-26219

MITTRA, R.
NASA Adaptive Multibeam Phased Array (AMPA): An application study
[NASA-CR-169125] p0079 N82-28503

MIYASAKA, K.
Effects of heat loss, preferential diffusion, and flame stretch on flame-front instability and extinction of propane/air mixtures
p0057 A82-32877

MIYOSHI, K.
Adhesion and friction of single-crystal diamond in contact with transition metals
p0103 A82-18680
Surface chemistry and wear behavior of single-crystal silicon carbide sliding against iron at temperatures to 1500 C in vacuum
[NASA-TP-1947] p0067 N82-19374
Friction and wear of iron in corrosive metal
[NASA-TP-1985] p0058 N82-20291
Influence of mineral oil and additives on microhardness and surface chemistry of magnesium oxide (001) surface
[NASA-TP-1986] p0067 N82-20316
Friction and surface chemistry of some ferrous-base metallic glasses
[NASA-TP-1991] p0059 N82-21301
Tribological properties and XPS studies of ion plated gold on nickel and iron
[NASA-TM-82814] p0059 N82-22344
Surface chemistry, microstructure and friction properties of some ferrous-base metallic glasses at temperatures to 750 C
[NASA-TP-2006] p0060 N82-22349
Correlation of tensile and shear strengths of metals with their friction properties
[NASA-TM-82828] p0060 N82-24325
Tribological properties of sintered polycrystalline and single crystal silicon carbide
[NASA-TM-82829] p0068 N82-24343
Influence of corrosive solutions on microhardness and chemistry of magnesium oxide /001/ surfaces
[NASA-TP-2040] p0102 N82-31691

- Occurrence of spherical ceramic debris in indentation and sliding contact [NASA-TP-2048] p0069 N82-32491
- MISNER, P. F.**
First results of material charging in the space environment [NASA-TN-84743] p0081 N82-24431
- MIZOHOTO, H.**
Lean-limit extinction of propane/air mixtures in the stagnation-point flow p0057 N82-28736
- MORNING, V.**
Conversion of acoustic energy by lossless liners p0154 N82-36195
- MOFFAT, R. J.**
Turbulent boundary layer heat transfer experiments - A separate effects study on a convexly-curved wall [ASME PAPER 81-HT-78] p0092 N82-10963
Turbulent boundary layer heat transfer experiments: Convex curvature effects including introduction and recovery [NASA-CR-3510] p0090 N82-17456
- MOGIA, R. C.**
Pollution reduction technology program small jet aircraft engines, phase 3 [NASA-CR-165386] p0023 N82-14095
ERDS fuel addendum: Pollution reduction technology program small jet aircraft engines, phase 3 [NASA-CR-165387] p0024 N82-14096
- MOORE, R. D.**
Performance of single-stage axial-flow transonic compressor with rotor and stator aspect ratios of 1.63 and 1.78, respectively, and with design pressure ratio of 1.82 [NASA-TP-1974] p0017 N82-19222
Performance of single-stage axial-flow transonic compressor with rotor and stator aspect ratios of 1.63 and 1.77, respectively, and with design pressure ratio of 2.05 [NASA-TP-2001] p0018 N82-22269
Rotor tip clearance effects on overall and blade-element performance of axial-flow transonic fan stage [NASA-TP-2049] p0020 N82-33389
- MOORE, T. J.**
Ultrasonic velocity for estimating density of structural ceramics [NASA-TN-82765] p0066 N82-14359
- MOORHEAD, P. E.**
Metal honeycomb to porous wireform substrate diffusion bond evaluation [NASA-TN-82793] p0110 N82-18612
- MORALES, W.**
Thermal and oxidative degradation studies of formulated C-ethers by gel-permeation chromatography [NASA-TP-1994] p0068 N82-21332
- MORENO, V.**
Nonlinear structural and life analyses of a combustor liner [NASA-TN-82846] p0111 N82-24501
- MORGAN, J. L.**
Effect of vacuum exhaust pressure on the performance of MHD ducts at high D-field [AIAA PAPER 82-0396] p0157 N82-20292
Effect of vacuum exhaust pressure on the performance of MHD ducts at high D-field [NASA-TN-82150] p0157 N82-13908
Results and comparison of Hall and DW duct experiments [NASA-TN-82864] p0157 N82-25961
- MORRIS, J. F.**
High thermal power density heat transfer [NASA-CASE-LEW-12950-1] p0087 N82-11395
- MORRIS, R. J.**
The three-dimensional boundary layer on a rotating helical blade p0009 N82-15459
- MOSS, J. E., JR.**
Exhaust emissions survey of a turbofan engine for flame holder swirl type augmentors at simulated altitude flight conditions [NASA-TN-82787] p0019 N82-25255
- MOYER, D. W.**
Effects of ultra-clean and centrifugal filtration on rolling-element bearing life [ASME PAPER 81-LUB-35] p0103 N82-18436
- MROG, T. S.,**
Magneto-hydrodynamics (MHD) Engineering Test Facility (ETF) 200 MWe power plant. Design Requirements Document (DRD) [NASA-TN-82705] p0099 N82-12446
- MULLER, A.**
Advanced stratified charge rotary aircraft engine design study [NASA-CR-165398] p0107 N82-27743
- MURFOLITTO, A. J.,**
Application of an airfoil stall flutter computer prediction program to a three-dimensional wing: Prediction versus experiment [NASA-CR-168586] p0007 N82-19169
- MUSE, D.**
Extended range stress intensity factor expressions for chevron-notched short bar and short rod fracture toughness specimens p0112 N82-40357
- MURALIDHARAN, U.**
Fatigue life prediction in bending from axial fatigue information [NASA-CR-165563] p0113 N82-20564
- MURATA, K.**
Maximum entropy image reconstruction from projections N82-11053
- MURDOCH, R. W.**
Computer modeling of fan-exit-splitter spacing effects on F100 response to distortion [NASA-CR-167879] p0025 N82-23246
- MURPHY, D. P.**
Analysis of crack propagation as an energy absorption mechanism in metal matrix composites [NASA-CR-165051] p0052 N82-14288
- MURTHY, K. M., S.**
Three dimensional flow field inside the passage of a low speed axial flow compressor rotor [AIAA PAPER 82-1006] p0011 N82-31964
- MURTHY, S. M., S.**
Water ingestion into jet engine axial compressors [AIAA PAPER 82-0196] p0030 N82-17836
- MYERS, D.**
Advanced stratified charge rotary aircraft engine design study [NASA-CR-165398] p0107 N82-27743
- MYSHENKO, V. V.,**
Investigation of a comb-type slow-wave structure for millimeter-wave masers N82-18368

N

- NAIK, S. K.**
Development of improved high temperature coatings for IN-792 + HF [NASA-CR-165395] p0063 N82-14333
- NAIENGER, J. J.**
Performance and operational economics estimates for a coal gasification combined-cycle cogeneration powerplant [NASA-TN-82729] p0120 N82-19672
- NATHAL, H. V.**
The influence of cobalt on the tensile and stress-rupture properties of the nickel-base superalloy MAR-M247 p0063 N82-47399
The influence of cobalt on the microstructure of the nickel-base superalloy MAR-M247 p0063 N82-47400
- NEEDLEMAN, W. H.**
Effects of ultra-clean and centrifugal filtration on rolling-element bearing life [ASME PAPER 81-LUB-35] p0103 N82-18436
- NEIL, J. T.**
Fabrication of turbine components and properties of sintered silicon nitride [ASME PAPER 82-GT-252] p0071 N82-35431
Fabrication of sinterable silicon nitride by injection molding p0071 N82-37015
- NELANDER, H. C.**
Real-time microcomputer simulation for space Shuttle/Centaur avionics p0033 N82-48245
- NELSON, H. D.**
Nonlinear analysis of rotor-bearing systems using component mode synthesis [ASME PAPER 82-GT-303] p0104 N82-35468

- WENAT-WASSER, S.
On finite deformation elasto-plasticity
p0116 A82-45869
- WESBITT, J. A.
Solute transport during the cyclic oxidation of
Ni-Cr-Al alloys
[NASA-CR-165544] p0064 A82-27462
- WRECHBAUER, H.
Overview study of Space Power Technologies for the
advanced energetics program
[NASA-CR-165269] p0132 A82-17606
- WROHMAN, H. E.
LV measurements with an advanced turboprop
p0097 A82-32690
- WROSTADTER, H. E.
Applications of the DOE/NASA wind turbine
engineering information system
p0122 A82-23696
- WRYLOFF, S.
Market assessment of photovoltaic power systems
for agricultural applications in Colombia
[NASA-CR-165524] p0134 A82-22770
- WG, Z.
IMPATT power building blocks for 20 GHz spaceborne
transmit amplifier
[AIAA 82-0498] p0086 A82-23566
- WICE, A. W.
NASA Redox system development project status
[NASA-TM-82665] p0123 A82-25637
- WIEDERDING, W. C.
High temperature electronic requirements in
aeropropulsion systems
[E-708] p0081 A82-15313
- WIELSON, C. E.
Advanced superposition methods for high speed
turbo-pump vibration analysis
[NASA-CR-165379] p0104 A82-11465
Liquid oxygen turbo-pump technology
[NASA-CR-165487] p0105 A82-11468
- WIMMONS, J. T.
Current legal and institutional issues in the
commercialization of phosphoric acid fuel cells
[NASA-CR-167867] p0136 A82-29719
- WIZANI, A. A.
Formation of oxides of nitrogen in monodisperse
spray combustion of hydrocarbon fuels
p0057 A82-37571
- WOLPI, J.
Market assessment of photovoltaic power systems
for agricultural applications in Nigeria
[NASA-CR-165511] p0133 A82-18698
- WONNAST, J. E.
Numerical simulation of sheath structure and
current-voltage characteristics of a
conductor-dielectric disk in a plasma
p0040 A82-15904
Numerical simulation of plasma insulator
interactions in space. Part 1: The self
consistent calculation
p0039 A82-14272
Numerical simulation of plasma insulator
interactions in space. Part 2: Dielectric
effects
p0039 A82-14273
- WORGREN, C. T.
Effect of fuel injector type on performance and
emissions of reverse-flow combustor
[NASA-TP-1945] p0016 A82-15040
- WROOD, E.
Advanced stratified charge rotary aircraft engine
design study
[NASA-CR-165398] p0107 A82-27743
- NOVAK, R. C.
Development of low modulus material for use in
ceramic gas path seal applications
[NASA-CR-165469] p0022 A82-10039
- NOVICK, A. S.
Small gas turbine combustor primary zone development
[AIAA PAPER 82-1159] p0103 A82-35036
Low NOx heavy fuel combustor concept program
addendum: Low/mid heating value gaseous fuel
evaluation
[NASA-CR-165615] p0055 A82-25338
Low NOx heavy fuel combustor concept
program
[NASA-CR-165367] p0136 A82-25635
- NUSSLE, R. C.
Experimental performance of the regenerator for
the Chrysler upgraded automotive gas turbine
engine
- [NASA-TM-82671] p0120 A82-21712
- NYLAND, T. W.
Microprocessor control system for 200-kilowatt
Mod-OA wind turbines
[NASA-TM-82711] p0120 A82-21710
- OBERLE, L. G.
A digital optical torque meter for high rotational
speed applications
[NASA-TM-82914] p0095 A82-31664
- OCONELL, J. E.
YF 102 in-duct combustor noise measurements with a
turbine nozzle, volume 1
[NASA-CR-165562-VOL-1] p0153 A82-21031
YF 102 in-duct combustor noise measurements with a
turbine nozzle, volume 2
[NASA-CR-165562-VOL-2] p0153 A82-21032
YF 102 in-duct combustor noise measurements with a
turbine nozzle, volume 3
[NASA-CR-165562-VOL-3] p0155 A82-21033
- ODONNELL, W. J.
A simplified design procedure for life prediction
of rocket thrust chambers
[AIAA PAPER 82-1251] p0043 A82-35087
Development of a simplified procedure for thrust
chamber life prediction
[NASA-CR-165585] p0044 A82-21253
- OHARA, J. B.
Fuel quality processing study, volume 1
[NASA-CR-165327-VOL-1] p0135 A82-24649
Fuel quality/processing study. Volume 2:
Appendix. Task 1 literature survey
[NASA-CR-165327-VOL-2] p0135 A82-24650
- OKRAM, W. C.
IMPATT power building blocks for 20 GHz spaceborne
transmit amplifier
[AIAA 82-0498] p0086 A82-23566
- OLIVER, J. E.
Undoped semi-insulating LEC GaAs - A model and a
mechanism
p0159 A82-13754
- OLSEN, R. C.
Modification of spacecraft potentials by thermal
electron emission on ATS-5
p0040 A82-16194
Field-aligned ion streams in the earth's midnight
region
p0140 A82-31009
The hidden ion population of the magnetosphere
p0140 A82-32630
- OLSEN, W. A., JR.
Aircraft icing research at NASA
[NASA-TM-82919] p0013 A82-30297
- OLSSON, W. J.
Performance deterioration due to acceptance
testing and flight loads; JT90 jet engine
diagnostic program
[NASA-CR-165572] p0027 A82-27309
B747/JT9D flight loads and their effect on engine
running clearances and performance
deterioration; BCAC MAIL/P and WA JT9D engine
diagnostics programs
[NASA-CR-165573] p0027 A82-28296
- ONEILL, G. E.
Mass Driver Two - A status report
p0046 A82-18191
- OPPENHEIM, A. K.
Secondary effects in combustion instabilities
leading to flashback
[AIAA PAPER 82-0037] p0056 A82-17746
Numerical modelling of turbulent flow in a
combustion tunnel
p0093 A82-27000
Numerical modeling of turbulent combustion in
premixed gases
p0056 A82-28708
Effects of internal heat transfer on the structure
of self-similar blast waves
p0093 A82-32225
- ORANGE, L.
Voltage gradients in solar array cavities as
possible breakdown sites in
spacecraft-charging-induced discharges
p0038 A82-18317
Voltage gradients in solar array cavities as
possible breakdown sites in
spacecraft-charging-induced discharges

ORIGINAL PAGE IS
OF POOR QUALITY

PERSONAL AUTHOR INDEX

PIERCE, W. S.

- [NASA-TM-82710] p0037 N82-11107
ORANGE, T. W.
 Crack displacements for J/I testing with compact specimens p0112 A82-40358
- OSTRACH, S.**
 Natural convection with combined driving forces p0093 A82-31445
- OTTENSON, D. A.**
 Aircraft sampling of the sulfate layer near the tropopause following the eruption of Mount St. Helens p0140 A82-37450
- OWEN, S. A., JR.**
 High-frequency high-voltage high-power DC-to-DC converters p0083 N82-12347
 Analysis of transistor and snubber turn-off dynamics in high-frequency high-voltage high-power converters [NASA-CR-168760] p0084 N82-22438
- P**
- PACIOREK, K. J. L.**
 Thermal oxidative degradation reactions of linear perfluoroalkyl ethers [NASA-TM-82874] p0068 N82-26468
- PACIOREK, K. L.**
 Thermal oxidative degradation reactions of perfluoroalkylethers [NASA-CR-165516] p0048 N82-12135
- PADOVAN, J.**
 Engine dynamic analysis with general nonlinear finite element codes. II - Bearing element implementation, overall numerical characteristics and benchmarking [ASME PAPER 82-GT-292] p0108 A82-35462
 On the solution of creep induced buckling in general structure p0115 A82-39514
 Self-adaptive closed constrained solution algorithms for nonlinear conduction p0094 A82-45157
 Engine dynamic analysis with general nonlinear finite element codes. Part 2: Bearing element implementation overall numerical characteristics and benchmarking [NASA-CR-167944] p0028 N82-33390
- PAGLIARO, P.**
 Preparation and evaluation of advanced electrocatalysts for phosphoric acid fuel cells [NASA-CR-165519] p0129 N82-12573
 Preparation and evaluation of advanced electrocatalysts for phosphoric acid fuel cells [NASA-CR-165594] p0132 N82-17615
- PANDYA, A.**
 Investigation of the tip-clearance flow inside and at the exit of a compressor rotor passage. I - Mean velocity field [ASME PAPER 82-GT-12] p0011 A82-35281
 Investigation of the tip clearance flow inside and at the exit of a compressor rotor passage [NASA-CR-169004] p0026 N82-25253
- PAPATHAKOS, L. C.**
 Aircraft sampling of the sulfate layer near the tropopause following the eruption of Mount St. Helens p0140 A82-37450
- PARIDON, C. A.**
 Reliability model for planetary gear [NASA-TM-82859] p0101 N82-28643
- PANKE, P. I.**
 Investigation and evaluation of a computer program to minimize three-dimensional flight time tracks [NASA-CR-168419] p0145 N82-17879
 Shaded computer graphic techniques for visualizing and interpreting analytic fluid flow models [NASA-CR-168418] p0145 N82-17880
- PARNER, H. W.**
 Barriers to the utilization of synthetic fuels for transportation [NASA-CR-165517] p0073 N82-13243
- PARKS, D. E.**
 Space Shuttle Orbiter charging [AIAA PAPER 82-0119] p0040 A82-17793
 'Bootstrap' charging of surfaces composed of multiple materials p0085 A82-18318
- NASCAP simulation of laboratory charging tests using multiple electron guns p0033 A82-18319**
Charging of a large object in low polar Earth orbit p0039 N82-14275
- PARSELL, J. K.**
 A pad perturbation method for the dynamic coefficients of tilting-pad journal bearings p0110 A82-14400
- PATER, R. H.**
 Novel improved PMR polyimides [NASA-TM-82733] p0049 N82-11117
- PATERSON, R. W.**
 Turbofan forced mixer-nozzle internal flowfield. Volume 1: A benchmark experimental study [NASA-CR-3492] p0090 N82-22458
- PAULOVICH, F. J.**
 Propeller flow visualization techniques p0096 N82-32672
- PELOSE, J. E.**
 Dynamic switch matrix for the TDMA satellite switching system [AIAA 82-0458] p0085 A82-23494
- PELOUCH, J. J., JR.**
 Systems integration p0042 N82-27371
- PENKO, P. F.**
 Summary and evaluation of the conceptual design study of a potential early commercial MHD power plant (CSPEC) [NASA-TM-82734] p0119 N82-16481
- PENNISI, P. J.**
 Improved plasma sprayed MCrAlY coatings for aircraft gas turbine applications p0065 A82-20742
 Tailored plasma sprayed MCrAlY coatings for aircraft gas turbine applications [NASA-CR-165234] p0064 A82-12360
- PENNLING, J. A.**
 Construction of solutions for some nonlinear two-point boundary value problems [NASA-TM-82937] p0144 N82-30949
- PERRASSO, H. M.**
 Dynamic switch matrix for the TDMA satellite switching system [AIAA 82-0458] p0085 A82-23494
- PERRINS, P. J.**
 Ozone and aircraft operations p0001 N82-21145
- PRESSAGNO, S. L.**
 Development of a high-temperature durable catalyst for use in catalytic combustors for advanced automotive gas turbine engines [NASA-CR-165396] p0130 N82-13510
- PETERS, W. H.**
 Digital imaging techniques in experimental stress analysis p0097 A82-34231
 Experimental boundary integral equation applications in speckle interferometry p0097 A82-36987
- PETERSON, D.**
 Development of a simplified procedure for thrust chamber life prediction [NASA-CR-165585] p0044 N82-21253
- PETERSON, D. H.**
 Study of multi-megawatt technology needs for photovoltaic space power systems. Volume 1: Executive summary [NASA-CR-165323-VOL-1] p0130 N82-14636
 Study of multi-megawatt technology needs for photovoltaic space power systems, volume 2 [NASA-CR-165323-VOL-2] p0130 N82-14637
- PHILIPPI, T. M.**
 International market assessment of stand-alone photovoltaic power systems for cottage industry applications [NASA-CR-165287] p0132 N82-16494
- PHILLIPS, B. M.**
 Resonance tube hazards in oxygen systems [NASA-TM-82801] p0072 N82-21415
- PHILLIPS, M.**
 Overview study of Space Power Technologies for the advanced energetics program [NASA-CR-165269] p0132 N82-17616
- PIERCE, W. S.**
 Extended range stress intensity factor expressions for chevron-notched short bar and short rod fracture toughness specimens

- PIKE, C. P. p0112 A82-40357
Agreement for NASA/OAST - USAF/AFSC space interdependency on spacecraft environment interaction
- PILLER, S. p0038 N82-14271
Automotive Stirling engine development program [NASA-CR-167907] p0164 N82-29235
- PIKE, V. W. p0041 A82-18312
Internal breakdown of charged spacecraft dielectrics
- PIRVICS, J. p0106 N82-20540
Spherical roller bearing analysis. SKF computer program SPHERBEAM. Volume I: Analysis [NASA-CR-165203]
- PITTS, L. p0055 A82-15732
Moderate temperature Na cells III - Electrochemical and structural studies of CrO.5VO.5S2 and its Na intercalates
Moderate temperature Na cells IV - VS2 and NbS2Cl2 as rechargeable cathodes in molten NaAlCl4 p0055 A82-15743
- PLATT, C. E. p0028 N82-33391
Structural tailoring of engine blades (STAEBL) [NASA-CR-167949]
- PLEASANT, R. L. p0130 N82-14636
Study of multi-megawatt technology needs for photovoltaic space power systems. Volume I: Executive summary [NASA-CR-165323-VOL-1]
Study of multi-megawatt technology needs for photovoltaic space power systems, volume 2 [NASA-CR-165323-VOL-2] p0130 N82-14637
Low-thrust chemical propulsion system propellant expulsion and thermal conditioning study. Executive summary [NASA-CR-165622] p0045 N82-24287
Low-thrust chemical propulsion system propellant expulsion and thermal conditioning study [NASA-CR-167841] p0045 N82-24288
- POESCHEL, R. L. p0046 A82-15434
30-cm mercury ion thruster technology
Characteristics of the IERC/Hughes J-series 30-cm engineering model thruster p0046 A82-15435
Retrofit and acceptance test of 30-cm ion thrusters [NASA-CR-165259] p0084 N82-12133
- POOR, R. B. p0125 N82-30710
Experience and assessment of the DOE-NASA Mod-1 2000-Kilowatt wind turbine generator at Boone, North Carolina [NASA-TN-82721]
- POPFEL, G. L. p0015 A82-37691
Optical tip clearance sensor for aircraft engine controls [AIAA PAPER 82-1131]
- PONOMSKI, J. S. p0043 A82-35087
A simplified design procedure for life prediction of rocket thrust chambers [AIAA PAPER 82-1251]
Development of a simplified procedure for thrust chamber life prediction [NASA-CR-165585] p0044 N82-21253
- PORTER, T. R. p0052 N82-20248
Environmental effects on defect growth in composite materials [NASA-CR-165213]
- POST, R. E. p0121 N82-22673
Light weight nickel battery plaque [NASA-CR-165585]
- POTTER, K. W. A82-13217
Illustration of a new test for detecting a shift in mean in precipitation series
- POWAGARE, H. p0011 A82-31964
Three dimensional flow field inside the passage of a low speed axial flow compressor rotor [AIAA PAPER 82-1006]
Three-dimensional flow field in the tip region of a compressor rotor passage. I - Mean velocity profiles and annulus wall boundary layer [ASME PAPER 82-GT-11] p0011 A82-35280
Three-dimensional flow field in the tip region of a compressor rotor passage. II - Turbulence properties [ASME PAPER 82-GT-234] p0011 A82-35416
- POWAGARE, H. p0091 N82-27686
Three dimensional flow field inside compressor rotor, including blade boundary layers [NASA-CR-169120]
- POWELL, C. E. p0028 N82-32370
Advanced turboprop testbed systems study. Volume I: Testbed program objectives and priorities, drive system and aircraft design studies, evaluation and recommendations and wind tunnel test plans [NASA-CR-167928-VOL-1]
- POWELL, E. A. p0028 N82-31328
Development of a spinning wave heat engine [NASA-CR-165611]
- POWELL, J. p0132 N82-17606
Overview study of Space Power Technologies for the advanced energetics program [NASA-CR-165269]
- POWELL, J. A. p0081 N82-15313
High temperature electronic requirements in aeropropulsion systems [E-708]
High-speed laser anemometer system for intrarotor flow mapping in turboachinery [NASA-TP-1663] p0095 N82-19521
- POWER, J. L. p0043 A82-15438
Measuring the spacecraft and environmental interactions of the 8-cm mercury ion thrusters on the P80-1 mission
- PRATHER, W. H. p0086 A82-43784
Wideband, high speed switch matrix development for SS-TDMA applications
- PRATT, T. K. p0028 N82-33391
Structural tailoring of engine blades (STAEBL) [NASA-CR-167949]
- PRATT, W. B. p0107 N82-27743
Advanced stratified charge rotary aircraft engine design study [NASA-CR-165398]
- PRINGLE, D. P. p0017 N82-21194
Preliminary results on performance testing of a turbocharged rotary combustion engine [NASA-TN-82772]
- PROFANT, B. D. p0063 N82-14333
Development of improved high temperature coatings for IN-792 + HF [NASA-CR-165395]
- PROKOPIUS, P. M. p0120 N82-19670
Phosphoric acid fuel cell technology status [NASA-TN-82791]
- PROTHON, D. p0136 N82-24725
Low NOx heavy fuel combustor concept program. Phase I: Combustion technology generation [NASA-CR-165482]
- PREBYSEWSKI, J. S. p0097 N82-22479
Thin film temperature sensors, phase 3 [NASA-CR-165476]
- PURVIS, C. K. p0037 N82-14251
SCATHA SSPM charging response: NASCAP predictions compared with data
Comparison of NASCAP modelling results with lumped circuit analysis p0037 N82-14255

Q

- QUACKENBUSH, C. L. p0071 A82-35431
Fabrication of turbine components and properties of sintered silicon nitride [ASME PAPER 82-GT-252]
Fabrication of sinterable silicon nitride by injection molding p0071 A82-37015
- QUAYLE, S. S. p0164 N82-18068
Fuel economy and exhaust emissions characteristics of diesel vehicles: Test results of a prototype fiat 131TC 2.4 liter automobile [NASA-CR-165535]

R

- RACKLEY, R. A. p0107 A82-11783
The AGT101 technology - An automotive alternative
AGT101 automotive gas turbine system development [AIAA PAPER 82-1166] p0108 A82-35039

- The AGT 101 advanced automotive gas turbine
[ASME PAPER 82-GT-72] p0108 A82-35321
- NADMAN, S.**
Modeling and Analysis of Power Processing Systems
(NAEPPS). Volume 2: Appendices
[NASA-CR-165539] p0145 A82-16748
- NADONSKI, M. A.**
CF6 Jet Engine Diagnostics Program: High pressure
compressor clearance investigation
[NASA-CR-165580] p0025 A82-21197
- NACEN, M. A.**
Research report: User's manual for computer
program AT81Y003 SHABERTH. Steady state and
transient thermal analysis of a shaft bearing
system including ball, cylindrical and tapered
roller bearings
[NASA-CR-165365] p0146 A82-31969
Research report: User's manual for computer
program AT81Y005. PLANETSYS, a computer program
for the steady state and transient thermal
analysis of a planetary power transmission system
[NASA-CR-165366] p0146 A82-31970
- NAHMAN, P.**
Mathematical models for the synthesis and
optimization of spiral bevel gear tooth surfaces
[NASA-CR-3553] p0106 A82-25516
- NAHMAN, S.**
A new approach to the minimum weight/loss design
of switching power converters p0082 A82-16831
Modeling and Analysis of Power Processing Systems
(NAEPPS). Volume 1: Technical report
[NASA-CR-165538] p0083 A82-14447
- NAJ, B.**
Experimental study of turbulence in blade end wall
corner region
[NASA-CR-169283] p0091 A82-31639
- NAJAN, M. S.**
Evidence for Pu-244 fission tracks in hibonites
from Murchison carbonaceous chondrite
p0166 A82-29316
- NAJENDRAN, A. M.**
A preliminary study of crack initiation and growth
at stress concentration sites
[NASA-CR-169358] p0115 A82-33738
- NAKAM, H. S. V.**
Experimental study of the effects of secondary air
on the emissions and stability of a lean
premixed combustor
[AIAA PAPER 82-1072] p0021 A82-34992
- NAKINS, P.**
Experimental verification of a computational
procedure for the design of TWT-refocuser-MDC
systems p0082 A82-16128
- NAKSEY, W.**
Developing a scalable inert gas ion thruster
[AIAA PAPER 82-1275] p0047 A82-37713
- NAKSEY, W. D.**
Inert gas ion thruster
[NASA-CR-165521] p0044 A82-21252
- NAKSON, W. F.**
Digital imaging techniques in experimental stress
analysis p0097 A82-34231
Experimental boundary integral equation
applications in speckle interferometry
p0097 A82-36987
- NAO, A. P.**
VLA observations of solar active regions at 6 cm
wavelength p0167 A82-10156
- NAO, P. V.**
A study of the nature of solid particle impact and
shape on the erosion morphology of ductile metals
[NASA-TN-82933] p0061 A82-33493
- NATAOCHAR, A. P.**
Operational performance of the
photovoltaic-powered grain mill and water pump
at Tanqaye, Upper Volta
[NASA-TN-82767] p0120 A82-19673
Design description of the Tanqaye Village
photovoltaic power system
[NASA-TN-82917] p0126 A82-33828
- NAUTIO, J. C.**
Adaptive rain fade compensation p0080 A82-27178
- NAVINDRABATH, B.**
Interaction of compressor rotor blade wake with
wall boundary layer/vortex in the end-wall region
[ASME PAPER 81-GT-1] p0010 A82-19301
- NAV, P. K.**
Characterization of advanced electric propulsion
systems
[AIAA PAPER 82-1246] p0071 A82-35083
Characterization of advanced electric propulsion
systems
[NASA-CR-167885] p0045 A82-26381
- NEAGAN, J. E.**
Failure analysis of a tool steel torque shaft
[NASA-TN-82758] p0058 A82-11184
- NECTOR, M. F., III**
Centaur capabilities for communications satellite
launches
[AIAA PAPER 82-0558] p0034 A82-36286
- NEEDY, D. R.**
Multigrid simulation of asymptotic curved-duct
flows using a semi-implicit numerical technique
p0010 A82-29003
- NEEDY, J. W.**
Finite-element modeling of layered, anisotropic
composite plates and shells: A review of recent
research p0113 A82-19563
- NEID, L.**
Performance of single-stage axial-flow transonic
compressor with rotor and stator aspect ratios
of 1.63 and 1.78, respectively, and with design
pressure ratio of 1.82
[NASA-TP-1974] p0017 A82-19222
Performance of single-stage axial-flow transonic
compressor with rotor and stator aspect ratios
of 1.63 and 1.77, respectively, and with design
pressure ratio of 2.05
[NASA-TP-2001] p0018 A82-22269
- NEID, M. A.**
Alkaline regenerative fuel cell systems for energy
storage p0042 A82-11706
Performance of advanced chromium electrodes for
the NASA Redox Energy Storage System
[NASA-TN-82724] p0118 A82-12574
Improved chromium electrodes for REDOX cells
[NASA-CASE-LEW-13653-1] p0121 A82-22672
Light weight nickel battery plaque
[NASA-CASE-LEW-13349-1] p0121 A82-22673
Chemical and electrochemical behavior of the
Cr(3)/Cr(2) half cell in the NASA Redox Energy
Storage System
[NASA-TN-82913] p0055 A82-33463
- NEILLY, M. J.**
Barriers to the utilization of synthetic fuels for
transportation
[NASA-CR-165517] p0073 A82-13243
- NEINMANN, J. J.**
Selected bibliography of NACA-NASA aircraft icing
publications
[NASA-TN-81651] p0014 A82-11053
Aircraft icing research at NASA
[NASA-TN-82919] p0013 A82-30297
- NEISENFELD, S.**
The 30/20 GHz flight experiment system, phase 2.
Volume 1: Executive summary
[NASA-CR-165409-VOL-1] p0078 A82-20362
The 30/20 GHz flight experiment system, phase 2.
Volume 2: Experiment system description
[NASA-CR-165409-VOL-2] p0078 A82-20363
The 30/20 GHz flight experiment system, phase 2.
Volume 3: Experiment system requirement document
[NASA-CR-165409-VOL-3] p0078 A82-20364
The 30/20 GHz flight experiment system, phase 2.
Volume 4: Experiment system development plan
[NASA-CR-165409-VOL-4] p0078 A82-20365
- NEKICK, R. J.**
Stabilizing platinum in phosphoric acid fuel cells
[NASA-CR-165483] p0130 A82-14628
Stabilizing platinum in phosphoric acid fuel cells
[NASA-CR-165606] p0136 A82-29718
- NEGSTORFF, G. W. P.**
Friction and wear of iron in corrosive metal
[NASA-TP-1985] p0058 A82-20291
- REYNOLDS, B.**
Effects of blade loading and rotation on
compressor rotor wake in end wall regions
[AIAA PAPER 82-0193] p0010 A82-22063
- REXY, B. J.**
Exhaust emissions reduction for intermittent
combustion aircraft engines

- [NASA-CR-167914] p0029 N82-33392
KNODE, D. L.
 On the prediction of swirling flowfields found in axisymmetric combustor geometries p0029 N82-12120
 Mean flowfields in axisymmetric combustor geometries with swirl [AIAA PAPER 82-0177] p0092 N82-17824
- KNOLIK, E. E.**
 Analytic investigation of effect of end-wall contouring on stator performance [NASA-TP-1943] p0003 N82-14051
- KIBERICH, J. J.**
 The 30/20 GHz flight experiment system, phase 2. Volume 1: Executive summary [NASA-CR-165409-VOL-1] p0078 N82-20362
 The 30/20 GHz flight experiment system, phase 2. Volume 2: Experiment system description [NASA-CR-165409-VOL-2] p0078 N82-20363
 The 30/20 GHz flight experiment system, phase 2. Volume 3: Experiment system requirement document [NASA-CR-165409-VOL-3] p0078 N82-20364
- KIBERICH, J. J.**
 The 30/20 GHz flight experiment system, phase 2. Volume 4: Experiment system development plan [NASA-CR-165409-VOL-4] p0078 N82-20365
- KICCA, J. J.**
 On determination of fibre fraction in continuous fibre composite materials p0051 N82-38133
- KICE, E. E.**
 Feasibility of an earth-to-space rail launcher system [IAF PAPER 82-46] p0033 N82-44659
 Preliminary feasibility assessment for Earth-to-space electromagnetic (Railgun) launchers [NASA-CR-167886] p0033 N82-29345
- KICE, E. J.**
 A shock wave approach to the noise of supersonic propellers [NASA-TN-82752] p0151 N82-16809
- KICE, W. J.**
 Preliminary results on performance testing of a turbocharged rotary combustion engine [NASA-TN-82772] p0017 N82-21194
 Real time pressure signal system for a rotary engine [NASA-CASE-LEW-13622-1] p0019 N82-26294
- KICH, S. E.**
 CF6 jet engine performance improvement: High pressure turbine active clearance control [NASA-CR-165556] p0027 N82-28297
- KICHERSON, D. W.**
 Analytical and experimental evaluation of biaxial contact stress p0071 N82-20741
 Oxidation stability of advanced reaction-bonded Si3N4 materials [ACS PAPER 52-B-80P] p0074 N82-33030
- KICHEY, A.**
 Automotive Stirling engine development program [NASA-CR-167907] p0164 N82-29235
- KIDLEBAUGH, S. H.**
 Dilution jet behavior in the turn section of a reverse flow combustor [AIAA PAPER 82-0192] p0021 N82-20291
 Effect of fuel injector type on performance and emissions of reverse-flow combustor [NASA-TP-1945] p0016 N82-15040
 Dilution jet behavior in the turn section of a reverse flow combustor [NASA-TN-82776] p0017 N82-19220
- KIGO, H. S.**
 Magnetohydrodynamics (MHD) Engineering Test Facility (ETF) 200 MWe power plant. Design Requirements Document (DRD) [NASA-TN-82705] p0099 N82-12446
- KOBACK, E.**
 Deposit formation in hydrocarbon fuels [ASME PAPER 82-GT-49] p0075 N82-35307
- KOBERTS, J. C.**
 Fabrication and wear test of a continuous fiber/particulate composite total surface hip replacement [NASA-TN-81746] p0066 N82-11211
 Tribological characteristics of a composite total-surface hip replacement [NASA-TP-1853] p0066 N82-16239
- KOBERTS, W. K.**
 Aircraft sampling of the sulfate layer near the tropopause following the eruption of Mount St. Helens p0140 N82-37450
- ROBERTSON, R. I.**
 Primary propulsion/large space system interaction study [NASA-CR-165277] p0044 N82-18315
- ROBINSON, J. W.**
 Oblique-incidence secondary emission from charged dielectrics p0039 N82-14227
 Mapping of electrical potential distributions with charged particle beams [NASA-CR-168556] p0084 N82-18508
- ROBINSON, P. A.**
 30-cm mercury ion thruster technology p0046 N82-15434
- ROBINSON, R. S.**
 Surface diffusion activation energy determination using ion beam microtexturing p0159 N82-21965
 Quasi-liquid states observed on ion beam microtextured surfaces p0159 N82-30335
 Ion-beam-induced topography and surface diffusion p0160 N82-46426
 Experimental simulation of biased solar arrays with the space plasma [NASA-CR-165485] p0157 N82-10880
 Electric thruster research [NASA-CR-165603] p0045 N82-24285
 Electric and magnetic fields [NASA-CR-165604] p0045 N82-20350
 Ion beam microtexturing and enhanced surface diffusion [NASA-CR-167948] p0065 N82-31509
- ROBSON, R.**
 A 10kW series resonant converter design, transistor characterization, and base-drive optimization [NASA-CR-165546] p0084 N82-17439
- ROBSON, R. E.**
 A 10-kw series resonant converter design, transistor characterization, and base-drive optimization p0086 N82-36927
- ROCHE, J. C.**
 Validation of the NASCAP model using spaceflight data [AIAA PAPER 82-0269] p0038 N82-17872
 Testing of a spacecraft model in a combined environment simulator p0033 N82-18310
 Testing of a spacecraft model in a combined environment simulator [NASA-TN-82723] p0037 N82-11106
- ROCK, S. H.**
 Sensor failure detection system [NASA-CR-165515] p0023 N82-13145
- ROCKWOOD, F. A.**
 Ceramic applications in turbine engines [NASA-CR-165197] p0164 N82-31158
- ROSLER, R. J.**
 The effect of rotor blade thickness and surface finish on the performance of a small axial flow turbine [ASME PAPER 82-GT-222] p0022 N82-35409
 The effect of rotor blade thickness and surface finish on the performance of a small axial flow turbine [NASA-TN-82726] J003 N82-13114
- ROFFE, G.**
 Experimental study of the effects of secondary air on the emissions and stability of a lean premixed combustor [AIAA PAPER 82-1072] p0021 N82-34992
- ROGERS, J.**
 Standing waves along a microwave generated surface wave plasma p0158 N82-26952
- ROGO, C.**
 Cooled variable nozzle radial turbine for rotor craft applications [NASA-CR-165397] p0028 N82-29323
- ROHN, D. A.**
 Multiroller traction drive speed reducer: Evaluation for automotive gas turbine engine [NASA-TP-2027] p0101 N82-26678

- ROHRBACH, C.**
Evaluation of wind tunnel performance testings of an advanced 45 deg swept 8-bladed propeller at Mach numbers from 0.45 to 0.85
[NASA-CR-3575] p0007 N82-19178
- ROLLWILLER, R. J.**
Lewis Research Center's coal-fired, pressurized, fluidized-bed reactor test facility
[NASA-TN-81616] p0087 N82-11397
Lewis pressurized, fluidized-bed combustion program. Data and calculated results
[NASA-TN-81767] p0124 N82-30704
- ROSMOSKI, G. R., JR.**
Mechanisms of deformation and fracture in high temperature low cycle fatigue of Rene 80 and IN 100
[NASA-CR-165498] p0113 N82-26706
- ROSE, J. H.**
Universal binding energy relations in metallic adhesion
[NASA-TN-82706] p0058 N82-11183
- ROSENBLAT, S.**
Eigenvalues of the Rayleigh-Benard and Marangoni problems
p0092 N82-13396
Nonlinear Marangoni convection in bounded layers. I - Circular cylindrical containers. II - Rectangular cylindrical containers
p0094 N82-39501
Surface-tension induced instabilities: Effects of lateral boundaries
[NASA-CR-165530] p0092 N82-11390
- ROSENBLIEB, J. W.**
Spherical roller bearing analysis. SKF computer program SPHERBFAN. Volume 3: Program correlation with full scale hardware tests
[NASA-CR-165205] p0106 N82-20542
- ROSFJORD, T.**
Low NO subx heavy fuel combustor concept program. Phase 1A: Coal gas addendum
[NASA-CR-165577] p0133 N82-18690
- ROSFJORD, T. J.**
Evaluation of fuel injection configurations to control carbon and soot formation in small GT combustors
[AIAA PAPER 82-1175] p0021 N82-35041
Investigation of soot and carbon formation in small gas turbine combustors
[NASA-CR-167853] p0025 N82-22267
- ROSWER, D. E.**
Experimental and theoretical studies of the laws governing condensate deposition from combustion gases
p0057 N82-28709
- ROSS, P. T.**
Combustor development for automotive gas turbines
[AIAA PAPER 82-1208] p0104 N82-35062
- ROSSMAGEL, S. H.**
Surface diffusion activation energy determination using ion beam microtexturing
p0159 N82-21965
Quasi-liquid states observed on ion beam microtextured surfaces
p0159 N82-30335
Ion-beam-induced topography and surface diffusion
p0160 N82-46426
- ROTH, S. P.**
A real time Pegasus propulsion system model for VSTOL piloted simulation evaluation
[AIAA PAPER 81-2663] p0020 N82-19221
A real time Pegasus propulsion system model for VSTOL piloted simulation evaluation
[NASA-TN-82770] p0016 N82-13144
A piecewise linear state variable technique for real time propulsion system simulation
[NASA-TN-82851] p0018 N82-24201
- ROWSE, J. H.**
Study of advanced propulsion systems for Small Transport Aircraft Technology (STAT) program
[NASA-CR-165610] p0026 N82-24202
- ROBIN, A. G.**
Validation of the NASCAP model using spaceflight data
[AIAA PAPER 82-0269] p0038 N82-17872
- ROPICH, H. W.**
Moderate temperature Na cells. IV - VS2 and NbS₂C12 as rechargeable cathodes in molten NaAlCl₄
p0055 N82-15743
- RUPPRECHT, S. D.**
Atomization and combustion properties of flashing injectors
[AIAA PAPER 82-0300] p0092 N82-17880
- RUSSELL, D. A.**
Testing of solar cell covers and encapsulants conducted in a simulated space environment
[NASA-CR-165475] p0139 N82-12571
- RUSSELL, L. H.**
Flow visualization study of the horseshoe vortex in a turbine stator cascade
[NASA-TP-1884] p0088 N82-30498
- RUSSELL, P.**
Low NO sub x heavy fuel combustor concept program
[NASA-CR-165512] p0129 N82-12572
- RUTLEDGE, S. K.**
Ion beam sputter deposited diamond like films
[NASA-TN-82873] p0069 N82-28445
- RYAN, C. R.**
Conversion and matched filter approximations for serial miniaus-shi't keyed modulation
p0080 N82-26713
Near optimum delay-line detection filters for serial detection of MSK signals
p0086 N82-43867
- RYAN, E. W.**
Thrust reverser for a long duct fan engine
[NASA-CASE-LEW-13199-1] p0019 N82-26293

S

- SAARI, D. P.**
MHD oxidant intermediate temperature ceramic heater study
[NASA-CR-165453] p0131 N82-15527
- SABERS, R. L.**
Low-thrust chemical propulsion system pump technology
[NASA-CR-165219] p0105 N82-13427
- SABOURIN, D.**
Baseband-processed SS-TDMA communication system architecture and design concepts
[AIAA 82-0482] p0079 N82-23508
- SAIN, H.**
A tensor approach to modeling of nonhomogeneous nonlinear systems
p0148 N82-19064
- SAIN, H. K.**
Alternatives for jet engine control
[NASA-CR-168894] p0026 N82-23247
- SALVINO, J. T.**
Rotor fragment protection program: Statistics on aircraft gas turbine engine rotor failures that occurred in U.S. commercial aviation during 1978
[NASA-CR-165388] p0027 N82-27316
- SAMANICH, M. E.**
QCSEE under-the-wing engine acoustic data
[NASA-TM-82691] p0019 N82-27311
- SANDERS, B. W.**
Tangential blowing for control of strong normal shock - Boundary layer interactions on inlet ramps
[AIAA PAPER 82-1082] p0005 N82-37684
- SANGER, W. L.**
The use of optimization techniques to design controlled diffusion compressor blading
[ASME PAPER 82-GT-149] p0022 N82-35373
The use of optimization techniques to design controlled diffusion compressor blading
[NASA-TM-82763] p0016 N82-14094
- SANTIAGO, J. P.**
Turbulence in argon shock waves
p0158 N82-11117
- SANE, J. M.**
Design of supercritical cascades with high solidity
[NASA-CR-165600] p0007 N82-22210
- SAVAGE, W.**
Optimal tooth numbers for compact standard spur gear sets
[ASME PAPER 81-DET-115] p0103 N82-19335
Reliability model for planetary gear
[NASA-TM-82859] p0101 N82-28643
The optimal design of involute gear teeth with unequal addenda
[NASA-TM-82866] p0101 N82-28645
- SAVINO, J. M.**
Effect of rotor configuration on guyed tower and foundation designs and estimated costs for intermediate site horizontal axis wind turbines
[NASA-TM-82804] p0121 N82-22649

- SAVITZ, F. H.
Planning satellite communication services and
spectrum-orbit utilization
[AIAA 82-0526] p0080 A82-23538
- SCHILLING, H.
Coaxial prime focus feeds for paraboloidal
reflectors
[NASA-CR-167934] p0078 N82-31585
- SCHMIDT, E. J.
VLA observations of solar active regions at 6 cm
wavelength
p0167 A82-10156
- Magnetic structure of a flaring region producing
impulsive microwave and hard X-ray bursts
p0167 A82-27323
- SCHMIDT, E.
Overview study of Space Power Technologies for the
advanced energetics program
[NASA-CR-165269] p0132 N82-17606
- SCHMIDT, G. F.
Development of battery separator composites
[NASA-CR-165508] p0128 N82-11547
- SCHNAUSS, E. R.
First results of material charging in the space
environment
[NASA-TM-84743] p0081 N82-24431
- SCHNEIDER, H. H.
Thermal expansion accommodation in a jet engine
frame
p0029 A82-11999
- SCHNEIDER, P. W.
Effect of a part span variable inlet guide vane on
T714 fan performance
[NASA-CR-165458] p0023 N82-12075
- SCHWENKE, G. W.
Representation and material charging response of
geoplasma environments
p0039 N82-14249
- Simulation of charging response of SCATHA (P78-2)
satellite
p0039 N82-14250
- SCROCK, E. J.
Preliminary results on performance testing of a
turbocharged rotary combustion engine
[NASA-TF-82772] p0017 N82-21194
- SCHOENMAN, L.
Propulsion system options for low-acceleration
orbit transfer
[AIAA PAPER 82-1196] p0047 A82-35056
- Fuel/oxidizer-rich high-pressure preburners
[NASA-CR-165404] p0073 N82-10245
- Low-thrust Isp sensitivity study
[NASA-CR-165621] p0045 N82-22309
- SCHUBERT, F. H.
Alkaline regenerative fuel cell systems for energy
storage
p0042 A82-11706
- Endurance test and evaluation of alkaline water
electrolysis cells
[NASA-CR-165424] p0130 N82-13508
- SCHULSCN, E. H.
Recrystallization and grain growth in NiAl
p0065 A82-44529
- SCHULTZ, D. F.
Gas-turbine critical research and advanced
technology support project
[NASA-TM-81708] p0118 N82-13509
- Techniques for enhancing durability and
equivalence ratio control in a rich-lean,
three-stage ground power gas turbine combustor
[NASA-TM-82922] p0124 N82-29717
- Gas turbine critical research and advanced
technology (CRTE) support project
[NASA-TM-82872] p0126 N82-31776
- SCHOON, S. R.
Effect of oxide films on hydrogen permeability of
candidate Stirling engine heater head tube alloys
[NASA-TM-82824] p0060 N82-24323
- SCHWAB, J. A.
Low NOx heavy fuel combustor concept program.
Phase 1: Combustion technology generation
[NASA-CR-165482] p0136 N82-24725
- Low and medium heating value coal gas catalytic
combustor characterization
[NASA-CR-165560] p0138 N82-32856
- SCHWAB, J. R.
Aerodynamic performance of high turning core
turbine vanes in a two-dimensional cascade
[AIAA PAPER 82-1288] p0005 A82-37716
- Aerodynamic performance of high turning core
turbine vanes in a two dimensional cascade
[NASA-TM-82894] p0004 N82-26240
- SCHWARTZ, H. J.
Progress on advanced dc and ac induction drives
for electric vehicles
[NASA-TM-82895] p0163 N82-31160
- SCHWENDEHANS, M. F.
Tangential blowing for control of strong normal
shock - Boundary layer interactions on inlet ramps
[AIAA PAPER 82-1082] p0005 A82-37604
- SCOPE, J. S.
The 30/20 GHz flight experiment system, phase 2.
Volume 1: Executive summary
[NASA-CR-165409-VOL-1] p0078 N82-20362
- The 30/20 GHz flight experiment system, phase 2.
Volume 2: Experiment system description
[NASA-CR-165409-VOL-2] p0078 N82-20363
- The 30/20 GHz flight experiment system, phase 2.
Volume 3: Experiment system requirement document
[NASA-CR-165409-VOL-3] p0078 N82-20364
- The 30/20 GHz flight experiment system, phase 2.
Volume 4: Experiment system development plan
[NASA-CR-165409-VOL-4] p0078 N82-20365
- SCOTT, W. G.
30/20 GHz communications satellite multibeam antenna
[AIAA 82-0449] p0079 A82-23486
- SEASHOLTZ, R. G.
High-speed laser anemometer system for intrarotor
flow mapping in turbomachinery
[NASA-TP-1663] p0095 N82-19521
- Comparison of laser anemometer measurements and
theory in an annular turbine cascade with
experimental accuracy determined by parameter
estimation
[NASA-TM-82860] p0005 N82-28250
- Laser anemometer using a Fabry-Perot
interferometer for measuring mean velocity and
turbulence intensity along the optical axis in
turbomachinery
[NASA-TM-82841] p0095 N82-28605
- Status of laser anemometry in turbomachinery
research at the Lewis Research Center
p0096 N82-32686
- SEASHOLTZ, R. G.
Laser anemometer measurements in an annular
cascade of core turbine vanes and comparison
with theory
[NASA-TP-2018] p0004 N82-26234
- SERENQUIST, R.
Low NO subx heavy fuel combustor concept program.
Phase 1A: Coal gas addendum
[NASA-CR-165577] p0133 N82-18690
- SERCALL, S. B.
Free electron lasers for transmission of energy in
space
[NASA-CR-165520] p0098 N82-25499
- SEIDEL, R. C.
Variable gain for a wind turbine pitch control
[NASA-TM-82751] p0119 N82-16478
- SENG, G. T.
Characterization of an Experimental Referee
Broadened Specification (ERBS) aviation turbine
fuel and ERBS fuel blends
[NASA-TM-82883] p0072 N82-32504
- SENGERS, J. V.
Toward the use of similarity theory in two-phase
choked flows
p0089 A82-16570
- SERAFINI, J. S.
LV measurements with an advanced turboprop
p0097 N82-32690
- SERAFINI, T. T.
High-temperature resins
p0051 A82-42657
- PMR polyimides-review and update
[NASA-TM-82821] p0068 N82-24342
- SESHADRI, K.
Experimental and theoretical studies of the laws
governing condensate deposition from combustion
gases
p0057 A82-28709
- SHALTENC, R. K.
Experience and assessment of the DOE-NASA Mod-1
2000-Kilowatt wind turbine generator at Boone,
North Carolina
[NASA-TM-82721] p0125 N82-30710
- SHALTENS, R. K.
Aluminum blade development for the Mod-0A

- 200-kilowatt wind turbine
[NASA-TM-82594] p0119 N82-14633
- SHANNON, J. L., JR.
Extended range stress intensity factor expressions
for chevron-notched short bar and short rod
fracture toughness specimens p0112 A82-40357
- SHAW, R.
Computer modeling of fan-exit-splitter spacing
effects on F100 response to distortion
[NASA-CR-167879] p0025 N82-23246
- SHAW, W. J.
The combined effects of Fe and H₂ on the
nitridation of silicon p0070 A82-42924
- Nitridation of silicon
[NASA-TM-82722] p0066 N82-15197
- SHAW, W. J.
Performance degradation of propeller/rotor systems
due to rime ice accretion
[AIAA PAPER 82-0286] p0014 A82-28322
- An experimental study of airfoil icing
characteristics [NASA-TM-82790] p0001 N82-17083
- Aircraft icing research at NASA
[NASA-TM-82919] p0013 N82-30297
- SHERRY, K. D.
Current legal and institutional issues in the
commercialization of phosphoric acid fuel cells
[NASA-CR-167867] p0136 N82-29719
- SHREVELEY, D. W.
Inexpensive cross-linked polymeric separators made
from water-soluble polymers p0048 A82-23778
- Method of making formulated plastic separators for
soluble electrode cells [NASA-CASE-LEW-12358-2] p0054 N82-21268
- Cross-linked polyvinyl alcohol films as alkaline
battery separators [NASA-TM-82802] p0054 N82-22327
- Advanced inorganic separators for alkaline batteries
[NASA-CASE-LEW-13171-1] p0124 N82-29708
- SHROGAN, Y.
A study of viscous flow in stator and rotor passages
[ASME PAPER 82-GT-248] p0011 A82-35427
- SHERLOCK, T. P.
Low NO sub x heavy fuel combustor concept program.
Phase IA: Combustion technology generation coal
gas fuels [NASA-CR-165614] p0055 N82-22326
- SHEU, Y. C.
The transmission or scattering of elastic waves by
an inhomogeneity of simple geometry: A
comparison of theories [NASA-CR-169034] p0079 N82-26526
- SHEYWIN, L.
Research report: User's manual for computer
program AT81Y003 SHABEPH. Steady state and
transient thermal analysis of a shaft bearing
system including ball, cylindrical and tapered
roller bearings [NASA-CR-165365] p0146 N82-31969
- Research report: User's manual for computer
program AT81Y005. PLANETSYS, a computer program
for the steady state and transient thermal
analysis of a planetary power transmission system
[NASA-CR-165366] p0146 N82-31970
- SHIGAKI, H.
Influence of mineral oil and additives on
microhardness and surface chemistry of magnesium
oxide (001) surface [NASA-TP-1986] p0067 N82-20316
- SHIM, C. I.
High temperature low cycle fatigue mechanisms for
nickel base and a copper base alloy [NASA-CR-3543] p0064 N82-26436
- SHIN, C. T.
Multigrad simulation of asymptotic curved-duct
flows using a semi-implicit numerical technique
p0010 A82-29003
- SHNATKOVA, A. A.
Motion of a rigid punch at the boundary of an
orthotropic viscoelastic half-plane A82-26436
- SHOAF, L.
Advanced turboprop tested systems study. Volume
1: Tested program objectives and priorities,
drive system and aircraft design studies,
evaluation and recommendations and wind tunnel
- test plans
[NASA-CR-167928-VOL-1] p0028 N82-32370
- SHORE, R. A.
Focal surfaces of offset dual-reflector antennas
p0080 A82-36265
- SIDI, A.
Acceleration of convergence of vector sequences
[NASA-TM-82931] p0149 N82-29075
- SIDIK, S. M.
Results of chopper-controlled discharge life
cycling studies on lead acid batteries
[NASA-TM-82912] p0124 N82-30700
- SIEBENHAAR, A.
Low-thrust chemical propulsion system pump
technology [NASA-CR-165219] p0105 N82-13427
- SIDDELL, R.
Heat transfer in cooled porous region with curved
boundary p0089 A82-14848
- Cauchy integral method for two-dimensional
solidification interface shapes p0089 A82-39899
- SIMMONS, F. A.
Thermal-barrier-coated turbine blade study
[NASA-CR-165351] p0023 N82-10040
- SIGMAN, R. K.
An iterative finite element-integral technique for
predicting sound radiation from turbofan inlets
in steady flight [AIAA PAPER 82-0124] p0030 A82-17796
- Acoustic properties of turbofan inlets
[NASA-CR-169016] p0153 N82-27090
- SIGNORELLI, R. A.
High temperature composites. Status and future
directions [NASA-TM-82929] p0051 N82-30336
- SIMON, T. M.
Turbulent boundary layer heat transfer experiments
- A separate effects study on a convexly-curved
wall [ASME PAPER 81-HT-78] p0092 A82-10963
- Turbulent boundary layer heat transfer
experiments: Convex curvature effects including
introduction and recovery [NASA-CR-3510] p0090 N82-17456
- SIMONHAU, R. J.
Toward the use of similarity theory in two-phase
choked flows p0089 A82-16570
- Effect of location in an array on heat transfer to
a cylinder in crossflow [NASA-TM-82797] p0087 N82-19493
- SIMONS, S.
Direct conversion of light to radio frequency energy
p0138 A82-11712
- SIMONS, S. M.
Phosphoric acid fuel cell technology status
[NASA-TM-82791] p0120 N82-19670
- SIMPSON, W. E.
V/STOL Tandem Fan transition section model test
[NASA-CR-165587] p0007 N82-21158
- SINCLAIR, J. M.
Impact resistance of fiber composites
p0112 A82-39852
- Durability/life of fiber composites in
hygrothermomechanical environments [NASA-TM-82749] p0049 N82-14287
- Prediction of composite hygral behavior made simple
[NASA-TM-82780] p0049 N82-16181
- Compression behavior of unidirectional fibrous
composite [NASA-TM-82833] p0050 N82-22313
- SINGER, J. R.
Current legal and institutional issues in the
commercialization of phosphoric acid fuel cells
[NASA-CR-167867] p0136 N82-29719
- SINGH, S.
Formation of oxides of nitrogen in monodisperse
spray combustion of hydrocarbon fuels p0057 A82-37571
- SISTO, F.
The influence of Coriolis forces on gyroscopic
motion of spinning blades [ASME PAPER 82-GT-163] p0030 A82-35384
- SITNIKOVA, M. V.
Dynamics of snow cover in mountain regions of the
Aral Sea basin, studied using satellite
photographs

SIVASHINSKY, G. I.

A82-27462

SIVASHINSKY, G. I.
On stability of premixed flames in stagnation -
Pcint flow p0057 A82-37574

SIVO, J. W.
Advanced 30/20 GHz communication satellites p0034 A82-12623

SKARILL, G.
A new antenna concept for satellite communications
[NASA-CR-167924] p0C79 N82-31584

SKINNER, A.
Work of fracture in aluminum metal-matrix composites p0053 A82-31339
Tensile properties of SiC/aluminum filamentary
composites - Thermal degradation effects p0053 A82-46220

SLADY, J. G.
Assessment of a 40-kilowatt stirling engine for
underground mining applications
[NASA-TM-82822] p0125 N82-30714

SLAVIK, B. J.
Rolling resistance of electric vehicle tires from
track tests [NASA-TM-82836] p0124 N82-28786
On the road performance tests of electric test
vehicle for correlation with road load simulator
[NASA-TM-82900] p0127 N82-33829

SLETTEN, C. J.
Focal surfaces of offset dual-reflector antennas p0080 A82-36265

SLICKER, J. M.
A PWM transistor inverter for an ac electric
vehicle drive p0085 A82-20744

SLINEY, E. E.
Performance of PTFE-lined composite journal bearings
[ASLE PAPER 82-AM-1A-1] p0104 A82-37854
Performance of PTFE-lined composite journal bearings
[NASA-TM-82779] p0048 N82-17263

SMIALEK, J. L.
Phase stability in plasma-sprayed, partially
stabilized zirconia-yttria p0070 A82-41552

SHENOVA, T. A.
Investigation of a comb-type slow-wave structure
for millimeter-wave masers A82-18368

SMITH, D. A.
Numerical comparisons of nonlinear convergence
accelerators p0149 A82-31438
Acceleration of convergence of vector sequences
[NASA-TM-82931] p0149 N82-29075

SMITH, G. T.
Environmental and High-Strain Rate effects on
composites for engine applications [NASA-TM-82882] p0051 N82-31449

SMITH, J. M.
End region and current consolidation effects upon
the performance of an MHD channel for the ETP
conceptual design [AIAA PAPER 82-0325] p0157 A82-17889
Effect of vacuum exhaust pressure on the
performance of MHD ducts at high B-field
[AIAA PAPER 82-0396] p0157 A82-20292
End region and current consolidation effects upon
the performance of an MHD channel for the ETP
conceptual design [NASA-TM-82744] p0157 N82-12943
Effect of vacuum exhaust pressure on the
performance of MHD ducts at high B-field
[NASA-TM-82750] p0157 N82-13908
Results and comparison of Hall and DW duct
experiments [NASA-TM-82864] p0157 N82-25961

SMITH, J. B.
Universal binding energy relations in metallic
adhesion [NASA-TM-82706] p0050 N82-11183

SMITH, J. T.
Fabrication of turbine components and properties
of sintered silicon nitride [ASME PAPER 82-GT-252] p0071 A82-35431

SMITH, R. J.
Strength advantages of chemically polished boron
fibers before and after reaction with aluminum
[NASA-TM-82806] p0049 N82-21258

SMITH, G. E.

Study of electrical and chemical propulsion
systems for auxiliary propulsion of large space
systems. Volume 1: Executive summary
[NASA-CR-165502-VOL-1] p0046 N82-11110

Study of electrical and chemical propulsion
systems for auxiliary propulsion of large space
systems, volume 2 [NASA-CR-165502-VOL-2] p0046 N82-11111

An insight into auxiliary propulsion requirements
of large space systems [NASA-TM-82827] p0042 N82-24286

SMITHERICK, J. J.
Effect of positive pulse charge waveforms on the
energy efficiency of lead-acid traction cells
[NASA-TM-82709] p0118 N82-10503
Design of a 35-kilowatt bipolar nickel-hydrogen
battery for low Earth orbit application
[NASA-TM-82844] p0123 N82-24647

SNOLL, A. E.
30/20 GHz communications satellite multibeam antenna
[AIAA 82-0449] p0079 A82-23486

SNOW, G. C.
High temperature durable catalyst development p0056 A82-20739
Development of a high-temperature durable catalyst
for use in catalytic combustors for advanced
automotive gas turbine engines [NASA-CR-165396] p0130 N82-13510

SNOW, W. R.
Mass Driver Two - A status report p0046 A82-18191
Mass driver reaction engine characteristics and
performance in earth orbital transfer missions p0046 A82-18199
A small scale lunar launcher for early lunar
material utilization p0032 A82-35617
The supply of lunar oxygen to low earth orbit p0032 A82-35618

SNIDER, A.
Heat transfer in cooled porous region with curved
boundary p0089 A82-14848

SOBEL, D. R.
Tube entrance heat transfer with deposit formation
[AIAA PAPER 82-0918] p0093 A82-31908

SOBIECHWY, H.
A computational design method for transonic
turbomachinery cascades [ASME PAPER 82-GT-117] p0022 A82-35348
CAS22 - FORTRAN program for fast design and
analysis of shock-free airfoil cascades using
fictitious-gas concept [NASA-CR-3507] p0006 N82-16044

SOCKOL, P. M.
Computational methods for internal flows with
emphasis on turbomachinery [NASA-TM-82764] p0003 N82-13113

SODA, M.
Effect of tangential traction and roughness on
crack initiation/propagation during rolling
contact p0103 A82-30022

SOLANO, F. R.
An experimental study of airfoil icing
characteristics [NASA-TM-82790] p0001 N82-17083

SOLOMON, A. S., P.
Atomization and combustion properties of flashing
injectors [AIAA PAPER 82-0300] p0092 A82-17880
Investigation of spray characteristics for
flashing injection of fuels containing dissolved
air and superheated fuels [NASA-CR-3563] p0027 N82-26295

SOLTIS, D. G.
Light weight nickel battery plague
[NASA-CASE-LEW-13349-1] p0121 N82-22673

SOMANO, R. B.
Raman study of the improper ferroelectric phase
transition in iron iodine boracite A82-30297

SOSOKA, D. J.
Cauchy integral method for two-dimensional
solidification interface shapes p0089 A82-39899

SOTOS, R. G.
An experimental study of airfoil icing

- characteristics
[NASA-TN-82790] p0001 N82-17003
- SOVEY, J. S.**
Ion beam textured graphite electrode plates
[NASA-CASE-LEW-12919-2] p0050 N82-26386
Texturing polymer surfaces by transfer casting
[NASA-CASE-LEW-13120-1] p0068 N82-28440
Surface texturing of fluoropolymers
[NASA-CASE-LEW-13028-1] p0070 N82-33521
- SOVIE, H. J.**
Comparative analysis of the conceptual design studies of potential early commercial MHD power plants (CSPEC)
[NASA-TN-82897] p0123 N82-27838
- SPADACCINI, L. J.**
Deposit formation in hydrocarbon fuels
[ASME PAPER 82-GT-49] p0075 A82-35307
- SPALVINS, T.**
Tribological properties and XPS studies of ion plated gold on nickel and iron
[NASA-TN-82814] p0059 N82-22344
Morphological and frictional behavior of sputtered MoS₂ films
[NASA-TN-82809] p0076 N82-22387
- SPEAR, D. A.**
Study of controlled diffusion stator blading. I. Aerodynamic and mechanical design report
[NASA-CF-165500] p0024 N82-16081
- SPERA, D. A.**
Applications of the DOE/NASA wind turbine engineering information system p0122 N82-23696
Calculation of guaranteed mean power from wind turbine generators p0122 N82-23699
- SPIZZER, M. B.**
Development of a large area space solar cell assembly
[NASA-CF-167929] p0137 N82-30706
- SRINIVASAN, M.**
Tribological properties of sintered polycrystalline and single crystal silicon carbide
[NASA-TN-82829] p0068 N82-24343
- SRIVATSA, S. K.**
Computations of soot and NO sub x emissions from gas turbine combustors
[NASA-CR-167930] p0139 N82-29777
- ST. GEORGE, E.**
Development of a dual-field heteropolar power converter
[NASA-CF-165168] p0084 N82-24424
- ST. JOHN, G. A.**
Oxidation and formation of deposit precursors in hydrocarbon fuels
[NASA-CR-165534] p0073 N82-18402
- STAHARA, S. S.**
Rapid approximate determination of nonlinear solutions - Application to aerodynamic flows and design/optimization problems p0012 A82-35571
- STAIGER, P. J.**
New features and applications of PRESTO, a computer code for the performance of regenerative, superheated steam turbine cycles
[NASA-TP-1954] p0119 N82-16477
Summary and evaluation of the conceptual design study of a potential early commercial MHD power plant (CSPEC)
[NASA-TN-82734] p0119 N82-16481
Integrated gasifier combined cycle polygeneration system to produce liquid hydrogen
[NASA-TN-82921] p0125 N82-30713
- STALLONE, M. J.**
Blade loss transient dynamic analysis of turbomachinery
[AIAA PAPER 82-1057] p0030 A82-34982
- STANG, D. B.**
Comparison of NASCAP modelling results with lumped circuit analysis p0037 N82-14255
- STANKIEWICZ, M.**
Experimental verification of a computational procedure for the design of TWT-refocuser-MDC systems p0082 A82-16128
Computer modeling of multiple-channel input signals and intermodulation losses caused by nonlinear traveling wave tube amplifiers
[NASA-TP-1999] p0082 N82-25441
- STANDARD, P. E.**
Validation of the NASCAP model using spaceflight data
[AIAA PAPER 82-0269] p0038 A82-17872
'Bootstrapping' charging of surfaces composed of multiple materials p0085 A82-18318
Representation and material charging response of geoplasma environments p0039 N82-14249
Simulation of charging response of SCATHA (P78-2) satellite p0039 N82-14250
Additional extensions to the NASCAP computer code, volume 1 [NASA-CR-167855] p0146 N82-25810
Additional extensions to the NASCAP computer code, volume 2 [NASA-CR-167856] p0040 N82-26377
- STAPLES, D.**
Market assessment of photovoltaic power systems for agricultural applications in Nigeria
[NASA-CR-165511] p0133 N82-18698
- STAPLETON, E. E.**
Development of an 1100 deg F capacitor p0083 N82-15315
- STARKE, H.**
Requirements for optimization of electrodes and electrolyte for the iron/chromium redox flow cell
[NASA-CR-165218] p0136 N82-25640
- STASKUS, J.**
SCATHA SSPM charging response: NASCAP predictions compared with data p0037 N82-14251
First results of material charging in the space environment
[NASA-TN-84743] p0081 N82-24431
- STASKUS, J. V.**
Testing of a spacecraft model in a combined environment simulator p0033 A82-18310
Testing of a spacecraft model in a combined environment simulator
[NASA-TN-82723] p0037 N82-11166
- STATON, D. V.**
Propulsion study for Small Transport Aircraft Technology (STAT)
[NASA-CR-165499] p0022 N82-10037
- STAUTER, R. C.**
The design and instrumentation of the Purdue annular cascade facility with initial data acquisition and analysis
[NASA-CR-167861] p0008 N82-26237
- STEARNS, E.**
Cost/benefit studies of advanced materials technologies for future aircraft turbine engines: Materials for advanced turbine engines
[NASA-CR-167849] p0026 N82-25254
- STECURA, S.**
Improved thermal barrier coating system
[NASA-CASE-LEW-13324-1] p0060 N82-26431
- STEPKO, G. L.**
Propeller flow visualization techniques p0096 N82-32672
- STEIGELMANN, W.**
Market assessment of photovoltaic power systems for agricultural applications in Mexico
[NASA-CR-165441] p0128 N82-10506
Market assessment of photovoltaic power systems for agricultural applications in Colombia
[NASA-CR-165524] p0134 N82-22770
- STEIN, C. K.**
Subsystems design and component development for the parabolic dish module for solar thermal power systems
[NASA-CR-168941] p0135 N82-24646
- STEINBERG, E.**
The NASA MERIT program - Developing new concepts for accurate flight planning
[AIAA PAPER 82-0340] p0014 A82-17894
- STEINER, G.**
Developing a scalable inert gas ion thruster
[AIAA PAPER 82-1275] p0047 A82-37713
- STEINGASS, H.**
Market assessment of photovoltaic power systems for agricultural applications in Morocco
[NASA-CR-165477] p0130 N82-14627
Market assessment of photovoltaic power systems for agricultural applications in Nigeria

ORIGINAL PAGE IS
OF POOR QUALITY

STEINKE, R. J.

PERSONAL AUTHOR INDEX

- [NASA-CF-165E11] p0133 N82-18698
- STEINKE, R. J.**
SITSIK: A computer code for predicting multistage axial flow compressor performance by a meanline stage stacking method
[NASA-TP-2023] p0018 N82-25250
- STEINWAGEL, K. H.**
Worldwide satellite market demand forecast
[NASA-CR-167918] p0079 N82-25423
- STENCEL, R. E.**
Ultraviolet observations of the 1980 eclipse of the symbiotic star CI Cygni
A82-27331
- STEVENSEN, K.**
Optically pumped high-pressure DF-CO₂ transfer laser
A82-10193
- STEPHENS, J. R.**
A status review of NASA's COSAM (Conservation Of Strategic Aerospace Materials) program
[NASA-TM-82852] p0060 N82-24326
- STEPKA, F. S.**
Thermal and flow analysis of a convection, air-cooled ceramic coated porous metal concept for turbine vanes
[ASME PAPER 81-HT-48] p0020 A82-10952
- STERN, B. A.**
Hybridized polymer matrix composite
[NASA-CR-165340] p0051 N82-12139
- STEYSON, A. R.**
Advanced ceramic coating development for industrial/utility gas turbines
[NASA-CR-169852] p0065 N82-33494
- STETZ, T. T.**
Flow through axially aligned sequential apertures of the orifice and Borda types
[ASME PAPER 81-HT-79] p0089 A82-10964
Flow through aligned sequential orifice type inlets
[NASA-TP-1967] p0087 N82-20467
Flows through sequential orifices with heated spacer reservoirs
[NASA-TM-82955] p0088 N82-24455
- STEVENS, M. J.**
Voltage gradients in solar array cavities as possible breakdown sites in spacecraft-charging-induced discharges
p0038 A82-18317
Voltage gradients in solar array cavities as possible breakdown sites in spacecraft-charging-induced discharges
[NASA-TM-82710] p0037 N82-11107
Analytical modeling of satellites in geosynchronous environment
p0037 N82-14258
Agreement for NASA/OAST - USAF/AFSC space interdependency on spacecraft environment interaction
p0038 N82-14271
Design practices for controlling spacecraft charging interactions
[NASA-TM-82781] p0038 N82-18311
Environmentally induced discharges on satellites
[NASA-TR-82849] p0038 N82-23261
First results of material charging in the space environment
[NASA-TM-84743] p0081 N82-24431
- STEVES, M. J.**
Use of charging control guidelines for geosynchronous satellite design studies
p0037 N82-14263
- STILLWELL, J. H.**
Conversion and matched filter approximations for serial minimum-shift keyed modulation
p0080 A82-26713
- STITT, L. E.**
NASA research in supersonic propulsion: A decade of progress
[NASA-TM-82862] p0019 N82-26300
- STOCHL, B. J.**
Assessment of steam-injected gas turbine systems and their potential application
[NASA-TM-82735] p0119 N82-18694
- STOCKNER, F. J.**
Experimental study of fuel heating at low temperatures in a wing tank model, volume 1
[NASA-CR-165391] p0073 N82-11224
Experiments on fuel heating for commercial aircraft
[NASA-TM-82878] p0072 N82-26483
Additional experiments on flowability improvements of aviation fuels at low temperatures, volume 2
- [NASA-CR-167912] p0074 N82-31546
- STOLOFF, W. S.**
Fatigue of Ni-Al-Mo aligned eutectics at elevated temperatures
p0052 A82-13403
- STOLP, P. C.**
Propulsion study for Small Transport Aircraft Technology (STAT)
[NASA-CR-165499] p0022 N82-10037
- STONE, J. E.**
NASA research in supersonic propulsion: A decade of progress
[NASA-TM-82862] p0019 N82-26300
- STONEHART, P.**
Survey on aging on electrodes and electrocatalysts in phosphoric acid fuel cells
[NASA-CR-165505] p0128 N82-11545
Preparation and evaluation of advanced electrocatalysts for phosphoric acid fuel cells
[NASA-CR-165519] p0129 N82-12573
Preparation and evaluation of advanced electrocatalysts for phosphoric acid fuel cells
[NASA-CR-165594] p0132 N82-17615
- STONESIFER, R. B.**
On a study of the $\Delta T/c$ and $C/asterisk/$ integrals for fracture analysis under non-steady creep
p0115 A82-36782
Moving singularity creep crack growth analysis with the $\Delta T/c$ and $C/asterisk/$ integrals
p0116 A82-40066
Creep crack-growth: A new path-independent T sub o and computational studies
[NASA-CR-168930] p0113 N82-24503
Creep crack-growth: A new path-independent integral (T sub c), and computational studies
[NASA-CR-167897] p0114 N82-29619
- STORAGE, A. F.**
Blade loss transient dynamic analysis of turbomachinery
[AIAA PAPER 82-1057] p0030 A82-34982
- STORN, R. S.**
Progress in ceramic component fabrication technology
[AIAA PAPER 82-1211] p0071 A82-35064
Net shape fabrication of Alpha Silicon Carbide turbine components
[ASME PAPER 82-GT-216] p0071 A82-35403
- STRACK, W. C.**
Future propulsion opportunities for computer airplanes
[NASA-TM-82880] p0018 N82-24203
Propulsion opportunities for future computer aircraft
[NASA-TM-82915] p0019 N82-26298
- STRAIGHT, D. H.**
Performance of a 2D-CD nonaxisymmetric exhaust nozzle on a turbojet engine at altitude
[NASA-TM-82881] p0005 N82-26241
- STRALISAN, A. J.**
Comparison of two and three dimensional flow computations with laser anemometer measurements in a transonic compressor rotor
[NASA-TM-82777] p0004 N82-15020
High-speed laser anemometer system for intrarotor flow mapping in turbomachinery
[NASA-TP-1663] p0095 N82-19521
- STERN, K. J.**
Permanent magnet properties of Mn-Al-C between -50 C and +150 C
p0085 A82-20505
- STUART, T. A.**
Modeling the full-bridge series-resonant power converter
p0086 A82-46385
- STUCKAS, K. J.**
Exhaust emissions reduction for intermittent combustion aircraft engines
[NASA-CR-167914] p0029 N82-33392
- STURGES, G. J.**
Advanced Low-Emissions Catalytic-Combustor Program, phase 1
[NASA-CR-159656] p0025 N82-22265
- SULLIVAN, R. E.**
Small gas turbine combustor primary zone development
[AIAA PAPER 82-1159] p0103 A82-35036
- SULLIVAN, T. L.**
A review of resonance response in large horizontal-axis wind turbines
p0122 N82-23711

- SUTCU, H.**
The influence of Coriolis forces on gyroscopic motion of spinning blades
[ASME PAPER 82-GT-163] p0030 A82-35384
- SWALLOE, D. W.**
MHD channel performance for potential early commercial MHD power plants p0158 A82-20750
- SWARTZ, C. K.**
Effects of processing and dopant on radiation damage removal in silicon solar cells
[NASA-TM-82892] p0042 A82-31443
- SYBERG, J.**
Aerodynamic analysis of VTOL inlets and definition of a short, blowing-lip inlet
[NASA-CR-165617] p0007 A82-22211
- SYVHNSON, H. T.**
Fuel quality processing study, volume 1
[NASA-CR-165127-VOL-1] p0135 A82-24649
- SEATKOWSKI, G. P.**
Design and verification of a multiple fault tolerant control system for STS applications using computer simulation
[AIAA 81-2173] p0035 A82-10124
Real-time computer simulation/emulation for verification of multi-fault-tolerant control of Centaur-in-Shuttle
[AIAA 81-2203] p0040 A82-13494
Real-time microcomputer simulation for space Shuttle/Centaur avionics p0033 A82-48245
- SZETELA, E. J.**
A heat exchanger computational procedure for temperature-dependent fouling
[ASME PAPER 81-HT-75] p0092 A82-10961
Tube entrance heat transfer with deposit formation
[AIAA PAPER 82-0918] p0093 A82-31908
Deposit formation in hydrocarbon fuels
[ASME PAPER 82-GT-49] p0075 A82-35307
Experimental study of external fuel vaporization
[ASME PAPER 82-GT-59] p0075 A82-35312
External fuel vaporization study
[NASA-CR-165513] p0073 A82-14371
- SZUCH, J. R.**
Advancements in real-time engine simulation technology
[AIAA PAPER 82-1075] p0021 A82-34995
Advancements in real-time engine simulation technology
[NASA-TM-82825] p0147 A82-22915
Automated procedure for developing hybrid computer simulations of turbofan engines. Part 1: General description
[NASA-TP-1851] p0146 A82-33020
- T**
- TABAKOFF, W.**
A study of viscous flow in stator and rotor passages
[ASME PAPER 82-GT-248] p0011 A82-35427
Three dimensional flow measurements in a turbine scroll
[NASA-CR-167920] p0009 A82-32310
- TACINA, R. R.**
Catalytic combustion of residual fuels
[NASA-TM-82731] p0118 A82-13504
- TAPT, W. J.**
Wideband, high speed switch matrix development for SS-TDMA applications p0086 A82-43784
- TANNANI, A. S.**
Evidence for Pu-244 fission tracks in hibonites from Murchison carbonaceous chondrite p0166 A82-29316
- TARTAGLIA, J. M.**
Fatigue of Ni-Al-Fe aligned eutectics at elevated temperatures p0052 A82-13403
- TAUSSIG, E.**
Overview study of Space Power Technologies for the advanced energetics program
[NASA-CR-165269] p0132 A82-17606
- TAUTZ, M. P.**
Validation of the NASCAP model using spaceflight data
[AIAA PAPER 82-0269] p0038 A82-17872
- TERTISHNYI, A. S.**
The use of a structural method to calculate the electrostatic field of a magnetron A82-18370
- TEVAARWERK, J. L.**
Traction contact performance evaluation at high speeds
[NASA-CR-165226] p0105 A82-16409
Stress evaluations under rolling/sliding contacts
[NASA-CR-165561] p0113 A82-17521
- TSVELDE, J. A.**
Experimental study of external fuel vaporization
[ASME PAPER 82-GT-59] p0075 A82-35312
External fuel vaporization study
[NASA-CR-165513] p0073 A82-14371
- THALLER, L. M.**
NASA Redox cell stack shunt current, pumping power, and cell performance tradeoffs
[NASA-TM-82686] p0054 A82-19333
Performance mapping studies in Redox flow cells
[NASA-TM-82707] p0120 A82-20668
Synthetic battery cycling techniques
[NASA-TM-82945] p0125 A82-30715
Nickel-hydrogen bipolar battery systems
[NASA-TM-82946] p0125 A82-30716
Design flexibility of Redox flow systems
[NASA-TM-82854] p0054 A82-31459
- THIEME, L. G.**
Jet impingement heat transfer enhancement for the GPU-3 Stirling engine
[NASA-TM-82727] p0163 A82-11993
- THOMAS, R. L.**
The NASA Lewis large wind turbine program
[NASA-TM-82761] p0119 A82-16495
- THOMPSON, W. T., JR.**
A FORTRAN program for calculating three dimensional, inviscid and rotational flows with shock waves in axial compressor blade rows: User's manual
[NASA-CR-3560] p0008 A82-26230
- THOMPSON, W. L.**
Nonlinear constitutive theory for turbine engine structural analysis p0112 A82-33744
- THOREN, R. J.**
Development report: Automatic System Test and Calibration (ASTAC) equipment
[NASA-CR-165403] p0129 A82-13505
- THRESHER, R. W.**
Wind turbine dynamics
[NASA-CP-2185] p0122 A82-23684
- THURLIN, R.**
Energy efficient engine: Turbine transition duct model technology report
[NASA-CR-167996] p0029 A82-33394
- TIEN, J. K.**
Effects of cobalt on structure, microchemistry and properties of a wrought nickel-base superalloy
p0065 A82-34973
Creep and rupture of an ODS alloy with high stress rupture ductility p0065 A82-40335
- TIEN, J. S.**
Transient catalytic combustor model
[NASA-CR-165324] p0129 A82-13507
- TIPTON, D. L.**
AGT100 turbomachinery
[AIAA PAPER 82-1207] p0108 A82-35061
- TOBIASON, A. R.**
NASA research programs responding to workshop recommendations A82-21146
- TONG, H.**
High temperature durable catalyst development
p0056 A82-20739
Development of a high-temperature durable catalyst for use in catalytic combustors for advanced automotive gas turbine engines
[NASA-CR-165396] p0130 A82-13510
Computer model of catalytic combustion/Stirling engine heater head
[NASA-CR-165378] p0134 A82-22666
- TORSTENSSON, J. R.**
On a free-electron-laser in a uniform magnetic field - A solution for arbitrarily strong electromagnetic radiation fields A82-28409
- TOVICHAKCHAIKUL, S.**
On the solution of creep induced buckling in general structure p0115 A82-39514

- Self-adaptive closed constrained solution algorithms for nonlinear conduction p0094 A82-45157
- TOWNSEND, D. P.**
Optimal tooth numbers for compact standard spur gear sets [ASME PAPER 81-DET-115] p0103 A82-19335
The optimal design of involute gear teeth with unequal addenda [NASA-TM-82866] p0101 N82-28645
Effect of shot peening on surface fatigue life of carburized and hardened AISI 9310 spur gears [NASA-TR-2047] p0102 N82-32736
- TRESSLER, R. E.**
Strength distributions of SiC ceramics after oxidation and oxidation under load [ACS PAPER 9-C-80C] p0071 A82-20143
Effects of oxidation and oxidation under load on strength distributions of Si3N4 [ACS PAPER 64-B-80] p0071 A82-35871
- TROTH, D. L.**
Low NOx heavy fuel combustor concept program addendum: Low/mid heating value gaseous fuel evaluation [NASA-CR-165615] p0055 N82-25338
Low NOx heavy fuel combustor concept program [NASA-CR-165367] p0136 N82-25635
- TRYON, H. B.**
Summary of electric vehicle dc motor-controller tests [NASA-TM-82863] p0082 N82-33636
- TSARNY, B. K.**
Dynamics of snow cover in mountain regions of the Aral Sea basin, studied using satellite photographs A82-27462
- TSENG, P. K.**
Detection of a change in the oxidation state on aluminum surface using angular correlation of positron annihilation radiation A82-30374
- TSUCHIYA, T.**
Water ingestion into jet engine axial compressors [AIAA PAPER 82-0196] p0030 A82-17836
- TUCKER, J. R.**
Exhaust emissions reduction for intermittent combustion aircraft engines [NASA-CR-167914] p0029 N82-33392
- TUNSTALL, B.**
Communications satellite systems capacity analysis [NASA-CR-167911] p0034 N82-27331
- TURNER, G. E.**
Comparison of two parallel/series flow turbofan propulsion concepts for supersonic V/STOL [AIAA PAPER 81-2637] p0020 A82-19214
Comparison of two parallel/series flow turbofan propulsion concepts for supersonic V/STOL [NASA-TM-82743] p0004 N82-18178
- V**
- VADYAK, J.**
Three-dimensional flow calculations including boundary layer effects for supersonic inlets at angle of attack [AIAA PAPER 82-0061] p0005 A82-19778
Calculation of the flow field including boundary layer effects for supersonic mixed compression inlets at angles of attack [NASA-CR-167941] p0009 N82-29269
- VALCO, G. J.**
Multi-junction high voltage concentrator solar cells p0043 A82-11796
Fabrication of multi-junction high voltage concentrator solar cells by integrated circuit technology p0127 A82-44957
- VALGORA, M.**
High power solar array switching regulation p0043 A82-11736
- VANEVELD, L.**
Secondary effects in combustion instabilities leading to flashback [AIAA PAPER 82-0037] p0056 A82-17746
- VANFOSSEN, G. J., JR.**
An experimental investigation into the feasibility of a thermoelectric heat flux gage [NASA-TM-82755] p0095 N82-14494
- Effect of location in an array on heat transfer to a cylinder in crossflow [NASA-TM-82797] p0087 N82-19493
- VARY, A.**
Metal honeycomb to porous wireform substrate diffusion bond evaluation [NASA-TM-82793] p0110 N82-18612
Interrelation of material microstructure, ultrasonic factors, and fracture toughness of two phase titanium alloy [NASA-TM-82810] p0110 N82-20551
- VASTA, V. M.**
Turbofan forced mixer-nozzle internal flowfield. Volume 2: Computational fluid dynamic predictions [NASA-CR-3493] p0091 N82-22459
- VATISTAS, G. M.**
Bluff-body flameholder wakes - A simple numerical solution [AIAA PAPER 82-1177] p0093 A82-35043
- VELUSAMY, T.**
Magnetic structure of a flaring region producing impulsive microwave and hard X-ray bursts p0167 A82-27323
- VERMES, G.**
Low NOx heavy fuel combustor concept program. Phase 1: Combustion technology generation [NASA-CR-165482] p0136 N82-24725
- VISSEK, T.**
Hybridized polymer matrix composite [NASA-CR-165340] p0051 N82-12139
- VITENBA, L. A.**
Method for predicting impulsive noise generated by wind turbine rotors [NASA-TM-82794] p0121 N82-21714
The NASA-LaRC wind turbine sound prediction code p0123 N82-23730
- Theoretical and experimental power from large horizontal-axis wind turbines [NASA-TM-82944] p0127 N82-33830
- VITTAL, B. V., M.**
Three dimensional flow measurements in a turbine scroll [NASA-CR-167920] p0009 N82-32310
- VOGAW, J. W.**
Advanced ceramic coating development for industrial/utility gas turbines [NASA-CR-169852] p0065 N82-33494
- VOLKONIRSKAYA, L. B.**
An attempt at magnetic-variation sounding in the Antarctic A82-25290
- VORRES, C. L.**
Acoustic microscopy of silicon carbide materials p0075 A82-33031
- W**
- WADE, R. F.**
Wideband, high speed switch matrix development for SS-TDMA applications p0086 A82-43784
- WAITE, W. A.**
Anion permselective membrane [NASA-CR-167872] p0137 N82-30711
- WAKABAYASHI, I.**
Low-thrust chemical propulsion system propellant expulsion and thermal conditioning study. Executive summary [NASA-CR-165622] p0045 N82-24287
Low-thrust chemical propulsion system propellant expulsion and thermal conditioning study [NASA-CR-167841] p0045 N82-24288
- WAKEFIELD, E. A.**
An assessment of alternative fuel cell designs for residential and commercial cogeneration p0138 A82-24695
- WALITT, L.**
Development of a locally mass flux conservative computer code for calculating 3-D viscous flow in turbomachines [NASA-CR-3539] p0007 N82-22214
- WALKER, B.**
Analytical and experimental investigation of the propagation and attenuation of sound in extended reaction lined ducts [AIAA PAPER 81-2014] p0153 A82-10454
- WALKER, B. E.**
The velocity field near the orifice of a Helmholtz resonator in grazing flow

- [NASA-CF-168548] p0153 N82-18994
WALKER, E. D.
 Propeller flow visualization techniques p0096 N82-32672
- WALKER, W. P.**
 Research and development program for non-linear structural modeling with advanced time-temperature dependent constitutive relationships [NASA-CR-165533] p0024 N82-16080
- WALKER, W. D.**
 Design study of a continuously variable roller cone traction CVT for electric vehicles [NASA-CR-159841] p0105 N82-12445
- WALSH, F.**
 Cathode catalyst for primary phosphoric fuel cells [NASA-CR-165198] p0134 N82-22675
- WALSH, K.**
 In-flight acoustic results from an advanced-dop 7u propeller at Mach numbers to C.8 [AIAA PAPER 82-1127] p0021 A82-35017
- WALTER, R. J.**
 Test results and facility description for a 40-kilowatt stirling engine [NASA-TM-82620] p0163 N82-13013
- WANG, S. S.**
 Boundary-layer effects in composite laminates: Free-edge stress singularities, part 6 [NASA-CR-165440] p0114 N82-26718
- WANG, A. J.**
 Vibrations of cantilevered shallow cylindrical shells of rectangular planform p0115 A82-11298
 Vibrations of twisted rotating blades [ASME PAPER 81-DET-127] p0115 A82-19341
- WANG, G.**
 Optically pumped high-pressure CF-CO2 transfer laser A82-10193
- WANG, H. T.**
 Interlaminar crack growth in fiber reinforced composites during fatigue, part 3 [NASA-CR-165434] p0114 N82-26715
- WANG, S. S.**
 Interface cracks in adhesively bounded lap-shear joints p0116 A82-46109
 Boundary-layer effects in composite laminates. I - Free-edge stress singularities. II - Free-edge stress solutions and basic characteristics p0116 A82-46806
 Boundary layer thermal stresses in angle-ply composite laminates, part 1 [NASA-CR-165412] p0113 N82-26713
 Analysis of cracks emanating from a circular hole in unidirectional fiber reinforced composites, part 2 [NASA-CF-165433] p0114 N82-26714
 Interlaminar crack growth in fiber reinforced composites during fatigue, part 3 [NASA-CF-165434] p0114 N82-26715
 Analysis of interface cracks in adhesively bonded lap shear joints, part 4 [NASA-CF-165432] p0114 N82-26716
 Edge delamination in angle-ply composite laminates, part 5 [NASA-CR-165439] p0114 N82-26717
- WANG, S. Y.**
 End region and current consolidation effects upon the performance of an MHD channel for the ETF conceptual design [AIAA PAPER 82-0325] p0157 A82-17809
 End region and current consolidation effects upon the performance of an MHD channel for the ETF conceptual design [NASA-TM-82744] p0157 N82-12943
 Effect of vacuum exhaust pressure on the performance of MHD ducts at high D-field [NASA-TM-82750] p0157 N82-13908
- WANG, S.-Y.**
 Effect of vacuum exhaust pressure on the performance of MHD ducts at high E-field [AIAA PAPER 82-0396] p0157 A82-20292
- WARD, J. W.**
 30-cm mercury ion thruster technology p0046 A82-15434
- WARNOCK, W.**
 Advanced turboprop testbed systems study. Volume 1: Testbed program objectives and priorities, drive system and aircraft design studies, evaluation and recommendations and wind tunnel test plans [NASA-CR-167928-VOL-1] p0028 N82-32370
- WATSON, G. K.**
 Ultrasonic velocity for estimating density of structural ceramics [NASA-TM-82765] p0066 N82-14359
- WATSON, T. L.**
 Tests of a D vented thrust deflecting nozzle behind a simulated turbofan engine [NASA-CR-3508] p0006 N82-17122
- WAWRO, S. W.**
 NC carbide structures in M(1c2)ar-M247 [NASA-CR-167892] p0064 N82-30374
- WEBER, R. E.**
 Development of battery separator composites [NASA-CR-165508] p0128 N82-11547
- WEBER, R. J.**
 NASA research activities in aeropropulsion [NASA-TM-82788] p0017 N82-16084
- WEDEVEN, L. D.**
 Effects of artificially produced defects on film thickness distribution in sliding EHD point contacts [NASA-TM-82732] p0099 N82-16412
 The influence of surface dents and grooves on traction in sliding EHD point contacts [NASA-TM-82943] p0102 N82-32734
- WEEKS, W. F.**
 Ground-truth observations of ice-covered North Slope Lakes imaged by radar [NASA-TM-84127] p0117 N82-18664
- WEIGAND, A. J.**
 Texturing polymer surfaces by transfer casting [NASA-CASE-LEW-13120-1] p0068 N82-28440
- WEINER, D.**
 Pockels-effect cell for gas-flow simulation [NASA-TP-2007] p0095 N82-23515
- WEINBERG, I.**
 Gallium arsenide solar cells-status and prospects for use in space p0043 A82-11765
 A theory of the n-i-p silicon solar cell p0128 A82-45055
 Effects of processing and dopant on radiation damage removal in silicon solar cells [NASA-TM-82892] p0042 N82-31443
- WEINBERGER, S. M.**
 Preliminary design development of 100 KW rotary power transfer device [NASA-CR-165431] p0084 N82-23395
- WEINERT, M.**
 Cessation of W/001/ - Work function lowering by multiple dipole formation A82-30002
- WEINGART, G.**
 Winding for the wind p0138 A82-37078
 Design, evaluation, and fabrication of low-cost composite blades for intermediate-size wind turbines [NASA-CR-165342] p0133 N82-18693
- WEINSTEIN, M.**
 Numerical analysis of confined turbulent flow p0093 A82-24748
- WEISER, V. G.**
 On the cause of the flat-spot phenomenon observed in silicon solar cells at low temperatures and low intensities p0043 A82-39599
 Advances in high output voltage silicon solar cells p0127 A82-44942
 On the cause of the flat spot phenomenon observed in silicon solar cells at low temperatures and low intensities p0044 A82-44965
 On the cause of the flat-spot phenomenon observed in silicon solar cells at low temperatures and low intensities [NASA-TM-82903] p0126 N82-31777
- WELTI, G. K.**
 Microwave intersatellite links for communications satellites p0036 A82-36925
- WRENELL, J. H.**
 Review of analysis methods for rotating systems with periodic coefficients p0135 N82-23702

- WENZEL, L. H.
Analytical investigation of nonrecoverable stall
[NASA-TM-82792] p0018 N82-21195
- WERLE, H. J.
Turbofan forced mixer-nozzle internal flow field.
Volume 2: Computational fluid dynamic predictions
[NASA-CF-3493] p0091 N82-22459
- WHEELER, D. R.
Refractory coatings and method of producing the same
[NASA-CASE-LEW-13169-1] p0060 N82-29415
Refractory coatings
[NASA-CASE-LEW-13169-2] p0061 N82-30371
- WHIPPLE, D. L.
Development of a laser velocimeter for a large
transonic wind tunnel p0096 N82-32688
- WHIPPLE, E. C.
Potentials of surfaces in space p0165 A82-23750
- WHITE, D. J.
Low NOx heavy fuel combustor concept program
[NASA-CR-167876] p0074 N82-26482
Low NOx heavy fuel combustor concept program
[NASA-CR-165481] p0138 N82-33827
- WHITE, J. W.
Application of steady state finite element and
transient finite difference theory to sound
propagation in a variable area duct: A
comparison with experiment
[NASA-TM-82678] p0151 N82-15847
- WHITELLY, S. R.
Impedance conversion using quantum limit
nonreciprocity for
superconductor-insulator-superconductor mixer
compensation p0159 A82-31276
Stationary state model for normal metal tunnel
junction phenomena p0159 A82-42912
- WHITLOW, J. B., JR.
NASA research in supersonic propulsion: A decade
of progress
[NASA-TM-82862] p0019 N82-26300
- WHITTENBERGER, J. D.
Comparative thermal fatigue resistance of several
oxide dispersion strengthened alloys p0062 A82-11399
Effects of nadic ester concentration and
processing on physical and mechanical properties
of BMR/Celion 6000 composites p0051 A82-27440
Long-term high-velocity oxidation and hot
corrosion testing of several NiCrAl and FeCrAl
base oxide dispersion strengthened alloys p0062 A82-37151
On determination of fibre fraction in continuous
fibre composite materials p0051 A82-38133
Crystallographic texture in
oxide-dispersion-strengthened alloys p0062 A82-40041
Application of a gripping system to test a
uniaxial graphite fiber reinforced composite
/BMR 15/Celion 6000/ in tension at 316 C p0051 A82-40796
Structure and creep rupture properties of
directionally solidified eutectic
 γ/γ -prime- α alloy p0062 A82-42774
- WIGGINS, J. V.
Primary propulsion/large space system interaction
study
[NASA-CF-165277] p0044 N82-18315
- WILBERS, L.
Cost/benefit studies of advanced materials
technologies for future aircraft turbine
engines: Materials for advanced turbine engines
[NASA-CF-167849] p0026 N82-25254
- WILCOCK, D. F.
Preliminary study of temperature measurement
techniques for Stirling engine reciprocating seals
[NASA-CF-165479] p0164 N82-11466
- WILHELMSSON, H.
On a free-electron-laser in a uniform magnetic
field - A solution for arbitrarily strong
electromagnetic radiation fields A82-28409
- WILKINS, W. J.
Pyrolytic graphite collector development program
- [NASA-CR-167909] p0052 N82-29363
- WILLEN, H. S.
Kevlar/PNR-15 polyimide matrix composite for a
complex shaped DC-9 drag reduction fairing
[AIAA PAPER 82-1047] p0002 A82-37678
- WILLIAMS, F. J.
Performance of PTFE-lined composite journal bearings
[ASLE PREPRINT 82-AM-1A-1] p0104 A82-37854
Performance of PTFE-lined composite journal bearings
[NASA-TM-82779] p0048 N82-17263
- WILLIAMS, J. H., JR.
Ultrasonic input-output for transmitting and
receiving longitudinal transducers coupled to
same face of isotropic elastic plate
[NASA-CR-3506] p0110 N82-18613
- WILLIAMS, J. E.
Combustor development for automotive gas turbines
[AIAA PAPER 82-1208] p0104 A82-35062
- WILLIAMS, M. H.
Diffraction by a finite strip p0150 A82-33605
Solution of the unsteady subsonic thin airfoil
problem p0012 A82-41267
- WILLIAMS, P. F.
Environmental effects on solar concentrator mirrors
A82-23394
- WILLIAMS, R. C.
Low speed testing of the inlets designed for a
tandem-fan V/STOL nacelle
[NASA-TM-82728] p0003 N82-11042
- WILLIAMS, R. T.
Effects of condensation and surface motion on the
structure of steady-state fronts A82-19360
- WILLIS, E. A.
Development potential of Intermittent Combustion
(I.C.) aircraft engines for commuter transport
applications
[NASA-TM-82869] p0019 N82-26297
- WILSON, C. A.
YF 102 in-duct combustor noise measurements with a
turbine nozzle, volume 1 p0153 N82-21031
[NASA-CR-165562-VOL-1]
YF 102 in-duct combustor noise measurements with a
turbine nozzle, volume 2 p0153 N82-21032
[NASA-CR-165562-VOL-2]
YF 102 in-duct combustor noise measurements with a
turbine nozzle, volume 3 p0155 N82-21033
[NASA-CR-165562-VOL-3]
- WILSON, J. M.
Advanced turboprop testbed systems study. Volume
1: Testbed program objectives and priorities,
drive system and aircraft design studies,
evaluation and recommendations and wind tunnel
test plans
[NASA-CR-167928-VOL-1] p0028 N82-32370
- WILSON, P. M.
High-frequency high-voltage high-power DC-to-DC
converters p0083 N82-12347
Analysis of transistor and snubber turn-off
dynamics in high-frequency high-voltage
high-power converters p0084 N82-22438
[NASA-CR-168760]
- WILSON, R. M.
Fatigue tests with a corrosive environment N82-13282
- WILSON, T. G.
High-frequency high-voltage high-power DC-to-DC
converters p0083 N82-12347
Analysis of transistor and snubber turn-off
dynamics in high-frequency high-voltage
high-power converters p0084 N82-22438
[NASA-CR-168760]
- WINNER, E.
Cessation of W/001/ - Work function lowering by
multiple dipole formation A82-30002
- WINNER, J. M.
Analytical and experimental evaluation of biaxial
contact stress p0071 A82-20741
- WINCHESTER, D. C.
Buoyancy effects on the temperature field in
downward spreading flames p0094 A82-41203

- WIMMILLER, J. R.**
Effect of rotor configuration on gayed tower and foundation designs and estimated costs for intermediate site horizontal axis wind turbines
[NASA-TM-82804] p0121 N82-22649
- WIMB, W. O.**
Regimes of traction in concentrated contact lubrication
[ASME PAPER 81-LUB-16] p0107 A82-18431
Some observations in high pressure rheology of lubricants
[ASME PAPER 81-LUB-17] p0070 A82-18432
Some observations in high pressure rheology of lubricants
[ASME PAPER 81-LUB-17] p0070 A82-18432
Preliminary study of temperature measurement techniques for Stirling engine reciprocating seals
[NASA-CR-165479] p0104 N82-11466
- WINDA, E. A.**
Tungsten fiber reinforced superalloy composite high temperature component design considerations
[NASA-TM-82811] p0049 N82-21259
- WINTER, J. M.**
Experimental performance of the regenerator for the Chrysler upgraded automotive gas turbine engine
[NASA-TM-82671] p0120 N82-21712
Comparative analysis of the conceptual design studies of potential early commercial MHD power plants (CSPEC)
[NASA-TM-82897] p0123 N82-27838
- WINTUCKY, E. G.**
Ion beam textured graphite electrode plates
[NASA-CASE-LEW-12919-2] p0050 N82-26386
- WIRSCHING, P. H.**
The application of probabilistic design theory to high temperature low cycle fatigue
[NASA-CR-165408] p0112 N82-14531
- WIRTH, G.**
Structure and creep rupture properties of directionally solidified eutectic gamma/gamma-prime-alpha alloy
p0062 A82-42774
- WISANDER, D. W.**
Fully plasma-sprayed compliant backed ceramic turbine seal
[NASA-CASE-LEW-13268-2] p0101 N82-26674
Fully plasma-sprayed compliant backed ceramic turbine seal
[NASA-CASE-LEW-13268-1] p0069 N82-29453
- WISEMAN, G.**
Numerical simulation of plasma insulator interactions in space. Part 1: The self consistent calculation
p0039 N82-14272
Numerical simulation of plasma insulator interactions in space. Part 2: Dielectric effects
p0039 N82-14273
- WISLER, D. C.**
Core compressor exit stage study. Volume 4: Data and performance report for the best stage configuration
[NASA-CR-165357] p0023 N82-14092
Core compressor exit stage study. Volume 5: Design and performance report for the Rotor C/Stator B configuration
[NASA-CF-165358] p0023 N82-14093
Core compressor exit stage study, volume 6
[NASA-CR-165553] p0027 N82-27310
- WISNIEWSKI, J. H.**
Dynamic switch matrix for the TEMSA satellite switching system
[AIAA 82-0458] p0085 A82-23494
- WOLF, H.**
Overview study of Space Power Technologies for the advanced energetics program
[NASA-CR-165269] p0132 N82-17606
- WONG, E. L.**
Effect of hydrocarbon fuel type on fuel
[NASA-TM-82916] p0072 N82-38460
- WONG, E. Y.**
Cold-air performance of a 15.41-cm-tip-diameter axial-flow power turbine with variable-area stator designed for a 75-kW automotive gas turbine engine
[NASA-TM-82644] p0024 N82-21193
- WOOD, B.**
Three dimensional flow measurements in a turbine scroll
[NASA-CR-167920] p0009 N82-32310
- WOODCOCK, G.**
Overview study of Space Power Technologies for the advanced energetics program
[NASA-CR-165269] p0132 N82-17606
- WOODS, R. E.**
40-kW phosphoric acid fuel cell field test - Project plan
p0128 A82-45325
- WOODWARD, R. P.**
Forward acoustic performance of a model turbofan designed for a high specific flow (QF-14)
[NASA-TP-1968] p0152 N82-21036
- WOOLETT, R. E.**
Thrust modulation methods for a subsonic V/STOL aircraft
[NASA-TM-82747] p0003 N82-13112
- WORSTELL, J. M.**
Quantitative separation of tetralin hydroperoxide from its decomposition products by high performance liquid chromatography
p0048 A82-15696
Deposit formation in liquid fuels. II - The effect of selected compounds on the storage stability of Jet A turbine fuel
p0074 A82-22240
Deposit formation in liquid fuels. I - Effect of coal-derived Lewis bases on storage stability of Jet A turbine fuel
p0074 A82-22241
Deposit formation in liquid fuels. III - The effect of selected nitrogen compounds on diesel fuel
p0074 A82-23238
- WU, C. H.**
Modeling and Analysis of Power Processing Systems (MAPPS). Volume 1: Technical report
[NASA-CR-165538] p0083 N82-14447
Modeling and Analysis of Power Processing Systems (MAPPS). Volume 2: Appendices
[NASA-CR-165539] p0145 N82-16748
- WU, C. J.**
A new approach to the minimum weight/loss design of switching power converters
p0082 A82-16831
- WU, J. C.**
Solutions of the compressible Navier-Stokes equations using the integral method
[AIAA PAPER 81-0046] p0093 A82-23832
A new numerical approach for compressible viscous flows
[NASA-CR-168842] p0090 N82-22455

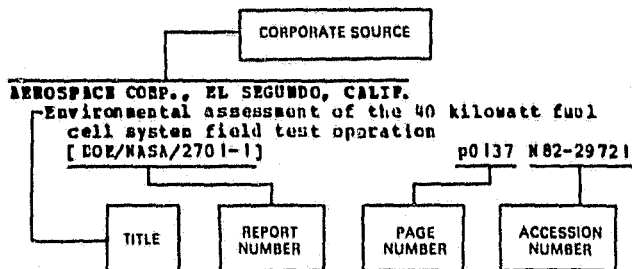
Y

- YAMAHOTO, T.**
Effect of tangential traction and roughness on crack initiation/propagation during rolling contact
p0103 A82-30022
Plastic deformation and wear process at a surface during unlubricated sliding
[NASA-TM-82820] p0102 N82-32735
Wear mechanism based on adhesion
[NASA-TP-2037] p0103 N82-32737
- YANG, S. H.**
Indentation law for composite laminates
[NASA-CR-165460] p0052 N82-15123
- YAU, J. F.**
Interface cracks in adhesively bonded lap-shear joints
p0116 A82-46109
Analysis of cracks emanating from a circular hole in unidirectional fiber reinforced composites, part 2
[NASA-CR-165433] p0114 N82-26714
Analysis of interface cracks in adhesively bonded lap shear joints, part 4
[NASA-CR-165438] p0114 N82-26716
- YBARRA, A. H.**
Low speed testing of the inlets designed for a tandem-fan V/STOL nacelle
[NASA-TM-82728] p0003 N82-11042
- YOUNG, S. G.**
Effect of aluminum phosphate additions on composition of three-component plasma-sprayed solid lubricant
[NASA-TP-1990] p0059 N82-21298

- Method of protecting a surface with a silicon-slurry/aluminide coating
[NASA-CASE-LEW-13343-1] p0068 N82-28441
- A study of the nature of solid particle impact and shape on the erosion morphology of ductile metals
[NASA-TM-82933] p0061 N82-33493
- YU, P. W.**
Undoped semi-insulating LEC GaAs - A model and a mechanism
p0159 A82-13758
- Compensation mechanism in liquid encapsulated Czochralski GaAs Importance of melt stoichiometry
p0086 A82-40403
- YU, Y.**
Power system design optimization using Lagrange multiplier techniques
p0085 A82-20743
- Analysis and design of a standardized control module for switching regulators
p0083 A82-46388
- Modeling and Analysis of Power Processing Systems (MAPPS). Volume 1: Technical report
[NASA-CR-165538] p0083 N82-14447
- Modeling and Analysis of Power Processing Systems (MAPPS). Volume 2: Appendices
[NASA-CR-165539] p0145 N82-16748
- YUHAS, D.**
Acoustic microscopy of silicon carbide materials
p0075 A82-33031
- YURKOVICH, S.**
A tensor approach to modeling of nonhomogeneous nonlinear systems
p0148 A82-19064
- Z**
- ZAPRAW, S.**
Integrated propulsion for near-Earth space missions. Volume 1: Executive summary
[NASA-CR-167889-VOL-1] p0045 N82-33424
- Integrated propulsion for near-Earth space missions. Volume 2: Technical
[NASA-CR-167889-VOL-2] p0046 N82-33425
- ZARLATYNSKY, I.**
Castable high temperature refractory materials
[NASA-CASE-LEW-13080-2] p0066 N82-11210
- Review of NASA progress in thermal barrier coatings for stationary gas turbines
[NASA-TM-81716] p0058 N82-17335
- Performance of laser glazed ZrO₂ TRCs in cyclic oxidation and corrosion burner test rigs
[NASA-TM-82830] p0059 N82-22346
- Method and apparatus for coating substrates using lasers
[NASA-CASE-LEW-13526-1] p0059 N82-22347
- ZARETSKY, E. V.**
Development of high-speed rolling-element bearings. A historical and technical perspective
[NASA-TM-82884] p0100 N82-24497
- Advances in high-speed rolling-element bearings
[NASA-TM-82910] p0101 N82-28644
- Precision of spiral-bevel gears
[NASA-TM-82888] p0102 N82-30552
- Kinematic precision of gear trains
[NASA-TM-82887] p0102 N82-32733
- Effect of shot peening on surface fatigue life of carburized and hardened AISI 9310 spur gears
[NASA-TP-2047] p0102 N82-32736
- ZEHID, I.**
Engine dynamic analysis with general nonlinear finite element codes. II - Bearing element implementation, overall numerical characteristics and benchmarking
[ASME PAPER 82-GT-292] p0108 A82-35462
- Engine dynamic analysis with general nonlinear finite element codes. Part 2: Bearing element implementation overall numerical characteristics and benchmarking
[NASA-CR-167944] p0028 N82-33390
- ZELLER, J.**
The role of modern control theory in the design of controls for aircraft turbine engines
[NASA-TM-82815] p0018 N82-22262
- ZICKWOLF, H. C., JR.**
Preliminary study, analysis and design for a power switch for digital engine actuators
[NASA-CR-159559] p0085 N82-23394
- ZIMMER, R. E.**
Conversion and matched filter approximations for serial minimum-shift keyed modulation
p0080 A82-26713
- Near optimum delay-line detection filters for serial detection of MSK signals
p0086 A82-43867
- ZINN, B. T.**
An iterative finite element-integral technique for predicting sound radiation from turbofan inlets in steady flight
[AIAA PAPER 82-0124] p0030 A82-17796
- Prediction of sound radiation from different practical jet engine inlets
[NASA-CR-165120] p0153 N82-16810
- Acoustic properties of turbofan inlets
[NASA-CR-169016] p0153 N82-27090
- Development of a spinning wave heat engine
[NASA-CR-165611] p0028 N82-31328
- ZIPP, B.**
Evaluation of the potential of the Stirling engine for heavy duty application
[NASA-CR-165473] p0128 N82-10505
- ZIMOCKEK, L. A.**
Advanced general aviation engine/airframe integration study
[NASA-CR-165565] p0025 N82-22268
- ZOLEZZI, B. A.**
Propulsion study for Small Transport Aircraft Technology (STAT)
[NASA-CR-165499] p0022 N82-10037

CORPORATE SOURCE INDEX

Typical Corporate Source Index Listing



The title of the document is used to provide a brief description of the subject matter. The page number and NASA or AIAA accession number are included in each entry to assist the user in locating the abstract in the abstract section. If applicable, a report number is also included as an aid in identifying the document.

A

- ACUREX CORP., MOUNTAIN VIEW, CALIF.**
High temperature durable catalyst development
p0056 N82-20739
Development of a high-temperature durable catalyst for use in catalytic combustors for advanced automotive gas turbine engines
[NASA-CR-165396] p0130 N82-13510
Computer model of catalytic combustion/Stirling engine heater head
[NASA-CR-165378] p0134 N82-22666
- AERONAUTICAL LIQUID ROCKET CO., SACRAMENTO, CALIF.**
Propulsion system options for low-acceleration orbit transfer
[AIAA PAPER 82-1196] p0047 N82-35056
Fuel/oxidizer-rich high-pressure preburners
[NASA-CR-165404] p0073 N82-10245
Low-thrust Isp sensitivity study
[NASA-CR-165621] p0045 N82-22309
Testing of fuel/oxidizer-rich, high-pressure preburners
[NASA-CR-165609] p0074 N82-24353
- AERONAUTICAL NUCLEAR SYSTEMS CO., SACRAMENTO, CALIF.**
Low-thrust chemical propulsion system pump technology
[NASA-CR-165219] p0105 N82-13427
- AEROSPACE CORP., EL SEGUNDO, CALIF.**
Environmental assessment of the 40 kilowatt fuel cell system field test operation
[DOE/NASA/2701-1] p0137 N82-29721
- AIR FORCE ACADEMY, COLO.**
Comparison of beam and shell theories for the vibrations of thin turbomachinery blades
[ASME PAPER 82-GT-223] p0115 N82-35408
- AIR FORCE GPHYSICS LAB., HANSCOM AFB, MASS.**
Validation of the NASCAP model using spaceflight data
[AIAA PAPER 82-0269] p0038 N82-17872
- AIRSEARCH CASTING CO., TORRANCE, CALIF.**
Oxidation stability of advanced reaction-bonded Si3N4 materials
[ACS PAPER 52-R-80P] p0074 N82-33030
- AIRSEARCH HFG. CO., PHOENIX, ARIZ.**
Pollution reduction technology program small jet aircraft engines, phase 3
[NASA-CR-165386] p0023 N82-14095
- ERBS fuel addendum: Pollution reduction technology program small jet aircraft engines, phase 3**
[NASA-CR-165387] p0024 N82-14096
- Advanced Gas Turbine (AGT) powertrain system initial development report**
[NASA-CR-165130] p0132 N82-16485
Advanced Gas Turbine (AGT) powertrain system development for automotive applications
[NASA-CR-165175] p0163 N82-16937
- AKRON UNIV., OHIO.**
Optimal tooth numbers for compact standard spur gear sets
[ASME PAPER 81-DET-115] p0103 N82-19335
Engine dynamic analysis with general nonlinear finite element codes. II - Bearing element implementation, overall numerical characteristics and benchmarking
[ASME PAPER 82-GT-292] p0108 N82-35462
On the solution of creep induced buckling in general structure
p0115 N82-39514
Self-adaptive closed constrained solution algorithms for nonlinear conduction
p0094 N82-45157
Engine dynamic analysis with general nonlinear finite element codes. Part 2: Bearing element implementation overall numerical characteristics and benchmarking
[NASA-CR-167944] p0028 N82-33390
- ALABAMA UNIV., HUNTSVILLE.**
Modification of spacecraft potentials by thermal electron emission on ATS-5
p0040 N82-16194
Field-aligned ion streams in the earth's midnight region
p0140 N82-31009
The hidden ion population of the magnetosphere
p0140 N82-32630
- ANDERSON (WILLIAM J.), NORTH OLMS TED, OHIO.**
Bearings: Technology and needs
[NASA-CR-167908] p0106 N82-26679
- APPLIED SOLAR ENERGY CORP., CITY OF INDUSTRY, CALIF.**
Thin foil silicon solar cells with coplanar back contacts
p0127 N82-44944
Development of thin wraparound junction silicon solar cells
[NASA-CR-165570] p0133 N82-18689
- ARINC RESEARCH CORP., ANNAPOLIS, MD.**
The 30/20 GHz communications satellite trunking network study
[NASA-CR-165467] p0078 N82-13302
- ARIZONA STATE UNIV., TEMPE.**
Flow distributions and discharge coefficient effects for jet array impingement with initial crossflow
[ASME PAPER 82-GT-156] p0011 N82-35379
Nonlinear analysis of rotor-bearing systems using component mode synthesis
[ASME PAPER 82-GT-303] p0104 N82-35468
Socioeconomic impact of photovoltaic power at Schuchuli, Arizona
[NASA-CR-165551] p0133 N82-19669
- ARIZONA UNIV., TUCSON.**
The application of probabilistic design theory to high temperature low cycle fatigue
[NASA-CR-165488] p0112 N82-14531
- ARMY AVIATION RESEARCH AND DEVELOPMENT COMMAND, CLEVELAND, OHIO.**
The effect of rotor blade thickness and surface finish on the performance of a small axial flow turbine
[NASA-TM-82726] p0003 N82-13114
Multiroller traction drive speed reducer: Evaluation for automotive gas turbine engine
[NASA-TP-2027] p0101 N82-26678
Tooth profile analysis of circular-cut, spiral-bevel gears
[NASA-TM-82840] p0101 N82-26681

- Reliability model for planetary gear
[NASA-TM-82859] p0101 N82-28643
A finite element stress analysis of spur gears
including fillet radii and rim thickness effects
[NASA-TM-82865] p0101 N82-28646
- ARMY AVIATION RESEARCH AND DEVELOPMENT COMMAND, ST.
LOUIS, MO.
Computer program for aerodynamic and blading
design of multistage axial-flow compressors
[NASA-TP-1946] p0016 N82-15039
Geometry and starvation effects in hydrodynamic
lubrication
[NASA-TM-82807] p0042 N82-20240
- ARMY COLD REGIONS RESEARCH AND ENGINEERING LAB.,
HANOVER, N. H.
Ground-truth observations of ice-covered North
Cape lakes imaged by radar
[NASA-TM-84127] p0117 N82-18664
- ARMY MATERIALS AND MECHANICS RESEARCH CENTER,
WATERTOWN, MASS.
On determination of fibre fraction in continuous
fibre composite materials p0051 A82-38133
- ARMY PROPULSION LAB., CLEVELAND, OHIO.
Surface geometry of circular cut spiral bevel
gears
[ASME PAPER 81-DET-114] p0108 A82-19334
Optimal tooth numbers for compact standard spur
gear sets
[ASME PAPER 81-DET-115] p0103 A82-19335
The effect of rotor blade thickness and surface
finish on the performance of a small axial
flow turbine
[ASME PAPER 82-GT-222] p0022 A82-35409
Nonlinear analysis of rotor-bearing systems
using component mode synthesis
[ASME PAPER 82-GT-303] p0104 A82-35468
- ASSOCIATES IN RURAL DEVELOPMENT, INC., BURLINGTON,
VT.
Market assessment of photovoltaic power systems
for agricultural applications in Colombia
[NASA-CR-165524] p0134 N82-22770
Application of photovoltaic electric power to
the rural education/communication needs of
developing countries
[NASA-CR-167894] p0137 N82-29720
- AUSTRALIAN NATIONAL UNIV., CANBERRA.
Feasibility of an earth-to-space rail launcher
system
[IAF PAPER P2-46] p0033 A82-44659
- AVCO-EVERETT RESEARCH LAB., MASS.
MHD channel performance for potential early
commercial MHD power plants p0158 A82-20750
- AVCO LYCING DIV., STRATFORD, CONN.
Development of improved high temperature
coatings for IN-792 + HP
[NASA-CR-165395] p0063 N82-14333
YP 102 in-duct combustor noise measurements with
a turbine nozzle, volume 1
[NASA-CR-165562-VOL-1] p0153 N82-21031
YP 102 in-duct combustor noise measurements with
a turbine nozzle, volume 2
[NASA-CR-165562-VOL-2] p0153 N82-21032
YP 102 in-duct combustor noise measurements with
a turbine nozzle, volume 3
[NASA-CR-165562-VOL-3] p0155 N82-21033
Small axial turbine stator technology program
[NASA-CR-165602] p0028 N82-32367
- B**
- BARCOCK AND WILCOX CO., BARBERTON, OHIO.
Comparative analysis of CCMHD power plants
p0158 A82-20747
- BALES-MCCOIN TRACTIONATIC, INC., EL PASO, TEX.
Design study of a continuously variable roller
cone traction CVT for electric vehicles
[NASA-CR-159841] p0105 N82-12445
- BATTELLE COLUMBUS LABS., OHIO.
Feasibility of an earth-to-space rail launcher
system
[IAF PAPER 82-46] p0033 A82-44659
Stress evaluations under rolling/sliding contacts
[NASA-CR-165561] p0113 N82-17521
Preliminary feasibility assessment for
Earth-to-space electromagnetic (Railgun)
launchers
[NASA-CR-167886] p0033 N82-29345
- BCHTEL NATIONAL, INC., SAN FRANCISCO, CALIF.
Comparative analysis of CCMHD power plants
p0158 A82-20747
- BEECH AIRCRAFT CORP., WICHITA, KANS.
Advanced general aviation engine/airframe
integration study
[NASA-CR-165565] p0025 N82-22268
- BEERS ASSOCIATES, INC., RESTON, VA.
Internal breakdown of charged spacecraft
dielectrics p0041 A82-18312
- BOEING AEROSPACE CO., SEATTLE, WASH.
Study of electrical and chemical propulsion
systems for auxiliary propulsion of large
space systems. Volume 1: Executive summary
[NASA-CR-165502-VOL-1] p0046 N82-11110
Study of electrical and chemical propulsion
systems for auxiliary propulsion of large
space systems, Volume 2
[NASA-CR-165502-VOL-2] p0044 N82-11111
- BOEING CO., SEATTLE, WASH.
The supply of lunar oxygen to low earth orbit
p0032 A82-35618
Testing of solar cell covers and encapsulants
conducted in a simulated space environment
[NASA-CR-165475] p0129 N82-12571
- BOEING COMMERCIAL AIRPLANE CO., SEATTLE, WASH.
Aerodynamic analysis of VTOL inlets and
definition of a short, blowing-lip inlet
[NASA-CR-165617] p0007 N82-22211
B747/JT9D flight loads and their effect on
engine running clearances and performance
deterioration; BCAC NAIL/P and WA JT9D engine
diagnostics programs
[NASA-CR-165573] p0027 N82-28296
- BOEING COMPUTER SERVICES CO., TUKWILA, WASH.
Hybrid and electric advanced vehicle systems
(heavy) simulation
[NASA-CR-165536] p0163 N82-16938
- BOEING MILITARY AIRPLANE DEVELOPMENT, SEATTLE, WASH.
Environmental effects on defect growth in
composite materials
[NASA-CR-165213] p0052 N82-20248
- BOEING VERTOL CO., PHILADELPHIA, PA.
Performance degradation of propeller/rotor
systems due to rime ice accretion
[AIAA PAPER 82-0286] p0014 A82-28322
On the automatic generation of FEM models for
complex gears - A work-in-progress report
p0109 A82-48243
- BURNS AND ROE, INC., WOODBURY, N. Y.
MHD oxidant intermediate temperature ceramic
heater study
[NASA-CR-165453] p0131 N82-15527
- C**
- CAIRO UNIV. (EGYPT).
Effects of internal heat transfer on the
structure of self-similar blast waves
p0093 A82-32225
- CALIFORNIA STATE UNIV., LOS ANGELES.
Electrostatic fuel conditioning of internal
combustion engines
[NASA-CR-169029] p0106 N82-26680
- CALIFORNIA UNIV., BERKELEY.
Secondary effects in combustion instabilities
leading to flashback
[AIAA PAPER 82-0037] p0056 A82-17746
Numerical modeling of turbulent combustion in
premixed gases p0056 A82-28708
- Impedance conversion using quantum limit
nonreciprocity for
superconductor-insulator-superconductor mixer
compensation p0159 A82-31276
- Effects of internal heat transfer on the
structure of self-similar blast waves
p0093 A82-32225
- On stability of premixed flames in stagnation -
Point flow p0057 A82-37574
- Stationary state model for normal metal tunnel
junction phenomena p0159 A82-42912
- Current legal and institutional issues in the
commercialization of phosphoric acid fuel cells
[NASA-CR-167867] p0136 N82-29719

- CALIFORNIA UNIV., BERKELEY. LAWRENCE BERKELEY LAB.
Numerical modeling of turbulent flow in a
combustion tunnel p0093 A82-27000
- CALIFORNIA UNIV., LA JOLLA.
Potentials of surfaces in space p0165 A82-23750
Shuttle to GEO propulsion tradeoffs
[AIAA PAPER 82-1245] p0034 A82-35082
- CALIFORNIA UNIV., LOS ANGELES.
Analytical and experimental investigation of the
propagation and attenuation of sound in
extended reaction lined ducts
[AIAA PAPER 81-2014] p0153 A82-10454
The velocity field near the orifice of a
Helmholtz resonator in grazing flow
[NASA-CR-168548] p0153 A82-18994
- CANTERBURY UNIV., CHRISTCHURCH (NEW ZEALAND).
Acoustic transmission in lined flow ducts - A
finite element eigenvalue problem p0154 A82-17663
- CARBORUNDUM CO., NIAGARA FALLS, N. Y.
Net shape fabrication of Alpha Silicon Carbide
turbine components
[ASME PAPER 82-GT-216] p0071 A82-35403
- CARNegie INSTITUTION OF WASHINGTON, D. C.
Evidence for Pu-244 fission tracks in hibonites
from Murchison carbonaceous chondrite
p0166 A82-29316
- CARRIER CORP., SYRACUSE, N.Y.
Measurement of oil film thickness for
application to elastomeric Stirling engine rod
seals
[ASME PAPER 81-LUB-9] p0107 A82-18426
- CASE WESTERN RESERVE UNIV., CLEVELAND, OHIO.
Multijunction high voltage concentrator solar
cells p0043 A82-11796
Dilution jet behavior in the turn section of a
reverse flow combustor
[AIAA PAPER 82-0192] p0021 A82-20291
Natural convection with combined driving forces
p0093 A82-31445
Electron beam induced damage in ITO coated Kapton
p0159 A82-41546
Fabrication of multijunction high voltage
concentrator solar cells by integrated circuit
technology p0127 A82-44957
The influence of cobalt on the tensile and
stress-rupture properties of the nickel-base
superalloy MAR-M247 p0063 A82-47399
The influence of cobalt on the microstructure of
the nickel-base superalloy MAR-M247 p0063 A82-47400
Transient catalytic combustor model
[NASA-CR-165324] p0129 A82-13507
Secondary electron emission yields p0038 A82-14226
Investigation and evaluation of a computer
program to minimize three-dimensional flight
time tracks
[NASA-CR-168419] p0145 A82-17879
Shaded computer graphic techniques for
visualizing and interpreting analytic fluid
flow models
[NASA-CR-168418] p0145 A82-17880
Fatigue life prediction in bending from axial
fatigue information
[NASA-CR-165563] p0113 A82-20564
Coaxial prime focus feeds for paraboloidal
reflectors
[NASA-CR-167934] p0078 A82-31585
- CELANESE RESEARCH CO., SUMMIT, N.J.
Creep and rupture of an ODS alloy with high
stress rupture ductility p0065 A82-40335
- CESSNA AIRCRAFT CO., VANDALIA, OHIO.
Impact of advanced propeller technology on
aircraft/mission characteristics of several
general aviation aircraft
[NASA-CR-167984] p0009 A82-33347
- CESSNA AIRCRAFT CO., WICHITA, KANS.
Advanced general aviation comparative
engine/airframe integration study
[NASA-CR-165564] p0025 A82-22263
- CHRYSLER CORP., DETROIT, MICH.
AGT-102 automotive gas turbine
- [NASA-CR-165353] p0105 A82-12444
CINCINNATI UNIV., OHIO.
Surface geometry of circular cut spiral bevel
gears
[ASME PAPER 81-DET-114] p0108 A82-19334
Numerical analysis of confined turbulent flow
p0093 A82-24748
Multigrid simulation of asymptotic curved-duct
flows using a semi-implicit numerical technique
p0010 A82-29003
A study of viscous flow in stator and rotor
passages
[ASME PAPER 82-GT-248] p0011 A82-35427
High temperature low cycle fatigue mechanisms
for nickel base and a copper base alloy
[NASA-CR-3543] p0064 A82-26436
Microstructural effects on the room and elevated
temperature low cycle fatigue behavior of
Waspaloy
[NASA-CR-165497] p0113 A82-26702
Mechanisms of deformation and fracture in high
temperature low cycle fatigue of Rene 80 and
IN 100
[NASA-CR-165498] p0113 A82-26706
On finite element stress analysis of spur gears
[NASA-CR-167938] p0107 A82-29607
Three dimensional flow measurements in a turbine
scroll
[NASA-CR-167920] p0009 A82-32310
CITY COLL. OF THE CITY UNIV. OF NEW YORK.
Numerical analysis of confined turbulent flow
p0093 A82-24748
CITY COLL. RESEARCH FOUNDATION, NEW YORK.
Experimental study of turbulence in blade end
wall corner region
[NASA-CR-169283] p0091 A82-31639
CLEVELAND STATE UNIV., OHIO.
Characteristic dynamic energy equations for
Stirling cycle analysis p0138 A82-11816
A theory of the n-i-p silicon solar cell
p0128 A82-45055
A multi-purpose method for analysis of spur gear
tooth loading
[NASA-CR-165163] p0104 A82-10401
CLIMAX MOLYBDENUM CO. OF MICHIGAN, ANN ARBOR.
Fatigue of Ni-Al-Mo aligned eutectics at
elevated temperatures p0052 A82-13403
COLORADO SCHOOL OF MINES, GOLDEN.
Quantitative separation of tetralin
hydroperoxide from its decomposition products
by high performance liquid chromatography
p0048 A82-15696
Deposit formation in liquid fuels. II - The
effect of selected compounds on the storage
stability of Jet A turbine fuel p0074 A82-22240
Deposit formation in liquid fuels. I - Effect of
coal-derived Lewis bases on storage stability
of Jet A turbine fuel p0074 A82-22241
Deposit formation in liquid fuels. III - The
effect of selected nitrogen compounds on
diesel fuel p0074 A82-23238
COLORADO STATE UNIV., FORT COLLINS.
Surface diffusion activation energy
determination using ion beam microtexturing
p0159 A82-21965
Quasi-liquid states observed on ion beam
microtextured surfaces p0159 A82-30335
Ion-beam-induced topography and surface diffusion
p0160 A82-46426
Experimental simulation of biased solar arrays
with the space plasma
[NASA-CR-165485] p0157 A82-10880
Electric thruster research
[NASA-CR-165603] p0045 A82-24285
Electric and magnetic fields
[NASA-CR-165604] p0045 A82-28350
Ion beam microtexturing and enhanced surface
diffusion
[NASA-CR-167948] p0065 A82-31509
COLUMBIA UNIV., NEW YORK.
Creep and rupture of an ODS alloy with high
stress rupture ductility p0065 A82-40335

- COMMUNICATIONS SATELLITE CORP., CLARKSBURG, MD.
High- and low-resistivity silicon solar cells
p0046 A82-11762
- Microwave intersatellite links for communications satellites
p0036 A82-36925
- Advances in high output voltage silicon solar cells
p0127 A82-44942
- COMPOSITES HORIZONS, POMONA, CALIF.
Hybridized polymer matrix composite
[NASA-CR-165340] p0051 N82-12139
- CONCORDIA UNIV., MONTREAL (QUEBEC).
Bluff-body flameholder wakes - A simple numerical solution
[AIAA PAPER 82-1177] p0093 A82-35043
- CONNECTICUT UNIV., STORRS.
Turbine endwall single cylinder program
[NASA-CR-169278] p0091 N82-31638
- CORNELL UNIV., ITHACA, N. Y.
Time resolved density measurements in premixed turbulent flames
[AIAA PAPER 82-0036] p0056 A82-22033
- Flame structure in a swirl stabilized combustor inferred by radiant emission measurements
p0056 A82-28694
- Exhaust gas measurements in a propane fueled swirl stabilized combustor
[NASA-CR-169293] p0091 N82-31641
- Flow process in combustors
[NASA-CR-169294] p0092 N82-31642
- CURTIS-WRIGHT CORP., WOOD-RIDGE, N.J.
Advanced stratified charge rotary aircraft engine design study
[NASA-CR-165398] p0107 N82-27743
- D**
- DARTMOUTH COLL., HANOVER, N.H.
Single pass rub phenomena - Analysis and experiment
[ASME PAPER 81-LUB-55] p0107 A82-18449
- Recrystallization and grain growth in NiAl
p0065 A82-44529
- DAYTON UNIV., OHIO.
Permanent magnet properties of Mn-Al-C between -50 C and +150 C
p0085 A82-20505
- Mathematical modeling of ice accretion on airfoils
[AIAA PAPER 82-0284] p0014 A82-27098
- Effect of heavy rain on aircraft
N82-21149
- A preliminary study of crack initiation and growth at stress concentration sites
[NASA-CR-169358] p0115 N82-33738
- DEPARTMENT OF ENERGY, WASHINGTON, D. C.
Development of a dual-field heteropolar power converter
[NASA-CR-165168] p0084 N82-24424
- DEPARTMENT OF TRANSPORTATION, CAMBRIDGE, MASS.
Fuel economy and exhaust emissions characteristics of diesel vehicles: Test results of a prototype fiat 131TC 2.4 liter automobile
[NASA-CR-165535] p0164 N82-18068
- DETROIT DIESEL ALLISON, INDIANAPOLIS, IND.
Propulsion study for Small Transport Aircraft Technology (STAT)
[NASA-CR-165499] p0022 N82-10037
- Propulsion study for Small Transport Aircraft Technology (STAT), Appendix B
[NASA-CR-165499-APP-B] p0022 N82-10038
- Low NOx heavy fuel combustor concept program addendum: Low/mid heating value gaseous fuel evaluation
[NASA-CR-165615] p0055 N82-25338
- Low NOx heavy fuel combustor concept program
[NASA-CR-165367] p0136 N82-25635
- Ceramic applications in turbine engines
[NASA-CR-165197] p0164 N82-31158
- DEUTSCHE FORSCHUNGS- UND VERSUCHSANSTALT FUER LUFT- UND RAUMFAHRT, COLOGNE (WEST GERMANY).
Structure and creep rupture properties of directionally solidified eutectic gamma/gamma-prime-alpha alloy
p0062 A82-42774
- D** CORP. SOURCE FOR DV488724INACTIVE
Market assessment of photovoltaic power systems for agricultural applications in Mexico
[NASA-CR-165441] p0128 N82-10506
- Market assessment of photovoltaic power systems for agricultural applications in Morocco
[NASA-CR-165477] p0130 N82-14627
- Market assessment of photovoltaic power systems for agricultural applications in Nigeria
[NASA-CR-165511] p0133 N82-18698
- Market assessment of photovoltaic power systems for agricultural applications in Colombia
[NASA-CR-165524] p0134 N82-22770
- Application of photovoltaic electric power to the rural education/communication needs of developing countries
[NASA-CR-167894] p0137 N82-29720
- DOUGLAS AIRCRAFT CO., INC., LONG BEACH, CALIF.
Kevlar/PMR-15 polyimide matrix composite for a complex shaped DC-9 drag reduction fairing
[AIAA PAPER 82-1047] p0002 A82-37678
- Kevlar/PMR-15 reduced drag DC-9 reverser stang fairing
[NASA-CR-165440] p0052 N82-31448
- Advanced turboprop testbed systems study
[NASA-CR-167895] p0014 N82-33375
- DREXEL UNIV., PHILADELPHIA, PA.
Work of fracture in aluminum metal-matrix composites
p0053 A82-31339
- Formation of oxides of nitrogen in monodisperse spray combustion of hydrocarbon fuels
p0057 A82-37571
- Tensile properties of SiC/aluminum filamentary composites - Thermal degradation effects
p0053 A82-46220
- DUKE UNIV., DURHAM, N. C.
Numerical comparisons of nonlinear convergence accelerators
p0149 A82-31438
- High-frequency high-voltage high-power DC-to-DC converters
p0083 N82-12347
- Analysis of transistor and snubber turn-off dynamics in high-frequency high-voltage high-power converters
[NASA-CR-168760] p0084 N82-22438
- DYNAMICS TECHNOLOGY, INC., TORRANCE, CALIF.
Mean flowfields in axisymmetric combustor geometries with swirl
[AIAA PAPER 82-0177] p0092 A82-17824
- Turbulence measurements in a confined jet using a six-orientation hot-wire probe technique
[AIAA PAPER 82-1262] p0094 A82-37710
- E**
- EATON CORP., SOUTHFIELD, MICH.
Small passenger car transmission test: Chevrolet Malibu 200C transmission with lockup
[NASA-CR-165182] p0105 N82-16410
- EATON ENGINEERING AND RESEARCH CENTER, SOUTHFIELD, MICH.
A PWM transistor inverter for an ac electric vehicle drive
p0085 A82-20744
- The ac propulsion system for an electric vehicle, phase I
[NASA-CR-165480] p0129 N82-13506
- Straight and chopped DC performance data for a reluctance EV-250AT motor with a General Electric EV-1 controller
[NASA-CR-165447] p0132 N82-17608
- Straight and chopped DC performance data for a General Electric 5BY436A1 DC shunt motor with a General Electric EV-1 controller
[NASA-CR-165507] p0085 N82-24425
- Small passenger car transmission test: Mercury Lynx ATX transmission
[NASA-CR-165510] p0106 N82-24496
- ECO, INC., CAMBRIDGE, MASS.
Cathode catalysts for primary phosphoric acid fuel cells
[NASA-CR-165578] p0134 N82-21709
- Cathode catalyst for primary phosphoric fuel cells
[NASA-CR-165198] p0134 N82-22675
- ECOLE NATIONALE SUPERIEURE DE MECHANIQUE ET D'AEROTECHNIQUE, POITIERS (FRANCE).
On stability of premixed flames in stagnation - Point flow
p0057 A82-37574

- EDDY (HOWARD), INC., BELLEVUE, WASH.**
Collection and dissemination of thermal energy storage system information for the pulp and paper industry
p0136 A82-24686
- EIC, INC., NEWTON, MASS.**
Moderate temperature Na cells, III - Electrochemical and structural studies of CrO₂SV0.5S2 and its Na intercalates
p0055 A82-15732
Moderate temperature Na cells IV - VS2 and NbS₂Cl₂ as rechargeable cathodes in molten NaAlCl₄
p0055 A82-15743
- ENERGY RESEARCH CORP., DANBURY, CONN.**
Technology development for phosphoric acid fuel cell powerplant, phase 2
[NASA-CR-165426] p0131 A82-16482
- ENGLISHMAN INDUSTRIES, INC., EDISON, N.J.**
Develop and test fuel cell powered on-site integrated total energy system. Phase 3: Full-scale power plant development
[NASA-CR-165328] p0117 A82-13490
Develop and test fuel cell powered on-site integrated total energy systems. Phase 3: Full-scale power plant development
[NASA-CR-165455] p0131 A82-16483
Develop and test fuel cell powered on-site integrated total energy systems. Phase 3: Full-scale power plant development
[NASA-CR-165568] p0135 A82-24648
Development and test fuel cell powered on-site integrated total energy systems. Phase 3: Full-scale power plant development
[NASA-CR-167898] p0137 A82-30705
- ENGINEERING SOCIETIES COMMISSION ON ENERGY, INC., WASHINGTON, D. C.**
Barriers to the utilization of synthetic fuels for transportation
[NASA-CR-165517] p0073 A82-13243
- ENVIRONMENTAL RESEARCH AND TECHNOLOGY, INC., CONCORD, MASS.**
A review of transhorizon propagation phenomena
p0079 A82-10679
- F**
- FLOW RESEARCH, INC., KENT, WASH.**
Finite volume calculation of three-dimensional potential flow around a propeller
[AIAA PAPER 82-0957] p0010 A82-31933
- FLUIDYNE ENGINEERING CORP., MINNEAPOLIS, MINN.**
MHD oxidant intermediate temperature ceramic heater study
[NASA-CR-165453] p0131 A82-15527
- FORD AEROSPACE AND COMMUNICATIONS CORP., PALO ALTO, CALIF.**
30/20 GHz communications satellite multibeam antenna
[AIAA 82-0449] p0079 A82-23486
Dynamic switch matrix for the TDMA satellite switching system
[AIAA 82-0458] p0085 A82-23494
- FORD MOTOR CO., DEARBORN, MICH.**
Advanced Gas Turbine (AGT) powertrain system initial development report
[NASA-CR-165130] p0132 A82-16485
- FUTURE SYSTEMS, INC., GAITHERSBURG, MD.**
Cross-impact study of foreign satellite communications on NASA's 30/20 GHz program
[NASA-CR-165154] p0078 A82-17420
- FWG ASSOCIATES, INC., TULLAHOCA, TENN.**
Design of prototype charged particle fog dispersal unit
[NASA-CR-3481] p0141 A82-16659
- G**
- GARRETT TURBINE ENGINE CO., PHOENIX, ARIZ.**
Analytical and experimental evaluation of biaxial contact stress
p0071 A82-20741
Oxidation stability of advanced reaction-bonded Si₃N₄ materials
[ACS PAPER 52-B-80P] p0074 A82-33030
AGT101 automotive gas turbine system development
[AIAA PAPER 82-1166] p0108 A82-35039
The AGT 101 advanced automotive gas turbine
[ASME PAPER 82-GT-72] p0108 A82-35321
- Design and development of a ceramic radial turbine for the AGT101
[AIAA PAPER 82-1209] p0109 A82-35480
Applications of high-temperature powder metal aluminum alloys to small gas turbines
p0065 A82-48244
Cooled variable-area radial turbine technology program
[NASA-CR-165408] p0024 A82-19221
Study of advanced propulsion systems for Small Transport Aircraft Technology (STAT) program
[NASA-CR-165610] p0026 A82-24202
Computations of soot and and NO sub x emissions from gas turbine combustors
[NASA-CR-167930] p0139 A82-29777
- GAS RESEARCH INST., CHICAGO, ILL.**
40-kW phosphoric acid fuel cell field test - Project plan
p0128 A82-45325
- GENERAL APPLIED SCIENCE LABS., INC., WESTBURY, N. Y.**
Experimental study of the effects of secondary air on the emissions and stability of a lean premixed combustor
[AIAA PAPER 82-1072] p0021 A82-34992
- GENERAL DYNAMICS/CONVAIR, SAN DIEGO, CALIF.**
Design and verification of a multiple fault tolerant control system for STS applications using computer simulation
[AIAA 81-2173] p0035 A82-10124
Real-time computer simulation/emulation for verification of multi-fault-tolerant control of Centaur-in-Shuttle
[AIAA 81-2283] p0040 A82-13494
Centaur capabilities for communications satellite launches
[AIAA PAPER 82-0558] p0034 A82-36286
Real-time microcomputer simulation for space Shuttle/Centaur avionics
p0033 A82-48245
- Study of multi-megawatt technology needs for photovoltaic space power systems. Volume 1: Executive summary
[NASA-CR-165323-VOL-1] p0130 A82-14636
Study of multi-megawatt technology needs for photovoltaic space power systems, volume 2
[NASA-CR-165323-VOL-2] p0130 A82-14637
Low-thrust chemical propulsion system propellant expulsion and thermal conditioning study.
Executive summary
[NASA-CR-165622] p0045 A82-24287
Low-thrust chemical propulsion system propellant expulsion and thermal conditioning study
[NASA-CR-167841] p0045 A82-24288
- GENERAL ELECTRIC CO., CINCINNATI, OHIO.**
Effects of vane/blade ratio and spacing on fan noise
[AIAA PAPER 81-2033] p0029 A82-10457
Thermal expansion accommodation in a jet engine frame
p0029 A82-11999
V/STOL propulsion control technology
[AIAA PAPER 81-2634] p0029 A82-16909
Turbine blade nonlinear structural and life analysis
[AIAA PAPER 82-1056] p0021 A82-34981
Blade loss transient dynamic analysis of turbomachinery
[AIAA PAPER 82-1057] p0030 A82-34982
NASA/General Electric broad-specification fuels combustion technology program - Phase I results and status
[AIAA PAPER 82-1089] p0021 A82-35000
Progress in the development of energy efficient engine components
[ASME PAPER 82-GT-275] p0030 A82-35450
Optical tip clearance sensor for aircraft engine controls
[AIAA PAPER 82-1131] p0015 A82-37691
Core compressor exit stage study. Volume 4: Data and performance report for the best stage configuration
[NASA-CR-165357] p0023 A82-14092
Core compressor exit stage study. Volume 5: Design and performance report for the Rotor C/Stator B configuration
[NASA-CR-165358] p0023 A82-14093
Demonstration of catalytic combustion with residual fuel
[NASA-CR-165369] p0131 A82-16484

- CF6 jet engine performance improvement: High pressure turbine roundness
[NASA-CR-165555] p0024 N82-17174
- CF6 Jet Engine Diagnostics Program: High pressure compressor clearance investigation
[NASA-CR-165580] p0025 N82-21197
- Thrust reverser for a long duct fan engine
[NASA-CASE-LEW-13199-1] p0019 N82-26293
- Core compressor exit stage study, volume 6
[NASA-CR-165553] p0027 N82-27310
- CF6 jet engine performance improvement: High pressure turbine active clearance control
[NASA-CR-165556] p0027 N82-28297
- The CF6 jet engine performance improvement: Low pressure turbine active clearance control
[NASA-CR-165557] p0029 N82-33393
- GENERAL ELECTRIC CO., EVENDALE, OHIO.**
Three-dimensional flow field in the tip region of a compressor rotor passage. I - Mean velocity profiles and annulus wall boundary layer
[ASME PAPER 82-GT-111] p0011 N82-35286
- Three-dimensional flow field in the tip region of a compressor rotor passage. II - Turbulence properties
[ASME PAPER 82-GT-234] p0011 N82-35416
- Cost/benefit studies of advanced materials technologies for future aircraft turbine engines: Materials for advanced turbine engines
[NASA-CR-167849] p0026 N82-25254
- GENERAL ELECTRIC CO., FAIRFIELD, CONN.**
Wideband, high speed switch matrix development for SS-TDMA applications
p0086 N82-43784
- GENERAL ELECTRIC CO., LYNN, MASS.**
Effects of vane/blade ratio and spacing on fan noise
[AIAA PAPER 81-2033] p0029 N82-10457
- TF34 Convertible Engine System Technology Program
p0022 N82-40521
- Effect of a part span variable inlet guide vane on TF34 fan performance
[NASA-CR-165458] p0023 N82-12075
- GENERAL ELECTRIC CO., PHILADELPHIA, PA.**
Comparative analysis of CCMHD power plants
p0158 N82-20747
- Adaptive rain fade compensation
p0080 N82-27178
- Preliminary design development of 100 KW rotary power transfer device
[NASA-CR-165431] p0084 N82-23395
- GENERAL ELECTRIC CO., SCHENECTADY, N. Y.**
Optical tip clearance sensor for aircraft engine controls
[AIAA PAPER 82-1131] p0015 N82-37691
- Low NOx heavy fuel combustor concept program, phase I
[NASA-CR-165449] p0135 N82-24651
- GENERAL ELECTRIC CO., ST. PETERSBURG, FLA.**
Thermal-barrier-coated turbine blade study
[NASA-CR-165351] p0023 N82-10040
- GENERAL ELECTRIC CO., SYRACUSE, N. Y.**
Low NO sub x heavy fuel combustor concept program phase IA gas tests
[NASA-CR-167877] p0055 N82-25337
- GENERAL MOTORS CORP., INDIANAPOLIS, IND.**
Acoustic microscopy of silicon carbide materials
p0075 N82-33031
- Small gas turbine combustor primary zone development
[AIAA PAPER 82-1159] p0103 N82-35036
- AGT 100 automotive gas turbine system development
[AIAA PAPER 82-1165] p0108 N82-35036
- AGT 100 turbomachinery
[AIAA PAPER 82-1207] p0108 N82-35061
- Combustor development for automotive gas turbines
[AIAA PAPER 82-1208] p0104 N82-35062
- GEORGIA INST. OF TECH., ATLANTA.**
An iterative finite element-integral technique for predicting sound radiation from turbfan inlets in steady flight
[AIAA PAPER 82-0124] p0030 N82-17796
- Regimes of traction in concentrated contact lubrication
[ASME PAPER 81-LUB-16] p0107 N82-18431
- Some observations in high pressure rheology of lubricants
[ASME PAPER 81-LUB-17] p0070 N82-18432
- Some observations in high pressure rheology of lubricants
[ASME PAPER 81-LUB-17] p0070 N82-18432
- Solutions of the compressible Navier-Stokes equations using the integral method
[AIAA PAPER 81-0046] p0093 N82-23832
- Path-independent integrals in finite elasticity and inelasticity, with body forces, inertia, and arbitrary crack-face conditions
p0115 N82-32303
- On a study of the $\Delta T/c$ and C^* integrals for fracture analysis under non-steady creep
p0115 N82-36782
- Moving singularity creep crack growth analysis with the $\Delta T/c$ and C^* integrals
p0116 N82-40066
- Preliminary study of temperature measurement techniques for Stirling engine reciprocating seals
[NASA-CR-165479] p0104 N82-11466
- Prediction of sound radiation from different practical jet engine inlets
[NASA-CR-165120] p0153 N82-16810
- A new numerical approach for compressible viscous flows
[NASA-CR-168842] p0090 N82-22455
- Creep crack-growth: A new path-independent T sub o and computational studies
[NASA-CR-168930] p0113 N82-24503
- Acoustic properties of turbfan inlets
[NASA-CR-169016] p0153 N82-27090
- Creep crack-growth: A new path-independent integral (T sub c), and computational studies
[NASA-CR-167897] p0114 N82-29619
- Development of a spinning wave heat engine
[NASA-CR-165611] p0028 N82-31328
- GILBERT/COMMONWEALTH, READING, PA.**
Magnetohydrodynamics (MHD) Engineering Test Facility (ETF) 200 Mwe power plant. Conceptual Design Engineering Report CDER. Volume 3: Costs and schedules
[NASA-CR-165452-VOL-3] p0128 N82-10495
- Magnetohydrodynamics (MHD) Engineering Test Facility (ETF) 200 Mwe power plant. Conceptual Design Engineering Report (CDER). Volume 1: Executive summary
[NASA-CR-165452-VOL-1] p0129 N82-12570
- Magnetohydrodynamics (MHD) Engineering Test Facility (ETF) 200 Mwe power plant Conceptual Design Engineering Report (CDER)
[NASA-CR-165452-VOL-5] p0132 N82-17603
- Magnetohydrodynamics (MHD) Engineering Test Facility (ETF) 200 Mwe power plant. Conceptual Design Engineering Report (CDER). Volume 4: Supplementary engineering data
[NASA-CR-165452-VOL-4] p0133 N82-18688
- Magnetohydrodynamics (MHD) Engineering Test Facility (ETF) 200 Mwe power plant. Conceptual Design Engineering Report (CDER). Volume 2: Engineering. Volume 3: Costs and schedules
[NASA-CR-165452-VOL-2] p0136 N82-27837
- GINER, INC., WALTHAM, MASS.**
Requirements for optimization of electrodes and electrolyte for the iron/chromium Redox flow cell
[NASA-CR-165218] p0136 N82-25640
- GTE LABS., INC., WALTHAM, MASS.**
Fabrication of turbine components and properties of sintered silicon nitride
[ASME PAPER 82-GT-252] p0071 N82-35431
- Fabrication of sinterable silicon nitride by injection molding
p0071 N82-37015

H

- HAMILTON STANDARD, WINDSOR LOCKS, CONN.**
Evaluation of wind tunnel performance testings of an advanced 45 deg swept 8-bladed propeller at Mach numbers from 0.45 to 0.85
[NASA-CR-3505] p0007 N82-19178
- HERSH ACOUSTICAL ENGINEERING, CHATSWORTH, CALIF.**
Analytical and experimental investigation of the propagation and attenuation of sound in extended reaction lined ducts
[AIAA PAPER 81-2014] p0153 N82-10454

- HUGHES AIRCRAFT CO., EL SEGUNDO, CALIF.**
The 30/20 GHz flight experiment system, phase 2.
Volume 1: Executive summary
[NASA-CR-165409-VOL-1] p0078 N82-20362
- The 30/20 GHz flight experiment system, phase 2.
Volume 2: Experiment system description
[NASA-CR-165409-VOL-2] p0078 N82-20363
- The 30/20 GHz flight experiment system, phase 2.
Volume 3: Experiment system requirement document
[NASA-CR-165409-VOL-3] p0078 N82-20364
- The 30/20 GHz flight experiment system, phase 2.
Volume 4: Experiment system development plan
[NASA-CR-165409-VOL-4] p0078 N82-20365
- HUGHES AIRCRAFT CO., MALIBU, CALIF.**
A 10-kw series resonant converter design, transistor characterization, and base-drive optimization
p0086 A82-36927
- HUGHES AIRCRAFT CO., TORRANCE, CALIF.**
Pyrolytic graphite collector development program
[NASA-CR-167909] p0052 N82-29363
- HUGHES RESEARCH LABS., MALIBU, CALIF.**
30-cm Mercury ion thruster technology
p0046 A82-15434
- Characteristics of the LoRC/Hughes J-series 30-cm engineering model thruster
p0046 A82-15435
- Retrofit and acceptance test of 30-cm ion thrusters
[NASA-CR-165259] p0044 N82-12133
- A 10kW series resonant converter design, transistor characterization, and base-drive optimization
[NASA-CR-165546] p0084 N82-17439
- I**
- IIT RESEARCH INST., CHICAGO, ILL.**
Thermal fatigue and oxidation data of TAZ-8A and M22 alloys and variations
[NASA-CR-165407] p0063 N82-10193
- International market assessment of stand-alone photovoltaic power systems for cottage industry applications
[NASA-CR-165287] p0132 N82-16494
- ILLINOIS UNIV., CHICAGO.**
Mathematical models for the synthesis and optimization of spiral bevel gear tooth surfaces
[NASA-CR-3553] p0106 N82-25516
- ILLINOIS UNIV., URBANA.**
Interface cracks in adhesively bounded lap-shear joints
p0116 A82-46109
- Boundary-layer effects in composite laminates. I - Free-edge stress singularities. II - Free-edge stress solutions and basic characteristics
p0116 A82-46806
- ILLINOIS UNIV., URBANA-CHAMPAIGN.**
Boundary layer thermal stresses in angle-ply composite laminates, part 1
[NASA-CR-165412] p0113 N82-26713
- Analysis of cracks emanating from a circular hole in unidirectional fiber reinforced composites, part 2
[NASA-CR-165433] p0114 N82-26714
- Interlaminar crack growth in fiber reinforced composites during fatigue, part 3
[NASA-CR-165434] p0114 N82-26715
- Analysis of interface cracks in adhesively bonded lap shear joints, part 4
[NASA-CR-165438] p0114 N82-26716
- Edge delamination in angle-ply composite laminates, part 5
[NASA-CR-165439] p0114 N82-26717
- Boundary-layer effects in composite laminates: Free-edge stress singularities, part 6
[NASA-CR-165440] p0114 N82-26718
- NASA Adaptive Multibeam Phased Array (AMPA): An application study
[NASA-CR-169125] p0079 N82-28503
- INSTITUT FUER THEORETISCHE STROMUNGSMECHANIK, GOETTINGEN (WEST GERMANY).**
A computational design method for transonic turbomachinery cascades
[ASME PAPER 82-GT-117] p0022 A82-35348
- INSTITUTE OF GAS TECHNOLOGY, CHICAGO, ILL.**
Stabilizing platinum in phosphoric acid fuel cells
[NASA-CR-165403] p0130 N82-14628
Stabilizing platinum in phosphoric acid fuel cells
[NASA-CR-165606] p0136 N82-29718
- IONICS, INC., WATERTOWN, MASS.**
Anion permselective membrane
[NASA-CR-167872] p0137 N82-30711
- J**
- JET PROPULSION LAB., CALIFORNIA INST. OF TECH., PASADENA.**
Evidence for Pu-244 fission tracks in hibonites from Murchison carbonaceous chondrite
p0166 A82-29316
- Raman study of the improper ferroelectric phase transition in iron iodine boracite
A82-30297
- Subsystems design and component development for the parabolic dish module for solar thermal power systems
[NASA-CR-168941] p0135 N82-24646
- K**
- KANSAS UNIV., LAWRENCE.**
Numerical simulation of sheath structure and current-voltage characteristics of a conductor-dielectric disk in a plasma
p0040 A82-15904
- Numerical simulation of plasma insulator interactions in space. Part 1: The self consistent calculation
p0039 N82-14272
- Numerical simulation of plasma insulator interactions in space. Part 2: Dielectric effects
p0039 N82-14273
- KANSAS UNIV. CENTER FOR RESEARCH, INC., LAWRENCE.**
Icing tunnel tests of a composite porous leading edge for use with a liquid anti-ice system
[NASA-CR-164966] p0014 N82-11052
- KARLSRUHE UNIV. (WEST GERMANY).**
Extended range stress intensity factor expressions for chevron-notched short bar and short rod fracture toughness specimens
p0112 A82-40357
- KENTUCKY UNIV., LEXINGTON.**
Buoyancy effects on the temperature field in downward spreading flames
p0094 A82-41203
- KMS FUSION, INC., ANN ARBOR, MICH.**
Free electron lasers for transmission of energy in space
[NASA-CR-165520] p0098 N82-25499
- L**
- LIFE SYSTEMS, INC., CLEVELAND, OHIO.**
Alkaline regenerative fuel cell systems for energy storage
p0042 A82-11706
- Endurance test and evaluation of alkaline water electrolysis cells
[NASA-CR-165424] p0130 N82-13508
- LITTLE (ARTHUR D.), INC., CAMBRIDGE, MASS.**
An assessment of the crash fire hazard of liquid hydrogen fueled aircraft
[NASA-CR-165526] p0013 N82-19196
- LWR COMMUNICATIONS, INC., HAUPPAUGE, N. Y.**
IMPATT power building blocks for 20 GHz spaceborne transmit amplifier
[ATAA 82-0498] p0086 A82-23566
- LOCKHEED-CALIFORNIA CO., BURBANK.**
Experimental study of fuel heating at low temperatures in a wing tank model, volume 1
[NASA-CR-165391] p0073 N82-11224
- Additional experiments on flowability improvements of aviation fuels at low temperatures, volume 2
[NASA-CR-167912] p0074 N82-31546
- LOCKHEED-GEORGIA CO., MARIETTA.**
Advanced turboprop testbed systems study. Volume 1: Testbed program objectives and priorities, drive system and aircraft design studies, evaluation and recommendations and wind tunnel test plans
[NASA-CR-167928-VOL-1] p0028 N82-32370
- LOWELL UNIV., MASS.**
Effect of gamma irradiation on the friction and

wear of ultrahigh molecular weight polyethylene
p0062 A82-10674

M

MARTIN MARIETTA AEROSPACE, DENVER, COLO.
An experiment to evaluate liquid hydrogen storage in space
A82-20748

Primary propulsion/large space system interaction study
[NASA-CR-165277] p0044 A82-18315

MARTIN MARIETTA CORP., BETHESDA, MD.
Cryogenic fluid management experiment
[NASA-CR-165495] p0039 A82-15117

MARYLAND UNIV., COLLEGE PARK.
VLA observations of solar active regions at 6 cm wavelength
p0167 A82-10156

Toward the use of similarity theory in two-phase choked flows
p0089 A82-16570

Time variability and structure of quiet sun sources at 6 cm wavelength
p0167 A82-26003

Magnetic structure of a flaring region producing impulsive microwave and hard X-ray bursts
p0167 A82-27323

MASSACHUSETTS INST. OF TECH., CAMBRIDGE.
Modeling parameter influences on MHD swirl combustion nozzle design
[AIAA PAPER 82-0984] p0011 A82-31947

Aerodynamic damping measurements in a transonic compressor
[ASME PAPER 82-GT-287] p0012 A82-35459

In-plane inertial coupling in tuned and severely mistuned bladed disks
[ASME PAPER 82-GT-288] p0012 A82-35460

Flow aerodynamics modeling of an MHD swirl combustor - Calculations and experimental verification
p0094 A82-44782

Conceptual design of superconducting magnet system for Magnetohydrodynamic (MHD) Engineering Test Facility (ETF) 200 MWe power plant
[NASA-CR-165053] p0105 A82-14520

Ultrasonic input-output for transmitting and receiving longitudinal transducers coupled to same face of isotropic elastic plate
[NASA-CR-3506] p0110 A82-18613

Review of analysis methods for rotating systems with periodic coefficients
p0135 A82-23702

A FORTRAN program for calculating three dimensional, inviscid and rotational flows with shock waves in axial compressor blade rows: User's manual
[NASA-CR-3560] p0008 A82-26230

MATHEMATICAL SCIENCES NORTHWEST, INC., BELLEVUE, WASH.
Overview study of Space Power Technologies for the advanced energetics program
[NASA-CR-165269] p0132 A82-17606

MAX-PLANCK-INSTITUT FUER STROEHUNGSPORSCHUNG, GOETTINGEN (WEST GERMANY).
Conversion of acoustic energy by lossless liners
p0154 A82-36195

MCDONNELL-DOUGLAS CORP., ST. LOUIS, MO.
Tests of a D vented thrust deflecting nozzle behind a simulated turbofan engine
[NASA-CR-3508] p0006 A82-17122

MECHANICAL TECHNOLOGY, INC., LATHAM, N. Y.
Development of C₆₀-graphite-Ag coatings for gas bearings to 427 C
p0108 A82-27079

Preliminary study of temperature measurement techniques for Stirling engine reciprocating seals
[NASA-CR-165479] p0104 A82-11466

Automotive Stirling engine development program
[NASA-CR-167907] p0164 A82-29235

Automotive Stirling Engine Mod 1 Design Review, volume 1
[NASA-CR-167935] p0164 A82-34311

Automotive Stirling Engine Mod 1 Design Review, volume 3
[NASA-CR-167997] p0164 A82-34312

MICHIGAN STATE UNIV., EAST LANSING.
Standing waves along a microwave generated surface wave plasma
p0158 A82-26952

MICHIGAN TECHNOLOGICAL UNIV., HOUGHTON.
Solute transport during the cyclic oxidation of Ni-Cr-Al alloys
[NASA-CR-165544] p0064 A82-27462

MINNESOTA UNIV., MINNEAPOLIS.
Turbulent boundary layer heat transfer experiments - A separate effects study on a convexly-curved wall
[ASME PAPER 81-HT-78] p0092 A82-10963

The acoustical structure of highly porous open-cell foams
p0154 A82-45165

MISSOURI UNIV., ROLLA.
Methods for the calculation of axial wave numbers in lined ducts with mean flow
p0153 A82-14044

Acoustic transmission in lined flow ducts - A finite element eigenvalue problem
p0154 A82-17663

Conversion and matched filter approximations for serial minimum-shift keyed modulation
p0080 A82-26713

Conversion of acoustic energy by lossless liners
p0154 A82-36195

MOTOROLA, INC., SCOTTSDALE, ARIZ.
Baseband-processed SS-TDMA communication system architecture and design concepts
[AIAA 82-0482] p0079 A82-23508

Near optimum delay-line detection filters for serial detection of MSK signals
p0086 A82-43867

MUNISING PAPER DIV., MENASH, WIS.
Development of battery separator composites
[NASA-CR-165508] p0128 A82-11547

N

NATIONAL ACADEMY OF SCIENCES - NATIONAL RESEARCH COUNCIL, WASHINGTON, D. C.
Nical ternary alloy having improved cyclic oxidation resistance
[NASA-CASE-LEW-13339-1] p0061 A82-31505

NATIONAL AERONAUTICS AND SPACE ADMINISTRATION, WASHINGTON, D. C.
Bibliography of NASA published reports on general aviation, 1975 to 1981
[NASA-TM-83307] p0001 A82-19132

NASA research programs responding to workshop recommendations
A82-21146

NATIONAL AERONAUTICS AND SPACE ADMINISTRATION, AMES RESEARCH CENTER, HOFFETT FIELD, CALIF.
A theory of the n-i-p silicon solar cell
p0128 A82-45055

NATIONAL AERONAUTICS AND SPACE ADMINISTRATION, LYNDON B. JOHNSON SPACE CENTER, HOUSTON, TEX.
Electromechanical actuators
A82-19148

NATIONAL BUREAU OF STANDARDS, WASHINGTON, D. C.
Non-noble catalysts and catalyst supports for phosphoric acid fuel cells
[NASA-CR-165289] p0137 A82-30722

NAVAL AIR PROPULSION TEST CENTER, TRENTON, N.J.
Rotor fragment protection program: Statistics on aircraft gas turbine engine rotor failures that occurred in U.S. commercial aviation during 1978
[NASA-CR-165388] p0027 A82-27316

NEW MEXICO UNIV., ALBUQUERQUE.
Study of the photovoltaic effect in thin film barium titanate
[NASA-CR-165081] p0131 A82-16479

NIELSEN ENGINEERING AND RESEARCH, INC., MOUNTAIN VIEW, CALIF.
Rapid approximate determination of nonlinear solutions - Application to aerodynamic flows and design/optimization problems
p0012 A82-35571

NORTHEASTERN UNIV., BOSTON, MASS.
Engine dynamic analysis with general nonlinear finite element codes. II - Bearing element implementation, overall numerical characteristics and benchmarking
[ASME PAPER 82-GT-292] p0108 A82-35462

NORTHROP CORP., HAWTHORNE, CALIF.

Tangential blowing for control of strong normal shock - Boundary layer interactions on inlet ramps
[AIAA PAPER 82-1082] p0005 A82-37684

NORTHWESTERN UNIV., EVANSTON, ILL.

Lean-limit extinction of propane/air mixtures in the stagnation-point flow p0057 A82-28736

Effects of heat loss, preferential diffusion, and flame stretch on flame-front instability and extinction of propane/air mixtures p0057 A82-32877

On the opening of premixed Bunsen flame tips p0057 A82-37570

On stability of premixed flames in stagnation - Point flow p0057 A82-37574

On finite deformation elasto-plasticity p0116 A82-45869

NOTRE DAME UNIV., IND.

Sound generated in a cascade by three-dimensional disturbances convected in a subsonic flow [AIAA PAPER 81-2046] p0153 A82-10460

A tensor approach to modeling of nonhomogeneous nonlinear systems p0148 A82-19064

Alternatives for jet engine control [NASA-CR-168894] p0026 A82-23247

NTL, INC., COLMACK, N.Y.

A new antenna concept for satellite communications [NASA-CR-167924] p0079 A82-31584

O**O'DONNELL AND ASSOCIATES, INC., PITTSBURGH, PA.**

A simplified design procedure for life prediction of rocket thrust chambers [AIAA PAPER 82-1251] p0043 A82-35087

Development of a simplified procedure for thrust chamber life prediction [NASA-CR-165585] p0044 A82-21253

OHIO STATE UNIV., COLUMBUS.

Vibrations of cantilevered shallow cylindrical shells of rectangular planform p0115 A82-11298

Vibrations of twisted rotating blades [ASME PAPER 81-DET-127] p0115 A82-19341

Aerodynamic characteristics of airfoils with ice accretions [AIAA PAPER 82-0282] p0010 A82-22081

Comparison of beam and shell theories for the vibrations of thin turbomachinery blades [ASME PAPER 82-GT-223] p0115 A82-35408

On ultrasonic factors and fracture toughness p0116 A82-42863

Rime ice accretion and its effect on airfoil performance [NASA-CR-165599] p0008 A82-24166

The orthogonal in-situ machining of single and polycrystalline aluminum and copper, volume I [NASA-CR-168929] p0076 A82-24361

The transmission or scattering of elastic waves by an inhomogeneity of simple geometry: A comparison of theories [NASA-CR-169034] p0079 A82-26526

OKLAHOMA STATE UNIV., STILLWATER.

On the prediction of swirling flowfields found in axisymmetric combustor geometries p0029 A82-12120

A simple finite difference procedure for the vortex controlled diffuser [AIAA PAPER 82-0109] p0030 A82-17788

Mean flowfields in axisymmetric combustor geometries with swirl [AIAA PAPER 82-0177] p0092 A82-17824

Modeling parameter influences on MHD swirl combustion nozzle design [AIAA PAPER 82-0984] p0011 A82-31947

Bluff-body flameholder wakes - A simple numerical solution [AIAA PAPER 82-1177] p0093 A82-35043

Turbulence measurements in a confined jet using a six-orientation hot-wire probe technique [AIAA PAPER 82-1262] p0094 A82-37710

Flow aerodynamics modeling of an MHD swirl combustor - Calculations and experimental

verification

Investigations of flowfields found in typical combustor geometries [NASA-CR-165061] p0090 A82-15360

Investigations of flowfields found in typical combustor geometries [NASA-CR-160585] p0090 A82-19495

Investigations of flowfields found in typical combustor geometries [NASA-CR-169295] p0092 A82-31643

OPERATIONS RESEARCH, INC., SILVER SPRING, MD.

Planning satellite communication services and spectrum-orbit utilization [AIAA 82-0526] p0080 A82-23538

P**PANELVISION CORP., PITTSBURGH, PA.**

Development of an 1100 deg F capacitor p0083 A82-15315

PARAGON PACIFIC, INC., EL SEGUNDO, CALIF.

Development report: Automatic System Test and Calibration (ASTAC) equipment [NASA-CF-165403] p0129 A82-13505

PARSONS (RALPH M.) CO., PASADENA, CALIF.

Fuel quality processing study, volume I [NASA-CR-165327-VOL-1] p0135 A82-24649

Fuel quality/processing study Volume 2: Appendix. Task 1 literature survey [NASA-CR-165327-VOL-2] p0135 A82-24650

PENNSYLVANIA STATE UNIV., UNIVERSITY PARK.

The three-dimensional boundary layer on a rotating helical blade p0009 A82-15459

Atomization and combustion properties of flashing injectors [AIAA PAPER 82-0300] p0092 A82-17880

Characteristics of the flow in the annulus-wall region of an axial-flow compressor rotor blade passage [AIAA PAPER 82-0413] p0009 A82-17933

Interaction of compressor rotor blade wake with wall boundary layer/vortex in the end-wall region [ASME PAPER 81-GR/GT-1] p0010 A82-19301

Strength distributions of SiC ceramics after oxidation and oxidation under load [ACS PAPER 9-C-80C] p0071 A82-20143

Anaerobic polymers as high vacuum leak sealants p0108 A82-21967

Effects of blade loading and rotation on compressor rotor wake in end wall regions [AIAA PAPER 82-0193] p0010 A82-22063

Measurement and prediction of mean velocity and turbulence structure in the near wake of an airfoil p0010 A82-26137

Three sensor hot wire/film technique for three dimensional mean and turbulence flow field measurement p0097 A82-30300

Three dimensional flow field inside the passage of a low speed axial flow compressor rotor [AIAA PAPER 82-1006] p0011 A82-31964

Three dimensional turbulent boundary layer development on a fan rotor blade [AIAA PAPER 82-1007] p0011 A82-31965

Three-dimensional flow field in the tip region of a compressor rotor passage. I - Mean velocity profiles and annulus wall boundary layer [ASME PAPER 82-GT-11] p0011 A82-35280

Investigation of the tip-clearance flow inside and at the exit of a compressor rotor passage. I - Mean velocity field [ASME PAPER 82-GT-12] p0011 A82-35281

Three-dimensional flow field in the tip region of a compressor rotor passage. II - Turbulence properties [ASME PAPER 82-GT-234] p0011 A82-35416

Effects of oxidation and oxidation under load on strength distributions of Si₃N₄ [ACS PAPER 69-B-80] p0071 A82-35871

Pressure pulsations above turbomolecular pumps p0076 A82-46430

Oblique-incidence secondary emission from charged dielectrics p0039 A82-14227

- Numerical analysis and FORTRAN program for the computation of the turbulent wakes of turbomachinery rotor blades, isolated airfoils and cascade of airfoils
[NASA-CR-3509] p0006 N82-18184
- Secondary electron emission from a charged dielectric in the presence of normal and oblique electric fields
[NASA-CR-168558] p0084 N82-18507
- Mapping of electrical potential distributions with charged particle beams
[NASA-CR-168556] p0084 N82-18508
- Application of an airfoil stall flutter computer prediction program to a three-dimensional wing: Prediction versus experiment
[NASA-CR-168586] p0007 N82-19169
- Three dimensional mean velocity and turbulence characteristics in the annulus wall region of an axial flow compressor rotor passage
[NASA-CR-169003] p0026 N82-25252
- Investigation of the tip clearance flow inside and at the exit of a compressor rotor passage
[NASA-CR-169004] p0026 N82-25253
- Investigation of spray characteristics for flashing injection of fuels containing dissolved air and superheated fuels
[NASA-CR-3563] p0027 N82-26295
- Three dimensional flow field inside compressor rotor, including blade boundary layers
[NASA-CR-169120] p0091 N82-27686
- PITTSBURGH UNIV.,**
Investigation into the role of NaCl deposited on oxide and metal substrates in the initiation of hot corrosion
[NASA-CR-165029] p0063 N82-13217
- POWER TRANSISTOR CO., TORRANCE, CALIF.**
Fast recovery, high voltage silicon diodes for AC motor controllers
p0086 N82-36926
- PRATT AND WHITNEY AIRCRAFT, EAST HARTFORD, CONN.**
Tailored plasma sprayed MCrAlY coatings for aircraft gas turbine applications
[NASA-CF-165234] p0064 N82-19360
- PRATT AND WHITNEY AIRCRAFT GROUP, EAST HARTFORD, CONN.**
Improved plasma sprayed MCrAlY coatings for aircraft gas turbine applications
p0065 N82-20742
- JIBE** high pressure compressor performance improvement
[NASA-CF-165531] p0104 N82-11467
- Low NO sub x heavy fuel combustor concept program
[NASA-CF-165512] p0129 N82-12572
- Sensor failure detection system
[NASA-CF-165515] p0023 N82-13145
- Study of controlled diffusion stator blading. 1. Aerodynamic and mechanical design report
[NASA-CF-165500] p0024 N82-16081
- JT9D** ceramic outer air seal system refinement program
[NASA-CF-165554] p0106 N82-18603
- Energy efficient engine shroudless, hollow fan blade technology report
[NASA-CF-165586] p0024 N82-21196
- Energy efficient engine exhaust mixer model technology
[NASA-CF-165459] p0025 N82-22264
- Advanced Low-Emissions Catalytic-Combustor Program, phase 1
[NASA-CF-159556] p0025 N82-22265
- Thin film temperature sensors, phase 3
[NASA-CF-165476] p0097 N82-22479
- Analysis of high load dampers
[NASA-CF-165503] p0026 N82-23248
- Preliminary study, analysis and design for a power switch for digital engine actuators
[NASA-CF-159559] p0085 N82-23394
- Performance deterioration due to acceptance testing and flight loads; JT9D jet engine diagnostic program
[NASA-CF-165572] p0027 N82-27309
- F747/JT9D flight loads and their effect on engine running clearances and performance deterioration; ECRC NAIL/E and WA JT9D engine diagnostics programs
[NASA-CF-165573] p0027 N82-28296
- Energy efficient engine: High pressure turbine uncooled rig technology report
[NASA-CF-165149] p0031 N82-32383
- Structural tailoring of engine blades (STAERL)
[NASA-CF-167949] p0028 N82-33391
- Energy efficient engine: Turbine transition duct model technology report
[NASA-CF-167996] p0029 N82-33394
- PRATT AND WHITNEY AIRCRAFT GROUP, WEST PALM BEACH, FLA.**
Computer modeling of fan-exit-splitter spacing effects on F100 response to distortion
[NASA-CF-167879] p0025 N82-23246
- PRC SYSTEMS SCIENCES CO., TUCSON, ARIZ.**
Gallium arsenide solar array subsystem study
[NASA-CF-167869] p0138 N82-32855
- PRINCETON UNIV., N. J.**
Mass Driver Two - A status report
p0046 N82-18191
- Mass driver reaction engine characteristics and performance in earth orbital transfer missions
p0046 N82-18199
- A small scale lunar launcher for early lunar material utilization
p0032 N82-35617
- The supply of lunar oxygen to low earth orbit
p0032 N82-35618
- PURDUE UNIV., LAFAYETTE, IND.**
Model degradation effects on sensor failure detection
p0148 N82-13143
- Water ingestion into jet engine axial compressors
[AIAA PAPER 82-0196] p0030 N82-17836
- Three-dimensional flow calculations including boundary layer effects for supersonic inlets at angle of attack
[AIAA PAPER 82-0061] p0005 N82-19778
- Diffraction by a finite strip
p0150 N82-33605
- Solution of the unsteady subsonic thin airfoil problem
p0012 N82-41267
- Indentation law for composite laminates
[NASA-CR-165460] p0052 N82-15123
- The design and instrumentation of the Purdue annular cascade facility with initial data acquisition and analysis
[NASA-CR-167861] p0008 N82-26237
- Effects of cobalt on the microstructure of Udimet 700
[NASA-CR-165605] p0064 N82-28409
- Calculation of the flow field including boundary layer effects for supersonic mixed compression inlets at angles of attack
[NASA-CR-167941] p0009 N82-29269
- MC carbide structures in M(Lc2)ar-H247
[NASA-CR-167892] p0064 N82-30374
- PURDUE UNIV., SCHOOL OF SCIENCE AT INDIANAPOLIS, IND.**
Application of a finite element algorithm for the solution of steady transonic Euler equations
[AIAA PAPER 82-0970] p0010 N82-31939
- Investigation of rotational transonic flows through ducts using a finite element scheme
[AIAA PAPER 82-1267] p0012 N82-37711

Q

- QUEENSBOROUGH COMMUNITY COLLEGE, BAYSIDE, N. Y.**
The influence of gamma prime on the recrystallization of an oxide dispersion strengthened superalloy - MA 6000E
p0062 N82-47393

R

- RASOR ASSOCIATES, INC., SUNNYVALE, CALIF.**
Jet impingement heat transfer enhancement for the GPU-3 Stirling engine
[NASA-TM-82727] p0163 N82-11993
- RENSSELAER POLYTECHNIC INST., TROY, N. Y.**
Fatigue of Ni-Al-Mo aligned eutectics at elevated temperatures
p0052 N82-13403
- Alignment of fluid molecules in an EHD contact
[ASLE PREPRINT 81-LC-5C-1] p0107 N82-18407
- Analysis of infrared emission from thin adsorbates

- Low temperature growth and electrical characterization of insulators for GaAs MISFETS [NASA-CR-164972] p0159 N82-11959
- RICE UNIV., HOUSTON, TEX.
Direct conversion of light to radio frequency energy p0138 A82-11712
- ROCKETDYNE, CANOGA PARK, CALIF.
Advanced superposition methods for high speed turbopump vibration analysis [NASA-CR-165379] p0104 N82-11465
- Liquid oxygen turbopump technology [NASA-CR-165487] p0105 N82-11468
- Reusable rocket engine maintenance study [NASA-CR-165569] p0044 N82-16172
- ROCKWELL INTERNATIONAL CORP., LOS ANGELES, CALIF.
Performance of PTFE-lined composite journal bearings [ASLE PREPRINT 82-AM-1A-1] p0104 A82-37854
- ROCKWELL INTERNATIONAL CORP., THOUSAND OAKS, CALIF.
Undoped semi-insulating LEC GaAs - A model and a mechanism p0159 A82-13754
- Stoichiometry-controlled compensation in liquid encapsulated Czochralski GaAs p0158 A82-17585
- Compensation mechanism in liquid encapsulated Czochralski GaAs Importance of melt stoichiometry p0086 A82-40403
- Effect of melt stoichiometry on twin formation in LEC GaAs p0160 A82-46517
- High purity low dislocation GaAs single crystals [NASA-CR-165593] p0159 N82-23030
- ROYAL AIRCRAFT ESTABLISHMENT, FARNBOROUGH (ENGLAND).
Fatigue tests with a corrosive environment N82-13282
- RUTGERS UNIV., NEW BRUNSWICK, N. J.
Turbulence in argon shock waves p0158 A82-11117
- S**
- SCIENTIFIC RESEARCH ASSOCIATES, INC., GLASTONBURY, CONN.
Turbofan forced mixer-nozzle internal flowfield. Volume 3: A computer code for 3-D mixing in axisymmetric nozzles [NASA-CR-3494] p0091 N82-22460
- SHD ASSOCIATES, INC., EVANSTON, ILL.
Eigenvalues of the Rayleigh-Benard and Marangoni problems p0092 A82-13396
- Nonlinear Marangoni convection in bounded layers. I - Circular cylindrical containers. II - Rectangular cylindrical containers p0094 A82-39501
- Surface-tension induced instabilities: Effects of lateral boundaries [NASA-CR-165530] p0092 N82-11390
- SKF TECHNOLOGY SERVICES, KING OF PRUSSIA, PA.
Spherical roller bearing analysis. SKF computer program SPHERBEAN. Volume 1: Analysis [NASA-CR-165203] p0106 N82-20540
- Spherical roller bearing analysis. SKF computer program SPHERBEAN. Volume 2: User's manual [NASA-CR-165204] p0106 N82-20541
- Spherical roller bearing analysis. SKF computer program SPHERBEAN. Volume 3: Program correlation with full scale hardware tests [NASA-CR-165205] p0106 N82-20542
- High speed cylindrical roller bearing analysis. SKF computer program CYBEAN. Volume 2: User's manual [NASA-CR-165364] p0146 N82-31968
- Research report: User's manual for computer program AT81Y003 SHAFERTH. Steady state and transient thermal analysis of a shaft bearing system including ball, cylindrical and tapered roller bearings [NASA-CR-165365] p0146 N82-31969
- Research report: User's manual for computer program AT81Y005. PLANETSYS, a computer program for the steady state and transient thermal analysis of a planetary power transmission system [NASA-CR-165366] p0146 N82-31970
- SOLAR ENERGY TECHNOLOGY, INC., BEDFORD, MASS.
Focal surfaces of offset dual-reflector antennas p0080 A82-36265
- SOLAR TURBINES INTERNATIONAL, SAN DIEGO, CALIF.
Low NOx heavy fuel combustor concept program [NASA-CR-167876] p0074 N82-26482
- Advanced ceramic coating development for industrial/utility gas turbines [NASA-CR-169852] p0065 N82-33494
- Low NOx heavy fuel combustor concept program [NASA-CR-165481] p0138 N82-33827
- SOMOSCAN, INC., BENSENVILLE, ILL.
Acoustic microscopy of silicon carbide materials p0075 A82-33031
- SOUTH CAROLINA UNIV., COLUMBIA.
Digital imaging techniques in experimental stress analysis p0097 A82-34231
- Experimental boundary integral equation applications in speckle interferometry p0097 A82-36987
- SOUTHWEST RESEARCH INST., SAN ANTONIO, TEX.
Study of vapor flow into a capillary acquisition device [NASA-CR-167883] p0091 N82-24452
- SPIRE CORP., BEDFORD, MASS.
Processing of silicon solar cells by ion implantation and laser annealing [NASA-CR-165283] p0128 N82-11546
- Development of a large area space solar cell assembly [NASA-CR-167929] p0137 N82-30706
- SRI INTERNATIONAL CORP., MENLO PARK, CALIF.
Oxidation and formation of deposit precursors in hydrocarbon fuels [NASA-CR-165534] p0073 N82-18402
- First results of material charging in the space environment [NASA-TN-84743] p0081 N82-24431
- STANFORD UNIV., CALIF.
Turbulent boundary layer heat transfer experiments - A separate effects study on a convexly-curved wall [ASME PAPER 81-HT-78] p0092 A82-10963
- Turbulent boundary layer heat transfer experiments: Convex curvature effects including introduction and recovery [NASA-CR-3510] p0090 N82-17456
- STEVENS INST. OF TECH., HOBOKEN, N. J.
The influence of Coriolis forces on gyroscopic motion of spinning blades [ASME PAPER 82-GT-163] p0030 A82-35384
- STERLING THERMAL MOTORS, INC., ANN ARBOR, MICH.
Evaluation of the potential of the Stirling engine for heavy duty application [NASA-CR-165473] p0128 N82-10505
- STONEHART ASSOCIATES, INC., MADISON, CONN.
Survey on aging on electrodes and electrocatalysts in phosphoric acid fuel cells [NASA-CR-165505] p0128 N82-11545
- Preparation and evaluation of advanced electrocatalysts for phosphoric acid fuel cells [NASA-CR-165519] p0129 N82-12573
- Preparation and evaluation of advanced electrocatalysts for phosphoric acid fuel cells [NASA-CR-165594] p0132 N82-17615
- STRUCTURAL COMPOSITES INDUSTRIES, INC., AZUSA, CALIF.
Winding for the wind p0138 A82-37078
- Design, evaluation, and fabrication of low-cost composite blades for intermediate-size wind turbines [NASA-CR-165342] p0133 N82-18693
- SYSTEMATICS GENERAL CORP., STERLING, VA.
Communications satellite systems capacity analysis [NASA-CR-167911] p0034 N82-27331
- SYSTEMS CONTROL, INC., PALO ALTO, CALIF.
Sensor failure detection system [NASA-CR-165515] p0023 N82-13145
- SYSTEMS SCIENCE AND SOFTWARE, LA JOLLA, CALIF.
Space Shuttle Orbiter charging [AIAA PAPER 82-0119] p0040 A82-17793
- Validation of the NASCAP model using spaceflight data [AIAA PAPER 82-0269] p0038 A82-17872

'Bootstrap' charging of surfaces composed of multiple materials p0085 A82-18318

NASCAP simulation of laboratory charging tests using multiple electron guns p0033 A82-18319

Differential charging of high-voltage spacecraft - The equilibrium potential of insulated surfaces p0041 A82-35547

Representation and material charging response of geoplasma environments p0039 A82-14249

Simulation of charging response of SCATHA (P78-2) satellite p0039 A82-14250

SYSTEMS SCIENCE AND SOFTWARE, SAN DIEGO, CALIF.

Charging of a large object in low polar Earth orbit p0039 A82-14275

Additional extensions to the NASCAP computer code, volume 1 [NASA-CR-167855] p0146 A82-25810

Additional extensions to the NASCAP computer code, volume 2 [NASA-CR-167856] p0040 A82-26377

Additional extensions to the NASCAP computer code, volume 3 [NASA-CR-167857] p0040 A82-26378

T

TANKSLEY (W. L.) AND ASSOCIATES, INC., BROOK PARK, OHIO.

Vibration analysis of three guyed tower designs for intermediate size wind turbines [NASA-CR-165589] p0137 A82-30709

TATA INST. OF FUNDAMENTAL RESEARCH, BOMBAY (INDIA).

Evidence for Pu-244 fission tracks in hibonites from Murchison carbonaceous chondrite p0166 A82-29316

TECHNION - ISRAEL INST. OF TECH., HAIFA.

Modified face seal for positive film stiffness [NASA-CASE-LEW-12989-1] p0099 A82-12442

TEL-AVIV UNIV. (ISRAEL).

On stability of premixed flames in stagnation - Point flow p0057 A82-37574

TELETYPE COE, TOLEDO, OHIO.

Cooled variable nozzle radial turbine for rotor craft applications [NASA-CR-165397] p0028 A82-29323

TELETYPE CONTINENTAL MOTORS, MOBILE, ALA.

Exhaust emissions reduction for intermittent combustion aircraft engines [NASA-CR-167914] p0029 A82-33392

TELETYPE CONTINENTAL MOTORS, MUSKEGON, MICH.

Lightweight diesel engine designs for commuter type aircraft [NASA-CR-165470] p0023 A82-11068

TENNESSEE UNIV. SPACE INST., TULLAHOMA.

'Coriolis resonance' within a rotating duct p0012 A82-37938

TEXAS A&M UNIV., COLLEGE STATION.

Performance degradation of propeller/rotor systems due to rime ice accretion [AIAA PAPER 82-0286] p0014 A82-28322

THERMO ELECTRON CORP., WALTHAM, MASS.

Evaluation of left ventricular assist device pump bladders cast from icn-sputtered polytetrafluorethylene mandrels [NASA-CR-167904] p0142 A82-23976

THERMO MECHANICAL SYSTEMS CO., CANOGA PARK, CALIF.

Development of a locally mass flux conservative computer code for calculating 3-D viscous flow in turbomachines [NASA-CR-3539] p0007 A82-22214

TOKYO UNIV. (JAPAN).

Effect of tangential traction and roughness on crack initiation/propagation during rolling contact p0103 A82-30022

TOLEDO UNIV., OHIO.

Aeroelastic characteristics of a cascade of mistuned blades in subsonic and supersonic flows [ASME PAPER 81-DET-122] p0021 A82-19337

The effects of controls and controllable and storage loads on the performance of stand-alone photovoltaic systems p0127 A82-45027

Modeling the full-bridge series-resonant power converter p0086 A82-46385

Numerical simulation of one-dimensional heat transfer in composite bodies with phase change [NASA-CR-165607] p0002 A82-22142

TRANSMISSION RESEARCH, INC., CLEVELAND, OHIO.

Traction contact performance evaluation at high speeds [NASA-CR-165226] p0105 A82-16409

TRIBON BEARING CO., CLEVELAND, OHIO.

Effects of ultra-clean and centrifugal filtration on rolling-element bearing life [ASME PAPER 81-IUB-35] p0103 A82-18436

TRW DEFENSE AND SPACE SYSTEMS GROUP, REDONDO BEACH, CALIF.

High power solar array switching regulation p0043 A82-11736

30/20 GHz demonstration system for improving orbit utilization p0080 A82-27189

Open-loop nanosecond-synchronization for wideband satellite communications p0036 A82-27224

Brushfire arc discharge model p0038 A82-14224

Integrated propulsion for near-Earth space missions. Volume 1: Executive summary [NASA-CR-167889-VOL-1] p0045 A82-33424

Integrated propulsion for near-Earth space missions. Volume 2: Technical [NASA-CR-167889-VOL-2] p0046 A82-33425

TRW, INC., CLEVELAND, OHIO.

Development of materials and process technology for dual alloy disks [NASA-CR-165224] p0063 A82-18370

TRW, INC., REDONDO BEACH, CALIF.

Shuttle to GEO propulsion tradeoffs [AIAA PAPER 82-1245] p0034 A82-25082

Chopper-controlled discharge life cycling studies on lead-acid batteries [NASA-CR-165616] p0134 A82-20661

TUSKEGEE INST., ALA.

Characterization of advanced electric propulsion systems [AIAA PAPER 82-1246] p0071 A82-35083

A comprehensive method for preliminary design optimization of axial gas turbine stages [AIAA PAPER 82-1264] p0030 A82-35091

Characterization of advanced electric propulsion systems [NASA-CR-167885] p0045 A82-26381

U

ULTRASYSTEMS, INC., IRVINE, CALIF.

Thermal oxidative degradation reactions of perfluoroalkylethers [NASA-CR-165516] p0048 A82-12135

UNITED AIR LINES, INC., SAN FRANCISCO, CALIF.

An automated system for global atmospheric sampling using B-747 airliners [NASA-CR-165264] p0139 A82-13554

UNITED TECHNOLOGIES CORP., EAST HARTFORD, CONN.

A heat exchanger computational procedure for temperature-dependent fouling [ASME PAPER 81-HT-75] p0092 A82-10961

NASA Broad Specification Fuels Combustion Technology program - Pratt and Whitney Aircraft Phase I results and status [AIAA PAPER 82-1088] p0021 A82-34999

Fracture mechanics criteria for turbine engine hot section components [NASA-CR-167896] p0027 A82-25257

Hot isostatically pressed manufacture of high strength MERL 76 disk and seal shapes [NASA-CR-165549] p0064 A82-26439

UNITED TECHNOLOGIES CORP., SOUTH WINDSOR, CONN.

Alkaline regenerative fuel cell systems for energy storage p0042 A82-11706

Low NO sub x heavy fuel combustor concept program [NASA-CR-165512] p0129 A82-12572

Electrochemical energy storage for an orbiting space station [NASA-CR-165436] p0132 A82-17607

Low NO subx heavy fuel combustor concept program. Phase 1A: Coal gas addendum [NASA-CR-165577] p0133 A82-18690

UNITED TECHNOLOGIES CORP., WEST PALM BEACH, FLA.

A real time Pegasus propulsion system model for
VSTOL piloted simulation evaluation
[AIAA PAPER 81-2663] p0020 A82-19221
UNITED TECHNOLOGIES RESEARCH CENTER, EAST HARTFORD,
CONN.

Tube entrance heat transfer with deposit formation
[AIAA PAPER 82-0918] p0093 A82-31908
Evaluation of fuel injection configurations to
control carbon and soot formation in small GT
combustors
[AIAA PAPER 82-1175] p0021 A82-35041
Deposit formation in hydrocarbon fuels
[ASME PAPER 82-GT-49] p0075 A82-35307
Experimental study of external fuel vaporization
[ASME PAPER 82-GT-59] p0075 A82-35312
Development of low modulus material for use in
ceramic gas path seal applications
[NASA-CR-165469] p0022 A82-10039

External fuel vaporization study
[NASA-CR-165513] p0073 A82-14371
Research and development program for non-linear
structural modeling with advanced
time-temperature dependent constitutive
relationships
[NASA-CR-165533] p0024 A82-16080

An experimental investigation of gapwise
periodicity and unsteady aerodynamic response
in an oscillating cascade. Volume 2: Data
report. Part 1: Text and mode 1 data
[NASA-CR-165457-VOL-2-P1-1] p0006 A82-18180

Mass and momentum turbulent transport
experiments with confined coaxial jets
[NASA-CR-165574] p0090 A82-19496

Investigation of soot and carbon formation in
small gas turbine combustors
[NASA-CR-167853] p0025 A82-22267

Turbofan forced mixer-nozzle internal flowfield.
Volume 1: A benchmark experimental study
[NASA-CR-3492] p0090 A82-22458

Turbofan forced mixer-nozzle internal flowfield.
Volume 2: Computational fluid dynamic
predictions
[NASA-CR-3493] p0091 A82-22459

Turbofan forced mixer-nozzle internal flowfield.
Volume 3: A computer code for 3-D mixing in
axisymmetric nozzles
[NASA-CR-3494] p0091 A82-22460

An experimental investigation of gapwise
periodicity and unsteady aerodynamic response
in an oscillating cascade. 1: Experimental
and theoretical results
[NASA-CR-3513] p0008 A82-26229

UNIVERSITIES SPACE RESEARCH ASSOCIATION, COLUMBIA,
MD.

CAS22 - FORTRAN program for fast design and
analysis of shock-free airfoil cascades using
fictitious-gas concept
[NASA-CR-3507] p0006 A82-16044

Design of supercritical cascades with high
solidity
[NASA-CR-165600] p0007 A82-22210

GRID3C: Computer program for generation of C
type multilevel, three dimensional and
boundary conforming periodic grids
[NASA-CR-167846] p0008 A82-26239

Fast generation of three-dimensional
computational boundary-conforming periodic
grids of C-type
[NASA-CR-165596] p0009 A82-28253

V

VARIAN ASSOCIATES, PALO ALTO, CALIF.
CM-VPE growth of Mg-doped GaAs
p0159 A82-38411

VIRGINIA POLYTECHNIC INST. AND STATE UNIV.,
BLACKSBURG.

A new approach to the minimum weight/loss design
of switching power converters
p0082 A82-16831

Power system design optimization using Lagrange
multiplier techniques
p0085 A82-20743

Analysis and design of a standardized control
module for switching regulators
p0083 A82-46388

Modeling and Analysis of Power Processing
Systems (MAPPS). Volume 1: Technical report
[NASA-CR-165538] p0083 A82-14447

Modeling and Analysis of Power Processing
Systems (MAPPS). Volume 2: Appendices
[NASA-CR-165539] p0145 A82-16748
Finite-element modeling of layered, anisotropic
composite plates and shells: A review of
recent research
p0113 A82-19563

Input filter compensation for switching regulators
[NASA-CR-169005] p0085 A82-25442

VIRGINIA UNIV., CHARLOTTESVILLE.
A pad perturbation method for the dynamic
coefficients of tilting-pad journal bearings
p0110 A82-14400

VOUGHT CORP., DALLAS, TEX.
V/VSTOL Tandem Fan transition section model test
[NASA-CR-165587] p0007 A82-21158

W

WESTERN UNION TELEGRAPH CO., MCLEAN, VA.
Worldwide satellite market demand forecast
[NASA-CR-167918] p0079 A82-25423

WESTINGHOUSE ELECTRIC CORP., CINCINNATI, OHIO.
Low NO sub x heavy fuel combustor concept
program. Phase 1A: Combustion technology
generation coal gas fuels
[NASA-CR-165614] p0055 A82-22326

Low NOx heavy fuel combustor concept program.
Phase 1: Combustion technology generation
[NASA-CR-165482] p0136 A82-24725

WESTINGHOUSE ELECTRIC CORP., LYMA, OHIO.
High voltage DC switchgear development for
multi-kw space power system: Aerospace
technology development of three types of solid
state power controllers for 200-1100VDC with
current ratings of 25, 50, and 80 amperes with
one type utilizing an electromechanical device
[NASA-CR-165413] p0083 A82-13357

WESTINGHOUSE ELECTRIC CORP., MADISON, PA.
Low and medium heating value coal gas catalytic
combustor characterization
[NASA-CR-165560] p0138 A82-32856

WESTINGHOUSE ELECTRIC CORP., PITTSBURGH, PA.
Development of an 1100 deg F capacitor
p0083 A82-15315

Evaluation of present thermal barrier coatings
for potential service in electric utility gas
turbines
[NASA-CR-165545] p0063 A82-18368

High voltage power transistor development
[NASA-CR-165547] p0084 A82-18506

Cell module and fuel conditioner development
[NASA-CR-165620] p0134 A82-21713

WESTINGHOUSE RESEARCH AND DEVELOPMENT CENTER,
PITTSBURGH, PA.
Ceramic thermal barrier coatings for gas turbine
engines
[ASME PAPER 82-GT-265] p0071 A82-35441

Cell module and fuel conditioner development
[NASA-CR-165462] p0130 A82-13511

Cell module and fuel conditioner development
[NASA-CR-165193] p0137 A82-30712

WICHITA STATE UNIV., KANS.
Numerical modeling of three-dimensional confined
flows
[NASA-CR-165583] p0158 A82-24078

WILLIAMS RESEARCH CORP., WALLED LAKE, WASH.
AGT-102 automotive gas turbine
[NASA-CR-165353] p0105 A82-12444

WRIGHT STATE UNIV., DAYTON, OHIO.
Undoped semi-insulating LEC GaAs - A model and a
mechanism
p0159 A82-13754

Compensation mechanism in liquid encapsulated
Czochralski GaAs Importance of melt
stoichiometry
p0086 A82-40403

WYOMING UNIV., LARAMIE.
Analysis of crack propagation as an energy
absorption mechanism in metal matrix composites
[NASA-CR-165051] p0052 A82-14288

Micromechanical predictions of crack propagation
and fracture energy in a single fiber
boron/aluminum model composite
[NASA-CR-168550] p0052 A82-18326

X

XXOX CORP., EL SEGUNDO, CALIF.

Power system design optimization using Lagrange
multiplier techniques

p0085 A82-20743

Analysis and design of a standardized control
module for switching regulators

p0083 A82-46388

XXOX ELECTRO-OPTICAL SYSTEMS, PASADENA, CALIF.

Developing a scalable inert gas ion thruster

[AIAA PAPER 82-1275]

p0047 A82-37713

Inert gas ion thruster

[NASA-CR-165521]

p0044 A82-21252

Y

YALE UNIV., NEW HAVEN, CONN.

Experimental and theoretical studies of the laws
governing condensate deposition from
combustion gases

p0057 A82-28709

Two dimensional stagnation point flow of a dusty
gas near an oscillating plate

p0012 A82-37535

CONTRACT NUMBER INDEX

DN3-241
 p0117 N82-13490
 p0131 N82-16483
 p0135 N82-24648
 p0137 N82-30705

DN3-248
 p0137 N82-29720

DN3-277
 p0138 N82-32856

DI-DH-JO-100026
 p0125 N82-30714

DNA001-79-C-0079
 p0033 A82-18319

EC-77-A-21-1011
 p0105 N82-16409

EC-77-A-31-1040
 p0164 N82-31158

EC-77-A-31-1044
 p0105 N82-12445

EC-77-A-21-10040
 p0164 N82-29235

EF-76-5-01-2479
 p0110 A82-14400

EF-77-A-01-2593
 p0058 N82-17335

EPA-68-02-3122
 p0056 A82-20739

EY-76-C-02-2749
 p0108 A82-27079

EZ-76-C-04-3737
 A82-23394

F04701-77-C-0062
 p0165 A82-23750
 p0140 A82-32630

F04701-80-C-0081
 p0081 N82-24431

F33615-77-C-5171
 p0074 A82-33030

F33615-78-C-2401
 p0030 A82-17836

F33615-80-C-1182
 p0086 A82-23566

F33615-81-C-1406
 p0086 A82-40403

F49620-76-C-0020
 p0057 A82-28709

NAGW-38
 p0166 A82-29316

NAG1-95
 p0131 N82-16479

NAG3-1 p0057 A82-37571
 NAG3-3 p0092 A82-10963
 p0090 N82-17456

NAG3-6 p0104 A82-35468

NAG3-13
 p0065 A82-44529

NAG3-22
 p0052 A82-13403

NAG3-26
 p0009 N82-32310

NAG3-26
 p0010 A82-22081
 p0008 N82-24166

NAG3-29
 p0138 A82-11712

NAG3-36
 p0115 A82-11298
 p0115 A82-19341
 p0115 A82-35408

NAG3-38
 p0115 A82-32303
 p0115 A82-36782
 p0116 A82-40066
 p0113 N82-24503
 p0114 N82-29619

NAG3-39
 p0113 N82-20564

NAG3-41
 p0112 N82-14531

NAG3-43
 p0159 A82-21965
 p0159 A82-30335
 p0160 A82-46426
 p0065 N82-31503

NAG3-44
 p0063 N82-13217

NAG3-47
 p0030 A82-35384

NAG3-48
 p0106 N82-25516

NAG3-53
 p0057 A82-28736
 p0057 A82-32877
 p0057 A82-37570
 p0057 A82-37574

NAG3-54
 p0115 A82-39514
 p0094 A82-45157

NAG3-57
 p0065 A82-34973
 p0064 N82-28409

NAG3-59
 p0064 N82-30374

NAG3-62
 p0030 A82-17836

NAG3-65
 p0014 A82-27098

NAG3-67
 p0153 N82-16810

NAG3-71
 p0014 N82-11052

NAG3-72
 p0002 N82-22142

NAG3-73
 p0106 N82-26680

NAG3-74
 p0029 A82-12120
 p0030 A82-17788
 p0092 A82-17824
 p0011 A82-31947
 p0093 A82-35043
 p0094 A82-37710
 p0094 A82-44782
 p0090 N82-15360
 p0090 N82-19495
 p0092 N82-31643

NAG3-75
 p0097 A82-34231
 p0097 A82-36987

NAG3-76
 p0071 A82-35083
 p0045 N82-26381

NAG3-81
 p0085 N82-25442

NAG3-86
 p0012 A82-37938

NAG3-88
 p0159 A82-31276
 p0159 A82-42912

NAG3-96
 p0028 N82-31328

NAG3-100
 p0105 N82-14520

NAG3-101
 p0145 N82-17879

NAG3-109
 p0014 A82-28322

NAG3-111
 p0136 N82-29719

NAG3-122
 p0091 N82-31639

NAG3-131
 p0093 A82-32225

NAG3-134
 p0116 A82-45869

NAG3-144
 p0128 A82-45055

NAG3-149
 p0079 N82-28503

NAG3-152
 p0165 A82-23750

NAG3-161
 p0154 A82-45165

NAG3-175
 p0159 N82-11959

NAG3-208
 p0113 N82-19563

NAG3-242
 p0014 A82-28322

NAG3-246
 p0115 N82-33738

NASA ORDER C-32817-D
 p0164 N82-18068

NASA ORDER C-41581-B
 p0027 N82-27316

NASA ORDER C-4270 D
 p0137 N82-29721

NASA ORDER C-46229-D
 p0137 N82-30722

NASA ORDER C-57307-D
 p0073 N82-13243

NASW-3336
 p0079 A82-10679

NAS1-15325
 p0027 N82-28296

NAS2-9281
 p0005 A82-37684

NAS3-2253
 p0007 N82-22210

NAS3-6465
 p0083 N82-15315

NAS3-10941
 p0083 N82-15315

NAS3-17787
 p0063 N82-10193

NAS3-17867
 p0139 N82-13554

NAS3-18547
 p0104 N82-10401

NAS3-19755
 p0029 N82-33392

NAS3-20070
 p0023 N82-14092
 p0023 N82-14093
 p0027 N82-27310

NAS3-20072
 p0064 N82-26439

NAS3-20074
 p0026 N82-25254

NAS3-20102
 p0083 A82-46388

NAS3-20405
 p0052 N82-20248

NAS3-20583
 p0128 N82-11547

NAS3-20629
 p0024 N82-17174
 p0027 N82-28297
 p0029 N82-33393

NAS3-20630
 p0104 N82-11467
 p0106 N82-18603

NAS3-20631
 p0025 N82-21197

NAS3-20632
 p0027 N82-27309
 p0027 N82-28296

NAS3-20643
 p0029 A82-11999
 p0030 A82-35450

NAS3-20646
 p0024 N82-21196
 p0025 N82-22264
 p0031 N82-32383
 p0029 N82-33394

NAS3-20769
 p0007 N82-19178

NAS3-20817
 p0084 N82-24424

NAS3-20819
 p0023 N82-14095
 p0024 N82-14096

NAS3-20821
 p0025 N82-22265

NAS3-20824
 p0106 N82-20540
 p0106 N82-20541
 p0106 N82-20542

NAS3-20834
 p0007 N82-22214

NAS3-20836
 p0012 A82-35571

NAS3-20951
 p0090 N82-22458
 p0091 N82-22459
 p0091 N82-22460

NAS3-21040
 p0046 A82-15434

NAS3-21051
 p0082 A82-16831
 p0085 A82-20743
 p0083 N82-14447
 p0145 N82-16748

NAS3-21052
 p0046 A82-15435

NAS3-21227
 p0127 A82-44942

NAS3-21276
 p0128 N82-11546

NAS3-21280
 p0046 A82-11762

NAS3-21285
 p0107 N82-27743

NAS3-21287
 p0130 N82-13508

NAS3-21293
 p0132 N82-17607

NAS3-21345
 p0044 N82-21252

NAS3-21351
 p0063 N82-18370

NAS3-21356
 p0105 N82-11461

NAS3-21357
 p0044 N82-12133

NAS3-21377
 p0071 A82-35441
 p0063 N82-18366

NAS3-21384
 p0051 N82-12139

NAS3-21500
 p0078 N82-17420

NAS3-21591
 A82-20748
 p0039 N82-15117

NAS3-21609
 p0011 A82-35427

NAS3-21624
 p0023 N82-12075

NAS3-21719
 p0009 N82-33347

NAS3-21726
 p0055 A82-1573
 p0055 A82-1574

NAS3-21727
 p0023 N82-1004

NAS3-21730
 p0065 A82-2074
 p0064 N82-1936

NAS3-21733
 p0006 N82-1712

NAS3-21745
 p0080 A82-271

NAS3-21753
 p0073 N82-102

NAS3-21755
 p0083 N82-133

NAS3-21762
 p0039 N82-142
 p0039 N82-142
 p0039 N82-142

NAS3-21763
 p0052 N82-314

NAS3-21809
 p0085 N82-233

NAS3-21843
 p0015 A82-376

NAS3-21900
 p0137 N82-307

NAS3-21933
 p0080 A82-271

NAS3-21940
 p0047 A82-350

NAS3-21949
 p0084 N82-185

NAS3-21951
 p0130 N82-140
 p0130 N82-140

NAS3-21952
 p0046 N82-111
 p0044 N82-111

NAS3-21955
 p0044 N82-183

NAS3-21960
 p0105 N82-134

NAS3-21961
 p0038 N82-142

NAS3-21971
 p0092 A82-105
 p0093 A82-319
 p0075 A82-35

NAS3-21974
 p0153 N82-210
 p0153 N82-210
 p0155 N82-210

NAS3-21975
 p0153 A82-10

NAS3-21977
 p0073 N82-11
 p0074 N82-3

NAS3-21995
 p0022 N82-10
 p0022 N82-10

ORIGINAL PAGE IS
OF POOR QUALITY

CONTRACT NUMBER INDEX

NAS3-21957	NAS3-22444	NAS3-22739	
p0026 N82-24202	p0047 A02-37713	p0025 N82-23246	p0097 A82-30300
NAS3-22002	NAS3-22461	NAS3-22762	p0006 N82-18184
p0097 N82-22479	p0079 N82-25423	p0103 A82-35036	MSG-3016
NAS3-22074	NAS3-22471	NAS3-22771	p0071 A82-20143
p0024 N82-19221	p0006 A02-36927	p0090 N82-19496	p0071 A82-35871
NAS3-22085	p0084 N82-17439	NAS3-22808	MSG-3019
p0038 N82-29323	NAS3-22476	p0113 N82-17521	p0056 A82-22033
NAS3-22108	p0142 N82-23976	NAS3-22876	p0056 A82-28694
p0024 N82-16081	NAS3-22477	p0047 A82-37713	p0091 N82-31641
NAS3-22019	p0132 N82-17606	NAS3-22882	p0092 N82-31642
p0006 N82-18180	NAS3-22480	p0033 A82-44659	MSG-3032
p0009 N82-26229	p0104 N82-11465	p0033 N82-29345	p0097 A82-30300
NAS3-22053	NAS3-22481	NAS3-22885	MSG-3036
p0030 A82-34982	p0023 N82-13145	p0080 A82-23538	p0030 A82-17796
NAS3-22055	NAS3-22482	NAS3-22887	p0153 N82-27090
p0024 N82-16080	p0013 N82-19196	p0079 N82-31584	MSG-3044
NAS3-22057	NAS3-22491	NAS3-22888	p0116 A82-46109
p0029 A82-16909	p0086 A82-23566	p0034 N82-27331	p0116 A82-46806
NAS3-22162	NAS3-22496	NAS3-22901	p0113 N82-26713
p0029 A82-10457	p0078 N82-13302	p0034 A82-36286	p0114 N82-26714
NAS3-22109	NAS3-22498	NAS3-22905	p0114 N82-26715
p0028 N82-32367	p0079 A82-23486	p0036 A82-36925	p0114 N82-26716
NAS3-22123	NAS3-22500	NAS3-22914	p0114 N82-26717
p0104 A82-37854	p0086 A82-43784	p0034 A82-36286	p0114 N82-26718
NAS3-22134	NAS3-22501	NAS3-22950	MSG-3048
p0022 N82-10039	p0085 A82-23494	p0083 A82-41845	p0148 A82-19064
NAS3-22143	NAS3-22502	NAS3-23157	p0026 N82-23247
p0109 A82-48247	p0079 A82-23508	p0106 N82-26679	MSG-3050
NAS3-22148	p0080 A82-26713	NAS3-33541	p0065 A82-40335
p0010 A82-31933	p0086 A82-43867	p0141 N82-16659	MSG-3075
NAS3-22149	NAS3-22505	NAS3-23481	p0011 A82-35379
p0023 N82-11068	p0052 N82-29363	p0040 A82-16194	MSG-3079
NAS3-22155	NAS3-22510	p0140 A82-32630	p0012 A82-35459
p0007 N82-21158	p0073 N82-18402	NAS7-10	p0012 A82-35460
NAS7-22171	NAS3-22517	p0135 N82-24646	MSG-3084
p0056 A82-28651	p0048 N82-12135	NAS8-30563	p0148 A82-13143
NAS3-22217	NAS3-22518	p0140 A82-31009	MSG-3105
p0046 A82-11762	p0026 N82-23248	NAS8-33982	p0110 A82-14400
NAS3-22220	NAS3-22524	p0140 A82-32630	MSG-3106
p0025 N82-22268	p0025 N82-22267	NBS-HA-1008	p0107 A82-18431
NAS3-22221	NAS3-22525	p0056 A82-28651	p0070 A82-18432
p0025 N82-22263	p0028 N82-33391	NGL-05-005-007	p0070 A82-18432
NAS3-22222	NAS3-22530	p0165 A82-23750	MSG-3107
p0129 N82-12571	p0041 A82-18312	NGL-39-009-007	p0057 A82-28709
NAS3-22224	NAS3-22532	p0097 A82-30300	p0012 A82-37535
p0159 A82-13754	p0006 N82-16044	NGR-21-002-199	MSG-3114
p0158 A82-17585	p0008 N82-26239	p0167 A82-10156	p0094 A82-41203
p0086 A82-40403	p0009 N82-20253	p0167 A82-27323	MSG-3122
p0160 A82-46517	NAS3-22536	NGR-21-022-199	p0048 A82-15696
p0159 N82-23030	p0040 A82-17793	p0167 A82-26003	p0074 A82-22240
NAS3-22226	p0038 A82-17872	NRC A-7435	p0074 A82-22241
p0128 N82-10505	p0085 A82-18318	p0093 A82-35043	p0074 A82-23238
NAS3-22228	p0033 A82-18319	NSF ATM-76-22415	MSG-3124
p0127 A82-44944	p0041 A82-35547	p0167 A82-26003	p0092 A82-10963
p0133 N82-18689	p0146 N82-25810	NSF ATM-77-14821	p0090 N82-17456
NAS3-22232	p0040 N82-26377	A82-19360	MSG-3128
p0159 A82-38411	p0040 N82-26378	NSF ATM-78-2176	p0053 A82-31339
NAS3-22236	NAS3-22539	p0167 A82-27323	p0053 A82-46220
p0137 N82-30706	p0086 A82-36926	NSF ATM-78-21762	MSG-3150
NAS3-22266	NAS3-22542	p0167 A82-10156	p0040 A82-16194
p0084 N82-23395	p0139 N82-29777	NSF ATM-80-13153	p0140 A82-31009
NAS3-22274	NAS3-22550	A82-19360	p0140 A82-32630
p0092 A82-13396	p0027 N82-25257	NSF CPE-79-23680	MSG-3157
p0094 A82-39501	NAS3-22647	p0056 A82-28651	p0083 N82-12347
p0092 N82-11390	p0074 N82-24353	NSF DMR-79-23573	p0084 N82-22438
NAS3-22277	NAS3-22649	A82-30002	MSG-3160
p0075 A82-35307	p0044 N82-21253	NSF ECS-79-23877	p0149 A82-31438
NAS3-22324	NAS3-22650	p0159 A82-31276	MSG-3164
p0035 A82-10124	p0045 A82-24287	p0159 A82-42912	p0076 N82-24361
p0040 A82-13494	p0045 A82-24288	NSF ENG-76-10232	MSG-3166
p0033 A82-48245	NAS3-22652	p0057 A82-37571	p0039 N82-14227
NAS3-22340	p0044 N82-16172	NSF ENG-78-12372	p0084 N82-18507
p0078 N82-20362	NAS3-22659	p0093 A82-32225	p0084 N82-18508
p0078 N82-20363	p0098 N82-25499	NSF MEA-80-11362	MSG-3169
p0078 N82-20364	NAS3-22661	p0154 A82-45165	p0057 A82-28709
p0078 N82-20365	p0034 A82-35082	MSG-317	MSG-3170
NAS3-22341	p0045 N82-33424	p0148 A82-13143	p0107 A82-18407
p0036 A82-27224	p0046 N82-33425	MSG-330	p0056 A82-21431
NAS3-22342	NAS3-22664	p0063 A82-47400	MSG-3171
p0078 N82-31585	p0091 N82-24452	MSG-398	p0148 A82-13143
NAS3-22343	NAS3-22665	p0167 A82-10156	MSG-3174
p0080 A82-36265	p0047 A82-35056	p0167 A82-26003	p0093 A82-24748
NAS3-22346	p0045 N82-22309	p0167 A82-27323	MSG-3176
p0028 N82-32370	NAS3-22667	MSG-3011	p0046 A82-18191
NAS3-22347	p0138 N82-32855	p0045 N82-24285	p0046 A82-18199
p0014 N82-33375	NAS3-22690	p0045 N82-28350	p0032 A82-35617
NAS3-22369	p0146 N82-31968	MSG-3012	p0032 A82-35618
p0007 N82-22211	p0146 N82-31969	p0010 A82-19301	MSG-3185
NAS3-22371	p0146 N82-31970	p0010 A82-22063	p0052 N82-15123
p0063 N82-14333		p0010 A82-26137	MSG-3186
			p0158 N82-24078

CONTRACT NUMBER INDEX

MSG-3188	p0108 A82-19334 p0107 A82-29607	MSG-3303	p0076 A82-46430 p0135 A82-23702	p0152 A82-21036 p0152 A82-22951 p0152 A82-31068 p0152 A82-32082 p0089 A82-32634	505-33-52	p0111 A82-21604					
MSG-3195	p0153 A82-10460	MSG-3304	p0007 A82-19169	505-32-12	505-33-62	p0049 A82-14287 p0052 A82-15123 p0049 A82-16181 p0018 A82-22266 p0050 A82-24300 p0113 A82-26713 p0114 A82-26714 p0114 A82-26715 p0114 A82-26716 p0114 A82-26717 p0114 A82-26718 p0112 A82-31707 p0112 A82-31706 p0028 A82-33391					
MSG-3196	p0157 A82-10880	MSG-3306	p0092 A82-17880 p0027 A82-26295	MSG-3307	p0093 A82-23832 p0090 A82-22455	p0049 A82-14287 p0052 A82-15123 p0049 A82-16181 p0018 A82-22266 p0050 A82-24300 p0113 A82-26713 p0114 A82-26714 p0114 A82-26715 p0114 A82-26716 p0114 A82-26717 p0114 A82-26718 p0112 A82-31707 p0112 A82-31706 p0028 A82-33391					
MSG-3197	p0159 A82-41546 p0038 A82-14226	MSG-3307	p0093 A82-23832 p0090 A82-22455	MSG-3311	p0005 A82-19778 p0009 A82-29269	p0049 A82-14287 p0052 A82-15123 p0049 A82-16181 p0018 A82-22266 p0050 A82-24300 p0113 A82-26713 p0114 A82-26714 p0114 A82-26715 p0114 A82-26716 p0114 A82-26717 p0114 A82-26718 p0112 A82-31707 p0112 A82-31706 p0028 A82-33391					
MSG-3207	p0145 A82-17080	MSG-5320	p0167 A82-10156 p0167 A82-27323	505-32-22	p0018 A82-25250	p0049 A82-14287 p0052 A82-15123 p0049 A82-16181 p0018 A82-22266 p0050 A82-24300 p0113 A82-26713 p0114 A82-26714 p0114 A82-26715 p0114 A82-26716 p0114 A82-26717 p0114 A82-26718 p0112 A82-31707 p0112 A82-31706 p0028 A82-33391					
MSG-3213	p0110 A82-18613	MSG-5320	p0167 A82-10156 p0167 A82-27323	505-32-32	p0016 A82-13143 p0016 A82-15040 p0087 A82-19494 p0072 A82-32504	p0049 A82-14287 p0052 A82-15123 p0049 A82-16181 p0018 A82-22266 p0050 A82-24300 p0113 A82-26713 p0114 A82-26714 p0114 A82-26715 p0114 A82-26716 p0114 A82-26717 p0114 A82-26718 p0112 A82-31707 p0112 A82-31706 p0028 A82-33391					
MSG-3212	p0009 A82-17933 p0011 A82-35280 p0011 A82-35281 p0011 A82-35416 p0026 A82-25252 p0026 A82-25253	N0014-80-C-0586	p0057 A82-37570	505-32-42	p0022 A82-10039 p0066 A82-15198 p0066 A82-15199 p0099 A82-16411 p0099 A82-16412 p0099 A82-16413 p0143 A82-16743 p0048 A82-17263 p0067 A82-20313 p0059 A82-21300 p0068 A82-21332 p0060 A82-24322 p0088 A82-24455 p0100 A82-25514 p0100 A82-25518 p0100 A82-25519 p0068 A82-26468 p0101 A82-28644 p0101 A82-28645 p0101 A82-28646 p0107 A82-29607 p0102 A82-30552 p0089 A82-32633 p0102 A82-32733 p0102 A82-32734	N00014-78-C-0547	p0071 A82-20741	505-32-52	p0004 A82-15020 p0006 A82-16044 p0149 A82-22922 p0149 A82-24859 p0008 A82-26239 p0005 A82-28247 p0009 A82-28253 p0005 A82-29270	505-33-12	p0058 A82-10195 p0058 A82-11182 p0048 A82-15119 p0066 A82-15197 p0059 A82-22346 p0064 A82-27462 p0061 A82-32461
MSG-3215	p0064 A82-27462	N00014-78-C-0547	p0071 A82-20741	505-32-68	p0018 A82-21195	p0058 A82-10195 p0058 A82-11182 p0048 A82-15119 p0066 A82-15197 p0059 A82-22346 p0064 A82-27462 p0061 A82-32461					
MSG-3217	p0052 A82-14288 p0052 A82-18326	N00014-78-C-0547	p0071 A82-20741	505-32-72	p0017 A82-15041 p0017 A82-16084 p0072 A82-27519 p0072 A82-28460 p0161 A82-32186 p0161 A82-32187 p0161 A82-32188 p0161 A82-32189	p0058 A82-10195 p0058 A82-11182 p0048 A82-15119 p0066 A82-15197 p0059 A82-22346 p0064 A82-27462 p0061 A82-32461					
MSG-3221	p0093 A82-31445	N00014-80-C-0586	p0057 A82-32877 p0057 A82-37574	505-32-82	p0095 A82-22481 p0095 A82-28605 p0095 A82-31664	p0058 A82-10195 p0058 A82-11182 p0048 A82-15119 p0066 A82-15197 p0059 A82-22346 p0064 A82-27462 p0061 A82-32461					
MSG-3227	p0056 A82-17746 p0093 A82-27000 p0056 A82-28708	N00014-80-G-0079	p0056 A82-28651	505-32-88	p0018 A82-21195	p0058 A82-10195 p0058 A82-11182 p0048 A82-15119 p0066 A82-15197 p0059 A82-22346 p0064 A82-27462 p0061 A82-32461					
MSG-3230	p0129 A82-13507	N00014-81-K-0438	A82-30002 N00024-76-C-5352 p0074 A82-33030	505-32-92	p0017 A82-19220	p0058 A82-10195 p0058 A82-11182 p0048 A82-15119 p0066 A82-15197 p0059 A82-22346 p0064 A82-27462 p0061 A82-32461					
MSG-3231	p0153 A82-14044 p0154 A82-17663 p0154 A82-36195	N00173-80-M-8575	p0056 A82-21431	505-32-98	p0017 A82-19220	p0058 A82-10195 p0058 A82-11182 p0048 A82-15119 p0066 A82-15197 p0059 A82-22346 p0064 A82-27462 p0061 A82-32461					
MSG-3234	p0008 A82-26230	W-7405-ZNG-48	p0056 A82-17746 p0093 A82-27000 p0056 A82-28708 A82-30002	505-32-00	p0117 A82-14552	p0058 A82-10195 p0058 A82-11182 p0048 A82-15119 p0066 A82-15197 p0059 A82-22346 p0064 A82-27462 p0061 A82-32461					
MSG-3236	p0153 A82-18994	146-40-18	p0093 A82-32225	307-90-00	p0117 A82-14552	p0058 A82-10195 p0058 A82-11182 p0048 A82-15119 p0066 A82-15197 p0059 A82-22346 p0064 A82-27462 p0061 A82-32461					
MSG-3238	p0091 A82-31638	307-90-00	p0117 A82-14552	p0016 A82-14090	p0016 A82-14090	p0058 A82-10195 p0058 A82-11182 p0048 A82-15119 p0066 A82-15197 p0059 A82-22346 p0064 A82-27462 p0061 A82-32461					
MSG-3246	p0062 A82-47397	500-42-62	p0003 A82-11043	500-42-62	p0003 A82-11043	p0058 A82-10195 p0058 A82-11182 p0048 A82-15119 p0066 A82-15197 p0059 A82-22346 p0064 A82-27462 p0061 A82-32461					
MSG-3253	p0107 A82-18449	500-55-12	p0003 A82-12043	500-55-12	p0003 A82-12043	p0058 A82-10195 p0058 A82-11182 p0048 A82-15119 p0066 A82-15197 p0059 A82-22346 p0064 A82-27462 p0061 A82-32461					
MSG-3257	p0138 A82-11816	503-04-72	p0009 A82-33347	503-04-72	p0009 A82-33347	p0058 A82-10195 p0058 A82-11182 p0048 A82-15119 p0066 A82-15197 p0059 A82-22346 p0064 A82-27462 p0061 A82-32461					
MSG-3263	p0064 A82-26436 p0113 A82-26702 p0113 A82-26706	505-03-22	p0025 A82-22265	505-03-22	p0025 A82-22265	p0058 A82-10195 p0058 A82-11182 p0048 A82-15119 p0066 A82-15197 p0059 A82-22346 p0064 A82-27462 p0061 A82-32461					
MSG-3265	p0009 A82-15459	505-04-82	p0007 A82-22214	505-04-82	p0007 A82-22214	p0058 A82-10195 p0058 A82-11182 p0048 A82-15119 p0066 A82-15197 p0059 A82-22346 p0064 A82-27462 p0061 A82-32461					
MSG-3266	p0011 A82-31564 p0011 A82-31965 p0091 A82-27686	505-15-22	p0017 A82-19220	505-15-22	p0017 A82-19220	p0058 A82-10195 p0058 A82-11182 p0048 A82-15119 p0066 A82-15197 p0059 A82-22346 p0064 A82-27462 p0061 A82-32461					
MSG-3267	p0010 A82-29003	505-31-32	p0068 A82-24342	505-31-32	p0068 A82-24342	p0058 A82-10195 p0058 A82-11182 p0048 A82-15119 p0066 A82-15197 p0059 A82-22346 p0064 A82-27462 p0061 A82-32461					
MSG-3269	p0116 A82-42862 p0079 A82-26526	505-32-2A	p0024 A82-16081 p0017 A82-19222 p0018 A82-22269 p0027 A82-27310	505-32-2A	p0024 A82-16081 p0017 A82-19222 p0018 A82-22269 p0027 A82-27310	p0058 A82-10195 p0058 A82-11182 p0048 A82-15119 p0066 A82-15197 p0059 A82-22346 p0064 A82-27462 p0061 A82-32461					
MSG-3280	p0158 A82-11117	505-32-2B	p0003 A82-14051 p0095 A82-14494 p0087 A82-19493 p0004 A82-26234 p0004 A82-26240 p0005 A82-28250 p0088 A82-30498 p0028 A82-32367	505-32-2B	p0003 A82-14051 p0095 A82-14494 p0087 A82-19493 p0004 A82-26234 p0004 A82-26240 p0005 A82-28250 p0088 A82-30498 p0028 A82-32367	p0058 A82-10195 p0058 A82-11182 p0048 A82-15119 p0066 A82-15197 p0059 A82-22346 p0064 A82-27462 p0061 A82-32461					
MSG-3281	p0086 A82-46385	505-32-6A	p0017 A82-18222 p0019 A82-25255	505-32-6A	p0017 A82-18222 p0019 A82-25255	p0058 A82-10195 p0058 A82-11182 p0048 A82-15119 p0066 A82-15197 p0059 A82-22346 p0064 A82-27462 p0061 A82-32461					
MSG-3283	p0108 A82-35462 p0028 A82-33390	505-32-6B	p0076 A82-20339 p0147 A82-22915 p0148 A82-30992 p0148 A82-31971 p0146 A82-33020	505-32-6B	p0076 A82-20339 p0147 A82-22915 p0148 A82-30992 p0148 A82-31971 p0146 A82-33020	p0058 A82-10195 p0058 A82-11182 p0048 A82-15119 p0066 A82-15197 p0059 A82-22346 p0064 A82-27462 p0061 A82-32461					
MSG-3285	p0008 A82-26237	505-32-02	p0151 A82-12890 p0151 A82-12891 p0151 A82-14881 p0151 A82-15847 p0006 A82-18184	505-32-02	p0151 A82-12890 p0151 A82-12891 p0151 A82-14881 p0151 A82-15847 p0006 A82-18184	p0058 A82-10195 p0058 A82-11182 p0048 A82-15119 p0066 A82-15197 p0059 A82-22346 p0064 A82-27462 p0061 A82-32461					
MSG-3290	p0040 A82-15904 p0039 A82-14272 p0039 A82-14273	505-32-02	p0151 A82-12890 p0151 A82-12891 p0151 A82-14881 p0151 A82-15847 p0006 A82-18184	505-32-02	p0151 A82-12890 p0151 A82-12891 p0151 A82-14881 p0151 A82-15847 p0006 A82-18184	p0058 A82-10195 p0058 A82-11182 p0048 A82-15119 p0066 A82-15197 p0059 A82-22346 p0064 A82-27462 p0061 A82-32461					
MSG-3292	p0150 A82-23605 p0012 A82-41267	505-32-02	p0151 A82-12890 p0151 A82-12891 p0151 A82-14881 p0151 A82-15847 p0006 A82-18184	505-32-02	p0151 A82-12890 p0151 A82-12891 p0151 A82-14881 p0151 A82-15847 p0006 A82-18184	p0058 A82-10195 p0058 A82-11182 p0048 A82-15119 p0066 A82-15197 p0059 A82-22346 p0064 A82-27462 p0061 A82-32461					
MSG-3294	p0009 A82-17759 p0010 A82-31939 p0012 A82-37711	505-32-02	p0151 A82-12890 p0151 A82-12891 p0151 A82-14881 p0151 A82-15847 p0006 A82-18184	505-32-02	p0151 A82-12890 p0151 A82-12891 p0151 A82-14881 p0151 A82-15847 p0006 A82-18184	p0058 A82-10195 p0058 A82-11182 p0048 A82-15119 p0066 A82-15197 p0059 A82-22346 p0064 A82-27462 p0061 A82-32461					
MSG-3295	p0030 A82-35091	505-32-02	p0151 A82-12890 p0151 A82-12891 p0151 A82-14881 p0151 A82-15847 p0006 A82-18184	505-32-02	p0151 A82-12890 p0151 A82-12891 p0151 A82-14881 p0151 A82-15847 p0006 A82-18184	p0058 A82-10195 p0058 A82-11182 p0048 A82-15119 p0066 A82-15197 p0059 A82-22346 p0064 A82-27462 p0061 A82-32461					
MSG-3299	p0158 A82-26952	505-32-02	p0151 A82-12890 p0151 A82-12891 p0151 A82-14881 p0151 A82-15847 p0006 A82-18184	505-32-02	p0151 A82-12890 p0151 A82-12891 p0151 A82-14881 p0151 A82-15847 p0006 A82-18184	p0058 A82-10195 p0058 A82-11182 p0048 A82-15119 p0066 A82-15197 p0059 A82-22346 p0064 A82-27462 p0061 A82-32461					
MSG-3301	p0108 A82-21967	505-32-02	p0151 A82-12890 p0151 A82-12891 p0151 A82-14881 p0151 A82-15847 p0006 A82-18184	505-32-02	p0151 A82-12890 p0151 A82-12891 p0151 A82-14881 p0151 A82-15847 p0006 A82-18184	p0058 A82-10195 p0058 A82-11182 p0048 A82-15119 p0066 A82-15197 p0059 A82-22346 p0064 A82-27462 p0061 A82-32461					

CONTRACT NUMBER INDEX

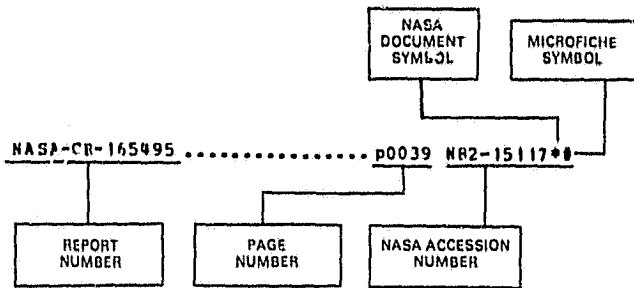
ORIGINAL PAGE IS
OF POOR QUALITY

p0038 N82-18311
p0038 N82-23261
p0069 N82-28445
p0082 N82-30474
506-56-12
p0049 N82-21260
506-61-22
p0081 N82-22439
508-52-12
p0074 N82-24343
510-53-12
p0026 N82-25254
p0064 N82-26439
510-55-12
p0006 N82-18180
p0008 N82-26229
510-57-1B
p0060 N82-24326
511-58-12
p0106 N82-25516
p0100 N82-25520
p0101 N82-26678
p0101 N82-26681
p0101 N82-28643
p0146 N82-31969
p0146 N82-31970
532-05-12
p0018 N82-24201
533-01-32
p0019 N82-26300
535-03-12
p0151 N82-16808
p0151 N82-16809
p0007 N82-19178
p0152 N82-21998
p0001 N82-26219
p0095 N82-31663
541-02-12
p0082 N82-25441
560-60-26
p0079 N82-25423
643-10-01
p0034 N82-27331
643-10-02
p0036 N82-25290
776-31-41
p0119 N82-14633
p0119 N82-16495
p0120 N82-21710
p0123 N82-26807
p0125 N82-30710
776-33-41
p0119 N82-16478
p0133 N82-18693
p0121 N82-21714
p0122 N82-23679
p0127 N82-33830
776-42-51
p0132 N82-16494
776-52-41
p0130 N82-14627
p0133 N82-19669
776-54-01
p0137 N82-29720
p0126 N82-33828
776-72-41
p0118 N82-12574
p0123 N82-25637
p0137 N82-30711
p0054 N82-31459
p0055 N82-33463
776-81-62
p0135 N82-24646
778-11-05
p0099 N82-12446
p0157 N82-12943
p0157 N82-13908
p0131 N82-15527
p0156 N82-24078
p0123 N82-25636
p0123 N82-26790
778-11-06
p0118 N82-13509
p0131 N82-16484
p0058 N82-17335
p0072 N82-21415
p0124 N82-29717
p0061 N82-30373
778-14-00
p0135 N82-24651
p0125 N82-30717

778-16-12
p0120 N82-19672
778-17-01
p0120 N82-19670
p0136 N82-29719
p0137 N82-29721
778-18-12
p0125 N82-30714
778-32-01
p0024 N82-21193
p0120 N82-21712
p0163 N82-26051
778-35-03
p0104 N82-11466
p0119 N82-18691
p0060 N82-24323
p0061 N82-30372
p0164 N82-34311
p0164 N82-34312
778-36-06
p0118 N82-10503
p0105 N82-12445
p0129 N82-13506
p0105 N82-16410
p0132 N82-17608
p0106 N82-24496
p0163 N82-31160
p0082 N82-33636
p0127 N82-33829
778-37-12
p0073 N82-13243
778-45-12
p0124 N82-30704
778-46-12
p0119 N82-16477
p0119 N82-18694
p0121 N82-23678
p0125 N82-30713
778-83-01
p0067 N82-11397

REPORT/ACCESSION NUMBER INDEX

Typical Report/Accession Number Index Listing



Listings in this index are arranged alphabetically by report number. The page number indicates the page in the abstract section in which the citation is located. The accession number denotes the number by which the citation is identified. An asterisk (*) indicates that the item is a NASA report. A pound sign (#) indicates that the item is available on microfiche.

ACFF-22-FR-1699A	p0014	NR2-33375**
ACS PAPER 9-C-80C	p0071	AB2-20143*
ACS PAPER 42-B-81	p0070	AB2-42366*
ACS PAPER 52-B-80P	p0074	AB2-33030*
ACS PAPER 69-R-80	p0071	AB2-35071*
AD-A 108342	p0117	NR2-10664**
AD-A 113767	p0027	NR2-27316**
ADL-85 161	p0013	NR2-19196**
AFGL-TR-81-0270	p0037	NR2-14213**
AIAA PAPER 81-0046	p0093	AB2-23832**
AIAA PAPER 81-0273	p0002	AB1-32548**
AIAA PAPER 81-2014	p0153	AB2-10454**
AIAA PAPER 81-2033	p0029	AB2-10457**
AIAA PAPER 81-2046	p0153	AB2-10460**
AIAA PAPER 81-2634	p0029	AB2-16909**
AIAA PAPER 81-2637	p0020	AB2-19214**
AIAA PAPER 81-2663	p0020	AB2-19221**
AIAA PAPER 82-0036	p0056	AB2-22033**
AIAA PAPER 82-0037	p0056	AB2-17746**
AIAA PAPER 82-0061	p0005	AB2-19778**
AIAA PAPER 82-0062	p0009	AB2-17759**
AIAA PAPER 82-0109	p0030	AB2-17788**
AIAA PAPER 82-0119	p0040	AB2-17793**
AIAA PAPER 82-0124	p0030	AB2-17796**
AIAA PAPER 82-0177	p0092	AB2-17824**
AIAA PAPER 82-0192	p0021	AB2-20291**
AIAA PAPER 82-0193	p0010	AB2-22063**
AIAA PAPER 82-0196	p0030	AB2-17836**
AIAA PAPER 82-0269	p0038	AB2-17872**
AIAA PAPER 82-0282	p0010	AB2-22081**
AIAA PAPER 82-0284	p0014	AB2-27098**
AIAA PAPER 82-0286	p0014	AB2-28322**
AIAA PAPER 82-0300	p0092	AB2-17880**
AIAA PAPER 82-0325	p0157	AB2-17889**
AIAA PAPER 82-0340	p0014	AB2-17894**
AIAA PAPER 82-0396	p0157	AB2-20292**
AIAA PAPER 82-0413	p0009	AB2-17933**
AIAA PAPER 82-0423	p0157	AB2-17941**
AIAA PAPER 82-0558	p0034	AB2-36286**
AIAA PAPER 82-0918	p0093	AB2-31908**
AIAA PAPER 82-0957	p0010	AB2-31933**
AIAA PAPER 82-0970	p0010	AB2-31939**
AIAA PAPER 82-0984	p0011	AB2-31947**
AIAA PAPER 82-1006	p0011	AB2-31964**
AIAA PAPER 82-1007	p0011	AB2-31965**
AIAA PAPER 82-1047	p0002	AB2-37678**
AIAA PAPER 82-1056	p0021	AB2-34981**

AIAA PAPER 82-1057	p0030	AB2-34982**
AIAA PAPER 82-1072	p0021	AB2-34992**
AIAA PAPER 82-1075	p0021	AB2-34995**
AIAA PAPER 82-1082	p0005	AB2-37684**
AIAA PAPER 82-1084	p0005	AB2-35195**
AIAA PAPER 82-1088	p0021	AB2-34999**
AIAA PAPER 82-1089	p0021	AB2-35000**
AIAA PAPER 82-1120	p0021	AB2-35017**
AIAA PAPER 82-1131	p0015	AB2-37691**
AIAA PAPER 82-1159	p0103	AB2-35036**
AIAA PAPER 82-1165	p0108	AB2-35038**
AIAA PAPER 82-1166	p0108	AB2-35039**
AIAA PAPER 82-1175	p0021	AB2-35041**
AIAA PAPER 82-1177	p0093	AB2-35043**
AIAA PAPER 82-1196	p0047	AB2-35056**
AIAA PAPER 82-1207	p0108	AB2-35061**
AIAA PAPER 82-1208	p0104	AB2-35062**
AIAA PAPER 82-1209	p0109	AB2-35480**
AIAA PAPER 82-1211	p0071	AB2-35064**
AIAA PAPER 82-1245	p0034	AB2-35082**
AIAA PAPER 82-1246	p0071	AB2-35083**
AIAA PAPER 82-1251	p0043	AB2-35087**
AIAA PAPER 82-1262	p0094	AB2-37710**
AIAA PAPER 82-1264	p0030	AB2-35091**
AIAA PAPER 82-1267	p0012	AB2-37711**
AIAA PAPER 82-1275	p0047	AB2-37713**
AIAA PAPER 82-1288	p0005	AB2-37716**
AIAA 81-2173	p0035	AB2-10124**
AIAA 81-2283	p0040	AB2-13494**
AIAA 82-0449	p0079	AB2-23486**
AIAA 82-0458	p0085	AB2-23494**
AIAA 82-0482	p0079	AB2-23508**
AIAA 82-0498	p0086	AB2-23566**
AIAA 82-0526	p0080	AB2-23538**
AIAA-PAPER-82-0122	p0151	NR2-14881**
AIAA-81-2627	p0003	NR2-11042**
AIAA-81-2637	p0004	NR2-18178**
AIAA-81-2663	p0016	NR2-13144**
AIAA-82-0192	p0017	NR2-19220**
AIRRESEARCH-21-3615	p0023	NR2-14095**
AIRRESEARCH-21-3619	p0024	NR2-14096**
AIRRESEARCH-31-3725	p0163	NR2-16937**
ASLE PREPRINT 81-LC-5C-1	p0107	AB2-18407**
ASLE PREPRINT 82-AM-1A-1	p0104	AB2-37854**
ASME PAPER 81-DET-114	p0108	AB2-19334**
ASME PAPER 81-DET-115	p0103	AB2-19335**
ASME PAPER 81-DET-122	p0021	AB2-19337**
ASME PAPER 81-DET-127	p0115	AB2-19341**
ASME PAPER 81-GR/GT-1	p0010	AB2-19301**
ASME PAPER 81-HT-48	p0020	AB2-10952**
ASME PAPER 81-HT-75	p0092	AB2-10961**
ASME PAPER 81-HT-78	p0092	AB2-10963**
ASME PAPER 81-HT-79	p0089	AB2-10964**
ASME PAPER 81-LUB-9	p0107	AB2-18426**
ASME PAPER 81-LUB-16	p0107	AB2-18431**
ASME PAPER 81-LUB-17	p0070	AB2-18432**
ASME PAPER 81-LUB-17	p0070	AB2-18432**
ASME PAPER 81-LUB-35	p0103	AB2-18436**
ASME PAPER 81-LUB-55	p0107	AB2-18449**
ASME PAPER 82-GT-11	p0011	AB2-35280**
ASME PAPER 82-GT-12	p0011	AB2-35281**
ASME PAPER 82-GT-49	p0075	AB2-35307**
ASME PAPER 82-GT-59	p0075	AB2-35312**
ASME PAPER 82-GT-72	p0108	AB2-35324**
ASME PAPER 82-GT-117	p0022	AB2-35348**
ASME PAPER 82-GT-149	p0022	AB2-35373**
ASME PAPER 82-GT-156	p0011	AB2-35379**
ASME PAPER 82-GT-163	p0030	AB2-35384**
ASME PAPER 82-GT-177	p0022	AB2-35389**
ASME PAPER 82-GT-216	p0071	AB2-35403**

REPORT/ACCESSION NUMBER INDEX

ORIGINAL PAGE IS
OF POOR QUALITY

ASME PAPER 82-GT-222	p0022	A82-35409**	DOE/NASA/0149-1	p0129	N82-12572**
ASME PAPER 82-GT-223	p0115	A82-35408**	DOE/NASA/0149-2	p0133	N82-18690**
ASME PAPER 82-GT-234	p0011	A82-35416**	DOE/NASA/0150-80/5	p0134	N82-22675**
ASME PAPER 82-GT-248	p0011	A82-35427**	DOE/NASA/0151-1	p0163	N82-16938**
ASME PAPER 82-GT-252	p0071	A82-35431**	DOE/NASA/0155-1	p0131	N82-16484**
ASME PAPER 82-GT-265	p0071	A82-35441**	DOE/NASA/0161-9	p0130	N82-13511**
ASME PAPER 82-GT-275	p0030	A82-35450**	DOE/NASA/0161-9A	p0134	N82-21713**
ASME PAPER 82-GT-284	p0022	A82-35456**	DOE/NASA/0161-10	p0137	N82-30712**
ASME PAPER 82-GT-287	p0012	A82-35459**	DOE/NASA/0167-80/1	p0163	N82-16237**
ASME PAPER 82-GT-288	p0012	A82-35460**	DOE/NASA/0176-81/3	p0128	N82-11545**
ASME PAPER 82-GT-292	p0108	A82-35462**	DOE/NASA/0176-81/4	p0129	N82-12573**
ASME PAPER 82-GT-303	p0104	A82-35468**	DOE/NASA/0176-81/5	p0122	N82-17615**
			DOE/NASA/0180-2	p0130	N82-14627**
AT81D006-VOL-1	p0106	N82-20540**	DOE/NASA/0180-3	p0128	N82-12506**
AT81D007-VOL-2	p0106	N82-20541**	DOE/NASA/0180-4	p0133	N82-18698**
AT81D008-VOL-3	p0106	N82-20542**	DOE/NASA/0180-5	p0134	N82-22770**
			DOE/NASA/0183-1	p0135	N82-24649**
AVRACCM-TR-80-C-21	p0016	N82-15039**	DOE/NASA/0183-1	p0135	N82-24650**
AVRACCM-TR-81-C-1	p0050	N82-30335**	DOE/NASA/0186-1	p0134	N82-22666**
AVRACCM-TR-81-C-7	p0016	N82-14090**	DOE/NASA/0197-1	p0132	N82-16494**
AVRACCM-TR-81-C-11	p0101	N82-26678**	DOE/NASA/0203-1	p0129	N82-13505**
AVRACCM-TR-82-C-2	p0049	N82-21260**	DOE/NASA/0204-1	p0137	N82-30711**
AVRACCM-TR-82-C-3	p0068	N82-24342**	DOE/NASA/0208-3	p0130	N82-14628**
AVRACCM-TR-82-C-6	p0101	N82-28643**	DOE/NASA/0208-4	p0136	N82-29718**
AVRACCM-TR-82-C-7	p0101	N82-28645**	DOE/NASA/0224-1	p0136	N82-27837**
AVRACCM-TR-82-C-8	p0101	N82-28646**	DOE/NASA/0224-1-VOL-1	p0129	N82-12570**
AVRACCM-TR-82-C-9	p0100	N82-25520**	DOE/NASA/0224-1-VOL-3	p0128	N82-10495**
AVRACCM-TR-82-C-05	p0101	N82-26681**	DOE/NASA/0224-1-VOL-4	p0133	N82-18688**
AVRACCM-TR-82-C-10	p0102	N82-32733**	DOE/NASA/0224-1-VOL-5	p0132	N82-17603**
AVRACCM-TR-82-C-11	p0102	N82-30552**	DOE/NASA/0227-1	p0104	N82-11466**
AVRACCM-TR-82-C-12	p0019	N82-26299**	DOE/NASA/0241-1	p0117	N82-13490**
AVRACCM-TR-82-C-17	p0042	N82-20240**	DOE/NASA/0241-2	p0131	N82-16483**
			DOE/NASA/0241-3	p0135	N82-24648**
BALES-MCCOIN-80-BMT-002	p0105	N82-12445**	DOE/NASA/0241-4	p0137	N82-30705**
			DOE/NASA/0277-1	p0138	N82-32856**
BCS-40357	p0163	N82-16938**	DOE/NASA/1011-35	p0058	N82-11184**
			DOE/NASA/1900-1	p0137	N82-30709**
C7SSHA-AD-217	p0025	N82-22263**	DOE/NASA/2593-24	p0118	N82-13509**
			DOE/NASA/2593-25	p0058	N82-17335**
CMZ-81-1	p0052	N82-15123**	DOE/NASA/2701-1	p0137	N82-29721**
CONF-810226	p0122	N82-23684**	DOE/NASA/2749-81/1	p0105	N82-12444**
CONF-810316	p0081	N82-15311**	DOE/NASA/2817-2	p0164	N82-18068**
			DOE/NASA/3230-1	p0129	N82-13507**
CRREL-81-19	p0117	N82-18664**	DOE/NASA/6229-2	p0137	N82-30722**
			DOE/NASA/7307-1	p0073	N82-13243**
CW-WR-81,021	p0107	N82-27743**	DOE/NASA/10350-32	p0061	N82-30373**
			DOE/NASA/10350-33-E-1313	p0124	N82-29717**
C4100-50	p0130	N82-14627**	DOE/NASA/10350-34	p0125	N82-30717**
C4100-50	p0133	N82-18698**	DOE/NASA/10769-20-REV-3	p0099	N82-12446**
			DOE/NASA/10769-21	p0119	N82-16481**
DDA-ADR-10096	p0132	N82-16485**	DOE/NASA/10769-22	p0157	N82-12943**
			DOE/NASA/10769-23	p0157	N82-13908**
EDA-EDR-10470	p0022	N82-10037**	DOE/NASA/10769-24	p0123	N82-25636**
EDA-EDR-10470-APP-B	p0022	N82-10038**	DOE/NASA/10769-25	p0157	N82-25961**
DDA-EDR-10594	p0136	N82-25635**	DOE/NASA/10769-26	p0123	N82-27838**
			DOE/NASA/10769-27	p0123	N82-26790**
			DOE/NASA/12726-9	p0123	N82-25637**
DE81-025058	p0081	N82-15311**	DOE/NASA/12726-11	p0054	N82-19333**
DE82-003288	p0120	N82-20668**	DOE/NASA/12726-13	p0120	N82-20668**
			DOE/NASA/12726-15	p0118	N82-12574**
DOE/JPL-1060-51	p0135	N82-24646**	DOE/NASA/12726-16	p0054	N82-31459**
DOE/NASA/150-81/7	p0134	N82-21709**	DOE/NASA/12726-17	p0055	N82-33463**
DOE/NASA/0032-15	p0164	N82-29235**	DOE/NASA/17088-3	p0120	N82-19670**
DOE/NASA/0032-16-VOL-1	p0164	N82-34311**	DOE/NASA/20270-1	p0117	N82-14552**
DOE/NASA/0032-18-VOL-3	p0164	N82-34312**	DOE/NASA/20305-7	p0119	N82-16495**
DOE/NASA/0035-1	p0105	N82-16409**	DOE/NASA/20305-8	p0123	N82-26807**
DOE/NASA/0037-80/2	p0122	N82-16485**	DOE/NASA/20320-34	p0119	N82-16478**
DOE/NASA/0050-1	p0133	N82-19669**	DOE/NASA/20320-36	p0121	N82-21714**
DOE/NASA/0067-79/7	p0131	N82-16482**	DOE/NASA/20320-37	p0122	N82-23679**
DOE/NASA/0083-1	p0130	N82-13510**	DOE/NASA/20320-38	p0110	N82-19550**
DOE/NASA/0097-80/1	p0136	N82-25640**	DOE/NASA/20320-39	p0121	N82-22649**
DOE/NASA/0100-1	p0133	N82-18693**	DOE/NASA/20320-41	p0127	N82-33830**
DOE/NASA/0107-3	p0131	N82-15527**	DOE/NASA/20366-2	p0125	N82-30710**
DOE/NASA/0109-1	p0065	N82-33494**	DOE/NASA/20370-20	p0119	N82-14633**
DOE/NASA/0111-1	p0136	N82-29719**	DOE/NASA/20370-22	p0120	N82-21710**
DOE/NASA/0115-80/1	p0105	N82-12445**	DOE/NASA/51040-27	p0163	N82-13013**
DOE/NASA/0123-3	p0132	N82-17608**	DOE/NASA/51040-30	p0024	N82-21193**
DOE/NASA/0123-4	p0085	N82-24425**	DOE/NASA/51040-32	p0120	N82-21712**
DOE/NASA/0124-6	p0105	N82-16410**	DOE/NASA/51040-33	p0163	N82-11993**
DOE/NASA/0124-7	p0106	N82-24496**	DOE/NASA/51040-34	p0003	N82-13114**
DOE/NASA/0125-1	p0129	N82-13506**	DOE/NASA/51040-35	p0066	N82-14359**
DOE/NASA/0145-1	p0138	N82-33827**	DOE/NASA/51040-36	p0119	N82-18691**
DOE/NASA/0145-2	p0074	N82-26482**	DOE/NASA/51040-38	p0060	N82-24323**
DOE/NASA/0146-1	p0136	N82-24725**	DOE/NASA/51040-39	p0061	N82-30372**
DOE/NASA/0146-2	p0055	N82-22326**	DOE/NASA/51040-40	p0163	N82-26051**
DOE/NASA/0147-1	p0135	N82-24651**	DOE/NASA/51044-22	p0118	N82-10503**
DOE/NASA/0147-2	p0055	N82-25337**	DOE/NASA/51044-24	p0124	N82-28786**
DOE/NASA/0148-1	p0136	N82-25635**	DOE/NASA/51044-25	p0127	N82-33829**
DOE/NASA/0148-2	p0055	N82-25338**	DOE/NASA/51044-26	p0124	N82-30700**

ORIGINAL PAGE IS
OF POOR QUALITY

REPORT/ACCESSION NUMBER INDEX

DOE/NA SA/5 1044-27	p0163	N82-31160**	E-1020	p0125	N82-30710**
DOE/NA SA/5 1044-28	p0082	N82-33636**	E-1022	p0049	N82-16181**
DOT-TSC-NASA-81-2	p0164	N82-18068**	E-1023	p0048	N82-15119**
D6-51418	p0007	N82-22211**	E-1024	p0037	N82-11106**
D180-2595-4-VOL-2	p0044	N82-11111**	E-1025	p0118	N82-12574**
D180-25956-3-VOL-1	p0046	N82-11110**	E-1026-5	p0066	N82-14359**
D180-2E590-1	p0129	N82-12571**	E-1027	p0003	N82-11043**
E-82-4	p0091	N82-31641**	E-1028	p0095	N82-23515**
E-116	p0049	N82-21260**	E-1029	p0020	N82-31329**
E-209	p0099	N82-16413**	E-1031	p0003	N82-11042**
E-2C9	p0100	N82-25518**	E-1032	p0120	N82-19672**
E-259	p0017	N82-19222**	E-1034	p0151	N82-12890**
E-276	p0095	N82-19521**	E-1035	p0102	N82-31691**
E-280	p0016	N82-15039**	E-1040	p0118	N82-13504**
E-334	p0018	N82-22269**	E-1042	p0099	N82-16412**
E-551	p0018	N82-25250**	E-1044	p0123	N82-25636**
E-556	p0016	N82-15040**	E-1045	p0049	N82-11117**
E-559	p0020	N82-33389**	E-1046	p0119	N82-16481**
E-573	p0152	N82-24942**	E-1047	p0119	N82-18694**
E-621	p0087	N82-11397**	E-1048	p0121	N82-23678**
E-626	p0111	N82-20566**	E-1050	p0066	N82-15199**
E-638	p0058	N82-20291**	E-1051	p0151	N82-16808**
E-646	p0151	N82-19944**	E-1053	p0151	N82-12891**
E-648	p0016	N82-13143**	E-1056	p0004	N82-18178**
E-654	p0067	N82-19374**	E-1057	p0157	N82-12943**
E-668	p0014	N82-11053**	E-1058	p0111	N82-16419**
E-678	p0059	N82-21300**	E-1059	p0149	N82-14849**
E-682	p0087	N82-20467**	E-1063	p0003	N82-13112**
E-687	p0111	N82-20565**	E-1065	p0049	N82-14287**
E-708	p0081	N82-15313**	E-1066	p0157	N82-13908**
E-709	p0066	N82-11211**	E-1067	p0119	N82-16478**
E-709	p0066	N82-16239**	E-1068	p0151	N82-16809**
E-711	p0058	N82-12216**	E-1069	p0099	N82-14519**
E-713	p0059	N82-21298**	E-1070	p0031	N82-19229**
E-719	p0003	N82-14051**	E-1071	p0095	N82-14494**
E-721	p0119	N82-16477**	E-1072	p0069	N82-32491**
E-722	p0082	N82-25441**	E-1073	p0072	N82-28460**
E-732	p0016	N82-14090**	E-1074	p0017	N82-15041**
E-737	p0118	N82-13509**	E-1076	p0066	N82-15198**
E-749	p0058	N82-17335**	E-1077	p0058	N82-11184**
E-757	p0095	N82-22481**	E-1078	p0003	N82-12043**
E-758	p0067	N82-19373**	E-1081	p0004	N82-16049**
E-777	p0152	N82-21036**	E-1082	p0119	N82-16495**
E-775	p0146	N82-33020**	E-1084	p0016	N82-14094**
E-828	p0117	N82-14552**	E-1085	p0003	N82-13113**
E-830	p0124	N82-30704**	E-1086	p0151	N82-14881**
E-871	p0163	N82-13013**	E-1089	p0120	N82-19673**
E-876	p0004	N82-26234**	E-1090	p0120	N82-19671**
E-897	p0100	N82-25511**	E-1096	p0016	N82-13146**
E-899	p0024	N82-21193**	E-1097	p0017	N82-21194**
E-915	p0088	N82-30498**	E-1098	p0143	N82-16743**
E-916	p0068	N82-22366**	E-1104	p0005	N82-29270**
E-919	p0059	N82-21301**	E-1106	p0162	N82-20006**
E-921	p0066	N82-15197**	E-1107	p0017	N82-19220**
E-936	p0102	N82-32736**	E-1110	p0048	N82-17263**
E-939	p0123	N82-25637**	E-1111	p0068	N82-24342**
E-941	p0004	N82-25213**	E-1112	p0038	N82-18311**
E-946	p0161	N82-32186**	E-1113	p0017	N82-16084**
E-947	p0161	N82-32187**	E-1114	p0001	N82-17083**
E-948	p0161	N82-32188**	E-1116	p0122	N82-23679**
E-949	p0161	N82-32189**	E-1118	p0103	N82-32737**
E-953	p0120	N82-21712**	E-1120	p0076	N82-20339**
E-955	p0019	N82-25255**	E-1121	p0099	N82-16411**
E-959	p0110	N82-18612**	E-1126	p0018	N82-21195**
E-960	p0151	N82-15847**	E-1128	p0121	N82-21714**
E-962	p0118	N82-11551**	E-1129	p0087	N82-17453**
E-967	p0054	N82-19333**	E-1131	p0087	N82-19493**
E-972	p0019	N82-27311**	E-1137	p0100	N82-20543**
E-975	p0067	N82-20316**	E-1138	p0076	N82-22386**
E-976	p0068	N82-21332**	E-1139	p0087	N82-19494**
E-982	p0017	N82-18222**	E-1140	p0072	N82-21415**
E-985	p0058	N82-10195**	E-1141	p0054	N82-22327**
E-990	p0020	N82-29324**	E-1142	p0110	N82-19550**
E-991	p0118	N82-10503**	E-1143	p0067	N82-20314**
E-993	p0058	N82-11183**	E-1144	p0152	N82-21998**
E-995	p0111	N82-11491**	E-1145	p0050	N82-22313**
E-999	p0058	N82-11182**	E-1146	p0049	N82-21258**
E-1001	p0060	N82-22349**	E-1147	p0042	N82-20240**
E-1002	p0101	N82-26678**	E-1149	p0067	N82-20313**
E-1003	p0037	N82-11107**	E-1150	p0076	N82-22387**
E-1004	p0016	N82-13144**	E-1151	p0110	N82-20551**
E-1005	p0120	N82-21710**	E-1152	p0049	N82-21259**
E-1007	p0004	N82-15020**	E-1155	p0050	N82-24300**
E-1013	p0005	N82-28247**	E-1156	p0111	N82-21604**
E-1017	p0081	N82-22439**	E-1161	p0059	N82-22344**
E-1018	p0081	N82-23397**	E-1162	p0018	N82-22262**
			E-1163	p0018	N82-22266**
			E-1168	p0102	N82-32735**
			E-1171	p0125	N82-30714**

REPORT/ACCESSION NUMBER INDEX

E-1175	p0050	N82-24297**	E-1345	p0102	N82-32734**
E-1176	p0060	N82-24323**	E-1346	p0127	N82-33830**
E-1177	p0147	N82-22915**	E-1351	p0125	N82-30715**
E-1178	p0096	N82-32662**	E-1352	p0125	N82-30716**
E-1181	p0069	N82-29458**	EDR-10383	p0164	N82-31158**
E-1182	p0067	N82-21331**	EDR-10950	p0055	N82-25338**
E-1185	p0042	N82-24286**	EE-273 (82) NASA-931-1	p0131	N82-16479**
E-1186	p0060	N82-24325**	ERC-TR-8101	p0129	N82-13506**
E-1189	p0095	N82-31664**	ERC-TR-8125	p0105	N82-16410**
E-1191	p0102	N82-32733**	ERC-TR-8175	p0132	N82-17608**
E-1192	p0076	N82-22388**	ERC-TR-8186	p0085	N82-24425**
E-1194	p0068	N82-24343**	ERC-TR-8191	p0106	N82-24496**
E-1195	p0059	N82-22346**	ERC#1054.36FR	p0159	N82-23030**
E-1196	p0102	N82-30552**	ESL-TR-79-23	p0025	N82-22265**
E-1198	p0100	N82-24497**	ES2-10247	p0117	N82-24525**
E-1199	p0069	N82-29459**	FBMHL-NAS-E-2	p0105	N82-14520**
E-1200	p0068	N82-26468**	FCR-3142	p0132	N82-17607**
E-1201	p0087	N82-22453**	FR-81-75/EE	p0134	N82-22666**
E-1202	p0089	N82-32634**	FR-10C20	p0128	N82-11546**
E-1204	p0061	N82-30372**	FR-10081	p0137	N82-30706**
E-1205	p0163	N82-27191**	FR-15596	p0025	N82-23246**
E-1207	p0060	N82-24322**	FSI-251	p0078	N82-17420**
E-1209	p0101	N82-26681**	GABRETT-21-3911	p0026	N82-24202**
E-1210	p0018	N82-24201**	GDC-AST-81-019-VOL-2	p0130	N82-14637**
E-1211	p0095	N82-28605**	GDC-NAS-82-001	p0045	N82-24287**
E-1212	p0152	N82-22951**	GDC-NAS-82-002	p0045	N82-24288**
E-1213	p0149	N82-22922**	GE-B81AEG288	p0027	N82-27310**
E-1214	p0123	N82-24647**	GE-8 ISDS4215	p0084	N82-23395**
F-1215	p0112	N82-24502**	GTR-3932	p0133	N82-18690**
E-1216	p0111	N82-24501**	G7782	p0113	N82-17521**
E-1217	p0004	N82-24165**	HMT-32	p0090	N82-17456**
E-1218	p0163	N82-26051**	IAP PAPER 82-46	p0033	N82-44659**
E-1219	p0038	N82-23261**	IAP PAPER 82-408	p0043	N82-44750**
E-1221	p0019	N82-26297**	IGT-61051	p0130	N82-14628**
E-1222	p0060	N82-24326**	IITRI-J06519	p0132	N82-16494**
E-1223	p0054	N82-31459**	IITRI-M06001-89	p0063	N82-10193**
E-1224	p0088	N82-24455**	ITR-1	p0115	N82-33738**
E-1225	p0100	N82-25519**	JPL-PUB-82-22	p0135	N82-24646**
E-1226	p0100	N82-25520**	KMSF-U-1185	p0098	N82-25499**
E-1228	p0005	N82-28250**	KU-FRI-464-3	p0014	N82-11052**
E-1229	p0036	N82-25290**	LG81ER0202-VOL-1	p0028	N82-32370**
E-1232	p0082	N82-33636**	LR-29935-VOL-1	p0073	N82-11224**
E-1233	p0157	N82-25961**	LYC-81-32-VOL-1	p0153	N82-21031**
E-1234	p0101	N82-28646**	LYC-81-32-VOL-2	p0153	N82-21032**
E-1235	p0101	N82-28645**	LYC-81-32-VOL-3	p0155	N82-21033**
E-1236	p0042	N82-29354**	LYC-82-15	p0028	N82-32367**
E-1238	p0050	N82-30335**	MCR-81-597	p0039	N82-15117**
E-1245	p0088	N82-26611**	MCR81-504	p0044	N82-18315**
E-1246	p0148	N82-30992**	MDC-A6930	p0006	N82-17122**
E-1247	p0126	N82-31776**	NE-TSPC-TR-82-11	p0008	N82-26237**
E-1249	p0069	N82-28445**	NSNW-1169	p0132	N82-17606**
E-1250	p0146	N82-31971**	MTI-80ASE142DR1-VOL-1	p0164	N82-34311**
E-1254	p0072	N82-26483**	MTI-91ASE229QT13	p0164	N82-29235**
E-1255	p0061	N82-30373**			
E-1256	p0018	N82-24203**			
E-1257	p0005	N82-26241**			
E-1260	p0072	N82-32504**			
E-1263	p0005	N82-28249**			
E-1264	p0095	N82-31663**			
E-1265	p0149	N82-24859**			
E-1269	p0001	N82-26219**			
E-1270	p0042	N82-31443**			
E-1272	p0044	N82-26240**			
E-1273	p0163	N82-31160**			
E-1276	p0112	N82-31708**			
E-1280	p0051	N82-30336**			
E-1282	p0126	N82-32853**			
E-1283	p0127	N82-33829**			
E-1284	p0089	N82-32633**			
E-1285	p0126	N82-32854**			
E-1286	p0126	N82-31777**			
E-1288	p0042	N82-27358**			
E-1289	p0061	N82-32461**			
E-1293	p0124	N82-30700**			
E-1294	p0123	N82-26790**			
E-1295	p0101	N82-28644**			
E-1298	p0061	N82-33493**			
E-1304	p0019	N82-26298**			
E-1305	p0126	N82-33828**			
E-1307	p0013	N82-30297**			
E-1308	p0125	N82-30713**			
E-1310	p0069	N82-30401**			
E-1316	p0152	N82-32082**			
E-1318	p0055	N82-33463**			
E-1322	p0082	N82-30474**			
E-1324	p0149	N82-29075**			
E-1326	p0125	N82-30717**			
E-1332	p0152	N82-31068**			
E-1335	p0144	N82-30949**			

MTI82-TR-4 p0104 N82-11466**
N364 p0141 N82-16659**
WAPC-PI-23 p0027 N82-27316**
NAS 1. 15:81694 p0100 N82-25518**
NAS 1. 15:81767 p0124 N82-30704**
NAS 1. 15:82644 p0024 N82-21193**
NAS 1. 15:82665 p0123 N82-25637**
NAS 1. 15:82671 p0120 N82-21712**
NAS 1. 15:82691 p0019 N82-27311**
NAS 1. 15:82707 p0120 N82-20668**
NAS 1. 15:82708 p0020 N82-29324**
NAS 1. 15:82711 p0120 N82-21710**
NAS 1. 15:82721 p0125 N82-30710**
NAS 1. 15:82736 p0121 N82-23678**
NAS 1. 15:82772 p0017 N82-21194**
NAS 1. 15:82784 p0122 N82-23679**
NAS 1. 15:82785 p0076 N82-20339**
NAS 1. 15:82787 p0019 N82-25255**
NAS 1. 15:82789 p0004 N82-25213**
NAS 1. 15:82792 p0018 N82-21195**
NAS 1. 15:82794 p0121 N82-21714**
NAS 1. 15:82798 p0100 N82-20543**
NAS 1. 15:82799 p0076 N82-22386**
NAS 1. 15:82801 p0072 N82-21415**
NAS 1. 15:82802 p0054 N82-22327**
NAS 1. 15:82804 p0121 N82-22649**
NAS 1. 15:82805 p0152 N82-21998**
NAS 1. 15:82806 p0049 N82-21258**
NAS 1. 15:82807 p0042 N82-20240**
NAS 1. 15:82808 p0067 N82-20313**
NAS 1. 15:82809 p0076 N82-22387**
NAS 1. 15:82810 p0110 N82-20551**
NAS 1. 15:82811 p0049 N82-21259**
NAS 1. 15:82812 p0050 N82-24300**
NAS 1. 15:82813 p0111 N82-21604**
NAS 1. 15:82814 p0059 N82-22344**
NAS 1. 15:82815 p0018 N82-22262**
NAS 1. 15:82816 p0018 N82-22266**
NAS 1. 15:82817 p0049 N82-21260**
NAS 1. 15:82819 p0067 N82-20314**
NAS 1. 15:82820 p0102 N82-32735**
NAS 1. 15:82821 p0068 N82-24342**
NAS 1. 15:82822 p0125 N82-30714**
NAS 1. 15:82823 p0050 N82-24297**
NAS 1. 15:82824 p0060 N82-24323**
NAS 1. 15:82825 p0147 N82-22915**
NAS 1. 15:82826 p0067 N82-21331**
NAS 1. 15:82827 p0042 N82-24286**
NAS 1. 15:82828 p0060 N82-24325**
NAS 1. 15:82829 p0068 N82-24343**
NAS 1. 15:82830 p0059 N82-22346**
NAS 1. 15:82831 p0112 N82-26701**
NAS 1. 15:82832 p0069 N82-29459**
NAS 1. 15:82833 p0050 N82-22313**
NAS 1. 15:82834 p0068 N82-26468**
NAS 1. 15:82835 p0087 N82-22453**
NAS 1. 15:82836 p0124 N82-28786**
NAS 1. 15:82837 p0061 N82-30372**
NAS 1. 15:82838 p0163 N82-27191**
NAS 1. 15:82839 p0060 N82-24322**
NAS 1. 15:82840 p0101 N82-26681**
NAS 1. 15:82841 p0095 N82-28605**
NAS 1. 15:82842 p0152 N82-22951**
NAS 1. 15:82843 p0149 N82-22922**
NAS 1. 15:82844 p0123 N82-24647**
NAS 1. 15:82845 p0112 N82-24502**
NAS 1. 15:82846 p0111 N82-24501**
NAS 1. 15:82847 p0004 N82-24165**
NAS 1. 15:82848 p0163 N82-26051**
NAS 1. 15:82849 p0038 N82-23261**
NAS 1. 15:82850 p0112 N82-31707**
NAS 1. 15:82851 p0018 N82-24201**
NAS 1. 15:82852 p0060 N82-24326**
NAS 1. 15:82853 p0076 N82-22388**
NAS 1. 15:82854 p0054 N82-31459**
NAS 1. 15:82855 p0088 N82-24455**
NAS 1. 15:82856 p0100 N82-25519**
NAS 1. 15:82857 p0100 N82-25520**
NAS 1. 15:82858 p0069 N82-29458**
NAS 1. 15:82859 p0101 N82-28643**
NAS 1. 15:82860 p0005 N82-28250**
NAS 1. 15:82861 p0036 N82-25290**
NAS 1. 15:82862 p0019 N82-26300**
NAS 1. 15:82863 p0082 N82-33636**
NAS 1. 15:82864 p0157 N82-25961**

NAS 1. 15:82865 p0101 N82-28646**
NAS 1. 15:82866 p0101 N82-28645**
NAS 1. 15:82867 p0042 N82-29354**
NAS 1. 15:82868 p0050 N82-30335**
NAS 1. 15:82869 p0019 N82-26297**
NAS 1. 15:82871 p0148 N82-30992**
NAS 1. 15:82872 p0126 N82-31776**
NAS 1. 15:82873 p0069 N82-28445**
NAS 1. 15:82874 p0146 N82-31971**
NAS 1. 15:82875 p0123 N82-25636**
NAS 1. 15:82877 p0019 N82-26299**
NAS 1. 15:82878 p0072 N82-26483**
NAS 1. 15:82879 p0061 N82-30373**
NAS 1. 15:82880 p0018 N82-24203**
NAS 1. 15:82881 p0005 N82-26241**
NAS 1. 15:82882 p0051 N82-31449**
NAS 1. 15:82883 p0072 N82-32504**
NAS 1. 15:82884 p0100 N82-24497**
NAS 1. 15:82885 p0005 N82-28249**
NAS 1. 15:82886 p0095 N82-31663**
NAS 1. 15:82887 p0102 N82-32733**
NAS 1. 15:82888 p0102 N82-30552**
NAS 1. 15:82889 p0149 N82-24859**
NAS 1. 15:82891 p0001 N82-26219**
NAS 1. 15:82892 p0042 N82-31443**
NAS 1. 15:82894 p0004 N82-26240**
NAS 1. 15:82895 p0163 N82-31160**
NAS 1. 15:82896 p0112 N82-31708**
NAS 1. 15:82897 p0123 N82-27838**
NAS 1. 15:82899 p0126 N82-32853**
NAS 1. 15:82900 p0127 N82-33829**
NAS 1. 15:82901 p0089 N82-32633**
NAS 1. 15:82902 p0126 N82-32854**
NAS 1. 15:82903 p0126 N82-31777**
NAS 1. 15:82904 p0042 N82-27358**
NAS 1. 15:82905 p0061 N82-32461**
NAS 1. 15:82906 p0123 N82-26807**
NAS 1. 15:82908 p0072 N82-27519**
NAS 1. 15:82909 p0123 N82-26790**
NAS 1. 15:82910 p0101 N82-28644**
NAS 1. 15:82911 p0088 N82-26611**
NAS 1. 15:82912 p0124 N82-30700**
NAS 1. 15:82913 p0055 N82-33463**
NAS 1. 15:82914 p0095 N82-31664**
NAS 1. 15:82915 p0019 N82-26298**
NAS 1. 15:82916 p0072 N82-28460**
NAS 1. 15:82917 p0126 N82-33828**
NAS 1. 15:82919 p0013 N82-30297**
NAS 1. 15:82921 p0125 N82-30713**
NAS 1. 15:82922 p0124 N82-29717**
NAS 1. 15:82924 p0152 N82-32082**
NAS 1. 15:82925 p0089 N82-32634**
NAS 1. 15:82927 p0096 N82-32662**
NAS 1. 15:82928 p0082 N82-30474**
NAS 1. 15:82929 p0051 N82-30336**
NAS 1. 15:82930 p0125 N82-30717**
NAS 1. 15:82931 p0149 N82-29075**
NAS 1. 15:82933 p0061 N82-33493**
NAS 1. 15:82936 p0152 N82-31066**
NAS 1. 15:82937 p0144 N82-30949**
NAS 1. 15:82942 p0069 N82-30401**
NAS 1. 15:82943 p0102 N82-32734**
NAS 1. 15:82944 p0127 N82-33830**
NAS 1. 15:82945 p0125 N82-30715**
NAS 1. 15:82946 p0125 N82-30716**
NAS 1. 15:84194 p0117 N82-24525**
NAS 1. 15:84207 p0015 N82-23241**
NAS 1. 15:84743 p0081 N82-24431**
NAS 1. 26:3492 p0090 N82-22458**
NAS 1. 26:3494 p0091 N82-22460**
NAS 1. 26:3513 p0008 N82-26229**
NAS 1. 26:3539 p0007 N82-22214**
NAS 1. 26:3543 p0064 N82-26436**
NAS 1. 26:3553 p0106 N82-25516**
NAS 1. 26:3560 p0008 N82-26230**
NAS 1. 26:3563 p0027 N82-26295**
NAS 1. 26:159559 p0085 N82-23394**
NAS 1. 26:159656 p0025 N82-22265**
NAS 1. 26:165149 p0031 N82-32383**
NAS 1. 26:165168 p0084 N82-24424**
NAS 1. 26:165197 p0164 N82-31158**
NAS 1. 26:165198 p0134 N82-22675**
NAS 1. 26:165203 p0106 N82-20540**
NAS 1. 26:165204 p0106 N82-20541**
NAS 1. 26:165205 p0106 N82-20542**
NAS 1. 26:165213 p0052 N82-20248**
NAS 1. 26:165218 p0136 N82-25640**
NAS 1. 26:165289 p0137 N82-30722**
NAS 1. 26:165327-VOL-1 p0135 N82-24649**

REPORT/ACCESSION NUMBER INDEX

NAS 1.26:165327-VOL-2	p0135	N82-24650**	NAS 1.26:167877	p0055	N82-25337**
NAS 1.26:165364	p0146	N82-31968**	NAS 1.26:167879	p0025	N82-23246**
NAS 1.26:165365	p0146	N82-31969**	NAS 1.26:167883	p0091	N82-24452**
NAS 1.26:165366	p0146	N82-31970**	NAS 1.26:167885	p0045	N82-26381**
NAS 1.26:165367	p0136	N82-25635**	NAS 1.26:167886	p0033	N82-29345**
NAS 1.26:165378	p0134	N82-22666**	NAS 1.26:167889-VOL-1	p0045	N82-33424**
NAS 1.26:165388	p0027	N82-27316**	NAS 1.26:167889-VOL-2	p0046	N82-33425**
NAS 1.26:165397	p0028	N82-29323**	NAS 1.26:167892	p0064	N82-30374**
NAS 1.26:165398	p0107	N82-27743**	NAS 1.26:167894	p0137	N82-29720**
NAS 1.26:165409-VOL-1	p0078	N82-20362**	NAS 1.26:167895	p0014	N82-33375**
NAS 1.26:165409-VOL-2	p0078	N82-20363**	NAS 1.26:167896	p0027	N82-25257**
NAS 1.26:165409-VOL-3	p0078	N82-20364**	NAS 1.26:167897	p0114	N82-29619**
NAS 1.26:165409-VOL-4	p0078	N82-20365**	NAS 1.26:167898	p0137	N82-30705**
NAS 1.26:165412	p0113	N82-26713**	NAS 1.26:167904	p0142	N82-23976**
NAS 1.26:165431	p0084	N82-23395**	NAS 1.26:167907	p0164	N82-29235**
NAS 1.26:165433	p0114	N82-26714**	NAS 1.26:167908	p0106	N82-26679**
NAS 1.26:165434	p0114	N82-26715**	NAS 1.26:167909	p0052	N82-29363**
NAS 1.26:165438	p0114	N82-26716**	NAS 1.26:167911	p0034	N82-27331**
NAS 1.26:165439	p0114	N82-26717**	NAS 1.26:167912	p0074	N82-31546**
NAS 1.26:165440	p0114	N82-26718**	NAS 1.26:167914	p0029	N82-33392**
NAS 1.26:165448	p0052	N82-31448**	NAS 1.26:167918	p0079	N82-25423**
NAS 1.26:165449	p0135	N82-24651**	NAS 1.26:167920	p0009	N82-32310**
NAS 1.26:165452-VOL-2	p0136	N82-27837**	NAS 1.26:167924	p0079	N82-31584**
NAS 1.26:165452-VOL-3	p0136	N82-27837**	NAS 1.26:167928-VOL-1	p0028	N82-32370**
NAS 1.26:165459	p0025	N82-22264**	NAS 1.26:167929	p0137	N82-30706**
NAS 1.26:165476	p0097	N82-22479**	NAS 1.26:167930	p0139	N82-29777**
NAS 1.26:165481	p0138	N82-33827**	NAS 1.26:167934	p0078	N82-31585**
NAS 1.26:165482	p0136	N82-24725**	NAS 1.26:167935	p0164	N82-34311**
NAS 1.26:165497	p0113	N82-26702**	NAS 1.26:167937	p0164	N82-34312**
NAS 1.26:165498	p0113	N82-26706**	NAS 1.26:167938	p0107	N82-29607**
NAS 1.26:165503	p0026	N82-23248**	NAS 1.26:167941	p0009	N82-29269**
NAS 1.26:165507	p0085	N82-24425**	NAS 1.26:167944	p0028	N82-33390**
NAS 1.26:165510	p0106	N82-24496**	NAS 1.26:167948	p0065	N82-31509**
NAS 1.26:165520	p0098	N82-25499**	NAS 1.26:167949	p0028	N82-33391**
NAS 1.26:165521	p0044	N82-21252**	NAS 1.26:167984	p0009	N82-33347**
NAS 1.26:165544	p0064	N82-27462**	NAS 1.26:167996	p0029	N82-33394**
NAS 1.26:165549	p0064	N82-26439**	NAS 1.26:168760	p0084	N82-22438**
NAS 1.26:165554	p0027	N82-27310**	NAS 1.26:168842	p0090	N82-22455**
NAS 1.26:165556	p0027	N82-28297**	NAS 1.26:168894	p0026	N82-23247**
NAS 1.26:165557	p0029	N82-33393**	NAS 1.26:168929	p0076	N82-24361**
NAS 1.26:165560	p0138	N82-32856**	NAS 1.26:168930	p0113	N82-24503**
NAS 1.26:165562-VOL-1	p0153	N82-21031**	NAS 1.26:168941	p0135	N82-24646**
NAS 1.26:165562-VOL-2	p0153	N82-21032**	NAS 1.26:169003	p0026	N82-25252**
NAS 1.26:165562-VOL-3	p0155	N82-21033**	NAS 1.26:169004	p0026	N82-25253**
NAS 1.26:165563	p0113	N82-20564**	NAS 1.26:169005	p0085	N82-25442**
NAS 1.26:165564	p0025	N82-22263**	NAS 1.26:169016	p0153	N82-27090**
NAS 1.26:165565	p0025	N82-22268**	NAS 1.26:169029	p0106	N82-26680**
NAS 1.26:165568	p0135	N82-24648**	NAS 1.26:169034	p0079	N82-25262**
NAS 1.26:165572	p0027	N82-27309**	NAS 1.26:169120	p0091	N82-27686**
NAS 1.26:165573	p0027	N82-28296**	NAS 1.26:169125	p0079	N82-28503**
NAS 1.26:165578	p0134	N82-21709**	NAS 1.26:169278	p0091	N82-31638**
NAS 1.26:165580	p0025	N82-21197**	NAS 1.26:169283	p0091	N82-31639**
NAS 1.26:165583	p0158	N82-24078**	NAS 1.26:169293	p0091	N82-31641**
NAS 1.26:165585	p0044	N82-21253**	NAS 1.26:169294	p0092	N82-31642**
NAS 1.26:165586	p0024	N82-21196**	NAS 1.26:169295	p0092	N82-31643**
NAS 1.26:165587	p0007	N82-21158**	NAS 1.26:169358	p0115	N82-33738**
NAS 1.26:165589	p0137	N82-30709**	NAS 1.26:169852	p0065	N82-33494**
NAS 1.26:165593	p0159	N82-23030**	NAS 1.26:185193	p0137	N82-30712**
NAS 1.26:165596	p0009	N82-28253**	NAS 1.55:2185	p0122	N82-23684**
NAS 1.26:165599	p0008	N82-24166**	NAS 1.60:1851	p0146	N82-33020**
NAS 1.26:165600	p0007	N82-22210**	NAS 1.60:1868	p0095	N82-22481**
NAS 1.26:165602	p0028	N82-32367**	NAS 1.60:1882	p0100	N82-25514**
NAS 1.26:165603	p0045	N82-24285**	NAS 1.60:1884	p0088	N82-30498**
NAS 1.26:165604	p0045	N82-28350**	NAS 1.60:1906	p0161	N82-32186**
NAS 1.26:165605	p0064	N82-28409**	NAS 1.60:1907	p0161	N82-32187**
NAS 1.26:165606	p0136	N82-29718**	NAS 1.60:1908	p0161	N82-32188**
NAS 1.26:165607	p0002	N82-22142**	NAS 1.60:1909	p0161	N82-32189**
NAS 1.26:165609	p0074	N82-24353**	NAS 1.60:1967	p0087	N82-20467**
NAS 1.26:165610	p0026	N82-24202**	NAS 1.60:1968	p0152	N82-21036**
NAS 1.26:165611	p0028	N82-31328**	NAS 1.60:1973	p0111	N82-20566**
NAS 1.26:165614	p0055	N82-22326**	NAS 1.60:1982	p0111	N82-20565**
NAS 1.26:165615	p0055	N82-25338**	NAS 1.60:1985	p0058	N82-20291**
NAS 1.26:165616	p0134	N82-20661**	NAS 1.60:1986	p0067	N82-20316**
NAS 1.26:165617	p0007	N82-22211**	NAS 1.60:1989	p0059	N82-21300**
NAS 1.26:165620	p0134	N82-21713**	NAS 1.60:1990	p0059	N82-21298**
NAS 1.26:165621	p0045	N82-22309**	NAS 1.60:1991	p0059	N82-21301**
NAS 1.26:165622	p0045	N82-24287**	NAS 1.60:1992	p0081	N82-22439**
NAS 1.26:167841	p0045	N82-24288**	NAS 1.60:1994	p0068	N82-21332**
NAS 1.26:167846	p0008	N82-26239**	NAS 1.60:1995	p0152	N82-24942**
NAS 1.26:167849	p0026	N82-25254**	NAS 1.60:1999	p0082	N82-25441**
NAS 1.26:167853	p0025	N82-22267**	NAS 1.60:2001	p0018	N82-22269**
NAS 1.26:167855	p0146	N82-25810**	NAS 1.60:2002	p0068	N82-22366**
NAS 1.26:167856	p0040	N82-26377**	NAS 1.60:2006	p0060	N82-22349**
NAS 1.26:167857	p0040	N82-26378**	NAS 1.60:2007	p0095	N82-23515**
NAS 1.26:167861	p0008	N82-26237**	NAS 1.60:2008	p0081	N82-23397**
NAS 1.26:167867	p0136	N82-29719**	NAS 1.60:2018	p0004	N82-26234**
NAS 1.26:167869	p0138	N82-32855**	NAS 1.60:2020	p0018	N82-25250**
NAS 1.26:167872	p0137	N82-30711**	NAS 1.60:2027	p0101	N82-26678**
NAS 1.26:167876	p0074	N82-26482**	NAS 1.60:2028	p0020	N82-31329**

NAS 1.60:2029 p0005 N82-29270**
 NAS 1.60:2030 p0005 N82-28247**
 NAS 1.60:2037 p0103 N82-32737**
 NAS 1.60:2040 p0102 N82-31691**
 NAS 1.60:2047 p0102 N82-32736**
 NAS 1.60:2048 p0069 N82-32491**
 NAS 1.60:2049 p0020 N82-33389**

 NASA-CASE-LEW-12131-3 p0099 N82-19540**
 NASA-CASE-LEW-12296-1 p0082 N82-26568**
 NASA-CASE-LEW-12358-2 p0054 N82-21268**
 NASA-CASE-LEW-12508-3 p0088 N82-24449**
 NASA-CASE-LEW-12582-1 p0094 N82-31450**
 NASA-CASE-LEW-12919-2 p0050 N82-26386**
 NASA-CASE-LEW-12938-1 p0020 N82-32366**
 NASA-CASE-LEW-12950-1 p0087 N82-11399**
 NASA-CASE-LEW-12989-1 p0099 N82-12442**
 NASA-CASE-LEW-13028-1 p0070 N82-33521**
 NASA-CASE-LEW-13080-2 p0066 N82-11210**
 NASA-CASE-LEW-13120-1 p0068 N82-28440**
 NASA-CASE-LEW-13169-1 p0060 N82-29415**
 NASA-CASE-LEW-13169-2 p0061 N82-30371**
 NASA-CASE-LEW-13171-1 p0124 N82-29708**
 NASA-CASE-LEW-13199-1 p0019 N82-26293**
 NASA-CASE-LEW-13268-1 p0069 N82-29453**
 NASA-CASE-LEW-13268-2 p0101 N82-26674**
 NASA-CASE-LEW-13282-1 p0081 N82-24415**
 NASA-CASE-LEW-13374-1 p0060 N82-26431**
 NASA-CASE-LEW-13339-1 p0061 N82-31505**
 NASA-CASE-LEW-13343-1 p0068 N82-28441**
 NASA-CASE-LEW-13349-1 p0121 N82-22673**
 NASA-CASE-LEW-13400-1 p0125 N82-31764**
 NASA-CASE-LEW-13401-1 p0124 N82-29709**
 NASA-CASE-LEW-13401-2 p0123 N82-24717**
 NASA-CASE-LEW-13426-1 p0126 N82-31769**
 NASA-CASE-LEW-13450-1 p0088 N82-25463**
 NASA-CASE-LEW-13495-1 p0082 N82-24432**
 NASA-CASE-LEW-13526-1 p0059 N82-22347**
 NASA-CASE-LEW-13622-1 p0019 N82-26294**
 NASA-CASE-LEW-13639-1 p0070 N82-33522**
 NASA-CASE-LEW-13653-1 p0121 N82-22672**
 NASA-CASE-LEW-13826-1 p0050 N82-26385**

 NASA-CR-2182 p0037 N82-14213**
 NASA-CR-2185 p0122 N82-23684**

 NASA-CR-3481 p0141 N82-16659**
 NASA-CR-3492 p0090 N82-22458**
 NASA-CR-3493 p0091 N82-22459**
 NASA-CR-3494 p0091 N82-22460**
 NASA-CR-3505 p0007 N82-19178**
 NASA-CR-3506 p0110 N82-18613**
 NASA-CR-3507 p0006 N82-16044**
 NASA-CR-3508 p0006 N82-17122**
 NASA-CR-3509 p0006 N82-18184**
 NASA-CR-3510 p0090 N82-17456**
 NASA-CR-3513 p0008 N82-26229**
 NASA-CR-3539 p0007 N82-22214**
 NASA-CR-3543 p0064 N82-26436**
 NASA-CR-3553 p0106 N82-25516**
 NASA-CR-3560 p0008 N82-26230**
 NASA-CR-3563 p0027 N82-26295**
 NASA-CR-159559 p0085 N82-23394**
 NASA-CF-159656 p0025 N82-22265**
 NASA-CF-159841 p0105 N82-12445**
 NASA-CF-164966 p0014 N82-11052**
 NASA-CF-164972 p0159 N82-11959**
 NASA-CR-165029 p0063 N82-13217**
 NASA-CR-165051 p0052 N82-14286**
 NASA-CR-165053 p0105 N82-14520**
 NASA-CR-165061 p0090 N82-15360**
 NASA-CR-165081 p0131 N82-16479**
 NASA-CR-165120 p0153 N82-16810**
 NASA-CR-165130 p0132 N82-16485**
 NASA-CR-165149 p0031 N82-32383**
 NASA-CR-165154 p0078 N82-17420**
 NASA-CR-165163 p0104 N82-10401**
 NASA-CF-165168 p0084 N82-24424**
 NASA-CR-165175 p0163 N82-16937**
 NASA-CR-165182 p0105 N82-16410**
 NASA-CR-165193 p0137 N82-30712**
 NASA-CR-165197 p0164 N82-31158**
 NASA-CR-165198 p0134 N82-22675**
 NASA-CR-165203 p0106 N82-20540**
 NASA-CR-165204 p0106 N82-20541**
 NASA-CR-165205 p0106 N82-20542**
 NASA-CR-165213 p0052 N82-20248**
 NASA-CR-165218 p0136 N82-25640**
 NASA-CR-165219 p0105 N82-13427**

NASA-CR-165224 p0063 N82-18370**
 NASA-CR-165226 p0105 N82-16409**
 NASA-CR-165234 p0064 N82-19360**
 NASA-CR-165259 p0044 N82-12133**
 NASA-CR-165264 p0139 N82-13554**
 NASA-CR-165269 p0132 N82-17606**
 NASA-CR-165277 p0044 N82-18315**
 NASA-CR-165283 p0128 N82-11546**
 NASA-CR-165287 p0132 N82-16494**
 NASA-CR-165289 p0137 N82-30722**
 NASA-CR-165323-VOL-1 p0130 N82-14636**
 NASA-CR-165323-VOL-2 p0130 N82-14637**
 NASA-CR-165324 p0129 N82-13507**
 NASA-CR-165327-VOL-1 p0135 N82-24649**
 NASA-CR-165327-VOL-2 p0135 N82-24650**
 NASA-CR-165328 p0117 N82-13490**
 NASA-CR-165340 p0051 N82-12139**
 NASA-CR-165342 p0133 N82-18693**
 NASA-CR-165351 p0023 N82-10040**
 NASA-CR-165353 p0105 N82-12444**
 NASA-CR-165357 p0023 N82-14092**
 NASA-CR-165358 p0023 N82-14093**
 NASA-CR-165364 p0146 N82-31968**
 NASA-CR-165365 p0146 N82-31969**
 NASA-CR-165366 p0146 N82-31970**
 NASA-CR-165367 p0136 N82-25635**
 NASA-CR-165369 p0131 N82-16484**
 NASA-CR-165378 p0134 N82-22666**
 NASA-CR-165379 p0104 N82-11465**
 NASA-CR-165386 p0023 N82-14095**
 NASA-CR-165387 p0024 N82-14096**
 NASA-CR-165388 p0027 N82-27316**
 NASA-CR-165391 p0073 N82-11224**
 NASA-CR-165395 p0063 N82-14333**
 NASA-CR-165396 p0130 N82-13510**
 NASA-CR-165397 p0028 N82-29323**
 NASA-CR-165398 p0107 N82-27743**
 NASA-CR-165403 p0129 N82-13505**
 NASA-CR-165404 p0073 N82-10245**
 NASA-CR-165407 p0063 N82-10193**
 NASA-CR-165408 p0024 N82-19221**
 NASA-CR-165409-VOL-1 p0078 N82-20362**
 NASA-CR-165409-VOL-2 p0078 N82-20363**
 NASA-CR-165409-VOL-3 p0078 N82-20364**
 NASA-CR-165409-VOL-4 p0078 N82-20365**
 NASA-CR-165412 p0113 N82-26713**
 NASA-CR-165413 p0083 N82-13357**
 NASA-CR-165424 p0130 N82-13508**
 NASA-CR-165426 p0131 N82-16482**
 NASA-CR-165431 p0064 N82-23395**
 NASA-CR-165433 p0114 N82-26714**
 NASA-CR-165434 p0114 N82-26715**
 NASA-CR-165436 p0132 N82-17607**
 NASA-CR-165438 p0114 N82-26716**
 NASA-CR-165439 p0114 N82-26717**
 NASA-CR-165440 p0114 N82-26718**
 NASA-CR-165441 p0128 N82-10506**
 NASA-CR-165447 p0132 N82-17608**
 NASA-CR-165448 p0052 N82-31448**
 NASA-CR-165449 p0135 N82-24651**
 NASA-CR-165452-VOL-1 p0129 N82-12570**
 NASA-CR-165452-VOL-2 p0136 N82-27837**
 NASA-CR-165452-VOL-3 p0128 N82-10495**
 NASA-CR-165452-VOL-4 p0136 N82-27837**
 NASA-CR-165452-VOL-5 p0133 N82-18688**
 NASA-CR-165453 p0132 N82-17603**
 NASA-CR-165453 p0131 N82-15527**
 NASA-CR-165455 p0131 N82-16483**
 NASA-CR-165457-VOL-2-PT-1 p0006 N82-18180**
 NASA-CR-165450 p0023 N82-12075**
 NASA-CR-165459 p0025 N82-22264**
 NASA-CR-165460 p0052 N82-15123**
 NASA-CR-165462 p0130 N82-13511**
 NASA-CR-165467 p0078 N82-13302**
 NASA-CR-165469 p0022 N82-10039**
 NASA-CR-165470 p0023 N82-11068**
 NASA-CR-165473 p0128 N82-10505**
 NASA-CR-165475 p0129 N82-12571**
 NASA-CR-165476 p0097 N82-22479**
 NASA-CR-165477 p0130 N82-14627**
 NASA-CR-165479 p0104 N82-11466**
 NASA-CR-165480 p0129 N82-13506**
 NASA-CR-165481 p0138 N82-33827**
 NASA-CR-165482 p0136 N82-24725**
 NASA-CR-165483 p0130 N82-14628**
 NASA-CR-165485 p0157 N82-10880**
 NASA-CR-165487 p0105 N82-11468**
 NASA-CR-165488 p0112 N82-14531**
 NASA-CR-165495 p0039 N82-15117**

NASA-CR-165497	p0113	N82-26702**	NASA-CR-167853	p0025	N82-22267**
NASA-CR-165498	p0113	N82-26706**	NASA-CR-167855	p0146	N82-25810**
NASA-CR-165499	p0022	N82-10037**	NASA-CR-167856	p0040	N82-26377**
NASA-CR-165499-APP-B	p0022	N82-10038**	NASA-CR-167857	p0040	N82-26378**
NASA-CR-165500	p0024	N82-16081**	NASA-CR-167861	p0008	N82-26237**
NASA-CR-165502-VOL-1	p0046	N82-11110**	NASA-CR-167867	p0136	N82-29719**
NASA-CR-165502-VOL-2	p0044	N82-11111**	NASA-CR-167869	p0138	N82-32855**
NASA-CR-165503	p0026	N82-23248**	NASA-CR-167872	p0137	N82-30711**
NASA-CR-165505	p0128	N82-11545**	NASA-CR-167876	p0074	N82-26482**
NASA-CR-165507	p0085	N82-24425**	NASA-CR-167877	p0055	N82-25337**
NASA-CR-165508	p0128	N82-11547**	NASA-CR-167879	p0025	N82-23246**
NASA-CR-165510	p0106	N82-24496**	NASA-CR-167883	p0091	N82-24452**
NASA-CR-165511	p0133	N82-18698**	NASA-CR-167885	p0045	N82-26381**
NASA-CR-165512	p0129	N82-12572**	NASA-CR-167886	p0033	N82-29345**
NASA-CR-165513	p0073	N82-14371**	NASA-CR-167889-VOL-1	p0045	N82-33424**
NASA-CR-165515	p0023	N82-13145**	NASA-CR-167889-VOL-2	p0046	N82-33425**
NASA-CR-165516	p0048	N82-12135**	NASA-CR-167892	p0064	N82-30374**
NASA-CR-165517	p0073	N82-13243**	NASA-CR-167894	p0137	N82-29720**
NASA-CR-165519	p0129	N82-12573**	NASA-CR-167895	p0014	N82-33375**
NASA-CR-165520	p0098	N82-25499**	NASA-CR-167896	p0027	N82-25257**
NASA-CR-165521	p0044	N82-21252**	NASA-CR-167897	p0114	N82-29619**
NASA-CR-165524	p0134	N82-22770**	NASA-CR-167898	p0137	N82-30705**
NASA-CR-165526	p0013	N82-19196**	NASA-CR-167904	p0142	N82-23976**
NASA-CR-165530	p0092	N82-11390**	NASA-CR-167907	p0164	N82-29235**
NASA-CR-165531	p0104	N82-11467**	NASA-CR-167908	p0106	N82-26679**
NASA-CR-165533	p0024	N82-16080**	NASA-CR-167909	p0052	N82-29363**
NASA-CR-165534	p0073	N82-18402**	NASA-CR-167911	p0034	N82-27331**
NASA-CR-165535	p0164	N82-18068**	NASA-CR-167912	p0074	N82-31546**
NASA-CR-165536	p0163	N82-16938**	NASA-CR-167914	p0029	N82-33392**
NASA-CR-165538	p0083	N82-14447**	NASA-CR-167918	p0079	N82-25423**
NASA-CR-165539	p0145	N82-16748**	NASA-CR-167920	p0009	N82-32310**
NASA-CR-165544	p0064	N82-27462**	NASA-CR-167923	p0137	N82-29721**
NASA-CR-165545	p0063	N82-18368**	NASA-CR-167924	p0079	N82-31584**
NASA-CR-165546	p0084	N82-17439**	NASA-CR-167928-VOL-1	p0028	N82-32370**
NASA-CR-165547	p0084	N82-18506**	NASA-CR-167929	p0137	N82-30706**
NASA-CR-165549	p0064	N82-26439**	NASA-CR-167930	p0139	N82-29777**
NASA-CR-165551	p0133	N82-19669**	NASA-CR-167934	p0078	N82-31585**
NASA-CR-165553	p0027	N82-27310**	NASA-CR-167935	p0164	N82-34311**
NASA-CR-165554	p0106	N82-18603**	NASA-CR-167938	p0107	N82-29607**
NASA-CR-165555	p0024	N82-17174**	NASA-CR-167941	p0009	N82-29269**
NASA-CR-165556	p0027	N82-28297**	NASA-CR-167944	p0028	N82-32438**
NASA-CR-165557	p0029	N82-33393**	NASA-CR-167948	p0065	N82-31509**
NASA-CR-165560	p0138	N82-32856**	NASA-CR-167949	p0028	N82-33391**
NASA-CR-165561	p0113	N82-17521**	NASA-CR-167984	p0009	N82-33347**
NASA-CR-165562-VOL-1	p0153	N82-21031**	NASA-CR-167996	p0029	N82-33394**
NASA-CR-165562-VOL-2	p0153	N82-21032**	NASA-CR-168418	p0145	N82-17880**
NASA-CR-165562-VOL-3	p0155	N82-21033**	NASA-CR-168419	p0145	N82-17879**
NASA-CR-165563	p0113	N82-20564**	NASA-CR-168548	p0153	N82-18994**
NASA-CR-165564	p0025	N82-22263**	NASA-CR-168550	p0052	N82-18326**
NASA-CR-165565	p0025	N82-22268**	NASA-CR-168556	p0084	N82-18508**
NASA-CR-165568	p0135	N82-24640**	NASA-CR-168558	p0084	N82-18507**
NASA-CR-165569	p0044	N82-16172**	NASA-CR-168585	p0090	N82-19495**
NASA-CR-165570	p0133	N82-18689**	NASA-CR-168586	p0007	N82-19169**
NASA-CR-165572	p0027	N82-27309**	NASA-CR-168760	p0084	N82-22438**
NASA-CR-165573	p0027	N82-28296**	NASA-CR-168842	p0090	N82-22455**
NASA-CR-165574	p0090	N82-19496**	NASA-CR-168894	p0026	N82-23247**
NASA-CR-165577	p0133	N82-18590**	NASA-CR-168929	p0076	N82-24361**
NASA-CR-165578	p0134	N82-21709**	NASA-CR-168930	p0113	N82-24503**
NASA-CR-165580	p0025	N82-21197**	NASA-CR-168941	p0135	N82-24646**
NASA-CR-165583	p0158	N82-24078**	NASA-CR-169003	p0026	N82-25252**
NASA-CR-165585	p0044	N82-21253**	NASA-CR-169004	p0026	N82-25253**
NASA-CR-165586	p0024	N82-21196**	NASA-CR-169005	p0085	N82-25442**
NASA-CR-165587	p0007	N82-21158**	NASA-CR-169016	p0153	N82-27090**
NASA-CR-165589	p0137	N82-30709**	NASA-CR-169029	p0106	N82-26680**
NASA-CR-165593	p0159	N82-23030**	NASA-CR-169034	p0079	N82-26526**
NASA-CR-165594	p0132	N82-17615**	NASA-CR-169120	p0091	N82-27686**
NASA-CR-165596	p0009	N82-28253**	NASA-CR-169125	p0079	N82-28503**
NASA-CR-165599	p0008	N82-24166**	NASA-CR-169278	p0091	N82-31638**
NASA-CR-165600	p0007	N82-22210**	NASA-CR-169283	p0091	N82-31639**
NASA-CR-165602	p0028	N82-32367**	NASA-CR-169293	p0091	N82-31641**
NASA-CR-165603	p0045	N82-24285**	NASA-CR-169294	p0092	N82-31642**
NASA-CR-165604	p0045	N82-28350**	NASA-CR-169295	p0092	N82-31643**
NASA-CR-165605	p0064	N82-28409**	NASA-CR-169358	p0115	N82-33738**
NASA-CR-165606	p0136	N82-29718**	NASA-CR-169852	p0065	N82-33494**
NASA-CR-165607	p0002	N82-22142**			
NASA-CR-165609	p0074	N82-24353**	NASA-TM-81616	p0087	N82-11397**
NASA-CR-165610	p0026	N82-24202**	NASA-TM-81635	p0151	N82-19944**
NASA-CR-165611	p0028	N82-31328**	NASA-TM-81651	p0014	N82-11053**
NASA-CR-165614	p0055	N82-22326**	NASA-TM-81693	p0099	N82-16413**
NASA-CR-165615	p0055	N82-25338**	NASA-TM-81694	p0100	N82-25518**
NASA-CR-165616	p0134	N82-20661**	NASA-TM-81708	p0118	N82-13509**
NASA-CR-165617	p0007	N82-22211**	NASA-TM-81716	p0058	N82-17335**
NASA-CR-165620	p0134	N82-21713**	NASA-TM-81746	p0066	N82-11211**
NASA-CR-165621	p0045	N82-22309**	NASA-TM-81766	p0117	N82-14552**
NASA-CR-165622	p0045	N82-24287**	NASA-TM-81767	p0124	N82-30704**
NASA-CR-167397	p0164	N82-34312**	NASA-TM-82594	p0119	N82-14633**
NASA-CR-167841	p0045	N82-24288**	NASA-TM-82620	p0163	N82-13013**
NASA-CR-167846	p0008	N82-26239**	NASA-TM-82644	p0024	N82-21193**
NASA-CR-167849	p0026	N82-25254**	NASA-TM-82665	p0123	N82-25637**

ORIGINAL PAGE IS
OF POOR QUALITY

REPORT/ACCESSION NUMBER INDEX

NASA-TM-82671	p0 120	N82-21712**	NASA-TM-82801	p0072	N82-21415**
NASA-TM-82678	p0 151	N82-15847**	NASA-TM-82802	p0054	N82-22327**
NASA-TM-82685	p0 118	N82-11551**	NASA-TM-82803	p0110	N82-19550**
NASA-TM-82686	p0054	N82-19333**	NASA-TM-82804	p0121	N82-22649**
NASA-TM-82691	p0019	N82-27311**	NASA-TM-82805	p0152	N82-21998**
NASA-TM-82699	p0017	N82-18222**	NASA-TM-82806	p0049	N82-21258**
NASA-TM-82704	p0058	N82-10195**	NASA-TM-82807	p0042	N82-20240**
NASA-TM-82705	p0099	N82-12446**	NASA-TM-82808	p0067	N82-20313**
NASA-TM-82706	p0058	N82-11183**	NASA-TM-82809	p0076	N82-22387**
NASA-TM-82707	p0 120	N82-20668**	NASA-TM-82810	p0110	N82-20551**
NASA-TM-82708	p0020	N82-29324**	NASA-TM-82811	p0049	N82-21259**
NASA-TM-82709	p0118	N82-10503**	NASA-TM-82812	p0050	N82-24300**
NASA-TM-82710	p0037	N82-11107**	NASA-TM-82813	p0111	N82-21604**
NASA-TM-82711	p0 120	N82-21710**	NASA-TM-82814	p0059	N82-22344**
NASA-TM-82713	p0 111	N82-11491**	NASA-TM-82815	p0018	N82-22262**
NASA-TM-82715	p0058	N82-11182**	NASA-TM-82816	p0018	N82-22266**
NASA-TM-82721	p0 125	N82-30710**	NASA-TM-82817	p0049	N82-21260**
NASA-TM-82722	p0066	N82-15197**	NASA-TM-82819	p0067	N82-20314**
NASA-TM-82723	p0037	N82-11106**	NASA-TM-82820	p0102	N82-32735**
NASA-TM-82724	p0118	N82-12574**	NASA-TM-82821	p0068	N82-24342**
NASA-TM-82725	p0003	N82-11043**	NASA-TM-82822	p0125	N82-30714**
NASA-TM-82726	p0003	N82-13114**	NASA-TM-82823	p0050	N82-24297**
NASA-TM-82727	p0 163	N82-11993**	NASA-TM-82824	p0060	N82-24323**
NASA-TM-82728	p0003	N82-11042**	NASA-TM-82825	p0147	N82-22915**
NASA-TM-82729	p0 120	N82-19672**	NASA-TM-82826	p0067	N82-21331**
NASA-TM-82730	p0151	N82-12890**	NASA-TM-82827	p0042	N82-24286**
NASA-TM-82731	p0 118	N82-13504**	NASA-TM-82828	p0060	N82-24325**
NASA-TM-82732	p0099	N82-16412**	NASA-TM-82829	p0068	N82-24343**
NASA-TM-82733	p0049	N82-11117**	NASA-TM-82830	p0059	N82-22346**
NASA-TM-82734	p0 119	N82-16481**	NASA-TM-82831	p0112	N82-26701**
NASA-TM-82735	p0119	N82-18694**	NASA-TM-82832	p0069	N82-29459**
NASA-TM-82736	p0 121	N82-23678**	NASA-TM-82833	p0050	N82-22313**
NASA-TM-82737	p0066	N82-15199**	NASA-TM-82834	p0068	N82-26468**
NASA-TM-82738	p0 151	N82-16808**	NASA-TM-82835	p0087	N82-22453**
NASA-TM-82740	p0058	N82-12216**	NASA-TM-82836	p0124	N82-28786**
NASA-TM-82741	p0 151	N82-12891**	NASA-TM-82837	p0061	N82-30372**
NASA-TM-82743	p0004	N82-18178**	NASA-TM-82838	p0163	N82-27191**
NASA-TM-82744	p0157	N82-12943**	NASA-TM-82839	p0060	N82-24322**
NASA-TM-82745	p0 111	N82-16419**	NASA-TM-82840	p0101	N82-26681**
NASA-TM-82746	p0 149	N82-14849**	NASA-TM-82841	p0095	N82-28605**
NASA-TM-82747	p0003	N82-13112**	NASA-TM-82842	p0152	N82-22951**
NASA-TM-82749	p0049	N82-14287**	NASA-TM-82843	p0149	N82-22922**
NASA-TM-82750	p0157	N82-13908**	NASA-TM-82844	p0123	N82-24647**
NASA-TM-82751	p0 119	N82-16478**	NASA-TM-82845	p0112	N82-24502**
NASA-TM-82752	p0 151	N82-16809**	NASA-TM-82846	p0111	N82-24501**
NASA-TM-82753	p0099	N82-14519**	NASA-TM-82847	p0004	N82-24165**
NASA-TM-82754	p0031	N82-19229**	NASA-TM-82848	p0163	N82-26051**
NASA-TM-82755	p0095	N82-14494**	NASA-TM-82849	p0038	N82-23261**
NASA-TM-82756	p0017	N82-15041**	NASA-TM-82850	p0112	N82-31707**
NASA-TM-82757	p0066	N82-15198**	NASA-TM-82851	p0018	N82-24201**
NASA-TM-82758	p0058	N82-11184**	NASA-TM-82852	p0060	N82-24326**
NASA-TM-82759	p0003	N82-12043**	NASA-TM-82853	p0076	N82-22388**
NASA-TM-82760	p0004	N82-16049**	NASA-TM-82854	p0054	N82-31459**
NASA-TM-82761	p0119	N82-16495**	NASA-TM-82855	p0088	N82-24455**
NASA-TM-82763	p0016	N82-14094**	NASA-TM-82856	p0100	N82-25519**
NASA-TM-82764	p0003	N82-13113**	NASA-TM-82857	p0100	N82-25520**
NASA-TM-82765	p0066	N82-14359**	NASA-TM-82858	p0069	N82-29458**
NASA-TM-82766	p0 151	N82-14881**	NASA-TM-82859	p0101	N82-28643**
NASA-TM-82767	p0 120	N82-19673**	NASA-TM-82860	p0005	N82-28250**
NASA-TM-82768	p0 120	N82-19671**	NASA-TM-82861	p0036	N82-25290**
NASA-TM-82769	p0048	N82-15119**	NASA-TM-82862	p0019	N82-26300**
NASA-TM-82770	p0016	N82-13144**	NASA-TM-82863	p0082	N82-33636**
NASA-TM-82771	p0016	N82-13146**	NASA-TM-82864	p0157	N82-25961**
NASA-TM-82772	p0017	N82-21194**	NASA-TM-82865	p0101	N82-28646**
NASA-TM-82773	p0143	N82-16743**	NASA-TM-82866	p0101	N82-28645**
NASA-TM-82775	p0162	N82-20006**	NASA-TM-82867	p0042	N82-29354**
NASA-TM-82776	p0017	N82-19220**	NASA-TM-82868	p0050	N82-30335**
NASA-TM-82777	p0004	N82-15020**	NASA-TM-82869	p0019	N82-26297**
NASA-TM-82779	p0048	N82-17263**	NASA-TM-82871	p0148	N82-30992**
NASA-TM-82780	p0049	N82-16181**	NASA-TM-82872	p0126	N82-31776**
NASA-TM-82781	p0038	N82-18311**	NASA-TM-82873	p0069	N82-28445**
NASA-TM-82783	p0119	N82-18691**	NASA-TM-82874	p0146	N82-31971**
NASA-TM-82784	p0 122	N82-23679**	NASA-TM-82875	p0123	N82-25636**
NASA-TM-82785	p0076	N82-29339**	NASA-TM-82877	p0019	N82-26299**
NASA-TM-82786	p0099	N82-16411**	NASA-TM-82878	p0072	N82-26483**
NASA-TM-82787	p0019	N82-25255**	NASA-TM-82879	p0061	N82-30373**
NASA-TM-82788	p0017	N82-16084**	NASA-TM-82880	p0018	N82-24203**
NASA-TM-82789	p0004	N82-25213**	NASA-TM-82881	p0005	N82-26241**
NASA-TM-82790	p0001	N82-17083**	NASA-TM-82882	p0051	N82-31449**
NASA-TM-82791	p0 120	N82-19670**	NASA-TM-82883	p0072	N82-32504**
NASA-TM-82792	p0018	N82-21195**	NASA-TM-82884	p0100	N82-24497**
NASA-TM-82793	p0110	N82-18612**	NASA-TM-82885	p0005	N82-28249**
NASA-TM-82794	p0 121	N82-21714**	NASA-TM-82886	p0095	N82-31663**
NASA-TM-82795	p0087	N82-17453**	NASA-TM-82887	p0102	N82-32733**
NASA-TM-82796	p0088	N82-28574**	NASA-TM-82888	p0102	N82-30552**
NASA-TM-82797	p0087	N82-19493**	NASA-TM-82889	p0149	N82-24859**
NASA-TM-82798	p0100	N82-20543**	NASA-TM-82891	p0001	N82-26219**
NASA-TM-82799	p0076	N82-22386**	NASA-TM-82892	p0042	N82-31443**
NASA-TM-82800	p0087	N82-19494**	NASA-TM-82894	p0004	N82-26205**

NASA-TM-82895 p0163 N82-31160**
 NASA-TM-82896 p0112 N82-31708**
 NASA-TM-82897 p0123 N82-27830**
 NASA-TM-82899 p0126 N82-32853**
 NASA-TM-82900 p0127 N82-33829**
 NASA-TM-82901 p0089 N82-32633**
 NASA-TM-82902 p0126 N82-32854**
 NASA-TM-82903 p0126 N82-31777**
 NASA-TM-82964 p0042 N82-27358**
 NASA-TM-82965 p0061 N82-32461**
 NASA-TM-82966 p0123 N82-26807**
 NASA-TM-82908 p0072 N82-27519**
 NASA-TM-82909 p0123 N82-26790**
 NASA-TM-82910 p0101 N82-28644**
 NASA-TM-82911 p0088 N82-26611**
 NASA-TM-82912 p0124 N82-30700**
 NASA-TM-82913 p0055 N82-33463**
 NASA-TM-82914 p0095 N82-31664**
 NASA-TM-82915 p0019 N82-26298**
 NASA-TM-82916 p0072 N82-28460**
 NASA-TM-82917 p0126 N82-33028**
 NASA-TM-82919 p0013 N82-30297**
 NASA-TM-82921 p0125 N82-30713**
 NASA-TM-82922 p0124 N82-29717**
 NASA-TM-82924 p0152 N82-32082**
 NASA-TM-82925 p0089 N82-32634**
 NASA-TM-82927 p0096 N82-32662**
 NASA-TM-82928 p0082 N82-30474**
 NASA-TM-82929 p0051 N82-30336**
 NASA-TM-82930 p0125 N82-30717**
 NASA-TM-82931 p0149 N82-29075**
 NASA-TM-82933 p0061 N82-33493**
 NASA-TM-82936 p0152 N82-31068**
 NASA-TM-82937 p0144 N82-30949**
 NASA-TM-82942 p0069 N82-30401**
 NASA-TM-82943 p0102 N82-32734**
 NASA-TM-82944 p0127 N82-33830**
 NASA-TM-82945 p0125 N82-30715**
 NASA-TM-82946 p0125 N82-30716**
 NASA-TM-83307 p0001 N82-19132**
 NASA-TM-84069 p0081 N82-15311**
 NASA-TM-84127 p0117 N82-18664**
 NASA-TM-84194 p0117 N82-24525**
 NASA-TM-84207 p0015 N82-23241**
 NASA-TM-84743 p0081 N82-24431**

 NASA-TP-1663 p0095 N82-19521**
 NASA-TP-1798 p0016 N82-13143**
 NASA-TP-1851 p0146 N82-33020**
 NASA-TP-1853 p0066 N82-16239**
 NASA-TP-1868 p0095 N82-22481**
 NASA-TP-1882 p0100 N82-25514**
 NASA-TP-1884 p0088 N82-30498**
 NASA-TP-1906 p0161 N82-32186**
 NASA-TP-1907 p0161 N82-32187**
 NASA-TP-1908 p0161 N82-32188**
 NASA-TP-1909 p0161 N82-32189**
 NASA-TP-1942 p0016 N82-14090**
 NASA-TP-1943 p0003 N82-14051**
 NASA-TP-1944 p0067 N82-19373**
 NASA-TP-1945 p0016 N82-15040**
 NASA-TP-1946 p0016 N82-15039**
 NASA-TP-1947 p0067 N82-19374**
 NASA-TP-1954 p0119 N82-16477**
 NASA-TP-1967 p0087 N82-20467**
 NASA-TP-1968 p0152 N82-21036**
 NASA-TP-1973 p0111 N82-20566**
 NASA-TP-1974 p0017 N82-19222**
 NASA-TP-1982 p0111 N82-20565**
 NASA-TP-1985 p0058 N82-20291**
 NASA-TP-1986 p0067 N82-20316**
 NASA-TP-1989 p0059 N82-21300**
 NASA-TP-1990 p0059 N82-21298**
 NASA-TP-1991 p0059 N82-21301**
 NASA-TP-1992 p0081 N82-22439**
 NASA-TP-1994 p0068 N82-21332**
 NASA-TP-1995 p0152 N82-24942**
 NASA-TP-1999 p0082 N82-25441**
 NASA-TP-2001 p0018 N82-22269**
 NASA-TP-2002 p0068 N82-22366**
 NASA-TP-2006 p0060 N82-22349**
 NASA-TP-2007 p0095 N82-23515**
 NASA-TP-2008 p0081 N82-23397**
 NASA-TP-2018 p0004 N82-26234**
 NASA-TP-2020 p0018 N82-25250**
 NASA-TP-2027 p0101 N82-26678**
 NASA-TP-2028 p0020 N82-31329**
 NASA-TP-2029 p0005 N82-29270**
 NASA-TP-2030 p0005 N82-28247**

NASA-TP-2037 p0103 N82-32737**
 NASA-TP-2040 p0102 N82-31691**
 NASA-TP-2047 p0102 N82-32736**
 NASA-TP-2048 p0069 N82-32491**
 NASA-TP-2049 p0020 N82-33389**

 NASA-1-4-W-1-111 p0079 N82-25423**

 ODAI-1403-12-81 p0044 N82-21253**

 PPI-3009-4 p0129 N82-13505**

 PR-1 p0163 N82-16937**

 PSU/TURBO-81-4 p0006 N82-18184**
 PSU/TURBO-82-2 p0026 N82-25252**
 PSU/TURBO-82-3 p0026 N82-25253**
 PSU/TURBO-82-4 p0091 N82-27686**

 PWA-5512-87 p0027 N82-27309**
 PWA-5512-88 p0027 N82-28296**
 PWA-5515-162 p0104 N82-11467**
 PWA-5515-165 p0106 N82-18603**
 PWA-5589-19 p0025 N82-22265**
 PWA-5594-92 p0031 N82-32383**
 PWA-5594-164 p0025 N82-22264**
 PWA-5594-199 p0024 N82-21196**
 PWA-5594-215 p0029 N82-33394**
 PWA-5642-21 p0064 N82-19360**
 PWA-5643-6 p0085 N82-23394**
 PWA-5698-28 p0024 N82-16081**
 PWA-5700-50 p0024 N82-16080**
 PWA-5708-26 p0097 N82-22479**
 PWA-5736-17 p0023 N82-13145**
 PWA-5772-23 p0027 N82-25257**
 PWA-5774-21 p0028 N82-33391**
 PWA-5779-10 p0026 N82-23248**

 PWA/5574-123 p0061 N82-26439**

 PYU-2115 p0073 N82-18402**

 QR-1 p0117 N82-13490**
 QR-2 p0131 N82-16483**
 QR-3 p0130 N82-14628**
 QR-3 p0135 N82-24648**
 QR-4 p0137 N82-30705**
 QR-7 p0129 N82-12573**
 QR-8 p0132 N82-17615**
 QR-9 p0134 N82-21713**

 QTR-3236 p0129 N82-12572**

 R-1489 p0084 N82-24424**

 REPT-21-4309 p0139 N82-29777**
 REPT-80ASB142DR1-VOL-3 p0164 N82-34312**
 REPT-81-9D1-HARD-R1 p0130 N82-13511**
 REPT-81-9D6-NASAC-R3 p0063 N82-18368**
 REPT-81-9F5-HTEAN-R5 p0084 N82-18506**
 REPT-111-2401-204 p0130 N82-14636**
 REPT-995 p0023 N82-11068**
 REPT-1759 p0028 N82-29323**
 REPT-2372-5009 p0044 N82-21252**
 REPT-61051 p0136 N82-29718**

 RF-05438 p0091 N82-31639**

 RI/RDB1-149 p0104 N82-11465**
 RI/RDB1-199 p0105 N82-11468**
 RI/RDB1-226 p0044 N82-16172**

 R80AEG314-VOL-4 p0023 N82-14092**
 R81-912929 p0091 N82-22460**
 R81-914618-27 p0008 N82-26223**
 R81-914618-28-VOL-2-PT-1 p0006 N82-18180**
 R81-915188-13 p0022 N82-10039**
 R81-915540-9 p0090 N82-19496**
 R81AEG030 p0023 N82-12075**
 R81AEG287-VOL-5 p0023 N82-14093**
 R81AEG590 p0131 N82-16484**
 R82AEB115 p0024 N82-17174**
 R82AEB189 p0025 N82-21197**
 R82AEB198 p0027 N82-28297**
 R82AEB462 p0029 N82-33393**

 SAR-3 p0063 N82-13217**

 SASR-2 p0090 N82-15360**

REPORT/ACCESSION NUMBER INDEX

SASR-3 p0090 N82-19495*#
 SASR-4 p0092 N82-31643*#
 SCG-810338P p0078 N82-20362*#
 SCG-810339R p0078 N82-20363*#
 SCG-810340R p0078 N82-20364*#
 SCG-810341P p0078 N82-20365*#
 SCG-810341R p0078 N82-20365*#
 SCI-81520 p0133 N82-18693*#
 SERI/CF-635-1238 p0122 N82-23684*#
 SKF-AT81C040 p0146 N82-31969*#
 SKF-AT81C044 p0146 N82-31970*#
 SKF-AT81C049-VOL-2 p0146 N82-31968*#
 SN-1020-A1-F p0048 N82-12135*#
 SR-34 p0007 N82-22214*#
 SRD-21-083 p0023 N82-10040*#
 SR81-R-476-1-21 p0138 N82-33827*#
 SR82-R-4792-28 p0065 N82-33494*#
 SR82-R-4994-08 p0074 N82-26482*#
 SSS-R-E1-5140 p0040 N82-26378*#
 SSS-R-82-5218 p0040 N82-26377*#
 SSS-R-82-5249-REV p0146 N82-25810*#
 SU-R102-6369 p0091 N82-24452*#
 TE200-230-82 p0142 N82-23976*#
 TOR-0081 (6506-1)-1 p0081 N82-24431*#
 TPR-12 p0026 N82-23247*#
 TR-81-C-29 p0003 N82-13114*#
 TR-104 p0079 N82-26526*#
 TR-376-16 p0130 N82-13508*#
 TRW-ER-8001-F p0063 N82-18370*#
 TRW-32660-6001-RU-01 p0083 N82-14447*#
 TRW-32660-6001-RU-01 p0145 N82-16740*#
 TRW-37255-6001-UT-VOL-1 p0045 N82-33424*#
 TRW-37255-6002-UT-VOL-2 p0046 N82-33425*#
 TR2-52200/2R-53085 p0007 N82-21158*#
 UAL-C-80-31-37 p0139 N82-13554*#
 UCLA-ENG-8-1-101 p0153 N82-18994*#
 UDR-TR-92-119 p0115 N82-33738*#
 US-PATENT-APPL-SN-025301 p0019 N82-26293*#
 US-PATENT-APPL-SN-060449 p0020 N82-32366*#
 US-PATENT-APPL-SN-073573 p0081 N82-24415*#
 US-PATENT-APPL-SN-092145 p0099 N82-19540*#
 US-PATENT-APPL-SN-096255 p0099 N82-19540*#
 US-PATENT-APPL-SN-102003 p0060 N82-23415*#
 US-PATENT-APPL-SN-102003 p0061 N82-30371*#
 US-PATENT-APPL-SN-122966 p0082 N82-26568*#
 US-PATENT-APPL-SN-145209 p0069 N82-29453*#
 US-PATENT-APPL-SN-161254 p0068 N82-28441*#
 US-PATENT-APPL-SN-191746 p0061 N82-30371*#
 US-PATENT-APPL-SN-199769 p0061 N82-31505*#
 US-PATENT-APPL-SN-202228 p0087 N82-11399*#
 US-PATENT-APPL-SN-218587 p0068 N82-28440*#
 US-PATENT-APPL-SN-218588 p0070 N82-33521*#
 US-PATENT-APPL-SN-219677 p0125 N82-31764*#
 US-PATENT-APPL-SN-219678 p0124 N82-29709*#
 US-PATENT-APPL-SN-235868 p0088 N82-24449*#
 US-PATENT-APPL-SN-238790 p0078 N82-29708*#
 US-PATENT-APPL-SN-310713 p0078 N82-11210*#
 US-PATENT-APPL-SN-325931 p0078 N82-26674*#
 US-PATENT-APPL-SN-328760 p0088 N82-25463*#
 US-PATENT-APPL-SN-350473 p0019 N82-26294*#
 US-PATENT-APPL-SN-350476 p0121 N82-22673*#
 US-PATENT-APPL-SN-352821 p0121 N82-22672*#
 US-PATENT-APPL-SN-358398 p0059 N82-22347*#
 US-PATENT-APPL-SN-359388 p0123 N82-24717*#
 US-PATENT-APPL-SN-364072 p0050 N82-26386*#
 US-PATENT-APPL-SN-368188 p0082 N82-24432*#
 US-PATENT-APPL-SN-371354 p0050 N82-26385*#
 US-PATENT-APPL-SN-375784 p0060 N82-26431*#

US-PATENT-APPL-SN-393588 p0126 N82-31769*#
 US-PATENT-APPL-SN-397281 p0054 N82-31450*#
 US-PATENT-APPL-SN-403378 p0070 N82-33522*#
 US-PATENT-APPL-SN-776146 p0054 N82-21268*#
 US-PATENT-APPL-SN-801290 p0099 N82-19540*#
 US-PATENT-APPL-SN-848428 p0054 N82-21268*#
 US-PATENT-APPL-SN-931090 p0099 N82-19540*#
 US-PATENT-CLASS-29-572 p0124 N82-29709*#
 US-PATENT-CLASS-60-39.07 p0020 N82-32366*#
 US-PATENT-CLASS-60-39.29 p0020 N82-32366*#
 US-PATENT-CLASS-60-226A p0019 N82-26293*#
 US-PATENT-CLASS-60-726 p0020 N82-32366*#
 US-PATENT-CLASS-136-249 p0124 N82-29709*#
 US-PATENT-CLASS-136-249 p0125 N82-31764*#
 US-PATENT-CLASS-148-1.5 p0124 N82-29709*#
 US-PATENT-CLASS-148-428 p0061 N82-31505*#
 US-PATENT-CLASS-204-38B p0070 N82-33521*#
 US-PATENT-CLASS-204-192C p0060 N82-29415*#
 US-PATENT-CLASS-204-192C p0061 N82-30371*#
 US-PATENT-CLASS-204-192E p0068 N82-28440*#
 US-PATENT-CLASS-204-192E p0070 N82-33521*#
 US-PATENT-CLASS-204-192EC p0068 N82-28440*#
 US-PATENT-CLASS-204-192EC p0070 N82-33521*#
 US-PATENT-CLASS-244-110B p0019 N82-26293*#
 US-PATENT-CLASS-264-22 p0068 N82-28440*#
 US-PATENT-CLASS-264-53 p0054 N82-21268*#
 US-PATENT-CLASS-264-216 p0054 N82-21268*#
 US-PATENT-CLASS-264-220 p0068 N82-28440*#
 US-PATENT-CLASS-264-453 p0054 N82-21268*#
 US-PATENT-CLASS-277-27 p0099 N82-12442*#
 US-PATENT-CLASS-277-40 p0099 N82-12442*#
 US-PATENT-CLASS-277-93R p0099 N82-12442*#
 US-PATENT-CLASS-315-3.5 p0082 N82-26568*#
 US-PATENT-CLASS-315-3.6 p0081 N82-24415*#
 US-PATENT-CLASS-315-3.6 p0082 N82-26568*#
 US-PATENT-CLASS-315-5.38 p0081 N82-24415*#
 US-PATENT-CLASS-330-43 p0082 N82-26568*#
 US-PATENT-CLASS-357-30 p0124 N82-29709*#
 US-PATENT-CLASS-357-30 p0125 N82-31764*#
 US-PATENT-CLASS-415-145 p0020 N82-32366*#
 US-PATENT-CLASS-415-174 p0099 N82-19540*#
 US-PATENT-CLASS-415-174 p0069 N82-29453*#
 US-PATENT-CLASS-415-178 p0020 N82-32366*#
 US-PATENT-CLASS-415-196 p0099 N82-19540*#
 US-PATENT-CLASS-420-445 p0061 N82-31505*#
 US-PATENT-CLASS-420-551 p0061 N82-31505*#
 US-PATENT-CLASS-420-588 p0061 N82-31505*#
 US-PATENT-CLASS-427-34 p0069 N82-29453*#
 US-PATENT-CLASS-427-115 p0054 N82-21268*#
 US-PATENT-CLASS-427-205 p0068 N82-28441*#
 US-PATENT-CLASS-427-244 p0054 N82-21268*#
 US-PATENT-CLASS-427-246 p0054 N82-21268*#
 US-PATENT-CLASS-427-253 p0068 N82-28441*#
 US-PATENT-CLASS-427-405 p0068 N82-28441*#
 US-PATENT-CLASS-427-423 p0069 N82-29453*#
 US-PATENT-CLASS-428-141 p0068 N82-28440*#
 US-PATENT-CLASS-428-141 p0070 N82-33521*#
 US-PATENT-CLASS-428-457 p0061 N82-30371*#
 US-PATENT-CLASS-428-472 p0061 N82-30371*#
 US-PATENT-CLASS-428-938 p0068 N82-28441*#
 US-PATENT-CLASS-428-941 p0068 N82-28441*#
 US-PATENT-CLASS-429-144 p0124 N82-29708*#
 US-PATENT-CLASS-429-251 p0124 N82-29708*#
 US-PATENT-CLASS-429-254 p0124 N82-29708*#
 US-PATENT-4,133,941 p0054 N82-21268*#
 US-PATENT-4,135,851 p0099 N82-19540*#
 US-PATENT-4,207,024 p0099 N82-19540*#
 US-PATENT-4,277,721 p0081 N82-24415*#
 US-PATENT-4,278,220 p0019 N82-26293*#
 US-PATENT-4,291,887 p0099 N82-12442*#
 US-PATENT-4,295,786 p0099 N82-19540*#
 US-PATENT-4,309,372 p0054 N82-21268*#
 US-PATENT-4,310,574 p0068 N82-28441*#
 US-PATENT-4,315,194 p0082 N82-26568*#
 US-PATENT-4,329,114 p0020 N82-32366*#
 US-PATENT-4,329,385 p0068 N82-28440*#
 US-PATENT-4,331,746 p0124 N82-29708*#
 US-PATENT-4,335,503 p0124 N82-29709*#
 US-PATENT-4,336,117 p0060 N82-29415*#
 US-PATENT-4,336,276 p0069 N82-29453*#
 US-PATENT-4,340,425 p0061 N82-31505*#
 US-PATENT-4,341,843 p0061 N82-30371*#
 US-PATENT-4,341,918 p0125 N82-31764*#
 US-PATENT-4,344,996 p0070 N82-33521*#
 UTRC/R81-915326-15 p0073 N82-14371*#
 UTRC/R82-915387-16 p0025 N82-22267*#

UMRE-DE-101-102-1	p0052	NO2-14288*0
UMRE-DR-201-101-1	p0052	NO2-18326*0
W-09170	p0052	NO2-29363*0
WARD-R1-C57	p0083	NO2-13357*0
WRC-R2-901-WARD-R1	p0137	NO2-30712*0

ORIGINAL PAGE IS
OF POOR QUALITY